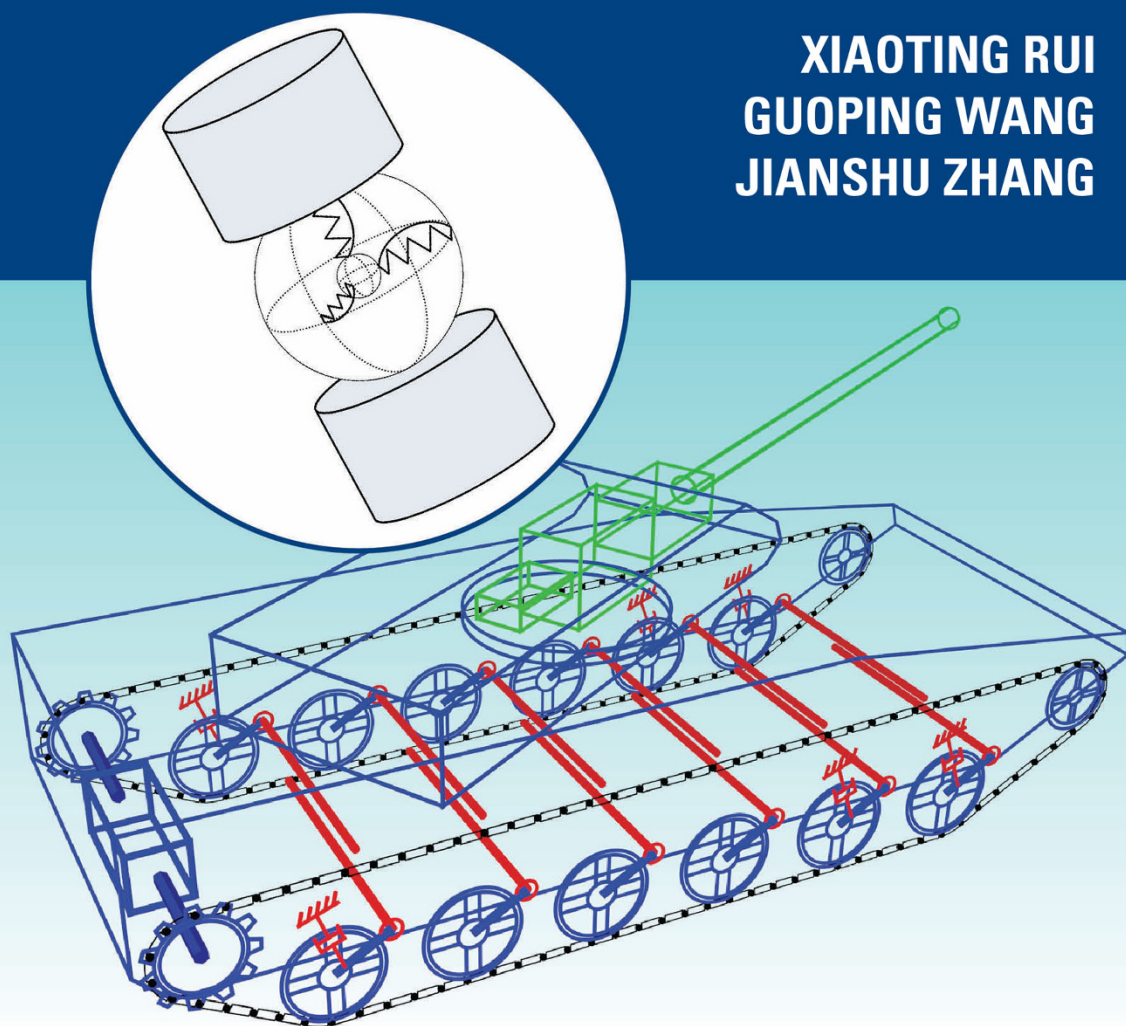


Transfer Matrix Method for Multibody Systems

Theory and Applications

XIAOTING RUI
GUOPING WANG
JIANSHU ZHANG



WILEY

**Transfer Matrix
Method for Multibody
Systems**

Transfer Matrix Method for Multibody Systems

Theory and Applications

Xiaoting Rui, Guoping Wang and Jianshu Zhang
Nanjing University of Science and Technology, P. R. China

WILEY

This edition first published 2019
© 2019 John Wiley & Sons Singapore Pte. Ltd.

All rights reserved. No part of this publication may be reproduced, stored in a retrieval system, or transmitted, in any form or by any means, electronic, mechanical, photocopying, recording or otherwise, except as permitted by law. Advice on how to obtain permission to reuse material from this title is available at <http://www.wiley.com/go/permissions>.

The right of Xiaoting Rui, Guoping Wang, Jianshu Zhang to be identified as the authors of this work has been asserted in accordance with law.

Registered Office(s)

John Wiley & Sons, Inc., 111 River Street, Hoboken, NJ 07030, USA
John Wiley & Sons Singapore Pte. Ltd, 1 Fusionopolis Walk, #07-01 Solaris South Tower, Singapore 138628

Editorial Office

The Atrium, Southern Gate, Chichester, West Sussex, PO19 8SQ, UK

For details of our global editorial offices, customer services, and more information about Wiley products visit us at www.wiley.com.

Wiley also publishes its books in a variety of electronic formats and by print-on-demand. Some content that appears in standard print versions of this book may not be available in other formats.

Limit of Liability/Disclaimer of Warranty

While the publisher and authors have used their best efforts in preparing this work, they make no representations or warranties with respect to the accuracy or completeness of the contents of this work and specifically disclaim all warranties, including without limitation any implied warranties of merchantability or fitness for a particular purpose. No warranty may be created or extended by sales representatives, written sales materials or promotional statements for this work. The fact that an organization, website, or product is referred to in this work as a citation and/or potential source of further information does not mean that the publisher and authors endorse the information or services the organization, website, or product may provide or recommendations it may make. This work is sold with the understanding that the publisher is not engaged in rendering professional services. The advice and strategies contained herein may not be suitable for your situation. You should consult with a specialist where appropriate. Further, readers should be aware that websites listed in this work may have changed or disappeared between when this work was written and when it is read. Neither the publisher nor authors shall be liable for any loss of profit or any other commercial damages, including but not limited to special, incidental, consequential, or other damages.

Library of Congress Cataloging-in-Publication Data

Names: Rui, Xiaoting, author. | Wang, Guoping, 1976 November 4– author. |
Zhang, Jianshu, 1986– author.

Title: Transfer matrix method for multibody systems : theory and applications
/ by Xiaoting Rui (Institute of Launch Dynamics, Nanjing University of Science and Technology, Nanjing, P.R. China),
Guoping Wang (Institute of Launch Dynamics, Nanjing University of Science and Technology, Nanjing,
P.R. China), Jianshu Zhang (Institute of Launch Dynamics, Nanjing University of Science and Technology,
Nanjing, P.R. China).

Description: Hoboken : Wiley, 2019. | Includes bibliographical references and index. |

Identifiers: LCCN 2017054874 (print) | LCCN 2018001943 (ebook) | ISBN
9781118724828 (pdf) | ISBN 9781118724835 (epub) | ISBN 9781118724804 (cloth)

Subjects: LCSH: Mechanics, Analytic. | Matrices. | Multibody systems.

Classification: LCC QA805 (ebook) | LCC QA805 .R824 2018 (print) | DDC 531/.16–dc23

LC record available at <https://lccn.loc.gov/2017054874>

Cover design by Wiley

Cover image: Courtesy of Xiaoting Rui

Set in 10/12pt Warnock by SPi Global, Pondicherry, India

Contents

Introduction	<i>xi</i>
About the Author	<i>xiii</i>
Foreword One for the Chinese Edition	<i>xv</i>
Foreword Two for the Chinese Edition	<i>xvii</i>
Foreword Three for the Chinese Edition	<i>xix</i>
Foreword Four for the Chinese Edition	<i>xxi</i>
Professor Rui's Method—Discrete Time Transfer Matrix Method for Multibody System Dynamics	<i>xxiii</i>
Preface	<i>xxv</i>
1 Introduction	1
1.1 The Status of the Multibody System Dynamics Method	1
1.2 The Transfer Matrix Method and the Finite Element Method	3
1.3 The Status of the Transfer Matrix Method for a Multibody System	5
1.4 Features of the Transfer Matrix Method for Multibody Systems	7
1.5 Launch Dynamics	12
1.6 Features of this Book	13
1.7 Sign Conventions	14
Part I Transfer Matrix Method for Linear Multibody Systems	19
2 Transfer Matrix Method for Linear Multibody Systems	21
2.1 Introduction	21
2.2 State Vector, Transfer Equation and Transfer Matrix	22
2.3 Overall Transfer Equation, Overall Transfer Matrix and Boundary Conditions	31
2.4 Characteristic Equation	32
2.5 Computation for State Vector and Vibration Characteristics	36
2.6 Vibration Characteristics of Multibody Systems	41
2.7 Eigenvalues of Damped Vibration	56
2.8 Steady-state Response to Forced Vibration	63
2.9 Steady-state Response of Forced Damped Vibration	70
3 Augmented Eigenvector and System Response	79
3.1 Introduction	79
3.2 Body Dynamics Equation and Parameter Matrices	80
3.3 Basic Theory of the Orthogonality of Eigenvectors	83

- 3.4 Augmented Eigenvectors and their Orthogonality 86
- 3.5 Examples of the Orthogonality of Augmented Eigenvectors 96
- 3.6 Transient Response of a Multibody System 102
- 3.7 Steady-state Response of a Damped Multibody System 111
- 3.8 Steady-state Response of a Multibody System 117
- 3.9 Static Response of a Multibody System 124

4 Transfer Matrix Method for Nonlinear and Multidimensional Multibody Systems 129

- 4.1 Introduction 129
- 4.2 Incremental Transfer Matrix Method for Nonlinear Systems 129
- 4.3 Finite Element Transfer Matrix Method for Two-dimensional Systems 140
- 4.4 Finite Element Riccati Transfer Matrix Method for Two-dimensional Nonlinear Systems 154
- 4.5 Fourier Series Transfer Matrix Method for Two-dimensional Systems 162
- 4.6 Finite Difference Transfer Matrix Method for Two-dimensional Systems 167
- 4.7 Transfer Matrix Method for Two-dimensional Systems 170

Part II Transfer Matrix Method for Multibody Systems 181

5 Transfer Matrix Method for Multi-rigid-body Systems 183

- 5.1 Introduction 183
- 5.2 State Vectors, Transfer Equations and Transfer Matrices 184
- 5.3 Overall Transfer Equation and Overall Transfer Matrix 185
- 5.4 Transfer Matrix of a Planar Rigid Body 185
- 5.5 Transfer Matrix of a Spatial Rigid Body 187
- 5.6 Transfer Matrix of a Planar Hinge 188
- 5.7 Transfer Matrix of a Spatial Hinge 189
- 5.8 Transfer Matrix of an Acceleration Hinge 192
- 5.9 Algorithm of the Transfer Matrix Method for Multibody Systems 193
- 5.10 Numerical Examples of Multibody System Dynamics 194

6 Transfer Matrix Method for Multi-flexible-body Systems 199

- 6.1 Introduction 199
- 6.2 State Vector, Transfer Equation and Transfer Matrix 200
- 6.3 Overall Transfer Equation and Overall Transfer Matrix 201
- 6.4 Transfer Matrix of a Planar Beam 201
- 6.5 Transfer Matrix of a Spatial Beam 205
- 6.6 Numerical Examples of Multi-flexible-body System Dynamics 211

Part III Discrete Time Transfer Matrix Method for Multibody Systems 217

7 Discrete Time Transfer Matrix Method for Multibody Systems 219

- 7.1 Introduction 219
- 7.2 State Vector, Transfer Equation and Transfer Matrix 221
- 7.3 Step-by-step Time Integration Method and Linearization 225
- 7.4 Transfer Matrix of a Planar Rigid Body 235

7.5	Transfer Matrices of Spatial Rigid Bodies	242
7.6	Transfer Matrices of Planar Hinges	251
7.7	Transfer Matrices of Spatial Hinges	256
7.8	Algorithm of the Discrete Time Transfer Matrix Method for Multibody Systems	259
7.9	Numerical Examples of Multibody System Dynamics	259
8	Discrete Time Transfer Matrix Method for Multi-flexible-body Systems	265
8.1	Introduction	265
8.2	Dynamics of a Flexible Body with Large Motion	266
8.3	State Vector, Transfer Equation and Transfer Matrix	276
8.4	Transfer Matrix of a Beam with Large Planar Motion	277
8.5	Transfer Matrices of Smooth Hinges Connected to a Beam with Large Planar Motion	282
8.6	Transfer Matrices of Spring Hinges Connected to a Beam with Large Planar Motion	286
8.7	Transfer Matrix of a Fixed Hinge Connected to a Beam	292
8.8	Dynamics Equation of a Spatial Large Motion Beam	296
8.9	Transfer Matrix of a Spatial Large Motion Beam	300
8.10	Transfer Matrices of Fixed Hinges Connected to a Beam with Large Spatial Motion	305
8.11	Transfer Matrices of Smooth Hinges Connected to a Beam with Large Spatial Motion	309
8.12	Transfer Matrices of Spring Hinges Connected to a Beam with Large Spatial Motion	313
8.13	Algorithm of the Discrete Time Transfer Matrix Method for Multi-flexible-body Systems	318
8.14	Planar Multi-flexible-body System Dynamics	318
8.15	Spatial Multi-flexible-body System Dynamics	322
9	Transfer Matrix Method for Controlled Multibody Systems	327
9.1	Introduction	327
9.2	Mixed Transfer Matrix Method for Multibody Systems	328
9.3	Finite Element Transfer Matrix Method for Multibody Systems	338
9.4	Finite Segment Transfer Matrix Method for Multibody Systems	341
9.5	Transfer Matrix Method for Controlled Multibody Systems I	348
9.6	Transfer Matrix Method for Controlled Multibody Systems II	362
10	Derivation and Computation of Transfer Matrices	377
10.1	Introduction	377
10.2	Derivation from Dynamics Equations	378
10.3	Derivation from an n th-order Differential Equation	388
10.4	Derivation from n First-order Differential Equations	398
10.5	Derivation from Stiffness Matrices	401
10.6	Computational Method of the Transfer Matrix	402
10.7	Improved Algorithm for Eigenvalue Problems	406
10.8	Properties of the Inverse Matrix of a Transfer Matrix	408
10.9	Riccati Transfer Matrix Method for Multibody Systems	417
10.10	Stability of the Transfer Matrix Method for Multibody Systems	428

11	Theorem to Deduce the Overall Transfer Equation Automatically	433
11.1	Introduction	433
11.2	Topology Figure of Multibody Systems	433
11.3	Automatic Deduction of the Overall Transfer Equation of a Closed-loop System	435
11.4	Automatic Deduction of the Overall Transfer Equation of a Tree System	435
11.5	Automatic Deduction of the Overall Transfer Equation of a General System	439
11.6	Automatic Deduction Theorem of the Overall Transfer Equation	442
11.7	Numerical Example of Closed-loop System Dynamics	443
11.8	Numerical Example of Tree System Dynamics	451
11.9	Numerical Example of Multi-level System Dynamics	470
11.10	Numerical Example of General System Dynamics	474

Part IV Applications of the Transfer Matrix Method for Multibody Systems 489

12	Dynamics of Multiple Launch Rocket Systems	491
12.1	Introduction	491
12.2	Launch Dynamics Model of the System and its Topology	492
12.3	State Vector, Transfer Equation and Transfer Matrix	496
12.4	Overall Transfer Equation of the System	502
12.5	Vibration Characteristics of the System	504
12.6	Dynamics Response of the System	506
12.7	Launch Dynamics Equation and Forces Acting on the System	512
12.8	Dynamics Simulation of the System and its Test Verifying	516
12.9	Low Rocket Consumption Technique for the System Test	533
12.10	High Launch Precision Technique for the System	541
13	Dynamics of Self-propelled Launch Systems	545
13.1	Introduction	545
13.2	Dynamics Model of the System and its Topology	545
13.3	State Vector, Transfer Equation and Transfer Matrix	549
13.4	Overall Transfer Equation of the System	555
13.5	Vibration Characteristics of the System	555
13.6	Dynamic Response of the System	557
13.7	Launch Dynamic Equations and Forces Analysis	563
13.8	Dynamics Simulation of the System and its Test Verifying	570
14	Dynamics of Shipboard Launch Systems	581
14.1	Introduction	581
14.2	Dynamics Model of Shipboard Launch Systems	581
14.3	State Vector, Transfer Equation and Transfer Matrix	583
14.4	Overall Transfer Equation of the System	587
14.5	Launch Dynamics Equation and Forces of the System	589
14.6	Solution of Shipboard Launch System Motion	598
14.7	Dynamics Simulation of the System and its Test Verifying	599
15	Transfer Matrix Library for Multibody Systems	607
15.1	Introduction	607
15.2	Springs	607

15.3	Rotary Springs	609
15.4	Elastic Hinges	610
15.5	Lumped Mass Vibrating in a Longitudinal Direction	611
15.6	Vibration of Rigid Bodies	612
15.7	Beam with Transverse Vibration	615
15.8	Shaft with Torsional Vibration	620
15.9	Rod with Longitudinal Vibration	621
15.10	Euler–Bernoulli Beam	622
15.11	Rectangular Plate	624
15.12	Disk	629
15.13	Strip Element of a Two-dimensional Thin Plate	635
15.14	Thick-walled Cylinder	638
15.15	Thin-walled Cylinder	640
15.16	Coordinate Transformation Matrix	642
15.17	Linearization and State Vectors	645
15.18	Spring and Damper Hinges Connected to Rigid Bodies	646
15.19	Smooth Hinges Connected to Rigid Bodies	648
15.20	Rigid Bodies Moving in a Plane	649
15.21	Spatial Rigid Bodies with Large Motion and Various Connections	651
15.22	Planar Beam with Large Motion	654
15.23	Spatial Beam with Large Motion	656
15.24	Fixed Hinges Connected to a Planar Beam with Large Motion	658
15.25	Fixed Hinges Connected to a Spatial Beam with Large Motion	660
15.26	Smooth Hinges Connected to a Beam with Large Planar Motion	663
15.27	Smooth Hinges Connected to a Beam with Large Spatial Motion	666
15.28	Elastic Hinges Connected to a Beam with Large Planar Motion	668
15.29	Elastic Hinges Connected to a Beam Moving in Space	672
15.30	Controlled Elements of a Linear System	675
15.31	Controlled Elements of a General Time-variable System	676
Appendix I		Rotation Formula Around an Axis 681
Appendix II		Orientation of a Body-fixed Coordinate System 683
Appendix III		List of Symbols 687
Appendix IV		International Academic Communion for the Transfer Matrix Method for Multibody Systems 693
References		707
Index		729

Introduction

The high programming transfer matrix method for multibody systems is introduced systematically for the first time in this book. It includes the transfer matrix method for multibody systems, the transfer matrix method for linear multibody systems and the discrete time transfer matrix method for general multibody systems developed by authors, and its applications in engineering technology. The automatic deduction theorem of the overall transfer equation of a multibody system is established. The overall transfer equations of all kinds of multibody systems are deduced manually or by computer, providing a totally new method and means for studying the dynamics of multibody systems.

The first part of the book develops the transfer matrix method for linear multibody systems. The deduction method for all kinds of transfer matrices is presented. The new concepts of the body dynamics equation, augmented operators and augmented eigenvectors of linear multibody systems are put forward. The natural vibration characteristics of complex multi-rigid-flexible-body systems are solved. The orthogonality of the augmented eigenvectors of a complex multi-rigid-flexible-body system is verified. The exact analysis of the dynamics response of complex multi-rigid-flexible-body systems is realized using the mode method. The second part of the book develops the general transfer matrix method for multibody systems. The third part illustrates the discrete time transfer matrix method for multibody systems and the transfer matrix method for controlled multibody systems. The derivation and computation method of the transfer matrix and theorem to deduce the overall transfer equation automatically are presented. Multi-rigid-body system dynamics, multi-rigid-flexible-body system dynamics and controlled multibody system dynamics are computed using the transfer matrix method for multibody systems. The fourth part of the book gives the practical application results for the transfer matrix method for multibody systems in some important engineering applications, including the launch dynamics of a multiple launch rocket system, the launch dynamics of self-propelled artillery and the launch dynamics of shipboard guns, which are the hotspots of weapon science in the international field at present. The numerous practical and research results presented demonstrate that these new theories and technologies are very effective for solving practical engineering problems. For example, the number of rockets consumed in testing the firing dispersion of a multiple launch rocket system is reduced 50–86% compared to the general testing method in many national high-tech engineering projects when the new technology is used. The firing dispersion of multiple launch rocket systems and self-propelled artillery are improved in many national high-tech engineering projects using the new technology to improve the firing precision of weapons. A library of transfer matrices of various basic mechanics elements and controlled elements has been formulated, including a library of transfer matrix methods for linear multibody systems, a library of general transfer matrix methods for multibody systems and a library of discrete time transfer matrix methods for multibody systems. It is easy to compile the various

types of multibody systems using these matrices. It is possible to model and compute complex multibody system dynamics with high computational speed without the global dynamics equation of the system.

This book can be used as a reference book by teachers, students and scientific researchers in the specialty of mechanical system dynamics. It can also be used as textbook for graduate students and as a reference book for science and technology researchers and engineers in the fields of weapons, aeronautics, astronautics, vehicles, shipping and robots.

About the Author

Professor Dr. Xiaoting Rui is presiding professor of mechanics at the Nanjing University of Science and Technology. He is a member of Chinese Academy of Sciences, a member of the Science and Technology Committee, vice-president of the Expert Committee of the General Armament Department of China and vice-president of the Applied Mechanics Society of the China Ordnance Society. He gained an outstanding person award from the Science Technology and Committee for the National Defense of China and gained a special award from the State Council of China. He is engaged in research and teaching in the field of launch dynamics and multibody system dynamics. He has completed over 20 large national and key scientific research projects, and has obtained four national



technological invention and national technological progress awards. He has published six books supported by the National Excellent Science and Technology Fund and 304 papers, including 218 papers indexed by SCI, EI and ISTP. He has won more than 30 book and paper prizes, including the China book prize, the China publishing prize and the Three One Hundred project prize. He has 64 national invention patents, and more than 40 students home and abroad from his group have gained postdoctoral and doctoral degrees. He has been guest editor of a special issue of *Advances in Mechanical Engineering* and guest co-editor of a special issue of *Multibody System Dynamics*. He is a member of the editorial committee of *Scientific Word Journal*, *Journal of ISRN Aerospace Engineering* and *Chinese Journal of Engineering*. He also is a member of the editorial committee of *Journal of Acta Armamentarii*, *Chinese Journal of Explosives & Propellants* and *Journal of Ordnance Industry Automation*. He was invited to lecture by famous scientists including Professor Werner Schiehlen (President of the International Union of Theoretical and Applied Mechanics), Professor Jens Wittenburg (developer of the Wittenburg method), Professor Erwin Stein (President of the German Mechanics Society), Professor Peter Eberhard (Head of the Institute of Engineering and Computational Mechanics at Stuttgart University), Professor Bodo Heimann (Head of the Robot Institute at Hannover University), Professor Dieter Bestle (Head of the Institute of Engineering and Vehicle Dynamics at Cottbus Technology University), Professor Klaus Thoma (Head of the Ernst-Mach Institute), Professor Edwin Kreuzer (President of Hamburg-Harburg Technology University). He has also been supported several times by key German Research Council projects, been guest professor at Stuttgart University, Karlsruhe University, Hannover University, the Ernst-Mach Institute, Cottbus Technology University and Hamburg-Harburg Technology University, and has given more than 50 invited

lectures at 16 universities and institutes in Europe and America. As a member of the Scientific Committees of several international conferences he has helped to organize and presided over conferences and given several invited keynote reports. His research results have won praise from members of the Academy of Sciences and the Academy of Engineering of China, America, Russia, Poland, India and Austria.

Foreword One for the Chinese Edition

Most mechanical systems can be considered as multibody systems composed of many rigid and flexible bodies jointed with hinges, in the fields of weapons, aeronautics, astronautics, vehicles, robots, and precision machinery. Development of the theory of multibody system dynamics rapidly in the recent 40 years has provided a powerful tool to study mechanical system dynamics. Various existing methods of multibody system dynamics have widely different styles; however, they have the following two same characteristics: (i) It is necessary to develop the global dynamics equations of systems. (ii) The order of the involved matrix of the global dynamics equations of systems is very high for a complex system, which makes the corresponding computational scale rather large. The classical transfer matrix method provides a simple and effective method to solve elastic structure mechanics problems for a one-dimensional linear system, but it cannot be used to solve the problems of vibration characteristics of a linear multi-rigid-flexible system and dynamics of a general multibody system. The coupling dynamic action between rigid bodies and flexible bodies makes the eigenvalue problem of linear multibody system non-orthogonal, which results in eigenvectors not satisfying the orthogonality in the ordinary sense. Now, the orthogonality of eigenvectors of a multibody system is a crucial requirement to analyze exactly the dynamics response of a linear multibody system with the classical mode method.

Having faced the abovementioned crucial problems at home and abroad in mechanical system dynamics, especially, in engineering, by creatively combining the transfer matrix method and modern computational methods, Professor Xiaoting Rui and his coauthors developed a new method for multibody system dynamics—the transfer matrix method of multibody systems in their monograph *Transfer Matrix Method of Multibody System and its Application*. The new method has the advantages of not requiring the global dynamics equations of system, high programming, low order of system matrix, and high computational efficiency. In the book, the study results of authors over many years are focused on, the concept and theory system of transfer matrix method of multibody systems are developed for the first time, and many creative research results are obtained. All methods developed by the authors of this book, such as transfer matrix method of linear multibody system, transfer matrix method of linear controlled multibody systems, and transfer matrix method of multidimensional systems, are expatiated systematically. The problem of rapid computation of the eigenvalue of a multi-rigid-flexible body system is solved, and the computational efficiency is improved greatly. The concepts of augmented eigenvector and augmented operator of multibody systems are presented, the orthogonality of augmented eigenvectors of multi-rigid-flexible body system is constructed for the first time, and the exact analysis of dynamics response of complex multibody systems is realized using the mode method. The discrete time transfer matrix method of multi-rigid-body systems, the discrete time transfer matrix method of multi-rigid-flexible-body systems, the discrete time transfer matrix method of controlled multibody systems, and the mixed method of transfer matrix method of multibody system with other mechanics methods are developed respectively, and the

rapid analysis of dynamics of complex multibody systems is realized using the transfer matrix method of multibody systems. These research results have been widely used to solve important engineering problems of every country with military power, such as, multiple launch rocket system, self-propelled artillery, and shipboard gun. The rapid analysis and forecast of dynamic performances of complex large multibody systems in modern engineering are realized. Strict testing technology substituting non-full charge loading rockets for full charge loading rockets in the testing of multiple launch rocket systems has been developed for the first time in the world. It has been directly verified that the technology is much better than the technology of Russia and other countries in the testing of multiple launch rocket systems. The firing dispersion of multiple launch rocket systems of national high-tech engineering projects has improved greatly. Important economic benefits have been produced. This shows that the method has powerful functions and wide application foreground.

The fact that the authors took 15 years to write the book and to rewrite the manuscripts three times shows their scientific spirit. Many famous scientists and research organizations at home and abroad have supported and shown interest in the research works of the authors for a long time. Invited by Professor Werner Schiehlen, President of International Union of Theoretical and Applied Mechanics; Professor Jens Wittenburg, Head of Engineering Mechanics Institute in Karlsruhe University; and more than 10 other famous scientists, and supported several times by key projects of the German Research Council (DFG), Professor Xiaoting Rui, guest professor of 5 universities in Europe, has given over 30 invited academic lectures about the contents of this book in 14 universities and institutes in Europe. Some members of the academy of science and the academy of engineering of several countries, including China, America, Russia, Poland, India, and Austria, have given him high appraisal.

This book has great value in theory and practicality. I believe that the publication of this book will surely enable the development of multibody system dynamics in theory and application, and provide a new powerful tool for dynamics design of mechanical systems.

Huang Wenhui
Mechanics Professor of Harbin Institute of Technology
The member of Chinese Academy of Engineering
People's Republic of China
November 18, 2007

Foreword Two for the Chinese Edition

The classical transfer matrix method was developed in the 1920s and used to study the linear system composed of elastic components, essentially applied to solve one-dimensional problems. Great research projects of the Chinese government and national defense have been accomplished recently over 10 years. Many difficult problems have been solved successfully and important breakthroughs in technology have been acquired. Tens of prizes for science and technology from the Chinese government, ministries, and commissions have been gained by the authors of this book, Professor Xiaoting Rui and others. In the process of accomplishing these works, the theory has been developed systematically by the authors as follows. The transfer matrix method of multibody system was developed in 1993 and was used to study the eigenvalue problem of a complex multibody launch system first. In 1997, the concept of augmented eigenvector and augmented operator was presented, the orthogonality of augmented eigenvectors of multibody system coupled with rigid and flexible bodies was developed, and the dynamics response of complex multibody launch systems was exactly analyzed first using the mode method. The discrete time transfer matrix method of multi-rigid-body systems was developed in 1998 while that of multi-rigid-flexible-body system was developed in 1999. It is utilized first to solve the dynamics problems of multi-rigid-body system and multi-rigid-flexible-body system using transfer matrix method of multibody system, and to study the dynamics of complex multibody launch systems using discrete time transfer matrix method of multibody system.

This book is a summarization of the transfer matrix method of multibody systems developed by the authors, and strives to expatiate on the basic principle, algorithm, and application of the method systematically. In this book, the transfer matrix method of linear multibody systems is introduced in the first part (Chapters 2–7), discrete time transfer matrix method of multibody systems is introduced in the second part (Chapters 8–11), and the application of transfer matrix method of multibody system is introduced in the third part (Chapters 12–14). Some contents of this book had been published in academic journals, mainly in Chinese. I believe that the teachers, students, and researchers of science and technology in the fields of mechanical system dynamics, weapons, and other engineering technology will surely benefit from this book.

I think the most worthy study from the authors of this book is not only the academic contents but also their excellent feature in research, addressing the main fields of construction of the national economy and national defense, combining science research with national construction and national defense, and combining theory with practice.

Huang Kezhi
Mechanics Professor of Tsinghua University
The member of Chinese Academy of Science
People's Republic of China
December 2007

Foreword Three for the Chinese Edition

The transfer matrix method was developed in the twentieth century to solve elastomechanical problems prior to the appearance of powerful computing facilities. The matrix notation supports modeling and analyzing mechanical systems with elastic elements, taking care of the various boundary conditions and initial conditions within the system and with respect to its environment. For the vibration analysis, a real and/or complex eigenvalue problem has to be solved as to what is computationally efficient because the elastic elements represent to some extent the system's configuration.

Multibody system dynamics has become a powerful tool in many engineering problems, such as, aviation, spacecraft, vehicles, robots, precision machinery, and biomechanics. A new method of multibody dynamics, namely, transfer matrix method of multibody systems, is presented by the authors. The method has four good characteristics: no necessity for the global dynamics equation of system, high programming, low order of matrix involved, and high efficiency. The new method is efficient for linear multi-rigid-flexible-body systems, nonlinear systems, time-variable systems, controlled multibody systems, and multi-dimensional systems. The method has been paid great attention, because many engineering problems of important mechanical systems were solved effectively using this method. And it is valuable to popularize the method.

The book entitled "Transfer Matrix Method of Multibody System and its Applications" authored by Professor Xiaoting Rui, Dr. Yun Laifeng, Professor Lu Yuqi, Dr. He Bin, and Dr. Wang Guoping contains a consistent view on the classical transfer matrix method, its extension to multibody systems with general topology, and applications to some important engineering problems. The book is organized in 3 parts with 14 chapters.

The first part is devoted to the transfer matrix method for linear mechanical systems. Chapter 1 presents an introduction to the topic and shows the relation between the transfer matrix method and the finite element method as well as the method of multibody systems. Chapter 2 applies the fundamentals of the transfer matrix method to linear elastic systems while in Chapter 3 the derivation and evaluation of transfer matrices is highlighted. Chapter 4 presents the vibration characteristics of linear mechanical systems resulting in real eigenvalue problems. In Chapter 5 rigid bodies are added to linear mechanical systems changing the eigenvalue problem to a complex one, the orthogonality of which is shown. Chapter 6 discusses the influence of damping and steady-state responses. Chapter 7 considers nonlinear mechanical systems introducing incremental transfer matrices.

The second part deals with nonlinear multibody systems and the related discrete time transfer matrices. Chapter 8 presents rigid multibody systems and the corresponding algorithms. Rigid-flexible multibody systems are treated in Chapter 9, especially considering Euler–Bernoulli beams as flexible bodies. Chapter 10 shows an extension to controlled dynamical systems based

on flexible bodies undergoing large displacements. Chapter 11 summarizes the transfer matrices for elements widely used in multibody dynamics.

The third part shows the application of the methods presented. Chapter 12 deals with the launch dynamics of multiple launch rocket systems. The excellent simulation results lead to a strong improvement of the firing precision and they reduce the costs of development and testing of rocket systems. Chapter 13 presents an application to self-propelled artillery systems and in Chapter 14 the launch dynamics of shipboard gun systems is investigated.

The leading author of this book, Professor Xiaoting Rui, visits the University of Stuttgart in Germany regularly. Thus, the many contributions of Professor Xiaoting Rui have been discussed thoroughly. It is most laudable that Professor Rui took the task of reviewing consistently his contributions published in many leading international journals, and put them together in one book in close cooperation with his four coauthors. I have no doubt that this book will be useful for students, scientists, and engineers who like to learn about an efficient method for the dynamical analysis of mechanical systems.

I wish the reader good success in his studies and a lot of benefit from this unique book on the latest developments of the transfer matrix method.



Werner Schiehlen
Professor of Mechanics
University of Stuttgart, Germany
November 20, 2007

Foreword Four for the Chinese Edition

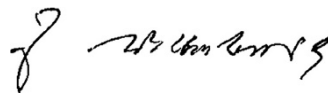
The book entitled “Transfer Matrix Method of Multibody System and its Applications” by the authors Professor Xiaoting Rui, Dr. Yun Laifeng, Professor Lu Yuqi, Dr. He Bin, and Dr. Wang Guoping is a thorough treatment of the subject. Starting from basic principles it leads in a systematic way to formalisms that enable readers to develop their own computer programs for treating dynamics problems of complex multibody systems composed of rigid and elastic bodies. Subjects of investigation are linear as well as nonlinear systems. In the case of linear systems one is interested in deformations under static loads, in eigenfrequencies and eigenforms, in steady-state vibrations with periodic excitation and with damping, and in the response to non-periodic excitation. By the method of discrete time transfer matrices nonlinear dynamics problems involving large motions of rigid bodies and large deformations of beams can be treated. The formalism presented aims at minimizing computation time so as to be applicable to very large systems.

The material is presented in 14 chapters that are divided into an introduction (Chapter 1) and in Parts I, II, and III. Part I (Chapters 2–7) is devoted to linear systems. Classical transfer matrices are formulated by various methods for basic elements of systems (point mass, spring, damper, rod under torsion, beam element) and for systems composed of such elements. Eigenfrequencies and eigenforms as well as the dynamic response to external excitation are discussed. Great room is given to the orthogonality of eigenforms. In Chapter 7 the relationship between transfer matrix and stiffness matrix is demonstrated for a finite plate element. Using the Riccati method incremental augmented transfer matrices are developed for systems of linear second-order differential equations with forcing functions.

Part II (Chapters 8–11) is devoted to the method of discrete time transfer matrices for nonlinear multibody systems. The material is presented in steps of increasing complexity. Chapter 8 deals with systems composed of rigid bodies interconnected by spherical and revolute joints and Chapter 9 with combinations of rigid and flexible bodies (beams undergoing large deformations). Both chapters begin with planar motions before treating the general case of three-dimensional motions. In Chapter 10 these methods are further generalized to include systems with control. In each of Chapters 2–10 the theory presented is illustrated by at least one non-trivial example. Various numerical algorithms are discussed. Chapter 11 presents a list of transfer matrices for some of the most frequent elements (springs, simple joints, rigid body, rod, beam and plate elements, coordinate transformations, etc.) and, in addition, a library of discrete time transfer matrices.

In Part III, in Chapters 12–14 applications of the theory to three highly complex military systems are described in some mathematical detail and with comments on the importance and quality of results. The three systems are a truck-based multiple launch rocket system, a tank with self-propelled artillery (two-phase interior ballistics and lateral vibrations of the gun), and a shipboard launch system.

The bibliography contains references to 360 Chinese and foreign books and articles. The book is 600 pages long. It is well organized. It is addressed to advanced students, researchers, and theoretically experienced engineers in practice.

A handwritten signature in black ink, appearing to read 'Jens Wittenburg', written in a cursive style.

Jens Wittenburg
Professor of University of Karlsruhe, Germany
November, 2007

Professor Rui's Method—Discrete Time Transfer Matrix Method for Multibody System Dynamics

Professor Rui developed a new method for simulating the dynamics of multibody systems. Typical examples of technical multibody systems are vehicles, robots, and machine mechanisms of all kinds. A multibody system consists of the following elements:

- bodies (rigid or deformable)
- kinematical joints interconnecting the bodies in an arbitrary configuration
- springs and dampers (linear or nonlinear)
- actuators
- a carrier vehicle on which the multibody system is mounted; the motion of this carrier vehicle is given.

The bodies of a multibody system undergo large motions. This has the consequence that the governing equations of motion to be formulated are nonlinear. It is this formulation that is the main problem of multibody system dynamics.

Over the last 35 years various methods have been developed. They differ from one another in

- the choice of variables
- the treatment of kinematical constraints
- the degree of reduction toward a minimal set of equations.

The common feature of all methods is that the system as a whole is considered. As a consequence, the equations are highly complex. The size of the coefficient matrix of the generalized accelerations depends on the total number of degrees of freedom of the system.

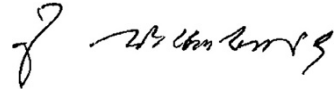
Professor Rui's method represents a totally new approach to the problems. It is a transfer matrix method. For individual elements of a multibody system (bodies, joints, springs, etc.) state vectors and transfer matrices are defined. The state vectors are composed of position and orientation variables relative to inertial space.

The transfer matrices relating the state vectors of individual elements are nonlinear, time-varying matrices that contain position and orientation variables at times t_i and t_{i-n} . The advantages of this method are the following:

- each type of element (rigid body, elastic rod, spring, etc.) is described by a standard type of transfer matrix that is developed only once;
- the transfer matrix of the system as a whole is the product of the transfer matrices of its elements. This formulation does not require special considerations for closed kinematical chains (with other methods this is a difficult problem);
- at each time step $t_i (i = 1, 2, \dots)$ the values of position and orientation variables of all bodies are calculated from the values at the previous time steps and from the boundary conditions.

The new method represents a generalization of the classical transfer matrix method of structural mechanics, where the transfer matrices are constants. In the special case of small oscillations of a multibody system around an equilibrium position the new method reduces to this classical method.

Professor Rui's method is very promising. It should be further developed and it should be applied to large technical multibody systems in order to demonstrate its accuracy and also in order to compare computation times with other methods.

A handwritten signature in black ink, appearing to read 'Jens Wittenburg', written in a cursive style.

Jens Wittenburg
Professor of University of Karlsruhe, Germany
October 1, 2000

Preface

Productions in the industries of weapons, ships, astronautics, aeronautics, machinery, vehicles including various modern tanks, artilleries, firearms, warships, submarines, planes, helicopters, missiles, launch vehicles, satellites, spaceships, aerospace vehicles, machine tools, trains, cars and electric cars, etc. are multibody systems composed of many bodies.

Multibody system dynamics (MSD) is one of the research focus areas in today's mechanics, and lays a significant foundation for the dynamics performance design as well as experiment design of industrial productions in engineering fields. Various multibody system dynamics methods (MSDMs) developed in the past 50 years have greatly promoted the development of modern science and engineering technology and provided many effective solutions for MSD. It was shown by many engineering practices that there is an urgent need for the theory of computation with high speed, the platform of numerical simulation and design with high efficiency, as well as methods of physical simulation and testing for MSD when the dynamics performance design and experiment design of multibody systems (MSs) are carried out. The following characteristics are the common problems faced by ordinary MSDMs: (i) It is necessary and rather complicated to develop the global dynamics equations of the system. (ii) The order of system matrix is proportional to the number of degrees of freedom (DOFs) of the system, which may become rather high for a complex multibody system. The computational speed decreases dramatically with the increase of the system scale, which has become an urgent problem to be solved. For example, for a multiple launch rocket system (MLRS) with 40 tubes, one needs to find out the optimal firing sequence to achieve the best firing accuracy from $40!$ (about 8.2×10^{47}) schemes, which is an amazing number. It can hardly meet the requirement of system dynamics design by using ordinary MSDMs, even when choosing the fastest computer in the world. This is because one has to first compute MSD for each of the schemes, showing how important it is to compute MSD in practical engineering design! In fact, fast computation will be a permanent research direction for complicated MSD. (iii) There was an urgent engineering demand for fast solution of the eigenvalue problems for complex multibody systems. However, one may encounter huge computational efforts and ill-conditioned problems due to large stiffness gradients by using the finite element method. Also, there was no universal approach for solving the eigenvalue problem of a linear multi-rigid-flexible-body system. (iv) For the dynamics coupling between rigid and flexible bodies, the eigenvalue problem of a multi-rigid-flexible-body system is usually non-self-conjugate, and the orthogonality of eigenvectors of the MS does not exist in an ordinary sense. Thus, the dynamics response of MSs cannot be precisely analyzed using the classical modal method. Consequently, several questions arise. Is it possible to study MSD without the global dynamics equations of the system and simplify the computational procedure of system dynamics? How can the computational scale for MSD be greatly reduced and thus the computational speed increased? How can dynamics performance design with a fast computational dynamics method be realized? How can the vibration characteristics of linear

MSs be computed? How can the orthogonality of eigenvectors for linear MSs be constructed and precise analysis of dynamics response realized with the modal method? How can experiments for complex mechanical systems be designed? These are urgent difficult problems noticed by most scientists and engineers around the world. And it is these urgent theoretical and engineering demands that rightly promote the rapid development of the transfer matrix method for multibody systems (MSTMM). According to my long-term study and engineering practice in launch dynamics and MSD, I have deeply perceived that it is primarily important to establish a new MSD method with high computational speed.

In order to avoid the global dynamics equations when studying MSD and increase computational speed regardless of the number of system DOFs, I first proposed the MSTMM to study MSD in my PhD thesis “Study on Launch Dynamics of Multibody Systems” in 1993, which was published in 1995, where the computational efficiency of MSD was greatly improved. Later on, many scholars and scientists made a lot of important contributions to the development of this method. By continuous improvement and engineering applications as well as extensive international academic exchanges during the past 25 years, the method has been developed into a novel stylized efficient dynamics method for general MSs. It has been applied to the dynamics analysis and design of various large mechanical systems that have received great attention from many scientists and engineers. Further, MSTMM plays an important role in the research, production, and testing process of many complex mechanical systems. Using this method, serious difficulties appearing in some projects of national high-tech engineering have been solved, and important technology breakthroughs have been achieved. All of these exhibit the strength and application prospect of MSTMM.

We took the lead in developing a strict testing technology using non-full charge loading test instead of full charge loading test for testing the firing precision of multiple launch rocket systems. The rocket consumption for testing the firing precision of a multiple launch rocket system has been greatly decreased, which used to be a crucial difficult problem for every country with military power. It has been verified by testing that the new technology is much better than that of Russia and other countries, and 12 million Yuan have been saved in each test of the multiple launch rocket system. In fact, a direct economic benefit of over hundred million Yuan has been saved. Another technology for improving the firing precision of weapons has also been developed. The firing precision of multiple launch rocket systems and self-propelled artilleries within the national high-tech engineering projects has been improved greatly using this new technology.

According to incomplete statistics to date, there have been six monographs published regarding MSTMM and its applications. Over 300 articles studying the method have been published in more than 100 journals by over 200 authors from over 60 work units. Moreover, over 10 software copyrights, 100 patents, and 4 national technology progress and invention awards related to MSTMM have been achieved, respectively. This method has been successfully applied to a wide range of engineering problems related to about 100 products and over 50 fields, including self-propelled artillery, shipborne gun, “metal storm” antiaircraft gun, spin tube gun, vehicular MLRS, airborne MLRS, shipborne MLRS, cannon on helicopters, tank, ultra-precision single-point diamond fly-cutting machine tool, spacecraft navigation and its vibration reduction system, launch vehicle, missile, aerospace aircraft, submarines, underwater towed systems, piezoelectric actuator, controlled flexible manipulators, intelligent flexible four-bar linkage devices, super long stay cable, earthquake resistant civil structures, immersed tunnel, robots, mobile concrete truck boom, vibrating screen, vibration compaction, road roller, wind turbine, wind turbine tower, gas turbine system, low pressure rotor of gas turbine, high pressure compressor of gas turbine, large-scale rotary machine, feeding platform, parachute-submissile, rocket projectile, vehicular missile, truck cranes, floating bridge, wing, five-axis CNC machine tool,

heavy duty longmen machine tool, machine tool spindle system, servo turret system, high pressure gas well system, diesel engine, roots blower with double rotor, ship's anti-vibration mounting system, ship pipeline system, bearing-rotor, vehicle suspension, etc.

There are mainly three stages in the development of MSTMM: transfer matrix method for linear multibody systems (linear MSTMM) (1993~), discrete time transfer matrix method for multibody systems (MSD-TMM) (1998~), and the new version of transfer matrix method for multibody systems (NV-MSTMM) (2013~).

In 1997, Rui et al. proposed the concept of “augmented eigenvector” and “augmented operator” for linear MSs, and constructed the orthogonality of augmented eigenvectors of linear multi-rigid-flexible-body systems. The exact analysis of dynamics response of a linear multi-rigid-flexible-body system using a modal method was achieved for the first time. Yun et al. (2006) proposed the transfer matrix method (TMM) for two-dimensional systems to analyze two-dimensional system dynamics by using pure TMM. Rui et al. (2006) also proposed the transfer matrix method for linear controlled MSs.

Rui et al. (1998) proposed and gradually improved the discrete time transfer matrix method for multi-rigid-body systems. In this method, the high efficiency of MSTMM and various time integration methods are combined. The constant transfer matrices and state vectors described by modal coordinates in linear MSTMM were extended into time-dependent transfer matrices and state vectors described by physical coordinates. Rui et al. (1999) proposed and gradually improved the discrete time transfer matrix method for multi-rigid-flexible-body systems. The Riccati transformation was then introduced by He et al. (2007) for solving the MSD composed of a huge number of elements. Rong et al. (2010) established the discrete time transfer matrix method for controlled MS. The dynamics of multi-rigid-body systems, multi-rigid-flexible-body systems, as well as controlled MSs, especially complex launching systems, were studied using MSTMM, which is suitable for time-variant, nonlinear systems with large motion, for the first time with fast computational speed and without global dynamics equations.

However, due to linearization of nonlinear functions in MSD-TMM, the time step size should be kept small to guarantee computational precision and stability. Rui et al. (2013) proposed the NV-MSTMM, where accelerations, angular accelerations, internal forces, and torques are selected as state variables of the state vectors. The local linearization is fully avoided while deducing the transfer equations of elements. In that sense, the transfer equations of elements and overall transfer equation of the system are exact, so MSTMM belongs to accurate analysis methods in theory.

Rui, Zhang, Xue Rui et al. (2011) introduced the topology figure and presented the automatic deduction theorem to deduce the overall transfer equation automatically. Zhou et al. (2016) proposed the deduction method for overall transfer equations of linear controlled MSs. Rui et al. (2006) proposed the mixed method of MSTMM with other MSD methods and the finite element method to take advantages of each of the methods. Rui et al. (2014) developed the visualized simulation and design software MSTMMSim with MSTMM executing as its core. This software has been applied to the dynamics computation of multiple launch rocket systems, self-propelled artilleries, tanks, and some other large mechanical systems.

This book is based on the “Transfer Matrix Method of Multibody System and its Applications” (Beijing: Science Press, 2008) written by the first author as the chief author. Additionally, over 100 papers published by the authors of the book during the last decade and the latest research results across the world in this field are incorporated into this book. The remarkable research findings of various state basic research development programs of China (973 Programs), exploration projects, pre-research fund projects, basic scientific research projects, cross-industry projects, etc. are included in this book. We strive to exhibit a self-contained system to introduce the basic theories, algorithms, latest developments, and applications of the transfer matrix method

for multibody systems. The book is organized in 4 parts with 15 chapters. Chapter 1 presents the characteristics of the transfer matrix method for multibody systems, the finite element method, and the multibody system dynamics methods.

The first part (Chapters 2–4) develops the transfer matrix method for linear multibody systems. It includes the fundamentals of the transfer matrix method for linear multi-rigid-flexible-body systems, the new concepts of the body dynamics equations and augmented eigenvectors, the methods to construct the orthogonality of augmented eigenvectors, to derivate transfer matrices, to evaluate vibration characteristics and dynamics response. Further, transfer matrix method of multi-dimensional systems and transfer matrix method for nonlinear systems are also introduced.

The second part (Chapters 5–6) introduces the new version of the transfer matrix method for multibody systems, where the accelerations and the internal forces are treated as the state variables of the connecting point. Both the transfer matrix method for multi-rigid-body systems and that for multi-flexible-body systems are introduced.

The third part (Chapters 7–11) develops the discrete time transfer matrix method for multibody systems. It includes discrete time transfer matrix method for multi-rigid-body systems, discrete time transfer matrix method for multi-rigid-flexible-body systems, transfer matrix method for controlled multibody systems, and a hybrid method of these with other dynamics methods. The derivation and computation methods of transfer matrices of elements, as well as the automatic derivation theorem of the overall transfer equation of the system, are also introduced.

The fourth part (Chapters 12–15) shows some practical engineering applications of the transfer matrix method for multibody systems in launch dynamics that are the hotspot in the international armament science at present. The new theories of launch dynamics of multiple launch rocket systems, launch dynamics of self-propelled artilleries, and launch dynamics of shipboard guns based on the transfer matrix method for multibody systems are developed. Excellent simulation results obtained by the theories lead to a strong improvement in the firing precision of weapons and a great decrease in costs for the testing of multiple launch rocket systems. Finally, a library of transfer matrices of various elements widely used in various multibody systems is provided.

Nearly 100 researchers have participated in the related research work of this book, and dozens of experts and scholars at home and abroad have made great contribution to this book. The four dynamicists, Professor Wenhui Huang, member of the Chinese Academy of Engineering; Professor Kezhi Huang, member of the Chinese Academy of Science; Professor Werner Schiehlen, President of International Union of Theoretical and Applied Mechanics, Professor Jens Wittenburg, Director of the Institute of Engineering Mechanics, Karlsruhe University, offered wonderful forewords for the first edition of the book. The two dynamicists, Professor Dieter Bestle, Cottbus Industrial University, and Professor Haiyan Hu, member of the Chinese Academy of Sciences from Beijing Institute of Technology, went through the whole manuscript of the book and made a recommendation for publication. The personnel who have participated in the work of this book include Associate Professor Fufeng Yang, Associate Professor Hailong Yu, Associate Professor Bao Rong, Associate Professor Bin He, Professor Laifeng Yun, Professor Laith K. Abbas, Lecturer Yan Wang, Lecturer Tao Chen, Dr. Weibo Wei, Dr. Jun Hong, Dr. Junyi He, Dr. Lei Ma, Dr. Zhihuan Zhan, Dr. Hao Xu, Dr. Binbin Feng, Dr. Wenbin Tang, Dr. Xue Rui, Dr. Feifei Liu, Dr. Heng Zhang, Dr. Chao Li, Dr. Junjie Gu, Dr. Haigen Yang, Dr. Minjiao Li, Dr. Qinbo Zhou, Dr. Qicheng Cha, Dr. Gangli Chen, Dr. Jian Gu, Dr. Tianxiong Tu, Dr. Lilin Gu, Dr. Bo Li, Dr. Yu Tao, Dr. Min Wei, Dr. Lu Sun, Dr. Hanjing Lu, Dr. Xun Wang, Professor Bin Hu, and Professor Ming Song. Science Publishing House and deputy editor Baoli Liu strongly supported the publication of this book. Monicka Simon, editor of Wiley publisher, gave the book an

elaborate editing and proofreading, and our family also gave us great understanding and support for our work.

I was invited and supported respectively by famous scientists including Professor Werner Schiehlen, President of International Union of Theoretical and Applied Mechanics; Professor Jens Wittenburg, Head of Engineering Mechanics Institute in Karlsruhe University; Professor Erwin Stein, President of Germany Mechanics Society; Professor Peter Eberhard, Head of Institute of Engineering and Computational Mechanics in Stuttgart University; Professor Klaus Thoma, Head of Ernst-Mach Institute; Professor Dieter Bestle, Head of Institute of Engineering Mechanics and Vehicle Dynamics in Cottbus Technology University; Professor Bodo Heimann, Head of Robot Institute in Hannover University; and Professor Edwin Kreuzer, President of Hamburg-Harburg Technology University. I was also supported several times by key projects of German Research Council (DFG), as guest professor of Stuttgart University, Karlsruhe University, Hannover University, Ernst-Mach Institute, Cottbus Technology University, and Hamburg-Harburg Technology University. Moreover, I was invited by dozens of famous dynamicists, such as, Professor Friedrich Pfeiffer, Chief Editor of Journal *Archive of Applied Mechanics*; Professor Peter Maisser, Head of Mechanic and Control Institute in Chemnitz Technology University; Professor Karl Popp, Head of Mechanics Institute in Hannover University; Professor Lutz Sperling of Engineering Mechanics Institute in Magdeburg University; Professor Joachim Lückel, Head of Mechanic Control Institute in Paderbor University; Professor Jorg Wauer of Engineering Mechanics Institute in Karlsruhe University and Professor Horst Irretier of Kassel University; Professor Peter Breedveld, Twente University; Professor Ahmed Shabana, University of Illinois at Chicago; and Professor Fen Wu, North Carolina State University. I was also invited by Harbin Engineering University, Xi'an Jiao Tong University, Xi'an Technological University, Suzhou University, Institute of automation of China weaponry and equipment group, Xi'an Modern Chemistry Research Institute, and Chongqing military representative Bureau. I have given over 80 invited academic lectures about the contents of this book in 20 universities and institutes in Europe and America, as well as in various international conferences about mechanics, machinery, and vibration.

I would like to express our great gratitude to the research organizations, institutions, scientists, experts, and our families, which sponsored, supported, and helped our research work, activities of academic exchange, and lectures at home and abroad. Special thanks are given to Professor Dieter Bestle. During his several academic visits to my institute summing up to about one year, he made a systematic study and development of the Rui method and made a lot of creative contributions to the book word by word. Professor Jens Wittenburg commented that "Rui method represents a totally new approach for simulating the dynamics of multibody system and is very promising." Professor Werner Schiehlen commented that "It is valuable to popularize the method." Professor John Herbst commented that "Transfer matrix method of multibody system is a totally new and original method for solving multibody system dynamics. It is very valuable to popularize Rui method in the study fields of multibody system dynamics and complicated mechanical engineering." I would like to dedicate the book to them. I wish that the transfer matrix method for multibody system will play a positive role in benefiting humankind. Any comments from professors and experts in various research fields on the book will be welcomed.

Professor Dr. Xiaoting Rui
Member of the Chinese Academy of Sciences
Presiding Professor of Mechanics in Nanjing University of Science & Technology
April 2018

1

Introduction

1.1 The Status of the Multibody System Dynamics Method

A *multibody system* (MS) is a system composed of many bodies, including rigid bodies, flexible bodies, lumped mass, etc., connected in various ways. The physical concept of an MS is ancient and unambiguous. In the construction of national defense and the economy, such as weaponry, shipping, aeronautics, astronautics, communications and mechanisms, many models of practice engineering, such as tanks, ships and warships, aircraft, carrier rockets, vehicles, robots, machine tools etc., can be regarded as MSs composed of rigid bodies, flexible bodies and lumped masses connected with various hinges [1–12].

In the 1950s to the 1960s, the concept of a multibody was either a multi-rigid-body or a multi-flexible-solid, therefore two totally different subjects, *multi-rigid-body system dynamics* (MRSD) [7, 9, 11] and the *finite element method* (FEM) [13], respectively, were developed almost independently. The infinite element method [14], presented in the mid-1970s, perhaps is a little supplement for the FEM. The basis of MRSD is the ancient dynamics and variation principle. The research objects of *multibody system dynamics* (MSD) [6, 8, 12] are a rigid body and flexible solid, which includes both the research objects of MRSD and the FEM. Since the dynamics equation of a rigid body rotating around a fixed point was established by Euler in 1765, rigid body theory has had more than 200 years of history and is very distinct. In the classical theory of rigid body dynamics developed since 1960s, only a few systems with more than two bodies, such as double pendulums and gyroscopes, have been studied. Complex *multi-rigid-body systems* (MRSs) composed of many rigid bodies moving on a large scale connected with various hinges has not been studied enough in flexible solid dynamics and the FEM. It is known that the model of the MRS is not a good enough mechanics model for practical problems. For example, a slender manipulator should not be modeled as a rigid body, and a slender tube of a rocket launcher and gun should also not be modeled as a rigid body in the study of launch dynamics. It is necessary to include the flexible body for further study of MSD. The *multi-rigid-flexible-body system* (MRFS) has become the main research direction in MSD and the main dynamics model for many engineering mechanism systems. The hybrid algorithm of the MRS and the FEM [10], developed by Professor Peter Eberhard of the University of Stuttgart and Dr. Bin Hu of the Mercedes-Benz Company in 2003, combines the highlight of multi-rigid-body dynamics and the FEM, and has the features of high computation efficiency and high computation accuracy when computing the dynamics of a flexible body with large motion using this method. It is one of the recommended advanced methods of contact dynamics.

Since the discovery of Hooke's law in 1660 to now, the solid theory has had more than 300 years of history and is very distinct. Beginning in the 1950s, the solid theory and

the deformation of elastic solids have progressed to finite deformation nonlinear elastic theory by elastic mechanics based on a formulation system [15]. However, the rigid body and its large motion have not been involved in elastic mechanics. It is necessary to have a unanimous opinion for the concept of solid rotation. The rotation of a rigid body is a characteristic quantity of global body movement of the rigid body and is independent of the origin of its translation coordinate system. How can we model the rotation of an elastic body, such as an elastic manipulator that has one end fixed on a rotational axis? The rotation of a point fixed on a deformable solid is used to describe the rotational displacement of the adjacent region of such a point, rather than to specify the characteristic quantity of the global movement of the whole solid. It is therefore necessary to include the rigid body in the further study of solid dynamics.

Multi-flexible-body system dynamics (MFSD) [6, 8, 12] is the current research focus in MSD. It differs not only from MRSD, but also from classical solid dynamics. Its main characteristic is coupling between the deformation and the global rigid motion of the body; the consideration of the flexible effect in the dynamics equations of MSs plays a key role. There are usually two methods of treating a flexible body. One is to model a flexible body using many rigid bodies connected by springs and dampers, and the other is to establish the dynamics equation of the flexible body directly and describe its deformation with the FEM, the *modal synthesis method* or the *hypothesis modal shape method*. The “*multi-flexible-body system*” emphasizes the two aspects of multi-body and flexibility. Multibody means that MFSD is the natural extension of MRSD, as usually there is large motion among bodies. Flexibility of body means that MFSD is the natural extension of solid dynamics; it makes the number of *degrees of freedom* (DOF) of the flexible body increase greatly and the relations between kinematics and dynamics more complex. The centrifugal forces and Coriolis forces acting on a body, caused by its large motion, affect its deformation and the deformation conversely affects the composite motion of the body. The coupling effect between large motion and deformation of the body is the core of MFSD.

Along with the development needs of engineering technology, many methods of MSD, such as the Wittenburg method [7], the Schiehlen method [6] and the Kane method [9] etc. [16–28], have been put forward and improved creatively by scholars and experts in the last 50 years. These methods provided effective computation means for various MSD, and greatly boosted the development of modern engineering technology. Based on the FEM and the *boundary element method* (BEM), the programming of structure dynamics analysis was realized. These theories provided powerful tools for complex structure dynamics. Various computational programs, such as SAP, NASTRAN and ANSYS, have been developed. Although the various methods of MSD have different styles, they all have the following two characteristics. First, it is vital to establish the global dynamic equation of the system, which is the most wonderful part of each MSD, marked by individual features, and is the most baffling part for ordinary technicians. Second, the order of the system matrix of the global dynamic equation of the system is not less than the number of degrees of freedom of the system and is very high for a complex system, resulting in a big problem regarding its computational scale. These two problems in the FEM and ordinary methods of MSD have been given great attention. First, it is not convenient to compute the *vibration characteristics* of complex MRFSs with a high stiffness gradient. Second, it is difficult to exactly analyze the system dynamic response because of a lack of *eigenvector orthogonality* of the general complex MRFS. The following academic and practical problems have been given great attention by dynamicists and engineers around the world [29–33]: avoiding the computation singularity caused by the computation ill-condition of a structure with a high stiffness gradient, finding the eigenvector orthogonality of general MRFS coupled with rigid bodies and flexible bodies, searching for efficient computational methods of MRFSD with high programmability, thinking of and designing dynamic launch system performance from the point of launch system dynamics.

To solve these problems can we develop a new way that is completely different from the study styles and features of ordinary MSD as follows: without the global dynamic equation of system, with a small computational scale and highly programmable? Motivated by the idea of the transfer between state vectors used in the classical *transfer matrix method* (TMM) [34–40], a totally new method with these features, the *transfer matrix method for multibody systems* (MSTMM) [3–5, 41–86], has been developed by the authors. The MSTMM applies to a linear multibody system, as well as a general multibody system, to compute their dynamic responses. In particular, the *vibration characteristics* of a linear multibody system can be solved by using the MSTMM. The technologies of dynamic design [87–121] are developed for improving the launch precision of launch systems, reducing the ammunition consumption of launch system tests, diagnosing faults, etc. These solved the important engineering problems of a series of national high-technique subjects, such as self-propelled artillery, shipboard launch systems, *multiple launch rocket systems* (MLRSs), missile sealift systems with ocean wave compensation, application of the strap-down inertial measurement unit of the gyroscope, and accelerometers with high precision. These injected new energy into and provided completely new methods for the development of launch dynamics and flight dynamics [122–200].

1.2 The Transfer Matrix Method and the Finite Element Method

The classical TMM was developed in the 1920s to analyze the vibration of one-dimensional linear systems with an elastic construct (see references [36–38]). Holzer (1921) first used the parameter method, named the Holzer method, to solve torsional vibration for shafts with multiple discs [201]. Myklestad (1944) used a similar method to determine the bend vibration modes of beams [202]. Proh (1945) improved the Holzer method, resulting in the so-called Myklestad method, to solve the transverse vibration of shafts [203]. With the development of computer and matrix operations, the Myklestad method was worked up to create the TMM. Thomson (1950) used the TMM to structure vibration of the general linear system [204]. Pestel (1963) published the first TMM book [36], *Matrix Method in Elastomechanics*. Many transfer matrices of elastic mechanics elements are given in this book. Rubin (1964) put forward the general method for the transfer matrix and the relationship between the transfer matrix and the frequency response matrix [205]. The TMM was used by many scholars and engineers, such as Targoff [206], Lin [207], Mercer [208], Lin [209], Mead [210, 211], Henderson [212], McDaniel [213, 214] and Murthy [215–217], to solve static and dynamic engineering problems for beams, beam-type multiple structures, skin-stringer panels, rib-skin structures, curved multi-span structures, cylindrical shells, stiffened rings, etc. Horner (1978) presented the Riccati TMM [218] to solve the numerical stability of boundary value problems. Huolang Fang (1990) used Fourier–Laplace transformation to derive the transfer matrix of three-dimensional viscoelastic groundsill floors with invariant mass density under harmonic loads and solve dynamics flexible coefficients of sandwich groundsills [219]. Using the theory of the Kelvin function, Xinzhu Zhou (2005) acquired the transfer matrix of an annulus plate element with invariant thickness in a Winckler groundsill and the overall transfer matrix of a symmetrical annulus plate with variable thickness [220]. The TMM has been used widely for a long time in structural dynamics, especially in rotor dynamics, because its order of frequency determinant is low. Consequently, it is very convenient to program and numerically compute. Ever since it came into being, the TMM, as one of the matrix methods, has been strongly bonded with numerical computers. The TMM is used widely in modern engineering and science in techniques such as optics, acoustics, electronics, surface science, robots, weaponry, aeronautics, astronautics, mechanisms, etc. However, the classical

TMM is not efficient for the vibration characteristics of the MRFS or for the dynamics of general MRSs and MRFSs with time-variant, nonlinear, large motion. It is an attractive research direction to combine the classical TMM with the modern algorithms to solve difficult problems of two- and three-dimensional dynamics systems with high computational speed.

The FEM is a numerical computational method for structure analysis that was developed in the 1930s. It discretizes a continuous elastic body into a set of finite elements, then an algebraic equation system can be assembled by analyzing these elements. Its main principle is to discretize a system into elements, substitute a straight segment for a bent one, and therefore make a complex and difficult problem into a simple and easy one. A huge renovation has taken place in engineering design and analysis due to the FEM because of its strong theory base, high comprehensibility and wide application fields, which are particularly suited to program design and numerical computation of highly complex structures. The application of FEM has been extended from planar elastic mechanics to spatial elastic mechanics and shells, from static forces equilibrium to stability, dynamics and waves. The analysis objects have extended from elastic materials to plastic, viscoelastic, viscoplastic and composite materials, from solid mechanics to hydrodynamics, heat transfer mechanics and continuous medium mechanics. Its action has been extended from analysis and checks to a combination of optimization with computer-aided design (CAD) in engineering analysis. Courant (1943) presented the approximate numerical solution by defining the subsection continuous function in the triangle region in his mathematics paper. Argyris (1950) analyzed the structure using the idea of grids. Clough computed airplane structure using triangle elements and named the FEM for the first time. Kang Feng (1956) then published his research paper on the FEM. It is because mathematicians engaged in the study of the FEM after the 1960s that the FEM had a strong mathematic foundation. Zienkiewicz and Ceung (1965) declared that the FEM can be used for all field problems computed in variation forms, so it was used and extended to a wider range of applications. It was used first in the field of aeronautics engineering, then in technique engineering, for example in mechanisms, vehicles, shipbuilding, construction, etc. The FEM has been extended from solid mechanics to subjects such as temperature field, flow field, electromagnetism field and vibration field. Along with the rapid development of computer technology, a lot of FEM computer software appeared, for example NASTRAN, DYTRAN, ASKA, SAP, MARC, ANSYS, ADINA, etc. The FEM has therefore become a widely accepted engineering analysis tool with a stable base [221]. However, the dynamics of a multi-rigid-body system or a multi-rigid-flexible-body system could not be solved merely by the FEM.

Both the TMM and the FEM developed slowly in their initial stages. From 1960 the two methods developed quickly because of the wide use of computers. They were first applied in the field of mechanics, especially in structural analysis. The matrix method has been a standard analysis tool of applied mathematicians for a long time. Sylvester (1848) first introduced the concept of matrix. Cayley (1855) presented matrix algebra for the first time in linear transformations. Although matrix algebra is a powerful tool in the operation of linear algebra, its application in structural analysis is seldom mentioned in references before 1940, nor is its application in other aspects of engineering technology. Why has the matrix method not been used widely in engineering technology in the long time since it came into being? One of reasons is that it takes too much time to calculate a practical engineering problem manually. The first computer ENIAC was developed in America in 1946. Computers greatly promoted the development of the TMM, the FEM and engineering techniques. The two methods were applied widely and were powerful tools for engineering technology.

It is clear that the TMM and the FEM were developed almost at the same time. The two methods are efficient for the statics and dynamics problems of complex structures. However, there are some differences between them. The classical TMM is used for the statics and dynamics problems of discrete or continuous one-dimensional systems that are linear, time-invariant

and have small vibrations. Its main features are modeling flexibility and high computational efficiency. The FEM is used for statics and dynamics problems of continuous multi-dimensional systems based upon the strategy of spatial discretization. Its main features are its powerful function and large computational scale. Even the sparsity of the mass matrix and the stiffness matrix of the system is utilized, the order of the system matrix is still very high for a complex structure consisting of a large number of elements and the computational speed of dynamics cannot meet the engineering requirement. It is one of the intended purposes of the FEM to reduce further the order of the system matrix to improve computational speed. The application of the FEM is wider than the application of the TMM mainly because the TMM is only efficient in nature for one-dimensional systems, whereas the FEM is efficient for one-dimensional, two-dimensional and three-dimensional systems. The FEM has therefore been developed more fully in theory and is used more widely in engineering. Because of its ability to deal with linear multi-rigid-flexible-body system dynamics, the application range of the TMM is being extended and it is being studied more fully and combined with other methods. We presented the TMM for a two-dimensional system in 2005 [74, 75], which makes it possible to study a two-dimensional system dynamics problem using the TMM alone. It is hoped to extend this method to three-dimensional system dynamics. Kumar (1986) presented the *discrete time transfer matrix method* (DTTMM) for time-variant structural dynamics [222]. Dokanish (1972) extended the research into the TMM and presented the *finite element transfer matrix method* by combining the FEM with the TMM [223]. If a two-dimensional plate is divided into finite stripe elements, the transfer matrix from state vectors of one end of the stripe plate to the other can be developed using the FEM. In this way, the system vibration is studied by the TMM and computational speed is improved with the same computation accuracy as the FEM [224, 225]. Some researchers, such as Ohga [226], Xue [227], Loewy [228, 229], etc., have improved the finite element transfer matrix method for studying structural dynamics. It has been verified by practice that combination of the TMM and the FEM is an inevitable result of the development of these two methods for efficiently solving complicated engineering problems. Although the TMM and the FEM are two mechanics methods that were developed independently almost at the same time 80 years ago, they have finally come together, just like a couple of lovers.

1.3 The Status of the Transfer Matrix Method for a Multibody System

To solve the urgent requirement of rapid computation of an eigenvalue problem in the engineering of a complicated launch system, the FEM came up against the following problems: lack of a general computational method for eigenvalues of a linear MS, an unacceptably large computational scale and the inevitable computation ill-condition problem caused by a complex system and a large stiffness gradient. We presented the concept of the MSTMM [41–54] and solved the computation of the eigenvalue problem for a complex launch system for the first time in 1993 [87–110]. The book *Launch Dynamics of Multibody Systems* [2] was published in 1995 and introduced systematically the linear MSTMM and its application in launch dynamics. The computation ill-condition of the eigenvalue problem was solved primarily and the computational efficiency of complex linear MSs was improved greatly by using the MSTMM. The dynamic coupling between rigid bodies and flexible bodies results in the following problems: non-self-conjugation of the eigenvalue problem of a linear MRFS, lack of normal eigenvector orthogonality and the difficulty of precisely analyzing the dynamic response of systems by the modal method. Inspired by the *orthogonality* of the eigenvectors of discrete systems and

continuous systems [230, 231], we presented the new concepts of an *augmented eigenvector* and an *augmented operator*, and constructed the orthogonality of augmented eigenvectors for the MRFS for the first time in 1997. The exact analysis of the dynamic response of a complex MRFS is realized using the modal method and the orthogonality of the MRFS [4, 50, 55–58]. The ordinary method of MSD is sometimes not enough for rapid dynamics computation in engineering design because it is necessary to develop the global dynamics equation of the system for this method and the computational speed decreases rapidly when the number of freedom of degrees of the system increases. From 1998 we presented and perfected the *discrete time transfer matrix method for multibody systems* (MSDTTMM) step by step, including the *discrete time transfer matrix method for multi-rigid-body systems* (MRSDDTTMM) for systems moving in plane and in space, which was presented in 1998 [3, 64–68]. Combining the advantages of the high computation efficiency of the TMM with the wide application of time-integration procedure, using the modern algorithm, the constant transfer matrix and state vector described by modal coordinates in the linear MSTMM are extended as the time variant transfer matrix and the state vector described by physical coordinates, respectively. We presented the *discrete time transfer matrix method for multi-rigid-flexible-body systems* in 1999 [65]. Besides the state variables involved in the state vectors of the MRSDDTTMM, the generalized coordinates which describe the deformation of the flexible elements are also collected in the state vectors, and the transfer matrix extended accordingly. The MSDTTMM was used to solve MRSD and MRFSD, especially complex launch system dynamics [87–117]. We presented the TMM for two-dimensional systems in 2005 and realized the dynamics analysis of two-dimensional systems using the MSTMM alone [74, 75]. We presented a hybrid method of the MSTMM and the eMSDM [71, 72], a hybrid method of the MSTMM and the FEM [76], the TMM for linear controlled MSs [77], the DTTMM for controlled MSs [78], the Riccati MSDTTMM in 2006 [79, 80] and the finite segment MSDTTMM in 2007 [81]. The dynamics analysis and rapid computation of MSs without global dynamics equations have therefore been realized.

With constant perfecting of the application of engineering and international academic exchange for 15 years, the MSTMM now combines the advantages of the high computational efficiency of the TMM and the wide application of the numerical integration procedure. It has become a totally new method with high programming and high efficiency, without constraint violation [66], and is very efficient for both of vibration analysis of linear MSs and general MSD. The MSTMM injected new energy into the development of launch dynamics and other engineering techniques. We presented a new theory and technique of launch dynamics of MSs [87–131] in 1995 based on the MSTMM. These have been used widely in the dynamic design of complex launch systems such as MLRSs, self-propelled launch systems and shipboard launch systems. These launch systems have been given great attention and developed quickly in many countries. It has been proved by many engineering practices that the launch dynamics of MSs are very effective and play an important role in the research, production and experimentation of many important engineering projects. Several difficult technology problems in important national areas have been solved, and distinct economic and social benefits obtained. As one of the applications of the launch dynamics of the MLRS, the strict dispersion test method of substituting the nonfull-charge loading test for the full-charge loading test was developed for the first time. Thus, the urgent and difficult problem of reducing the number of rockets consumed in MLRS dispersion tests has been solved. It has been verified by tests that the new technology is much better than the existing technology. The economic benefit is large, for example the fees saved in one test may be more than 12 million Yuan for some launch systems. A new technique for improving the firing dispersion has been developed, and the firing dispersion of MLRSs and self-propelled launch systems greatly improved. These results demonstrate the powerful function and wide application area of the MSTMM.

The first TMM book, *Matrix Methods in Elastomechanics* [36], was published in 1963 by Professor Eduard Pestel, Professor Jens Wittenburg's teacher. It played the same important role in the development of the TMM as *Dynamics of Systems of Rigid Bodies* [7], published by Professor Wittenburg in 1977, did in the development of MSD. Invited by Professor Wittenburg and Professor Pestel's successor, Professor Rui worked as a guest professor at Karlsruhe University and the Mechanics Institute of Hannover University, where Professor Pestel had worked. We expanded the TMM for structure mechanics, founded by Professor Pestel, into the MSTMM that applies for the study of MSD, to which Professor Wittenburg is one of the most important contributors.

1.4 Features of the Transfer Matrix Method for Multibody Systems

1.4.1 Research Objectives of the Transfer Matrix Method for Multibody Systems

The MSTMM is a method for studying MSD using transfer matrices. Its research objective is the MS composed of many bodies connected by various hinges. MSs are universal dynamics models used widely in weaponry, shipping, aeronautics, astronautics, communications and machinery industries. The MSTMM is very efficient in solving the problems of vibration characteristics, orthogonality and the dynamic response of linear MSs. It is also very effective in the dynamics of a general time-variant nonlinear multibody system undergoing large motion and control. The classical TMM can be regarded as a special case of the MSTMM under the conditions of linear, time-invariant and small vibration.

The transfer matrix uncovers the inherent mechanics property of different points of a system. For example, it describes the relationship of different state vectors under modal coordinates for the eigenvalue problem and that under physical coordinates for steady-state response in linear time-invariant MSs, and the relationship of different state vectors under physical coordinates in general MSs with nonlinear, time-variant, large motion.

1.4.1.1 Linear MSTMM

It is of important theoretical and practical significance to compute the vibration characteristics of the MRFS rapidly and accurately. For multi-rigid-flexible-body systems such as multiple-launch-rocket systems, launching frequency (launching number per second) is one of required tactics. Only when the eigenfrequencies of a launch system match the launching frequency can the dynamics performance of the launch system be good enough. Rapid computation of the eigenvalue problem is an important basis of the dynamics design and scientific experiments of launch systems. By developing the transfer matrices of rigid bodies, flexible bodies and various hinges, high computational speed can be ensured and computation ill-conditions can be overcome because of the lower-order of the matrix in the MSTMM.

The dynamic coupling between rigid bodies and flexible bodies results in nonself-conjugation of the eigenvalue problem of the linear MRFS, lack of normal eigenvector orthogonality and the difficulty of analyzing precisely the dynamic response of systems by the modal method. In fact, a solution to the orthogonality theory of eigenvectors of the complex MRFS is urgently needed. The orthogonality of eigenvectors of the MRFS is a precondition to compute exactly the dynamic response of systems using the modal synthesis method, and to make the dynamic response converge quickly even when few mode shapes are adopted. By presenting new concepts of augmented eigenvectors, that is, the *augmented operator* and *body dynamics equation* of the MRFS, the problem of the orthogonality of eigenvectors is solved. It has been shown that the orthogonality of augmented eigenvectors of the MRFS is satisfied automatically. The augmented eigenvectors are easy to be set up, and their structures are quite concise. They contain modal

coordinates of displacements, angular displacements, discrete variables and continuous variables. They are composed of the motion state of every body element, and the number of state variables is equal to the number of body dynamics equations of the system. These important characteristics differ from those of ordinary eigenvectors.

If using the MSTMM to study MRFSD, the global dynamics equation of the system is not always required. In Chapter 3 we propose a new concept of the body dynamics equations of MSs. They are much simpler than the global dynamics equation of a system, and are the sum of the body dynamics equations of every body element. The constrained equations between the body elements and dynamics equations of the hinge elements are not needed in the MSTMM. Using the orthogonality of augmented eigenvectors and the vibration characteristics of the system, transforming the body dynamics equations of the system into motion differential equations of the system in principal coordinates, the system dynamic response and dynamic analysis of MSs can be easily obtained using the modal method. Using the extended MSTMM, the steady-state response and deformation and force under the static load of MSs can be obtained by direct computation of matrix algebra instead of differential equations.

1.4.1.2 MSDTTMM

The linear MSTMM is efficient for linear MSs, but inapplicable to general MSs that are time-variant, nonlinear and have large motion. The MSDTTMM is developed by combining the TMM with a modern numerical integration procedure. It is efficient for general MSs that are time-variant, nonlinear and have large motion. The linear MSTMM can be regarded as a special case of the MSDTTMM that is linear, time invariant and has small vibrations.

The MSDTTMM includes the MSDTTMM for MRSs, the MSDTTMM for MRFSSs, hybrid methods of the MSTMM and other mechanical methods, the Riccati MSDTTMM, etc. The MSTMM and other mechanics methods can be combined to increase their functions. For example, the mixed method of the MSTMM and the FEM combines the advantages of the MSTMM with the simple form and high computation efficiency of the FEM, resulting in a powerful function that is effective for multi-dimensional problems. This method increases the computational efficiency of the FEM and is efficient for various complicated multi-dimensional linear MSs, nonlinear systems and time-variant systems. Mixed methods of the MSTMM and MSD combine the advantages of the MSTMM, the Wittenburg method, the Schiehlen method, the Kane method, the classical mechanics method and the analytic mechanics method, etc. It will bring high computational efficiency if we embed the MSTMM into various FEM software packages. Many practical examples show that these methods not only are effective for various MSs, but also have higher computation efficiency compared with other dynamics methods. The Riccati MSDTTMM, developed by a combination of the MSDTTMM with the Riccati transformation, is effective even for huge MSs with many elements. In principle, the MSTMM can be used together with any mechanical method, such as various MSD, the FEM, the classical mechanics method and the analytic mechanics method. It can be embedded in various commercial software packages, such as the SAP series, NASTRAN, ANSYS and ADMAS. This shows that it is compatible and complementary with other dynamics methods rather than contradictory, and has broad application potential.

1.4.1.3 MSTMM for Controlled Systems

Based on the MSTMM, there are two cases for dealing with control elements of controlled MSs. First, if control forces can be expressed by the state of the system of the previous time step, such as delay-controlled MSs, then control forces can be regarded as external forces located in their row matrix of the transfer matrix and controlled systems can be studied in a similar way to that

used in the MSTMM for uncontrolled systems. Second, if the control force is relative to the present state of the system, such as in real-time control systems, then each control characteristic parameter of the system should be regarded as a special mechanics characteristic parameter to develop the transfer matrix of the control element, and the controlled system can be studied in a similar way to that used in the MSTMM for uncontrolled systems.

1.4.2 Transfer Matrix Method for Multibody Systems

The basic idea of the MSTMM is to break up a complicated MS into elements including bodies and hinges whose dynamics properties can be readily expressed in matrix form. The library of transfer matrices can be readily developed in advance. The positions of bodies and hinges are considered equivalent. These element matrices are considered as building blocks that, when assembled according to the structure of the system, will provide the dynamics properties of the entire system. The *overall transfer matrix* and the *overall transfer equation* of the system can be obtained by successive multiplications of the transfer matrices of the elements according to the conventions provided in this book.

For vibration analysis of linear MSs, the body dynamics equations of a system can be obtained by listing in order the body dynamics equations of every body element in standard form in an inertial coordinates system. It is usually very simple and easy to establish the body dynamics because the relationship between this body element and any other elements in kinematics and dynamics does not need to be considered. The *eigenequation* of the system can be obtained by taking boundary conditions into overall transfer equation of the system. The *eigenfrequencies* of the system can be obtained by solving the eigenequation of the system. A state vector of boundary ends can be obtained by solving the overall transfer equation using a corresponding eigenfrequency. The state vectors of all other points and augmented eigenvectors of the system can be obtained by solving the transfer equations of the elements. The generalized coordinates and dynamic response of the system can be obtained by solving the dynamics equations of the system using the orthogonality of the augmented vectors. The interactions among the body elements are reflected in the vibration characteristics and their effect on the dynamic responses of the system. The solution procedures of the linear MSTMM are shown in Figure 1.1.

The solution procedure for the MSDTTMM is shown in Figure 1.2 for the dynamics of a general MS that is time-variant, nonlinear and has large motion and control. First, letting $i = 1$ and taking boundary conditions into the overall transfer equation of the system, the state vectors of the boundary at time t_i can be obtained by solving the overall transfer matrix of the system. Then the state vectors of every hinge point and the system dynamics at time t_i can be obtained by applying the transfer equations of the elements. Lastly, the time history of the system dynamics can be obtained by letting $i = i + 1$ and repeating the above process until the required time T .

The order of the system matrix of the MSTMM is much lower than that of the ordinary dynamics method. For example, the order of the system matrix of the chain system is only dependent on the highest order of the matrix of elements. This is the important feature of the MSTMM that differs from the ordinary MSDM. Why does an originally complex matter become so simple? Because the “hinge” and the “body” are considered to have equivalent positions in the MSTMM and therefore it is not necessary to deal with the “hinge” in the way of an ordinary MSDM.

It is necessary to point out that the linear MSTMM is essentially different from the MSDTTMM, which will be discussed in detail in the following chapters.

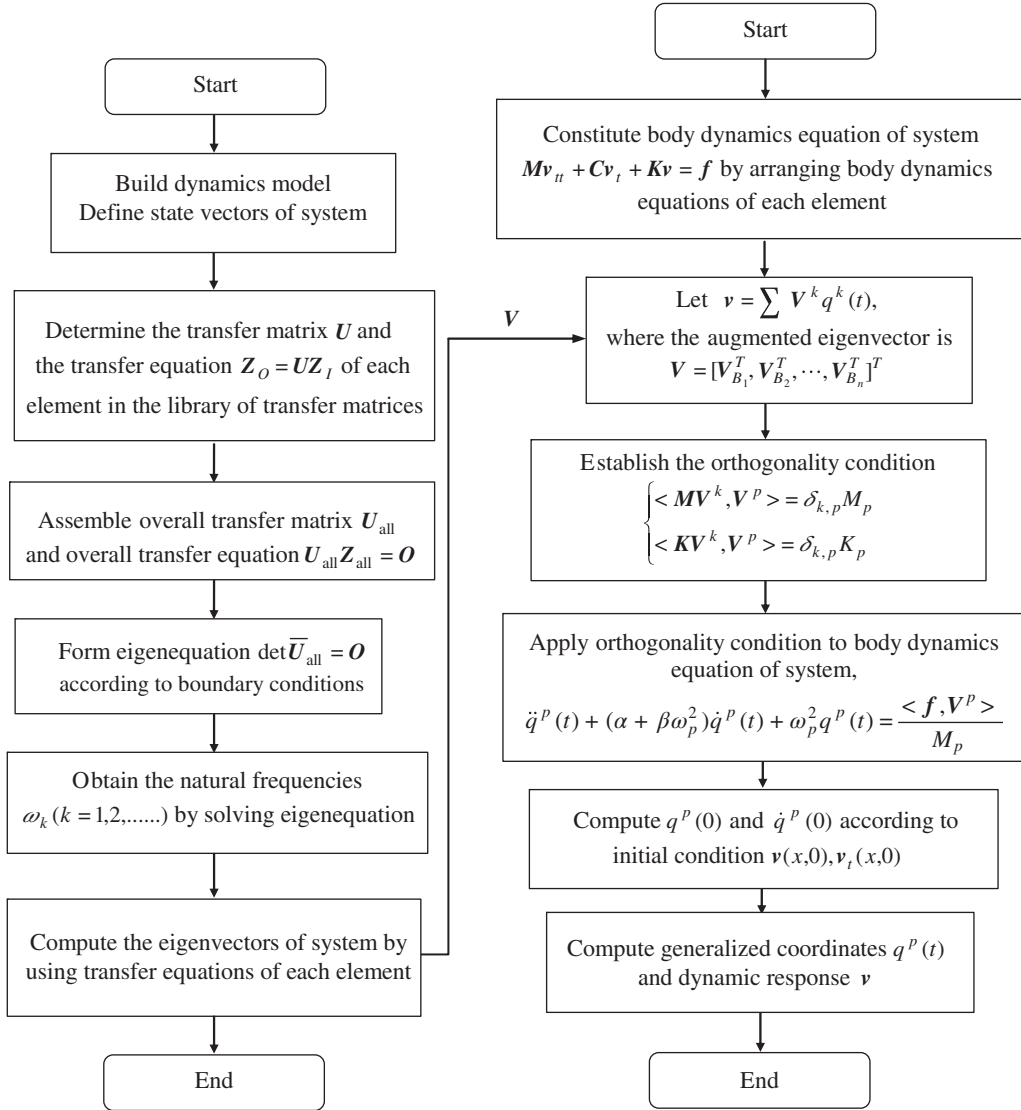
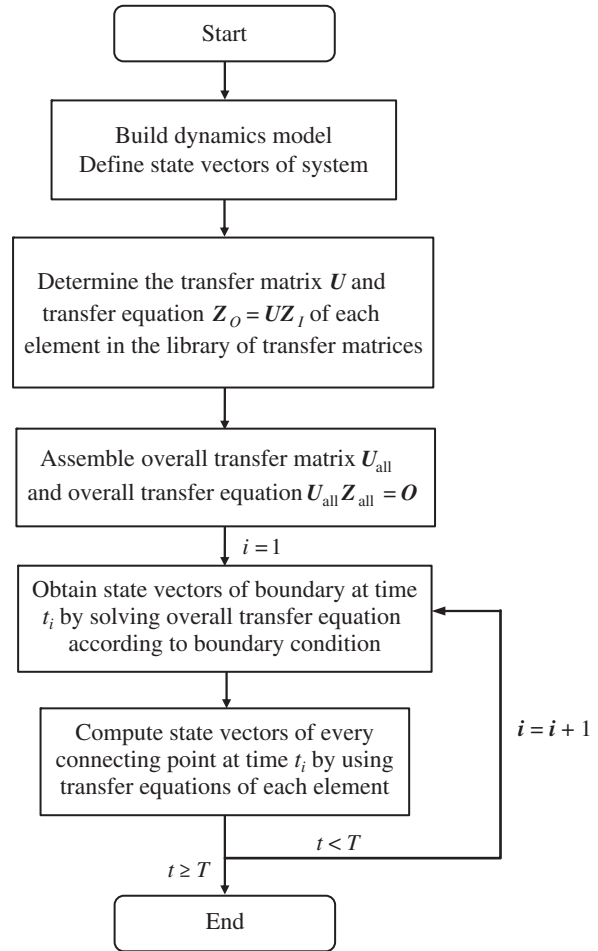


Figure 1.1 Vibration characteristics and dynamics response procedure.

1.4.3 Features of the Transfer Matrix Method for Multibody Systems

The characteristics of the ordinary MSDM are as follows:

- 1) The global dynamics equations of the system are necessary and are usually hybrid equations composed of ordinary differential equations expressing rigid body motion and partial differential equations expressing flexible body motion, as well as algebraic (or ordinary differential) equations describing constraints. They have to be re-deduced, which is complex, if the elements of the system change.
- 2) The order of the system matrix is high and usually equal to the number of degrees of freedom of the system, so the computational scale is huge for complex MSD.

Figure 1.2 The MSDTTMM procedure.

- 3) It is complicated to solve the *dynamic response* of the MRFS because generally most scholars and engineers convert the partial differential equations into ordinary differential equations by using separating variables using the *assumed modes method* and also convert algebraic equations into ordinary differential equations, then solve them all together; The true mode is unknown in these methods, resulting in a unclear difference between the assumed mode and the true mode, and obviously this affects the solution precision of the dynamic response.

The characteristics of the MSTMM are as follows:

- 1) There is no need for global dynamic equations of the system, so the complex procedures for developing the global dynamics equations will be avoided forever.
- 2) The order of the system matrix is independent of the number of degrees of freedom of the system, for example the order of the system matrix only depends on the highest order of the element matrices for the chain system. The MSTMM has much smaller computational scale and much faster computational speed because of its lower order of system matrix, so the computational ill-condition of the eigenvalue is avoided.
- 3) Wide application fields and powerful functions. The research objectives of the classical TMM are two kinds of linear elastic structural systems: linear discrete systems composed of springs

and lumped masses, and continuous systems composed of elastic solid components. It is hard to deal with general MSs for the classical TMM. The computation of the vibration characteristics of the complex MRFS is easy for the MSTMM and is difficult for ordinary dynamics methods.

- 4) If using the MSDTTMM, MSD can usually be obtained by solving algebraic equations instead of differential equations. The dynamics of linear time-invariant MSs can be obtained by solving the body dynamics equations of the system. The dynamics of time-variant MSs can be obtained by solving the transfer equations of the system. It is easy to understand and apply the MSTMM.
- 5) High programming. The overall transfer matrix can be deduced automatically using the transfer matrices of the elements with the standard form according to the topology of the system. Once the transfer matrix has been derived for the given motion and connection model, it can then be used for any MS with the corresponding motion and connection model. In fact, various transfer matrices of elements can be found directly from the transfer matrix library given in this book. The dynamics modeling and analysis of MSs become flexible, concise and quite simple. This work can be done efficiently by a computer because the computational scale is small.
- 6) It is only necessary to solve ordinary differential equations to obtain the dynamic response of an MRFS. The true mode of the system can be obtained with a much higher accuracy either by the TMM for the MRFS or directly by modal test. Thus, a high-precision dynamic response can be achieved.

Because of these characteristics, the MSTMM has played a very important role in the dynamics design and testing in aeronautics, astronautics, vehicles, robots, machinery etc.

1.5 Launch Dynamics

Launch dynamics [1, 2, 132] is a subject that studies the forces acting on a launch system and the consequent motion of the system during the launching process. It is involved in interior ballistics, external ballistics, middle ballistics, aerodynamics, launch systems dynamics, MSD, vibration theory, test technology, etc. and is closely related to modern science and technology. The theory and technology of launch dynamics have become a research hot topic and increasing attention has been given to the field of modern launch science and technology at home and abroad. This has been one of the main special subjects in all International Symposium of Ballistics and American Guns Dynamics Conferences.

The entire trajectory of a projectile may be divided into two stages: the launching process and free flight. The trajectory of projectile flight with zero attack angles under standard conditions is a plane curve called the ideal trajectory in exterior ballistics [133]. The factors that are not considered in the ballistics equations of an ideal trajectory are called disturbance factors. These factors make the real trajectory deviate from its ideal trajectory. The initial disturbance of a projectile is given by the initial values of the 12 motion parameters of the exterior ballistics equations of a rigid projectile with six degrees of freedom, including three initial rotation angles of initial swing angle Φ_0 , the initial deflection angle Ψ_0 , the initial spin angle γ_0 and the corresponding angular velocity $\dot{\Phi}_0$, $\dot{\Psi}_0$, $\dot{\gamma}_0$, the initial position coordinate r_0 and the corresponding velocity v_0 in three directions at the launch end [1]. The initial disturbance of a projectile is caused by the combined effect of various factors in the launch process, for example the projectile, launcher, propellant and environment. The results of study of the initial disturbance of a projectile provide technology support for the design and evaluation of the dynamic performances of a launch

system by optimizing the structure parameters. The vibration characteristics of the launch system are one of the main study components of launch dynamics. It has been proved in practice that a reasonable dynamics model of a launch system should be the MRFS and the tubes of the launch system have to be treated as elastic bodies. For example, the dynamic performance of the MLRS is affected greatly by the ratio of eigenfrequencies to running launch frequencies. In the launch test of a launch system, in order to evaluate the performances scientifically, to decrease the ammunition consumption significantly and to improve the performances of the launch system via the implementation of dynamics design, it is first necessary to compute rapidly the vibration characteristics and exactly analyze the dynamic responses of the MRFS for the launch system. A number of difficulties have to be solved to achieve this. First, too high an order of matrix causes the computation to fail because of the huge computational scale of the vibration characteristics of the MRFS and the inevitable computational ill-condition problem of a high stiffness gradient system when using ordinary methods. Second, coupling of rigid and flexible bodies causes the non-self-conjugate problem of the eigenvalue of the MS and the lack of the orthogonality of the eigenvectors of the system under ordinary means so the modal method cannot be used to analyze exactly the dynamic response of the system.

It has been proved by theory and experiment that the launch orders of the MLRS have a great influence on its launch dispersion. The reason for this is that different launch orders will result in different vibration characteristics, different initial disturbances and different launch dispersions of projectiles. The vibration characteristics and the ratio of eigenfrequencies to launch frequencies of a running-fire MLRS have a great influence on its dynamic performance. Rapid and exact computation of the vibration characteristics of the MLRS is of great importance and has become one of the key topics of the launch dynamics of the MLRS. The total mass of rockets is usually larger than the mass of tubes in the MLRS. The mass influences the vibration characteristics of the MLRS, which are different for each rocket. To scientifically evaluate and improve the dynamic performance of the MLRS, it is necessary to find the quantitative relationship between the structural parameters and the vibration characteristics, and match the eigenfrequency with the launch frequencies by changing the structure parameters of the MLRS.

The main methods of studying the vibration characteristics of a system are the FEM, the modal analysis method and the modal synthesis method. The FEM and the MSDM, for example the Wittenburg method and the Kane method, are important in studying launch dynamics. Generally speaking, these methods are efficient for computing complex engineering systems. At the same time, it is usually difficult to study the vibration characteristics of the mechanism system because of the large computational scale of these methods.

It is an urgent requirement in the area of launch dynamics to seek methods to improve the dynamics modeling precision and reduce the computational scale for the dynamics of MSs. Based on the MSTMM, the authors have developed new theory for the launch dynamics of MSs. Many difficult problems related to high-technique engineering have been solved successfully because the theory of the launch dynamics of MSs developed based on the MSTMM expounds launch dynamics in a totally new way and injects new energy into its development.

1.6 Features of this Book

The characteristics of this book are as follows:

- 1) The MSTMM and its theory system are originated and systemically introduced. A totally new method is obtained to compute MSD with high computational speed and without global dynamics equations of the system.

- 2) The MSTMM is established for linear systems, multi-dimensional systems, controlled systems, time-variant MRSs, time-variant MRFSSs, and time-variant controlled systems. These methods are used for dynamics analysis of linear time-invariant systems and general time-variant nonlinear MSs undergoing large motion and control, and provide a powerful means for forecasting the dynamics performances of general mechanical systems.
- 3) Using the new theory and method for the eigenvalue problem and dynamics design provided by the MSTMM, the problems of computational ill-condition and the huge computational scale of MRFSSs arising in important projects have been overcome and computational efficiency has been increased.
- 4) New concepts of augmented eigenvector, augmented operator and body dynamics equations of MSs are presented, and the orthogonality of the eigenvectors of the MRFSS proved for the first time. We solve the difficulty of analyzing exactly the dynamic response of the system using the modal method because of the nonself-conjugation of the eigenvalues of MSs and the lack of orthogonality of the eigenvectors of the system under ordinary means caused by coupling of rigid and flexible bodies. The dynamic response of the MRFSS is analyzed precisely and the dynamics design of important engineering products, such as the launch system, etc., is realized.
- 5) The library of transfer matrices of MSs is established for the first time. The transfer matrices of various elements involved in linear system dynamics and general MSs are given systematically. The MS required can be readily assembled by using the transfer matrices of elements in the library and MSD can be studied easily.
- 6) Based on the MSTMM, the theory, technology and simulation systems of the launch dynamics of MSs are established, including the launch dynamics of MLRSs, self-propelled launch systems and shipboard launch systems, indicating that launch dynamics have entered the practical stage. The initial disturbance theory of a projectile is presented to improve launch precision and decrease experimental consumption of projectiles for launch systems by studying the launch dynamics. This theory is the basis for accurate forecasting and evaluation of the dynamic performance of the launch system.
- 7) Using the MSTMM, technologies for improving the launch precision of the launch system and decreasing projectile consumption in strict tests are presented for the first time.
- 8) The MSTMM and its application results have been appraised by the government appraisal commission that the MSTMM possesses original innovativeness and many proprietary intellectual properties, leads launch dynamics research into practical stage, achieves international leading level, has brought great social, economic and military benefits and has broad application prospects. Professor Rui has given over 50 invited lectures in 16 universities and institutes, and has been invited to international conferences by scientists such as Professor Werner Schiehlen, former President of International Union of Theoretical and Applied Mechanics.

1.7 Sign Conventions

According to the features of the MSTMM, the sign conventions in this book are as follows:

- 1) Mechanics elements. Mechanics elements are classified into two types, “bodies” and “hinges”, and are numbered uniformly. “Bodies” include rigid bodies, flexible bodies, lumped masses, etc. “Hinges” are the links between bodies, including elastic hinges, smooth hinges, prismatic hinges, fixed hinges and damping hinges. A hinge is considered as massless and its mass is totally included in its inboard body and outboard body.
- 2) State vector. For a nonboundary end, the first and second subscripts i and j ($i, j \neq 0$) in a state vector $\mathbf{z}_{i,j}$ of the end denote the sequence numbers of the adjacent body element and hinge

element, respectively. Only one of the boundary ends of a MS is called the root, and all of the other boundary ends are considered as the tips. In the state vectors of boundary ends of root and tips $\mathbf{z}_{i,0}$, the second subscript $j = 0$ and the first subscript i stand for the sequence number of the elements of root and tips involved.

- 3) Transfer direction. The transfer direction of a system is always from its tip to its root.
- 4) Input end and output end. Every body element has only a single output end, and all of the other ends are considered as input ends. Along the transfer direction, the nodes entering into the element are called the input ends of the element and are denoted by I_i ($i = 1, 2, \dots, n$), and the node leaving from the element is called the output end of the element and is denoted by O . There are sometimes several elements in a transfer path. The connection point between elements is the output end of its inboard element and the input end of its outboard element. It is denoted by $P_{i,j}$, where the first subscript i indicates the sequence number of the body element and the second subscript j indicates the sequence number of the hinge. Sometimes the connection point $P_{i,j}$ is denoted by (i, j) .
- 5) Coordinate systems. The stationary inertial Cartesian coordinate system is used to describe the motion of the elements of a multibody system. In order to easily describe the motion of the system, some inertial coordinate systems with different orientations are used according to research objects, and the orientation relations between different coordinate systems are described with direction cosine matrices. The parameters of transfer matrices are described in body-fixed coordinate systems for a linear time-invariant system. The origin of the coordinate system of an element is at the input end for an element with a single input end or at the first input end for an element with more than one input end. For a nonlinear, time-variant system in the MSDTTMM the body-fixed coordinate system $o_2x_2y_2z_2$ of an element is uniquely determined in the inertial Cartesian coordinate system $oxyz$. The space-three axes inertial coordinate system is used as the reference system, and the space-three angles (1-2-3) [71] are used to describe the orientation of the rigid body.
- 6) Position coordinates and coordinates cross-product matrix. For a rigid body element, C , D and E denote the mass center, the action point of the external force and the torque center of the external torque (torque center for short), respectively. The coordinates of any point of the rigid body in its body-fixed coordinate system located at its input end are denoted with a column matrix and boldface italic letter \mathbf{l} . For example, in the body-fixed coordinate system of a rigid body, the position coordinates of the output end O are $\mathbf{l}_{IO} = [b_1, b_2, b_3]^T$, the position coordinates of the mass center C are $\mathbf{l}_{IC} = [c_{c1}, c_{c2}, c_{c3}]^T$, the position coordinates of the action point D of the external force are $\mathbf{l}_{ID} = [d_1, d_2, d_3]^T$, and the position coordinates of the torque center E are $\mathbf{l}_{IE} = [e_1, e_2, e_3]^T$. The coordinates of the input ends I_n ($n = 1, 2, \dots, N$) and the output end O are denoted as $\mathbf{l}_{I_n} = [a_{1,n}, a_{2,n}, a_{3,n}]^T$ and $\mathbf{l}_{IO} = [b_1, b_2, b_3]^T$, respectively, and these are decomposed in the body-fixed coordinate system located at the first input end of the body element.

The cross-product matrix of the position vectors is denoted by the symbol $\tilde{\mathbf{l}}$, for example

$$\tilde{\mathbf{l}}_{I,O} = \begin{bmatrix} 0 & -b_3 & b_2 \\ b_3 & 0 & -b_1 \\ -b_2 & b_1 & 0 \end{bmatrix}, \quad \tilde{\mathbf{l}}_{I,C} = \begin{bmatrix} 0 & -c_{c3} & c_{c2} \\ c_{c3} & 0 & -c_{c1} \\ -c_{c2} & c_{c1} & 0 \end{bmatrix} \quad (1.1)$$

- 7) Physical coordinates and modal coordinates of displacement, position coordinate, angular displacement, rotation angle, torque and force. For linear systems, boldface italic lowercase $\mathbf{r} = [x, y, z]^T$, $\boldsymbol{\theta} = [\theta_x, \theta_y, \theta_z]^T$, $\mathbf{m} = [m_x, m_y, m_z]^T$ and $\mathbf{q} = [q_x, q_y, q_z]^T$ denote the column matrices of linear displacements, angular displacements, internal torques (except damping torque) and internal forces (except damping force), respectively, of a connection

point relative to the equilibrium position of the system in the inertial coordinate system under physical coordinates. Boldface italic capitals $\mathbf{R} = [X, Y, Z]^T$, $\boldsymbol{\Theta} = [\theta_x, \theta_y, \theta_z]^T$, $\mathbf{M} = [M_x, M_y, M_z]^T$ and $\mathbf{Q} = [Q_x, Q_y, Q_z]^T$ denote the corresponding column matrices of linear displacements \mathbf{r} , angular displacements $\boldsymbol{\theta}$, internal torques \mathbf{m} and internal forces \mathbf{q} , respectively, under modal coordinates.

The physical coordinates can be expressed with modal coordinates as follows:

$$\begin{cases} \mathbf{r} = \sum_{k=1}^n \mathbf{R}^k q^k(t), & \boldsymbol{\theta} = \sum_{k=1}^n \boldsymbol{\Theta}^k q^k(t) \\ \mathbf{m} = \sum_{k=1}^n \mathbf{M}^k q^k(t), & \mathbf{q} = \sum_{k=1}^n \mathbf{Q}^k q^k(t) \end{cases} \quad (1.2)$$

where k denotes the order of the modal, n denotes the number of degrees of freedom of the system, t is time and $q^k(t)$ denotes the generalized coordinates.

For general time-variant and nonlinear MSSs, $\mathbf{r}_{IO} = [x_{IO}, y_{IO}, z_{IO}]^T$, $\mathbf{l}_{IO} = [b_1, b_2, b_3]^T$, $\boldsymbol{\theta} = [\theta_x, \theta_y, \theta_z]^T$, $\mathbf{q}_I = [q_{x,I}, q_{y,I}, q_{z,I}]^T$, $\mathbf{q}_{2,I} = [q_{x_2,I}, q_{y_2,I}, q_{z_2,I}]^T$, $\mathbf{m}_I = [m_{x,I}, m_{y,I}, m_{z,I}]^T$ and $\mathbf{m}_{2,I} = [m_{x_2,I}, m_{y_2,I}, m_{z_2,I}]^T$ denote the column matrices of the position vectors of output end O relative to I , rotation angles, internal forces and internal torques of point I relative to the three-space axes inertial coordinate system and the body-fixed coordinate system under physical coordinates, respectively. $\mathbf{r}_{IC} = [x_{IC}, y_{IC}, z_{IC}]^T$ and $\mathbf{l}_{IC} = [c_{c1}, c_{c2}, c_{c3}]^T$ denote the column matrices of the position vectors of mass center C with respect to I in an inertial coordinate system and a body-fixed coordinate system, respectively, and \mathbf{A} denotes the transformation matrix from a body-fixed coordinate system to an inertial coordinate system. From the definition of a transformation matrix, it can be inferred that $\mathbf{r}_{IO} = \mathbf{A}\mathbf{l}_{IO}$, $\mathbf{q}_I = \mathbf{A}\mathbf{q}_{2,I}$ and $\mathbf{m}_I = \mathbf{A}\mathbf{m}_{2,I}$.

- 8) Conventions for the positive direction for displacement, position coordinate, angular displacement, rotation angle, torque and force (Figures 1.3 and 1.4). Positive displacements and position coordinates x, y, z and angular displacements and rotation angles $\theta_x, \theta_y, \theta_z$ at the input and output ends coincide with the positive directions of the coordinate system.

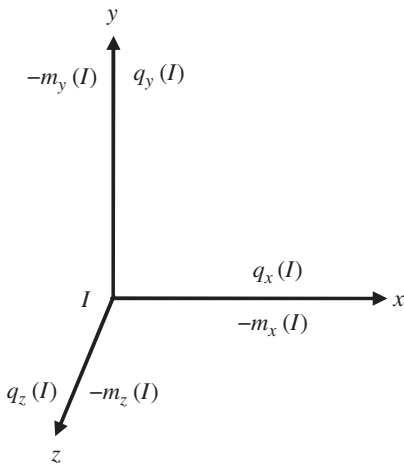


Figure 1.3 Positive direction convention of torques and forces at the input end.

Inboard forces q_x, q_y, q_z and outboard torques m_x, m_y, m_z acting on the elements are positive (negative) if their vectors are in the positive (negative) directions of the coordinate system, and outboard forces q_x, q_y, q_z and inboard torques m_x, m_y, m_z acting on the elements are positive (negative) if their vectors are in the negative (positive) directions.

- 9) Bold italic lowercase $\mathbf{z}_{i,j}$ and bold italic capital $\mathbf{Z}_{i,j}$ denote the state vectors of the connection point $P_{i,j}$ under physical coordinates and modal coordinates, respectively, that is:

$$\begin{cases} \mathbf{z}_{i,j} = [x, y, z, \theta_x, \theta_y, \theta_z, m_x, m_y, m_z, q_x, q_y, q_z]_{i,j}^T \\ \mathbf{Z}_{i,j} = [X, Y, Z, \Theta_x, \Theta_y, \Theta_z, M_x, M_y, M_z, Q_x, Q_y, Q_z]_{i,j}^T \end{cases} \quad (1.3)$$

For describing and writing conveniently, bold italic capital \mathbf{Z}_I and \mathbf{Z}_O denote the state vectors of the input

and output ends, respectively, of the body element with only two ends. $\mathbf{Z}_{i \sim i+k, j \sim j+k}$ and $\mathbf{Z}_{i, j \sim j+k}$ denote the state vectors of $k+1$ connection points $P_{i,j}, P_{i+1,j+1}, \dots, P_{i+k,j+k}$ and $P_{i,j}, P_{i,j+1}, \dots, P_{i,j+k}$, respectively, of the body element with more than two ends. Generally speaking, as the state variants of the state vector, displacements include linear displacements and angular displacements, position coordinates include position coordinates and rotation angles, and forces include forces and the torques. To keep things simple, these will not be explained again.

- 10) Bold italic capital \mathbf{U}_i denotes the transfer matrix of the element whose sequence number is i . Bold italic capital $\mathbf{U}_{k,j}$ denotes a partitioned matrix of a transfer matrix, where the subscripts k and j are the sequence numbers of the row and column, respectively, of the partitioned matrix in the transfer matrix. The transfer matrix \mathbf{U}_{i-k} and the partitioned matrix \mathbf{u}_{i-k} are the resultants of continued multiplication of the transfer matrices of all elements in the transfer path from element i to element k of the system. Lowercase $u_{k,j}$ or $u_{k,j}$ denote an element of a transfer matrix, where k and j represent the row and column numbers, respectively, of the element in the transfer matrix.
- 11) Bold italic capital \mathbf{I}_n denotes a unit matrix of order n , bold italic capital $\mathbf{O}_{m \times n}$ denotes a zero matrix with m rows and n columns, and \mathbf{O}_n denotes a zero column matrix with n rows.
- 12) Bold italic capital \mathbf{V} denotes an augmented eigenvector of the system, \mathbf{V}^k denotes the augmented eigenvector corresponding to the k th order modal and bold italic lowercase \mathbf{v} denotes the column matrix of corresponding physical coordinates, that is

$$\mathbf{v} = \sum_{k=1}^n \mathbf{V}^k q^k \quad (1.4)$$

where $q^k (k=1, 2, \dots, n)$ denotes the k th generalized coordinate, and \mathbf{v}_t and \mathbf{v}_{tt} denote the first- and second-order derivatives of \mathbf{v} with respect to time t , respectively, F_i or F_i denotes the external force acting on the i th element, f_i denotes the external force (including the external torque) acting on the i th element and \mathbf{f} denotes the column matrix of the external force of the system.

- 13) According to the writing standard that the operators should be expressed using standardized form, the bold capital standardized forms \mathbf{M} , \mathbf{K} and \mathbf{C} denote the augmented operator matrices presented in this book.
- 14) $\delta_{k,p}$ denotes the Kronecker operator

$$\delta_{k,p} = \begin{cases} 0 & k \neq p \\ 1 & k = p \end{cases} \quad (1.5)$$

where k and p are natural numbers.

- 15) Bold italic type is used for vectors and matrices.
- 16) The *International System of Units* (SI) is used in the examples and problems throughout the book. In this system, the three basic units are the meter (distance), the kilogram (mass) and the second (time). The unit of force called the *newton* is derived from these three basic units.

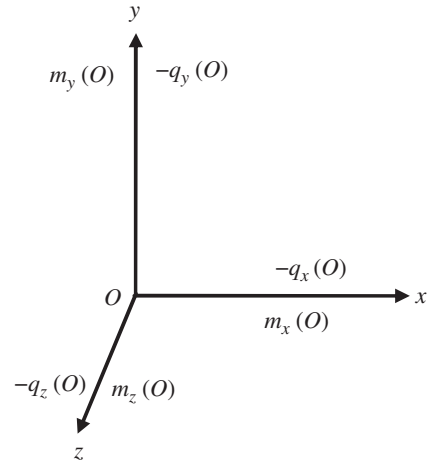


Figure 1.4 Positive direction convention of torques and forces at the output end.

Part I

Transfer Matrix Method for Linear Multibody Systems

Linear multibody systems are the most popular dynamics model encountered in the field of engineering areas such as weaponry, robotics, aeronautics, astronautics, and machinery, etc. Research and engineering technicians are concerned with common dynamic problems related to linear multibody systems that mainly include eigenvalue problems, vibration characteristics, steady state response of the system, orthogonality of the eigenvectors, and the solution of the dynamics response, etc. The transfer matrix method for linear multibody systems (LMSTMM) is developed in this part, the concepts of body dynamics equations, augmented eigenvectors, and augmented operators proposed by the authors are introduced, and the orthogonality of the augmented eigenvectors of multi-rigid-flexible-body systems is verified, which provides the readers the basic theory and techniques for solving the dynamics of linear multibody systems by using the LMSTMM. In this way, the vibration characteristics and the dynamics response of the linear multibody systems could be determined precisely, free from suffering numerical ill-condition problems. The basic theory and the chief distinguishing features of the LMSTMM are introduced in Chapter 2. The concept of the body dynamics equations, the augmented operators, the augmented eigenvectors, and the verification of their orthogonality are provided in Chapter 3, followed by the solution of the transient dynamics response of the LMSTMM based on the mode method. The transfer matrix methods for nonlinear and multidimensional multibody systems are briefly introduced in Chapter 4.

In the first part of this book, the distinguishing features of the LMSTMM compared with traditional multibody system dynamics methods are revealed: there is no need for the global dynamics equations, the orders of the matrices involved are very low, the computational scale is rather small, the dynamics modelling is flexible, and the solution procedures are reasonably concise and suited for coding.

2

Transfer Matrix Method for Linear Multibody Systems

2.1 Introduction

Strictly speaking, various engineering mechanism systems, such as machine tools, weaponry, carrier rockets, airplanes and vehicles as well as electromechanical systems with controllers, are nonlinear and time-variant multi-flexible-body systems (MFSs). However, the accuracy could also be achieved in many situations even if a linear model of a multi-rigid-flexible-body system is used for an engineering project as then it becomes easy to solve actual engineering problems. The dynamics model of linear MRFSSs has therefore become one of the most popular, most important and most practical physical models in engineering fields such as weaponry, shipping, aeronautics, astronautics, communications, general machineries etc. The problems of linear multibody system dynamics (MSD) that are of interest to scientists and engineers include eigenvalue problems, vibration characteristics, steady-state responses, the orthogonality of eigenvectors and the dynamic responses of linear multibody systems (MSs).

Vibration characteristics are one of the most important dynamics characteristics of mechanical systems. It is hard to obtain justifiable *dynamic performance* of the mechanical system if the vibration characteristics cannot be solved or pre-estimated exactly when designing it. It is therefore very important to express exactly the vibration characteristics of MRFSSs. For example, it has been shown by theory and experiment that the dynamic performance and *firing precision* of a multiple launch rocket system (MLRS) are influenced greatly by its vibration characteristics, *firing frequency* and *firing orders*. This is because different vibration characteristics of the MLRS induced by different firing orders lead to different *initial disturbances* of the rockets and different firing precision of the MLRS. To appraise the dynamics characteristics of a mechanical system scientifically, it is necessary to compute the vibration characteristics of the system exactly, therefore the exact expression of the vibration characteristics of the MRFS is an important component of MSD. If a quantitative relationship between the population parameters of the structure and the vibration characteristics can be developed for a weapons system, the vibration characteristics can be modified according to our prediction by changing the population parameters, and this offers a good base for the design of weapons with high firing precision. Evaluating the vibration characteristics of a MRFS exactly, including eigenfrequency, eigenvector and damping ratio, is the precondition to solve exactly the dynamic response of the MRFS under arbitrary excitation by using the modal analysis method. At present, the approaches used in researching the vibration characteristics of mechanical systems include the finite element method (FEM), the modal analysis method and the modal synthesis method. We have to deal with problems such as high-order matrices, huge computational scale and computational ill-condition problems when computing the vibration characteristics of a complex MRFS by using ordinary mechanics methods. It is an important long-term aim

in this field to reduce greatly the computational scale and avoid computational ill-condition problems. The transfer matrix method for linear multibody systems has been developed by the authors and their co-workers, thus the problems of huge computational scale and computational ill-condition are avoided when the vibration characteristics are evaluated.

The basic idea of using the transfer matrix method for multibody system (MSTMM) to study MSD is as follows. A complicated MS can be broken up into elements containing bodies (rigid bodies, flexible bodies, lumped masses, etc.) and hinges (joints, ball-and-sockets, pins, springs, rotary springs, dampers and rotary dampers, etc.) with simple dynamics properties that can be readily expressed in matrix form. These matrices of elements are considered as the building blocks that provide the dynamics properties of the entire system when they are assembled according to the topology structure of the system, and are therefore called transfer matrices. The matrix formulation of any topology structure of the system is superbly adapted for consumption by computers. Furthermore the concise matrix notation brings to light basic properties of MSs formerly obscured in a mass of algebraic baroque. In particular, in the MSTMM the positions of bodies and hinges are considered equivalent in transfer matrices, and the order of the system matrix is independent of the number of degrees of freedom (DOF) of the system and dependent only on the order of the dynamics equations of the elements, which is totally different from ordinary MSD and results in a very low order of system matrix and very high computational speed. It is therefore not difficult to compute huge MSD with high DOF. A common type of MS occurring in engineering practice consists of a number of elements linked together end to end in the form of a chain, such as beams, turbine-generator shafts, crankshafts, etc. The MSTMM is ideally suitable for such systems and the overall transfer matrix of the system can be obtained automatically by successive multiplications of matrices of elements to assemble the element. In the MSTMM, the overall transfer matrix of the system can be deduced automatically by using the transfer matrices of each element. The *characteristic equation* can be obtained from the overall transfer equation by using the boundary conditions of the system, from which the vibration characteristics can be computed.

In this chapter, the basic principles of the MSTMM developed by the authors, the *eigenvalue problem* [4, 41, 43–46] and *steady-state response* of *undamped systems* and *damped systems*, including discrete and continuous MSs, and hybrid systems coupling discrete and continuous MSs composed of rigid bodies, lumped masses, beams, rods, shafts and so forth, are introduced. The dynamics problems of the flexible plate will be introduced in Chapter 4.

2.2 State Vector, Transfer Equation and Transfer Matrix

2.2.1 State Vector

The *state vector* at a point i of an MS is defined as a column matrix denoting the mechanics state of the point. The *state variables* of the state vector include the *displacements* of the point (including angular displacements) and the *internal forces* (including internal torques). Based on the sign conventions used in this book, \mathbf{z} denotes the state vector under *physics coordinates* and \mathbf{Z} denotes the state vector under *modal coordinates*. The state vectors of different points are distinguished from each other by using different subscripts. For a nonboundary end, the first and second subscripts i and j ($i, j \neq 0$) in a state vector $\mathbf{z}_{i,j}$ of the end denote the sequence numbers of the adjacent body element and hinge element, respectively. For a boundary end, the second subscript $j = 0$ in the state vector $\mathbf{z}_{i,j}$, that is, the second subscript 0 means boundary end and the first subscript i in the state vector $\mathbf{z}_{i,0}$ of the boundary end stands for the sequence number of the element involved.

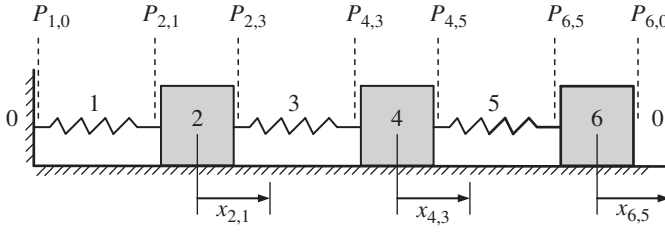


Figure 2.1 Spring-mass chain system.

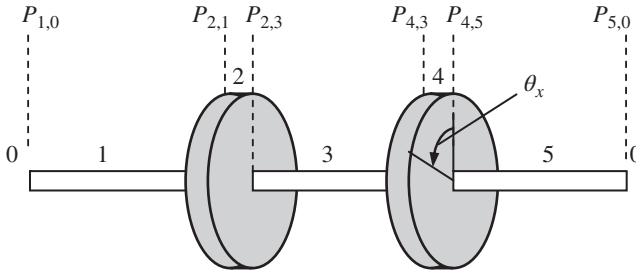


Figure 2.2 Torsion vibration system of shaft disks.

A chain system composed of three springs and three lumped masses with longitudinal vibration is shown in Figure 2.1. Consider the elements 1 and 6 as the root and tip of the system, respectively. According to the sign conventions used in this book, the transfer direction is from the tip to the root of the system, elements are numbered from 1 to 6 in sequence and the two boundary ends are numbered 0. The state vector at the connection point $P_{i,j}$ is defined as

$$\mathbf{z}_{i,j} = [x, q_x]_{i,j}^T \quad (2.1)$$

where $x_{i,j}$ and $q_{xi,j}$ are the displacement and internal forces of point $P_{i,j}$ in the *inertia coordinate system*, respectively, subscripts i and j are the sequence numbers of the adjacent body element and hinge element, respectively, and superscript T means transposition. In other words, the state vector consists of displacement and corresponding internal force for a longitudinal vibration system.

A torsion vibration system composed of an elastic massless shaft and disks concentrated at different points along its length is shown in Figure 2.2. Analogous to the longitudinal vibration system, the state vector is defined as

$$\mathbf{z}_{i,j} = [\theta_x, m_x]_{i,j}^T \quad (2.2)$$

where $\theta_{xi,j}$ and $m_{xi,j}$ are the angular displacement and corresponding internal torque of point $P_{i,j}$ in the *inertia coordinate system*, respectively. The state vector is composed of angular displacement and corresponding internal torque for the torsion vibration system.

A step beam system transversely vibrating in a plane is shown in Figure 2.3, and the state vector of the connection point $P_{i,j}$ is defined as

$$\mathbf{z}_{i,j} = [y, \theta_z, m_z, q_y]_{i,j}^T \quad (2.3)$$

where $y_{i,j}$ and $\theta_{zi,j}$ are the displacement and the angular displacement of point $P_{i,j}$ in the y axis and about the z axis in the *inertia coordinate system*, respectively, and $m_{zi,j}$ and $q_{yi,j}$ are the

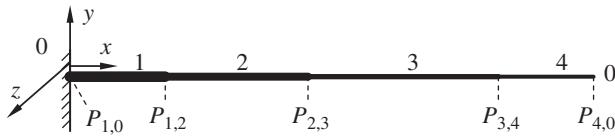


Figure 2.3 Transverse vibration of a step beam system.

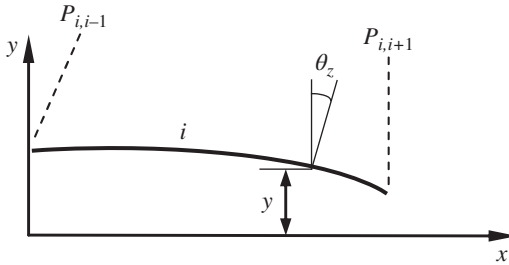


Figure 2.4 Transverse vibration of an elastic beam.

corresponding internal torque and internal shear force of point $P_{i,j}$ in the same inertia coordinate system, respectively, as shown in Figure 2.4.

The state vector of an arbitrary point P_{x_i} of the beam is defined as

$$\mathbf{z}_{x_i} = [y, \theta_z, m_z, q_y]_{x_i}^T \quad (0 < x_i \leq l_i, i = 1, 2, 3, 4) \quad (2.4)$$

where l_i is the length of the i th beam element.

Notice the order of the state variables in the state vectors: the displacements are placed in the upper half of the column and the forces in the lower, in such a way that the forces and the corresponding displacements (i.e., y and q_y , θ_z and m_z) are in positions that are mirror images of each other about the center of the column. This arrangement has advantages that will be appreciated later.

A spatial small vibration rigid body numbered i with one input end and one output end is shown in Figure 2.5, and the state vectors at the input and output ends are defined as

$$\begin{cases} \mathbf{z}_{I,i} = [x, y, z, \theta_x, \theta_y, \theta_z, m_x, m_y, m_z, q_x, q_y, q_z]_{I,i}^T \\ \mathbf{z}_{O,i} = [x, y, z, \theta_x, \theta_y, \theta_z, m_x, m_y, m_z, q_x, q_y, q_z]_{O,i}^T \end{cases} \quad (2.5)$$

The general principles used to define state vectors are as follows:

- 1) The geometric position and mechanics state of each connection point of the system can be described completely.
- 2) The number of state variables involved is as less as possible.
- 3) It is convenient to build up the transfer equations.

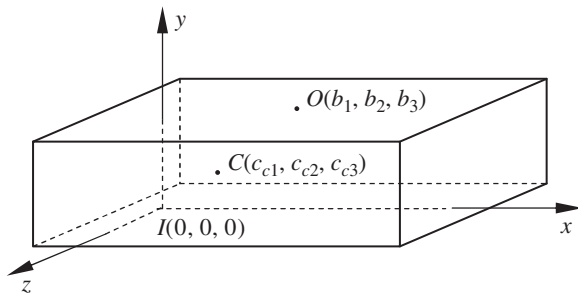
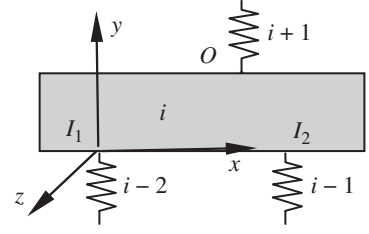


Figure 2.5 Rigid body with one input end and one output end.

Figure 2.6 Planar motion rigid body with two input ends and one output end.



For instance, a planar motion rigid body numbered i with two input ends and one output end is shown in Figure 2.6. The two input ends are connected with hinges $i-2$ and $i-1$, respectively, and the output end is connected with hinge $i+1$. The state vectors of each connection point are defined as

$$\begin{cases} \mathbf{z}_{i,i-2} = [x, y, \theta_z, m_z, q_x, q_y]_{i,i-2}^T \\ \mathbf{z}_{i,i-1} = [x, y, \theta_z, m_z, q_x, q_y]_{i,i-1}^T \\ \mathbf{z}_{i,i+1} = [x, y, \theta_z, m_z, q_x, q_y]_{i,i+1}^T \end{cases} \quad (2.6a)$$

There are only three independent variables in the six displacement variants of the state vectors at the two input ends. Therefore, the state vector of the input end of the rigid body is defined as

$$\mathbf{z}_{I,i} = [x_{i,i-2}, y_{i,i-2}, \theta_{zi,i-2}, m_{zi,i-2}, q_{xi,i-2}, q_{yi,i-2}, m_{zi,i-1}, q_{xi,i-1}, q_{yi,i-1}]_{I,i}^T \quad (2.6b)$$

or

$$\mathbf{z}_{I,i} = \mathbf{E}_1 \mathbf{z}_{i,i-2} + \mathbf{E}_2 \mathbf{z}_{i,i-1} \quad (2.6c)$$

where

$$\mathbf{E}_1 = \begin{bmatrix} \mathbf{I}_6 \\ \mathbf{O}_{3 \times 6} \end{bmatrix}, \quad \mathbf{E}_2 = \begin{bmatrix} \mathbf{O}_{6 \times 3} & \mathbf{O}_{6 \times 3} \\ \mathbf{O}_{3 \times 3} & \mathbf{I}_3 \end{bmatrix} \quad (2.6d)$$

Nine independent variables in $\mathbf{z}_{I,i}$ are used to describe completely the geometric and mechanics state of the input ends of the rigid body, including total state variables at the first input end $\mathbf{z}_{i,i-2}$ and three forces and torques in the state variables of the second input end $\mathbf{z}_{i,i-1}$. None is dispensable.

2.2.2 State Vector under Modal Coordinates

The response of undamped free vibration of MSs can be obtained by superposition of *principal modals*. The state vector of the system corresponding to *eigenfrequency* ω_k under the k th modal can be expressed as

$$\mathbf{z} = \mathbf{Z}^k e^{i\omega_k t} \quad \text{or} \quad \mathbf{z} = \mathbf{Z} e^{i\omega t} \quad (2.7)$$

where i is the imaginary unit and \mathbf{Z}^k is the state vector under the k th modal coordinates, whose variables are displacements and internal forces corresponding to eigenfrequency ω_k .

According to the sign conventions used in this book, \mathbf{Z}^k should be written as $\mathbf{Z}_{i,j}^k$. For conciseness, the superscript k of $\mathbf{Z}_{i,j}^k$ will be omitted and the term is abbreviated as $\mathbf{Z}_{i,j}$ when

Table 2.1 State vectors under modal coordinates and corresponding physics coordinates

Research objects	State vectors	
Spring-mass system	Physics coordinates	$\mathbf{z}_{i,j} = [x, q_x]_{i,j}^T$
	Modal coordinates	$\mathbf{Z}_{i,j} = [X, Q_x]_{i,j}^T$
Torsion vibration system	Physics coordinates	$\mathbf{z}_{i,j} = [\theta_x, m_x]_{i,j}^T$
	Modal coordinates	$\mathbf{Z}_{i,j} = [\Theta_x, M_x]_{i,j}^T$
Transverse vibration beam	Physics coordinates	$\mathbf{z}_{x_i} = [y, \theta_z, m_z, q_y]_{x_i}^T$
	Modal coordinates	$\mathbf{Z}_{x_i} = [Y, \Theta_z, M_z, Q_y]_{x_i}^T$
Rigid body with one input end and one output end	Physics coordinates	$\mathbf{z}_{l,i} = [x, y, z, \theta_x, \theta_y, \theta_z, m_x, m_y, m_z, q_x, q_y, q_z]_{l,i}^T$
		$\mathbf{z}_{O,i} = [x, y, z, \theta_x, \theta_y, \theta_z, m_x, m_y, m_z, q_x, q_y, q_z]_{O,i}^T$
	Modal coordinates	$\mathbf{Z}_{l,i} = [X, Y, Z, \Theta_x, \Theta_y, \Theta_z, M_x, M_y, M_z, Q_x, Q_y, Q_z]_{l,i}^T$
		$\mathbf{z}_{O,i} = [X, Y, Z, \Theta_x, \Theta_y, \Theta_z, M_x, M_y, M_z, Q_x, Q_y, Q_z]_{O,i}^T$

the modal orders are not emphasized. The detailed forms of the state vectors under modal and physics coordinates are shown in Table 2.1.

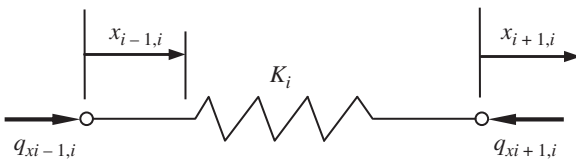
2.2.3 Transfer Equation and Transfer Matrix

To introduce the basic principles of MSTMM, *transfer equations* and *transfer matrices* of some basic mechanics elements are introduced here. Various transfer matrices of other elements involved in general MSs and their derivation methods are introduced in Chapter 10 and subsequent chapters.

2.2.3.1 Transfer Matrix of a Longitudinal Vibration Spring

The transfer equation and the transfer matrix of a longitudinal spring that is used in the chain spring-mass system shown in Figure 2.1 are introduced. The free-body diagram of the massless spring, as well as the positive directions of the displacements of its two ends and the forces acting on these two ends, are shown in Figure 2.7. We assume that the dynamic system is undergoing simple harmonic vibration and the eigenfrequency is denoted by ω . The stiffness of the spring is K_i and the state vectors of the input and output ends are $\mathbf{z}_{i-1,i}$ and $\mathbf{z}_{i+1,i}$, respectively. From the equilibrium of forces acting on the spring and the stiffness property of the spring we obtain

$$\begin{cases} q_{xi+1,i} = q_{xi-1,i} \\ -q_{xi+1,i} - K_i(x_{i+1,i} - x_{i-1,i}) = 0 \end{cases} \quad (2.8)$$

**Figure 2.7** Free-body diagram of a spring.

Equation (2.8) can be rewritten in the form

$$\begin{cases} x_{i+1,i} = x_{i-1,i} - \frac{1}{K_i} q_{xi-1,i} \\ q_{xi+1,i} = q_{xi-1,i} \end{cases} \quad (2.9)$$

For simple harmonic vibration we have

$$\mathbf{z} = \mathbf{Z}e^{i\omega t} \quad (2.10)$$

Substituting Equation (2.10) into Equation (2.9) results in the corresponding equations in the modal coordinate, notated in a matrix form as

$$\begin{bmatrix} X \\ Q_x \end{bmatrix}_{i+1,i} = \begin{bmatrix} 1 & -\frac{1}{K_i} \\ 0 & 1 \end{bmatrix} \begin{bmatrix} X \\ Q_x \end{bmatrix}_{i-1,i} \quad (2.11)$$

or

$$\mathbf{Z}_{i+1,i} = \mathbf{U}_i \mathbf{Z}_{i-1,i} \quad (2.12)$$

where

$$\mathbf{U}_i = \begin{bmatrix} 1 & -\frac{1}{K_i} \\ 0 & 1 \end{bmatrix} \quad (2.13)$$

Equation (2.12) describes the relation of state vectors between the two ends of the spring. It means that the state vector of the output end $\mathbf{Z}_{i+1,i}$ of the element numbered i can be expressed using the state vector of the input end $\mathbf{Z}_{i-1,i}$ by using matrix \mathbf{U}_i . Therefore Equation (2.11) or Equation (2.12) is called the transfer equation of the spring. The bold italic capital \mathbf{U}_i is the transfer matrix of the spring i .

2.2.3.2 Transfer Matrix of Longitudinal Vibration Lumped Mass

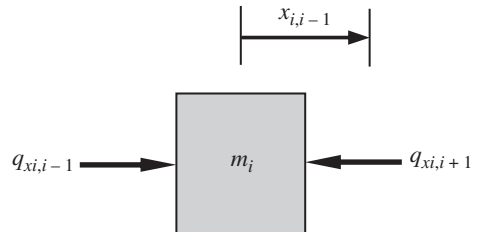
The free-body diagram of lumped mass m_i in the longitudinal vibration system of Figure 2.1 is shown in Figure 2.8. The displacements at the left and right ends are equal, that is

$$x_{i,i+1} = x_{i,i-1} \quad (2.14)$$

According to Newton's second law, we obtain

$$m_i \ddot{x}_{i,i-1} = q_{xi,i-1} - q_{xi,i+1} \quad (2.15)$$

Figure 2.8 Free-body diagram of a lumped mass.



Combining Equations (2.14) and (2.15) yields

$$\begin{cases} x_{i,i+1} = x_{i,i-1} \\ q_{x_{i,i+1}} = -m_i \ddot{x}_{i,i-1} + q_{x_{i,i-1}} \end{cases} \quad (2.16)$$

For the lumped mass m_i with simple harmonic vibration, substituting Equation (2.10) in Equation (2.16) and compacting the results in a matrix form, we have

$$\begin{bmatrix} X \\ Q_x \end{bmatrix}_{i,i+1} = \begin{bmatrix} 1 & 0 \\ m_i \omega^2 & 1 \end{bmatrix} \begin{bmatrix} X \\ Q_x \end{bmatrix}_{i,i-1} \quad (2.17)$$

that is,

$$\mathbf{Z}_{i,i+1} = \mathbf{U}_i \mathbf{Z}_{i,i-1} \quad (2.18)$$

Equation (2.18) is the transfer equation of the longitudinal vibration lumped mass, where

$$\mathbf{U}_i = \begin{bmatrix} 1 & 0 \\ m_i \omega^2 & 1 \end{bmatrix} \quad (2.19)$$

is the transfer matrix of the lumped mass.

2.2.3.3 Transfer Matrix of a Torsion Vibration Massless Shaft

The free-body diagram of the massless shafts with uniform cross-section in a torsion vibration system of Figure 2.2 is shown in Figure 2.9. From the equilibrium of the internal torsion moments of its two ends, we have

$$m_{xi+1,i} = m_{xi-1,i} \quad (2.20)$$

From the mechanics of materials

$$\theta_{xi+1,i} = \theta_{xi-1,i} + \frac{m_{xi-1,i} l_i}{(GJ_p)_i} \quad (2.21)$$

where G and GJ_p are the shear modulus of material and the torsion stiffness of the shaft, respectively.

Considering Equation (2.10), notate Equations (2.19) and (2.20) using the matrix, and then the transfer equation of the torsion vibration massless shaft can be obtained:

$$\mathbf{Z}_{i+1,i} = \mathbf{U}_i \mathbf{Z}_{i-1,i}$$

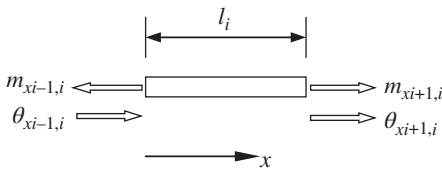


Figure 2.9 Free-body diagram of a shaft.

where

$$\mathbf{U}_i = \begin{bmatrix} 1 & \frac{l}{(GJ_p)_i} \\ 0 & 1 \end{bmatrix} \quad (2.22)$$

is the transfer matrix of the torsion vibration massless shaft.

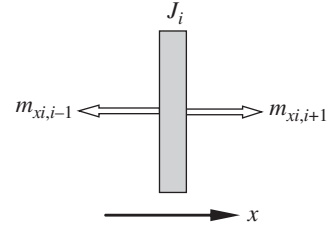


Figure 2.10 Free-body diagram of a disk.

2.2.3.4 Transfer Matrix of a Disk

The free-body diagram of the rigid disks in the torsion vibration system of Figure 2.2, whose rotational inertia is J_i , is shown in Figure 2.10. The twist angles of its two ends are equal, that is,

$$\theta_{xi,i+1} = \theta_{xi,i-1} \quad (2.23)$$

The rotation equation is

$$m_{xi,i+1} = m_{xi,i-1} + J_i \ddot{\theta}_{xi,i-1} \quad (2.24)$$

Considering Equation (2.10) and rewriting Equations (2.23) and (2.24) in matrix form, the transfer equation can be obtained:

$$\mathbf{Z}_{i,i+1} = \mathbf{U}_i \mathbf{Z}_{i,i-1}$$

where

$$\mathbf{U}_i = \begin{bmatrix} 1 & 0 \\ -\omega^2 J_i & 1 \end{bmatrix} \quad (2.25)$$

is the transfer matrix of the torsion vibration rigid disk.

2.2.3.5 Transfer Matrix of a Planar Transverse Vibration Massless Elastic Beam

The free-body diagram of a planar transverse vibration massless elastic beam is shown in Figure 2.11. Its length and bending stiffness are l_i and EI_i , respectively, and its displacements

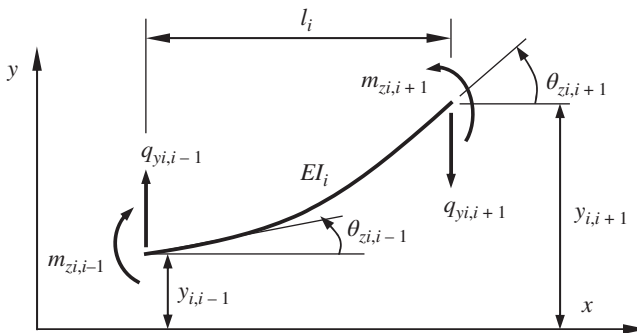


Figure 2.11 Free-body diagram of a transverse vibration elastic beam.

and internal forces of its two ends are given based on the sign conventions. From the equilibrium condition of forces and moments, we obtain

$$\begin{cases} q_{y_{i,i-1}} - q_{y_{i,i+1}} = 0 \\ -m_{z_{i,i-1}} + m_{z_{i,i+1}} - q_{y_{i,i+1}} l_i = 0 \end{cases} \quad (2.26)$$

According to the elementary theory of a beam, in the body-fixed coordinate system with origin the input end of the beam, the displacement and slope of the output end are

$$y = \frac{m_z l^2}{2EI} - \frac{q_y l^3}{3EI} \quad (2.27)$$

$$\theta_z = \frac{m_z l}{EI} - \frac{q_y l^2}{2EI} \quad (2.28)$$

where EI and l are the flexural rigidity and length.

Applying the above equations and taking note of the displacement $y_{i,i-1}$ and slope $\theta_{z_{i,i-1}}$ of the input end $P_{i,i-1}$, the displacement and the slope of the output end in the inertial coordinate system can be written as

$$\begin{cases} y_{i,i+1} = y_{i,i-1} + \theta_{z_{i,i-1}} l_i + m_{z_{i,i+1}} \frac{l_i^2}{2EI_i} - q_{y_{i,i+1}} \frac{l_i^3}{3EI_i} \\ \theta_{z_{i,i+1}} = \theta_{z_{i,i-1}} + m_{z_{i,i+1}} \frac{l_i}{EI_i} - q_{y_{i,i+1}} \frac{l_i^2}{2EI_i} \end{cases} \quad (2.29)$$

Combining Equations (2.26) and (2.29) yields

$$\begin{cases} y_{i,i+1} = y_{i,i-1} + l_i \theta_{z_{i,i-1}} + \frac{l_i^2}{2EI_i} m_{z_{i,i-1}} + \frac{l_i^3}{6EI_i} q_{y_{i,i-1}} \\ \theta_{z_{i,i+1}} = \theta_{z_{i,i-1}} + \frac{l_i}{EI_i} m_{z_{i,i-1}} + \frac{l_i^2}{2EI_i} q_{y_{i,i-1}} \\ m_{z_{i,i+1}} = m_{z_{i,i-1}} + l_i q_{y_{i,i-1}} \\ q_{y_{i,i+1}} = q_{y_{i,i-1}} \end{cases} \quad (2.30)$$

Furthermore, considering Equation (2.10) and rewriting Equation (2.30) in matrix form, the transfer equation can be deduced as

$$\mathbf{Z}_{i,i+1} = \mathbf{U}_i \mathbf{Z}_{i,i-1}$$

where

$$\mathbf{U}_i = \begin{bmatrix} 1 & l_i & \frac{l_i^2}{2EI_i} & \frac{l_i^3}{6EI_i} \\ 0 & 1 & \frac{l_i}{EI_i} & \frac{l_i^2}{2EI_i} \\ 0 & 0 & 1 & l_i \\ 0 & 0 & 0 & 1 \end{bmatrix} \quad (2.31)$$

is the transfer matrix of the planar transverse vibration massless elastic beam.

It can be seen clearly that the transfer matrix describes the relation between the mechanics states of different space points at the same time. It transfers the state vectors from $Z_{i,j}$ of point $P_{i,j}$ to $Z_{m,n}$ of point $P_{m,n}$ of the system. That is, it transfers the state from one place to another, so the transfer matrix is also called the state transform matrix. Generally speaking, for a simple-harmonic vibration system with frequency ω , the transfer matrix is a function of ω , that is, $U_i = U_i(\omega)$.

2.3 Overall Transfer Equation, Overall Transfer Matrix and Boundary Conditions

2.3.1 Overall Transfer Equation and Overall Transfer Matrix

A vibration system comprising n elements is used as an example, as shown in Figure 2.12, to show how to deduce the *overall transfer equation* and *overall transfer matrix* of the system. There are $n + 1$ connection points and two boundary ends, and $Z_{1,0}, Z_{n,0}$ are the boundary state vectors.

The transfer equations of the n elements are

$$\begin{cases} Z_{2,1} = U_1 Z_{1,0} \\ Z_{2,3} = U_2 Z_{2,1} \\ \vdots \\ Z_{n,0} = U_n Z_{n-1,n} \end{cases} \quad (2.32)$$

The overall transfer equation of the system is

$$Z_{n,0} = U_{1-n} Z_{1,0} \quad (2.33)$$

where

$$U_{1-n} = U_n U_{n-1} \cdots U_{i+1} U_i U_{i-1} \cdots U_3 U_2 U_1 \quad (2.34)$$

is the overall transfer matrix of the system, which is obtained by successively multiplying each element's transfer matrix of the system in sequence.

In the overall transfer equation, apart from the boundary state vectors no state vectors of other connection points are involved.

2.3.2 Boundary Conditions

The state vectors at the boundaries are composed of displacements and internal forces, and the number m of its components is always an even number. Generally, the components of state

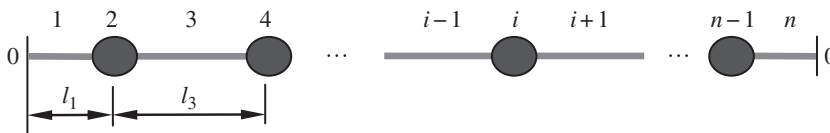


Figure 2.12 An elastic beam with several lumped masses.

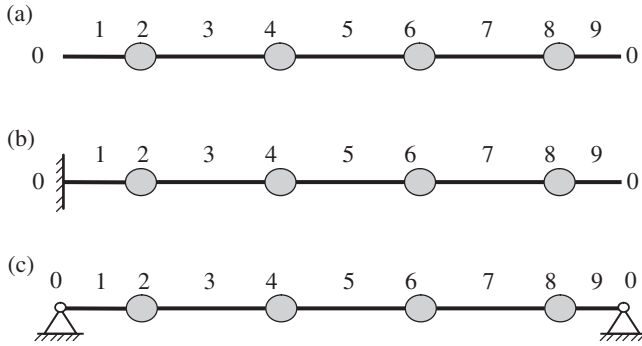


Figure 2.13 Examples of boundary conditions.

vectors at the boundaries are partly unknown. For homogeneous *boundary conditions*, half of the components are zeros and the others are unknown. Examples are as follows:

- 1) In the transverse vibration system shown in Figure 2.13a, both ends of points $P_{1,0}$ and $P_{9,0}$ are free, and the internal forces and the internal moments are zero, whereas displacements are unknown. The boundary conditions are

$$\mathbf{Z}_{1,0} = [Y, \theta_z, 0, 0]_{1,0}^T, \quad \mathbf{Z}_{9,0} = [Y, \theta_z, 0, 0]_{9,0}^T \quad (2.35)$$

- 2) Point $P_{1,0}$ is fixed and point $P_{9,0}$ is free, as shown in Figure 2.13b. The boundary conditions are

$$\mathbf{Z}_{1,0} = [0, 0, M_z, Q_y]_{1,0}^T, \quad \mathbf{Z}_{9,0} = [Y, \theta_z, 0, 0]_{9,0}^T \quad (2.36)$$

- 3) If both points $P_{1,0}$ and $P_{9,0}$ are simply supported, as shown in Figure 2.13c, the boundary conditions are

$$\mathbf{Z}_{1,0} = [0, \theta_z, 0, Q_y]_{1,0}^T, \quad \mathbf{Z}_{9,0} = [0, \theta_z, 0, Q_y]_{9,0}^T \quad (2.37)$$

2.4 Characteristic Equation

For the transverse vibration system shown in Figure 2.12 the overall transfer Equation (2.33) of the system can be written as

$$\begin{bmatrix} Y \\ \theta_z \\ M_z \\ Q_y \end{bmatrix}_{n,0} = \begin{bmatrix} u_{11} & u_{12} & u_{13} & u_{14} \\ u_{21} & u_{22} & u_{23} & u_{24} \\ u_{31} & u_{32} & u_{33} & u_{34} \\ u_{41} & u_{42} & u_{43} & u_{44} \end{bmatrix} \begin{bmatrix} Y \\ \theta_z \\ M_z \\ Q_y \end{bmatrix}_{1,0} \quad (2.38)$$

where the components u_{ij} ($i, j = 1, 2, 3, 4$) of the transfer matrix are functions of the eigenfrequencies of the system.

Applying the boundary conditions, the following two homogeneous equation can be obtained

$$\mathbf{U}' \mathbf{Z}'_{1,0} = \mathbf{0} \quad (2.39)$$

where $\mathbf{Z}'_{1,0}$ consists of the two unknown components of state vector $\mathbf{Z}_{1,0}$.

A nontrivial solution of the system is possible if and only if $\mathbf{Z}'_{1,0} \neq \mathbf{0}$, so the value of the determinant of matrix \mathbf{U}' is zero, that is

$$\Delta = \det \mathbf{U}' = 0 \quad (2.40)$$

where $\det \mathbf{U}'$ is a function of ω and Equation (2.40) is the *characteristic equation* of the system. For an undamped system, Equation (2.40) is usually known as the frequency equation and its roots are the eigenfrequencies of the system. For a damped system, the unknown components of the transfer matrix are complex numbers and the solutions of Equation (2.40) $\lambda = -\lambda^r + i\lambda^i$ are called eigenvalues. The real part $-\lambda^r$ is related to the magnitude of damping, and the imaginary part λ^i is related to the eigenfrequency of the damped system. For the three kinds of boundary conditions mentioned above, the frequency equations of the undamped system are discussed as follows.

- 1) Both ends of $P_{1,0}$ and $P_{9,0}$ are free boundaries, as shown in Figure 2.13a. Substituting boundary condition Equation (2.35) into Equation (2.38), we obtain

$$\begin{bmatrix} Y \\ \Theta_z \\ 0 \\ 0 \end{bmatrix}_{9,0} = \begin{bmatrix} u_{11} & u_{12} & u_{13} & u_{14} \\ u_{21} & u_{22} & u_{23} & u_{24} \\ u_{31} & u_{32} & u_{33} & u_{34} \\ u_{41} & u_{42} & u_{43} & u_{44} \end{bmatrix} \begin{bmatrix} Y \\ \Theta_z \\ 0 \\ 0 \end{bmatrix}_{1,0} \quad (2.41)$$

Picking out the third and fourth formulas of the homogeneous equations and rewriting them in form of Equation (2.39), we obtain

$$\begin{bmatrix} 0 \\ 0 \end{bmatrix} = \begin{bmatrix} u_{31} & u_{32} \\ u_{41} & u_{42} \end{bmatrix} \begin{bmatrix} Y \\ \Theta_z \end{bmatrix}_{1,0} \quad (2.42)$$

If there exist nontrivial solutions of the system, namely $[Y, \Theta_z]_{1,0}^T \neq \mathbf{0}$, then the frequency equation can be obtained:

$$\begin{vmatrix} u_{31} & u_{32} \\ u_{41} & u_{42} \end{vmatrix} = 0 \quad (2.43)$$

- 2) Point $P_{1,0}$ is fixed and point $P_{9,0}$ is free, as shown in Figure 2.13b. The frequency equation is obtained using the proposed method:

$$\begin{vmatrix} u_{33} & u_{34} \\ u_{43} & u_{44} \end{vmatrix} = 0 \quad (2.44)$$

- 3) Both ends of $P_{0,1}$ and $P_{9,0}$ are simply supported, as shown in Figure 2.13c. The frequency equation is obtained using the proposed method:

$$\begin{vmatrix} u_{12} & u_{14} \\ u_{32} & u_{34} \end{vmatrix} = 0 \quad (2.45)$$

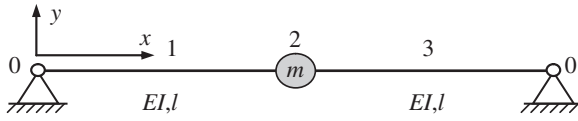


Figure 2.14 A massless elastic simply supported beam with a lumped mass at the midpoint.

Example 2.1 Find the eigenfrequencies of the simply supported beam system composed of a massless elastic beam and a lumped mass at the midpoint, as shown in Figure 2.14.

Solution

The state vectors $\mathbf{Z}_{1,0}, \mathbf{Z}_{2,1}, \mathbf{Z}_{2,3}, \mathbf{Z}_{3,0}$ are defined as $\mathbf{Z} = [Y, \theta_z, M_z, Q_y]^T$ and the transfer equations of the three elements are

$$\mathbf{Z}_{2,1} = \mathbf{U}_1 \mathbf{Z}_{1,0}, \quad \mathbf{Z}_{2,3} = \mathbf{U}_2 \mathbf{Z}_{2,1}, \quad \mathbf{Z}_{3,0} = \mathbf{U}_3 \mathbf{Z}_{2,3} \quad (\text{a})$$

where \mathbf{U}_1 and \mathbf{U}_3 are determined by Equation (2.31) and \mathbf{U}_2 is derived as follows.

Recall that the displacements, angular displacements and internal moments on the two ends of a lumped mass are continuous, thus

$$y_{2,3} = y_{2,1}, \quad \theta_{z2,3} = \theta_{z2,1}, \quad m_{z2,3} = m_{z2,1} \quad (\text{b})$$

The free-body diagram of the lumped mass is shown in Figure 2.15. From the equilibrium of forces acting on the lumped mass we obtain

$$q_{y2,3} = q_{y2,1} - m\ddot{y}_{2,1} \quad (\text{c})$$

Combining Equations (b) and (c), $\ddot{y}_{2,1} = -\omega^2 y_{2,1}$ is developed from Equation (2.10), thus the transfer matrix is

$$\mathbf{U}_2 = \begin{bmatrix} 1 & 0 & 0 & 0 \\ 0 & 1 & 0 & 0 \\ 0 & 0 & 1 & 0 \\ m\omega^2 & 0 & 0 & 1 \end{bmatrix} \quad (\text{d})$$

According to Equation (a), we obtain

$$\mathbf{Z}_{3,0} = \mathbf{U}_3 \mathbf{U}_2 \mathbf{U}_1 \mathbf{Z}_{1,0} \quad (\text{e})$$

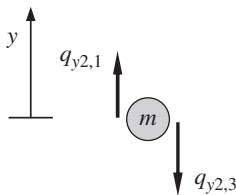


Figure 2.15 Free-body diagram of a mass.

that is

$$\begin{bmatrix} Y \\ \Theta_z \\ M_z \\ Q_y \end{bmatrix}_{3,0} = \begin{bmatrix} 1 + \frac{m\omega^2 l^3}{6EI} & 2l + \frac{m\omega^2 l^4}{6EI} & \frac{2l^2}{EI} + \frac{m\omega^2 l^5}{12(EI)^2} & \frac{4l^3}{3EI} + \frac{m\omega^2 l^6}{36(EI)^2} \\ \frac{m\omega^2 l^2}{2EI} & 1 + \frac{m\omega^2 l^3}{2EI} & \frac{2l}{EI} + \frac{m\omega^2 l^4}{4(EI)^2} & \frac{2l^2}{EI} + \frac{m\omega^2 l^5}{12(EI)^2} \\ m\omega^2 l & m\omega^2 l^2 & 1 + \frac{m\omega^2 l^3}{2EI} & 2l + \frac{m\omega^2 l^4}{6EI} \\ m\omega^2 & m\omega^2 l & \frac{m\omega^2 l^2}{2EI} & 1 + \frac{m\omega^2 l^3}{6EI} \end{bmatrix} \begin{bmatrix} Y \\ \Theta_z \\ M_z \\ Q_y \end{bmatrix}_{1,0} \quad (f)$$

Substituting the boundary conditions

$$Y_{1,0} = M_{z1,0} = 0, \quad Y_{3,0} = M_{z3,0} = 0 \quad (g)$$

into Equation (e), we obtain

$$\begin{bmatrix} 0 \\ \Theta_z \\ 0 \\ Q_y \end{bmatrix}_{3,0} = \begin{bmatrix} 1 + \frac{m\omega^2 l^3}{6EI} & 2l + \frac{m\omega^2 l^4}{6EI} & \frac{2l^2}{EI} + \frac{m\omega^2 l^5}{12(EI)^2} & \frac{4l^3}{3EI} + \frac{m\omega^2 l^6}{36(EI)^2} \\ \frac{m\omega^2 l^2}{2EI} & 1 + \frac{m\omega^2 l^3}{2EI} & \frac{2l}{EI} + \frac{m\omega^2 l^4}{4(EI)^2} & \frac{2l^2}{EI} + \frac{m\omega^2 l^5}{12(EI)^2} \\ m\omega^2 l & m\omega^2 l^2 & 1 + \frac{m\omega^2 l^3}{2EI} & 2l + \frac{m\omega^2 l^4}{6EI} \\ m\omega^2 & m\omega^2 l & \frac{m\omega^2 l^2}{2EI} & 1 + \frac{m\omega^2 l^3}{6EI} \end{bmatrix} \begin{bmatrix} 0 \\ \Theta_z \\ 0 \\ Q_y \end{bmatrix}_{1,0} \quad (h)$$

$\Theta_{z1,0}$ and $Q_{y1,0}$ have nonzero solutions only when the following equation is satisfied

$$\begin{vmatrix} 2l + \frac{m\omega^2 l^4}{6EI} & \frac{4l^3}{3EI} + \frac{m\omega^2 l^6}{36(EI)^2} \\ m\omega^2 l^2 & 2l + \frac{m\omega^2 l^4}{6EI} \end{vmatrix} = 0 \quad (i)$$

By solving Equation (i), the eigenfrequency can be obtained:

$$\omega = \sqrt{\frac{6EI}{ml^3}} \quad (j)$$

Example 2.2 Find the eigenfrequencies of the 2 DOF spring-mass system shown in Figure 2.16.

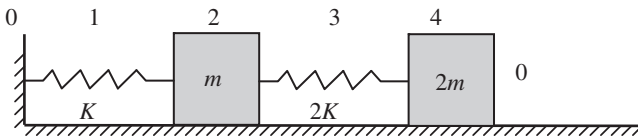


Figure 2.16 A 2 DOF spring-mass system.

Solution

The state vectors $\mathbf{Z}_{1,0}$, $\mathbf{Z}_{2,1}$, $\mathbf{Z}_{2,3}$, $\mathbf{Z}_{4,3}$ and $\mathbf{Z}_{4,0}$ are defined in the form of $\mathbf{Z} = [X, Q_x]^T$.

The transfer matrices of the elements are.

$$\mathbf{U}_1 = \begin{bmatrix} 1 & -\frac{1}{K} \\ 0 & 1 \end{bmatrix}, \quad \mathbf{U}_2 = \begin{bmatrix} 1 & 0 \\ m\omega^2 & 1 \end{bmatrix}, \quad \mathbf{U}_3 = \begin{bmatrix} 1 & -\frac{1}{2K} \\ 0 & 1 \end{bmatrix}, \quad \mathbf{U}_4 = \begin{bmatrix} 1 & 0 \\ 2m\omega^2 & 1 \end{bmatrix} \quad (\text{a})$$

The overall transfer matrix is

$$\mathbf{U} = \mathbf{U}_4 \mathbf{U}_3 \mathbf{U}_2 \mathbf{U}_1 = \begin{bmatrix} 1 - \frac{m\omega^2}{2K} & -\frac{1}{2K} \left(3 - \frac{m\omega^2}{K} \right) \\ m\omega^2 \left(3 - \frac{m\omega^2}{K} \right) & \left(1 - \frac{m\omega^2}{K} \right)^2 - \frac{2m\omega^2}{K} \end{bmatrix} \quad (\text{b})$$

Substituting the boundary conditions

$$\mathbf{Z}_{1,0} = [0, Q_x]_{1,0}^T, \quad \mathbf{Z}_{4,0} = [X, 0]_{4,0}^T \quad (\text{c})$$

into the overall transfer equation of the system, we obtain

$$\begin{bmatrix} X \\ 0 \end{bmatrix}_{4,0} = \begin{bmatrix} 1 - \frac{m\omega^2}{2K} & -\frac{1}{2K} \left(3 - \frac{m\omega^2}{K} \right) \\ m\omega^2 \left(3 - \frac{m\omega^2}{K} \right) & \left(1 - \frac{m\omega^2}{K} \right)^2 - \frac{2m\omega^2}{K} \end{bmatrix} \begin{bmatrix} 0 \\ Q_x \end{bmatrix}_{1,0} \quad (\text{d})$$

Therefore, the frequency equation is

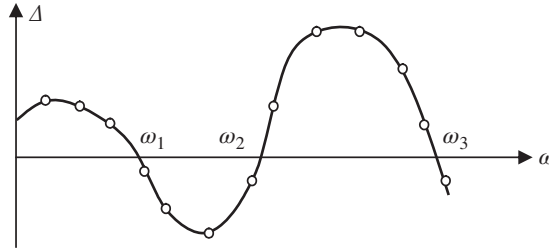
$$\left(1 - \frac{m\omega^2}{K} \right)^2 - \frac{2m\omega^2}{K} = 0 \quad (\text{e})$$

resulting in

$$\omega_1^2 = (2 - \sqrt{3}) \frac{K}{m}, \quad \omega_2^2 = (2 + \sqrt{3}) \frac{K}{m} \quad (\text{f})$$

2.5 Computation for State Vector and Vibration Characteristics

The computation for the *eigenfrequencies* of a vibration system involves matrix multiplication. For a simple mass-spring system, only simple multiplication of second-order square matrices is involved. However, because of the high order of matrices for a complex system, the calculation by hand is very difficult and a computer has to be used. The computation of the eigenfrequencies of a system is usually done by combining the step-by-step scanning method and the dichotomy method, which is carried out by a computer. First, a series of tentative frequencies determined by the selected step should be chosen, such as ω , $\omega + \Delta\omega$, $\omega + 2\Delta\omega$, \dots . The determinant value Δ of the characteristic equation (2.40) under each tentative frequency is then computed. If the Δ values corresponding to two adjacent tentative frequencies have opposite signs, there must be at least one frequency between them satisfying $\Delta = 0$. Thus, one of the regions of system eigenfrequencies is obtained. The eigenfrequencies can then be found using dichotomy in the regions. Setting ω as the horizontal axis and Δ as the vertical axis, we can obtain a point at this coordinate system for each tentative computation. Linking these points, the curve of $\omega - \Delta(\omega)$ can be obtained, as shown in Figure 2.17. The intersection points of the curve and the axis of abscissa correspond to eigenfrequencies ω_k ($k = 1, 2, 3, \dots$).

Figure 2.17 Plot of $\omega - \Delta(\omega)$.

Example 2.3 Find the eigenfrequencies of the systems for three kinds of boundary conditions, as shown in Figure 2.13, then plot the $\omega - \Delta(\omega)$ curves. The parameters are given as follows: $m_2 = m_8 = m$, $m_4 = m_6 = 3m$, $l_1 = l_3 = l_5 = l_7 = l_9 = l$, $EI_1 = EI_9 = EI$, $EI_3 = EI_5 = EI_7 = 2EI$, where $m = 1\text{kg}$, $l = 1\text{m}$, $EI = 1\text{N}\cdot\text{m}^2$.

Solution

Select tentative frequencies ω and $\omega + \Delta\omega, \dots$, and let $\omega = 0$ and $\Delta\omega = 0.2$. Substitute the tentative frequencies and the structure parameters into the transfer matrices $\mathbf{U}_i (i = 1, 2, \dots, 9)$ of each element, and obtain the overall transfer matrix by successive multiplication of these matrices $\mathbf{U} = \mathbf{U}_9 \mathbf{U}_8 \mathbf{U}_7 \mathbf{U}_6 \mathbf{U}_5 \mathbf{U}_4 \mathbf{U}_3 \mathbf{U}_2 \mathbf{U}_1$. Compute the determinant value using Equations (2.43), (2.44) and (2.45), respectively. Plot the $\omega - \Delta(\omega)$ curves shown in Figure 2.18. Search the eigenfrequencies using the dichotomy in the regions of roots. The computation results are shown in Table 2.2.

The components of the overall transfer matrix \mathbf{U} are known once the eigenfrequencies of the system have been obtained. Once the state vectors of the boundaries have been obtained, the state vectors of the other connection points can be determined using Equation (2.46):

$$\begin{cases} \mathbf{Z}_{i,i-1} = \mathbf{U}_{i-1} \cdots \mathbf{U}_2 \mathbf{U}_1 \mathbf{Z}_{1,0} & (i \text{ is the sequence number of body}) \\ \mathbf{Z}_{i-1,i} = \mathbf{U}_{i-1} \cdots \mathbf{U}_2 \mathbf{U}_1 \mathbf{Z}_{1,0} & (i \text{ is the sequence number of hinge}) \end{cases} \quad (2.46)$$

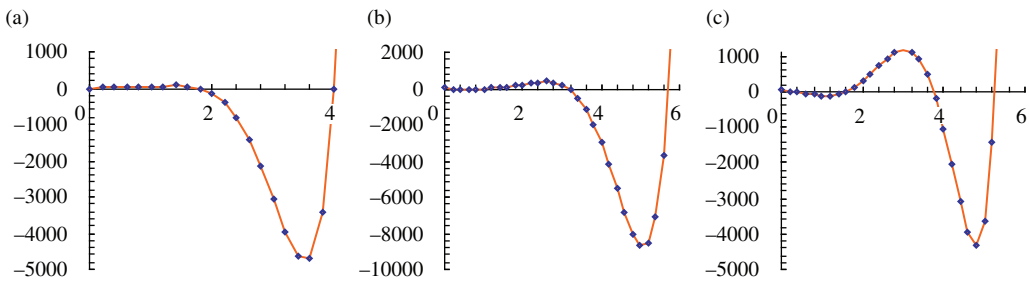


Figure 2.18 The $\omega - \Delta(\omega)$ curves under the three kinds of boundary conditions: (a) free-free, (b) fixed-free and (c) both simply supported.

Table 2.2 Computation results of eigenfrequencies under the three boundary conditions (rad/s)

Boundary conditions			
Order		Free-Free	Fixed-Free
1		0	0.146
2		0	1.080
3		1.789	3.144
4		4.000	5.731
			Both simply supported
			0.343
			1.593
			3.754
			5.274

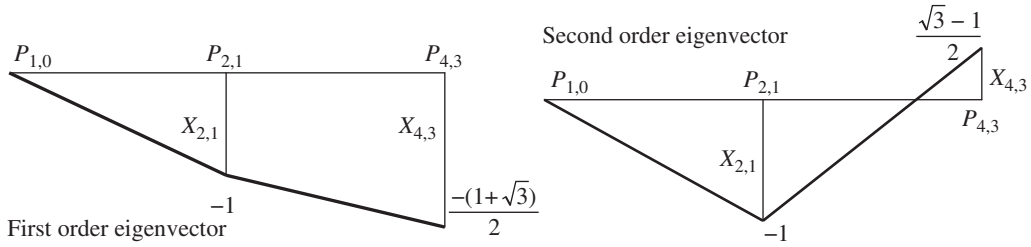


Figure 2.19 The eigenvectors of the 2 DOF spring-mass system.

The state vectors at the boundaries can be obtained by solving $m/2$ homogeneous equations $\mathbf{U}'\mathbf{Z}'_{1,0} = \mathbf{0}$ of the overall equation. For example, the 2 DOF spring-mass system in Example 2.2, shown in Figure 2.16, has the overall transfer equation

$$\begin{bmatrix} X \\ 0 \end{bmatrix}_{4,0} = \begin{bmatrix} u_{11} & u_{12} \\ u_{21} & u_{22} \end{bmatrix} \begin{bmatrix} 0 \\ Q_x \end{bmatrix}_{1,0} \quad (2.47)$$

where the homogeneous equation is $u_{22}Q_{x1,0} = 0$. When $\omega = \omega_1$ or $\omega = \omega_2$, $u_{22} = \left(1 - \frac{m\omega^2}{K}\right)^2 - \frac{2m\omega^2}{K} = 0$. Thus, $Q_{x1,0}$ may be an arbitrary number. Usually, $Q_{x1,0} = 1$, that is, $\mathbf{Z}_{1,0} = [0, 1]^T$. Substituting this into Equation (2.47), the state vector at another boundary is obtained, $\mathbf{Z}_{4,0} = \left[-\frac{1}{2K}\left(3 - \frac{m\omega^2}{K}\right), 0\right]^T$. The state vectors at each connection point can be obtained successively using the transfer equations of each element as follows:

$$\mathbf{Z}_{2,1} = \mathbf{U}_1\mathbf{Z}_{1,0}, \quad \mathbf{Z}_{2,3} = \mathbf{U}_2\mathbf{Z}_{2,1}, \quad \mathbf{Z}_{4,3} = \mathbf{U}_3\mathbf{Z}_{2,3} \quad (2.48)$$

Equation (2.48) can be rewritten as

$$\mathbf{Z}_{2,1} = \mathbf{U}_1\mathbf{Z}_{1,0}, \quad \mathbf{Z}_{2,3} = \mathbf{U}_2\mathbf{U}_1\mathbf{Z}_{1,0}, \quad \mathbf{Z}_{4,3} = \mathbf{U}_3\mathbf{U}_2\mathbf{U}_1\mathbf{Z}_{1,0} \quad (2.49)$$

Thus, all the state vectors of the system are obtained. Then, the k th order *eigenvector* of the system corresponding to the eigenfrequency ω_k is

$$[X_{2,1}^k, X_{4,3}^k]^T \quad (2.50)$$

The computation results of the eigenvectors are shown in Figure 2.19 (assume the spring stiffness $K = 1$).

Example 2.4 Find the eigenvectors of the simply-simply supported systems shown in Figure 2.13c. The parameters are the same as in Example 2.3.

Solution

According to the boundary conditions and overall transfer equation, we get

$$\begin{bmatrix} 0 \\ \Theta_z \\ 0 \\ Q_y \end{bmatrix}_{9,0} = \begin{bmatrix} u_{11} & u_{12} & u_{13} & u_{14} \\ u_{21} & u_{22} & u_{23} & u_{24} \\ u_{31} & u_{32} & u_{33} & u_{34} \\ u_{41} & u_{42} & u_{43} & u_{44} \end{bmatrix} \begin{bmatrix} 0 \\ \Theta_z \\ 0 \\ Q_y \end{bmatrix}_{1,0} \quad (a)$$

In Equation (a), the first and third equations are homogeneous equations, that is

$$\begin{bmatrix} 0 \\ 0 \end{bmatrix} = \begin{bmatrix} u_{12} & u_{14} \\ u_{32} & u_{34} \end{bmatrix} \begin{bmatrix} \Theta_z \\ Q_y \end{bmatrix}_{1,0} \quad (b)$$

Let $\Theta_{z1,0} = 1$, then $Q_{y1,0} = -\frac{u_{12}}{u_{14}} (u_{14} \neq 0)$ (or $Q_{y1,0} = -\frac{u_{32}}{u_{34}} (u_{34} \neq 0)$), so

$$\mathbf{Z}_{1,0} = \begin{bmatrix} 0 & 1 & 0 & -\frac{u_{12}}{u_{14}} \end{bmatrix}^T, \quad \mathbf{Z}_{9,0} = \mathbf{U}\mathbf{Z}_{1,0} \quad (c)$$

The state vectors at the connection points are

$$\begin{cases} \mathbf{Z}_{i,i-1} = \mathbf{U}_{i-1} \cdots \mathbf{U}_2 \mathbf{U}_1 \mathbf{Z}_{1,0} & (i = 2, 4, 6, 8) \\ \mathbf{Z}_{i-1,i} = \mathbf{U}_{i-1} \cdots \mathbf{U}_2 \mathbf{U}_1 \mathbf{Z}_{1,0} & (i = 3, 5, 7, 9) \end{cases} \quad (d)$$

The state vectors of arbitrary points at the beams are

$$\mathbf{Z}_{i,x_i} = \mathbf{U}_{i,x_i} \mathbf{Z}_{i-1,i} \quad (i = 1, 3, 5, 7, 9) \quad (e)$$

where

$$\mathbf{U}_{i,x_i} = \begin{bmatrix} 1 & x_i & \frac{x_i^2}{2EI_i} & \frac{x_i^3}{6EI_i} \\ 0 & 1 & \frac{x_i}{EI_i} & \frac{x_i^2}{2EI_i} \\ 0 & 0 & 1 & x_i \\ 0 & 0 & 0 & 1 \end{bmatrix} \quad (f)$$

x_i is the distance between an arbitrary point and the input of beam i .

There is a k th order eigenvector corresponding to the eigenfrequency ω_k

$$[Y_k(x_1), Y_{1,2}^k, Y^k(x_3), Y_{3,4}^k, Y^k(x_5), Y_{5,6}^k, Y^k(x_7), Y_{7,8}^k, Y^k(x_9), Y_{9,0}^k]^T \quad (g)$$

The computational results of the eigenvectors are shown in Figure 2.20.

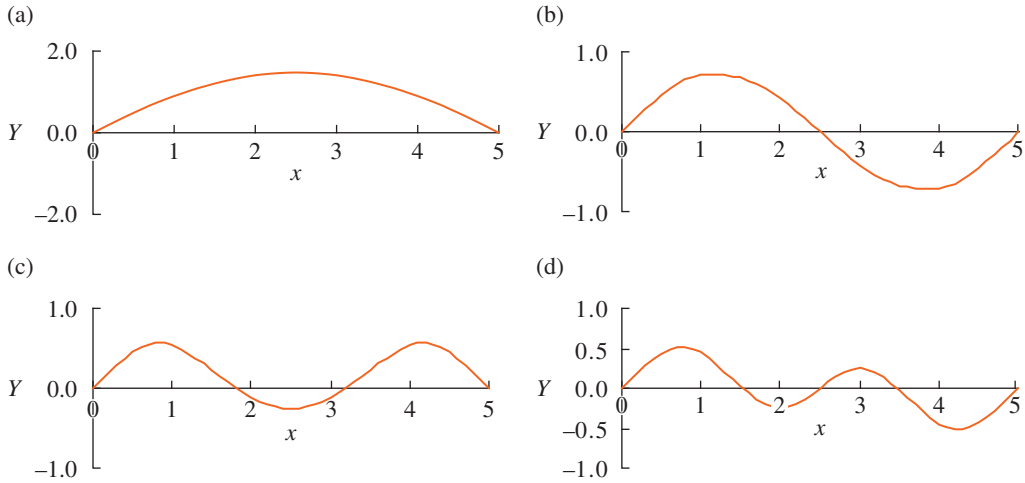


Figure 2.20 The eigenvectors of a simply-simply supported system: (a) first-order eigenvector, (b) second-order eigenvector, (c) third-order eigenvector and (d) fourth-order eigenvector.

Example 2.5 Find the eigenvectors of a free-free beam system corresponding to the eigenfrequencies $\omega_1 = \omega_2 = 0$ shown in Figure 2.13a. The parameters are the same as in Example 2.3.

Solution

According to the boundary conditions and overall transfer equation, we obtain

$$\begin{bmatrix} Y \\ \Theta_z \\ 0 \\ 0 \end{bmatrix}_{9,0} = \begin{bmatrix} u_{11} & u_{12} & u_{13} & u_{14} \\ u_{21} & u_{22} & u_{23} & u_{24} \\ u_{31} & u_{32} & u_{33} & u_{34} \\ u_{41} & u_{42} & u_{43} & u_{44} \end{bmatrix} \begin{bmatrix} Y \\ \Theta_z \\ 0 \\ 0 \end{bmatrix}_{1,0} \quad (a)$$

It can be proved that the overall transfer equation \mathbf{U} is an upper triangular matrix when $\omega_1 = \omega_2 = 0$, the homogeneous equations of which are

$$\begin{bmatrix} 0 \\ 0 \end{bmatrix} = \begin{bmatrix} u_{31} & u_{32} \\ u_{41} & u_{42} \end{bmatrix} \begin{bmatrix} Y \\ \Theta_z \end{bmatrix}_{1,0} = \begin{bmatrix} 0 & 0 \\ 0 & 0 \end{bmatrix} \begin{bmatrix} Y \\ \Theta_z \end{bmatrix}_{1,0} \quad (b)$$

Therefore, $\mathbf{Z}'_{1,0} = [Y, \Theta_z]_{1,0}^T$ is an arbitrary vector. Let $\mathbf{Z}'_{1,0} = [1, 0]^T$ and $\mathbf{Z}'_{1,0} = [0, 1]^T$ correspond to $\omega_1 = 0$ and $\omega_2 = 0$, respectively. Using a method similar to that in Example 2.4, all the state vectors of the system can be obtained. The computational results of the eigenvectors are shown in Figure 2.21. It can be seen from Figure 2.21 that the eigenvector corresponding to $\omega_1 = 0$ expresses the translation motion of the global system, while the eigenvector corresponding to $\omega_2 = 0$ expresses the rotation of the global system. Both eigenvectors are rigid body motion of the global system as a result of the free-free boundary conditions.

An MRFS has many or even infinite eigenfrequencies. When a system vibrates freely with a certain eigenfrequency, the system appears to have synchronous motion, called *principal vibration*. The vibration shape of the system under the principal vibration is called the *principal mode shape*, or *mode*. A free vibration of the system with initial disturbance can be regarded as a superposition of some principal vibrations. For the generalized coordinates selected, the coordinates of the motion differential equation are mutually independent and are called *principal coordinates*. Using the principal coordinates, the vibration of the MRFS can be regarded as superposition of the vibration of many single DOF systems, and the analysis method is called the *mode superposition method*.

It is well known that the displacement is sufficient to describe the vibration of a lumped mass. It is necessary to describe the vibration of the rigid body utilizing the displacements of an arbitrary point of the rigid body and the angular displacements around the point. The longitudinal

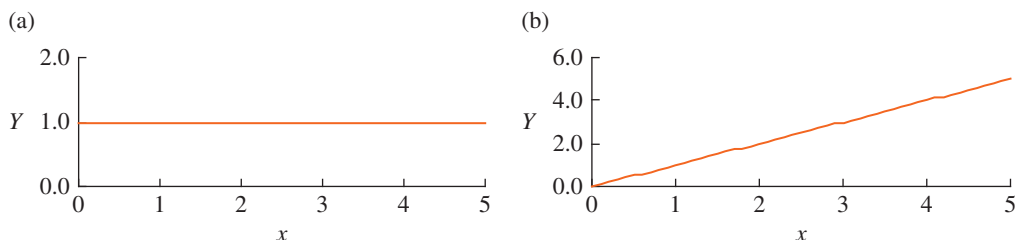


Figure 2.21 The eigenvectors of the free-free beam system corresponding to $\omega_1 = \omega_2 = 0$: (a) first-order eigenvector and (b) second-order eigenvector.

displacement of an arbitrary point from its equilibrium position is adequate to describe the longitudinal vibration of a rod, and the angular displacement of a section from its equilibrium position is adequate to describe the torsional vibration of a shaft. It is necessary to describe the transverse vibration of an Euler–Bernoulli beam using the transverse displacement of an arbitrary point from its equilibrium position. The transverse vibration of a Timoshenko beam can be described using the transverse displacement of an arbitrary point from its equilibrium position and the angular displacement of the arbitrary section from its equilibrium position. The principal mode shape of the system (hereinafter called the mode shape or mode) describes the vibration shape of the system under principal vibration, and it is merely the proportional relation of vibrating displacement of each part in the system. The same mode shape can be expressed in many forms with the difference of an arbitrary nonzero constant factor. When we plot the mode shapes, the rules are as follows:

- 1) When a system is vibrating in only one direction, for example the spring-mass system with longitudinal vibration, the rotation shaft with torsional vibration and the beam with transverse vibration, the sequence number i of the discrete body elements or the physical coordinate x of the continuous body elements is expressed by the x axis and the motion of the system is expressed by the y axis.
- 2) For a planar motion system, the motion state of the system is described in the planar coordinate system OXY , and the axes of abscissa and ordinate express the physics coordinates and motion state separately, by using the solid line to express the stationary state of the system and dashed lines to express the vibration mode. If the information cannot be fully expressed by the two statutes above, it needs to be expressed with a thin dashed line and explained by text notes. For example, when the transverse vibration mode of a Timoshenko beam is portrayed, the thin solid line expresses the transverse displacement of an arbitrary point from its equilibrium position, and the thin dashed line expresses the angular displacement of any section from its equilibrium position.
- 3) For a spatial motion system, the motion state of the system is described by three planar coordinate systems OXY , OYZ and OZX . The illustration principle of each coordinate system is the same as in (2).

2.6 Vibration Characteristics of Multibody Systems

2.6.1 Vibration Characteristics of Discrete Systems

Example 2.6 Find the vibration characteristics of a MS composed of four rigid bodies, four springs and four torsional springs, as shown in Figure 2.22, using the following data:

$$m_2 = m_4 = m_6 = m_8 = 1\text{kg}, \quad l_2 = l_4 = l_6 = l_8 = 0.1\text{m}, \quad K_{x,1} = K_{x,3} = K_{x,5} = K_{x,7} = 1\text{kN/m},$$

$$K_{y,1} = K_{y,3} = K_{y,5} = K_{y,7} = 50\text{kN/m}, \quad K'_{z,1} = K'_{z,3} = K'_{z,5} = K'_{z,7} = 4\text{kN}\cdot\text{m/rad}$$

The rigid bodies vibrate longitudinally in the direction of the x axis, vibrate transversely in the direction of the y axis and rotate about the z axis with small amplitudes.

Solution

According to the numbers of the elements shown in Figure 2.22, the state vectors of the connection points are defined as $Z_{1,0}$, $Z_{2,1}$, $Z_{2,3}$, $Z_{4,3}$, $Z_{4,5}$, $Z_{6,5}$, $Z_{6,7}$, $Z_{8,7}$ and $Z_{8,0}$, and the form of each vector is $Z = [X, Y, \theta_z, M_z, Q_x, Q_y]^T$.

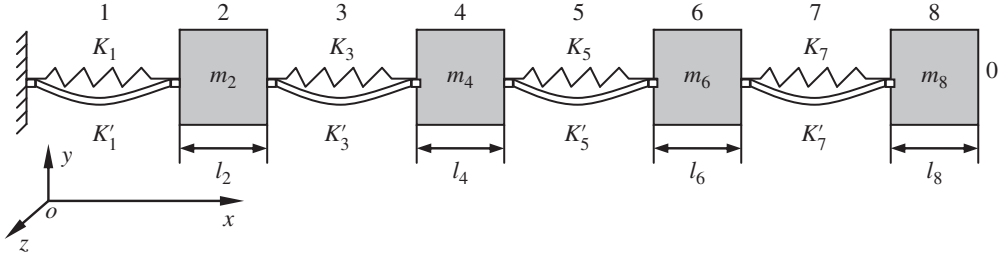


Figure 2.22 Chain discrete system.

The transfer matrices of each element are developed. The elements 1, 3, 5 and 7 are planar elastic hinges that are composed of two springs in both directions and a torsional spring in a single direction connected in parallel. According to Equation (10.39) this yields the transfer matrix

$$\mathbf{U}_i = \begin{bmatrix} \mathbf{I}_3 & \mathbf{U}_{1,2} \\ \mathbf{O}_{3 \times 3} & \mathbf{I}_3 \end{bmatrix}, \quad \mathbf{U}_{1,2} = \begin{bmatrix} 0 & -\frac{1}{K_{x,i}} & 0 \\ 0 & 0 & -\frac{1}{K_{y,i}} \\ \frac{1}{K'_{z,i}} & 0 & 0 \end{bmatrix} \quad (i = 1, 3, 5, 7) \quad (\text{a})$$

From Equation (10.10) the transfer matrices of rigid bodies 2, 4, 6 and 8 are obtained

$$\mathbf{U}_i = \begin{bmatrix} 1 & 0 & -b_2 & 0 & 0 & 0 \\ 0 & 1 & b_1 & 0 & 0 & 0 \\ 0 & 0 & 1 & 0 & 0 & 0 \\ -m_i\omega^2(b_2 - c_{c2}) & m_i\omega^2(b_1 - c_{c1}) & -\omega^2[J_i - m_i(b_2c_{c2} + b_1c_{c1})] & 1 & -b_2 & b_1 \\ m_i\omega^2 & 0 & -m_i\omega^2c_{c2} & 0 & 1 & 0 \\ 0 & m_i\omega^2 & m_i\omega^2c_{c1} & 0 & 0 & 1 \end{bmatrix} \quad (i = 2, 4, 6, 8) \quad (\text{b})$$

where $b_1 = l_i$, $c_{c1} = \frac{l_i}{2}$, $b_2 = c_{c2} = 0$ and $J_i = \frac{m_i l_i^2}{6} + \frac{m_i l_i^2}{4} = \frac{5}{12} m_i l_i^2$.

The transfer equations of the elements are

$$\begin{cases} \mathbf{Z}_{2,1} = \mathbf{U}_1 \mathbf{Z}_{1,0}, \mathbf{Z}_{2,3} = \mathbf{U}_2 \mathbf{Z}_{2,1}, \mathbf{Z}_{4,3} = \mathbf{U}_3 \mathbf{Z}_{2,3}, \mathbf{Z}_{4,5} = \mathbf{U}_4 \mathbf{Z}_{4,3} \\ \mathbf{Z}_{6,5} = \mathbf{U}_5 \mathbf{Z}_{4,5}, \mathbf{Z}_{6,7} = \mathbf{U}_6 \mathbf{Z}_{6,5}, \mathbf{Z}_{8,7} = \mathbf{U}_7 \mathbf{Z}_{6,7}, \mathbf{Z}_{8,0} = \mathbf{U}_8 \mathbf{Z}_{8,7} \end{cases} \quad (\text{c})$$

The overall transfer equation of the system is

$$\mathbf{Z}_{8,0} = \mathbf{U}_8 \mathbf{U}_7 \mathbf{U}_6 \mathbf{U}_5 \mathbf{U}_4 \mathbf{U}_3 \mathbf{U}_2 \mathbf{U}_1 \mathbf{Z}_{1,0} = \mathbf{U} \mathbf{Z}_{1,0} \quad (\text{d})$$

Substituting the boundary conditions

$$\mathbf{Z}_{1,0} = [0, 0, 0, M_z, Q_x, Q_y]_{1,0}^T, \quad \mathbf{Z}_{8,0} = [X, Y, \theta_z, 0, 0, 0]_{8,0}^T \quad (\text{e})$$

Table 2.3 Computational results of eigenfrequencies

Mode	1	2	3	4	5	6
Eigenfrequencies/(rad/s)	10.98	31.62	48.45	59.43	64.24	196.47
Mode	7	8	9	10	11	12
Eigenfrequencies/(rad/s)	334.78	417.66	727.58	1606.10	2394.15	2916.31

into Equation (d) yields the characteristic equation

$$\Delta = \begin{vmatrix} u_{44} & u_{45} & u_{46} \\ u_{54} & u_{55} & u_{56} \\ u_{64} & u_{65} & u_{66} \end{vmatrix} \quad (f)$$

Solving Equation (f), the eigenfrequencies ω_k ($k = 1, 2, \dots, 12$) can be obtained. The results are presented in Table 2.3. For each ω_k , solve the following equations:

$$\begin{bmatrix} u_{44} & u_{45} & u_{46} \\ u_{54} & u_{55} & u_{56} \\ u_{64} & u_{65} & u_{66} \end{bmatrix} \begin{bmatrix} M_z \\ Q_x \\ Q_y \end{bmatrix}_{1,0} = \begin{bmatrix} 0 \\ 0 \\ 0 \end{bmatrix} \quad (g)$$

From reference [232], the algebraic cofactor of each element in a certain row of the coefficient matrix is regarded as the solution of the corresponding unknown quantity (when the roots are not all zero), that is to say, for equations

$$\mathbf{A}\mathbf{x} = \mathbf{0} \quad (h)$$

where \mathbf{A} is a square matrix with n order and its rank is $n - 1$, the algebraic cofactors of each element in the i th row are not all zero.

A nonzero solution of Equation (h) is

$$\mathbf{x} = \begin{bmatrix} x_1 \\ x_2 \\ \vdots \\ x_n \end{bmatrix} = \begin{bmatrix} A_{i,1} \\ A_{i,2} \\ \vdots \\ A_{i,n} \end{bmatrix} \quad (i)$$

where $A_{i,j}$ ($j = 1, 2, \dots, n$) is the algebraic cofactor of element $a_{i,j}$.

Using the above method, the state vector $\mathbf{Z}_{1,0}$ at the left boundary of the system can be obtained, and all the state vectors are determined from transfer equations of every element. The eigenvectors of the system also can be determined, as shown in Figure 2.23. The computational results show that the first four eigenvectors of the system only show longitudinal vibration, and the latter eight eigenvectors show transversal and torsional vibrations.

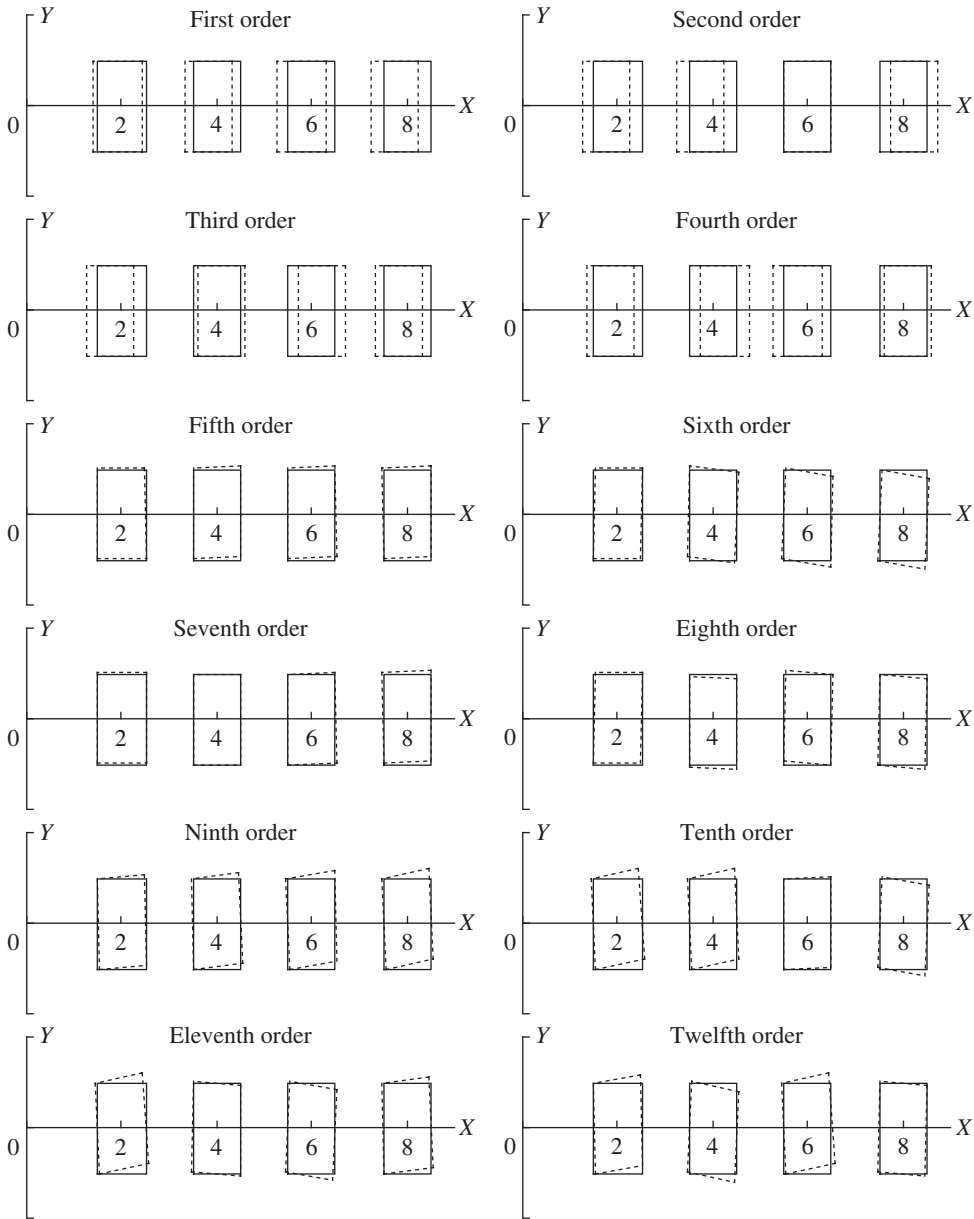


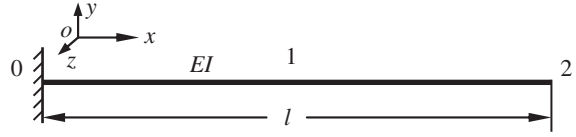
Figure 2.23 Eigenvectors of the discrete system.

2.6.2 Vibration Characteristics of Continuous Systems

Example 2.7 Find the vibration characteristics of the uniform Euler–Bernoulli beam with transverse vibration.

Solution

As shown in Figure 2.24, an Euler–Bernoulli beam with uniform cross-section vibrates transversely in a plane. One end of the beam is fixed and the other is free. The state vectors at

Figure 2.24 Elastic beam with uniform cross-section.

the two ends are $\mathbf{Z}_{1,0}$ and $\mathbf{Z}_{1,2}$, and the state vector at an arbitrary point on the beam is \mathbf{Z}_x in the form of $\mathbf{Z} = [Y, \theta_z, M_z, Q_y]^T$. Equation (10.61) is the transfer matrix of the beam.

The overall transfer equation is

$$\mathbf{Z}_{1,2} = \mathbf{U}_{x=1} \mathbf{Z}_{1,0} = \mathbf{U} \mathbf{Z}_{1,0} \quad (2.51)$$

By substituting the boundary conditions

$$\mathbf{Z}_{1,2} = [Y, \theta_z, 0, 0]^T_{1,2}, \quad \mathbf{Z}_{1,0} = [0, 0, M_z, Q_y]^T_{1,0} \quad (2.52)$$

into Equation (2.51), the characteristic equation will be obtained:

$$\Delta = \begin{vmatrix} u_{33} & u_{34} \\ u_{43} & u_{44} \end{vmatrix} = \begin{vmatrix} S(\lambda l) & \frac{T(\lambda l)}{\lambda} \\ \lambda V(\lambda l) & S(\lambda l) \end{vmatrix} \quad (2.53)$$

that is,

$$\cosh \lambda l \cos \lambda l = -1 \quad (2.54)$$

Solving it, the eigenfrequencies $\omega_k (k=1, 2, \dots)$ and corresponding λ_k are obtained. For each ω_k , let $Q_{x1,0} = 1$, $M_{z1,0} = -\frac{u_{34}}{u_{33}} = -\frac{u_{44}}{u_{43}} = -\frac{T(\lambda_k l)}{\lambda_k S(\lambda_k l)}$ or let $M_{z1,0} = 1$, $Q_{x1,0} = -\frac{u_{43}}{u_{44}} = -\frac{u_{33}}{u_{34}} = -\frac{\lambda_k V(\lambda_k l)}{S(\lambda_k l)}$. The reason for this is that the elements of the determinant in Equation (2.53) may be zeros; sometimes all the elements in a row are zeros. After the state vector $\mathbf{Z}_{1,0}$ at the left boundary of the system is determined, the state vector \mathbf{Z}_x at an arbitrary point on the beam can be obtained from $\mathbf{Z}_x^k = \mathbf{U}_x(\omega_k) \mathbf{Z}_{1,0}^k (0 < x \leq l)$. The eigenvector of the system can be written as

$$Y^k(x) = \frac{S(\lambda_k l) V(\lambda_k x) - T(\lambda_k l) U(\lambda_k x)}{EI \lambda_k^3 S(\lambda_k l)} \quad (2.55)$$

Let the cross-section of the beam be a rectangle with width $b = 0.01\text{m}$ and height $h = 0.01\text{m}$. Let the length $l = 1\text{m}$, the material density $\rho = 7.8 \times 10^3 \text{kg/m}^3$ and the elastic modulus $E = 200 \text{GN/m}^2$. The mass per unit length is $\bar{m} = 0.78 \text{kg/m}$ and the bending stiffness of the beam is $EI = E \cdot b h^3 = 166.67 \text{N} \cdot \text{m}^2$. From $\lambda = \sqrt[4]{\bar{m} \omega^2 / EI}$ and $\cosh(\lambda l) \cos(\lambda l) = -1$, the eigenfrequencies $\omega_k (k=1, 2, \dots)$ can be obtained. The results of the first eight modes are given in Table 2.4, and the corresponding eigenvectors are illustrated in Figure 2.25.

Table 2.4 Computational results of eigenfrequencies

Order	1	2	3	4	5	6	7	8
ω_k (rad/s)	51.40	322.1	901.9	1767.3	2921.5	4364.2	6095.4	8115.2
$\lambda_k l$	1.8751	4.6941	7.8548	10.9955	14.1372	17.2788	20.4204	23.5619

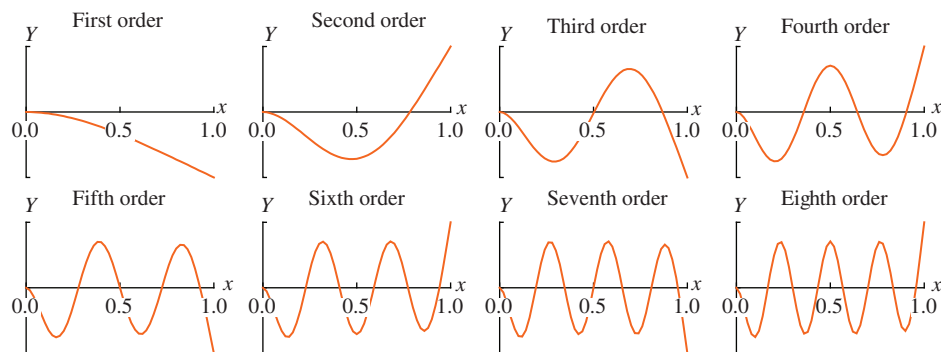


Figure 2.25 Eigenvectors of the continuous system.

Example 2.8 By using the model of the Timoshenko beam and the parameters of Example 2.7, find the eigenfrequencies and the eigenvectors. Let the shear stiffness $GA_s = 6.664 \times 10^6$ N and the radius of gyration of the cross-section with respect to the neutral line $\rho_z = 0.029$ m.

Solution

Substituting these parameters into Equation (10.60), the overall transfer matrix can be obtained. Because the state vectors and boundary conditions are the same as those in Example 2.7, the solution procedure is similar to that in Example 2.7. The computational results of first eight eigenfrequencies $\omega_k (k = 1, 2, \dots)$ and eigenvectors are obtained as shown in Table 2.5 and Figure 2.26, respectively.

Comparing the computational results between Examples 2.7 and 2.8, it is concluded that the vibration characteristics of the Timoshenko beam are almost the same as those of the Euler–Bernoulli beam, and the difference slightly increases at higher frequencies. The computational results obtained in the two situations diverge when increasing the area of the cross-section or decreasing the length of the beam. As a result, when the length/diameter ratio for

Table 2.5 Computational results of eigenfrequencies

Order	1	2	3	4	5	6	7	8
ω_k (rad/s)	51.40	321.9	900.7	1763.1	2910.4	4340.2	6049.5	8035.2

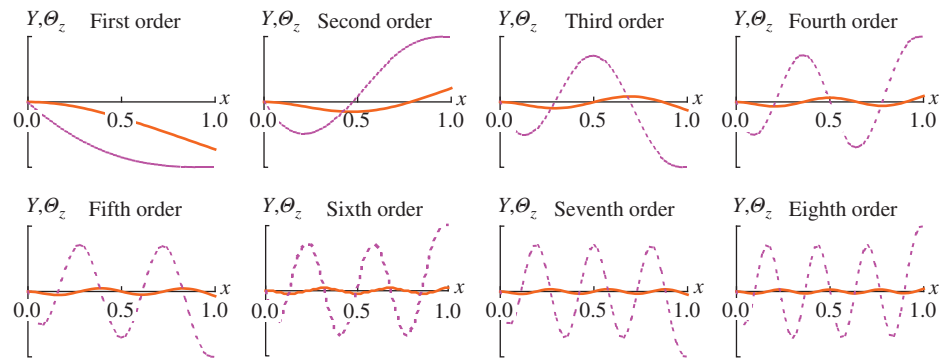



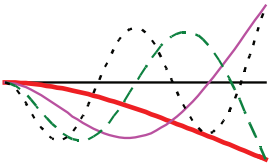

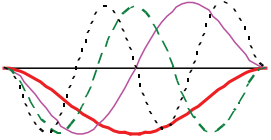
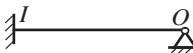
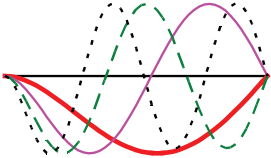

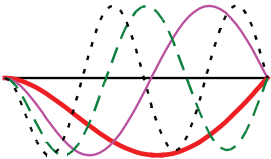

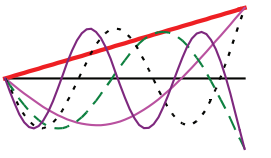
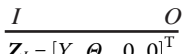
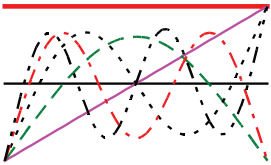
Figure 2.26 Eigenvectors of the Timoshenko beam.

a beam is very large ($L/D > 10$) and the frequencies are not high, the difference between the Euler–Bernoulli beam and the Timoshenko beam is small.

The frequency equations, their roots and the corresponding eigenvectors of the Euler–Bernoulli beam with uniform cross-section are shown in Table 2.6 under several different boundary conditions. The angular displacement of the Euler–Bernoulli beam is just the derivative of the displacement with respect to coordinate x (but it is not so for the Timoshenko beam), therefore Table 2.6 only provides the eigenvectors of displacement.

A straight rod with uniform cross-section and longitudinal vibration has mass per unit length \bar{m} , length l and tensile stiffness EA . The state vectors $\mathbf{Z}_{1,0}$, \mathbf{Z}_{x_1} and $\mathbf{Z}_{1,2}$ are defined in the form of




Table 2.6 Vibration characteristics of a Euler–Bernoulli beam with uniform cross-section

Boundary condition	Frequency equation		$\lambda_k l$	Eigenvector
 $\mathbf{Z}_I = [0, 0, M_z, Q_y]_I^T$ $\mathbf{Z}_O = [Y, \theta_z, 0, 0]_O^T$	$\cosh \lambda l \cos \lambda l = -1$	1	1.8751	
		2	4.6941	
		3	7.8548	
		4	10.9955	
 $\mathbf{Z}_I = [0, 0, M_z, Q_y]_I^T$ $\mathbf{Z}_O = [0, 0, M_z, Q_y]_O^T$	$\cosh \lambda l \cos \lambda l = 1$	1	4.7300	
		2	7.8532	
		3	10.9956	
		4	14.1372	
 $\mathbf{Z}_I = [0, 0, M_z, Q_y]_I^T$ $\mathbf{Z}_O = [0, \theta_z, 0, Q_y]_O^T$	$\sinh \lambda l = 0$	1	3.9266	
		2	7.0686	
		3	10.2102	
		4	13.3518	
 $\mathbf{Z}_I = [0, \theta_z, 0, Q_y]_I^T$ $\mathbf{Z}_O = [0, \theta_z, 0, Q_y]_O^T$	$\tanh \lambda l - \tan \lambda l = 0$	1	3.1416	
		2	6.2832	
		3	9.4248	
		4	12.5664	
 $\mathbf{Z}_I = [0, \theta_z, 0, Q_y]_I^T$ $\mathbf{Z}_O = [Y, \theta_z, 0, 0]_O^T$	$\tanh \lambda l - \tan \lambda l = 0$	1	0	
		2	3.9266	
		3	7.0686	
		4	10.2102	
		5	13.3518	
 $\mathbf{Z}_I = [Y, \theta_z, 0, 0]_I^T$ $\mathbf{Z}_O = [Y, \theta_z, 0, 0]_O^T$	$\cosh \lambda l \cos \lambda l = 1$	1	0	
		2	0	
		3	4.7300	
		4	7.8532	
		5	10.995	
		6	14.1372	

$\mathbf{Z} = [X, Q_x]^T$ and Equation (10.66) is the transfer matrix. The overall transfer equation is $\mathbf{Z}_{1,2} = \mathbf{U}_{x_1=l} \mathbf{Z}_{1,0}$ and the frequency equation can be obtained according to the boundary conditions; consequently, the eigenfrequencies $\omega_k (k = 1, 2, \dots)$ and state vectors at an arbitrary point can be solved. The frequency equations and the roots of the first four eigenvectors and the corresponding functions of the eigenvectors of a straight rod with uniform cross-section are shown in Table 2.7 under various simple boundary conditions.




An elastic shaft with uniform cross-section and torsional vibration has length l , material density ρ , polar moment of inertia of cross-section J_p and torsional stiffness GJ_p . The state vectors $\mathbf{Z}_{1,0}$, \mathbf{Z}_x and $\mathbf{Z}_{1,2}$ are defined as $\mathbf{Z} = [\Theta_x, M_x]^T$ and the transfer matrix is given by Equation (10.46b). The overall transfer equation is $\mathbf{Z}_{1,2} = \mathbf{U}_{x=l} \mathbf{Z}_{1,0}$. The frequency equations and the first four roots as well as corresponding mode functions are shown in Table 2.8 under various simple boundary conditions.

Table 2.7 Vibration characteristics of a straight rod with uniform cross-section

Boundary condition	Frequency equation	$\beta_k l$	Function of eigenvector
 $\mathbf{Z}_I = [0, Q_x]_I^T$ $\mathbf{Z}_O = [0, Q_x]_O^T$	$\frac{\sin \beta l}{\beta} = 0$	$\beta_k l = k\pi$ ($k = 1, 2, \dots$)	$X(x_1) = c_k \sin \beta_k x_1$
 $\mathbf{Z}_I = [0, Q_x]_I^T$ $\mathbf{Z}_O = [X, 0]_O^T$	$\cos \beta l = 0$	$\beta_k l = \left(k - \frac{1}{2}\right)\pi$ ($k = 1, 2, \dots$)	$X(x_1) = c_k \sin \beta_k x_1$
 $\mathbf{Z}_I = [X, 0]_I^T$ $\mathbf{Z}_O = [X, 0]_O^T$	$\beta \sin \beta l = 0$	$\beta_k l = (k-1)\pi$ ($k = 1, 2, \dots$)	$X(x_1) = c_k \cos \beta_k x_1$

Note: c_k is an arbitrary nonzero constant.

Table 2.8 Vibration characteristics of an elastic shaft with uniform cross-section

Boundary condition	Frequency equation	$\gamma_k l$	Function of eigenvector
 $\mathbf{Z}_I = [0, M_x]_I^T$ $\mathbf{Z}_O = [0, M_x]_O^T$	$\frac{\sin \gamma l}{\gamma} = 0$	$\gamma_k l = k\pi$ ($k = 1, 2, \dots$)	$\Theta_x(x) = c_k \sin \gamma_k x$
 $\mathbf{Z}_I = [0, M_x]_I^T$ $\mathbf{Z}_O = [\Theta_x, 0]_O^T$	$\cos \gamma l = 0$	$\gamma_k l = \left(k - \frac{1}{2}\right)\pi$ ($k = 1, 2, \dots$)	$\Theta_x(x) = c_k \sin \gamma_k x$
 $\mathbf{Z}_I = [\Theta_x, 0]_I^T$ $\mathbf{Z}_O = [\Theta_x, 0]_O^T$	$\gamma \sin \gamma l = 0$	$\gamma_k l = (k-1)\pi$ ($k = 1, 2, \dots$)	$\Theta_x(x) = c_k \cos \gamma_k x$

Note: c_k is an arbitrary nonzero constant.

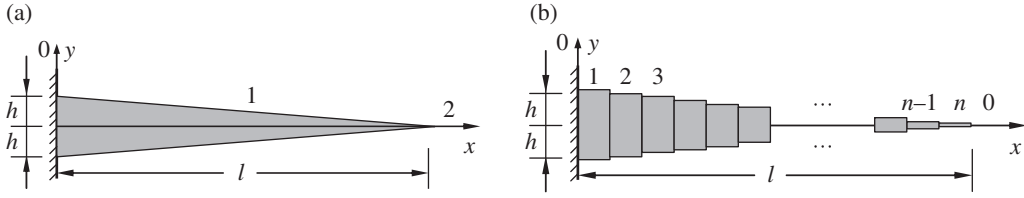


Figure 2.27 Transverse vibration of nonuniform beam.

Example 2.9 Find the eigenfrequencies of the cantilever Euler–Bernoulli beam.

Solution

A nonuniform beam vibrating transversely with one end fixed and the other free is shown in Figure 2.27a. In Figure 2.27b, the nonuniform beam is regarded as a multi-step beam composed of n sections with uniform cross-section and equal length. The problem can be solved by using the transfer matrix of a uniform beam. The state vectors $\mathbf{Z}_{1,0}, \mathbf{Z}_{1,2}, \dots, \mathbf{Z}_{i-1,i}, \dots, \mathbf{Z}_{n,0}$ are defined in the form of $\mathbf{Z} = [Y, \theta_z, M_z, Q_y]^T$. The transfer equation of each beam section is $\mathbf{Z}_{i,i+1} = \mathbf{U}_i \mathbf{Z}_{i-1,i}$ ($i = 1, 2, \dots, n-1$), where \mathbf{U}_i is the transfer matrix of the i th beam section. The overall transfer equation is

$$\mathbf{Z}_{n,0} = \mathbf{U}_n \mathbf{U}_{n-1} \cdots \mathbf{U}_i \cdots \mathbf{U}_2 \mathbf{U}_1 \mathbf{Z}_{1,0} = \mathbf{U} \mathbf{Z}_{1,0} \quad (2.56a)$$

Substituting the boundary conditions

$$\mathbf{Z}_{n,0} = [Y, \theta_z, 0, 0]_{n,0}^T, \quad \mathbf{Z}_{1,0} = [0, 0, M_z, Q_y]_{1,0}^T \quad (2.56b)$$

into the overall transfer equation, the characteristic equation is obtained

$$\Delta = \begin{vmatrix} u_{33} & u_{34} \\ u_{43} & u_{44} \end{vmatrix} = 0 \quad (2.56c)$$

Therefore, the vibration characteristics of the nonuniform beam vibrating transversely can be obtained by the proposed same approach.

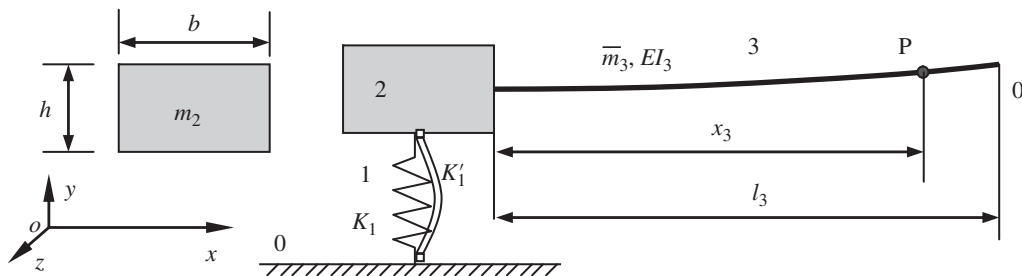
Assume the cross-section of the beam is a rectangle with width $b = 0.01\text{m}$ and root height $2h = 0.02\text{m}$. The length is $l = 1\text{m}$, and the material density of the steel, modulus of elasticity and shear elastic modulus are $\rho = 7.8 \times 10^3 \text{kg/m}^3$, $E = 200 \text{GN/m}^2$ and $G = 80 \text{GN/m}^2$, respectively. The shape factors of the rectangular cross-section are $\kappa_s = 1/0.833$, $n = 100$ and $n = 10$. The computational results of eigenfrequencies for the nonuniform beam are shown in Table 2.9, where the error is a relative error with respect to the results of the Timoshenko beam for $n = 100$.

2.6.3 Vibration Characteristics of a Hybrid System of Rigid and Flexible Bodies

Example 2.10 Find the vibration characteristics of MRFS in Figure 2.28. The MRFS is composed of an elastic hinge, a rigid body and an Euler–Bernoulli beam vibrating in a plane. The displacement of the connection point between the rigid body and the spring in the direction of the x axis is neglected, and the longitudinal displacement of the beam is not considered.

Table 2.9 Computational results of eigenfrequencies for a nonuniform beam

Order	Timoshenko beam			Euler-Bernoulli beam			
	$n = 100$		$n = 10$	$n = 100$		$n = 10$	
	ω_k (rad/s)	ω_k (rad/s)		ω_k (rad/s)	Error (%)	ω_k (rad/s)	Error (%)
1	155.3	150.6	-3.03	155.4	0.06	150.6	-3.03
2	443.8	367.1	-17.28	444.1	0.07	367.3	-17.24
3	873.7	621.4	-28.88	874.6	0.10	621.8	-28.83
4	1440.9	1120.3	-22.25	1443.1	0.15	1121.8	-22.15
5	2134.4	1873.3	-12.23	2138.9	0.21	1877.6	-12.03
6	2928.5	2831.6	-3.31	2936.1	0.26	2840.2	-3.02
7	3779.9	3682.2	-2.58	3791.3	0.30	3692.4	-2.31
8	4696.3	4728.8	0.69	4713.7	0.37	4754.5	1.24

**Figure 2.28** A multi-rigid-flexible-body system.

The stiffness of the spring is K_1 and the torsional stiffness of the connection point is K'_1 . The mass of the rigid body m_2 is distributed uniformly. The width is b and the height is h . The bending stiffness, length and the mass per unit length of the beam are EI_3 , l_3 and \bar{m}_3 , respectively.

Solution

Define the connection point between the spring and the ground as the input end of the system, and the free end of the beam as the output end of system. From input end to output end, each element is numbered in sequence along the transfer direction. The ground, planar elastic hinge, rigid body and the beam with the free end are numbered 0, 1, 2, 3 and 0, respectively. The state vectors $\mathbf{Z}_{1,0}, \mathbf{Z}_{2,1}, \mathbf{Z}_{2,3}, \mathbf{Z}_{x_3} (0 < x_3 < l_3), \mathbf{Z}_{3,0}$ are defined as $\mathbf{Z} = [X, Y, \theta_z, M_z, Q_x, Q_y]^T$. The transfer matrices of each element are expressed as follows:

$$\mathbf{U}_1 = \begin{bmatrix} \mathbf{I}_3 & \mathbf{U}_{1,2} \\ \mathbf{O}_{3 \times 3} & \mathbf{I}_3 \end{bmatrix}, \quad \mathbf{U}_{1,2} = \begin{bmatrix} 0 & 0 & 0 \\ 0 & 0 & -1/K_1 \\ 1/K'_1 & 0 & 0 \end{bmatrix} \quad (2.57)$$

$$\mathbf{U}_2 = \begin{bmatrix} 1 & 0 & -b_2 & 0 & 0 & 0 \\ 0 & 1 & b_1 & 0 & 0 & 0 \\ 0 & 0 & 1 & 0 & 0 & 0 \\ -m_2\omega^2(b_2 - c_{c2}) & m_2\omega^2(b_1 - c_{c1}) & -\omega^2[J_2 - m_2(b_2c_{c2} + b_1c_{c1})] & 1 & -b_2 & b_1 \\ m_2\omega^2 & 0 & -m_2\omega^2c_{c2} & 0 & 1 & 0 \\ 0 & m_2\omega^2 & m_2\omega^2c_{c1} & 0 & 0 & 1 \end{bmatrix} \quad (2.58)$$

$$\mathbf{U}_3 = \begin{bmatrix} 1 & 0 & 0 & 0 & 0 & 0 \\ 0 & S(\lambda x_3) & \frac{T(\lambda x_3)}{\lambda} & \frac{U(\lambda x_3)}{EI_3\lambda^2} & 0 & \frac{V(\lambda x_3)}{EI_3\lambda^3} \\ 0 & \lambda V(\lambda x_3) & S(\lambda x_3) & \frac{T(\lambda x_3)}{EI_3\lambda} & 0 & \frac{U(\lambda x_3)}{EI_3\lambda^2} \\ 0 & EI_3\lambda^2 U(\lambda x_3) & EI_3\lambda V(\lambda x_3) & S(\lambda x_3) & 0 & \frac{T(\lambda x_3)}{\lambda} \\ \bar{m}_3\omega^2 x_3 & 0 & 0 & 0 & 1 & 0 \\ 0 & EI_3\lambda^3 T(\lambda x_3) & EI_3\lambda^2 U(\lambda x_3) & \lambda V(\lambda x_3) & 0 & S(\lambda x_3) \end{bmatrix}_{x_3=l_3} \quad (2.59)$$

where

$$b_1 = \frac{b}{2}, b_2 = \frac{h}{2}, c_{c1} = 0, c_{c2} = \frac{h}{2}, J_2 = \frac{m_2(b^2 + h^2)}{12} + \frac{m_2 h^2}{4} = m_2 \frac{b^2 + 4h^2}{12}, \lambda = \sqrt[4]{\bar{m}_3\omega^2/(EI_3)}$$

The overall transfer equation is

$$\mathbf{Z}_{3,0} = \mathbf{U}_3 \mathbf{U}_2 \mathbf{U}_1 \mathbf{Z}_{1,0} = \mathbf{U} \mathbf{Z}_{1,0} \quad (2.60)$$

Substituting the boundary conditions

$$\mathbf{Z}_{3,0} = [X, Y, \theta_z, 0, 0, 0]_{3,0}^T, \mathbf{Z}_{1,0} = [0, 0, 0, M_z, Q_x, Q_y]_{1,0}^T \quad (2.61)$$

into Equation (2.60) results in the characteristic equation

$$\Delta = \begin{vmatrix} u_{44} & u_{45} & u_{46} \\ u_{54} & u_{55} & u_{56} \\ u_{64} & u_{65} & u_{66} \end{vmatrix} = 0 \quad (2.62)$$

from which the eigenfrequencies $\omega_k (k = 1, 2, \dots)$ can be obtained. For each ω_k , the state vector $\mathbf{Z}_{1,0}$ at the input end of the system can be determined by solving the equations

$$\begin{bmatrix} u_{44} & u_{45} & u_{46} \\ u_{54} & u_{55} & u_{56} \\ u_{64} & u_{65} & u_{66} \end{bmatrix} \begin{bmatrix} M_z \\ Q_x \\ Q_y \end{bmatrix}_{1,0} = 0 \quad (2.63)$$

The state vector at an arbitrary point and the eigenvectors of the system can be obtained by using the transfer equations $\mathbf{Z}_{2,1} = \mathbf{U}_1 \mathbf{Z}_{1,0}$, $\mathbf{Z}_{2,3} = \mathbf{U}_2 \mathbf{Z}_{2,1}$ and $\mathbf{Z}_{x_3} = \mathbf{U}_{x_3} \mathbf{Z}_{2,3} (0 < x_3 \leq l_3)$.

If $K_1 = 1 \text{ kN/m}$, $K'_1 = 0.15 \text{ kN}\cdot\text{m/rad}$, $m_2 = 7.8 \text{ kg}$, $b = 0.1 \text{ m}$, $h = 0.1 \text{ m}$, $EI_3 = 166.67 \text{ N}\cdot\text{m}^2$, $l_3 = 1 \text{ m}$ and $\bar{m}_3 = 0.78 \text{ kg/m}$, by substituting these parameters into Equations (2.59)–(2.63),

Table 2.10 Computational results of eigenfrequencies

Order	1	2	3	4	5	6	7	8	9	10
ω_k (rad/s)	10.7	20.7	143.7	372.0	925.7	1783.3	2934.0	4374.8	6104.8	8123.8

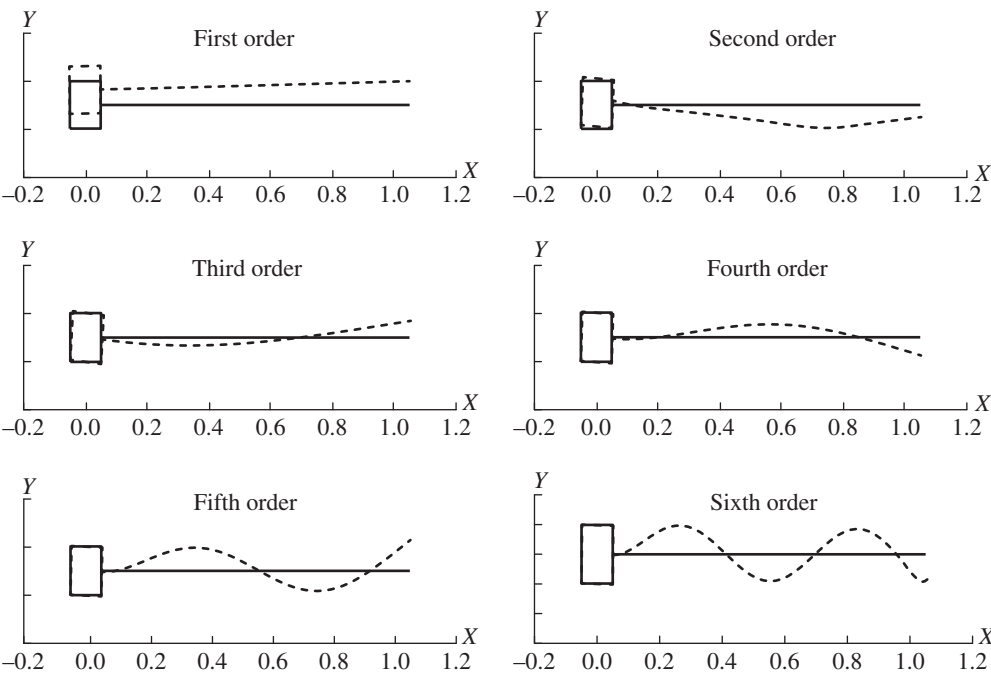


Figure 2.29 Eigenvectors of the hybrid system of rigid and flexible Bodies.

the vibration characteristics of the system can be determined. The first ten eigenfrequencies are presented in Table 2.10, and the first six eigenvectors are illustrated in Figure 2.29. The first mode represents the transverse vibration and torsional vibration of rigid body 2 with beam 3, while the second mode is the torsional vibration of rigid body 2 with beam 3. The higher modes are associated with transverse vibration of beam 3.

Discussion

- 1) If the system only includes element 1 and element 2, the eigenfrequencies should be $\omega_1 = \sqrt{K_1/m_2} = 11.3$ rad/s and $\omega_2 = \sqrt{K'_1/J_2} = 67.9$ rad/s. However, the first two eigenfrequencies are $\omega_1 = 10.7$ rad/s and $\omega_2 = 20.7$ rad/s, respectively. The reason is that the mass of element 3 increases the total mass and the total moment of inertia of the system, which results in a decrease in the basic frequencies.
- 2) The computational results of the eigenfrequencies of a cantilever beam are shown in the second row of Table 2.11. Compared with Table 2.10, the eigenfrequencies of the higher modes are closer to those of the cantilever beam. Let the mass of rigid body 2 be $m_2 = 7800$ kg. The computational results are shown in the third row of Table 2.11. Compared with the cantilever beam, the mass of rigid body 2 is much larger and the higher-order eigenfrequencies can be

Table 2.11 Eigenfrequencies comparison for $m_2 \rightarrow \infty$ and cantilever beam (rad/s)

Order	1	2	3	4	5	6	7	8	9	10
Cantilever beam	–	–	51.40	322.1	901.9	1767.3	2921.5	4364.2	6095.4	8115.2
$m_2 = 7800 \text{ kg}$	0.3580	2.138	51.63	322.1	901.9	1767.3	2921.5	4364.2	6095.5	8115.3

Table 2.12 Computational results of eigenfrequencies when $K'_1 \rightarrow \infty$ (rad/s)

Order	1	2	3	4	5	6	7	8	9
$K'_1 \rightarrow \infty$	10.78	52.96	325.1	904.8	1770.2	2924.4	4367.1	6098.4	8118.2

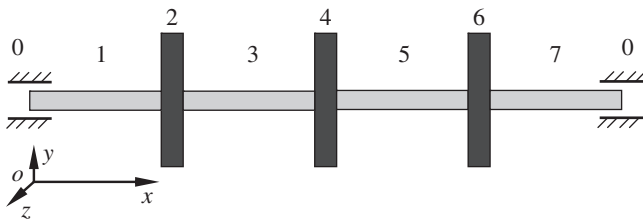
substituted by the eigenfrequencies of the cantilever beam. The lower-order eigenfrequencies of the system can be substituted by $\omega_1 = \sqrt{K'_1/m_2} = 0.358 \text{ rad/s}$ and $\omega_2 = \sqrt{K'_1/J_2} = 2.148 \text{ rad/s}$.

- 3) If $K'_1 \rightarrow \infty$ in the system, the rigid body and beam can only vibrate vertically but cannot move horizontally. The eigenfrequencies are shown in Table 2.12. It is obvious that the eigenfrequencies are closer to that of the cantilever beam along with the increasing order of the mode.

Example 2.11 As shown in Figure 2.30, a torsional vibration system composed of four shafts and three disks can rotate around the x axis, and its two ends are free. Let the length of the four shafts be $l_1 = 1.2\text{m}$, $l_3 = 0.6\text{m}$, $l_5 = 0.5\text{m}$ and $l_7 = 1.0\text{m}$, respectively, and the radius of the cross-sections are $r_1 = r_7 = 0.01\text{m}$ and $r_3 = r_5 = 0.02\text{m}$, respectively. The moments of inertia of the three disks are $J_2 = J_6 = 0.312\text{kg}\cdot\text{m}^2$ and $J_4 = 0.936\text{kg}\cdot\text{m}^2$, respectively. The shafts' density is $\rho = 7.8 \times 10^3\text{kg/m}^3$, and their shear elastic modulus is $G = 80\text{GN/m}^2$. Find (1) the vibration characteristics of the system and (2) the eigenfrequencies of the system when the mass of the shafts is not considered.

Solution

- 1) The sequence number of the system is shown in Figure 2.30. The state vectors $\mathbf{Z}_{1,0}, \mathbf{Z}_{2,1}, \mathbf{Z}_{2,3}, \mathbf{Z}_{4,3}, \mathbf{Z}_{4,5}, \mathbf{Z}_{6,5}, \mathbf{Z}_{6,7}, \mathbf{Z}_{7,0}$ and \mathbf{Z}_{x_i} ($0 < x_i \leq l_i, i = 1, 3, 5, 7$) are defined in the form of $\mathbf{Z} = [\Theta_x, M_x]^T$. The transfer matrices of the elements are

**Figure 2.30** A torsional vibration system.

$$\mathbf{U}_{x_i} = \begin{bmatrix} \cos \gamma_i x_i & \frac{1}{\gamma_i (GJ_p)_i} \sin \gamma_i x_i \\ -\gamma_i (GJ_p)_i \sin \gamma_i x_i & \cos \gamma_i x_i \end{bmatrix} \quad (i = 1, 3, 5, 7) \quad (\text{a})$$

$$\mathbf{U}_i = \begin{bmatrix} 1 & 0 \\ -J_i \omega^2 & 1 \end{bmatrix} \quad (i = 2, 4, 6) \quad (\text{b})$$

where $\gamma_i = \sqrt{(\rho J_p)_i \omega^2 / (GJ_p)_i} = \sqrt{\rho_i \omega^2 / G_i}$

The overall transfer equation is

$$\mathbf{Z}_{7,0} = \mathbf{U}_7 \mathbf{U}_6 \mathbf{U}_5 \mathbf{U}_4 \mathbf{U}_3 \mathbf{U}_2 \mathbf{U}_1 \mathbf{Z}_{1,0} = \mathbf{U} \mathbf{Z}_{1,0} \quad (\text{c})$$

Substituting the boundary condition

$$\mathbf{Z}_{7,0} = [\Theta_x, 0]^T_{7,0}, \quad \mathbf{Z}_{1,0} = [\Theta_x, 0]^T_{1,0} \quad (\text{d})$$

into Equation (c), the characteristic equation is obtained:

$$\Delta = u_{21} = 0 \quad (\text{e})$$

The first eight eigenfrequencies are computed in Table 2.13 and the first four eigenvectors are shown in Figure 2.31.

- 2) When the mass of shafts is not considered, that is, $\rho_i \rightarrow 0$ or $\gamma_i \rightarrow 0$ ($i = 1, 3, 5, 7$), the transfer matrix is

$$\mathbf{U}_i = \begin{bmatrix} 1 & \frac{l_i}{(GJ_p)_i} \\ 0 & 1 \end{bmatrix} \quad (i = 1, 3, 5, 7)$$

The computational process is the same as (1), and the results are shown in Table 2.14.

Table 2.13 Computational results of eigenfrequencies

Order	1	2	3	4	5	6	7	8
ω_k (rad/s)	0	340.0	446.2	4192.9	5031.4	12576.7	15092.0	16777.1

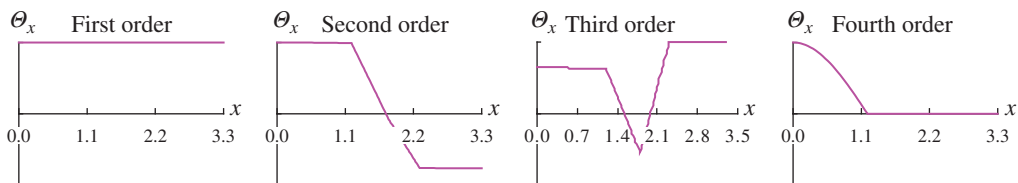


Figure 2.31 Eigenvectors of the torsional vibration system.

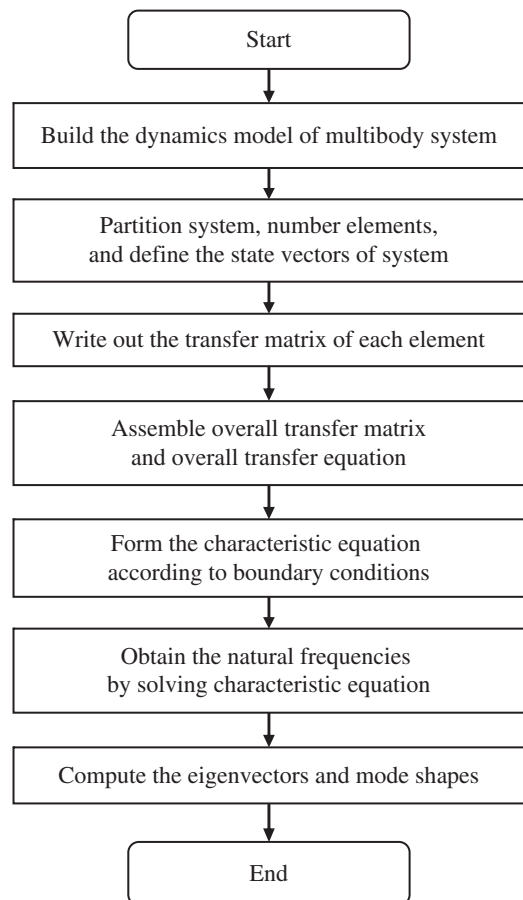
Table 2.14 Computational results of eigenfrequencies without considering the mass of the shaft

Order	1	2	3
ω_k (rad/s)	0	340.3	446.4

2.6.4 Procedure to Compute the Vibration Characteristics of a Multibody System

A general procedure to compute the vibration characteristics of MRFS is shown in Figure 2.32. The detailed procedures are as follows.

- 1) Develop the dynamics model of the MRFS. Break up the whole MRFS into various elements. Define the state vectors of each element.
- 2) The transfer matrices of each element are written according to the dynamics equations of each element, the transfer direction and the connection styles with other elements.
- 3) According to the topology of the system, the overall transfer equation and the overall transfer matrix are deduced automatically. For chain systems, the overall transfer matrix can be obtained only by successively multiplying the transfer matrices of the elements. The

Figure 2.32 Procedure to compute the vibration characteristics of the MRFS.

unknown variables in the overall transfer equation are the state vectors at the boundary points of the system, and the elements of the overall transfer matrix are functions of the structural parameters and eigenfrequencies of the system.

- 4) Construct the characteristic equation by substituting the boundary conditions into the overall transfer equation.
- 5) The eigenfrequencies $\omega_k (k = 1, 2, \dots)$ of the system are determined by solving the characteristic equation.
- 6) For each eigenfrequency ω_k , the state vectors at the boundary points can be evaluated by solving the overall transfer equation. The state vectors and eigenvectors of each point in the system can be obtained by using the transfer equations of each element.

2.7 Eigenvalues of Damped Vibration

2.7.1 Damping Model

2.7.1.1 Viscous Damping

A spring-damper system is shown in Figure 2.33. The spring coefficient and the viscous damping coefficient are K and C , respectively, and the spring and damping force $P(t)$ is expressed by

$$P(t) = Kx + C\dot{x} \quad (2.64)$$

where x is the elongation (deformation) and \dot{x} is the motion speed.

When the system vibrates harmonically with $x = A \cos \Omega t$, frequency Ω and amplitude A , the energy dissipated per cycle is

$$\int_0^{2\pi/\Omega} P(t)\dot{x}dt = \pi A^2 C \Omega \quad (2.65)$$

Obviously, the energy dissipated per cycle is proportional to the exciting frequency Ω .

2.7.1.2 Structural Damping

The damping coefficient may vary with the exciting frequency Ω as

$$C(\Omega) = K \frac{g}{\Omega} \quad (2.66)$$

This kind of damping is called structural damping, where K is the spring coefficient and g is a constant between 0.005 and 0.015. The damping coefficient of an aircraft structure behaves in this way. It has been proved by Veubeke [233] that this kind of damping is nonexistent in physics. The relationship between force and displacement for this kind of damping is

$$P(t) = Kx(t) + \frac{Kg}{\pi} \int_{-\infty}^{+\infty} x(\tau) \frac{1}{\tau - t} d\tau \quad (2.67)$$

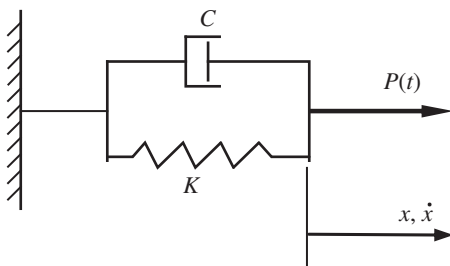


Figure 2.33 Spring-damper system.

The current damping force of the structure damping satisfying Equation (2.66) depends on the behavior of the displacement x in the past, present and future. Obviously, such a physical phenomenon does not exist. However, the concept of structural damping is acceptable if the frequency is confined to a certain range. When the spring-damper system undergoes harmonic vibration,

$$x = A \cos \Omega t \quad (2.68)$$

According to Equations (2.64) and (2.66), we obtain

$$P(t) = A(K \cos \Omega t - Kg \sin \Omega t) \quad (2.69)$$

Then, the energy dissipated per cycle

$$\int_0^{2\pi/\Omega} P(t) \dot{x} dt = \pi A^2 Kg \quad (2.70)$$

is a constant independent of the frequency Ω .

2.7.1.3 Complex Impedance

Rewrite Equation (2.68) as

$$x = \text{Re}(Ae^{i\Omega t}) \quad (2.71)$$

where Re represents the real part of the complex expression in the parentheses.

Substituting Equation (2.71) into Equation (2.64) yields

$$P(t) = \text{Re}[(K + iC\Omega)Ae^{i\Omega t}] \quad (2.72)$$

Analogous to a typical expression in the electric theory

$$\bar{z}(\Omega) = K + iC\Omega \quad (2.73)$$

is called the complex impedance of viscous damping. Similarly, the complex impedance for structure damping is

$$\bar{z}(\Omega) = K(1 + ig) \quad (2.74)$$

The concepts of complex shear modulus and complex Young's modulus can be developed from Equation (2.74). If Poisson's ratio is still a real number, we have

$$\bar{G} = G(1 + ig) \quad (2.75)$$

$$\bar{E} = E(1 + ig) \quad (2.76)$$

In Equations (2.74) and (2.76), G is the shear modulus, E is Young's modulus and $g = 0.005\text{--}0.010$ for a welded structure.

2.7.2 Free Vibration of a Damped System

2.7.2.1 Damped Spring-Mass System

The equation of free vibration for a damped spring-mass system, as shown in Figure 2.34, is

$$m\ddot{x} + C\dot{x} + Kx = 0 \quad (2.77)$$

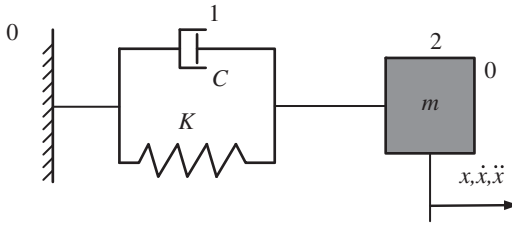


Figure 2.34 Damped spring-mass system.

Its solution has the form

$$x(t) = e^{-\lambda^r t} (A \cos \lambda^i t + B \sin \lambda^i t) \quad (2.78)$$

where the damping rate λ^r and the eigenfrequency λ^i are determined by Equation (2.77), and the constants A and B are determined by the initial conditions x_0 and \dot{x}_0 .

To determine λ^r and λ^i , Equation (2.78) is differentiated twice with respect to time, yielding

$$\dot{x}(t) = e^{-\lambda^r t} [(-A\lambda^r + B\lambda^i) \cos \lambda^i t + (-B\lambda^r - A\lambda^i) \sin \lambda^i t] \quad (2.79)$$

$$\ddot{x}(t) = e^{-\lambda^r t} \left\{ \left[A(\lambda^{r^2} - \lambda^{i^2}) - 2B\lambda^i \lambda^r \right] \cos \lambda^i t + \left[B(\lambda^{r^2} - \lambda^{i^2}) + 2A\lambda^i \lambda^r \right] \sin \lambda^i t \right\} \quad (2.80)$$

Substituting Equations (2.78), (2.79) and (2.80) into Equation (2.77) yields

$$e^{-\lambda^r t} \left\{ \left[m(\lambda^{r^2} - \lambda^{i^2})A - 2m\lambda^i \lambda^r B - C\lambda^r A + C\lambda^i B + KA \right] \cos \lambda^i t + \left[m(\lambda^{r^2} - \lambda^{i^2})B + 2m\lambda^i \lambda^r A - C\lambda^r B - C\lambda^i A + KB \right] \sin \lambda^i t \right\} = 0 \quad (2.81)$$

Equation (2.81) holds true regardless of initial conditions, so

$$\begin{cases} m(\lambda^{r^2} - \lambda^{i^2}) - C\lambda^r + K = 0 \\ 2m\lambda^i \lambda^r - C\lambda^i = 0 \end{cases} \quad (2.82)$$

that is,

$$\begin{cases} \lambda^r = \frac{C}{2m} \\ \lambda^{i^2} = \frac{K}{m} - \left(\frac{C}{2m} \right)^2 = \omega^2 - \lambda^{r^2} \end{cases} \quad (2.83)$$

where $\omega = \sqrt{K/m}$ is the eigenfrequency corresponding to the undamped system.

Applying the initial conditions $x(t)|_{t=0} = x_0$, $\dot{x}(t)|_{t=0} = \dot{x}_0$, the expressions for the constants A and B are

$$\begin{cases} A = x_0 \\ B = \frac{\dot{x}_0 + \lambda^r x_0}{\lambda^i} \end{cases} \quad (2.84)$$

Only when λ^i is real, that is, when $\lambda^{i^2} = \omega^2 - \lambda^{r^2}$ is positive, can the solution of Equation (2.77) exist, namely Equation (2.78) is valid. This means $\frac{K}{m} - \left(\frac{C}{2m} \right)^2 > 0$, namely $C < 2\sqrt{mK}$. The system where the damping coefficient C is less than $2\sqrt{mK}$ is called a light damped system. Most structures and mechanics systems may be regarded as light damped systems.

2.7.2.2 Complex Solution of Vibration

Let

$$x = \text{Re}(\bar{X}e^{\lambda t}) \quad (2.85)$$

where \bar{X} is a complex amplitude and λ is a complex eigenvalue with dimension $1/s$.

Substituting Equation (2.85) into Equation (2.77) yields the characteristic equation of the system

$$m\lambda^2 + C\lambda + K = 0 \quad (2.86)$$

The complex eigenvalue can also be obtained:

$$\lambda_{1,2} = -\frac{C}{2m} \pm i\sqrt{\frac{K}{m} - \left(\frac{C}{2m}\right)^2} = -\lambda^r + i\lambda^i \quad (2.87)$$

Under the light damped situation ($C < 2\sqrt{mK}$), this result coincides with Equation (2.83). Therefore, the solution of Equation (2.77) is

$$x(t) = \bar{X}_1 e^{\lambda_1 t} + \bar{X}_2 e^{\lambda_2 t}$$

According to the Eulerian formula $e^{\lambda_{1,2}t} = e^{-\lambda^r t \pm i\lambda^i t} = e^{-\lambda^r t}(\cos\lambda^i t \pm i\sin\lambda^i t)$, the solution of Equation (2.77) can be written as

$$x(t) = e^{-\lambda^r t} [(\bar{X}_1 + \bar{X}_2)\cos\lambda^i t + i(\bar{X}_1 - \bar{X}_2)\sin\lambda^i t] \quad (2.88)$$

Because the right-hand side of Equation (2.88) must be real, \bar{X}_1 and \bar{X}_2 must be conjugate complex numbers. Let $\bar{X}_{1,2} = (A \mp iB)/2$, then Equation (2.88) is reduced to Equation (2.78). Using the complex form, the expression of $\lambda = -\lambda^r + i\lambda^i$ can be easily obtained for common cases (not confined to light damped systems). The complex amplitude of a physics quantity under modal coordinates is denoted by a capital with a bar over it.

2.7.3 Transfer Matrix Method for Free Vibration of Damped Multibody Systems

2.7.3.1 Complex Transfer Matrix

The forces of both ends of the spring-damper system are equal, as shown in Figure 2.35, yielding

$$q_{x,O_C} = q_{x,I_C} = -C_i(\dot{x}_{i+1,i} - \dot{x}_{i-1,i}) \quad (2.89)$$

The complex amplitudes of the forces are

$$\bar{Q}_{x,O_C} = \bar{Q}_{x,I_C} = -C_i\lambda(\bar{X}_{i+1,i} - \bar{X}_{i-1,i}) \quad (2.90)$$

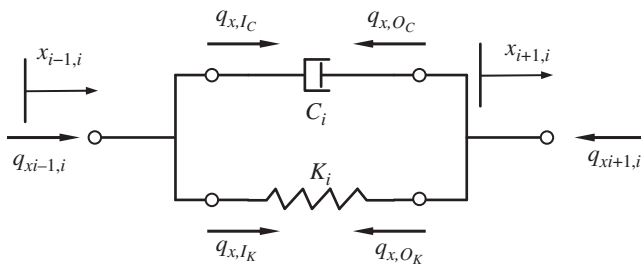


Figure 2.35 Free-body diagram of a spring-damper system.

The complex elastic force is

$$\bar{Q}_{x,O_K} = \bar{Q}_{x,I_K} = -K_i(\bar{X}_{i+1,i} - \bar{X}_{i-1,i}) \quad (2.91)$$

The complex internal forces at the two ends of the spring-damper system are

$$\bar{Q}_{xi+1,i} = \bar{Q}_{xi-1,i} = \bar{Q}_{x,I_C} + \bar{Q}_{x,I_K} = -(K_i + C_i\lambda)(\bar{X}_{i+1,i} - \bar{X}_{i-1,i})$$

hence

$$\bar{X}_{i+1,i} = \bar{X}_{i-1,i} - \frac{1}{K_i + C_i\lambda} \bar{Q}_{xi-1,i}$$

The complex transfer equation is

$$\bar{\mathbf{Z}}_{i+1,i} = \bar{\mathbf{U}}_i \bar{\mathbf{Z}}_{i-1,i} \quad (2.92a)$$

where

$$\bar{\mathbf{Z}} = \begin{bmatrix} \bar{X} \\ \bar{Q}_x \end{bmatrix}, \quad \bar{\mathbf{U}}_i = \begin{bmatrix} 1 & -\frac{1}{K_i + C_i\lambda} \\ 0 & 1 \end{bmatrix} \quad (2.92b)$$

$\bar{\mathbf{U}}_i$ is the complex transfer matrix of the spring-damper.

For a lumped mass in a damped system, as shown in Figure 2.36, the relationship of displacements and forces between the two ends is

$$\begin{cases} \bar{X}_{i,i+1} = \bar{X}_{i,i-1} \\ \bar{Q}_{xi,i+1} = \bar{Q}_{xi,i-1} - m_i\lambda^2 \bar{X}_{i,i-1} \end{cases}$$

or

$$\bar{\mathbf{Z}}_{i,i+1} = \bar{\mathbf{U}}_i \bar{\mathbf{Z}}_{i,i-1} \quad (2.93a)$$

where

$$\bar{\mathbf{Z}} = \begin{bmatrix} \bar{X} \\ \bar{Q}_x \end{bmatrix}, \quad \bar{\mathbf{U}}_i = \begin{bmatrix} 1 & 0 \\ -m_i\lambda^2 & 1 \end{bmatrix} \quad (2.93b)$$

$\bar{\mathbf{U}}_i$ is the complex transfer matrix of the lumped mass.

2.7.3.2 Real and Imaginary Parts of the Complex Transfer Matrix

The complex state vectors and the complex transfer matrix can be split into real and imaginary parts and identified using the superscripts “ r ” and “ i ”, respectively. Then

$$\begin{cases} \bar{\mathbf{Z}} = \mathbf{Z}^r + i\mathbf{Z}^i \\ \bar{\mathbf{U}} = \mathbf{U}^r + i\mathbf{U}^i \end{cases} \quad (2.94)$$

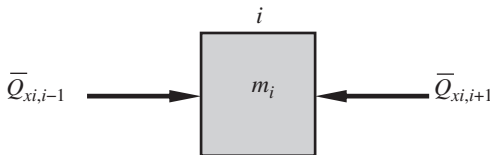


Figure 2.36 Free-body diagram of a lumped mass in a damped system.

therefore

$$\bar{\mathbf{Z}}_O = \bar{\mathbf{U}}_i \bar{\mathbf{Z}}_I$$

$$\mathbf{Z}_O^r + i\mathbf{Z}_O^i = (\mathbf{U}_i^r + i\mathbf{U}_i^i)(\mathbf{Z}_I^r + i\mathbf{Z}_I^i) = (\mathbf{U}_i^r \mathbf{Z}_I^r - \mathbf{U}_i^i \mathbf{Z}_I^i) + i(\mathbf{U}_i^r \mathbf{Z}_I^i + \mathbf{U}_i^i \mathbf{Z}_I^r)$$

which can be rewritten in a matrix form as

$$\begin{bmatrix} \mathbf{Z}^r \\ \mathbf{Z}^i \end{bmatrix}_O = \begin{bmatrix} \mathbf{U}^r & -\mathbf{U}^i \\ \mathbf{U}^i & \mathbf{U}^r \end{bmatrix}_i \begin{bmatrix} \mathbf{Z}^r \\ \mathbf{Z}^i \end{bmatrix}_I \quad (2.95)$$

Substituting $\lambda = -\lambda^r + i\lambda^i$ into Equation (2.92b), the transfer matrix of the spring-damper becomes

$$\bar{\mathbf{U}} = \begin{bmatrix} 1 & -\frac{1}{K + C(-\lambda^r + i\lambda^i)} \\ 0 & 1 \end{bmatrix} = \begin{bmatrix} 1 & -\frac{K - C\lambda^r}{(K - C\lambda^r)^2 + (C\lambda^i)^2} \\ 0 & 1 \end{bmatrix} + i \begin{bmatrix} 0 & \frac{C\lambda^i}{(K - C\lambda^r)^2 + (C\lambda^i)^2} \\ 0 & 0 \end{bmatrix} \quad (2.96)$$

Rewriting in the form of Equation (2.95) yields

$$\mathbf{U} = \begin{bmatrix} 1 & u_{12}^r & 0 & -u_{12}^i \\ 0 & 1 & 0 & 0 \\ 0 & u_{12}^i & 1 & u_{12}^r \\ 0 & 0 & 0 & 1 \end{bmatrix} \quad (2.97)$$

where

$$u_{12}^r = -\frac{K - C\lambda^r}{(K - C\lambda^r)^2 + (C\lambda^i)^2}, \quad u_{12}^i = \frac{C\lambda^i}{(K - C\lambda^r)^2 + (C\lambda^i)^2}$$

Similarly, the transfer matrix of the lumped mass is described as

$$\mathbf{U} = \begin{bmatrix} 1 & 0 & 0 & 0 \\ u_{21}^r & 1 & -u_{21}^i & 0 \\ 0 & 0 & 1 & 0 \\ u_{21}^i & 0 & u_{21}^r & 1 \end{bmatrix} \quad (2.98)$$

where $u_{21}^r = -m(\lambda^{r^2} - \lambda^{i^2})$ and $u_{21}^i = 2m\lambda^r\lambda^i$.

According to Equation (2.95) the state vector now consists of four elements:

$$\bar{\mathbf{Z}} = \begin{bmatrix} \mathbf{Z}^r \\ \mathbf{Z}^i \end{bmatrix} = [X^r, Q_x^r, X^i, Q_x^i]^T$$

When square matrices of the type in Equation (2.95) are multiplied, the result is a square matrix of the same type. This can be proved as follows:

$$\begin{bmatrix} \mathbf{A} & -\mathbf{B} \\ \mathbf{B} & \mathbf{A} \end{bmatrix} \begin{bmatrix} \mathbf{C} & -\mathbf{D} \\ \mathbf{D} & \mathbf{C} \end{bmatrix} = \begin{bmatrix} \mathbf{AC} - \mathbf{BD} & -(\mathbf{AD} + \mathbf{BC}) \\ \mathbf{AD} + \mathbf{BC} & \mathbf{AC} - \mathbf{BD} \end{bmatrix} = \begin{bmatrix} \mathbf{E} & -\mathbf{F} \\ \mathbf{F} & \mathbf{E} \end{bmatrix} \quad (2.99)$$

It is therefore necessary to carried out only half of the matrix multiplications.

2.7.3.3 Characteristic Equation

For the system shown in Figure 2.34, according to Equations (2.92) and (2.93), the overall transfer equation is obtained:

$$\bar{Z}_{2,3} = \bar{U}_2 \bar{U}_1 \bar{Z}_{0,1} = \bar{U} \bar{Z}_{0,1} \quad (2.100)$$

$$\bar{U} = \bar{U}_2 \bar{U}_1 = \begin{bmatrix} 1 & 0 \\ -m\lambda^2 & 1 \end{bmatrix} \begin{bmatrix} 1 & -\frac{1}{K+C\lambda} \\ 0 & 1 \end{bmatrix} = \begin{bmatrix} 1 & -\frac{1}{K+C\lambda} \\ -m\lambda^2 & 1 + \frac{m\lambda^2}{K+C\lambda} \end{bmatrix} \quad (2.101)$$

Substituting the boundary conditions $\bar{X}_{1,0} = \bar{Q}_{x2,3} = 0$ into the overall transfer equation, the characteristic equation of the system is obtained:

$$1 + \frac{m\lambda^2}{K+C\lambda} = 0 \quad \text{or} \quad m\lambda^2 + C\lambda + K = 0 \quad (2.102)$$

Substituting $\lambda = -\lambda^r + i\lambda^i$ into Equation (2.102) yields

$$\left(m\lambda^{r^2} - m\lambda^{i^2} - C\lambda^r + K \right) + i(C\lambda^i - 2m\lambda^r\lambda^i) = 0$$

therefore

$$\lambda^r = \frac{C}{2m}, \quad \lambda^i = \pm \sqrt{\frac{K}{m} - \left(\frac{C}{2m}\right)^2} \quad (2.103)$$

The complex eigenvalue of the damped system is obtained by solving the characteristic equation of the system.

By repeating the above process with Equation (2.95), the overall transfer equation can be deduced as

$$\begin{bmatrix} X^r \\ Q_x^r \\ X^i \\ Q_x^i \end{bmatrix}_{2,3} = \begin{bmatrix} 1 & u_{12}^r & 0 & -u_{12}^i \\ u_{21}^r & a & -u_{21}^i & -b \\ 0 & u_{12}^i & 1 & u_{12}^r \\ u_{21}^i & b & u_{21}^r & a \end{bmatrix} \begin{bmatrix} X^r \\ Q_x^r \\ X^i \\ Q_x^i \end{bmatrix}_{1,0} \quad (2.104)$$

where

$$a = u_{21}^r u_{12}^r + 1 - u_{21}^i u_{12}^i, \quad b = u_{21}^r u_{12}^i + u_{21}^i u_{12}^r \quad (2.105)$$

Substituting the boundary conditions $X_{1,0}^r = X_{1,0}^i = Q_{x2,3}^r = Q_{x2,3}^i = 0$ into Equation (2.104) yields

$$\begin{cases} aQ_x^r - bQ_x^i = 0 \\ bQ_x^r + aQ_x^i = 0 \end{cases} \quad (2.106)$$

A nonzero solution of the system is possible if and only if

$$\begin{vmatrix} a & -b \\ b & a \end{vmatrix} = a^2 + b^2 = 0 \quad (2.107)$$

Both a and b are real numbers, therefore $a = b = 0$. By solving Equation (2.105), the complex eigenvalues of the system are obtained, which are identical to those in Equation (2.103).

The characteristic equation of a complex multibody damped system can be obtained by using the two methods described. It can be seen from the above example that there are two unknown parameters λ^r and λ^i in the characteristic equation for a damped system, but only one unknown parameter of eigenfrequency in the characteristic equation for an undamped system. The numerical computation of eigenvalue problems for damped systems is therefore more difficult than for undamped systems. However, the TMM provides a powerful tool to compute the steady-state response of the forced vibration of a damped system.

2.8 Steady-state Response to Forced Vibration

After evaluating the eigenfrequencies and eigenvectors of a system using the TMM, the dynamic response of system including the *transient response* and *steady-state response* to an arbitrary excitation can be solved. The system subjected to a simple-harmonic excitation with frequency Ω will vibrate steadily with frequency Ω , and both the amplitude and phase of vibration depend on Ω . Based on this principle, the TMM can be applied to study the steady-state forced vibration and the deformations and corresponding forces of static state of the system ($\Omega = 0$).

2.8.1 Extended Transfer Matrix

In a system of spring-mass steady-state vibration with frequency Ω , as shown in Figure 2.39, the lumped masses are subjected to simple-harmonic excitations $F_2 \cos \Omega t$, $F_4 \cos \Omega t$ and $F_6 \cos \Omega t$, respectively. Find the amplitude of the steady-state responses of the system.

First, develop the *extended transfer matrix* of a lumped mass. The displacements of two ends of a lumped mass are equal, namely

$$X_{i,i+1} = X_{i,i-1} \quad (2.108)$$

As shown in Figure 2.38, from the equilibrium of the internal forces of the two ends, external force and inertia force, we get

$$Q_{x,i,i+1} = Q_{x,i,i-1} + m_i \Omega^2 X_{i,i-1} + F_i \quad (2.109)$$

Equations (2.108) and (2.109) can be expressed in matrix notation as

$$\begin{bmatrix} X \\ Q_x \end{bmatrix}_{i,i+1} = \begin{bmatrix} 1 & 0 \\ m_i \Omega^2 & 1 \end{bmatrix} \begin{bmatrix} X \\ Q_x \end{bmatrix}_{i,i-1} + \begin{bmatrix} 0 \\ F_i \end{bmatrix} \quad (2.110)$$

Equation (2.110) can be rewritten as an extended transfer equation

$$\begin{bmatrix} X \\ Q_x \\ 1 \end{bmatrix}_{i,i+1} = \begin{bmatrix} 1 & 0 & 0 \\ m_i \Omega^2 & 1 & F_i \\ 0 & 0 & 1 \end{bmatrix} \begin{bmatrix} X \\ Q_x \\ 1 \end{bmatrix}_{i,i-1} \quad (2.111)$$

Notate the state vector $\hat{\mathbf{Z}}$ and transfer matrix $\hat{\mathbf{U}}$ of forced vibration lumped mass as

$$\hat{\mathbf{Z}} = \begin{bmatrix} X \\ Q_x \\ 1 \end{bmatrix}, \quad \hat{\mathbf{U}}_i = \begin{bmatrix} 1 & 0 & 0 \\ m_i \Omega^2 & 1 & F_i \\ 0 & 0 & 1 \end{bmatrix}$$

Then, Equation (2.111) is expressed as

$$\hat{\mathbf{Z}}_{i,i+1} = \hat{\mathbf{U}}_i \hat{\mathbf{Z}}_{i,i-1} \quad (2.112)$$

where the state vector $\hat{\mathbf{Z}}_{i,i+1}$ with components $X_{i,i+1}$, $Q_{x,i,i+1}$ and additional “1” is called the extended state vector of point $P_{i,i+1}$ and the transfer matrix $\hat{\mathbf{U}}_i$ is called the extended transfer matrix of lumped mass i .

Similar to Equation (2.111) for a lumped mass, the extended transfer equation of a spring i can be written as

$$\begin{bmatrix} X \\ Q_x \\ 1 \end{bmatrix}_{i+1,i} = \begin{bmatrix} 1 & -1/K_i & 0 \\ 0 & 1 & 0 \\ 0 & 0 & 1 \end{bmatrix} \begin{bmatrix} X \\ Q_x \\ 1 \end{bmatrix}_{i-1,i} \quad (2.113)$$

2.8.2 Steady-state Response to Forced Vibrations

Similar to the method for solving the eigenfrequencies and eigenvectors of a system, the overall transfer equation of a steady-state vibration system can be obtained using the transfer equations of elements:

$$\hat{\mathbf{Z}}_{6,0} = \hat{\mathbf{U}}_6 \hat{\mathbf{U}}_5 \hat{\mathbf{U}}_4 \hat{\mathbf{U}}_3 \hat{\mathbf{U}}_2 \hat{\mathbf{U}}_1 \hat{\mathbf{Z}}_{1,0} = \hat{\mathbf{U}} \hat{\mathbf{Z}}_{1,0} \quad (2.114)$$

Notate the extended transfer matrix of element i as

$$\hat{\mathbf{U}}_i = \begin{bmatrix} \mathbf{U}_i & \mathbf{f}_i \\ \mathbf{0} & 1 \end{bmatrix} \quad (2.115)$$

It can be proved that

$$\hat{\mathbf{U}} = \hat{\mathbf{U}}_n \hat{\mathbf{U}}_{n-1} \cdots \hat{\mathbf{U}}_2 \hat{\mathbf{U}}_1 = \begin{bmatrix} \mathbf{U} & \mathbf{f} \\ \mathbf{0} & 1 \end{bmatrix} \quad (2.116)$$

If the sign of continued multiplication is used, which is defined as

$$\prod_{k=i}^n \mathbf{U}_k = \mathbf{U}_n \mathbf{U}_{n-1} \cdots \mathbf{U}_{i+1} \mathbf{U}_i \quad (2.117)$$

then

$$\begin{cases} \mathbf{U} = \mathbf{U}_n \mathbf{U}_{n-1} \cdots \mathbf{U}_2 \mathbf{U}_1 = \prod_{k=1}^n \mathbf{U}_k \\ \mathbf{f} = \left(\prod_{k=2}^n \mathbf{U}_k \right) \mathbf{f}_1 + \left(\prod_{k=3}^n \mathbf{U}_k \right) \mathbf{f}_2 + \cdots + \mathbf{U}_n \mathbf{f}_{n-1} + \mathbf{f}_n = \sum_{i=2}^n \left[\left(\prod_{k=i}^n \mathbf{U}_k \right) \mathbf{f}_{i-1} \right] \end{cases} \quad (2.118)$$

where the form of \mathbf{U} is the same as the overall transfer matrix of the free vibrations system. However, the frequency in \mathbf{U} is not the eigenfrequencies ω but the excitation frequency Ω of the exciting forces, that is, $\mathbf{U} = \mathbf{U}(\Omega)$.

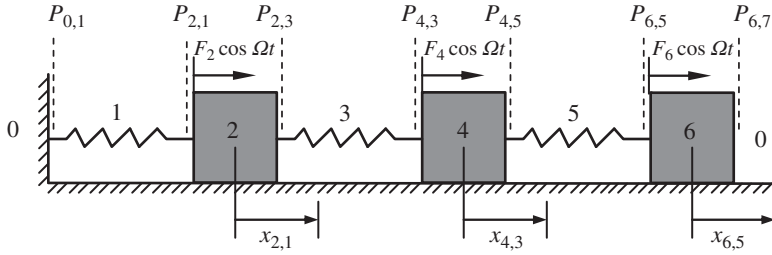
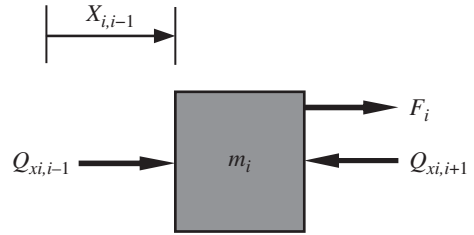


Figure 2.37 Forced vibration system of spring-mass.

Figure 2.38 Free-body diagram of a lumped mass in an undamped system.



Equation (2.114) can be expressed as

$$\begin{bmatrix} X \\ Q_x \\ 1 \end{bmatrix}_{6,0} = \begin{bmatrix} u_{11} & u_{12} & u_{13} \\ u_{21} & u_{22} & u_{23} \\ 0 & 0 & 1 \end{bmatrix} \begin{bmatrix} X \\ Q_x \\ 1 \end{bmatrix}_{1,0}$$

that is

$$\begin{cases} X_{6,0} = u_{11}X_{1,0} + u_{12}Q_{x1,0} + u_{13} \\ Q_{x6,0} = u_{21}X_{1,0} + u_{22}Q_{x1,0} + u_{23} \end{cases} \quad (2.119)$$

When Ω is not equal to any of the eigenfrequencies ω , the unknown variables of Equation (2.119) can be easily solved with the boundary conditions. The boundary conditions of the system shown in Figure 2.37 are

$$X_{1,0} = Q_{x6,0} = 0$$

Substituting this into Equation (2.119) gives

$$X_{6,0} = u_{13} - \frac{u_{12}u_{23}}{u_{22}}, \quad Q_{x1,0} = -\frac{u_{23}}{u_{22}} \quad (2.120)$$

The state vectors, including the forces and displacements of an arbitrary point in the system, can be obtained by using the transfer matrices of the elements.

Example 2.12 The 2-DOFs spring-mass system is acted on by a harmonic force $F \cos \Omega t$ on the lumped mass m_4 , as shown in Figure 2.39. Find the steady-state response of the system.

Solution

According to Equations (2.111) and (2.113)

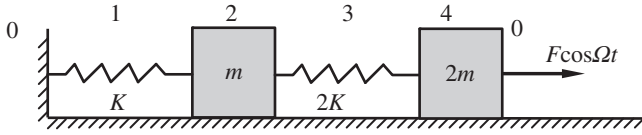


Figure 2.39 A forced vibration of the 2 DOF spring-mass system.

$$\hat{\mathbf{Z}}_{2,1} = \hat{\mathbf{U}}_1 \hat{\mathbf{Z}}_{1,0}, \quad \hat{\mathbf{Z}}_{2,3} = \hat{\mathbf{U}}_2 \hat{\mathbf{Z}}_{2,1}, \quad \hat{\mathbf{Z}}_{4,3} = \hat{\mathbf{U}}_3 \hat{\mathbf{Z}}_{2,3}, \quad \hat{\mathbf{Z}}_{4,0} = \hat{\mathbf{U}}_4 \hat{\mathbf{Z}}_{4,3} \quad (\text{a})$$

$$\hat{\mathbf{U}}_1 = \begin{bmatrix} 1 & -1/K & 0 \\ 0 & 1 & 0 \\ 0 & 0 & 1 \end{bmatrix}, \quad \hat{\mathbf{U}}_2 = \begin{bmatrix} 1 & 0 & 0 \\ m\Omega^2 & 1 & 0 \\ 0 & 0 & 1 \end{bmatrix} \quad (\text{b})$$

$$\hat{\mathbf{U}}_3 = \begin{bmatrix} 1 & -1/(2K) & 0 \\ 0 & 1 & 0 \\ 0 & 0 & 1 \end{bmatrix}, \quad \hat{\mathbf{U}}_4 = \begin{bmatrix} 1 & 0 & 0 \\ 2m\Omega^2 & 1 & F \\ 0 & 0 & 1 \end{bmatrix}$$

therefore

$$\hat{\mathbf{Z}}_{4,0} = \hat{\mathbf{U}}_4 \hat{\mathbf{U}}_3 \hat{\mathbf{U}}_2 \hat{\mathbf{U}}_1 \hat{\mathbf{Z}}_{1,0} = \hat{\mathbf{U}} \hat{\mathbf{Z}}_{1,0} \quad (\text{c})$$

$$\hat{\mathbf{U}} = \hat{\mathbf{U}}_4 \hat{\mathbf{U}}_3 \hat{\mathbf{U}}_2 \hat{\mathbf{U}}_1 = \begin{bmatrix} 1 - \frac{m\Omega^2}{2K} & \frac{1}{2K} \left(\frac{m\Omega^2}{K} - 3 \right) & 0 \\ m\Omega^2 \left(3 - \frac{m\Omega^2}{K} \right) & \left(\frac{m\Omega^2}{K} \right)^2 - \frac{4m\Omega^2}{K} + 1 & F \\ 0 & 0 & 1 \end{bmatrix} \quad (\text{d})$$

Substituting the boundary conditions $X_{1,0} = Q_{x4,0} = 0$ into Equation (c) gives

$$Q_{x1,0} = -\frac{F}{\left(\frac{m\Omega^2}{K} \right)^2 - \frac{4m\Omega^2}{K} + 1}, \quad X_{4,0} = \frac{F}{2K} \cdot \frac{3 - \frac{m\Omega^2}{K}}{\left(\frac{m\Omega^2}{K} \right)^2 - \frac{4m\Omega^2}{K} + 1} \quad (\text{e})$$

In addition,

$$X_{2,1} = \frac{F}{K} \cdot \frac{1}{\left(\frac{m\Omega^2}{K} \right)^2 - \frac{4m\Omega^2}{K} + 1}, \quad X_{4,3} = \frac{F}{2K} \cdot \frac{3 - \frac{m\Omega^2}{K}}{\left(\frac{m\Omega^2}{K} \right)^2 - \frac{4m\Omega^2}{K} + 1} \quad (\text{f})$$

The steady-state response is

$$x_{2,1} = X_{2,1} \cos \Omega t, \quad x_{4,3} = X_{4,3} \cos \Omega t \quad (\text{g})$$

The variation of the vibration amplitudes of the two lumped masses with the excitation frequency is shown in Figure 2.40. The amplitudes of $X_{2,1}$ and $X_{4,3}$ will tend to be infinitely larger

if $\left(\frac{m\Omega^2}{K} \right)^2 - \frac{4m\Omega^2}{K} + 1$ tends to zero, that is, when the excitation frequency is equal to one of the eigenfrequencies of the system then $\Omega = \omega_1$ or $\Omega = \omega_2$ resonance will occur.

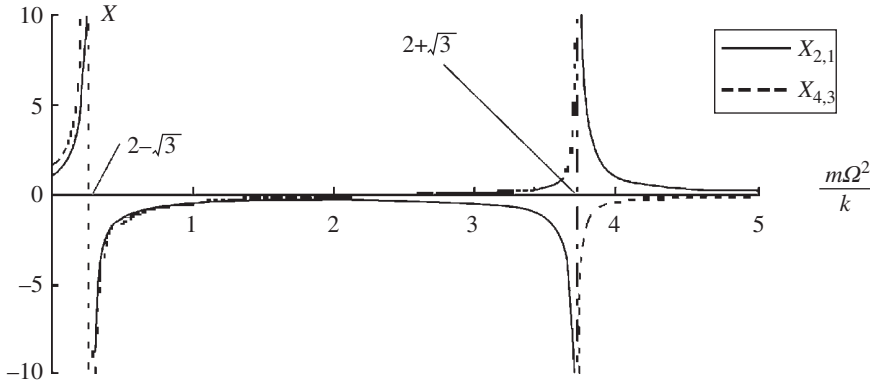


Figure 2.40 The frequency response of the 2-DOFs spring-mass system.

2.8.3 Forced Vibration of a Massless Beam

A transverse vibration massless beam subjected to a uniformly distributed harmonic load $P_i \cos \Omega t$ is shown in Figure 2.41. From the equilibrium of forces and moments acting on the beam we get

$$\begin{cases} Q_{y,i,i+1} = Q_{y,i,i-1} + P_i l_i \cdot 1 \\ M_{z,i,i+1} = M_{z,i,i-1} + l_i \cdot Q_{y,i,i-1} + \frac{P_i l_i^2}{2} \cdot 1 \end{cases} \quad (2.121)$$

According to the Euler–Bernoulli beam theory,

$$\begin{cases} Y_{i,i+1} = Y_{i,i-1} + l_i \cdot \theta_{z,i,i-1} + \frac{l_i^2}{2EI_i} \cdot M_{z,i,i-1} + \frac{l_i^3}{6EI_i} \cdot Q_{y,i,i-1} + \frac{P_i l_i^4}{24EI_i} \cdot 1 \\ \theta_{z,i,i+1} = \theta_{z,i,i-1} + \frac{l_i}{EI_i} \cdot M_{z,i,i-1} + \frac{l_i^2}{2EI_i} \cdot Q_{y,i,i-1} + \frac{P_i l_i^3}{6EI_i} \cdot 1 \end{cases} \quad (2.122)$$

Combining Equation (2.121) with Equation (2.122), the transfer equation of the beam can be described as

$$\hat{\mathbf{Z}}_{i,i+1} = \hat{\mathbf{U}}_i \hat{\mathbf{Z}}_{i,i-1} \quad (2.123a)$$

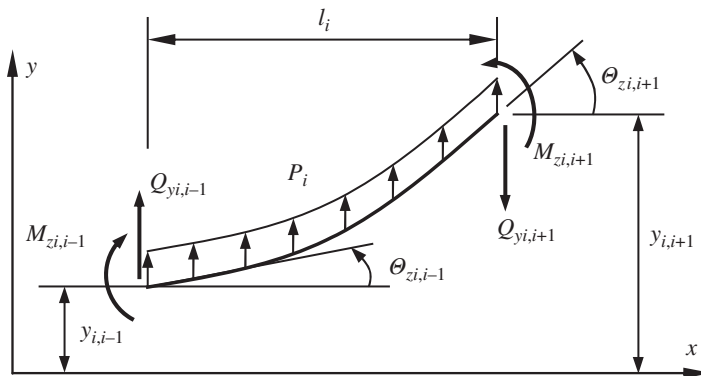


Figure 2.41 A transverse forced vibration beam.

where

$$\hat{\mathbf{Z}} = \begin{bmatrix} Y \\ \theta_z \\ M_z \\ Q_y \\ 1 \end{bmatrix}, \quad \hat{\mathbf{U}}_i = \begin{bmatrix} 1 & l_i & \frac{l_i^2}{2EI_i} & \frac{l_i^3}{6EI_i} & \frac{P_i l_i^4}{24EI_i} \\ 0 & 1 & \frac{l_i}{EI_i} & \frac{l_i^2}{2EI_i} & \frac{P_i l_i^3}{6EI_i} \\ 0 & 0 & 1 & l_i & \frac{P_i l_i^2}{2} \\ 0 & 0 & 0 & 1 & P_i l_i \\ 0 & 0 & 0 & 0 & 1 \end{bmatrix} \quad (2.123b)$$

$\hat{\mathbf{U}}_i$ is the extended transfer matrix of a vibration transverse massless beam subjected to a uniformly distributed harmonic load $P_i \cos \Omega t$ and $\hat{\mathbf{Z}}$ is the extended state vector of an arbitrary point of the beam.

Example 2.13 A simply supported fixed massless beam is subjected to a uniformly distributed static load P and a concentrated moment $M = Pl^2$, as shown in Figure 2.42, with length $3l$ and bending stiffness EI . It is supported by a spring one-third of the distance along its length. Find the deformation and distribution of the bending moment and the shear force of the beam.

Solution

Divide the beam into two parts. The left-hand side is numbered 1, the right-hand side is numbered 3 and the spring is numbered 2. The two input ends, as well as the output end, are numbered 0. From the left to the right of the beam, the extended state vectors are defined as $\hat{\mathbf{z}}_{1,0}$, $\hat{\mathbf{z}}_{1,2}$, $\hat{\mathbf{z}}_{3,2}$ and $\hat{\mathbf{z}}_{3,0}$.

According to Equations (2.123a) and (2.123b),

$$\hat{\mathbf{z}}_{1,2} = \hat{\mathbf{U}}_1 \hat{\mathbf{z}}_{1,0}, \quad \hat{\mathbf{z}}_{3,0} = \hat{\mathbf{U}}_3 \hat{\mathbf{z}}_{3,2} \quad (a)$$

$$\hat{\mathbf{U}}_1 = \begin{bmatrix} 1 & l & \frac{l^2}{2EI} & \frac{l^3}{6EI} & -\frac{Pl^4}{24EI} \\ 0 & 1 & \frac{l}{EI} & \frac{l^2}{2EI} & -\frac{Pl^3}{6EI} \\ 0 & 0 & 1 & l & -\frac{Pl^2}{2EI} \\ 0 & 0 & 0 & 1 & -Pl \\ 0 & 0 & 0 & 0 & 1 \end{bmatrix}, \quad \hat{\mathbf{U}}_3 = \begin{bmatrix} 1 & 2l & \frac{2l^2}{EI} & \frac{4l^3}{3EI} & 0 \\ 0 & 1 & \frac{2l}{EI} & \frac{2l^2}{EI} & 0 \\ 0 & 0 & 1 & 2l & 0 \\ 0 & 0 & 0 & 1 & 0 \\ 0 & 0 & 0 & 0 & 1 \end{bmatrix} \quad (b)$$

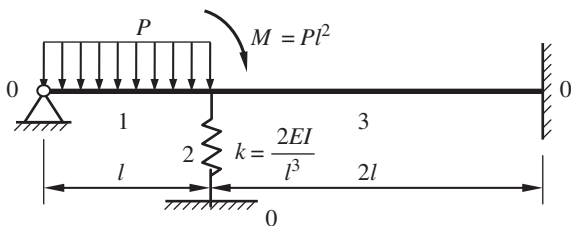


Figure 2.42 A beam under static load.

It is easy to obtain

$$\hat{\mathbf{z}}_{3,2} = \hat{\mathbf{U}}_2 \hat{\mathbf{z}}_{1,2}, \quad \hat{\mathbf{U}}_2 = \begin{bmatrix} 1 & 0 & 0 & 0 & 0 \\ 0 & 1 & 0 & 0 & 0 \\ 0 & 0 & 1 & 0 & Pl^2 \\ -\frac{2EI}{l^3} & 0 & 0 & 1 & 0 \\ 0 & 0 & 0 & 0 & 1 \end{bmatrix} \quad (c)$$

therefore

$$\hat{\mathbf{z}}_{3,0} = \hat{\mathbf{U}}_3 \hat{\mathbf{U}}_2 \hat{\mathbf{U}}_1 \hat{\mathbf{z}}_{1,0} = \hat{\mathbf{U}} \hat{\mathbf{z}}_{1,0} \quad (d)$$

Substituting the boundary conditions, the equation becomes

$$\begin{bmatrix} 0 \\ 0 \\ m_z \\ q_y \\ 1 \end{bmatrix}_{3,0} = \begin{bmatrix} u_{11} & u_{12} & u_{13} & u_{14} & u_{15} \\ u_{21} & u_{22} & u_{23} & u_{24} & u_{25} \\ u_{31} & u_{32} & u_{33} & u_{34} & u_{35} \\ u_{41} & u_{42} & u_{43} & u_{44} & u_{45} \\ 0 & 0 & 0 & 0 & 1 \end{bmatrix} \begin{bmatrix} 0 \\ \theta_z \\ 0 \\ q_y \\ 1 \end{bmatrix}_{1,0} \quad (e)$$

$\hat{\mathbf{z}}_{1,0}$ can be obtained by solving the first two nonhomogeneous equations. Then, the state vector at an arbitrary point of the system can be computed using ordinary methods. If $l = 1\text{m}$, $EI = 200\text{N}\cdot\text{m}^2$ and $P = 10\text{N/m}$, the computation results of the distribution of deformation, bending moment and shear force of the beam are shown in Figure 2.43.

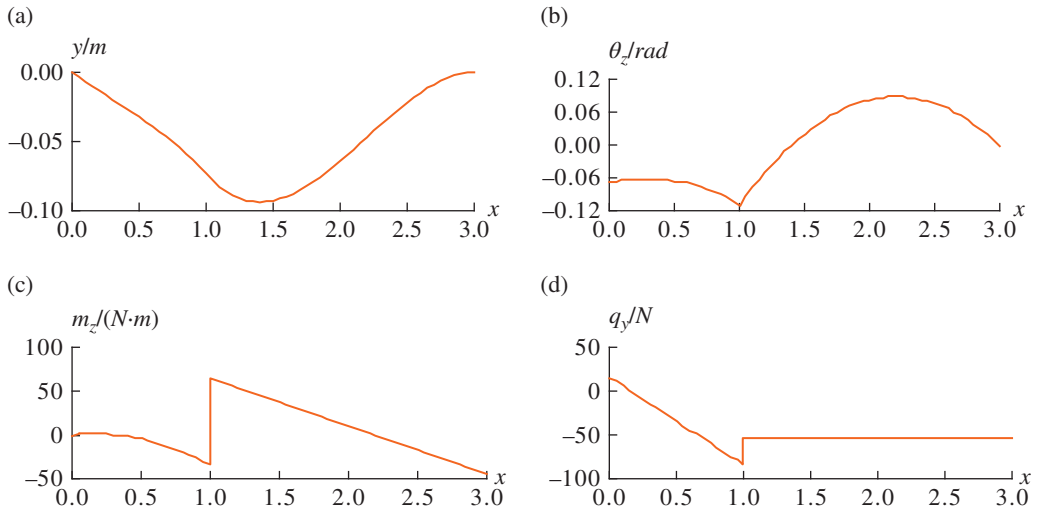


Figure 2.43 Computation results of deformation and distribution of moment and shear force: (a) displacement, (b) angular displacement, (c) bending moment and (d) shear force.

2.9 Steady-state Response of Forced Damped Vibration

2.9.1 Response to Some Typical Excitations

2.9.1.1 Transient Response to an Impulse

The lumped mass of the damped system of Figure 2.34 is excited by an impulse G at time t_0 , and thereby it assumes the initial velocity

$$\dot{x}_0 = \frac{G}{m} \quad (2.124)$$

with $x_0 = 0$, and the ensuing motion of mass m is given by Equations (2.78) and (2.84)

$$x(t) = \frac{G}{m\lambda^i} e^{-\lambda^r(t-t_0)} \sin \lambda^i(t-t_0) \quad (t \geq t_0) \quad (2.125)$$

2.9.1.2 Response to an Arbitrary Time-variant Force

The lumped mass m of the damped system shown in Figure 2.34 is subjected to an arbitrary time-variant force $F(t)$ and an impulse $F(t)d\tau$ produces a velocity increment $F(t)d\tau/m$ at time τ . According to Equation (2.125), for $t \geq \tau$ the motion increment of mass m ($x_0 = \dot{x}_0 = 0$) due to the impulse is

$$dx(t) = \frac{F(\tau)}{m\lambda^i} e^{-\lambda^r(t-\tau)} \sin \lambda^i(t-\tau) d\tau \quad (2.126)$$

The resulting motion of m is obtained by integrating Equation (2.126) with respect to τ in time $\tau \geq 0$

$$x(t) = \frac{1}{m\lambda^i} \int_0^t F(\tau) e^{-\lambda^r(t-\tau)} \sin \lambda^i(t-\tau) d\tau \quad (2.127)$$

If at time $t = 0$ the initial conditions are nonzero, the motion of mass m is

$$x(t) = e^{-\lambda^r t} \left(x_0 \cos \lambda^i t + \frac{\dot{x}_0 + \lambda^r x_0}{\lambda^i} \sin \lambda^i t \right) + \frac{1}{m\lambda^i} \int_0^t F(\tau) e^{-\lambda^r(t-\tau)} \sin \lambda^i(t-\tau) d\tau \quad (2.128)$$

2.9.1.3 Steady-state Forced Vibration of a Viscous Damping System

The lumped mass m of the viscous damped system shown in Figure 2.44 is subjected to a harmonic force with frequency, Ω , $F(t) = F \cos \Omega t$, which can also be represented as the real part of a complex function, that is

$$F(t) = \text{Re}(F e^{i\Omega t}) = \text{Re}[F(\cos \Omega t + i \sin \Omega t)] = F \cos \Omega t$$

The differential motion equation of lumped mass m is

$$m\ddot{x} + C\dot{x} + Kx = \text{Re}(F e^{i\Omega t}) \quad (2.129)$$

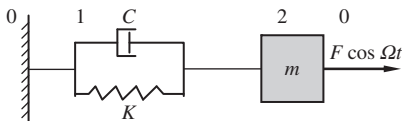


Figure 2.44 Viscous damped system.

The particular solution of the differential Equation (2.129) which describes the steady-state vibration of m is

$$x = \text{Re}(\bar{X} e^{i\Omega t}) \quad (2.130)$$

where \bar{X} is the complex amplitude of the steady-state forced vibration.

Substituting Equation (2.130) into Equation (2.129) gives

$$(-m\Omega^2 + iC\Omega + K)\bar{X}e^{i\Omega t} = Fe^{i\Omega t} \quad \text{or} \quad (-m\Omega^2 + iC\Omega + K)\bar{X} = F \quad (2.131)$$

from which

$$\bar{X} = \frac{F}{K - m\Omega^2 + iC\Omega} \quad (2.132)$$

The physics meaning of Equation (2.131) can be represented in the complex plane shown in Figure 2.45. If the displacement vector is \bar{X} , the spring force $k\bar{X}$ is parallel to \bar{X} . The effect of multiplication by i is to rotate the vector \bar{X} counterclockwise through 90° so that the direction of the damping force $iC\Omega\bar{X}$ is at 90° to \bar{X} . The direction of inertia force $-m\Omega^2\bar{X}$ is opposite to that of \bar{X} .

From Figure 2.45, the magnitude $|\bar{X}|$ and the phase-lag angle α should satisfy

$$\begin{cases} |\bar{X}| \sqrt{(K - m\Omega^2)^2 + C^2\Omega^2} = F \\ \tan \alpha = \frac{C\Omega}{K - m\Omega^2} \end{cases} \quad (2.133)$$

therefore $\bar{X} = |\bar{X}|e^{-i\alpha}$. (Note: a minus sign is positioned before α .) Substituting this into Equation (2.130) gives

$$x = \text{Re}(\bar{X}e^{i\Omega t}) = |\bar{X}|\text{Re}(e^{i(\Omega t - \alpha)}) = |\bar{X}|\cos(\Omega t - \alpha) \quad (2.134)$$

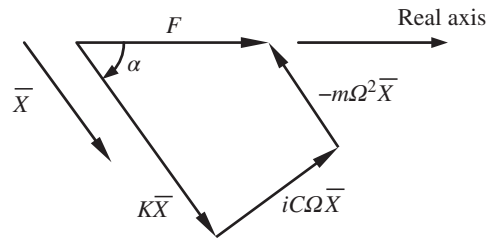
Introducing the eigenfrequency of undamped free vibration $\omega = \sqrt{K/m}$ and dimensionless damping ratio $\zeta = \frac{C}{2\sqrt{mK}}$, from Equation (2.134) the magnitude $|\bar{X}|$ and the phase-lag angle α can be written as

$$|\bar{X}| = \frac{F}{K}M, \quad \tan \alpha = \frac{2\zeta(\Omega/\omega)}{1 - (\Omega/\omega)^2} \quad (2.135)$$

$$M = \frac{1}{\sqrt{[1 - (\Omega/\omega)^2]^2 + 4\zeta^2(\Omega/\omega)^2}} \quad (2.136)$$

where F/K is the static deformation of the system under a static load F , as shown in Figure 2.44, and M is the dynamic magnification factor.

Figure 2.45 Force vectors in the complex plane.



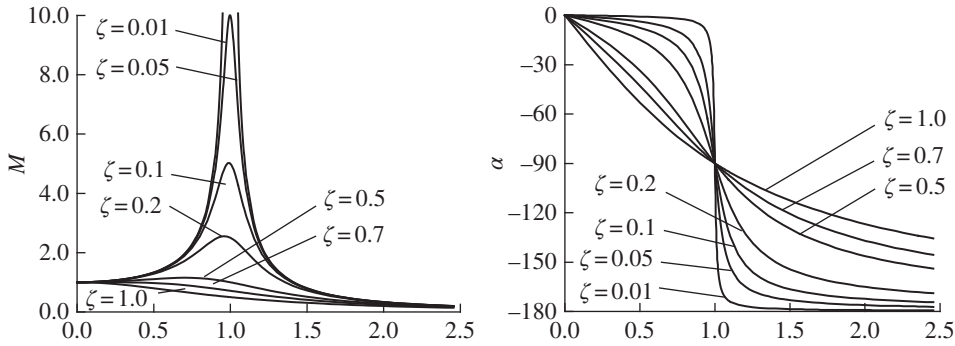


Figure 2.46 Frequency response curves of forced damped vibration.

The frequency response curves of the system with forced damped vibration are plotted in Figure 2.46, which shows how M and α vary with Ω/ω . We call this the amplitude resonance when M is a maximum, which is the case for the excitation frequency $\Omega_M = \omega \sqrt{1 - 2\zeta^2} < \omega$. Then, for a lightly damped system, we have $M = \left(2\zeta \sqrt{1 - \zeta^2}\right)^{-1}$ or $M \approx (2\zeta)^{-1}$. The condition at which $F(t)$ and $\dot{x}(t)$ are in phase is called phase resonance, which occurs for $\Omega = \omega$ when $\alpha = \pi/2$. It can be seen clearly from Figure 2.46 that for light damping the phase-lag angle is very sensitive to frequency changes near $\Omega = \omega$, therefore this offers an ideal way to determine experimentally the phase-resonance frequency ω .

2.9.1.4 Steady-state Vibration of a System with Structural Damping

The differential equation of motion of a lumped mass m is

$$m\ddot{x} + \frac{Kg}{\Omega}\dot{x} + Kx = \text{Re}(Fe^{i\Omega t}) \quad (2.137)$$

For the steady-state solution $x = \text{Re}(\bar{X} \cdot e^{i\Omega t})$, we obtain

$$\bar{X} = \frac{F}{K - m\Omega^2 + igK} \quad (2.138)$$

We obtain

$$x = \frac{F}{K} M \cos(\Omega t - \alpha) \quad (2.139)$$

where

$$\begin{cases} M = \frac{1}{\sqrt{[1 - (\Omega/\omega)^2]^2 + g^2}} \\ \alpha = \arctan \frac{g}{1 - (\Omega/\omega)^2} \end{cases} \quad (2.140)$$

Similar to viscous damping, phase resonance occurs for $\Omega = \omega$ for a structural damping system. However, the amplitude resonance M of viscous damping systems occurs for $\Omega < \omega$, but is $\Omega = \omega$

for a structural damping system when M also reaches its maximum. It is noteworthy and indicative of the physical shortcoming of the concept of structure damping that $\alpha = tg^{-1}g \neq 0$ for $\Omega = 0$.

2.9.2 Complex Extended Transfer Matrix and Steady-state Response

2.9.2.1 Complex Extended Transfer Matrix

Now let us compute the steady-state vibration of the system of Figure 2.44 using the MSTMM. The complex transfer matrix of the spring-damper in parallel connection was found for the free vibrations in Equation (2.92), where λ is in the form of $\lambda = -\lambda^r + i\lambda^i$. If we consider steady-state forced vibrations $\lambda = i\Omega$ and add an extra column to the transfer matrix, the extended transfer matrix relating the complex extended state vectors $\hat{\bar{Z}}_I$ and $\hat{\bar{Z}}_O$ is obtained:

$$\begin{bmatrix} \bar{X} \\ \bar{Q}_x \\ 1 \end{bmatrix}_{2,1} = \begin{bmatrix} 1 & -1/(K + iC\Omega) & 0 \\ 0 & 1 & 0 \\ 0 & 0 & 1 \end{bmatrix} \begin{bmatrix} \bar{X} \\ \bar{Q}_x \\ 1 \end{bmatrix}_{1,0} \quad (2.141)$$

Similarly, according to Equation (2.92) the extended transfer equation of a lumped mass is

$$\begin{bmatrix} \bar{X} \\ \bar{Q}_x \\ 1 \end{bmatrix}_{2,0} = \begin{bmatrix} 1 & 0 & 0 \\ m\Omega^2 & 1 & \bar{F} \\ 0 & 0 & 1 \end{bmatrix} \begin{bmatrix} \bar{X} \\ \bar{Q}_x \\ 1 \end{bmatrix}_{2,1} \quad (2.142)$$

therefore the overall transfer equation of the system of Figure 2.44 is

$$\begin{bmatrix} \bar{X} \\ \bar{Q}_x \\ 1 \end{bmatrix}_{2,0} = \begin{bmatrix} 1 & 0 & 0 \\ m\Omega^2 & 1 & \bar{F} \\ 0 & 0 & 1 \end{bmatrix} \begin{bmatrix} 1 & -1/(K + iC\Omega) & 0 \\ 0 & 1 & 0 \\ 0 & 0 & 1 \end{bmatrix} \begin{bmatrix} \bar{X} \\ \bar{Q}_x \\ 1 \end{bmatrix}_{1,0} = \begin{bmatrix} 1 & -1/(K + iC\Omega) & 0 \\ m\Omega^2 & 1 - m\Omega^2/(K + iC\Omega) & \bar{F} \\ 0 & 0 & 1 \end{bmatrix} \begin{bmatrix} \bar{X} \\ \bar{Q}_x \\ 1 \end{bmatrix}_{1,0}$$

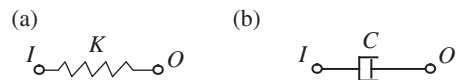
Substituting the boundary conditions $\bar{X}_{1,0} = \bar{Q}_{x2,0} = 0$ into the above formula yields

$$\begin{cases} \bar{Q}_{x1,0} = \frac{-\bar{F}}{1 - m\Omega^2/(K + iC\Omega)} \\ \bar{X}_{2,0} = \frac{\bar{F}}{K - m\Omega^2 + iC\Omega} \end{cases}$$

which coincides with Equation (2.132).

Two further examples of extended transfer matrices are given as follows. One is Equation (2.143) for a spring with stiffness K , shown in Figure 2.47a, and the other is

Figure 2.47 Spring and damper: (a) spring with stiffness K and (b) damper with complex stiffness $iC\Omega$.



Equation (2.144) for a damper with complex stiffness $iC\Omega$, shown in Figure 2.47b. The elements of the state vectors have been written above the corresponding column of the transfer matrix.

$$\hat{\mathbf{U}} = \begin{matrix} \bar{X} & \bar{Q}_x & 1 \\ \begin{bmatrix} 1 & -1/K & 0 \\ 0 & 1 & 0 \\ 0 & 0 & 1 \end{bmatrix} \end{matrix} \quad \text{or} \quad \hat{\mathbf{U}} = \begin{matrix} X^r & Q_x^r & X^i & Q_x^i & 1 \\ \begin{bmatrix} 1 & -1/K & 0 & 0 & 0 \\ 0 & 1 & 0 & 0 & 0 \\ 0 & 0 & 1 & -1/K & 0 \\ 0 & 0 & 0 & 1 & 0 \\ 0 & 0 & 0 & 0 & 1 \end{bmatrix} \end{matrix} \quad (2.143)$$

$$\hat{\mathbf{U}} = \begin{matrix} \bar{X} & \bar{Q}_x & 1 \\ \begin{bmatrix} 1 & -1/(iC\Omega) & 0 \\ 0 & 1 & 0 \\ 0 & 0 & 1 \end{bmatrix} \end{matrix} \quad \text{or} \quad \hat{\mathbf{U}} = \begin{matrix} X^r & Q_x^r & X^i & Q_x^i & 1 \\ \begin{bmatrix} 1 & 0 & 0 & -1/(C\Omega) & 0 \\ 0 & 1 & 0 & 0 & 0 \\ 0 & 1/(C\Omega) & 1 & 0 & 0 \\ 0 & 0 & 0 & 1 & 0 \\ 0 & 0 & 0 & 0 & 1 \end{bmatrix} \end{matrix} \quad (2.144)$$

2.9.2.2 Steady-state Response

If we use the extended transfer matrices in their real form, as in Equation (2.95), the form of the extended state vector is

$$\hat{\mathbf{Z}} = \begin{bmatrix} \mathbf{Z}^r \\ \mathbf{Z}^i \\ 1 \end{bmatrix}$$

and the transfer equation is

$$\begin{bmatrix} \mathbf{Z}^r \\ \mathbf{Z}^i \\ 1 \end{bmatrix}_O = \begin{bmatrix} \mathbf{U}^r & -\mathbf{U}^i & \mathbf{f}^r \\ \mathbf{U}^i & \mathbf{U}^r & \mathbf{f}^i \\ \mathbf{0} & \mathbf{0} & 1 \end{bmatrix} \begin{bmatrix} \mathbf{Z}^r \\ \mathbf{Z}^i \\ 1 \end{bmatrix}_I \quad \text{or} \quad \hat{\mathbf{Z}}_O = \hat{\mathbf{U}} \hat{\mathbf{Z}}_I \quad (2.145)$$

The overall transfer matrix is obtained by multiplying the extended transfer matrix of each element in sequence:

$$\hat{\mathbf{Z}}_{n,0} = \hat{\mathbf{U}}_n \hat{\mathbf{U}}_{n-1} \cdots \hat{\mathbf{U}}_2 \hat{\mathbf{U}}_1 \hat{\mathbf{Z}}_{1,0} = \hat{\mathbf{U}} \hat{\mathbf{Z}}_{1,0} \quad (2.146)$$

where the overall transfer matrix $\hat{\mathbf{U}}$ still has the matrix form of Equation (2.145).

Similar to the case for an undamped system, in the boundary state vectors of the damped system there are also $m/2$ components equal to zero. The beam is fixed at the input end and simply supported at the output end, so the corresponding boundary conditions are

$$\begin{cases} \hat{\mathbf{Z}}_{1,0} = [0, 0, M_z^r, Q_y^r, 0, 0, M_z^i, Q_y^i, 1]^T \\ \hat{\mathbf{Z}}_{n,0} = [0, \theta_z^r, 0, Q_y^r, 0, \theta_z^i, 0, Q_y^i, 1]^T \end{cases} \quad (2.147)$$

The overall transfer equation can be expressed explicitly as

$$\begin{bmatrix} 0 \\ \theta_z^r \\ 0 \\ Q_y^r \\ 0 \\ \theta_z^i \\ 0 \\ Q_y^i \\ 1 \end{bmatrix}_{n,0} = \begin{bmatrix} u_{11} & u_{12} & u_{13} & u_{14} & -u_{51} & -u_{52} & -u_{53} & -u_{54} & f_1^r \\ u_{21} & u_{22} & u_{23} & u_{24} & -u_{61} & -u_{62} & -u_{63} & -u_{64} & f_2^r \\ u_{31} & u_{32} & u_{33} & u_{34} & -u_{71} & -u_{72} & -u_{73} & -u_{74} & f_3^r \\ u_{41} & u_{42} & u_{43} & u_{44} & -u_{81} & -u_{82} & -u_{83} & -u_{84} & f_4^r \\ u_{51} & u_{52} & u_{53} & u_{54} & u_{11} & u_{12} & u_{13} & u_{14} & f_1^i \\ u_{61} & u_{62} & u_{63} & u_{64} & u_{21} & u_{22} & u_{23} & u_{24} & f_2^i \\ u_{71} & u_{72} & u_{73} & u_{74} & u_{31} & u_{32} & u_{33} & u_{34} & f_3^i \\ u_{81} & u_{82} & u_{83} & u_{84} & u_{41} & u_{42} & u_{43} & u_{44} & f_4^i \\ 0 & 0 & 0 & 0 & 0 & 0 & 0 & 0 & 1 \end{bmatrix} \begin{bmatrix} 0 \\ 0 \\ M_z^r \\ Q_y^r \\ 0 \\ 0 \\ M_z^i \\ Q_y^i \\ 1 \end{bmatrix}_{1,0} \quad (2.148)$$

that is

$$\begin{bmatrix} u_{13} & u_{14} & -u_{53} & -u_{54} \\ u_{33} & u_{34} & -u_{73} & -u_{74} \\ u_{53} & u_{54} & u_{13} & u_{14} \\ u_{73} & u_{74} & u_{33} & u_{34} \end{bmatrix} \begin{bmatrix} M_z^r \\ Q_y^r \\ M_z^i \\ Q_y^i \end{bmatrix}_{1,0} = \begin{bmatrix} -f_1^r \\ -f_3^r \\ -f_1^i \\ -f_3^i \end{bmatrix} \quad (2.149)$$

This can be written as

$$\mathbf{U}_x \mathbf{Z}_x = \mathbf{f}_x \quad (2.150)$$

so

$$\mathbf{Z}_x = \mathbf{U}_x^{-1} \mathbf{f}_x \quad (2.151)$$

Knowing the state vector \mathbf{Z}_x at the input end, the other state vectors can be computed by the method described earlier.

Example 2.14 The damping torsion system shown in Figure 2.48 is used to understand the advantages of the MSTMM. r_3 is the damping of a rotor damper and C_4 is the damping of an electromagnetic coupling damper. The spring K_6 with complex impedance $\bar{z}_6 = K_6(1 + i g_6)$ has strong structural damping to keep the phase independent on the exciting frequency. Disks J_5 and J_7 are acted on by torques $M_5 = M_5^c \cos \Omega t + M_5^s \sin \Omega t = -0.75 \cos \Omega t + 0.70 \sin \Omega t$ and $M_7 = M_7^c \cos \Omega t + M_7^s \sin \Omega t = 0.20 \cos \Omega t + 0.60 \sin \Omega t$, respectively, and $\Omega^2 = 0.8$. Find the steady-state response of the system.

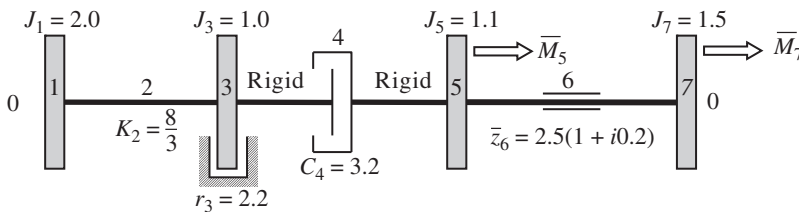


Figure 2.48 Damping torsion system.

Solution

Because the exciting torques M_5 and M_7 are given in their cosine and sine components, it is necessary to transform these into their corresponding real and imaginary components, that is

$$\begin{aligned} M^c \cos \Omega t + M^s \sin \Omega t &= \operatorname{Re}(\bar{M} e^{i\Omega t}) = \operatorname{Re}[(M^r + iM^i)(\cos \Omega t + i \sin \Omega t)] \\ &= \operatorname{Re}[(M^r \cos \Omega t - M^i \sin \Omega t) + i(M^r \sin \Omega t + M^i \cos \Omega t)] \end{aligned} \quad (a)$$

therefore $M^r = M^c$, $M^i = -M^s$ and

$$M_5^r = M_5^c = -0.75, M_5^i = -M_5^s = -0.70, M_7^r = M_7^c = 0.20, M_7^i = -M_7^s = -0.60 \quad (b)$$

The extended transfer matrices of each element in real form are

$$\begin{aligned} \hat{\mathbf{U}}_1 &= \begin{bmatrix} 1 & 0 & 0 & 0 & 0 \\ -J_1 \Omega^2 & 1 & 0 & 0 & 0 \\ 0 & 0 & 1 & 0 & 0 \\ 0 & 0 & -J_1 \Omega^2 & 1 & 0 \\ 0 & 0 & 0 & 0 & 1 \end{bmatrix}, \hat{\mathbf{U}}_3 = \begin{bmatrix} 1 & 0 & 0 & 0 & 0 \\ -J_3 \Omega^2 & 1 & -r_3 \Omega & 0 & 0 \\ 0 & 0 & 1 & 0 & 0 \\ r_3 \Omega & 0 & -J_3 \Omega^2 & 1 & 0 \\ 0 & 0 & 0 & 0 & 1 \end{bmatrix} \\ \hat{\mathbf{U}}_5 &= \begin{bmatrix} 1 & 0 & 0 & 0 & 0 \\ -J_5 \Omega^2 & 1 & 0 & 0 & -M_5^r \\ 0 & 0 & 1 & 0 & 0 \\ 0 & 0 & -J_5 \Omega^2 & 1 & -M_5^i \\ 0 & 0 & 0 & 0 & 1 \end{bmatrix}, \hat{\mathbf{U}}_7 = \begin{bmatrix} 1 & 0 & 0 & 0 & 0 \\ -J_7 \Omega^2 & 1 & 0 & 0 & -M_7^r \\ 0 & 0 & 1 & 0 & 0 \\ 0 & 0 & -J_7 \Omega^2 & 1 & -M_7^i \\ 0 & 0 & 0 & 0 & 1 \end{bmatrix} \\ \hat{\mathbf{U}}_2 &= \begin{bmatrix} 1 & -1/K_2 & 0 & 0 & 0 \\ 0 & 1 & 0 & 0 & 0 \\ 0 & 0 & 1 & -1/K_2 & 0 \\ 0 & 0 & 0 & 1 & 0 \\ 0 & 0 & 0 & 0 & 1 \end{bmatrix}, \hat{\mathbf{U}}_4 = \begin{bmatrix} 1 & 0 & 0 & 1/(C_4 \Omega) & 0 \\ 0 & 1 & 0 & 0 & 0 \\ 0 & -1/(C_4 \Omega) & 1 & 0 & 0 \\ 0 & 0 & 0 & 1 & 0 \\ 0 & 0 & 0 & 0 & 1 \end{bmatrix} \\ \hat{\mathbf{U}}_6 &= \begin{bmatrix} 1 & \frac{1}{K_6(1+g_6^2)} & 0 & \frac{g_6}{K_6(1+g_6^2)} & 0 \\ 0 & 1 & 0 & 0 & 0 \\ 0 & -\frac{g_6}{K_6(1+g_6^2)} & 1 & \frac{1}{K_6(1+g_6^2)} & 0 \\ 0 & 0 & 0 & 1 & 0 \\ 0 & 0 & 0 & 0 & 1 \end{bmatrix} \end{aligned} \quad (c)$$

Table 2.15 Computation results of the forced damped vibration of the system

Sequence number i	1	3	5	7
$\theta_{xi,i-1}^r$	0.2271	0.0908	-0.1034	-0.0801
$\theta_{xi,i-1}^i$	0.3826	0.1530	0.4106	0.3191

The overall transfer equation is

$$\hat{\mathbf{Z}}_{7,0} = \hat{\mathbf{U}}_7 \hat{\mathbf{U}}_6 \hat{\mathbf{U}}_5 \hat{\mathbf{U}}_4 \hat{\mathbf{U}}_3 \hat{\mathbf{U}}_2 \hat{\mathbf{U}}_1 \hat{\mathbf{Z}}_{1,0} = \hat{\mathbf{U}} \hat{\mathbf{Z}}_{1,0} \quad (\text{d})$$

Substituting the boundary conditions

$$M_{x7,0}^r = M_{x7,0}^i = M_{x1,0}^r = M_{x1,0}^i = 0 \quad (\text{e})$$

into Equation (d) yields

$$\begin{bmatrix} \theta_x^r \\ \theta_x^i \end{bmatrix}_{1,0} = \begin{bmatrix} u_{21} & u_{23} \\ u_{41} & u_{43} \end{bmatrix}^{-1} \begin{bmatrix} -u_{25} \\ -u_{45} \end{bmatrix} \quad (\text{f})$$

The motion of each disk is

$$\theta_x = \text{Re}(\bar{\theta}_x e^{i\Omega t}) = \text{Re}[(\theta_x^r + i\theta_x^i)(\cos\Omega t + i\sin\Omega t)] = \theta_x^r \cos\Omega t - \theta_x^i \sin\Omega t \quad (\text{g})$$

The computation results for θ_x^r and θ_x^i of the four disks are shown in Table 2.15.

3

Augmented Eigenvector and System Response

3.1 Introduction

By presenting the new concepts of the *body dynamics equation* of the body element and the body dynamics equations of a system in the transfer matrix method for multibody systems (MSTMM), the complicated *global dynamics equation* of a system is no longer needed in solving multiple rocket launch system dynamics (MRLSD). The body dynamics equations of a system are merely the assemblage of the body dynamics equations of the body elements of the system, which are totally different from the global dynamic equations of the system. It is also not necessary to consider the connection relations among body elements of the system because they have been considered in the overall transfer matrix and vibration characteristics of the system. There are uniform forms of body dynamics equations for various body elements, therefore there are very simple forms of body dynamics equations of systems for multi-rigid-flexible-body systems (MRFSs). These make the writing and derivation of dynamics equations and solving the dynamics response more convenient.

The *orthogonality* of eigenvectors of MRFSs is the pre-condition to calculate the dynamics response of the system accurately and makes the dynamics response quickly converge to the precision required by engineering in limited modals. For example, to assess scientifically and improve the performance of weapon systems, and to greatly reduce the consumption of ammunition in the test and realize the dynamics design of a weapons system, it is necessary to compute the vibration characteristics of the launch system and analyze precisely the dynamics response of the weapons system. However, the eigenvectors do not possess conventional orthogonality because of nonself-conjugation of the eigenvalues of the MRFS caused by the dynamic coupling between the rigid and flexible bodies of the system. It is therefore difficult to precisely analyze the dynamics response of the system using the *modal analysis method*. Finding the orthogonal eigenvectors of a complex MRFS became a worldwide complex problem except for several special and simple dynamics models [230, 234].

To solve the problems of the orthogonality of eigenvectors and accurate analyses of the dynamics response of MRFSs, new concepts such as the *body dynamics equation*, *augmented eigenvector* and *augmented operator* of MRFSs were proposed (section 3.4), and it has been shown by the authors that the *orthogonality of augmented eigenvectors* can be satisfied automatically [4, 50, 55–63]. Exact analysis of the dynamics responses for linear MRFSs are also realized. These provide the basic theory and approach for solving systematically the problems of linear multibody system dynamics (MSD). The augmented eigenvector can be obtained by successively writing the modal coordinates of the corresponding displacements and angular displacements of

body elements. It contains discrete and continuous variables. Its number of variables is equal to the number of body dynamics equations of the system. Its construction process is simple, convenient and programmable. These are important features of augmented eigenvectors which are different from ordinary eigenvectors. Using the orthogonality of augmented eigenvectors and the vibration characteristics of the system, the body dynamics equations of body elements, which cannot be solved directly, can be solved by translating them into the differential equations of motion independent to each other under principal coordinates. This ensures the very high computational speed of multi-rigid-flexible-body systems dynamics (MRFSD).

The following topics are introduced in this chapter: the basic theory of the orthogonality of eigenvectors, new concepts such as the body dynamics equation, the augmented eigenvector and the augmented operator of MRFSSs, verification of the orthogonality of augmented eigenvectors, which is satisfied automatically, solving the transient responses of MRFSSs to any excitations using augmented eigenvectors [60–63], and solving steady-state and static responses of MRFSSs.

3.2 Body Dynamics Equation and Parameter Matrices

3.2.1 Body Dynamics Equation of Body Elements

Any multibody system (MS) may be composed of body elements such as lumped masses, rigid bodies, flexible bodies and others connected by various hinges. It can be shown that the dynamics equation of any body element i can be written in the matrix form

$$\mathbf{M}_i \mathbf{v}_{i,tt} + \mathbf{C}_i \mathbf{v}_{i,t} + \mathbf{K}_i \mathbf{v}_i = \mathbf{f}_i \quad (3.1)$$

Equation (3.1) is the body dynamics equation, which is originally presented in the MSTMM, where, \mathbf{M}_i , \mathbf{C}_i , \mathbf{K}_i , \mathbf{v}_i and \mathbf{f}_i are the parameter matrices of body element i . \mathbf{M}_i is the parameter matrix of mass and denotes the mass distribution of the body element. \mathbf{v}_i is a column matrix composed of displacements and angular displacements indicating the motion state of the body element. The subscript t denotes differentiation with respect to time. \mathbf{K}_i is the parameter matrix of stiffness and denotes all internal forces acting on the body elements and their points of action except the damping forces and damping torque when it acts on \mathbf{v}_i . \mathbf{C}_i is the parameter matrix of damping and denotes the damping forces and damping torques acting on the body elements and their points of action when it acts on $\mathbf{v}_{i,t}$. \mathbf{f}_i is the column matrix of external forces and external torques acting on the body element.

If the damping forces are included in the external forces, Equation (3.1) can be written as

$$\mathbf{M}_i \mathbf{v}_{i,tt} + \mathbf{K}_i \mathbf{v}_i = \mathbf{f}_i \quad (3.2)$$

The body dynamics equations and the parameter matrices of typical body elements, such as lumped masses, rigid bodies and elastic bodies, are discussed in the following sections.

3.2.2 Parameter Matrices of Typical Elements

3.2.2.1 Parameter Matrix of a Lumped Mass Vibrating in Space

The body dynamics equation of a lumped mass vibrating in space is

$$\mathbf{M}_i \ddot{\mathbf{r}}_i - \mathbf{q}_{L,i} + \mathbf{q}_{o,i} = \mathbf{F}_i \quad (3.3)$$

where

$$\mathbf{M}_i = \begin{bmatrix} m_i & 0 & 0 \\ 0 & m_i & 0 \\ 0 & 0 & m_i \end{bmatrix}, \quad \mathbf{r}_i = \begin{bmatrix} x_{I,i} \\ y_{I,i} \\ z_{I,i} \end{bmatrix}, \quad \mathbf{q}_{I,i} = \begin{bmatrix} q_{x,I,i} \\ q_{y,I,i} \\ q_{z,I,i} \end{bmatrix}, \quad \mathbf{q}_{O,i} = \begin{bmatrix} q_{x,O,i} \\ q_{y,O,i} \\ q_{z,O,i} \end{bmatrix}, \quad \mathbf{F}_i = \begin{bmatrix} F_{x,i} \\ F_{y,i} \\ F_{z,i} \end{bmatrix} \quad (3.4)$$

m_i is the mass of lumped mass i , $\mathbf{q}_{I,i}$ and $\mathbf{q}_{O,i}$ are the column matrices of internal force acting on the input end I and output end O , and \mathbf{F}_i is the column matrix of external force acting on the lumped mass i .

A linear operator D^3 is defined as

$$\begin{cases} D^3|_I x_{I,i} = q_{x,I,i} \\ D^3|_I y_{I,i} = q_{y,I,i} \\ D^3|_I z_{I,i} = q_{z,I,i} \end{cases}, \quad \begin{cases} D^3|_O x_{I,i} = q_{x,O,i} \\ D^3|_O y_{I,i} = q_{y,O,i} \\ D^3|_O z_{I,i} = q_{z,O,i} \end{cases} \quad (3.5)$$

The physical meaning of the operator D^3 is that the action of D^3 on the displacement of a connection point of the system results in corresponding internal forces at the connection point except the damping force, that is

$$D^3|_I \mathbf{r}_i = D^3|_I \begin{bmatrix} x_{I,i} \\ y_{I,i} \\ z_{I,i} \end{bmatrix} = \begin{bmatrix} q_{x,I,i} \\ q_{y,I,i} \\ q_{z,I,i} \end{bmatrix} = \mathbf{q}_{I,i}, \quad D^3|_O \mathbf{r}_i = \mathbf{q}_{O,i} \quad (3.6)$$

Using the linear operator, D^3 , Equation (3.3) can be reformed as Equation (3.2), where the detailed parameter matrices are

$$\mathbf{v}_i = \mathbf{r}_i = \begin{bmatrix} x_{I,i} \\ y_{I,i} \\ z_{I,i} \end{bmatrix}, \quad \mathbf{f}_i = \mathbf{F}_i = \begin{bmatrix} F_{x,i} \\ F_{y,i} \\ F_{z,i} \end{bmatrix}$$

$$\mathbf{K}_i = \begin{bmatrix} -D^3|_{I,i} + D^3|_{O,i} & 0 & 0 \\ 0 & -D^3|_{I,i} + D^3|_{O,i} & 0 \\ 0 & 0 & -D^3|_{I,i} + D^3|_{O,i} \end{bmatrix} \quad (3.7)$$

3.2.2.2 Parameter Matrix of a Rigid Body Vibrating in Space

For a rigid body i vibrating in space with N input and L output ends, the motion can be described by linear displacements $\mathbf{r}_i = [x_{I,i}, y_{I,i}, z_{I,i}]^T$ and angular displacements $\boldsymbol{\theta}_i = [\theta_{x,I,i}, \theta_{y,I,i}, \theta_{z,I,i}]^T$ of the first input end I_1 . The motion equation of the mass center of the rigid body is

$$m_i \ddot{\mathbf{r}}_C \sum_{n=1}^N \mathbf{q}_{I_n,i} - \sum_{l=1}^L \mathbf{q}_{O_l,i} + \mathbf{F}_i \quad (3.8)$$

The rotation equation of the rigid body rotating about I_1 is

$$\mathbf{J}_{I_1,i} \ddot{\boldsymbol{\theta}}_i = - \sum_{n=1}^N \mathbf{m}_{I_n,i} + \sum_{l=1}^L \mathbf{m}_{O_l,i} + \sum_{n=2}^N \tilde{\mathbf{l}}_{I_1 I_n,i} \mathbf{q}_{I_n,i} - \sum_{l=1}^L \tilde{\mathbf{l}}_{I_1 O_l,i} \mathbf{q}_{O_l,i} + \mathbf{m}_i + \tilde{\mathbf{l}}_{I_1 D,i} \mathbf{F}_i - \mathbf{m}_i \tilde{\mathbf{l}}_{I_1 C,i} \ddot{\mathbf{r}}_i \quad (3.9)$$

where \mathbf{m}_i is the external principal moment acting on the rigid body, \mathbf{F}_i is the principal vector of external force (contains the damping force) acting on the rigid body and $\tilde{\mathbf{l}}_{l_1 D, i} \mathbf{F}_i$ is the moment of the principal vector of external force with respect to point I_1 . $\mathbf{m}_{l_n, i}$ is the internal moment of the n th input end of the rigid body, $\mathbf{m}_{O_l, i}$ is the internal moment of the l th output end of the rigid body and $\mathbf{J}_{l_1, i}$ is the moment of inertia matrix of the rigid body with respect to point I_1 . D is the simplified center of external force (center of moment).

The displacement of the mass center is

$$\mathbf{r}_C = \mathbf{r}_i - \tilde{\mathbf{l}}_{l_1 C, i} \boldsymbol{\theta}_i \quad (3.10)$$

The acceleration of the mass center is

$$\ddot{\mathbf{r}}_C = \ddot{\mathbf{r}}_i - \tilde{\mathbf{l}}_{l_1 C, i} \ddot{\boldsymbol{\theta}}_i \quad (3.11)$$

Substituting Equation (3.11) into Equation (3.8), we obtain

$$m_i \ddot{\mathbf{r}}_i - m_i \tilde{\mathbf{l}}_{l_1 C, i} \ddot{\boldsymbol{\theta}}_i - \sum_{n=1}^N \mathbf{q}_{l_n, i} + \sum_{l=1}^L \mathbf{q}_{O_l, i} = \mathbf{F}_i \quad (3.12)$$

Rewriting Equation (3.9) yields

$$m_i \tilde{\mathbf{l}}_{l_1 C, i} \ddot{\mathbf{r}}_i + \mathbf{J}_{l_1, i} \ddot{\boldsymbol{\theta}}_i + \sum_{n=1}^N \mathbf{m}_{l_n, i} - \sum_{l=1}^L \mathbf{m}_{O_l, i} - \sum_{n=2}^N \tilde{\mathbf{l}}_{l_1 l_n, i} \mathbf{q}_{l_n, i} + \sum_{l=1}^L \tilde{\mathbf{l}}_{l_1 O_l, i} \mathbf{q}_{O_l, i} = \mathbf{m}_i + \tilde{\mathbf{l}}_{l_1 D, i} \mathbf{F}_i \quad (3.13)$$

Combining Equations (3.12) and (3.13) and rewriting the body dynamics equation in the form of Equation (3.2) yields the parameter matrices

$$\mathbf{M}_i = \begin{bmatrix} m_i \mathbf{I}_3 & -m_i \tilde{\mathbf{l}}_{l_1 C, i} \\ m_i \tilde{\mathbf{l}}_{l_1 C, i} & \mathbf{J}_{l_1, i} \end{bmatrix}, \quad \mathbf{v}_i = \begin{bmatrix} \mathbf{r}_i \\ \boldsymbol{\theta}_i \end{bmatrix}, \quad \mathbf{f}_i = \begin{bmatrix} \mathbf{F}_i \\ \mathbf{m}_i + \tilde{\mathbf{l}}_{l_1 D, i} \mathbf{F}_i \end{bmatrix}$$

$$\mathbf{K}_i = \begin{bmatrix} -\sum_{n=1}^N \mathbf{I}_3 \mathbf{D}^3|_{l_n, i} + \sum_{l=1}^L \mathbf{I}_3 \mathbf{D}^3|_{O_l, i} & \mathbf{O}_{3 \times 3} \\ -\sum_{n=2}^N \tilde{\mathbf{l}}_{l_1 l_n, i} \mathbf{D}^3|_{l_n, i} + \sum_{l=1}^L \tilde{\mathbf{l}}_{l_1 O_l, i} \mathbf{D}^3|_{O_l, i} & \sum_{n=1}^N \mathbf{I}_3 \mathbf{D}^1|_{l_n, i} - \sum_{l=1}^L \mathbf{I}_3 \mathbf{D}^1|_{O_l, i} \end{bmatrix} \quad (3.14)$$

where \mathbf{D}^1 is a linear operator that denotes all internal moments of the body element at the connection point except the damping force, in which case it acts on the angular displacement of this point, namely

$$\begin{cases} \mathbf{D}^1|_I \theta_{x, l, i} = m_{x, l, i} \\ \mathbf{D}^1|_I \theta_{y, l, i} = m_{y, l, i} \\ \mathbf{D}^1|_I \theta_{z, l, i} = m_{z, l, i} \end{cases}, \quad \begin{cases} \mathbf{D}^1|_O \theta_{x, l, i} = m_{x, O, i} \\ \mathbf{D}^1|_O \theta_{y, l, i} = m_{y, O, i} \\ \mathbf{D}^1|_O \theta_{z, l, i} = m_{z, O, i} \end{cases} \quad (3.15)$$

3.2.2.3 Parameter Matrix of a Beam Undergoing Transversal, Longitudinal and Torsional Vibrations

It can be shown that the dynamics equations for an Euler–Bernoulli beam with uniform cross-section undergoing transversal, longitudinal and torsional vibrations are

$$(EI)_{z,i} \frac{\partial^4 y}{\partial x_1^4} + \bar{m}_i \frac{\partial^2 y}{\partial t^2} = f_y(x_1, t) - \frac{\partial}{\partial x_1} m_z(x_1, t) \quad (0 \leq x_1 \leq l_i) \quad (3.16)$$

$$(EI)_{y,i} \frac{\partial^4 z}{\partial x_1^4} + \bar{m}_i \frac{\partial^2 z}{\partial t^2} = f_z(x_1, t) + \frac{\partial}{\partial x_1} m_y(x_1, t) \quad (0 \leq x_1 \leq l_i) \quad (3.17)$$

$$\bar{m}_i \frac{\partial^2 x}{\partial t^2} - (EA)_i \frac{\partial^2 x}{\partial x_1^2} = f_x(x_1, t) \quad (0 \leq x_1 \leq l_i) \quad (3.18)$$

$$(\rho J_p)_i \frac{\partial^2 \theta_x}{\partial t^2} - (GJ_p)_i \frac{\partial^2 \theta_x}{\partial x_1^2} = m_x(x_1, t) \quad (0 \leq x_1 \leq l_i) \quad (3.19)$$

where $y(x_1, t)$, $z(x_1, t)$ and $x(x_1, t)$ denote the transverse and longitudinal displacements of any point on the beam relative to its equilibrium position, respectively. $\theta_x(x_1, t)$ is the torsion angle of an arbitrary cross-section on the beam relative to its equilibrium position. $f_x(x_1, t)$, $f_y(x_1, t)$ and $f_z(x_1, t)$ denote the components of an external distributional force on the beam in the x , y and z directions, respectively. $m_x(x_1, t)$, $m_y(x_1, t)$ and $m_z(x_1, t)$ are the components of an external distributed moment on the beam in the x , y and z directions, respectively.

The parameter matrices of the beam with transverse, longitudinal and torsional vibration simultaneously can be obtained by combining Equations (3.16) to (3.19) and writing them in the form of Equation (3.2):

$$\mathbf{v}_i = \begin{bmatrix} x \\ \theta_x \\ y \\ z \end{bmatrix}, \quad \mathbf{M}_i = \begin{bmatrix} \bar{m}_i & 0 & 0 & 0 \\ 0 & (\rho J_p)_i & 0 & 0 \\ 0 & 0 & \bar{m}_i & 0 \\ 0 & 0 & 0 & \bar{m}_i \end{bmatrix}, \quad \mathbf{f}_i = \begin{bmatrix} f_x(x_1, t) \\ m_x(x_1, t) \\ f_y(x_1, t) - \frac{\partial}{\partial x_1} m_z(x_1, t) \\ f_z(x_1, t) - \frac{\partial}{\partial x_1} m_y(x_1, t) \end{bmatrix}$$

$$\mathbf{K}_i = \begin{bmatrix} -(EA)_i \frac{\partial^2}{\partial x_1^2} & 0 & 0 & 0 \\ 0 & -(GJ_p)_i \frac{\partial^2}{\partial x_1^2} & 0 & 0 \\ 0 & 0 & (EI)_{z,i} \frac{\partial^4}{\partial x_1^4} & 0 \\ 0 & 0 & 0 & EI_{y,i} \frac{\partial^4}{\partial x_1^4} \end{bmatrix} \quad (0 \leq x_1 \leq l_i) \quad (3.20)$$

3.3 Basic Theory of the Orthogonality of Eigenvectors

3.3.1 Inner Product Space

Definition 3.1 Assuming V is a linear space in the real number field, define a real function of two variables in V , which is called the inner product, denoted by, $\langle \alpha, \beta \rangle$ if it has the following characteristics:

- 1) $\langle \alpha, \beta \rangle = \langle \beta, \alpha \rangle$ (exchangeability)
- 2) $\langle k\alpha, \beta \rangle = k \langle \alpha, \beta \rangle$ (homogeneity)

- 3) $\langle \alpha + \beta, \gamma \rangle = \langle \alpha, \gamma \rangle + \langle \beta, \gamma \rangle$ (distributivity)
 4) $\langle \alpha, \alpha \rangle \geq 0$, where $\langle \alpha, \alpha \rangle = 0$ if and only if $\alpha = 0$ (positive definite characteristic)

where α, β and γ are arbitrary vectors in V , and k is an arbitrary real number. Then, the linear space V is called the inner product space.

In a n -dimensional linear space R^n , the inner product of vectors

$$\alpha_1 = [a_1, a_2, \dots, a_n]^T, \quad \alpha_2 = [b_1, b_2, \dots, b_n]^T$$

is defined as

$$\langle \alpha_1, \alpha_2 \rangle = a_1 b_1 + a_2 b_2 + \dots + a_n b_n \quad (3.21)$$

The linear space R^n constitutes an inner product space with a finite dimension, and is called an Euclidean space.

In space $C(a, b)$ constituted by all real continuous functions in the closed interval $[a, b]$, the inner product of two functions $f(x)$ and $g(x)$ in $C(a, b)$ is defined as

$$\langle f(x), g(x) \rangle = \int_a^b f(x)g(x) dx \quad (3.22)$$

Then, $C(a, b)$ constitutes an (infinite-dimensional) inner product space.

Example 3.1 When the inner product space V is constituted by the mixed vector

$$v = \begin{bmatrix} \alpha \\ f \end{bmatrix} = [\alpha_1, \alpha_2, \dots, \alpha_m, f_1(x), f_2(x), \dots, f_n(x)]^T \quad (3.23)$$

composed of an arbitrary element $\alpha = [\alpha_1, \alpha_2, \dots, \alpha_m]^T$ in R^m and an arbitrary element $f = [f_1(x), f_2(x), \dots, f_n(x)]^T$ in $C^n(a, b)$, the inner product in space V is defined as

$$\langle v_1, v_2 \rangle = \langle \alpha, \beta \rangle + \langle f, g \rangle = \sum_{i=1}^m \alpha_i \beta_i + \sum_{i=1}^n \int_{a_i}^{b_i} f_i(x)g_i(x)dx \quad (3.24)$$

where V is an inner product space.

Definition 3.2 Non-negative real number $\sqrt{\langle \alpha, \alpha \rangle}$ is called the length of vector α , denoted by $|\alpha|$.

Definition 3.3 The angle $\angle(\alpha, \beta)$ between two nonzero vectors α, β is defined as

$$\angle(\alpha, \beta) = \arccos \frac{\langle \alpha, \beta \rangle}{|\alpha| \cdot |\beta|} \quad (0 \leq \angle(\alpha, \beta) \leq \pi) \quad (3.25)$$

Definition 3.4 If the inner product of two vectors α, β is zero, namely

$$\langle \alpha, \beta \rangle = 0 \quad (3.26)$$

then α, β are called orthogonal or mutually perpendicular, denoted by $\alpha \perp \beta$.

3.3.2 Conjugate Transformation and Symmetric Transformation

Definition 3.5 Supposing V and V' are two linear spaces in real number field P . σ is a mapping from V to V' if σ satisfies

- 1) $\sigma(\alpha + \beta) = \sigma(\alpha) + \sigma(\beta), \forall \alpha, \beta \in V$
 2) $\sigma(k\alpha) = k\sigma(\alpha), \forall \alpha \in V, \forall k \in P$

Hence, σ is called a linear mapping (or linear operator). In particular, the linear mapping from V to itself is called a linear transformation and the linear mapping from V to the basic field P is called a linear function.

Definition 3.6 Let σ be an arbitrary linear transformation in the n -dimensional Euclidean space, and its matrix in a standard orthogonal base $\mathbf{e}_1, \mathbf{e}_2, \dots, \mathbf{e}_n$ of V is A . Then, for A' , the corresponding linear transformation σ' is the conjugate (linear) transformation σ in the base $\mathbf{e}_1, \mathbf{e}_2, \dots, \mathbf{e}_n$. σ' is also called the transpose transformation of σ .

Symmetry transformation can be defined according to the definition of conjugate transformation. Symmetry transformation means the transformation σ and its conjugate transformation σ' are the same linear transformation, that is, $\sigma = \sigma'$. The necessary and sufficient condition for σ being a symmetry transformation in the inner product space V is that, for any arbitrary vectors α and β in V , there are

$$\langle \sigma(\alpha), \beta \rangle = \langle \alpha, \sigma(\beta) \rangle \quad (3.27)$$

It can be seen from Definition 3.5 that the definition of linear transformation is stricter than the definition of linear operator, but the symmetry of “operator” is enough and the symmetry of “transformation” is not needed for some situations. The following will expand the concept of “conjugate” and “symmetry” to linear operators, namely the conjugate operator and symmetry operator.

Definition 3.7 Let L and H be linear operators in the inner product space V . For any vectors of α, β in V , if there are

$$\langle L(\alpha), \beta \rangle = \langle \alpha, H(\beta) \rangle \quad (3.28)$$

then L and H are mutual conjugate operators. H is called the conjugate operator of L (or L is the conjugate operator of H) denoted by $H = L'$ (or $L = H'$). Furthermore, if

$$\langle L(\alpha), \beta \rangle = \langle \alpha, L(\beta) \rangle \quad (3.29)$$

then L is called a symmetry operator.

If $\mathbf{e}_1, \mathbf{e}_2, \dots, \mathbf{e}_n$ is a standard orthogonal base in the n -dimensional Euclidean space, σ' is the conjugate transformation of σ and

$$\langle \sigma(\mathbf{e}_j), \mathbf{e}_k \rangle = \langle \mathbf{e}_j, \sigma'(\mathbf{e}_k) \rangle \quad (3.30)$$

If σ is a linear transformation in the n -dimensional Euclidean space V , then the necessary and sufficient condition for τ being the conjugate transformation of σ is that for any vectors of α and β there are

$$\langle \sigma(\alpha), \beta \rangle = \langle \alpha, \tau(\beta) \rangle \quad (3.31)$$

Example 3.2 L is a linear operator in the inner product space $C'(a, b)$, which is composed of all infinite differential functions in the closed interval $[a, b]$. Find the necessary conditions for L being a symmetry operator in following situations:

- 1) L denotes the second-order derivative of a function, namely, there are $L(f(x)) = f''(x)$ for any arbitrary function $f(x)$ in $C'(a, b)$.
- 2) L denotes the fourth-order derivative of a function, namely, there are $L(f(x)) = f^{(4)}(x)$ for any arbitrary function $f(x)$ in $C'(a, b)$.

Solution

If L is a symmetry operator, then for arbitrary functions $f(x)$ and $g(x)$ in $C'(a, b)$ there are

$$\langle L(f(x)), g(x) \rangle = \langle f(x), L(g(x)) \rangle \quad (3.32)$$

1) If L denotes the second-order differential, according to integration by parts

$$\begin{aligned} \langle L(f(x)), g(x) \rangle &= \langle f''(x), g(x) \rangle = \int_a^b f''(x)g(x)dx = f'(x)g(x)\Big|_a^b - \int_a^b f'(x)g'(x)dx \\ \langle f(x), L(g(x)) \rangle &= \langle f(x), g''(x) \rangle = \int_a^b f(x)g''(x)dx = f(x)g'(x)\Big|_a^b - \int_a^b f'(x)g'(x)dx \end{aligned}$$

According to Equation (3.32), the necessary condition can be obtained:

$$f'(x)g(x)\Big|_a^b = f(x)g'(x)\Big|_a^b \quad (3.33)$$

2) Similarly, if L denotes the fourth-order differential

$$\begin{aligned} \langle L(f(x)), g(x) \rangle &= f'''(x)g(x)\Big|_a^b - f''(x)g'(x)\Big|_a^b + \int_a^b f''(x)g''(x)dx \\ \langle f(x), L(g(x)) \rangle &= f(x)g'''(x)\Big|_a^b - f'(x)g''(x)\Big|_a^b + \int_a^b f''(x)g''(x)dx \end{aligned} \quad (3.34)$$

According to Equation (3.32), the necessary condition can be obtained

$$f'''(x)g(x)\Big|_a^b - f''(x)g'(x)\Big|_a^b = f(x)g'''(x)\Big|_a^b - f'(x)g''(x)\Big|_a^b \quad (3.35)$$

Example 3.2 shows that in the space $C'(a, b)$ the linear operators of the second- or fourth-order derivatives are not symmetrical in general and the operators are symmetrical only in the space constructed by the functions that satisfy limited boundary conditions in $C'(a, b)$, for example limit the boundary conditions as $f(a)=f(b)=0$ or $f(a)=f'(b)=0$ in (1), and limit the boundary conditions as $f(a)=f(b)=f'(a)=f'(b)$ or $f(a)=f'(a)=f''(b)=f'''(b)=0$ in (2).

It can be seen from the basic theory of orthogonality of augmented eigenvectors how to construct a linear operator T which is symmetrical in the linear space V and to make the eigenvectors orthogonal with T in V . In other words, a new linear operator and a new eigenvector can be found that are different in a conventional sense and satisfy the symmetry automatically in the definition field. It is shown in the following that the eigenvectors and operators based on the above body dynamics equations are the new eigenvectors and operators.

3.4 Augmented Eigenvectors and their Orthogonality

In this section the new concept of augmented eigenvectors of MSs and their construction methods is introduced and it is verified that they satisfy orthogonality automatically.

3.4.1 Augmented Eigenvectors

The uniform expression of the body dynamics equation for any body element in a MS without considering damping forces is

$$\mathbf{M}_i \mathbf{v}_{i,tt} + \mathbf{K}_i \mathbf{v}_i = \mathbf{f}_i \quad (3.36)$$

and the uniform expression of the body dynamics equation of the MS is

$$\mathbf{M} \mathbf{v}_{tt} + \mathbf{K} \mathbf{v} = \mathbf{f} \quad (3.37)$$

where

$$\mathbf{M} = \begin{bmatrix} \mathbf{M}_{B_1} & & & \\ & \mathbf{M}_{B_2} & & \\ & & \ddots & \\ & & & \mathbf{M}_{B_n} \end{bmatrix}, \quad \mathbf{K} = \begin{bmatrix} \mathbf{K}_{B_1} & & & \\ & \mathbf{K}_{B_2} & & \\ & & \ddots & \\ & & & \mathbf{K}_{B_n} \end{bmatrix}, \quad \mathbf{v} = \begin{bmatrix} \mathbf{v}_{B_1} \\ \mathbf{v}_{B_2} \\ \vdots \\ \mathbf{v}_{B_n} \end{bmatrix}, \quad \mathbf{f} = \begin{bmatrix} \mathbf{f}_{B_1} \\ \mathbf{f}_{B_2} \\ \vdots \\ \mathbf{f}_{B_n} \end{bmatrix} \quad (3.38)$$

\mathbf{M} and \mathbf{K} are augmented operators presented originally in MSTMM, \mathbf{v} is the column matrix of the displacement coordinates of the system, \mathbf{f} is the column matrix of the external force of the system, the subscripts B_1, B_2, \dots and B_n are the sequence numbers of the body elements, and $\mathbf{M}_{B_i}, \mathbf{K}_{B_i}, \mathbf{v}_{B_i}$ and \mathbf{f}_{B_i} are the parameter matrices of body element B_i .

A new concept of augmented eigenvector V of the MS is defined as the column matrix of the modal coordinate corresponding to displacement coordinates of the MS:

$$\mathbf{V}^K = \left[\mathbf{V}_{B_1}^{kT}, \mathbf{V}_{B_2}^{kT}, \dots, \mathbf{V}_{B_n}^{kT} \right]^T \quad (k = 1, 2, \dots) \quad (3.39)$$

The augmented eigenvectors \mathbf{V}^k include the modal coordinates of displacements and angular displacements of each discrete element and the mode shape of each continuous element corresponding to the k th eigenfrequency ω_k of the system.

Applying modal technology, assume that

$$\mathbf{v} = \sum_{k=1}^{\infty} \mathbf{V}^k q^k(t) \quad (3.40)$$

where $q^k(t)$ is a generalized coordinate and the superscript k is the modal order.

The eigenvector covers only discrete variables for a discrete system or continuous functions for a continuous system. The two variables are included in the augmented eigenvector of a MRFS to describe discrete elements and continuous elements. They are different from the ordinary eigenfunctions of a continuous system and the eigenvectors of a discrete system. The eigenvectors for a discrete system consist only of discrete variables, while those for a continuous system consist only of continuous functions. However, both the discrete variables and the continuous functions should be included in the eigenvectors for a multi-rigid-flexible-body system which consists of discrete elements (rigid bodies) and continuous elements (flexible bodies) at the same time, and such an eigenvector is called the augmented eigenvector in this book. The eigenvectors for a discrete system, as well as those for a continuous system, are just special cases of the augmented eigenvector of a general MRFS. Substituting Equation (3.39) into Equation (3.37) yields

$$\sum_{k=1}^{\infty} \mathbf{M} \mathbf{V}^k \ddot{q}^k(t) + \sum_{k=1}^{\infty} \mathbf{K} \mathbf{V}^k q^k(t) = \mathbf{f} \quad (3.41)$$

For free vibration, namely $\mathbf{f} = \mathbf{0}$,

$$\sum_{k=1}^{\infty} \mathbf{M} \mathbf{V}^k \ddot{q}^k(t) + \sum_{k=1}^{\infty} \mathbf{K} \mathbf{V}^k q^k(t) = \mathbf{0} \quad (3.42)$$

Example 3.3 Write the global dynamics equation, the body dynamics equations and the augmented eigenvector of the free vibration system shown in Figure 3.1. The system is composed of an elastic joint, a rigid body and a uniform beam with constant section. The elasticity coefficients of the elastic joint in the x and y axes and the torsional stiffness in the z axis are $K_{x,1}$, $K_{y,1}$ and $K'_{z,1}$, respectively. The mass, width and height of the rigid body and the moment of inertia with respect to the spring connection point are m_2 , b , h and J_2 , respectively. The length, mass density per unit length, longitudinal stiffness and bending stiffness of the beam are l_3 , \bar{m}_3 , EA_3 and EI_3 , respectively

Solution

The free end of the beam is taken as the output end and the connection point of the spring and the ground is regarded as the input end. From the input to the output ends, the element numbers of the ground, elastic joint, rigid body, beam and free boundary are 0, 1, 2, 3 and 0, respectively. The column matrix of displacement of element 2 is $\mathbf{v}_2 = [x_{2,1}(t), y_{2,1}(t), \theta_{z2,1}(t)]^T$. The column matrix of displacement of an arbitrary point $P(x_3)$ on the beam is $\mathbf{v}_3 = [x(x_3, t), y(x_3, t)]^T$ ($0 < x_3 \leq l_3$). It can be proved that there are global dynamics equations of the undamped system vibrating in the plane

$$\left\{ \begin{array}{l} m_2 \ddot{x}_{2,1} - m_2 c_{c2} \ddot{\theta}_{z2,1} + K_{x,1} x_{2,1} - EA_3 \frac{\partial x(0, t)}{\partial x_3} = 0 \\ m_2 \ddot{y}_{2,1} + m_2 c_{c1} \ddot{\theta}_{z2,1} + K_{y,1} y_{2,1} + EI_3 \frac{\partial^3 y(0, t)}{\partial x_3^3} = 0 \\ -m_2 c_{c2} \ddot{x}_{2,1} + m_2 c_{c1} \ddot{y}_{2,1} + J_2 \ddot{\theta}_{z2,1} + K'_1 \theta_{z2,1} \\ - b_2 EA_3 \frac{\partial x(0, t)}{\partial x_3} - EI_3 \frac{\partial^2 y(0, t)}{\partial x_3^2} + b_1 EI_3 \frac{\partial^3 y(0, t)}{\partial x_3^3} = 0 \\ \bar{m}_3 \frac{\partial^2 x(x_3, t)}{\partial t^2} - EA_3 \frac{\partial^2 x(x_3, t)}{\partial x_3^2} = 0 \quad (0 \leq x_3 \leq l_3) \\ \bar{m}_3 \frac{\partial^2 y(x_3, t)}{\partial t^2} + EI_3 \frac{\partial^4 y(x_3, t)}{\partial x_3^4} = 0 \quad (0 \leq x_3 \leq l_3) \end{array} \right. \quad (3.43)$$

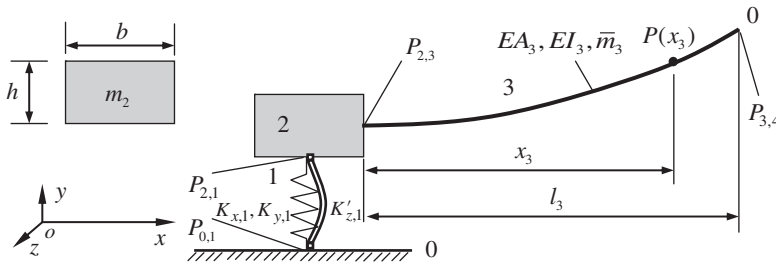


Figure 3.1 An MRFS vibrating in a plane.

The body dynamics equation of the system can be obtained using the MSTMM

$$\begin{bmatrix} \mathbf{M}_2 \\ \mathbf{M}_3 \end{bmatrix} \begin{bmatrix} \mathbf{v}_2 \\ \mathbf{v}_3 \end{bmatrix}_{tt} + \begin{bmatrix} \mathbf{K}_2 \\ \mathbf{K}_3 \end{bmatrix} \begin{bmatrix} \mathbf{v}_2 \\ \mathbf{v}_3 \end{bmatrix} = \mathbf{0} \quad (3.44)$$

where

$$\mathbf{M}_2 = \begin{bmatrix} m_2 & 0 & -m_2 c_{c2} \\ 0 & m_2 & m_2 c_{c1} \\ -m_2 c_{c2} & m_2 c_{c1} & J_2 \end{bmatrix}, \quad \mathbf{M}_3 = \begin{bmatrix} \bar{m}_3 & 0 \\ 0 & \bar{m}_3 \end{bmatrix} \quad (3.45)$$

$$\mathbf{K}_2 = \begin{bmatrix} -D^3|_{I,2} + D^3|_{O,2} & 0 & 0 \\ 0 & -D^3|_{I,2} + D^3|_{O,2} & 0 \\ -b_2 D^3|_{O,2} & b_1 D^3|_{O,2} & D^1|_{I,2} - D^1|_{O,2} \end{bmatrix}, \quad \mathbf{K}_3 = \begin{bmatrix} -EA_3 \frac{\partial^2}{\partial x_3^2} & 0 \\ 0 & EI_3 \frac{\partial^4}{\partial x_3^4} \end{bmatrix} \quad (3.46)$$

The augmented eigenvectors of the system are

$$\mathbf{V}^k = \begin{bmatrix} \mathbf{V}_2^k \\ \mathbf{V}_3^k \end{bmatrix} = [X_{2,1}^k, Y_{2,1}^k, \Theta_{z2,1}^k, X^k(x_3), Y^k(x_3)]^T \quad (k = 1, 2, \dots) \quad (3.47)$$

Obviously, the body dynamics equations of the system are just the combination of the body dynamics equation of each body element of the system. Their form is simple and convenient to write. The augmented eigenvectors include three discrete variables and two continuous functions used to describe the motion of rigid body 2 and beam 3, respectively.

3.4.2 Orthogonality of Augmented Eigenvectors

The orthogonality of the augmented eigenvectors $\mathbf{V}^k (k = 1, 2, \dots)$ with respect to \mathbf{M} and \mathbf{K} indicates that

$$\langle \mathbf{M} \mathbf{V}^k, \mathbf{V}^p \rangle = \delta_{k,p} M_p, \quad \langle \mathbf{K} \mathbf{V}^k, \mathbf{V}^p \rangle = \delta_{k,p} K_p \quad (3.48)$$

where $M_p, K_p = \omega_p^2 M_p$ and ω_p are the modal mass, modal stiffness and eigenfrequency of the system of p order, respectively.

It can be proved that the orthogonality Equation (3.48) can be satisfied by the augmented eigenvectors $\mathbf{V}^k (k = 1, 2, \dots)$ introduced in this book, and this is a very important characteristic of augmented eigenvectors.

For free vibration, the generalized coordinate $q^k(t)$ is a harmonic function with eigenfrequency ω_k , thus Equation (3.41) becomes

$$\sum_{k=1}^{+\infty} [-\omega_k^2 \mathbf{M} \mathbf{V}^k + \mathbf{K} \mathbf{V}^k] q^k(t) = \mathbf{0} \quad (3.49)$$

where $q^k(t)$ is mutually independent, therefore

$$-\omega_k^2 \mathbf{M} \mathbf{V}^k + \mathbf{K} \mathbf{V}^k = \mathbf{0} \quad (3.50)$$

namely

$$\omega_k^2 \mathbf{M} \mathbf{V}^k = \mathbf{K} \mathbf{V}^k \quad (k = 1, 2, \dots) \quad (3.51)$$

If augmented eigenvectors $\mathbf{V}^k (k = 1, 2, \dots)$ are symmetrical with respect to operators \mathbf{M} and \mathbf{K} , namely

$$\begin{cases} \langle \mathbf{M} \mathbf{V}^k, \mathbf{V}^p \rangle = \langle \mathbf{V}^k, \mathbf{M} \mathbf{V}^p \rangle \\ \langle \mathbf{K} \mathbf{V}^k, \mathbf{V}^p \rangle = \langle \mathbf{V}^k, \mathbf{K} \mathbf{V}^p \rangle \end{cases} \quad (3.52)$$

then

$$\begin{aligned} \omega_k^2 \langle \mathbf{M} \mathbf{V}^k, \mathbf{V}^p \rangle &= \langle \omega_k^2 \mathbf{M} \mathbf{V}^k, \mathbf{V}^p \rangle = \langle \mathbf{K} \mathbf{V}^k, \mathbf{V}^p \rangle \\ &= \langle \mathbf{V}^k, \mathbf{K} \mathbf{V}^p \rangle = \langle \mathbf{V}^k, \omega_p^2 \mathbf{M} \mathbf{V}^p \rangle = \omega_p^2 \langle \mathbf{M} \mathbf{V}^k, \mathbf{V}^p \rangle \end{aligned}$$

namely

$$(\omega_k^2 - \omega_p^2) \langle \mathbf{M} \mathbf{V}^k, \mathbf{V}^p \rangle = 0 \quad (3.53)$$

For $\omega_k^2 \neq \omega_p^2$, this leads to

$$\langle \mathbf{M} \mathbf{V}^k, \mathbf{V}^p \rangle = \delta_{k,p} M_p$$

Similarly

$$\langle \mathbf{K} \mathbf{V}^k, \mathbf{V}^p \rangle = \delta_{k,p} K_p$$

In summary, whether the augmented eigenvectors of a system do or do not satisfy the orthogonality, namely whether Equation (3.52) holds or not, depends on whether or not the augmented eigenvectors \mathbf{V}^k of a MS are symmetrical to the augmented operators \mathbf{M} and \mathbf{K} .

3.4.3 Symmetry of Augmented Eigenvectors about Augmented Operator \mathbf{M}

The inner products related to the augmented eigenvectors could be decomposed as

$$\langle \mathbf{M} \mathbf{V}^k, \mathbf{V}^p \rangle = \sum_{B_i} \langle \mathbf{M}_{B_i} \mathbf{V}_{B_i}^k, \mathbf{V}_{B_i}^p \rangle, \quad \langle \mathbf{K} \mathbf{V}^k, \mathbf{V}^p \rangle = \sum_{B_i} \langle \mathbf{K}_{B_i} \mathbf{V}_{B_i}^k, \mathbf{V}_{B_i}^p \rangle \quad (3.54)$$

where \sum_{B_i} denotes the summation of the inner product corresponding to each body element. \mathbf{M}_{B_i} is always a real symmetrical matrix for any kind of body element, that is

$$\mathbf{M}_{B_i}^T = \mathbf{M}_{B_i} \quad (3.55)$$

therefore

$$\langle \mathbf{M}_{B_i} \mathbf{V}_{B_i}^k, \mathbf{V}_{B_i}^p \rangle = \langle \mathbf{V}_{B_i}^k, \mathbf{M}_{B_i}^T \mathbf{V}_{B_i}^p \rangle = \langle \mathbf{V}_{B_i}^k, \mathbf{M}_{B_i} \mathbf{V}_{B_i}^p \rangle \quad (3.56)$$

or

$$\langle \mathbf{M} \mathbf{V}^k, \mathbf{V}^p \rangle = \sum_{B_i} \langle \mathbf{M}_{B_i} \mathbf{V}_{B_i}^k, \mathbf{V}_{B_i}^p \rangle = \sum_{B_i} \langle \mathbf{V}_{B_i}^k, \mathbf{M}_{B_i} \mathbf{V}_{B_i}^p \rangle = \langle \mathbf{V}^k, \mathbf{M} \mathbf{V}^p \rangle \quad (3.57)$$

The parameter matrix of the mass of each body element is a real symmetrical matrix, and the augmented eigenvectors are symmetrical about the augmented operator \mathbf{M} and the first formula in Equation (3.52) holds automatically.

3.4.4 Symmetry of Augmented Eigenvectors about Augmented Operators K

The symmetry of \mathbf{V}_{B_i} about \mathbf{K}_{B_i} will be discussed as follows. For simplicity, the \mathbf{K}_{B_i} involved in Equations (3.7), (3.14) and (3.20) which correspond to a lumped mass, a rigid body and a beam, respectively, are selected to illustrate the ideas.

3.4.4.1 $\langle \mathbf{K}_{B_i} \mathbf{V}_{B_i}^k, \mathbf{V}_{B_i}^p \rangle$ of a Lumped Mass Vibrating in Space

For a lumped mass with spatial vibrations

$$\mathbf{K}_{B_i} = \begin{bmatrix} -D^3|_{I,B_i} + D^3|_{O,B_i} & 0 & 0 \\ 0 & -D^3|_{I,B_i} + D^3|_{O,B_i} & 0 \\ 0 & 0 & -D^3|_{I,B_i} + D^3|_{O,B_i} \end{bmatrix}, \quad \mathbf{V}_{B_i} = \begin{bmatrix} X_{I,B_i} \\ Y_{I,B_i} \\ Z_{I,B_i} \end{bmatrix} \quad (3.58)$$

$$\begin{aligned} \langle \mathbf{K}_{B_i} \mathbf{V}_{B_i}^k, \mathbf{V}_{B_i}^p \rangle &= \left\langle \begin{bmatrix} -Q_{x,I,B_i}^k + Q_{x,O,B_i}^k \\ -Q_{y,I,B_i}^k + Q_{y,O,B_i}^k \\ -Q_{z,I,B_i}^k + Q_{z,O,B_i}^k \end{bmatrix}, \begin{bmatrix} X_{I,B_i}^p \\ Y_{I,B_i}^p \\ Z_{I,B_i}^p \end{bmatrix} \right\rangle \\ &= -Q_{x,I,B_i}^k X_{I,B_i}^p - Q_{y,I,B_i}^k Y_{I,B_i}^p - Q_{z,I,B_i}^k Z_{I,B_i}^p + Q_{x,O,B_i}^k X_{I,B_i}^p + Q_{y,O,B_i}^k Y_{I,B_i}^p + Q_{z,O,B_i}^k Z_{I,B_i}^p \end{aligned}$$

Let $\mathbf{R}_{I,B_i}^T = [X_{I,B_i}, Y_{I,B_i}, Z_{I,B_i}]^T$ and $\mathbf{R}_{O,B_i}^T = [X_{O,B_i}, Y_{O,B_i}, Z_{O,B_i}]^T$. According to the continuous condition of a lumped mass $\mathbf{R}_{I,B_i}^T = \mathbf{R}_{O,B_i}^T$, so

$$\langle \mathbf{K}_{B_i} \mathbf{V}_{B_i}^k, \mathbf{V}_{B_i}^p \rangle = -\left(\mathbf{R}_{I,B_i}^p\right)^T \mathbf{Q}_{I,B_i}^k + \left(\mathbf{R}_{O,B_i}^p\right)^T \mathbf{Q}_{O,B_i}^k \quad (3.59)$$

where $\mathbf{Q}_{I,B_i} = [Q_{x,I,B_i}, Q_{y,I,B_i}, Q_{z,I,B_i}]^T$ and $\mathbf{Q}_{O,B_i} = [Q_{x,O,B_i}, Q_{y,O,B_i}, Q_{z,O,B_i}]^T$ denote the internal force of the system at the input and output ends, respectively, except for damping forces, which are correlated to the connected relations of a lumped mass in an MS.

For example, when a lumped mass B_i is connected to the lumped masses $B_i - 2$ and $B_i + 2$ by springs $B_i - 1$ and $B_i + 1$ in the input and output ends, respectively, we obtain

$$\begin{cases} \mathbf{Q}_{I,B_i} = [Q_{x,B_i,B_i-1}, Q_{y,B_i,B_i-1}, Q_{z,B_i,B_i-1}]^T = -[K_{B_i-1}](\mathbf{R}_{B_i,B_i-1} - \mathbf{R}_{B_i-2,B_i-1}) \\ \mathbf{Q}_{O,B_i} = [Q_{x,B_i,B_i+1}, Q_{y,B_i,B_i+1}, Q_{z,B_i,B_i+1}]^T = -[K_{B_i+1}](\mathbf{R}_{B_i+2,B_i+1} - \mathbf{R}_{B_i,B_i+1}) \end{cases} \quad (3.60)$$

where

$$[K_{B_i-1}] = \begin{bmatrix} K_{x,B_i-1} & 0 & 0 \\ 0 & K_{y,B_i-1} & 0 \\ 0 & 0 & K_{z,B_i-1} \end{bmatrix}, \quad \mathbf{R}_{B_i,B_i-1} = \begin{bmatrix} X_{B_i,B_i-1} \\ Y_{B_i,B_i-1} \\ Z_{B_i,B_i-1} \end{bmatrix}, \quad \mathbf{R}_{B_i-2,B_i-1} = \begin{bmatrix} X_{B_i-2,B_i-1} \\ Y_{B_i-2,B_i-1} \\ Z_{B_i-2,B_i-1} \end{bmatrix}$$

$$[K_{B_i+1}] = \begin{bmatrix} K_{x,B_i+1} & 0 & 0 \\ 0 & K_{y,B_i+1} & 0 \\ 0 & 0 & K_{z,B_i+1} \end{bmatrix}, \quad \mathbf{R}_{B_i+2,B_i+1} = \begin{bmatrix} X_{B_i+2,B_i+1} \\ Y_{B_i+2,B_i+1} \\ Z_{B_i+2,B_i+1} \end{bmatrix}, \quad \mathbf{R}_{B_i,B_i+1} = \begin{bmatrix} X_{B_i,B_i+1} \\ Y_{B_i,B_i+1} \\ Z_{B_i,B_i+1} \end{bmatrix}$$

Substituting Equation (3.60) into Equation (3.59) yields

$$\begin{aligned} \langle \mathbf{K}_{B_i} \mathbf{V}_{B_i}^k, \mathbf{V}_{B_i}^p \rangle &= \left(\mathbf{R}_{B_i,B_i-1}^p \right)^T [K_{B_i-1}] \mathbf{R}_{B_i,B_i-1}^k + \left(\mathbf{R}_{B_i,B_i+1}^p \right)^T [K_{B_i+1}] \mathbf{R}_{B_i,B_i+1}^k \\ &\quad - \left(\mathbf{R}_{B_i,B_i-1}^p \right)^T [K_{B_i-1}] \mathbf{R}_{B_i-2,B_i-1}^k - \left(\mathbf{R}_{B_i,B_i+1}^p \right)^T [K_{B_i+1}] \mathbf{R}_{B_i+2,B_i+1}^k \end{aligned} \quad (3.61)$$

The superscripts k and p are symmetrical for the first two terms and unsymmetrical for the last two terms in Equation (3.61), therefore \mathbf{V}_{B_i} is unsymmetrical about \mathbf{K}_{B_i} in general. The signs of $\langle \mathbf{K}_{B_i} \mathbf{V}_{B_i}^k, \mathbf{V}_{B_i}^p \rangle$ are opposite, corresponding to the input and output ends.

3.4.4.2 $\langle \mathbf{K}_{B_i} \mathbf{V}_{B_i}^k, \mathbf{V}_{B_i}^p \rangle$ of a Rigid Body Vibrating in Space

For a rigid body vibrating in space with N input and L output ends

$$\begin{aligned} \mathbf{K}_{B_i} &= \begin{bmatrix} -\sum_{n=1}^N \mathbf{I}_3 \mathbf{D}^3|_{I_n, B_i} + \sum_{l=1}^L \mathbf{I}_3 \mathbf{D}^3|_{O_l, B_i} & \mathbf{O}_{3 \times 3} \\ -\sum_{n=2}^N \tilde{\mathbf{I}}_{I_1 I_n} \mathbf{D}^3|_{I_n, B_i} + \sum_{l=1}^L \tilde{\mathbf{I}}_{I_1 O_l} \mathbf{D}^3|_{O_l, B_i} & \sum_{n=1}^N \mathbf{I}_3 \mathbf{D}^1|_{I_n, B_i} - \sum_{l=1}^L \mathbf{I}_3 \mathbf{D}^1|_{O_l, B_i} \end{bmatrix}, \quad \mathbf{V}_{B_i} = \begin{bmatrix} \mathbf{R}_{I_1, B_i} \\ \boldsymbol{\theta}_{I_1, B_i} \end{bmatrix} \\ \langle \mathbf{K}_{B_i} \mathbf{V}_{B_i}^k, \mathbf{V}_{B_i}^p \rangle &= - \left(\mathbf{R}_{I_1, B_i}^p \right)^T \sum_{n=1}^N \mathbf{Q}_{I_n, B_i}^k + \left(\boldsymbol{\theta}_{I_1, B_i}^p \right)^T \sum_{n=2}^N \tilde{\mathbf{I}}_{I_1 I_n, B_i} \mathbf{Q}_{I_n, B_i}^k + \left(\boldsymbol{\theta}_{I_1, B_i}^p \right)^T \sum_{n=1}^N \mathbf{M}_{I_n, B_i}^k \\ &\quad + \left(\mathbf{R}_{I_1, B_i}^p \right)^T \sum_{l=1}^L \mathbf{Q}_{O_l, B_i}^k + \left(\boldsymbol{\theta}_{I_1, B_i}^p \right)^T \sum_{l=1}^L \tilde{\mathbf{I}}_{I_1 O_l, B_i} \mathbf{Q}_{O_l, B_i}^k - \left(\boldsymbol{\theta}_{I_1, B_i}^p \right)^T \sum_{l=1}^L \mathbf{M}_{O_l, B_i}^k \end{aligned}$$

According to the geometry relations of a rigid body

$$\mathbf{R}_{I_1, B_i}^p - \tilde{\mathbf{I}}_{I_1 I_n, B_i} \boldsymbol{\theta}_{I_1, B_i}^p = \mathbf{R}_{I_n, B_i}^p, \quad \mathbf{R}_{I_1, B_i}^p - \tilde{\mathbf{I}}_{I_1 O_l, B_i} \boldsymbol{\theta}_{I_1, B_i}^p = \mathbf{R}_{O_l, B_i}^p, \quad \boldsymbol{\theta}_{I_1, B_i}^p = \boldsymbol{\theta}_{I_n, B_i}^p = \boldsymbol{\theta}_{O_l, B_i}^p$$

therefore

$$\begin{aligned} \langle \mathbf{K}_{B_i} \mathbf{V}_{B_i}^k, \mathbf{V}_{B_i}^p \rangle &= - \sum_{n=1}^N \left[\left(\mathbf{R}_{I_1, B_i}^p - \tilde{\mathbf{I}}_{I_1 I_n, B_i} \boldsymbol{\theta}_{I_1, B_i}^p \right)^T \mathbf{Q}_{I_n, B_i}^k - \left(\boldsymbol{\theta}_{I_n, B_i}^p \right)^T \mathbf{M}_{I_n, B_i}^k \right] \\ &\quad + \sum_{l=1}^L \left[\left(\mathbf{R}_{I_1, B_i}^p - \tilde{\mathbf{I}}_{I_1 O_l, B_i} \boldsymbol{\theta}_{I_1, B_i}^p \right)^T \mathbf{Q}_{O_l, B_i}^k - \left(\boldsymbol{\theta}_{O_l, B_i}^p \right)^T \mathbf{M}_{O_l, B_i}^k \right] \\ &= - \sum_{n=1}^N \left\{ \left[\mathbf{R}_{I_n, B_i}^p \right]^T \mathbf{Q}_{O_l, B_i}^k - \left[\boldsymbol{\theta}_{I_n, B_i}^p \right]^T \mathbf{M}_{I_n, B_i}^k \right\} + \sum_{l=1}^L \left\{ \left[\mathbf{R}_{O_l, B_i}^p \right]^T \mathbf{Q}_{O_l, B_i}^k - \left[\boldsymbol{\theta}_{O_l, B_i}^p \right]^T \mathbf{M}_{O_l, B_i}^k \right\} \end{aligned} \quad (3.62)$$

Equations (3.62) and (3.59) have the same form and physical meaning, but the signs of $\langle \mathbf{K}_{B_i} \mathbf{V}_{B_i}^k, \mathbf{V}_{B_i}^p \rangle$ are opposite, corresponding to the input and output ends.

3.4.4.3 $\langle K_{B_i} V_{B_i}^k, V_{B_i}^p \rangle$ of a Beam Simultaneously Vibrating Transversely, Longitudinally and Torsionally

For a Euler–Bernoulli beam with uniform and constant sections simultaneously vibrating transversely, longitudinally and torsionally, we have

$$K_{B_i} = \begin{bmatrix} -EA_{B_i} \frac{\partial^2}{\partial x_{B_i}^2} & 0 & 0 & 0 \\ 0 & -(GJ_p)_{B_i} \frac{\partial^2}{\partial x_{B_i}^2} & 0 & 0 \\ 0 & 0 & EI_{z,B_i} \frac{\partial^4}{\partial x_{B_i}^4} & 0 \\ 0 & 0 & 0 & EI_{y,B_i} \frac{\partial^4}{\partial x_{B_i}^4} \end{bmatrix}, \quad V_{B_i} = \begin{bmatrix} X(x_{B_i}) \\ \Theta_x(x_{B_i}) \\ Y(x_{B_i}) \\ Z(x_{B_i}) \end{bmatrix} \quad (3.63)$$

Thus

$$\begin{aligned} & \langle K_{B_i} V_{B_i}^k, V_{B_i}^p \rangle \\ &= - \int_0^l X^p(x_{B_i}) EA_{B_i} \frac{d^2 X^k(x_{B_i})}{dx_{B_i}^2} dx_{B_i} - \int_0^l \Theta_x^p(x_{B_i}) (GJ_p)_{B_i} \frac{d^2 \Theta_x^k(x_{B_i})}{dx_{B_i}^2} dx_{B_i} \\ &+ \int_0^l Y^p(x_{B_i}) EI_{z,B_i} \frac{d^4 Y^k(x_{B_i})}{dx_{B_i}^4} dx_{B_i} + \int_0^l Z^p(x_{B_i}) EI_{y,B_i} \frac{d^4 Z^k(x_{B_i})}{dx_{B_i}^4} dx_{B_i} \\ &= -X^p(x_{B_i}) EA_{B_i} \frac{dX^k(x_{B_i})}{dx_{B_i}} \Big|_0^l + \int_0^l \frac{dX^p(x_{B_i})}{dx_{B_i}} EA_{B_i} \frac{dX^k(x_{B_i})}{dx_{B_i}} dx_{B_i} \\ &- \Theta_x^p(x_{B_i}) (GJ_p)_{B_i} \frac{d\Theta_x^k(x_{B_i})}{dx_{B_i}} \Big|_0^l + \int_0^l \frac{d\Theta_x^p(x_{B_i})}{dx_{B_i}} (GJ_p)_{B_i} \frac{d\Theta_x^k(x_{B_i})}{dx_{B_i}} dx_{B_i} \\ &+ Y^p(x_{B_i}) EI_{z,B_i} \frac{d^3 Y^k(x_{B_i})}{dx_{B_i}^3} \Big|_0^l - \frac{dY^p(x_{B_i})}{dx_{B_i}} EI_{z,B_i} \frac{d^2 Y^k(x_{B_i})}{dx_{B_i}^2} \Big|_0^l + \int_0^l \frac{d^2 Y^p(x_{B_i})}{dx_{B_i}^2} EI_{z,B_i} \frac{d^2 Y^k(x_{B_i})}{dx_{B_i}^2} dx_{B_i} \\ &+ Z^p(x_{B_i}) EI_{y,B_i} \frac{d^3 Z^k(x_{B_i})}{dx_{B_i}^3} \Big|_0^l - \frac{dZ^p(x_{B_i})}{dx_{B_i}} EI_{y,B_i} \frac{d^2 Z^k(x_{B_i})}{dx_{B_i}^2} \Big|_0^l + \int_0^l \frac{d^2 Z^p(x_{B_i})}{dx_{B_i}^2} EI_{y,B_i} \frac{d^2 Z^k(x_{B_i})}{dx_{B_i}^2} dx_{B_i} \end{aligned}$$

By the constitutive relations of a beam, we obtain

$$\begin{aligned} \langle K_{B_i} V_{B_i}^k, V_{B_i}^p \rangle &= - \left[\left(R_{I,B_i}^p \right)^T Q_{I,B_i}^k - \left(\Theta_{I,B_i}^p \right)^T M_{I,B_i}^k \right] + \left[\left(R_{O,B_i}^p \right)^T Q_{O,B_i}^k - \left(\Theta_{O,B_i}^p \right)^T M_{O,B_i}^k \right] \\ &+ \int_0^l \frac{dX^p(x_{B_i})}{dx_{B_i}} EA_{B_i} \frac{dX^k(x_{B_i})}{dx_{B_i}} dx_{B_i} + \int_0^l \frac{d\Theta_x^p(x_{B_i})}{dx_{B_i}} (GJ_p)_{B_i} \frac{d\Theta_x^k(x_{B_i})}{dx_{B_i}} dx_{B_i} \\ &+ \int_0^l \frac{d^2 Y^p(x_{B_i})}{dx_{B_i}^2} EI_{z,B_i} \frac{d^2 Y^k(x_{B_i})}{dx_{B_i}^2} dx_{B_i} + \int_0^l \frac{d^2 Z^p(x_{B_i})}{dx_{B_i}^2} EI_{y,B_i} \frac{d^2 Z^k(x_{B_i})}{dx_{B_i}^2} dx_{B_i} \end{aligned} \quad (3.64)$$

It can be seen from Equation (3.64) that the superscripts k and p are symmetrical for the four integral terms of the right-hand side and unsymmetrical for terms related to the ends of the beam in general. These terms have the same physical meaning as Equation (3.59), and the signs of $\langle K_{B_i} V_{B_i}^k, V_{B_i}^p \rangle$ are opposite, corresponding to the input and output ends.

It can be seen from this discussion about the three kinds of typical body elements that V_{B_i} is unsymmetrical about K_{B_i} in general and the signs of $\langle K_{B_i} V_{B_i}^k, V_{B_i}^p \rangle$ are opposite, corresponding to the input and output ends. The stiffness parameter matrix K_{B_i} of a body element is an unsymmetrical matrix and the orthogonality of the augmented eigenvector V about augmented operator K should be proved from the point view of the system. We will prove V is symmetrical about K from the connection relations of the hinge elements and the boundary conditions of the system. For a rigid body, lumped mass or beam, the general unsymmetrical term about superscripts k and p of $\langle K_{B_i} V_{B_i}^k, V_{B_i}^p \rangle$ is

$$\left[(R_P^p)^T Q_P^k - (\Theta_P^p)^T M_P^k \right] \quad (3.65)$$

where the subscript P denotes the connection point.

These terms are all the products of internal force and displacement of the connection point or internal moment and angular displacement, and the signs are always negative for the input end and positive for the output end of the body element:

$$\begin{aligned} \langle K V^k, V^p \rangle &= \sum_{B_i} \langle K_{B_i} V_{B_i}^k, V_{B_i}^p \rangle \\ &= - \sum_{P_I} \left[(R_{P_I}^p)^T Q_{P_I}^k - (\Theta_{P_I}^p)^T M_{P_I}^k \right] + \sum_{P_O} \left[(R_{P_O}^p)^T Q_{P_O}^k - (\Theta_{P_O}^p)^T M_{P_O}^k \right] + S \end{aligned} \quad (3.66)$$

where P_I and P_O are the set constituted by the input and output ends, respectively, of all body elements in the system, P_I and P_O are the elements corresponding to P_I and P_O , and S is the summation of symmetrical terms about k and p in $\langle K_{B_i} V_{B_i}^k, V_{B_i}^p \rangle$.

For an MRFS composed of rigid bodies, lumped masses and beams connected by various hinges, the connection points are the input end (or output end) of one element and the output end (or input end) of another, except for the boundary ends. Hence, only the parameters of the input and output ends of the body elements are involved for the first two terms of the right-hand side of Equation (3.66), which can be classified into the following six cases in which k and p are symmetrical.

- 1) The input end of a body element is the input boundary of the system.

Such a point is denoted by P in the first term of the right-hand side of Equation (3.64), $P_I = P \in P_I$, therefore for homogeneous boundary conditions there are always

$$- \left[(R_{P_I}^p)^T Q_{P_I}^k - (\Theta_{P_I}^p)^T M_{P_I}^k \right] \Big|_{P_I=P} = 0 \quad (3.67)$$

Obviously, k and p are symmetrical in Equation (3.67).

- 2) The output end of the body element is the output boundary of the system.

Such a point is denoted by P in the second term on the right-hand side of Equation (3.66), $P_O = P \in P_O$, therefore for homogeneous boundary conditions there are always

$$\left[(R_{P_O}^p)^T Q_{P_O}^k - (\Theta_{P_O}^p)^T M_{P_O}^k \right] \Big|_{P_O=P} = 0 \quad (3.68)$$

Obviously, k and p are symmetrical in Equation (3.68).

- 3) The input end of the body element is the output end of another body element.

This point is denoted by P in the first term on the right-hand side of Equation (3.66), $P_I = P \in \mathbf{P}_I$. This point is also denoted by P in the second term on the right-hand side of Equation (3.66), $P_O = P \in \mathbf{P}_O$:

$$\begin{aligned} & - \left[(\mathbf{R}_{P_I}^p)^T \mathbf{Q}_{P_I}^k - (\boldsymbol{\theta}_{P_I}^p)^T \mathbf{M}_{P_I}^k \right] \Big|_{P_I=P} + \left[(\mathbf{R}_{P_O}^p)^T \mathbf{Q}_{P_O}^k - (\boldsymbol{\theta}_{P_O}^p)^T \mathbf{M}_{P_O}^k \right] \Big|_{P_O=P} \\ & = - \left[(\mathbf{R}_P^p)^T \mathbf{Q}_P^k - (\boldsymbol{\theta}_P^p)^T \mathbf{M}_P^k \right] + \left[(\mathbf{R}_P^p)^T \mathbf{Q}_P^k - (\boldsymbol{\theta}_P^p)^T \mathbf{M}_P^k \right] = 0 \end{aligned} \quad (3.69)$$

Obviously, k and p are symmetrical in Equation (3.69).

- 4) The input end of the body element is the output end of the hinge element.

This point is denoted by B_I in the first term of the right-hand side of Equation (3.66) and the input end of the body element. The output end of the hinge element is denoted by J_O . B_I and J_O are the same points, namely $P_I = B_I = J_O \in \mathbf{P}_I$. Suppose that the input end of the hinge element is J_I and this must be the output end of the other body element. This point is included in the second term of the right-hand side of Equation (3.66), namely, $P_O = J_I \in \mathbf{P}_O$. Since the internal forces (moments) are always equal for the input and output ends of the hinge element, namely

$$\mathbf{Q}_{J_O}^k = \mathbf{Q}_{J_I}^k, \quad \mathbf{M}_{J_O}^k = \mathbf{M}_{J_I}^k \quad (3.70)$$

then

$$\begin{aligned} & - \left[(\mathbf{R}_{P_I}^p)^T \mathbf{Q}_{P_I}^k - (\boldsymbol{\theta}_{P_I}^p)^T \mathbf{M}_{P_I}^k \right] \Big|_{P_I=B_I=J_O} + \left[(\mathbf{R}_{P_O}^p)^T \mathbf{Q}_{P_O}^k - (\boldsymbol{\theta}_{P_O}^p)^T \mathbf{M}_{P_O}^k \right] \Big|_{P_O=J_I} \\ & = - \left[(\mathbf{R}_{J_O}^p)^T \mathbf{Q}_{J_O}^k - (\boldsymbol{\theta}_{J_O}^p)^T \mathbf{M}_{J_O}^k \right] + \left[(\mathbf{R}_{J_I}^p)^T \mathbf{Q}_{J_I}^k - (\boldsymbol{\theta}_{J_I}^p)^T \mathbf{M}_{J_I}^k \right] \\ & = - \left[(\mathbf{R}_{J_O}^p)^T - (\mathbf{R}_{J_I}^p)^T \right] \mathbf{Q}_{J_I}^k + \left[(\boldsymbol{\theta}_{J_O}^p)^T - (\boldsymbol{\theta}_{J_I}^p)^T \right] \mathbf{M}_{J_I}^k \end{aligned} \quad (3.71)$$

For a linear system, the internal force and the internal moment are linearly correlated to the deformations of the hinge in the following forms

$$\mathbf{R}_{J_I} - \mathbf{R}_{J_O} = [\mathbf{K}_J]^{-1} \mathbf{Q}_{J_I}, \quad \boldsymbol{\theta}_{J_O} - \boldsymbol{\theta}_{J_I} = [\mathbf{K}'_J]^{-1} \mathbf{M}_{J_I} \quad (3.72)$$

where $[\mathbf{K}_J]$ and $[\mathbf{K}'_J]$ denote the stiffness coefficient matrices of the hinge element J . They are the real constant symmetrical matrix

$$[\mathbf{K}_J] = [\mathbf{K}_J]^T, \quad [\mathbf{K}'_J] = [\mathbf{K}'_J]^T.$$

Substituting Equation (3.58) into Equation (3.57), we obtain

$$\begin{aligned} & - \left[(\mathbf{R}_{P_I}^p)^T \mathbf{Q}_{P_I}^k - (\boldsymbol{\theta}_{P_I}^p)^T \mathbf{M}_{P_I}^k \right] \Big|_{P_I=B_I=J_O} + \left[(\mathbf{R}_{P_O}^p)^T \mathbf{Q}_{P_O}^k - (\boldsymbol{\theta}_{P_O}^p)^T \mathbf{M}_{P_O}^k \right] \Big|_{P_O=J_I} \\ & = ([\mathbf{K}_J]^{-1} \mathbf{Q}_{J_I}^p)^T \mathbf{Q}_{J_I}^k + ([\mathbf{K}'_J]^{-1} \mathbf{M}_{J_I}^p)^T \mathbf{M}_{J_I}^k \\ & = (\mathbf{Q}_{J_I}^p)^T [\mathbf{K}_J]^{-1} \mathbf{Q}_{J_I}^k + (\mathbf{M}_{J_I}^p)^T [\mathbf{K}'_J]^{-1} \mathbf{M}_{J_I}^k \end{aligned} \quad (3.73)$$

Obviously, k and p are symmetrical in Equation (3.73).

- 5) The output end of a body element is the input end of another body element.
The proof of this is the same as (3), and k and p are symmetrical.
- 6) The output end of a body element is the input end of the hinge element.
The proof of this is similar to (4), where k and p are symmetrical, and we will not discuss this in detail.

In summary, the superscripts k and p in Equation (3.66) are symmetrical for a real system, therefore the augmented eigenvector is symmetrical about the augmented operator \mathbf{K} and the second equation in Equation (3.52) is satisfied automatically.

3.5 Examples of the Orthogonality of Augmented Eigenvectors

Augmented eigenvector orthogonality covers the orthogonality of the *eigenfunctions* of a continuous system and the *eigenvectors* of a discrete system, thus both of them can be regarded as special cases of the orthogonality for augmented eigenvectors of MRFS.

Example 3.4 Prove that the augmented eigenvector of the chain discrete system shown in Figure 2.22 satisfies the orthogonality.

Solution

There are four rigid bodies in this system, and the free vibration equation of each rigid body can be written in the form of Equation (3.2), namely

$$\mathbf{M}_i = \begin{bmatrix} m_i & 0 & -m_i c_{c2} \\ 0 & m_i & m_i c_{c1} \\ -m_i c_{c2} & m_i c_{c1} & J_i \end{bmatrix}, \quad \mathbf{v}_i = \begin{bmatrix} x_{i,i-1} \\ y_{i,i-1} \\ \theta_{zi,i-1} \end{bmatrix}$$

$$\mathbf{K}_i = \begin{bmatrix} -D^3|_{L,i} + D^3|_{O,i} & 0 & 0 \\ 0 & -D^3|_{L,i} + D^3|_{O,i} & 0 \\ -b_2 D^3|_{O,i} & b_1 D^3|_{O,i} & D^1|_{L,i} - D^1|_{O,i} \end{bmatrix} \quad (i = 2, 4, 6, 8) \quad (3.74)$$

According to the definition, the augmented operators \mathbf{M} and \mathbf{K} along with augmented eigenvector \mathbf{V} are

$$\mathbf{M} = \begin{bmatrix} \mathbf{M}_2 & & & \\ & \mathbf{M}_4 & & \\ & & \mathbf{M}_6 & \\ & & & \mathbf{M}_8 \end{bmatrix}, \quad \mathbf{K} = \begin{bmatrix} \mathbf{K}_2 & & & \\ & \mathbf{K}_4 & & \\ & & \mathbf{K}_6 & \\ & & & \mathbf{K}_8 \end{bmatrix}, \quad \mathbf{V} = \begin{bmatrix} \mathbf{V}_2 \\ \mathbf{V}_4 \\ \mathbf{V}_6 \\ \mathbf{V}_8 \end{bmatrix} \quad (3.75)$$

therefore

$$\begin{aligned}
\langle \mathbf{K}\mathbf{V}^k, \mathbf{V}^p \rangle &= \sum_{i=2,4,6,8} \langle \mathbf{K}_i \mathbf{V}_i^k, \mathbf{V}_i^p \rangle \\
&= \sum_{i=2,4,6,8} \left\langle \begin{bmatrix} -Q_{xi,i-1}^k + Q_{xi,i+1}^k \\ -Q_{yi,i-1}^k + Q_{yi,i+1}^k \\ -b_2 Q_{xi,i+1}^k + b_1 Q_{yi,i+1}^k + M_{zi,i-1}^k - M_{zi,i+1}^k \end{bmatrix}, \begin{bmatrix} X_{i,i-1}^p \\ Y_{i,i-1}^p \\ \Theta_{zi,i-1}^p \end{bmatrix} \right\rangle \\
&= \sum_{i=2,4,6,8} \left[-Q_{xi,i-1}^k X_{i,i-1}^p + Q_{xi,i+1}^k (X_{i,i-1}^p - b_2 \Theta_{zi,i-1}^p) \right. \\
&\quad \left. - Q_{yi,i-1}^k Y_{i,i-1}^p + Q_{yi,i+1}^k (Y_{i,i-1}^p + b_1 \Theta_{zi,i-1}^p) + M_{zi,i-1}^k \Theta_{zi,i-1}^p - M_{zi,i+1}^k \Theta_{zi,i-1}^p \right]
\end{aligned}$$

Consider the *geometry relations* of two ends for the body elements 2, 4, 6 and 8, and the *constitutive relations* of the elements 1, 3, 5 and 7:

$$\begin{cases} X_{i,i-1}^p - b_2 \Theta_{zi,i-1}^p = X_{i,i+1}^p \\ Y_{i,i-1}^p + b_1 \Theta_{zi,i-1}^p = Y_{i,i+1}^p \\ \Theta_{zi,i-1}^p = \Theta_{zi,i+1}^p \end{cases} \quad (i=2,4,6,8) \quad (3.76)$$

$$\begin{cases} Q_{xi-1,i}^k = Q_{xi+1,i}^k = K_{x,i} (X_{i-1,i}^k - X_{i+1,i}^k) \\ Q_{yi-1,i}^k = Q_{yi+1,i}^k = K_{y,i} (Y_{i-1,i}^k - Y_{i+1,i}^k) \\ M_{zi-1,i}^k = M_{zi+1,i}^k = -K'_{z,i} (\Theta_{zi-1,i}^k - \Theta_{zi+1,i}^k) \end{cases} \quad (i=1,3,5,7) \quad (3.77)$$

and the boundary conditions

$$\begin{cases} X_{1,0}^p = 0 \\ Y_{1,0}^p = 0 \\ \Theta_{z1,0}^p = 0 \end{cases}, \begin{cases} Q_{x8,0}^k = 0 \\ Q_{y8,0}^k = 0 \\ M_{z8,0}^k = 0 \end{cases} \quad (3.78)$$

then

$$\begin{aligned}
\langle \mathbf{K}\mathbf{V}^k, \mathbf{V}^p \rangle &= \sum_{i=2,4,6,8} \left[-Q_{xi,i-1}^k X_{i,i-1}^p - Q_{yi,i-1}^k Y_{i,i-1}^p + M_{zi,i-1}^k \Theta_{zi,i-1}^p + Q_{xi,i+1}^k X_{i,i+1}^p \right. \\
&\quad \left. + Q_{yi,i+1}^k Y_{i,i+1}^p - M_{zi,i+1}^k \Theta_{zi,i+1}^p \right] \\
&= \sum_{i=1,3,5,7} \left[Q_{xi-1,i}^k (X_{i-1,i}^p - X_{i+1,i}^p) + Q_{yi-1,i}^k (Y_{i-1,i}^p - Y_{i+1,i}^p) - M_{zi-1,i}^k (\Theta_{zi-1,i}^p - \Theta_{zi+1,i}^p) \right] \\
&= \sum_{i=1,3,5,7} \left[K_{x,i} (X_{i-1,i}^k - X_{i+1,i}^k) (X_{i-1,i}^p - X_{i+1,i}^p) + K_{y,i} (Y_{i-1,i}^k - Y_{i+1,i}^k) (Y_{i-1,i}^p - Y_{i+1,i}^p) \right. \\
&\quad \left. + K'_{z,i} (\Theta_{zi-1,i}^k - \Theta_{zi+1,i}^k) (\Theta_{zi-1,i}^p - \Theta_{zi+1,i}^p) \right]
\end{aligned}$$

It can be seen from the above equations that the value of $\langle \mathbf{K}\mathbf{V}^k, \mathbf{V}^p \rangle$ is invariable if we exchange the position of the superscripts k and p , therefore the augmented eigenvector \mathbf{V} is symmetrical about the augmented operator \mathbf{K} . Because the augmented eigenvector \mathbf{V} is always symmetrical about the augmented operator \mathbf{M} , the orthogonality of the augmented eigenvectors \mathbf{V} is satisfied automatically.

Example 3.5 Prove that the augmented eigenvector of a Euler–Bernoulli beam with uniform cross-section and transverse vibration satisfies the orthogonality.

Solution

There is an equation of transverse free vibration in plane for a Euler–Bernoulli beam with length l , mass density per unit length \bar{m} and bending stiffness EI :

$$EI \frac{\partial^4 y}{\partial x_1^4} + \bar{m} \frac{\partial^2 y}{\partial t^2} = 0 \quad (0 \leq x_1 \leq l) \quad (3.79)$$

Rewriting Equation (3.79) in the form of the body dynamics equation in Equation (3.37) gives

$$\mathbf{M} = [\bar{m}], \mathbf{K} = \left[EI \frac{\partial^4}{\partial x_1^4} \right], \mathbf{v} = [y(x_1, t)] \quad (0 \leq x_1 \leq l) \quad (3.80)$$

where $y(x_1, t)$ denotes the transverse displacement of an arbitrary point of the beam relative to its equilibrium position.

The augmented eigenvector is

$$\mathbf{V}^k = [Y^k(x_1)] \quad (0 \leq x_1 \leq l, k = 1, 2, \dots) \quad (3.81)$$

therefore

$$\langle \mathbf{M} \mathbf{V}^k, \mathbf{V}^p \rangle = \int_0^l \bar{m} Y^k(x_1) \cdot Y^p(x_1) dx_1 + \int_0^l \bar{m} \rho_z^2 \Theta_z^k(x_1) \cdot \Theta_z^p(x_1) dx_1 = \langle \mathbf{V}^k, \mathbf{M} \mathbf{V}^p \rangle$$

$$\begin{aligned} \langle \mathbf{K} \mathbf{V}^k, \mathbf{V}^p \rangle &= \langle EI \frac{d^4 Y^k(x_1)}{dx_1^4}, Y^p(x_1) \rangle = \int_0^l EI \frac{d^4 Y^k(x_1)}{dx_1^4} Y^p(x_1) dx_1 \\ &= EI \frac{d^3 Y^k(x_1)}{dx_1^3} Y^p(x_1) \Big|_0^l - EI \frac{d^2 Y^k(x_1)}{dx_1^2} \frac{dY^p(x_1)}{dx_1} \Big|_0^l + \int_0^l EI \frac{d^2 Y^k(x_1)}{dx_1^2} \frac{d^2 Y^p(x_1)}{dx_1^2} dx_1 \end{aligned}$$

Consider the constitutive relations of a Euler–Bernoulli beam:

$$EI \frac{d^3 Y^k(x_1)}{dx_1^3} = Q_y^k(x_1), \quad EI \frac{d^2 Y^k(x_1)}{dx_1^2} = M_z^k(x_1), \quad \frac{dY^p(x_1)}{dx_1} = \Theta_z^p(x_1)$$

therefore

$$\langle \mathbf{K} \mathbf{V}^k, \mathbf{V}^p \rangle = Q_y^k(x_1) Y^p(x_1) \Big|_0^l - M_z^k(x_1) \Theta_z^p(x_1) \Big|_0^l + \int_0^l EI \frac{d^2 Y^k(x_1)}{dx_1^2} \frac{d^2 Y^p(x_1)}{dx_1^2} dx_1$$

The following equations are satisfied for the six kinds of boundary conditions in Table 2.7:

$$Q_y^k(x_1) Y^p(x_1) \Big|_0^l = 0, \quad M_z^k(x_1) \Theta_z^p(x_1) \Big|_0^l = 0$$

namely

$$\langle \mathbf{K} \mathbf{V}^k, \mathbf{V}^p \rangle = \int_0^l EI \frac{d^2 Y^k(x_1)}{dx_1^2} \cdot \frac{d^2 Y^p(x_1)}{dx_1^2} dx_1$$

It can be seen from these equations that the value of $\langle \mathbf{K} \mathbf{V}^k, \mathbf{V}^p \rangle$ is invariable if we exchange the superscripts k and p , therefore the augmented eigenvector \mathbf{V} of a Euler–Bernoulli beam with

transverse free vibration in a plane is symmetrical about the augmented operators \mathbf{M} and \mathbf{K} , and satisfies the orthogonality.

Example 3.6 Prove that the augmented eigenvector of a Timoshenko beam with uniform cross-section and transverse vibration satisfies the orthogonality.

Solution

There are equations for a homogenous Timoshenko beam with uniform cross-section and free transverse vibration in a plane:

$$\begin{cases} \bar{m} \frac{\partial^2 y}{\partial t^2} - GA_s \frac{\partial^2 y}{\partial x_1^2} + GA_s \frac{\partial \theta_z}{\partial x_1} = 0 \\ \bar{m} \rho_z^2 \frac{\partial^2 \theta_z}{\partial t^2} - EI_z \frac{\partial^2 \theta_z}{\partial x_1^2} - GA_s \frac{\partial y}{\partial x_1} + GA_s \theta_z = 0 \end{cases} \quad (0 \leq x_1 \leq l) \quad (3.82)$$

Write the above equation in body dynamics equations form as Equation (3.37), namely

$$\mathbf{M} = \begin{bmatrix} \bar{m} & 0 \\ 0 & \bar{m} \rho_z^2 \end{bmatrix}, \quad \mathbf{K} = \begin{bmatrix} -GA_s \frac{\partial^2}{\partial x_1^2} & GA_s \frac{\partial}{\partial x_1} \\ -GA_s \frac{\partial}{\partial x_1} & -EI_z \frac{\partial^2}{\partial x_1^2} + GA_s \end{bmatrix}, \quad \mathbf{v} = \begin{bmatrix} y(x_1, t) \\ \theta_z(x_1, t) \end{bmatrix} \quad (0 \leq x_1 \leq l) \quad (3.83)$$

where $y(x_1, t)$ denotes the transverse displacement of an arbitrary point on the beam relative to its equilibrium position, and $\theta_z(x_1, t)$ denotes the angular displacement of arbitrary cross-section on the beam relative to its equilibrium position.

The augmented eigenvector is

$$\mathbf{V}^k = \begin{bmatrix} Y^k(x_1) \\ \Theta_z^k(x_1) \end{bmatrix} \quad (0 \leq x_1 \leq l, k = 1, 2, \dots) \quad (3.84)$$

therefore

$$\begin{aligned} \langle \mathbf{M} \mathbf{V}^k, \mathbf{V}^p \rangle &= \int_0^l \bar{m} Y^k(x_1) \cdot Y^p(x_1) dx_1 + \int_0^l \bar{m} \rho_z^2 \Theta_z^k(x_1) \cdot \Theta_z^p(x_1) dx_1 = \langle \mathbf{V}^k, \mathbf{M} \mathbf{V}^p \rangle \\ \langle \mathbf{K} \mathbf{V}^k, \mathbf{V}^p \rangle &= \left\langle \begin{bmatrix} -GA_s \frac{d^2 Y^k(x_1)}{dx_1^2} + GA_s \frac{d \Theta_z^k(x_1)}{dx_1} \\ -GA_s \frac{d Y^k(x_1)}{dx_1} - EI_z \frac{d^2 \Theta_z^k(x_1)}{dx_1^2} + GA_s \Theta_z^k(x_1) \end{bmatrix}, \begin{bmatrix} Y^p(x_1) \\ \Theta_z^p(x_1) \end{bmatrix} \right\rangle \\ &= - \int_0^l GA_s \frac{d^2 Y^k(x_1)}{dx_1^2} Y^p(x_1) dx_1 + \int_0^l GA_s \left[\frac{d \Theta_z^k(x_1)}{dx_1} Y^p(x_1) - \frac{d Y^k(x_1)}{dx_1} \Theta_z^p(x_1) \right] dx_1 \\ &\quad - \int_0^l EI_z \frac{d^2 \Theta_z^k(x_1)}{dx_1^2} \Theta_z^p(x_1) dx_1 + \int_0^l GA_s \Theta_z^k(x_1) \Theta_z^p(x_1) dx_1 \\ &= Y^p(x_1) GA_s \left[\Theta_z^k(x_1) - \frac{d Y^k(x_1)}{dx_1} \right] \Big|_0^l - EI_z \frac{d \Theta_z^k(x_1)}{dx_1} \Theta_z^p(x_1) \Big|_0^l \end{aligned}$$

$$\begin{aligned}
& + \int_0^l GA_s \frac{dY^k(x_1)}{dx_1} \frac{dY^p(x_1)}{dx_1} dx_1 - \int_0^l GA_s \left[\theta_z^k(x_1) \frac{dY^p(x_1)}{dx_1} + \theta_z^p(x_1) \frac{dY^k(x_1)}{dx_1} \right] dx_1 \\
& + \int_0^l EI_z \frac{d\theta_z^k(x_1)}{dx_1} \frac{d\theta_z^p(x_1)}{dx_1} dx_1 + \int_0^l GA_s \theta_z^k(x_1) \theta_z^p(x_1) dx_1
\end{aligned}$$

Consider the constitutive relations of a Timoshenko beam:

$$GA_s \left[\theta_z^k(x_1) - \frac{dY^k(x_1)}{dx_1} \right] = Q_y^k(x_1), \quad EI_z \frac{d\theta_z^k(x_1)}{dx_1} = M_z^k(x_1)$$

Consequently

$$Y^p(x_1) GA_s \left[\theta_z^k(x_1) - \frac{dY^k(x_1)}{dx_1} \right] \Big|_0^l - EI_z \frac{d\theta_z^k(x_1)}{dx_1} \theta_z^p(x_1) \Big|_0^l = Y^p(x_1) Q_y^k(x_1) \Big|_0^l - M_z^k(x_1) \theta_z^p(x_1) \Big|_0^l$$

Similarly, the following equations are satisfied for the six kinds of boundary conditions in Table 2.7:

$$Y^p(x_1) Q_y^k(x_1) \Big|_0^l = 0, \quad M_z^k(x_1) \theta_z^p(x_1) \Big|_0^l = 0$$

therefore

$$\begin{aligned}
& \langle \mathbf{K} \mathbf{V}^k, \mathbf{V}^p \rangle \\
& = \int_0^l GA_s \frac{dY^k(x_1)}{dx_1} \frac{dY^p(x_1)}{dx_1} dx_1 - \int_0^l GA_s \left[\theta_z^k(x_1) \frac{dY^p(x_1)}{dx_1} + \theta_z^p(x_1) \frac{dY^k(x_1)}{dx_1} \right] dx_1 \\
& + \int_0^l EI_z \frac{d\theta_z^k(x_1)}{dx_1} \frac{d\theta_z^p(x_1)}{dx_1} dx_1 + \int_0^l GA_s \theta_z^k(x_1) \theta_z^p(x_1) dx_1 \\
& = \int_0^l GA_s \left[\theta_z^k(x_1) - \frac{dY^k(x_1)}{dx_1} \right] \left[\theta_z^p(x_1) - \frac{dY^p(x_1)}{dx_1} \right] dx_1 + \int_0^l EI_z \frac{d\theta_z^k(x_1)}{dx_1} \frac{d\theta_z^p(x_1)}{dx_1} dx_1 \\
& = \langle \mathbf{V}^k, \mathbf{K} \mathbf{V}^p \rangle
\end{aligned}$$

As a result, the augmented eigenvector \mathbf{V} of a Timoshenko beam with uniform cross-section and transverse vibration in a plane is symmetrical about the augmented operators \mathbf{M} and \mathbf{K} , and satisfies the orthogonality.

Augmented operator \mathbf{M} is symmetrical matrix, and the augmented eigenvector \mathbf{V} is symmetrical about the augmented operator \mathbf{M} automatically. The symmetry of \mathbf{V} about \mathbf{K} will be validated by following examples.

Example 3.7 Prove that the augmented eigenvector of the chain multi-rigid-flexible-body system shown in Figure 3.1 satisfies the orthogonality.

Solution

The body dynamics equations and augmented operators \mathbf{M} and \mathbf{K} of the system shown in Figure 3.1 are written out in Example 3.3. The augmented eigenvector \mathbf{V} of the system is

$$\mathbf{V}^k = \begin{bmatrix} \mathbf{V}_2^k \\ \mathbf{V}_3^k \end{bmatrix} = [X_{2,1}^k, Y_{2,1}^k, \theta_{z2,1}^k, X^k(x_3), Y^k(x_3)]^T \quad (3.85)$$

therefore

$$\begin{aligned}
\langle \mathbf{K}\mathbf{V}^k, \mathbf{V}^p \rangle &= \langle \mathbf{K}_2 \mathbf{V}_2^k, \mathbf{V}_2^p \rangle + \langle \mathbf{K}_3 \mathbf{V}_3^k, \mathbf{V}_3^p \rangle \\
&= \left\langle \begin{bmatrix} -Q_{x2,1}^k + Q_{x2,3}^k \\ -Q_{y2,1}^k + Q_{y2,3}^k \\ -b_2 Q_{x2,3}^k + b_1 Q_{y2,3}^k + M_{z2,1}^k - M_{z2,3}^k \end{bmatrix}, \begin{bmatrix} X_{2,1}^p \\ Y_{2,1}^p \\ \Theta_{z2,1}^p \end{bmatrix} \right\rangle + \left\langle \begin{bmatrix} -EA_3 \frac{d^2 X^k(x_3)}{dx_3^2} \\ EI_3 \frac{d^4 Y^k(x_3)}{dx_3^4} \end{bmatrix}, \begin{bmatrix} X^p(x_3) \\ Y^p(x_3) \end{bmatrix} \right\rangle \\
&= -Q_{x2,1}^k X_{2,1}^p + Q_{x2,3}^k X_{2,1}^p - Q_{y2,1}^k Y_{2,1}^p + Q_{y2,3}^k Y_{2,1}^p - b_2 Q_{x2,3}^k \Theta_{z2,1}^p + b_1 Q_{y2,3}^k \Theta_{z2,1}^p \\
&\quad + M_{z2,1}^k \Theta_{z2,1}^p - M_{z2,3}^k \Theta_{z2,1}^p + \int_0^{l_3} \left[-EA_3 \frac{d^2 X^k(x_3)}{dx_3^2} X^p(x_3) + EI_3 \frac{d^4 Y^k(x_3)}{dx_3^4} Y^p(x_3) \right] dx_3 \\
&= -Q_{x2,1}^k X_{2,1}^p - Q_{y2,1}^k Y_{2,1}^p + M_{z2,1}^k \Theta_{z2,1}^p \\
&\quad + Q_{x2,3}^k (X_{2,1}^p - b_2 \Theta_{z2,1}^p) + Q_{y2,3}^k (Y_{2,1}^p + b_1 \Theta_{z2,1}^p) - M_{z2,3}^k \Theta_{z2,1}^p \\
&\quad - EA_3 \frac{dX^k(x_3)}{dx_3} X^p(x_3) \Big|_0^{l_3} + EI_3 \frac{d^3 Y^k(x_3)}{dx_3^3} Y^p(x_3) \Big|_0^{l_3} - EI_3 \frac{d^2 Y^k(x_3)}{dx_3^2} \frac{dY^p(x_3)}{dx_3} \Big|_0^{l_3} \\
&\quad + \int_0^{l_3} EA_3 \frac{dX^k(x_3)}{dx_3} \frac{dX^p(x_3)}{dx_3} dx_3 + \int_0^{l_3} EI_3 \frac{d^2 Y^k(x_3)}{dx_3^2} \frac{d^2 Y^p(x_3)}{dx_3^2} dx_3
\end{aligned}$$

According to the geometry relations of the rigid body and the constitutive relations of a Euler–Bernoulli beam with uniform cross-section

$$\begin{aligned}
X_{2,3}^p &= X_{2,1}^p - b_2 \Theta_{z2,1}^p, \quad Y_{2,3}^p = Y_{2,1}^p + b_1 \Theta_{z2,1}^p, \quad \Theta_{z2,3}^p = \Theta_{z2,1}^p \\
EI_3 \frac{d^3 Y^k(x_3)}{dx_3^3} &= Q_y^k(x_3), \quad EI_3 \frac{d^2 Y^k(x_3)}{dx_3^2} = M_z^k(x_3), \quad \frac{dY^p(x_3)}{dx_3} = \Theta_z^p(x_3) \\
-EA_3 \frac{dX^k(x_3)}{dx_3} &= Q_x^k(x_3)
\end{aligned} \tag{3.86}$$

Hence,

$$\begin{aligned}
\langle \mathbf{K}\mathbf{V}^k, \mathbf{V}^p \rangle &= -Q_{x2,1}^k X_{2,1}^p - Q_{y2,1}^k Y_{2,1}^p + M_{z2,1}^k \Theta_{z2,1}^p + Q_{x2,3}^k X_{2,3}^p + Q_{y2,3}^k Y_{2,3}^p - M_{z2,3}^k \Theta_{z2,3}^p \\
&\quad + Q_x^k(x_3) X^p(x_3) \Big|_0^{l_3} + Q_y^k(x_3) Y^p(x_3) \Big|_0^{l_3} - M_z^k(x_3) \Theta_z^p(x_3) \Big|_0^{l_3} \\
&\quad + \int_0^{l_3} EA_3 \frac{dX^k(x_3)}{dx_3} \frac{dX^p(x_3)}{dx_3} dx_3 + \int_0^{l_3} EI_3 \frac{d^2 Y^k(x_3)}{dx_3^2} \frac{d^2 Y^p(x_3)}{dx_3^2} dx_3
\end{aligned}$$

Consider the connection relations

$$\begin{aligned}
X_{2,3}^p &= X^p(x_3) \Big|_{x_3=0}, \quad Y_{2,3}^p = Y^p(x_3) \Big|_{x_3=0}, \quad \Theta_{z2,3}^p = \Theta_z^p(x_3) \Big|_{x_3=0} \\
Q_{x2,3}^k &= Q_x^k(x_3) \Big|_{x_3=0}, \quad Q_{y2,3}^k = Q_y^k(x_3) \Big|_{x_3=0}, \quad M_{z2,3}^k = M_z^k(x_3) \Big|_{x_3=0}
\end{aligned} \tag{3.87}$$

According to the constitutive relations of planar elastic hinges

$$\begin{cases} Q_{x2,1}^k = Q_{x1,0}^k = -K_{x,1} (X_{2,1}^k - X_{1,0}^k) \\ Q_{y2,1}^k = Q_{y1,0}^k = -K_{y,1} (X_{2,1}^k - Y_{1,0}^k) \\ M_{z2,1}^k = M_{z1,0}^k = K_1' (\Theta_{z2,1}^k - \Theta_{z1,0}^k) \end{cases} \tag{3.88}$$

and the boundary conditions

$$\begin{cases} X_{1,0}^p = 0, & Y_{1,0}^p = 0, & \Theta_{z1,0}^p = 0 \\ Q_x^k(x_3)|_{x_3=l_3} = 0, & Q_y^k(x_3)|_{x_3=l_3} = 0, & M_z^k(x_3)|_{x_3=l_3} = 0 \end{cases} \quad (3.89)$$

then

$$\begin{aligned} & \langle \mathbf{K}\mathbf{V}^k, \mathbf{V}^p \rangle \\ &= -Q_{x2,1}^k X_{2,1}^p - Q_{y2,1}^k Y_{2,1}^p + M_{z2,1}^k \Theta_{z2,1}^p \\ &+ \int_0^{l_3} EA_3 \frac{dX^k(x_3)}{dx_3} \frac{dX^p(x_3)}{dx_3} dx_3 + \int_0^{l_3} EI_3 \frac{d^2 Y^k(x_3)}{dx_3^2} \frac{d^2 Y^p(x_3)}{dx_3^2} dx_3 \\ &+ Q_{x2,3}^k X_{2,3}^p - Q_x^k(x_3) X^p(x_3)|_{x_3=0} + Q_{y2,3}^k Y_{2,3}^p - Q_y^k(x_3) Y^p(x_3)|_{x_3=0} \\ &- M_{z2,3}^k \Theta_{z2,3}^p + M_z^k(x_3) \Theta_z^p(x_3)|_{x_3=0} \\ &+ Q_x^k(x_3) X^p(x_3)|_{x_3=l_3} + Q_y^k(x_3) Y^p(x_3)|_{x_3=l_3} - M_z^k(x_3) \Theta_z^p(x_3)|_{x_3=l_3} \\ &= -Q_{x2,1}^k X_{2,1}^p - Q_{y2,1}^k Y_{2,1}^p + M_{z2,1}^k \Theta_{z2,1}^p \\ &+ \int_0^{l_3} EA_3 \frac{dX^k(x_3)}{dx_3} \frac{dX^p(x_3)}{dx_3} dx_3 + \int_0^{l_3} EI_3 \frac{d^2 Y^k(x_3)}{dx_3^2} \frac{d^2 Y^p(x_3)}{dx_3^2} dx_3 \\ &= K_{x,1} (X_{2,1}^k - X_{0,1}^k) X_{2,1}^p + K_{y,1} (Y_{2,1}^k - Y_{0,1}^k) Y_{2,1}^p + K_1' (\Theta_{z2,1}^k - \Theta_{z0,1}^k) \Theta_{z2,1}^p \\ &+ \int_0^{l_3} EA_3 \frac{dX^k(x_3)}{dx_3} \frac{dX^p(x_3)}{dx_3} dx_3 + \int_0^{l_3} EI_3 \frac{d^2 Y^k(x_3)}{dx_3^2} \frac{d^2 Y^p(x_3)}{dx_3^2} dx_3 \\ &= K_{x,1} X_{2,1}^k X_{2,1}^p + K_{y,1} Y_{2,1}^k Y_{2,1}^p + K_1' \Theta_{z2,1}^k \Theta_{z2,1}^p \\ &+ \int_0^{l_3} EA_3 \frac{dX^k(x_3)}{dx_3} \frac{dX^p(x_3)}{dx_3} dx_3 + \int_0^{l_3} EI_3 \frac{d^2 Y^k(x_3)}{dx_3^2} \frac{d^2 Y^p(x_3)}{dx_3^2} dx_3 \\ &= \langle \mathbf{V}^k, \mathbf{K}\mathbf{V}^p \rangle \end{aligned}$$

It is obvious that \mathbf{V} is symmetrical about \mathbf{K} , therefore the augmented eigenvector \mathbf{V} of the system satisfies the orthogonality.

3.6 Transient Response of a Multibody System

The body dynamics equation of an undamped MRFS is

$$\mathbf{M}\nu_{tt} + \mathbf{K}\nu = \mathbf{f} \quad (3.90)$$

The physical coordinate of the dynamics response may be expanded using augmented eigenvectors \mathbf{V}^k as

$$\nu = \sum_{k=1}^n \mathbf{V}^k q^k(t) \quad (3.91)$$

Substituting Equation (3.91) into Equation (3.90) yields

$$\sum_{k=1}^n \mathbf{M} \mathbf{V}^k \ddot{q}^k(t) + \sum_{k=1}^n \mathbf{K} \mathbf{V}^k q^k(t) = \mathbf{f} \quad (3.92)$$

Take the inner product for both sides of Equation (3.92) using augmented eigenvectors \mathbf{V}^p ($p = 1, 2, \dots, n$) and the orthogonality of the augmented eigenvectors:

$$\langle \mathbf{M} \mathbf{V}^k, \mathbf{V}^p \rangle = \delta_{k,p} M_p, \quad \langle \mathbf{K} \mathbf{V}^k, \mathbf{V}^p \rangle = \delta_{k,p} K_p \quad (3.93)$$

The generalized coordinate equations of the system can be obtained:

$$\ddot{q}^p(t) + \omega_p^2 q^p(t) = \frac{\langle \mathbf{f}, \mathbf{V}^p \rangle}{M_p} \quad (p = 1, 2, \dots, n) \quad (3.94)$$

Assume that the initial conditions of the MRFS are

$$\mathbf{v}(t)|_{t=0} = \mathbf{v}_0, \quad \dot{\mathbf{v}}(t)|_{t=0} = \dot{\mathbf{v}}_0 \quad (3.95)$$

This yields

$$\mathbf{v}(t)|_{t=0} = \sum_{k=1}^n \mathbf{V}^k q^k(t)|_{t=0} = \sum_{k=1}^n \mathbf{V}^k q_0^k = \mathbf{v}_0, \quad \dot{\mathbf{v}}(t)|_{t=0} = \sum_{k=1}^n \mathbf{V}^k \dot{q}^k(t)|_{t=0} = \sum_{k=1}^n \mathbf{V}^k \dot{q}_0^k = \dot{\mathbf{v}}_0 \quad (3.96)$$

$$\langle \mathbf{v}_0, \mathbf{M} \mathbf{V}^p \rangle = \langle \mathbf{M} \mathbf{V}^p, \mathbf{V}^p \rangle q_0^p = M_p q_0^p, \quad \langle \dot{\mathbf{v}}_0, \mathbf{M} \mathbf{V}^p \rangle = \langle \mathbf{M} \mathbf{V}^p, \mathbf{V}^p \rangle \dot{q}_0^p = M_p \dot{q}_0^p \quad (3.97)$$

We obtain

$$q^p(t)|_{t=0} = q_0^p = \frac{\langle \mathbf{v}_0, \mathbf{M} \mathbf{V}^p \rangle}{M_p}, \quad \dot{q}^p(t)|_{t=0} = \dot{q}_0^p = \frac{\langle \dot{\mathbf{v}}_0, \mathbf{M} \mathbf{V}^p \rangle}{M_p} \quad (p = 1, 2, \dots, n) \quad (3.98)$$

Equation (3.94) is the forced vibration equation of the system in generalized principal coordinates. The eigenfrequencies ω_p ($p = 1, 2, \dots, n$) and the corresponding augmented eigenvectors \mathbf{V}^p can be acquired using the method illustrated above. The generalized coordinates $q^p(t)$ ($p = 1, 2, \dots, n$) can be obtained by integrating Equation (3.94) with respect to time one by one. The dynamics response of the system can be determined by Equation (3.91). Note that $f_p(t) = \langle \mathbf{f}, \mathbf{V}^p \rangle$ is a single-valued function depending only on time t , and the solutions of generalized coordinates are found out as

$$q^p(t) = q_0^p \cos \omega_p t + \frac{\dot{q}_0^p}{\omega_p} \sin \omega_p t + \frac{1}{M_p \omega_p} \int_0^t f_p(\tau) \sin \omega_p(t - \tau) d\tau \quad (3.99)$$

therefore the dynamics response of the system is

$$\mathbf{v} = \sum_{p=1}^n \mathbf{V}^p \left[q_0^p \cos \omega_p t + \frac{\dot{q}_0^p}{\omega_p} \sin \omega_p t + \frac{1}{M_p \omega_p} \int_0^t f_p(\tau) \sin \omega_p(t - \tau) d\tau \right] \quad (3.100)$$

Example 3.8 For the system shown in Example 2.10, an initial velocity of 1 m/s of the rigid body 2 is acquired by a downward impact load. The initial displacement, rightward and leftward velocities, and angular velocity are zero. Compute the displacement of the free end of beam 3 within 10 s.

Solution

The vibration characteristics of the system were calculated in Example 2.10. The body dynamics equation, augmented operator and augmented eigenvector of the system are

$$\begin{bmatrix} M_2 \\ M_3 \end{bmatrix} \begin{bmatrix} v_2 \\ v_3 \end{bmatrix}_{tt} + \begin{bmatrix} K_2 \\ K_3 \end{bmatrix} \begin{bmatrix} v_2 \\ v_3 \end{bmatrix} = \mathbf{0} \quad (3.101)$$

where

$$M_2 = \begin{bmatrix} m_2 & 0 & -m_2 c_{c2} \\ 0 & m_2 & m_2 c_{c1} \\ -m_2 c_{c2} & m_2 c_{c1} & J_2 \end{bmatrix}, \quad M_3 = \begin{bmatrix} \bar{m}_3 l_3 & 0 \\ 0 & \bar{m}_3 \end{bmatrix} \quad (3.102)$$

$$K_2 = \begin{bmatrix} -D^3|_{I,2} + D^3|_{O,2} & 0 & 0 \\ 0 & -D^3|_{I,2} + D^3|_{O,2} & 0 \\ -b_2 D^3|_{O,2} & b_1 D^3|_{O,2} & D^1|_{I,2} - D^1|_{O,2} \end{bmatrix}$$

$$K_3 = \begin{bmatrix} -D^3|_{I,3} + D^3|_{O,3} & 0 \\ 0 & EI_3 \frac{\partial^4}{\partial x_3^4} \end{bmatrix} \quad (3.103)$$

$$V^k = \begin{bmatrix} V_2^k \\ V_3^k \end{bmatrix} = [X_{2,1}^k, Y_{2,1}^k, \Theta_{z2,1}^k, X^k(x_3), Y^k(x_3)]^T \quad (k = 1, 2, \dots) \quad (3.104)$$

The modal mass M_p ($p = 1, 2, \dots$) given by Equation (3.48) is

$$M_p = m_2 \left[(X_{2,1}^p)^2 + (Y_{2,1}^p)^2 \right] - 2m_2 c_{c2} X_{2,1}^p \Theta_{z2,1}^p + 2m_2 c_{c1} Y_{2,1}^p \Theta_{z2,1}^p + J_2 (\Theta_{z2,1}^p)^2 \\ + \bar{m}_3 \int_0^{l_3} \{ [X^p(x_3)]^2 + [Y^p(x_3)]^2 \} dx_3 \quad (3.105)$$

The initial conditions of the system are

$$v_0 = [0, 0, 0, 0, 0]^T, \quad \dot{v}_0 = [0, -1, 0, 0, 0]^T \quad (3.106)$$

Considering Equation (3.96) yields

$$q_0^p = 0, \quad \dot{q}_0^p = \frac{-m_2 Y_{2,1}^p - m_2 c_{c1} \Theta_{z2,1}^p}{M_p} \quad (p = 1, 2, \dots) \quad (3.107)$$

Substituting Equation (3.107) into Equation (3.100), the dynamics response of the system is

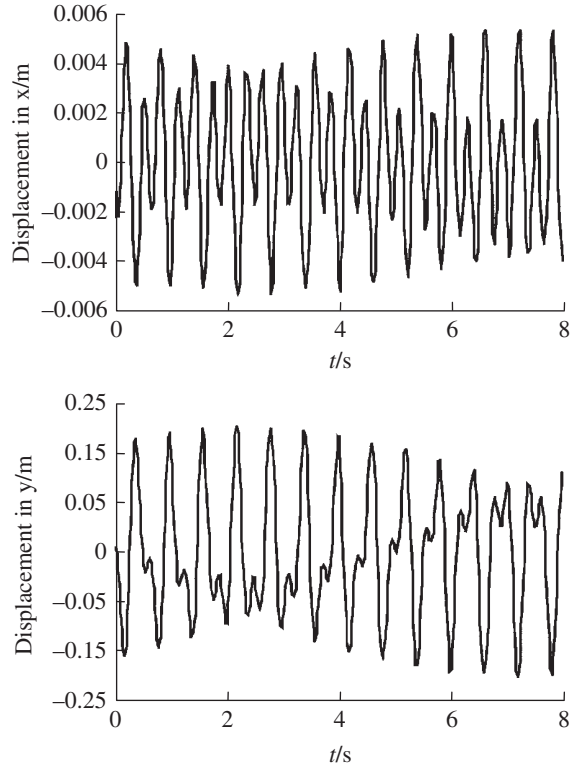
$$v = \sum_{p=1}^{\infty} V^p \frac{\dot{q}_0^p}{\omega_p} \sin \omega_p t \quad (3.108)$$

The displacement of the free end of beam 3 is

$$x(l_3) = \sum_{p=1}^{\infty} X^p(l_3) \frac{\dot{q}_0^p}{\omega_p} \sin \omega_p t, \quad y(l_3) = \sum_{p=1}^{\infty} Y^p(l_3) \frac{\dot{q}_0^p}{\omega_p} \sin \omega_p t \quad (3.109)$$

Dynamics simulation of the system reveals that the computational dynamics response of the system using only the first three eigenvectors is accurate enough. The time history of the displacement of the free end of beam 3 obtained by computation using the first three eigenvectors is shown in Figure 3.2.

Figure 3.2 Time history of the displacement of the free end of beam 3.



Example 3.9 The planar vibration system shown in Figure 3.3 is composed of spring 1 with elastic coefficient K , lumped mass 2 with mass m and beam 3 with uniform cross-section, length l , mass per length \bar{m} and bending stiffness EI . The lumped mass 2 is constrained by a smooth guideway and moves only up and down. The left end of beam 3 is fixed to body 2 at the point Q , and the right end is free. At the initial time $t = 0$, beam 3 has no deformation and the spring is elongated by 0.1 m. There are neither external excitations nor damping forces acting this system. The system is motionless at the initial time. Determine the motion of the free end of the beam.

Solution

The dynamics response of the system is computed by three methods: the analytical method, Kane's method and the MSTMM.

1) Analytical method

As shown in Figure 3.3, $y(x, t)$ denotes the displacement of an arbitrary point P on the beam. The vibration equation of the beam is

$$\bar{m} \frac{\partial^2 y}{\partial t^2} + EI \frac{\partial^4 y}{\partial x^4} = 0 \quad (3.110)$$

The boundary conditions are

$$\begin{cases} \left. \frac{\partial y(x, t)}{\partial x} \right|_{x=0} = 0, \left. \frac{\partial^2 y(x, t)}{\partial x^2} \right|_{x=l} = 0, \left. \frac{\partial^3 y(x, t)}{\partial x^3} \right|_{x=l} = 0 \\ \left. m \frac{\partial^2 y(x, t)}{\partial t^2} \right|_{x=0} + EI \left. \frac{\partial^3 y(x, t)}{\partial x^3} \right|_{x=0} + Ky(x, t)|_{x=0} = 0 \end{cases} \quad (3.111)$$

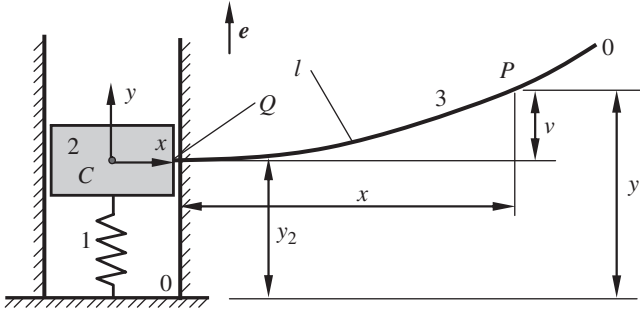


Figure 3.3 A planar vibration system composed of a spring, lumped mass and beam.

The initial conditions are

$$y(x, t)|_{t=0} = f(x), \quad \left. \frac{\partial y(x, t)}{\partial t} \right|_{t=0} = g(x) \quad (3.112)$$

where $f(x) = 0.1$ and $g(x) = 0$ ($0 \leq x \leq l$).

The solution satisfying the initial conditions and boundary conditions is

$$y(x, t) = \sum_{i=1}^{\infty} [Y_i(x)(A_i \sin \omega_i t + B_i \cos \omega_i t)] \quad (3.113)$$

where $\omega_i = (\lambda_i/l)^2 \sqrt{EI/\bar{m}}$

$$Y_i(x) = \sin \frac{\lambda_i x}{l} - \sinh \frac{\lambda_i x}{l} + \alpha_i \cos \frac{\lambda_i x}{l} + \beta_i \cosh \frac{\lambda_i x}{l} \quad (3.114)$$

$$\alpha_i = -\frac{\sin \lambda_i + \sinh \lambda_i + \frac{2\bar{m}lEI\lambda_i^3 \cosh \lambda_i}{mEI\lambda_i^4 - k\bar{m}l^4}}{\cos \lambda_i + \cosh \lambda_i}, \quad \beta_i = \frac{\sin \lambda_i + \sinh \lambda_i - \frac{2\bar{m}lEI\lambda_i^3 \cosh \lambda_i}{mEI\lambda_i^4 - k\bar{m}l^4}}{\cos \lambda_i + \cosh \lambda_i}$$

$$A_i = \frac{\int_0^l g(x) Y_i(x) dx + \frac{m}{\bar{m}} g(0) Y_i(0)}{\omega_i \int_0^l Y_i^2(x) dx + \frac{m\omega_i}{\bar{m}} Y_i^2(0)} = 0$$

$$B_i = \frac{\int_0^l f(x) Y_i(x) dx + \frac{m}{\bar{m}} f(0) Y_i(0)}{\int_0^l Y_i^2(x) dx + \frac{m}{\bar{m}} Y_i^2(0)} = \frac{0.1 \times \left[\int_0^l Y_i(x) dx + \frac{m}{\bar{m}} Y_i(0) \right]}{\int_0^l Y_i^2(x) dx + \frac{m}{\bar{m}} Y_i^2(0)}$$

$\lambda_i (i = 1, 2, \dots, \infty)$ are the roots of the transcendental equation

$$\left(\lambda^4 - \frac{k\bar{m}l^4}{mEI} \right) (1 + \cos \lambda \cdot \cosh \lambda) + \frac{\bar{m}l\lambda^3}{m} (\cosh \lambda \cdot \sin \lambda + \sinh \lambda \cdot \cos \lambda) = 0 \quad (3.115)$$

2) Kane's method [9]

The displacement y of a point P on the beam can be written as $y = y_2 + v$, where y_2 is the displacement of lumped mass 2 and $v = \sum_{i=1}^{\infty} \bar{Y}_i(x) q_i(t)$ denotes the displacement of point P with

respect to the lumped mass 2. $q_i(t)$ are the generalized coordinates and $\bar{Y}_i(x)$ are the eigenfunctions of the cantilever beam, that is

$$\bar{Y}_i(x) = \cosh \frac{\lambda_i x}{l} - \cos \frac{\lambda_i x}{l} - \frac{\cosh \lambda_i + \cos \lambda_i}{\sinh \lambda_i + \sin \lambda_i} \left(\sinh \frac{\lambda_i x}{l} - \sin \frac{\lambda_i x}{l} \right) \quad (i = 1, 2, \dots) \quad (3.116)$$

The generalized velocities u_1, u_2, \dots, u_{1+n} are defined as $u_1 = \dot{y}_2$ and $u_{1+i} = \dot{q}_i$ ($i = 1, 2, \dots, n$), which yields $n + 1$ kinematics equations of the system:

$$\begin{cases} \dot{y}_2 = u_1 \\ \dot{q}_i = u_{1+i} \quad (i = 1, 2, \dots, n) \end{cases} \quad (3.117)$$

As shown in Figure 3.3, with base vector \mathbf{e} , the velocities of mass centers, C , P and Q of lumped mass 2 have the expressions

$$\mathbf{V}^C = u_1 \mathbf{e}, \quad \mathbf{V}^P = \left(u_1 + \sum_{i=1}^{\infty} \bar{Y}_i u_{1+i} \right) \mathbf{e}, \quad \mathbf{V}^Q = \mathbf{V}^C = u_1 \mathbf{e} \quad (3.118)$$

The partial velocities in Equations (3.116) to (3.118) are shown in Table. 3.1. The accelerations \mathbf{a}^C and \mathbf{a}^P of point C and point P can be written as

$$\mathbf{a}^C = \dot{u}_1 \mathbf{e}, \quad \mathbf{a}^P = \left(\dot{u}_1 + \sum_{i=1}^{\infty} \bar{Y}_i \dot{u}_{1+i} \right) \mathbf{e} \quad (3.119)$$

The generalized inertia force becomes

$$\mathbf{F}_r^* = -m \mathbf{V}_r^C \cdot \mathbf{a}^C - \bar{m} \int_0^l \mathbf{V}_r^P \cdot \mathbf{a}^P dx \quad (3.120)$$

Substituting the formula of partial velocity and acceleration into Equation (3.120) yields

$$\begin{cases} \mathbf{F}_1^* = -(m + \bar{m}l) \dot{u}_1 - \sum_{i=1}^n C_i \dot{u}_{1+i} \\ \mathbf{F}_{1+j}^* = -C_j \dot{u}_1 - \sum_{i=1}^n D_{ij} \dot{u}_{1+i} \end{cases} \quad (3.121)$$

where, $\bar{m}l = \bar{m} \int_0^l dx$, $C_i = \bar{m} \int_0^l \bar{Y}_i dx = \frac{2\bar{m}l(\cosh \lambda_i + \cos \lambda_i)}{\lambda_i(\sinh \lambda_i + \sin \lambda_i)}$ and $D_{ij} = \bar{m} \int_0^l \bar{Y}_i \bar{Y}_j dx = \bar{m}l \delta_{i,j}$.

There is no external force acting on the system. Hence, the generalized active force becomes

$$\mathbf{F}_r = -\mathbf{V}_r^C \cdot \mathbf{e} k y_2 - \mathbf{V}_r^Q \cdot \mathbf{e} EI \frac{\partial^3 v}{\partial x^3} \Big|_{x=0} - \int_0^l \mathbf{V}_r^P \cdot \mathbf{e} \frac{\partial^2}{\partial x^2} \left(EI \frac{\partial^2 v}{\partial x^2} \right) dx \quad (3.122)$$

Table 3.1 Generalized speed corresponding to partial velocity

r	u_r	Partial velocity		
		V^C	V^P	V^Q
1	u_1	\mathbf{e}	\mathbf{e}	\mathbf{e}
$1+j$	u_{1+j}	0	$\bar{Y}_j \mathbf{e}$	0

Substituting the partial velocity (Equation (3.118)), acceleration (Equation (3.119)) and $v = \sum_{i=1}^n \bar{Y}_i q_i$ into Equation (3.122) and making use of partial integration yields

$$\begin{cases} F_1 = -ky_2 \\ F_{1+j} = -\sum_{i=1}^n E_{ij} q_i \quad (j = 1, 2, \dots, n) \end{cases} \quad (3.123)$$

where $E_{ij} = EI \int_0^l \bar{Y}_i \bar{Y}_j dx = \frac{EI \lambda_i^4}{l^3} \delta_{i,j}$.

Substituting generalized inertia force (Equation (3.120)) and generalized active force (Equation (3.122)) into dynamics equation $F_r + F_r^* = 0$, and rewriting Equation (3.123) yields

$$\begin{cases} (m + \bar{m}l) \dot{u}_1 + \sum_{i=1}^n C_i \dot{u}_{1+i} + ky_2 = 0 \\ C_i \dot{u}_i + m \dot{u}_{1+i} + \frac{EI \lambda_i^4}{l^3} q_i = 0 \quad (i = 1, 2, \dots, n) \end{cases} \quad (3.124)$$

Regard the initial conditions

$$\begin{cases} y_2|_{t=0} = 0.1 \\ q_i|_{t=0} = 0.0 \quad (i = 1, 2, \dots, n) \end{cases}, \begin{cases} u_1|_{t=0} = 0.0 \\ u_{1+i}|_{t=0} = 0.0 \quad (i = 1, 2, \dots, n) \end{cases} \quad (3.125)$$

Equations (3.117) and (3.124) can be solved by a Runge–Kutta method, resulting in the time responses of, $y_2(t)$, $q_i(t)$, $u_1(t)$ and $u_{1+i}(t)$. Then the displacement of any point on the beam can be computed:

$$y(x, t) = y_2(t) + \sum_{i=1}^n \bar{Y}_i(x) q_i(t) \quad (3.126)$$

3) MSTMM

Let the connection point of spring 1 and the ground 0 be the input end, and the free end 0 of the beam be the output end. Define the state vectors $Z_{1,0}$, $Z_{2,1}$, $Z_{2,3}$, Z_x ($0 < x \leq l$) in the form of $Z = [Y, \Theta_z, M_z, Q_v]^T$. The transfer equation of each element is

$$Z_{2,1} = U_1 Z_{1,0}, \quad Z_{2,3} = U_2 Z_{2,1}, \quad Z_x = U_x Z_{2,3} \quad (0 < x \leq l) \quad (3.127)$$

The transfer matrices of the elements are

$$U_1 = \begin{bmatrix} 1 & 0 & 0 & -1/K \\ 0 & 1 & 0 & 0 \\ 0 & 0 & 1 & 0 \\ 0 & 0 & 0 & 1 \end{bmatrix}, \quad U_2 = \begin{bmatrix} 1 & 0 & 0 & 0 \\ 0 & 1 & 0 & 0 \\ 0 & 0 & 1 & 0 \\ m\omega^2 & 0 & 0 & 1 \end{bmatrix}$$

$$U_x = \begin{bmatrix} S(\lambda x) & \frac{T(\lambda x)}{\lambda} & \frac{U(\lambda x)}{EI\lambda^2} & \frac{V(\lambda x)}{EI\lambda^3} \\ \lambda V(\lambda x) & S(\lambda x) & \frac{T(\lambda x)}{EI\lambda} & \frac{U(\lambda x)}{EI\lambda^2} \\ EI\lambda^2 U(\lambda x) & EI\lambda V(\lambda x) & S(\lambda x) & \frac{T(\lambda x)}{\lambda} \\ EI\lambda^3 T(\lambda x) & EI\lambda^2 U(\lambda x) & \lambda V(\lambda x) & S(\lambda x) \end{bmatrix} \quad (3.128)$$

where $\lambda = \sqrt[4]{\bar{m}\omega^2/(EI)}$ and $S(x)$, $T(x)$, $U(x)$, $V(x)$ is the Крылов function [235]. The overall transfer equation of the system is

$$\mathbf{Z}_{x=l} = \mathbf{U}_{x=l} \mathbf{U}_2 \mathbf{U}_1 \mathbf{Z}_{1,0} = \mathbf{U} \mathbf{Z}_{1,0} \quad (3.129)$$

Substituting the boundary conditions

$$\mathbf{Z}_{x=l} = [Y, \Theta_z, 0, 0]_{x=l}^T, \quad \mathbf{Z}_{1,0} = [0, 0, M_z, Q_y]_{1,0}^T \quad (3.130)$$

into the overall transfer equation yields the characteristic equation

$$\begin{vmatrix} u_{33} & u_{34} \\ u_{43} & u_{44} \end{vmatrix} = 0 \quad (3.131)$$

The eigenfrequencies ω_k ($k = 1, 2, \dots$) can be solved numerically. For each eigenfrequency ω_k , the state vector $\mathbf{Z}_{1,0}$ can be solved from Equation (3.129). The state vector of an arbitrary point and the eigenvector of the system can be obtained by solving Equation (3.127).

Let $y_{2,1}(t)$ denote the displacements of lumped mass 2 and $y_3(x, t)$ ($0 < x \leq l$) denote the displacements of point P . The body dynamics equations of the system are

$$\mathbf{M}\mathbf{v}_{tt} + \mathbf{K}\mathbf{v} = 0 \quad (3.132)$$

where

$$\mathbf{M} = \begin{bmatrix} m & 0 \\ 0 & \bar{m} \end{bmatrix}, \quad \mathbf{K} = \begin{bmatrix} -D^3|_{l,2} + D^3|_{0,2} & 0 \\ 0 & EI \frac{\partial^4}{\partial x^4} \end{bmatrix}, \quad \mathbf{v} = \begin{bmatrix} y_{2,1}(t) \\ y_3(x, t) \end{bmatrix}$$

Let $\mathbf{v} = \sum_{k=1}^{\infty} \mathbf{V}^k q^k(t)$, where $\mathbf{V}^k = [Y_{2,1}^k, Y_3^k(x)]^T$ and $q^k(t)$ is the augmented eigenvector and corresponding generalized coordinate. Using the orthogonality of augmented eigenvector, Equation (132) becomes

$$\ddot{q}^p(t) + \omega_p^2 q^p(t) = 0 \quad (p = 1, 2, \dots) \quad (3.133)$$

The initial conditions are

$$q^p(t)|_{t=0} = \frac{\langle \mathbf{M}[0.1, 0.1]^T, \mathbf{V}^p \rangle}{M_p}, \quad \dot{q}^p(t)|_{t=0} = 0 \quad (3.134)$$

The generalized coordinates $q^p(t)$ ($p = 1, 2, \dots$) can be obtained using numerical integrals of Equation (3.133).

Take $K = 615.86 \text{ N/m}$, $m = 15.6 \text{ kg}$, $l = 5 \text{ m}$, $\bar{m} = 6.24 \text{ kg/m}$, and $EI = 213.33 \text{ N}\cdot\text{m}^2$. The computational results of the eigenfrequencies obtained by the three methods are shown in Table 3.2.

Table 3.2 Computational results of eigenfrequency (rad/s)

Mode	1	2	3	4	5	6	7	8
Analytical method	0.8136	4.0820	6.7085	15.2696	29.0900	47.5685	70.6657	98.3774
Kane's method	0.8223	5.1534	—	14.4298	28.2766	46.7432	69.8263	97.5259
MSTMM	0.8136	4.0820	6.7085	15.2696	29.0900	47.5685	70.6657	98.3774

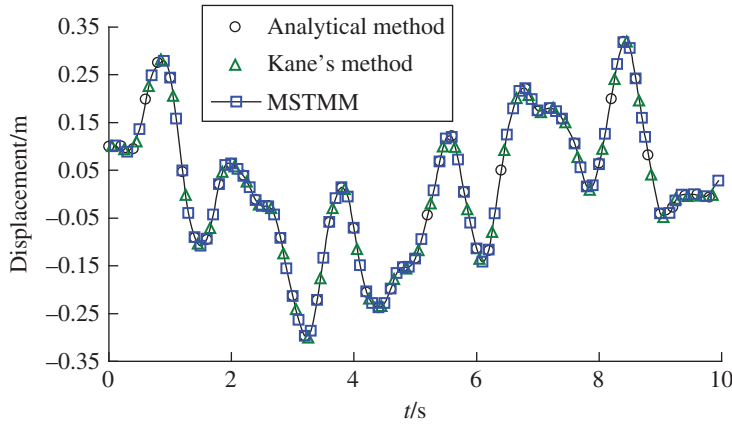


Figure 3.4 The time history of displacement of the free end of the beam.

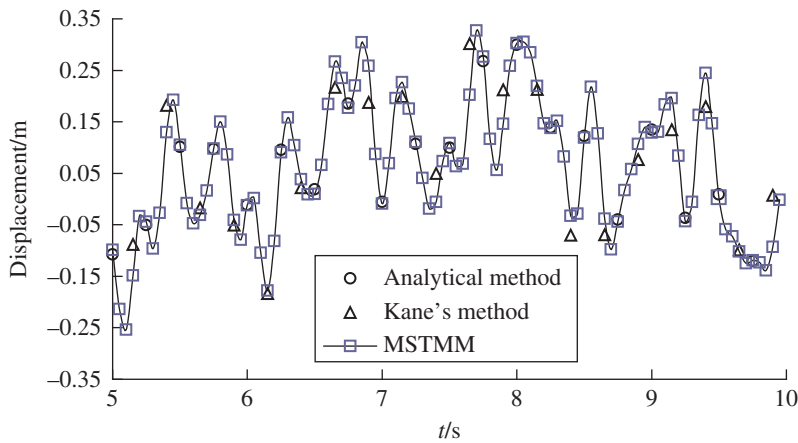


Figure 3.5 The time history of displacement at the free end of beam for $K_i = 10000 \text{ N/m}$.

Obviously the MSTMM belongs to the exact solution. Kane's method belongs to one of approximate methods because the vibration characteristics of the system are replaced by that of a cantilever beam in this example.

The time history of the displacement of point 4 obtained by computation using the three methods is shown in Figure 3.4. The modals are the first 10 orders for the analytical method (\circ), $(1 + n)$ ($n = 4$) orders for Kane's method (\triangle) and the first five orders for the MSTMM (\boxplus). The computational results are shown in Figure 3.5 for $K = 10000 \text{ N/m}$. Clearly, the results obtained by the MSTMM coincide with the analytical solution, but the results obtained by Kane's method are close to the analytical solution only in the first case.

To find the analytical solution is complicated, and impossible for the general complex system. The process of Kane's method is complex. The computation for the MSTMM is easy and has high computational accuracy.

3.7 Steady-state Response of a Damped Multibody System

3.7.1 Treatment of the Damping Forces in a Multibody System

The body dynamics equation of a viscous-damped MRFS is

$$\mathbf{M}\mathbf{v}_{tt} + \mathbf{C}\mathbf{v}_t + \mathbf{K}\mathbf{v} = \mathbf{f} \quad (3.135)$$

where \mathbf{C} is the damping augmented operator of the system.

Substituting $\mathbf{v} = \sum_{k=1}^n \mathbf{V}^k q^k(t)$ into Equation (3.135) yields

$$\sum_{k=1}^n \mathbf{M}\mathbf{V}^k \ddot{q}^k(t) + \sum_{k=1}^n \mathbf{C}\mathbf{V}^k \dot{q}^k(t) + \sum_{k=1}^n \mathbf{K}\mathbf{V}^k q^k(t) = \mathbf{f} \quad (3.136)$$

Taking the inner product for \mathbf{V}^p ($p = 1, 2, \dots, n$) on both sides of Equation (3.136) yields

$$M_p \ddot{q}^p(t) + \sum_{k=1}^n \langle \mathbf{C}\mathbf{V}^k, \mathbf{V}^p \rangle \dot{q}^k(t) + K_p q^p(t) = f_p(t) \quad (p = 1, 2, \dots, n) \quad (3.137)$$

General speaking, the augmented eigenvector is not orthogonal with respect to the damping augmented operator \mathbf{C} , namely for $k \neq p$ the equation $\langle \mathbf{C}\mathbf{V}^k, \mathbf{V}^p \rangle = 0$ does not always hold. Thus, the coordinates in Equation (3.137) are still coupled. Taking the system shown in Figure 3.6 as an example, it is easy to write the damping augmented operator of this system:

$$\mathbf{C} = \begin{bmatrix} C & 0 & 0 \\ 0 & 0 & 0 \\ 0 & 0 & 0 \end{bmatrix} \quad (3.138)$$

The augmented eigenvectors \mathbf{V}^k ($k = 1, 2, 3$) of the system are

$$\mathbf{V}^1 = \begin{bmatrix} 1 \\ 2 \\ 1 \end{bmatrix}, \quad \mathbf{V}^2 = \begin{bmatrix} 1 \\ 0 \\ -1 \end{bmatrix}, \quad \mathbf{V}^3 = \begin{bmatrix} 1 \\ -1 \\ 1 \end{bmatrix} \quad (3.139)$$

Noting that $C_{kp} = \langle \mathbf{C}\mathbf{V}^k, \mathbf{V}^p \rangle$, then

$$[C_{kp}] = \begin{bmatrix} C & C & C \\ C & C & C \\ C & C & C \end{bmatrix} \quad (3.140)$$

Obviously, $[C_{kp}]$ is not a diagonal matrix, namely, for $k \neq p$, $\langle \mathbf{C}\mathbf{V}^k, \mathbf{V}^p \rangle \neq 0$.

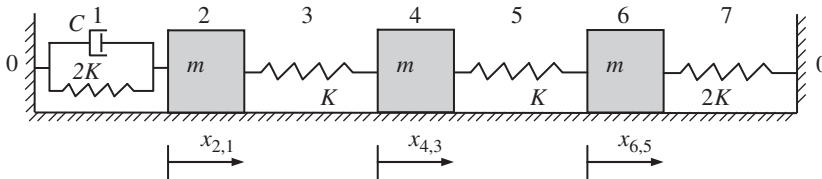


Figure 3.6 A damped system with three degrees of freedom.

The vibration analysis is extremely complex since the coordinates are coupled in Equation (3.137). To use the modal analysis used for the undamped system, the following approximate methods for engineering are applied.

3.7.1.1 Neglecting all the Nondiagonal Elements of Matrix $[C_{kp}]$

The procedure in practice is to let

$$\langle \mathbf{C}\mathbf{V}^k, \mathbf{V}^p \rangle = \delta_{k,p} C_p \quad (3.141)$$

The matrix $[C_{kp}]$ become a diagonal matrix

$$[C_{kp}] = \begin{bmatrix} C_1 & & & \\ & C_2 & & \\ & & \ddots & \\ & & & C_p \\ & & & & \ddots \end{bmatrix} \quad (3.142)$$

where C_p is the damping coefficient of the p th-order principal mode, which is known as the p th-order *mode damping* or *modal damping*.

Hence, Equation (3.137) is decoupled and the p th equation becomes

$$M_p \ddot{q}^p(t) + C_p \dot{q}^p(t) + K_p q^p(t) = f_p(t) \quad (3.143)$$

Both sides of Equation (3.143) are divided by M_p , then let

$$\frac{C_p}{M_p} = 2\zeta_p \omega_p \quad (3.144)$$

Then Equation (3.143) becomes

$$\ddot{q}^p(t) + 2\zeta_p \omega_p \dot{q}^p(t) + \omega_p^2 q^p(t) = f_p(t)/M_p \quad (3.145)$$

where ζ_p is the p th-order *mode damping ratio* or *modal damping ratio*.

A fairly good approximate solution can usually be obtained with this treatment for general engineering problems.

3.7.1.2 Assumption of Proportional Damping

In this method, the damping parameter matrix is assumed to be proportional to the mass and stiffness parameter matrices

$$\mathbf{C} = \alpha \mathbf{M} + \beta \mathbf{K} \quad (3.146)$$

where α and β are constants.

By using the orthogonality of augmented eigenvectors, we obtain

$$\begin{aligned} & \sum_{k=1}^n \langle \mathbf{C}\mathbf{V}^k, \mathbf{V}^p \rangle \dot{q}^k(t) \\ &= \sum_{k=1}^n \langle \alpha \mathbf{M}\mathbf{V}^k, \mathbf{V}^p \rangle \dot{q}^k(t) + \sum_{k=1}^n \langle \beta \mathbf{K}\mathbf{V}^k, \mathbf{V}^p \rangle \dot{q}^k(t) = (\alpha M_p + \beta K_p) \dot{q}^p(t) \end{aligned} \quad (3.147)$$

Obviously Equation (3.147) is decoupled and thus

$$C_p = \alpha M_p + \beta K_p \quad (3.148)$$

By rewriting Equation (3.144), we obtain

$$\zeta_p = \frac{C_p}{2\omega_p M_p} = \frac{1}{2} \left(\frac{\alpha}{\omega_p} + \beta \omega_p \right) \quad (3.149)$$

The first and second terms on the right-hand side of Equation (3.149) are inversely proportional and proportional, respectively, to the eigenfrequency ω_p . Hence, α and β affect mainly low and high frequencies, respectively.

3.7.1.3 Determine each Mode Damping Ratio by Experiment

Until now the mechanisms of damping have not been clear, and it has been difficult to measure or compute accurately the practical damping matrix. The mode damping ratio is usually measured directly by experiment when $\zeta_p \leq 0.2$ ($p = 1, 2, \dots, n$) in practice and then each parameter in Equation (3.145) is obtained.

3.7.1.4 Take Damping as an External Force

If the external force vector \mathbf{f} acting on MRFS relates to the displacement, velocity and other parameters of the system, the inner product $\langle \mathbf{f}, \mathbf{V}^p \rangle$ will contain the generalized coordinates $q^p(t)$ and the terms corresponding to dampings in Equation (3.137) may be treated as external forces, namely

$$f_p(t, q^1, q^2, \dots, q^n, \dot{q}^1, \dot{q}^2, \dots, \dot{q}^n) = \langle \mathbf{f}, \mathbf{V}^p \rangle - \sum_{k=1}^n \langle \mathbf{C} \mathbf{V}^k, \mathbf{V}^p \rangle \dot{q}^k(t) \quad (p = 1, 2, \dots, n) \quad (3.150)$$

Then, Equation (3.137) becomes

$$\ddot{q}^p(t) + \omega_p^2 q^p(t) = \frac{f_p(t, q^1, q^2, \dots, q^n, \dot{q}^1, \dot{q}^2, \dots, \dot{q}^n)}{M_p} \quad (p = 1, 2, \dots, n) \quad (3.151)$$

In fact, Equation (3.151) has not been decoupled. If the value f_p in any time is instead given by its value the previous time, the computation and programming may be simplified greatly. It is impossible to decouple completely the dynamics equations for many practical engineering applications because of their time variance and nonlinearity, therefore this approach is very useful.

3.7.1.5 Damping Linear Operator

For convenience, the *damping linear operator* can be defined as follows for complex MRFS:

$$\begin{cases} d^3|_I x_{I,i} = q_{x,I,i}^d \\ d^3|_I y_{I,i} = q_{y,I,i}^d \\ d^3|_I z_{I,i} = q_{z,I,i}^d \end{cases}, \quad \begin{cases} d^3|_O x_{O,i} = q_{x,O,i}^d \\ d^3|_O y_{O,i} = q_{y,O,i}^d \\ d^3|_O z_{O,i} = q_{z,O,i}^d \end{cases} \quad (3.152)$$

$$\begin{cases} d^1|_I \theta_{x,I,i} = m_{x,I,i}^d \\ d^1|_I \theta_{y,I,i} = m_{y,I,i}^d \\ d^1|_I \theta_{z,I,i} = m_{z,I,i}^d \end{cases} \quad \begin{cases} d^1|_O \theta_{x,O,i} = m_{x,O,i}^d \\ d^1|_O \theta_{y,O,i} = m_{y,O,i}^d \\ d^1|_O \theta_{z,O,i} = m_{z,O,i}^d \end{cases} \quad (3.153)$$

where i is the sequence number of the body element, I and O denote the input and output ends, and, q_x^d, q_y^d and q_z^d and, m_x^d, m_y^d and m_z^d denote damping forces and damping moments.

The combination of the damping linear operator d^3 and the displacement of a point of a body element results in the damping force acting on this point, while the combination of the operator d^1 and an angular displacement of a point of a body element leads to the damping moment acting on this point. For example, using the linear operator d^3 , the damping force acting on the body element of sequence number i in the system shown in Figure 3.5 can be written as

$$d^3|_{I,i} x_{i,i-1} = q_{x,i,i-1}^d = -C_{i-1}(\dot{x}_{i,i-1} - \dot{x}_{i-2,i-1}), \quad d^3|_{O,i} x_{i,i-1} = q_{x,i,i+1}^d = -C_{i+1}(\dot{x}_{i+2,i+1} - \dot{x}_{i,i+1}) \quad (3.154)$$

The damping augmented operator of the system is

$$C = \begin{bmatrix} -d^3|_{I,2} + d^3|_{O,2} & 0 & 0 \\ 0 & -d^3|_{I,4} + d^3|_{O,4} & 0 \\ 0 & 0 & -d^3|_{I,6} + d^3|_{O,6} \end{bmatrix} \quad (3.155)$$

3.7.2 Steady-state Response of a Damped Multibody System

3.7.2.1 Approximate Solution of the Dynamics Responses of a Multibody System

According to the approximate treatment methods for damping discussed in Section 3.7.1, the solution of differential Equation (3.145) in term of generalized coordinates is obtained as follows

$$q^p(t) = e^{-\zeta_p \omega_p t} \left(q_0^p \cos \omega_{d,p} t + \frac{\dot{q}_0^p + \zeta_p \omega_p q_0^p}{\omega_{d,p}} \sin \omega_{d,p} t \right) + \frac{1}{M_p \omega_{d,p}} \int_0^t f_p(\tau) e^{-\zeta_p \omega_p (t-\tau)} \sin \omega_{d,p} (t-\tau) d\tau \quad (3.156)$$

where

$$\omega_{d,p} = \omega_p \sqrt{1 - \zeta_p^2} \quad (3.157)$$

$\omega_{d,p}$ is the p th-order damped eigenfrequency.

Substituting $q^p(t)$ into

$$v = \sum_{p=1}^n V^p q^p(t)$$

gives the dynamics response of the system to arbitrary excitation.

3.7.2.2 The General Solution of Dynamics Responses of MRFS

The general steps for solving the dynamic response of a damped MRFS to arbitrary excitation using the mode superposition method are as follows.

- 1) Compute the vibration characteristic of the undamped system.
- 2) Write the body dynamics equations of the system and construct the augmented eigenvectors of the undamped system.

- 3) Decouple the body dynamics equations of the system using the orthogonality of the augmented eigenvectors and transform the partial differential equations to ordinary differential equations, dealing with the damping according to the methods described in Section 3.7.1.
- 4) Compute the initial conditions and excitation force under the generalized coordinates.
- 5) Compute the generalized coordinates of the system.
- 6) Compute the dynamics responses in physical coordinates using generalized coordinates and augmented eigenvectors.

Example 3.10 The system shown in Figure 3.7 is similar to that in Example 3.9. However, a damper in parallel to spring 1 is added and damping of the beam is considered. The viscous damping coefficient of the damper is C and the internal friction damping coefficient of the beam is C' . All the other physical parameters are the same as for Example 3.9. At the initial time, beam 3 has no deformation, the spring is elongated by 0.1 m and an external force $F_2 = F \sin \Omega t$ acts on the lumped mass 2, which moves from rest. Find the dynamics response of the system.

Solution

The vibration characteristics of the undamped system corresponding to this system have already been obtained in Example 3.9. The body dynamics equation of the system is

$$\mathbf{M}\mathbf{v}_{tt} + \mathbf{C}\mathbf{v}_t + \mathbf{K}\mathbf{v} = \mathbf{f} \quad (3.158)$$

where

$$\mathbf{M} = \begin{bmatrix} m & 0 \\ 0 & \bar{m} \end{bmatrix}, \quad \mathbf{v} = \begin{bmatrix} y_{2,1}(t) \\ y_3(x, t) \end{bmatrix}, \quad \mathbf{f} = \begin{bmatrix} F_2 \\ 0 \end{bmatrix}$$

$$\mathbf{C} = \begin{bmatrix} -d^3|_{l,2} + d^3|_{0,2} & 0 \\ 0 & C' \frac{\partial^4}{\partial x^4} \end{bmatrix}, \quad \mathbf{K} = \begin{bmatrix} -D^3|_{l,2} + D^3|_{0,2} & 0 \\ 0 & EI \frac{\partial^4}{\partial x^4} \end{bmatrix}$$

Let $\mathbf{v} = \sum_{k=1}^{\infty} \mathbf{V}^k q^k(t)$, where $\mathbf{V}^k = [Y_{2,1}^k, Y_3^k(x)]^T$ is an augmented eigenvector and $q^k(t)$ is the corresponding generalized coordinate. Using the orthogonality of the augmented eigenvector, Equation (3.158) becomes

$$\ddot{q}^p(t) + \sum_{k=1}^{\infty} \frac{\langle \mathbf{C}\mathbf{V}^k, \mathbf{V}^p \rangle \dot{q}^k(t)}{M_p} + \omega_p^2 q^p(t) = \frac{\langle \mathbf{f}, \mathbf{V}^p \rangle}{M_p} \quad (p = 1, 2, \dots) \quad (3.159)$$

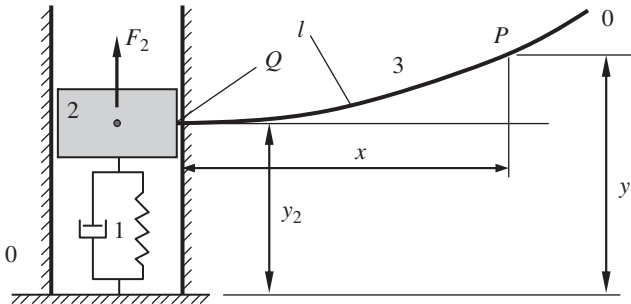


Figure 3.7 A damped system vibrating in a plane.

It can be proved that

$$\langle \mathbf{C}\mathbf{V}^k, \mathbf{V}^p \rangle = CY_{2,1}^k Y_{2,1}^p + C' \int_0^l \frac{d^2 Y^k(x)}{dx^2} \frac{d^2 Y^p(x)}{dx^2} dx \quad (3.160)$$

due to

$$\langle \mathbf{K}\mathbf{V}^k, \mathbf{V}^p \rangle = KY_{2,1}^k Y_{2,1}^p + EI \int_0^l \frac{d^2 Y^k(x)}{dx^2} \frac{d^2 Y^p(x)}{dx^2} dx = M_p \omega_p^2 \delta_{kp} \quad (3.161)$$

namely

$$\int_0^l \frac{d^2 Y^k(x)}{dx^2} \frac{d^2 Y^p(x)}{dx^2} dx = \frac{M_p \omega_p^2 \delta_{kp} - KY_{2,1}^k Y_{2,1}^p}{EI}$$

Equation (3.160) can be rewritten as

$$\frac{\langle \mathbf{C}\mathbf{V}^k, \mathbf{V}^p \rangle}{M_p} = \left(C - \frac{C'K}{EI} \right) \frac{Y_{2,1}^k Y_{2,1}^p}{M_p} + \frac{C'}{EI} \omega_p^2 \delta_{kp} \quad (3.162)$$

Substituting Equation (3.162) into Equation (3.159) yields

$$\ddot{q}^p(t) + \sum_{k=1}^{\infty} \left[\left(C - \frac{C'K}{EI} \right) \frac{Y_{2,1}^k Y_{2,1}^p}{M_p} + \frac{C'}{EI} \omega_p^2 \delta_{kp} \right] \dot{q}^k(t) + \omega_p^2 q^p(t) = \frac{Y_{2,1}^p}{M_p} F \sin \Omega t \quad (p = 1, 2, \dots) \quad (3.163)$$

The initial conditions are

$$q^p|_{t=0} = \frac{\langle \mathbf{M}[0.1, 0.1]^T, \mathbf{V}^p \rangle}{M_p}, \quad \dot{q}^p|_{t=0} = 0 \quad (p = 1, 2, \dots) \quad (3.164)$$

The generalized coordinate $q^p(t)$ can be obtained by integrating Equation (3.163) and considering the initial conditions of Equation (3.164). The dynamics response of the system is thus obtained

by $\mathbf{v} = \sum_{p=1}^{\infty} \mathbf{V}^p q^p(t)$. Three simplified methods are used to solve Equation (3.163) as follows.

1) Approximate solution

With the first n th modes, let $\langle \mathbf{C}\mathbf{V}^k, \mathbf{V}^p \rangle = \delta_{k,p} C_p$, namely

$$\sum_{k=1}^n \left[\left(C - \frac{C'K}{EI} \right) \frac{Y_{2,1}^k Y_{2,1}^p}{M_p} + \frac{C'}{EI} \omega_p^2 \delta_{kp} \right] = \left(C - \frac{C'K}{EI} \right) \frac{Y_{2,1}^p Y_{2,1}^p}{M_p} + \frac{C'}{EI} \omega_p^2 = 2\zeta_p \omega_p \quad (3.165)$$

Then Equation (3.163) becomes

$$\ddot{q}^p(t) + 2\zeta_p \omega_p \dot{q}^p(t) + \omega_p^2 q^p(t) = \frac{Y_{2,1}^p}{M_p} F \sin \Omega t \quad (p = 1, 2, \dots, n) \quad (3.166)$$

2) Quasi exact solution

On the basis of Equation (3.165), let $\sum_{k=1, k \neq p}^n \left[\left(C - \frac{C'K}{EI} \right) \frac{Y_{2,1}^k Y_{2,1}^p}{M_p} + \frac{C'}{EI} \omega_p^2 \delta_{kp} \right] \dot{q}^k(t) = r_0^p(t)$

then Equation (3.163) may be reformulated as

$$\ddot{q}^p(t) + 2\zeta_p \omega_p \dot{q}^p(t) + \omega_p^2 q^p(t) = \frac{Y_{2,1}^p}{M_p} F \sin \Omega t - r_0^p(t) \quad (p = 1, 2, \dots, n) \quad (3.167)$$

Take the value of $r_{0-}^p(t)$ at the time of the last step when integrating Equation (3.167).

3) Exact solution

Rewrite Equation (3.163) directly as

$$\ddot{q}^p(t) + 2\zeta_p\omega_p\dot{q}^p(t) + \omega_p^2q^p(t) = \frac{Y_{2,1}^p}{M_p}F \sin\Omega t - \sum_{k=1, k \neq p}^n \left(C - \frac{C'K}{EI} \right) \frac{Y_{2,1}^k Y_{2,1}^p}{M_p} \dot{q}^k(t) \quad (p=1, 2, \dots, n) \quad (3.168)$$

Numerically integrate n ordinary differential equations of two orders together.

If $K = 615.86 \text{ N/m}$, $C = 5.0 \text{ kg/s}$, $m = 15.6 \text{ kg}$, $l = 5 \text{ m}$, $\bar{m} = 6.24 \text{ kg/m}$, $EI = 213.33 \text{ N m}^2$, $C' = 1.0 \text{ kg m}^3/\text{s}$, $F = 20 \text{ N}$, $\Omega = 0.5 \text{ rad/s}$, and $n = 10$, the computational results of the time histories of the displacements of the lumped mass 2 and the free end of the beam obtained by three methods are shown in Figures 3.8a and b, respectively.

For the same parameters except for $C = 40 \text{ kg/s}$, $C' = 8 \text{ kg m}^3/\text{s}$ and $\Omega = 0.5 \text{ rad/s}$, the computational results are shown in Figures 3.8c and d, respectively. In this situation, the damping is too large to belong to micro-damping, so the first method is no longer applicable. The accuracy of the second method is high enough because the results obtained by the second and third methods are almost identical.

3.8 Steady-state Response of a Multibody System

3.8.1 Steady-state Response of a Multibody System to Harmonic Excitation

3.8.1.1 Steady-state Response of a Single DOF System to Harmonic Excitation

The dynamics equation of a damped system with a single DOF under a harmonic force $F(t) = F^c \cos\Omega t + F^s \sin\Omega t$ is

$$m\ddot{x}_t + C\dot{x}_t + Kx = F(t) \quad (3.169)$$

Note that if $F(t) = F \cos(\Omega t + \alpha)$, then

$$F = \sqrt{(F^c)^2 + (F^s)^2}, \quad \tan\alpha = \frac{-F^s}{F^c} \quad (3.170)$$

where F and α are the amplitude and phase of the exciting force $F(t)$, respectively. $F^c = F \cos\alpha$, $F^s = -F \sin\alpha$.

$F(t)$ can be written as

$$F(t) = \text{Re}\left(Fe^{i(\Omega t + \alpha)}\right) = \text{Re}\left(\bar{F}e^{i\Omega t}\right) \quad (3.171)$$

where $\bar{F} = Fe^{i\alpha}$.

Then Equation (3.69) can be written as

$$m\ddot{x}_t + C\dot{x}_t + Kx = \text{Re}\left(Fe^{i(\Omega t + \alpha)}\right) \quad \text{or} \quad m\ddot{x}_t + C\dot{x}_t + Kx = \text{Re}\left(\bar{F}e^{i\Omega t}\right) \quad (3.172)$$

The steady-state solution of Equation (3.172) is $x = \text{Re}(\bar{X}e^{i\Omega t})$, where \bar{X} is the complex amplitude of forced vibration. Substituting this into Equation (3.172) yields

$$\bar{X} = \frac{Fe^{i\alpha}}{K - m\Omega^2 + iC\Omega} = \frac{F}{K} \frac{e^{i\alpha}}{1 - m\Omega^2/K + iC\Omega/K} = \frac{F}{K} Me^{i(\alpha - \beta)} \quad (3.173)$$

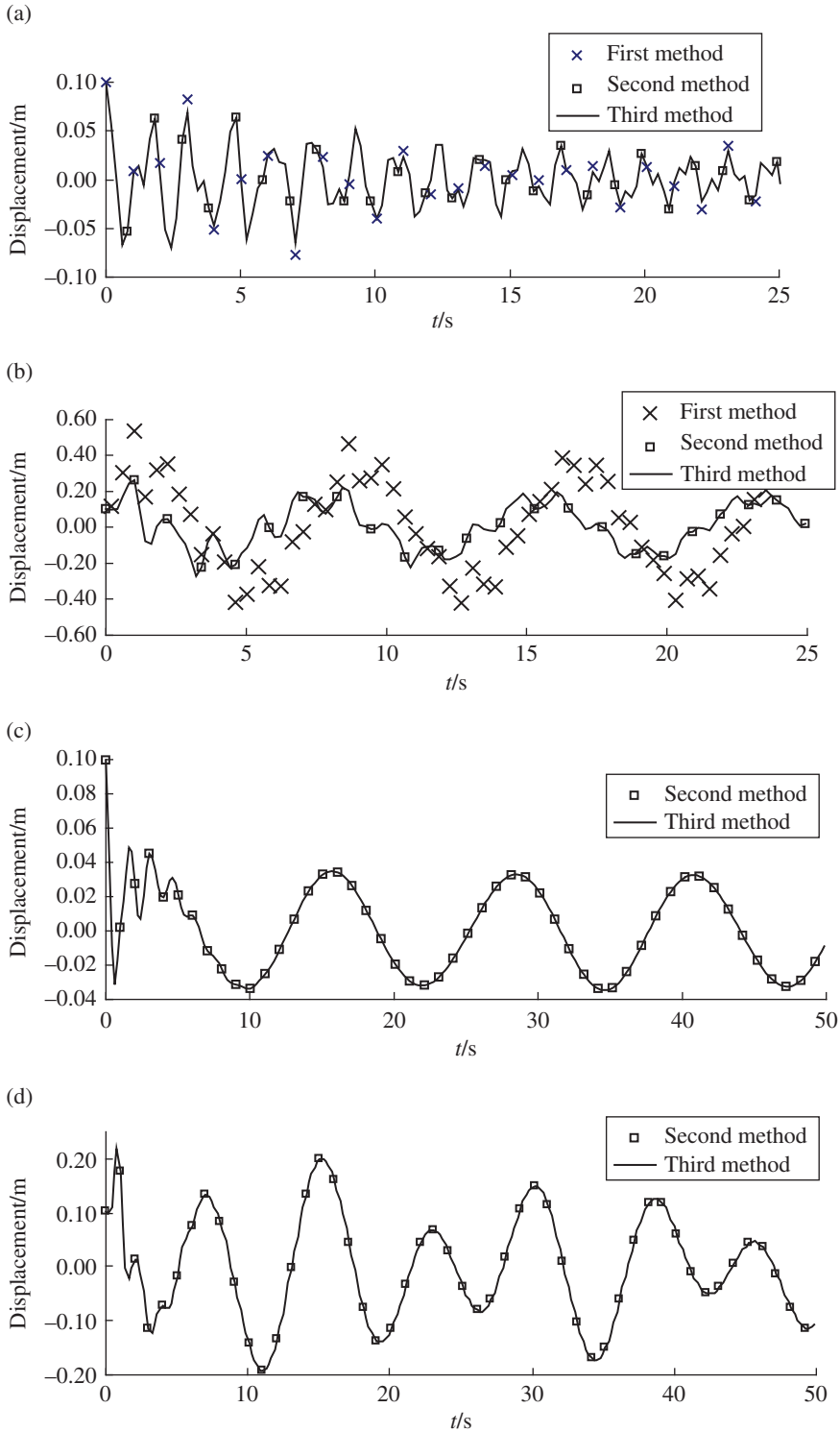


Figure 3.8 The computational result of the dynamics response of a damped plane vibration system: (a) time history of displacement of lumped mass 2, (b) time history of displacement of the free end of beam 3, (c) time history of displacement of lumped mass 2 and (d) time history of displacement of the free end of beam 3.

where

$$M = \frac{1}{\sqrt{\left(1 - \frac{\Omega^2}{\omega_n^2}\right)^2 + \left(2\zeta \frac{\Omega}{\omega_n}\right)^2}}, \quad \tan \beta = \frac{2\zeta \Omega \omega_n}{\omega_n^2 - \Omega^2}, \quad \omega_n = \sqrt{\frac{K}{m}}, \quad \zeta = \frac{C}{2\sqrt{Km}} \quad (3.174)$$

M is the magnification factor of the dynamic vibration amplitude and β is the phase-lag angle of response x relative exciting force $F(t)$.

The steady-state response of the system is

$$x = \operatorname{Re}(\bar{X} e^{i\Omega t}) = \frac{M}{K} F^c \cos(\Omega t - \beta) + \frac{M}{K} F^s \sin(\Omega t - \beta) \quad (3.175)$$

3.8.1.2 Steady-state Response of a MRFS to Harmonic Excitation

The body dynamics equation of a damped MRFS under an external force $f(t) = f^c \cos \Omega t + f^s \sin \Omega t$ is

$$\mathbf{M} \mathbf{v}_{tt} + \mathbf{C} \mathbf{v}_t + \mathbf{K} \mathbf{v} = f^c \cos \Omega t + f^s \sin \Omega t \quad (3.176)$$

Note that $f(t)$ cannot be written in the form of $f(t) = f \cos(\Omega t + \alpha)$. However, using the orthogonality of the augmented eigenvectors and the simplification treatment for damping, we can obtain

$$M_p \ddot{q}^p(t) + C_p \dot{q}^p(t) + K_p q^p(t) = \langle f^c, V^p \rangle \cos \Omega t + \langle f^s, V^p \rangle \sin \Omega t \quad (3.177)$$

Note that if $f_p^c = \langle f^c, V^p \rangle$, $f_p^s = \langle f^s, V^p \rangle$, $F_p(t) = f_p^c \cos \Omega t + f_p^s \sin \Omega t$, then

$$M_p \ddot{q}^p(t) + C_p \dot{q}^p(t) + K_p q^p(t) = F_p(t) \quad (3.178)$$

Comparing Equation (3.178) with Equation (3.169), and using the results of section 3.8.1.1, yields

$$q^p(t) = \frac{M^p}{K_p} \left[f_p^c \cos(\Omega t - \beta^p) + f_p^s \sin(\Omega t - \beta^p) \right] \quad (3.179)$$

where

$$M^p = \frac{1}{\sqrt{\left(1 - \frac{\Omega^2}{\omega_p^2}\right)^2 + \left(2\zeta_p \frac{\Omega}{\omega_p}\right)^2}}, \quad \tan \beta^p = \frac{2\zeta_p \Omega \omega_p}{\omega_p^2 - \Omega^2} \quad (3.180)$$

M^p is the magnification factor of the vibration amplitude of p th-order and β^p is the phase-lag angle of principal coordinate $q^p(t)$ of p th-order relative to exciting force $F_p(t)$.

The steady-state response of the system is then

$$\mathbf{v} = \sum_{p=1}^{\infty} V^p q^p(t) = \sum_{p=1}^{\infty} V^p \frac{M^p}{K_p} \left[f_p^c \cos(\Omega t - \beta^p) + f_p^s \sin(\Omega t - \beta^p) \right] \quad (3.181)$$

3.8.1.3 Solve the Steady-state Response of an MRFS under Harmonic Excitation Using the Extended MSTMM

The solution of the steady-state response of an MRFS under harmonic excitation using the extended MSTMM has been discussed in Chapter 2. The computational time needed for this method is less than that for the method used in section 3.8.1.2. Only the calculation of the extended transfer matrices should be carried out, and the vibration characteristic of the system does not need to be solved. The approximate treatment for damping is necessary and only the approximate solution can be obtained if using the method used in section 3.8.1.2. The extended MSTMM results in an exact solution of the system.

3.8.2 Steady-state Response of a Multibody System to Periodic Excitation

The body dynamics equation of a damped MRFS is

$$\mathbf{M}\mathbf{v}_{tt} + \mathbf{C}\mathbf{v}_t + \mathbf{K}\mathbf{v} = \mathbf{f}(t) \quad (3.182)$$

If the external force $\mathbf{f}(t)$ is a function of period $2T$, it can be expanded using Fourier series as follows

$$\mathbf{f}(t) = \frac{1}{2}\mathbf{f}_0^c + \sum_{k=1}^{\infty} \left(\mathbf{f}_k^c \cos \frac{k\pi}{T}t + \mathbf{f}_k^s \sin \frac{k\pi}{T}t \right) \quad (3.183)$$

where

$$\begin{cases} \mathbf{f}_k^c = \frac{1}{T} \int_{-T}^T \mathbf{f}(t) \cos \frac{k\pi}{T}t dt & (k = 0, 1, 2, \dots) \\ \mathbf{f}_k^s = \frac{1}{T} \int_{-T}^T \mathbf{f}(t) \sin \frac{k\pi}{T}t dt & (k = 1, 2, \dots) \end{cases} \quad (3.184)$$

$\mathbf{f}_0^c, \mathbf{f}_k^c, \mathbf{f}_k^s (k = 1, 2, \dots)$ are constant column matrices.

With the method used in part (3) of section 3.8.1 the steady-state responses $\mathbf{v}^0, \mathbf{v}^k (k = 1, 2, \dots)$ can be obtained by solving the following equations

$$\begin{aligned} \mathbf{M}\mathbf{v}_{tt}^0 + \mathbf{C}\mathbf{v}_t^0 + \mathbf{K}\mathbf{v}^0 &= \frac{1}{2}\mathbf{f}_0^c \\ \mathbf{M}\mathbf{v}_{tt}^k + \mathbf{C}\mathbf{v}_t^k + \mathbf{K}\mathbf{v}^k &= \mathbf{f}_k^c \cos \frac{k\pi}{T}t + \mathbf{f}_k^s \sin \frac{k\pi}{T}t \quad (k = 1, 2, \dots) \end{aligned} \quad (3.185)$$

The steady-state response of the system $\mathbf{v} = \mathbf{v}^0 + \sum_{k=1}^{\infty} \mathbf{v}^k$ can be obtained by superposition of $\mathbf{v}^0, \mathbf{v}^k (k = 1, 2, \dots)$.

It should be pointed out that this process is only the mathematical explanation to solve steady-state response, and the practical method of solving $\mathbf{v}^0, \mathbf{v}^k (k = 1, 2, \dots)$ is still by extended transfer matrix method. For example in part (3) in section 3.8.1, the external force \mathbf{F}_2 appears in the extended transfer matrix $\tilde{\mathbf{U}}_2$ in the form of $\bar{\mathbf{F}}_2 = \mathbf{F}_2^c - i\mathbf{F}_2^s$, and the external force \mathbf{F}_5 appears in the extended transfer matrix $\tilde{\mathbf{U}}_5$ in the form of $\bar{\mathbf{F}}_5 = \mathbf{F}_5^c - i\mathbf{F}_5^s$. Equation (3.182) is solved rather than directly using Equation (3.183). We still use the above-mentioned MRFS to explain the solving process.

In the above example, assume that

$$\mathbf{F}_2 = \mathbf{F}_2(t) = \begin{bmatrix} F_{x,2} \\ F_{y,2} \end{bmatrix} F_2(t), \quad \mathbf{F}_5 = \mathbf{F}_5(t) = \begin{bmatrix} F_{x,5} \\ F_{y,5} \end{bmatrix} F_5(t) \quad (3.186)$$

where

$$\begin{cases} F_2(t) = \frac{1}{2}F_{2,0}^c + \sum_{k=1}^{\infty} \left(F_{2,k}^c \cos \frac{k\pi}{T}t + F_{2,k}^s \sin \frac{k\pi}{T}t \right) \\ F_5(t) = \frac{1}{2}F_{5,0}^c + \sum_{k=1}^{\infty} \left(F_{5,k}^c \cos \frac{k\pi}{T}t + F_{5,k}^s \sin \frac{k\pi}{T}t \right) \end{cases} \quad (3.187)$$

$$\begin{cases} F_{2,k}^c = \frac{1}{T} \int_{-T}^T F_2(t) \cos \frac{k\pi}{T}t dt & (k=0,1,\dots) \\ F_{2,k}^s = \frac{1}{T} \int_{-T}^T F_2(t) \sin \frac{k\pi}{T}t dt & (k=1,2,\dots) \end{cases}, \begin{cases} F_{5,k}^c = \frac{1}{T} \int_{-T}^T F_5(t) \cos \frac{k\pi}{T}t dt & (k=0,1,\dots) \\ F_{5,k}^s = \frac{1}{T} \int_{-T}^T F_5(t) \sin \frac{k\pi}{T}t dt & (k=1,2,\dots) \end{cases} \quad (3.188)$$

$F_{2,k}^c, F_{5,k}^c (k=0,1,2,\dots)$ and $F_{2,k}^s, F_{5,k}^s (k=1,2,\dots)$ are constant real numbers.

Substituting Equation (3.187) into Equation (3.186) yields

$$F_2 = \frac{1}{2} \begin{bmatrix} F_{x,2} & F_{2,0}^c \\ F_{y,2} & F_{2,0}^c \end{bmatrix} + \sum_{k=1}^{\infty} \left(\begin{bmatrix} F_{x,2} & F_{2,k}^c \\ F_{y,2} & F_{2,k}^c \end{bmatrix} \cos \frac{k\pi}{T}t + \begin{bmatrix} F_{x,2} & F_{2,k}^s \\ F_{y,2} & F_{2,k}^s \end{bmatrix} \sin \frac{k\pi}{T}t \right) \quad (3.189)$$

$$F_5 = \frac{1}{2} \begin{bmatrix} F_{x,5} & F_{5,0}^c \\ F_{y,5} & F_{5,0}^c \end{bmatrix} + \sum_{k=1}^{\infty} \left(\begin{bmatrix} F_{x,5} & F_{5,k}^c \\ F_{y,5} & F_{5,k}^c \end{bmatrix} \cos \frac{k\pi}{T}t + \begin{bmatrix} F_{x,5} & F_{5,k}^s \\ F_{y,5} & F_{5,k}^s \end{bmatrix} \sin \frac{k\pi}{T}t \right) \quad (3.190)$$

Note that if

$$\Omega_k = \frac{k\pi}{T}$$

$$F_{2,0}^c = \frac{1}{2} \begin{bmatrix} F_{x,2} & F_{2,0}^c \\ F_{y,2} & F_{2,0}^c \end{bmatrix}, \quad F_{2,k}^c = \begin{bmatrix} F_{x,2} & F_{2,k}^c \\ F_{y,2} & F_{2,k}^c \end{bmatrix}, \quad F_{2,k}^s = \begin{bmatrix} F_{x,2} & F_{2,k}^s \\ F_{y,2} & F_{2,k}^s \end{bmatrix}$$

$$F_{5,0}^c = \frac{1}{2} \begin{bmatrix} F_{x,5} & F_{5,0}^c \\ F_{y,5} & F_{5,0}^c \end{bmatrix}, \quad F_{5,k}^c = \begin{bmatrix} F_{x,5} & F_{5,k}^c \\ F_{y,5} & F_{5,k}^c \end{bmatrix}, \quad F_{5,k}^s = \begin{bmatrix} F_{x,5} & F_{5,k}^s \\ F_{y,5} & F_{5,k}^s \end{bmatrix}$$

then

$$\begin{cases} F_2 = F_{2,0}^c + \sum_{k=1}^{\infty} (F_{2,k}^c \cos \Omega_k t + F_{2,k}^s \sin \Omega_k t) \\ F_5 = F_{5,0}^c + \sum_{k=1}^{\infty} (F_{5,k}^c \cos \Omega_k t + F_{5,k}^s \sin \Omega_k t) \end{cases} \quad (3.191)$$

Using the same method and steps as in part (3) of section 3.8.1, the steady-state response \mathbf{v}^0 of the system under the static load $F_{2,0}^c$ and $F_{5,0}^c$ is solved first. Then the steady-state responses $\mathbf{v}^k (k=1,2,\dots)$ under the harmonic forces $F_{2,k}$ and $F_{5,k}$ with frequency Ω_k are computed one by one, and finally the steady-state response of the system excited by an external force with a period of $2T$ is obtained as

$$\mathbf{v} = \mathbf{v}^0 + \sum_{k=1}^{\infty} \mathbf{v}^k$$

Example 3.11 Solve the steady-state response of the system in Example 3.10 using the extended MSTMM.

Solution

Define the extended state vectors $\hat{\mathbf{Z}}_{1,0}$, $\hat{\mathbf{Z}}_{2,1}$, $\hat{\mathbf{Z}}_{2,3}$, $\hat{\mathbf{Z}}_{3,0}$ as

$$\hat{\mathbf{Z}} = \begin{bmatrix} Y^r & \boldsymbol{\theta}_z^r & M_z^r & Q_y^r & Y^i & \boldsymbol{\theta}_z^i & M_z^i & Q_y^i & 1 \end{bmatrix}^T \quad (3.192)$$

The extended transfer equations of the corresponding elements are

$$\hat{\mathbf{Z}}_{2,1} = \hat{\mathbf{U}}_1 \hat{\mathbf{Z}}_{1,0}, \quad \hat{\mathbf{Z}}_{2,3} = \hat{\mathbf{U}}_2 \hat{\mathbf{Z}}_{2,1}, \quad \hat{\mathbf{Z}}_{3,0} = \hat{\mathbf{U}}_3 \hat{\mathbf{Z}}_{2,3} \quad (3.193)$$

where $\hat{\mathbf{U}}_1$, $\hat{\mathbf{U}}_2$ and $\hat{\mathbf{U}}_3$ are extended transfer matrices of hinge 1, body 2 and body 3, respectively:

$$\hat{\mathbf{U}}_1 = \begin{bmatrix} \mathbf{U}^r & -\mathbf{U}^i & \mathbf{O}_{4 \times 1} \\ \mathbf{U}^i & \mathbf{U}^r & \mathbf{O}_{4 \times 1} \\ \mathbf{O}_{1 \times 4} & \mathbf{O}_{1 \times 4} & 1 \end{bmatrix} \quad (3.194)$$

$$\mathbf{U}^r = \begin{bmatrix} 1 & 0 & 0 & -K/(K^2 + C^2\Omega^2) \\ 0 & 1 & 0 & 0 \\ 0 & 0 & 1 & 0 \\ 0 & 0 & 0 & 1 \end{bmatrix}, \quad \mathbf{U}^i = \begin{bmatrix} 0 & 0 & 0 & C\Omega/(K^2 + C^2\Omega^2) \\ 0 & 0 & 0 & 0 \\ 0 & 0 & 0 & 0 \\ 0 & 0 & 0 & 0 \end{bmatrix}$$

$$\hat{\mathbf{U}}_2 = \begin{bmatrix} \mathbf{U}^r & \mathbf{O}_{4 \times 4} & \mathbf{O}_{4 \times 1} \\ \mathbf{O}_{4 \times 4} & \mathbf{U}^r & \mathbf{f}^i \\ \mathbf{O}_{1 \times 4} & \mathbf{O}_{1 \times 4} & 1 \end{bmatrix}, \quad \mathbf{U}^r = \begin{bmatrix} 1 & 0 & 0 & 0 \\ 0 & 1 & 0 & 0 \\ 0 & 0 & 1 & 0 \\ m\Omega^2 & 0 & 0 & 1 \end{bmatrix}, \quad \mathbf{f}^i = \begin{bmatrix} 0 \\ 0 \\ 0 \\ -F \end{bmatrix} \quad (3.195)$$

$$\hat{\mathbf{U}}_3 = \hat{\mathbf{U}}_{x_3=l} = \begin{bmatrix} \mathbf{U}^r & -\mathbf{U}^i & \mathbf{O}_{4 \times 1} \\ \mathbf{U}^i & \mathbf{U}^r & \mathbf{O}_{4 \times 1} \\ \mathbf{O}_{1 \times 4} & \mathbf{O}_{1 \times 4} & 1 \end{bmatrix}_{x_3=l} \quad (3.196)$$

$$\mathbf{U}^r = \begin{bmatrix} u_{11}^r & u_{12}^r & u_{13}^r & u_{14}^r \\ u_{21}^r & u_{22}^r & u_{23}^r & \\ u_{31}^r & u_{32}^r & & \\ u_{41}^r & & & \end{bmatrix}, \quad \mathbf{U}^i = \begin{bmatrix} u_{11}^i & u_{12}^i & u_{13}^i & u_{14}^i \\ u_{21}^i & u_{22}^i & u_{23}^i & \\ u_{31}^i & u_{32}^i & & \\ u_{41}^i & & & \end{bmatrix}$$

symmetrical *symmetrical*

$$\begin{bmatrix} u_{11}^r \\ u_{11}^i \end{bmatrix} = \begin{bmatrix} u_{22}^r \\ u_{22}^i \end{bmatrix} = \begin{bmatrix} S^r \\ S^i \end{bmatrix}, \quad \begin{bmatrix} u_{12}^r \\ u_{12}^i \end{bmatrix} = \frac{1}{\alpha^2 + \beta^2} \begin{bmatrix} \alpha & \beta \\ -\beta & \alpha \end{bmatrix} \begin{bmatrix} T^r \\ T^i \end{bmatrix}$$

$$\begin{bmatrix} u_{13}^r \\ u_{13}^i \end{bmatrix} = \frac{1}{\bar{m}\Omega^2} \begin{bmatrix} \alpha & -\beta \\ \beta & \alpha \end{bmatrix}^2 \begin{bmatrix} U^r \\ U^i \end{bmatrix}, \quad \begin{bmatrix} u_{14}^r \\ u_{14}^i \end{bmatrix} = \frac{1}{\bar{m}\Omega^2} \begin{bmatrix} \alpha & -\beta \\ \beta & \alpha \end{bmatrix} \begin{bmatrix} V^r \\ V^i \end{bmatrix}$$

$$\begin{bmatrix} u_{21}^r \\ u_{21}^i \end{bmatrix} = \begin{bmatrix} \alpha & -\beta \\ \beta & \alpha \end{bmatrix} \begin{bmatrix} V^r \\ V^i \end{bmatrix}, \quad \begin{bmatrix} u_{23}^r \\ u_{23}^i \end{bmatrix} = \frac{1}{\bar{m}\Omega^2} \begin{bmatrix} \alpha & -\beta \\ \beta & \alpha \end{bmatrix}^3 \begin{bmatrix} T^r \\ T^i \end{bmatrix}$$

$$\begin{bmatrix} u_{31}^r \\ u_{31}^i \end{bmatrix} = \begin{bmatrix} EI & -C'\Omega \\ C'\Omega & EI \end{bmatrix} \begin{bmatrix} \alpha & -\beta \\ \beta & \alpha \end{bmatrix}^2 \begin{bmatrix} U^r \\ U^i \end{bmatrix}, \quad \begin{bmatrix} u_{32}^r \\ u_{32}^i \end{bmatrix} = \begin{bmatrix} EI & -C'\Omega \\ C'\Omega & EI \end{bmatrix} \begin{bmatrix} \alpha & -\beta \\ \beta & \alpha \end{bmatrix} \begin{bmatrix} V^r \\ V^i \end{bmatrix}$$

$$\begin{aligned}
\begin{bmatrix} u_{41}^r \\ u_{41}^i \end{bmatrix} &= \begin{bmatrix} EI & -C'\Omega \\ C'\Omega & EI \end{bmatrix} \begin{bmatrix} \alpha & -\beta \\ \beta & \alpha \end{bmatrix}^3 \begin{bmatrix} T^r \\ T^i \end{bmatrix} \\
\alpha &= \sqrt[4]{r} \sqrt{\frac{1}{2} \left(1 + \sqrt{\frac{\gamma}{2}} \right)}, \quad \beta = -\sqrt[4]{r} \sqrt{\frac{1}{2} \left(1 - \sqrt{\frac{\gamma}{2}} \right)} \\
r &= -\frac{\bar{m}\Omega^2}{\sqrt{(EI)^2 + (C'\Omega)^2}}, \quad \gamma = 1 + \frac{EI}{\sqrt{(EI)^2 + (C'\Omega)^2}} \\
\begin{cases} S^r = \frac{1}{2}(\cosh\alpha x \cos\beta x + \cosh\beta x \cos\alpha x), & S^i = \frac{1}{2}(\sinh\alpha x \sin\beta x - \sinh\beta x \sin\alpha x) \\ T^r = \frac{1}{2}(\sinh\alpha x \cos\beta x + \cosh\beta x \sin\alpha x), & T^i = \frac{1}{2}(\cosh\alpha x \sin\beta x - \sinh\beta x \cos\alpha x) \\ U^r = \frac{1}{2}(\cosh\alpha x \cos\beta x - \cosh\beta x \cos\alpha x), & U^i = \frac{1}{2}(\sinh\alpha x \sin\beta x + \sinh\beta x \sin\alpha x) \\ V^r = \frac{1}{2}(\sinh\alpha x \cos\beta x - \cosh\beta x \sin\alpha x), & V^i = \frac{1}{2}(\cosh\alpha x \sin\beta x - \sinh\beta x \cos\alpha x) \end{cases}
\end{aligned}$$

The overall transfer matrix is

$$\hat{\mathbf{Z}}_{3,0} = \hat{\mathbf{U}}_3 \hat{\mathbf{U}}_2 \hat{\mathbf{U}}_1 \hat{\mathbf{Z}}_{1,0} = \hat{\mathbf{U}} \hat{\mathbf{Z}}_{1,0} \quad (3.197)$$

Substituting the boundary conditions

$$\begin{cases} \hat{\mathbf{Z}}_{1,0} = \begin{bmatrix} 0 & 0 & M_z^r & Q_y^r & 0 & 0 & M_z^i & Q_y^i & 1 \end{bmatrix}_{1,0}^T \\ \hat{\mathbf{Z}}_{3,0} = \begin{bmatrix} Y^r & \Theta_z^r & 0 & 0 & Y^i & \Theta_z^i & 0 & 0 & 1 \end{bmatrix}_{3,0}^T \end{cases} \quad (3.198)$$

into Equation (3.197), we obtain

$$\begin{bmatrix} 0 \\ 0 \\ 0 \\ 0 \end{bmatrix} = \begin{bmatrix} u_{33} & u_{34} & u_{37} & u_{38} \\ u_{43} & u_{44} & u_{47} & u_{48} \\ u_{73} & u_{74} & u_{77} & u_{78} \\ u_{83} & u_{84} & u_{87} & u_{88} \end{bmatrix} \begin{bmatrix} M_z^r \\ Q_y^r \\ M_z^i \\ Q_y^i \end{bmatrix}_{1,0} + \begin{bmatrix} u_{39} \\ u_{49} \\ u_{79} \\ u_{89} \end{bmatrix} \quad (3.199)$$

namely

$$\begin{bmatrix} M_z^r \\ Q_y^r \\ M_z^i \\ Q_y^i \end{bmatrix}_{1,0} = - \begin{bmatrix} u_{33} & u_{34} & u_{37} & u_{38} \\ u_{43} & u_{44} & u_{47} & u_{48} \\ u_{73} & u_{74} & u_{77} & u_{78} \\ u_{83} & u_{84} & u_{87} & u_{88} \end{bmatrix}^{-1} \begin{bmatrix} u_{39} \\ u_{49} \\ u_{79} \\ u_{89} \end{bmatrix} \quad (3.200)$$

Thus, $\hat{\mathbf{Z}}_{1,0}$ is determined. $\hat{\mathbf{Z}}_{2,1}$, $\hat{\mathbf{Z}}_{2,3}$ and $\hat{\mathbf{Z}}_{3,0}$ can be obtained via the transfer equations given in (3.193). Finally, the steady-state response of the free end of beam is computed, namely

$$y_{3,0} = Y_{3,0}^r \cos\Omega t - Y_{3,0}^i \sin\Omega t \quad (3.201)$$

If $C = 40 \text{ kg/s}$, $C' = 8 \text{ kg m}^3/\text{s}$ and $\Omega = 0.5 \text{ rad/s}$, the computational results of the steady-state response of the free end of beam are obtained as shown in Figure 3.9. The dotted line in Figure 3.9 is the exact solution of the transient response of the system. Note that the latter part

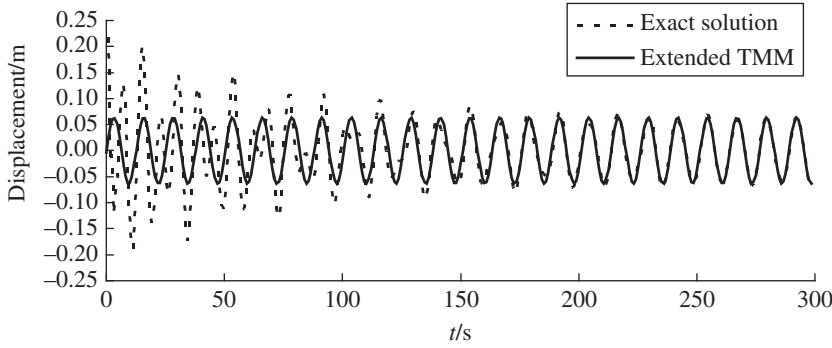


Figure 3.9 Steady-state response of the free end of the beam.

of the dotted line, which denotes the steady-state response, is almost identical to the results obtained by the extended MSTMM.

3.9 Static Response of a Multibody System

Static force can be treated as a periodic force of frequency $\Omega = 0$. The steady-state response of MRFS to a static force can be solved as a periodic force. The effect of the inertia and damping of such a system need not to be considered. This greatly reduces the order of matrices and the computational scale.

Example 3.12 A barrel assembly contains a gun breech, a gun tube and a muzzle brake, as shown in Figure 3.11. They are fixed to each other and can be regarded as a rigid body, nonuniform cross-section beam and rigid body, respectively. The barrel assembly is connected to the front and back hoops. Compute the static deflection of the barrel assembly under gravity using the MSTMM.

Solution

The gun tube is regarded as six uniform cross-section beams and each one has a different cross-section, as shown in Figure 3.10.

The state vectors, $\hat{\mathbf{z}}_{1,0}$, $\hat{\mathbf{z}}_{1,2}$, $\hat{\mathbf{z}}_{2,0}$, $\hat{\mathbf{z}}_{0,3}$, $\hat{\mathbf{z}}_{3,0}$, $\hat{\mathbf{z}}_{0,4}$, $\hat{\mathbf{z}}_{4,5}$, $\hat{\mathbf{z}}_{5,6}$, $\hat{\mathbf{z}}_{6,7}$, $\hat{\mathbf{z}}_{8,7}$ and $\hat{\mathbf{z}}_{8,0}$ are defined as

$$\hat{\mathbf{z}} = [y, \quad \theta_z, \quad m_z, \quad q_y, \quad 1]^T \quad (3.202)$$

The extended matrix of each element is

$$\begin{cases} \hat{\mathbf{z}}_{1,2} = \hat{\mathbf{U}}_1 \hat{\mathbf{z}}_{1,0}, & \hat{\mathbf{z}}_{2,0} = \hat{\mathbf{U}}_2 \hat{\mathbf{z}}_{1,2}, & \hat{\mathbf{z}}_{3,0} = \hat{\mathbf{U}}_3 \hat{\mathbf{z}}_{0,3}, & \hat{\mathbf{z}}_{4,5} = \hat{\mathbf{U}}_4 \hat{\mathbf{z}}_{0,4} \\ \hat{\mathbf{z}}_{5,6} = \hat{\mathbf{U}}_5 \hat{\mathbf{z}}_{4,5}, & \hat{\mathbf{z}}_{6,7} = \hat{\mathbf{U}}_6 \hat{\mathbf{z}}_{5,6}, & \hat{\mathbf{z}}_{8,7} = \hat{\mathbf{U}}_7 \hat{\mathbf{z}}_{6,7}, & \hat{\mathbf{z}}_{8,0} = \hat{\mathbf{U}}_8 \hat{\mathbf{z}}_{8,7} \end{cases} \quad (3.203)$$

where

$$\hat{\mathbf{U}}_i = \begin{bmatrix} 1 & b & 0 & 0 & 0 \\ 0 & 1 & 0 & 0 & 0 \\ 0 & 0 & 1 & b & (c_c - b)m_i g \cos \theta_1 \\ 0 & 0 & 0 & 1 & -m_i g \cos \theta_1 \\ 0 & 0 & 0 & 0 & 1 \end{bmatrix} \quad (i = 1, 8) \quad (3.204)$$

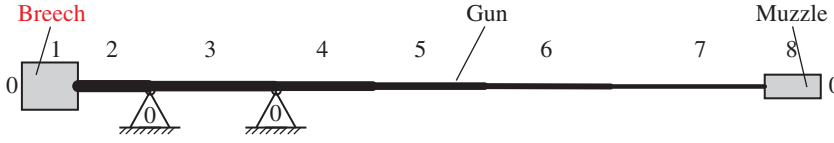


Figure 3.10 Mechanics model of a barrel assembly for static deformation.

$$\hat{\mathbf{U}}_i = \hat{\mathbf{U}}_{x_i = l_i} = \begin{bmatrix} 1 & x_i & \frac{x_i^2}{2EI_i} & \frac{x_i^3}{6EI_i} & -\frac{\bar{m}_i g \cos \theta_1}{24EI_i} x_i^4 \\ 0 & 1 & \frac{x_i}{EI_i} & \frac{x_i^2}{2EI_i} & -\frac{\bar{m}_i g \cos \theta_1}{6EI_i} x_i^3 \\ 0 & 0 & 1 & x_i & -\frac{\bar{m}_i g \cos \theta_1}{2} x_i^2 \\ 0 & 0 & 0 & 1 & -\bar{m}_i g \cos \theta_1 x_i \\ 0 & 0 & 0 & 0 & 1 \end{bmatrix}_{x_i = l_i} \quad (i = 2, 3, 4, 5, 6, 7) \quad (3.205)$$

$\hat{\mathbf{U}}_1$ and $\hat{\mathbf{U}}_8$ are the transfer matrices of the gun breech and muzzle brake, respectively. $\hat{\mathbf{U}}_2, \hat{\mathbf{U}}_3, \dots, \hat{\mathbf{U}}_7$ are the transfer matrices of each beam section of the tube, respectively. m_i is the mass of the rigid body, b is the coordinate of the output end in the body-fixed coordinate system with the input end as the origin, c_c is the coordinate of the mass center, g is the gravity acceleration, θ_1 is the firing angle of the artillery, l_i is the length of the beam section, EI_i is bending stiffness and \bar{m}_i is the mass per length of the beam i .

Consider Equation (3.203)

$$\hat{\mathbf{z}}_{8,0} = H_1 \hat{\mathbf{z}}_{0,4}, \quad \hat{\mathbf{z}}_{3,0} = H_2 \hat{\mathbf{z}}_{0,3}, \quad \hat{\mathbf{z}}_{2,0} = H_3 \hat{\mathbf{z}}_{1,0} \quad (3.206)$$

where

$$H_1 = \hat{\mathbf{U}}_8 \hat{\mathbf{U}}_7 \hat{\mathbf{U}}_6 \hat{\mathbf{U}}_5 \hat{\mathbf{U}}_4, \quad H_2 = \hat{\mathbf{U}}_3, \quad H_3 = \hat{\mathbf{U}}_2 \hat{\mathbf{U}}_1$$

H_1, H_2 and H_3 are all known square matrices of fifth order, denoted by

$$H_i = \begin{bmatrix} h_{11}^{(i)} & h_{12}^{(i)} & h_{13}^{(i)} & h_{14}^{(i)} & h_{15}^{(i)} \\ h_{21}^{(i)} & h_{22}^{(i)} & h_{23}^{(i)} & h_{24}^{(i)} & h_{25}^{(i)} \\ h_{31}^{(i)} & h_{32}^{(i)} & h_{33}^{(i)} & h_{34}^{(i)} & h_{35}^{(i)} \\ h_{41}^{(i)} & h_{42}^{(i)} & h_{43}^{(i)} & h_{44}^{(i)} & h_{45}^{(i)} \\ 0 & 0 & 0 & 0 & 1 \end{bmatrix} \quad (i = 1, 2, 3) \quad (3.207)$$

$P_{2,3}$ and $P_{3,4}$ are regarded as simply supported points, whose displacement in the y direction is 0. The angular displacements and the moments at the left and right ends of points $P_{2,3}$ and $P_{3,4}$ are equal, namely

$$\begin{cases} \hat{\mathbf{z}}_{0,3} = [0, \theta_{z2,3}, m_{z2,3}, q_{y0,3}, 1]^T \\ \hat{\mathbf{z}}_{2,0} = [0, \theta_{z2,3}, m_{z2,3}, q_{y2,0}, 1]^T \end{cases}, \quad \begin{cases} \hat{\mathbf{z}}_{0,4} = [0, \theta_{z3,4}, m_{z3,4}, q_{y0,4}, 1]^T \\ \hat{\mathbf{z}}_{3,0} = [0, \theta_{z3,4}, m_{z3,4}, q_{y3,0}, 1]^T \end{cases} \quad (3.208)$$

$P_{1,0}$ and $P_{8,0}$ are the free boundaries, therefore

$$\begin{cases} \hat{\mathbf{z}}_{1,0} = [y_{1,0}, \theta_{z1,0}, 0, 0, 1]^T \\ \hat{\mathbf{z}}_{8,0} = [y_{8,0}, \theta_{z8,0}, 0, 0, 1]^T \end{cases} \quad (3.209)$$

Substitute Equations (3.208) and (3.209) into Equation (3.206), and rearrange Equation (3.206) as follows

$$\begin{bmatrix}
 1 & 0 & -h_{12}^{(1)} & -h_{13}^{(1)} & -h_{14}^{(1)} & 0 & 0 & 0 & 0 & 0 & 0 & 0 \\
 0 & 1 & -h_{22}^{(1)} & -h_{23}^{(1)} & -h_{24}^{(1)} & 0 & 0 & 0 & 0 & 0 & 0 & 0 \\
 0 & 0 & -h_{32}^{(1)} & -h_{33}^{(1)} & -h_{34}^{(1)} & 0 & 0 & 0 & 0 & 0 & 0 & 0 \\
 0 & 0 & -h_{42}^{(1)} & -h_{43}^{(1)} & -h_{44}^{(1)} & 0 & 0 & 0 & 0 & 0 & 0 & 0 \\
 0 & 0 & 0 & 0 & 0 & 0 & -h_{12}^{(2)} & -h_{13}^{(2)} & -h_{14}^{(2)} & 0 & 0 & 0 \\
 0 & 0 & 1 & 0 & 0 & 0 & -h_{22}^{(2)} & -h_{23}^{(2)} & -h_{24}^{(2)} & 0 & 0 & 0 \\
 0 & 0 & 0 & 1 & 0 & 0 & -h_{32}^{(2)} & -h_{33}^{(2)} & -h_{34}^{(2)} & 0 & 0 & 0 \\
 0 & 0 & 0 & 0 & 0 & 1 & -h_{42}^{(2)} & -h_{43}^{(2)} & -h_{44}^{(2)} & 0 & 0 & 0 \\
 0 & 0 & 0 & 0 & 0 & 0 & 0 & 0 & 0 & 0 & -h_{11}^{(3)} & -h_{12}^{(3)} \\
 0 & 0 & 0 & 0 & 0 & 0 & 1 & 0 & 0 & 0 & -h_{21}^{(3)} & -h_{22}^{(3)} \\
 0 & 0 & 0 & 0 & 0 & 0 & 0 & 1 & 0 & 0 & -h_{31}^{(3)} & -h_{32}^{(3)} \\
 0 & 0 & 0 & 0 & 0 & 0 & 0 & 0 & 1 & 0 & -h_{41}^{(3)} & -h_{42}^{(3)}
 \end{bmatrix}
 \begin{bmatrix}
 y_{8,0} \\
 \theta_{z8,0} \\
 \theta_{z3,4} \\
 m_{z3,4} \\
 q_{y0,4} \\
 q_{y3,0} \\
 \theta_{z2,3} \\
 m_{z2,3} \\
 q_{y0,3} \\
 q_{y2,0} \\
 y_{1,0} \\
 \theta_{z1,0}
 \end{bmatrix}
 =
 \begin{bmatrix}
 h_{15}^{(1)} \\
 h_{25}^{(1)} \\
 h_{35}^{(1)} \\
 h_{45}^{(1)} \\
 h_{15}^{(2)} \\
 h_{25}^{(2)} \\
 h_{35}^{(2)} \\
 h_{45}^{(2)} \\
 h_{15}^{(3)} \\
 h_{25}^{(3)} \\
 h_{35}^{(3)} \\
 h_{45}^{(3)}
 \end{bmatrix}
 \quad (3.210)$$

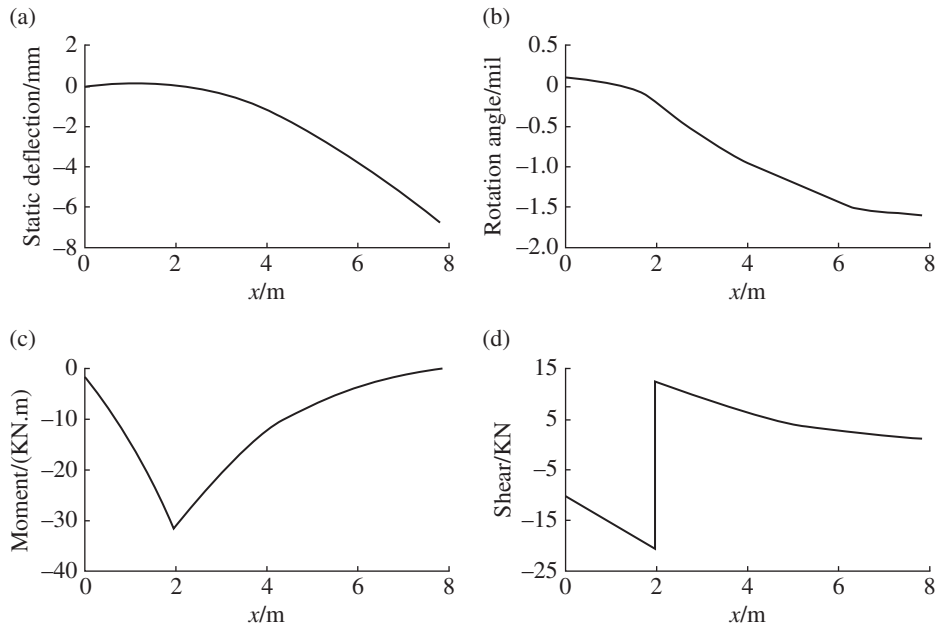


Figure 3.11 Computational results of the static response of the gun tube: (a) the static deflection of the gun tube, (b) the rotation angle of the gun tube, (c) the moment of the gun tube and (d) the shear force of the gun tube.

By solving Equation (3.210), $y_{8,0}$, $\theta_{z8,0}$, $\theta_{z3,4}$, $m_{z3,4}$, $q_{y0,4}$, $q_{y3,0}$, $\theta_{z2,3}$, $m_{z2,3}$, $q_{y0,3}$, $q_{y2,0}$, $y_{1,0}$ and $\theta_{z1,0}$ can be obtained, then $\hat{z}_{1,0}$, $\hat{z}_{2,0}$, $\hat{z}_{0,3}$, $\hat{z}_{3,0}$, $\hat{z}_{0,4}$ and $\hat{z}_{8,0}$ can be obtained from Equations (3.208) and (3.209). The state vector of the arbitrary connection points can be computed through the transfer equations. The static deflection $y(x)$, the rotation angle $\theta_z(x)$, the internal moment $m_z(x)$ and the internal force $q_y(x)$ of any of the points on the gun tube can be determined. The static deflection of the gun tube is obtained. The distribution of displacement, rotation angle, internal moment and internal force along the axis of the gun tube for certain barrels is shown in Figure 3.11a–d.

4

Transfer Matrix Method for Nonlinear and Multidimensional Multibody Systems

4.1 Introduction

Nowadays, *nonlinear science* is developing rapidly, bringing an unprecedented challenge to almost all disciplines and fields. Any physical system is nonlinear as long as it is analyzed precisely enough. Considering a real physical system as a linear system means that its main performance can be represented precisely enough by an approximate linear system. “Precisely enough” means the difference between the real system and an ideal linear system is so insignificant that it can be neglected for a particular matter. Whether to model a real physical system as linear or nonlinear depends on the specified requirements and conditions.

Essentially, the transfer matrix method for multibody systems (MSTMM) transforms the problems of developing the differential dynamics equation and its solution into problems of developing the transfer equation describing the relation between the state vectors of input and output ends and its solution. The transfer direction is unidirectional and one-dimensional for the classical transfer matrix method (TMM). The methods for dealing with the tree system, closed-loop system and framework system, which are common in engineering, are studied in Chapter 11. These are also one-dimensional methods.

In this chapter, the strategies to solve the dynamics of nonlinear multibody systems by using the MSTMM are introduced. The following topics are included: solving the steady-state response of a nonlinear system by using the increment MSTMM and iterative algorithms [236] and studying the dynamics response and eigenvalue problem of a nonlinear system by using the finite element transfer matrix method for a multibody system (FE-MSTMM). The FE-MSTMM combines the advantages of the FEM (its powerful ability to deal with complex structures) and the TMM (its high computational efficiency). Then the MSTMM for the dynamics analysis of a two-dimensional system [74, 75] is introduced, which was developed by the authors. A two-dimensional system is divided into some regions and a transfer direction is chosen, then the state vectors and their transfer relations between the start point and end point in the region are established. The FE-MSTMM has a higher computational efficiency compared with the FEM and can be extended to three-dimensional problems.

4.2 Incremental Transfer Matrix Method for Nonlinear Systems

The linearization of a vibration system not only makes the mathematics solution simple, but also provides satisfactory results for many engineering problems. For example, problems such as the physical explanation of resonance phenomena and the relations between the eigenfrequencies

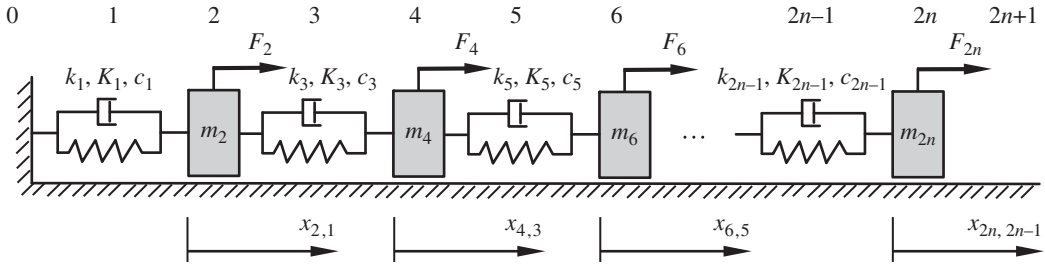


Figure 4.1 An n degrees of freedom vibration system.

or eigenvectors and system parameters etc. can be solved satisfactorily by linear vibration theory. However, such a linearization strategy is sometimes extensively adopted where nonlinear terms are abandoned without verification, resulting in significant computational errors and even essential mistakes. It has been proved by experience that it is impossible to replace the analysis of every vibration system using the linear theory. Even a quasi-linear system has essential differences compared with a linear one, regarding the theoretical analysis methods and the vibration characteristics.

The incremental TMM [236] for the steady-state response of nonlinear systems under periodic excitation is introduced in this section. This method is similar to the ordinary TMM, the only difference being that increases in state variables are used to describe the problem and the state variables of the system are extended to Fourier series. The transfer matrix is composed of the increments which are related to Fourier coefficients.

Consider the nonlinear system with n degrees of freedom, as shown in Figure 4.1, which is composed of n lumped masses connected by springs and dampers. The spring and the damper at the left are fixed to the wall (sequence number 0), while the right (sequence number $2n + 1$) lumped mass $2n$ is free. Nonlinearity may exist in both the spring and damping characteristics. For convenience, however, we will consider here only cases in which nonlinearity exists in spring characteristics. The m_i , F_i and Ω denote the mass of the lumped mass i , force and excitation frequency, respectively. k_i , $K_i = K_i(x)$ and c_i denote the linear part and nonlinear characteristics of the spring coefficients and the viscous damping coefficient of element i , which is composed of springs and dampers. The displacement x and the internal force q_x are state variables. Figure 4.2a and b show the analysis of forces of the elements composed of springs and dampers and the lumped mass, respectively.

According to the analysis of forces shown in Figure 4.2a, we obtain

$$\begin{cases} q_{xi-1,i} = q_{xi+1,i} \\ q_{xi-1,i} = -k_i(x_{i+1,i} - x_{i-1,i}) - K_i(x_{i+1,i} - x_{i-1,i}) - c_i \left(\frac{dx_{i+1,i}}{dt} - \frac{dx_{i-1,i}}{dt} \right) \end{cases} \quad (4.1)$$

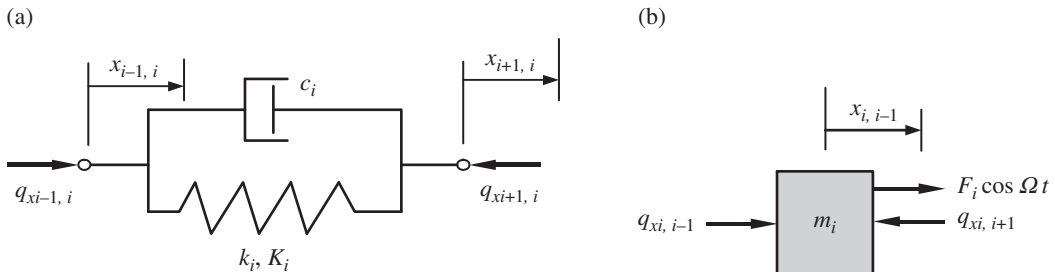


Figure 4.2 The force analysis of a single component: (a) spring and damper; (b) mass.

The force analysis in Figure 4.2b yields

$$\begin{cases} x_{i,i+1} = x_{i,i-1} \\ q_{x_{i,i-1}} - q_{x_{i,i+1}} = m_i \frac{d^2 x_{i,i-1}}{dt^2} - F_i \cos \Omega t \end{cases} \quad (4.2)$$

Let $\tau = \Omega t$, then Equations (4.1) and (4.2) become

$$\begin{cases} q_{x_{i-1,i}} = q_{x_{i+1,i}} \\ q_{x_{i-1,i}} = -k_i(x_{i+1,i} - x_{i-1,i}) - K_i(x_{i+1,i} - x_{i-1,i}) - c_i \Omega (\dot{x}_{i+1,i} - \dot{x}_{i-1,i}) \end{cases} \quad (4.3)$$

$$\begin{cases} x_{i,i+1} = x_{i,i-1} \\ q_{x_{i,i-1}} - q_{x_{i,i+1}} = m_i \Omega^2 \ddot{x}_{i,i-1} - F_i \cos \tau \end{cases} \quad (4.4)$$

where the ‘.’ over x means differentiation with respect to τ .

To develop the incremental method using the TMM for solving Equations (4.3) and (4.4), assume that the stable state response of Ω has the approximate solution (x, q_x, Ω) . The solution of the linear system or the solution of Ω that is far from the resonant point can be considered as an approximate solution.

We will propose a method which enables us to obtain, starting from this solution, a solution more accurate for a case in which the parameters are kept constant, or a solution valid for a case in which some parameters (here Ω will be considered as a variable parameter) are slightly varied. For instance, we can determine the response curve first by improving the accuracy of an initial solution, and then by obtaining solutions successively for varied Ω . Designate the initial solution as (x, q_x, Ω) and try to obtain an improved solution (x', q'_x, Ω') from this solution. Assume that the improved solution (x', q'_x, Ω') can be obtained by adding the increment $(\Delta x, \Delta q_x, \Delta \Omega)$ to the initial values as follows.

Replace (x, q_x, Ω) in Equations (4.3) and (4.4) with Equation (4.5), and omit terms with higher order infinitesimals. We obtain

$$\begin{cases} x' = x + \Delta x \\ q'_x = q_x + \Delta q_x \\ \Omega' = \Omega + \Delta \Omega \end{cases} \quad (4.5)$$

$$\begin{cases} \Delta q_{x_{i-1,i}} = \Delta q_{x_{i+1,i}} \\ \Delta q_{x_{i-1,i}} = -k_i(\Delta x_{i+1,i} - \Delta x_{i-1,i}) - \frac{\partial K_i}{\partial x} \Big|_{x=x_{i+1,i}-x_{i-1,i}} (\Delta x_{i+1,i} - \Delta x_{i-1,i}) \\ \quad - c_i \Omega (\Delta \dot{x}_{i+1,i} - \Delta \dot{x}_{i-1,i}) - c_i \Delta \Omega (\dot{x}_{i+1,i} - \dot{x}_{i-1,i}) + R_i \end{cases} \quad (4.6)$$

$$\begin{cases} \Delta x_{i,i+1} = \Delta x_{i,i-1} \\ \Delta q_{x_{i,i-1}} - \Delta q_{x_{i,i+1}} = 2m_i \Omega \Delta \Omega \ddot{x}_{i,i-1} + m_i \Omega^2 \Delta \ddot{x}_{i,i-1} + S_i \end{cases} \quad (4.7)$$

where

$$\begin{cases} R_i = -q_{x_{i-1,i}} - k_i(x_{i+1,i} - x_{i-1,i}) - K_i(x_{i+1,i} - x_{i-1,i}) - c_i \Omega (\dot{x}_{i+1,i} - \dot{x}_{i-1,i}) \\ S_i = -q_{x_{i,i-1}} + q_{x_{i,i+1}} + m_i \Omega^2 \ddot{x}_{i,i-1} - F_i \cos \tau \end{cases} \quad (4.8)$$

are terms retained to improve convergence.

Solving Equations (4.6) and (4.7), $(\Delta x, \Delta q_x, \Delta \Omega)$ and the improved solution (x', q'_x, Ω') can be obtained. Fourier series is used to solve Equations (4.6) and (4.7). The incremental state vector and incremental transfer matrix are introduced according to Equation (4.6).

The initial solution in Equation (4.6) is developed into Fourier series of the form:

$$\left\{ \begin{array}{l} x_{i-1,i} = a_{i-1,i,0} + \sum_{j=1}^{\infty} (a_{i-1,i,j} \cos j\tau + b_{i-1,i,j} \sin j\tau) \\ x_{i+1,i} = a_{i+1,i,0} + \sum_{j=1}^{\infty} (a_{i+1,i,j} \cos j\tau + b_{i+1,i,j} \sin j\tau) \\ q_{x_{i-1,i}} = g_{i-1,i,0} + \sum_{j=1}^{\infty} (g_{i-1,i,j} \cos j\tau + h_{i-1,i,j} \sin j\tau) \\ q_{x_{i+1,i}} = g_{i+1,i,0} + \sum_{j=1}^{\infty} (g_{i+1,i,j} \cos j\tau + h_{i+1,i,j} \sin j\tau) \end{array} \right. \quad (4.9)$$

Since the initial solutions $x_{i-1,i}$, $x_{i+1,i}$, $q_{x_{i-1,i}}$ and $q_{x_{i+1,i}}$ are known quantities, the Fourier coefficients a , b , g and h in Equation (4.9) are also known.

Similarly, the unknown increments Δx and Δq_x are also extended to Fourier series

$$\left\{ \begin{array}{l} \Delta x_{i-1,i} = \Delta a_{i-1,i,0} + \sum_{j=1}^{\infty} (\Delta a_{i-1,i,j} \cos j\tau + \Delta b_{i-1,i,j} \sin j\tau) \\ \Delta x_{i+1,i} = \Delta a_{i+1,i,0} + \sum_{j=1}^{\infty} (\Delta a_{i+1,i,j} \cos j\tau + \Delta b_{i+1,i,j} \sin j\tau) \\ \Delta q_{x_{i-1,i}} = \Delta g_{i-1,i,0} + \sum_{j=1}^{\infty} (\Delta g_{i-1,i,j} \cos j\tau + \Delta h_{i-1,i,j} \sin j\tau) \\ \Delta q_{x_{i+1,i}} = \Delta g_{i+1,i,0} + \sum_{j=1}^{\infty} (\Delta g_{i+1,i,j} \cos j\tau + \Delta h_{i+1,i,j} \sin j\tau) \end{array} \right. \quad (4.10)$$

where the Fourier coefficients Δa , Δb , Δg and Δh are unknown quantities.

As long as these unknown quantities can be obtained, the increments $\Delta x_{i-1,i}$, $\Delta x_{i+1,i}$, $\Delta q_{x_{i-1,i}}$ and $\Delta q_{x_{i+1,i}}$ can be determined according to Equation (4.10). To determinate these quantities, Equations (4.9) and (4.10) are substituted into Equation (4.6) and applying the *harmonic balance principle*, we obtain

$$\left\{ \begin{array}{l} \Delta g_{i-1,i,j} = \Delta g_{i+1,i,j} \quad (j = 0, 1, 2, \dots) \\ \Delta h_{i-1,i,j} = \Delta h_{i+1,i,j} \quad (j = 1, 2, \dots) \\ \Delta g_{i-1,i,j} = -k_i (\Delta a_{i+1,i,j} - \Delta a_{i-1,i,j}) - \sum_{l=0}^{\infty} A_{i,l,j} (\Delta a_{i+1,i,l} - \Delta a_{i-1,i,l}) - \sum_{l=1}^{\infty} B_{i,l,j} (\Delta b_{i+1,i,l} - \Delta b_{i-1,i,l}) \\ \quad - j c_i \Omega (\Delta b_{i+1,i,j} - \Delta b_{i-1,i,j}) - j c_i \Delta \Omega (b_{i+1,i,j} - b_{i-1,i,j}) + R_{i,j}^c \quad (j = 0, 1, 2, \dots) \\ \Delta h_{i-1,i,j} = -k_i (\Delta b_{i+1,i,j} - \Delta b_{i-1,i,j}) - \sum_{l=0}^{\infty} C_{i,l,j} (\Delta a_{i+1,i,l} - \Delta a_{i-1,i,l}) - \sum_{l=1}^{\infty} D_{i,l,j} (\Delta b_{i+1,i,l} - \Delta b_{i-1,i,l}) \\ \quad + j c_i \Omega (\Delta a_{i+1,i,j} - \Delta a_{i-1,i,j}) + j c_i \Delta \Omega (a_{i+1,i,j} - a_{i-1,i,j}) + R_{i,j}^s \quad (j = 1, 2, \dots) \end{array} \right. \quad (4.11)$$

since

$$R_i = R_{i,0}^c + \sum_{j=1}^{\infty} \left(R_{i,j}^c \cos j\tau + R_{i,j}^s \sin j\tau \right)$$

where

$$\begin{cases} R_{i,0}^c = \frac{1}{2\pi} \int_0^{2\pi} R_i d\tau \\ R_{i,j}^c = \frac{1}{\pi} \int_0^{2\pi} R_i \cos j\tau d\tau, \quad R_{i,j}^s = \frac{1}{\pi} \int_0^{2\pi} R_i \sin j\tau d\tau \quad (j=1,2,\dots) \end{cases} \quad (4.12a)$$

Let

$$w(j, \tau, x) = \left. \frac{\partial K_i}{\partial x} \right|_{x=x_{i+1,i}-x_{i-1,i}} \left[(\Delta a_{i+1,i,0} - \Delta a_{i-1,i,0}) + \sum_{j=1}^{\infty} (\Delta a_{i+1,i,j} - \Delta a_{i-1,i,j}) \cos j\tau + \sum_{j=1}^{\infty} (\Delta b_{i+1,i,j} - \Delta b_{i-1,i,j}) \sin j\tau \right]$$

then

$$\begin{aligned} w(j, \tau, x) &= \frac{1}{2\pi} \int_0^{2\pi} w(l, \tau, x) d\tau + \sum_{j=1}^{\infty} \frac{1}{\pi} \left[\int_0^{2\pi} w(l, \tau, x) \cos j\tau d\tau \right] \cos j\tau \\ &\quad + \sum_{j=1}^{\infty} \frac{1}{\pi} \left[\int_0^{2\pi} w(l, \tau, x) \sin j\tau d\tau \right] \sin j\tau \end{aligned}$$

where the Fourier coefficients are given as

$$\begin{aligned} \frac{1}{2\pi} \int_0^{2\pi} w(l, \tau, x) d\tau &= \frac{1}{2\pi} \int_0^{2\pi} \frac{\partial K_i}{\partial x} (\Delta a_{i+1,i,0} - \Delta a_{i-1,i,0}) d\tau \\ &\quad + \frac{1}{2\pi} \int_0^{2\pi} \frac{\partial K_i}{\partial x} \sum_{l=1}^{\infty} (\Delta a_{i+1,i,l} - \Delta a_{i-1,i,l}) \cos l\tau d\tau \\ &\quad + \frac{1}{2\pi} \int_0^{2\pi} \frac{\partial K_i}{\partial x} \sum_{l=1}^{\infty} (\Delta b_{i+1,i,l} - \Delta b_{i-1,i,l}) \sin l\tau d\tau \\ &= \sum_{l=0}^{\infty} \frac{1}{2\pi} \int_0^{2\pi} \frac{\partial K_i}{\partial x} \cos l\tau d\tau (\Delta a_{i+1,i,l} - \Delta a_{i-1,i,l}) \\ &\quad + \sum_{l=1}^{\infty} \frac{1}{2\pi} \int_0^{2\pi} \frac{\partial K_i}{\partial x} \sin l\tau d\tau (\Delta b_{i+1,i,l} - \Delta b_{i-1,i,l}) \end{aligned}$$

$$\begin{aligned}
\frac{1}{\pi} \int_0^{2\pi} w(l, \tau, x) \cos j\tau \, d\tau &= \sum_{l=0}^{\infty} \frac{1}{\pi} \int_0^{2\pi} \frac{\partial K_i}{\partial x} \cos l\tau \cos j\tau \, d\tau (\Delta a_{i+1,i,l} - \Delta a_{i-1,i,l}) \\
&\quad + \sum_{l=1}^{\infty} \frac{1}{\pi} \int_0^{2\pi} \frac{\partial K_i}{\partial x} \sin l\tau \cos j\tau \, d\tau (\Delta b_{i+1,i,l} - \Delta b_{i-1,i,l}) \\
\frac{1}{\pi} \int_0^{2\pi} w(l, \tau, x) \sin j\tau \, d\tau &= \sum_{l=0}^{\infty} \frac{1}{\pi} \int_0^{2\pi} \frac{\partial K_i}{\partial x} \cos l\tau \sin j\tau \, d\tau (\Delta a_{i+1,i,l} - \Delta a_{i-1,i,l}) \\
&\quad + \sum_{l=1}^{\infty} \frac{1}{\pi} \int_0^{2\pi} \frac{\partial K_i}{\partial x} \sin l\tau \sin j\tau \, d\tau (\Delta b_{i+1,i,l} - \Delta b_{i-1,i,l})
\end{aligned}$$

therefore

$$\left\{ \begin{aligned} A_{i,l,0} &= \frac{1}{2\pi} \int_0^{2\pi} \frac{\partial K_i}{\partial x} \cos l\tau \, d\tau \quad (l=0,1,2,\dots) \\ B_{i,l,0} &= \frac{1}{2\pi} \int_0^{2\pi} \frac{\partial K_i}{\partial x} \sin l\tau \, d\tau \quad (l=1,2,\dots) \\ A_{i,l,j} &= \frac{1}{\pi} \int_0^{2\pi} \frac{\partial K_i}{\partial x} \cos l\tau \cos j\tau \, d\tau \quad (l=0,1,2,\dots; j=1,2,\dots) \\ B_{i,l,j} &= \frac{1}{\pi} \int_0^{2\pi} \frac{\partial K_i}{\partial x} \sin l\tau \cos j\tau \, d\tau \quad (l=1,2,\dots; j=1,2,\dots) \\ C_{i,l,j} &= \frac{1}{\pi} \int_0^{2\pi} \frac{\partial K_i}{\partial x} \cos l\tau \sin j\tau \, d\tau \quad (l=0,1,2,\dots; j=1,2,\dots) \\ D_{i,l,j} &= \frac{1}{\pi} \int_0^{2\pi} \frac{\partial K_i}{\partial x} \sin l\tau \sin j\tau \, d\tau \quad (l=1,2,\dots; j=1,2,\dots) \end{aligned} \right. \quad (4.12b)$$

in Equations (4.12a) and (4.12b), $\frac{\partial K_i}{\partial x}$ and R_i are obtained by substituting $x = x_{i+1,i} - x_{i-1,i}$ into them.

To denote Equation (4.11) in matrix form, define the incremental state vectors at the connection points $P_{i-1,i}$ and $P_{i+1,i}$, respectively

$$\left\{ \begin{aligned} \Delta \mathbf{z}_{i-1,i} &= [\Delta a_{i-1,i,0}, \Delta g_{i-1,i,0}, \Delta a_{i-1,i,1}, \Delta b_{i-1,i,1}, \Delta g_{i-1,i,1}, \Delta h_{i-1,i,1}, \dots, \Delta \Omega, 1]^T \\ \Delta \mathbf{z}_{i+1,i} &= [\Delta a_{i+1,i,0}, \Delta g_{i+1,i,0}, \Delta a_{i+1,i,1}, \Delta b_{i+1,i,1}, \Delta g_{i+1,i,1}, \Delta h_{i+1,i,1}, \dots, \Delta \Omega, 1]^T \end{aligned} \right. \quad (4.13)$$

which are similar to the extended state vectors in the ordinary TMM.

Equation (4.11) is denoted as the incremental transfer equation of a component which is composed of parallel dampers and springs,

$$\Delta \mathbf{z}_{i+1,i} = \mathbf{U}_i \Delta \mathbf{z}_{i-1,i} \quad (4.14)$$

where \mathbf{U}_i corresponds to the transfer matrix in the ordinary TMM and is called the incremental transfer matrix of the component that is composed of parallel dampers and springs.

Equation (4.11) becomes

$$\left\{ \begin{aligned} & \left(k_i + A_{i,0,0} \right) \Delta a_{i+1,i,0} + \sum_{l=1}^{\infty} A_{i,l,0} \Delta a_{i+1,i,l} + \sum_{l=1}^{\infty} B_{i,l,0} \Delta b_{i+1,i,l} \\ &= \left(k_i + A_{i,0,0} \right) \Delta a_{i-1,i,0} + \sum_{l=1}^{\infty} A_{i,l,0} \Delta a_{i-1,i,l} + \sum_{l=1}^{\infty} B_{i,l,0} \Delta b_{i-1,i,l} + R_{i,0}^c - \Delta g_{i-1,i,0} \\ & \Delta g_{i+1,i,0} = \Delta g_{i-1,i,0} \\ & k_i \Delta a_{i+1,i,j} + \sum_{l=0}^{\infty} A_{i,l,j} \Delta a_{i+1,i,l} + \sum_{l=1}^{\infty} B_{i,l,j} \Delta b_{i+1,i,l} + j c_i \Omega \Delta b_{i+1,i,j} + j c_i \Delta \Omega b_{i+1,i,j} \\ &= k_i \Delta a_{i-1,i,j} + \sum_{l=0}^{\infty} A_{i,l,j} \Delta a_{i-1,i,l} + \sum_{l=1}^{\infty} B_{i,l,j} \Delta b_{i-1,i,l} + j c_i \Omega \Delta b_{i-1,i,j} + j c_i \Delta \Omega b_{i-1,i,j} \\ & \quad - \Delta g_{i-1,i,j} + R_{i,j}^c \\ & k_i \Delta b_{i+1,i,j} + \sum_{l=0}^{\infty} C_{i,l,j} \Delta a_{i+1,i,l} + \sum_{l=1}^{\infty} D_{i,l,j} \Delta b_{i+1,i,l} - j c_i \Omega \Delta a_{i+1,i,j} - j c_i \Delta \Omega a_{i+1,i,j} \\ &= k_i \Delta b_{i-1,i,j} + \sum_{l=0}^{\infty} C_{i,l,j} \Delta a_{i-1,i,l} + \sum_{l=1}^{\infty} D_{i,l,j} \Delta b_{i-1,i,l} - j c_i \Omega \Delta a_{i-1,i,j} - j c_i \Delta \Omega a_{i-1,i,j} \\ & \quad - \Delta h_{i-1,i,j} + R_{i,j}^s \\ & \Delta g_{i+1,i,j} = \Delta g_{i-1,i,j} \\ & \Delta h_{i+1,i,j} = \Delta h_{i-1,i,j} \end{aligned} \right\} (j = 1, 2, \dots)$$

namely

$$\mathbf{U}_{i,0} \Delta \mathbf{z}_{i+1,i} = \mathbf{U}_{i,1} \Delta \mathbf{z}_{i-1,i} \quad (4.15)$$

where

$$\begin{aligned} \Delta \mathbf{z}_{i+1,i} &= [\Delta a_{i+1,i,0}, \Delta g_{i+1,i,0}, \dots, \Delta a_{i+1,i,j}, \Delta b_{i+1,i,j}, \Delta g_{i+1,i,j}, \Delta h_{i+1,i,j}, \dots, \Delta \Omega, 1]^T \\ \Delta \mathbf{z}_{i-1,i} &= [\Delta a_{i-1,i,0}, \Delta g_{i-1,i,0}, \dots, \Delta a_{i-1,i,j}, \Delta b_{i-1,i,j}, \Delta g_{i-1,i,j}, \Delta h_{i-1,i,j}, \dots, \Delta \Omega, 1]^T \\ \mathbf{U}_{i,0} &= \begin{bmatrix} k_i + A_{i,0,0} & 0 & \cdots & A_{i,j,0} & B_{i,j,0} & 0 & 0 & \cdots & 0 & 0 \\ 0 & 1 & \cdots & 0 & 0 & 0 & 0 & \cdots & 0 & 0 \\ \vdots & \vdots & \ddots & \vdots & \vdots & \vdots & \vdots & \vdots & \vdots & \vdots \\ A_{i,0,j} & 0 & \cdots & k_i + A_{i,j,j} & B_{i,j,j} + j c_i \Omega & 0 & 0 & \cdots & j c_i b_{i+1,i,j} & 0 \\ C_{i,0,j} & 0 & \cdots & C_{i,j,j} - j c_i \Omega & k_i + D_{i,j,j} & 0 & 0 & \cdots & -j c_i a_{i+1,i,j} & 0 \\ 0 & 0 & \cdots & 0 & 0 & 1 & 0 & \cdots & 0 & 0 \\ 0 & 0 & \cdots & 0 & 0 & 0 & 1 & \cdots & 0 & 0 \\ \vdots & \vdots & \vdots & \vdots & \vdots & \vdots & \vdots & \ddots & \vdots & \vdots \\ 0 & 0 & \cdots & 0 & 0 & 0 & 0 & \cdots & 1 & 0 \\ 0 & 0 & \cdots & 0 & 0 & 0 & 0 & \cdots & 0 & 1 \end{bmatrix} \end{aligned}$$

$$\mathbf{U}_{i,I} = \begin{bmatrix} k_i + A_{i,0,0} & -1 & \cdots & A_{i,j,0} & B_{i,j,0} & 0 & 0 & \cdots & 0 & R_{i,0}^c \\ 0 & 1 & \cdots & 0 & 0 & 0 & 0 & \cdots & 0 & 0 \\ \vdots & \vdots & \ddots & \vdots & \vdots & \vdots & \vdots & \vdots & \vdots & \vdots \\ A_{i,0,j} & 0 & \cdots & k_i + A_{i,j,j} & B_{i,j,j} + jc_i\Omega & -1 & 0 & \cdots & jc_i b_{i-1,i,j} & R_{i,j}^c \\ C_{i,0,j} & 0 & \cdots & C_{i,j,j} - jc_i\Omega & k_i + D_{i,j,j} & 0 & -1 & \cdots & -jc_i a_{i-1,i,j} & R_{i,j}^s \\ 0 & 0 & \cdots & 0 & 0 & 1 & 0 & \cdots & 0 & 0 \\ 0 & 0 & \cdots & 0 & 0 & 0 & 1 & \cdots & 0 & 0 \\ \vdots & \vdots & \vdots & \vdots & \vdots & \vdots & \vdots & \ddots & \vdots & \vdots \\ 0 & 0 & \cdots & 0 & 0 & 0 & 0 & \cdots & 1 & 0 \\ 0 & 0 & \cdots & 0 & 0 & 0 & 0 & \cdots & 0 & 1 \end{bmatrix}$$

The incremental transfer matrix of the component composed of a parallel damper and spring is

$$\mathbf{U}_i = \mathbf{U}_{i,O}^{-1} \mathbf{U}_{i,I} \quad (4.16)$$

As an example, consider the case in which only the harmonic components are retained. The incremental state vectors in Equation (4.13) are

$$\begin{cases} \Delta \mathbf{z}_{i-1,i} = [\Delta a_{i-1,i,1}, \Delta b_{i-1,i,1}, \Delta g_{i-1,i,1}, \Delta h_{i-1,i,1}, \Delta \Omega, 1]^T \\ \Delta \mathbf{z}_{i+1,i} = [\Delta a_{i+1,i,1}, \Delta b_{i+1,i,1}, \Delta g_{i+1,i,1}, \Delta h_{i+1,i,1}, \Delta \Omega, 1]^T \end{cases} \quad (4.17)$$

The corresponding incremental transfer matrix is $\mathbf{U}_i = \mathbf{U}_{i,O}^{-1} \mathbf{U}_{i,I}$, where

$$\mathbf{U}_{i,O} = \begin{bmatrix} k_i + A_{i,1,1} & B_{i,1,1} + c_i\Omega & 0 & 0 & c_i b_{i+1,i,1} & 0 \\ C_{i,1,1} - c_i\Omega & k_i + D_{i,1,1} & 0 & 0 & -c_i a_{i+1,i,1} & 0 \\ 0 & 0 & 1 & 0 & 0 & 0 \\ 0 & 0 & 0 & 1 & 0 & 0 \\ 0 & 0 & 0 & 0 & 1 & 0 \\ 0 & 0 & 0 & 0 & 0 & 1 \end{bmatrix}$$

$$\mathbf{U}_{i,I} = \begin{bmatrix} k_i + A_{i,1,1} & B_{i,1,1} + c_i\Omega & -1 & 0 & c_i b_{i-1,i,1} & R_{i,1}^c \\ C_{i,1,1} - c_i\Omega & k_i + D_{i,1,1} & 0 & -1 & -c_i a_{i-1,i,1} & R_{i,1}^s \\ 0 & 0 & 1 & 0 & 0 & 0 \\ 0 & 0 & 0 & 1 & 0 & 0 \\ 0 & 0 & 0 & 0 & 1 & 0 \\ 0 & 0 & 0 & 0 & 0 & 1 \end{bmatrix} \quad (4.18)$$

According to Equation (4.7) the incremental transfer matrix of the lumped mass is introduced. Similarly, with Equations (4.9) and (4.10) and the harmonic balance principle, Equation (4.7) becomes

$$\begin{cases} \Delta a_{i,i+1,j} = \Delta a_{i,i-1,j} \quad (j = 0, 1, 2, \dots) \\ \Delta b_{i,i+1,j} = \Delta b_{i,i-1,j} \quad (j = 1, 2, \dots) \\ \Delta g_{i,i+1,j} = \Delta g_{i,i-1,j} + 2j^2 m_i \Omega \Delta \Omega a_{i,i-1,j} + j^2 m_i \Omega^2 \Delta a_{i,i-1,j} - S_{i,j}^c \quad (j = 0, 1, 2, \dots) \\ \Delta h_{i,i+1,j} = \Delta h_{i,i-1,j} + 2j^2 m_i \Omega \Delta \Omega b_{i,i-1,j} + j^2 m_i \Omega^2 \Delta b_{i,i-1,j} - S_{i,j}^s \quad (j = 1, 2, \dots) \end{cases} \quad (4.19)$$

where

$$\begin{cases} S_{i,0}^c = \frac{1}{2\pi} \int_0^{2\pi} S_i d\tau \\ S_{i,j}^c = \frac{1}{\pi} \int_0^{2\pi} S_i \cos j\tau d\tau, \quad S_{i,j}^s = \frac{1}{\pi} \int_0^{2\pi} S_i \sin j\tau d\tau \quad (j=1,2,\dots) \end{cases} \quad (4.20)$$

To express Equation (4.19) in matrix form, incremental state vectors at the connection points $P_{i-1,i}$ and $P_{i+1,i}$ are defined as

$$\begin{cases} \Delta \mathbf{z}_{i,i-1} = [\Delta a_{i,i-1,0}, \Delta g_{i,i-1,0}, \Delta a_{i,i-1,1}, \Delta b_{i,i-1,1}, \Delta g_{i,i-1,1}, \Delta h_{i,i-1,1}, \dots, \Delta \Omega, 1]^T \\ \Delta \mathbf{z}_{i,i+1} = [\Delta a_{i,i+1,0}, \Delta g_{i,i+1,0}, \Delta a_{i,i+1,1}, \Delta b_{i,i+1,1}, \Delta g_{i,i+1,1}, \Delta h_{i,i+1,1}, \dots, \Delta \Omega, 1]^T \end{cases} \quad (4.21)$$

Then Equation (4.19) is written as incremental transfer equation of the lumped mass:

$$\Delta \mathbf{z}_{i,i+1} = \mathbf{U}_i \Delta \mathbf{z}_{i,i-1} \quad (4.22)$$

where \mathbf{U}_i is the incremental transfer matrix of the lumped mass:

$$\mathbf{U}_i = \begin{bmatrix} 1 & 0 & \cdots & 0 & 0 & 0 & 0 & \cdots & 0 & 0 \\ 0 & 1 & \cdots & 0 & 0 & 0 & 0 & \cdots & 0 & -S_{i,0}^c \\ \vdots & \vdots & \ddots & \vdots & \vdots & \vdots & \vdots & \vdots & \vdots & \vdots \\ 0 & 0 & \cdots & 1 & 0 & 0 & 0 & \cdots & 0 & 0 \\ 0 & 0 & \cdots & 0 & 1 & 0 & 0 & \cdots & 0 & 0 \\ 0 & 0 & \cdots & j^2 m_i \Omega^2 & 0 & 1 & 0 & \cdots & 2j^2 m_i \Omega a_{i,i-1,j} & -S_{i,j}^c \\ 0 & 0 & \cdots & 0 & j^2 m_i \Omega^2 & 0 & 1 & \cdots & 2j^2 m_i \Omega b_{i,i-1,j} & -S_{i,j}^s \\ \vdots & \vdots & \vdots & \vdots & \vdots & \vdots & \vdots & \ddots & \vdots & \vdots \\ 0 & 0 & \cdots & 0 & 0 & 0 & 0 & \cdots & 1 & 0 \\ 0 & 0 & \cdots & 0 & 0 & 0 & 0 & \cdots & 0 & 1 \end{bmatrix} \quad (4.23)$$

As an example, consider the case in which only harmonic components are retained. The incremental state vectors in Equation (4.21) yield

$$\begin{cases} \Delta \mathbf{z}_{i,i-1} = [\Delta a_{i,i-1,1}, \Delta b_{i,i-1,1}, \Delta g_{i,i-1,1}, \Delta h_{i,i-1,1}, \Delta \Omega, 1]^T \\ \Delta \mathbf{z}_{i,i+1} = [\Delta a_{i,i+1,1}, \Delta b_{i,i+1,1}, \Delta g_{i,i+1,1}, \Delta h_{i,i+1,1}, \Delta \Omega, 1]^T \end{cases} \quad (4.24)$$

The corresponding incremental transfer matrix is

$$\mathbf{U}_i = \begin{bmatrix} 1 & 0 & 0 & 0 & 0 & 0 \\ 0 & 1 & 0 & 0 & 0 & 0 \\ m_i \Omega^2 & 0 & 1 & 0 & 2m_i \Omega a_{i,i-1,1} & -S_{i,j}^c \\ 0 & m_i \Omega^2 & 0 & 1 & 2m_i \Omega b_{i,i-1,1} & -S_{i,j}^s \\ 0 & 0 & 0 & 0 & 1 & 0 \\ 0 & 0 & 0 & 0 & 0 & 1 \end{bmatrix} \quad (4.25)$$

Combine Equations (4.14) and (4.22), using the steps of the multibody system TMM to obtain the stable state response of a multi-degree-of-freedom system. Thus, the incremental TMM has been fully established. To explain how to use this method, in the following the solution process of the steady-state response for n degrees of freedom (DOF) system will be introduced, as shown in Figure 4.1. According to the system structure, the state vectors $\Delta \mathbf{z}_{0,1}$, $\Delta \mathbf{z}_{2,1}$, $\Delta \mathbf{z}_{2,3}$, $\Delta \mathbf{z}_{4,3}$, $\Delta \mathbf{z}_{4,5}$, ..., $\Delta \mathbf{z}_{2n,2n+1}$ are defined in the same form as Equations (4.13) or (4.21), and the transfer equation yields

$$\begin{cases} \Delta \mathbf{z}_{2,1} = \mathbf{U}_1 \Delta \mathbf{z}_{0,1} \\ \Delta \mathbf{z}_{2,3} = \mathbf{U}_2 \Delta \mathbf{z}_{2,1} \\ \vdots \\ \Delta \mathbf{z}_{2n,2n-1} = \mathbf{U}_{2n-1} \Delta \mathbf{z}_{2n-2,2n-1} \\ \Delta \mathbf{z}_{2n,2n+1} = \mathbf{U}_{2n} \Delta \mathbf{z}_{2n,2n-1} \end{cases} \quad (4.26)$$

where \mathbf{U}_1 , \mathbf{U}_3 , ..., \mathbf{U}_{2n-1} are the incremental transfer matrices of components 1, 3, ..., $2n-1$, respectively, which are composed of parallel dampers and springs. \mathbf{U}_2 , \mathbf{U}_4 and \mathbf{U}_{2n} are the incremental transfer matrices of lumped masses 2, 4, ..., $2n$, respectively.

The overall transfer equation is obtained by successively multiplying each transfer matrix in sequence

$$\Delta \mathbf{z}_{2n,2n+1} = \mathbf{U}_{2n} \mathbf{U}_{2n-1} \cdots \mathbf{U}_2 \mathbf{U}_1 \Delta \mathbf{z}_{0,1} = \mathbf{U} \Delta \mathbf{z}_{0,1} \quad (4.27)$$

where \mathbf{U} is the overall transfer matrix.

From the boundary conditions, parts of the state variables in $\Delta \mathbf{z}_{0,1}$ and $\Delta \mathbf{z}_{2n,2n+1}$ are zeros, that is

$$\begin{cases} \Delta a_{0,1,j} = 0, \quad \Delta g_{2n,2n+1,j} = 0 & (j = 0, 1, 2, \dots) \\ \Delta b_{0,1,j} = 0, \quad \Delta h_{2n,2n+1,j} = 0 & (j = 1, 2, \dots) \end{cases} \quad (4.28)$$

Therefore, the problem is simplified to solve Equation (4.27) under the condition of Equation (4.28). Solving Equation (4.27), the unknown state variables in $\Delta \mathbf{z}_{0,1}$, $\Delta \mathbf{z}_{2n,2n+1}$ and the boundary incremental state vectors $\Delta \mathbf{z}_{0,1}$ and $\Delta \mathbf{z}_{2n,2n+1}$ can be determined. Finally, the state vectors of all the connected points can be obtained through the transfer equations of all components. Substituting these increments into the initial solution, according to Equations (4.10) and (4.5), the improved solution can be evaluated. If this improved solution cannot satisfy the accuracy, take the improved solution as the new initial solution, and the new increments can be evaluated by repeating the process to solve Equation (4.27) until the improved solution satisfies the accuracy.

As an example, take Equation (4.18) as the incremental transfer matrices of the component composed of parallel dampers and springs, and Equation (4.25) as the incremental transfer matrices of the lumped mass, respectively. Using the boundary conditions in Equation (4.28), Equation (4.27) becomes

$$\begin{bmatrix} \Delta a_{2n,2n+1,1} \\ \Delta b_{2n,2n+1,1} \\ 0 \\ 0 \\ \Delta \Omega \\ 1 \end{bmatrix} = \begin{bmatrix} u_{11} & u_{12} & u_{13} & u_{14} & u_{15} & u_{16} \\ u_{12} & u_{22} & u_{23} & u_{24} & u_{25} & u_{26} \\ u_{31} & u_{32} & u_{33} & u_{34} & u_{35} & u_{36} \\ u_{41} & u_{42} & u_{43} & u_{44} & u_{45} & u_{46} \\ 0 & 0 & 0 & 0 & 1 & 0 \\ 0 & 0 & 0 & 0 & 0 & 1 \end{bmatrix} \begin{bmatrix} 0 \\ 0 \\ \Delta g_{0,1,1} \\ \Delta h_{0,1,1} \\ \Delta \Omega \\ 1 \end{bmatrix} \quad (4.29)$$

where u_{ij} is the element of the overall transfer matrix.

Let $\Delta\Omega = 0$ in Equation (4.29). A more precise improved solution corresponding to the original excitation frequency Ω can be found by solving Equation (4.29). If this improved solution still does not satisfy the precision, the repeated step could be carried out. If $\Delta\Omega (\neq 0)$ is a given value in Equation (4.29), the improved solution corresponding to excitation frequency $\Omega + \Delta\Omega$ can be obtained. If this improved solution still does not satisfy the precision, repeat the same step.

Example 4.1 [236] The case for $n = 3$ is shown in Figure 4.1. Suppose the nonlinearity of the spring to be

$$K_i(x) = \varepsilon_i x^3$$

The parameters of the system are

$$\begin{cases} m_1 = 1.0, & m_2 = 1.63, & m_3 = 1.0 \\ c_1 = c_2 = c_3 = 0.001 \\ k_1 = k_2 = k_3 = 1.0 \\ \varepsilon_1 = \varepsilon_2 = \varepsilon_3 = 0.001 \\ F_1 = F_2 = 0, & F_3 = 0.1 \end{cases}$$

Solution

For these values of the parameters, the eigenfrequencies of the system are

$$\omega_1 = 0.402, \quad \omega_2 = 1.206, \quad \omega_3 = 1.616$$

1) Analysis of harmonic oscillations

Using this method, we retain the components up to the third order, and adopt Ω as the varying parameter. The results obtained for Ω between 0.0 and 2.0 are shown in Figure 4.3. In the figure, $X_{i,k}$ denotes the amplitudes of the k th order harmonic component of the i th mass, and the stable and unstable oscillations are denoted by solid and dashed lines, respectively. To check the validity of this method, we determine the steady-state oscillations by numerical integration of the equations of motion and decompose them into harmonic as well as third-order harmonic components. These results are shown by “○” in Figure 4.3 (Note that such circles look just like dots as a result of their small size especially when they intersect the solid or the dotted lines). From this figure it is found that the solutions obtained by the proposed method agree well with those obtained by numerical integration. Thus, the validity of this method is confirmed.

2) Analysis of subharmonic oscillations

Putting $\Omega t = l\tau$ (l is a positive integer) instead of $\Omega t = \tau$ in Equations (4.1) and (4.2), and treating it the same way as before, we can analyze the subharmonic oscillation of the order of $1/l$ or super subharmonic oscillation of the order of j/l (j is a positive integer). The results obtained for subharmonic oscillation of the order of $1/3$ are shown in Figure 4.4. In the figure, $X_{i,k/3}$ denotes the amplitude of the order of $k/3$ subharmonic oscillation, while $X_{i,k}$ denotes the amplitudes of harmonic oscillation. To check the validity of this method, the steady-state oscillation by numerical integration of the equation of motion is determined and decomposed into subharmonic and harmonic components. These computation results are shown by “○” in Figure 4.4 (Note that such circles look just like dots as a result of their small size especially when they intersect the solid or the dotted lines). It has been shown that the solutions obtained by the

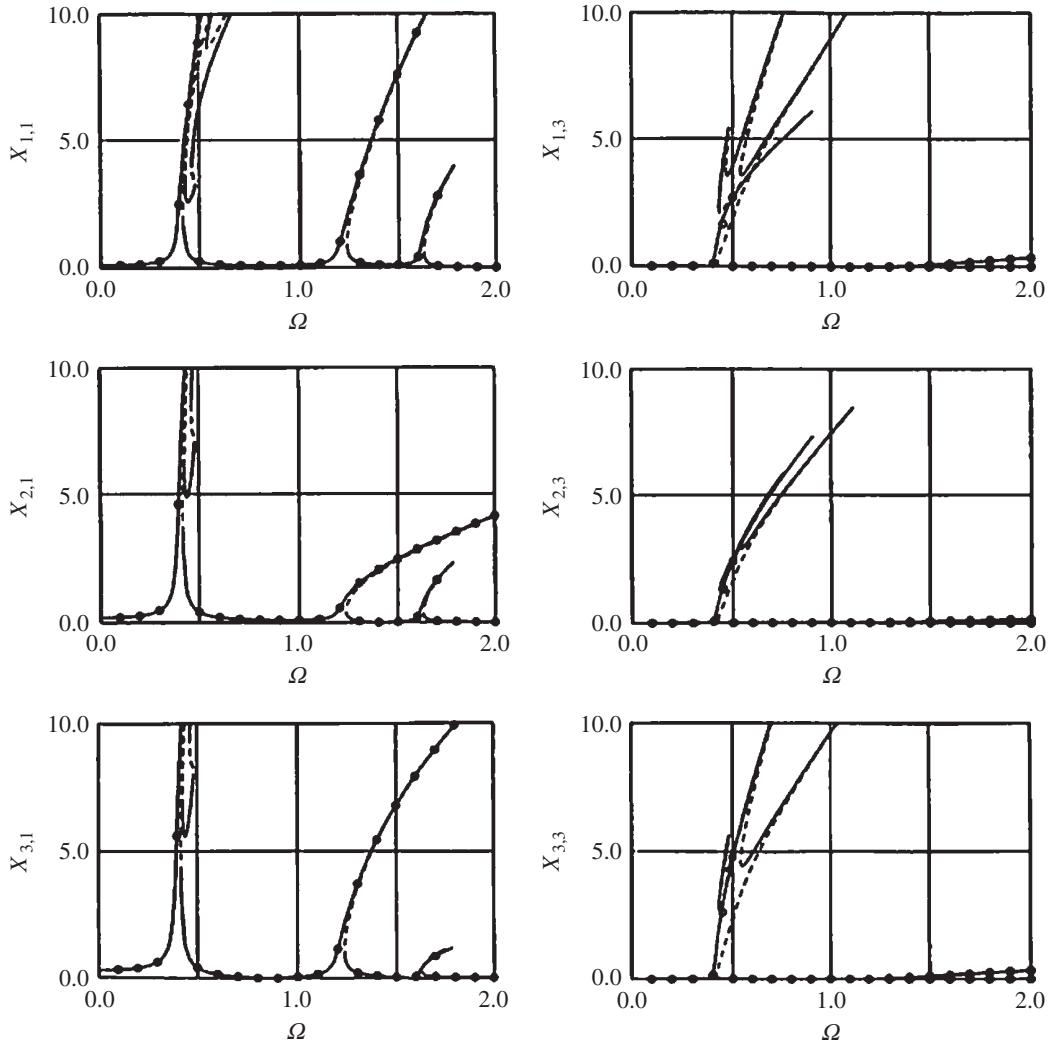


Figure 4.3 Response curves of harmonic oscillations.

proposed method agree well with those obtained by numerical integration. Thus, the validity of this method is confirmed. It is noted that near the second resonance point, the subharmonic oscillation of the order of $1/3$ occurs and its resonance varies in a complex way. This may be due to internal resonance.

4.3 Finite Element Transfer Matrix Method for Two-dimensional Systems

FEM is the most widely used and powerful tool for structural analysis. However, many nodes used in a very complex structure induce huge matrices which need to be managed and dealt with. The computation cost is huge, and systems with large stiffness gradients usually are accompanied by computational “ill-condition”, which leads to computational difficulties. Therefore, the problem of how to increase the computation speed and avoid computational

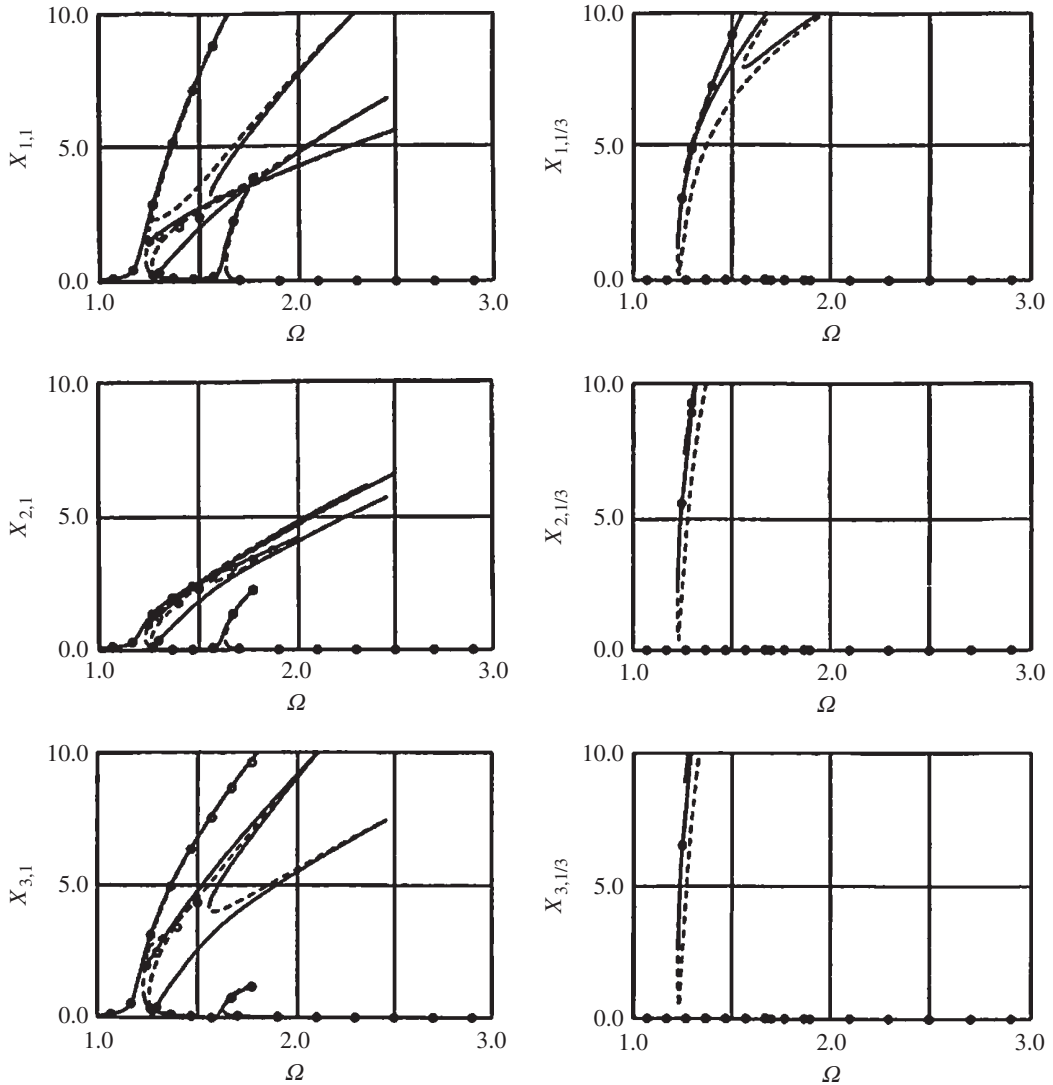


Figure 4.4 Response curves of subharmonic oscillations.

“ill-condition” is one of the eternal topics for FEM research. The two-dimensional structure is divided into finite regions along the transfer direction, and each region is divided again into finite elements. FEM is used to develop the matrix relations of state variables at the two ends of strips. Consequently, it is solved by the TMM. The FE-TMM can be developed [237] by combining the FEM with the TMM, which greatly reduces the computational costs compared with using the FEM only. The FE-TMM has not only the strong power of the FEM, but also the high efficiency of the TMM in dealing with complicated structures.

4.3.1 Differential Equation of the Transverse Vibration of a Thin Plate

The object enclosed in the surfaces of two parallel planes and a vertical cylinder or prism is called a flat plate, or simple plate, in elastic mechanics where the thickness is much less than the size of the bottom surface, as shown in Figure 4.5. h is the thickness of the plate. The middle plane that

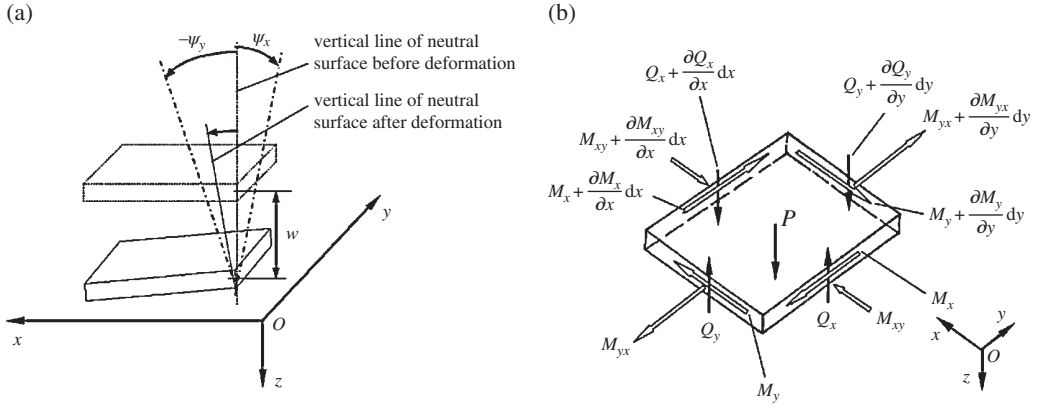


Figure 4.5 Rectangular element of a plate.

bisects the thickness h is a neutral surface. The neutral surface is assumed to coincide with the oxy plane and the z axis is vertical downwards. The displacements of any point along the x , y and z axes are denoted by u , v and w , respectively.

Assuming that the original cross-section is still a plane after deformation, this yields

$$\begin{cases} w(z) = w \\ u(z) = u_0 + z\psi_x \\ v(z) = v_0 + z\psi_y \end{cases} \quad (4.30)$$

where u_0 and v_0 are the displacements of elements on the neutral surface of the plate, ψ_x is the angular displacement around the x axis and ψ_y is the angular displacement around the y axis.

Shear deformations are

$$\gamma_{xz} = \frac{\partial w}{\partial x} + \psi_x, \quad \gamma_{yz} = \frac{\partial w}{\partial y} + \psi_y \quad (4.31)$$

where γ_{xz} is the angular displacement of element $dx dz$ and γ_{yz} is the angular displacement of element $dy dz$.

Figure 4.5b shows the forces on the element $dx dy$ under transverse vibration. P is the exciting force distributed on the unit area, ρ is the material density and $\rho h \frac{\partial^2 w}{\partial t^2}$ is the inertial force on the unit area. According to the condition of moment equilibrium along the y and x axes, and the condition of force equilibrium along the z axis on the rectangular element, the equilibrium equations are

$$\begin{cases} \frac{\partial}{\partial x} M_x + \frac{\partial}{\partial y} M_{yx} = Q_x \\ \frac{\partial}{\partial x} M_{xy} + \frac{\partial}{\partial y} M_y = Q_y \\ \frac{\partial}{\partial x} Q_x + \frac{\partial}{\partial y} Q_y - \rho h \frac{\partial^2 w}{\partial t^2} = -P \end{cases} \quad (4.32)$$

where

$$\begin{cases} M_x = \int_{-h/2}^{h/2} z \sigma_x dz, & M_y = \int_{-h/2}^{h/2} z \sigma_y dz \\ M_{xy} = \int_{-h/2}^{h/2} z \tau_{xy} dz, & M_{yx} = \int_{-h/2}^{h/2} z \tau_{yx} dz \\ Q_x = \int_{-h/2}^{h/2} \tau_{xz} dz, & Q_y = \int_{-h/2}^{h/2} \tau_{yz} dz \end{cases} \quad (4.33)$$

M_x and M_y are the bending moments, M_{yx} and M_{xy} are the rotational moments, and Q_x and Q_y are the shear forces.

If the ratio of thickness to the least character size of the plate is greater than 1/5, the plate is called a thick plate, while if the ratio of thickness to the least character size of the plate is less than 1/80, the plate is called a membrane plate. If the ratio of thickness to the least character size of the plate is between 1/5 and 1/80, the plate is called a thin plate. For a thin plate, bending deformation is mainly generated when all the outside loads are vertical to the neutral surface, and the displacements along the z axis of all the points on the neutral surface are called deflections of the plate. If the ratio of deflection to thickness is less than or equal to 1/5, the problem belongs to small deflection theory.

Kirchhoff's hypothesis is fundamental assumptions in the development linear elastic, small-deformation theory for the bending of thin plates. The assumptions are:

- 1) The straight lines, initially normal to the middle plane before bending, remain straight and normal to the middle plane during the deformation, and the length of such an element does not alter. Due to the assumption, $\gamma_{xz} = 0$, $\gamma_{yz} = 0$ and $\varepsilon_z = 0$.
- 2) σ_z , the stress normal to the middle plane, is small compared with other stress components (σ_x , σ_y and τ_{xy}) and may be neglected in the stress-strain relations.
- 3) When the thin plate is bending and deforming, all the points in the neutral surface have only vertical displacement w but no displacement along the x and y axes, that is, $u(z)|_{z=0} = 0$, $v(z)|_{z=0} = 0$, and $w(z)|_{z=0} = w(x, y)$.

Now deduce the differential equation of the transverse vibration of a thin plate. From Kirchhoff's hypothesis $\gamma_{xz} = \gamma_{yz} = 0$ and Equation (4.31)

$$\psi_x = -\frac{\partial w}{\partial x}, \quad \psi_y = -\frac{\partial w}{\partial y} \quad (4.34)$$

Equations (4.32) and (4.33) still apply. Considering bending deformation only, Equation (4.30) becomes

$$u = -z \frac{\partial w}{\partial x}, \quad v = -z \frac{\partial w}{\partial y} \quad (4.35)$$

then

$$\begin{cases} \varepsilon_x = \frac{\partial u}{\partial x} = -z \frac{\partial^2 w}{\partial x^2} \\ \varepsilon_y = \frac{\partial v}{\partial y} = -z \frac{\partial^2 w}{\partial y^2} \\ \gamma_{xy} = \frac{\partial u}{\partial y} + \frac{\partial v}{\partial x} = -2z \frac{\partial^2 w}{\partial x \partial y} \end{cases} \quad (4.36)$$

The stress–strain relation of the thin bending plate is

$$\boldsymbol{\sigma} = \begin{bmatrix} \sigma_x \\ \sigma_y \\ \tau_{xy} \end{bmatrix} = \frac{E}{1-\mu^2} \begin{bmatrix} 1 & \mu & 0 \\ \mu & 1 & 0 \\ 0 & 0 & (1-\mu)/2 \end{bmatrix} \begin{bmatrix} \varepsilon_x \\ \varepsilon_y \\ \gamma_{xy} \end{bmatrix} = \mathbf{E}\boldsymbol{\varepsilon} \quad (4.37)$$

Substituting Equation (4.37) into Equation (4.33) and taking the integration, we obtain

$$\begin{bmatrix} M_x \\ M_y \\ M_{xy} \end{bmatrix} = -D \begin{bmatrix} 1 & \mu & 0 \\ \mu & 1 & 0 \\ 0 & 0 & 1-\mu \end{bmatrix} \begin{bmatrix} \partial^2 w / \partial x^2 \\ \partial^2 w / \partial y^2 \\ \partial^2 w / \partial x \partial y \end{bmatrix} \quad (4.38)$$

where $D = \frac{Eh^3}{12(1-\mu^2)}$ is the *bending stiffness of the thin plate*.

Substituting Equation (4.38) into the first two formulas of Equation (4.32) yields

$$\begin{cases} Q_x = -D \frac{\partial}{\partial x} \left(\frac{\partial^2 w}{\partial x^2} + \frac{\partial^2 w}{\partial y^2} \right) \\ Q_y = -D \frac{\partial}{\partial y} \left(\frac{\partial^2 w}{\partial x^2} + \frac{\partial^2 w}{\partial y^2} \right) \end{cases} \quad (4.39)$$

Substituting Equation (4.39) into the last formula of Equation (4.32), the dynamic differential equation of the thin plate is obtained as

$$\Delta^2 w = \frac{P}{D} - \frac{\rho h \partial^2 w}{D \partial t^2} \quad (4.40)$$

where Δ^2 is the operator $\left(\frac{\partial^2}{\partial x^2} + \frac{\partial^2}{\partial y^2} \right)^2$.

4.3.2 Triangular Elements

Triangular or rectangular elements are usually used while analyzing the transverse vibration of a thin plate using the FEM. Using three nodal triangular elements and local *Cartesian coordinates*, the *oxy* plane is assumed to coincide with the neutral surface of the thin plate. As shown in Figure 4.6, the three nodes are numbered in sequence, and the *oy* axis is coincident with the line connected by nodes ① and ②.

In each node, displacement w and angular displacements θ_x and θ_y are denoted by $\boldsymbol{\delta}$

$$\boldsymbol{\delta}_i = \begin{bmatrix} w_i \\ \theta_{xi} \\ \theta_{yi} \end{bmatrix} = \left[w_i, \left(\frac{\partial w}{\partial y} \right)_i, - \left(\frac{\partial w}{\partial x} \right)_i \right]^T \quad (4.41)$$

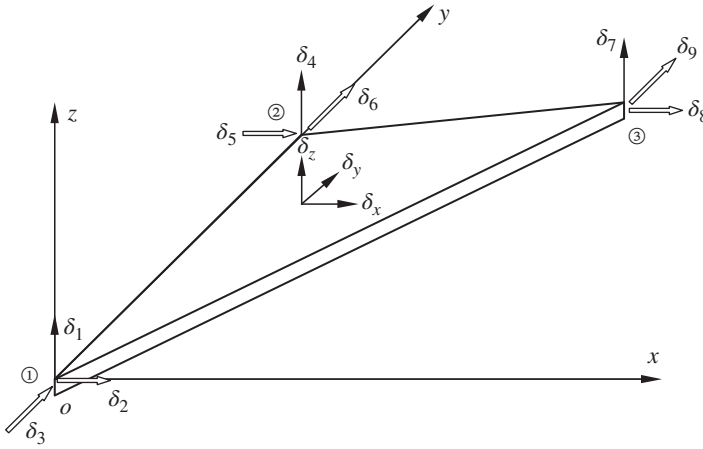


Figure 4.6 Triangle element of a thin plate.

The displacement vector of the element is

$$\delta^e = [w_1, \theta_{x1}, \theta_{y1}, \dots, w_3, \theta_{x3}, \theta_{y3}]^T = [\delta_1, \delta_2, \delta_3, \dots, \delta_7, \delta_8, \delta_9]^T \quad (4.42)$$

and the nodal force is

$$F_i = [W_i, m_{\theta_{xi}}, m_{\theta_{yi}}]^T \quad (4.43)$$

where W_i is the force along the z axis, and $m_{\theta_{xi}}$ and $m_{\theta_{yi}}$ are the nodal moments. These parameters do not have simple relations with the bending moment M_x of this node, and their dimensions are also different.

The element displacement δ^e has nine unknown quantities. Therefore, the function of displacement includes nine parameters that have symmetry with respect to x and y . Normally, let

$$w(x, y) = a_1 + a_2x + a_3y + a_4x^2 + a_5xy + a_6y^2 + a_7x^3 + a_8(x^2y + xy^2) + a_9y^3 = \mathbf{d}^T \mathbf{a} \quad (4.44)$$

where

$$\mathbf{d} = [1, x, y, x^2, xy, y^2, x^3, (x^2y + xy^2), y^3]^T \quad (4.45)$$

$$\mathbf{a} = [a_1, a_2, \dots, a_8, a_9]^T \quad (4.46)$$

\mathbf{a} is an unknown constant column vector that is determined by the nodal state of the element, that is

$$\begin{cases} \text{at node 1, } (x_1, y_1) = (0, 0): & w(x, y) = \delta_1, \frac{\partial w(x, y)}{\partial y} = \delta_2, -\frac{\partial w(x, y)}{\partial x} = \delta_3 \\ \text{at node 2, } (x_2, y_2) = (0, y_2): & w(x, y) = \delta_4, \frac{\partial w(x, y)}{\partial y} = \delta_5, -\frac{\partial w(x, y)}{\partial x} = \delta_6 \\ \text{at node 3, } (x_3, y_3) = (x_3, y_3): & w(x, y) = \delta_7, \frac{\partial w(x, y)}{\partial y} = \delta_8, -\frac{\partial w(x, y)}{\partial x} = \delta_9 \end{cases} \quad (4.47)$$

We obtain

$$\delta^e = \mathbf{n} \mathbf{a} \quad (4.48)$$

where

$$\mathbf{n} = \begin{bmatrix} 1 & 0 & 0 & 0 & 0 & 0 & 0 & 0 & 0 \\ 0 & 0 & 1 & 0 & 0 & 0 & 0 & 0 & 0 \\ 0 & -1 & 0 & 0 & 0 & 0 & 0 & 0 & 0 \\ 1 & 0 & y_2 & 0 & 0 & y_2^2 & 0 & 0 & y_2^3 \\ 0 & 0 & 1 & 0 & 0 & 2y_2 & 0 & 0 & 3y_2^2 \\ 0 & -1 & 0 & 0 & -y_2 & 0 & 0 & -y_2^2 & 0 \\ 1 & x_3 & y_3 & x_3^2 & x_3y_3 & y_3^2 & x_3^3 & x_3^2y_3 + x_3y_3^2 & y_3^3 \\ 0 & 0 & 1 & 0 & x_3 & 2y_3 & 0 & 2x_3y_3 + x_3^2 & 3y_3^2 \\ 0 & -1 & 0 & -2x_3 & -y_3 & 0 & -3x_3^2 & -(y_3^2 + 2x_3y_3) & 0 \end{bmatrix} \quad (4.49)$$

$\mathbf{a} = \mathbf{n}^{-1}\boldsymbol{\delta}^e$ can be evaluated from Equation (4.48), and substituting this into Equation (4.44) yields

$$w(x, y) = \mathbf{d}^T \mathbf{a} = \mathbf{d}^T \mathbf{n}^{-1} \boldsymbol{\delta}^e = \mathbf{N} \boldsymbol{\delta}^e \quad (4.50)$$

where \mathbf{N} is a matrix of *shape functions*

$$\mathbf{N} = \mathbf{d}^T \mathbf{n}^{-1} \quad (4.51)$$

In Equation (4.50), the deflection function $w(x, y)$ of the element is denoted by nodal displacement. In order to deduce the stiffness matrix, Equation (4.50) is substituted into Equation (4.36) and the strain vector of the element expressed by the nodal displacement can be determined as

$$\begin{aligned} \boldsymbol{\varepsilon} &= \begin{bmatrix} \varepsilon_x \\ \varepsilon_y \\ \gamma_{xy} \end{bmatrix} = -z \begin{bmatrix} \partial^2 w / \partial x^2 \\ \partial^2 w / \partial y^2 \\ 2\partial^2 w / (\partial x \partial y) \end{bmatrix} = -z \begin{bmatrix} \partial^2 (\cdot) / \partial x^2 \\ \partial^2 (\cdot) / \partial y^2 \\ 2\partial^2 (\cdot) / (\partial x \partial y) \end{bmatrix} \mathbf{N} \boldsymbol{\delta}^e = -z \begin{bmatrix} \partial^2 (\mathbf{d}^T) / \partial x^2 \\ \partial^2 (\mathbf{d}^T) / \partial y^2 \\ 2\partial^2 (\mathbf{d}^T) / (\partial x \partial y) \end{bmatrix} \mathbf{n}^{-1} \boldsymbol{\delta}^e \\ &= -z \begin{bmatrix} 0 & 0 & 0 & 2 & 0 & 0 & 6x & 2y & 0 \\ 0 & 0 & 0 & 0 & 0 & 2 & 0 & 2x & 6y \\ 0 & 0 & 0 & 0 & 2 & 0 & 0 & 4(x+y) & 0 \end{bmatrix} \mathbf{n}^{-1} \boldsymbol{\delta}^e = \mathbf{B}_1 \mathbf{n}^{-1} \boldsymbol{\delta}^e = \mathbf{B} \boldsymbol{\delta}^e \end{aligned} \quad (4.52)$$

where

$$\mathbf{B} = \mathbf{B}_1 \mathbf{n}^{-1} \quad (4.53)$$

The stress vector of the element denoted by nodal displacement can be obtained from Equation (4.37)

$$\boldsymbol{\sigma} = \mathbf{E} \boldsymbol{\varepsilon} = \mathbf{E} \mathbf{B} \boldsymbol{\delta}^e \quad (4.54)$$

4.3.3 The Finite Element Dynamic Equation of a Thin Plate

All the nodal displacements of the whole elements of a thin plate are taken to be generalized coordinates of the thin plate and the Lagrange equation is used to set up the dynamic equation. With Equation (4.50), the deflection function becomes

$$w(x, y, t) = \mathbf{N}(x, y) \boldsymbol{\delta}(t) \quad (4.55)$$

The *kinetic energy* of the thin plate is calculated by neglecting the contributions of the in-plane displacement components u and v , namely

$$T^e = \frac{1}{2} \int_V \rho \dot{w}^2 dV = \frac{1}{2} \dot{\boldsymbol{\delta}}^{eT} \int_S \rho h \mathbf{N}^T \mathbf{N} dx dy \dot{\boldsymbol{\delta}}^e = \frac{1}{2} \dot{\boldsymbol{\delta}}^{eT} \mathbf{M}^e \dot{\boldsymbol{\delta}}^e \quad (4.56)$$

where

$$\mathbf{M}^e = \int_S \rho h \mathbf{N}^T \mathbf{N} dx dy \quad (4.57)$$

\mathbf{M}^e is the consistent mass matrix of the thin plate element, ρ is the material density and ρh is the mass of the unit area.

The elastic *potential energy* of an element can be determined from Equations (4.52) and (4.54)

$$\Pi^e = \frac{1}{2} \int_V \boldsymbol{\epsilon}^T \boldsymbol{\sigma} dV = \frac{1}{2} \boldsymbol{\delta}^{eT} \int_S \mathbf{B}^T \mathbf{E} \mathbf{B} dx dy \boldsymbol{\delta}^e = \frac{1}{2} \boldsymbol{\delta}^{eT} \mathbf{K}^e \boldsymbol{\delta}^e \quad (4.58)$$

where

$$\mathbf{K}^e = \int_S \mathbf{B}^T \mathbf{E} \mathbf{B} dx dy \quad (4.59)$$

\mathbf{K}^e is called the stiffness matrix of the thin plate element.

If there is a distributed load $P(x, y, t)$ acting on the element and it is vertical to the plane, according to the principle of virtual work the nodal load is

$$\mathbf{P}^e = \int_S \mathbf{N}^T P dx dy \quad (4.60)$$

To develop the overall equation, the expression of each element in local coordinates has to be transformed into global coordinates. Here we only need to transfer \mathbf{M}^e and \mathbf{K}^e by the following transfer matrix

$$\boldsymbol{\lambda}^e = \begin{bmatrix} \lambda_1 & & \\ & \lambda_2 & \\ & & \lambda_3 \end{bmatrix} \quad (4.61)$$

where

$$\lambda_i = \begin{bmatrix} 1 & 0 & 0 \\ 0 & l_{ox} & m_{ox} \\ 0 & l_{oy} & m_{oy} \end{bmatrix}_i \quad (4.62)$$

(l_{ox}, m_{ox}) and (l_{oy}, m_{oy}) are the direction cosines of local coordinates ox and oy in the global coordinates, respectively.

After the coordinate transformation, the kinetic and potential energies of the whole system, expressed by generalized coordinates of the global nodal displacement, are obtained. The transferred matrices are also denoted by \mathbf{M}^e and \mathbf{K}^e for simplicity, that is

$$T = \sum T^e = \sum \frac{1}{2} \dot{\boldsymbol{\delta}}^{eT} \mathbf{M}^e \dot{\boldsymbol{\delta}}^e = \frac{1}{2} \dot{\boldsymbol{\delta}}^T \mathbf{M} \dot{\boldsymbol{\delta}} \quad (4.63)$$

$$\Pi = \sum \Pi^e = \sum \frac{1}{2} \delta^{eT} K^e \delta^e = \frac{1}{2} \delta^T K \delta \quad (4.64)$$

where δ is $3n \times 1$ -dimensional column matrix of displacement of n nodes in turn, and M and K are $3n \times 3n$ -dimensional matrices.

As T and Π are quadratic homogeneous polynomials, M and K can be constructed by adding the related terms together. Because the parameters of one point are only related to its surrounding elements, M and K are sparse diagonally dominant matrices.

Using the Lagrange equation

$$\frac{d}{dt} \left(\frac{\partial(T - \Pi)}{\partial \dot{\delta}} \right) - \frac{\partial(T - \Pi)}{\partial \delta} = P \quad (4.65)$$

the differential equation of motion of the whole thin plate established by FEM is

$$M\ddot{\delta} + K\delta = P \quad (4.66)$$

As mentioned before, the direction of P^e is the same as the direction of nodal displacement, therefore P is the column matrix of the generalized force of the system.

To obtain the eigenfrequency of a thin plate under the condition of small amplitude, let

$$\delta = \Phi \sin \omega t \quad (4.67)$$

Substituting this into Equation (4.66) and assuming $P = 0$, the free vibration equation becomes

$$(K - \omega^2 M) \Phi = 0 \quad (4.68)$$

where Φ is the eigenvector.

4.3.4 Finite Element Transfer Matrix Method of Two-dimensional Systems

Now we take a rectangular thin plate as an example of the analysis steps for the FE-TMM. As shown in Figure 4.7a, the neutral surface is coincident with the oxy plane, taking the x axis as the transfer direction and dividing the plate into n equal strips along the transfer direction. Dividing each strip into $m - 1$ triangular elements, gives $2m$ nodes and $2m \times 3$ degrees of freedom. According to the TMM, for the i th strip the column matrix of nodal displacement of the AD side is the state vector of the input end, and the BE side is the output end. If the plate is not rectangular, to compute this easily let the index of the state vector of the input and output ends be equal. Of course, other methods exist, such as generalized inverse matrix [238].

Obviously, the input end of the i th strip is the output end of the $i - 1$ th strip. The subscript $(i, i - 1)$ is used to denote the input end of the i th strip and the subscript $(i, i + 1)$ is used to denote the output end of the i th strip. In short, the section between the i th strip and the $i - 1$ th strip can be defined as the i th section. The subscript $(i, i - 1)$ is used to denote the output end of the i th section and the subscript $(i - 1, i)$ is used to describe the input end of the i th section. The external force acting on the i th strip is ignored and the external force on the i th strip only acts on the nodes in the section.

The characteristics of the FE-TMM include the fact that it is not necessary to develop the dynamic equation of the whole system and only the finite element equation of strips needs to be developed. Taking the i th strip as an example, after dividing it into right-angled triangle elements, as shown in Figure 4.7b, it is easy to see that the matrix n is nonsingular. According to the boundary conditions of the top and bottom sides of the thin plate, the rows and columns which correspond to the displacement variables can be omitted, with 0 DOF at the plate boundaries (take the simply supported end w as an example) while developing M and K .

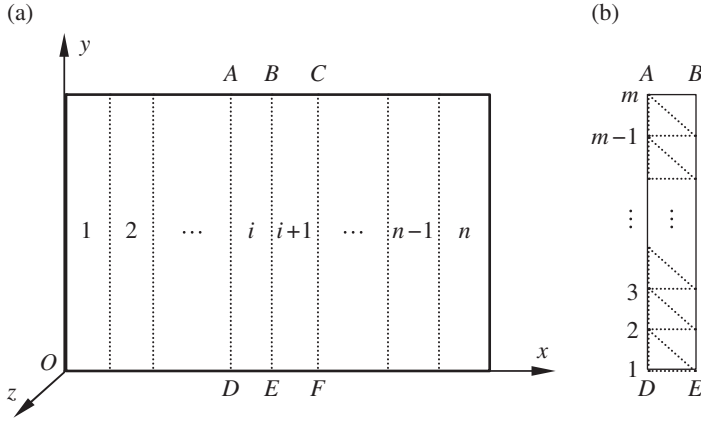


Figure 4.7 Finite element partition of a thin plate.

Assuming the boundary conditions of top and bottom sides are consistent, the conditions of each strip are the same. The force that acts on the nodes of the input end of element i is taken to be the nodal load of element $i-1$, and the force acting on the nodes of the output end of element $i-1$ is taken to be the nodal load of element i . These two forces are equal and opposite. The column matrices of displacement are denoted by $\delta_{i,i-1}$ and $\delta_{i,i+1}$. The equilibrium equation of the i th strip is

$$K_i \begin{bmatrix} \delta_{i,i-1} \\ \delta_{i,i+1} \end{bmatrix} - \omega^2 M_i \begin{bmatrix} \delta_{i,i-1} \\ \delta_{i,i+1} \end{bmatrix} = \begin{bmatrix} Q_{i,i-1} \\ Q_{i,i+1} \end{bmatrix} \quad (4.69)$$

where

$$\delta_{i,i-1} = \begin{bmatrix} \delta_1 \\ \delta_2 \\ \vdots \\ \delta_m \end{bmatrix}_{i,i-1}, \quad \delta_{i,i+1} = \begin{bmatrix} \delta_1 \\ \delta_2 \\ \vdots \\ \delta_m \end{bmatrix}_{i,i+1} \quad (4.70)$$

These matrices are $3m \times 1$ -dimensional. If there exist zeros in δ_1 and δ_m , they are omitted. Simplifying Equation (4.69), this yields

$$S_i \begin{bmatrix} \delta_{i,i-1} \\ \delta_{i,i+1} \end{bmatrix} = \begin{bmatrix} Q_{i,i-1} \\ Q_{i,i+1} \end{bmatrix} \quad (4.71)$$

where $S_i = K_i - \omega^2 M_i$ is the dynamic matrix of the i th strip.

After partitioning we obtain

$$\begin{bmatrix} S_{11} & S_{12} \\ S_{21} & S_{22} \end{bmatrix}_i \begin{bmatrix} \delta_{i,i-1} \\ \delta_{i,i+1} \end{bmatrix} = \begin{bmatrix} Q_{i,i-1} \\ Q_{i,i+1} \end{bmatrix} \quad (4.72)$$

and through simple calculation this gives

$$\begin{bmatrix} \delta \\ Q \end{bmatrix}_{i,i+1} = \begin{bmatrix} U_{11} & U_{12} \\ U_{21} & U_{22} \end{bmatrix}_i \begin{bmatrix} \delta \\ -Q \end{bmatrix}_{i,i-1} = U_i \begin{bmatrix} \delta \\ -Q \end{bmatrix}_{i,i-1} \quad (4.73)$$

where

$$\begin{cases} \mathbf{U}_{11,i} = -\mathbf{S}_{12,i}^{-1}\mathbf{S}_{11,i} \\ \mathbf{U}_{12,i} = -\mathbf{S}_{12,i}^{-1} \\ \mathbf{U}_{21,i} = \mathbf{S}_{21,i} - \mathbf{S}_{22,i}\mathbf{S}_{12,i}^{-1}\mathbf{S}_{11,i} \\ \mathbf{U}_{22,i} = -\mathbf{S}_{22,i}\mathbf{S}_{12,i}^{-1} \end{cases} \quad (4.74)$$

4.3.5 Solving Vibration Characteristics using the Finite Element Transfer Matrix Method

External load is not considered while computing the free vibration, that is to say, there is no external load at the section (node). Considering the displacement of the two ends of the section is continuous, this yields

$$\begin{bmatrix} \delta \\ -\mathbf{Q} \end{bmatrix}_{i,i-1} = \begin{bmatrix} \delta \\ \mathbf{Q} \end{bmatrix}_{i-1,i} \quad (4.75)$$

Substituting Equation (4.75) into Equation (4.73), and denoting $\mathbf{Z} = [\delta, \mathbf{Q}]^T$, the transfer equation yields

$$\mathbf{Z}_{i,i+1} = \mathbf{U}_i \mathbf{Z}_{i-1,i} \quad (4.76)$$

Finally, the overall transfer equation of the thin plate is

$$\mathbf{Z}_{n,n+1} = \mathbf{U}_n \mathbf{U}_{n-1} \cdots \mathbf{U}_2 \mathbf{U}_1 \mathbf{Z}_{0,1} = \mathbf{U} \mathbf{Z}_{0,1} \quad (4.77)$$

After partitioning \mathbf{U} , this becomes

$$\begin{bmatrix} \delta \\ \mathbf{Q} \end{bmatrix}_{n,n+1} = \begin{bmatrix} \mathbf{U}_{11} & \mathbf{U}_{12} \\ \mathbf{U}_{21} & \mathbf{U}_{22} \end{bmatrix} \begin{bmatrix} \delta \\ \mathbf{Q} \end{bmatrix}_{0,1} \quad (4.78)$$

Introducing the boundary condition of two sides, the frequency equation is obtained. For instance, the left side is fixed and right side is free, which means

$$\delta_{0,1} = \mathbf{0}, \quad \mathbf{Q}_{n,n+1} = \mathbf{0} \quad (4.79)$$

Substituting into Equation (4.78) yields

$$\mathbf{U}_{22} \mathbf{Q}_{0,1} = \mathbf{0} \quad (4.80)$$

so the frequency equation is

$$|\mathbf{U}_{22}| = 0 \quad (4.81)$$

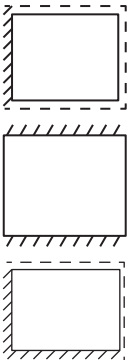
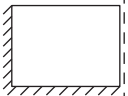
When one order frequency is determined, $\mathbf{Q}_{0,1}$ and state vector $\mathbf{Z}_{0,1}$ can be evaluated from Equations (4.80) and (4.79), respectively, and then $\mathbf{Z}_{1,2}$ is obtained from Equation (4.76), so all the state vectors can be determined in turn.

Example 4.2 [237] The square plate of uniform thickness is divided into four strips with equal width. Let $\mu = 0.3$ and compute the first three orders of its eigenfrequencies (y axis).

Solution

The results are presented in Table 4.1 and compared with reference [239]. From the table it can be concluded that although the number of the divided strips is few, the accuracy of results is acceptable, and because the four strips are exactly the same, we only need to compute the transfer matrix of one strip. As a result, the computing speed is improved.

Table 4.1 Eigenfrequencies of a square plate of equal thickness

Boundary condition	J	λ_{1j}		λ_{1j}		λ_{1j}		λ_{1j}	
		FE-TMM	Reference [239]	FE-TMM	Reference [239]	FE-TMM	Reference [239]	FE-TMM	Reference [239]
	1	19.74	19.72	49.40	49.30	99.34	98.60	171.27	167.88
	2	49.35	49.30	78.99	78.88	128.84	128.10	200.50	197.20
	3	98.67	98.60	128.46	128.10	177.05	177.48	250.21	246.40
	1	23.65	23.65	58.77	58.65	114.27	113.20	193.02	187.80
	2	51.69	51.95	86.27	86.30	141.86	140.80	219.49	215.50
	3	100.31	101.20	134.04	134.20	189.44	188.10	271.66	262.80
	1	22.23	22.42	26.52	27.30	44.05	45.40	81.10	82.10
	2	61.25	61.62	67.32	68.75	88.08	91.45	126.06	129.10
	3	120.19	120.80	126.89	128.82	149.63	153.85	189.17	194.45
	1	27.14	27.25	61.11	61.10	116.25	115.20	193.71	189.20
	2	60.69	61.10	93.11	93.20	147.30	146.20	229.64	220.20
	3	114.67	115.20	146.17	146.40	199.28	198.30	278.94	271.10

Note: $\omega_{i,j} = \lambda_{i,j} \frac{1}{l^2} \sqrt{\frac{Eh^2}{12\rho(1-\mu^2)}}$ [240], i is the sequence number of the mode along the x axis and j is the sequence number of the mode along the y axis.

4.3.6 Steady-state Response using the Finite Element Transfer Matrix Method

When computing the steady-state response, suppose the external loads only act on the section (node). Considering the displacement of the two ends of the section to be continuous, \mathbf{P} denotes the vector of the generalized external force column matrix, and so according to Equation (4.75)

$$\begin{bmatrix} \delta \\ -\mathbf{Q} \end{bmatrix}_{i,i-1} = \begin{bmatrix} \delta \\ \mathbf{Q} + \mathbf{P} \end{bmatrix}_{i-1,i} \quad (4.82)$$

Substituting the equation above into Equation (4.73) leads to

$$\begin{bmatrix} \delta \\ \mathbf{Q} \end{bmatrix}_{i,i+1} = \begin{bmatrix} \mathbf{u}_{11} & \mathbf{u}_{12} \\ \mathbf{u}_{21} & \mathbf{u}_{22} \end{bmatrix}_i \begin{bmatrix} \delta \\ \mathbf{Q} \end{bmatrix}_{i-1,i} + \begin{bmatrix} \mathbf{u}_{12,i} \mathbf{P}_{i,i-1} \\ \mathbf{u}_{22,i} \mathbf{P}_{i,i-1} \end{bmatrix} \quad (4.83)$$

or

$$\mathbf{Z}_{i,i+1} = \mathbf{u}_i \mathbf{Z}_{i-1,i} + \mathbf{f}_i \quad (4.84)$$

Let $\hat{\mathbf{Z}} = [\delta, \mathbf{Q}, 1]^T$, so we have

$$\hat{\mathbf{Z}}_{i,i+1} = \mathbf{u}_i \hat{\mathbf{Z}}_{i-1,i} \quad (4.85)$$

where

$$\mathbf{U}_i = \begin{bmatrix} \mathbf{U}_{11} & \mathbf{U}_{12} & \mathbf{U}_{12,i} \mathbf{P}_{i,i-1} \\ \mathbf{U}_{21} & \mathbf{U}_{22} & \mathbf{U}_{22,i} \mathbf{P}_{i,i-1} \\ \mathbf{O}_{1 \times 3m} & \mathbf{O}_{1 \times 3m} & 1 \end{bmatrix} \quad (4.86)$$

Example 4.3 [241] A cantilever rectangular plate with a quadrate hole and bevel edge, $E = 7.06 \times 10^4 \text{ MPa}$ and $\nu = 0.33$, has side length of the quadrate hole of 0.2 m , $h = 2 \text{ cm}$ and other dimensions as shown in Figure 4.8. Find the displacement of A and B when the distributed load is $P = 2 \text{ kN/m}^2$.

Solution

Considering the plate as shown in Figure 4.8, which is divided into rectangular area 1 and nonregular area 2, apply the FE-TMM in area 1 and the FEM in area 2. Use the section $n+1$ to denote the intersection of the two regions. Areas 1 and 2 have the same nodes on the intersection surface $n+1$ and their elements are the same type, as shown in Figure 4.9.

The FE-TMM is applied to the regular area 1, which is divided into n strips. The right boundary state vector and left boundary state vector of area 1 yield the transfer equation as follows

$$\begin{bmatrix} \delta_{n,n+1}^L \\ \mathbf{Q}_{n,n+1}^L \end{bmatrix} = \begin{bmatrix} \mathbf{U}_{11} & \mathbf{U}_{12} \\ \mathbf{U}_{21} & \mathbf{U}_{22} \end{bmatrix} \begin{bmatrix} \delta_{0,1} \\ \mathbf{Q}_{0,1} \end{bmatrix} + \begin{bmatrix} \mathbf{f}' \\ \mathbf{f}'' \end{bmatrix} \quad (\text{a})$$

where $\delta_{n,n+1}^L$ and $\mathbf{Q}_{n,n+1}^L$ are the displacement and internal force vector on the left side of section $n+1$, respectively. $\delta_{0,1}$ and $\mathbf{Q}_{0,1}$ are the displacement and internal force vector on the left boundary of the whole structure, respectively.

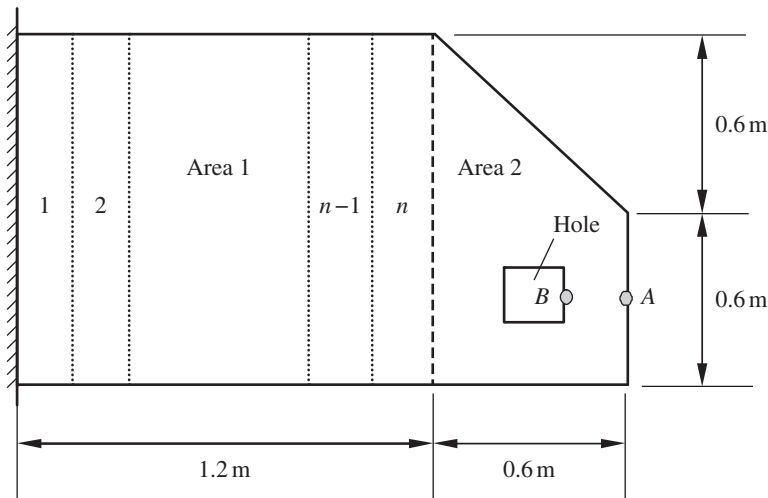


Figure 4.8 Plate structure.

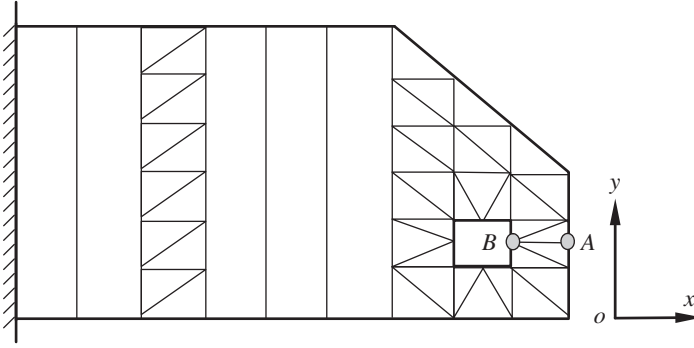


Figure 4.9 Plate and structure portion of a plate.

The FEM is applied to the nonregular area 2. The internal force vector on the right side of section $n + 1$ should be treated as the external force when area 2 is studied alone.

$$\begin{bmatrix} K_{11} & K_{12} \\ K_{21} & K_{22} \end{bmatrix} \begin{bmatrix} \delta_{n,n+1}^R \\ \delta \end{bmatrix} = \begin{bmatrix} P' \\ P'' \end{bmatrix} + \begin{bmatrix} Q_{n,n+1}^R \\ \mathbf{0} \end{bmatrix} \quad (b)$$

where $\delta_{n,n+1}^R$ and $Q_{n,n+1}^R$ are the displacement and the internal force vectors on the right side of section $n + 1$, respectively. δ is the nodal displacement vector in area 2 excluding $\delta_{n,n+1}^R$, and P' and P'' are the subvectors of the nodal load vector P .

In section $n + 1$, according to the continuous condition of displacement and internal force, this yields

$$\delta_{n,n+1}^R = \delta_{n,n+1}^L, \quad Q_{n,n+1}^R = -Q_{n,n+1}^L \quad (c)$$

Substituting Equation (c) into Equation (a), we obtain $\delta_{n,n+1}^R$ and $Q_{n,n+1}^R$. Substituting the results into Equation (b), we obtain

$$\begin{bmatrix} K_{11}U_{11} + U_{21} & K_{12} \\ K_{21}U_{11} & K_{22} \end{bmatrix} \begin{bmatrix} \delta_{0,1} \\ \delta \end{bmatrix} + \begin{bmatrix} K_{11}U_{12} + U_{22} & I \\ K_{21}U_{12} & I \end{bmatrix} \begin{bmatrix} Q_{0,1} \\ \mathbf{0} \end{bmatrix} = \begin{bmatrix} P' - K_{11}f' - f'' \\ P'' - K_{21}f' \end{bmatrix} \quad (d)$$

Taking into account the boundary conditions and substituting the known parts of $\delta_{0,1}$ and $Q_{0,1}$ into the above equation, we obtain the unknown parts of $\delta_{0,1}$ and $Q_{0,1}$ as well as the unknown displacement δ . Next, using $\delta_{0,1}$ and $Q_{0,1}$ for transfer calculating, the displacements and internal forces at the nodes of each part in area 1 can be evaluated.

Using the FEM and FE-TMM respectively, the computational results are shown in Table 4.2. Herein, the FE-TMM has the same computational accuracy as the FEM, but it takes less computational time and has higher computational efficiency.

Table 4.2 Computation results of FE-TMM and FEM

Results Method	A			B			Computational time (s)
	w (cm)	θ_x (rad)	θ_y (rad)	w (cm)	θ_x (rad)	θ_y (rad)	
FEM	4.2207	0.0017	-0.0314	3.5949	0.0014	-0.0312	80
FE-TMM	4.2110	0.0016	-0.0311	3.5726	0.0014	-0.0310	58

4.4 Finite Element Riccati Transfer Matrix Method for Two-dimensional Nonlinear Systems

The analysis of a geometrically nonlinear structure has been a subject of considerable interest for several decades. When dealing with the transient analysis of structures with large displacement under general excitation by a direct integration method such as the Wilson- θ method on a computer, the matrices obtained by the FEM are usually very large, which leads to low computational efficiency. For this reason, various techniques have been suggested to reduce the order of the matrices. The FE-TMM, introduced in the previous section is one of these techniques. In this method, the size of the stiffness and mass matrices is equal to the number of the degrees of freedom in the subsystem, hence these matrices are much smaller than those obtained by the ordinary FEM. This method has been successfully applied to various linear static, free vibration, dynamic response and nonlinear static problems. By combining the FE-TMM and the Riccati TMM [225], we can carry out the transient analysis of nonlinear structure dynamics with large displacement under general excitation, where the time integration of the incremental equations could be solved by the Wilson- θ method. The improved Newton–Raphson method is employed in equilibrium iterative procedures of each time step, and the Riccati transformation of the state vector is proposed to avoid the propagation of round-off errors occurring in recursive multiplications of the transfer matrices.

4.4.1 Incremental Equilibrium Equation and Direct Integration Method

The governing equation for a dynamic problem in FEM at time t is

$$M\ddot{\mathbf{v}}(t) + C\dot{\mathbf{v}}(t) + \mathbf{F}(t) = \mathbf{R}(t) \quad (4.87)$$

where M and C are mass and damping matrices, and $\ddot{\mathbf{v}}(t)$, $\dot{\mathbf{v}}(t)$, $\mathbf{F}(t)$ and $\mathbf{R}(t)$ are the acceleration, velocity, nodal elastic force and nodal external force vectors, respectively, of all the nodes of the system at time t .

At time $t + \theta\Delta t$ (Δt is the time step, θ is the parameter that for stability control, $\theta \geq 1$), from Equation (4.87) we can get

$$M\ddot{\mathbf{v}}(t + \theta\Delta t) + C\dot{\mathbf{v}}(t + \theta\Delta t) + \mathbf{F}(t + \theta\Delta t) = \mathbf{R}(t + \theta\Delta t) \quad (4.88)$$

Equation (4.88) is a nonlinear equation for a geometrically nonlinear structure problem. In the analysis of nonlinear structures, the linearization of equations of motion usually uses the following approximation

$$\mathbf{F}(t + \theta\Delta t) = \mathbf{F}(t) + \mathbf{K}_T(t)\Delta\mathbf{v} \quad (4.89)$$

where $\Delta\mathbf{v}$ is the vector of incremental displacement in time interval $\theta\Delta t$, with $\Delta\mathbf{v} = \mathbf{v}(t + \theta\Delta t) - \mathbf{v}(t)$, and $\mathbf{K}_T(t)$ is the tangent stiffness matrix at time t [225].

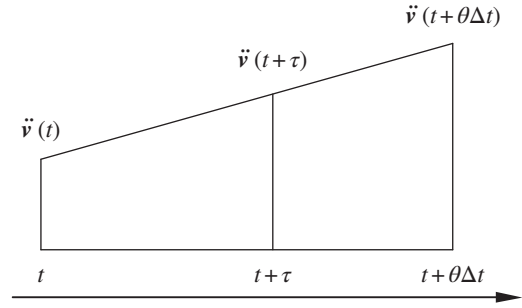
Substituting Equation (4.89) into Equation (4.88) and then subtracting Equation (4.87) gives the incremental equilibrium equation from time t to $t + \theta\Delta t$

$$M\Delta\ddot{\mathbf{v}} + C\Delta\dot{\mathbf{v}} + \mathbf{K}_T\Delta\mathbf{v} = \Delta\mathbf{R} \quad (4.90)$$

where $\Delta\mathbf{R} = \mathbf{R}(t + \theta\Delta t) - \mathbf{R}(t)$.

Solve Equation (4.90) using the Wilson- θ method [242]. The Wilson- θ method is based on the linear acceleration method, namely an assumption is made that the acceleration varies according to the linear rule in time $t \sim t + \theta\Delta t$, as shown in Figure 4.10.

Figure 4.10 Assumption of the linear variation of acceleration.



τ is a time variable start from time t , and for $0 \leq \tau \leq \theta\Delta t$ the acceleration inside this range can be obtained according to the linear assumption of acceleration

$$\ddot{v}(t+\tau) = \ddot{v}(t) + \frac{\tau}{\theta\Delta t} [\ddot{v}(t+\theta\Delta t) - \ddot{v}(t)] \quad (4.91)$$

Integrating Equation (4.91) yields

$$\dot{v}(t+\tau) = \dot{v}(t) + \tau \ddot{v}(t) + \frac{\tau^2}{2\theta\Delta t} [\ddot{v}(t+\theta\Delta t) - \ddot{v}(t)] \quad (4.92)$$

$$v(t+\tau) = v(t) + \tau \dot{v}(t) + \frac{\tau^2}{2} \ddot{v}(t) + \frac{\tau^3}{6\theta\Delta t} [\ddot{v}(t+\theta\Delta t) - \ddot{v}(t)] \quad (4.93)$$

In Equations (4.92) and (4.93), let $\tau = \theta\Delta t$, then we obtain

$$\dot{v}(t+\theta\Delta t) = \dot{v}(t) + \frac{\theta\Delta t}{2} [\ddot{v}(t+\theta\Delta t) + \ddot{v}(t)] \quad (4.94)$$

$$v(t+\theta\Delta t) = v(t) + \theta\Delta t \dot{v}(t) + \frac{(\theta\Delta t)^2}{6} [\ddot{v}(t+\theta\Delta t) + 2\ddot{v}(t)] \quad (4.95)$$

The acceleration and velocity at time $t+\theta\Delta t$ can be determined from Equations (4.94) and (4.95)

$$\ddot{v}(t+\theta\Delta t) = \frac{6}{(\theta\Delta t)^2} [v(t+\theta\Delta t) - v(t)] - \frac{6}{\theta\Delta t} \dot{v}(t) - 2\ddot{v}(t) \quad (4.96)$$

$$\dot{v}(t+\theta\Delta t) = \frac{3}{\theta\Delta t} [v(t+\theta\Delta t) - v(t)] - 2\dot{v}(t) - \frac{\theta\Delta t}{2} \ddot{v}(t) \quad (4.97)$$

namely

$$\Delta\ddot{v} = \ddot{v}(t+\theta\Delta t) - \ddot{v}(t) = \frac{6}{(\theta\Delta t)^2} \Delta v - \frac{6}{\theta\Delta t} \dot{v}(t) - 3\ddot{v}(t) \quad (4.98)$$

$$\Delta\dot{v} = \dot{v}(t+\theta\Delta t) - \dot{v}(t) = \frac{3}{\theta\Delta t} \Delta v - 3\dot{v}(t) - \frac{\theta\Delta t}{2} \ddot{v}(t) \quad (4.99)$$

Substituting Equations (4.98) and (4.99) into Equation (4.90) yields

$$H\Delta v = \Delta G \quad (4.100)$$

where

$$\mathbf{H} = \frac{6}{(\theta\Delta t)^2}\mathbf{M} + \frac{3}{\theta\Delta t}\mathbf{C} + \mathbf{K}_T \quad (4.101)$$

$$\Delta\mathbf{G} = \Delta\mathbf{R} + \mathbf{M} \left[\frac{6}{\theta\Delta t}\dot{\mathbf{v}}(t) + 3\ddot{\mathbf{v}}(t) \right] + \mathbf{C} \left[3\dot{\mathbf{v}}(t) + \frac{\theta\Delta t}{2}\ddot{\mathbf{v}}(t) \right] \quad (4.102)$$

Equation (4.100) only has one unknown variable $\Delta\mathbf{v}$, and we can solve it to obtain the acceleration, velocity and displacements of all the nodes in the system at time $t + \Delta t$

$$\ddot{\mathbf{v}}(t + \Delta t) = \frac{6}{\theta(\theta\Delta t)^2}\Delta\mathbf{v} - \frac{6}{\theta^2\Delta t}\dot{\mathbf{v}}(t) + \left(1 - \frac{3}{\theta}\right)\ddot{\mathbf{v}}(t) \quad (4.103)$$

$$\dot{\mathbf{v}}(t + \Delta t) = \dot{\mathbf{v}}(t) + \frac{\Delta t}{2}[\ddot{\mathbf{v}}(t + \Delta t) + \ddot{\mathbf{v}}(t)] \quad (4.104)$$

$$\mathbf{v}(t + \Delta t) = \mathbf{v}(t) + \Delta t\dot{\mathbf{v}}(t) + \frac{\Delta t^2}{6}[\ddot{\mathbf{v}}(t + \Delta t) + 2\ddot{\mathbf{v}}(t)] \quad (4.105)$$

It is necessary to point out that $\Delta\mathbf{v}$ obtained from Equation (4.100) is only an approximation of incremental displacements. To obtain a more precise solution, a series of iterations is generally used, and the determined solutions $\Delta\mathbf{v}$, $\Delta\dot{\mathbf{v}}$ and $\Delta\ddot{\mathbf{v}}$ are substituted into Equation (4.90), then the approximation of incremental vectors of external force can be obtained:

$$\Delta\mathbf{R}' = \mathbf{M}\Delta\ddot{\mathbf{v}} + \mathbf{C}\Delta\dot{\mathbf{v}} + \mathbf{K}_T\Delta\mathbf{v}$$

The difference between the real incremental vector of external force and the approximation of external force is called the unbalanced force:

$$\delta\Delta\mathbf{R} = \Delta\mathbf{R} - \Delta\mathbf{R}' = \mathbf{R}(t + \theta\Delta t) - \mathbf{R}(t) - (\mathbf{M}\Delta\ddot{\mathbf{v}} + \mathbf{C}\Delta\dot{\mathbf{v}} + \mathbf{K}_T\Delta\mathbf{v})$$

Replacing $\Delta\mathbf{G}$ in Equation (4.100) by $\delta\Delta\mathbf{R}$, we obtain

$$\mathbf{H}\delta\Delta\mathbf{v} = \delta\Delta\mathbf{R}$$

and the correction $\delta\Delta\mathbf{v}$, hence

$$\Delta\mathbf{v}' = \Delta\mathbf{v} + \delta\Delta\mathbf{v}$$

However, because $\Delta\mathbf{v}$ in Equation (4.100) has a large number of elements, the order of the corresponding matrix \mathbf{H} is very large, and this iterative process needs a lot of computation time. Take the thin plate shown in Figure 4.11 as an example. If the plate is divided into n strips, and each strip is divided into $2m$ triangular elements, then the elements number of $\Delta\mathbf{v}$ is $3(n+1)(m+1)$ while the corresponding matrix \mathbf{H} is a square matrix with $3(n+1)(m+1)$ orders.

4.4.2 Finite Element Riccati Transfer Matrix Method for Two-dimensional Nonlinear Systems

Without loss of generality, consider the plate shown in Figure 4.11.

4.4.2.1 Transfer Matrix of a Strip

Ignore the external load acting on the i th strip and consider that the external load acts only on nodes, then the transfer equation [226] of the i th strip is

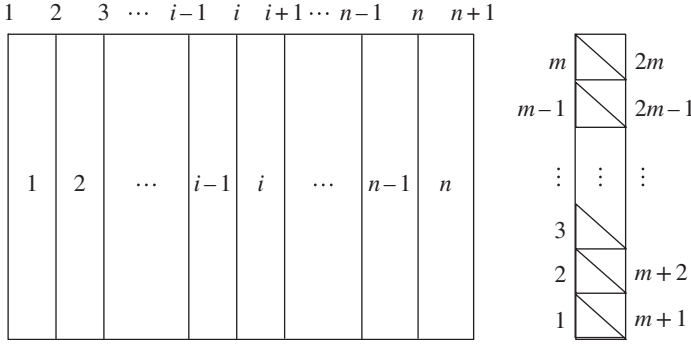


Figure 4.11 Finite element partition of a plane plate.

$$\begin{bmatrix} \Delta \mathbf{v} \\ \Delta \mathbf{Q} \end{bmatrix}_{i,i+1} = \begin{bmatrix} \mathbf{U}_{11} & \mathbf{U}_{12} \\ \mathbf{U}_{21} & \mathbf{U}_{22} \end{bmatrix}_i \begin{bmatrix} \Delta \mathbf{v} \\ -\Delta \mathbf{Q} \end{bmatrix}_{i,i-1} \quad (4.106)$$

where

$$\begin{cases} \mathbf{U}_{11} = -\mathbf{H}_{12}^{-1} \mathbf{H}_{11} \\ \mathbf{U}_{12} = -\mathbf{H}_{12}^{-1} \\ \mathbf{U}_{21} = \mathbf{H}_{21} - \mathbf{H}_{22} \mathbf{H}_{12}^{-1} \mathbf{H}_{11} \\ \mathbf{U}_{22} = -\mathbf{H}_{22} \mathbf{H}_{12}^{-1} \end{cases}$$

$\Delta \mathbf{v}_{i,i+1}$, $\Delta \mathbf{Q}_{i,i+1}$ and $\Delta \mathbf{v}_{i,i-1}$, $\Delta \mathbf{Q}_{i,i-1}$ are incremental vectors of displacement and nodal elastic force on the output ends and input ends of the i th strip from t to $t + \theta \Delta t$, and \mathbf{H}_{11} , \mathbf{H}_{12} , \mathbf{H}_{21} , \mathbf{H}_{22} are the submatrices of matrix \mathbf{H} (local) in Equation (4.100).

The transfer matrix of the i th section is

$$\begin{bmatrix} \Delta \mathbf{v} \\ -\Delta \mathbf{Q} \end{bmatrix}_{i,i-1} = \begin{bmatrix} \mathbf{I} & \mathbf{O} \\ \mathbf{O} & \mathbf{I} \end{bmatrix} \begin{bmatrix} \Delta \mathbf{v} \\ \Delta \mathbf{Q} \end{bmatrix}_{i-1,i} + \begin{bmatrix} \mathbf{0} \\ \Delta \mathbf{P} \end{bmatrix}_i \quad (4.107)$$

where, $\Delta \mathbf{v}_{i,i-1}$, $\Delta \mathbf{Q}_{i,i-1}$, $\Delta \mathbf{v}_{i,i+1}$ and $\Delta \mathbf{Q}_{i,i+1}$ are incremental vectors of displacement and nodal elastic force on the input ends of the i th strip and the output ends of the $(i-1)$ th strip from t to $t + \theta \Delta t$, and $\Delta \mathbf{P}$ is the generalized load incremental vector acting on the i th section.

Substituting Equation (4.107) into Equation (4.106) yields

$$\begin{bmatrix} \Delta \mathbf{v} \\ \Delta \mathbf{Q} \end{bmatrix}_{i,i+1} = \begin{bmatrix} \mathbf{U}_{11} & \mathbf{U}_{12} \\ \mathbf{U}_{21} & \mathbf{U}_{22} \end{bmatrix}_i \begin{bmatrix} \Delta \mathbf{v} \\ \Delta \mathbf{Q} \end{bmatrix}_{i-1,i} + \begin{bmatrix} \mathbf{U}_{12} \Delta \mathbf{P} \\ \mathbf{U}_{22} \Delta \mathbf{P} \end{bmatrix}_i \quad (4.108a)$$

or

$$\Delta \mathbf{z}_{i,i+1} = \mathbf{U}_i \Delta \mathbf{z}_{i-1,i} + \Delta \mathbf{f}_i \quad (4.108b)$$

Equation (4.108) describes the relation of incremental state vectors of the sections $i+1$ and i , which is usually described as follows

$$\begin{bmatrix} \Delta \mathbf{v} \\ \Delta \mathbf{Q} \\ 1 \end{bmatrix}_{i,i+1} = \begin{bmatrix} \mathbf{U}_{11} & \mathbf{U}_{12} & \mathbf{U}_{12} \Delta \mathbf{P} \\ \mathbf{U}_{21} & \mathbf{U}_{22} & \mathbf{U}_{22} \Delta \mathbf{P} \\ \mathbf{0} & \mathbf{0} & 1 \end{bmatrix}_i \begin{bmatrix} \Delta \mathbf{v} \\ \Delta \mathbf{Q} \\ 1 \end{bmatrix}_{i-1,i} \quad (4.109a)$$

or

$$\Delta \hat{\mathbf{z}}_{i,i+1} = \hat{\mathbf{U}}_i \Delta \hat{\mathbf{z}}_{i-1,i} \quad (4.109b)$$

Equation (4.109) is the transfer equation of the i th strip and $\hat{\mathbf{U}}_i$ is the transfer matrix of the i th strip.

$\Delta \mathbf{v}$ can be obtained from Equation (4.109) by using the ordinary TMM with boundary conditions. Both Equations (4.109) and (4.100) can be applied to achieve $\Delta \mathbf{v}$: using Equation (4.100) we only need to solve a single large equation once, while using Equation (4.109) we need to solve all the transfer equations step by step to get $\Delta \mathbf{v}_{i,i+1}$. However, the order of corresponding matrix \mathbf{H} of Equation (4.109) is much less than the order of the matrix when using Equation (4.100). Taking Figure 4.9 as an example, if Equation (4.109) is used the dimension is only $6(m+1)+1$, which is much less than the dimension of \mathbf{H} , which is $3(n+1)(m+1)$.

4.4.2.2 Riccati Transformation of Incremental State Vectors

To reduce the propagation of round-off errors in the ordinary TMM, the Riccati transformation of incremental state vectors is proposed. Rearranging and repartitioning Equation (4.109) we obtain

$$\begin{bmatrix} \Delta \mathbf{z}_a \\ \Delta \mathbf{z}_b \end{bmatrix}_{i,i+1} = \begin{bmatrix} T_{11} & T_{12} \\ T_{21} & T_{22} \end{bmatrix}_i \begin{bmatrix} \Delta \mathbf{z}_a \\ \Delta \mathbf{z}_b \end{bmatrix}_{i-1,i} + \begin{bmatrix} \Delta \mathbf{f}_a \\ \Delta \mathbf{f}_b \end{bmatrix}_i \quad (4.110)$$

where $\Delta \mathbf{z}_a$ contains half of the elements, which are already known, of incremental state vectors at the input boundary and $\Delta \mathbf{z}_b$ contains the other half of the unknown incremental state variables.

A general Riccati transformation at the i th section is

$$\Delta \mathbf{z}_{ai-1,i} = \mathbf{S}_i \Delta \mathbf{z}_{bi-1,i} + \Delta \mathbf{e}_i \quad (4.111)$$

where \mathbf{S}_i is the Riccati transfer matrix and vector $\Delta \mathbf{e}_i$ is associated with external force. From Equations (4.110) and (4.111), we obtain

$$\Delta \mathbf{z}_{ai,i+1} = \mathbf{S}_{i+1} \Delta \mathbf{z}_{bi,i+1} + \Delta \mathbf{e}_{i+1} \quad (4.112)$$

where

$$\begin{cases} \mathbf{S}_{i+1} = (\mathbf{T}_{11}\mathbf{S} + \mathbf{T}_{12})_i (\mathbf{T}_{21}\mathbf{S} + \mathbf{T}_{22})_i^{-1} \\ \Delta \mathbf{e}_{i+1} = (\mathbf{T}_{11}\Delta \mathbf{e} + \Delta \mathbf{f}_a)_i - \mathbf{S}_{i+1} (\mathbf{T}_{21}\Delta \mathbf{e} + \Delta \mathbf{f}_b)_i \end{cases} \quad (4.113)$$

Equation (4.113) shows the general recursive relations for \mathbf{S}_i and $\Delta \mathbf{e}_i$.

First, \mathbf{S}_1 and $\Delta \mathbf{e}_1$ are obtained by using the input boundary conditions. Then \mathbf{S}_i and $\Delta \mathbf{e}_i$ of the whole structure can be obtained in turn by using Equation (4.113), hence

$$\Delta \mathbf{z}_{an,n+1} = \mathbf{S}_{n+1} \Delta \mathbf{z}_{bn,n+1} + \Delta \mathbf{e}_{n+1} \quad (4.114)$$

According to the output boundary conditions (parts of state variables are known in $\Delta \mathbf{z}_{n,n+1}$), by substituting these variables into Equation (4.114) the unknown state variables in $\Delta \mathbf{z}_{n,n+1}$ can be evaluated. After the incremental state vector $\Delta \mathbf{z}_{n,n+1}$ at the output boundary of the whole structure has been solved, the incremental state vector $\Delta \mathbf{z}_{i-1,i}$ on any section i can be evaluated from Equations (4.114) and (4.111) as follows

$$\Delta \mathbf{z}_{bi-1,i} = (\mathbf{T}_{21}\mathbf{S} + \mathbf{T}_{22})_i^{-1} [\Delta \mathbf{z}_{bi,i+1} - (\mathbf{T}_{21}\Delta \mathbf{e} + \Delta \mathbf{f}_b)_i] \quad (4.115)$$

4.4.2.3 Iterative Procedure

Because the approximation of Equation (4.89) was used, the incremental state vectors obtained from the above are only approximations of the accurate incremental state vectors. Hence, a modified Newton–Raphson method is applied to iterate for dynamic equilibrium equations. The iterative procedure is as follows:

- 1) Let initial $\Delta \mathbf{v}^{(0)}$ be equal to the solution of Equation (4.100) or the solution of TMM in (1), $j = 0$.
- 2) The unbalanced force $\delta \Delta \mathbf{R}^{(j)}$ is calculated using the following equation

$$\delta \Delta \mathbf{R}^{(j)} = \mathbf{R}(t + \theta \Delta t) - \mathbf{R}(t) - \left(\mathbf{M} \Delta \ddot{\mathbf{v}}^{(j)} + \mathbf{C} \Delta \dot{\mathbf{v}}^{(j)} + \mathbf{K}_T \Delta \mathbf{v}^{(j)} \right) \quad (4.116)$$

- 3) Replacing $\Delta \mathbf{G}$ in Equation (4.100) by $\delta \Delta \mathbf{R}^{(j)}$, we obtain

$$\mathbf{H} \delta \Delta \mathbf{v}^{(j+1)} = \delta \Delta \mathbf{R}^{(j)}$$

Using FE-RTM as described above, the $(j + 1)$ th correction $\delta \Delta \mathbf{v}^{(j+1)}$ is obtained.

- 4) The correction $\delta \Delta \mathbf{v}^{(j+1)}$ is added to $\Delta \mathbf{v}^{(j)}$ to obtain the j th approximation

$$\Delta \mathbf{v}^{(j+1)} = \Delta \mathbf{v}^{(j)} + \delta \Delta \mathbf{v}^{(j+1)}$$

- 5) $j = j + 1$.
- 6) Repeat iterations (2)–(5) until the unbalanced forces become sufficiently small.
- 7) Using Equations (4.103)–(4.105), the displacement, velocity and acceleration at time $t + \Delta t$ are obtained.

4.4.3 Numerical Examples

To review the computational accuracy and efficiency of the finite element Riccati TMM, this method is used to compute the dynamic response of armor plate with and without stiffeners under impact load, and these results are compared with those obtained by ordinary FEM.

Example 4.4 [225] Find the dynamic response of a clamped square plate subjected to a suddenly applied uniform pressure. The size of the plate is $244 \times 244 \times 0.635$ cm, the material density is $2.524 \times 10^3 \text{ kg/m}^3$, Young's modulus is $E = 6.895 \times 10^4 \text{ MPa}$, Poisson's ratio is $\nu = 0.23$ and the uniform pressure is 479 N/m^2 .

Solution

As shown in Figure 4.12, a quarter of the plate is divided into 6×8 elements. Assume the time step is $\Delta t = 0.0015$ s. The time history results of the displacement at the center of the plate using the FE-RTMM and the FEM are shown in Figure 4.13. The FE-RTMM and the FEM use the same mesh grid sizes when solving the problem and the computational results prove both methods are completely consistent. Table 4.3 shows comparisons of the average computation time for each time step between the FE-RTMM and the FEM. It is obvious that the computational time using the FE-RTM is half that for the FEM.

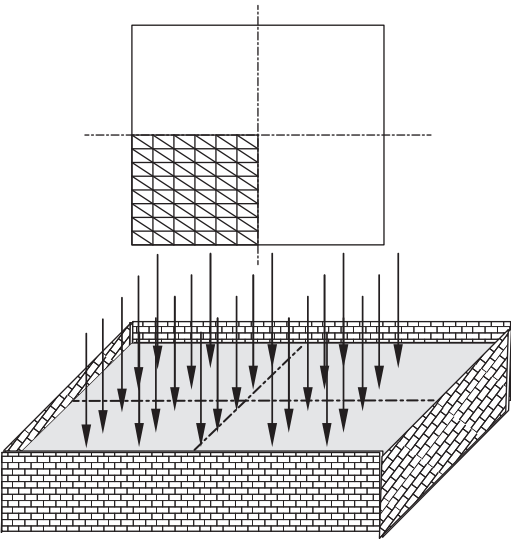


Figure 4.12 Clamped square plate and the mesh of the finite elements.

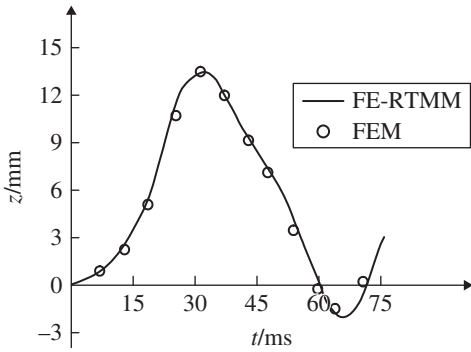


Figure 4.13 Displacement of the center of a clamped plate.

Table 4.3 Comparison of computational time for Example 4.4

Method	Computational time of each step (s)
FE-RTMM	346
FEM	700

Example 4.5 [227] Find the dynamic response of a clamped square plate structure subjected to a suddenly applied uniform pressure (479N/m^2), as shown in Figure 4.14.

Solution

There are seven and five stiffeners in the x and y directions of the plate, respectively. The stiffeners have axial strength $EA = 11 \times 10^6\text{N}$ and bending stiffness $EI_y = 9\text{ N}\cdot\text{m}^2$ and $EI_z = 40\text{ N}\cdot\text{m}^2$. The dimensions, thickness and material of the plate are identical with those in Example 4.4.

Figure 4.14 Clamped stiffened square plate.

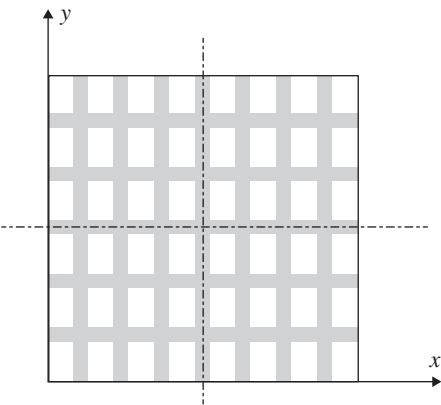


Figure 4.15 Displacement of the center of a clamped stiffened square plate.

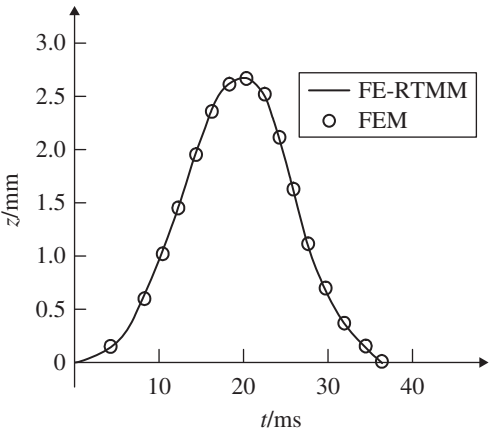


Table 4.4 Comparison of computational time for Example 4.5

Method	Computational time of each step (s)
FE-RTMM	200
FEM	365

A quarter of the plate structure is divided into 4×6 plate elements and 24 beam elements. Both the FE-RTMM and the FEM have the same time step, $\Delta t = 0.002s$. The dynamic responses of the deformation at a central point computed by the two methods are shown in Figure 4.15. The differences between the results are too small to distinguish in the figure. The average computation time taken for each time step is shown in Table 4.4.

These two examples indicate that the FE-RTMM method has the same computational accuracy as the FEM when the same element mesh pattern are employed, but the computational efficiency of the FE-RTMM is higher than that of the FEM.

4.5 Fourier Series Transfer Matrix Method for Two-dimensional Systems

The *Fourier series TMM* combines the Fourier series and the TMM, and extends the bivariate function $f(x, y)$ to the following form using a double Fourier series:

$$f(x, y) = \sum_{m, n} f_m(y) g_n(x)$$

$f_m(y)$ and $g_n(x)$ are usually selected to be trigonometric function systems when they are adopted to solve a two-dimensional problem of elastic bodies. If the y axis is chosen as the transfer direction, $f_m(y)$ is only required to ensure continuous differentiable conditions and $g_n(x)$ still belongs to the trigonometric function system. Because of the orthogonality of the function $g_n(x)$, a partial differential equation can be transformed into an ordinary differential equation about the y axis, and then the transfer matrix about function $f_m(y)$ can be determined.

The temperature change inside an elastic body can bring expansion or shrinkage of its volume. The stress inside an elastic body due to the change of temperature is called thermal stress. In the following, the problem of the thermal stress of a thin plate is used to illustrate the Fourier series TMM.

The problem of the thermal stress of a thin plate is a plane stress problem. The displacements and stresses of elements in thin plates are shown in Figure 4.16. Here, u is the displacement along the x axis, v is the displacement along the y axis, $\partial v / \partial x$, $\partial u / \partial y$ are angular displacements, σ_x , σ_y are normal stresses of the x and y axes, and τ_{xy} , τ_{yx} are the corresponding tangent stresses. According to the assumption of plane stress in elastic mechanics, when the external force is zero, the equilibrium equations of the elements are

$$\begin{aligned} \frac{\partial}{\partial x} \sigma_x + \frac{\partial}{\partial y} \tau_{yx} &= 0 \\ \frac{\partial}{\partial x} \tau_{xy} + \frac{\partial}{\partial y} \sigma_y &= 0 \\ \tau_{xy} &= \tau_{yx} \end{aligned} \quad (4.117)$$

Normal strains ε_x , ε_y and shear strains γ_{xy} are

$$\begin{aligned} \varepsilon_x &= \frac{\partial u}{\partial x} \\ \varepsilon_y &= \frac{\partial v}{\partial y} \end{aligned}$$

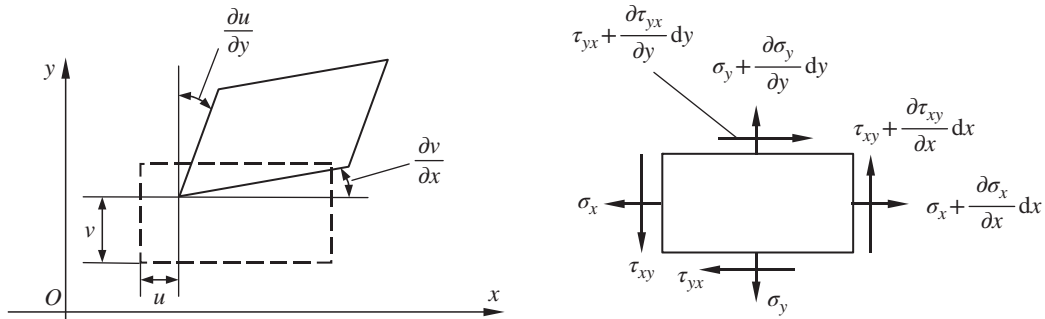


Figure 4.16 Displacement and stress of the element of a thin plate.

$$\gamma_{xy} = \gamma_{yx} = \frac{\partial v}{\partial x} + \frac{\partial u}{\partial y} \quad (4.118)$$

Assume the height of plate is h . If the linear elastic material is isotropic, the relationships between thermal stress and strain are

$$\begin{aligned} \varepsilon_x &= \frac{1}{E} (\sigma_x - \mu \sigma_y) + \alpha T \\ \varepsilon_y &= \frac{1}{E} (\sigma_y - \mu \sigma_x) + \alpha T \\ \gamma_{xy} &= \frac{2(1+\mu)}{E} \tau_{xy} \end{aligned} \quad (4.119)$$

where E is Young's modulus, μ is Poisson's ratio, T is the variable of temperature ($T = T(x, y)$) and α is the linear thermal expansion coefficient of an elastic body.

The expressions of the stress components in terms of strain components can be obtained by solving Equation (4.119):

$$\begin{bmatrix} \sigma_x \\ \sigma_y \\ \tau_{xy} \end{bmatrix} = \begin{bmatrix} \frac{E}{1-\mu^2} & \mu \frac{E}{1-\mu^2} & 0 \\ \mu \frac{E}{1-\mu^2} & \frac{E}{1-\mu^2} & 0 \\ 0 & 0 & \frac{E}{2(1+\mu)} \end{bmatrix} \begin{bmatrix} \varepsilon_x \\ \varepsilon_y \\ \gamma_{xy} \end{bmatrix} - \frac{E}{1-\mu} \alpha T \begin{bmatrix} 1 \\ 1 \\ 0 \end{bmatrix} \quad (4.120)$$

The stress of the difference in temperature of a rectangular thin plate is considered. Its two sides are free along the x axis and its displacement along the y axis can be ignored, as shown in Figure 4.17. If the y axis is the transfer direction, the terms on the left-hand side of equation are derivatives with respect to y . The derivatives with respect to x are on the right-hand side of the equation. At first, the following equation can be obtained from Equation (4.118) and the third equation of Equation (4.120)

$$\frac{\partial}{\partial y} u = -\frac{\partial}{\partial x} v + \frac{2(1+\mu)}{E} \tau_{xy} \quad (4.121)$$

From the second formula of Equation (4.120),

$$\frac{\partial}{\partial y} v = -\mu \frac{\partial}{\partial x} u + \frac{1-\mu^2}{E} \sigma_y + \alpha(1+\mu)T \quad (4.122)$$

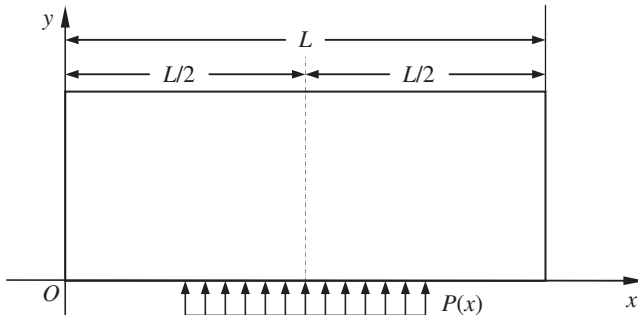


Figure 4.17 Temperature difference in the stress of a thin rectangle plate.

From the second formula of equilibrium Equation (4.117),

$$\frac{\partial}{\partial y}\sigma_y = -\frac{\partial}{\partial x}\tau_{xy} \quad (4.123)$$

Hence, the three equations about u , v , σ_y and τ_{xy} have been found. To find $\frac{\partial}{\partial y}\tau_{xy}$, the following equation can be obtained from the first formula of Equation (4.120)

$$\sigma_x = \frac{E}{1-\mu^2} \left[\frac{\partial}{\partial x}u + \mu \frac{\partial}{\partial y}v - \alpha(1+\mu)T \right]$$

Substituting Equation (4.122) into the above equation

$$\sigma_x = E \frac{\partial}{\partial x}u + \mu\sigma_y - E\alpha T \quad (4.124)$$

Substituting Equation (4.124) into the first formula of Equation (4.117) and using the third equation of Equation (4.117)

$$\frac{\partial}{\partial y}\tau_{xy} = -E \frac{\partial^2}{\partial x^2}u - \mu \frac{\partial}{\partial x}\sigma_y + E\alpha \frac{\partial}{\partial x}T \quad (4.125)$$

Combining Equations (4.121) to (4.123) and Equation (4.125), we can obtain the partial differential equations

$$\frac{\partial}{\partial y} \begin{bmatrix} u \\ v \\ \sigma_y \\ \tau_{xy} \end{bmatrix} = \begin{bmatrix} 0 & -\frac{\partial}{\partial x} & 0 & \frac{2(1+\mu)}{E} \\ -\mu \frac{\partial}{\partial x} & 0 & \frac{1-\mu^2}{E} & 0 \\ 0 & 0 & 0 & -\frac{\partial}{\partial x} \\ -E \frac{\partial^2}{\partial x^2} & 0 & -\mu \frac{\partial}{\partial x} & 0 \end{bmatrix} \begin{bmatrix} u \\ v \\ \sigma_y \\ \tau_{xy} \end{bmatrix} + \alpha \begin{bmatrix} 0 \\ (1+\mu)T \\ 0 \\ E \frac{\partial}{\partial x}T \end{bmatrix} \quad (4.126)$$

These equations do not now contain σ_x and the explicit Equation (4.124) of σ_x has been obtained. After solving the other variables, σ_x can be determined directly by substituting into Equation (4.124). All the nonzero elements of the matrix can be arranged in the black squares of a chessboard (see section 10.8). This arrangement can bring computational advantages.

The unknown functions in Equation (4.126) of a rectangular thin plate can be extended to Fourier series

$$\begin{cases} u(x,y) = u_0(y) + \sum u_m(y)\cos\beta x + \sum \tilde{u}_m(y)\sin\beta x \\ v(x,y) = v_0(y) + \sum v_m(y)\sin\beta x + \sum \tilde{v}_m(y)\cos\beta x \\ \tau_{xy}(x,y) = \tau_{xy0}(y) + \sum \tau_{xym}(y)\cos\beta x + \sum \tilde{\tau}_{xym}(y)\sin\beta x \\ \sigma_y(x,y) = \sigma_{y0}(y) + \sum \sigma_{ym}(y)\sin\beta x + \sum \tilde{\sigma}_{ym}(y)\cos\beta x \end{cases} \quad (4.127)$$

and

$$\sigma_x(x,y) = \sigma_{x0}(y) + \sum \sigma_{xm}(y)\sin\beta x + \sum \tilde{\sigma}_{xm}(y)\cos\beta x \quad (4.128)$$

where $\beta = m\pi/L$ ($m = 1, 2, 3, \dots$), L is the width of the thin plate in the x axis and m is the ordinal number of the series term.

The varying temperature field can be denoted as

$$T(x, y) = T_0(y) + \sum T_m(y) \sin \beta x + \sum \tilde{T}_m(y) \cos \beta x \quad (4.129)$$

The external load at boundary $y = 0$ can be described as

$$P(x) = P_0 + \sum P_m(y) \sin \beta x + \sum \tilde{P}_m(y) \cos \beta x \quad (4.130)$$

More simply, assume the temperature field $T(x, y)$ and external load $P(x)$ are symmetric about center line $x = L/2$ of the thin plate, so $\tilde{P}_m = 0$ and $\tilde{T}_m(y) = 0$, $u(x, y)$ and $\tau(x, y)$ are anti-symmetric about the center line, and the rest are symmetric. According to the boundary conditions, all the terms marked with wave lines are equal to zero; we can obtain the ordinary differential equations about the series coefficients using the orthogonality of the trigonometric series

$$\frac{d}{dy} \begin{bmatrix} u_m \\ v_m \\ \sigma_{ym} \\ \tau_{xym} \end{bmatrix} = \begin{bmatrix} 0 & -\beta & 0 & \frac{2(1+\mu)}{E} \\ \mu\beta & 0 & \frac{1-\mu^2}{E} & 0 \\ 0 & 0 & 0 & \beta \\ E\beta^2 & 0 & -\mu\beta & 0 \end{bmatrix} \begin{bmatrix} u_m \\ v_m \\ \sigma_{ym} \\ \tau_{xym} \end{bmatrix} + \alpha \begin{bmatrix} 0 \\ (1+\mu)T_m \\ 0 \\ E\beta T_m \end{bmatrix} \quad (4.131)$$

and the m th term of series of normal stress σ_x

$$\sigma_{xm} = -E\beta u_m + \mu\sigma_{ym} - \alpha ET_m \quad (4.132)$$

Replacing v_m with $-v_m$, and letting the matrix of the system be symmetric about the minor diagonal

$$\frac{d}{dy} \begin{bmatrix} u_m \\ -v_m \\ \sigma_{ym} \\ \tau_{xym} \end{bmatrix} = \begin{bmatrix} 0 & \beta & 0 & \frac{2(1+\mu)}{E} \\ -\mu\beta & 0 & -\frac{1-\mu^2}{E} & 0 \\ 0 & 0 & 0 & \beta \\ E\beta^2 & 0 & -\mu\beta & 0 \end{bmatrix} \begin{bmatrix} u_m \\ -v_m \\ \sigma_{ym} \\ \tau_{xym} \end{bmatrix} + \alpha \begin{bmatrix} 0 \\ -(1+\mu)T_m \\ 0 \\ E\beta T_m \end{bmatrix} \quad (4.133)$$

Let

$$A = \begin{bmatrix} 0 & \beta & 0 & \frac{2(1+\mu)}{E} \\ -\mu\beta & 0 & -\frac{1-\mu^2}{E} & 0 \\ 0 & 0 & 0 & \beta \\ E\beta^2 & 0 & -\mu\beta & 0 \end{bmatrix} \quad (4.134)$$

Its Jordan standard form is

$$B^{-1}AB = \begin{bmatrix} -\beta & 1 & 0 & 0 \\ 0 & -\beta & 0 & 0 \\ 0 & 0 & \beta & 1 \\ 0 & 0 & 0 & \beta \end{bmatrix} \quad (4.135)$$

where \mathbf{B} is the transformation matrix

$$\mathbf{B} = \begin{bmatrix} 1+\mu & -2/\beta & 1+\mu & (1-\mu)/\beta \\ 1+\mu & (1-\mu)/\beta & -(1+\mu) & 2/\beta \\ E\beta & 0 & E\beta & -E \\ -E\beta & E & E\beta & 0 \end{bmatrix} \quad (4.136)$$

Therefore, the general term of $e^{\mathbf{B}^{-1}\mathbf{A}By}$ is

$$\mathbf{C}_n = \frac{y^n}{n!} (\mathbf{B}^{-1}\mathbf{A}\mathbf{B})^n = \begin{bmatrix} \frac{(-1)^n}{n!} y^n \beta^n & \frac{(-1)^{n-1}}{(n-1)!} y^n \beta^{n-1} & & \\ & \frac{(-1)^n}{n!} y^n \beta^n & & \\ & & \frac{1}{n!} y^n \beta^n & \frac{1}{(n-1)!} y^n \beta^{n-1} \\ & & & \frac{1}{n!} y^n \beta^n \end{bmatrix} \quad (4.137)$$

After summing, this yields

$$e^{\mathbf{B}^{-1}\mathbf{A}By} = \sum_{n=0}^{\infty} \mathbf{C}_n = \begin{bmatrix} \cosh\beta y - \sinh\beta y & y(\cosh\beta y - \sinh\beta y) & & \\ & \cosh\beta y - \sinh\beta y & & \\ & & \cosh\beta y + \sinh\beta y & y(\cosh\beta y + \sinh\beta y) \\ & & & \cosh\beta y + \sinh\beta y \end{bmatrix} \quad (4.138)$$

Therefore the transfer matrix of the coefficients in a Fourier expansion of internal displacement and stress of the thin plate with load acting on the edge is

$$\mathbf{U}_m(y) = e^{\mathbf{A}y} = \mathbf{B}e^{\mathbf{B}^{-1}\mathbf{A}By}\mathbf{B}^{-1} = \begin{bmatrix} \cosh\beta y + \frac{1+\mu}{2}\beta y \sinh\beta y & \frac{1+\mu}{2}\beta y \cosh\beta y + \frac{1-\mu}{2}\sinh\beta y & u_{13} & u_{14} \\ \frac{1-\mu}{2}\sinh\beta y - \frac{1+\mu}{2}\beta y \cosh\beta y & \cosh\beta y - \frac{1+\mu}{2}\beta y \sinh\beta y & u_{23} & \\ \frac{E}{2}\beta^2 y \sinh\beta y & \frac{E}{2}\beta(\beta y \cosh\beta y - \sinh\beta y) & & \\ \frac{E}{2}\beta(\beta y \cosh\beta y + \sinh\beta y) & & \text{symmetry} & \end{bmatrix} \quad (4.139)$$

where

$$u_{13} = -\frac{(1+\mu)^2}{2E} y \sinh\beta y, \quad u_{14} = \frac{(1+\mu)^2}{2E} \left(\frac{3-\mu}{1+\mu\beta} \sinh\beta y + y \cosh\beta y \right) \\ u_{23} = \frac{(1+\mu)^2}{2E} \left(y \cosh\beta y - \frac{3-\mu}{1+\mu\beta} \sinh\beta y \right)$$

Define the state vector as

$$\mathbf{Z}_m(y) = [u_m(y), -v_m(y), \sigma_{ym}(y), \tau_{xym}(y)]^T \quad (4.140)$$

To obtain the corresponding coefficients of the extended function of stress due to temperature difference, the nonhomogeneous solution of Equation (4.133) needs to be found

$$\mathbf{Z}_m(y) = \mathbf{U}_m(y)\mathbf{Z}_m(0) + \mathbf{U}_m(y) \int_0^y \mathbf{U}_m(-\xi) \mathbf{F}_m(\xi) d\xi \quad (4.141)$$

where $\mathbf{F}_m(\xi)$ is the nonhomogeneous column matrix in Equation 4.133.

If temperature difference is linearly distributed

$$T_m(y) = T_{0m} + K_{Tm}y \quad (4.142)$$

The nonhomogeneous terms are

$$\mathbf{F}_m(y) = \begin{bmatrix} 0 \\ -\alpha(1+\mu)(T_{0m} + K_{Tm}y) \\ 0 \\ E\beta\alpha(T_{0m} + K_{Tm}y) \end{bmatrix} \quad (4.143)$$

Note that $\mathbf{U}_m(-y) = e^{-Ay}$ (namely $[e^{Ay}]^{-1}$), which can be obtained merely by adding a minus sign to each element in the black grids in matrix $\mathbf{U}_m(y) = e^{Ay}$.

The coefficient of the series term of normal stress is

$$\sigma_{xm} = -E\beta u_m + \mu\sigma_{ym} - \alpha E(T_{0m} + K_{Tm}y) \quad (4.144)$$

4.6 Finite Difference Transfer Matrix Method for Two-dimensional Systems

The finite difference TMM is a method which combines the finite difference method and the TMM. Again taking the problem of the thermal stress of the rectangular thin plate as an example, consider the y axis as the transfer direction and replace derivation with the finite difference method in the x axis. Herein the plane is not divided into grids, but into strips along the transfer direction, so this method is also called the strip method.

As shown in Figure 4.18, the plate is divided into n areas by $n+1$ parallels with equal width in a thin plate structure whose boundaries are $x=0$ and $x=L$. The distance between parallels is Δx . According to the variables found in differential Equation (4.126) in section 4.5, the variables in each parallel are defined as follows:

$$\mathbf{u}(y) = \begin{bmatrix} u_0(y) \\ u_1(y) \\ \vdots \\ u_k(y) \\ \vdots \\ u_n(y) \end{bmatrix}, \quad \mathbf{v}(y) = \begin{bmatrix} v_0(y) \\ v_1(y) \\ \vdots \\ v_k(y) \\ \vdots \\ v_n(y) \end{bmatrix}, \quad \boldsymbol{\sigma}_y(y) = \begin{bmatrix} \sigma_{y0}(y) \\ \sigma_{y1}(y) \\ \vdots \\ \sigma_{yk}(y) \\ \vdots \\ \sigma_{yn}(y) \end{bmatrix}, \quad \boldsymbol{\tau}_{xy}(y) = \begin{bmatrix} \tau_{xy0}(y) \\ \tau_{xy1}(y) \\ \vdots \\ \tau_{xyk}(y) \\ \vdots \\ \tau_{xyn}(y) \end{bmatrix} \quad (4.145)$$

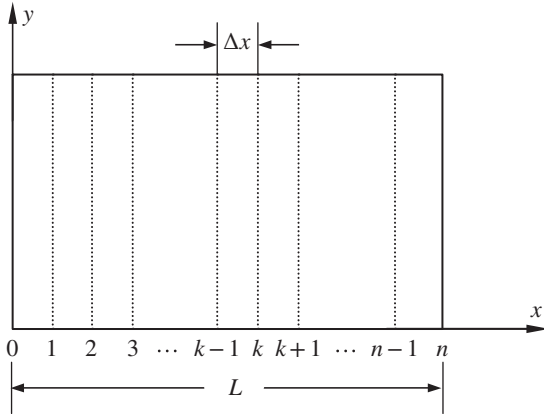


Figure 4.18 Strip element partition of a thin plane rectangle plate.

The derivative of x is denoted in the form of an intermediate difference

$$\frac{\partial u_k}{\partial x} \approx \frac{(-u_{k-1} + u_{k+1})}{2\Delta x} \quad (4.146)$$

$$\frac{\partial^2 u_k}{\partial x^2} \approx \frac{(u_{k-1} - 2u_k + u_{k+1})}{\Delta x^2} \quad (4.147)$$

At the boundaries $x=0$ and $x=L$, the forward and backward differences are applied, respectively, that is

$$\frac{\partial u_0}{\partial x} \approx \frac{-u_0 + u_1}{\Delta x} \quad (4.148)$$

$$\frac{\partial u_n}{\partial x} \approx \frac{-u_{n-1} + u_n}{\Delta x} \quad (4.149)$$

To ensure difference accuracy, the extension of the forward and backward difference of the second-order derivative is

$$\frac{\partial^2}{\partial x^2} = \frac{1}{\Delta x^2} \left(\Delta^2 \mp \Delta^3 + \frac{11}{12} \Delta^4 \mp \frac{5}{6} \Delta^5 + \dots \right) \quad (4.150)$$

where Δ is the difference operator. Two formulas are involved in the above equation, where the first formula corresponds to the forward difference operator while the second formula corresponds to the backward difference operator.

If only the first two terms are chosen, this becomes

$$\frac{\partial^2 u_0}{\partial x^2} \approx \frac{2u_0 - 5u_1 + 4u_2 - u_3}{\Delta x^2} \quad (4.151)$$

$$\frac{\partial^2 u_n}{\partial x^2} \approx \frac{2u_{n-3} - 5u_{n-2} + 4u_{n-1} - u_n}{\Delta x^2} \quad (4.152)$$

The partial derivatives of $v(y)$, $\tau_{xy}(y)$ and $\tau_{xy}(y)$ with respect to x are calculated in the same way as used in the above equations. Therefore, the first-order difference matrix D_1 can be written

from Equations (4.146), (4.148) and (4.149), and the second-order difference matrix D_2 can be written from Equations (4.147), (4.151) and (4.152):

$$D_1 = \frac{1}{2\Delta x} \begin{bmatrix} -2 & 2 & & & \\ -1 & 0 & 1 & & \\ & -1 & 0 & 1 & \\ & & & \ddots & \\ & & & & -1 & 0 & 1 \\ & & & & & -2 & 2 \end{bmatrix} \quad (4.153)$$

$$D_2 = \frac{1}{\Delta x^2} \begin{bmatrix} 2 & -5 & 4 & -1 & & & \\ 1 & -2 & 1 & & & & \\ & 1 & -2 & 1 & & & \\ & & & \ddots & & & \\ & & & & 1 & -2 & 1 \\ & & & & & 1 & -2 & 1 \\ & & & & & & 2 & -5 & 4 & -1 \end{bmatrix} \quad (4.154)$$

Replacing derivation with finite difference, and considering Equation (4.126), we can obtain the differential equations of the state vectors with $4(n+1)$ dimensions

$$\frac{d}{dy} \begin{bmatrix} u(y) \\ v(y) \\ \sigma_y(y) \\ \tau_{xy}(y) \end{bmatrix} = \begin{bmatrix} \mathbf{O} & -D_1 & \mathbf{O} & \frac{2(1+\mu)}{E}I \\ -\mu D_1 & \mathbf{O} & \frac{1-\mu^2}{E}I & \mathbf{O} \\ \mathbf{O} & \mathbf{O} & \mathbf{O} & -D_1 \\ -ED_2 & \mathbf{O} & -\mu D_1 & \mathbf{O} \end{bmatrix} \begin{bmatrix} u(y) \\ v(y) \\ \sigma_y(y) \\ \tau_{xy}(y) \end{bmatrix} + \alpha \begin{bmatrix} \mathbf{O} \\ (1+\mu)I \\ \mathbf{O} \\ ED_1 \end{bmatrix} \mathbf{t} \quad (4.155)$$

where

$$\mathbf{t} = [T_0(y), T_1(y), \dots, T_{n-1}(y), T_n(y)]^T \quad (4.156)$$

Vector \mathbf{t} denotes the varying temperature on each single parameter line.

Let

$$A = \begin{bmatrix} \mathbf{O} & -D_1 & \mathbf{O} & \frac{2(1+\mu)}{E}I \\ -\mu D_1 & \mathbf{O} & \frac{1-\mu^2}{E}I & \mathbf{O} \\ \mathbf{O} & \mathbf{O} & \mathbf{O} & -D_1 \\ -ED_2 & \mathbf{O} & -\mu D_1 & \mathbf{O} \end{bmatrix}, Z_m(y) = \begin{bmatrix} u(y) \\ v(y) \\ \sigma_y(y) \\ \tau_{xy}(y) \end{bmatrix}, F(y) = \alpha \begin{bmatrix} \mathbf{O} \\ (1+\mu)I \\ \mathbf{O} \\ ED_1 \end{bmatrix} \mathbf{t} \quad (4.157)$$

Hence, the transfer matrix is

$$U(y) = e^{Ay} \quad (4.158)$$

The transfer equation is

$$\mathbf{Z}(y) = \mathbf{U}(y)\mathbf{Z}(0) + \mathbf{U}(y) \int_0^y \mathbf{U}(-\xi)\mathbf{F}(\xi)d\xi \quad (4.159)$$

The corresponding normal stress σ_x can be computed by Equation (4.160)

$$\sigma_x(y) = [\sigma_{x0}(y), \sigma_{x1}(y), \dots, \sigma_{xn-1}(y), \sigma_{xn}(y)]^T = E\mathbf{D}_1\mathbf{u}(y) + \mu\sigma_y(y) - \alpha Et \quad (4.160)$$

4.7 Transfer Matrix Method for Two-dimensional Systems

A beam is usually treated as a one-dimensional system [36] consisting of several lumped masses and massless elastic beam sections when studying the structural dynamic problems of an elastic beam using the classic TMM. In fact, this model with lumped masses and massless elastic beam sections is also widely used in the FEM and the discrete element method [243, 244]. To exert the high computational efficiency of the TMM, the dynamic problems of two-dimensional systems, such as the vibration characteristics of a thin plate, will be studied using only the TMM, and the TMM of two-dimensional systems developed by author introduced [74, 75]. The problem of the natural vibration characteristics of a thin plate which has transverse vibration is taken as an example. The thin plate is divided into grids of two-dimensional structure which consist of several lumped masses (or small rigid bodies) and massless elastic beam sections. The method can be extended to solve other complex two-dimensional systems directly, and can also be developed to form a three-dimensional matrix method to solve spatial problems.

4.7.1 Model and State Vector of Two-dimensional Systems

As shown in Figure 4.19, there is a rectangle thin plate whose four edges are $x = 0$, $x = a$, $y = 0$, $y = b$. We will consider only its transverse vibration along the z axis. As shown in Figure 4.20, the plate is divided into n isometric strips along the x axis, and each strip is divided into m grids along the y axis. In this way, the plate is divided into $n \times m$ grid elements. The dashed lines in the figure denote the edges of the grids. The mass of each grid is treated as a lumped mass located at its center, and the elastic effect between two contiguous lumped masses is equivalent to the massless elastic beam which links the two lumped masses. Therefore, the rectangle thin plate is equivalent to a plane network structure consisting of $n \times m$ lumped masses, $n \times (m + 1)$ beams along the x axis and $(n + 1) \times m$ beams along the y axis, which vibrates along the z axis. The direction of the x axis is chosen to be the main transfer direction and the direction of the y axis is chosen to be the assistant transfer direction. From the following process to establish the transfer equations of the two-dimensional system, it can be seen that the dynamic problems for

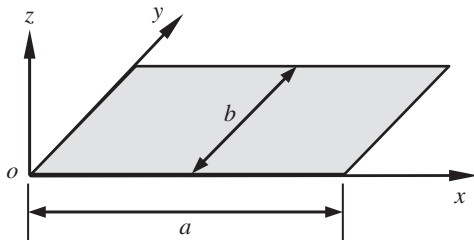
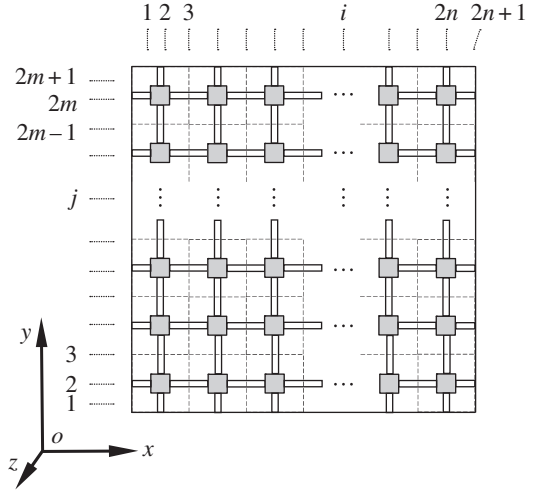


Figure 4.19 Rectangular thin plate.

Figure 4.20 Element partition of a rectangular thin plate.



two-dimensional systems can be researched using the classical TMM, as long as the transfer matrix of the strip substructure in the x axis direction can be established.

The state vectors of each connection point are defined as

$$\mathbf{Z} = [Z, \theta_x, \theta_y, M_x, M_y, Q_z]^T \quad (4.161)$$

where Z , θ_x , θ_y , M_x , M_y and Q_z are the modal coordinates of the displacement along the z direction, the angular displacement around the x and y directions, the internal momentum along the x and y directions, and the internal force along the z direction, respectively.

The sequence numbers of the columns and rows of elements are denoted by i and j , respectively. The sequence numbers of the elements are denoted by (i, j) . The state vectors of each connection point in the j th row ($j = 2, 4, \dots, 2m$) are denoted by $\mathbf{Z}_{(i,i+1),j}$ ($i = 0, 2, \dots, 2n$) and $\mathbf{Z}_{(i,i-1),j}$ ($i = 2, 4, \dots, 2n+2$). The first subscript in the parentheses denotes the sequence number of the column where the body element is located, the second subscript denotes the sequence number of the column where the hinge element is located and the subscript outside the parentheses denotes the sequence number of the corresponding connection point row. The state vectors of each connection point on the i th column ($i = 2, 4, \dots, 2n$) are denoted by $\mathbf{Z}_{i,(j,j+1)}$ ($j = 2, 4, \dots, 2m-2$) and $\mathbf{Z}_{i,(j,j-1)}$ ($j = 4, 6, \dots, 2m$). The first and second subscripts in the parentheses denote the sequence numbers of the body element and hinge element rows, respectively. The subscript outside the parentheses denotes the sequence number of the corresponding connection point column.

In the main transfer direction, elements $(i+1, j)$ are all hinge elements when $i = 0, 2, \dots, 2n$, and the state vectors of the input ends of the hinge elements in the $i+1$ th column are defined as

$$\mathbf{Z}_{i,i+1} = [\mathbf{Z}_{(i,i+1),2}^T, \mathbf{Z}_{(i,i+1),4}^T, \dots, \mathbf{Z}_{(i,i+1),2m}^T]^T \quad (4.162)$$

Elements $(i-1, j)$ are all hinges when $i = 2, \dots, 2n+2$. The state vectors of the output ends of the joint elements in the $i-1$ th column are defined as

$$\mathbf{Z}_{i,i-1} = [\mathbf{Z}_{(i,i-1),2}^T, \mathbf{Z}_{(i,i-1),4}^T, \dots, \mathbf{Z}_{(i,i-1),2m}^T]^T \quad (4.163)$$

4.7.2 The Transfer Matrix and the Transfer Equation of the Strip Element

When $i = 1, 3, 5, \dots, 2n + 1$, the strip elements in the i th column consist of m parallel massless elastic beams along the x axis. It is easy to obtain the transfer equation and transfer matrix of the strip elements in the i th column

$$\mathbf{Z}_{i+1,i} = \mathbf{U}_i \mathbf{Z}_{i-1,i} \quad (4.164)$$

$$\mathbf{U}_i = \begin{bmatrix} \mathbf{U}_{i,2} & & & \\ & \mathbf{U}_{i,4} & & \\ & & \ddots & \\ & & & \mathbf{U}_{i,2m} \end{bmatrix} \quad (4.165)$$

where

$$\mathbf{U}_{i,j} = \begin{bmatrix} 1 & 0 & -x & 0 & -\frac{x^2}{2EI_{i,j}} & \frac{x^3}{6EI_{i,j}} \\ 0 & 1 & 0 & \frac{x}{(GJ_p)_{i,j}} & 0 & 0 \\ 0 & 0 & 1 & 0 & \frac{x}{EI_{i,j}} & -\frac{x^2}{2EI_{i,j}} \\ 0 & 0 & 0 & 1 & 0 & 0 \\ 0 & 0 & 0 & 0 & 1 & -x \\ 0 & 0 & 0 & 0 & 0 & 1 \end{bmatrix}_{x=l_{i,j}} \quad (4.166)$$

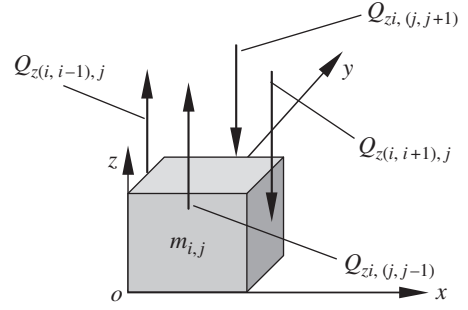
$$EI_{i,j} = E \frac{b}{m} \frac{h^3}{12(1-\mu^2)}, \quad (GJ_p)_{i,j} = G\beta h^3 \frac{b}{m}$$

$$l_{i,j} = \begin{cases} \frac{a}{2n} & (i = 1, 2n + 1) \\ \frac{a}{n} & (i = 3, 5, \dots, 2n - 1) \end{cases} \quad (j = 2, 4, 6, \dots, 2m)$$

$\mathbf{U}_{i,j}$ ($i = 1, 3, 5, \dots, 2n + 1, j = 2, 4, 6, \dots, 2m$) is the transfer matrix of the single elastic beam, and (i, j) , $EI_{i,j}$, $l_{i,j}$, $(GJ_p)_{i,j}$ are the bending stiffness, length and torsional stiffness of beam (i, j) respectively. E is Young's modulus, h is the thickness of the plate, μ is Poisson's ratio, G is the shear elastic modulus and β is determined by the ratio of the length to width in the rectangle section, $\beta = 0.333$ when the corresponding ratio is greater than 10 [245].

When $i = 2, 4, 6, \dots, 2n$, the strip elements in the i th column consist of m lumped masses and $m + 1$ massless elastic beams in series sequentially along the y axis. The transfer equation of this strip element is similar to Equation (4.164), as follows

$$\mathbf{Z}_{i,i+1} = \mathbf{U}_i \mathbf{Z}_{i,i-1} \quad (4.167)$$

Figure 4.21 Force analysis of a lumped mass element.

The transfer equation of a single lumped mass inside the network is the precondition of deriving Equation (4.167). The single lumped mass inside the network contains three input ends and one output end, and the transfer equation is derived as follows. The forces acting on the lumped mass are shown in Figure 4.21. According to the displacement continuous conditions and the force equilibrium of the lumped mass at the both input and output ends

$$\begin{bmatrix} Z \\ \theta_x \\ \theta_y \\ M_x \\ M_y \\ Q_z \end{bmatrix}_{(i,i+1),j} = \begin{bmatrix} Z \\ \theta_x \\ \theta_y \\ M_x - J_{xi,j}\omega^2\theta_x \\ M_y - J_{yi,j}\omega^2\theta_y \\ Q_z + m_{i,j}\omega^2 Z \end{bmatrix}_{(i,i-1),j} + \begin{bmatrix} 0 \\ 0 \\ 0 \\ M_x \\ M_y \\ Q_z \end{bmatrix}_{i,(j,j-1)} + \begin{bmatrix} 0 \\ 0 \\ 0 \\ -M_x \\ -M_y \\ -Q_z \end{bmatrix}_{i,(j,j+1)} \quad (4.168)$$

where

$$m_{i,j} = \rho h \frac{a b}{n m}, J_{xi,j} = \frac{1}{12} m_{i,j} \left(\frac{b^2}{m^2} + h^2 \right), J_{yi,j} = \frac{1}{12} m_{i,j} \left(\frac{a^2}{n^2} + h^2 \right)$$

$m_{i,j}$ is the mass of lumped mass (i, j) , and $J_{xi,j}$ and $J_{yi,j}$ are the moments of inertia relative to the x and y axes, respectively.

Because of the transfer equation of beam $(i, j-1)$

$$\begin{bmatrix} Z \\ \theta_x \\ \theta_y \\ M_x \\ M_y \\ Q_z \end{bmatrix}_{i,(j,j-1)} = \begin{bmatrix} 1 & y & 0 & \frac{y^2}{2EI_{i,j-1}} & 0 & \frac{y^3}{6EI_{i,j-1}} \\ 0 & 1 & 0 & \frac{y}{EI_{i,j-1}} & 0 & \frac{y^2}{2EI_{i,j-1}} \\ 0 & 0 & 1 & 0 & \frac{y}{(GJ_p)_{i,j-1}} & 0 \\ 0 & 0 & 0 & 1 & 0 & y \\ 0 & 0 & 0 & 0 & 1 & 0 \\ 0 & 0 & 0 & 0 & 0 & 1 \end{bmatrix}_{y=l_{i,j-1}} \begin{bmatrix} Z \\ \theta_x \\ \theta_y \\ M_x \\ M_y \\ Q_z \end{bmatrix}_{i,(j-2,j-1)}$$

hence

$$\begin{aligned}
 \begin{bmatrix} M_x \\ M_y \\ Q_z \end{bmatrix}_{i,(j,j-1)} &= \begin{bmatrix} -\frac{6EI_{i,j-1}}{l_{i,j-1}^2} & \frac{4EI_{i,j-1}}{l_{i,j-1}} & 0 \\ 0 & 0 & \frac{(GJ_p)_{i,j-1}}{l_{i,j-1}} \\ -\frac{12EI_{i,j-1}}{l_{i,j-1}^3} & \frac{6EI_{i,j-1}}{l_{i,j-1}^2} & 0 \end{bmatrix} \begin{bmatrix} Z \\ \theta_x \\ \theta_y \end{bmatrix}_{i,(j,j-1)} \\
 &+ \begin{bmatrix} \frac{6EI_{i,j-1}}{l_{i,j-1}^2} & \frac{2EI_{i,j-1}}{l_{i,j-1}} & 0 \\ 0 & 0 & -\frac{(GJ_p)_{i,j-1}}{l_{i,j-1}} \\ \frac{12EI_{i,j-1}}{l_{i,j-1}^3} & \frac{6EI_{i,j-1}}{l_{i,j-1}^2} & 0 \end{bmatrix} \begin{bmatrix} Z \\ \theta_x \\ \theta_y \end{bmatrix}_{i,(j-2,j-1)}
 \end{aligned}$$

Applying similar steps, the equations arising from the transfer equation of the beam element $(i,j+1)$ are

$$\begin{aligned}
 \begin{bmatrix} -M_x \\ -M_y \\ -Q_z \end{bmatrix}_{i,(j,j+1)} &= \begin{bmatrix} \frac{6EI_{i,j+1}}{l_{i,j+1}^2} & \frac{4EI_{i,j+1}}{l_{i,j+1}} & 0 \\ 0 & 0 & \frac{(GJ_p)_{i,j+1}}{l_{i,j+1}} \\ -\frac{12EI_{i,j+1}}{l_{i,j+1}^3} & -\frac{6EI_{i,j+1}}{l_{i,j+1}^2} & 0 \end{bmatrix} \begin{bmatrix} Z \\ \theta_x \\ \theta_y \end{bmatrix}_{i,(j,j+1)} \\
 &+ \begin{bmatrix} -\frac{6EI_{i,j+1}}{l_{i,j+1}^2} & \frac{2EI_{i,j+1}}{l_{i,j+1}} & 0 \\ 0 & 0 & -\frac{(GJ_p)_{i,j+1}}{l_{i,j+1}} \\ \frac{12EI_{i,j+1}}{l_{i,j+1}^3} & -\frac{6EI_{i,j+1}}{l_{i,j+1}^2} & 0 \end{bmatrix} \begin{bmatrix} Z \\ \theta_x \\ \theta_y \end{bmatrix}_{i,(j+2,j+1)}
 \end{aligned}$$

Considering the geometric relationship of each connection point and substituting each of the above equations into Equation (4.168), the transfer equation of a single lumped mass inside the network is

$$\mathbf{Z}_{(i,i+1),j} = \mathbf{U}_{i,j} \left[\mathbf{Z}_{(i,i-1),j-2}^T, \mathbf{Z}_{(i,i-1),j}^T, \mathbf{Z}_{(i,i-1),j+2}^T \right]^T \quad (4.169)$$

where

$$\mathbf{U}_{i,j} = [\mathbf{U}_{i,j,-2}, \mathbf{U}_{i,j,0}, \mathbf{U}_{i,j,+2}] \quad (4.170)$$

$$\mathbf{U}_{i,j,-2} = \begin{bmatrix} \mathbf{O}_{3 \times 3} & \mathbf{O}_{3 \times 3} \\ \mathbf{U}_{-2,2,1} & \mathbf{O}_{3 \times 3} \end{bmatrix}, \mathbf{U}_{i,j,0} = \begin{bmatrix} \mathbf{I}_3 & \mathbf{O}_{3 \times 3} \\ \mathbf{U}_{0,2,1} & \mathbf{I}_3 \end{bmatrix}, \mathbf{U}_{i,j,+2} = \begin{bmatrix} \mathbf{O}_{3 \times 3} & \mathbf{O}_{3 \times 3} \\ \mathbf{U}_{+2,2,1} & \mathbf{O}_{3 \times 3} \end{bmatrix} \quad (4.171)$$

$$\mathbf{U}_{0,2,1} = \begin{bmatrix} -\frac{6EI_{i,j-1}}{l_{i,j-1}^2} + \frac{6EI_{i,j+1}}{l_{i,j+1}^2} & \frac{4EI_{i,j-1}}{l_{i,j-1}} + \frac{4EI_{i,j+1}}{l_{i,j+1}} - J_{xi,j}\omega^2 & 0 \\ 0 & 0 & \frac{(GJ_p)_{i,j-1}}{l_{i,j-1}} + \frac{(GJ_p)_{i,j+1}}{l_{i,j+1}} - J_{yi,j}\omega^2 \\ m_{i,j}\omega^2 - \frac{12EI_{i,j-1}}{l_{i,j-1}^3} - \frac{12EI_{i,j+1}}{l_{i,j+1}^3} & \frac{6EI_{i,j-1}}{l_{i,j-1}^2} - \frac{6EI_{i,j+1}}{l_{i,j+1}^2} & 0 \end{bmatrix} \quad (4.172a)$$

$$\mathbf{U}_{-2,2,1} = \begin{bmatrix} \frac{6EI_{i,j-1}}{l_{i,j-1}^2} & \frac{2EI_{i,j-1}}{l_{i,j-1}} & 0 \\ 0 & 0 & -\frac{(GJ_p)_{i,j-1}}{l_{i,j-1}} \\ \frac{12EI_{i,j-1}}{l_{i,j-1}^3} & \frac{6EI_{i,j-1}}{l_{i,j-1}^2} & 0 \end{bmatrix},$$

$$\mathbf{U}_{+2,2,1} = \begin{bmatrix} -\frac{6EI_{i,j+1}}{l_{i,j+1}^2} & \frac{2EI_{i,j+1}}{l_{i,j+1}} & 0 \\ 0 & 0 & -\frac{(GJ_p)_{i,j+1}}{l_{i,j+1}} \\ \frac{12EI_{i,j+1}}{l_{i,j+1}^3} & -\frac{6EI_{i,j+1}}{l_{i,j+1}^2} & 0 \end{bmatrix} \quad (4.172b)$$

$$EI_{i,j-1} = EI_{i,j+1} = E \frac{a h^3}{n 12(1-\mu^2)}, (GJ_p)_{i,j-1} = (GJ_p)_{i,j+1} = G\beta h^3 \frac{a}{n}$$

$$l_{i,j} = \begin{cases} \frac{b}{2m} & (j = 1, 2m+1) \\ \frac{b}{m} & (j = 3, 5, \dots, 2m-1) \end{cases} \quad (i = 2, 4, \dots, 2n)$$

Equation (4.169) is called the transfer equation of single lumped mass inside the network. The transfer equation of the lumped mass on the edges, for instance $j = 2$ or $j = 2m$, includes the boundary condition at the boundary $y = 0$ or $y = b$.

Using a similar method as used to derive Equation (4.169), at the boundary $y = 0$, namely $j = 2$, the transfer equation can be written as

$$\mathbf{Z}_{(i,i+1),2} = \mathbf{U}_{i,2} \left[\mathbf{Z}_{(i,i-1),2}^T, \mathbf{Z}_{(i,i-1),4}^T \right]^T \quad (4.173)$$

and at the boundary $y = b$, when $j = 2m$, the transfer equation can be written as

$$\mathbf{Z}_{(i,i+1),2m} = \mathbf{U}_{i,2m} \left[\mathbf{Z}_{(i,i-1),2m-2}^T, \mathbf{Z}_{(i,i-1),2m}^T \right]^T \quad (4.174)$$

where

$$\mathbf{U}_{i,2} = [\mathbf{U}_{i,2,0} \mathbf{U}_{i,2,+2}] \quad (4.175)$$

$$\mathbf{U}_{i,2m} = [\mathbf{U}_{i,2m,-2} \mathbf{U}_{i,2m,0}] \quad (4.176)$$

Submatrix $\mathbf{U}_{i,2,+2}$ in Equation (4.175) is given in Equation (4.171c). Submatrix $\mathbf{U}_{i,2m,-2}$ in Equation (4.176) is given in Equation (4.171a). However, to determine $\mathbf{U}_{i,2,0}$ and $\mathbf{U}_{i,2m,0}$ in Equations (4.175) and (4.176), the boundary conditions at $y = 0$ and $y = b$ must be considered.

For instance, the boundary $y = 0$ is simply supported, so the transfer equation of beam $(i, 1)$ can be written as

$$\begin{bmatrix} Z \\ \theta_x \\ \theta_y \\ M_x \\ M_y \\ Q_z \end{bmatrix}_{i,(2,1)} = \begin{bmatrix} 1 & y & 0 & \frac{y^2}{2EI_{i,1}} & 0 & \frac{y^3}{6EI_{i,1}} \\ 0 & 1 & 0 & \frac{y}{EI_{i,1}} & 0 & \frac{y^2}{2EI_{i,1}} \\ 0 & 0 & 1 & 0 & \frac{y}{(GJ_p)_{i,1}} & 0 \\ 0 & 0 & 0 & 1 & 0 & y \\ 0 & 0 & 0 & 0 & 1 & 0 \\ 0 & 0 & 0 & 0 & 0 & 1 \end{bmatrix}_{y=l_{i,1}} \begin{bmatrix} 0 \\ \theta_x \\ 0 \\ 0 \\ M_y \\ Q_z \end{bmatrix}_{i,(0,1)}$$

that is

$$\begin{bmatrix} M_x \\ M_y \\ Q_z \end{bmatrix}_{i,(2,1)} = \begin{bmatrix} -\frac{3EI_{i,1}}{l_{i,1}^2} & \frac{3EI_{i,1}}{l_{i,1}} & 0 \\ 0 & 0 & \frac{(GJ_p)_{i,1}}{l_{i,1}} \\ -\frac{3EI_{i,1}}{l_{i,1}^3} & \frac{3EI_{i,1}}{l_{i,1}^2} & 0 \end{bmatrix} \begin{bmatrix} Z \\ \theta_x \\ \theta_y \end{bmatrix}_{i,(2,1)}$$

We obtain

$$\mathbf{U}_{i,2,0} = \begin{bmatrix} \mathbf{I}_3 & \mathbf{O}_{3 \times 3} \\ \mathbf{U}_{0,2,1}^{j=2} & \mathbf{I}_3 \end{bmatrix} \quad (4.177)$$

$$\mathbf{U}_{0,2,1}^{j=2} = \begin{bmatrix} -\frac{3EI_{i,j-1}}{l_{i,j-1}^2} + \frac{6EI_{i,j+1}}{l_{i,j+1}^2} & \frac{3EI_{i,j-1}}{l_{i,j-1}} + \frac{4EI_{i,j+1}}{l_{i,j+1}} - J_{xi,j}\omega^2 & 0 \\ 0 & 0 & \frac{(GJ_p)_{i,j-1}}{l_{i,j-1}} + \frac{(GJ_p)_{i,j+1}}{l_{i,j+1}} - J_{yi,j}\omega^2 \\ m_{i,j}\omega^2 - \frac{3EI_{i,j-1}}{l_{i,j-1}^3} - \frac{12EI_{i,j+1}}{l_{i,j+1}^3} & \frac{3EI_{i,j-1}}{l_{i,j-1}^2} - \frac{6EI_{i,j+1}}{l_{i,j+1}^2} & 0 \end{bmatrix} \quad (4.178)$$

If the boundary $y = b$ is also simply supported, then

$$\mathbf{U}_{i,2m,0} = \begin{bmatrix} \mathbf{I}_3 & \mathbf{O}_{3 \times 3} \\ \mathbf{U}_{0,2,1}^{j=2m} & \mathbf{I}_3 \end{bmatrix} \quad (4.179)$$

$$\mathbf{U}_{0,2,1}^{j=2m} = \begin{bmatrix} -\frac{6EI_{i,j-1}}{l_{i,j-1}^2} + \frac{3EI_{i,j+1}}{l_{i,j+1}^2} & \frac{4EI_{i,j-1}}{l_{i,j-1}} + \frac{3EI_{i,j+1}}{l_{i,j+1}} - J_{xi,j}\omega^2 & 0 \\ 0 & 0 & \frac{(GJ_p)_{i,j-1}}{l_{i,j-1}} + \frac{(GJ_p)_{i,j+1}}{l_{i,j+1}} - J_{yi,j}\omega^2 \\ m_{i,j}\omega^2 - \frac{12EI_{i,j-1}}{l_{i,j-1}^3} - \frac{3EI_{i,j+1}}{l_{i,j+1}^3} & \frac{6EI_{i,j-1}}{l_{i,j-1}^2} - \frac{3EI_{i,j+1}}{l_{i,j+1}^2} & 0 \end{bmatrix} \quad (4.180)$$

Similarly, $\mathbf{U}_{i,2,0}$ and $\mathbf{U}_{i,2m,0}$ in Equations (4.175) and (4.176) under other boundary conditions can be obtained:

$$\mathbf{U}_{i,2,0} = \begin{bmatrix} \mathbf{I}_3 & \mathbf{O}_{3 \times 3} \\ \mathbf{U}_{0,2,1}^{j=2} & \mathbf{I}_3 \end{bmatrix}, \mathbf{U}_{i,2m,0} = \begin{bmatrix} \mathbf{I}_3 & \mathbf{O}_{3 \times 3} \\ \mathbf{U}_{0,2,1}^{j=2m} & \mathbf{I}_3 \end{bmatrix} \quad (4.181)$$

If the boundaries of $y = 0$ and $y = b$ are clamped, both $\mathbf{U}_{0,2,1}^{j=2}$ and $\mathbf{U}_{0,2,1}^{j=2m}$ can be determined by Equation (4.172a). If the boundaries of $y = 0$ and $y = b$ are free, $\mathbf{U}_{0,2,1}^{j=2}$ and $\mathbf{U}_{0,2,1}^{j=2m}$ are determined by both Equations (4.182) and (4.183):

$$\mathbf{U}_{0,2,1}^{j=2} = \begin{bmatrix} \frac{6EI_{i,j+1}}{l_{i,j+1}^2} & \frac{4EI_{i,j+1}}{l_{i,j+1}} - J_{xi,j}\omega^2 & 0 \\ 0 & 0 & \frac{(GJ_p)_{i,j+1}}{l_{i,j+1}} - J_{yi,j}\omega^2 \\ m_{i,j}\omega^2 - \frac{12EI_{i,j+1}}{l_{i,j+1}^3} & -\frac{6EI_{i,j+1}}{l_{i,j+1}^2} & 0 \end{bmatrix} \quad (4.182)$$

$$\mathbf{U}_{0,2,1}^{j=2m} = \begin{bmatrix} -\frac{6EI_{i,j-1}}{l_{i,j-1}^2} & \frac{4EI_{i,j-1}}{l_{i,j-1}} - J_{xi,j}\omega^2 & 0 \\ 0 & 0 & \frac{(GJ_p)_{i,j-1}}{l_{i,j-1}} - J_{yi,j}\omega^2 \\ m_{i,j}\omega^2 - \frac{12EI_{i,j-1}}{l_{i,j-1}^3} & \frac{6EI_{i,j-1}}{l_{i,j-1}^2} & 0 \end{bmatrix} \quad (4.183)$$

Therefore, the transfer matrix \mathbf{U}_i in Equation (4.167) can be obtained from Equations (4.169), (4.173) and (4.174),

$$\mathbf{U}_i = \begin{bmatrix} \mathbf{U}_{i,2,0} & \mathbf{U}_{i,2,+2} & & & \\ \mathbf{U}_{i,4,-2} & \mathbf{U}_{i,4,0} & \mathbf{U}_{i,4,+2} & & \\ & \mathbf{U}_{i,6,-2} & \mathbf{U}_{i,6,0} & \mathbf{U}_{i,6,+2} & \\ & & \ddots & \ddots & \ddots \\ & & & \mathbf{U}_{i,2m-2,-2} & \mathbf{U}_{i,2m-2,0} & \mathbf{U}_{i,2m-2,+2} \\ & & & & \mathbf{U}_{i,2m,-2} & \mathbf{U}_{i,2m,0} \end{bmatrix} \quad (4.184)$$

4.7.3 Boundary Conditions and Characteristic Equations

Equations (4.164) and (4.167) give rise to the overall transfer equation

$$\mathbf{Z}_{2n+2,2n+1} = \mathbf{U}_{2n+1} \mathbf{U}_{2n} \cdots \mathbf{U}_2 \mathbf{U}_1 \mathbf{Z}_{0,1} = \mathbf{U} \mathbf{Z}_{0,1} \quad (4.185)$$

Applying boundary conditions, the boundary state vectors $\mathbf{Z}_{0,1}$ and $\mathbf{Z}_{2n+2,2n+1}$ can be evaluated from Equation (4.185). For instance, assume the boundaries $x = 0$ and $x = a$ are both simply supported:

$$\mathbf{Z}_{0,1} = \begin{bmatrix} 0, & 0, & \theta_{y(0,1),2}, M_{x(0,1),2}, & 0, & Q_{z(0,1),2}, & \cdots, & 0, & 0, & \theta_{y(0,1),2m}, M_{x(0,1),2m}, & 0, & Q_{z(0,1),2m} \end{bmatrix}^T \quad (4.186)$$

$$\mathbf{Z}_{2n+2,2n+1} = \begin{bmatrix} 0, & 0, & \theta_{y(2n+2,2n+1),2}, & M_{x(2n+2,2n+1),2}, & 0, & Q_{z(2n+2,2n+1),2}, & \cdots, \\ 0, & 0, & \theta_{y(2n+2,2n+1),2m}, & M_{x(2n+2,2n+1),2m}, & 0, & Q_{z(2n+2,2n+1),2m} \end{bmatrix}^T \quad (4.187)$$

In other words, the $1, 2, 5, 7, 8, 11, \dots, 6m-5, 6m-4, 6m-1$ th elements, $3m$ in total, in boundary state vectors $\mathbf{Z}_{0,1}$ and $\mathbf{Z}_{2n+2,2n+1}$ are zero. Therefore, the characteristic equations can be determined by substituting Equations (4.186) and (4.187) into Equation (4.185):

$$\begin{bmatrix} u_{1,3} & u_{1,4} & u_{1,6} & u_{1,9} & u_{1,10} & u_{1,12} & \cdots & u_{1,6m-3} & u_{1,6m-2} & u_{1,6m} \\ u_{2,3} & u_{2,4} & u_{2,6} & u_{2,9} & u_{2,10} & u_{2,12} & \cdots & u_{2,6m-3} & u_{2,6m-2} & u_{2,6m} \\ u_{5,3} & u_{5,4} & u_{5,6} & u_{5,9} & u_{5,10} & u_{5,12} & \cdots & u_{5,6m-3} & u_{5,6m-2} & u_{5,6m} \\ u_{7,3} & u_{7,4} & u_{7,6} & u_{7,9} & u_{7,10} & u_{7,12} & \cdots & u_{7,6m-3} & u_{7,6m-2} & u_{7,6m} \\ u_{8,3} & u_{8,4} & u_{8,6} & u_{8,9} & u_{8,10} & u_{8,12} & \cdots & u_{8,6m-3} & u_{8,6m-2} & u_{8,6m} \\ u_{11,3} & u_{11,4} & u_{11,6} & u_{11,9} & u_{11,10} & u_{11,12} & \cdots & u_{11,6m-3} & u_{11,6m-2} & u_{11,6m} \\ \vdots & \vdots & \vdots & \vdots & \vdots & \vdots & \ddots & \vdots & \vdots & \vdots \\ u_{6m-5,3} & u_{6m-5,4} & u_{6m-5,6} & u_{6m-5,9} & u_{6m-5,10} & u_{6m-5,12} & \cdots & u_{6m-5,6m-3} & u_{6m-5,6m-2} & u_{6m-5,6m} \\ u_{6m-4,3} & u_{6m-4,4} & u_{6m-4,6} & u_{6m-4,9} & u_{6m-4,10} & u_{6m-4,12} & \cdots & u_{6m-4,6m-3} & u_{6m-4,6m-2} & u_{6m-4,6m} \\ u_{6m-1,3} & u_{6m-1,4} & u_{6m-1,6} & u_{6m-1,9} & u_{6m-1,10} & u_{6m-1,12} & \cdots & u_{6m-1,6m-3} & u_{6m-1,6m-2} & u_{6m-1,6m} \end{bmatrix} = 0 \quad (4.188)$$

The eigenfrequencies of each order of the system can be obtained by solving the characteristic equations. The corresponding boundary state vectors $\mathbf{Z}_{0,1}$ and $\mathbf{Z}_{2n+2,2n+1}$ can be determined by substituting the eigenfrequencies of each order into Equation (4.185), and the eigenvectors which correspond to the eigenfrequencies can be obtained by using the transfer equations of each strip element.

If $x = 0$ and $x = a$ are clamped or free boundaries, the eigenfrequencies and eigenvectors in the relevant boundary conditions can be easily evaluated by re-determining the boundary state vectors $\mathbf{Z}_{0,1}$ and $\mathbf{Z}_{2n+2,2n+1}$ in Equations (4.186) and (4.187) using the corresponding boundary conditions and substituting them into the overall transfer equation.

4.7.4 Numerical Examples

Example 4.6 Let $a = b = 1\text{m}$, $h = 0.002\text{m}$, $E = 200\text{GN/m}^2$, $G = 80\text{GN/m}^2$, $\mu = 0.25$, $\rho = 7.8 \times 10^3\text{kg/m}^3$ and $m = n = 8$, according to the above-mentioned method. Compute numerically the eigenfrequency ω_{ij} of the transverse vibration of the fully-simply-supported plate by solving Equation (4.188). Subscript i is the order number of the modal along the x axis and subscript j is the order number of the modal along the y axis.

Solution

The eigenfrequencies computed by the analytical solution and the TMM of the two-dimensional system are shown in Table 4.5, and parts of the mode shapes associated with the relevant nature frequencies computed by the TMM are shown in Figure 4.22.

Table 4.5 Computational results of the eigenfrequencies of the fully-simply-supported plate

ω_{ij} (rad/s)	$i = 1$			$i = 2$			$i = 3$		
	TMM	Analytical	Error (%)	TMM	Analytical	Error (%)	TMM	Analytical	Error (%)
$j = 1$	65.19	59.60	9.4	153.29	149.00	2.9	288.29	298.00	-3.3
$j = 2$	153.29	149.00	2.9	245.61	238.40	3.0	378.56	387.40	-2.3
$j = 3$	288.29	298.00	-3.3	378.56	387.40	-2.3	507.14	536.41	-5.5

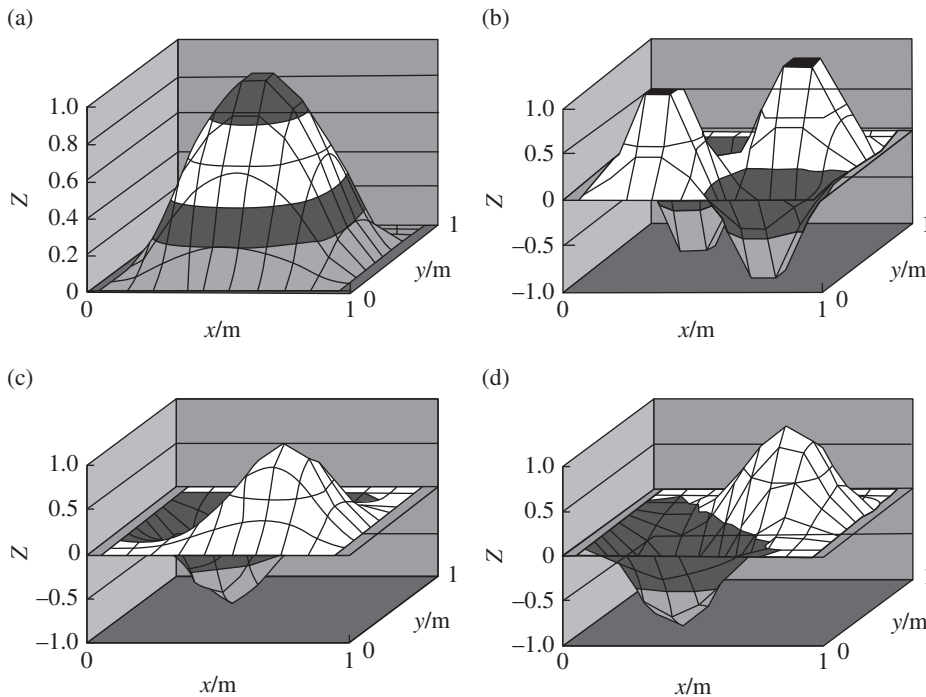


Figure 4.22 Computational results of mode shape corresponding to different frequencies of the fully simply supported plate: (a) mode shape corresponding to $\omega_{1,1} = 65.19\text{ rad/s}$; (b) mode shape corresponding to $\omega_{2,2} = 245.61\text{ rad/s}$; (c) mode shape corresponding to $\omega_{1,2} = 153.29\text{ rad/s}$; (d) mode shape corresponding to $\omega_{2,1} = 153.29\text{ rad/s}$.

Example 4.7 If $y=0$ and $y=b$ are simply supported boundaries, and $x=0$ and $x=a$ are clamped boundaries, compute the eigenfrequency of the system. Let $a = 1\text{m}$, $b = 0.5\text{m}$, $m = 5$, and $n = 8$. The other parameters are kept constant. The comparison of the computational results of the eigenfrequencies obtained by the TMM of a two-dimensional system and the results given in reference [245] are shown in Table 4.6. Some mode shapes of eigenfrequencies are shown in Figure 4.23.

Table 4.6 Computational results of the eigenfrequencies of the plate with two simply-supported edges and two clamped edges

ω_{ij} (rad/s)	$i = 1$			$i = 2$			$i = 3$		
	TMM	Reference [239]	Error (%)	TMM	Reference [239]	Error (%)	TMM	Reference [239]	Error (%)
$j = 1$	174.65	166.67	4.8	303.32	286.24	6.0	483.91	467.40	3.5
$j = 2$	519.75	517.22	0.5	637.60	623.81	2.2	806.86	800.75	0.8
$j = 3$	1086.56	1107.52	-1.9	1241.08	1210.48	2.5	1315.15	1381.08	-4.8
$j = 4$	1947.21	1940.87	0.3	2005.70	2040.82	-1.7	2185.04	2205.68	-0.9

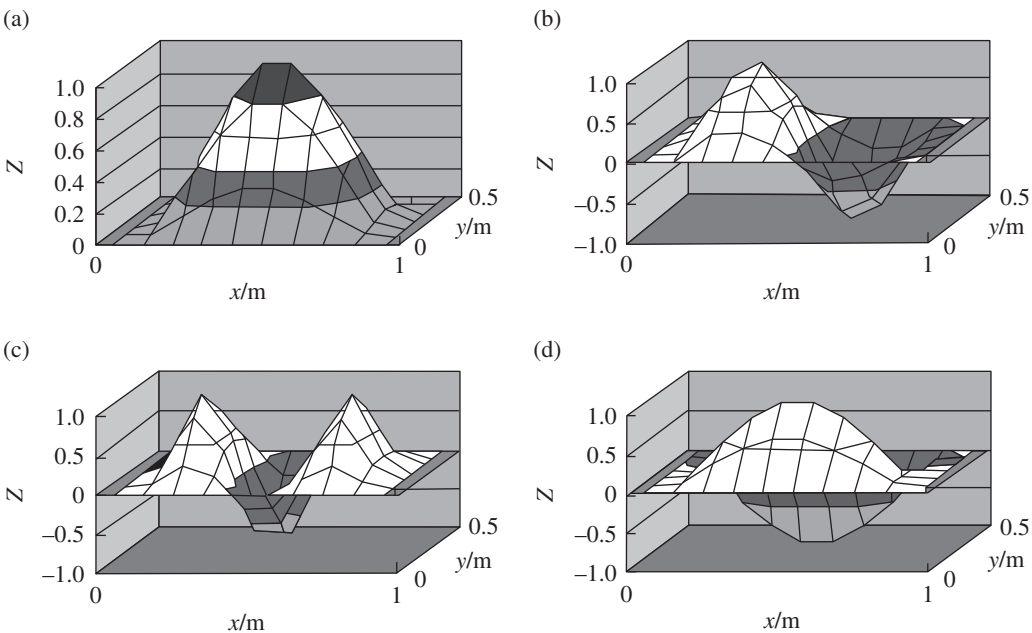


Figure 4.23 Computational results of mode shape corresponding to different frequencies of the plate whose two edges are simply supported and two edges are clamped: (a) mode shape corresponding to $\omega_{1,1} = 174.65 \text{ rad/s}$; (b) mode shape corresponding to $\omega_{2,1} = 303.32 \text{ rad/s}$; (c) mode shape corresponding to $\omega_{3,1} = 483.91 \text{ rad/s}$; (d) mode shape corresponding to $\omega_{1,2} = 519.75 \text{ rad/s}$.

Part II

Transfer Matrix Method for Multibody Systems

In order to avoid the global dynamics equations and increase the computational efficiency for multibody system dynamics (MSD), the transfer matrix method of multibody system (MSTMM) has been developed and applied very widely in research and engineering. It differs from ordinary methods in multibody system dynamics with respect to the features that there is no need for a global dynamics equation, and it uses low-order matrices for high computational efficiency. For linear multibody systems, the solution of MSTMM is exact even if continuous elements like beams are involved. The discrete time MSTMM, however, has to use local linearization. In order to release the method from such approximations, a novel version of MSTMM is developed where translational and angular accelerations, on the one hand, and internal forces and moments, on the other hand, are used as state variables. Already linear relationships among these quantities are utilized, which results in new element transfer matrices and algorithms making the study of multibody systems as simple as the study of single bodies. This approach also allows combining MSTMM with any general numerical integration procedure. Two chapters are provided in this part: the transfer matrix method for multi-rigid-body systems is introduced in Chapter 5 and the transfer matrix method for multi-flexible-body systems is presented in Chapter 6.

5

Transfer Matrix Method for Multi-rigid-body Systems

5.1 Introduction

Multibody system dynamics methods (MSDMs) have developed rapidly in the last 50 years and provide powerful tools for studying the dynamics of various mechanical systems. Although the various classical MSDMs have different styles, at the same time almost all of them share the following characteristics: first, it is necessary to develop the global dynamics equations of the system, and they have to be deduced again if the system's topological structure is changed; second, the order of the global dynamics equations is not less than the number of degrees of freedom of the system, which may become very high for complex systems resulting in a rather long computational time.

The approach proposed in this chapter is different from the above and has a different origin. In 1986, Kumar and Sankar developed a discrete time transfer matrix method (DTTMM) for the structural dynamics of time-variant systems by combining the transfer matrix method with a numerical integration procedure. In 1989, Rui and others extended the transfer matrix method to multibody systems (MSTMM) for vibration analysis of linear multi-rigid-flexible-body systems by developing new transfer matrices, where eigenvalues of linear multi-rigid-flexible-body systems can be computed easily and with high precision. For general nonlinear multi-rigid-body and multi-rigid-flexible-body systems, the discrete time transfer matrix method of multibody systems (MSDTTMM) was developed by combining the MSTMM with a numerical integration procedure.

To improve computational precision and simplify the transfer matrices of the MSTMM, a novel MSTMM is presented in this chapter. The translational and angular accelerations together with internal forces and moments are taken as new state variables instead of position coordinates in the original MSTMM. This results in totally different transfer matrices of elements and algorithms compared with the original MSTMM. The proposed method expands the advantages of the MSTMM by allowing more sophisticated numerical integration procedures such as the Runge–Kutta method to be used: no global dynamics equations of the system are required, matrices have low order, setup of global transfer equation is highly programmable and solution allows high computational precision since linearization is not required anymore. The new method is simple, straightforward, efficient, practical and provides a powerful tool for multibody system dynamics (MSD).

5.2 State Vectors, Transfer Equations and Transfer Matrices

For simplicity, a chain multibody system is taken as an example in the following. The new state vectors of the input ends and output ends of any rigid bodies and hinges moving in space are defined as

$$\mathbf{z} = [\ddot{x} \ \ddot{y} \ \ddot{z} \ \dot{\Omega}_x \ \dot{\Omega}_y \ \dot{\Omega}_z \ m_x \ m_y \ m_z \ q_x \ q_y \ q_z \ 1]^T \quad (5.1)$$

or

$$\mathbf{z} = [\ddot{\mathbf{r}}^T \ \dot{\boldsymbol{\Omega}}^T \ \mathbf{m}^T \ \mathbf{q}^T \ 1]^T \quad (5.2)$$

where

$$\ddot{\mathbf{r}} = \begin{bmatrix} \ddot{x} \\ \ddot{y} \\ \ddot{z} \end{bmatrix}, \quad \dot{\boldsymbol{\Omega}} = \begin{bmatrix} \dot{\Omega}_x \\ \dot{\Omega}_y \\ \dot{\Omega}_z \end{bmatrix}, \quad \mathbf{m} = \begin{bmatrix} m_x \\ m_y \\ m_z \end{bmatrix}, \quad \mathbf{q} = \begin{bmatrix} q_x \\ q_y \\ q_z \end{bmatrix} \quad (5.3)$$

$\ddot{x}, \ddot{y}, \ddot{z}, \dot{\Omega}_x, \dot{\Omega}_y$ and $\dot{\Omega}_z$ are the absolute accelerations of the connection end with respect to the inertial reference system $oxyz$ and the corresponding absolute angular accelerations in the directions of x, y and $z, m_x, m_y, m_z, q_x, q_y$ and q_z are the corresponding internal torques and internal forces in the same reference system, respectively, and $\ddot{\mathbf{r}}, \dot{\boldsymbol{\Omega}}, \mathbf{m}$ and \mathbf{q} are the column vectors of absolute accelerations, absolute angular accelerations, internal torques and internal forces in $oxyz$, respectively.

For a chain system moving in a plane, the state vectors of the input ends and output ends of any rigid bodies and hinges are defined as

$$\mathbf{z} = [\ddot{x} \ \ddot{y} \ \dot{\Omega}_z \ m_z \ q_x \ q_y \ 1]^T \quad (5.4)$$

or

$$\mathbf{z} = [\ddot{\mathbf{r}}^T \ \dot{\Omega}^T \ \mathbf{m}^T \ \mathbf{q}^T \ 1]^T \quad (5.5)$$

where

$$\ddot{\mathbf{r}} = \begin{bmatrix} \ddot{x} \\ \ddot{y} \end{bmatrix}, \quad \dot{\Omega} = \dot{\Omega}_z, \quad \mathbf{m} = m_z, \quad \mathbf{q} = \begin{bmatrix} q_x \\ q_y \end{bmatrix} \quad (5.6)$$

Then the dynamics equations of the j th element can be assembled into a single transfer equation

$$\mathbf{z}_{j,O}(t_i) = \mathbf{U}_j(t_i)\mathbf{z}_{j,I}(t_i) \quad (5.7)$$

The transfer equation describes the transfer relationship between the state vectors at two ends of the j th element and has a similar form to but total different contents from a general transfer equation used in the original MSTMM. Here, the matrix $\mathbf{U}_j(t_i)$ is the transfer matrix of the j th element which is known at time instant t_i . Its order is always (13×13) for any dynamics of a chain multi-rigid-body system moving in space or (7×7) for any dynamics of a chain multi-rigid-body system moving in a plane.

5.3 Overall Transfer Equation and Overall Transfer Matrix

According to Newton's third law, the state vector of the output end of an inboard element is equal to the state vector of the input end of an outboard element for any two adjoining elements in a multibody system. So, the overall transfer equation and transfer matrix of the system, which relates the state vectors at boundaries of the system, can be assembled for any chain multibody system as follows:

$$\mathbf{z}_{n,O} = \mathbf{U}_{1-n} \mathbf{z}_{1,I} \quad (5.8)$$

$$\mathbf{U}_{1-n} = \mathbf{U}_n \cdots \mathbf{U}_2 \mathbf{U}_1 \quad (5.9)$$

It can be seen clearly from the overall transfer equation that the order of the overall transfer matrix of the system is equal to the order of the transfer matrix of an element for a chain system, and it does not increase even if the degrees of freedom of the system increase. Irrespective of the size of a multibody system, the highest order of the overall transfer matrix is the same as the order of the transfer matrix of a single body, that is, (13×13) for the dynamics of a chain multi-rigid-body system moving in space or (7×7) for the dynamics of a chain multi-rigid-body system moving in a plane. The matrices involved in the new MSTMM are therefore always small, which greatly reduces the computational time and the memory storage requirement.

5.4 Transfer Matrix of a Planar Rigid Body

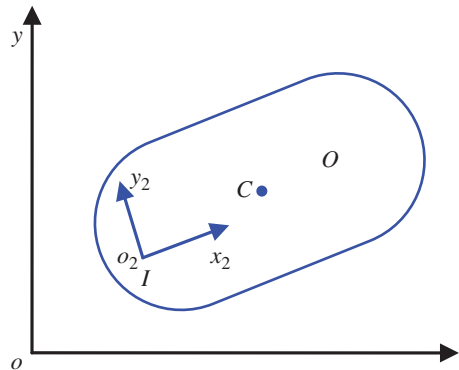
A planar rigid body with a single input end and a single output end is shown in Figure 5.1, where points I , O and C denote the inboard end, outboard end and mass center of the rigid body, respectively. The subscript 2 denotes the body-fixed coordinate system whose origin O_2 coincides with the inboard end I of the rigid body, while oxy is the inertial coordinate system. The structural parameters of the rigid body are represented in a body-fixed coordinate system.

Geometrical equations can be obtained

$$\mathbf{r}_K = \mathbf{r}_I + \mathbf{r}_{IK} \quad (5.10)$$

where \mathbf{r}_K and \mathbf{r}_I are the global position vectors, decomposed in the inertial coordinate system, of point K and the input end I , respectively. The same formula also applies for the output end O and

Figure 5.1 Planar rigid body.



the mass center C . \mathbf{r}_{IK} is the position vector of point K with respect to the input end I , decomposed in the inertial coordinate system.

Using the Newton–Euler method, the dynamics equations of the rigid body can be deduced

$$m\ddot{\mathbf{r}}_C = \mathbf{q}_I - \mathbf{q}_O + \mathbf{f}_C \quad (5.11)$$

$$J_I \dot{\dot{\Omega}}_I + m x_{IC} \ddot{y}_I - m y_{IC} \ddot{x}_I = m_C + m_O - m_I - x_{IO} q_{y,O} + y_{IO} q_{x,O} + x_{IC} f_{y,C} - y_{IC} f_{x,C} \quad (5.12)$$

where m and $\ddot{\mathbf{r}}_C = [\ddot{x}_C \ \ddot{y}_C]^T$ are the mass and the column vector of the absolute acceleration of the mass center, respectively, $\mathbf{q}_I = [q_{x,I} \ q_{y,I}]^T$ and $\mathbf{q}_O = [q_{x,O} \ q_{y,O}]^T$ are the column vectors of internal forces acting on points I and O , $\mathbf{f}_C = [f_{x,C} \ f_{y,C}]^T$ and $\mathbf{m}_C = [m_C]$ are the column vectors of external force and the external torque acting on the mass center of the rigid body, J_I is the moment of inertia with respect to point I , $\mathbf{m}_I = [m_I]$ and $\mathbf{m}_O = [m_O]$ are the column vectors of internal torques acting on the points I and O , $[x_{IO} \ y_{IO}]^T$ and $[x_{IC} \ y_{IC}]^T$ are the column vectors of position vectors from I to O and to C , respectively, and \ddot{x}_I and \ddot{y}_I are the components of the column vector of the absolute acceleration of point I , which can be denoted compactly as $\ddot{\mathbf{r}}_I = [\ddot{x}_I \ \ddot{y}_I]^T$.

The rotation of any point of the same rigid body is uniform and can be expressed as

$$\dot{\Omega}_O = \dot{\Omega}_I \quad (5.13)$$

Equations (5.10) to (5.12) can be rewritten as

$$\ddot{\mathbf{r}}_O = \ddot{\mathbf{r}}_I + \mathbf{E}_1 \dot{\Omega}_I + \mathbf{E}_2 \quad (5.14)$$

$$\mathbf{q}_O = \mathbf{q}_I + \mathbf{E}_3 \ddot{\mathbf{r}}_I + \mathbf{E}_4 \dot{\Omega}_I + \mathbf{E}_5 \quad (5.15)$$

$$\mathbf{m}_O = \mathbf{m}_I + \mathbf{E}_6 \mathbf{q}_O + \mathbf{E}_7 \ddot{\mathbf{r}}_I + \mathbf{E}_8 \dot{\Omega}_I + \mathbf{E}_9 \quad (5.16)$$

where

$$\begin{aligned} \mathbf{E}_1 &= \begin{bmatrix} -y_{IO} \\ x_{IO} \end{bmatrix}, \mathbf{E}_2 = \begin{bmatrix} -x_{IO} \Omega_I^2 \\ -y_{IO} \Omega_I^2 \end{bmatrix}, \mathbf{E}_3 = \begin{bmatrix} -m & 0 \\ 0 & -m \end{bmatrix}, \mathbf{E}_4 = \begin{bmatrix} m y_{IC} \\ -m x_{IC} \end{bmatrix} \\ \mathbf{E}_5 &= \begin{bmatrix} m x_{IC} \Omega_I^2 + f_{x,C} \\ m y_{IC} \Omega_I^2 + f_{y,C} \end{bmatrix}, \mathbf{E}_6 = \begin{bmatrix} -y_{IO} & x_{IO} \end{bmatrix}, \mathbf{E}_7 = \begin{bmatrix} -m y_{IC} & m x_{IC} \end{bmatrix} \\ \mathbf{E}_8 &= [J_I], \mathbf{E}_9 = [-m_C + y_{IC} f_{x,C} - x_{IC} f_{y,C}] \end{aligned}$$

Combining Equations (5.13) to (5.16), the transfer equation and transfer matrix of a rigid body moving in a plane can be obtained

$$\mathbf{z}_O = \mathbf{U} \mathbf{z}_I \quad (5.17)$$

$$\mathbf{U} = \begin{bmatrix} \mathbf{I}_2 & \mathbf{E}_1 & \mathbf{O}_{2 \times 1} & \mathbf{O}_{2 \times 2} & \mathbf{E}_2 \\ \mathbf{O}_{1 \times 2} & \mathbf{I}_1 & \mathbf{O}_{1 \times 1} & \mathbf{O}_{1 \times 2} & \mathbf{O}_{1 \times 1} \\ \mathbf{E}_6 \mathbf{E}_3 + \mathbf{E}_7 & \mathbf{E}_6 \mathbf{E}_4 + \mathbf{E}_8 & \mathbf{I}_1 & \mathbf{E}_6 & \mathbf{E}_6 \mathbf{E}_5 + \mathbf{E}_9 \\ \mathbf{E}_3 & \mathbf{E}_4 & \mathbf{O}_{2 \times 1} & \mathbf{I}_2 & \mathbf{E}_5 \\ \mathbf{O}_{1 \times 2} & \mathbf{O}_{1 \times 1} & \mathbf{O}_{1 \times 1} & \mathbf{O}_{1 \times 2} & 1 \end{bmatrix} \quad (5.18)$$

where \mathbf{z}_O and \mathbf{z}_I are the state vectors of the inboard end I and outboard end O on the rigid body defined in Equation (5.4), and the order of the transfer matrix of the rigid body moving in a plane is (7×7) .

5.5 Transfer Matrix of a Spatial Rigid Body

A spatial rigid body with a single input end and a single output end is shown in Figure 5.2, where points I , O and C denote the inboard end, outboard end and mass center of the rigid body, respectively. The subscript 2 denotes the body-fixed coordinate system whose origin O_2 coincides with the inboard end I of the rigid body, while xyz is the inertial coordinate system. The structural parameters of the rigid body are represented in a body-fixed coordinate system.

Geometrical equations can be obtained

$$\mathbf{r}_K = \mathbf{r}_I + \mathbf{A}_I \mathbf{l}_{IK} \quad (5.19)$$

where \mathbf{r}_K and \mathbf{l}_{IK} are the column vectors of the position coordinate of point K with respect to the inertial coordinate system and the body-fixed coordinate system, respectively. The same formula applies for points O and C . \mathbf{A}_I is direction cosine matrix of input end I with respect to the global reference system.

Using the Newton–Euler method, the dynamics equations of the rigid body can be deduced

$$m\ddot{\mathbf{r}}_C = \mathbf{q}_I - \mathbf{q}_O + \mathbf{f}_C \quad (5.20)$$

$$\dot{\mathbf{G}}_I = -\tilde{\mathbf{r}}_{IO}\mathbf{q}_O + \mathbf{m}_O - \mathbf{m}_I + \mathbf{m}_C - m\tilde{\mathbf{r}}_{IC}\ddot{\mathbf{r}}_I + \tilde{\mathbf{r}}_{IC}\mathbf{f}_C \quad (5.21)$$

where m and $\ddot{\mathbf{r}}_C$ are the mass and the column vector of mass center absolute acceleration of the rigid body, \mathbf{q}_I and \mathbf{q}_O are the column vectors of internal forces acting on points I and O , \mathbf{f}_C and \mathbf{m}_C are the column vectors of external force and the external torque acting on the mass center of the rigid body, \mathbf{G}_I is the column vector of moment of momentum with respect to point I , \mathbf{m}_I and \mathbf{m}_O are the column vectors of internal torques acted on points I and O , \mathbf{r}_{IO} and \mathbf{r}_{IC} are the column vectors of position vectors from I to O and to C , respectively, and $\ddot{\mathbf{r}}_I$ is the column vector of the absolute acceleration of point I .

The rotation of any point of the same rigid body is uniform and can be expressed as

$$\dot{\mathbf{\Omega}}_O = \dot{\mathbf{\Omega}}_I \quad (5.22)$$

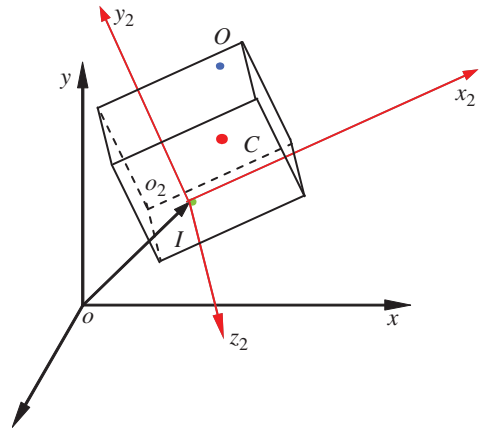
Equations (5.19) to (5.21) can be rewritten as

$$\ddot{\mathbf{r}}_O = \ddot{\mathbf{r}}_I + \mathbf{E}_1 \dot{\mathbf{\Omega}}_I + \mathbf{E}_2 \quad (5.23)$$

$$\mathbf{q}_O = \mathbf{q}_I + \mathbf{E}_3 \ddot{\mathbf{r}}_I + \mathbf{E}_4 \dot{\mathbf{\Omega}}_I + \mathbf{E}_5 \quad (5.24)$$

$$\mathbf{m} = \mathbf{m}_I + \mathbf{E}_6 \mathbf{q}_O + \mathbf{E}_7 \ddot{\mathbf{r}}_I + \mathbf{E}_8 \dot{\mathbf{\Omega}}_I + \mathbf{E}_9 \quad (5.25)$$

Figure 5.2 Spatial rigid body.



where

$$\begin{aligned} E_1 &= -\tilde{\mathbf{r}}_{IO}, E_2 = \tilde{\mathbf{\Omega}}_I \tilde{\mathbf{\Omega}}_I \mathbf{r}_{IO}, E_3 = -m\mathbf{I}_3, E_4 = m\tilde{\mathbf{r}}_{IC}, E_5 = \mathbf{f}_C - m\tilde{\mathbf{\Omega}}_I \tilde{\mathbf{\Omega}}_I \mathbf{r}_{IC} \\ E_6 &= \tilde{\mathbf{r}}_{IO}, E_7 = m\tilde{\mathbf{r}}_{IC}, E_8 = \mathbf{A}_I \mathbf{J}_I \mathbf{A}_I^T, E_9 = -m_C - \tilde{\mathbf{r}}_{IC} \mathbf{f}_C + \mathbf{A}_I \tilde{\mathbf{\omega}}_I \mathbf{J}_I \tilde{\mathbf{\omega}}_I \end{aligned}$$

Combining Equations (5.22) to (5.25), the transfer equation and the transfer matrix of a rigid body moving in space can be obtained

$$\mathbf{z}_O = \mathbf{U} \mathbf{z}_I \quad (5.26)$$

$$\mathbf{U} = \begin{bmatrix} \mathbf{I}_3 & \mathbf{E}_1 & \mathbf{O}_{3 \times 3} & \mathbf{O}_{3 \times 3} & \mathbf{E}_2 \\ \mathbf{O}_{3 \times 3} & \mathbf{I}_3 & \mathbf{O}_{3 \times 3} & \mathbf{O}_{3 \times 3} & \mathbf{O}_{3 \times 1} \\ \mathbf{E}_6 \mathbf{E}_3 + \mathbf{E}_7 & \mathbf{E}_6 \mathbf{E}_4 + \mathbf{E}_8 & \mathbf{I}_3 & \mathbf{E}_6 & \mathbf{E}_6 \mathbf{E}_5 + \mathbf{E}_9 \\ \mathbf{E}_3 & \mathbf{E}_4 & \mathbf{O}_{3 \times 3} & \mathbf{I}_3 & \mathbf{E}_5 \\ \mathbf{O}_{1 \times 3} & \mathbf{O}_{1 \times 3} & \mathbf{O}_{1 \times 3} & \mathbf{O}_{1 \times 3} & 1 \end{bmatrix} \quad (5.27)$$

where \mathbf{z}_O and \mathbf{z}_I are the state vector of the inboard end I and outboard end O on the rigid body defined in Equation (5.1), and the order of the transfer matrix of the rigid body moving in space is (13×13) .

5.6 Transfer Matrix of a Planar Hinge

For a smooth pin hinge j , whose inboard body $j-1$ and outboard body $j+1$ are moving in a plane, its mass and size are neglected. The position coordinates of its two ends, as well as the corresponding time derivatives, are equal. Newton's third law of motion says that internal forces acting on its two ends are equal in magnitude but opposite in directions. The "smooth" here means that the internal torques are equal to zeros. Thus the following four groups of equations are obtained.

$$\ddot{\mathbf{r}}_{j+1,j} = \ddot{\mathbf{r}}_{j-1,j} \quad (5.28)$$

$$\mathbf{q}_{j+1,j} = \mathbf{q}_{j-1,j} \quad (5.29)$$

$$\mathbf{m}_{j+1,j} = \mathbf{m}_{j-1,j} \quad (5.30)$$

$$\mathbf{m}_{j-1,j} = \mathbf{0} \quad (5.31)$$

For a smooth pin hinge j whose outboard body's outboard hinge is also a smooth pin hinge

$$\mathbf{m}_{j+1,j+2} = \mathbf{0} \quad (5.32)$$

The transfer equation for an outboard rigid body of a smooth pin hinge j is

$$\mathbf{z}_{j+1,j+2} = \mathbf{U}_{j+1} \mathbf{z}_{j+1,j} \quad (5.33)$$

The state vectors and transfer matrix in the form of a partitioned matrix are

$$\mathbf{z}_{j+1,j+2} = \begin{bmatrix} \ddot{\mathbf{r}} \\ \dot{\mathbf{\Omega}} \\ \mathbf{m} \\ \mathbf{q} \\ 1 \end{bmatrix}_{j+1,j+2}, \quad \mathbf{z}_{j+1,j} = \begin{bmatrix} \ddot{\mathbf{r}} \\ \dot{\mathbf{\Omega}} \\ \mathbf{m} \\ \mathbf{q} \\ 1 \end{bmatrix}_{j+1,j}, \quad \mathbf{U}_{j+1} = \begin{bmatrix} \mathbf{u}_{1,1} & \mathbf{u}_{1,2} & \mathbf{u}_{1,3} & \mathbf{u}_{1,4} & \mathbf{u}_{1,5} \\ \mathbf{u}_{2,1} & \mathbf{u}_{2,2} & \mathbf{u}_{2,3} & \mathbf{u}_{2,4} & \mathbf{u}_{2,5} \\ \mathbf{u}_{3,1} & \mathbf{u}_{3,2} & \mathbf{u}_{3,3} & \mathbf{u}_{3,4} & \mathbf{u}_{3,5} \\ \mathbf{u}_{4,1} & \mathbf{u}_{4,2} & \mathbf{u}_{4,3} & \mathbf{u}_{4,4} & \mathbf{u}_{4,5} \\ \mathbf{O}_{1 \times 2} & \mathbf{O}_{1 \times 1} & \mathbf{O}_{1 \times 1} & \mathbf{O}_{1 \times 2} & 1 \end{bmatrix}_{j+1} \quad (5.34)$$

The relation of internal moments between the input and output ends of a rigid body is

$$\mathbf{m}_{j+1,j+2} = \mathbf{u}_{3,1}\ddot{\mathbf{r}}_{j+1,j} + \mathbf{u}_{3,2}\dot{\mathbf{Q}}_{j+1,j} + \mathbf{u}_{3,3}\mathbf{m}_{j+1,j} + \mathbf{u}_{3,4}\mathbf{q}_{j+1,j} + \mathbf{u}_{3,5} \quad (5.35)$$

where $\mathbf{u}_{m,n}$ is the corresponding partitioned submatrix of \mathbf{U}_{j+1} , the transfer matrix of the outboard body, given in Equation (5.34).

Substituting the above equations into Equation (5.32), the relation of angular accelerations between the input and output ends of the hinge can be obtained

$$\dot{\mathbf{Q}}_{j+1,j} = -\mathbf{u}_{3,2}^{-1}\mathbf{u}_{3,1}\ddot{\mathbf{r}}_{j-1,j} - \mathbf{u}_{3,2}^{-1}\mathbf{u}_{3,3}\mathbf{m}_{j-1,j} - \mathbf{u}_{3,2}^{-1}\mathbf{u}_{3,4}\mathbf{q}_{j-1,j} - \mathbf{u}_{3,2}^{-1}\mathbf{u}_{3,5} \quad (5.36)$$

Combining Equations (5.28) to (5.30) and (5.36) the transfer equation and the transfer matrix of a smooth pin hinge j moving in a plane can be obtained

$$\mathbf{z}_{j+1,j} = \mathbf{U}_j \mathbf{z}_{j-1,j} \quad (5.37)$$

$$\mathbf{U}_j = \begin{bmatrix} \mathbf{I}_2 & \mathbf{O}_{2 \times 1} & \mathbf{O}_{2 \times 1} & \mathbf{O}_{2 \times 2} & \mathbf{O}_{2 \times 1} \\ -\mathbf{u}_{3,2}^{-1}\mathbf{u}_{N_j,3,1} & \mathbf{O}_{1 \times 1} & \mathbf{O}_{1 \times 1} & -\mathbf{u}_{3,2}^{-1}\mathbf{u}_{3,4} & -\mathbf{u}_{3,2}^{-1}\mathbf{u}_{3,5} \\ \mathbf{O}_{1 \times 2} & \mathbf{O}_{1 \times 1} & \mathbf{I}_1 & \mathbf{O}_{1 \times 2} & \mathbf{O}_{1 \times 1} \\ \mathbf{O}_{2 \times 2} & \mathbf{O}_{2 \times 1} & \mathbf{O}_{2 \times 1} & \mathbf{I}_2 & \mathbf{O}_{2 \times 1} \\ \mathbf{O}_{1 \times 2} & \mathbf{O}_{1 \times 1} & \mathbf{O}_{1 \times 1} & \mathbf{O}_{1 \times 2} & 1 \end{bmatrix} \quad (5.38)$$

5.7 Transfer Matrix of a Spatial Hinge

5.7.1 Transfer Equation of a Smooth Ball-and-socket Hinge

Similarly, for a smooth ball-and-socket hinge j , whose inboard body $j-1$ and outboard body $j+1$ are moving in space, its mass and size are also neglected. The position coordinates of its two ends, as well as the corresponding time derivatives, are equal. The internal torques are equal to zeros. Thus the following four groups of equations are obtained.

$$\ddot{\mathbf{r}}_{j+1,j} = \ddot{\mathbf{r}}_{j-1,j} \quad (5.39)$$

$$\mathbf{q}_{j+1,j} = \mathbf{q}_{j-1,j} \quad (5.40)$$

$$\mathbf{m}_{j+1,j} = \mathbf{m}_{j-1,j} \quad (5.41)$$

$$\mathbf{m}_{j-1,j} = \mathbf{0} \quad (5.42)$$

For a smooth ball-and-socket hinge j whose outboard body's outboard hinge is also a smooth ball-and-socket hinge

$$\mathbf{m}_{j+1,j+2} = \mathbf{0} \quad (5.43)$$

The transfer equation for an outboard rigid body of a smooth ball-and-socket hinge j is

$$\mathbf{z}_{j+1,j+2} = \mathbf{U}_{j+1} \mathbf{z}_{j+1,j} \quad (5.44)$$

The state vectors and transfer matrix in the form of a partitioned matrix are

$$\mathbf{z}_{j+1,j+2} = \begin{bmatrix} \ddot{\mathbf{r}} \\ \dot{\mathbf{Q}} \\ \mathbf{m} \\ \mathbf{q} \\ 1 \end{bmatrix}_{j+1,j+2}, \quad \mathbf{z}_{j+1,j} = \begin{bmatrix} \ddot{\mathbf{r}} \\ \dot{\mathbf{Q}} \\ \mathbf{m} \\ \mathbf{q} \\ 1 \end{bmatrix}_{j+1,j}, \quad \mathbf{U}_{j+1} = \begin{bmatrix} \mathbf{u}_{1,1} & \mathbf{u}_{1,2} & \mathbf{u}_{1,3} & \mathbf{u}_{1,4} & \mathbf{u}_{1,5} \\ \mathbf{u}_{2,1} & \mathbf{u}_{2,2} & \mathbf{u}_{2,3} & \mathbf{u}_{2,4} & \mathbf{u}_{2,5} \\ \mathbf{u}_{3,1} & \mathbf{u}_{3,2} & \mathbf{u}_{3,3} & \mathbf{u}_{3,4} & \mathbf{u}_{3,5} \\ \mathbf{u}_{4,1} & \mathbf{u}_{4,2} & \mathbf{u}_{4,3} & \mathbf{u}_{4,4} & \mathbf{u}_{4,5} \\ \mathbf{O}_{1 \times 3} & \mathbf{O}_{1 \times 3} & \mathbf{O}_{1 \times 3} & \mathbf{O}_{1 \times 3} & 1 \end{bmatrix}_{j+1} \quad (5.45)$$

The relation of internal moments between the input and output ends of a rigid body is

$$\mathbf{m}_{j+1,j+2} = \mathbf{u}_{3,1}\ddot{\mathbf{r}}_{j+1,j} + \mathbf{u}_{3,2}\dot{\mathbf{Q}}_{j+1,j} + \mathbf{u}_{3,3}\mathbf{m}_{j+1,j} + \mathbf{u}_{3,4}\mathbf{q}_{j+1,j} + \mathbf{u}_{3,5} \quad (5.46)$$

where $\mathbf{u}_{m,n}$ is the corresponding partitioned submatrix of \mathbf{U}_{j+1} , the transfer matrix of the outboard body, given in Equation (5.45).

Substituting the above equations into Equation (5.43), the relation of angular accelerations between the input and output ends of the hinge can be obtained

$$\dot{\mathbf{Q}}_{j+1,j} = -\mathbf{u}_{3,2}^{-1}\mathbf{u}_{3,1}\ddot{\mathbf{r}}_{j-1,j} - \mathbf{u}_{3,2}^{-1}\mathbf{u}_{3,3}\mathbf{m}_{j-1,j} - \mathbf{u}_{3,2}^{-1}\mathbf{u}_{3,4}\mathbf{q}_{j-1,j} - \mathbf{u}_{3,2}^{-1}\mathbf{u}_{3,5} \quad (5.47)$$

Combining Equations (5.39) to (5.41) and (5.47), the transfer equation and transfer matrix of a smooth ball-and-socket hinge j can be obtained

$$\mathbf{z}_{j+1,j} = \mathbf{U}_j \mathbf{z}_{j-1,j} \quad (5.48)$$

$$\mathbf{U}_j = \begin{bmatrix} \mathbf{I}_3 & \mathbf{O}_{3 \times 3} & \mathbf{O}_{3 \times 3} & \mathbf{O}_{3 \times 3} & \mathbf{O}_{3 \times 1} \\ -\mathbf{u}_{3,2}^{-1}\mathbf{u}_{3,1} & \mathbf{O}_{3 \times 3} & -\mathbf{u}_{3,2}^{-1}\mathbf{u}_{3,3} & -\mathbf{u}_{3,2}^{-1}\mathbf{u}_{3,4} & -\mathbf{u}_{3,2}^{-1}\mathbf{u}_{3,5} \\ \mathbf{O}_{3 \times 3} & \mathbf{O}_{3 \times 3} & \mathbf{I}_3 & \mathbf{O}_{3 \times 3} & \mathbf{O}_{3 \times 1} \\ \mathbf{O}_{3 \times 3} & \mathbf{O}_{3 \times 3} & \mathbf{O}_{3 \times 3} & \mathbf{I}_3 & \mathbf{O}_{3 \times 1} \\ \mathbf{O}_{1 \times 3} & \mathbf{O}_{1 \times 3} & \mathbf{O}_{1 \times 3} & \mathbf{O}_{1 \times 3} & 1 \end{bmatrix} \quad (5.49)$$

5.7.2 Transfer Equation of a Smooth Pin Hinge Moving in Space

A smooth pin hinge j whose inboard rigid body is $j-1$ and outboard rigid body is $j+1$ is shown in Figure 5.3. The position coordinates, as well as the corresponding time derivatives, and internal forces are equal, and the internal torque is equal to zero along the relative-rotation axis. If the relative rotation angle of the smooth pin hinge j is denoted by θ_j , then there are the following five groups of equations

$$\ddot{\mathbf{r}}_{j+1,j} = \ddot{\mathbf{r}}_{j-1,j} \quad (5.50)$$

$$\mathbf{q}_{j+1,j} = \mathbf{q}_{j-1,j} \quad (5.51)$$

$$\mathbf{H}_1 \mathbf{A}_{j+1,j}^T \dot{\mathbf{Q}}_{j+1,j} = \mathbf{H}_1 \mathbf{A}_{j+1,j}^T \dot{\mathbf{Q}}_{j-1,j} + \mathbf{H}_1 \mathbf{A}_{j+1,j}^T \tilde{\mathbf{Q}}_{j+1,j} \mathbf{A}_{j+1,j} \boldsymbol{\omega}_r \quad (5.52)$$

$$\mathbf{m}_{j+1,j} = \mathbf{m}_{j-1,j} \quad (5.53)$$

$$\mathbf{H}_2 \mathbf{A}_{j+1,j}^T \mathbf{m}_{j-1,j} = 0 \quad (5.54)$$

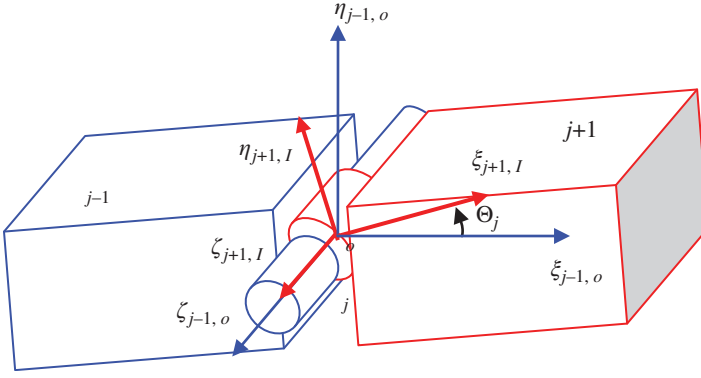


Figure 5.3 Smooth pin hinge moving in space.

where

$$\mathbf{H}_1 = \begin{bmatrix} 1 & 0 & 0 \\ 0 & 1 & 0 \end{bmatrix}, \mathbf{H}_2 = [0 \ 0 \ 1], \boldsymbol{\omega}_r = [0 \ 0 \ \dot{\Theta}_j]^T$$

$\mathbf{A}_{j+1,j}$ is the direction cosine matrix of the input-end body-fixed coordinate system of body element $j+1$.

For a smooth pin hinge j whose outboard body's outboard hinge is also a pin hinge

$$\mathbf{H}_2 \mathbf{A}_{j+1,j+2}^T \mathbf{m}_{j+1,j+2} = 0 \quad (5.55)$$

where $\mathbf{A}_{j+1,j+2}$ is the direction cosine matrix of the output-end body-fixed coordinate system of body element $j+1$.

The transfer equation for an outboard rigid body $j+1$ of the smooth pin hinge j is

$$\mathbf{z}_{j+1,j+2} = \mathbf{U}_{j+1} \mathbf{z}_{j+1,j} \quad (5.56)$$

The state vectors and transfer matrix in the form of a partitioned matrix are

$$\mathbf{z}_{j+1,j+2} = \begin{bmatrix} \ddot{\mathbf{r}} \\ \dot{\mathbf{\Omega}} \\ \mathbf{m} \\ \mathbf{q} \\ 1 \end{bmatrix}_{j+1,j+2}, \quad \mathbf{z}_{j+1,j} = \begin{bmatrix} \ddot{\mathbf{r}} \\ \dot{\mathbf{\Omega}} \\ \mathbf{m} \\ \mathbf{q} \\ 1 \end{bmatrix}_{j+1,j}, \quad \mathbf{U}_{j+1} = \begin{bmatrix} \mathbf{u}_{1,1} & \mathbf{u}_{1,2} & \mathbf{u}_{1,3} & \mathbf{u}_{1,4} & \mathbf{u}_{1,5} \\ \mathbf{u}_{2,1} & \mathbf{u}_{2,2} & \mathbf{u}_{2,3} & \mathbf{u}_{2,4} & \mathbf{u}_{2,5} \\ \mathbf{u}_{3,1} & \mathbf{u}_{3,2} & \mathbf{u}_{3,3} & \mathbf{u}_{3,4} & \mathbf{u}_{3,5} \\ \mathbf{u}_{4,1} & \mathbf{u}_{4,2} & \mathbf{u}_{4,3} & \mathbf{u}_{4,4} & \mathbf{u}_{4,5} \\ \mathbf{O}_{1 \times 3} & \mathbf{O}_{1 \times 3} & \mathbf{O}_{1 \times 3} & \mathbf{O}_{1 \times 3} & 1 \end{bmatrix}_{j+1} \quad (5.57)$$

The relation of internal moments between the input and output ends of a rigid body $j+1$ is

$$\mathbf{m}_{j+1,j+2} = \mathbf{u}_{3,1} \ddot{\mathbf{r}}_{j+1,j} + \mathbf{u}_{3,2} \dot{\mathbf{\Omega}}_{j+1,j} + \mathbf{u}_{3,3} \mathbf{m}_{j+1,j} + \mathbf{u}_{3,4} \mathbf{q}_{j+1,j} + \mathbf{u}_{3,5} \quad (5.58)$$

where $\mathbf{u}_{m,n}$ is the corresponding partitioned submatrix of \mathbf{U}_{j+1} , the transfer matrix of the outboard body, given in Equation (5.57).

Substituting the above equations into Equation (5.52), the relation of angular accelerations between the input and output ends of a smooth pin hinge j can be obtained

$$\dot{\mathbf{\Omega}}_{j+1,j} = \mathbf{E}_0^{-1} \mathbf{E}_1 \ddot{\mathbf{r}}_{j-1,j} + \mathbf{E}_0^{-1} \mathbf{E}_2 \dot{\mathbf{\Omega}}_{j-1,j} + \mathbf{E}_0^{-1} \mathbf{E}_3 \mathbf{m}_{j-1,j} + \mathbf{E}_0^{-1} \mathbf{E}_4 \mathbf{q}_{j-1,j} + \mathbf{E}_0^{-1} \mathbf{E}_5 \quad (5.59)$$

where

$$\begin{aligned} E_0 &= \begin{bmatrix} H_1 A_{j+1,j}^T \\ -H_2 A_{j+1,j+2}^T \mathbf{u}_{3,2} \end{bmatrix}, E_1 = \begin{bmatrix} \mathbf{O}_{2 \times 3} \\ H_2 A_{j+1,j+2}^T \mathbf{u}_{3,1} \end{bmatrix}, E_2 = \begin{bmatrix} H_1 A_{j+1,j}^T \\ \mathbf{O}_{1 \times 3} \end{bmatrix} \\ E_3 &= \begin{bmatrix} \mathbf{O}_{2 \times 3} \\ H_2 A_{j+1,j+2}^T \mathbf{O}_{3,3} \end{bmatrix}, E_4 = \begin{bmatrix} \mathbf{O}_{2 \times 3} \\ H_2 A_{j+1,j+2}^T \mathbf{u}_{3,4} \end{bmatrix}, E_5 = \begin{bmatrix} H_1 A_{j+1,j}^T \tilde{\mathbf{Q}}_{j-1,j} A_{j+1,j} \boldsymbol{\omega}_r \\ H_2 A_{j+1,j+2}^T \mathbf{u}_{3,5} \end{bmatrix} \end{aligned}$$

Combining Equations (5.50), (5.51), (5.53) and (5.59) and adjusting their sequences according to the configuration of the state vector, the transfer equation and transfer matrix of the smooth pin hinge j can be obtained

$$\mathbf{z}_{j+1,j} = \mathbf{U}_j \mathbf{z}_{j-1,j} \quad (5.60)$$

$$\mathbf{U}_j = \begin{bmatrix} \mathbf{I}_3 & \mathbf{O}_{3 \times 3} & \mathbf{O}_{3 \times 3} & \mathbf{O}_{3 \times 3} & \mathbf{O}_{3 \times 1} \\ E_0^{-1} E_1 & E_0^{-1} E_2 & E_0^{-1} E_3 & E_0^{-1} E_4 & E_0^{-1} E_5 \\ \mathbf{O}_{3 \times 3} & \mathbf{O}_{3 \times 3} & \mathbf{I}_3 & \mathbf{O}_{3 \times 3} & \mathbf{O}_{3 \times 1} \\ \mathbf{O}_{3 \times 3} & \mathbf{O}_{3 \times 3} & \mathbf{O}_{3 \times 3} & \mathbf{I}_3 & \mathbf{O}_{3 \times 1} \\ \mathbf{O}_{1 \times 3} & \mathbf{O}_{1 \times 3} & \mathbf{O}_{1 \times 3} & \mathbf{O}_{1 \times 3} & 1 \end{bmatrix} \quad (5.61)$$

5.8 Transfer Matrix of an Acceleration Hinge

An acceleration hinge is a totally new concept that can be considered to be a fictitious hinge presented in the new MSTMM. The acceleration hinge describes the elastic internal forces, elastic internal torques, damping internal forces and damping internal torques due to the relative deformation of the hinge.

The acceleration and angular acceleration of the output end of an acceleration hinge can be obtained from the transfer matrix of its outboard bodies. The processes to deduce the transfer matrix are similar for a smooth hinge and an acceleration hinge.

The internal forces and torques of the elastic hinge are treated as torques acting on its inboard and outboard bodies, respectively.

As stated previously, once the action and reaction forces of an elastic hinge are treated as part of the external forces acting on the connected body elements, the elastic hinge can be dealt with as an acceleration hinge.

For an acceleration hinge j moving in space, whose inboard body $j-1$ and outboard body $j+1$ are all rigid bodies moving in space, the internal forces and torques are zeros at its two ends. Thus the following four groups of equations can be obtained:

$$\mathbf{q}_{j+1,j} = \mathbf{q}_{j-1,j} \quad (5.62)$$

$$\mathbf{q}_{j-1,j} = \mathbf{0} \quad (5.63)$$

$$\mathbf{m}_{j+1,j} = \mathbf{m}_{j-1,j} \quad (5.64)$$

$$\mathbf{m}_{j-1,j} = \mathbf{0} \quad (5.65)$$

For an acceleration hinge j whose outboard body's outboard hinge is also an acceleration hinge

$$\mathbf{q}_{j+1,j+2} = \mathbf{0} \quad (5.66)$$

$$\mathbf{m}_{j+1,j+2} = \mathbf{0} \quad (5.67)$$

The transfer equation for the outboard rigid body of the acceleration hinge j is

$$\mathbf{z}_{j+1,j+2} = \mathbf{U}_{j+1} \mathbf{z}_{j+1,j} \quad (5.68)$$

The state vectors and transfer matrix in the form of a partitioned matrix are

$$\mathbf{z}_{j+1,j+2} = \begin{bmatrix} \ddot{\mathbf{r}} \\ \dot{\mathbf{Q}} \\ \mathbf{m} \\ \mathbf{q} \\ 1 \end{bmatrix}_{j+1,j+2}, \quad \mathbf{z}_{j+1,j} = \begin{bmatrix} \ddot{\mathbf{r}} \\ \dot{\mathbf{Q}} \\ \mathbf{m} \\ \mathbf{q} \\ 1 \end{bmatrix}_{j+1,j}, \quad \mathbf{U}_{j+1} = \begin{bmatrix} \mathbf{u}_{1,1} & \mathbf{u}_{1,2} & \mathbf{u}_{1,3} & \mathbf{u}_{1,4} & \mathbf{u}_{1,5} \\ \mathbf{u}_{2,1} & \mathbf{u}_{2,2} & \mathbf{u}_{2,3} & \mathbf{u}_{2,4} & \mathbf{u}_{2,5} \\ \mathbf{u}_{3,1} & \mathbf{u}_{3,2} & \mathbf{u}_{3,3} & \mathbf{u}_{3,4} & \mathbf{u}_{3,5} \\ \mathbf{u}_{4,1} & \mathbf{u}_{4,2} & \mathbf{u}_{4,3} & \mathbf{u}_{4,4} & \mathbf{u}_{4,5} \\ \mathbf{O}_{1 \times 3} & \mathbf{O}_{1 \times 3} & \mathbf{O}_{1 \times 3} & \mathbf{O}_{1 \times 3} & 1 \end{bmatrix}_{j+1} \quad (5.69)$$

The relation of internal moments between the input and output ends of a rigid body is

$$\mathbf{m}_{j+1,j+2} = \mathbf{u}_{3,1}\ddot{\mathbf{r}}_{j+1,j} + \mathbf{u}_{3,2}\dot{\mathbf{Q}}_{j+1,j} + \mathbf{u}_{3,3}\mathbf{m}_{j+1,j} + \mathbf{u}_{3,4}\mathbf{q}_{j+1,j} + \mathbf{u}_{3,5} \quad (5.70)$$

where $\mathbf{u}_{m,n}$ is the corresponding partitioned submatrix of \mathbf{U}_{j+1} , the transfer matrix of the outboard body, given in Equation (5.69).

Substituting the above equations into Equation (5.67), the relation of angular accelerations between the input and output ends of the hinge can be obtained

$$\dot{\mathbf{Q}}_{j+1,j} = -\mathbf{u}_{3,2}^{-1}\mathbf{u}_{3,1}\ddot{\mathbf{r}}_{j-1,j} - \mathbf{u}_{3,2}^{-1}\mathbf{u}_{3,3}\mathbf{m}_{j-1,j} - \mathbf{u}_{3,2}^{-1}\mathbf{u}_{3,4}\mathbf{q}_{j-1,j} - \mathbf{u}_{3,2}^{-1}\mathbf{u}_{3,5} \quad (5.71)$$

In the same way, we can obtain

$$\ddot{\mathbf{r}}_{j+1,j} = -\mathbf{u}_{4,1}^{-1}\mathbf{u}_{4,2}\dot{\mathbf{Q}}_{j-1,j} - \mathbf{u}_{4,1}^{-1}\mathbf{u}_{4,3}\mathbf{m}_{j-1,j} - \mathbf{u}_{4,1}^{-1}\mathbf{u}_{4,4}\mathbf{q}_{j-1,j} - \mathbf{u}_{4,1}^{-1}\mathbf{u}_{4,5} \quad (5.72)$$

Combining Equations (5.62), (5.64), (5.71) and (5.72), the transfer equation and transfer matrix of acceleration hinge j can be obtained

$$\mathbf{z}_{j+1,j} = \mathbf{U}_j \mathbf{z}_{j-1,j} \quad (5.73)$$

$$\mathbf{U}_j = \begin{bmatrix} \mathbf{O}_{3 \times 3} & -\mathbf{u}_{4,1}^{-1}\mathbf{u}_{4,2} & -\mathbf{u}_{4,1}^{-1}\mathbf{u}_{4,3} & -\mathbf{u}_{4,1}^{-1}\mathbf{u}_{4,4} & -\mathbf{u}_{4,1}^{-1}\mathbf{u}_{4,5} \\ -\mathbf{u}_{3,2}^{-1}\mathbf{u}_{3,1} & \mathbf{O}_{3 \times 3} & -\mathbf{u}_{3,2}^{-1}\mathbf{u}_{3,3} & -\mathbf{u}_{3,2}^{-1}\mathbf{u}_{3,4} & -\mathbf{u}_{3,2}^{-1}\mathbf{u}_{3,5} \\ \mathbf{O}_{3 \times 3} & \mathbf{O}_{3 \times 3} & \mathbf{I}_3 & \mathbf{O}_{3 \times 3} & \mathbf{O}_{3 \times 1} \\ \mathbf{O}_{3 \times 3} & \mathbf{O}_{3 \times 3} & \mathbf{O}_{3 \times 3} & \mathbf{I}_3 & \mathbf{O}_{3 \times 1} \\ \mathbf{O}_{1 \times 3} & \mathbf{O}_{1 \times 3} & \mathbf{O}_{1 \times 3} & \mathbf{O}_{1 \times 3} & 1 \end{bmatrix} \quad (5.74)$$

It can be proved and understood easily that the transfer equation and transfer matrix of an acceleration hinge moving in a plane are similar, corresponding to Equations (5.73) and (5.74), respectively, moving in space.

5.9 Algorithm of the Transfer Matrix Method for Multibody Systems

The algorithms of the new MSTMM and the original MSTMM are different because of the different state vectors defined in the two situations. Following the formulations given above, the motion quantities of a multibody system at different time instants for different subsystems can be obtained as follows:

- 1) Decide the initial conditions and system properties of the multibody system.
- 2) Set $i = 1$.
- 3) Knowing the initial conditions $\mathbf{r}(t_{i-1})$, $\dot{\mathbf{r}}(t_{i-1})$, $\boldsymbol{\theta}(t_{i-1})$, $\dot{\boldsymbol{\theta}}(t_{i-1})$, etc. and the system properties at time t_{i-1} , formulate the transfer matrix for each subsystem and the overall transfer matrix.

- 4) Apply boundary conditions to the end state vectors of the system and calculate the unknown quantities in the boundary state vectors as a function of the elements of the overall transfer matrix.
- 5) Knowing all the elements in the boundary state vector, the state vectors of each subsystem at time instant t_{i-1} can be computed by successive multiplication of the transfer matrices using the transfer equation of the elements.
- 6) By using the initial conditions $\mathbf{r}(t_{i-1})$, $\dot{\mathbf{r}}(t_{i-1})$, $\boldsymbol{\theta}(t_{i-1})$ and $\dot{\boldsymbol{\theta}}(t_{i-1})$, and the computed values of the accelerations $\ddot{\mathbf{r}}_{i-1}$ and angular accelerations $\ddot{\boldsymbol{\theta}}_{i-1}$ at t_{i-1} , compute the values of position coordinates $\mathbf{r}(t_i)$, velocities $\dot{\mathbf{r}}(t_i)$, orientation angles $\boldsymbol{\theta}(t_i)$ and $\dot{\boldsymbol{\theta}}(t_i)$, etc. at time t_i using any numerical integration procedures, for example the Runge–Kutta method.
- 7) Let $i = i + 1$, use the computed values of the last step as the initial conditions, and return to step 3. This procedure is repeated until the final time step is achieved.

5.10 Numerical Examples of Multibody System Dynamics

To verify the new MSTMM, the dynamics of a pendulum system consisting of three rigid body moving in space and the dynamics of space mechanical arm system are numerically calculated by the proposed method and the Newton–Euler method, respectively.

5.10.1 Dynamics of a Spatial Multibody System with Ball-and-socket Hinges

A spatial three pendulum system with three rigid bodies moving in space and connected by three smooth ball-and-socket hinges under the effect of gravity is shown in Figure 5.4. The body elements and the hinge elements are numbered: 0, 2 and 4 denote the sequence numbers of the smooth ball-and-socket hinges, and 1, 3 and 5 denote the sequence numbers of the body elements. The structure parameters of the three rigid bodies are the same. The coordinates of the mass center and the output point, the moment of inertia relative to the input-end body-fixed coordinate system, are

$$\begin{bmatrix} c_1 \\ c_2 \\ c_3 \end{bmatrix} = \begin{bmatrix} 0.5 \\ 0 \\ 0 \end{bmatrix} \text{ m}, \quad \begin{bmatrix} d_1 \\ d_2 \\ d_3 \end{bmatrix} = \begin{bmatrix} 1 \\ 0 \\ 0 \end{bmatrix} \text{ m}, \quad J_I = \begin{bmatrix} \frac{1}{6} & 0 & 0 \\ 0 & \frac{5}{12} & 0 \\ 0 & 0 & \frac{5}{12} \end{bmatrix} \text{ kg}\cdot\text{m}^2$$

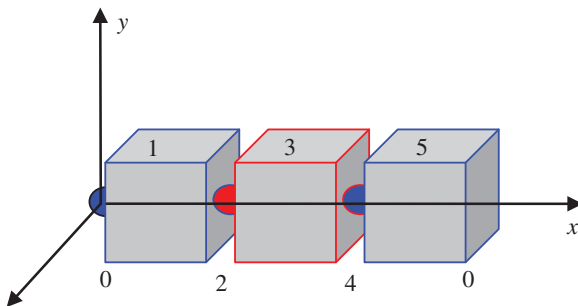
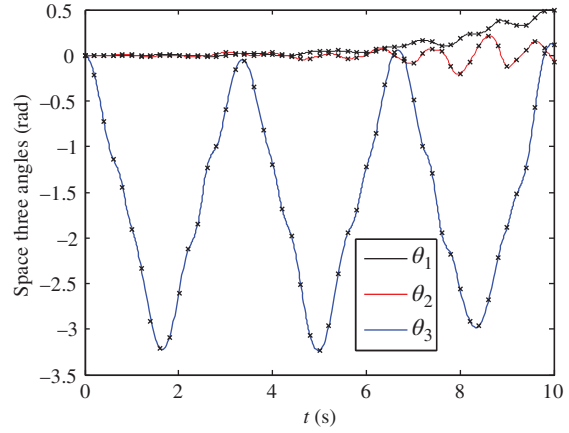


Figure 5.4 Dynamics model of a spatial three-pendulum system.

Figure 5.5 Time history of the space three angles of body element 1.



The initial conditions of the system are

$$\begin{bmatrix} \theta_1 \\ \theta_2 \\ \theta_3 \end{bmatrix}_2 = \begin{bmatrix} \theta_1 \\ \theta_2 \\ \theta_3 \end{bmatrix}_4 = \begin{bmatrix} \theta_1 \\ \theta_2 \\ \theta_3 \end{bmatrix}_6 = \begin{bmatrix} 0 \\ 0 \\ 0 \end{bmatrix} \text{ rad}, \quad \begin{bmatrix} \dot{\theta}_1 \\ \dot{\theta}_2 \\ \dot{\theta}_3 \end{bmatrix}_2 = \begin{bmatrix} \dot{\theta}_1 \\ \dot{\theta}_2 \\ \dot{\theta}_3 \end{bmatrix}_4 = \begin{bmatrix} 0 \\ 0 \\ 0 \end{bmatrix} \text{ rad/s}, \quad \begin{bmatrix} \dot{\theta}_1 \\ \dot{\theta}_2 \\ \dot{\theta}_3 \end{bmatrix}_6 = \begin{bmatrix} 0 \\ 0.1 \\ 0 \end{bmatrix} \text{ rad/s}$$

where $[\theta_1 \ \theta_2 \ \theta_3]_j^T$ represents the space three angles (x - y - z) of body element j .

The overall transfer equation and the overall transfer matrix and boundary conditions of the system are

$$\mathbf{z}_{5,0} = \mathbf{U}_{1-5} \mathbf{z}_{1,0}$$

$$\mathbf{U}_{1-5} = \mathbf{U}_5 \mathbf{U}_4 \mathbf{U}_3 \mathbf{U}_2 \mathbf{U}_1$$

$$\mathbf{z}_{1,0} = [0 \ 0 \ 0 \ \dot{\Omega}_x \ \dot{\Omega}_y \ \dot{\Omega}_z \ 0 \ 0 \ 0 \ q_x \ q_y \ q_z \ 1]^T_{1,0}$$

$$\mathbf{z}_{5,0} = [\ddot{x} \ \ddot{y} \ \ddot{z} \ \dot{\Omega}_x \ \dot{\Omega}_y \ \dot{\Omega}_z \ 0 \ 0 \ 0 \ 0 \ 0 \ 0 \ 1]^T_{5,0}$$

The time histories of the space three angles of rigid body 1 of the system obtained by the proposed method and by the Newton–Euler method are shown in Figure 5.5, represented with ‘line’ and ‘x’ respectively. It can be seen clearly from Figure 5.5 that the computational results of the two methods are in good agreement.

5.10.2 Dynamics of a Spatial Multibody System with Pin Hinges

A spatial mechanical arm system with three rigid bodies moving in space and connected by three smooth pin hinges under the effect of gravity is shown in Figure 5.6. The body elements and the hinge elements are numbered uniformly: 0, 2 and 4 denote the sequence numbers of the smooth pin elements, and 1, 3 and 5 denote the sequence numbers of the body elements. The structure parameters of the three rigid bodies are the same. The coordinates of the mass center and the output point, the moment of inertia relative to the input-end body-fixed coordinate system, are

$$\begin{bmatrix} c_1 \\ c_2 \\ c_3 \end{bmatrix} = \begin{bmatrix} 0.5 \\ 0 \\ 0 \end{bmatrix} \text{ m}, \quad \begin{bmatrix} d_1 \\ d_2 \\ d_3 \end{bmatrix} = \begin{bmatrix} 1 \\ 0 \\ 0 \end{bmatrix} \text{ m}, \quad \mathbf{J}_I = \begin{bmatrix} \frac{1}{6} & 0 & 0 \\ 0 & \frac{5}{12} & 0 \\ 0 & 0 & \frac{5}{12} \end{bmatrix} \text{ kg} \cdot \text{m}^2$$

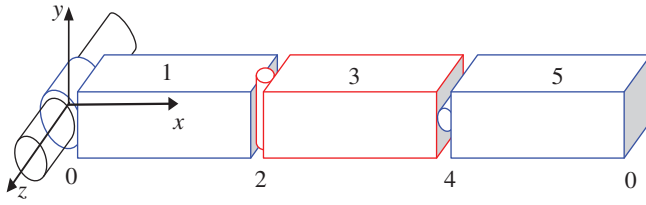


Figure 5.6 Spatial 3 degrees of freedom arm.

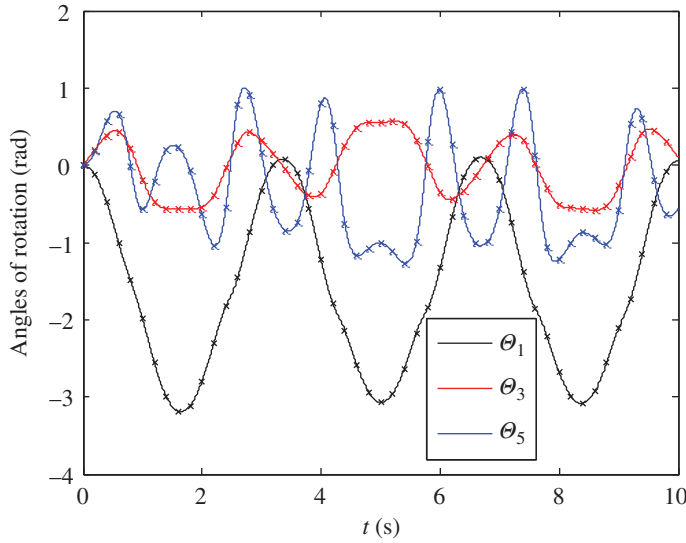


Figure 5.7 Time history of the relative rotation angles of the three pin hinges.

The relative rotation angle of pin element j is Θ_j and the initial conditions of the system are

$$\Theta_1 = \Theta_3 = \Theta_5 = 0 \text{ rad}, \quad \dot{\Theta}_1 = \dot{\Theta}_5 = 0 \text{ rad/s}, \quad \dot{\Theta}_3 = 1 \text{ rad/s}$$

The overall transfer equation and the overall transfer matrix and boundary conditions of the system are

$$\mathbf{z}_{5,0} = \mathbf{U}_{1-5} \mathbf{z}_{1,0}$$

$$\mathbf{U}_{1-5} = \mathbf{U}_5 \mathbf{U}_4 \mathbf{U}_3 \mathbf{U}_2 \mathbf{U}_1$$

$$\mathbf{z}_{1,0} = [0 \ 0 \ 0 \ 0 \ 0 \ \dot{\Omega}_z \ m_x \ m_y \ 0 \ q_x \ q_y \ q_z \ 1]^T_{1,0}$$

$$\mathbf{z}_{5,0} = [\ddot{x} \ \ddot{y} \ \ddot{z} \ \dot{\Omega}_x \ \dot{\Omega}_y \ \dot{\Omega}_z \ 0 \ 0 \ 0 \ 0 \ 0 \ 0 \ 1]^T_{5,0}$$

The time histories of the relative rotation angles of the three pin hinges of the system obtained by the proposed method and by the Newton–Euler method are shown in Figure 5.7, represented with ‘line’ and ‘x’ respectively. It can be seen clearly from Figure 5.7 that the computational results of the two methods are in good agreement.

5.10.3 Dynamics of a Spatial Multibody System with Spring and Damping Hinges

Here we choose a multibody system the same as the one given in section 5.10.2 to illustrate the use of spring and damping hinges moving in space. The only difference between the dynamic model in this section and that in section 5.10.2 is that the original smooth pin hinges are

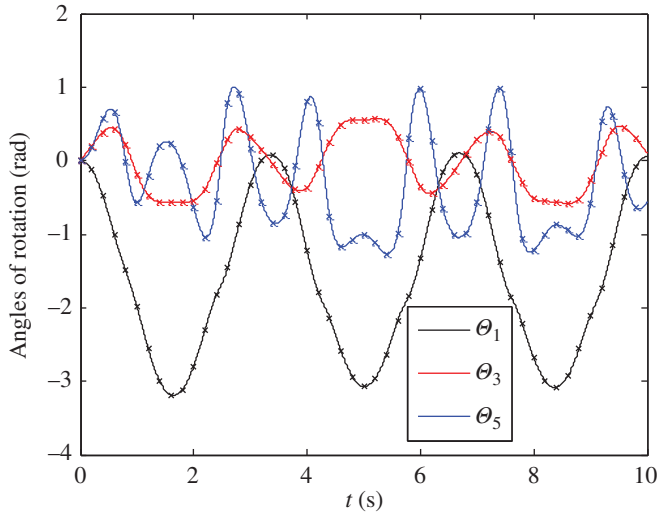


Figure 5.8 Time history of the relative rotation angles of the three hinges.

substituted by corresponding spring and damping hinges. The corresponding coefficients of the springs and dampers are appropriately selected according to the dynamical parameters of the system. One appropriate group of coefficients is

$$k_s = 100000 \text{ N/m} \quad c_s = 0 \text{ N/(m} \cdot \text{s}^{-1})$$

$$k_r = 100000 \text{ N} \cdot \text{m/rad} \quad c_r = 0 \text{ N} \cdot \text{m/(rad} \cdot \text{s}^{-1})$$

where k_s and c_s are the coefficients of the springs and dampers, and k_r and c_r are the coefficients of the rotary springs and dampers, which are used to simulate the connection relationship of the original smooth pin hinges.

The time histories of the relative rotation angles of the three hinges obtained by the smooth pin hinge model and by the elastic and damping hinges model are shown in Figure 5.8, represented with 'line' and 'x' respectively. It can be seen clearly from Figure 5.8 that the computational results of the two models are in good agreement.

6

Transfer Matrix Method for Multi-flexible-body Systems

6.1 Introduction

The transfer matrix method for multi-rigid-body systems was introduced in Chapter 5. The translational and angular accelerations together with internal forces and moments are taken as new state variables instead of position coordinates in the original transfer matrix method for multibody systems (MSTMM). This results in totally different transfer matrices of elements and algorithms compared with the original MSTMM. The proposed method expands the advantages of the MSTMM by allowing more sophisticated numerical integration procedures to be used, such as the Runge–Kutta method: no global dynamics equations of the system are required, matrices have low order, setup of the global transfer equation is highly programmable, and solution allows high computational precision since linearization is not required anymore. The new method is simple, straightforward, efficient, practical and provides a powerful tool for multibody system dynamics (MSD).

The dynamics of a multi-rigid-flexible-body system could also be solved by the transfer matrix method, in a way that is similar to dealing with a multi-rigid-body system. Hereafter, the way to study the dynamics of a multi-rigid-flexible-body system by using the transfer matrix method is called the transfer matrix method for multi-flexible-body systems, which is introduced in this chapter.

The floating frame of reference formulation is used while modeling a flexible body, which satisfies the assumption of small deformation. Using the small deformation assumption and the modal superposition method, the partial dynamics equations of the flexible body can be discretized into ordinary differential equations about the generalized coordinates. Then we can proceed to the next step, that is, to deduce the transfer equation and the corresponding transfer matrix of the flexible body.

The translational and angular accelerations together with internal forces and moments are taken as new state variables for flexible bodies. Recall that the same state variables are used in the transfer matrix method for multi-rigid-body systems. However, the form of the transfer equations in the transfer matrix method for multi-flexible-body systems will be a little different from that of the transfer equations in the transfer matrix method for multi-rigid-body systems due to consideration of the deformation of the flexible bodies. There are two kinds of transfer equations in the transfer matrix method for multi-flexible-body systems: the first is used to assemble the overall transfer equations of the system and the second is used to solve the deformation acceleration of each flexible body. The division of the transfer equations of flexible bodies makes it much simpler to analyze a general multibody system which consists of rigid bodies and flexible bodies using the transfer matrix method for multibody systems.

6.2 State Vector, Transfer Equation and Transfer Matrix

For simplicity, a chain multibody system is taken as an example to sketch the ideas of the transfer matrix method for multi-flexible-body systems. The new state vectors of the input and output ends of any flexible bodies and hinges moving in space are defined as

$$\mathbf{z} = [\ddot{x} \ \ddot{y} \ \ddot{z} \ \dot{\Omega}_x \ \dot{\Omega}_y \ \dot{\Omega}_z \ m_x \ m_y \ m_z \ q_x \ q_y \ q_z \ 1]^T \quad (6.1)$$

or

$$\mathbf{z} = [\dot{\mathbf{r}}^T \ \dot{\boldsymbol{\Omega}}^T \ \mathbf{m}^T \ \mathbf{q}^T \ 1]^T \quad (6.2)$$

where

$$\dot{\mathbf{r}} = \begin{bmatrix} \ddot{x} \\ \ddot{y} \\ \ddot{z} \end{bmatrix}, \quad \dot{\boldsymbol{\Omega}} = \begin{bmatrix} \dot{\Omega}_x \\ \dot{\Omega}_y \\ \dot{\Omega}_z \end{bmatrix}, \quad \mathbf{m} = \begin{bmatrix} m_x \\ m_y \\ m_z \end{bmatrix}, \quad \mathbf{q} = \begin{bmatrix} q_x \\ q_y \\ q_z \end{bmatrix} \quad (6.3)$$

$\ddot{x}, \ddot{y}, \ddot{z}, \dot{\Omega}_x, \dot{\Omega}_y$ and $\dot{\Omega}_z$ are the absolute accelerations of the connection point with respect to the inertial reference system $oxyz$ and the corresponding absolute angular accelerations in the directions of x, y and z , m_x, m_y, m_z, q_x, q_y and q_z are the corresponding internal torques and internal forces in the same reference system, respectively, and $\dot{\mathbf{r}}, \dot{\boldsymbol{\Omega}}, \mathbf{m}$ and \mathbf{q} are the column vectors of absolute accelerations, absolute angular accelerations, internal torques and internal forces in $oxyz$, respectively.

For a chain system moving in a plane, the new state vectors of the input ends and output ends of any flexible bodies and hinges are defined as

$$\mathbf{z} = [\ddot{x} \ \ddot{y} \ \dot{\Omega}_z \ m_z \ q_x \ q_y \ 1]^T \quad (6.4)$$

or

$$\mathbf{z} = [\dot{\mathbf{r}}^T \ \dot{\boldsymbol{\Omega}}^T \ \mathbf{m}^T \ \mathbf{q}^T \ 1]^T \quad (6.5)$$

where

$$\dot{\mathbf{r}} = \begin{bmatrix} \ddot{x} \\ \ddot{y} \end{bmatrix}, \quad \dot{\boldsymbol{\Omega}} = \dot{\Omega}_z, \quad \mathbf{m} = m_z, \quad \mathbf{q} = \begin{bmatrix} q_x \\ q_y \end{bmatrix}, \quad (6.6)$$

Then the dynamics equations of the j th flexible element can be assembled into two transfer equations

$$\mathbf{z}_{j,O}(t_i) = \mathbf{U}_j(t_i) \mathbf{z}_{j,I}(t_i) \quad (6.7)$$

$$\ddot{\mathbf{q}}_j = \hat{\mathbf{U}}_j \mathbf{z}_{j,I} \quad (6.8)$$

The transfer Equation (6.7) describes the transfer relationship between the state vectors at two ends of the j th element and the transfer Equation (6.8) is used to evaluate the deformation acceleration of the flexible body. Here, the matrix $\mathbf{U}_j(t_i)$ is the transfer matrix of the j th element which is known at time instant t_i . Its order is always (13×13) for any dynamics of a chain multi-rigid-body system moving in space or (7×7) for any dynamics of a chain multi-rigid-body system moving in a plane.

6.3 Overall Transfer Equation and Overall Transfer Matrix

According to Newton's third law, the state vector of the output end of an inboard element is equal to the state vector of the input end of an outboard element for any two adjoining elements in a multibody system. The overall transfer equation and transfer matrix of the system, which relates the state vectors at the boundaries of the system, can therefore be assembled for any chain multibody system as follows:

$$\mathbf{z}_{n,O} = \mathbf{U}_{1-n} \mathbf{z}_{1,I} \quad (6.9)$$

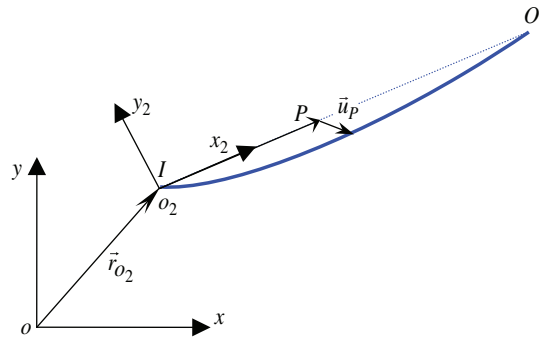
$$\mathbf{U}_{1-n} = \mathbf{U}_n \cdots \mathbf{U}_2 \mathbf{U}_1 \quad (6.10)$$

It can be seen from the overall transfer equation and the overall transfer matrix that the order of the overall transfer matrix of the system is equal to the order of the transfer matrix of an element for a chain system, and it does not increase even if the degrees of freedom of the system increase. Irrespective of the size of a multibody system, the highest order of the overall transfer matrix is the same as the order of the transfer matrix of a single body, that is, (13×13) for the dynamics of a chain multibody system moving in space or (7×7) for the dynamics of a chain multibody system moving in a plane. The matrices involved in the new MSTMM are therefore always small, which greatly reduces the computational time and the memory storage requirement.

6.4 Transfer Matrix of a Planar Beam

A planar flexible beam is shown in Figure 6.1, where $o_2x_2y_2z_2$ is the floating frame of the flexible body and $oxyz$ is the global inertial coordinate system. If there is no deformation of the flexible beam, the axis of the beam will coincide with o_2x_2 and the input point I of the beam will coincide with o_2 . Any point P on the beam is identified by its abscissa $\xi \in [0, l]$ in $o_2x_2y_2z_2$, where the abscissa of the input point is 0, the mass center is ξ_C and the output point is l . l is also the length of the flexible beam. $\bar{f}_\xi(\xi, t)$ and $\bar{f}_\eta(\xi, t)$ are used to represent the distributed external forces acting on the flexible beam. $u(\xi, t)$ and $v(\xi, t)$ are the deformations of the beam along the directions of o_2x_2 and o_2y_2 , respectively. The absolute accelerations, absolute angular accelerations, internal moments and internal forces of the input point or output point of the beam are denoted as $\ddot{\mathbf{r}}_I(\ddot{\mathbf{r}}_O)$, $\ddot{\theta}_{z,I}(\ddot{\theta}_{z,O})$, $m_{z,I}(m_{z,O})$ and $\mathbf{q}_I(\mathbf{q}_O)$, respectively, which are represented in $oxyz$. According to the sign conventions, the positive directions of \mathbf{q}_I and $m_{z,O}$ coincide with the positive directions of the axes of $oxyz$, while the positive directions of \mathbf{q}_O and $m_{z,I}$ coincide with the negative direction of the axes of $oxyz$.

Figure 6.1 A planar beam with large motion.



6.4.1 Deformation Mode of a Flexible Beam

The free vibration differential equations of a flexible beam are

$$\rho A \frac{\partial^2 u}{\partial t^2} - \frac{\partial}{\partial \xi} \left(EA \frac{\partial u}{\partial \xi} \right) = 0, \quad \rho A \frac{\partial^2 v}{\partial t^2} + \frac{\partial^2}{\partial \xi^2} \left(EI_z \frac{\partial^2 v}{\partial \xi^2} \right) = 0 \quad (6.11)$$

The inherent mode shapes and eigenvalues of the flexible beam along o_2x_2 and o_2y_2 are denoted by $\phi(\xi)$ and λ_ϕ , $\varphi(\xi)$ and λ_φ , respectively. The orders of $\phi(\xi)$ and $\varphi(\xi)$ are noted as n_ϕ and n_φ , respectively, the value of which depends on the convergence of the specific dynamical system. Let

$$\hat{\mathbf{M}}_{\phi,\phi} = \int_0^l \rho A \phi \phi^T d\xi, \quad \hat{\mathbf{M}}_{\varphi,\varphi} = \int_0^l \rho A \varphi \varphi^T d\xi \quad (6.12)$$

$$\hat{\mathbf{K}}_{\phi,\phi} = \int_0^l EA \phi' \phi'^T d\xi, \quad \hat{\mathbf{K}}_{\varphi,\varphi} = \int_0^l EI_z \varphi'' \varphi''^T d\xi \quad (6.13)$$

It can be verified that $\hat{\mathbf{M}}_{\phi,\phi}$, $\hat{\mathbf{M}}_{\varphi,\varphi}$, $\hat{\mathbf{K}}_{\phi,\phi}$ and $\hat{\mathbf{K}}_{\varphi,\varphi}$ are all diagonal matrices and satisfy the following relationships

$$\hat{\mathbf{K}}_{\phi,\phi} = \text{diag}(\lambda_\phi) \hat{\mathbf{M}}_{\phi,\phi}, \quad \hat{\mathbf{K}}_{\varphi,\varphi} = \text{diag}(\lambda_\varphi) \hat{\mathbf{M}}_{\varphi,\varphi} \quad (6.14)$$

As a result of the couplings among the vibrations in different directions and the large motion of the beam, the following constant parameters are defined

$$\hat{\mathbf{M}}_{\phi,I} = \int_0^l \rho A \phi d\xi, \quad \hat{\mathbf{M}}_{\varphi,I} = \int_0^l \rho A \varphi d\xi \quad (6.15)$$

$$\hat{\mathbf{M}}_{\phi,\xi} = \int_0^l \rho A \phi \xi d\xi, \quad \hat{\mathbf{M}}_{\varphi,\xi} = \int_0^l \rho A \varphi \xi d\xi \quad (6.16)$$

$$\hat{\mathbf{M}}_{\phi,\varphi} = \int_0^l \rho A \phi \varphi^T d\xi, \quad \hat{\mathbf{K}}_{j,\phi,\varphi} = \int_0^l \varphi_j' EA \phi' \varphi'^T d\xi \quad (6.17)$$

6.4.2 Dynamics Equation of a Planar Beam

For an arbitrary point P on the axis of a flexible beam, the orientation angle, absolute angular velocity and the absolute angular acceleration are, respectively

$$\theta_P = \theta_{o_2} + \frac{\partial}{\partial \xi} v, \quad \dot{\theta}_P = \dot{\theta}_{o_2} + \frac{\partial^2}{\partial \xi \partial t} v, \quad \ddot{\theta}_P = \ddot{\theta}_{o_2} + \frac{\partial^3}{\partial \xi \partial t^2} v \quad (6.18)$$

The position vector from the origin of $oxyz$ to point P is

$$\mathbf{r}_P = \mathbf{r}_{o_2} + \mathbf{A}_{o_2}(\mathbf{L} + \mathbf{u}) \quad (6.19)$$

where \mathbf{A}_{o_2} is the direction cosine matrix of $o_2x_2y_2z_2$ with respect to $oxyz$, which satisfies

$$\mathbf{A}_{o_2} = \mathbf{I} \cos \theta_{o_2} + \mathbf{D} \sin \theta_{o_2}, \quad \dot{\mathbf{A}}_{o_2} = \mathbf{A}_{o_2} \mathbf{D} \dot{\theta}_{o_2}, \quad \ddot{\mathbf{A}}_{o_2} = \mathbf{A}_{o_2} \mathbf{D} \ddot{\theta}_{o_2} - \mathbf{A}_{o_2} \dot{\theta}_{o_2}^2 \quad (6.20)$$

$$\mathbf{L} = \mathbf{H}_1 \xi, \quad \mathbf{u} = \mathbf{H}_1 \mathbf{u} + \mathbf{H}_2 v + \mathbf{H}_3 w \quad (6.21)$$

$$\mathbf{H}_1 = [1 \ 0]^T, \quad \mathbf{H}_2 = [0 \ 1]^T \quad (6.22)$$

$$\mathbf{D} = \begin{bmatrix} 0 & -1 \\ 1 & 0 \end{bmatrix} \quad (6.23)$$

The absolute velocity and acceleration of point P can be easily obtained by differentiating Equation (6.19) with respect to time

$$\dot{\mathbf{r}}_P = \dot{\mathbf{r}}_{o_2} + \mathbf{A}_{o_2} [\mathbf{D}(\mathbf{L} + \mathbf{u})\dot{\theta}_{o_2} + \dot{\mathbf{u}}] \quad (6.24)$$

$$\ddot{\mathbf{r}}_P = \ddot{\mathbf{r}}_{o_2} + \mathbf{A}_{o_2} [\mathbf{D}(\mathbf{L} + \mathbf{u})\ddot{\theta}_{o_2} + \ddot{\mathbf{u}} + 2\mathbf{D}\dot{\mathbf{u}}\dot{\theta}_{o_2} - (\mathbf{L} + \mathbf{u})\dot{\theta}_{o_2}^2] \quad (6.25)$$

The translational equation and the rotation equation of the beam, which makes up the dynamics equations governing the large motion of the beam, can be deduced based on the theorems of momentum and moment, respectively, as follows

$$\int_0^l \rho A [\mathbf{A}_{o_2}^T \ddot{\mathbf{r}}_{o_2} + \mathbf{D}(\mathbf{L} + \mathbf{u})\ddot{\theta}_{o_2} + \ddot{\mathbf{u}} + 2\mathbf{D}\dot{\mathbf{u}}\dot{\theta}_{o_2} - (\mathbf{L} + \mathbf{u})\dot{\theta}_{o_2}^2] d\xi \quad (6.26)$$

$$= \mathbf{f}_{o_2} + \mathbf{A}_{o_2}^T \mathbf{q}_I - \mathbf{A}_{o_2}^T \mathbf{q}_O$$

$$\int_0^l (\mathbf{L} + \mathbf{u})^T [(\mathbf{L} + \mathbf{u})\ddot{\theta}_{o_2} + \mathbf{D}^T \ddot{\mathbf{u}} + 2\dot{\mathbf{u}}\dot{\theta}_{o_2}] \rho A d\xi + m(\mathbf{L}_C + \mathbf{u}_C)^T \mathbf{D}^T \mathbf{A}_{o_2}^T \ddot{\mathbf{r}}_{o_2} \quad (6.27)$$

$$= m_{z,o_2} + m_{z,O} - m_{z,I} + (\mathbf{L}_I + \mathbf{u}_I)^T \mathbf{D}^T \mathbf{A}_{o_2}^T \mathbf{q}_I - (\mathbf{L}_O + \mathbf{u}_O)^T \mathbf{D}^T \mathbf{A}_{o_2}^T \mathbf{q}_O$$

where

$$\mathbf{f}_{o_2} = [f_{\xi,o_2} \ f_{\eta,o_2}]^T, \ m_{z,o_2} = \int_0^l \bar{f}_\eta \xi d\xi \quad (6.28)$$

$$f_{\xi,o_2} = \int_0^l \bar{f}_\xi d\xi, \ f_{\eta,o_2} = \int_0^l \bar{f}_\eta d\xi \quad (6.29)$$

The dynamics equations governing the longitudinal vibration and the transverse vibration of the beam are, respectively

$$\begin{aligned} & \rho A \mathbf{H}_1^T [\mathbf{A}_{o_2}^T \ddot{\mathbf{r}}_{o_2} + \mathbf{D}(\mathbf{L} + \mathbf{u})\ddot{\theta}_{o_2} + \ddot{\mathbf{u}} + 2\mathbf{D}\dot{\mathbf{u}}\dot{\theta}_{o_2} - (\mathbf{L} + \mathbf{u})\dot{\theta}_{o_2}^2] \\ &= \frac{\partial}{\partial \xi} \left(EA \frac{\partial \mathbf{u}}{\partial \xi} \right) + \bar{f}_\xi + \mathbf{H}_1^T \mathbf{A}_{o_2}^T \mathbf{q}_I \delta(\xi - 0) - \mathbf{H}_1^T \mathbf{A}_{o_2}^T \mathbf{q}_O \delta(\xi - l) \end{aligned} \quad (6.30)$$

$$\begin{aligned} & \rho A \mathbf{H}_2^T [\mathbf{A}_{o_2}^T \ddot{\mathbf{r}}_{o_2} + \mathbf{D}(\mathbf{L} + \mathbf{u})\ddot{\theta}_{o_2} + \ddot{\mathbf{u}} + 2\mathbf{D}\dot{\mathbf{u}}\dot{\theta}_{o_2} - (\mathbf{L} + \mathbf{u})\dot{\theta}_{o_2}^2] \\ &= -\frac{\partial^2}{\partial \xi^2} \left(EI_z \frac{\partial^2 \nu}{\partial \xi^2} \right) + \bar{f}_\eta + \mathbf{H}_2^T \mathbf{A}_{o_2}^T \mathbf{q}_I \delta(\xi - 0) - \mathbf{H}_2^T \mathbf{A}_{o_2}^T \mathbf{q}_O \delta(\xi - l) + \frac{\partial}{\partial \xi} \left(EA \frac{\partial \mathbf{u}}{\partial \xi} \frac{\partial \nu}{\partial \xi} \right) \end{aligned} \quad (6.31)$$

The last term of Equation (6.31) is used to take the effects of the axial force on the transverse vibration into consideration.

For an arbitrary point P on the axis of the flexible beam, we define

$$\ddot{\mathbf{R}}_P = \begin{bmatrix} \ddot{\mathbf{r}}_P \\ \ddot{\theta}_P \end{bmatrix}, \ \mathbf{Q}_P = \begin{bmatrix} m_{z,P} \\ \mathbf{q}_P \end{bmatrix} \quad (6.32)$$

To carry out the next step, the deformation of the beam is expanded into the form of modal superposition. Substituting the discretized deformation into the dynamics equations of the

beam described by partial differential equations, we can obtain the governing equations of the beam in the form of ordinary differential equations. The dynamics equations governing the large motion and the vibration of the beam are, respectively

$$\mathbf{a}_{1,1}\ddot{\mathbf{R}}_{o_2} + \mathbf{a}_{1,2}\ddot{\mathbf{q}} + \mathbf{a}_{1,3}\mathbf{Q}_I + \mathbf{a}_{1,4}\mathbf{Q}_O + \mathbf{a}_{1,5} = \mathbf{0} \quad (6.33)$$

$$\mathbf{a}_{2,1}\ddot{\mathbf{R}}_{o_2} + \mathbf{a}_{2,2}\ddot{\mathbf{q}} + \mathbf{a}_{2,3}\mathbf{Q}_I + \mathbf{a}_{2,4}\mathbf{Q}_O + \mathbf{a}_{2,5} = \mathbf{0} \quad (6.34)$$

where

$$\mathbf{a}_{1,1} = \begin{bmatrix} m\mathbf{A}_{o_2}^T & D\left(\mathbf{H}_1 m\xi_C + \mathbf{H}_1 \hat{\mathbf{M}}_{\phi,I}^T \hat{\mathbf{q}}_\phi + \mathbf{H}_2 \hat{\mathbf{M}}_{\phi,I}^T \hat{\mathbf{q}}_\phi\right) \\ m(\mathbf{L}_C + \mathbf{u}_C)^T D^T \mathbf{A}_{o_2}^T & J_{o_2} + 2\hat{\mathbf{M}}_{\phi,\xi}^T \hat{\mathbf{q}}_\phi + \hat{\mathbf{q}}_\phi^T \hat{\mathbf{M}}_{\phi,\phi} \hat{\mathbf{q}}_\phi + \hat{\mathbf{q}}_\phi^T \hat{\mathbf{M}}_{\phi,\varphi} \hat{\mathbf{q}}_\varphi \end{bmatrix} \quad (6.35)$$

$$\mathbf{a}_{1,2} = \begin{bmatrix} \mathbf{H}_1 \hat{\mathbf{M}}_{\phi,I}^T & \mathbf{H}_2 \hat{\mathbf{M}}_{\phi,I}^T \\ -\hat{\mathbf{q}}_\varphi^T \hat{\mathbf{M}}_{\phi,\varphi}^T & \hat{\mathbf{M}}_{\phi,\xi}^T + \hat{\mathbf{q}}_\phi^T \hat{\mathbf{M}}_{\phi,\varphi} \end{bmatrix} \quad (6.36)$$

$$\mathbf{a}_{1,3} = \begin{bmatrix} \mathbf{0} & -\mathbf{A}_{o_2}^T \\ 1 & -(\mathbf{L}_I + \mathbf{u}_I)^T D^T \mathbf{A}_{o_2}^T \end{bmatrix}, \quad \mathbf{a}_{1,4} = \begin{bmatrix} \mathbf{0} & \mathbf{A}_{o_2}^T \\ -1 & (\mathbf{L}_O + \mathbf{u}_O)^T D^T \mathbf{A}_{o_2}^T \end{bmatrix} \quad (6.37)$$

$$\mathbf{a}_{1,5} = \begin{bmatrix} 2D\left(\mathbf{H}_1 \hat{\mathbf{M}}_{\phi,I}^T \dot{\hat{\mathbf{q}}}_\phi + \mathbf{H}_2 \hat{\mathbf{M}}_{\phi,I}^T \dot{\hat{\mathbf{q}}}_\phi\right) \dot{\theta}_{o_2} - \left(\mathbf{H}_1 m\xi_C + \mathbf{H}_1 \hat{\mathbf{M}}_{\phi,I}^T \hat{\mathbf{q}}_\phi + \mathbf{H}_2 \hat{\mathbf{M}}_{\phi,I}^T \hat{\mathbf{q}}_\phi\right) \dot{\theta}_{o_2}^2 - \mathbf{f}_{o_2} \\ 2\dot{\theta}_{o_2} \left(\hat{\mathbf{M}}_{\phi,\xi}^T \dot{\hat{\mathbf{q}}}_\phi + \hat{\mathbf{q}}_\phi^T \hat{\mathbf{M}}_{\phi,\phi} \dot{\hat{\mathbf{q}}}_\phi + \hat{\mathbf{q}}_\phi^T \hat{\mathbf{M}}_{\phi,\varphi} \dot{\hat{\mathbf{q}}}_\varphi\right) - m_{z,o_2} \end{bmatrix} \quad (6.38)$$

$$\mathbf{a}_{2,1} = \begin{bmatrix} \hat{\mathbf{M}}_{\phi,I} \mathbf{H}_1^T \mathbf{A}_{o_2}^T & -\hat{\mathbf{M}}_{\phi,\varphi} \hat{\mathbf{q}}_\varphi \\ \hat{\mathbf{M}}_{\phi,I} \mathbf{H}_2^T \mathbf{A}_{o_2}^T & \hat{\mathbf{M}}_{\phi,\xi} + \hat{\mathbf{M}}_{\phi,\varphi}^T \hat{\mathbf{q}}_\phi \end{bmatrix}, \quad \mathbf{a}_{2,2} = \begin{bmatrix} \hat{\mathbf{M}}_{\phi,\phi} \\ \hat{\mathbf{M}}_{\phi,\varphi} \end{bmatrix} \quad (6.39)$$

$$\mathbf{a}_{2,3} = \begin{bmatrix} \mathbf{0} & -\phi(0) \mathbf{H}_1^T \mathbf{A}_{o_2}^T \\ \mathbf{0} & -\varphi(0) \mathbf{H}_2^T \mathbf{A}_{o_2}^T \end{bmatrix}, \quad \mathbf{a}_{2,4} = \begin{bmatrix} \mathbf{0} & \phi(l) \mathbf{H}_1^T \mathbf{A}_{o_2}^T \\ \mathbf{0} & \varphi(l) \mathbf{H}_2^T \mathbf{A}_{o_2}^T \end{bmatrix} \quad (6.40)$$

$$\mathbf{a}_{2,5} = \begin{bmatrix} \hat{\mathbf{K}}_{\phi,\phi} \hat{\mathbf{q}}_\phi - \mathbf{f}_\xi - 2\hat{\mathbf{M}}_{\phi,\varphi} \dot{\hat{\mathbf{q}}}_\varphi \dot{\theta}_{o_2} - \left(\hat{\mathbf{M}}_{\phi,\xi} + \hat{\mathbf{M}}_{\phi,\varphi} \hat{\mathbf{q}}_\phi\right) \dot{\theta}_{o_2}^2 \\ \hat{\mathbf{K}}_{\phi,\varphi} \hat{\mathbf{q}}_\varphi - \mathbf{f}_\eta + 2\hat{\mathbf{M}}_{\phi,\varphi}^T \dot{\hat{\mathbf{q}}}_\phi \dot{\theta}_{o_2} - \hat{\mathbf{M}}_{\phi,\varphi} \hat{\mathbf{q}}_\phi \dot{\theta}_{o_2}^2 + \hat{\mathbf{f}} \end{bmatrix} \quad (6.41)$$

$$J_{o_2} = \int_0^l \xi^2 \rho A d\xi, \quad \mathbf{f}_\xi = \int_0^l \phi \bar{\mathbf{f}}_\xi d\xi, \quad \mathbf{f}_\eta = \int_0^l \varphi \bar{\mathbf{f}}_\eta d\xi \quad (6.42)$$

$$\hat{\mathbf{f}}_j = \hat{\mathbf{q}}_\phi^T \hat{\mathbf{K}}_{j,\phi,\varphi} \hat{\mathbf{q}}_\varphi \quad (6.43)$$

6.4.3 Deduction of the Transfer Equation of a Planar Beam

The kinematics Equations (6.18) and (6.25) of the beam can be combined and rewritten in the following form

$$\ddot{\mathbf{R}}_P = \mathbf{B}_{1,P} \ddot{\mathbf{R}}_{o_2} + \mathbf{B}_{2,P} \ddot{\mathbf{q}} + \mathbf{B}_{3,P} \quad (6.44)$$

where

$$\mathbf{B}_{1,P} = \begin{bmatrix} \mathbf{I} & \mathbf{A}_{o_2} D(\mathbf{L} + \mathbf{u}) \\ \mathbf{0}^T & 1 \end{bmatrix}_P, \quad \mathbf{B}_{2,P} = \begin{bmatrix} \mathbf{A}_{o_2} \mathbf{H}_1 \phi^T & \mathbf{A}_{o_2} \mathbf{H}_2 \varphi^T \\ \mathbf{0}^T & \varphi'^T \end{bmatrix}_P \quad (6.45)$$

$$\mathbf{B}_{3,P} = \begin{bmatrix} 2\mathbf{A}_{o_2} \mathbf{D} \dot{\mathbf{u}} \dot{\theta}_{o_2} - \mathbf{A}_{o_2} (\mathbf{L} + \mathbf{u}) \dot{\theta}_{o_2}^2 \\ 0 \end{bmatrix}_P \quad (6.46)$$

Then for the input and output points of the beam we have

$$\ddot{\mathbf{R}}_I = \mathbf{B}_{1,I} \ddot{\mathbf{R}}_{o_2} + \mathbf{B}_{2,I} \ddot{\mathbf{q}} + \mathbf{B}_{3,I} \quad (6.47)$$

$$\ddot{\mathbf{R}}_O = \mathbf{B}_{1,O} \ddot{\mathbf{R}}_{o_2} + \mathbf{B}_{2,O} \ddot{\mathbf{q}} + \mathbf{B}_{3,O} \quad (6.48)$$

Define the form of the state vector \mathbf{z} of the connecting points of the beam, including the input and output points, as

$$\mathbf{z} = [\ddot{x} \ \ddot{y} \ \ddot{\theta}_z \ m_z \ q_x \ q_y \ 1]^T \quad (6.49)$$

which can be rewritten simplified as

$$\mathbf{z} = [\ddot{\mathbf{R}}^T \ \mathbf{Q}^T \ 1]^T \quad (6.50)$$

Combining Equations (6.33), (6.34), (6.47) and (6.48), the transfer equation of the planar beam can be obtained, namely

$$\mathbf{z}_O = \mathbf{U} \mathbf{z}_I, \quad \ddot{\mathbf{q}} = \hat{\mathbf{U}} \mathbf{z}_I \quad (6.51)$$

The corresponding transfer matrices are

$$\mathbf{U} = \begin{bmatrix} \mathbf{E}_{14} & \mathbf{E}_{12} \mathbf{E}_{10} & \mathbf{E}_{15} \\ -\mathbf{E}_7^{-1} \mathbf{E}_5 & -\mathbf{E}_7^{-1} \mathbf{E}_6 & -\mathbf{E}_7^{-1} \mathbf{E}_8 \\ \mathbf{0}^T & \mathbf{0}^T & 1 \end{bmatrix}, \quad \hat{\mathbf{U}} = [\mathbf{E}_9 \ \mathbf{E}_{10} \ \mathbf{E}_{11}] \quad (6.52)$$

where

$$\mathbf{E}_1 = \mathbf{a}_{1,2} - \mathbf{a}_{1,1} \mathbf{B}_{1,I}^{-1} \mathbf{B}_{2,I}, \quad \mathbf{E}_2 = \mathbf{a}_{1,5} - \mathbf{a}_{1,1} \mathbf{B}_{1,I}^{-1} \mathbf{B}_{3,I} \quad (6.53)$$

$$\mathbf{E}_3 = \mathbf{a}_{2,2} - \mathbf{a}_{2,1} \mathbf{B}_{1,I}^{-1} \mathbf{B}_{2,I}, \quad \mathbf{E}_4 = \mathbf{a}_{2,5} - \mathbf{a}_{2,1} \mathbf{B}_{1,I}^{-1} \mathbf{B}_{3,I} \quad (6.54)$$

$$\mathbf{E}_5 = \mathbf{a}_{1,1} \mathbf{B}_{1,I}^{-1} - \mathbf{E}_1 \mathbf{E}_3^{-1} \mathbf{a}_{2,1} \mathbf{B}_{1,I}^{-1}, \quad \mathbf{E}_6 = \mathbf{a}_{1,3} - \mathbf{E}_1 \mathbf{E}_3^{-1} \mathbf{a}_{2,3} \quad (6.55)$$

$$\mathbf{E}_7 = \mathbf{a}_{1,4} - \mathbf{E}_1 \mathbf{E}_3^{-1} \mathbf{a}_{2,4}, \quad \mathbf{E}_8 = \mathbf{E}_2 - \mathbf{E}_1 \mathbf{E}_3^{-1} \mathbf{E}_4 \quad (6.56)$$

$$\mathbf{E}_9 = \mathbf{E}_3^{-1} \mathbf{a}_{2,4} \mathbf{E}_7^{-1} \mathbf{E}_5 - \mathbf{E}_3^{-1} \mathbf{a}_{2,1} \mathbf{B}_{1,I}^{-1} \quad (6.57)$$

$$\mathbf{E}_{10} = \mathbf{E}_3^{-1} \mathbf{a}_{2,4} \mathbf{E}_7^{-1} \mathbf{E}_6 - \mathbf{E}_3^{-1} \mathbf{a}_{2,3}, \quad \mathbf{E}_{11} = \mathbf{E}_3^{-1} \mathbf{a}_{2,4} \mathbf{E}_7^{-1} \mathbf{E}_8 - \mathbf{E}_3^{-1} \mathbf{E}_4 \quad (6.58)$$

$$\mathbf{E}_{12} = \mathbf{B}_{2,O} - \mathbf{B}_{1,O} \mathbf{B}_{1,I}^{-1} \mathbf{B}_{2,I}, \quad \mathbf{E}_{13} = \mathbf{B}_{3,O} - \mathbf{B}_{1,O} \mathbf{B}_{1,I}^{-1} \mathbf{B}_{3,I} \quad (6.59)$$

$$\mathbf{E}_{14} = \mathbf{B}_{1,O} \mathbf{B}_{1,I}^{-1} + \mathbf{E}_{12} \mathbf{E}_9, \quad \mathbf{E}_{15} = \mathbf{E}_{12} \mathbf{E}_{11} + \mathbf{E}_{13} \quad (6.60)$$

6.5 Transfer Matrix of a Spatial Beam

A spatial flexible beam is shown in Figure 6.2, where $o_2x_2y_2z_2$ is the floating frame of the flexible body and $oxyz$ is the global inertial coordinate system. If there is no deformation of the flexible beam, the axis of the beam will coincide with o_2x_2 and the input point I of the beam will coincide with o_2 . Any point P on the beam is identified by its abscissa $\xi \in [0, l]$ in $o_2x_2y_2z_2$, where the abscissa of the input point is 0, the mass center is ξ_C and the output point is l . l is also the length of the flexible beam. $\bar{f}_\xi(\xi, t)$, $\bar{f}_\eta(\xi, t)$ and $\bar{f}_\zeta(\xi, t)$ are used to represent the distributed external forces acting on the flexible beam and $u(\xi, t)$, $v(\xi, t)$ and $w(\xi, t)$ the deformations of the beam

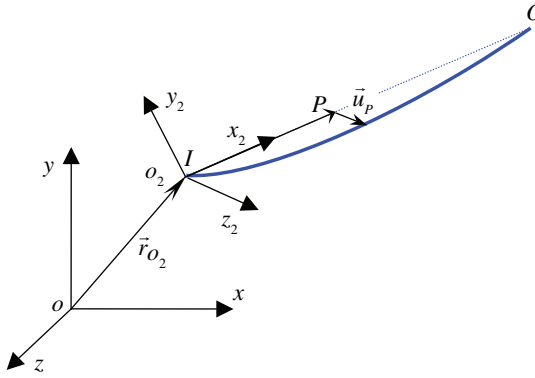


Figure 6.2 A spatial beam with large motion.

in the directions of o_2x_2 , o_2y_2 and o_2z_2 , respectively. The absolute accelerations, absolute angular accelerations, internal moments and internal forces of the input or output point of the beam are denoted by $\ddot{\mathbf{r}}_I(\ddot{\mathbf{r}}_O)$, $\dot{\mathbf{\Omega}}_I(\dot{\mathbf{\Omega}}_O)$, $\mathbf{m}_I(\mathbf{m}_O)$ and $\mathbf{q}_I(\mathbf{q}_O)$, respectively, which are represented in $oxyz$. According to the sign convention, the positive directions of \mathbf{q}_I and \mathbf{m}_O coincide with the positive directions of the axes of $oxyz$, while the positive directions of \mathbf{q}_O and \mathbf{m}_I coincide with the negative direction of the axes of $oxyz$.

6.5.1 Deformation Mode of a Flexible Beam

The free vibration differential equations of a flexible beam are

$$\rho A \frac{\partial^2 u}{\partial t^2} - \frac{\partial}{\partial \xi} \left(EA \frac{\partial u}{\partial \xi} \right) = 0 \quad (6.61)$$

$$\rho A \frac{\partial^2 v}{\partial t^2} + \frac{\partial^2}{\partial \xi^2} \left(EI_z \frac{\partial^2 v}{\partial \xi^2} \right) = 0, \quad \rho A \frac{\partial^2 w}{\partial t^2} + \frac{\partial^2}{\partial \xi^2} \left(EI_y \frac{\partial^2 w}{\partial \xi^2} \right) = 0 \quad (6.62)$$

The inherent mode shapes and eigenvalues of the flexible beam along o_2x_2 , o_2y_2 and o_2z_2 are denoted by $\phi(\xi)$ and λ_ϕ , $\varphi(\xi)$ and λ_φ , and $\psi(\xi)$ and λ_ψ , respectively. The orders of $\phi(\xi)$, $\varphi(\xi)$ and $\psi(\xi)$ are n_ϕ , n_φ and n_ψ , respectively, the value of which depends on the convergence of the specific dynamical system. Let

$$\hat{\mathbf{M}}_{\phi,\phi} = \int_0^l \rho A \phi \phi^T d\xi, \quad \hat{\mathbf{M}}_{\varphi,\varphi} = \int_0^l \rho A \varphi \varphi^T d\xi, \quad \hat{\mathbf{M}}_{\psi,\psi} = \int_0^l \rho A \psi \psi^T d\xi \quad (6.63)$$

$$\hat{\mathbf{K}}_{\phi,\phi} = \int_0^l EA \phi' \phi'^T d\xi, \quad \hat{\mathbf{K}}_{\varphi,\varphi} = \int_0^l EI_z \varphi'' \varphi''^T d\xi, \quad \hat{\mathbf{K}}_{\psi,\psi} = \int_0^l EI_y \psi'' \psi''^T d\xi \quad (6.64)$$

It can be verified that $\hat{\mathbf{M}}_{\phi,\phi}$, $\hat{\mathbf{M}}_{\varphi,\varphi}$, $\hat{\mathbf{M}}_{\psi,\psi}$, $\hat{\mathbf{K}}_{\phi,\phi}$, $\hat{\mathbf{K}}_{\varphi,\varphi}$ and $\hat{\mathbf{K}}_{\psi,\psi}$ are all diagonal matrices that satisfy the following relationships

$$\hat{\mathbf{K}}_{\phi,\phi} = \text{diag}(\lambda_\phi) \hat{\mathbf{M}}_{\phi,\phi}, \quad \hat{\mathbf{K}}_{\varphi,\varphi} = \text{diag}(\lambda_\varphi) \hat{\mathbf{M}}_{\varphi,\varphi}, \quad \hat{\mathbf{K}}_{\psi,\psi} = \text{diag}(\lambda_\psi) \hat{\mathbf{M}}_{\psi,\psi} \quad (6.65)$$

As a result of the couplings among the vibrations in different directions and the large motion of the beam, the following constant parameters are defined

$$\hat{M}_{\phi,I} = \int_0^l \rho A \phi d\xi, \quad \hat{M}_{\varphi,I} = \int_0^l \rho A \varphi d\xi, \quad \hat{M}_{\psi,I} = \int_0^l \rho A \psi d\xi \quad (6.66)$$

$$\hat{M}_{\phi,\xi} = \int_0^l \rho A \phi \xi d\xi, \quad \hat{M}_{\varphi,\xi} = \int_0^l \rho A \varphi \xi d\xi, \quad \hat{M}_{\psi,\xi} = \int_0^l \rho A \psi \xi d\xi \quad (6.67)$$

$$\hat{M}_{\phi,\varphi} = \int_0^l \rho A \phi \varphi^T d\xi, \quad \hat{M}_{\phi,\psi} = \int_0^l \rho A \phi \psi^T d\xi, \quad \hat{M}_{\varphi,\psi} = \int_0^l \rho A \varphi \psi^T d\xi \quad (6.68)$$

$$\hat{K}_{j,\phi,\varphi} = \int_0^l \varphi'_j E A \phi' \varphi'^T d\xi, \quad \hat{K}_{j,\phi,\psi} = \int_0^l \psi'_j E A \phi' \psi'^T d\xi \quad (6.69)$$

6.5.2 Dynamics Equation of a Spatial Beam

For an arbitrary point P on the axis of a flexible beam, the rotation angle caused by the deformation of the beam is

$$\theta(\xi, t) = \begin{bmatrix} 0 & -\frac{\partial}{\partial \xi} w & \frac{\partial}{\partial \xi} v \end{bmatrix}^T \quad (6.70)$$

which is represented in $o_2x_2y_2z_2$.

The direction cosine matrix, angular velocity and angular acceleration of the body fixed coordinate system of this point with respect to $oxyz$ are, respectively

$$A_P = A_{o_2} \left(I + \tilde{\theta}_P \right) \quad (6.71)$$

$$\Omega_P = \Omega_{o_2} + A_{o_2} \dot{\theta}_P \quad (6.72)$$

$$\dot{\Omega}_P = \dot{\Omega}_{o_2} + A_{o_2} \ddot{\theta}_P + \tilde{\Omega}_{o_2} A_{o_2} \dot{\theta}_P \quad (6.73)$$

which are all represented in $oxyz$. A_{o_2} is the direction cosine matrix of $o_2x_2y_2z_2$ with respect to $oxyz$.

The position vector from the origin of $oxyz$ to point P is

$$r_P = r_{o_2} + A_{o_2} (L + u) \quad (6.74)$$

where

$$L = H_1 \xi \quad u = H_1 u + H_2 v + H_3 w \quad (6.75)$$

$$H_1 = [1 \ 0 \ 0]^T, \quad H_2 = [0 \ 1 \ 0]^T, \quad H_3 = [0 \ 0 \ 1]^T \quad (6.76)$$

The absolute velocity and acceleration of point P can be easily obtained by differentiating Equation (6.19) with respect to time

$$\dot{r}_P = \dot{r}_{o_2} + A_{o_2} \tilde{\omega}_{o_2} (L + u) + A_{o_2} \dot{u} \quad (6.77)$$

$$\ddot{r}_P = \ddot{r}_{o_2} + A_{o_2} \tilde{\omega}_{o_2} \tilde{\omega}_{o_2} (L + u) - A_{o_2} \left(\tilde{L} + \tilde{u} \right) \dot{\omega}_{o_2} + 2A_{o_2} \tilde{\omega}_{o_2} \dot{u} + A_{o_2} \ddot{u} \quad (6.78)$$

The translational equation and the rotation equation of the beam, which make up the dynamics equations governing the large motion of the beam, can be deduced based on the theorems of momentum and moment, respectively, as follows

$$\begin{aligned} & \int_0^l \rho A \left[\mathbf{A}_{o_2}^T \ddot{\mathbf{r}}_{o_2} + \tilde{\boldsymbol{\omega}}_{o_2} \tilde{\boldsymbol{\omega}}_{o_2} (\mathbf{L} + \mathbf{u}) - \left(\tilde{\mathbf{L}} + \tilde{\mathbf{u}} \right) \dot{\boldsymbol{\omega}}_{o_2} + 2\tilde{\boldsymbol{\omega}}_{o_2} \dot{\mathbf{u}} + \ddot{\mathbf{u}} \right] d\xi \\ & = \mathbf{f}_{o_2} + \mathbf{A}_{o_2}^T \mathbf{q}_I - \mathbf{A}_{o_2}^T \mathbf{q}_O \end{aligned} \quad (6.79)$$

$$\begin{aligned} & \int_0^l \left(\tilde{\mathbf{L}} + \tilde{\mathbf{u}} \right) \left[\tilde{\boldsymbol{\omega}}_{o_2} \tilde{\boldsymbol{\omega}}_{o_2} (\mathbf{L} + \mathbf{u}) - \left(\tilde{\mathbf{L}} + \tilde{\mathbf{u}} \right) \dot{\boldsymbol{\omega}}_{o_2} + 2\tilde{\boldsymbol{\omega}}_{o_2} \dot{\mathbf{u}} + \ddot{\mathbf{u}} \right] \rho A d\xi + m \left(\tilde{\mathbf{L}}_C + \tilde{\mathbf{u}}_C \right) \mathbf{A}_{o_2}^T \ddot{\mathbf{r}}_{o_2} \\ & + J_\xi \mathbf{H}_1 \mathbf{H}_1^T \dot{\boldsymbol{\omega}}_{o_2} + J_\xi \mathbf{H}_1^T \boldsymbol{\omega}_{o_2} \tilde{\boldsymbol{\omega}}_{o_2} \mathbf{H}_1 \\ & = \mathbf{m}_{o_2} + \mathbf{A}_{o_2}^T \mathbf{m}_O - \mathbf{A}_{o_2}^T \mathbf{m}_I + \left(\tilde{\mathbf{L}}_I + \tilde{\mathbf{u}}_I \right) \mathbf{A}_{o_2}^T \mathbf{q}_I - \left(\tilde{\mathbf{L}}_O + \tilde{\mathbf{u}}_O \right) \mathbf{A}_{o_2}^T \mathbf{q}_O \end{aligned} \quad (6.80)$$

where

$$\mathbf{f}_{o_2} = [f_{\xi, o_2} \quad f_{\eta, o_2} \quad f_{\zeta, o_2}]^T, \quad \mathbf{m}_{o_2} = \left[\int_0^l \bar{m}_\xi d\xi \quad - \int_0^l \bar{f}_\xi \xi d\xi \quad \int_0^l \bar{f}_\eta \xi d\xi \right] \quad (6.81)$$

$$f_{\xi, o_2} = \int_0^l \bar{f}_\xi d\xi, \quad f_{\eta, o_2} = \int_0^l \bar{f}_\eta d\xi, \quad f_{\zeta, o_2} = \int_0^l \bar{f}_\zeta d\xi \quad (6.82)$$

The dynamics equations governing the longitudinal vibration and the transverse vibration of the beam are, respectively

$$\begin{aligned} & \rho A \left[\mathbf{H}_1^T \mathbf{A}_{o_2}^T \ddot{\mathbf{r}}_{o_2} + \mathbf{H}_1^T \tilde{\boldsymbol{\omega}}_{o_2} \tilde{\boldsymbol{\omega}}_{o_2} (\mathbf{L} + \mathbf{u}) - \mathbf{H}_1^T \left(\tilde{\mathbf{L}} + \tilde{\mathbf{u}} \right) \dot{\boldsymbol{\omega}}_{o_2} + 2\mathbf{H}_1^T \tilde{\boldsymbol{\omega}}_{o_2} \dot{\mathbf{u}} + \ddot{\mathbf{u}} \right] \\ & = \frac{\partial}{\partial \xi} \left(EA \frac{\partial \mathbf{u}}{\partial \xi} \right) + \bar{f}_\xi + \mathbf{H}_1^T \mathbf{A}_{o_2}^T \mathbf{q}_I \delta(\xi - 0) - \mathbf{H}_1^T \mathbf{A}_{o_2}^T \mathbf{q}_O \delta(\xi - l) \end{aligned} \quad (6.83)$$

$$\begin{aligned} & \rho A \left[\mathbf{H}_2^T \mathbf{A}_{o_2}^T \ddot{\mathbf{r}}_{o_2} + \mathbf{H}_2^T \tilde{\boldsymbol{\omega}}_{o_2} \tilde{\boldsymbol{\omega}}_{o_2} (\mathbf{L} + \mathbf{u}) - \mathbf{H}_2^T \left(\tilde{\mathbf{L}} + \tilde{\mathbf{u}} \right) \dot{\boldsymbol{\omega}}_{o_2} + 2\mathbf{H}_2^T \tilde{\boldsymbol{\omega}}_{o_2} \dot{\mathbf{u}} + \ddot{\mathbf{v}} \right] \\ & = - \frac{\partial^2}{\partial \xi^2} \left(EI_z \frac{\partial^2 \mathbf{v}}{\partial \xi^2} \right) + \bar{f}_\eta + \mathbf{H}_2^T \mathbf{A}_{o_2}^T \mathbf{q}_I \delta(\xi - 0) - \mathbf{H}_2^T \mathbf{A}_{o_2}^T \mathbf{q}_O \delta(\xi - l) + \frac{\partial}{\partial \xi} \left(EA \frac{\partial \mathbf{u}}{\partial \xi} \frac{\partial \mathbf{v}}{\partial \xi} \right) \end{aligned} \quad (6.84)$$

$$\begin{aligned} & \rho A \left[\mathbf{H}_3^T \mathbf{A}_{o_2}^T \ddot{\mathbf{r}}_{o_2} + \mathbf{H}_3^T \tilde{\boldsymbol{\omega}}_{o_2} \tilde{\boldsymbol{\omega}}_{o_2} (\mathbf{L} + \mathbf{u}) - \mathbf{H}_3^T \left(\tilde{\mathbf{L}} + \tilde{\mathbf{u}} \right) \dot{\boldsymbol{\omega}}_{o_2} + 2\mathbf{H}_3^T \tilde{\boldsymbol{\omega}}_{o_2} \dot{\mathbf{u}} + \ddot{\mathbf{w}} \right] \\ & = - \frac{\partial^2}{\partial \xi^2} \left(EI_y \frac{\partial^2 \mathbf{w}}{\partial \xi^2} \right) + \bar{f}_\zeta + \mathbf{H}_3^T \mathbf{A}_{o_2}^T \mathbf{q}_I \delta(\xi - 0) - \mathbf{H}_3^T \mathbf{A}_{o_2}^T \mathbf{q}_O \delta(\xi - l) + \frac{\partial}{\partial \xi} \left(EA \frac{\partial \mathbf{u}}{\partial \xi} \frac{\partial \mathbf{w}}{\partial \xi} \right) \end{aligned} \quad (6.85)$$

The last term of Equation (6.31) is used to take the effects of the axial force on the transverse vibration into consideration. The same applies in Equation (6.85).

For an arbitrary point P on the axis of the flexible beam, we can define

$$\ddot{\mathbf{R}}_P = \begin{bmatrix} \ddot{\mathbf{r}}_P \\ \dot{\boldsymbol{\omega}}_P \end{bmatrix}, \quad \mathbf{Q}_P = \begin{bmatrix} \mathbf{m}_P \\ \mathbf{q}_P \end{bmatrix} \quad (6.86)$$

To carry out the next step, the deformation of the beam is expanded into the form of modal superposition. Substituting the discretized deformation into the dynamics equations of the beam described by partial differential equations, we can obtain the governing equations of the beam in the form of ordinary differential equations. The dynamics equations governing the large motion and the vibration of the beam are, respectively

$$\mathbf{a}_{1,1} \ddot{\mathbf{R}}_{o_2} + \mathbf{a}_{1,2} \ddot{\mathbf{q}} + \mathbf{a}_{1,3} \mathbf{Q}_I + \mathbf{a}_{1,4} \mathbf{Q}_O + \mathbf{a}_{1,5} = \mathbf{0} \quad (6.87)$$

$$\mathbf{a}_{2,1} \ddot{\mathbf{R}}_{o_2} + \mathbf{a}_{2,2} \ddot{\mathbf{q}} + \mathbf{a}_{2,3} \mathbf{Q}_I + \mathbf{a}_{2,4} \mathbf{Q}_O + \mathbf{a}_{2,5} = \mathbf{0} \quad (6.88)$$

where

$$\left\{ \begin{array}{l} \mathbf{a}_{1,1}(1,1) = m\mathbf{A}_{o_2}^T \quad \mathbf{a}_{1,1}(1,2) = -\left(\tilde{H}_1 m \xi_C + \tilde{H}_1 \hat{M}_{\phi,I}^T \hat{\mathbf{q}}_\phi + \tilde{H}_2 \hat{M}_{\phi,I}^T \hat{\mathbf{q}}_\phi + \tilde{H}_3 \hat{M}_{\psi,I}^T \hat{\mathbf{q}}_\psi\right) \mathbf{A}_{o_2}^T \\ \mathbf{a}_{1,1}(2,1) = m\left(\tilde{L}_C + \tilde{u}_C\right) \mathbf{A}_{o_2}^T \\ \mathbf{a}_{1,1}(2,2) = -\left(-J_\xi H_1 H_1^T + J_{o_2} \tilde{H}_1 \tilde{H}_1\right. \\ \quad + \tilde{H}_1 \tilde{H}_1 \hat{\mathbf{q}}_\phi^T \hat{M}_{\phi,\phi}^T \hat{\mathbf{q}}_\phi + \tilde{H}_2 \tilde{H}_2 \hat{\mathbf{q}}_\phi^T \hat{M}_{\phi,\phi}^T \hat{\mathbf{q}}_\phi + \tilde{H}_3 \tilde{H}_3 \hat{\mathbf{q}}_\psi^T \hat{M}_{\psi,\psi}^T \hat{\mathbf{q}}_\psi \\ \quad + 2\tilde{H}_1 \tilde{H}_1 \hat{M}_{\phi,\xi}^T \hat{\mathbf{q}}_\phi + \left(\tilde{H}_1 \tilde{H}_2 + \tilde{H}_2 \tilde{H}_1\right) \hat{M}_{\phi,\xi}^T \hat{\mathbf{q}}_\phi + \left(\tilde{H}_1 \tilde{H}_3 + \tilde{H}_3 \tilde{H}_1\right) \hat{M}_{\psi,\xi}^T \hat{\mathbf{q}}_\psi \\ \quad + \left(\tilde{H}_1 \tilde{H}_2 + \tilde{H}_2 \tilde{H}_1\right) \hat{\mathbf{q}}_\phi^T \hat{M}_{\phi,\phi}^T \hat{\mathbf{q}}_\phi + \left(\tilde{H}_1 \tilde{H}_3 + \tilde{H}_3 \tilde{H}_1\right) \hat{\mathbf{q}}_\phi^T \hat{M}_{\phi,\psi}^T \hat{\mathbf{q}}_\psi \\ \quad \left. + \left(\tilde{H}_2 \tilde{H}_3 + \tilde{H}_3 \tilde{H}_2\right) \hat{\mathbf{q}}_\phi^T \hat{M}_{\phi,\psi}^T \hat{\mathbf{q}}_\psi\right) \mathbf{A}_{o_2}^T \end{array} \right. \quad (6.89)$$

$$\left\{ \begin{array}{l} \mathbf{a}_{1,2}(1,1) = H_1 \hat{M}_{\phi,I}^T \quad \mathbf{a}_{1,2}(1,2) = H_2 \hat{M}_{\phi,I}^T \quad \mathbf{a}_{1,2}(1,3) = H_3 \hat{M}_{\psi,I}^T \\ \mathbf{a}_{1,2}(2,1) = \tilde{H}_1 H_1 \hat{M}_{\phi,\xi}^T + \tilde{H}_1 H_1 \hat{\mathbf{q}}_\phi^T \hat{M}_{\phi,\phi}^T + \tilde{H}_2 H_1 \hat{\mathbf{q}}_\phi^T \hat{M}_{\phi,\phi}^T + \tilde{H}_3 H_1 \hat{\mathbf{q}}_\psi^T \hat{M}_{\psi,\psi}^T \\ \mathbf{a}_{1,2}(2,2) = \tilde{H}_1 H_2 \hat{M}_{\phi,\xi}^T + \tilde{H}_1 H_2 \hat{\mathbf{q}}_\phi^T \hat{M}_{\phi,\phi}^T + \tilde{H}_2 H_2 \hat{\mathbf{q}}_\phi^T \hat{M}_{\phi,\phi}^T + \tilde{H}_3 H_2 \hat{\mathbf{q}}_\psi^T \hat{M}_{\psi,\psi}^T \\ \mathbf{a}_{1,2}(2,3) = \tilde{H}_1 H_3 \hat{M}_{\psi,\xi}^T + \tilde{H}_1 H_3 \hat{\mathbf{q}}_\phi^T \hat{M}_{\phi,\psi}^T + \tilde{H}_2 H_3 \hat{\mathbf{q}}_\phi^T \hat{M}_{\phi,\psi}^T + \tilde{H}_3 H_3 \hat{\mathbf{q}}_\psi^T \hat{M}_{\psi,\psi}^T \end{array} \right. \quad (6.90)$$

$$\mathbf{a}_{1,3} = \begin{bmatrix} \mathbf{0} & -\mathbf{A}_{o_2}^T \\ \mathbf{A}_{o_2}^T & -\left(\tilde{L}_I + \tilde{u}_I\right) \mathbf{A}_{o_2}^T \end{bmatrix}, \quad \mathbf{a}_{1,4} = \begin{bmatrix} \mathbf{0} & \mathbf{A}_{o_2}^T \\ -\mathbf{A}_{o_2}^T & \left(\tilde{L}_O + \tilde{u}_O\right) \mathbf{A}_{o_2}^T \end{bmatrix} \quad (6.91)$$

$$\left\{ \begin{array}{l} \mathbf{a}_{1,5}(1,1) = -\mathbf{f}_{o_2} + 2\tilde{\omega}_{o_2} \left(H_1 \hat{M}_{\phi,I}^T \dot{\hat{\mathbf{q}}}_\phi + H_2 \hat{M}_{\phi,I}^T \dot{\hat{\mathbf{q}}}_\phi + H_3 \hat{M}_{\psi,I}^T \dot{\hat{\mathbf{q}}}_\psi \right) \\ \quad + \tilde{\omega}_{o_2} \tilde{\omega}_{o_2} \left(H_1 m \xi_C + H_1 \hat{M}_{\phi,I}^T \hat{\mathbf{q}}_\phi + H_2 \hat{M}_{\phi,I}^T \hat{\mathbf{q}}_\phi + H_3 \hat{M}_{\psi,I}^T \hat{\mathbf{q}}_\psi \right) \\ \mathbf{a}_{1,5}(2,1) = J_\xi H_1^T \omega_{o_2} \tilde{\omega}_{o_2} H_1 - \mathbf{m}_{o_2} \\ \quad + \tilde{H}_1 \tilde{\omega}_{o_2} \tilde{\omega}_{o_2} \left(H_1 J_{o_2} + H_1 \hat{M}_{\phi,\xi}^T \hat{\mathbf{q}}_\phi + H_2 \hat{M}_{\phi,\xi}^T \hat{\mathbf{q}}_\phi + H_3 \hat{M}_{\psi,\xi}^T \hat{\mathbf{q}}_\psi \right) \\ \quad + \left(\tilde{H}_1 \tilde{\omega}_{o_2} \tilde{\omega}_{o_2} H_1 \hat{M}_{\phi,\xi}^T \hat{\mathbf{q}}_\phi + \tilde{H}_2 \tilde{\omega}_{o_2} \tilde{\omega}_{o_2} H_1 \hat{M}_{\phi,\xi}^T \hat{\mathbf{q}}_\phi + \tilde{H}_3 \tilde{\omega}_{o_2} \tilde{\omega}_{o_2} H_1 \hat{M}_{\psi,\xi}^T \hat{\mathbf{q}}_\psi \right) \\ \quad + \tilde{H}_1 \tilde{\omega}_{o_2} \tilde{\omega}_{o_2} H_1 \hat{\mathbf{q}}_\phi^T \hat{M}_{\phi,\phi}^T \hat{\mathbf{q}}_\phi + \tilde{H}_2 \tilde{\omega}_{o_2} \tilde{\omega}_{o_2} H_2 \hat{\mathbf{q}}_\phi^T \hat{M}_{\phi,\phi}^T \hat{\mathbf{q}}_\phi + \tilde{H}_3 \tilde{\omega}_{o_2} \tilde{\omega}_{o_2} H_3 \hat{\mathbf{q}}_\psi^T \hat{M}_{\psi,\psi}^T \hat{\mathbf{q}}_\psi \\ \quad + \left(\tilde{H}_1 \tilde{\omega}_{o_2} \tilde{\omega}_{o_2} H_2 + \tilde{H}_2 \tilde{\omega}_{o_2} \tilde{\omega}_{o_2} H_1 \right) \hat{\mathbf{q}}_\phi^T \hat{M}_{\phi,\phi}^T \hat{\mathbf{q}}_\phi \\ \quad + \left(\tilde{H}_1 \tilde{\omega}_{o_2} \tilde{\omega}_{o_2} H_3 + \tilde{H}_3 \tilde{\omega}_{o_2} \tilde{\omega}_{o_2} H_1 \right) \hat{\mathbf{q}}_\phi^T \hat{M}_{\phi,\psi}^T \hat{\mathbf{q}}_\psi \\ \quad + \left(\tilde{H}_2 \tilde{\omega}_{o_2} \tilde{\omega}_{o_2} H_3 + \tilde{H}_3 \tilde{\omega}_{o_2} \tilde{\omega}_{o_2} H_2 \right) \hat{\mathbf{q}}_\phi^T \hat{M}_{\phi,\psi}^T \hat{\mathbf{q}}_\psi \\ \quad + 2 \left(\tilde{H}_1 \tilde{\omega}_{o_2} H_1 \hat{M}_{\phi,\xi}^T \dot{\hat{\mathbf{q}}}_\phi + \tilde{H}_1 \tilde{\omega}_{o_2} H_2 \hat{M}_{\phi,\xi}^T \dot{\hat{\mathbf{q}}}_\phi + \tilde{H}_1 \tilde{\omega}_{o_2} H_3 \hat{M}_{\psi,\xi}^T \dot{\hat{\mathbf{q}}}_\psi \right) \\ \quad + 2 \left(\tilde{H}_1 \tilde{\omega}_{o_2} H_1 \hat{\mathbf{q}}_\phi^T \hat{M}_{\phi,\phi}^T \dot{\hat{\mathbf{q}}}_\phi + \tilde{H}_2 \tilde{\omega}_{o_2} H_2 \hat{\mathbf{q}}_\phi^T \hat{M}_{\phi,\phi}^T \dot{\hat{\mathbf{q}}}_\phi + \tilde{H}_3 \tilde{\omega}_{o_2} H_3 \hat{\mathbf{q}}_\psi^T \hat{M}_{\psi,\psi}^T \dot{\hat{\mathbf{q}}}_\psi \right) \\ \quad + 2 \left(\tilde{H}_1 \tilde{\omega}_{o_2} H_2 \hat{\mathbf{q}}_\phi^T \hat{M}_{\phi,\phi}^T \dot{\hat{\mathbf{q}}}_\phi + \tilde{H}_2 \tilde{\omega}_{o_2} H_1 \hat{\mathbf{q}}_\phi^T \hat{M}_{\phi,\phi}^T \dot{\hat{\mathbf{q}}}_\phi \right) \\ \quad + 2 \left(\tilde{H}_1 \tilde{\omega}_{o_2} H_3 \hat{\mathbf{q}}_\phi^T \hat{M}_{\phi,\psi}^T \dot{\hat{\mathbf{q}}}_\psi + \tilde{H}_3 \tilde{\omega}_{o_2} H_1 \hat{\mathbf{q}}_\phi^T \hat{M}_{\phi,\psi}^T \dot{\hat{\mathbf{q}}}_\psi \right) \\ \quad + 2 \left(\tilde{H}_2 \tilde{\omega}_{o_2} H_3 \hat{\mathbf{q}}_\phi^T \hat{M}_{\phi,\psi}^T \dot{\hat{\mathbf{q}}}_\psi + \tilde{H}_3 \tilde{\omega}_{o_2} H_2 \hat{\mathbf{q}}_\phi^T \hat{M}_{\phi,\psi}^T \dot{\hat{\mathbf{q}}}_\psi \right) \end{array} \right. \quad (6.92)$$

$$\mathbf{a}_{2,1} = \begin{bmatrix} \hat{\mathbf{M}}_{\phi,I} \mathbf{H}_1^T \mathbf{A}_{o_2}^T - \left(\hat{\mathbf{M}}_{\phi,\xi} \mathbf{H}_1^T \tilde{\mathbf{H}}_1 + \hat{\mathbf{M}}_{\phi,\phi} \hat{\mathbf{q}}_{\phi} \mathbf{H}_1^T \tilde{\mathbf{H}}_1 + \hat{\mathbf{M}}_{\phi,\varphi} \hat{\mathbf{q}}_{\varphi} \mathbf{H}_1^T \tilde{\mathbf{H}}_2 + \hat{\mathbf{M}}_{\phi,\psi} \hat{\mathbf{q}}_{\psi} \mathbf{H}_1^T \tilde{\mathbf{H}}_3 \right) \mathbf{A}_{o_2}^T \\ \hat{\mathbf{M}}_{\varphi,I} \mathbf{H}_2^T \mathbf{A}_{o_2}^T - \left(\hat{\mathbf{M}}_{\varphi,\xi} \mathbf{H}_2^T \tilde{\mathbf{H}}_1 + \hat{\mathbf{M}}_{\phi,\varphi}^T \hat{\mathbf{q}}_{\phi} \mathbf{H}_2^T \tilde{\mathbf{H}}_1 + \hat{\mathbf{M}}_{\varphi,\varphi} \hat{\mathbf{q}}_{\varphi} \mathbf{H}_2^T \tilde{\mathbf{H}}_2 + \hat{\mathbf{M}}_{\varphi,\psi} \hat{\mathbf{q}}_{\psi} \mathbf{H}_2^T \tilde{\mathbf{H}}_3 \right) \mathbf{A}_{o_2}^T \\ \hat{\mathbf{M}}_{\psi,I} \mathbf{H}_3^T \mathbf{A}_{o_2}^T - \left(\hat{\mathbf{M}}_{\psi,\xi} \mathbf{H}_3^T \tilde{\mathbf{H}}_1 + \hat{\mathbf{M}}_{\phi,\psi}^T \hat{\mathbf{q}}_{\phi} \mathbf{H}_3^T \tilde{\mathbf{H}}_1 + \hat{\mathbf{M}}_{\varphi,\psi}^T \hat{\mathbf{q}}_{\varphi} \mathbf{H}_3^T \tilde{\mathbf{H}}_2 + \hat{\mathbf{M}}_{\psi,\psi} \hat{\mathbf{q}}_{\psi} \mathbf{H}_3^T \tilde{\mathbf{H}}_3 \right) \mathbf{A}_{o_2}^T \end{bmatrix} \quad (6.93)$$

$$\mathbf{a}_{2,2} = \begin{bmatrix} \hat{\mathbf{M}}_{\phi,\phi} \\ \hat{\mathbf{M}}_{\varphi,\varphi} \\ \hat{\mathbf{M}}_{\psi,\psi} \end{bmatrix}, \quad \mathbf{a}_{2,3} = \begin{bmatrix} 0 & -\phi(0) \mathbf{H}_1^T \mathbf{A}_{o_2}^T \\ 0 & -\varphi(0) \mathbf{H}_2^T \mathbf{A}_{o_2}^T \\ 0 & -\psi(0) \mathbf{H}_3^T \mathbf{A}_{o_2}^T \end{bmatrix}, \quad \mathbf{a}_{2,4} = \begin{bmatrix} 0 & \phi(l) \mathbf{H}_1^T \mathbf{A}_{o_2}^T \\ 0 & \varphi(l) \mathbf{H}_2^T \mathbf{A}_{o_2}^T \\ 0 & \psi(l) \mathbf{H}_3^T \mathbf{A}_{o_2}^T \end{bmatrix} \quad (6.94)$$

$$\left\{ \begin{array}{l} \mathbf{a}_{2,5}(1,1) = \hat{\mathbf{K}}_{\phi,\phi} \hat{\mathbf{q}}_{\phi} - \mathbf{f}_{\xi} + \hat{\mathbf{M}}_{\phi,\xi} \mathbf{H}_1^T \tilde{\omega}_{o_2} \tilde{\omega}_{o_2} \mathbf{H}_1 \\ \quad + \hat{\mathbf{M}}_{\phi,\phi} \hat{\mathbf{q}}_{\phi} \mathbf{H}_1^T \tilde{\omega}_{o_2} \tilde{\omega}_{o_2} \mathbf{H}_1 + \hat{\mathbf{M}}_{\phi,\varphi} \hat{\mathbf{q}}_{\varphi} \mathbf{H}_1^T \tilde{\omega}_{o_2} \tilde{\omega}_{o_2} \mathbf{H}_2 + \hat{\mathbf{M}}_{\phi,\psi} \hat{\mathbf{q}}_{\psi} \mathbf{H}_1^T \tilde{\omega}_{o_2} \tilde{\omega}_{o_2} \mathbf{H}_3 \\ \quad + 2\hat{\mathbf{M}}_{\phi,\phi} \dot{\hat{\mathbf{q}}}_{\phi} \mathbf{H}_1^T \tilde{\omega}_{o_2} \mathbf{H}_1 + 2\hat{\mathbf{M}}_{\phi,\varphi} \dot{\hat{\mathbf{q}}}_{\varphi} \mathbf{H}_1^T \tilde{\omega}_{o_2} \mathbf{H}_2 + 2\hat{\mathbf{M}}_{\phi,\psi} \dot{\hat{\mathbf{q}}}_{\psi} \mathbf{H}_1^T \tilde{\omega}_{o_2} \mathbf{H}_3 \\ \mathbf{a}_{2,5}(2,1) = \hat{\mathbf{K}}_{\varphi,\varphi} \hat{\mathbf{q}}_{\varphi} - \mathbf{f}_{\eta} + \hat{\mathbf{M}}_{\xi,\varphi} \mathbf{H}_2^T \tilde{\omega}_{o_2} \tilde{\omega}_{o_2} \mathbf{H}_1 \\ \quad + \hat{\mathbf{M}}_{\phi,\varphi}^T \hat{\mathbf{q}}_{\phi} \mathbf{H}_2^T \tilde{\omega}_{o_2} \tilde{\omega}_{o_2} \mathbf{H}_1 + \hat{\mathbf{M}}_{\varphi,\varphi} \hat{\mathbf{q}}_{\varphi} \mathbf{H}_2^T \tilde{\omega}_{o_2} \tilde{\omega}_{o_2} \mathbf{H}_2 + \hat{\mathbf{M}}_{\varphi,\psi} \hat{\mathbf{q}}_{\psi} \mathbf{H}_2^T \tilde{\omega}_{o_2} \tilde{\omega}_{o_2} \mathbf{H}_3 \\ \quad + 2\hat{\mathbf{M}}_{\phi,\varphi}^T \dot{\hat{\mathbf{q}}}_{\phi} \mathbf{H}_2^T \tilde{\omega}_{o_2} \mathbf{H}_1 + 2\hat{\mathbf{M}}_{\varphi,\varphi} \dot{\hat{\mathbf{q}}}_{\varphi} \mathbf{H}_2^T \tilde{\omega}_{o_2} \mathbf{H}_2 + 2\hat{\mathbf{M}}_{\varphi,\psi} \dot{\hat{\mathbf{q}}}_{\psi} \mathbf{H}_2^T \tilde{\omega}_{o_2} \mathbf{H}_3 + \hat{\mathbf{f}}_{\varphi} \\ \mathbf{a}_{2,5}(3,1) = \hat{\mathbf{K}}_{\psi,\psi} \hat{\mathbf{q}}_{\psi} - \mathbf{f}_{\zeta} + \hat{\mathbf{M}}_{\psi,\xi} \mathbf{H}_3^T \tilde{\omega}_{o_2} \tilde{\omega}_{o_2} \mathbf{H}_1 \\ \quad + \hat{\mathbf{M}}_{\phi,\psi}^T \hat{\mathbf{q}}_{\phi} \mathbf{H}_3^T \tilde{\omega}_{o_2} \tilde{\omega}_{o_2} \mathbf{H}_1 + \hat{\mathbf{M}}_{\varphi,\psi}^T \hat{\mathbf{q}}_{\varphi} \mathbf{H}_3^T \tilde{\omega}_{o_2} \tilde{\omega}_{o_2} \mathbf{H}_2 + \hat{\mathbf{M}}_{\psi,\psi} \hat{\mathbf{q}}_{\psi} \mathbf{H}_3^T \tilde{\omega}_{o_2} \tilde{\omega}_{o_2} \mathbf{H}_3 \\ \quad + 2\hat{\mathbf{M}}_{\phi,\psi}^T \dot{\hat{\mathbf{q}}}_{\phi} \mathbf{H}_3^T \tilde{\omega}_{o_2} \mathbf{H}_1 + 2\hat{\mathbf{M}}_{\varphi,\psi}^T \dot{\hat{\mathbf{q}}}_{\varphi} \mathbf{H}_3^T \tilde{\omega}_{o_2} \mathbf{H}_2 + 2\hat{\mathbf{M}}_{\psi,\psi} \dot{\hat{\mathbf{q}}}_{\psi} \mathbf{H}_3^T \tilde{\omega}_{o_2} \mathbf{H}_3 + \hat{\mathbf{f}}_{\psi} \end{array} \right. \quad (6.95)$$

$$J_{o_2} = \int_0^l \rho A \xi^2 d\xi, \quad \mathbf{f}_{\xi} = \int_0^l \bar{f}_{\xi} \phi d\xi, \quad \mathbf{f}_{\eta} = \int_0^l \bar{f}_{\eta} \varphi d\xi, \quad \mathbf{f}_{\zeta} = \int_0^l \bar{f}_{\zeta} \psi d\xi \quad (6.96)$$

$$\hat{\mathbf{f}}_{\varphi,j} = \hat{\mathbf{q}}_{\phi}^T \hat{\mathbf{K}}_{j,\phi,\varphi} \hat{\mathbf{q}}_{\varphi}, \quad \hat{\mathbf{f}}_{\psi,j} = \hat{\mathbf{q}}_{\phi}^T \hat{\mathbf{K}}_{j,\phi,\psi} \hat{\mathbf{q}}_{\psi} \quad (6.97)$$

6.5.3 Deduction of the Transfer Equation of a Spatial Beam

The kinematics Equations (6.73) and (6.25) of the beam can be rewritten as

$$\ddot{\mathbf{R}}_P = \mathbf{B}_{1,P} \ddot{\mathbf{R}}_{o_2} + \mathbf{B}_{2,P} \ddot{\mathbf{q}} + \mathbf{B}_{3,P} \quad (6.98)$$

where

$$\mathbf{B}_{1,P} = \begin{bmatrix} \mathbf{I} & -\mathbf{A}_{o_2} (\tilde{\mathbf{L}} + \tilde{\mathbf{u}}) \mathbf{A}_{o_2}^T \\ 0 & \mathbf{I} \end{bmatrix}_P, \quad \mathbf{B}_{2,P} = \begin{bmatrix} \mathbf{A}_{o_2} \mathbf{H}_1 \phi^T & \mathbf{A}_{o_2} \mathbf{H}_2 \varphi^T & \mathbf{A}_{o_2} \mathbf{H}_3 \psi^T \\ 0 & \mathbf{A}_{o_2} \mathbf{H}_3 \varphi'^T & -\mathbf{A}_{o_2} \mathbf{H}_2 \psi'^T \end{bmatrix}_P \quad (6.99)$$

$$\mathbf{B}_{3,P} = \begin{bmatrix} \mathbf{A}_{o_2} \tilde{\omega}_{o_2} \tilde{\omega}_{o_2} (\mathbf{L} + \mathbf{u}) + 2\mathbf{A}_{o_2} \tilde{\omega}_{o_2} \dot{\mathbf{u}} \\ \tilde{\omega}_{o_2} \mathbf{A}_{o_2} \dot{\theta} \end{bmatrix}_P \quad (6.100)$$

Then for the input and output points of the beam we have

$$\ddot{\mathbf{R}}_I = \mathbf{B}_{1,I} \ddot{\mathbf{R}}_{o_2} + \mathbf{B}_{2,I} \ddot{\mathbf{q}} + \mathbf{B}_{3,I} \quad (6.101)$$

$$\ddot{\mathbf{R}}_O = \mathbf{B}_{1,O} \ddot{\mathbf{R}}_{o_2} + \mathbf{B}_{2,O} \ddot{\mathbf{q}} + \mathbf{B}_{3,O} \quad (6.102)$$

The form of the state vector \mathbf{z} of the connecting points of the beam, including the input and output points, is defined as

$$\mathbf{z} = \begin{bmatrix} \ddot{\mathbf{r}}^T & \dot{\boldsymbol{\Omega}}^T & \mathbf{m}^T & \mathbf{q}^T & 1 \end{bmatrix}^T \quad (6.103)$$

where

$$\ddot{\mathbf{r}} = \begin{bmatrix} \ddot{x} \\ \ddot{y} \\ \ddot{z} \end{bmatrix}, \quad \dot{\boldsymbol{\Omega}} = \begin{bmatrix} \Omega_x \\ \Omega_y \\ \Omega_z \end{bmatrix}, \quad \mathbf{m} = \begin{bmatrix} m_x \\ m_y \\ m_z \end{bmatrix}, \quad \mathbf{q} = \begin{bmatrix} q_x \\ q_y \\ q_z \end{bmatrix}$$

Combining Equations (6.33), (6.34), (6.47) and (6.48), the transfer equation of the spatial beam can be obtained, namely

$$\mathbf{z}_O = \mathbf{U} \mathbf{z}_I, \quad \ddot{\mathbf{q}} = \hat{\mathbf{U}} \mathbf{z}_I \quad (6.104)$$

The corresponding transfer matrices are

$$\mathbf{U} = \begin{bmatrix} \mathbf{E}_{14} & \mathbf{E}_{12} \mathbf{E}_{10} & \mathbf{E}_{15} \\ -\mathbf{E}_7^{-1} \mathbf{E}_5 & -\mathbf{E}_7^{-1} \mathbf{E}_6 & -\mathbf{E}_7^{-1} \mathbf{E}_8 \\ \mathbf{0}^T & \mathbf{0}^T & 1 \end{bmatrix}, \quad \hat{\mathbf{U}} = [\mathbf{E}_9 \quad \mathbf{E}_{10} \quad \mathbf{E}_{11}] \quad (6.105)$$

where

$$\mathbf{E}_1 = \mathbf{a}_{1,2} - \mathbf{a}_{1,1} \mathbf{B}_{1,I}^{-1} \mathbf{B}_{2,I}, \quad \mathbf{E}_2 = \mathbf{a}_{1,5} - \mathbf{a}_{1,1} \mathbf{B}_{1,I}^{-1} \mathbf{B}_{3,I} \quad (6.106)$$

$$\mathbf{E}_3 = \mathbf{a}_{2,2} - \mathbf{a}_{2,1} \mathbf{B}_{1,I}^{-1} \mathbf{B}_{2,I}, \quad \mathbf{E}_4 = \mathbf{a}_{2,5} - \mathbf{a}_{2,1} \mathbf{B}_{1,I}^{-1} \mathbf{B}_{3,I} \quad (6.107)$$

$$\mathbf{E}_5 = \mathbf{a}_{1,1} \mathbf{B}_{1,I}^{-1} - \mathbf{E}_1 \mathbf{E}_3^{-1} \mathbf{a}_{2,1} \mathbf{B}_{1,I}^{-1}, \quad \mathbf{E}_6 = \mathbf{a}_{1,3} - \mathbf{E}_1 \mathbf{E}_3^{-1} \mathbf{a}_{2,3} \quad (6.108)$$

$$\mathbf{E}_7 = \mathbf{a}_{1,4} - \mathbf{E}_1 \mathbf{E}_3^{-1} \mathbf{a}_{2,4}, \quad \mathbf{E}_8 = \mathbf{E}_2 - \mathbf{E}_1 \mathbf{E}_3^{-1} \mathbf{E}_4 \quad (6.109)$$

$$\mathbf{E}_9 = \mathbf{E}_3^{-1} \mathbf{a}_{2,4} \mathbf{E}_7^{-1} \mathbf{E}_5 - \mathbf{E}_3^{-1} \mathbf{a}_{2,1} \mathbf{B}_{1,I}^{-1} \quad (6.110)$$

$$\mathbf{E}_{10} = \mathbf{E}_3^{-1} \mathbf{a}_{2,4} \mathbf{E}_7^{-1} \mathbf{E}_6 - \mathbf{E}_3^{-1} \mathbf{a}_{2,3}, \quad \mathbf{E}_{11} = \mathbf{E}_3^{-1} \mathbf{a}_{2,4} \mathbf{E}_7^{-1} \mathbf{E}_8 - \mathbf{E}_3^{-1} \mathbf{E}_4 \quad (6.111)$$

$$\mathbf{E}_{12} = \mathbf{B}_{2,O} - \mathbf{B}_{1,O} \mathbf{B}_{1,I}^{-1} \mathbf{B}_{2,I}, \quad \mathbf{E}_{13} = \mathbf{B}_{3,O} - \mathbf{B}_{1,O} \mathbf{B}_{1,I}^{-1} \mathbf{B}_{3,I} \quad (6.112)$$

$$\mathbf{E}_{14} = \mathbf{B}_{1,O} \mathbf{B}_{1,I}^{-1} + \mathbf{E}_{12} \mathbf{E}_9, \quad \mathbf{E}_{15} = \mathbf{E}_{12} \mathbf{E}_{11} + \mathbf{E}_{13} \quad (6.113)$$

6.6 Numerical Examples of Multi-flexible-body System Dynamics

To illustrate the procedure of how to solve the dynamics of the system using the transfer equations of elements, the dynamics of a hub–beam system and the dynamical system of a hub–beam system with a rigid body at the end of it are carried out.

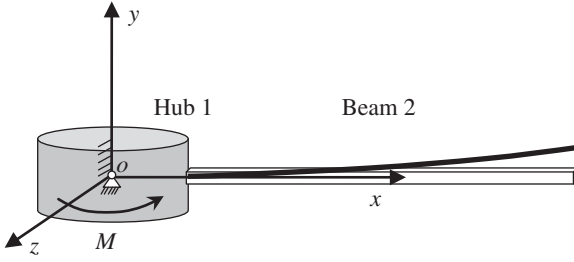


Figure 6.3 The hub-beam system.

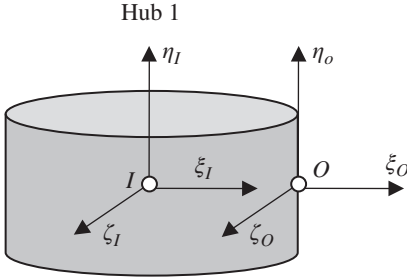


Figure 6.4 The coordinates system of the hub.

6.6.1 Dynamics of a Hub-beam System

The hub-beam system is shown in Figure 6.3, where $oxyz$ is the global inertial coordinate system. The hub is numbered 1 and the beam 2. The body fixed coordinate systems of the input and output points of the hub are shown in Figure 6.4 and those of the beam can be seen in Figure 6.2. The input point of the hub is connected to the global inertial coordinate system through a pin, which can rotate around the axis of oy , the beam is fixed on the hub, and its output end is free. An external moment M along the spin axis is applied to the hub as the driving force. The dynamic response of the system can be solved under zero initial conditions.

The overall transfer equations of this system are

$$\mathbf{z}_{2,O} = \mathbf{U}_2 \mathbf{U}_1 \mathbf{z}_{1,I} \quad (6.114)$$

$$\ddot{\mathbf{q}}_j = \hat{\mathbf{U}}_j \mathbf{z}_{j,I} \quad (j = 2) \quad (6.115)$$

where \mathbf{U}_1 and \mathbf{U}_2 are the transfer matrices of elements 1 and 2, respectively. $\mathbf{z}_{1,I}$ is the state vector of the input point of element 1 and $\mathbf{z}_{2,O}$ is the state vector of the output point of element 2. Equation (6.115) represents the attendant transfer equation of each flexible body element of the system, by which we can obtain the general acceleration of the deformation of each flexible body element after all the state vectors of the system are acquired. $\mathbf{z}_{1,I}$ and $\mathbf{z}_{2,O}$ both belong to the state vectors of the boundaries of the system, which satisfy

$$\mathbf{z}_{1,I} = [0 \ 0 \ 0 \ 0 \ \dot{\Omega}_y \ 0 \ m_x \ 0 \ m_z \ q_x \ q_y \ q_z \ 1]_{1,I}^T \quad (6.116)$$

$$\mathbf{z}_{2,O} = [\ddot{x} \ \ddot{y} \ \ddot{z} \ \dot{\Omega}_x \ \dot{\Omega}_y \ \dot{\Omega}_z \ 0 \ 0 \ 0 \ 0 \ 0 \ 0 \ 1]_{2,O}^T \quad (6.117)$$

The state vectors of the boundaries of the system can be obtained by substituting the boundary conditions of Equations (6.116) and (6.117) into the overall transfer Equation (6.114) of the system, and then all the state vectors of the system can be determined using the transfer equation of each element of the system. Choosing the fourth-order Runge-Kutta method, one of the numerical methods for ordinary differential equations, we can conduct the dynamical simulation of the system easily.

The physical parameters of the system are as follows. The length of beam is $l = 5$ m, the area of the cross-section is $A = 7.3 \times 10^{-5} \text{ m}^2$, the moment of inertia of the cross-section is $I_y = I_z = 8.218 \times 10^{-9} \text{ m}^4$, the density of the material is $\rho = 2.76667 \times 10^3 \text{ kg/m}^3$, the elasticity modulus is $E = 6.895 \times 10^{10} \text{ N/m}^2$, the radius of the hub is $a = 1$ m, the mass of the hub is $m = 10$ kg and the matrix of the moment of inertia of the hub is $\mathbf{J} = \text{diag}(5,5,5) \text{ kg}\cdot\text{m}^2$. The external moment acting on the hub is given as shown in Figure 6.5. The responses of the rotational angular velocity of the hub, and the longitudinal and transversal deformations of the end of the beam are shown in Figures 6.6, 6.7 and 6.8, respectively.

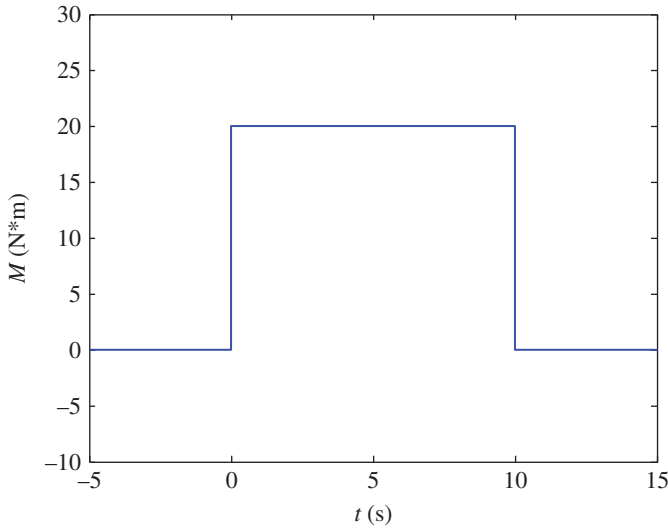


Figure 6.5 The external moment acting on the hub.

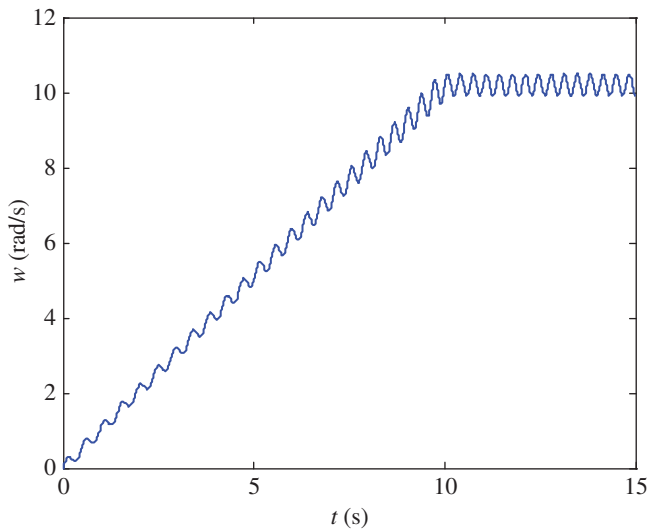


Figure 6.6 The rotational angular velocity of the hub.

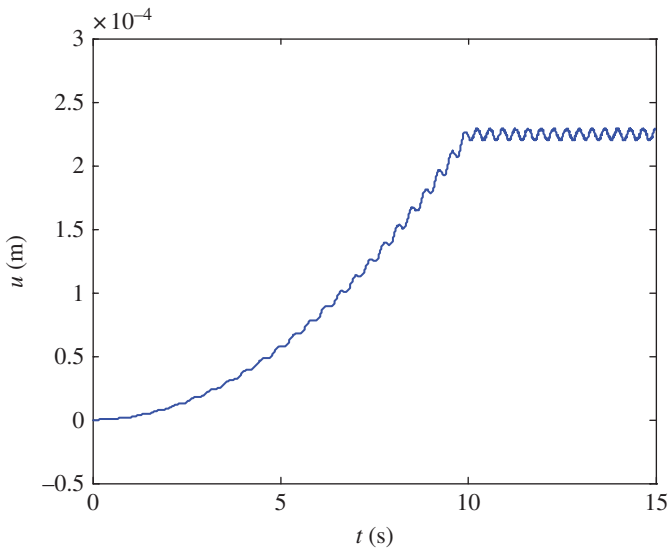


Figure 6.7 The longitudinal deformation of the end of the beam.

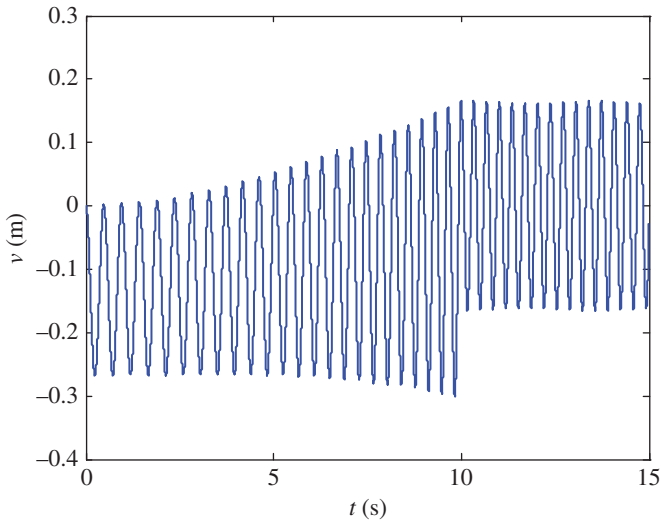


Figure 6.8 The deformation of the beam along O_2Z_2 .

6.6.2 Dynamics of a Hub-beam System with a Rigid Body

The hub-beam system with a rigid body at the end is shown in Figure 6.9. The terminal rigid body is numbered 3, and the body fixed coordinate systems of its input and output points are shown in Figure 6.10. The rigid body is fixed on the beam, which is numbered 2.

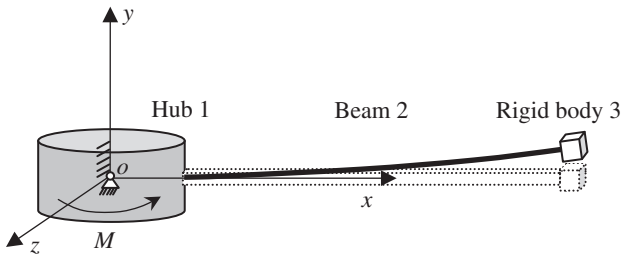


Figure 6.9 A hub-beam system with a terminal rigid body.

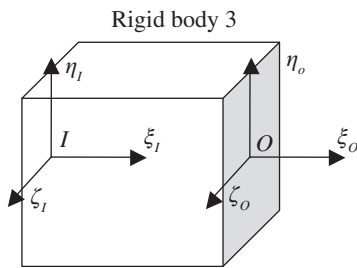


Figure 6.10 The coordinates system of the terminal rigid body.

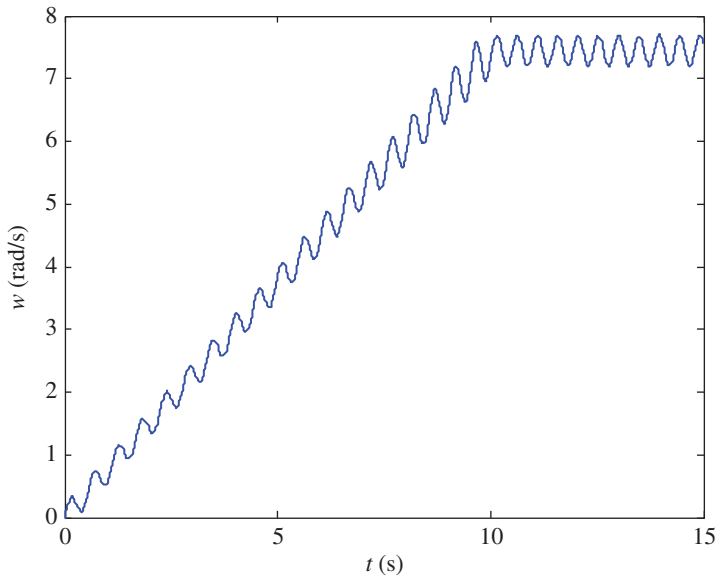


Figure 6.11 The rotational angular velocity of the hub.

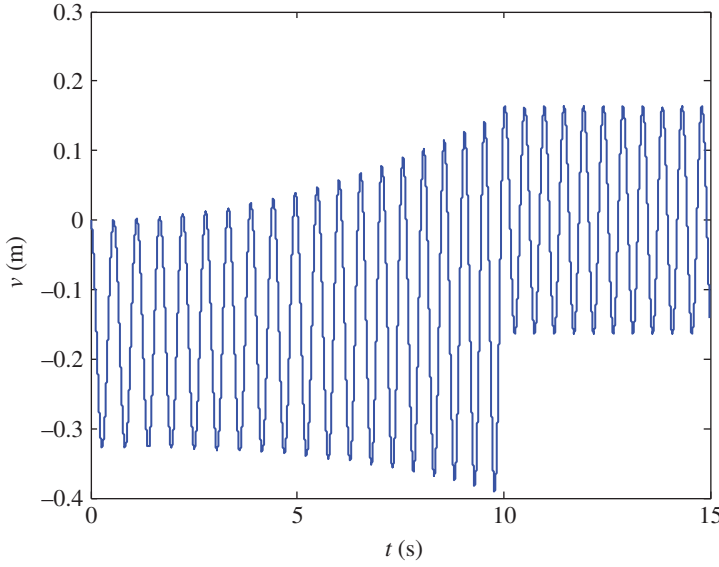


Figure 6.12 The deformation of the beam along o_2z_2 .

Just as in previous section, an external moment M along the spin axis is applied on the hub as the driving force. The dynamic response of the system can be solved under zero initial conditions.

The overall transfer equations of the system are

$$\mathbf{z}_{3,O} = \mathbf{U}_3 \mathbf{U}_2 \mathbf{U}_1 \mathbf{z}_{1,I} \quad (6.118)$$

$$\ddot{\mathbf{q}}_j = \hat{\mathbf{U}}_j \mathbf{z}_{j,I} \quad (j = 2) \quad (6.119)$$

where \mathbf{U}_1 , \mathbf{U}_2 and \mathbf{U}_3 are the transfer matrix of elements 1, 2 and 3, respectively. $\mathbf{z}_{1,I}$ is the state vector of the input point of element 1 and $\mathbf{z}_{3,O}$ is the state vector of the output point of element 3. The meaning of Equation (6.119) is the same as that of Equation (6.115). $\mathbf{z}_{1,I}$ and $\mathbf{z}_{3,O}$ both belong to the state vectors of the boundaries of the system, which satisfy

$$\mathbf{z}_{1,I} = [0 \ 0 \ 0 \ 0 \ \dot{\Omega}_y \ 0 \ m_x \ 0 \ m_z \ q_x \ q_y \ q_z \ 1]^T_{1,I} \quad (6.120)$$

$$\mathbf{z}_{3,O} = [\ddot{x} \ \ddot{y} \ \ddot{z} \ \dot{\Omega}_x \ \dot{\Omega}_y \ \dot{\Omega}_z \ 0 \ 0 \ 0 \ 0 \ 0 \ 0 \ 1]^T_{3,O} \quad (6.121)$$

The state vectors of the boundaries of the system can be obtained by substituting the boundary conditions of Equations (6.120) and (6.121) into the overall transfer Equation (6.118) of the system, and then all the state vectors of the system can be determined using the transfer equation of each element of the system.

It is assumed that the terminal rigid body is given with a mass of 0.2 kg and zero moment of inertia. All the other parameters are the same as those given in section 6.6.1. The responses of the rotational angular velocity of the hub and the transversal deformations of the end of the beam are shown in Figures 6.11 and 6.12, respectively.

Part III

Discrete Time Transfer Matrix Method for Multibody Systems

The *discrete time transfer matrix method for multibody systems* (MSDTTMM) is introduced in this part (Chapters 7 to 11). This method is used to solve multi-rigid-body system dynamics, multi-rigid-flexible-body system dynamics and controlled multibody system dynamics. In Chapter 7, the discrete time transfer matrix method for multi-rigid-body systems is introduced. The discrete time transfer matrix method for multi-rigid-flexible-body systems is given in Chapter 8. The transfer matrix method for controlled multibody systems and the mixed transfer matrix method as well as other methods are presented in Chapter 9. The derivation and computation method for transfer matrices is introduced in Chapter 10. The theorem to deduce the overall transfer equation automatically is introduced in Chapter 11.

The MSDTTMM can be used to compute the dynamics of general multibody systems that are *time-variant* and *nonlinear*, and have *large motion* and control. This method has the following features: no global dynamic equation of the system, low order of matrix, small computational scale, modeling flexibility and high programmability. It can be used with any mechanical method, including all kinds of multibody system dynamics. The basic theory and characteristics of the MSDTTMM are introduced in this part. The efficiency and feasibility of the proposed method are validated by some numerical examples compared with other dynamic methods. In the MSDTTMM, the dynamic equations of elements are linearized and discretized in the time domain. The defined state vector is different from the transfer matrix method for linear multibody systems, and even the elements of state vectors at the two ends of a joint are different in some cases. This is because the state vector of linear multibody systems is denoted by modal coordinate parameters, but in the MSDTTMM only the state vectors of flexible bodies and joints connecting flexible bodies contain generalized coordinates corresponding to modal coordinates. For instance, the definition of the state vectors of the input and output ends of a joint connecting a rigid body and a flexible body are different in the MSDTTMM, but in the transfer matrix method for linear multibody systems they are the same.

The essential difference between the MSDTTMM and the transfer matrix method for linear multibody systems is that the transfer matrix for the latter is a constant matrix, while the transfer matrix in the MSDTTMM is time variant. The state variables of state vectors in the MSDTTMM are physical coordinate parameters (system motion) corresponding to the positions of the connection points, while for the latter they are physical coordinate parameters (steady-state response) or modal coordinate parameters (eigenvalue problem) with respect to displacement.

7

Discrete Time Transfer Matrix Method for Multibody Systems

7.1 Introduction

7.1.1 Characteristics of Ordinary Multibody System Dynamics Methods

With the development of modern industrial technology, many complex mechanical systems have appeared, such as weaponry, aeronautics, astronautics, vehicles, robots and precision machines, which are composed of many components with large relative motion. Under the condition of strong engineering demands, a new branch, namely multibody system dynamics, appeared. The numerical simulation of complex mechanical systems became possible with the appearance and development of the computer. Multibody system dynamics is an engineering application essential to the study of mechanical system dynamics, and systems consisting of many bodies undergoing large relative motion are its main study object. In general, the components of multibody systems include bodies and joints. Body components include rigid bodies, flexible bodies and lumped masses. A system is a multi-rigid-body system if the bodies involved are all rigid bodies, it is a multi-flexible-body system if the bodies involved are all flexible bodies and a multi-rigid-flexible-body system if both rigid bodies and flexible bodies are involved. The joints are the components connecting the bodies.

The deduction of the dynamic equations of multibody systems and their numerical solutions are two main research areas of multibody system dynamics. Generally, there are two major methods for deriving dynamic equations, and their basic forms are different. The first method uses *Lagrangian equations* of the first kind, in which Lagrange multipliers are used to define unknown generalized constraint forces and obtain an augmented formulation. This approach leads to a mixed set of nonlinear differential and algebraic equations that have to be solved simultaneously, and it is the theoretical foundation of some commercial analysis software, such as ADAMS and DADS. It must solve a set of *differential-algebraic equations*. The second method describes the motion using a set of first-order differential equations (kinematics and dynamics) with a minimal set of unknown variables without constraint forces. From a point of view of computational efficiency, its numerical solution is more sophisticated. Differential-algebraic equations can be transformed into a new form with a minimal number of coordinates, and a typical code is the MBOSS [246] developed by Arizona University.

With developments in engineering technology, researchers are still proposing and improving various multibody system dynamics methods, which are promoting the development of modern

engineering technology. These methods have different forms, but in general they all have the two same characteristics:

- 1) It is necessary to build the global dynamic equations of the system, which is the most interesting and brilliant part of various methods, but is also the difficult part for engineers.
- 2) The orders of matrices involved in the global dynamic equations of the system are rather high (generally speaking not less than the degrees of freedom (DOFs) of the system). It has become one of the main research directions in multibody system dynamics to search for a new method to reduce the orders of relevant matrices and to avoid computational difficulty caused by high matrix order.

7.1.2 Features of the Discrete Time Transfer Matrix Method for Multibody Systems

To improve the computational efficiency of multibody system dynamics, a new method, the discrete time transfer matrix method for multibody systems (MSDTTMM) [3, 64–68], has been developed, which is different from other ordinary methods of multibody system dynamics. This method combines the advantages of the transfer matrix method and *numerical integration*. The dynamics equations of typical elements are derived first, followed by their discretization and linearization in the time domain based on the basic thought of numerical integration. Then the transfer matrices of these elements are obtained. The overall transfer equation and overall transfer matrix of the multibody system can be assembled. The system motion can be obtained using step-by-step time integration. The method is suitable for linear time-variable, nonlinear, large motion and general multibody systems. Compared with ordinary multibody system dynamics methods, the MSDTTMM has the following features:

- 1) The global dynamic equations of a system are not needed, hence its application and computation are very convenient.
- 2) The order of involved matrices is much lower than for ordinary multibody system dynamics methods. For example, the order of relevant matrices for chain multibody systems is determined only by the highest order of differential equations of its subsystems. The computational cost is small, resulting in high computational efficiency.
- 3) It provides a flexible modeling instrument and the modeling procedure is highly programmable. The modeling of a multibody system looks like building blocks, the overall transfer matrix of the system can be assembled by the transfer matrices of each element directly, and its solution procedure is very simple and straightforward.
- 4) Complex multibody systems, such as branch, closed-loop or network systems, can be conveniently dealt with by this method in a similar way to the transfer matrix method for linear multibody systems.
- 5) The study method for multi-flexible-body systems and the MRFS is the same as that for multi-rigid-body systems.
- 6) The transfer matrix is always a real number matrix, even when considering dampers. This simplifies the numerical algorithm.
- 7) The natural frequency of linear multibody systems can be obtained easily by using the MSDTTMM, and the transfer matrix method for linear multibody systems can be regarded as a special case.
- 8) An arbitrary appropriate numerical integration method can be introduced into the MSDTTMM, which gives the method some flexibility.

The basic principles, steps and algorithm of the MSDTTMM developed by the authors are introduced in this chapter, and the transfer matrices of typical elements are deduced.

7.2 State Vector, Transfer Equation and Transfer Matrix

Enlightened by the idea of matrix “transfer” in the transfer matrix method for linear *time-invariant systems*, the concepts of state vector, transfer equation and transfer matrix for *nonlinear time-variant systems* are introduced in this section. These new concepts are not the same as those in the transfer matrix method for linear time-invariant systems. We start to address these concepts with a simple example.

Figure 7.1 shows a chain multi-DOF system composed of springs and lumped masses moving along the ox axis. As shown in Figure 7.2, each spring and the lumped mass on its right can be regarded as a subsystem. The position coordinate of the left side of spring j is denoted by $x_{j-1,j}$, the corresponding force is denoted by $q_{j-1,j}$. Their positive direction is the same as the positive direction of the ox axis, and the position coordinate of the right side of spring j is denoted by $x_{j+1,j}$, the force is denoted by $q_{j+1,j}$ and their positive direction is the same as the negative direction of the ox axis. For a massless spring, we have

$$q_{j-1,j} = q_{j+1,j} \quad (7.1)$$

and for a linear spring, according to Hooke's law, we obtain

$$q_{j-1,j} = -K_j(x_{j+1,j} - x_{j-1,j} - l_j) \quad (7.2)$$

where l_j is the initial length of the spring and K_j is the stiffness coefficient.

For lumped mass $j+1$, the position coordinate of its left side is denoted by $x_{j+1,j}$ and the corresponding force denoted by $q_{j+1,j}$. Their positive direction is the same as the positive direction of the ox axis, and the position coordinate of its right side is denoted by $x_{j+1,j+2}$. The force is denoted by $q_{j+1,j+2}$ and the positive direction is the same as the negative direction of the ox axis. According to *Newton's second law of motion*, we obtain

$$q_{j+1,j+2} = q_{j+1,j} - m_{j+1}\ddot{x}_{c_{j+1}} + f_{j+1} \quad (7.3)$$

where m_{j+1} is the mass of body $j+1$ and f_{j+1} is the external force acting on the body.

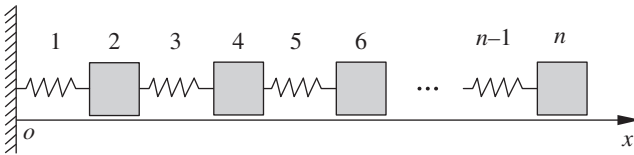
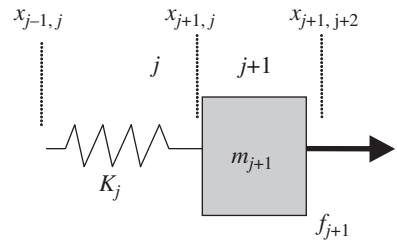


Figure 7.1 A chain system with multiple DOFs.

Figure 7.2 Subsystem model.



There are many numerical methods which describe \ddot{x} and \dot{x} as linear functions of x . For example, by using the Taylor series, we find

$$x_{c_{j+1}}(t_i) = x_{c_{j+1}}(t_{i-1}) + \dot{x}_{c_{j+1}}(t_{i-1})\Delta T + \frac{\ddot{x}_{c_{j+1}}(\xi)}{2}\Delta T^2 \approx x_{c_{j+1}}(t_{i-1}) + \dot{x}_{c_{j+1}}(t_{i-1})\Delta T + \frac{\ddot{x}_{c_{j+1}}(t_i)}{2}\Delta T^2$$

$$\dot{x}_{c_{j+1}}(t_i) = \dot{x}_{c_{j+1}}(t_{i-1}) + \ddot{x}_{c_{j+1}}(\xi)\Delta T \approx \dot{x}_{c_{j+1}}(t_{i-1}) + \ddot{x}_{c_{j+1}}(t_i)\Delta T$$

$\ddot{x}_{c_{j+1}}$ and $\dot{x}_{c_{j+1}}$ can be expressed as linear functions of $x_{c_{j+1}}$:

$$\ddot{x}_{c_{j+1}}(t_i) = \frac{2}{\Delta T^2}x_{c_{j+1}}(t_i) - \frac{2}{\Delta T^2}[x_{c_{j+1}}(t_{i-1}) + \dot{x}_{c_{j+1}}(t_{i-1})\Delta T] \quad (7.4)$$

$$\dot{x}_{c_{j+1}}(t_i) = \frac{2}{\Delta T}x_{c_{j+1}}(t_i) - \frac{2}{\Delta T}x_{c_{j+1}}(t_{i-1}) - \dot{x}_{c_{j+1}}(t_{i-1}) \quad (7.5)$$

where $\Delta T = t_i - t_{i-1}$ is a time step.

Substituting Equation (7.4) into Equation (7.3) yields

$$q_{j+1,j+2} = -m_{j+1}\frac{2}{\Delta T^2}x_{c_{j+1}}(t_i) + q_{j+1,j} + m_{j+1}\frac{2}{\Delta T^2}[x_{c_{j+1}}(t_{i-1}) + \dot{x}_{c_{j+1}}(t_{i-1})\Delta T] + f_{j+1} \quad (7.6)$$

According to the continuous condition of displacement of lumped mass, this becomes

$$x_{j+1,j+2} = x_{j+1,j} = x_{c_{j+1}} \quad (7.7)$$

Combining Equations (7.1) and (7.2) yields

$$\begin{bmatrix} x \\ q \\ 1 \end{bmatrix}_{j+1,j} = \begin{bmatrix} 1 & -1/K_j & l_j \\ 0 & 1 & 0 \\ 0 & 0 & 1 \end{bmatrix} \begin{bmatrix} x \\ q \\ 1 \end{bmatrix}_{j-1,j} \quad (7.8)$$

The state vector at the connection point is defined as

$$\mathbf{z} = [x, \quad q, \quad 1]^T \quad (7.9)$$

Equation (7.8) can be written as

$$\mathbf{z}_{j+1,j} = \mathbf{U}_j \mathbf{z}_{j-1,j} \quad (7.10)$$

where

$$\mathbf{U}_j = \begin{bmatrix} 1 & -1/K_j & l_j \\ 0 & 1 & 0 \\ 0 & 0 & 1 \end{bmatrix} \quad (7.11)$$

Equation (7.8) or Equation (7.10) is the transfer equation of a spring, and Equation (7.11) is the transfer matrix of a spring. Combining Equations (7.6) and (7.7) yields

$$\begin{bmatrix} x \\ q \\ 1 \end{bmatrix}_{j+1,j+2} = \begin{bmatrix} 1 & 0 & 0 \\ -\frac{2m_{j+1}}{\Delta T^2} & 1 & \frac{2m_{j+1}}{\Delta T^2}[x_{j+1,j+2}(t_{i-1}) + \dot{x}_{j+1,j+2}(t_{i-1})\Delta T] + f_{j+1} \\ 0 & 0 & 1 \end{bmatrix} \begin{bmatrix} x \\ q \\ 1 \end{bmatrix}_{j+1,j} \quad (7.12)$$

namely

$$\mathbf{z}_{j+1,j+2} = \mathbf{U}_{j+1} \mathbf{z}_{j+1,j} \quad (7.13)$$

where

$$\mathbf{U}_{j+1} = \begin{bmatrix} 1 & 0 & 0 \\ -\frac{2m_{j+1}}{\Delta T^2} & 1 & \frac{2m_{j+1}}{\Delta T^2} [\dot{x}_{j+1,j+2}(t_{i-1}) + \dot{x}_{j+1,j+2}(t_{i-1})\Delta T] + f_{j+1} \\ 0 & 0 & 1 \end{bmatrix} \quad (7.14)$$

Equation (7.12) or Equation (7.13) is the transfer equation of a lumped mass, and Equation (7.14) is the transfer matrix of a lumped mass.

According to Equations (7.10) and (7.13), the transfer equation of the subsystem including the spring and lumped mass is

$$\mathbf{z}_{j+1,j+2} = \mathbf{U}_{j+1 \leftarrow j} \mathbf{z}_{j-1,j} \quad (7.15)$$

where $\mathbf{U}_{j+1 \leftarrow j}$ is the transfer matrix of the subsystem:

$$\mathbf{U}_{j+1 \leftarrow j} = \mathbf{U}_{j+1} \mathbf{U}_j \quad (7.16)$$

that is

$$\mathbf{U}_{j+1 \leftarrow j} = \begin{bmatrix} 1 & -1/K_j & l_j \\ -\frac{2m_{j+1}}{\Delta T^2} & 1 + \frac{2m_{j+1}}{\Delta T^2 K_j} & \frac{2m_{j+1}}{\Delta T^2} [\dot{x}_{j+1,j+2}(t_{i-1}) + \dot{x}_{j+1,j+2}(t_{i-1})\Delta T - l_j] + f_{j+1} \\ 0 & 0 & 1 \end{bmatrix} \quad (7.17)$$

By simply assembling the transfer matrices of the subsystems, the overall transfer equation of the chain multibody system shown in Figure 7.1 is

$$\mathbf{z}_{n,n+1} = \mathbf{U}_{n \leftarrow n-1} \mathbf{U}_{n-2 \leftarrow n-3} \cdots \mathbf{U}_{4 \leftarrow 3} \mathbf{U}_{2 \leftarrow 1} \mathbf{z}_{0,1} \quad (7.18)$$

The overall transfer matrix of the system is

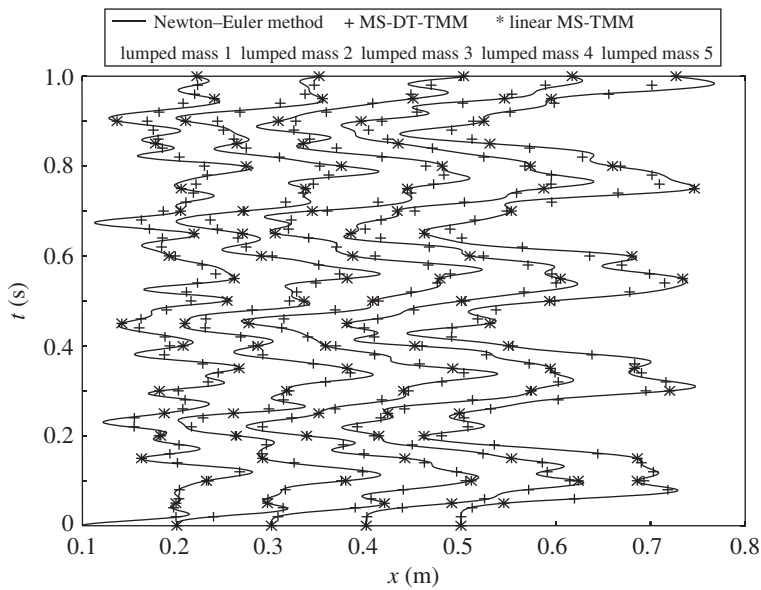
$$\mathbf{U} = \mathbf{U}_{n \leftarrow n-1} \mathbf{U}_{n-2 \leftarrow n-3} \cdots \mathbf{U}_{4 \leftarrow 3} \mathbf{U}_{2 \leftarrow 1} \quad (7.19)$$

Substituting the boundary conditions $q_{n,n+1} = 0$, $x_{0,1} = 0$ and the initial condition at time t_0 into Equation (7.18), the unknown quantities of state vectors of the system boundary at time t_1 can be obtained. For the chain multibody system shown in Figure 7.1, $x_{n,n+1}$ and $q_{0,1}$ at time t_1 can be determined. The dynamics of all elements can be computed by using Equation (7.15), which can be considered as the initial condition for computing the dynamic response at time t_2 . The system dynamic response at an arbitrary time point is determined via the iterative method.

For the model shown in Figure 7.1, we choose $n = 10$, with structure parameters and initial conditions according to Table 7.1. The computational results of motion by the transfer matrix method for linear multibody systems, the MSDTTMM and the Newton mechanics method, respectively, are shown in Figure 7.3. The solid line denotes the results computed by the Newton mechanics method, the symbol + denotes the results computed by the MSDTTMM and the symbol * denotes the results computed by the transfer matrix method for linear multibody systems. The results obtained by these three methods have good agreement and validate the proposed method.

Table 7.1 Structure parameters and initial conditions

Spring number	1	3	5	7	9
Stiffness K (N/m)	1000	1000	1000	1000	1000
Initial length l (m)	0.1	0.1	0.1	0.1	0.1
Lumped mass number	2	4	6	8	10
Mass m (kg)	0.1	0.1	0.1	0.1	0.1
External force f (N)	100	0	0	0	0
Initial displacement x_0 (m)	0.1	0.2	0.3	0.4	0.5
Initial velocity \dot{x}_0 (m/s)	0	0	0	0	0

**Figure 7.3** Computational results by three methods.

The state vector of a rigid body moving in space is defined as

$$\mathbf{z} = [x, y, z, \theta_x, \theta_y, \theta_z, m_x, m_y, m_z, q_x, q_y, q_z, 1]^T \quad (7.20)$$

where $x, y, z, \theta_x, \theta_y$ and θ_z are the position coordinates of the connection point with respect to the inertial coordinate system and the corresponding rotation angles about the x, y and z axes. m_x, m_y, m_z, q_x, q_y and q_z are the corresponding internal moments and forces in the same coordinate system.

The state vector of a rigid body moving in a plane is defined as

$$\mathbf{z} = [x, y, \theta, m, q_x, q_y, 1]^T \quad (7.21)$$

For the body element j with one input end and one output end, the transfer equation which relates the state vectors at its two points is

$$\mathbf{z}_{j,j+1} = \mathbf{U}_j \mathbf{z}_{j,j-1} \quad (7.22)$$

The transfer equation which relates the state vectors at the two points of a joint j is

$$\mathbf{z}_{j+1,j} = \mathbf{U}_j \mathbf{z}_{j-1,j} \quad (7.23)$$

where \mathbf{U}_j is the transfer matrix of element j .

For a chain system composed of n elements, the overall transfer equation which relates the state vectors at the two points can be obtained by using Equations (7.22) and (7.23) repeatedly,

$$\mathbf{z}_{n,n+1} = \mathbf{U} \mathbf{z}_{0,1} \quad (7.24)$$

where

$$\mathbf{U} = \mathbf{U}_n \mathbf{U}_{n-1} \cdots \mathbf{U}_2 \mathbf{U}_1 \quad (7.25)$$

\mathbf{U} is the overall transfer matrix of the system.

Once the overall transfer matrix of the system is obtained, the boundary conditions of the system can be applied and the unknown quantities in the boundary state vectors can be computed. The state vectors of each element at time t_i can be obtained using Equations (7.22) and (7.23) repeatedly and the system motion at time t_i can be obtained. The entire procedure can be repeated for time t_{i+1} and so on.

7.3 Step-by-step Time Integration Method and Linearization

The linear MSTMM is established based on the fact that the internal forces at the same point are equal in magnitude, opposite in direction and act on different objects, resulting in a linear relationship between different points' state vectors. For a nonlinear system, this linear relationship does not exist. Even for a linear time-variant system, this linear relationship also does not exist. If we still want to use the transfer matrix method to study the dynamics of such a system, the linear relationship of state vectors between different points must be developed. Therefore, two questions must be answered: the first is whether physically nonlinear relations of state vectors involving transcendent functions or other complex relations can be expressed as linear forms; the second is how these complex relations can be linearly expressed to make the computation convergent and stable. The answers which come from modern science are affirmative. In fact, the increment transfer matrix method of a nonlinear time-variant system was presented in Chapter 4 to compute the steady-state response. For a time-variant system, during the physical process of any computational time step size, if the time step size is small enough the relationship among many physical quantities can be approximately expressed by linear formulas. Modern numerical integral methods [222, 242, 247, 248] provide many linear forms to ensure computational convergence and stability. This section introduces these linearization methods of motion parameters and special functions that are based on step-by-step time integration methods.

7.3.1 Linearization of Velocity (Angular Velocity) and Acceleration (Angular Acceleration)

In dynamic equations of general elements, the unknown quantities include velocities (angular velocities), accelerations (angular accelerations), trigonometric functions and internal forces at connection points, as well as cross terms, high-order terms and so on. For the free vibration of linear time-invariant multibody systems, the state vectors satisfy the following relation:

$$\mathbf{z} = \mathbf{Z} e^{i\omega t}$$

where z is the physical coordinate and Z is the corresponding modal coordinate.

We can obtain

$$\dot{z} = i\omega Z e^{i\omega t}, \quad \ddot{z} = -\omega^2 Z e^{i\omega t} \quad (7.26)$$

If the motion of a multibody system is aperiodic, Equation (7.26) does not exist. In order to develop the transfer matrix of an element, its dynamic equation must be linearized. Using numerical integral methods, velocity \dot{z} (angular velocity) and acceleration \ddot{z} (angular acceleration) can be expressed as linear functions of the position coordinate (angular coordinate), that is

$$\ddot{z}(t_i) = A(t_{i-1})z(t_i) + B_z(t_{i-1}) \quad (7.27)$$

$$\dot{z}(t_i) = C(t_{i-1})z(t_i) + D_z(t_{i-1}) \quad (7.28)$$

where $A(t_{i-1})$, $B_z(t_{i-1})$, $C(t_{i-1})$ and $D_z(t_{i-1})$ at time t_i are known functions with respect to time t_{i-1} , and can be summarized as A , B_z , C and D_z .

Based on the linearization of velocities, accelerations and other variables in a small time segment during time interval $\Delta T = t_i - t_{i-1}$, the nonlinear dynamic equation at time t_i can be expressed by linear formulas of the motion variables at time t_i . The quantities above can be determined using the following methods.

7.3.2 Step-by-step Time Integration Method

7.3.2.1 Forward-Euler Method

According to the Taylor expansion theorem, $x(t_i)$ can be approximately expressed as

$$x(t_i) = x(t_{i-1}) + \dot{x}(t_{i-1})\Delta T + \frac{\ddot{x}(t_i)}{2}\Delta T^2 \quad (7.29)$$

From Equation (7.30), it follows that

$$\ddot{x}(t_i) = \frac{2}{\Delta T^2}x(t_i) - \frac{2}{\Delta T^2}[x(t_{i-1}) + \dot{x}(t_{i-1})\Delta T] \quad (7.30)$$

Thus, the acceleration can be expressed approximately by the first-order difference as $\ddot{x}(t_i) = [\dot{x}(t_i) - \dot{x}(t_{i-1})]/\Delta T$ from Equation (7.30), that is

$$\dot{x}(t_i) = \frac{2}{\Delta T}x(t_i) - \left[\frac{2}{\Delta T}x(t_{i-1}) + \dot{x}(t_{i-1}) \right] \quad (7.31)$$

By comparing Equations (7.30) and (7.31) with Equations (7.27) and (7.28), we obtain

$$\begin{aligned} A &= \frac{2}{\Delta T^2}, \quad B_x = -\frac{2}{\Delta T^2}[x(t_{i-1}) + \dot{x}(t_{i-1})\Delta T] \\ C &= \frac{2}{\Delta T}, \quad D_x = -\left[\frac{2}{\Delta T}x(t_{i-1}) + \dot{x}(t_{i-1}) \right] \end{aligned} \quad (7.32)$$

7.3.2.2 Newmark- β Method

Expanding the variable $x(t_i)$ at time t_{i-1} by Taylor expansion theorem yields

$$x(t_i) = x(t_{i-1}) + \dot{x}(t_{i-1})\Delta T + \frac{\ddot{x}(\xi)}{2}\Delta T^2, \quad \xi \in [t_{i-1}, t_i] \quad (7.33)$$

Let

$$\ddot{x}(\xi) = (1 - 2\beta)\ddot{x}(t_{i-1}) + 2\beta\ddot{x}(t_i) \quad (7.34)$$

then

$$\ddot{x}(t_i) = \frac{1}{\beta \Delta T^2} x(t_i) + \frac{1}{\beta \Delta T^2} \left[-x(t_{i-1}) - \dot{x}(t_{i-1}) \Delta T - \left(\frac{1}{2} - \beta \right) \ddot{x}(t_{i-1}) \Delta T^2 \right] \quad (7.35)$$

The velocity can be expressed by using Taylor expansion theorem as

$$\dot{x}(t_i) = \dot{x}(t_{i-1}) + \ddot{x}(\xi) \Delta T \quad (7.36)$$

Let

$$\ddot{x}(\xi) = (1 - \gamma) \ddot{x}(t_{i-1}) + \gamma \ddot{x}(t_i) \quad (7.37)$$

Substituting Equations (7.35) and (7.37) into Equation (7.36) yields

$$\dot{x}(t_i) = \frac{\gamma}{\beta \Delta T} x(t_i) + \dot{x}(t_{i-1}) + (1 - \gamma) \ddot{x}(t_{i-1}) \Delta T + \gamma B(t_i) \Delta T \quad (7.38)$$

From Equations (7.35) and (7.38) we obtain

$$A = \frac{1}{\beta \Delta T^2}, \quad B_x = A \left[-x(t_{i-1}) - \dot{x}(t_{i-1}) \Delta T - \left(\frac{1}{2} - \beta \right) \ddot{x}(t_{i-1}) \Delta T^2 \right] \quad (7.39)$$

$$C = \frac{\gamma}{\beta \Delta T}, \quad D_x = \dot{x}(t_{i-1}) + (1 - \gamma) \ddot{x}(t_{i-1}) \Delta T + \gamma B_x \Delta T$$

The Newmark- β method originates from the trapezoid method, where only the first and second-order derivatives of the Taylor series are adopted. The two parameters γ and β are used to compensate the contributions of the abandoned higher-order quantities. If γ and β have different values, many formulas can be obtained. When $\gamma = 1/2$ and $\beta = 1/4$, this is the average acceleration method. $\beta = 0$ leads to the constant acceleration method (center difference method), and $\beta = 1/6$ yields the linear acceleration method. It can be proved that if $\gamma \geq 1/2$, $\beta \geq \gamma/2$, and the formulas are unconditionally stable. If the value of β is increased, the computational precision will be reduced, and if $\beta = 1/12$, the computational precision is the highest, but the formula is conditionally stable. Newmark has pointed out that $\gamma < 1/2$ induces negative damping to a linear system, i.e. the vibration amplitude will be amplified in the integral computation. When $\gamma > 1/2$, artificial damp will be introduced and finally induce reduction in the vibration amplitude. Generally, let $\gamma \geq 1/2$. The most common choice is to let $\gamma = 1/2$ and then change β accordingly, so the method is called the Newmark- β method. If $\gamma = 1$ and $\beta = 0.5$, this is the Forward-Euler method.

7.3.2.3 Wilson- θ Method

The Wilson- θ method was developed on the basis of the linear acceleration assumption. The parameter $\theta \geq 1$ can be introduced in the time interval $[t, t + \theta \Delta T]$, assuming acceleration is linear with respect to time, as shown in Figure 7.4.

A set of equations at time $t + \theta \Delta T$, called predicted equations, is deduced first. Then the correction equations of displacement, velocity and acceleration at time $t + \theta \Delta T$ are deduced. When $\theta = 1$, this is the linear acceleration method. If τ is the time variable limited by $0 \leq \tau \leq \theta \Delta T$, the acceleration during this time interval can be written as $\ddot{x}_{n+\tau} = \ddot{x}_n + (\ddot{x}_{n+\theta} - \ddot{x}_n) \tau / (\theta \Delta T)$, according to the assumption of linear acceleration. Later the acceleration can be integrated in $[0, \tau]$.

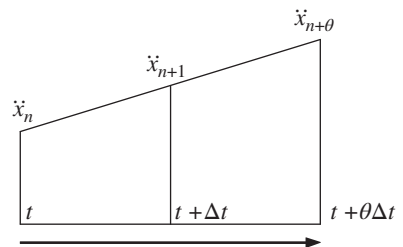


Figure 7.4 Linear acceleration.

$$\dot{x}_{n+\tau} = \dot{x}_n + \ddot{x}_n \tau + \frac{\tau^2}{2\theta\Delta T}(\ddot{x}_{n+\theta} - \ddot{x}_n) \quad (7.40)$$

$$x_{n+\tau} = x_n + \dot{x}_n \tau + \frac{\tau^2}{2}\ddot{x}_n + \frac{\tau^3}{6\theta\Delta T}(\ddot{x}_{n+\theta} - \ddot{x}_n) \quad (7.41)$$

If $\tau = \theta\Delta T$, according to Equations (7.40) and (7.41), the velocity and displacement at time $t + \theta\Delta T$ can be computed by the following two formulas

$$\dot{x}_{n+\theta} = \dot{x}_n + \frac{\theta\Delta T}{2}(\ddot{x}_{n+\theta} + \ddot{x}_n) \quad (7.42)$$

$$x_{n+\theta} = x_n + \theta\Delta T\dot{x}_n + \frac{(\theta\Delta T)^2}{6}(\ddot{x}_{n+\theta} + 2\ddot{x}_n) \quad (7.43)$$

Combining Equations (7.42) and (7.43) yields

$$\ddot{x}_{n+\theta} = \frac{6}{(\theta\Delta T)^2}x_{n+\theta} - \frac{6}{(\theta\Delta T)^2}\left[x_n + \theta\Delta T\dot{x}_n + \frac{(\theta\Delta T)^2}{3}\ddot{x}_n\right] \quad (7.44)$$

$$\dot{x}_{n+\theta} = \frac{3}{\theta\Delta T}x_{n+\theta} - \frac{3}{\theta\Delta T}x_n - 2\dot{x}_n - \frac{\theta\Delta T}{2}\ddot{x}_n \quad (7.45)$$

According to Equations (7.44) and (7.45), we obtain

$$A = \frac{6}{(\theta\Delta T)^2}, \quad B_x = -A \left[x_n + \theta\Delta T\dot{x}_n + \frac{(\theta\Delta T)^2}{3}\ddot{x}_n \right]$$

$$C = \frac{3}{\theta\Delta T}, \quad D_x = -\frac{3}{\theta\Delta T}x_n - 2\dot{x}_n - \frac{\theta\Delta T}{2}\ddot{x}_n \quad (7.46)$$

7.3.2.4 Houbolt Method

The basic idea of the Houbolt method is that the velocity and acceleration at $t + \Delta T$ can be expressed approximately by the position coordinates of four points at previous times $(n-2, n-1, n, n+1)$, as shown in Figure 7.5. The relative coordinate $\zeta = t/\Delta T$ is introduced, and x_{n-2} , x_{n-1} , x_n and x_{n+1} are the position coordinates corresponding to $\zeta = 0, 1, 2$ and 3 , respectively. When $0 \leq \zeta \leq 3$, the position coordinate $x(\zeta)$ can be expressed approximately by the *Lagrange interpolation polynomial*:

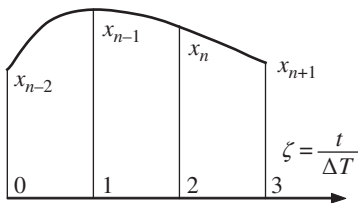


Figure 7.5 Houbolt method.

$$x(\zeta) = \frac{1}{6}\zeta(\zeta-1)(\zeta-2)x_{n+1} - \frac{1}{2}\zeta(\zeta-1)(\zeta-3)x_n$$

$$+ \frac{1}{2}\zeta(\zeta-2)(\zeta-3)x_{n-1} - \frac{1}{6}(\zeta-1)(\zeta-2)(\zeta-3)x_{n-2} \quad (7.47)$$

It is not difficult to figure out the rules of this interpolation polynomial: any individual term of this polynomial is the product of a position coordinate function and three terms

of the four basic functions ζ , $(\zeta - 1)$, $(\zeta - 2)$ and $(\zeta - 3)$. Its coefficients are obtained by the value of the function $x(\zeta)$ corresponding to each point. The first- and second-order derivatives of $x(\zeta)$ are

$$\begin{aligned} \frac{d}{dt}x(\zeta) &= \frac{1}{6\Delta t}[(\zeta - 1)(\zeta - 2) + \zeta(\zeta - 1) + \zeta(\zeta - 2)]x_{n+1} \\ &\quad - \frac{1}{2\Delta t}[(\zeta - 1)(\zeta - 3) + \zeta(\zeta - 3) + \zeta(\zeta - 1)]x_n \\ &\quad + \frac{1}{2\Delta t}[(\zeta - 2)(\zeta - 3) + \zeta(\zeta - 3) + \zeta(\zeta - 2)]x_{n-1} \\ &\quad - \frac{1}{6\Delta t}[(\zeta - 2)(\zeta - 3) + (\zeta - 1)(\zeta - 3) + (\zeta - 1)(\zeta - 2)]x_{n-2} \end{aligned} \quad (7.48)$$

$$\frac{d^2}{dt^2}x(\zeta) = \frac{1}{\Delta t^2}(\zeta - 1)x_{n+1} - \frac{1}{\Delta t^2}(3\zeta - 4)x_n + \frac{1}{\Delta t^2}(3\zeta - 5)x_{n-1} - \frac{1}{\Delta t^2}(\zeta - 2)x_{n-2} \quad (7.49)$$

If $\zeta = 3$, then

$$\begin{aligned} A &= \frac{2}{\Delta T^2}, \quad B_x = -\frac{1}{\Delta T^2}(5x_n - 4x_{n-1} + x_{n-2}) \\ C &= \frac{11}{6\Delta T}, \quad D_x = -\frac{1}{6\Delta T}(18x_n - 9x_{n-1} + 2x_{n-2}) \end{aligned} \quad (7.50)$$

Three previous time points are used in this linearization method, hence the first and second steps cannot be implemented in these formulations. The method can only be used if the information for three time points is known. This is the disadvantage of the multistep method. The two-step and single-step Houbolt methods are described here. Equation (7.50) yields

$$\ddot{x}_{n+1} = \frac{2}{\Delta T^2}x_{n+1} - \frac{1}{\Delta T^2}[4x_n - 2x_{n-1} + (x_n - 2x_{n-1} + x_{n-2})] \quad (7.51)$$

$$\dot{x}_{n+1} = \frac{11}{6\Delta T}x_{n+1} - \frac{1}{6\Delta T}[16x_n - 5x_{n-1} + (2x_n - 4x_{n-1} + 2x_{n-2})] \quad (7.52)$$

as

$$x_n = x_{n-1} + \dot{x}_{n-1}\Delta T + \frac{\ddot{x}_{n-1}}{2}\Delta T^2 \quad (7.53)$$

$$x_{n-2} = x_{n-1} - \dot{x}_{n-1}\Delta T + \frac{\ddot{x}_{n-1}}{2}\Delta T^2 \quad (7.54)$$

Adding Equations (7.53) and (7.54), then

$$x_n - 2x_{n-1} + x_{n-2} = \ddot{x}_{n-1}\Delta T^2 \quad (7.55)$$

Substituting Equation (7.55) into Equations (7.51) and (7.52), the linearization coefficients of the two-step Houbolt method can be obtained:

$$\begin{aligned} A &= \frac{2}{\Delta T^2}, \quad B_x = -\frac{1}{\Delta T^2}(4x_n - 2x_{n-1} + \ddot{x}_{n-1}\Delta T^2) \\ C &= \frac{11}{6\Delta T}, \quad D_x = -\frac{1}{6\Delta T}(16x_n - 5x_{n-1} + 2\ddot{x}_{n-1}\Delta T^2) \end{aligned} \quad (7.56)$$

As

$$\begin{aligned} x_{n+1} &= x_n + \dot{x}_n\Delta T + \frac{\ddot{x}(\xi)}{2}\Delta T^2 = x_n + \dot{x}_n\Delta T + \left(\frac{\ddot{x}_{n+1}}{6} + \frac{\ddot{x}_n}{3}\right)\Delta T^2 \\ x_{n+1} &= x_n + \dot{x}(\xi)\Delta T + \frac{\ddot{x}_n}{2}\Delta T^2 = x_n + \frac{1}{3}(\dot{x}_{n+1} + 2\dot{x}_n)\Delta T + \frac{1}{2}\ddot{x}_n\Delta T^2 \end{aligned} \quad (7.57)$$

then

$$\ddot{x}_{n+1} = \frac{6}{\Delta T^2} x_{n+1} - \frac{2}{\Delta T^2} (3x_n + 3\dot{x}_n \Delta T + \ddot{x}_n \Delta T^2) \quad (7.58)$$

$$\dot{x}_{n+1} = \frac{3}{\Delta T} x_{n+1} - \frac{1}{2\Delta T} (6x_n + 4\dot{x}_n \Delta T + 3\ddot{x}_n \Delta T^2) \quad (7.59)$$

Therefore, the linearization coefficients of the one-step Houbolt method become

$$\begin{aligned} A &= \frac{6}{\Delta T^2}, \quad B_x = -\frac{2}{\Delta T^2} (3x_n + 3\dot{x}_n \Delta T + \ddot{x}_n \Delta T^2) \\ C &= \frac{3}{\Delta T}, \quad D_x = -\frac{1}{2\Delta T} (6x_n + 4\dot{x}_n \Delta T + 3\ddot{x}_n \Delta T^2) \end{aligned} \quad (7.60)$$

In summary, the higher-order Houbolt method can be constructed by a higher-order Lagrange interpolation polynomial.

For different step-by-step time integration methods, different formulations of A , B_z , C and D_z can be obtained. Linearization coefficient formulations for different step-by-step time integration methods are shown in Table 7.2.

Table 7.2 Linearization coefficient for different step-by-step time integration methods

Method	A	B_z
TMM	$-\omega^2$	0
Forward–Euler	$\frac{2}{\Delta T^2}$	$-\frac{2}{\Delta T^2} [z(t_{i-1}) + \Delta T \dot{z}(t_{i-1})]$
Newmark- β	$\frac{1}{\beta \Delta T^2}$	$-\frac{1}{\beta \Delta T^2} \left[z(t_{i-1}) + \Delta T \dot{z}(t_{i-1}) + \left(\frac{1}{2} - \beta \right) \Delta T^2 \ddot{z}(t_{i-1}) \right]$
Wilson- θ	$\frac{6}{(\theta \Delta T)^2}$	$-\frac{6}{(\theta \Delta T)^2} \left[z(t_{i-1}) + \theta \Delta T \dot{z}(t_{i-1}) + \frac{(\theta \Delta T)^2}{3} \ddot{z}(t_{i-1}) \right]$
Houbolt for $i \geq 3$	$\frac{2}{\Delta T^2}$	$-\frac{1}{\Delta T^2} (5z(t_{i-1}) - 4z(t_{i-2}) + z(t_{i-3}))$
Houbolt for $i = 2$	$\frac{2}{\Delta T^2}$	$-\frac{1}{\Delta T^2} [4z(t_{i-1}) - 2z(t_{i-2}) + \Delta T^2 \ddot{z}(t_{i-2})]$
Houbolt for $i = 1$	$\frac{6}{\Delta T^2}$	$-\frac{2}{\Delta T^2} [3z(t_{i-1}) + 3\Delta T \dot{z}(t_{i-1}) + \Delta T^2 \ddot{z}(t_{i-1})]$
Method	C	D_z
TMM	0	0
Forward–Euler	$\frac{2}{\Delta T}$	$-\frac{1}{\Delta T} [2z(t_{i-1}) + \Delta T \dot{z}(t_{i-1})]$
Newmark- β	$\frac{\gamma}{\beta \Delta T}$	$\dot{z}(t_{i-1}) + \Delta T [(1-\gamma)\ddot{z}(t_{i-1}) + \gamma B_z]$
Wilson- θ	$\frac{3}{\theta \Delta T}$	$-\frac{3}{\theta \Delta T} \left[z(t_{i-1}) + \frac{2\theta \Delta T}{3} \dot{z}(t_{i-1}) + \frac{(\theta \Delta T)^2}{3} \ddot{z}(t_{i-1}) \right]$
Houbolt for $i \geq 3$	$\frac{11}{6\Delta T}$	$-\frac{1}{6\Delta T} [18z(t_{i-1}) - 9z(t_{i-2}) + 2z(t_{i-3})]$
Houbolt for $i = 2$	$\frac{11}{6\Delta T}$	$-\frac{1}{6\Delta T} [16z(t_{i-1}) - 5z(t_{i-2}) + 2\Delta T^2 \ddot{z}(t_{i-2})]$
Houbolt for $i = 1$	$\frac{3}{\Delta T}$	$-\frac{1}{2\Delta T} [6z(t_{i-1}) + 4\Delta T \dot{z}(t_{i-1}) + 3\Delta T^2 \ddot{z}(t_{i-1})]$

Let the variable z represent a column matrix, such as the position coordinates $\mathbf{r} = [x, y, z]^T$ or orientation angles $\boldsymbol{\theta} = [\theta_x, \theta_y, \theta_z]^T$. At present, of the four linearization coefficients, A and C are irrespective of the state vector coefficient z , hence their expressions are invariant. B_z and D_z , however, should be rewritten as column matrices \mathbf{B}_r and \mathbf{D}_r or \mathbf{B}_θ and \mathbf{D}_θ , respectively. For example, in the Newmark- β method

$$\begin{aligned}\mathbf{B}_r &= -\frac{1}{\beta\Delta T^2} \left[\mathbf{r}(t_{i-1}) + \Delta T \dot{\mathbf{r}}(t_{i-1}) + \left(\frac{1}{2} - \beta \right) \Delta T^2 \ddot{\mathbf{r}}(t_{i-1}) \right] \\ \mathbf{D}_r &= \dot{\mathbf{r}}(t_{i-1}) + \Delta T [(1-\gamma)\ddot{\mathbf{r}}(t_{i-1}) + \gamma\mathbf{B}_r] \\ \mathbf{B}_\theta &= -\frac{1}{\beta\Delta T^2} \left[\boldsymbol{\theta}(t_{i-1}) + \Delta T \dot{\boldsymbol{\theta}}(t_{i-1}) + \left(\frac{1}{2} - \beta \right) \Delta T^2 \ddot{\boldsymbol{\theta}}(t_{i-1}) \right] \\ \mathbf{D}_\theta &= \dot{\boldsymbol{\theta}}(t_{i-1}) + \Delta T [(1-\gamma)\ddot{\boldsymbol{\theta}}(t_{i-1}) + \gamma\mathbf{B}_\theta]\end{aligned}$$

7.3.3 Linearization of Nonlinear Functions

Correct to ΔT^2 , we expand the trigonometric functions at time t_i as an explicit function of previous time t_{i-1} by the Taylor expansion theorem, that is

$$\begin{aligned}\sin\theta(t_i) &= \sin[\theta(t_{i-1}) + \Delta\theta] = \bar{s} + o(\Delta T^2) \\ \cos\theta(t_i) &= \cos[\theta(t_{i-1}) + \Delta\theta] = \bar{c} + o(\Delta T^2)\end{aligned}\tag{7.61}$$

where

$$\begin{aligned}\bar{s} &= \sin\theta(t_{i-1}) \left\{ 1 - \frac{1}{2} [\dot{\theta}(t_{i-1})\Delta T]^2 \right\} + \cos\theta(t_{i-1}) \left[\dot{\theta}(t_{i-1})\Delta T + \frac{1}{2}\ddot{\theta}(t_{i-1})\Delta T^2 \right] \\ \bar{c} &= \cos\theta(t_{i-1}) \left\{ 1 - \frac{1}{2} [\dot{\theta}(t_{i-1})\Delta T]^2 \right\} - \sin\theta(t_{i-1}) \left[\dot{\theta}(t_{i-1})\Delta T + \frac{1}{2}\ddot{\theta}(t_{i-1})\Delta T^2 \right]\end{aligned}\tag{7.62}$$

In the geometric relationship from input end to output end, which includes trigonometric functions, the trigonometric functions can be linearized by the second-order Taylor expansion, that is

$$\sin\theta(t_i) = \cos\theta(t_{i-1})\theta(t_i) + \sin\theta(t_{i-1}) - \theta(t_{i-1})\cos\theta(t_{i-1}) - \frac{1}{2}\sin\theta(t_{i-1})[\dot{\theta}(t_{i-1})\Delta T]^2\tag{7.63}$$

$$\cos\theta(t_i) = -\sin\theta(t_{i-1})\theta(t_i) + \cos\theta(t_{i-1}) + \theta(t_{i-1})\sin\theta(t_{i-1}) - \frac{1}{2}\cos\theta(t_{i-1})[\dot{\theta}(t_{i-1})\Delta T]^2\tag{7.64}$$

For higher-order terms in body dynamic equations, the second-order terms can be expressed approximately as linear functions, that is

$$\mathbf{a}(t_i)\mathbf{b}(t_i) = \mathbf{a}(t_{i-1})\mathbf{b}(t_i) + \mathbf{a}(t_i)\mathbf{b}(t_{i-1}) - \mathbf{a}(t_{i-1})\mathbf{b}(t_{i-1}) + \dot{\mathbf{a}}(t_{i-1})\dot{\mathbf{b}}(t_{i-1})\Delta T^2\tag{7.65}$$

The linear expression of a third-order function is

$$\begin{aligned}\mathbf{a}(t_i)\mathbf{b}(t_i)\mathbf{c}(t_i) &= \mathbf{a}(t_{i-1})\mathbf{b}(t_{i-1})\mathbf{c}(t_i) + \mathbf{a}(t_{i-1})\mathbf{b}(t_i)\mathbf{c}(t_{i-1}) + \mathbf{a}(t_i)\mathbf{b}(t_{i-1})\mathbf{c}(t_{i-1}) - 2\mathbf{a}(t_{i-1})\mathbf{b}(t_{i-1})\mathbf{c}(t_{i-1}) \\ &\quad + [\dot{\mathbf{a}}(t_{i-1})\dot{\mathbf{b}}(t_{i-1})\mathbf{c}(t_{i-1}) + \dot{\mathbf{a}}(t_{i-1})\mathbf{b}(t_{i-1})\dot{\mathbf{c}}(t_{i-1}) + \mathbf{a}(t_{i-1})\dot{\mathbf{b}}(t_{i-1})\dot{\mathbf{c}}(t_{i-1})]\Delta T^2\end{aligned}\tag{7.66}$$

The above expansion formulations neglect the effect of terms that are higher than ΔT^3 order. For higher-order terms, their linearization expression can be obtained by using the same method.

The linearization expression of a general polynomial can be written as

$$a(\ddot{x}_i, \dot{x}_i, x_i, t_i) = \prod_{j=1}^n f_j(\ddot{x}_i, \dot{x}_i, x_i, t_i) = \sum_{j=1}^n \bar{f}_j f_j(\ddot{x}_i, \dot{x}_i, x_i, t_i) + \bar{F} \quad (7.67)$$

where \bar{f}_j ($j = 1, \dots, n$) and \bar{F} at time t_i are constants or functions of variables at previous times.

Substituting differential for finite difference

$$f_j(\ddot{x}_i, \dot{x}_i, x_i, t_i) - f_j(\ddot{x}_{i-1}, \dot{x}_{i-1}, x_{i-1}, t_{i-1}) = \dot{f}_j(\ddot{x}_{i-1}, \dot{x}_{i-1}, x_{i-1}, t_{i-1}) \Delta T \quad (7.68)$$

yields

$$a(\ddot{x}_i, \dot{x}_i, x_i, t_i) = \sum_{j=1}^n \left[\prod_{k=1, k \neq j}^n f_k(\ddot{x}_{i-1}, \dot{x}_{i-1}, x_{i-1}, t_{i-1}) \right] f_j(\ddot{x}_i, \dot{x}_i, x_i, t_i) - (n-1)a(\ddot{x}_{i-1}, \dot{x}_{i-1}, x_{i-1}, t_{i-1}) + \sum_{1 \leq j < k \leq n} \left[\dot{f}_j(\ddot{x}_{i-1}, \dot{x}_{i-1}, x_{i-1}, t_{i-1}) \dot{f}_k(\ddot{x}_{i-1}, \dot{x}_{i-1}, x_{i-1}, t_{i-1}) \Delta T^2 \prod_{\substack{l=1 \\ l \neq j, l \neq k}}^n \dot{f}_l(\ddot{x}_{i-1}, \dot{x}_{i-1}, x_{i-1}, t_{i-1}) \right] \quad (7.69)$$

Hence

$$\begin{aligned} \bar{f}_j &= \prod_{k=1, k \neq j}^n f_k(\ddot{x}_{i-1}, \dot{x}_{i-1}, x_{i-1}, t_{i-1}) \\ \bar{F} &= -(n-1)a(\ddot{x}_{i-1}, \dot{x}_{i-1}, x_{i-1}, t_{i-1}) + \sum_{1 \leq j < k \leq n} \left[\dot{f}_j(\ddot{x}_{i-1}, \dot{x}_{i-1}, x_{i-1}, t_{i-1}) \dot{f}_k(\ddot{x}_{i-1}, \dot{x}_{i-1}, x_{i-1}, t_{i-1}) \Delta T^2 \prod_{\substack{l=1 \\ l \neq j, l \neq k}}^n \dot{f}_l(\ddot{x}_{i-1}, \dot{x}_{i-1}, x_{i-1}, t_{i-1}) \right] \end{aligned} \quad (7.70)$$

Linearization formulas of the trigonometric functions $\sin \theta(t_i)$, $\cos \theta(t_i)$ and higher-order functions $a(t_i)b(t_i)$ and $a(t_i)b(t_i)c(t_i)$ are used to derive the transfer matrices of elements. For convenience, all of these formulations are listed in Table 7.3.

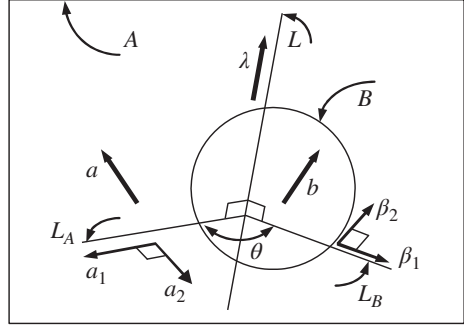
7.3.4 Linearization of Coordinate Transformation Matrices

The angular motion of a rigid body with respect to a fixed point can be realized by three rotations along three spatial fixed axes successively. The proof can be found in Appendix A.

A motion of a rigid body B relative to reference frame A is shown in Figure 7.6, where \mathbf{a} is any vector fixed in reference system A , and \mathbf{b} is a vector fixed on rigid body B . Before B rotates relative to A , $\mathbf{b} = \mathbf{a}$. One fixed point's 3 DOF rotation can be described by three angles which rotate in sequence around three arbitrary non-coplanar axes. Herein we consider the angles

Table 7.3 Linearization formulas of trigonometric functions and higher order functions

Function	Linearization formulas
$\sin \theta(t_i)$	$\sin \theta(t_{i-1}) \left\{ 1 - \frac{1}{2} [\dot{\theta}(t_{i-1}) \Delta T]^2 \right\} + \cos \theta(t_{i-1}) \left[\dot{\theta}(t_{i-1}) \Delta T + \frac{1}{2} \ddot{\theta}(t_{i-1}) \Delta T^2 \right]$
$\cos \theta(t_i)$	$\cos \theta(t_{i-1}) \left\{ 1 - \frac{1}{2} [\dot{\theta}(t_{i-1}) \Delta T]^2 \right\} - \sin \theta(t_{i-1}) \left[\dot{\theta}(t_{i-1}) \Delta T + \frac{1}{2} \ddot{\theta}(t_{i-1}) \Delta T^2 \right]$
$\sin \theta(t_i)$	$\cos \theta(t_{i-1}) \theta(t_i) + G_2, G_2 = \sin \theta(t_{i-1}) \left\{ 1 - \frac{1}{2} [\dot{\theta}(t_{i-1}) \Delta T]^2 \right\} - \theta(t_{i-1}) \cos \theta(t_{i-1})$
$\cos \theta(t_i)$	$-\sin \theta(t_{i-1}) \theta(t_i) + G_1, G_1 = \cos \theta(t_{i-1}) \left\{ 1 - \frac{1}{2} [\dot{\theta}(t_{i-1}) \Delta T]^2 \right\} + \theta(t_{i-1}) \sin \theta(t_{i-1})$
$a(t_i)b(t_i)$	$a(t_{i-1})b(t_i) + a(t_i)b(t_{i-1}) - a(t_{i-1})b(t_{i-1}) + \dot{a}(t_{i-1})\dot{b}(t_{i-1})\Delta T^2$
$a(t_i)b(t_i)c(t_i)$	$a(t_{i-1})b(t_{i-1})c(t_i) + a(t_{i-1})b(t_i)c(t_{i-1}) + a(t_i)b(t_{i-1})c(t_{i-1}) - 2a(t_{i-1})b(t_{i-1})c(t_{i-1})$ $+ [\dot{a}(t_{i-1})\dot{b}(t_{i-1})c(t_{i-1}) + \dot{a}(t_{i-1})b(t_{i-1})\dot{c}(t_{i-1}) + a(t_{i-1})\dot{b}(t_{i-1})\dot{c}(t_{i-1})] \Delta T^2$

Figure 7.6 Simple rotation.

$\theta_x, \theta_y, \theta_z$ that rotate in sequence around three spatial fixed axes in inertial coordinates. Therefore, the transform matrix, from the body-fixed coordinate system to the inertial coordinate system, can be expressed by trigonometric functions of angles $\theta_x, \theta_y, \theta_z$ as follows:

$$\mathbf{A} = \mathbf{A}_z \mathbf{A}_y \mathbf{A}_x = \begin{bmatrix} c_y c_z & s_x c_y c_z - c_x s_z & c_x s_y c_z + s_x s_z \\ c_y s_z & s_x s_y s_z + c_x c_z & c_x s_y s_z - s_x c_z \\ -s_y & s_x c_y & c_x c_y \end{bmatrix} \quad (7.71)$$

Where

$$\mathbf{A}_x = \begin{bmatrix} 1 & 0 & 0 \\ 0 & c_x & -s_x \\ 0 & s_x & c_x \end{bmatrix}, \mathbf{A}_y = \begin{bmatrix} c_y & 0 & s_y \\ 0 & 1 & 0 \\ -s_y & 0 & c_y \end{bmatrix}, \mathbf{A}_z = \begin{bmatrix} c_z & -s_z & 0 \\ s_z & c_z & 0 \\ 0 & 0 & 1 \end{bmatrix} \quad (7.72)$$

$$s_r = \sin \theta_r, \quad c_r = \cos \theta_r \quad (r = x, y, z)$$

Using multiple Taylor expansion, for transform matrix $A(t_i)$ at t_{i-1} , keeping second-order terms, we obtain

$$\begin{aligned}
 A(t_i) = & A(t_{i-1}) + \frac{\partial A(t_{i-1})}{\partial \theta_x} \Delta \theta_x + \frac{\partial A(t_{i-1})}{\partial \theta_y} \Delta \theta_y + \frac{\partial A(t_{i-1})}{\partial \theta_z} \Delta \theta_z \\
 & + \frac{1}{2!} \left\{ \frac{\partial^2 A(t_{i-1})}{\partial \theta_x^2} \Delta \theta_x^2 + \frac{\partial^2 A(t_{i-1})}{\partial \theta_y^2} \Delta \theta_y^2 + \frac{\partial^2 A(t_{i-1})}{\partial \theta_z^2} \Delta \theta_z^2 + \left[\frac{\partial^2 A(t_{i-1})}{\partial \theta_x \partial \theta_y} + \frac{\partial^2 A(t_{i-1})}{\partial \theta_y \partial \theta_x} \right] \Delta \theta_x \Delta \theta_y \right. \\
 & \left. + \left[\frac{\partial^2 A(t_{i-1})}{\partial \theta_x \partial \theta_z} + \frac{\partial^2 A(t_{i-1})}{\partial \theta_z \partial \theta_x} \right] \Delta \theta_x \Delta \theta_z + \left[\frac{\partial^2 A(t_{i-1})}{\partial \theta_y \partial \theta_z} + \frac{\partial^2 A(t_{i-1})}{\partial \theta_z \partial \theta_y} \right] \Delta \theta_y \Delta \theta_z \right\}
 \end{aligned} \tag{7.73}$$

According to Equation (7.71)

$$\frac{\partial A(t_i)}{\partial \theta_x} = A_z(t_i) A_y(t_i) \frac{\partial A_x(t_i)}{\partial \theta_x} = A(t_i) \begin{bmatrix} 0 & 0 & 0 \\ 0 & 0 & -1 \\ 0 & 1 & 0 \end{bmatrix} \tag{7.74}$$

$$\frac{\partial A(t_i)}{\partial \theta_y} = A_z(t_i) \frac{\partial A_y(t_i)}{\partial \theta_y} A_x(t_i) = A(t_i) \begin{bmatrix} 0 & s_x & c_x \\ -s_x & 0 & 0 \\ -c_x & 0 & 0 \end{bmatrix} \tag{7.75}$$

$$\frac{\partial A(t_i)}{\partial \theta_z} = \frac{\partial A_z(t_i)}{\partial \theta_z} A_y(t_i) A_x(t_i) = A(t_i) \begin{bmatrix} 0 & -c_x c_y & s_x c_y \\ c_x c_y & 0 & s_y \\ -s_x c_y & -s_y & 0 \end{bmatrix} \tag{7.76}$$

Let

$$T_1 = \begin{bmatrix} 1 \\ 0 \\ 0 \end{bmatrix}, \quad T_2 = \begin{bmatrix} 0 \\ c_x \\ -s_x \end{bmatrix}, \quad T_3 = \begin{bmatrix} -s_y \\ s_x c_y \\ c_x c_y \end{bmatrix} \tag{7.77}$$

Then

$$\frac{\partial A(t_i)}{\partial \theta_x} = A(t_i) \tilde{T}_1(t_i), \quad \frac{\partial A(t_i)}{\partial \theta_y} = A(t_i) \tilde{T}_2(t_i), \quad \frac{\partial A(t_i)}{\partial \theta_z} = A(t_i) \tilde{T}_3(t_i) \tag{7.78}$$

Similarly, it is easy to prove that

$$\frac{\partial^2 A(t_i)}{\partial \theta_x^2} = A(t_i) \tilde{T}_1^2(t_i), \quad \frac{\partial^2 A(t_i)}{\partial \theta_y^2} = A(t_i) \tilde{T}_2^2(t_i), \quad \frac{\partial^2 A(t_i)}{\partial \theta_z^2} = A(t_i) \tilde{T}_3^2(t_i) \tag{7.79}$$

Combining Equations (7.71) and (7.78) yields

$$\frac{\partial^2 A(t_i)}{\partial \theta_x \partial \theta_y} = \frac{\partial^2 A(t_i)}{\partial \theta_y \partial \theta_x} = A_z(t_i) \frac{\partial A_y(t_i)}{\partial \theta_y} \frac{\partial A_x(t_i)}{\partial \theta_x} = A(t_i) \tilde{T}_2(t_i) \tilde{T}_1(t_i) \tag{7.80}$$

$$\frac{\partial^2 A(t_i)}{\partial \theta_y \partial \theta_z} = \frac{\partial^2 A(t_i)}{\partial \theta_z \partial \theta_y} = \frac{\partial A_z(t_i)}{\partial \theta_z} \frac{\partial A_y(t_i)}{\partial \theta_y} A_x(t_i) = A(t_i) \tilde{T}_3(t_i) \tilde{T}_2(t_i) \tag{7.81}$$

$$\frac{\partial^2 \mathbf{A}(t_i)}{\partial \theta_z \partial \theta_x} = \frac{\partial^2 \mathbf{A}(t_i)}{\partial \theta_x \partial \theta_z} = \frac{\partial \mathbf{A}_z(t_i)}{\partial \theta_z} \mathbf{A}_y(t_i) \frac{\partial \mathbf{A}_x(t_i)}{\partial \theta_x} = \mathbf{A}(t_i) \tilde{\mathbf{T}}_3(t_i) \tilde{\mathbf{T}}_1(t_i) \quad (7.82)$$

Let

$$\Delta \theta_x^2 = [\Delta T \dot{\theta}_x(t_{i-1})]^2, \Delta \theta_y^2 = [\Delta T \dot{\theta}_y(t_{i-1})]^2, \Delta \theta_z^2 = [\Delta T \dot{\theta}_z(t_{i-1})]^2$$

$$\Delta \theta_x \Delta \theta_y = \Delta T^2 \dot{\theta}_x(t_{i-1}) \dot{\theta}_y(t_{i-1}), \Delta \theta_y \Delta \theta_z = \Delta T^2 \dot{\theta}_y(t_{i-1}) \dot{\theta}_z(t_{i-1}), \Delta \theta_x \Delta \theta_z = \Delta T^2 \dot{\theta}_x(t_{i-1}) \dot{\theta}_z(t_{i-1})$$

Substituting Equations (7.78) to (7.82) into Equation (7.73) yields

$$\mathbf{A}(t_i) = \mathbf{A}(t_{i-1}) \tilde{\mathbf{T}}_1(t_{i-1}) \theta_x(t_i) + \mathbf{A}(t_{i-1}) \tilde{\mathbf{T}}_2(t_{i-1}) \theta_y(t_i) + \mathbf{A}(t_{i-1}) \tilde{\mathbf{T}}_3(t_{i-1}) \theta_z(t_i) + \boldsymbol{\Phi}(t_{i-1}) \quad (7.83)$$

where

$$\begin{aligned} \boldsymbol{\Phi}(t_{i-1}) = & \mathbf{A}(t_{i-1}) \{ \mathbf{I} - \tilde{\mathbf{T}}_1(t_{i-1}) \theta_x(t_{i-1}) - \tilde{\mathbf{T}}_2(t_{i-1}) \theta_y(t_{i-1}) - \tilde{\mathbf{T}}_3(t_{i-1}) \theta_z(t_{i-1}) \\ & + \left[\frac{1}{2} \tilde{\mathbf{T}}_1^2(t_{i-1}) \dot{\theta}_x^2(t_{i-1}) + \frac{1}{2} \tilde{\mathbf{T}}_2^2(t_{i-1}) \dot{\theta}_y^2(t_{i-1}) + \frac{1}{2} \tilde{\mathbf{T}}_3^2(t_{i-1}) \dot{\theta}_z^2(t_{i-1}) + \tilde{\mathbf{T}}_2(t_{i-1}) \tilde{\mathbf{T}}_1(t_{i-1}) \dot{\theta}_y(t_{i-1}) \dot{\theta}_x(t_{i-1}) \right. \\ & \left. + \tilde{\mathbf{T}}_3(t_{i-1}) \tilde{\mathbf{T}}_2(t_{i-1}) \dot{\theta}_z(t_{i-1}) \dot{\theta}_y(t_{i-1}) + \tilde{\mathbf{T}}_3(t_{i-1}) \tilde{\mathbf{T}}_1(t_{i-1}) \dot{\theta}_z(t_{i-1}) \dot{\theta}_x(t_{i-1}) \right] \Delta T^2 \} \end{aligned} \quad (7.84)$$

7.4 Transfer Matrix of a Planar Rigid Body

A multi-rigid-body system is a system composed of several rigid bodies connected by all kinds of joints. Based on the MSDTTMM, once the transfer matrices of the elements are obtained, the multibody system dynamics can be computed and studied by simple programming matrix operations. It is important to point out that the transfer matrices of these elements remain the same for any multi-rigid-body systems and do not change with the structural variation of the multi-rigid-body system. The method provides flexibility in the modeling and computation of the dynamics of multibody systems with varying configuration, and this is one of the characteristics of the proposed method compared with any other method of multibody system dynamics. In this section, the dynamic equations of a rigid body are derived relative to the inertial coordinate system $oxyz$. The series uniform transfer equations and transfer matrices are deduced according to the input and output situations of all kinds of rigid bodies.

7.4.1 Planar Rigid Body with One Input End and One Output End

For the planar rigid body shown in Figure 7.7 the input end is I , the output end is O and the mass center is C . The inertial coordinate system is oxy and the body-fixed coordinate system is $O_2x_2y_2$ with origin I . In the coordinate system $O_2x_2y_2$, the position coordinates of O are (b_1, b_2) and for the mass center C they are (c_{c1}, c_{c2}) . The body-fixed coordinate system is obtained by rotating $o_1x_1y_1$ about the z_2 axis with angle θ . Hence,

$$\theta_O = \theta_I = \theta \quad (7.85)$$

$$\mathbf{x}_C = \mathbf{x}_I + c_{c1} \mathbf{c}_I - c_{c2} \mathbf{s}_I = \mathbf{x}_I + \mathbf{x}_{IC} \quad (7.86)$$

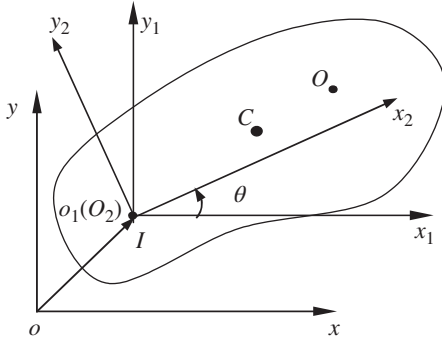


Figure 7.7 Rigid body moving in a plane with one input and one output end.

$$y_C = y_I + c_{c1}s_I + c_{c2}c_I = y_I + y_{IC} \quad (7.87)$$

$$x_O = x_I + b_1c_I - b_2s_I = x_I + x_{IO} \quad (7.88)$$

$$y_O = y_I + b_1s_I + b_2c_I = y_I + y_{IO} \quad (7.89)$$

where

$$s_I = \sin \theta_I, c_I = \cos \theta_I$$

$$x_{IC} = c_{c1}c_I - c_{c2}s_I \approx c_{c1}\bar{c} - c_{c2}\bar{s}$$

$$y_{IC} = c_{c1}s_I + c_{c2}c_I \approx c_{c1}\bar{s} + c_{c2}\bar{c}$$

$$x_{IO} = b_1c_I - b_2s_I \approx b_1\bar{c} - b_2\bar{s}$$

$$y_{IO} = b_1s_I + b_2c_I \approx b_1\bar{s} + b_2\bar{c}$$

The external forces and moments acting on the rigid body are equivalent to the external forces and moments acting on the mass center of the rigid body. Therefore, we only consider the external forces and moments acting on the mass center of rigid bodies in the following analysis. The motion equation of the mass center is

$$m\ddot{x}_C = q_{x,I} - q_{x,O} + f_{x,C} \quad (7.90)$$

$$m\ddot{y}_C = q_{y,I} - q_{y,O} + f_{y,C} \quad (7.91)$$

where m is the mass of the rigid body and (x_C, y_C) are the position coordinates relative to the inertial coordinate system, while $q_{x,I}$ and $q_{y,I}$ are internal forces acting on the input end of the rigid body, and $q_{x,O}$ and $q_{y,O}$ are internal forces acting on the output end. $f_{x,C}$ and $f_{y,C}$ are external forces acting on the mass center of the rigid body.

According to the theorem of absolute angular momentum with respect to moving point I

$$\frac{d\mathbf{G}_I}{dt} + m\mathbf{r}_{IC} \times \mathbf{a}_I = \mathbf{M} \quad (7.92)$$

The projection of Equation (7.92) on the inertial coordinate system can be written as

$$J_I\ddot{\theta}_I + mx_{IC}\ddot{y}_I - my_{IC}\ddot{x}_I = -m_I + m_O + m_C + q_{x,O}y_{IO} - q_{y,O}x_{IO} - f_{x,C}y_{IC} + f_{y,C}x_{IC} \quad (7.93)$$

where $\mathbf{G}_I = J_I\dot{\theta}_I$ is the absolute moment of momentum of the rigid body with respect to origin I of the body-fixed coordinate system, and J_I is the rotational inertia relative to point I . $\dot{\theta}_I$ is the

absolute angular velocity of the rigid body. \mathbf{r}_{IC} is the radius vector of the mass center C of the rigid body with respect to the point I , and \mathbf{a}_I is the absolute acceleration of point I .

Linearizing Equations (7.88) and (7.89) using Equations (7.63) and (7.64) yields

$$x_O = x_I - y_{IO}(t_{i-1})\theta_I + b_1 G_1 - b_2 G_2 \quad (7.94)$$

$$y_O = y_I + x_{IO}(t_{i-1})\theta_I + b_1 G_2 + b_2 G_1 \quad (7.95)$$

Substituting Equations (7.86) and (7.87) into Equations (7.90) and (7.91), and linearizing using Equations (7.27), (7.63) and (7.64), we obtain

$$q_{x,O} = -mAx_I + mAy_{IC}(t_{i-1})\theta_I + q_{x,I} + u_{57} \quad (7.96)$$

$$q_{y,O} = -mAy_I - mAx_{IC}(t_{i-1})\theta_I + q_{y,I} + u_{67} \quad (7.97)$$

Substituting Equations (7.96) and (7.97) into Equation (7.93), and linearizing using Equation (7.27), we obtain

$$m_O = u_{41}x_I + u_{42}y_I + u_{43}\theta_I + m_I + u_{45}q_{x,I} + u_{46}q_{y,I} + u_{47} \quad (7.98)$$

Combining Equations (7.85) and (7.95) to (7.98), the transfer equation of the rigid body moving in a plane with one input and one output end can be expressed as

$$\mathbf{z}_O = \mathbf{U} \mathbf{z}_I \quad (7.99)$$

The state vector is

$$\mathbf{z} = [x, y, \theta, m, q_x, q_y, 1]^T \quad (7.100)$$

and the transfer matrix is

$$\mathbf{U} = \begin{bmatrix} 1 & 0 & -y_{IO}(t_{i-1}) & 0 & 0 & 0 & b_1 G_1 - b_2 G_2 \\ 0 & 1 & x_{IO}(t_{i-1}) & 0 & 0 & 0 & b_1 G_2 + b_2 G_1 \\ 0 & 0 & 1 & 0 & 0 & 0 & 0 \\ u_{41} & u_{42} & u_{43} & 1 & u_{45} & u_{46} & u_{47} \\ -mA & 0 & mAy_{IC}(t_{i-1}) & 0 & 1 & 0 & u_{57} \\ 0 & -mA & -mAx_{IC}(t_{i-1}) & 0 & 0 & 1 & u_{67} \\ 0 & 0 & 0 & 0 & 0 & 0 & 1 \end{bmatrix} \quad (7.101)$$

where

$$\begin{aligned} u_{41} &= mA(y_{IO} - y_{IC}), u_{42} = -mA(x_{IO} - x_{IC}), u_{45} = -y_{IO}, u_{46} = x_{IO} \\ u_{43} &= -mAx_{IC}(t_{i-1})x_{IO} - mAy_{IC}(t_{i-1})y_{IO} + J_I A \\ u_{47} &= -m_C + u_{67}x_{IO} - u_{57}y_{IO} + J_I B_\theta + (mB_{y_I} - f_{y,C})x_{IC} + (f_{x,C} - mB_{x_I})y_{IC} \\ u_{57} &= f_{x,C} - mA(c_{c1}G_1 - c_{c2}G_2) - mB_{x_C} \\ u_{67} &= f_{y,C} - mA(c_{c1}G_2 + c_{c2}G_1) - mB_{y_C} \\ x_{IC}(t_{i-1}) &= (c_{c1}c_I - c_{c2}s_I)|_{t_{i-1}}, y_{IC}(t_{i-1}) = (c_{c1}s_I + c_{c2}c_I)|_{t_{i-1}}, \\ x_{IO}(t_{i-1}) &= (b_1c_I - b_2s_I)|_{t_{i-1}}, y_{IO}(t_{i-1}) = (b_1s_I + b_2c_I)|_{t_{i-1}} \end{aligned} \quad (7.103)$$

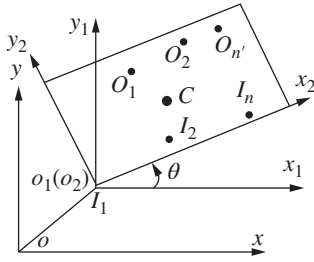


Figure 7.8 Rigid body with multiple input and multiple output ends moving in a plane.

7.4.2 Planar Rigid Body with Multiple Input and Multiple Output Ends

In this section, we derive the transfer equations and transfer matrices of rigid bodies with multiple input and multiple output ends, rigid bodies with one input end and multiple output ends, and rigid bodies with one output end and multiple input ends. For rigid bodies with multiple input and multiple output ends, we cannot obtain the main transfer equation from one point to another point. Only the matrix relation between input and output ends can be obtained.

Figure 7.8 is the dynamic model of a rigid body moving in a plane. Assuming the input ends are I_1, I_2, \dots, I_n and the output ends are $O_1, O_2, \dots, O_{n'}$, the mass center is C . The inertial coordinate system is oxy . The coordinate system $o_1x_1y_1$ is fixed on the first input end I_1 , and parallels the inertial coordinate system. The coordinate system $O_2x_2y_2$ is the body-fixed coordinate system and its origin is the same as $o_1x_1y_1$. The position coordinates of the input and output ends in the coordinate system $O_2x_2y_2$ are $(a_{1,1}, a_{2,1}), (a_{1,2}, a_{2,2}), \dots, (a_{1,n}, a_{2,n})$ and $(b_{1,1}, b_{2,1}), (b_{1,2}, b_{2,2}), \dots, (b_{1,n'}, b_{2,n'})$, respectively. The position coordinates of the mass center of the rigid body in the coordinate system $O_2x_2y_2$ are (c_{c1}, c_{c2}) .

Suppose we rotate $o_1x_1y_1$ by angle θ to obtain body-fixed coordinate $O_2x_2y_2$. If $n = n' = 1$, it is a one input end and one output end rigid body. When $n = 1$ and $n' > 1$, it is a rigid body with one input end and multiple output ends. When $n > 1$ and $n' = 1$, it is a rigid body with multiple input ends and one output end. When $n > 1$ and $n' > 1$, it is a rigid body with multiple input ends and multiple output ends.

Similarly to Equations (7.85) to (7.89), considering Equations (7.63) and (7.64) we obtain

$$\theta_{I_j} = \theta_{I_1} \quad (j = 2, 3, \dots, n) \quad (7.104)$$

$$\theta_{O_j} = \theta_{I_1} \quad (j = 1, 2, \dots, n') \quad (7.105)$$

$$\begin{bmatrix} x_C \\ y_C \end{bmatrix} = \begin{bmatrix} x_{I_1} \\ y_{I_1} \end{bmatrix} + \begin{bmatrix} -y_{I_1 C}(t_{i-1}) \\ x_{I_1 C}(t_{i-1}) \end{bmatrix} \theta_{I_1}(t_i) + \begin{bmatrix} c_{c1}G_1 - c_{c2}G_2 \\ c_{c1}G_2 + c_{c2}G_1 \end{bmatrix} \quad (7.106)$$

$$\begin{bmatrix} x_{I_j} \\ y_{I_j} \end{bmatrix} = \begin{bmatrix} x_{I_1} \\ y_{I_1} \end{bmatrix} + \begin{bmatrix} -y_{I_1 I_j}(t_{i-1}) \\ x_{I_1 I_j}(t_{i-1}) \end{bmatrix} \theta_{I_1}(t_i) + \begin{bmatrix} a_{1,j}G_1 - a_{2,j}G_2 \\ a_{1,j}G_2 + a_{2,j}G_1 \end{bmatrix} \quad (j = 2, 3, \dots, n) \quad (7.107)$$

$$\begin{bmatrix} x_{O_j} \\ y_{O_j} \end{bmatrix} = \begin{bmatrix} x_{I_1} \\ y_{I_1} \end{bmatrix} + \begin{bmatrix} -y_{I_1 O_j}(t_{i-1}) \\ x_{I_1 O_j}(t_{i-1}) \end{bmatrix} \theta_{I_1}(t_i) + \begin{bmatrix} b_{1,j}G_1 - b_{2,j}G_2 \\ b_{1,j}G_2 + b_{2,j}G_1 \end{bmatrix} \quad (j = 1, 2, 3, \dots, n') \quad (7.108)$$

where

$$x_{I_1 C} = c_{c1}c_{I_1} - c_{c2}s_{I_1} \approx c_{c1}\bar{c} - c_{c2}\bar{s} \quad (7.109)$$

$$y_{I_1 C} = c_{c1}s_{I_1} + c_{c2}c_{I_1} \approx c_{c1}\bar{s} + c_{c2}\bar{c} \quad (7.110)$$

$$x_{I_1 I_j} = a_{1,j}c_{I_1} - a_{2,j}s_{I_1} \approx a_{1,j}\bar{c} - a_{2,j}\bar{s} \quad (j = 2, 3, \dots, n) \quad (7.111)$$

$$y_{I_1 I_j} = a_{1,j}s_{I_1} + a_{2,j}c_{I_1} \approx a_{1,j}\bar{s} + a_{2,j}\bar{c} \quad (j = 2, 3, \dots, n) \quad (7.112)$$

$$x_{I_1 O_j} = b_{1,j}c_{I_1} - b_{2,j}s_{I_1} \approx b_{1,j}\bar{c} - b_{2,j}\bar{s} \quad (j = 1, 2, \dots, n') \quad (7.113)$$

$$y_{I_1 O_j} = b_{1,j}s_{I_1} + b_{2,j}c_{I_1} \approx b_{1,j}\bar{s} + b_{2,j}\bar{c} \quad (j = 1, 2, \dots, n') \quad (7.114)$$

(x_C, y_C) are the position coordinates of the mass center of a rigid body with respect to the inertial coordinate system. (x_{I_j}, y_{I_j}) and (x_{O_j}, y_{O_j}) are the position coordinates of the input end I_j and the output end O_j in the inertial coordinate system.

In the following analysis, we only consider the external force and external moment acting on the mass center of the rigid body. According to the dynamic equation of the mass center of a rigid body

$$m\ddot{x}_C = \sum_{j=1}^n q_{x,I_j} - \sum_{j=1}^{n'} q_{x,O_j} + f_{x,C} \quad (7.115)$$

$$m\ddot{y}_C = \sum_{j=1}^n q_{y,I_j} - \sum_{j=1}^{n'} q_{y,O_j} + f_{y,C} \quad (7.116)$$

where m is the mass of the rigid body, q_{x,I_j} and q_{y,I_j} are the internal forces acting on the input end of the rigid body, q_{x,O_j} and q_{y,O_j} are the internal forces acting on the output end of the rigid body, and $f_{x,C}$ and $f_{y,C}$ are the external forces acting on the mass center of the rigid body.

Based on the theorem of the absolute angular momentum on the moving momentum center, which is the first input end I_1 , we obtain

$$\frac{d\mathbf{G}_{I_1}}{dt} + m\mathbf{r}_{I_1C} \times \mathbf{a}_{I_1} = \sum \mathbf{r}_{I_1i} \times \mathbf{f}_i \quad (7.117)$$

The projection of Equation (7.117) on the inertial coordinate system can be written as

$$\begin{aligned} J_{I_1} \ddot{\theta}_{I_1} + mx_{I_1C} \ddot{y}_{I_1} - my_{I_1C} \ddot{x}_{I_1} = & - \sum_{j=1}^n m_{I_j} + \sum_{j=1}^{n'} m_{I_{O_j}} + m_C - \sum_{j=1}^n q_{x,I_j} y_{I_1 I_j} + \sum_{j=1}^n q_{y,I_j} x_{I_1 I_j} \\ & + \sum_{j=1}^{n'} q_{x,O_j} y_{I_1 O_j} - \sum_{j=1}^{n'} q_{y,O_j} x_{I_1 O_j} - f_{x,C} y_{I_1 C} + f_{y,C} x_{I_1 C} \end{aligned} \quad (7.118)$$

Substituting Equations (7.27), (7.106), (7.63) and (7.64) into Equations (7.115) and (7.116) yields

$$\sum_{j=1}^{n'} q_{x,O_j} = -mAx_{I_1} + mAy_{I_1C}(t_{i-1})\theta_{I_1}(t_i) + \sum_{j=1}^n q_{x,I_j} + f_{x,C} - mA(c_{c1}G_1 - c_{c2}G_2) - mB_{x,C} \quad (7.119)$$

$$\sum_{j=1}^{n'} q_{y,O_j} = -mAy_{I_1} - mAx_{I_1C}(t_{i-1})\theta_{I_1}(t_i) + \sum_{j=1}^n q_{y,I_j} + f_{y,C} - mA(c_{c1}G_2 + c_{c2}G_1) - mB_{y,C} \quad (7.120)$$

Substituting Equations (7.27), (7.119) and (7.120) into Equation (7.118) yields

$$\begin{aligned} \sum_{j=1}^{n'} m_{O_j} + \sum_{j=1}^{n'} q_{x,O_j} y_{I_1 O_j} - \sum_{j=1}^{n'} q_{y,O_j} x_{I_1 O_j} = & -my_{I_1C}Ax_{I_1} + mx_{I_1C}Ay_{I_1} + J_{I_1}A\theta_{I_1} + \sum_{j=1}^n m_{I_j} \\ & + \sum_{j=2}^n q_{x,I_j} y_{I_1 I_j} - \sum_{j=2}^n q_{y,I_j} x_{I_1 I_j} - m_C + J_{I_1}B_{\theta_{I_1}} + (mB_{y_{I_1}} - f_{y,C})x_{I_1C} - (mB_{x_{I_1}} - f_{x,C})y_{I_1C} \end{aligned} \quad (7.121)$$

Equations (7.107) and (7.104) can be written in matrix form

$$\mathbf{U}_{I_1 I_1} \mathbf{z}_{I_1} + \mathbf{U}_{I_1 I_j} \mathbf{z}_{I_j} = \mathbf{0}_3 \quad (j = 2, 3, \dots, n) \quad (7.122)$$

where

$$\mathbf{U}_{I_1 I_1} = \begin{bmatrix} 1 & 0 & -y_{I_1 I_j}(t_{i-1}) & 0 & 0 & 0 & a_{1,j}G_1 - a_{2,j}G_2 \\ 0 & 1 & x_{I_1 I_j}(t_{i-1}) & 0 & 0 & 0 & a_{1,j}G_2 + a_{2,j}G_1 \\ 0 & 0 & 1 & 0 & 0 & 0 & 0 \end{bmatrix}_{I_j} \quad (j = 2, 3, \dots, n) \quad (7.123)$$

$$\mathbf{U}_{I_1} = [-\mathbf{I}_3 \quad \mathbf{0}_{3 \times 4}] \quad (7.124)$$

Equations (7.105) and (7.108) can be written in matrix form

$$\mathbf{U}_{O_j I_1} \mathbf{z}_{I_1} + \mathbf{U}_{I_1 O_j} \mathbf{z}_{O_j} = \mathbf{0}_3 \quad (j = 1, 2, \dots, n') \quad (7.125)$$

where

$$\mathbf{U}_{O_j I_1} = \begin{bmatrix} 1 & 0 & -y_{I_1 O_j}(t_{i-1}) & 0 & 0 & 0 & b_{1,j}G_1 - b_{2,j}G_2 \\ 0 & 1 & x_{I_1 O_j}(t_{i-1}) & 0 & 0 & 0 & b_{1,j}G_2 + b_{2,j}G_1 \\ 0 & 0 & 1 & 0 & 0 & 0 & 0 \end{bmatrix} \quad (j = 1, 2, \dots, n') \quad (7.126)$$

Equations (7.119) to (7.121) can be written in matrix form

$$\mathbf{U}_{I_1}^4 \mathbf{z}_{I_1} + \mathbf{U}_{I_2}^4 \mathbf{z}_{I_2} + \dots + \mathbf{U}_{I_n}^4 \mathbf{z}_{I_n} + \mathbf{U}_{O_1}^4 \mathbf{z}_{O_1} + \mathbf{U}_{O_2}^4 \mathbf{z}_{O_2} + \dots + \mathbf{U}_{O_{n'}}^4 \mathbf{z}_{O_{n'}} = \mathbf{0}_3 \quad (7.127)$$

where

$$\mathbf{U}_{I_1}^4 = \begin{bmatrix} -my_{I_1 C}A & mx_{I_1 C}A & J_{I_1}A & 1 & 0 & 0 & u_{47, I_1} \\ -mA & 0 & mA y_{I_1 C}(t_{i-1}) & 0 & 1 & 0 & u_{57, I_1} \\ 0 & -mA & -mA x_{I_1 C}(t_{i-1}) & 0 & 0 & 1 & u_{67, I_1} \end{bmatrix} \quad (7.128)$$

$$u_{47, I_1} = -m_C + J_{I_1} B_\theta + (mB_{y_{I_1}} - f_{y, C})x_{I_1, C} - (mB_{x_{I_1}} - f_{x, C})y_{I_1, C}$$

$$u_{57, I_1} = f_{x, C} - mA(c_{c1}G_1 - c_{c2}G_2) - mB_{x_C}$$

$$u_{67, I_1} = f_{y, C} - mA(c_{c1}G_2 + c_{c2}G_1) - mB_{y_C}$$

$$\mathbf{U}_{I_j}^4 = \begin{bmatrix} 0 & 0 & 0 & 1 & y_{I_1 I_j} & -x_{I_1 I_j} & 0 \\ 0 & 0 & 0 & 0 & 1 & 0 & 0 \\ 0 & 0 & 0 & 0 & 0 & 1 & 0 \end{bmatrix} \quad (j = 2, 3, \dots, n) \quad (7.129)$$

$$\mathbf{U}_{O_j}^4 = - \begin{bmatrix} 0 & 0 & 0 & 1 & y_{I_1 O_j} & -x_{I_1 O_j} & 0 \\ 0 & 0 & 0 & 0 & 1 & 0 & 0 \\ 0 & 0 & 0 & 0 & 0 & 1 & 0 \end{bmatrix} \quad (j = 1, 2, \dots, n') \quad (7.130)$$

The state vector of the rigid body with multiple input ends and multiple output ends can be defined as

$$\mathbf{z} = \left[\mathbf{z}_{I_1}^T, \mathbf{z}_{I_2}^T, \dots, \mathbf{z}_{I_n}^T, \mathbf{z}_{O_1}^T, \mathbf{z}_{O_2}^T, \dots, \mathbf{z}_{O_{n'}}^T \right]^T \quad (7.131)$$

According to Equations (7.122), (7.125) and (7.127), the transfer equation of the rigid body with multiple input ends and multiple output ends is

$$\mathbf{U}\mathbf{z} = \mathbf{0}_{3n+3n'} \quad (7.132)$$

The transfer matrix is

$$\mathbf{U} = \begin{bmatrix} \mathbf{U}_{I_1 I_2} & \mathbf{U}_{I_1} & \mathbf{O}_{3 \times 7} & \cdots & \mathbf{O}_{3 \times 7} & \mathbf{O}_{3 \times 7} & \mathbf{O}_{3 \times 7} & \cdots & \mathbf{O}_{3 \times 7} \\ \mathbf{U}_{I_3 I_1} & \mathbf{O}_{3 \times 7} & \mathbf{U}_{I_1} & \cdots & \mathbf{O}_{3 \times 7} & \mathbf{O}_{3 \times 7} & \mathbf{O}_{3 \times 7} & \cdots & \mathbf{O}_{3 \times 7} \\ \vdots & \vdots & \vdots & \ddots & \vdots & \vdots & \vdots & & \vdots \\ \mathbf{U}_{I_n I_1} & \mathbf{O}_{3 \times 7} & \mathbf{O}_{3 \times 7} & \cdots & \mathbf{U}_{I_1} & \mathbf{O}_{3 \times 7} & \mathbf{O}_{3 \times 7} & \cdots & \mathbf{O}_{3 \times 7} \\ \mathbf{U}_{O_1 I_1} & \mathbf{O}_{3 \times 7} & \mathbf{O}_{3 \times 7} & \cdots & \mathbf{O}_{3 \times 7} & \mathbf{U}_{I_1} & \mathbf{O}_{3 \times 7} & \cdots & \mathbf{O}_{3 \times 7} \\ \mathbf{U}_{O_2 I_1} & \mathbf{O}_{3 \times 7} & \mathbf{O}_{3 \times 7} & \cdots & \mathbf{O}_{3 \times 7} & & \mathbf{U}_{I_1} & \cdots & \mathbf{O}_{3 \times 7} \\ \vdots & \vdots & \vdots & & \vdots & \vdots & \vdots & \ddots & \vdots \\ \mathbf{U}_{O_n I_1} & \mathbf{O}_{3 \times 7} & \mathbf{O}_{3 \times 7} & \cdots & \mathbf{O}_{3 \times 7} & \mathbf{O}_{3 \times 7} & \mathbf{O}_{3 \times 7} & \cdots & \mathbf{U}_{I_1} \\ \mathbf{U}_{I_1}^4 & \mathbf{U}_{I_2}^4 & \mathbf{U}_{I_3}^4 & \cdots & \mathbf{U}_{O_n}^4 & \mathbf{U}_{O_1}^4 & \mathbf{U}_{O_2}^4 & \cdots & \mathbf{U}_{O_{n'}}^4 \end{bmatrix} \quad (7.133)$$

Similarly, the transfer equations and transfer matrices of the rigid body with multiple input ends and one output end, and the rigid body with one input end and multiple output ends can be obtained, which are provided in the following sections without the detailed deduction procedures.

7.4.2.1 Transfer Equation and Transfer Matrix of a Rigid Body moving in a Plane with Multiple Input Ends and One Output End

State vector

$$\mathbf{z} = \left[\mathbf{z}_{I_1}^T, \mathbf{z}_{I_2}^T, \dots, \mathbf{z}_{I_n}^T, \mathbf{z}_{O_1}^T \right]^T \quad (7.134)$$

Transfer equation

$$\mathbf{U}\mathbf{z} = \mathbf{0}_{3n+3} \quad (7.135)$$

Transfer matrix

$$\mathbf{U} = \begin{bmatrix} \mathbf{U}_{I_2 I_1} & \mathbf{U}_{I_1} & \mathbf{O}_{3 \times 7} & \cdots & \mathbf{O}_{3 \times 7} & \mathbf{O}_{3 \times 7} \\ \mathbf{U}_{I_3 I_1} & \mathbf{O}_{3 \times 7} & \mathbf{U}_{I_1} & \cdots & \mathbf{O}_{3 \times 7} & \mathbf{O}_{3 \times 7} \\ \vdots & \vdots & \vdots & \ddots & \vdots & \vdots \\ \mathbf{U}_{I_n I_1} & \mathbf{O}_{3 \times 7} & \mathbf{O}_{3 \times 7} & \cdots & \mathbf{U}_{I_1} & \mathbf{O}_{3 \times 7} \\ \mathbf{U}_{O_1 I_1} & \mathbf{O}_{3 \times 7} & \mathbf{O}_{3 \times 7} & \cdots & \mathbf{O}_{3 \times 7} & \mathbf{U}_{I_1} \\ \mathbf{U}_{I_1}^4 & \mathbf{U}_{I_2}^4 & \mathbf{U}_{I_3}^4 & \cdots & \mathbf{U}_{I_n}^4 & \mathbf{U}_{O_1}^4 \end{bmatrix} \quad (7.136)$$

All submatrices are the same as those in Equation (7.133).

For computation convenience, \mathbf{z}_{O_1} can be expressed by $\mathbf{z}_{I_1}, \dots, \mathbf{z}_{I_n}$ as

$$\mathbf{z}_{O_1} = \begin{bmatrix} \mathbf{U}_{O_1 I_1} \mathbf{z}_{I_1} \\ \begin{bmatrix} 1 & -y_{I_1 O_1} & x_{I_1 O_1} \\ 0 & 1 & 0 \\ 0 & 0 & 1 \end{bmatrix} \left(\mathbf{U}_{I_1}^4 \mathbf{z}_{I_1} + \mathbf{U}_{I_2}^4 \mathbf{z}_{I_2} + \dots + \mathbf{U}_{I_n}^4 \mathbf{z}_{I_n} \right) \\ 1 \end{bmatrix} \quad (7.137)$$

7.4.2.2 Transfer Equation and Transfer Matrix of a Rigid Body Moving in a Plane with One Input End and Multiple Output Ends

State vector

$$\mathbf{z} = \left[\mathbf{z}_{I_1}^T, \mathbf{z}_{O_1}^T, \mathbf{z}_{O_2}^T, \dots, \mathbf{z}_{O_{n'}}^T \right]^T \quad (7.138)$$

Transfer equation

$$\mathbf{U} \mathbf{z} = \mathbf{0}_{2n'+4} \quad (7.139)$$

Transfer matrix

$$\mathbf{U} = \begin{bmatrix} \mathbf{U}_{O_1 I_1} & \mathbf{U}_{I_1} & \mathbf{O}_{3 \times 7} & \dots & \mathbf{O}_{3 \times 7} \\ \mathbf{U}_{O_2 I_1} & \mathbf{O}_{3 \times 7} & \mathbf{U}_{I_1} & \dots & \mathbf{O}_{3 \times 7} \\ \vdots & \vdots & \vdots & \ddots & \vdots \\ \mathbf{U}_{O_{n'} I_1} & \mathbf{O}_{3 \times 7} & \mathbf{O}_{3 \times 7} & \dots & \mathbf{U}_{I_1} \\ \mathbf{U}_{I_1}^4 & \mathbf{U}_{O_1}^4 & \mathbf{U}_{O_2}^4 & \dots & \mathbf{U}_{O_{n'}}^4 \end{bmatrix} \quad (7.140)$$

All submatrices are the same as those in Equation (7.133).

For computation convenience, \mathbf{z}_{I_1} can be expressed by $\mathbf{z}_{O_1}, \dots, \mathbf{z}_{O_{n'}}$ as

$$\mathbf{z}_{I_1} = \begin{bmatrix} \mathbf{R} \mathbf{z}_{O_1} \\ -\mathbf{U}_{I_1}^4 \begin{bmatrix} \mathbf{I}_3 \\ \mathbf{O}_{4 \times 3} \end{bmatrix} \mathbf{R} \mathbf{z}_{O_1} - \mathbf{U}_{I_1}^4 \begin{bmatrix} \mathbf{O}_{6 \times 1} \\ 1 \end{bmatrix} - \left(\mathbf{U}_{O_1}^4 \mathbf{z}_{O_1} + \mathbf{U}_{O_2}^4 \mathbf{z}_{O_2} + \dots + \mathbf{U}_{O_{n'}}^4 \mathbf{z}_{O_{n'}} \right) \\ 1 \end{bmatrix} \quad (7.141)$$

where

$$\mathbf{R} = \begin{bmatrix} 1 & 0 & y_{I_1 O_1}(t_{i-1}) & 0 & 0 & 0 & -b_{1,1}G_1 + b_{2,1}G_2 \\ 0 & 1 & -x_{I_1 O_1}(t_{i-1}) & 0 & 0 & 0 & -b_{1,1}G_2 - b_{2,1}G_1 \\ 0 & 0 & 1 & 0 & 0 & 0 & 0 \end{bmatrix}$$

7.5 Transfer Matrices of Spatial Rigid Bodies

In this book, the spatial motion of a multibody system is studied in the inertial coordinate system using three spatial angles about the x - y - z axis defined in reference [9], which is very convenient for the transformation of state vectors.

7.5.1 Spatial Rigid Body with One Input End and One Output End

The column matrix of the angular velocity of a rigid body with respect to the inertial coordinate system in the body-fixed coordinate system of a rigid body is

$$\omega = [\omega_x, \omega_y, \omega_z]^T \quad (7.142)$$

and its skew symmetric matrix is

$$\tilde{\omega} \equiv \begin{bmatrix} 0 & -\omega_z & \omega_y \\ \omega_z & 0 & -\omega_x \\ -\omega_y & \omega_x & 0 \end{bmatrix} \quad (7.143)$$

The first-order derivative with respect to time of transformation matrix A defined in Equation (7.71) is

$$\dot{A} = \begin{bmatrix} \dot{a}_{xx} & \dot{a}_{xy} & \dot{a}_{xz} \\ \dot{a}_{yx} & \dot{a}_{yy} & \dot{a}_{yz} \\ \dot{a}_{zx} & \dot{a}_{zy} & \dot{a}_{zz} \end{bmatrix}$$

The dynamics equation and transfer matrix are deduced using the three spatial axis angles about x - y - z , that is

$$\begin{bmatrix} \omega_x \\ \omega_y \\ \omega_z \end{bmatrix} = \begin{bmatrix} \dot{\theta}_x - s_y \dot{\theta}_z \\ c_x \dot{\theta}_y + s_x c_y \dot{\theta}_z \\ -s_x \dot{\theta}_y + c_x c_y \dot{\theta}_z \end{bmatrix} = \begin{bmatrix} 1 & 0 & -s_y \\ 0 & c_x & s_x c_y \\ 0 & -s_x & c_x c_y \end{bmatrix} \begin{bmatrix} \dot{\theta}_x \\ \dot{\theta}_y \\ \dot{\theta}_z \end{bmatrix} = H \begin{bmatrix} \dot{\theta}_x \\ \dot{\theta}_y \\ \dot{\theta}_z \end{bmatrix} \quad (7.144)$$

where

$$H = \begin{bmatrix} 1 & 0 & -s_y \\ 0 & c_x & s_x c_y \\ 0 & -s_x & c_x c_y \end{bmatrix}$$

It can be proved that

$$\dot{A} \equiv A \tilde{\omega} \quad (7.145)$$

$$\ddot{A} \equiv \dot{A} \tilde{\omega} + A \dot{\tilde{\omega}} = A (\tilde{\omega} \tilde{\omega} + \dot{\tilde{\omega}}) \quad (7.146)$$

The first-order derivative with respect to the time of the angular velocity ω of the rigid body in the inertial coordinate system is

$$\dot{\omega} = [\dot{\omega}_x, \dot{\omega}_y, \dot{\omega}_z]^T \quad (7.147)$$

The time derivative of Equation (7.144) is

$$\begin{bmatrix} \dot{\omega}_x \\ \dot{\omega}_y \\ \dot{\omega}_z \end{bmatrix} = \dot{H} \begin{bmatrix} \dot{\theta}_x \\ \dot{\theta}_y \\ \dot{\theta}_z \end{bmatrix} + H \begin{bmatrix} \ddot{\theta}_x \\ \ddot{\theta}_y \\ \ddot{\theta}_z \end{bmatrix} \quad (7.148)$$

where

$$\dot{H} = \begin{bmatrix} 0 & 0 & -c_y \dot{\theta}_y \\ 0 & -s_x \dot{\theta}_x & c_x c_y \dot{\theta}_x - s_x s_y \dot{\theta}_y \\ 0 & -c_x \dot{\theta}_x & -s_x c_y \dot{\theta}_x - c_x s_y \dot{\theta}_y \end{bmatrix} \quad (7.149)$$

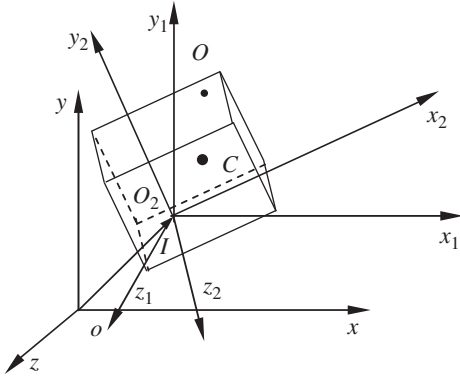


Figure 7.9 Rigid body moving in space.

For a rigid body moving in space, as shown in Figure 7.9, the column vectors of the rotation angle and positions are defined as $\theta = [\theta_x, \theta_y, \theta_z]^T$ and $r = [x, y, z]^T$, respectively. For the input end and output end

$$\theta_O = \theta_I = \theta \quad (7.150)$$

$$r_O = r_I + A l_{IO} \quad (7.151)$$

where A is the coordinate transformation matrix from $O_2 x_2 y_2 z_2$ to $o_1 x_1 y_1 z_1$.

If only the external force and moment acting on the mass center of the rigid body are considered, according to the motion equation of the mass center

$$m \ddot{r}_C = q_I - q_O + f_C \quad (7.152)$$

where m is the mass of the rigid body and r_C is the radius vector of the mass center of the rigid body with respect to the origin of the inertial coordinate system. q_I is the internal force acting on the input end of the rigid body, q_O is the internal force acting on the output end of rigid body and f_C is the external force acting on the mass center of the rigid body.

The projection of Equation (7.152) on the inertial coordinate system can be written as

$$m \begin{bmatrix} \ddot{x} \\ \ddot{y} \\ \ddot{z} \end{bmatrix}_C = \begin{bmatrix} q_x \\ q_y \\ q_z \end{bmatrix}_I - \begin{bmatrix} q_x \\ q_y \\ q_z \end{bmatrix}_O + \begin{bmatrix} f_x \\ f_y \\ f_z \end{bmatrix}_C \quad (7.153)$$

where $[x, y, z]^T_C$ is the coordinate column matrix of the mass center of the rigid body with respect to the inertial coordinate system:

$$r_C = r_I + A l_{IC} \quad (7.154)$$

According to the theorem of absolute angular momentum to the moving momentum center, we obtain

$$\frac{dG_I}{dt} = -m_I + m_O - r_{IO} \times q_O - m r_{IC} \times a_I + m_C + r_{IC} \times f_C \quad (7.155)$$

The projection of Equation (7.155) on the inertial coordinate system can be written as

$$A\dot{\mathbf{J}}\dot{\boldsymbol{\omega}} + \dot{A}\mathbf{J}\boldsymbol{\omega} = - \begin{bmatrix} m_x \\ m_y \\ m_z \end{bmatrix}_I + \begin{bmatrix} m_x \\ m_y \\ m_z \end{bmatrix}_O - \tilde{\mathbf{r}}_{IO} \begin{bmatrix} q_x \\ q_y \\ q_z \end{bmatrix}_O + \tilde{\mathbf{r}}_{IC} \left(\begin{bmatrix} f_x \\ f_y \\ f_z \end{bmatrix}_C - m \begin{bmatrix} \ddot{x} \\ \ddot{y} \\ \ddot{z} \end{bmatrix}_I \right) + \begin{bmatrix} m_x \\ m_y \\ m_z \end{bmatrix}_C \quad (7.156)$$

$$\mathbf{J} = \begin{bmatrix} J_{xx} & -J_{xy} & -J_{xz} \\ -J_{xy} & J_{yy} & -J_{yz} \\ -J_{xz} & -J_{yz} & J_{zz} \end{bmatrix} \quad (7.157)$$

where $\mathbf{r}_{IC} = A\mathbf{l}_{IC}$, $\mathbf{r}_{IO} = A\mathbf{l}_{IO}$ and \mathbf{G}_I is the absolute moment of momentum of the rigid body with respect to point I . \mathbf{m}_I and \mathbf{m}_O are the internal moments acting on points I and O , respectively, \mathbf{q}_O is the internal forces acting on point O , \mathbf{m}_C is the external moment acting on the mass center of the rigid body, \mathbf{a}_I is the acceleration of the point I and \mathbf{J} is the inertia matrix of the rigid body with respect to point I in the body-fixed coordinate system.

The transfer matrix is now derived. Substituting Equation (7.83) into Equation (7.151), we obtain

$$\begin{bmatrix} x \\ y \\ z \end{bmatrix}_O = [\mathbf{I}_3 \ \boldsymbol{\Psi}_{IO} \ \mathbf{O}_{3 \times 3} \ \mathbf{O}_{3 \times 3} \ \boldsymbol{\Phi}(t_{i-1})\mathbf{l}_{IO}] \mathbf{z}_I \quad (7.158)$$

where

$$\boldsymbol{\Psi}_{IO} = A(t_{i-1}) \left[\tilde{\mathbf{T}}_1(t_{i-1})\mathbf{l}_{IO} \ \tilde{\mathbf{T}}_2(t_{i-1})\mathbf{l}_{IO} \ \tilde{\mathbf{T}}_3(t_{i-1})\mathbf{l}_{IO} \right]$$

$\boldsymbol{\Phi}(t_{i-1})$, \mathbf{T}_1 , \mathbf{T}_2 , \mathbf{T}_3 and \mathbf{z}_I can be obtained by Equations (7.84), (7.77) and (7.20), respectively.

Equation (7.150) can be written as

$$\boldsymbol{\theta}_O = [\mathbf{O}_{3 \times 3} \ \mathbf{I}_3 \ \mathbf{O}_{3 \times 3} \ \mathbf{O}_{3 \times 3} \ \mathbf{O}_{3 \times 1}] \mathbf{z}_I \quad (7.159)$$

Linearizing the left-hand terms of Equation (7.153) yields

$$m(A\mathbf{r}_C + \mathbf{B}_{r_C}) = \begin{bmatrix} q_x \\ q_y \\ q_z \end{bmatrix}_I - \begin{bmatrix} q_x \\ q_y \\ q_z \end{bmatrix}_O + \begin{bmatrix} f_x \\ f_y \\ f_z \end{bmatrix}_C \quad (7.160)$$

Replacing the subscript O in Equation (7.158) by C , we obtain

$$\mathbf{r}_C = \mathbf{r}_I + \boldsymbol{\Psi}_{IC}\boldsymbol{\theta}_I + \boldsymbol{\Phi}(t_{i-1})\mathbf{l}_{IC} \quad (7.161)$$

Substituting Equation (7.161) into Equation (7.160) yields

$$\begin{bmatrix} q_x \\ q_y \\ q_z \end{bmatrix}_O = [-mA\mathbf{I}_3 \ -mA\boldsymbol{\Psi}_{IC} \ \mathbf{O}_{3 \times 3} \ \mathbf{I}_3 \ \mathbf{U}_{45}] \mathbf{z}_I \quad (7.162)$$

where

$$\mathbf{U}_{45} = [f_x, f_y, f_z]_C^T - mA\boldsymbol{\Phi}(t_{i-1})\mathbf{l}_{IC} - m\mathbf{B}_{r_C}$$

The coordinate column matrix of angular acceleration in the body-fixed coordinate system can be obtained, that is

$$\begin{aligned} \begin{bmatrix} \dot{\omega}_x \\ \dot{\omega}_y \\ \dot{\omega}_z \end{bmatrix} &= \begin{bmatrix} 0 & 0 & c_y \dot{\theta}_y \\ 0 & -s_x \dot{\theta}_x & c_x c_y \dot{\theta}_x - s_x s_y \dot{\theta}_y \\ 0 & -c_x \dot{\theta}_x & -s_x c_y \dot{\theta}_x - c_x s_y \dot{\theta}_y \end{bmatrix} \begin{bmatrix} \dot{\theta}_x \\ \dot{\theta}_y \\ \dot{\theta}_z \end{bmatrix} + \begin{bmatrix} 1 & 0 & -s_y \\ 0 & c_x & s_x c_y \\ 0 & -s_x & c_x c_y \end{bmatrix} \begin{bmatrix} \ddot{\theta}_x \\ \ddot{\theta}_y \\ \ddot{\theta}_z \end{bmatrix} \\ &= \begin{bmatrix} 0 \\ -s_x \\ -c_x \end{bmatrix} \dot{\theta}_x \dot{\theta}_y + \begin{bmatrix} -c_y \\ -s_x s_y \\ -c_x s_y \end{bmatrix} \dot{\theta}_y \dot{\theta}_z + \begin{bmatrix} 0 \\ c_x c_y \\ -s_x c_y \end{bmatrix} \dot{\theta}_x \dot{\theta}_z + \begin{bmatrix} 1 & 0 & -s_y \\ 0 & c_x & s_x c_y \\ 0 & -s_x & c_x c_y \end{bmatrix} \begin{bmatrix} \ddot{\theta}_x \\ \ddot{\theta}_y \\ \ddot{\theta}_z \end{bmatrix} \end{aligned}$$

Let

$$T_{12} = \begin{bmatrix} 0 \\ -s_x \\ -c_x \end{bmatrix}, T_{23} = \begin{bmatrix} -c_y \\ -s_x s_y \\ -c_x s_y \end{bmatrix}, T_{13} = \begin{bmatrix} 0 \\ c_x c_y \\ -s_x c_y \end{bmatrix} \quad (7.163)$$

then the coordinate column matrix of angular acceleration in the body-fixed coordinate system can be rewritten as

$$\dot{\omega} = T_{12} \dot{\theta}_x \dot{\theta}_y + T_{23} \dot{\theta}_y \dot{\theta}_z + T_{13} \dot{\theta}_x \dot{\theta}_z + T_1 \ddot{\theta}_x + T_2 \ddot{\theta}_y + T_3 \ddot{\theta}_z \quad (7.164)$$

Combining Equations (7.144) and (7.77) yields

$$\omega = [T_1 \quad T_2 \quad T_3] \begin{bmatrix} \dot{\theta}_x \\ \dot{\theta}_y \\ \dot{\theta}_z \end{bmatrix} \quad (7.165)$$

According to Equations (7.145), (7.164) and (7.165)

$$\begin{aligned} AJ\dot{\omega} + \dot{A}J\omega &= AJ(T_{12} \dot{\theta}_x \dot{\theta}_y + T_{23} \dot{\theta}_y \dot{\theta}_z + T_{13} \dot{\theta}_x \dot{\theta}_z + T_1 \ddot{\theta}_x + T_2 \ddot{\theta}_y + T_3 \ddot{\theta}_z) \\ &\quad + (A\tilde{T}_3 \dot{\theta}_z + A\tilde{T}_2 \dot{\theta}_y + A\tilde{T}_1 \dot{\theta}_x)J(T_1 \dot{\theta}_x + T_2 \dot{\theta}_y + T_3 \dot{\theta}_z) \end{aligned} \quad (7.166)$$

Let

$$H_1 = A[\tilde{T}_1 J T_1 \quad \tilde{T}_2 J T_2 \quad \tilde{T}_3 J T_3] \quad (7.167)$$

$$H_2 = A[J T_{12} + \tilde{T}_1 J T_2 + \tilde{T}_2 J T_1 \quad J T_{23} + \tilde{T}_2 J T_3 + \tilde{T}_3 J T_2 \quad J T_{13} + \tilde{T}_1 J T_3 + \tilde{T}_3 J T_1] \quad (7.168)$$

then

$$AJ\dot{\omega} + \dot{A}J\omega = \kappa_4 \theta_I(t_i) + \kappa_5 \quad (7.169)$$

where

$$\kappa_4 = AJHA + (H_1 \kappa_1 + H_2 \kappa_2)C \quad (7.170)$$

$$\kappa_5 = AJHB_{\theta_I} + (H_1 \kappa_x + H_2 \kappa_z) \kappa_3 + H_1 \begin{bmatrix} \ddot{\theta}_x^2 \\ \ddot{\theta}_y^2 \\ \ddot{\theta}_z^2 \end{bmatrix} \Delta T^2 + H_2 \begin{bmatrix} \ddot{\theta}_x \ddot{\theta}_y \\ \ddot{\theta}_y \ddot{\theta}_z \\ \ddot{\theta}_z \ddot{\theta}_x \end{bmatrix} \Delta T^2 \quad (7.171)$$

$$\kappa_1 = 2 \begin{bmatrix} \dot{\theta}_x & 0 & 0 \\ 0 & \dot{\theta}_y & 0 \\ 0 & 0 & \dot{\theta}_z \end{bmatrix}_{t_{i-1}}, \kappa_2 = \begin{bmatrix} \dot{\theta}_y & \dot{\theta}_x & 0 \\ 0 & \dot{\theta}_z & \dot{\theta}_y \\ \dot{\theta}_z & 0 & \dot{\theta}_x \end{bmatrix}_{t_{i-1}}, \kappa_3 = D_{\theta_i} - \frac{1}{2} \dot{\theta}(t_{i-1})$$

Substituting Equations (7.27) and (7.169) into Equation (7.156) yields

$$\begin{bmatrix} m_x \\ m_y \\ m_z \end{bmatrix}_O = [U_{31} \ U_{32} \ I_3 \ U_{34} \ U_{35}] z_I \quad (7.172)$$

where

$$\begin{aligned} U_{31} &= mA(\tilde{r}_{IC} - \tilde{r}_{IO}), \\ U_{32} &= \kappa_4 - mA\tilde{r}_{IO}\Psi_{IC}, \\ U_{34} &= \tilde{r}_{IO}, \\ U_{35} &= \kappa_5 - m_C + \tilde{r}_{IC}(mB_{r_i} - f_C) + \tilde{r}_{IO}U_{45} \end{aligned}$$

Combining Equations (7.158), (7.159), (7.162) and (7.172), the transfer equation of a rigid body moving in space with one input end and one output end can be obtained:

$$z_O = Uz_I \quad (7.173)$$

The transfer matrix is

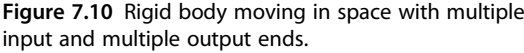
$$U = \begin{bmatrix} I_3 & \Psi_{IO} & O_{3 \times 3} & O_{3 \times 3} & \Phi(t_{i-1})I_{IO} \\ O_{3 \times 3} & I_3 & O_{3 \times 3} & O_{3 \times 3} & O_{3 \times 1} \\ U_{31} & U_{32} & I_3 & U_{34} & U_{35} \\ -mA I_3 & -mA \Psi_{IC} & O_{3 \times 3} & I_3 & U_{45} \\ O_{1 \times 3} & O_{1 \times 3} & O_{1 \times 3} & O_{1 \times 3} & 1 \end{bmatrix} \quad (7.174)$$

7.5.2 Spatial Rigid Body with Multiple Input and Multiple Output Ends

7.5.2.1 Transfer Equation and Transfer Matrix of a Rigid Body moving in Space with Multiple Input and Multiple Output Ends

The dynamics model of a rigid body moving in space with multiple input and multiple output ends is shown in Figure 7.10. I_1, I_2, \dots, I_n are input ends, O_1, O_2, \dots, O_m are output ends and C is the mass center of the rigid body. The inertial coordinate system is xyz . The origin of the coordinate system $o_1x_1y_1z_1$ is the first input end I_1 of the rigid body, which is parallel to the inertial coordinate system. The origin of the body-fixed coordinate system $O_2x_2y_2z_2$ is the same as the coordinate system $o_1x_1y_1z_1$. The coordinates of the input and output ends in the body-fixed coordinate system $O_2x_2y_2z_2$ are $(a_{1,j}, a_{2,j}, a_{3,j})$ and $(b_{1,j}, b_{2,j}, b_{3,j})$, respectively, and the coordinates of the mass center are (c_{c1}, c_{c2}, c_{c3}) . Then;

$$\begin{cases} \theta_{x,O_j} = \theta_{x,I_i} \\ \theta_{y,O_j} = \theta_{y,I_i} \quad (i = 1, 2, \dots, n \quad j = 1, 2, \dots, m) \\ \theta_{z,O_j} = \theta_{z,I_i} \end{cases} \quad (7.175)$$



$$(7.176)$$

$$(7.177)$$

$$(7.178)$$

where $[x, y, z]_I^T (j = 1, 2, \dots, n)$ and $[x, y, z]_O^T (j = 1, 2, \dots, m)$ are the coordinates column matrices of the input and output ends in the inertial coordinate system, \mathbf{r}_C is the vector of the mass center relative to the origin of the inertial coordinate system, $[x, y, z]_C^T$ are the coordinates column matrix of the mass center of the rigid body in the inertial coordinate system and \mathbf{A} is the transformation matrix from the coordinate system $O_2x_2y_2z_2$ to $o_1x_1y_1z_1$.

Linearizing Equations (7.175) and (7.176) yields

$$(7.179)$$

where

$(j = 1, 2, \dots, m)$

Linearizing Equations (7.175) and (7.177) yields

$$(7.180)$$

where

$$(j = 2, 3, \dots, n)$$

According to the dynamic equation of the mass center of the rigid body, we obtain

$$m\ddot{\mathbf{r}}_C = \sum_{j=1}^n \mathbf{q}_{I_j} - \sum_{j=1}^m \mathbf{q}_{O_j} + \mathbf{f}_C \quad (7.181)$$

Projecting Equation (7.181) into the inertial coordinate system yields

$$m \begin{bmatrix} \ddot{x} \\ \ddot{y} \\ \ddot{z} \end{bmatrix}_C = \sum_{j=1}^n \begin{bmatrix} q_x \\ q_y \\ q_z \end{bmatrix}_{I_j} - \sum_{j=1}^m \begin{bmatrix} q_x \\ q_y \\ q_z \end{bmatrix}_{O_j} + \begin{bmatrix} f_x \\ f_y \\ f_z \end{bmatrix}_C \quad (7.182)$$

where m is the mass of the rigid body. $\mathbf{q}_{I_j} (j=1,2,\dots,n)$ are the internal forces at the input ends and $\mathbf{q}_{O_j} (j=1,2,\dots,m)$ are the internal forces at the output ends. \mathbf{f}_C is the external force acting on the rigid body mass center.

According to the theorem of absolute angular momentum to the moving momentum center, the dynamics equation of a rigid body with multiple input and multiple output ends can be written as

$$\frac{d\mathbf{G}_{I_1}}{dt} = - \sum_{j=1}^n \mathbf{m}_{I_j} + \sum_{j=1}^m \mathbf{m}_{O_j} + \sum_{j=1}^n \mathbf{r}_{I_1 I_j} \times \mathbf{q}_{I_j} - \sum_{j=1}^m \mathbf{r}_{I_1 O_j} \times \mathbf{q}_{O_j} - \mathbf{r}_{I_1 C} \times m\mathbf{a}_{I_1} + \mathbf{m}_C + \mathbf{r}_{I_1 C} \times \mathbf{f}_C \quad (7.183)$$

Projecting Equation (7.183) into the inertial coordinate system yields

$$\begin{aligned} \frac{d}{dt}(\mathbf{A}\mathbf{J}\boldsymbol{\omega}) = & - \sum_{j=1}^n \begin{bmatrix} m_x \\ m_y \\ m_z \end{bmatrix}_{I_j} + \sum_{j=1}^m \begin{bmatrix} m_x \\ m_y \\ m_z \end{bmatrix}_{O_j} + \sum_{j=1}^n \tilde{\mathbf{r}}_{I_1 I_j} \begin{bmatrix} q_x \\ q_y \\ q_z \end{bmatrix}_{I_j} - \sum_{j=1}^m \tilde{\mathbf{r}}_{I_1 O_j} \begin{bmatrix} q_x \\ q_y \\ q_z \end{bmatrix}_{O_j} \\ & + \tilde{\mathbf{r}}_{I_1 C} \left(\begin{bmatrix} f_x \\ f_y \\ f_z \end{bmatrix}_C - m \begin{bmatrix} \ddot{x} \\ \ddot{y} \\ \ddot{z} \end{bmatrix}_{I_1} \right) + \begin{bmatrix} m_x \\ m_y \\ m_z \end{bmatrix}_C \end{aligned} \quad (7.184)$$

where

$$\mathbf{r}_{I_1 C} = \mathbf{A}\mathbf{I}_{I_1 C}$$

$$\mathbf{r}_{I_1 I_j} = \mathbf{A}\mathbf{I}_{I_1 I_j} \quad (j=1,2,\dots,n)$$

$$\mathbf{r}_{I_1 O_j} = \mathbf{A}\mathbf{I}_{I_1 O_j} \quad (j=1,2,\dots,m)$$

Linearizing Equations (7.182) and (7.184) yields

$$\mathbf{U}_{I_1}^4 \mathbf{z}_{I_1} + \mathbf{U}_{I_2}^4 \mathbf{z}_{I_2} + \dots + \mathbf{U}_{I_n}^4 \mathbf{z}_{I_n} + \mathbf{U}_{O_1}^4 \mathbf{z}_{O_1} + \mathbf{U}_{O_2}^4 \mathbf{z}_{O_2} + \dots + \mathbf{U}_{O_m}^4 \mathbf{z}_{O_m} = \mathbf{0}_6 \quad (7.185)$$

where

$$\begin{aligned} \mathbf{U}_{I_1}^4 = & \begin{bmatrix} m\mathbf{A}\tilde{\mathbf{r}}_{I_1 C} & \boldsymbol{\kappa}_4 & \mathbf{I}_3 & \mathbf{O}_{3 \times 3} & -\mathbf{m}_C + \boldsymbol{\kappa}_5 - \tilde{\mathbf{r}}_{I_1 C}(\mathbf{f}_C - m\mathbf{B}_{r_{I_1}}) \\ -m\mathbf{A}\mathbf{I}_3 & -m\mathbf{A}\boldsymbol{\Psi}_{I_1 C} & \mathbf{O}_{3 \times 3} & \mathbf{I}_3 & -m\mathbf{A}\boldsymbol{\Phi}(t_{i-1})\mathbf{I}_{I_1 C} + (\mathbf{f}_C - m\mathbf{B}_{r_C}) \end{bmatrix} \\ \mathbf{U}_{I_j}^4 = & \begin{bmatrix} \mathbf{O}_{3 \times 3} & \mathbf{O}_{3 \times 3} & \mathbf{I}_3 & -\tilde{\mathbf{r}}_{I_1 I_j} & \mathbf{O}_{3 \times 1} \\ \mathbf{O}_{3 \times 3} & \mathbf{O}_{3 \times 3} & \mathbf{O}_{3 \times 3} & \mathbf{I}_3 & \mathbf{O}_{3 \times 1} \end{bmatrix} \quad (j=2,3,\dots,n) \\ \mathbf{U}_{O_j}^4 = & \begin{bmatrix} \mathbf{O}_{3 \times 3} & \mathbf{O}_{3 \times 3} & -\mathbf{I}_3 & \tilde{\mathbf{r}}_{I_1 O_j} & \mathbf{O}_{3 \times 1} \\ \mathbf{O}_{3 \times 3} & \mathbf{O}_{3 \times 3} & \mathbf{O}_{3 \times 3} & -\mathbf{I}_3 & \mathbf{O}_{3 \times 1} \end{bmatrix} \quad (j=1,2,\dots,m) \end{aligned}$$

The state vector of a rigid body with multiple input ends and multiple output ends can be defined as

$$\mathbf{z} = \left[\mathbf{z}_{I_1}^T, \mathbf{z}_{I_2}^T, \dots, \mathbf{z}_{I_n}^T, \mathbf{z}_{O_1}^T, \mathbf{z}_{O_2}^T, \dots, \mathbf{z}_{O_m}^T \right]^T \quad (7.186)$$

Combining Equations (7.179), (7.180) and (7.185), the transfer equation of a rigid body with multiple input ends and multiple output ends can be obtained

$$\mathbf{U}\mathbf{z} = \mathbf{0}_{6n+6m} \quad (7.187)$$

The transfer matrix is

$$\mathbf{U} = \begin{bmatrix} \mathbf{U}_{I_2 I_1} & \mathbf{U}_{I_1} & \mathbf{O}_{6 \times 13} & \cdots & \mathbf{O}_{6 \times 13} & \mathbf{O}_{6 \times 13} & \mathbf{O}_{6 \times 13} & \cdots & \mathbf{O}_{6 \times 13} \\ \mathbf{U}_{I_3 I_1} & \mathbf{O}_{6 \times 13} & \mathbf{U}_{I_1} & \cdots & \mathbf{O}_{6 \times 13} & \mathbf{O}_{6 \times 13} & \mathbf{O}_{6 \times 13} & \cdots & \mathbf{O}_{6 \times 13} \\ \vdots & \vdots & \vdots & \ddots & \vdots & \vdots & \vdots & & \vdots \\ \mathbf{U}_{I_n I_1} & \mathbf{O}_{6 \times 13} & \mathbf{O}_{6 \times 13} & \cdots & \mathbf{U}_{I_1} & \mathbf{O}_{6 \times 13} & \mathbf{O}_{6 \times 13} & \cdots & \mathbf{O}_{6 \times 13} \\ \mathbf{U}_{O_1 I_1} & \mathbf{O}_{6 \times 13} & \mathbf{O}_{6 \times 13} & \cdots & \mathbf{O}_{6 \times 13} & \mathbf{U}_{I_1} & \mathbf{O}_{6 \times 13} & \cdots & \mathbf{O}_{6 \times 13} \\ \mathbf{U}_{O_2 I_1} & \mathbf{O}_{6 \times 13} & \mathbf{O}_{6 \times 13} & \cdots & \mathbf{O}_{6 \times 13} & \mathbf{O}_{6 \times 13} & \mathbf{U}_{I_1} & \cdots & \mathbf{O}_{6 \times 13} \\ \vdots & \vdots & \vdots & & \vdots & \vdots & \vdots & \ddots & \vdots \\ \mathbf{U}_{O_m I_1} & \mathbf{O}_{6 \times 13} & \mathbf{O}_{6 \times 13} & \cdots & \mathbf{O}_{6 \times 13} & \mathbf{O}_{6 \times 13} & \mathbf{O}_{6 \times 13} & \cdots & \mathbf{U}_{I_1} \\ \mathbf{U}_{I_1}^4 & \mathbf{U}_{I_2}^4 & \mathbf{U}_{I_3}^4 & \cdots & \mathbf{U}_{I_n}^4 & \mathbf{U}_{O_1}^4 & \mathbf{U}_{O_2}^4 & \cdots & \mathbf{U}_{O_m}^4 \end{bmatrix} \quad (7.188)$$

In a similar manner, the transfer equations and transfer matrices of a rigid body with multiple input ends and one output end, and a rigid body with one input end and multiple output ends can be found. The results are given in the following sections.

7.5.2.2 Transfer Matrix of a Rigid Body with Multiple Input Ends and One Output End

State vector

$$\mathbf{z} = \left[\mathbf{z}_{I_1}^T, \mathbf{z}_{I_2}^T, \dots, \mathbf{z}_{I_n}^T, \mathbf{z}_{O_1}^T \right]^T \quad (7.189)$$

Transfer equation

$$\mathbf{U}\mathbf{z} = \mathbf{0}_{6n+6} \quad (7.190)$$

Transfer matrix

$$\mathbf{U} = \begin{bmatrix} \mathbf{U}_{I_2 I_1} & \mathbf{U}_{I_1} & \mathbf{O}_{6 \times 13} & \cdots & \mathbf{O}_{6 \times 13} & \mathbf{O}_{6 \times 13} \\ \mathbf{U}_{I_3 I_1} & \mathbf{O}_{6 \times 13} & \mathbf{U}_{I_1} & \cdots & \mathbf{O}_{6 \times 13} & \mathbf{O}_{6 \times 13} \\ \vdots & \vdots & \vdots & \ddots & \vdots & \vdots \\ \mathbf{U}_{I_n I_1} & \mathbf{O}_{6 \times 13} & \mathbf{O}_{6 \times 13} & \cdots & \mathbf{U}_{I_1} & \mathbf{O}_{6 \times 13} \\ \mathbf{U}_{O_1 I_1} & \mathbf{O}_{6 \times 13} & \mathbf{O}_{6 \times 13} & \cdots & \mathbf{O}_{6 \times 13} & \mathbf{U}_{I_1} \\ \mathbf{U}_{I_1}^4 & \mathbf{U}_{I_2}^4 & \mathbf{U}_{I_3}^4 & \cdots & \mathbf{U}_{I_n}^4 & \mathbf{U}_{O_1}^4 \end{bmatrix} \quad (7.191)$$

All submatrices are the same as those in Equation (7.188).

For ease of calculation, \mathbf{z}_{O_1} can be expressed by $\mathbf{z}_{I_1}, \dots, \mathbf{z}_{I_n}$, hence

$$\mathbf{z}_{O_1} = \begin{bmatrix} \mathbf{U}_{O_1 I_1} \mathbf{z}_{I_1} \\ \begin{bmatrix} \mathbf{I}_3 & \tilde{\mathbf{r}}_{I_1 O_1} \\ \mathbf{O}_{3 \times 3} & \mathbf{I}_3 \end{bmatrix} \left(\mathbf{U}_{I_1}^4 \mathbf{z}_{I_1} + \mathbf{U}_{I_2}^4 \mathbf{z}_{I_2} + \dots + \mathbf{U}_{I_n}^4 \mathbf{z}_{I_n} \right) \\ 1 \end{bmatrix} \quad (7.192)$$

7.5.2.3 Transfer Matrix of a Rigid Body with One Input End and Multiple Output Ends

State vector

$$\mathbf{z} = \left[\mathbf{z}_{I_1}^T, \mathbf{z}_{O_1}^T, \mathbf{z}_{O_2}^T, \dots, \mathbf{z}_{O_m}^T \right]^T \quad (7.193)$$

Transfer equation

$$\mathbf{U}\mathbf{z} = \mathbf{0}_{6m+6} \quad (7.194)$$

Transfer matrix

$$\mathbf{U} = \begin{bmatrix} \mathbf{U}_{O_1 I_1} & \mathbf{U}_{I_1} & \mathbf{O}_{6 \times 13} & \cdots & \mathbf{O}_{6 \times 13} \\ \mathbf{U}_{O_2 I_1} & \mathbf{O}_{6 \times 13} & \mathbf{U}_{I_1} & \cdots & \mathbf{O}_{6 \times 13} \\ \vdots & \vdots & \vdots & \ddots & \vdots \\ \mathbf{U}_{O_m I_1} & \mathbf{O}_{6 \times 13} & \mathbf{O}_{6 \times 13} & \cdots & \mathbf{U}_{I_1} \\ \mathbf{U}_{I_1}^4 & \mathbf{U}_{O_1}^4 & \mathbf{U}_{O_2}^4 & \cdots & \mathbf{U}_{O_m}^4 \end{bmatrix} \quad (7.195)$$

All submatrices are the same as those in Equation (7.188).

For ease of calculation, \mathbf{z}_{I_1} can be expressed by $\mathbf{z}_{O_1}, \dots, \mathbf{z}_{O_m}$, hence

$$\mathbf{z}_{I_1} = \begin{bmatrix} \mathbf{R}_1 \mathbf{z}_{O_1} \\ -\mathbf{R}_2 \mathbf{z}_{O_1} - \mathbf{R}_3 - \left(\mathbf{U}_{O_1}^4 \mathbf{z}_{O_1} + \mathbf{U}_{O_2}^4 \mathbf{z}_{O_2} + \dots + \mathbf{U}_{O_m}^4 \mathbf{z}_{O_m} \right) \\ 1 \end{bmatrix} \quad (7.196)$$

where

$$\mathbf{R}_1 = \begin{bmatrix} \mathbf{I}_3 & -\Psi_{I_1 O_1} & \mathbf{O}_{3 \times 3} & \mathbf{O}_{3 \times 3} & -\Phi(t_{i-1}) \mathbf{l}_{I_1 O_1} \\ \mathbf{O}_{3 \times 3} & \mathbf{I}_3 & \mathbf{O}_{3 \times 3} & \mathbf{O}_{3 \times 3} & \mathbf{O}_{3 \times 3} \end{bmatrix}$$

$$\mathbf{R}_2 = \begin{bmatrix} m A \tilde{\mathbf{r}}_{I_1 C} & \kappa_4 \\ -m A \mathbf{I}_3 & -m A \Psi_{I_1 C} \end{bmatrix} \mathbf{R}_1, \quad \mathbf{R}_3 = \begin{bmatrix} -\mathbf{m}_C + \kappa_5 - \tilde{\mathbf{r}}_{I_1 C} \left(\mathbf{f}_C - m \mathbf{B}_{r_{I_1}} \right) \\ -m A \Phi(t_{i-1}) \mathbf{l}_{I_1 C} + (\mathbf{f}_C - m \mathbf{B}_{r_C}) \end{bmatrix}$$

7.6 Transfer Matrices of Planar Hinges

The interaction (such as damper, spring, driven constraint or motion and contact) between different bodies can be regarded as a force element in the ordinary dynamics methods of multibody systems. However, in MSDTTMM, the interactions between different bodies can be regarded as hinges, and that makes dynamic modeling more convenient and flexible.

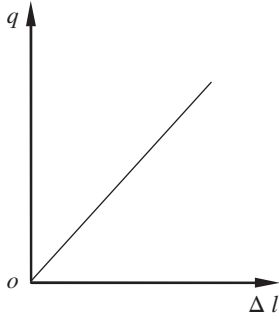


Figure 7.11 Linear spring force model.

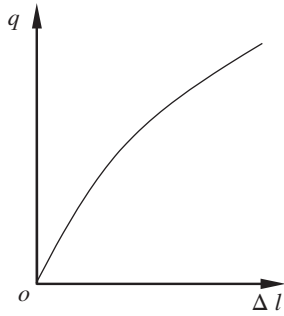


Figure 7.12 Nonlinear spring force model.

7.6.1 Elastic Hinges

Here, the elastic hinge consists of linear (or nonlinear) spring hinges and linear (or nonlinear) rotary spring hinges. Figures 7.11 and 7.12 illustrate the models for linear spring and nonlinear spring forces, respectively.

Ignore the mass and the initial length of the spring and assume

$$\mathbf{q} = K_1 \Delta \mathbf{l} + K_2 \Delta \mathbf{l}^3 \quad (7.197)$$

where $|\Delta \mathbf{l}| = \sqrt{(x_O - x_I)^2 + (y_O - y_I)^2}$ is the change in length of a spring in the xy plane. O denotes the output end and I denotes the input end. \mathbf{q} is the spring force, and K_1 and K_2 are the stiffness coefficients of a nonlinear spring.

Projection of Equation (7.197) into the ox and oy directions results in

$$\begin{cases} -q_{x,I} = K_1(x_O - x_I) + K_2[(x_O - x_I)^3 + (y_O - y_I)^2(x_O - x_I)] \\ -q_{y,I} = K_1(y_O - y_I) + K_2[(x_O - x_I)^2(y_O - y_I) + (y_O - y_I)^3] \end{cases} \quad (7.198)$$

Substituting Equation (7.66) into Equation (7.198) yields

$$\begin{cases} -q_{x,I} = a_1(x_O - x_I) + a_2(y_O - y_I) + a_3 \\ -q_{y,I} = b_1(x_O - x_I) + b_2(y_O - y_I) + b_3 \end{cases} \quad (7.199)$$

where

$$\begin{aligned} a_1 &= K_1 + 3K_2[x_O(t_{i-1}) - x_I(t_{i-1})]^2 + K_2[y_O(t_{i-1}) - y_I(t_{i-1})]^2 \\ a_2 &= 2K_2[y_O(t_{i-1}) - y_I(t_{i-1})][x_O(t_{i-1}) - x_I(t_{i-1})] \\ a_3 &= K_2\{-2[x_O(t_{i-1}) - x_I(t_{i-1})]^3 + 3[\dot{x}_O(t_{i-1}) - \dot{x}_I(t_{i-1})]^2[x_O(t_{i-1}) - x_I(t_{i-1})]\Delta T^2 \\ &\quad + [\dot{y}_O(t_{i-1}) - \dot{y}_I(t_{i-1})]^2[x_O(t_{i-1}) - x_I(t_{i-1})]\Delta T^2 - 2[y_O(t_{i-1}) - y_I(t_{i-1})]^2[x_O(t_{i-1}) - x_I(t_{i-1})] \\ &\quad + 2[\dot{y}_O(t_{i-1}) - \dot{y}_I(t_{i-1})][\dot{x}_O(t_{i-1}) - \dot{x}_I(t_{i-1})][y_O(t_{i-1}) - y_I(t_{i-1})]\Delta T^2\} \\ b_1 &= 2K_2[y_O(t_{i-1}) - y_I(t_{i-1})][x_O(t_{i-1}) - x_I(t_{i-1})] \\ b_2 &= K_1 + K_2[x_O(t_{i-1}) - x_I(t_{i-1})]^2 + 3K_2[y_O(t_{i-1}) - y_I(t_{i-1})]^2 \\ b_3 &= K_2\{-2[y_O(t_{i-1}) - y_I(t_{i-1})]^3 + 3[\dot{y}_O(t_{i-1}) - \dot{y}_I(t_{i-1})]^2[y_O(t_{i-1}) - y_I(t_{i-1})]\Delta T^2 \\ &\quad + [\dot{x}_O(t_{i-1}) - \dot{x}_I(t_{i-1})]^2[y_O(t_{i-1}) - y_I(t_{i-1})]\Delta T^2 - 2[x_O(t_{i-1}) - x_I(t_{i-1})]^2[y_O(t_{i-1}) - y_I(t_{i-1})] \\ &\quad + 2[\dot{y}_O(t_{i-1}) - \dot{y}_I(t_{i-1})][\dot{x}_O(t_{i-1}) - \dot{x}_I(t_{i-1})][x_O(t_{i-1}) - x_I(t_{i-1})]\Delta T^2\} \end{aligned}$$

According to Equation (7.199), we obtain

$$x_O = x_I + \frac{\Delta_{11}}{\Delta} q_{x,I} + \frac{\Delta_{12}}{\Delta} q_{y,I} + \frac{\Delta_{13}}{\Delta} \quad (7.200)$$

$$y_O = y_I + \frac{\Delta_{21}}{\Delta} q_{x,I} + \frac{\Delta_{22}}{\Delta} q_{y,I} + \frac{\Delta_{23}}{\Delta} \quad (7.201)$$

where

$$\Delta = \begin{vmatrix} a_1 & a_2 \\ b_1 & b_2 \end{vmatrix}$$

$$\Delta_{11} = \begin{vmatrix} -1 & a_2 \\ 0 & b_2 \end{vmatrix}, \Delta_{12} = \begin{vmatrix} 0 & a_2 \\ -1 & b_2 \end{vmatrix}, \Delta_{13} = \begin{vmatrix} -a_3 & a_2 \\ -b_3 & b_2 \end{vmatrix}$$

$$\Delta_{21} = \begin{vmatrix} a_1 & -1 \\ b_1 & 0 \end{vmatrix}, \Delta_{22} = \begin{vmatrix} a_1 & 0 \\ b_1 & -1 \end{vmatrix}, \Delta_{23} = \begin{vmatrix} a_1 & -a_3 \\ b_1 & -b_3 \end{vmatrix}$$

The moment of a nonlinear rotary spring is

$$m_I = K'_1(\theta_O - \theta_I) + K'_2(\theta_O - \theta_I)^3 \quad (7.202)$$

where K'_1 and K'_2 are the stiffness coefficients.

Similarly, linearizing Equation (7.202), we obtain

$$\theta_O = \theta_I + \frac{m_I}{K'_1 + 3K'_2[\theta_O(t_{i-1}) - \theta_I(t_{i-1})]^2}$$

$$- \frac{K'_2 \left\{ 3[\dot{\theta}_O(t_{i-1}) - \dot{\theta}_I(t_{i-1})]^2 [\theta_O(t_{i-1}) - \theta_I(t_{i-1})] \Delta T^2 - 2[\theta_O(t_{i-1}) - \theta_I(t_{i-1})]^3 \right\}}{K'_1 + 3K'_2[\theta_O(t_{i-1}) - \theta_I(t_{i-1})]^2} \quad (7.203)$$

For linear spring and rotary spring hinges whose masses are neglected, we obtain

$$q_{x,O} = q_{x,I} \quad (7.204)$$

$$q_{y,O} = q_{y,I} \quad (7.205)$$

$$m_O = m_I \quad (7.206)$$

Rewriting Equations (7.200), (7.201) and (7.203) to (7.206) in terms of matrices, the transfer equation of a spring moving in a plane is

$$\mathbf{z}_O = \mathbf{U} \mathbf{z}_I \quad (7.207)$$

The state vector is

$$\mathbf{z} = [x, y, \theta, m, q_x, q_y, 1]^T$$

and the transfer matrix is

$$U = \begin{bmatrix} 1 & 0 & 0 & 0 & \frac{\Delta_{11}}{\Delta} & \frac{\Delta_{12}}{\Delta} & \frac{\Delta_{13}}{\Delta} \\ 0 & 1 & 0 & 0 & \frac{\Delta_{21}}{\Delta} & \frac{\Delta_{22}}{\Delta} & \frac{\Delta_{23}}{\Delta} \\ 0 & 0 & 1 & u_{34} & 0 & 0 & u_{37} \\ 0 & 0 & 0 & 1 & 0 & 0 & 0 \\ 0 & 0 & 0 & 0 & 1 & 0 & 0 \\ 0 & 0 & 0 & 0 & 0 & 1 & 0 \\ 0 & 0 & 0 & 0 & 0 & 0 & 1 \end{bmatrix} \quad (7.208)$$

where

$$u_{34} = \frac{1}{K'_1 + 3K'_2(\theta_O(t_{i-1}) - \theta_I(t_{i-1}))^2}$$

$$u_{37} = -\frac{K'_2 \left[3(\dot{\theta}_O(t_{i-1}) - \dot{\theta}_I(t_{i-1}))^2 (\theta_O(t_{i-1}) - \theta_I(t_{i-1})) \Delta T^2 - 2(\theta_O(t_{i-1}) - \theta_I(t_{i-1}))^3 \right]}{K'_1 + 3K'_2(\theta_O(t_{i-1}) - \theta_I(t_{i-1}))^2}$$

For a linear spring, that is, $K_2 = K'_2 = 0$, the transfer matrix can be derived from Equation (7.208) as

$$\mathbf{U}_i = \begin{bmatrix} \mathbf{I}_3 & \mathbf{U}_{1,2} & \mathbf{O}_{3 \times 1} \\ \mathbf{O}_{3 \times 3} & \mathbf{I}_3 & \mathbf{O}_{3 \times 1} \\ \mathbf{O}_{1 \times 3} & \mathbf{O}_{1 \times 3} & 1 \end{bmatrix}, \quad \mathbf{U}_{1,2} = \begin{bmatrix} 0 & -\frac{1}{K_1} & 0 \\ 0 & 0 & -\frac{1}{K_1} \\ \frac{1}{K'_1} & 0 & 0 \end{bmatrix} \quad (7.209)$$

7.6.2 Damper Hinges

For a viscous damper, the viscous damped forces and damped moment are

$$q_x = -C_d(\dot{x}_O - \dot{x}_I), \quad q_y = -C_d(\dot{y}_O - \dot{y}_I), \quad m = C'_d(\dot{\theta}_O - \dot{\theta}_I) \quad (7.210)$$

where C_d and C'_d are the damping coefficients of translational dampers and rotary dampers, respectively.

Linearizing Equation (7.210), we obtain

$$x_O = x_I - \frac{1}{C_d C} q_{x,I} + \frac{D_{x_I} - D_{x_O}}{C} \quad (7.211)$$

$$y_O = y_I - \frac{1}{C_d C} q_{y,I} + \frac{D_{y_I} - D_{y_O}}{C} \quad (7.212)$$

$$\theta_O = \theta_I + \frac{1}{C'_d C} m_I - \frac{D_{\theta_I} - D_{\theta_O}}{C} \quad (7.213)$$

From Equations (7.211) to (7.213), the transfer equation of a viscous damper hinge moving in a plane is

$$\mathbf{z}_O = \mathbf{U} \mathbf{z}_I \quad (7.214)$$

The state vector is

$$\mathbf{z} = [x, y, \theta, m, q_x, q_y, 1]^T$$

and the transfer matrix is

$$\mathbf{U} = \begin{bmatrix} 1 & 0 & 0 & 0 & u_{15} & 0 & u_{17} \\ 0 & 1 & 0 & 0 & 0 & u_{26} & u_{27} \\ 0 & 0 & 1 & u_{34} & 0 & 0 & u_{37} \\ 0 & 0 & 0 & 1 & 0 & 0 & 0 \\ 0 & 0 & 0 & 0 & 1 & 0 & 0 \\ 0 & 0 & 0 & 0 & 0 & 1 & 0 \\ 0 & 0 & 0 & 0 & 0 & 0 & 1 \end{bmatrix} \quad (7.215)$$

where

$$\begin{aligned} u_{15} &= -\frac{1}{C_d C}, & u_{26} &= -\frac{1}{C_d C}, & u_{34} &= \frac{1}{C'_d C} \\ u_{17} &= \frac{D_{x_I} - D_{x_O}}{C}, & u_{27} &= \frac{D_{y_I} - D_{y_O}}{C}, & u_{37} &= -\frac{D_{\theta_I} - D_{\theta_O}}{C} \end{aligned}$$

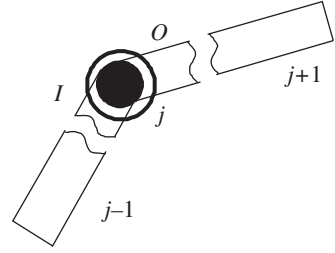


Figure 7.13 Model of a smooth hinge.

7.6.3 Smooth Hinges

For the smooth hinge shown in Figure 7.13, at the two ends the position coordinates and internal forces are equal and the internal torques are constant zero:

$$x_O = x_I, y_O = y_I, q_{y,O} = q_{y,I}, q_{x,O} = q_{x,I}, m_O = m_I = 0 \quad (7.216)$$

The numbers of inboard and outboard bodies of the smooth hinge j are $j-1$ and $j+1$, respectively. In the following, the rotation angle θ_O of the outboard body $j+1$ of a smooth hinge is discussed for two cases.

7.6.3.1 Smooth Hinge whose Outboard is a Rigid Body and with Internal Torques at the Output End of Zero

If another point of the outboard rigid body is also connected to a smooth hinge or a free boundary, then we can obtain the transfer equation of the outboard rigid body of the smooth hinge

$$0 = u_{41}x_O + u_{42}y_O + u_{43}\theta_O + u_{45}q_{x,O} + u_{46}q_{y,O} + u_{47} \quad (7.217)$$

where u_{41} , u_{42} , u_{43} , u_{45} , u_{46} and u_{47} are elements of the transfer matrix of the outboard rigid body.

Substituting Equation (7.216) into Equation (7.217) yields

$$\theta_O = -\frac{u_{41}}{u_{43}}x_I - \frac{u_{42}}{u_{43}}y_I - \frac{u_{45}}{u_{43}}q_{x,I} - \frac{u_{46}}{u_{43}}q_{y,I} - \frac{u_{47}}{u_{43}} \quad (7.218)$$

Combining Equations (7.216) and (7.218), and referring to the state vectors defined by Equation (7.21), we obtain the transfer equation of the smooth hinge whose outboard is a rigid body and whose internal torques of the output end are zero, namely

$$\mathbf{z}_O = \mathbf{U} \mathbf{z}_I$$

The transfer matrix is

$$\mathbf{U} = \begin{bmatrix} 1 & 0 & 0 & 0 & 0 & 0 & 0 \\ 0 & 1 & 0 & 0 & 0 & 0 & 0 \\ -\frac{u_{41}}{u_{43}} & -\frac{u_{42}}{u_{43}} & 0 & 0 & -\frac{u_{45}}{u_{43}} & -\frac{u_{46}}{u_{43}} & -\frac{u_{47}}{u_{43}} \\ 0 & 0 & 0 & 0 & 0 & 0 & 0 \\ 0 & 0 & 0 & 0 & 1 & 0 & 0 \\ 0 & 0 & 0 & 0 & 0 & 1 & 0 \\ 0 & 0 & 0 & 0 & 0 & 0 & 1 \end{bmatrix} \quad (7.219)$$

In Equation (7.219), the element $u_{4,4}$ could also be written as “1”. However, if we set $u_{4,4} = 0$, the computational precision will be improved. According to the above derivation, if the internal

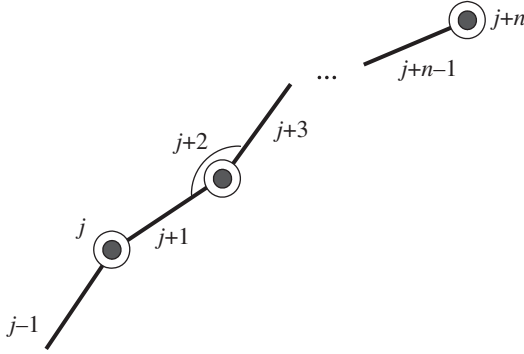


Figure 7.14 Model of a multibody system.

moments of the outboard body at the two ends of the smooth hinge are equal to zero, the above transfer equation and transfer matrix are valid.

7.6.3.2 Smooth Hinge whose Outboard is a Rigid Body and with Nonzero Internal Torques at the Output End

The output end of the outboard rigid body of a smooth hinge is connected to an elastic hinge or a damper hinge, as shown in Figure 7.14. Among the outboard elements of the smooth hinge, if there is such an element whose internal moment is always zero or with free boundaries, then the transfer equation of this smooth hinge can be deduced in the following way. The transfer equation of the subsystem from the smooth hinge to the hinge whose internal moment is zero can be derived as

$$\mathbf{z}_{j+n-1,j+n} = \mathbf{U}' \mathbf{z}_{j+1,j}$$

The transfer matrix is

$$\mathbf{U}' = \mathbf{U}_{j+n-1} \mathbf{U}_{j+n-2} \cdots \mathbf{U}_{j+2} \mathbf{U}_{j+1} \quad (7.220)$$

where $\mathbf{U}_{j+1}, \mathbf{U}_{j+2}, \dots, \mathbf{U}_{j+n-2}, \mathbf{U}_{j+n-1}$ are the transfer matrices of the outboard elements of the smooth hinge.

Because the internal moments in the state vectors $\mathbf{z}_{j+1,j}$ of the output end of the smooth hinge and the state vector $\mathbf{z}_{j+n-1,j+n}$ of the output end of the subsystem are all equal to zero, we can obtain the transfer equation and transfer matrix of the smooth hinge which are similar to the form of Equation (7.219), where, $u_{41}, u_{42}, \dots, u_{47}$ are elements of the transfer matrix \mathbf{U}' .

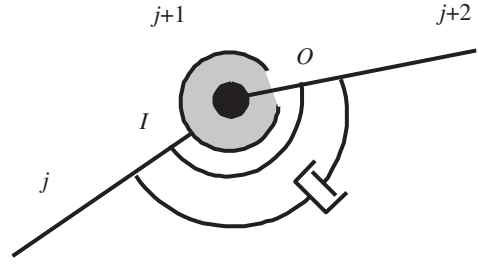
7.7 Transfer Matrices of Spatial Hinges

7.7.1 Elastic and Damper Hinges

The elastic damper hinge is composed of a linear spring hinge with a parallel connected damper, combining a rotary spring with a parallel connected damper. As shown in Figure 7.15, element $j+1$ is the elastic joint and damper, whose inboard body and outboard body are rigid bodies j and $j+2$, respectively. According to the force equilibrium at points O and I , we obtain

$$\begin{bmatrix} q_x \\ q_y \\ q_z \end{bmatrix}_I + \mathbf{C}_d \left(\frac{d}{dt} \mathbf{r}_O - \frac{d}{dt} \mathbf{r}_I \right) + \mathbf{K} (\mathbf{r}_O - \mathbf{r}_I) = \begin{bmatrix} 0 \\ 0 \\ 0 \end{bmatrix} \quad (7.221)$$

Figure 7.15 Elastic and damper hinges.



where

$$\mathbf{K} = \begin{bmatrix} K_x & 0 & 0 \\ 0 & K_y & 0 \\ 0 & 0 & K_z \end{bmatrix}, \quad \mathbf{C}_d = \begin{bmatrix} C_{d,x} & 0 & 0 \\ 0 & C_{d,y} & 0 \\ 0 & 0 & C_{d,z} \end{bmatrix}$$

K_x , K_y and K_z are the stiffness coefficients of the spring along the three axes of the inertial coordinate system, respectively, and $C_{d,x}$, $C_{d,y}$ and $C_{d,z}$ are the damper coefficients of the translation damper in the three axes of the inertial coordinate system, respectively.

Linearizing the velocity item yields

$$\mathbf{r}_O = [\mathbf{I}_3 \quad \mathbf{O}_{3 \times 3} \quad \mathbf{O}_{3 \times 3} \quad \mathbf{U}_{14} \quad \mathbf{U}_{15}] \mathbf{z}_I \quad (7.222)$$

where

$$\mathbf{U}_{14} = -(\mathbf{K} + \mathbf{C}_d \mathbf{C})^{-1}, \quad \mathbf{U}_{15} = -(\mathbf{K} + \mathbf{C}_d \mathbf{C})^{-1} \mathbf{C}_d (\mathbf{D}_{r_I} - \mathbf{D}_{r_O})$$

and \mathbf{z}_I is defined as in Equation (7.20).

For the rotational spring and damper we obtain

$$\mathbf{K}'(\boldsymbol{\theta}_O - \boldsymbol{\theta}_I) + \mathbf{C}'_d (\mathbf{A}_O \mathbf{H}_O \dot{\boldsymbol{\theta}}_O - \mathbf{A}_I \mathbf{H}_I \dot{\boldsymbol{\theta}}_I) - \begin{bmatrix} m_x \\ m_y \\ m_z \end{bmatrix}_I = \begin{bmatrix} 0 \\ 0 \\ 0 \end{bmatrix} \quad (7.223)$$

where

$$\mathbf{K}' = \begin{bmatrix} K'_x & 0 & 0 \\ 0 & K'_y & 0 \\ 0 & 0 & K'_z \end{bmatrix}, \quad \mathbf{C}'_d = \begin{bmatrix} C'_{d,x} & 0 & 0 \\ 0 & C'_{d,y} & 0 \\ 0 & 0 & C'_{d,z} \end{bmatrix}$$

The definitions of \mathbf{A} and \mathbf{H} can be seen in Equations (7.71) and (7.144). K'_x , K'_y and K'_z are the stiffness coefficients of the rotational spring along the three axes of the inertial system, respectively, and $C'_{d,x}$, $C'_{d,y}$ and $C'_{d,z}$ are the damper coefficients of the rotational damper about the three axes of the inertial system, respectively.

Linearizing Equation (7.223), we obtain

$$\boldsymbol{\theta}_O = [\mathbf{O}_{3 \times 3} \quad \mathbf{U}_{22} \quad \mathbf{U}_{23} \quad \mathbf{O}_{3 \times 3} \quad \mathbf{U}_{25}] \mathbf{z}_I \quad (7.224)$$

where

$$\begin{aligned} \mathbf{U}_{22} &= (\mathbf{K}' + \mathbf{C}'_d \mathbf{A}_O \mathbf{H}_O \mathbf{C})^{-1} (\mathbf{K}' + \mathbf{C}'_d \mathbf{A}_I \mathbf{H}_I \mathbf{C}) \\ \mathbf{U}_{23} &= (\mathbf{K}' + \mathbf{C}'_d \mathbf{A}_O \mathbf{H}_O \mathbf{C})^{-1} \\ \mathbf{U}_{25} &= (\mathbf{K}' + \mathbf{C}'_d \mathbf{A}_O \mathbf{H}_O \mathbf{C})^{-1} \mathbf{C}'_d (\mathbf{A}_I \mathbf{H}_I \mathbf{D}_{\theta_I} - \mathbf{A}_O \mathbf{H}_O \mathbf{D}_{\theta_O}) \end{aligned}$$

The transfer equation of the spring joint and damper moving in space can be written as

$$\mathbf{z}_O = \mathbf{U} \mathbf{z}_I$$

The transfer matrix is

$$\mathbf{U} = \begin{bmatrix} \mathbf{I}_3 & \mathbf{O}_{3 \times 3} & \mathbf{O}_{3 \times 3} & \mathbf{U}_{14} & \mathbf{U}_{15} \\ \mathbf{O}_{3 \times 3} & \mathbf{U}_{22} & \mathbf{U}_{23} & \mathbf{O}_{3 \times 3} & \mathbf{U}_{25} \\ \mathbf{O}_{3 \times 3} & \mathbf{O}_{3 \times 3} & \mathbf{I}_3 & \mathbf{O}_{3 \times 3} & \mathbf{O}_{3 \times 1} \\ \mathbf{O}_{3 \times 3} & \mathbf{O}_{3 \times 3} & \mathbf{O}_{3 \times 3} & \mathbf{I}_3 & \mathbf{O}_{3 \times 1} \\ \mathbf{O}_{1 \times 3} & \mathbf{O}_{1 \times 3} & \mathbf{O}_{1 \times 3} & \mathbf{O}_{1 \times 3} & 1 \end{bmatrix} \quad (7.225)$$

7.7.2 Smooth Ball-and-socket Hinge whose Outboard is a Rigid Body and with Internal Torques at the Output End of Zero

For a smooth ball-and-socket hinge, using a similar method as for the smooth hinge moving in a plane, its mass and size can be neglected. The position coordinates and internal forces are equal and the internal moments are constant zero at its two ends, that is

$$\mathbf{r}_O = \mathbf{r}_I, \begin{bmatrix} q_x \\ q_y \\ q_z \end{bmatrix}_O = \begin{bmatrix} q_x \\ q_y \\ q_z \end{bmatrix}_I, \begin{bmatrix} m_x \\ m_y \\ m_z \end{bmatrix}_O = \begin{bmatrix} m_x \\ m_y \\ m_z \end{bmatrix}_I = \begin{bmatrix} 0 \\ 0 \\ 0 \end{bmatrix} \quad (7.226)$$

The $j-1$ and $j+1$ denote the numbers of the inboard body and outboard body of the smooth ball-and-socket hinge j . For a smooth ball-and-socket hinge, if its outboard is a rigid body and the internal moment of the output end of this rigid body is zero, then by using the transfer equation of the outboard body of the smooth ball-and-socket joint, we obtain:

$$\mathbf{0}_3 = [\mathbf{U}_{31} \ \mathbf{U}_{32} \ \mathbf{I}_3 \ \mathbf{U}_{34} \ \mathbf{U}_{35}] \mathbf{z}_O \quad (7.227)$$

where \mathbf{U}_{31} , \mathbf{U}_{32} , \mathbf{U}_{34} and \mathbf{U}_{35} are submatrices of the transfer matrix of the smooth ball-and-socket joint's outboard body. \mathbf{z}_O is defined in Equation (7.20).

Substituting Equation (7.226) into Equation (7.227) yields

$$\boldsymbol{\theta}_O = -\mathbf{U}_{32}^{-1} \mathbf{U}_{31} \begin{bmatrix} x \\ y \\ z \end{bmatrix}_I - \mathbf{U}_{32}^{-1} \mathbf{U}_{34} \begin{bmatrix} q_x \\ q_y \\ q_z \end{bmatrix}_I - \mathbf{U}_{32}^{-1} \mathbf{U}_{35} \quad (7.228)$$

Combining Equations (7.226) and (7.228), the state vectors are derived by Equation (7.20), and the transfer equation of the smooth ball-and-socket joint can be derived as

$$\mathbf{z}_O = \mathbf{U} \mathbf{z}_I \quad (7.229)$$

The transfer matrix is

$$\mathbf{U} = \begin{bmatrix} \mathbf{I}_3 & \mathbf{O}_{3 \times 3} & \mathbf{O}_{3 \times 3} & \mathbf{O}_{3 \times 3} & \mathbf{O}_{3 \times 1} \\ -\mathbf{U}_{32}^{-1} \mathbf{U}_{31} & \mathbf{O}_{3 \times 3} & \mathbf{O}_{3 \times 3} & -\mathbf{U}_{32}^{-1} \mathbf{U}_{34} & -\mathbf{U}_{32}^{-1} \mathbf{U}_{35} \\ \mathbf{O}_{3 \times 3} & \mathbf{O}_{3 \times 3} & \mathbf{O}_{3 \times 3} & \mathbf{O}_{3 \times 3} & \mathbf{O}_{3 \times 1} \\ \mathbf{O}_{3 \times 3} & \mathbf{O}_{3 \times 3} & \mathbf{O}_{3 \times 3} & \mathbf{I}_3 & \mathbf{O}_{3 \times 1} \\ \mathbf{O}_{1 \times 3} & \mathbf{O}_{1 \times 3} & \mathbf{O}_{1 \times 3} & \mathbf{O}_{1 \times 3} & 1 \end{bmatrix} \quad (7.230)$$

7.7.3 Smooth Ball-and-socket Hinge whose Outboard is a Rigid Body and with Nonzero Internal Torques at the Output End

If the internal moment of the output end of the outboard rigid body of the smooth ball-and-socket joint is nonzero, the transfer matrix and transfer equation of smooth ball-and-socket joint can be obtained by using the same method as in section 7.6.3. The form is the same as in Equation (7.220).

7.8 Algorithm of the Discrete Time Transfer Matrix Method for Multibody Systems

The algorithm to compute multi-rigid-body system dynamics using MSDTTMM is as follows:

- 1) Determine the initial conditions and the boundary conditions of the system and set $i = 1$.
- 2) Compute the coefficients A, B_z (or \mathbf{B}_z), C, D_z (or \mathbf{D}_z), $\mathbf{A}, \Phi, \mathbf{T}_1, \mathbf{T}_2, \mathbf{T}_3, \bar{s}, \bar{c}$ etc. at time t_i for each connecting element by the linearization method, and determine the initial conditions $\mathbf{z}(t_{i-1}), \dot{\mathbf{z}}(t_{i-1})$ and $\ddot{\mathbf{z}}(t_{i-1})$ at time t_i as well as the system parameters.
- 3) Formulate the transfer matrix for each subsystem and the overall transfer matrix at time t_i , respectively.
- 4) Apply the boundary conditions and the overall transfer equation to compute the unknown quantities in the boundary state vectors at time t_i .
- 5) By using the transfer equations of each element, compute the state vectors of each element at time t_i .
- 6) Use the state vectors at time t_i to compute the first- and second-order derivatives of the position coordinates and rotation angles with respect to time.
- 7) Let $i = i + 1$, use the computational result of the last step as the initial conditions, and return to step (2). This procedure is repeated until the final time step is accomplished.

7.9 Numerical Examples of Multibody System Dynamics

7.9.1 Chain Multibody System Dynamics

For the chain multibody system shown in Figure 7.16, the transfer equations of hinge element j and body element $j + 1$ are

$$\mathbf{z}_{j+1,j} = \mathbf{U}_j \mathbf{z}_{j-1,j}, \mathbf{z}_{j+1,j+2} = \mathbf{U}_{j+1} \mathbf{z}_{j+1,j} \quad (7.231)$$

where \mathbf{U}_j and \mathbf{U}_{j+1} are the transfer matrices of hinge j and body $j + 1$.

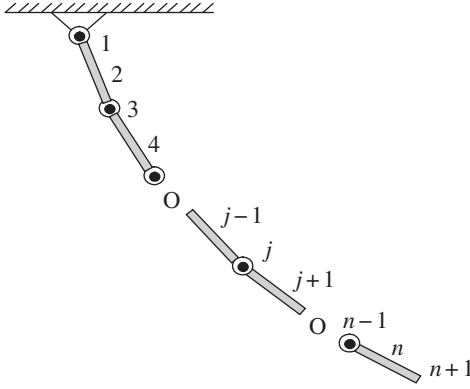


Figure 7.16 Chain multibody system.

The overall transfer equation of the system can be assembled by only using the transfer matrices of these elements, that is

$$\mathbf{z}_{n,n+1} = \mathbf{U} \mathbf{z}_{2,1} \quad (7.232)$$

where the overall transfer matrix is

$$\mathbf{U} = \mathbf{U}_n \mathbf{U}_{n-1} \cdots \mathbf{U}_j \cdots \mathbf{U}_3 \mathbf{U}_2 \quad (7.233)$$

For a chain multibody system, the overall transfer matrix of the system can be obtained by successive multiplication of the transfer matrices of the elements. The order of the overall transfer matrix of the system is equal to the highest order of the transfer matrices of the elements, and it does not change as the number of DOFs in the system increases. For a chain multi-rigid-body system moving in a plane, the highest order of the transfer matrix is (7×7) , while for a chain multi-rigid-body system moving in space, the highest order is (13×13) .

Substituting the boundary conditions into the overall transfer equation of the system, the unknown quantities in the state vectors of the system boundaries can be computed. The state vectors and the motion quantities of each element at time t_i can be computed by repeatedly using the corresponding transfer equations of elements. The quantities of velocity, angular velocity, acceleration and angular acceleration at time t_i can be obtained. Repeating the entire procedure can allow the system motion to be obtained.

7.9.2 Numerical Example of a Chain Multi-rigid-body System Moving in a Plane

Example 7.1 A dynamic model of three pendulums composed of rigid bodies which are connected by smooth hinges moving in a plane under the effect of gravity is shown in Figure 7.17. From top to bottom the elements are (1) a smooth hinge, (2) a rigid bar, (3) a smooth hinge, (4) a rigid bar, (5) a smooth hinge and (6) a rigid bar. The output end of rigid body (6) is denoted by (7). The three rigid bars have the same structural parameters and initial conditions, as shown in Figure 7.17. m , l and J_C are the mass, length and moment of inertia with respect to the mass center, respectively. Solve the motion of the system under the effect of gravity.

Solution

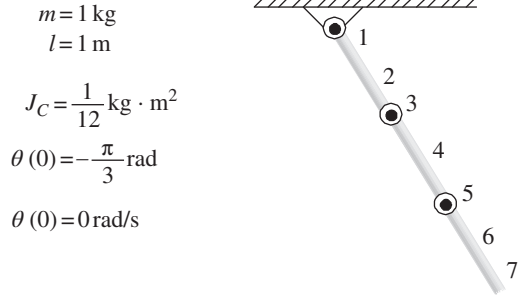
The dynamics of this system are computed and compared using two methods.

1) MSDTTMM solution

The overall transfer equation of the system is

$$\mathbf{z}_{6,7} = \mathbf{U}_6 \mathbf{U}_5 \mathbf{U}_4 \mathbf{U}_3 \mathbf{U}_2 \mathbf{z}_{2,1} = \mathbf{U} \mathbf{z}_{2,1} \quad (7.234)$$

Figure 7.17 Three-pendulum system moving in a plane.



where $\mathbf{U}_6, \mathbf{U}_4, \mathbf{U}_2$ are determined by Equation (7.101), while $\mathbf{U}_5, \mathbf{U}_3$ are determined by Equation (7.219).

The boundary conditions are

$$\begin{cases} \mathbf{z}_{2,1} = [0, 0, \theta, 0, q_x, q_y, 1]_{2,1}^T \\ \mathbf{z}_{6,7} = [x, y, \theta, 0, 0, 0, 1]_{6,7}^T \end{cases} \quad (7.235)$$

By substituting the boundary conditions into Equation (7.233), the unknown quantities in state vector $\mathbf{z}_{2,1}$ can be obtained. The state vectors and the motion quantities of each element at time t_i can be computed using the corresponding transfer equations of elements. The quantities of velocity, angular velocity, acceleration and angular acceleration at time t_i are then obtained from Equations (7.27) and (7.28), respectively.

2) Analytical mechanics method solution

By using the analytical mechanics method, the global dynamic equations of n pendulums are

$$\mathbf{A} \begin{bmatrix} \ddot{\theta}_1 \\ \ddot{\theta}_2 \\ \vdots \\ \ddot{\theta}_n \end{bmatrix} = -\mathbf{B} \begin{bmatrix} \dot{\theta}_1^2 \\ \dot{\theta}_2^2 \\ \vdots \\ \dot{\theta}_n^2 \end{bmatrix} - \begin{bmatrix} gl_1(m_1/2 + m_2 + \cdots + m_n)\cos\theta_1 \\ gl_1(m_2/2 + m_3 + \cdots + m_n)\cos\theta_2 \\ \vdots \\ gl_n(m_n/2)\cos\theta_n \end{bmatrix} \quad (7.236)$$

where

$$\mathbf{A} = [a_{ij}], \mathbf{B} = [b_{ij}]$$

$$a_{jj} = \left(\frac{m_j}{4} + m_{j+1} + \cdots + m_n \right) l_j^2 + J_{C_j} \quad (j = 1, 2, \dots, n)$$

$$a_{ij} = a_{ji} = l_i l_j \left(\frac{m_j}{2} + m_{j+1} + \cdots + m_n \right) \cos(\theta_i - \theta_j) \quad (1 \leq i < j \leq n)$$

$$b_{jj} = 0 \quad (j = 1, 2, \dots, n)$$

$$b_{ij} = -b_{ji} = l_i l_j \left(\frac{m_j}{2} + m_{j+1} + \cdots + m_n \right) \sin(\theta_i - \theta_j) \quad (1 \leq i < j \leq n)$$

The subscript j on l_j , m_j and θ_j denotes the number of the bar $2j$.

The computational results using the MSDTTMM and analytical mechanics methods are shown in Figure 7.18. The results of the two methods are in good agreement, which validates the proposed method for solving multi-rigid-body system dynamics.

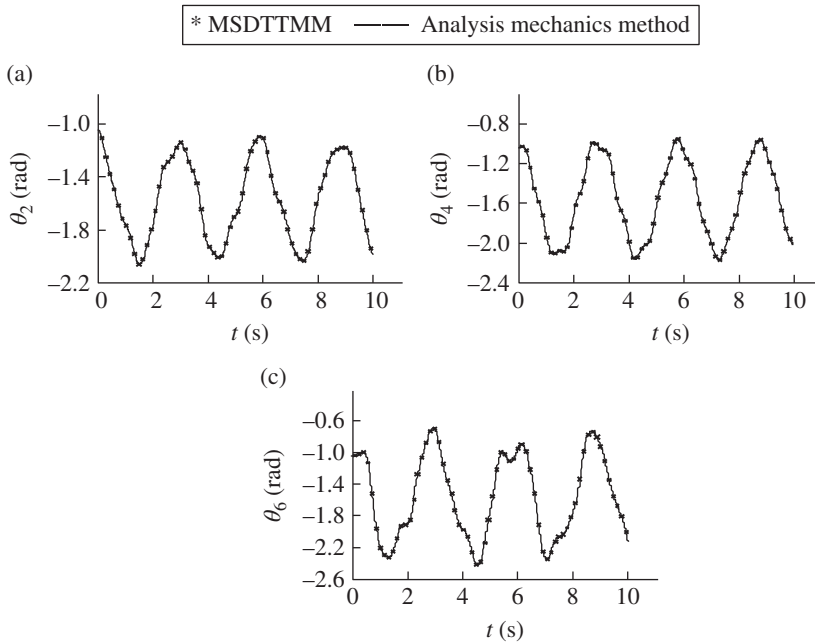


Figure 7.18 Time history of angles of a three-pendulum system moving in a plane: (a) orientation angle of rigid body 2, (b) orientation angle of rigid body 4 and (c) orientation angle of rigid body 6.

7.9.3 Numerical Example of a Chain Multi-rigid-body System Moving in Space

Example 7.2 The dynamics model of three pendulums composed of three rigid bodies connected by smooth ball-and-socket joints under the effect of gravity is shown in Figure 7.19. The structural parameters of the three rigid bodies are the same. For example, the parameters of body 2 are

$$m = 1 \text{ kg}, \begin{bmatrix} x \\ y \\ z \end{bmatrix}_{2,C} = \begin{bmatrix} 0.5 \\ 0 \\ 0 \end{bmatrix} \text{ m}, \begin{bmatrix} x \\ y \\ z \end{bmatrix}_{2,O} = \begin{bmatrix} 1 \\ 0 \\ 0 \end{bmatrix} \text{ m}, J = \begin{bmatrix} \frac{1}{6} & 0 & 0 \\ 0 & \frac{5}{12} & 0 \\ 0 & 0 & \frac{5}{12} \end{bmatrix} \text{ kg} \cdot \text{m}^2$$

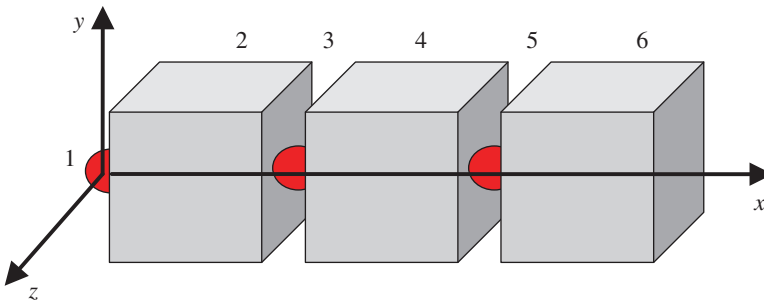
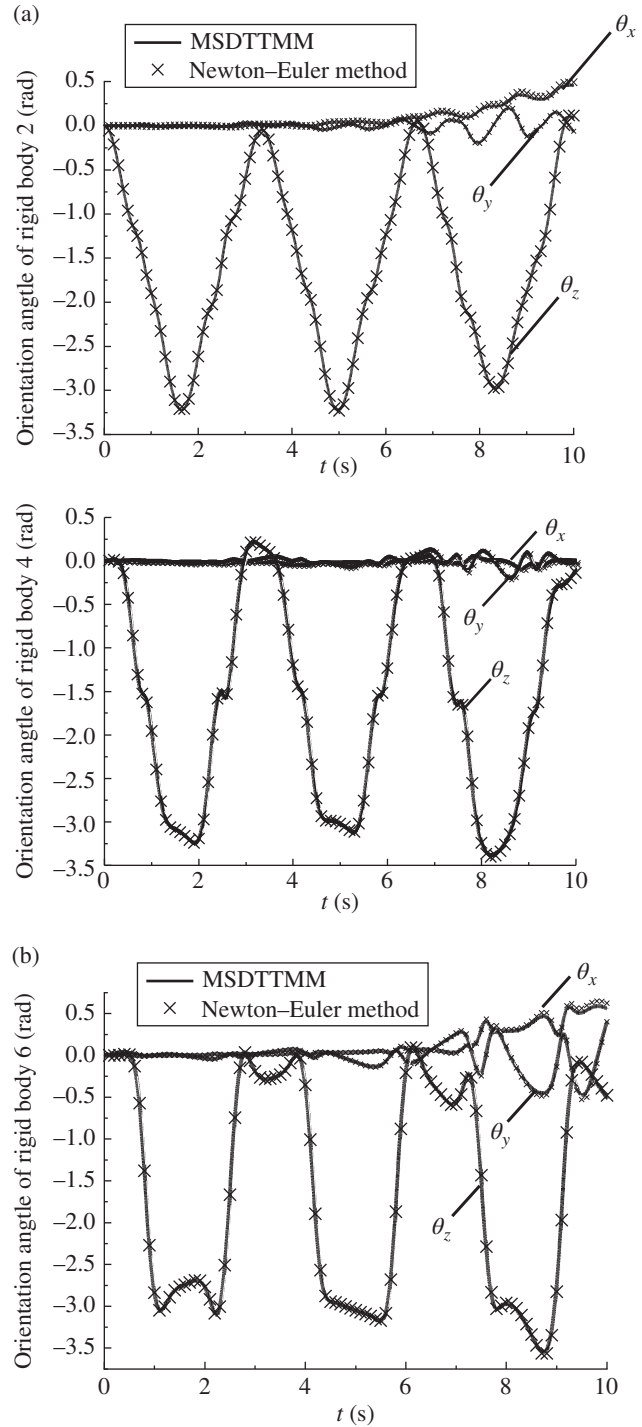


Figure 7.19 Three rigid bars connected by smooth ball-and-socket joints.

Figure 7.20 Time histories of orientation angles of a multi-rigid-body system: (a) computational results of time histories of orientation angles of rigid body 2 and rigid body 4, and (b) computational results of time history of orientation angle of rigid body 6.



The motion of the system is computed under the following initial conditions:

$$\begin{bmatrix} \theta_x \\ \theta_y \\ \theta_z \end{bmatrix}_{2,1} = \begin{bmatrix} \theta_x \\ \theta_y \\ \theta_z \end{bmatrix}_{4,3} = \begin{bmatrix} \theta_x \\ \theta_y \\ \theta_z \end{bmatrix}_{6,5} = \begin{bmatrix} 0 \\ 0 \\ 0 \end{bmatrix} \text{ rad}, \begin{bmatrix} \dot{\theta}_x \\ \dot{\theta}_y \\ \dot{\theta}_z \end{bmatrix}_{2,1} = \begin{bmatrix} \dot{\theta}_x \\ \dot{\theta}_y \\ \dot{\theta}_z \end{bmatrix}_{4,3} = \begin{bmatrix} 0 \\ 0 \\ 0 \end{bmatrix} \text{ rad/s}, \begin{bmatrix} \dot{\theta}_x \\ \dot{\theta}_y \\ \dot{\theta}_z \end{bmatrix}_{6,5} = \begin{bmatrix} 0 \\ 0.1 \\ 0 \end{bmatrix} \text{ rad/s}$$

Solution

The overall transfer equation of the system is

$$\mathbf{z}_{6,7} = \mathbf{U}_6 \mathbf{U}_5 \mathbf{U}_4 \mathbf{U}_3 \mathbf{U}_2 \mathbf{z}_{2,1} = \mathbf{U} \mathbf{z}_{2,1} \quad (7.237)$$

where \mathbf{U}_6 , \mathbf{U}_4 and \mathbf{U}_2 are determined by Equation (7.174), and \mathbf{U}_5 and \mathbf{U}_3 are determined by Equation (7.230).

The boundary conditions are

$$\begin{cases} \mathbf{z}_{2,1} = [0, 0, 0, \theta_x, \theta_y, \theta_z, 0, 0, 0, q_x, q_y, q_z, 1]^T_{2,1} \\ \mathbf{z}_{6,7} = [x, y, z, \theta_x, \theta_y, \theta_z, 0, 0, 0, 0, 0, 0, 1]^T_{6,7} \end{cases} \quad (7.238)$$

The dynamics of the multibody system are computed by MSDTTMM and the Newton–Euler method. The computational results of the two methods are in good agreement, as shown in Figure 7.20, which validates the proposed method for solving multi-rigid-body system dynamics.

8

Discrete Time Transfer Matrix Method for Multi-flexible-body Systems

8.1 Introduction

Generally speaking, for many engineering problems, a dynamics model of a multi-rigid-body system (MRS) cannot meet the demand of engineering accuracy. For example, to implement the dynamic design required for precision firing of artillery and rocket launchers, the gun barrel and the guider of the rocket launcher have to be treated as elastic bodies to meet the demands of engineering accuracy [1, 249]. Therefore, the dynamics models of artillery systems and rocket launchers have to be treated as *multi-rigid-flexible-body systems* (MRFSs). MRFSs are systems composed of rigid and flexible bodies undergoing large motion connected by various hinges. In MRFSs, not only are the elasticity and damping of connection points, as well as the large motion of body elements, considered, but also the coupling of deformation and large motion of the elements. The MRFS is the refinement, natural extension and further development of the physical model of the MRS. Using ordinary methods of multi-body system dynamics, the derivation of the global dynamic equations of the MRFS is rather more complicated than those of the MRS, and the computational scale and cost are also greater, while the theory of MRFS dynamics is not as perfect that of MRS dynamics. How to establish the dynamic equations of general MRFSs and improve computational speed is one of the primary research directions in MRFS dynamics.

The description for the motion of a flexible body system can be divided into two categories: absolute and relative. Absolute description is related to the motion variables of each body under an inertial coordinate system. Relative description builds a local body-fixed coordinate system for each body respectively, and decomposes the body motion into two parts: global motion of a rigid body along with the local body-fixed coordinate system and deformation motion of a rigid body relative to the local body-fixed coordinate system. The equations of motion can be established directly by using these two motion variables. A flexible body has infinite degrees of freedom (DOFs), and there are some methods to deal with elastic deformation in multibody system dynamics, such as the *Rayleigh–Ritz method*, the *finite segment method*, the *finite element method* (FEM) and the *modal analysis method*. There are various ways to select the generalized coordinates of a multibody system, including the *hybrid coordinate approach*, the *corotational coordinate approach* and the *absolute nodal coordinate approach*.

Based on the discrete time transfer matrix method for multibody systems (MSDTTMM), as introduced in Chapter 7, this chapter introduces the discrete time transfer matrix method (DTTMM) for an MRFS [61, 69–73], including dynamic equations, state vectors, transfer equations and transfer matrices of planar and spatial flexible bodies, transfer matrices of various

hinges, the algorithm and examples of the DTTMM for the MRFS. The results indicate that the DTTMM for the MRFS is not only valid for the dynamics of the MRFS, but also very efficient due to the following features: no need for global dynamics equations of the system and high computational speed.

8.2 Dynamics of a Flexible Body with Large Motion

In rigid body dynamics, the general motion of a rigid body can be decomposed into the translation of the body-fixed coordinate system and the relative rotation of the body-fixed coordinate system with respect to its origin. To eliminate the inertia coupling between the translation and rotation at the acceleration, the principal axes of inertia of the rigid body are selected as the body-fixed coordinate system to produce the inertial tensor in diagonal form. When the flexible body moves, the relative positions of all points of the body are time-varying and its motion is described exactly using the continuum mechanics method. Usually, we cannot use one uniform body-fixed coordinate system and for each flexible body we use one floating frame or floating coordinate system described by the Cartesian coordinate system. The origin and the orientation of coordinate axes of the floating coordinate system are time-varying with respect to the flexible body. The principles of choosing the floating frame are not only to try to reduce or eliminate the coupling between the overall motion of the flexible body and relative deformation motion in order to decouple the equations of motion, but also to linearize the relative deformation motion of the flexible body and describe the relative deformation motion by a first-order function.

8.2.1 Kinematics of a Flexible Body

Using the floating frame of reference formulation, the translational motion is described by body-fixed coordinate system $o_1x_1y_1z_1$, which is parallel to the inertia coordinate system, and the large rotation is described by body-fixed coordinate system $O_2x_2y_2z_2$, which takes o_1 as the origin. The motion of a flexible body can be decomposed into the large motion of the body-fixed coordinate system and the motion of deformation with respect to the body-fixed coordinate system.

The schematic decomposition diagrams of the motion of a flexible body, from position 1 to position 4, are shown in Figure 8.1. First, the flexible body is assumed to be a rigid body, and the initial position 1 translates to 2, then rotates to 3 around an arbitrary point on the flexible body. The flexible body finally undergoes deformation motion to position 4. As shown in Figure 8.2, the position vector of arbitrary point j on the flexible body can be expressed as

$$\mathbf{r}_j = \mathbf{r}_{O_2} + \mathbf{r}_{O_2j} \quad (8.1)$$

where \mathbf{r}_j is the position vector of an arbitrary point j on the flexible body with respect to the inertia coordinate system and \mathbf{r}_{O_2} is the position vector of the origin of body-fixed coordinate system with respect to the origin of the inertia coordinate system. \mathbf{r}_{O_2j} is the position vector of point j on the flexible body with respect to the origin of the body-fixed coordinate system.

\mathbf{r}_{O_2j} can be decomposed into the undeformed position vector \mathbf{l}_{O_2j} and the deformable vector \mathbf{u}_j

$$\mathbf{r}_{O_2j} = \mathbf{l}_{O_2j} + \mathbf{u}_j \quad (8.2)$$

therefore

$$\mathbf{r}_j = \mathbf{r}_{O_2} + \mathbf{l}_{O_2j} + \mathbf{u}_j \quad (8.3)$$

Figure 8.1 Decomposition of flexible body motion.

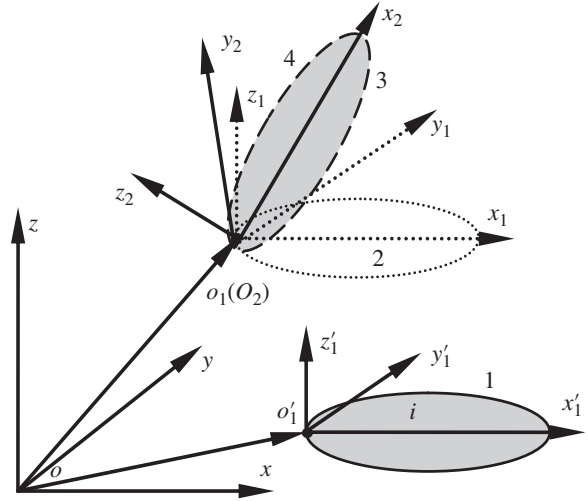
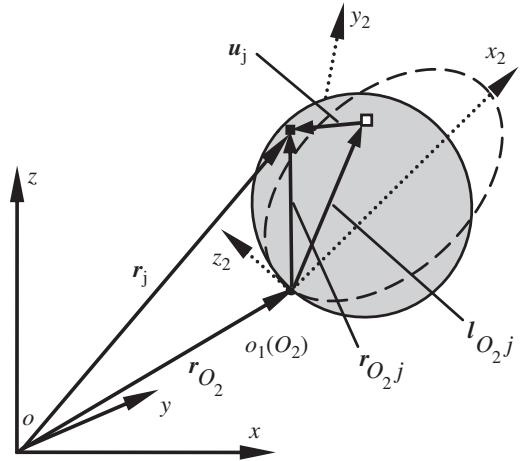


Figure 8.2 Position description of an arbitrary point on a flexible body.



For a flexible body with large planar motion, projecting Equation (8.3) onto the inertia coordinate system yields

$$\begin{bmatrix} x \\ y \end{bmatrix}_j = \begin{bmatrix} x \\ y \end{bmatrix}_{O_2} + A \left(\begin{bmatrix} b_1 \\ b_2 \end{bmatrix} + \begin{bmatrix} u \\ v \end{bmatrix}_j \right) \quad (8.4)$$

where

$$A = \begin{bmatrix} c & -s \\ s & c \end{bmatrix} \quad (8.5)$$

A is the transformation matrix of planar motion, and $[b_1, b_2]_j^T$ and $[u, v]_j^T$ are the column matrices of \mathbf{l}_{O_2j} and \mathbf{u}_j , respectively, in the body-fixed coordinate system.

Differentiating Equation (8.4) with respect to time, the absolute velocities of point j on the flexible body can be obtained

$$\begin{bmatrix} \dot{x} \\ \dot{y} \end{bmatrix}_j = \begin{bmatrix} \dot{x} \\ \dot{y} \end{bmatrix}_{O_2} + \dot{\mathbf{A}} \left(\begin{bmatrix} b_1 \\ b_2 \end{bmatrix} + \begin{bmatrix} u \\ v \end{bmatrix}_j \right) + \mathbf{A} \begin{bmatrix} \dot{u} \\ \dot{v} \end{bmatrix}_j \quad (8.6)$$

where

$$\dot{\mathbf{A}} = \frac{\partial \mathbf{A}}{\partial \theta} \dot{\theta} \quad (8.7)$$

$$\frac{\partial \mathbf{A}}{\partial \theta} = \begin{bmatrix} -s & -c \\ c & -s \end{bmatrix} \quad (8.8)$$

Hence Equation (8.6) can be written as

$$\begin{bmatrix} \dot{x} \\ \dot{y} \end{bmatrix}_j = \begin{bmatrix} \dot{x} \\ \dot{y} \end{bmatrix}_{O_2} + \frac{\partial \mathbf{A}}{\partial \theta} \left(\begin{bmatrix} b_1 \\ b_2 \end{bmatrix} + \begin{bmatrix} u \\ v \end{bmatrix}_j \right) \dot{\theta} + \mathbf{A} \begin{bmatrix} \dot{u} \\ \dot{v} \end{bmatrix}_j \quad (8.9)$$

or

$$\begin{bmatrix} \dot{x} \\ \dot{y} \end{bmatrix}_j = \begin{bmatrix} \mathbf{I}_2 & \frac{\partial \mathbf{A}}{\partial \theta} \left(\begin{bmatrix} b_1 \\ b_2 \end{bmatrix} + \begin{bmatrix} u \\ v \end{bmatrix}_j \right) \mathbf{A} \end{bmatrix} [\dot{x}_{O_2}, \dot{y}_{O_2}, \dot{\theta}, \dot{u}_j, \dot{v}_j]^T \quad (8.10)$$

Differentiating Equation (8.4) twice with respect to time, the absolute accelerations of point j on a flexible body are as follows

$$\begin{bmatrix} \ddot{x} \\ \ddot{y} \end{bmatrix}_j = \begin{bmatrix} \ddot{x} \\ \ddot{y} \end{bmatrix}_{O_2} + \ddot{\mathbf{A}} \left(\begin{bmatrix} b_1 \\ b_2 \end{bmatrix} + \begin{bmatrix} u \\ v \end{bmatrix}_j \right) + 2 \frac{\partial \mathbf{A}}{\partial \theta} \left(\begin{bmatrix} \dot{u} \\ \dot{v} \end{bmatrix}_j \right) \dot{\theta} + \mathbf{A} \begin{bmatrix} \ddot{u} \\ \ddot{v} \end{bmatrix}_j \quad (8.11)$$

According to Equation (8.7),

$$\ddot{\mathbf{A}} = \frac{\partial^2 \mathbf{A}}{\partial \theta^2} \dot{\theta}^2 + \frac{\partial \mathbf{A}}{\partial \theta} \ddot{\theta} \quad (8.12)$$

where

$$\frac{\partial^2 \mathbf{A}}{\partial \theta^2} = -\mathbf{A} \quad (8.13)$$

therefore

$$\ddot{\mathbf{A}} = -\mathbf{A} \dot{\theta}^2 + \frac{\partial \mathbf{A}}{\partial \theta} \ddot{\theta} \quad (8.14)$$

Thus Equation (8.11) can be rewritten as

$$\begin{bmatrix} \ddot{x} \\ \ddot{y} \end{bmatrix}_j = \begin{bmatrix} \ddot{x} \\ \ddot{y} \end{bmatrix}_{O_2} - \mathbf{A} \dot{\theta}^2 \left(\begin{bmatrix} b_1 \\ b_2 \end{bmatrix} + \begin{bmatrix} u \\ v \end{bmatrix}_j \right) + \frac{\partial \mathbf{A}}{\partial \theta} \ddot{\theta} \left(\begin{bmatrix} b_1 \\ b_2 \end{bmatrix} + \begin{bmatrix} u \\ v \end{bmatrix}_j \right) + 2 \frac{\partial \mathbf{A}}{\partial \theta} \left(\begin{bmatrix} \dot{u} \\ \dot{v} \end{bmatrix}_j \right) \dot{\theta} + \mathbf{A} \begin{bmatrix} \ddot{u} \\ \ddot{v} \end{bmatrix}_j \quad (8.15)$$

It is clear that the first term on the right-hand side of Equation (8.15) is the average translation acceleration of the flexible body, the second term is the normal acceleration of rotation, the third term is the tangent acceleration of rotation, the fourth term is Coriolis acceleration and the fifth term is relative deformation acceleration.

Similarly, for an elastic body with large spatial motion, by projecting Equation (8.3) onto the inertia coordinate system and differentiating it with respect to time, the positions, absolute velocities and absolute accelerations of point j on a flexible body can be obtained:

$$\begin{bmatrix} x \\ y \\ z \end{bmatrix}_j = \begin{bmatrix} x \\ y \\ z \end{bmatrix}_{O_2} + \mathbf{A} \left(\begin{bmatrix} b_1 \\ b_2 \\ b_3 \end{bmatrix} + \begin{bmatrix} u \\ v \\ w \end{bmatrix}_j \right) \quad (8.16)$$

$$\begin{bmatrix} \dot{x} \\ \dot{y} \\ \dot{z} \end{bmatrix}_j = \begin{bmatrix} \dot{x} \\ \dot{y} \\ \dot{z} \end{bmatrix}_{O_2} + \dot{\mathbf{A}} \left(\begin{bmatrix} b_1 \\ b_2 \\ b_3 \end{bmatrix} + \begin{bmatrix} u \\ v \\ w \end{bmatrix}_j \right) + \mathbf{A} \begin{bmatrix} \dot{u} \\ \dot{v} \\ \dot{w} \end{bmatrix}_j \quad (8.17)$$

$$\begin{bmatrix} \ddot{x} \\ \ddot{y} \\ \ddot{z} \end{bmatrix}_j = \begin{bmatrix} \ddot{x} \\ \ddot{y} \\ \ddot{z} \end{bmatrix}_{O_2} + \ddot{\mathbf{A}} \left(\begin{bmatrix} b_1 \\ b_2 \\ b_3 \end{bmatrix} + \begin{bmatrix} u \\ v \\ w \end{bmatrix}_j \right) + 2\dot{\mathbf{A}} \begin{bmatrix} \dot{u} \\ \dot{v} \\ \dot{w} \end{bmatrix}_j + \mathbf{A} \begin{bmatrix} \ddot{u} \\ \ddot{v} \\ \ddot{w} \end{bmatrix}_j \quad (8.18)$$

where $[b_1, b_2, b_3]_j^T$ and $[u, v, w]_j^T$ are coordinate column matrices of \mathbf{I}_{O_2j} and \mathbf{u}_j , respectively, in the body-fixed coordinate system. \mathbf{A} is the transformation matrix of the coordinate system. For an element with large spatial motion, we obtain

$$\mathbf{A} = \begin{bmatrix} c_y c_z & s_x c_y c_z - c_x s_z & c_x s_y c_z + s_x s_z \\ c_y s_z & s_x s_y s_z + c_x c_z & c_x s_y s_z - s_x c_z \\ -s_y & s_x c_y & c_x c_y \end{bmatrix} \quad (8.19)$$

8.2.2 Discretization and Generalized Coordinates of a Flexible Body

After the dynamic equations of planar motion of a flexible body with elastic deformation have been derived, the transfer matrix of a flexible body can be developed. The motion of the flexible body is determined by two groups of generalized coordinates which describe the motion of the reference coordinate system and the elastic deformation. The translation and rotation of the floating frame of the flexible body are described in the generalized coordinates of the body-fixed coordinate system, and the deformation of the flexible body with respect to the body-fixed coordinate system are described using the generalized coordinates of elastic deformation. There are several methods describing the deformation of an elastic body [242].

Rayleigh–Ritz method The assumed displacement field, which satisfies the compatibility and completeness, is constructed for an elastic body. The assumed displacement field is described by $\Psi(x, y, z)$, which describes the deformation of the elastic body and can be partitioned as $\Psi = [\Psi_1 \ \Psi_2 \ \cdots \ \Psi_n]$. The deformation of each point on the body \mathbf{u} can be expressed as

$$\mathbf{u} = \Psi \mathbf{Q}(t) \quad (8.20)$$

where $\mathbf{Q}(t)$ are the generalized coordinates of elastic deformation.

This is the most basic method for the approximation of the deformation of a continuous body in elastic mechanics. For complex shape, boundary and load, it is extremely difficult to construct a displacement field that is suitable for the entire flexible body.

Finite element method This method is a kind of piecewise Rayleigh–Ritz method. Its basic idea is to discretize the continuous body into a group of finite elements which connect with each other according to a certain mode. Because the elements can be assembled with different connections and may have different shapes, FEM can formulate the body with complex shape, boundary and load.

By the rapid development of computer performances, FEM has become a powerful tool to analyze and compute engineering structures and general elastic bodies. When the actual object is simulated approximately using FEM, displacement of infinite particles on the elastic body is described by the shape function of the finite element node displacements. Deformation \mathbf{u}_j of an arbitrary point on element j of the body can be expressed as

$$\mathbf{u}_j = \mathbf{N}_j \mathbf{u}'_j \quad (8.21)$$

where \mathbf{N}_j is the deformation pattern of element j (or assumed displacement field), which is called the shape function of element j , and \mathbf{u}'_j is the node displacement of the element.

After assembling all the elements, the displacements of all the nodes construct generalized coordinates of the elastic body. The infinite DOFs of modeling can be reduced into finite DOFs of modeling using FEM. Usually, the remaining number of DOFs is still considerably large to guarantee the computational precision.

Component mode synthesis method In structure dynamic analysis, the displacement (deformation) of an object which changes with time is often described using its mode coordinates, that is

$$\mathbf{u} = \mathbf{\Psi} \mathbf{Q}(t) \quad (8.22)$$

where $\mathbf{\Psi} = [\mathbf{\Psi}_1 \ \mathbf{\Psi}_2 \ \cdots \ \mathbf{\Psi}_n]$ is the mode matrix, $\mathbf{Q}(t)$ are generalized coordinates and n is the mode number.

The advantages of the component mode synthesis method are:

- 1) The computational scale could be reduced by the modal truncation according to aprioristic response characteristics and required precision. In some cases, low-order modes have more contribution to the response, for example some elastic mechanical arms can take the first one or two modes and satellite solar panels usually need to take the first five or six modes. For a fluid–solid coupling system, where high-order modes play an important role, we could also truncate off the less contributive modes to maximally reduce the solution scale.
- 2) The mode synthesis technique makes it more convenient to study the vibration of a large-scale complex system.
- 3) The results of the mode test are applied directly, so the theory and numerical analysis closely integrate with the experimental data.

8.2.3 Dynamic Equations of a Flexible Body with Large Planar Motion

There are some basic assumptions in linear elasticity mechanics:

- 1) *Continuity assumption.* The volume of the entire object is filled with the mediums which compose this object, without any space.

- 2) *Entire elasticity assumption.* The object completely obeys Hooke's law, that is, strain is directly proportional to the stress components which cause the strain, namely, the elastic constant does not change with the stress components or strain components.
- 3) *Homogeneity assumption.* The entire object is composed of identical material.
- 4) *Isotropy assumption.* The characteristics of the object in each direction are all the same, that is to say elastic constant does not change with direction.
- 5) *Small deformation assumption.* Suppose that each deformation is far smaller than the original size of the object, namely the strain is far smaller than 1, therefore when we establish the balance equation after object deformation, we may use the size before the deformation to replace the size after the deformation without causing appreciable error.

The planar and spatial dynamic equations of an elastic body can be derived on the basis of these five assumptions.

The force analysis of infinitesimal element of an elastic body with large planar motion is shown in Figure 8.3a. Projecting the absolute acceleration of an arbitrary point j on the elastic body to body-fixed coordinate system $O_2x_2y_2$, this yields

$$\begin{bmatrix} \ddot{x} \\ \ddot{y} \end{bmatrix}_{2,j} = \mathbf{A}^T \begin{bmatrix} \ddot{x} \\ \ddot{y} \end{bmatrix}_j \quad (8.23)$$

According to Newton's second law,

$$dx_2 dy_2 \rho \ddot{x}_{2,j} = \left(\sigma_x + \frac{\partial \sigma_x}{\partial x_2} dx_2 - \sigma_x \right) dy_2 + \left(\tau_{yx} + \frac{\partial \tau_{yx}}{\partial y_2} dy_2 - \tau_{yx} \right) dx_2 + f_{2,x} dx_2 dy_2 \quad (8.24)$$

which can be simplified as

$$\rho \ddot{x}_{2,j} = \frac{\partial \sigma_x}{\partial x_2} + \frac{\partial \tau_{yx}}{\partial y_2} + f_{2,x} \quad (8.25)$$

Similarly,

$$\rho \ddot{y}_{2,j} = \frac{\partial \sigma_y}{\partial y_2} + \frac{\partial \tau_{xy}}{\partial x_2} + f_{2,y} \quad (8.26)$$

where σ and τ are normal stress and shear stress, respectively, and their directions are distinguished by the subscripts (Figure 8.3a). $f_{2,x}$ is the distribution of external force and ρ is area mass density per unit surface. The subscript 2 denotes variables in body-fixed coordinate system $O_2x_2y_2$.

According to elasticity mechanics, the constitutive equation of planar isotropic linear elastic material, that is, generalized Hooke's law, can be written as

$$\sigma_x = 2G\varepsilon_x + \lambda(\varepsilon_x + \varepsilon_y) \quad (8.27)$$

$$\sigma_y = 2G\varepsilon_y + \lambda(\varepsilon_x + \varepsilon_y) \quad (8.28)$$

$$\tau_{yx} = \tau_{xy} = 2G\gamma_{xy} = 2G\gamma_{yx} \quad (8.29)$$

where λ is the Lamé constant, $G = \frac{E}{2(1+\mu)}$, $\lambda = \frac{E\mu}{(1+\mu)(1-2\mu)}$, E is Young's modulus and μ is Poisson's ratio. ε and γ are normal strain and shear strain, respectively.

The kinematic equations of small deformation and isotropic linear elastic material are

$$\varepsilon_x = \frac{\partial u}{\partial x_2} \quad (8.30)$$

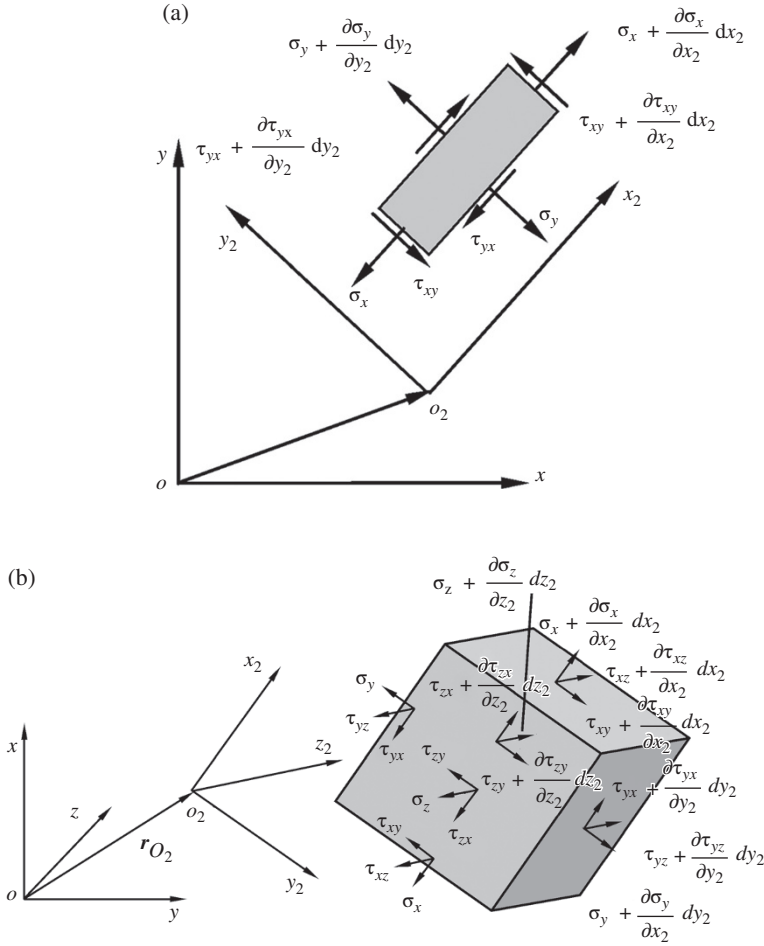


Figure 8.3 Force analysis of an infinitesimal element of an elastic body: (a) force analysis of an infinitesimal element of a planar elastic body and (b) force analysis of an infinitesimal element of a spatial elastic body.

$$\varepsilon_y = \frac{\partial v}{\partial y_2} \quad (8.31)$$

$$\gamma_{yx} = \gamma_{xy} = \frac{1}{2} \left(\frac{\partial u}{\partial y_2} + \frac{\partial v}{\partial x_2} \right) \quad (8.32)$$

Substituting Equations (8.27) to (8.32) into Equations (8.25) and (8.26), we obtain

$$\rho \ddot{x}_{2,j} = (\lambda + G) \left(\frac{\partial^2 u}{\partial x_2^2} + \frac{\partial^2 v}{\partial x_2 \partial y_2} \right) + G \left(\frac{\partial^2 u}{\partial x_2^2} + \frac{\partial^2 v}{\partial y_2^2} \right) + f_{2,x} \quad (8.33)$$

$$\rho \ddot{y}_{2,j} = (\lambda + G) \left(\frac{\partial^2 v}{\partial y_2^2} + \frac{\partial^2 u}{\partial y_2 \partial x_2} \right) + G \left(\frac{\partial^2 v}{\partial y_2^2} + \frac{\partial^2 u}{\partial x_2^2} \right) + f_{2,y} \quad (8.34)$$

The dynamic equations of flexible body deformation with large planar motion are Equations (8.33) and (8.34). These are different from the dynamic equations of a planar elastic

body with small displacement. Here, the acceleration expression includes not only the deformation acceleration, but also the characteristic quantity of the motion of a body-fixed coordinate system, such as the angular acceleration of the body-fixed coordinate system.

Because the motion of a flexible body is described by the large motion of a floating frame and the deformation relative to the moving reference frame, respectively, we should take into account the equations governing the motion of the floating frame of reference. Assume mid-point j in Equation (8.15) is mass center C of the flexible body, hence,

$$\begin{bmatrix} \ddot{x} \\ \ddot{y} \end{bmatrix}_C = \begin{bmatrix} \ddot{x} \\ \ddot{y} \end{bmatrix}_{O_2} - \mathbf{A}\dot{\theta}^2 \left(\begin{bmatrix} c_{c1} \\ c_{c2} \end{bmatrix} + \begin{bmatrix} u \\ v \end{bmatrix}_C \right) + \frac{\partial \mathbf{A}}{\partial \theta} \ddot{\theta} \left(\begin{bmatrix} c_{c1} \\ c_{c2} \end{bmatrix} + \begin{bmatrix} u \\ v \end{bmatrix}_C \right) + 2 \frac{\partial \mathbf{A}}{\partial \theta} \left(\begin{bmatrix} \dot{u} \\ \dot{v} \end{bmatrix}_C \right) \dot{\theta} + \mathbf{A} \begin{bmatrix} \ddot{u} \\ \ddot{v} \end{bmatrix}_C \quad (8.35)$$

where

$$\begin{bmatrix} c_{c1} \\ c_{c2} \end{bmatrix} = \frac{1}{m} \int_V \begin{bmatrix} b_1 \\ b_2 \end{bmatrix} \rho dV, \quad \begin{bmatrix} u \\ v \end{bmatrix}_C = \frac{1}{m} \int_V \begin{bmatrix} u \\ v \end{bmatrix} \rho dV$$

$$\begin{bmatrix} \dot{u} \\ \dot{v} \end{bmatrix}_C = \frac{1}{m} \int_V \begin{bmatrix} \dot{u} \\ \dot{v} \end{bmatrix} \rho dV, \quad \begin{bmatrix} \ddot{u} \\ \ddot{v} \end{bmatrix}_C = \frac{1}{m} \int_V \begin{bmatrix} \ddot{u} \\ \ddot{v} \end{bmatrix} \rho dV$$

The mass center motion equation of the flexible body with large planar motion becomes

$$m \begin{bmatrix} \ddot{x} \\ \ddot{y} \end{bmatrix}_C = \sum \begin{bmatrix} f_x \\ f_y \end{bmatrix} \quad (8.36)$$

Setting the origin O_2 of the body-fixed coordinate system to be the momentum center, using the theorem of the absolute angular momentum of the particle system with respect to the moving momentum center yields

$$\frac{d\mathbf{G}_{O_2}}{dt} + m\mathbf{r}_{O_2C} \times \mathbf{a}_{O_2} = \mathbf{M} \quad (8.37)$$

where $\mathbf{G}_{O_2} = \int \mathbf{r}_{O_2j} \times \dot{\mathbf{r}}_{O_2j} \rho dx_2 dy_2$ is the absolute moment of momentum of the flexible body of large planar motion with respect to point O_2 . \mathbf{r}_{O_2C} is the radius vector of mass center C of the flexible body with respect to point O_2 . m is the mass of the flexible body, \mathbf{a}_{O_2} is the acceleration of point O_2 and \mathbf{M} is the principal moment of the external forces.

In the body-fixed coordinate system $O_2x_2y_2$,

$$\frac{d\mathbf{G}_{O_2}}{dt} = \frac{d}{dt} \int [(x_2 + u)^2 + (y_2 + v)^2] \dot{\theta} \rho dx_2 dy_2 + \frac{d}{dt} \int [(x_2 + u)\dot{v} - (y_2 + v)\dot{u}] \rho dx_2 dy_2 \quad (8.38)$$

Rearranging Equation (8.38), this becomes

$$\frac{d\mathbf{G}_{O_2}}{dt} = 2\dot{\theta} \int [(x_2 + u)\dot{u} + (y_2 + v)\dot{v}] \rho dx_2 dy_2 + \int |\mathbf{r}_{jO_2}|^2 \ddot{\theta} \rho dx_2 dy_2 + \int [(x_2 + u)\ddot{v} - (y_2 + v)\ddot{u}] \rho dx_2 dy_2 \quad (8.39)$$

8.2.4 Dynamic Equations of a Flexible Body with Large Spatial Motion

Similar to the derivation of the dynamic equations of a flexible body with large planar motion, the force analysis of an infinitesimal element of a flexible body with large spatial motion is shown in Figure 8.3b. Projecting the absolute acceleration of an arbitrary point j on the flexible body to the body-fixed coordinate system $O_2x_2y_2z_2$, we obtain

$$\begin{bmatrix} \ddot{x} \\ \ddot{y} \\ \ddot{z} \end{bmatrix}_{2,j} = \mathbf{A}^T \begin{bmatrix} \ddot{x} \\ \ddot{y} \\ \ddot{z} \end{bmatrix}_j \quad (8.40)$$

where \mathbf{A} is the transformation matrix of the coordinate system, which is shown in Equation (8.19).

According to Newton's law of motion, we obtain

$$\begin{aligned} dx_2 dy_2 dz_2 \rho \ddot{x}_{2,j} = & \left(\sigma_x + \frac{\partial \sigma_x}{\partial x_2} dx_2 - \sigma_x \right) dy_2 dz_2 + \left(\tau_{yx} + \frac{\partial \tau_{yx}}{\partial y_2} dy_2 - \tau_{yx} \right) dx_2 dz_2 \\ & + \left(\tau_{zx} + \frac{\partial \tau_{zx}}{\partial z_2} dz_2 - \tau_{zx} \right) dx_2 dy_2 + f_{2,x} dx_2 dy_2 dz_2 \end{aligned} \quad (8.41)$$

This can be simplified to

$$\rho \ddot{x}_{2,j} = \frac{\partial \sigma_x}{\partial x_2} + \frac{\partial \tau_{yx}}{\partial y_2} + \frac{\partial \tau_{zx}}{\partial z_2} + f_{2,x} \quad (8.42)$$

Similarly, for the y_2 and z_2 directions we obtain

$$\rho \ddot{y}_{2,j} = \frac{\partial \tau_{xy}}{\partial x_2} + \frac{\partial \sigma_y}{\partial y_2} + \frac{\partial \tau_{zy}}{\partial z_2} + f_{2,y} \quad (8.43)$$

$$\rho \ddot{z}_{2,j} = \frac{\partial \tau_{xz}}{\partial x_2} + \frac{\partial \tau_{yz}}{\partial y_2} + \frac{\partial \sigma_z}{\partial z_2} + f_{2,z} \quad (8.44)$$

where σ and τ are the normal stress and shear stress, and their directions are distinguished by the subscripts (Figure 8.3b). $f_{2,x}$, $f_{2,y}$ and $f_{2,z}$ are the distributed external forces components, respectively, ρ is the mass density and subscript 2 denotes parameters expressed in the body-fixed coordinate system $O_2x_2y_2z_2$.

According to the theory of elasticity, the constitutive equations of three-dimensional isotropic linear elastic materials can be written as:

$$\sigma_x = 2G\varepsilon_x + \lambda(\varepsilon_x + \varepsilon_y + \varepsilon_z) \quad (8.45)$$

$$\sigma_y = 2G\varepsilon_y + \lambda(\varepsilon_x + \varepsilon_y + \varepsilon_z) \quad (8.46)$$

$$\sigma_z = 2G\varepsilon_z + \lambda(\varepsilon_x + \varepsilon_y + \varepsilon_z) \quad (8.47)$$

$$\tau_{yx} = \tau_{xy} = 2G\gamma_{xy} = 2G\gamma_{yx} \quad (8.48)$$

$$\tau_{zx} = \tau_{xz} = 2G\gamma_{xz} = 2G\gamma_{zx} \quad (8.49)$$

$$\tau_{yz} = \tau_{zy} = 2G\gamma_{yz} = 2G\gamma_{yz} \quad (8.50)$$

The kinematics equations of an isotropic linear elastic material for small deformation are

$$\varepsilon_x = \frac{\partial u}{\partial x_2} \quad (8.51)$$

$$\varepsilon_y = \frac{\partial v}{\partial y_2} \quad (8.52)$$

$$\varepsilon_z = \frac{\partial w}{\partial z_2} \quad (8.53)$$

$$\gamma_{yx} = \gamma_{xy} = \frac{1}{2} \left(\frac{\partial u}{\partial y_2} + \frac{\partial v}{\partial x_2} \right) \quad (8.54)$$

$$\gamma_{yz} = \gamma_{zy} = \frac{1}{2} \left(\frac{\partial v}{\partial z_2} + \frac{\partial w}{\partial y_2} \right) \quad (8.55)$$

$$\gamma_{zx} = \gamma_{xz} = \frac{1}{2} \left(\frac{\partial u}{\partial z_2} + \frac{\partial w}{\partial x_2} \right) \quad (8.56)$$

Substituting Equations (8.45) to (8.56) into Equations (8.42) and (8.44), we obtain

$$\rho \ddot{x}_{2,j} = (\lambda + G) \left(\frac{\partial^2 u}{\partial x_2^2} + \frac{\partial^2 v}{\partial x_2 \partial y_2} + \frac{\partial^2 w}{\partial x_2 \partial z_2} \right) + G \left(\frac{\partial^2 u}{\partial x_2^2} + \frac{\partial^2 u}{\partial y_2^2} + \frac{\partial^2 u}{\partial z_2^2} \right) + f_{2,x} \quad (8.57)$$

$$\rho \ddot{y}_{2,j} = (\lambda + G) \left(\frac{\partial^2 v}{\partial y_2^2} + \frac{\partial^2 u}{\partial y_2 \partial x_2} + \frac{\partial^2 w}{\partial y_2 \partial z_2} \right) + G \left(\frac{\partial^2 v}{\partial y_2^2} + \frac{\partial^2 v}{\partial x_2^2} + \frac{\partial^2 v}{\partial z_2^2} \right) + f_{2,y} \quad (8.58)$$

$$\rho \ddot{z}_{2,j} = (\lambda + G) \left(\frac{\partial^2 w}{\partial z_2^2} + \frac{\partial^2 u}{\partial z_2 \partial x_2} + \frac{\partial^2 v}{\partial z_2 \partial y_2} \right) + G \left(\frac{\partial^2 w}{\partial z_2^2} + \frac{\partial^2 w}{\partial x_2^2} + \frac{\partial^2 w}{\partial y_2^2} \right) + f_{2,z} \quad (8.59)$$

The dynamic equations of the deformation of a flexible body with large spatial motion are defined by Equations (8.57) to (8.59). Similar to Equations (8.33) and (8.34), the acceleration expressions given by Equations (8.57) to (8.59) include the deformation acceleration and the characteristic quantity of the motion of the body-fixed coordinate system.

Similar to the derivation of the equation of motion of the mass center of a flexible body with large planar motion, mid-point j in Equation (8.18) is assumed to be the mass center C of a flexible body, therefore

$$\begin{bmatrix} \ddot{x} \\ \ddot{y} \\ \ddot{z} \end{bmatrix}_C = \begin{bmatrix} \ddot{x} \\ \ddot{y} \\ \ddot{z} \end{bmatrix}_{O_2} + \ddot{\mathbf{A}} \left(\begin{bmatrix} c_{c1} \\ c_{c2} \\ c_{c3} \end{bmatrix} + \begin{bmatrix} u \\ v \\ w \end{bmatrix}_C \right) + 2\dot{\mathbf{A}} \begin{bmatrix} \dot{u} \\ \dot{v} \\ \dot{w} \end{bmatrix}_C + \mathbf{A} \begin{bmatrix} \ddot{u} \\ \ddot{v} \\ \ddot{w} \end{bmatrix}_C \quad (8.60)$$

where

$$\begin{bmatrix} c_{c1} \\ c_{c2} \\ c_{c3} \end{bmatrix} = \frac{1}{m} \int_V \begin{bmatrix} b_1 \\ b_2 \\ b_3 \end{bmatrix} \rho dV, \quad \begin{bmatrix} u \\ v \\ w \end{bmatrix}_C = \frac{1}{m} \int_V \begin{bmatrix} u \\ v \\ w \end{bmatrix} \rho dV$$

$$\begin{bmatrix} \dot{u} \\ \dot{v} \\ \dot{w} \end{bmatrix}_C = \frac{1}{m} \int_V \begin{bmatrix} \dot{u} \\ \dot{v} \\ \dot{w} \end{bmatrix} \rho dV, \quad \begin{bmatrix} \ddot{u} \\ \ddot{v} \\ \ddot{w} \end{bmatrix}_C = \frac{1}{m} \int_V \begin{bmatrix} \ddot{u} \\ \ddot{v} \\ \ddot{w} \end{bmatrix} \rho dV$$

The mass center motion equation of a flexible body moving in space is

$$m \begin{bmatrix} \ddot{x} \\ \ddot{y} \\ \ddot{z} \end{bmatrix}_C = \sum \begin{bmatrix} f_x \\ f_y \\ f_z \end{bmatrix} \quad (8.61)$$

Let the origin O_2 of the body-fixed coordinate system be the moment center. Using the theorem of the absolute angular momentum of a particle system with respect to the moving moment center, the rotational equation of a flexible body with large spatial motion is

$$\frac{d\mathbf{G}_{O_2}}{dt} + m\mathbf{r}_{O_2C} \times \mathbf{a}_{O_2} = \mathbf{M} \quad (8.62)$$

where $\mathbf{G}_{O_2} = \int \mathbf{r}_{O_2j} \times \dot{\mathbf{r}}_{O_2j} \rho dx_2 dy_2$ is the absolute momentum moment of the flexible body with large spatial motion with respect to point O_2 . The meanings of the other terms are the same as in Equation (8.37).

8.3 State Vector, Transfer Equation and Transfer Matrix

The definition of a state vector of a rigid body in the MRFS is the same as in the DTTMM for an MRS, as developed in Chapter 7. For the definition of the state vector of a flexible body, the physical variables that reflect the relative deformation of a flexible body must be considered in addition to the state variables in the state vectors of a rigid body. The deformation of a flexible body is described using the modal analysis method and the deformation of an arbitrary point on the flexible body, which is a function of time, can be described by generalized coordinates corresponding to eigenvectors. Therefore, by the addition of generalized coordinates which describe the deformation of a flexible body to the definition of the state vector of a rigid body, the state vector of a flexible body can be obtained.

The state vector of a flexible body moving in a plane is

$$\mathbf{z} = [x, y, \theta, m, q_x, q_y, q^1, q^2, \dots, q^n, 1]^T \quad (8.63)$$

The state vector of a flexible body moving in space is

$$\mathbf{z} = [x, y, z, \theta_x, \theta_y, \theta_z, m_x, m_y, m_z, q_x, q_y, q_z, q^1, q^2, \dots, q^n, 1]^T \quad (8.64)$$

where $x, y, z, \theta_x, \theta_y, \theta_z$ and $m_x, m_y, m_z, q_x, q_y, q_z$ are similar to the terms in the state vectors of a rigid body, while $x, y, z, \theta_x, \theta_y$ and θ_z are the position coordinates of the origin and its orientation angles of the floating frame, respectively. m_x, m_y, m_z, q_x, q_y and q_z are the internal moments and internal forces projected to x, y and z , respectively. q^1, q^2, \dots, q^n are the generalized coordinates which describe the deformation using the modal analysis method, and the superscript n is the highest order of the modes.

Similar to the DTTMM for MRSSs, by linearization of the dynamic equations of the flexible body element the transfer equation which connects the different connection points of a flexible body is

$$\mathbf{z}_O = \mathbf{U} \mathbf{z}_I \quad (8.65)$$

where the transfer matrix \mathbf{U} at the current time is known or can be obtained by iterative computation.

Compared with the DTTMM for MRSs, the DTTMM for MRFSs has a similar approach, but there are two important differences:

- 1) The deformation effect of flexible body must be considered in the DTTMM for an MRFS, therefore the state vector and transfer matrix of a flexible body have generalized coordinates which describe the deformation and its correlated terms with respect to the state vector and transfer matrix of a rigid body.
- 2) In an MRS, the body and hinge have the same number of state variables (at least as a chain system), but in an MRFS the state vector of the hinge is determined by the characteristics and transfer direction of the two ends of the hinge. Readers should pay attention to these differences, which will be seen in Section 8.5.

8.4 Transfer Matrix of a Beam with Large Planar Motion

Using the description of the deformation and dynamic equations of motion of a flexible body in Section 8.2, the dynamic equations of a Euler–Bernoulli beam can be obtained:

$$\bar{m}\dot{\theta} \int_0^l 2u\dot{u}dx_2 + \bar{m}\ddot{\theta} \int_0^l (u^2 + x_2^2)dx_2 + \bar{m} \int_0^l x_2\ddot{u}dx_2 + m\ddot{y}_{O_2}x_{O_2C} - m\ddot{x}_{O_2}y_{O_2C} = \sum_p m_p \quad (8.66)$$

$$\frac{\partial q_{2,y}(x_2, t)}{\partial x_2} = f_{2,y}(x_2, t) - \bar{m} \left(\ddot{u} + x_2\ddot{\theta} - u\dot{\theta}^2 + \ddot{y}_{O_2} \cos\theta - \ddot{x}_{O_2} \sin\theta \right) \quad (8.67)$$

$$\frac{\partial q_{2,x}(x_2, t)}{\partial x_2} = f_{2,x}(x_2, t) - \bar{m} \left(-\ddot{\theta}u - 2\dot{\theta}\dot{u} - \dot{\theta}^2 x_2 + \ddot{y}_{O_2} \sin\theta + \ddot{x}_{O_2} \cos\theta \right) \quad (8.68)$$

where u is the transverse deformation of the beam, l is the length of the beam, \bar{m} is the mass per unit length and m is the mass of the beam, $m = \bar{m}l$. $f_{2,x}(x_2, t)$ and $f_{2,y}(x_2, t)$ are the distributed external forces acting on the beam projected to x_2 and y_2 , respectively, and $\sum_p m_p$ is the sum of moments of all the forces and the moment acting on the beam with respect to point O_2 .

By the modal analysis method, the mode shapes of the component with small deformation, which satisfy the boundary condition, can be obtained directly. Using the modal analysis method, the transverse deformation u of the beam in Equations (8.66) to (8.68) can be expressed as

$$u(x_2, t) = \sum_{k=1}^{\infty} \sin \frac{k\pi x_2}{l} q^k(t) \quad (8.69)$$

Using the finite-order mode shape to describe the solution of the system, for example let $n = 3$,

$$u(x_2, t) = \sum_{k=1}^3 \sin \frac{k\pi x_2}{l} q^k(t) \quad (8.70)$$

Substituting Equation (8.70) into Equation (8.67), integrated along the axial direction of the Euler–Bernoulli beam with uniform cross-section, this yields

$$q_{2,y}(l,t) - q_{2,y}(0,t) = \int_0^l f_{2,y}(x_2,t) dx_2 - \bar{m} \int_0^l \left(\sin \frac{\pi x_2}{l} \ddot{q}^1 + \sin \frac{2\pi x_2}{l} \ddot{q}^2 + \sin \frac{3\pi x_2}{l} \ddot{q}^3 \right) dx_2$$

$$- \bar{m} \int_0^l x_2 \ddot{\theta} dx_2 + \bar{m} \int_0^l \dot{\theta}^2 \left(\sin \frac{\pi x_2}{l} q^1 + \sin \frac{2\pi x_2}{l} q^2 + \sin \frac{3\pi x_2}{l} q^3 \right) dx_2 - (\ddot{y}_{O_2} \cos \theta - \ddot{x}_{O_2} \sin \theta) \bar{m} \int_0^l dx_2 \quad (8.71)$$

namely

$$q_{2,y}(l,t) = q_{2,y}(0,t) + \int_0^l f_{2,y}(x_2,t) dx_2 - m(\ddot{y}_{O_2} \cos \theta - \ddot{x}_{O_2} \sin \theta)$$

$$- \frac{2m}{\pi} \ddot{q}^1 - \frac{2m}{3\pi} \ddot{q}^3 - \frac{ml}{2} \ddot{\theta} + m\dot{\theta}^2 \left(\frac{2}{\pi} q^1 + \frac{2}{3\pi} q^3 \right) \quad (8.72)$$

Substituting Equations (8.27) and (8.28) into Equation (8.72) and rearranging yields

$$q_{2,y}(l,t) = m\bar{s}Ax_{O_2} - m\bar{c}Ay_{O_2} + \left\{ -\frac{lA}{2} + \frac{4C}{\pi} \left[\dot{\theta} \left(q^1 + \frac{1}{3} q^3 \right) \right]_{t_{i-1}} \right\} m\theta + q_{2,y}(0,t)$$

$$+ \frac{2m}{\pi} \left[-A + \dot{\theta}^2_{t_{i-1}} \right] q^1 + \frac{2m}{3\pi} \left[-A + \dot{\theta}^2_{t_{i-1}} \right] q^3$$

$$- \frac{2m}{\pi} \left(B_{q^1} + \frac{1}{3} B_{q^3} \right) - \frac{ml}{2} B_\theta + \frac{4mD_\theta}{\pi} \left[\dot{\theta} \left(q^1 + \frac{1}{3} q^3 \right) \right]_{t_{i-1}}$$

$$- \frac{4m}{\pi} \left[\dot{\theta}^2 \left(q^1 + \frac{1}{3} q^3 \right) \right]_{t_{i-1}} - m\bar{c}B_{y_{O_2}} + m\bar{s}B_{x_{O_2}} + \int_0^l f_{2,y}(x_2,t) dx_2 \quad (8.73)$$

Similarly, from Equation (8.68),

$$q_{2,x}(l,t) = -m\bar{c}Ax_{O_2} - m\bar{s}Ay_{O_2} + \left[\frac{2A}{\pi} \left(q^1 + \frac{1}{3} q^3 \right)_{t_{i-1}} + \frac{4C}{\pi} \left(\dot{q}^1 + \frac{1}{3} \dot{q}^3 \right)_{t_{i-1}} + lC\dot{\theta}_{t_{i-1}} \right] m\theta$$

$$+ q_{2,x}(0,t) + \frac{2m}{\pi} (\ddot{\theta}_{t_{i-1}} + 2C\dot{\theta}_{t_{i-1}}) q^1 + \frac{2m}{3\pi} (\ddot{\theta}_{t_{i-1}} + 2C\dot{\theta}_{t_{i-1}}) q^3$$

$$+ \frac{2m}{\pi} B_\theta \left(q^1 + \frac{1}{3} q^3 \right)_{t_{i-1}} - \frac{2m}{\pi} \ddot{\theta}_{t_{i-1}} \left(q^1 + \frac{1}{3} q^3 \right)_{t_{i-1}} + \frac{4mD_\theta}{\pi} \left(\dot{q}^1 + \frac{1}{3} \dot{q}^3 \right)_{t_{i-1}}$$

$$+ \frac{4m}{\pi} \dot{\theta}_{t_{i-1}} \left(D_{q^1} + \frac{1}{3} D_{q^3} \right) - \frac{4m}{\pi} \dot{\theta}_{t_{i-1}} \left(\dot{q}^1 + \frac{1}{3} \dot{q}^3 \right)_{t_{i-1}} + ml\dot{\theta}_{t_{i-1}} \left(D_\theta - \frac{\dot{\theta}_{t_{i-1}}}{2} \right)$$

$$- m\bar{s}B_{y_{O_2}} - m\bar{c}B_{x_{O_2}} + \int_0^l f_{2,x}(x_2,t) dx_2 \quad (8.74)$$

Equations (8.73) and (8.74) can be rewritten as

$$q_{2,y}(l,t) = \zeta_{1,1}x_{O_2} + \zeta_{1,2}y_{O_2} + \zeta_{1,3}\theta + q_{2,y}(0,t) + \zeta_{1,7}q^1 + \zeta_{1,9}q^3 + \zeta_{1,10} \quad (8.75)$$

$$q_{2,x}(l,t) = \zeta_{2,1}x_{O_2} + \zeta_{2,2}y_{O_2} + \zeta_{2,3}\theta + q_{2,x}(0,t) + \zeta_{2,7}q^1 + \zeta_{2,9}q^3 + \zeta_{2,10} \quad (8.76)$$

where

$$\begin{aligned}
\zeta_{1,1} &= m\bar{s}A, \quad \zeta_{1,2} = -m\bar{c}A, \quad \zeta_{1,3} = m \left\{ -\frac{lA}{2} + \frac{4C}{\pi} \left[\dot{\theta} \left(q^1 + \frac{1}{3}q^3 \right) \right]_{t_{i-1}} \right\} \\
\zeta_{2,1} &= -m\bar{c}A, \quad \zeta_{2,2} = -m\bar{s}A, \quad \zeta_{2,3} = m \left[\frac{2A}{\pi} \left(q^1 + \frac{1}{3}q^3 \right)_{t_{i-1}} + \frac{4C}{\pi} \left(\dot{q}^1 + \frac{1}{3}\dot{q}^3 \right)_{t_{i-1}} + lC\dot{\theta}_{t_{i-1}} \right] \\
\zeta_{1,7} &= \frac{2m}{\pi} \left(-A + \dot{\theta}_{t_{i-1}}^2 \right), \quad \zeta_{2,7} = \frac{2m}{\pi} (\ddot{\theta}_{t_{i-1}} + 2C\dot{\theta}_{t_{i-1}}), \quad \zeta_{1,9} = \frac{1}{3}\zeta_{1,7}, \quad \zeta_{2,9} = \frac{1}{3}\zeta_{2,7} \\
\zeta_{1,10} &= -\frac{2m}{\pi} \left(B_{q^1} + \frac{1}{3}B_{q^3} \right) - \frac{ml}{2}B_{\theta} + \frac{4mD_{\theta}}{\pi} \left[\dot{\theta} \left(q^1 + \frac{1}{3}q^3 \right) \right]_{t_{i-1}} - \frac{4m}{\pi} \left[\dot{\theta}^2 \left(q^1 + \frac{1}{3}q^3 \right) \right]_{t_{i-1}} \\
&\quad - m\bar{c}B_{y_{O_2}} + m\bar{s}B_{x_{O_2}} + \int_0^l f_{2,y}(x_2, t) dx_2 \\
\zeta_{2,10} &= \frac{2m}{\pi} B_{\theta} \left(q^1 + \frac{1}{3}q^3 \right)_{t_{i-1}} - \frac{2m}{\pi} \ddot{\theta}_{t_{i-1}} \left(q^1 + \frac{1}{3}q^3 \right)_{t_{i-1}} + \frac{4mD_{\theta}}{\pi} \left(\dot{q}^1 + \frac{1}{3}\dot{q}^3 \right)_{t_{i-1}} \\
&\quad + \frac{4m}{\pi} \dot{\theta}_{t_{i-1}} \left(D_{q^1} + \frac{1}{3}D_{q^3} \right) - \frac{4m}{\pi} \dot{\theta}_{t_{i-1}} \left(\dot{q}^1 + \frac{1}{3}\dot{q}^3 \right)_{t_{i-1}} + ml\dot{\theta}_{t_{i-1}} \left(D_{\theta} - \frac{\dot{\theta}_{t_{i-1}}}{2} \right) \\
&\quad - m\bar{s}B_{y_{O_2}} - m\bar{c}B_{x_{O_2}} + \int_0^l f_{2,x}(x_2, t) dx_2
\end{aligned}$$

Discretizing Equation (8.66) gives

$$\begin{aligned}
&mA \left[-\frac{l\bar{s}}{2} - \frac{2\bar{c}}{\pi} \left(q^1 + \frac{1}{3}q^3 \right)_{t_{i-1}} \right] x_{O_2} + mA \left[\frac{l\bar{c}}{2} - \frac{2\bar{s}}{\pi} \left(q^1 + \frac{1}{3}q^3 \right)_{t_{i-1}} \right] y_{O_2} \\
&+ m \left[(q^1\dot{q}^1 + q^2\dot{q}^2 + q^3\dot{q}^3)_{t_{i-1}} C + \frac{A}{2} (q^1q^1 + q^2q^2 + q^3q^3)_{t_{i-1}} + \frac{A}{3}l^2 \right] \theta \\
&+ m \left\{ [\dot{\theta}(\dot{q}^1 + q^1C) + \ddot{\theta}q^1]_{t_{i-1}} + \frac{lA}{\pi} - \frac{2}{\pi} (\bar{s}\ddot{y}_{O_2} + \bar{c}\ddot{x}_{O_2})_{t_{i-1}} \right\} q^1 \\
&+ m \left\{ [\dot{\theta}(\dot{q}^2 + q^2C) + \ddot{\theta}q^2]_{t_{i-1}} - \frac{lA}{2\pi} \right\} q^2 \\
&+ m \left\{ [\dot{\theta}(\dot{q}^3 + q^3C) + \ddot{\theta}q^3]_{t_{i-1}} + \frac{lA}{3\pi} - \frac{2}{3\pi} (\bar{s}\ddot{y}_{O_2} + \bar{c}\ddot{x}_{O_2})_{t_{i-1}} \right\} q^3 \\
&+ m(q^1\dot{q}^1 + q^2\dot{q}^2 + q^3\dot{q}^3)_{t_{i-1}} (D_{\theta} - 2\dot{\theta}_{t_{i-1}}) \\
&+ m\dot{\theta}_{t_{i-1}} (q^1D_{q^1} + q^2D_{q^2} + q^3D_{q^3})_{t_{i-1}} + m(q^1q^1 + q^2q^2 + q^3q^3)_{t_{i-1}} \left(\frac{B_{\theta}}{2} - \ddot{\theta}_{t_{i-1}} \right) \\
&+ \frac{ml^2}{3}B_{\theta} + \frac{ml}{\pi} \left(B_{q^1} - \frac{B_{q^2}}{2} + \frac{B_{q^3}}{3} \right) + \frac{ml}{2} (\bar{c}B_{y_{O_2}} - \bar{s}B_{x_{O_2}}) \\
&- \frac{2m}{\pi} \bar{s} \left(q^1 + \frac{1}{3}q^3 \right)_{t_{i-1}} (B_{y_{O_2}} - \ddot{y}_{O_2})_{t_{i-1}} - \frac{2m}{\pi} \bar{c} \left(q^1 + \frac{1}{3}q^3 \right)_{t_{i-1}} (B_{x_{O_2}} - \ddot{x}_{O_2})_{t_{i-1}} \\
&= \sum_p m_p
\end{aligned} \tag{8.77}$$

Equation (8.77) can be rewritten as

$$\xi_1 x_{O_2} + \xi_2 y_{O_2} + \xi_3 \theta + \xi_7 q^1 + \xi_8 q^2 + \xi_9 q^3 + \xi_{10} = \sum_p m_p \quad (8.78)$$

where

$$\begin{aligned} \xi_1 &= mA \left[-\frac{l\bar{s}}{2} - \frac{2\bar{c}}{\pi} \left(q^1 + \frac{1}{3} q^3 \right) \right]_{t_{i-1}}, \\ \xi_2 &= mA \left[\frac{l\bar{c}}{2} - \frac{2\bar{s}}{\pi} \left(q^1 + \frac{1}{3} q^3 \right) \right]_{t_{i-1}}, \\ \xi_3 &= m \left[(q^1 \dot{q}^1 + q^2 \dot{q}^2 + q^3 \dot{q}^3)_{t_{i-1}} C + \frac{A}{2} (q^1 q^1 + q^2 q^2 + q^3 q^3)_{t_{i-1}} + \frac{A}{3} l^2 \right], \\ \xi_7 &= m \left\{ [\dot{\theta}(\dot{q}^1 + q^1 C) + \ddot{\theta} q^1]_{t_{i-1}} + \frac{LA}{\pi} - \frac{2}{\pi} (\bar{s} \ddot{y}_{O_2} + \bar{c} \ddot{x}_{O_2})_{t_{i-1}} \right\}, \\ \xi_8 &= m \left\{ [\dot{\theta}(\dot{q}^2 + q^2 C) + \ddot{\theta} q^2]_{t_{i-1}} - \frac{LA}{2\pi} \right\}, \\ \xi_9 &= m \left\{ [\dot{\theta}(\dot{q}^3 + q^3 C) + \ddot{\theta} q^3]_{t_{i-1}} + \frac{LA}{3\pi} - \frac{2}{3\pi} (\bar{s} \ddot{y}_{O_2} + \bar{c} \ddot{x}_{O_2})_{t_{i-1}} \right\}, \\ \xi_{10} &= m (q^1 \dot{q}^1 + q^2 \dot{q}^2 + q^3 \dot{q}^3)_{t_{i-1}} (D_\theta - 2\dot{\theta}_{t_{i-1}}) + m \dot{\theta}_{t_{i-1}} (q^1 D_{q^1} + q^2 D_{q^2} + q^3 D_{q^3})_{t_{i-1}} \\ &\quad + m (q^1 q^1 + q^2 q^2 + q^3 q^3)_{t_{i-1}} \left(\frac{B_\theta}{2} - \ddot{\theta}_{t_{i-1}} \right) + \frac{ml^2}{3} B_\theta + \frac{ml}{\pi} \left(B_{q^1} - \frac{B_{q^2}}{2} + \frac{B_{q^3}}{3} \right) \\ &\quad + \frac{ml}{2} (\bar{c} B_{y_{O_2}} - \bar{s} B_{x_{O_2}}) - \frac{2m}{\pi} \bar{s} \left(q^1 + \frac{1}{3} q^3 \right)_{t_{i-1}} (B_{y_{O_2}} - \ddot{y}_{O_2})_{t_{i-1}} \\ &\quad - \frac{2m}{\pi} \bar{c} \left(q^1 + \frac{1}{3} q^3 \right)_{t_{i-1}} (B_{x_{O_2}} - \ddot{x}_{O_2})_{t_{i-1}} \end{aligned} \quad (8.79)$$

If the distributed external force acting on the beam is f , and the distributed external moment is m' , then

$$\sum_p m_p = -l q_{2,y}(l, t) - m(0, t) + m(l, t) + \int_0^l x_2 f_{2,y}(x_2, t) dx_2 - \int_0^l u f_{2,x}(x_2, t) dx_2 + \int_0^l m'(x_2, t) dx_2 \quad (8.80)$$

For small deformation, eliminating the moment $\int_0^l u f_{2,x}(x_2, t) dx_2$, which is caused by axial distributed force, yields

$$\sum_p m_p = -l q_{2,y}(l, t) - m(0, t) + m(l, t) + \int_0^l x_2 f_{2,y}(x_2, t) dx_2 + \int_0^l m'(x_2, t) dx_2 \quad (8.81)$$

Substituting Equation (8.81) into Equation (8.78) yields

$$\begin{aligned} m(l, t) &= m(0, t) + l q_{2,y}(l, t) + \xi_1 x_{O_2} + \xi_2 y_{O_2} + \xi_3 \theta + \xi_7 q^1 + \xi_8 q^2 + \xi_9 q^3 + \xi_{10} \\ &\quad - \int_0^l x_2 f_{2,y}(x_2, t) dx_2 - \int_0^l m'(x_2, t) dx_2 \end{aligned} \quad (8.82)$$

$$\begin{aligned}
m(l, t) = & (\xi_1 + l\zeta_{1,1})x_{O_2} + (\xi_2 + l\zeta_{1,2})y_{O_2} + (\xi_3 + l\zeta_{1,3})\theta + (\xi_7 + l\zeta_{1,7})q^1 + \xi_8q^2 + (\xi_9 + l\zeta_{1,9})q^3 \\
& + (\xi_{10} + l\zeta_{1,10}) + m(0, t) + lq_{2,y}(0, t) - \int_0^l x_2 f_{2,y}(x_2, t) dx_2 - \int_0^l m'(x_2, t) dx_2
\end{aligned} \tag{8.83}$$
$$m(l, t) = u_{4,1}x_{O_2} + u_{4,2}y_{O_2} + u_{4,3}\theta + m(0, t) + u_{4,5}q_x(0, t) + u_{4,6}q_y(0, t) + u_{4,7}q^1 + u_{4,8}q^2 + u_{4,9}q^3 + u_{4,10} \quad (8.84)$$
$$\begin{aligned} q_x(l,t) &= q_{2,x}(l,t)\cos\theta - q_{2,y}(l,t)\sin\theta = q_{2,x}(l,t)\bar{c} - q_{2,y}(l,t)\bar{s} \\ q_y(l,t) &= q_{2,x}(l,t)\sin\theta + q_{2,y}(l,t)\cos\theta = q_{2,x}(l,t)\bar{s} + q_{2,y}(l,t)\bar{c} \end{aligned} \quad (8.85)$$
$$\begin{aligned}
q_x(l,t) &= -mA x_{O_2} + (\bar{c}\zeta_{2,3} - \bar{s}\zeta_{1,3})\theta + q_x(0,t) + (\bar{c}\zeta_{2,7} - \bar{s}\zeta_{1,7})q^1 \\
&\quad + (\bar{c}\zeta_{2,9} - \bar{s}\zeta_{1,9})q^3 + (\bar{c}\zeta_{2,10} - \bar{s}\zeta_{1,10}) \\
q_y(l,t) &= -mA y_{O_2} + (\bar{s}\zeta_{2,3} + \bar{c}\zeta_{1,3})\theta + q_y(0,t) + (\bar{s}\zeta_{2,7} + \bar{c}\zeta_{1,7})q^1 \\
&\quad + (\bar{s}\zeta_{2,9} + \bar{c}\zeta_{1,9})q^3 + (\bar{s}\zeta_{2,10} + \bar{c}\zeta_{1,10})
\end{aligned} \tag{8.86}$$
$$\begin{aligned} q_x(l,t) &= u_{5,1}x_{O_2} + u_{5,3}\theta + q_x(0,t) + u_{5,7}q^1 + u_{5,9}q^3 + u_{5,10} \\ q_y(l,t) &= u_{6,2}y_{O_2} + u_{6,3}\theta + q_y(0,t) + u_{6,7}q^1 + u_{6,9}q^3 + u_{6,10} \end{aligned} \quad (8.87)$$

The state vector of the planar beam can be defined as

From Equation (8.88), considering that the generalized coordinates of the two ends of the beam are equal, the transfer equation of the planar Euler–Bernoulli beam with large motion yields

The transfer matrix is

[illegible]

where

$$u_{1,3} = -ls, \quad u_{1,10} = l(c + \theta s), \quad u_{2,3} = lc, \quad u_{2,10} = l(s - \theta c)$$

$$u_{4,j} = l\zeta_{1,j} + \xi_j \quad (j = 1, 2, 3, 7, 9)$$

$$u_{4,5} = -l\bar{s}, \quad u_{4,6} = l\bar{c}, \quad u_{4,8} = \xi_8$$

$$u_{4,10} = l\zeta_{1,10} + \xi_{10} - \int_0^l x_2 f_{2,y}(x_2, t) dx_2 - \int_0^l m'(x_2, t) dx_2$$

$$u_{5,1} = -mA, \quad u_{5,j} = \bar{c}\zeta_{2,j} - \bar{s}\zeta_{1,j} \quad (j = 3, 7, 9, 10)$$

$$u_{6,2} = -mA, \quad u_{6,j} = \bar{s}\zeta_{2,j} + \bar{c}\zeta_{1,j} \quad (j = 3, 7, 9, 10)$$

8.5 Transfer Matrices of Smooth Hinges Connected to a Beam with Large Planar Motion

The transfer matrices and state vectors of the hinges of MRFSs are determined by the characteristics and transfer direction of the connected bodies, which are different from those in MRSs. There are four kinds of smooth hinges: (1) the outboard body and the inboard body are both rigid, (2) the inboard body is flexible and the outboard body is rigid, (3) the inboard body is rigid and the outboard body is flexible, and (4) both the outboard body and the inboard body are flexible. The transfer matrices of smooth hinges whose outboard body is a beam or rigid body are discussed in the following sections.

8.5.1 Smooth Hinges whose Outboard Body is a Beam

The transfer matrices of smooth hinges whose outboard body is a beam and inboard body is a beam or rigid body are derived as follows. Because x, y, q_x and q_y in the two ends of smooth hinge are equal, and m is zero, we only need to determine θ and $q^k (k = 1, 2, \dots, n)$ of the output end of the smooth hinge.

According to the rotation equation of the beam element, we obtain

$$q_{2,y}(x_2, t) = EI \frac{\partial^3 u}{\partial x_2^3} - \rho I \left(\frac{\partial^3 u}{\partial x_2 \partial t^2} + \ddot{\theta} \right) + m'(x_2, t)$$

Substituting this equation into Equation (8.67), the vibration equation of the beam is

$$EI \frac{\partial^4 u}{\partial x_2^4} - \rho I \frac{\partial^4 u}{\partial x_2^2 \partial t^2} + \bar{m} \left(\frac{\partial^2 u}{\partial t^2} - u \dot{\theta}^2 + x_2 \ddot{\theta} + \ddot{y}_{O_2} \cos \theta - \ddot{x}_{O_2} \sin \theta \right) = f_{2,y}(x_2, t) - \frac{\partial}{\partial x_2} m'(x_2, t) \quad (8.91)$$

Substituting Equation (8.70) into Equation (8.91) yields

$$\begin{aligned} & EI \sum_{k=1}^3 \frac{k^4 \pi^4}{l^4} \sin \frac{k\pi x_2}{l} q^k(t) + \rho I \sum_{k=1}^3 \frac{k^2 \pi^2}{l^2} \sin \frac{k\pi x_2}{l} \ddot{q}^k(t) + \bar{m} \sum_{k=1}^3 \sin \frac{k\pi x_2}{l} \ddot{q}^k(t) \\ & - \bar{m} \dot{\theta}^2 \sum_{k=1}^3 \sin \frac{k\pi x_2}{l} q^k(t) + \bar{m} x_2 \ddot{\theta} + \bar{m} \ddot{y}_{O_2} \cos \theta - \bar{m} \ddot{x}_{O_2} \sin \theta = f_{2,y}(x_2, t) - \frac{\partial}{\partial x_2} m'(x_2, t) \end{aligned} \quad (8.92)$$

Multiplying both sides of Equation (8.92) by $\sin \frac{p\pi x_2}{l}$ ($p = 1, 2, 3$) and integrating along x_2 gives

$$EI \frac{p^4 \pi^4}{l^4} \frac{l}{2} q^p(t) + \rho I \frac{p^2 \pi^2}{l^2} \frac{l}{2} \ddot{q}^p(t) + \bar{m} \frac{l}{2} \ddot{q}^p(t) - \bar{m} \dot{\theta}^2 \frac{l}{2} q^p(t) + (-1)^{p-1} \bar{m} \frac{l^2}{p\pi} \ddot{\theta} + [1 - (-1)^p] \bar{m} \frac{l}{p\pi} (\ddot{y}_{O_2} \cos \theta - \ddot{x}_{O_2} \sin \theta) = \int_0^l \left[f_{2,y}(x_2, t) - \frac{\partial}{\partial x_2} m'(x_2, t) \right] \sin \frac{p\pi x_2}{l} dx_2 \quad (8.93)$$

Let

$$\begin{aligned} D_{kk} &= \frac{l}{2} \left[EI \frac{k^4 \pi^4}{l^4} - \bar{m} \dot{\theta}^2(t_{i-1}) \right] + \frac{l}{2} \left(\rho I \frac{k^2 \pi^2}{l^2} + \bar{m} \right) A \quad (k = 1, 2, 3) \\ D_{k4} &= (-1)^{k-1} \bar{m} \frac{l^2}{k\pi} A - \bar{m} l \dot{\theta}(t_{i-1}) q^k(t_{i-1}) C \quad (k = 1, 2, 3) \\ D_{41} &= u_{4,7}, \quad D_{42} = u_{4,8}, \quad D_{43} = u_{4,9}, \quad D_{44} = u_{4,3} \\ H_{k1} &= \left[1 - (-1)^k \right] \bar{m} \frac{l}{k\pi} \bar{s} A \quad (k = 1, 2, 3), \quad H_{k2} = - \left[1 - (-1)^k \right] \bar{m} \frac{l}{k\pi} \bar{c} A \quad (k = 1, 2, 3) \\ H_{k5} &= \int_0^l \left[f_{2,y}(x_2, t) - \frac{\partial}{\partial x_2} m'(x_2, t) \right] \sin \frac{k\pi x_2}{l} dx_2 - \frac{l}{2} \left(\bar{m} + \rho I \frac{k^2 \pi^2}{l^2} \right) B_{q^k} - \bar{m} l \dot{\theta}^2(t_{i-1}) q^k(t_{i-1}) \\ &\quad - (-1)^{k-1} \frac{\bar{m} l^2}{k\pi} B_{\theta} - \left[1 - (-1)^k \right] \frac{\bar{m} l}{k\pi} \left(\bar{c} B_{y_{O_2}} - \bar{s} B_{x_{O_2}} \right) + \bar{m} l \dot{\theta}(t_{i-1}) q^k(t_{i-1}) D_{\theta} \quad (k = 1, 2, 3) \\ H_{41} &= -u_{4,1}, \quad H_{42} = -u_{4,2}, \quad H_{43} = -u_{4,5}, \quad H_{44} = -u_{4,6}, \quad H_{45} = -u_{4,10} \end{aligned}$$

where $u_{4,1}, u_{4,2}, \dots, u_{4,10}$ are the elements of the transfer matrix of the outboard beam.

Linearizing Equation (8.93) yields

$$\begin{cases} D_{11}q^1 & + D_{14}\theta = H_{11}x_{O_2} + H_{12}y_{O_2} & + H_{15} \\ D_{22}q^2 & + D_{24}\theta = H_{21}x_{O_2} + H_{22}y_{O_2} & + H_{25} \\ D_{33}q^3 + D_{34}\theta & = H_{31}x_{O_2} + H_{32}y_{O_2} & + H_{35} \\ D_{41}q^1 + D_{42}q^2 + D_{43}q^3 + D_{44}\theta & = H_{41}x_{O_2} + H_{42}y_{O_2} + H_{43}q_x + H_{44}q_y + H_{45} \end{cases} \quad (8.94)$$

Using the Cramer rule yields

$$\begin{bmatrix} q^1 \\ q^2 \\ q^3 \\ \theta \end{bmatrix} = \begin{bmatrix} \Delta_{11}/\Delta & \Delta_{12}/\Delta & \Delta_{13}/\Delta & \Delta_{14}/\Delta \\ \Delta_{21}/\Delta & \Delta_{22}/\Delta & \Delta_{23}/\Delta & \Delta_{24}/\Delta \\ \Delta_{31}/\Delta & \Delta_{32}/\Delta & \Delta_{33}/\Delta & \Delta_{34}/\Delta \\ \Delta_{41}/\Delta & \Delta_{42}/\Delta & \Delta_{43}/\Delta & \Delta_{44}/\Delta \end{bmatrix} \begin{bmatrix} x_{O_2} \\ y_{O_2} \\ q_x \\ q_y \end{bmatrix} + \begin{bmatrix} \Delta_{15}/\Delta \\ \Delta_{25}/\Delta \\ \Delta_{35}/\Delta \\ \Delta_{45}/\Delta \end{bmatrix} \quad (8.95)$$

where

$$\Delta = \begin{vmatrix} D_{11} & D_{14} \\ & D_{22} & D_{24} \\ & & D_{33} & D_{34} \\ D_{41} & D_{42} & D_{43} & D_{44} \end{vmatrix}$$

$$\Delta_{1j} = \begin{vmatrix} H_{1i} & & D_{14} \\ H_{2i} & D_{22} & D_{24} \\ H_{3i} & D_{33} & D_{34} \\ H_{4i} & D_{42} & D_{43} & D_{44} \end{vmatrix}, \quad \Delta_{2j} = \begin{vmatrix} D_{11} & H_{1i} & D_{14} \\ & H_{2i} & D_{24} \\ & H_{3i} & D_{33} & D_{34} \\ D_{41} & H_{4i} & D_{43} & D_{44} \end{vmatrix}$$

$$\Delta_{3j} = \begin{vmatrix} D_{11} & & H_{1i} & D_{14} \\ & D_{22} & H_{2i} & D_{24} \\ & & H_{3i} & D_{34} \\ D_{41} & D_{42} & H_{4i} & D_{44} \end{vmatrix}, \quad \Delta_{4j} = \begin{vmatrix} D_{11} & & & H_{1i} \\ & D_{22} & & H_{2i} \\ & & D_{33} & H_{3i} \\ D_{41} & D_{42} & D_{43} & H_{4i} \end{vmatrix} \quad (j = 1, 2, 3, 4, 5)$$

To reduce computational cost, we usually do not use the Cramer rule to solve the linear equations. Instead, we simplify Equation (8.94) with transformations to make the coefficient matrix on the left-hand side of the equation into a unit matrix and obtain Equation (8.98).

For a smooth hinge whose outboard body is a beam, the transfer matrices are deduced for two cases: the inboard body is a beam and the inboard body is a rigid body. The deduction is accomplished based upon an assumption that the output end of the outboard body is also connected with another smooth hinge. If the output end of the outboard body is not connected with another smooth hinge, we can deduce the transfer matrices in a similar way.

8.5.1.1 Smooth Hinge whose Outboard and Inboard Bodies are Beams

If the highest order of the modes $n = 3$, the state vectors of the input and output ends of the smooth hinge whose inboard and outboard bodies are beams are defined respectively as

$$\mathbf{z}_I = [x, y, \theta, m, q_x, q_y, q^1, q^2, q^3, 1]^T, \quad \mathbf{z}_O = [x, y, \theta, m, q_x, q_y, q^1, q^2, q^3, 1]^T \quad (8.96)$$

The transfer equation is

$$\mathbf{z}_O = \mathbf{U}\mathbf{z}_I \quad (8.97)$$

The transfer matrix is

[illegible]

8.5.1.2 Smooth Hinge whose Outboard Body is a Beam and whose Inboard Body is a Rigid Body

For a smooth hinge whose outboard body is a beam and whose inboard body is a rigid body, the transfer matrix of the smooth hinge can be obtained by eliminating the columns corresponding to the generalized coordinates in Equation (8.98). The state vectors of the input and output ends of this smooth hinge are, respectively,

$$\mathbf{z}_I = [x, y, \theta, m, q_x, q_y, 1]^T \quad \text{and} \quad \mathbf{z}_O = [x, y, \theta, m, q_x, q_y, q^1, q^2, q^3, 1]^T \quad (8.99)$$

The transfer equation is

$$\mathbf{z}_O = \mathbf{U} \mathbf{z}_I \quad (8.100)$$

Eliminating columns 7–9 in Equation (8.98), the transfer matrix of this smooth hinge is

$$\mathbf{U} = \begin{bmatrix} 1 & 0 & 0 & 0 & 0 & 0 & 0 \\ 0 & 1 & 0 & 0 & 0 & 0 & 0 \\ \Delta_{41}/\Delta & \Delta_{42}/\Delta & 0 & 0 & \Delta_{43}/\Delta & \Delta_{44}/\Delta & \Delta_{45}/\Delta \\ 0 & 0 & 0 & 0 & 0 & 0 & 0 \\ 0 & 0 & 0 & 0 & 1 & 0 & 0 \\ 0 & 0 & 0 & 0 & 0 & 1 & 0 \\ \Delta_{11}/\Delta & \Delta_{12}/\Delta & 0 & 0 & \Delta_{13}/\Delta & \Delta_{14}/\Delta & \Delta_{15}/\Delta \\ \Delta_{21}/\Delta & \Delta_{22}/\Delta & 0 & 0 & \Delta_{23}/\Delta & \Delta_{24}/\Delta & \Delta_{25}/\Delta \\ \Delta_{31}/\Delta & \Delta_{32}/\Delta & 0 & 0 & \Delta_{33}/\Delta & \Delta_{34}/\Delta & \Delta_{35}/\Delta \\ 0 & 0 & 0 & 0 & 0 & 0 & 1 \end{bmatrix} \quad (8.101)$$

8.5.2 Smooth Hinge whose Outboard Body is a Rigid Body

8.5.2.1 Smooth Hinge whose Inboard Body is a Rigid Body

The smooth hinge whose outboard and inboard bodies are rigid is discussed in Chapter 7. The state vectors of the input and output ends of the smooth hinge whose outboard and inboard bodies are rigid are defined respectively as

$$\mathbf{z}_I = [x, y, \theta, m, q_x, q_y, 1]^T, \quad \mathbf{z}_O = [x, y, \theta, m, q_x, q_y, 1]^T \quad (8.102)$$

The transfer matrix is Equation (7.219).

8.5.2.2 Smooth Hinge whose Inboard Body is a Beam

The derivation of the transfer matrix of smooth hinge whose outboard body is a rigid body and whose inboard body is a beam is the same as Equation (7.219). The state vectors of the input and output ends of this smooth hinge are defined respectively as

$$\mathbf{z}_I = [x, y, \theta, m, q_x, q_y, q^1, q^2, q^3, 1]^T \quad \text{and} \quad \mathbf{z}_O = [x, y, \theta, m, q_x, q_y, 1]^T \quad (8.103)$$

The transfer equation is

$$\mathbf{z}_O = \mathbf{U} \mathbf{z}_I \quad (8.104)$$

Inserting three columns with zero elements behind the sixth column in Equation (7.219), the transfer matrix of this smooth hinge can be obtained:

$$\mathbf{U} = \begin{bmatrix} 1 & 0 & 0 & 0 & 0 & 0 & 0 & 0 & 0 & 0 \\ 0 & 1 & 0 & 0 & 0 & 0 & 0 & 0 & 0 & 0 \\ -\frac{u_{4,1}}{u_{4,3}} & -\frac{u_{4,2}}{u_{4,3}} & 0 & 0 & -\frac{u_{4,5}}{u_{4,3}} & -\frac{u_{4,6}}{u_{4,3}} & 0 & 0 & 0 & -\frac{u_{4,7}}{u_{4,3}} \\ 0 & 0 & 0 & 0 & 0 & 0 & 0 & 0 & 0 & 0 \\ 0 & 0 & 0 & 0 & 1 & 0 & 0 & 0 & 0 & 0 \\ 0 & 0 & 0 & 0 & 0 & 1 & 0 & 0 & 0 & 0 \\ 0 & 0 & 0 & 0 & 0 & 0 & 0 & 0 & 0 & 0 \end{bmatrix} \quad (8.105)$$

The meanings of the elements in this equation are the same as in Equation (7.219).

8.6 Transfer Matrices of Spring Hinges Connected to a Beam with Large Planar Motion

Similarly to the smooth hinges connected to a beam with large planar motion introduced in section 8.5, there are four kinds of spring hinges connected to a beam with large planar motion: (1) both of the outboard and inboard bodies are rigid, (2) the inboard body is flexible and the outboard body is rigid, (3) the inboard body is rigid and the outboard body is flexible, and (4) both the outboard and inboard bodies are flexible. The transfer matrix of the spring hinge whose outboard and inboard bodies are rigid bodies with planar motion was given in Chapter 7. Here the transfer matrix of a spring hinge connected to a flexible body with planar motion is discussed.

8.6.1 Dynamic Equation of a Spring Hinge Connected to a Beam with Planar Motion

Similarly to section 7.6, the spring hinge includes a linear (or nonlinear) spring and a torsional spring.

The mass of the spring is omitted. According to Equations (7.200) and (7.201), we obtain

$$x_O = x_I + \frac{\Delta_{11}}{\Delta} q_{x,I} + \frac{\Delta_{12}}{\Delta} q_{y,I} + \frac{\Delta_{13}}{\Delta} \quad (8.106)$$

$$y_O = y_I + \frac{\Delta_{21}}{\Delta} q_{x,I} + \frac{\Delta_{22}}{\Delta} q_{y,I} + \frac{\Delta_{23}}{\Delta} \quad (8.107)$$

The variables are the same as in section 7.6.1.

For a nonlinear torsional spring,

$$m_I = K'_1 (\theta'_O - \theta'_I) + K'_2 (\theta'_O - \theta'_I)^3 \quad (8.108)$$

where

$$\theta'_I = \theta_I + \frac{\partial u_2(x_2, t)}{\partial x_2} \Big|_I, \quad \theta'_O = \theta_O + \frac{\partial u_2(x_2, t)}{\partial x_2} \Big|_O \quad (8.109)$$

K'_1 and K'_2 are the stiffness coefficients of a nonlinear torsional spring, θ'_I and θ'_O are the orientation angles of the input and output ends of the torsional spring, respectively, θ_I and θ_O are

the orientation angles of the inboard and outboard bodies of the torsional spring, respectively, and $\partial u_2(x_2, t)/\partial x_2|_I$ and $\partial u_2(x_2, t)/\partial x_2|_O$ are rotation angles caused by the deformation of the inboard and outboard bodies of torsional spring. If the inboard or outboard body of the torsional spring is rigid, then $\partial u_2(x_2, t)/\partial x_2|_I = 0$ or $\partial u_2(x_2, t)/\partial x_2|_O = 0$.

Linearizing Equation (8.108) yields

$$\theta_O + \frac{\partial u_2(x_2, t)}{\partial x_2}|_O = \theta_I + \frac{\partial u_2(x_2, t)}{\partial x_2}|_I + \lambda_1 m_I - \lambda_2 \quad (8.110)$$

where

$$\lambda_1 = \frac{1}{K'_1 + 3K'_2(\theta'_O - \theta'_I)_{t_{i-1}}^2}, \quad \lambda_2 = \frac{K'_2 \left[3(\dot{\theta}'_O - \dot{\theta}'_I)_{t_{i-1}}^2 (\theta'_O - \theta'_I)_{t_{i-1}} \Delta T^2 - 2(\theta'_O - \theta'_I)_{t_{i-1}}^3 \right]}{K'_1 + 3K'_2(\theta'_O - \theta'_I)_{t_{i-1}}^2}$$

For the massless spring and the massless torsional spring, Newton's third law of motion tells us that

$$q_{x,O} = q_{x,I}, \quad q_{y,O} = q_{y,I}, \quad m_O = m_I \quad (8.111)$$

8.6.2 Transfer Matrix of a Spring Hinge whose Inboard and Outboard Bodies are Beams moving in a Plane

For a spring hinge whose inboard and outboard bodies are beams moving in a plane, it is necessary to determine the relation between the angular orientation θ and the generalized coordinates $q^k (k = 1, 2, \dots, n)$ of the output end of the spring hinge and the state vector of the input end. Using the modal expansion, the transverse deformation u of a beam becomes

$$u(x_2, t) = \sum_{k=1}^n Y^k(x_2) q^k(t) \quad (8.112)$$

Substituting Equation (8.112) into the equation of vibration Equation (8.91) of the outboard beam, we obtain

$$\begin{aligned} EI \sum_{k=1}^n \frac{\partial^4}{\partial x_2^4} Y^k(x_2) q^k(t) - \rho I \sum_{k=1}^n \frac{\partial^2}{\partial x_2^2} Y^k(x_2) \ddot{q}^k(t) + \bar{m} \sum_{k=1}^n Y^k(x_2) \ddot{q}^k(t) \\ - \bar{m} \dot{\theta}^2 \sum_{k=1}^n Y^k(x_2) q^k(t) + \bar{m} x_2 \ddot{\theta} + \bar{m} \ddot{y}_{O_2} \cos \theta - \bar{m} \ddot{x}_{O_2} \sin \theta = f(x_2, t) - \frac{\partial}{\partial x_2} m'(x_2, t) \end{aligned} \quad (8.113)$$

Let

$$\begin{aligned} {}^4s_{k,k'} = \int_0^l \frac{dY^{k(4)}}{dx_2^{(4)}} Y^{k'}(x_2) dx_2, \quad {}^2s_{k,k'} = \int_0^l \frac{dY^{k(2)}}{dx_2^{(2)}} Y^{k'}(x_2) dx_2, \quad {}^1Y = \frac{dY^k(x_2)}{dx_2} \\ s_k^0 = \int_0^l Y^k(x_2) dx_2, \quad s_{k,k'} = \int_0^l Y^k(x_2) Y^{k'}(x_2) dx_2, \quad s_k^1 = \int_0^l Y^k(x_2) x_2 dx_2 \end{aligned} \quad (8.114)$$

Multiplying both sides of Equation (8.113) by $Y^{k'}(x_2)$ ($k' = 1, 2, \dots, n$) and integrating along x_2 , we obtain

$$EI \left[\sum_{k=1}^n s_{k,k'} q^k(t) \right] - \rho I \left[\sum_{k=1}^n s_{k,k'} \ddot{q}^k(t) \right] + \bar{m} \sum_{k=1}^n s_{k,k'} \ddot{q}^k(t) - \bar{m} \dot{\theta}^2 \sum_{k=1}^n s_{k,k'} q^k(t) + \bar{m} s_{k'}^1 \ddot{\theta} + \bar{m} \bar{s}_{k'}^0 \ddot{y}_{O_2} \cos \theta - \bar{m} \bar{s}_{k'}^0 \ddot{x}_{O_2} \sin \theta = \int_0^l Y^{k'}(x_2) f(x_2, t) dx_2 - \int_0^l Y^{k'}(x_2) \frac{\partial}{\partial x_2} m'(x_2, t) dx_2 \quad (8.115)$$

Linearizing Equation (8.115) yields

$$\begin{aligned} & \sum_{k=1}^n \left(s_{k,k'} EI - s_{k,k'} \rho I A + \bar{m} s_{k,k'} A - \bar{m} s_{k,k'} \dot{\theta}_{t_{i-1}}^2 \right) q^k(t_i) + \bar{m} \left(s_{k'}^1 A - 2C \sum_{k=1}^n s_{k,k'} q_{t_{i-1}}^k \dot{\theta}_{t_{i-1}} \right) \theta(t_i) \\ &= \bar{m} \bar{s}_{k'}^0 A x_{O_2}(t_i) - \bar{m} \bar{s}_{k'}^0 A y_{O_2}(t_i) + \int_0^l Y^{k'}(x_2) f(x_2, t) dx_2 - \int_0^l Y^{k'}(x_2) \frac{\partial}{\partial x_2} m'(x_2, t) dx_2 \\ & - \bar{m} \left\{ \sum_{k=1}^n s_{k,k'} B_{q^k} - \sum_{k=1}^n s_{k,k'} \left(2q_{t_{i-1}}^k \dot{\theta}_{t_{i-1}} D_\theta - 2q^k(t_{i-1}) \dot{\theta}_{t_{i-1}}^2 \right) + s_{k'}^1 B_\theta + \bar{s} s_{k'}^0 B_{y_{O_2}} - \bar{c} s_{k'}^0 B_{x_{O_2}} \right\} \\ & + \rho I \sum_{k=1}^n s_{k,k'} B_{q^k} \quad (k' = 1, 2, \dots, n) \end{aligned} \quad (8.116)$$

Substituting Equation (8.112) into Equation (8.110) yields

$$\sum_{k=1}^n {}^1 Y^k(x_2) q^k(t_i) |_O + \theta_O = \theta_I + \sum_{k=1}^n {}^1 Y^k(x_2) q^k(t_i) |_I + \lambda_1 m_I - \lambda_2 \quad (8.117)$$

Let

$$\begin{aligned} A_{k',k} &= {}^4 s_{k,k'} EI - {}^2 s_{k,k'} \rho I A + \bar{m} s_{k,k'} A - \bar{m} s_{k,k'} \dot{\theta}_{t_{i-1}}^2, \quad A_{n+1,k} = {}^1 Y_O^k, \quad (k = 1, 2, \dots, n) \\ A_{k',n+1} &= \bar{m} \left(s_{k'}^1 A - 2C \sum_{k=1}^n s_{k,k'} q_{t_{i-1}}^k \dot{\theta}_{t_{i-1}} \right), \quad A_{n+1,n+1} = 1 \\ B_{k',1} &= \bar{m} \bar{s}_{k'}^0 A, \quad B_{k',2} = -\bar{m} \bar{s}_{k'}^0 A, \quad B_{k',k} = 0, \quad (k = 3, 4, \dots, 4+n) \\ B_{k',5+n} &= \int_0^l Y^{k'}(x_2) f(x_2, t) dx_2 - \int_0^l Y^{k'}(x_2) \frac{\partial}{\partial x_2} m'(x_2, t) dx_2 + \rho I \sum_{k=1}^n s_{k,k'} B_{q^k} \\ & - \bar{m} \left\{ \sum_{k=1}^n s_{k,k'} B_{q^k} - \sum_{k=1}^n s_{k,k'} \left(2q_{t_{i-1}}^k \dot{\theta}_{t_{i-1}} D_\theta - 2q^k(t_{i-1}) \dot{\theta}_{t_{i-1}}^2 \right) + s_{k'}^1 B_\theta + \bar{s} s_{k'}^0 B_{y_{O_2}} - \bar{c} s_{k'}^0 B_{x_{O_2}} \right\} \\ B_{n+1,1} &= 0, \quad B_{n+1,2} = 0, \quad B_{n+1,3} = 1, \quad B_{n+1,4} = \lambda_1 \\ B_{n+1,4+k} &= {}^1 Y_I^k, \quad (k = 1, 2, \dots, n) \\ B_{n+1,5+n} &= -\lambda_2 \end{aligned}$$

where $k' = 1, 2, \dots, n$.

The x , y and m of the two ends of the state vectors of the spring hinge are equal.

$$\begin{aligned}
 & \begin{bmatrix} A_{1,1} & A_{1,2} & \cdots & A_{1,n} & A_{1,n+1} \\ A_{2,1} & A_{2,2} & \cdots & A_{2,n} & A_{2,n+1} \\ \vdots & \vdots & \ddots & \vdots & \vdots \\ A_{n,1} & A_{n,2} & \cdots & A_{n,n} & A_{n,n+1} \\ A_{n+1,1} & A_{n+1,2} & \cdots & A_{n+1,n} & A_{n+1,n+1} \end{bmatrix} \begin{bmatrix} q^1 \\ q^2 \\ \vdots \\ q^n \\ \theta \end{bmatrix}_O \\
 &= \begin{bmatrix} B_{1,1} & B_{1,2} & B_{1,3} & B_{1,4} & B_{1,4+1} & \cdots & B_{1,4+n} & B_{1,5+n} \\ B_{2,1} & B_{2,2} & B_{2,3} & B_{2,4} & B_{2,4+1} & \cdots & B_{2,4+n} & B_{2,5+n} \\ \vdots & \vdots & \vdots & \vdots & \vdots & \ddots & \vdots & \vdots \\ B_{n,1} & B_{n,2} & B_{n,3} & B_{n,4} & B_{n,4+1} & \cdots & B_{n,4+n} & B_{n,5+n} \\ B_{n+1,1} & B_{n+1,2} & B_{n+1,3} & B_{n+1,4} & B_{n+1,4+1} & \cdots & B_{n+1,4+n} & B_{n+1,5+n} \end{bmatrix} \begin{bmatrix} x \\ y \\ \theta \\ m \\ q^1 \\ \vdots \\ q^n \\ 1 \end{bmatrix}_I \quad (8.118)
 \end{aligned}$$

Solving Equation (8.118) for the state variables θ and q^k ($k = 1, 2, \dots, n$) of the output end in terms of the state variables x , y , θ , m and q^k of the input end and applying the Cramer rule for simplicity, we obtain

$$\begin{aligned}
 & \begin{bmatrix} q^1 \\ q^2 \\ \vdots \\ q^n \\ \theta \end{bmatrix}_O = \begin{bmatrix} \Delta'_{1,1}/\Delta' & \cdots & \Delta'_{1,4}/\Delta' & \Delta'_{1,4+1}/\Delta' & \cdots & \Delta'_{1,4+1+n}/\Delta' \\ \Delta'_{2,1}/\Delta' & \cdots & \Delta'_{2,4}/\Delta' & \Delta'_{2,4+1}/\Delta' & \cdots & \Delta'_{2,4+1+n}/\Delta' \\ \vdots & \ddots & \vdots & \vdots & \ddots & \vdots \\ \Delta'_{n+1,1}/\Delta' & \cdots & \Delta'_{n+1,4}/\Delta' & \Delta'_{n+1,4+1}/\Delta' & \cdots & \Delta'_{n+1,4+1+n}/\Delta' \end{bmatrix} \begin{bmatrix} x \\ y \\ \theta \\ m \\ q^1 \\ \vdots \\ q^n \\ 1 \end{bmatrix}_I \quad (8.119)
 \end{aligned}$$

where

$$\Delta' = \begin{bmatrix} A_{1,1} & A_{1,2} & \cdots & A_{1,n} & A_{1,n+1} \\ A_{2,1} & A_{2,2} & \cdots & A_{2,n} & A_{2,n+1} \\ \vdots & \vdots & \ddots & \vdots & \vdots \\ A_{n,1} & A_{n,2} & \cdots & A_{n,n} & A_{n,n+1} \\ A_{n+1,1} & A_{n+1,2} & \cdots & A_{n+1,n} & A_{n+1,n+1} \end{bmatrix}$$

$$\Delta'_{k,i} = \begin{bmatrix} A_{1,1} & \cdots & A_{1,k-1} & B_{1,i} & A_{1,k+1} & \cdots & A_{1,n+1} \\ A_{2,1} & \cdots & A_{2,k-1} & B_{2,i} & A_{2,k+1} & \cdots & A_{2,n+1} \\ \vdots & \ddots & \vdots & \vdots & \vdots & \ddots & \vdots \\ A_{n,1} & \cdots & A_{n,k-1} & B_{n,i} & A_{n,k+1} & \cdots & A_{n,n+1} \\ A_{n+1,1} & \cdots & A_{n+1,k-1} & B_{n+1,i} & A_{n+1,k+1} & \cdots & A_{n+1,n+1} \end{bmatrix} \quad \begin{pmatrix} k = 1, 2, \dots, n+1 \\ i = 1, 2, \dots, n+5 \end{pmatrix}$$

For example,

$$\Delta'_{1,i} = \begin{bmatrix} B_{1,i} & A_{1,2} & \cdots & A_{1,n} & A_{1,n+1} \\ B_{2,i} & A_{2,2} & \cdots & A_{2,n} & A_{2,n+1} \\ \vdots & \vdots & \ddots & \vdots & \vdots \\ B_{n,i} & A_{n,2} & \cdots & A_{n,n} & A_{n,n+1} \\ B_{n+1,i} & A_{n+1,2} & \cdots & A_{n+1,n} & A_{n+1,n+1} \end{bmatrix}, \Delta'_{2,i} = \begin{bmatrix} A_{1,1} & B_{1,i} & \cdots & A_{1,n} & A_{1,n+1} \\ A_{2,1} & B_{2,i} & \cdots & A_{2,n} & A_{2,n+1} \\ \vdots & \vdots & \ddots & \vdots & \vdots \\ A_{n,1} & B_{n,i} & \cdots & A_{n,n} & A_{n,n+1} \\ A_{n+1,1} & B_{n+1,i} & \cdots & A_{n+1,n} & A_{n+1,n+1} \end{bmatrix}$$

Therefore, the transfer equation of a spring hinge whose inboard and outboard bodies are beams is

$$\mathbf{z}_O = \mathbf{U} \mathbf{z}_I \quad (8.120)$$

where the definition of the state vectors is the same as for the state vectors of the beam, that is

$$\mathbf{z}_O = [x, y, \theta, m, q_x, q_y, q^1, q^2, \dots, q^n, 1]^T \text{ and } \mathbf{z}_I = [x, y, \theta, m, q_x, q_y, q^1, q^2, \dots, q^n, 1]^T$$

The transfer matrix is

$$\mathbf{U} = \begin{bmatrix} 1 & 0 & 0 & 0 & \frac{\Delta_{11}}{\Delta} & \frac{\Delta_{12}}{\Delta} & 0 & \cdots & 0 & \frac{\Delta_{13}}{\Delta} \\ 0 & 1 & 0 & 0 & \frac{\Delta_{21}}{\Delta} & \frac{\Delta_{22}}{\Delta} & 0 & \cdots & 0 & \frac{\Delta_{23}}{\Delta} \\ \frac{\Delta'_{n+1,1}}{\Delta'} & \frac{\Delta'_{n+1,2}}{\Delta'} & \frac{\Delta'_{n+1,3}}{\Delta'} & \frac{\Delta'_{n+1,4}}{\Delta'} & 0 & 0 & \frac{\Delta'_{n+1,4+1}}{\Delta'} & \cdots & \frac{\Delta'_{n+1,4+n}}{\Delta'} & \frac{\Delta'_{n+1,4+(1+n)}}{\Delta'} \\ 0 & 0 & 0 & 1 & 0 & 0 & 0 & \cdots & 0 & 0 \\ 0 & 0 & 0 & 0 & 1 & 0 & 0 & \cdots & 0 & 0 \\ 0 & 0 & 0 & 0 & 0 & 1 & 0 & \cdots & 0 & 0 \\ \frac{\Delta'_{1,1}}{\Delta'} & \frac{\Delta'_{1,2}}{\Delta'} & \frac{\Delta'_{1,3}}{\Delta'} & \frac{\Delta'_{1,4}}{\Delta'} & 0 & 0 & \frac{\Delta'_{1,4+1}}{\Delta'} & \cdots & \frac{\Delta'_{1,4+n}}{\Delta'} & \frac{\Delta'_{1,4+(1+n)}}{\Delta'} \\ \vdots & \vdots & \vdots & \vdots & \vdots & \vdots & \vdots & \ddots & \vdots & \vdots \\ \frac{\Delta'_{n,1}}{\Delta'} & \frac{\Delta'_{n,2}}{\Delta'} & \frac{\Delta'_{n,3}}{\Delta'} & \frac{\Delta'_{n,4}}{\Delta'} & 0 & 0 & \frac{\Delta'_{n,4+1}}{\Delta'} & \cdots & \frac{\Delta'_{n,4+n}}{\Delta'} & \frac{\Delta'_{n,4+(1+n)}}{\Delta'} \\ 0 & 0 & 0 & 0 & 0 & 0 & 0 & \cdots & 0 & 1 \end{bmatrix} \quad (8.121)$$

8.6.3 Transfer Matrix of a Spring Hinge whose Inboard Body is Rigid and whose Outboard Body is a Beam moving in a Plane

If the inboard body of a spring hinge is rigid body, according to the above analysis we know $\partial u_2(x_2, t)/\partial x_2|_I = 0$ and according to Equation (8.117) this becomes

$$\sum_{k=1}^n Y^k(x_2) q^k(t_i)|_O + \theta_O = \theta_I + \lambda_1 m_I - \lambda_2 \quad (8.122)$$

Similarly, combining Equations (8.116) and (8.122), let θ and q^k ($k = 1, 2, \dots, n$) in the state vector of the spring hinge output end be expressed as a linear representation of x, y, θ, m and q^k in the state vector of the input end. Using the Cramer rule, the transfer matrix of a spring hinge whose inboard body is rigid and whose outboard body is a beam moving in plane can be obtained. The state vectors of the input and output points of this spring hinge are

$$\mathbf{z}_I = [x, y, \theta, m, q_x, q_y, 1]^T \text{ and } \mathbf{z}_O = [x, y, \theta, m, q_x, q_y, q^1, q^2, \dots, q^n, 1]^T \quad (8.123)$$

The transfer equation is

$$\mathbf{z}_O = \mathbf{U} \mathbf{z}_I \quad (8.124)$$

The transfer matrix is

$$\mathbf{U} = \begin{bmatrix} 1 & 0 & 0 & 0 & \Delta_{11}/\Delta & \Delta_{12}/\Delta & \Delta_{13}/\Delta \\ 0 & 1 & 0 & 0 & \Delta_{21}/\Delta & \Delta_{22}/\Delta & \Delta_{23}/\Delta \\ \frac{\Delta'_{n+1,1}}{\Delta'} & \frac{\Delta'_{n+1,2}}{\Delta'} & \frac{\Delta'_{n+1,3}}{\Delta'} & \frac{\Delta'_{n+1,4}}{\Delta'} & 0 & 0 & \frac{\Delta'_{n+1,5+n}}{\Delta'} \\ 0 & 0 & 0 & 1 & 0 & 0 & 0 \\ 0 & 0 & 0 & 0 & 1 & 0 & 0 \\ 0 & 0 & 0 & 0 & 0 & 1 & 0 \\ \frac{\Delta'_{1,1}}{\Delta'} & \frac{\Delta'_{1,2}}{\Delta'} & \frac{\Delta'_{1,3}}{\Delta'} & \frac{\Delta'_{1,4}}{\Delta'} & 0 & 0 & \frac{\Delta'_{1,5+n}}{\Delta'} \\ \frac{\Delta'_{2,1}}{\Delta'} & \frac{\Delta'_{2,2}}{\Delta'} & \frac{\Delta'_{2,3}}{\Delta'} & \frac{\Delta'_{2,4}}{\Delta'} & 0 & 0 & \frac{\Delta'_{2,5+n}}{\Delta'} \\ \vdots & \vdots & \vdots & \vdots & \vdots & \vdots & \vdots \\ \frac{\Delta'_{n,1}}{\Delta'} & \frac{\Delta'_{n,2}}{\Delta'} & \frac{\Delta'_{n,3}}{\Delta'} & \frac{\Delta'_{n,4}}{\Delta'} & 0 & 0 & \frac{\Delta'_{n,5+n}}{\Delta'} \\ 0 & 0 & 0 & 0 & 0 & 0 & 1 \end{bmatrix} \quad (8.125)$$

where the meaning of all the elements is the same as in Equation (8.121), except that we let $B_{n+1,k+4} = 0$ ($k = 1, 2, \dots, n$) during the computation.

8.6.4 Transfer Matrix of a Spring Hinge whose Inboard Body is a Beam and whose Outboard Body is a Rigid Body Moving in Plane

If the outboard body of spring hinge is a rigid body, according to the above analysis we know $\partial u_2(x_2, t)/\partial x_2|_I = 0$, and according to Equation (8.117)

$$\theta_O = \theta_I + \sum_{k=1}^n Y'^k(x_2) q^k(t_i)|_I + \lambda_1 m_I - \lambda_2 \quad (8.126)$$

Similarly, combining Equations (8.106), (8.107), (8.111) and (8.126), the transfer matrix of a spring hinge whose inboard body is a beam and whose outboard body is a rigid body moving in a plane can be obtained.

The state vectors of the input and output ends of a spring hinge whose inboard body is beam and whose outboard body is a rigid body moving in a plane are

$$\mathbf{z}_I = [x, y, \theta, m, q_x, q_y, q^1, q^2, \dots, q^n, 1]^T \text{ and } \mathbf{z}_O = [x, y, \theta, m, q_x, q_y, 1]^T \quad (8.127)$$

The transfer equation is

$$\mathbf{z}_O = \mathbf{U} \mathbf{z}_I \quad (8.128)$$

The transfer matrix is

$$\mathbf{U} = \begin{bmatrix} 1 & 0 & 0 & 0 & \Delta_{11}/\Delta & \Delta_{12}/\Delta & 0 & 0 & \dots & 0 & \Delta_{13}/\Delta \\ 0 & 1 & 0 & 0 & \Delta_{21}/\Delta & \Delta_{22}/\Delta & 0 & 0 & \dots & 0 & \Delta_{23}/\Delta \\ 0 & 0 & 1 & \lambda_1 & 0 & 0 & {}^1Y^1(x_2) & {}^1Y^2(x_2) & \dots & {}^1Y^n(x_2) & -\lambda_2 \\ 0 & 0 & 0 & 1 & 0 & 0 & 0 & 0 & \dots & 0 & 0 \\ 0 & 0 & 0 & 0 & 1 & 0 & 0 & 0 & \dots & 0 & 0 \\ 0 & 0 & 0 & 0 & 0 & 1 & 0 & 0 & \dots & 0 & 0 \\ 0 & 0 & 0 & 0 & 0 & 0 & 0 & 0 & \dots & 0 & 1 \end{bmatrix} \quad (8.129)$$

8.7 Transfer Matrix of a Fixed Hinge Connected to a Beam

There are three kinds of fixed hinges connected to a beam moving in a plane: (1) both the outboard and inboard bodies are flexible, (2) the outboard body is flexible and the inboard body is rigid, and (3) the outboard body is rigid and the inboard body is flexible.

8.7.1 Transfer Matrix of a Fixed Hinge whose Inboard and Outboard Bodies are Beams Moving in a Plane

For a fixed hinge whose inboard and outboard bodies are Euler–Bernoulli beams moving in a plane, its position coordinates, internal forces and internal moments are equal at the input and output ends. The relation between θ of the output end and q^k ($k = 1, 2, \dots, n$) of the state vectors of input end needs to be derived.

For a fixed hinge whose inboard and outboard bodies are beams moving in a plane, the relation of orientation angles at the input and output ends is

$$\theta_O = \theta_I + \frac{\partial u_2(l_2, t)}{\partial x_2} \Big|_I = \theta_I + \sum_{k=1}^n \frac{\partial Y_I^k(l_2)}{\partial x_2} q_I^k(t_i) \quad (8.130)$$

where θ_I and θ_O are the orientation angles of the fixed hinge at the input and output ends, respectively. $\partial u_2(l_2, t)/\partial x_2|_I$ is the rotation angle caused by the deformation of inboard beam, Y_I^k and q_I^k are the mode shape function and generalized coordinates that describe the deformation of inboard beam, and the superscript n is the highest order of the modes. If the inboard body is rigid, then $\partial u_2(l_2, t)/\partial x_2|_I = 0$.

Similar to section 8.6.2, the transverse deformation u of the beam can be expressed by modal superposition. Substituting it into the vibration equation of the outboard Euler–Bernoulli beam, integrating along axial direction and linearizing, we obtain

$$\begin{aligned} & \sum_{k=1}^n \left({}^4s_{k,k'} EI - {}^2s_{k,k'} \rho I A + \bar{m} s_{k,k'} A - \bar{m} s_{k,k'} \dot{\theta}_{O,t_{i-1}}^2 \right) q_O^k(t_i) \\ &= \bar{m} \bar{c} s_k^0 A x_{O_2}(t_i) - \bar{m} \bar{s} s_k^0 A y_{O_2}(t_i) - \bar{m} \left(s_{k'}^1 A - 2C \sum_{k=1}^n s_{k,k'} q_{t_{i-1}}^k \dot{\theta}_{O,t_{i-1}} \right) \theta_O(t_i) \\ &+ \int_0^l Y_O^{k'}(x_2) f(x_2, t) dx_2 - \int_0^l Y_O^{k'}(x_2) \frac{\partial}{\partial x_2} m'(x_2, t) dx_2 - \bar{m} \left\{ \sum_{k=1}^n s_{k,k'} B_{q^k} \right. \\ &- \sum_{k=1}^n s_{k,k'} \left(2q_{t_{i-1}}^k \dot{\theta}_{O,t_{i-1}} D_{\theta_O} - 2q^k(t_{i-1}) \dot{\theta}_{O,t_{i-1}}^2 \right) + s_{k'}^1 B_{\theta_O} + \bar{s} s_k^0 B_{y_{O_2}} - \bar{c} s_k^0 B_{x_{O_2}} \Big\} \\ &+ \rho I \sum_{k=1}^n {}^2s_{k,k'} B_{q^k} \quad (k' = 1, 2, \dots, n) \end{aligned} \quad (8.131)$$

where θ_O is the orientation angle of the fixed hinge at the output end, that is, the rotation angle of the body-fixed coordinate system of its outboard beam. $Y_O^{k'}$ and q_O^k are the mode shape function and generalized coordinates describing the deformation of the outboard beam. The meanings of the other elements are the same as in Equation (8.116).

Substituting Equation (8.130) into Equation (8.131) gives

$$\begin{aligned} & \sum_{k=1}^n \left({}^4s_{k,k'} EI - {}^2s_{k,k'} \rho I A + \bar{m} s_{k,k'} A - \bar{m} s_{k,k'} \dot{\theta}_{O,t_{i-1}}^2 \right) q_O^k(t_i) \\ &= \bar{m} \bar{c} s_k^0 A x_{O_2}(t_i) - \bar{m} \bar{s} s_k^0 A y_{O_2}(t_i) - \bar{m} \left(s_{k'}^1 A - 2C \sum_{k=1}^n s_{k,k'} q_{t_{i-1}}^k \dot{\theta}_{O,t_{i-1}} \right) \theta_I(t_i) \\ &- \sum_{j=1}^n \bar{m} \left(s_{k'}^1 A - 2C \sum_{k=1}^{n_O} s_{k,k'} q_{t_{i-1}}^k \dot{\theta}_{O,t_{i-1}} \right) \frac{\partial Y_I^j(l_2)}{\partial x_2} q_I^j(t_i) + \int_0^l Y_O^{k'}(x_2) f(x_2, t) dx_2 \\ &- \int_0^l Y_O^{k'}(x_2) \frac{\partial}{\partial x_2} m'(x_2, t) dx_2 - \bar{m} \left\{ \sum_{k=1}^n s_{k,k'} B_{q^k} - \sum_{k=1}^n s_{k,k'} \left(2q_{t_{i-1}}^k \dot{\theta}_{O,t_{i-1}} D_{\theta_O} - 2q^k(t_{i-1}) \dot{\theta}_{O,t_{i-1}}^2 \right) \right. \\ &+ s_{k'}^1 B_{\theta_O} + \bar{s} s_k^0 B_{y_{O_2}} - \bar{c} s_k^0 B_{x_{O_2}} \Big\} + \rho I \sum_{k=1}^n {}^2s_{k,k'} B_{q^k} \quad (k' = 1, 2, \dots, n) \end{aligned} \quad (8.132)$$

Let

$$\begin{aligned}
 \mathbf{M} &= \begin{bmatrix} m_{11} & m_{12} & \cdots & m_{1n} \\ m_{21} & m_{22} & \cdots & m_{2n} \\ \vdots & \vdots & \ddots & \vdots \\ m_{n1} & m_{n2} & \cdots & m_{nn} \end{bmatrix}, \quad \mathbf{N}_1 = \begin{bmatrix} n_{11} & n_{12} & n_{13} \\ n_{21} & n_{22} & n_{23} \\ \vdots & \vdots & \vdots \\ n_{n1} & n_{n2} & n_{n3} \end{bmatrix}, \quad \mathbf{N}_2 = \begin{bmatrix} n_{14} & n_{15} & \cdots & n_{1(n+3)} \\ n_{24} & n_{25} & \cdots & n_{2(n+3)} \\ \vdots & \vdots & \ddots & \vdots \\ n_{n4} & n_{n5} & \cdots & n_{n(n+3)} \end{bmatrix} \\
 \mathbf{N}_3 &= [n_{1(n+4)} \quad n_{2(n+4)} \quad \cdots \quad n_{n(n+4)}]^T \\
 m_{k'k} &= {}^4s_{k,k'}EI - {}^2s_{k,k'}\rho IA + \bar{m}s_{k,k'}A - \bar{m}s_{k,k'}\dot{\theta}_{O,t_{i-1}}^2 \\
 n_{k'1} &= \bar{m}\bar{c}s_{k'}^0A, n_{k'2} = -\bar{m}\bar{s}s_{k'}^0A, n_{k'3} = -\bar{m}\left(s_{k'}^1A - 2C\sum_{k=1}^n s_{k,k'}q_{t_{i-1}}^k\dot{\theta}_{O,t_{i-1}}\right) \\
 n_{k'(j+3)} &= -\bar{m}\left(s_{k'}^1A - 2C\sum_{k=1}^{n_O} s_{k,k'}q_{t_{i-1}}^k\dot{\theta}_{O,t_{i-1}}\right)\frac{\partial Y_I^j(l_2)}{\partial x_2} \\
 n_{k'(n_I+3+1)} &= \int_0^l Y^{k'}(x_2)f(x_2,t)dx_2 - \int_0^l Y^{k'}(x_2)\frac{\partial}{\partial x_2}m'(x_2,t)dx_2 + \rho I\sum_{k=1}^n {}^2s_{k,k'}B_{q^k} \\
 &\quad - \bar{m}\left\{\sum_{k=1}^n s_{k,k'}B_{q^k} - \sum_{k=1}^n s_{k,k'}\left(2q_{t_{i-1}}^k\dot{\theta}_{O,t_{i-1}}D_{\theta_O} - 2q^k(t_{i-1})\dot{\theta}_{O,t_{i-1}}^2\right) + s_{k'}^1B_{\theta_O}\right. \\
 &\quad \left.+ \bar{s}s_{k'}^0B_{y_{O_2}} - \bar{c}s_{k'}^0B_{x_{O_2}}\right\} \quad (k,k',j=1,2,\dots,n)
 \end{aligned}$$

then

$$[q^1, q^2, \dots, q^n]^T_O = \mathbf{M}^{-1}\mathbf{N}_1[x, y, \theta]^T + \mathbf{M}^{-1}\mathbf{N}_2[q^1, q^2, \dots, q^n]^T_I + \mathbf{M}^{-1}\mathbf{N}_3 \quad (8.133)$$

The transfer equation of the fixed hinge whose inboard and outboard bodies are beams moving in a plane is denoted as

$$\mathbf{z}_O = \mathbf{U}\mathbf{z}_I \quad (8.134)$$

The state vectors are

$$\mathbf{z}_I = [x, y, \theta, m, q_x, q_y, q^1, q^2, \dots, q^n, 1]^T \text{ and } \mathbf{z}_O = [x, y, \theta, m, q_x, q_y, q^1, q^2, \dots, q^n, 1]^T$$

The transfer matrix is

$$\mathbf{U} = \begin{bmatrix} \mathbf{I}_3 & \mathbf{O}_{3 \times 3} & \mathbf{U}_{13} & \mathbf{O}_{3 \times 1} \\ \mathbf{O}_{3 \times 3} & \mathbf{I}_3 & \mathbf{O}_{3 \times n} & \mathbf{O}_{3 \times 1} \\ \mathbf{M}^{-1}\mathbf{N}_1 & \mathbf{O}_{n \times 3} & \mathbf{M}^{-1}\mathbf{N}_2 & \mathbf{M}^{-1}\mathbf{N}_3 \\ \mathbf{O}_{1 \times 3} & \mathbf{O}_{1 \times 3} & \mathbf{O}_{1 \times n} & 1 \end{bmatrix} \quad (8.135)$$

where

$$\mathbf{U}_{13} = \begin{bmatrix} 0 & \cdots & 0 \\ 0 & \cdots & 0 \\ \partial Y_I^1(l_2)/\partial x_2 & \cdots & \partial Y_I^n(l_2)/\partial x_2 \end{bmatrix}$$

8.7.2 Transfer Matrix of a Fixed Hinge whose Inboard Body is a Rigid Body and whose Outboard Body is a Beam

For a beam with transverse vibration fixed on the rigid body, the position coordinates, orientation angles, internal forces and internal moments of the fixed hinge are equal at its input and output ends. Similar to section 8.5, but eliminating columns corresponding to generalized coordinates which describe the deformation of the inboard beam in Equation (8.135), the transfer equation of the fixed hinge whose inboard body is a rigid body and whose outboard body is a beam is

$$\mathbf{z}_O = \mathbf{U} \mathbf{z}_I \quad (8.136)$$

The state vectors are

$$\mathbf{z}_I = [x, y, \theta, m, q_x, q_y, 1]^T \text{ and } \mathbf{z}_O = [x, y, \theta, m, q_x, q_y, q^1, q^2, \dots, q^n, 1]^T$$

The transfer matrix is

$$\mathbf{U} = \begin{bmatrix} \mathbf{I}_3 & \mathbf{O}_{3 \times 3} & \mathbf{O}_{3 \times 1} \\ \mathbf{O}_{3 \times 3} & \mathbf{I}_3 & \mathbf{O}_{3 \times 1} \\ \mathbf{M}^{-1} \mathbf{N}_1 & \mathbf{O}_{3 \times 3} & \mathbf{M}^{-1} \mathbf{N}_3 \\ \mathbf{O}_{1 \times 3} & \mathbf{O}_{1 \times 3} & 1 \end{bmatrix} \quad (8.137)$$

where the meaning of all elements is the same as in Equation (8.135).

8.7.3 Transfer Matrix of a Fixed Hinge whose Inboard Body is a Beam and whose Outboard Body is a Rigid Body

The derivation of the transfer matrix of a fixed hinge whose inboard body is a beam and whose outboard body is rigid is the same as in section 8.5, except some rows in Equation (8.135) corresponding to the generalized coordinates which describe the deformation of the outboard beam need to be eliminated.

The transfer equation and transfer matrix of the fixed hinge whose inboard body is beam and whose outboard body is rigid can be obtained as

$$\mathbf{z}_O = \mathbf{U} \mathbf{z}_I \quad (8.138)$$

The state vectors are

$$\mathbf{z}_I = [x, y, \theta, m, q_x, q_y, q^1, q^2, \dots, q^n, 1]^T \text{ and } \mathbf{z}_O = [x, y, \theta, m, q_x, q_y, 1]^T$$

The transfer matrix is

$$\mathbf{U} = \begin{bmatrix} \mathbf{I}_3 & \mathbf{O}_{3 \times 3} & \mathbf{U}_{13} & \mathbf{O}_{3 \times 1} \\ \mathbf{O}_{3 \times 3} & \mathbf{I}_3 & \mathbf{O}_{3 \times n} & \mathbf{O}_{3 \times 1} \\ \mathbf{O}_{1 \times 3} & \mathbf{O}_{1 \times 3} & \mathbf{O}_{1 \times n} & 1 \end{bmatrix} \quad (8.139)$$

where the meaning of all elements is the same as in Equation (8.135).

8.8 Dynamics Equation of a Spatial Large Motion Beam

The Euler–Bernoulli beam theory assumptions are:

- 1) The cross-section of the beam which is perpendicular to the central line before deformation doesn't distort after the deformation (rigid cross-section hypothesis).
- 2) The cross-section after the deformation is still perpendicular to the axis after the deformation. The distributed load acting on the beam includes the distributed external force \mathbf{f} , the distribution inertia force \mathbf{f}' and the distributed moment $\bar{\mathbf{m}}$.

For the spatial beam shown in Figure 8.4, based on the equilibrium condition of forces

$$\mathbf{q} + \mathbf{f} dx_2 = \mathbf{q} + \frac{\partial \mathbf{q}}{\partial x_2} dx_2 + \mathbf{f}' dx_2 \quad (8.140)$$

Based on the equilibrium condition of moment acting on the output end of the element, we have

$$\mathbf{m} + d\mathbf{x}_2 \times \mathbf{q} + \frac{d\mathbf{x}_2}{2} \times \mathbf{f} dx_2 = \bar{\mathbf{m}} dx_2 + \mathbf{m} + \frac{\partial \mathbf{m}}{\partial x_2} dx_2 + \frac{d\mathbf{x}_2}{2} \times \mathbf{f}' dx_2 \quad (8.141)$$

Neglecting the second-order small quantities and according to Equations (8.140) and (8.141), we obtain

$$\frac{\partial \mathbf{q}}{\partial x_2} = \mathbf{f} - \mathbf{f}' \quad (8.142)$$

$$\frac{d\mathbf{x}_2}{|d\mathbf{z}_2|} \times \mathbf{q} = \frac{\partial \mathbf{m}}{\partial x_2} + \bar{\mathbf{m}} \quad (8.143)$$

The geometric relationship of the beam element is

$$\begin{bmatrix} \alpha_{2,y} \\ \alpha_{2,z} \end{bmatrix} = \frac{\partial}{\partial x_2} \begin{bmatrix} -w \\ v \end{bmatrix} \quad (8.144)$$

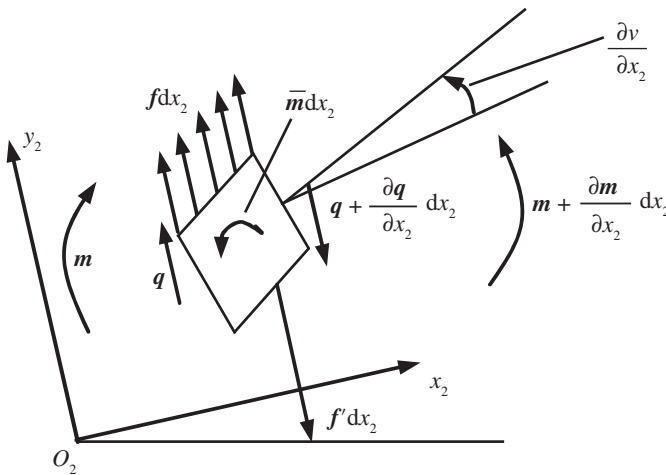


Figure 8.4 Model of a beam element.

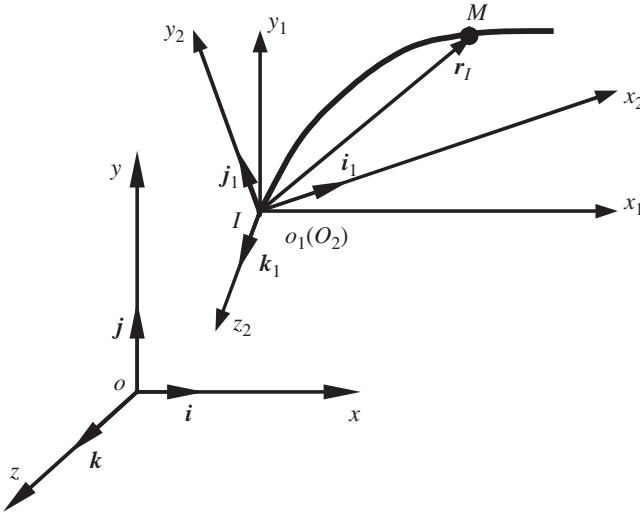


Figure 8.5 Body-fixed coordinate system of a beam.

where v and w are the components of deformation of an arbitrary point on the central line of the beam along axes y_2 and z_2 , respectively. $\alpha_{2,y}$ and $\alpha_{2,z}$ are components of the rotation angle caused by beam deformation along axes y_2 and z_2 , respectively.

According to material mechanics,

$$\begin{bmatrix} m_{2,y} \\ m_{2,z} \end{bmatrix} = EI \frac{\partial}{\partial x_2} \begin{bmatrix} \alpha_{2,y} \\ \alpha_{2,z} \end{bmatrix} = EI \frac{\partial^2}{\partial x_2^2} \begin{bmatrix} -w \\ v \end{bmatrix} \quad (8.145)$$

As shown in Figure 8.5, $oxyz$ is the inertia coordinate system and $O_2x_2y_2z_2$ is the body-fixed coordinate system of the beam, whose origin is fixed on one end of the beam. The coordinate axis O_2x_2 and the direction of the axis of the undeformed beam coincide. The motion of the beam can be decomposed into rigid motion and deformation motion. Here, the undeformed position is the position when the beam only undergoes rigid motion without deformation.

The coordinates of an arbitrary point of the beam in the inertia coordinate system $oxyz$ are

$$\begin{bmatrix} x \\ y \\ z \end{bmatrix} = \begin{bmatrix} x \\ y \\ z \end{bmatrix}_I + \mathbf{A} \begin{bmatrix} x_2 \\ v \\ w \end{bmatrix} \quad (8.146)$$

From Equation (8.146), the absolute velocity and absolute acceleration of this point are

$$\begin{bmatrix} \dot{x} \\ \dot{y} \\ \dot{z} \end{bmatrix} = \begin{bmatrix} \dot{x} \\ \dot{y} \\ \dot{z} \end{bmatrix}_I + \dot{\mathbf{A}} \begin{bmatrix} x_2 \\ v \\ w \end{bmatrix} + \mathbf{A} \begin{bmatrix} 0 \\ \dot{v} \\ \dot{w} \end{bmatrix} \quad (8.147)$$

$$\begin{bmatrix} \ddot{x} \\ \ddot{y} \\ \ddot{z} \end{bmatrix} = \begin{bmatrix} \ddot{x} \\ \ddot{y} \\ \ddot{z} \end{bmatrix}_I + \ddot{\mathbf{A}} \begin{bmatrix} x_2 \\ v \\ w \end{bmatrix} + 2\dot{\mathbf{A}} \begin{bmatrix} 0 \\ \dot{v} \\ \dot{w} \end{bmatrix} + \mathbf{A} \begin{bmatrix} 0 \\ \ddot{v} \\ \ddot{w} \end{bmatrix} \quad (8.148)$$

Projecting Equation (8.142) to the inertia coordinate system leads to

$$\frac{\partial}{\partial x_2} \begin{bmatrix} q_x \\ q_y \\ q_z \end{bmatrix} = \begin{bmatrix} f_x \\ f_y \\ f_z \end{bmatrix} - m(x_2) \begin{bmatrix} \ddot{x} \\ \ddot{y} \\ \ddot{z} \end{bmatrix} \quad (8.149)$$

Substituting Equation (8.145) into Equation (8.143), we obtain

$$q_{2,z} = \frac{\partial}{\partial x_2} \left(EI_{2,y} \frac{\partial^2}{\partial x_2^2} w \right) - \bar{m}_{2,y} \quad (8.150)$$

$$q_{2,y} = \frac{\partial}{\partial x_2} \left(EI_{2,z} \frac{\partial^2}{\partial x_2^2} v \right) + \bar{m}_{2,z} \quad (8.151)$$

Substituting Equations (8.150) and (8.151) into Equation (8.142), the transverse vibration equations of the beam, yields

$$\frac{\partial}{\partial x_2} \left[\frac{\partial}{\partial x_2} \left(EI_{2,z} \frac{\partial^2}{\partial x_2^2} v \right) + \bar{m}_{2,z} \right] = f_{2,y} - m(x_2) [0 \ 1 \ 0] \mathbf{A}^T \begin{bmatrix} \ddot{x} \\ \ddot{y} \\ \ddot{z} \end{bmatrix} \quad (8.152)$$

$$\frac{\partial}{\partial x_2} \left[\frac{\partial}{\partial x_2} \left(EI_{2,y} \frac{\partial^2}{\partial x_2^2} w \right) - \bar{m}_{2,y} \right] = f_{2,z} - m(x_2) [0 \ 0 \ 1] \mathbf{A}^T \begin{bmatrix} \ddot{x} \\ \ddot{y} \\ \ddot{z} \end{bmatrix} \quad (8.153)$$

The theorem of the absolute angular momentum of a particle system with respect to the moving point is

$$\frac{d\mathbf{G}_I}{dt} + \mathbf{r}_{IC} \times m\mathbf{a}_I = \sum_j \mathbf{r}_{Ij} \times \mathbf{f}_j \quad (8.154)$$

where

$$\mathbf{G}_I = \int_0^l \mathbf{r}_I(x_2) \times m(x_2) \mathbf{v}_I(x_2) dx_2 \quad (8.155)$$

$$\mathbf{r}_I(x_2) = [\mathbf{i}_1 \ \mathbf{j}_1 \ \mathbf{k}_1] \begin{bmatrix} x_2 \\ v \\ w \end{bmatrix} = [\mathbf{i} \ \mathbf{j} \ \mathbf{k}] \mathbf{A} \begin{bmatrix} x_2 \\ v \\ w \end{bmatrix} \quad (8.156)$$

$$\begin{aligned} \mathbf{v}_I(x_2) &= \frac{d}{dt} \mathbf{r}_{IM} = [\mathbf{i} \ \mathbf{j} \ \mathbf{k}] \left(\dot{\mathbf{A}} \begin{bmatrix} x_2 \\ v \\ w \end{bmatrix} + \mathbf{A} \begin{bmatrix} 0 \\ \dot{v} \\ \dot{w} \end{bmatrix} \right) = [\mathbf{i} \ \mathbf{j} \ \mathbf{k}] \mathbf{A} \left(\tilde{\boldsymbol{\omega}} \begin{bmatrix} x_2 \\ v \\ w \end{bmatrix} + \begin{bmatrix} 0 \\ \dot{v} \\ \dot{w} \end{bmatrix} \right) \\ &= [\mathbf{i}_1 \ \mathbf{j}_1 \ \mathbf{k}_1] \left(\tilde{\boldsymbol{\omega}} \begin{bmatrix} x_2 \\ v \\ w \end{bmatrix} + \begin{bmatrix} 0 \\ \dot{v} \\ \dot{w} \end{bmatrix} \right) \end{aligned} \quad (8.157)$$

$$\mathbf{r}_I(x_2) \times \mathbf{v}_I(x_2) = [\mathbf{i}_1 \ \mathbf{j}_1 \ \mathbf{k}_1] \tilde{\mathbf{r}}_I \left(\tilde{\boldsymbol{\omega}} \begin{bmatrix} x_2 \\ v \\ w \end{bmatrix} + \begin{bmatrix} 0 \\ \dot{v} \\ \dot{w} \end{bmatrix} \right) = [\mathbf{i} \ \mathbf{j} \ \mathbf{k}] \mathbf{A} \left[\tilde{\mathbf{r}}_I \left(\tilde{\boldsymbol{\omega}} \begin{bmatrix} x_2 \\ v \\ w \end{bmatrix} + \begin{bmatrix} 0 \\ \dot{v} \\ \dot{w} \end{bmatrix} \right) \right] \quad (8.158)$$

\mathbf{G}_I is the absolute moment of momentum of a particle system with respect to the input end I , $(\mathbf{i}, \mathbf{j}, \mathbf{k})$ are three base vectors of the inertia coordinate system and $(\mathbf{i}_1, \mathbf{j}_1, \mathbf{k}_1)$ are three base vectors of the body-fixed coordinate system.

Substituting Equation (8.158) into Equation (8.155), in the inertia coordinate system, gives

$$\mathbf{G}_I = [\mathbf{i} \ \mathbf{j} \ \mathbf{k}] \int_0^l m(x_2) \left\{ \mathbf{A} \tilde{\mathbf{r}}_I \tilde{\boldsymbol{\omega}} \begin{bmatrix} x_2 \\ v \\ w \end{bmatrix} + \mathbf{A} \tilde{\mathbf{r}}_I \begin{bmatrix} 0 \\ \dot{v} \\ \dot{w} \end{bmatrix} \right\} dx_2 = [\mathbf{i} \ \mathbf{j} \ \mathbf{k}] \mathbf{A} \int_0^l m(x_2) \left\{ -\tilde{\mathbf{r}}_I \tilde{\mathbf{r}}_I \boldsymbol{\omega} + \tilde{\mathbf{r}}_I \begin{bmatrix} 0 \\ \dot{v} \\ \dot{w} \end{bmatrix} \right\} dx_2 \quad (8.159)$$

therefore

$$\begin{aligned} \frac{d\mathbf{G}_I}{dt} = & [\mathbf{i} \ \mathbf{j} \ \mathbf{k}] \mathbf{A} \left\{ \tilde{\boldsymbol{\omega}} \int_0^l m(x_2) \mathbf{J}_1 \boldsymbol{\omega} dx_2 + \tilde{\boldsymbol{\omega}} \int_0^l m(x_2) \tilde{\mathbf{r}}_I \begin{bmatrix} 0 \\ \dot{v} \\ \dot{w} \end{bmatrix} dx_2 + \frac{d}{dt} \int_0^l m(x_2) \mathbf{J}_1 \boldsymbol{\omega} dx_2 \right. \\ & \left. + \frac{d}{dt} \int_0^l m(x_2) \tilde{\mathbf{r}}_I \begin{bmatrix} 0 \\ \dot{v} \\ \dot{w} \end{bmatrix} dx_2 \right\} \end{aligned} \quad (8.160)$$

where

$$\mathbf{J}_1 = -\tilde{\mathbf{r}}_I \tilde{\mathbf{r}}_I = \begin{bmatrix} v^2 + w^2 & -x_2 v & -x_2 w \\ -x_2 v & w^2 + x_2^2 & -vw \\ -x_2 w & -vw & x_2^2 + v^2 \end{bmatrix} \quad (8.161)$$

In the inertia coordinate system, $\mathbf{r}_{IC} \times m\mathbf{a}_I$ can be expressed as

$$\mathbf{r}_{IC} \times m\mathbf{a}_I = m[\mathbf{i} \ \mathbf{j} \ \mathbf{k}] \tilde{\mathbf{r}}_{IC} \begin{bmatrix} \ddot{x}_I \\ \ddot{y}_I \\ \ddot{z}_I \end{bmatrix} \quad (8.162)$$

where

$$\tilde{\mathbf{r}}_{IC} = \begin{bmatrix} 0 & -z_{IC} & y_{IC} \\ z_{IC} & 0 & -x_{IC} \\ -y_{IC} & x_{IC} & 0 \end{bmatrix} \quad (8.163)$$

Substituting Equations (8.160) and (8.162) into Equation (8.154), the rotation equations of the beam in the inertia coordinate system can be found:

$$\begin{aligned}
 A \left\{ \tilde{\omega} \int_0^l m(x_2) J_1 \omega dx_2 + \tilde{\omega} \int_0^l m(x_2) \tilde{r}_I \begin{bmatrix} 0 \\ \dot{v} \\ \dot{w} \end{bmatrix} dx_2 + \frac{d}{dt} \int_0^l m(x_2) J_1 \omega dx_2 + \frac{d}{dt} \int_0^l m(x_2) \tilde{r}_I \begin{bmatrix} 0 \\ \dot{v} \\ \dot{w} \end{bmatrix} dx_2 \right\} \\
 + m \tilde{r}_{IC} \begin{bmatrix} \ddot{x}_I \\ \ddot{y}_I \\ \ddot{z}_I \end{bmatrix} = A \sum_j \tilde{r}_{Ij} \begin{bmatrix} f_{2,x} \\ f_{2,y} \\ f_{2,z} \end{bmatrix}_j
 \end{aligned} \quad (8.164)$$

Using the transformation matrix, the rotation equations of the beam in the body-fixed coordinate system can be obtained:

$$\begin{aligned}
 \tilde{\omega} \int_0^l m(x_2) J_1 \omega dx_2 + \tilde{\omega} \int_0^l m(x_2) \tilde{r}_I \begin{bmatrix} 0 \\ \dot{v} \\ \dot{w} \end{bmatrix} dx_2 + \frac{d}{dt} \int_0^l m(x_2) J_1 \omega dx_2 + \frac{d}{dt} \int_0^l m(x_2) \tilde{r}_I \begin{bmatrix} 0 \\ \dot{v} \\ \dot{w} \end{bmatrix} dx_2 \\
 + m A^T \tilde{r}_{IC} \begin{bmatrix} \ddot{x}_I \\ \ddot{y}_I \\ \ddot{z}_I \end{bmatrix} = \sum_j \tilde{r}_{Ij} \begin{bmatrix} f_{2,x} \\ f_{2,y} \\ f_{2,z} \end{bmatrix}_j
 \end{aligned} \quad (8.165)$$

8.9 Transfer Matrix of a Spatial Large Motion Beam

Consider the transverse vibration of a Euler–Bernoulli beam with large spatial motion. The state vector is defined as

$$\mathbf{z} = [x, y, z, \theta_x, \theta_y, \theta_z, m_x, m_y, m_z, q_x, q_y, q_z, q^1, q^2, \dots, q^n, 1]^T \quad (8.166)$$

For the uniform beam with uniform cross-section $m(x_2) = \bar{m}$, the length of the beam is l and the mass is $m = \bar{m}l$.

Let

$$\mathbf{r}_{iO_2} = A[x_2, v, w]^T, \mathbf{r}_i = \mathbf{r}_I + \mathbf{r}_{iO_2} \quad (8.167)$$

and combine Equations (8.27) and (8.28) as

$$\ddot{\mathbf{r}}_{iO_2}(t_i) = A \mathbf{r}_{iO_2}(t_i) + \mathbf{B}_{r_{iO_2}} \quad (8.168)$$

$$[\ddot{x}, \ddot{y}, \ddot{z}]_I^T = \ddot{\mathbf{r}}_I = A \mathbf{r}_I(t_i) + \mathbf{B}_{r_I} \quad (8.169)$$

In the inertia coordinate system, considering Equation (8.146) and integrating Equation (8.149) in the limit $[0, l]$, we obtain

$$\begin{aligned}
 \begin{bmatrix} q_x \\ q_y \\ q_z \end{bmatrix}_O &= \begin{bmatrix} q_x \\ q_y \\ q_z \end{bmatrix}_I + \int_0^l \begin{bmatrix} f_x \\ f_y \\ f_z \end{bmatrix} dx_2 - m \begin{bmatrix} \ddot{x} \\ \ddot{y} \\ \ddot{z} \end{bmatrix}_I - \int_0^l \bar{m} \left(A(t_i) \begin{bmatrix} x_2 \\ v \\ w \end{bmatrix} \right)_{tt} dx_2 \\
 &= \begin{bmatrix} q_x \\ q_y \\ q_z \end{bmatrix}_I + \int_0^l \begin{bmatrix} f_x \\ f_y \\ f_z \end{bmatrix} dx_2 - mA \begin{bmatrix} x(t_i) \\ y(t_i) \\ z(t_i) \end{bmatrix}_I - mB_{r_I} - \bar{m}A \int_0^l A(t_i) \begin{bmatrix} x_2 \\ v \\ w \end{bmatrix} dx_2 - \bar{m} \int_0^l B_{r_{iO_2}} dx_2
 \end{aligned} \tag{8.170}$$

Let

$$v(x_2, t) = \sum_{k=1}^n Y^k(x_2) q^k(t), \quad w(x_2, t) = \sum_{k=1}^n Z^k(x_2) q^k(t). \tag{8.171}$$

Then

$$\begin{aligned}
 \int_0^l A(t_i) \begin{bmatrix} x_2 \\ v \\ w \end{bmatrix} dx_2 &= \left[\left(A\tilde{T}_1 \int_0^l \begin{bmatrix} x_2 \\ v \\ w \end{bmatrix} dx_2 \right)_{t_{i-1}} \left(A\tilde{T}_2 \int_0^l \begin{bmatrix} x_2 \\ v \\ w \end{bmatrix} dx_2 \right)_{t_{i-1}} \left(A\tilde{T}_3 \int_0^l \begin{bmatrix} x_2 \\ v \\ w \end{bmatrix} dx_2 \right)_{t_{i-1}} \right] \begin{bmatrix} \theta_x \\ \theta_y \\ \theta_z \end{bmatrix}_{t_i} \\
 &+ \Phi(t_{i-1}) \int_0^l \begin{bmatrix} x_2 \\ v \\ w \end{bmatrix}_{t_{i-1}} dx_2 + \sum_{k=1}^n \left(\int_0^l A(t_{i-1}) \begin{bmatrix} 0 \\ Y^k(x_2) \\ Z^k(x_2) \end{bmatrix} dx_2 \right) q^k(t_i) - A(t_{i-1}) \int_0^l \begin{bmatrix} 0 \\ v \\ w \end{bmatrix}_{t_{i-1}} dx_2
 \end{aligned} \tag{8.172}$$

Substituting Equations (8.172) and (8.171) into Equation (8.170) and rearranging it yields

$$\begin{bmatrix} q_x \\ q_y \\ q_z \end{bmatrix}_O = U_{41} \begin{bmatrix} x \\ y \\ z \end{bmatrix}_I + U_{42} \begin{bmatrix} \theta_x \\ \theta_y \\ \theta_z \end{bmatrix} + \begin{bmatrix} q_x \\ q_y \\ q_z \end{bmatrix}_I + U_{45} \begin{bmatrix} q_1 \\ q_2 \\ \vdots \\ q_n \end{bmatrix} + U_{46} \tag{8.173}$$

where

$$\begin{aligned}
 U_{41} &= -mAI \\
 U_{42} &= -\bar{m}AA(t_{i-1}) \left[\tilde{T}_1 \int_0^l \begin{bmatrix} x_2 \\ v \\ w \end{bmatrix} dx_2 \quad \tilde{T}_2 \int_0^l \begin{bmatrix} x_2 \\ v \\ w \end{bmatrix} dx_2 \quad \tilde{T}_3 \int_0^l \begin{bmatrix} x_2 \\ v \\ w \end{bmatrix} dx_2 \right]_{t_{i-1}}
 \end{aligned}$$

$$\begin{aligned}
\mathbf{U}_{45} &= -\bar{m}\mathbf{A}\mathbf{A}(t_{i-1}) \left[\int_0^l \begin{bmatrix} 0 \\ Y^1(x_2) \\ Z^1(x_2) \end{bmatrix} dx_2 \int_0^l \begin{bmatrix} 0 \\ Y^2(x_2) \\ Z^2(x_2) \end{bmatrix} dx_2 \cdots \int_0^l \begin{bmatrix} 0 \\ Y^n(x_2) \\ Z^n(x_2) \end{bmatrix} dx_2 \right] \\
\mathbf{U}_{46} &= \int_0^l \begin{bmatrix} f_x \\ f_y \\ f_z \end{bmatrix} dx_2 - \mathbf{m}\mathbf{B}\mathbf{r}_1 - \bar{m}\mathbf{A}\Phi(t_{i-1}) \int_0^l \begin{bmatrix} x_2 \\ v \\ w \end{bmatrix}_{t_{i-1}} dx_2 + \bar{m}\mathbf{A}\mathbf{A}(t_{i-1}) \int_0^l \begin{bmatrix} 0 \\ v \\ w \end{bmatrix}_{t_{i-1}} dx_2 - \bar{m} \int_0^l \mathbf{B}_{r_i, O_2} dx_2
\end{aligned} \tag{8.174}$$

Linearize the rotation equation of the beam in the inertia coordinate system and let

$$\mathbf{h}_2 = \int_0^l \bar{m}\mathbf{J}_1 \omega dx_2, \quad \mathbf{h}_3 = \int_0^l \bar{m}\tilde{\mathbf{r}}_I \begin{bmatrix} 0 \\ \dot{v} \\ \dot{w} \end{bmatrix} dx_2, \quad \mathbf{h}_4 = m\tilde{\mathbf{r}}_{IC}\ddot{\mathbf{r}}_1 \tag{8.175}$$

From Equation (8.154), if the beam is only excited by the distributed external force \mathbf{f} and the distributed external moment $\bar{\mathbf{m}}$, the rotation equation of the beam in the inertia coordinate system can be written as

$$\begin{aligned}
\frac{d\mathbf{G}_I}{dt} + \mathbf{h}_4 &= \frac{d}{dt} [[i \ j \ k] \mathbf{A}(\mathbf{h}_2 + \mathbf{h}_3)] + \mathbf{h}_4 \\
&= \mathbf{A} \int_0^l \begin{bmatrix} \bar{m}_{2,x} \\ \bar{m}_{2,y} \\ \bar{m}_{2,z} \end{bmatrix} dx_2 + \mathbf{A} \int_0^l \sum_j \tilde{\mathbf{r}}_{Ij} \begin{bmatrix} f_{2,x} \\ f_{2,y} \\ f_{2,z} \end{bmatrix}_j dx_2 - \mathbf{A}\tilde{\mathbf{r}}_{IO}(t_i) \mathbf{A}^T \begin{bmatrix} q_x(t_i) \\ q_y(t_i) \\ q_z(t_i) \end{bmatrix}_O - \begin{bmatrix} m_x(t_i) \\ m_y(t_i) \\ m_z(t_i) \end{bmatrix}_I + \begin{bmatrix} m_x(t_i) \\ m_y(t_i) \\ m_z(t_i) \end{bmatrix}_O
\end{aligned} \tag{8.176}$$

$$\begin{aligned}
\begin{bmatrix} m_x(t_i) \\ m_y(t_i) \\ m_z(t_i) \end{bmatrix}_O &= \frac{d}{dt} [[i \ j \ k] \mathbf{A}(\mathbf{h}_2 + \mathbf{h}_3)] + \mathbf{h}_4 - \mathbf{A} \int_0^l \begin{bmatrix} \bar{m}_{2,x} \\ \bar{m}_{2,y} \\ \bar{m}_{2,z} \end{bmatrix} dx_2 \\
&\quad - \mathbf{A} \int_0^l \sum_j \tilde{\mathbf{r}}_{Ij} \begin{bmatrix} f_{2,x} \\ f_{2,y} \\ f_{2,z} \end{bmatrix}_j dx_2 + \mathbf{A}\tilde{\mathbf{r}}_{IO}(t_i) \mathbf{A}^T \begin{bmatrix} q_x(t_i) \\ q_y(t_i) \\ q_z(t_i) \end{bmatrix}_O + \begin{bmatrix} m_x(t_i) \\ m_y(t_i) \\ m_z(t_i) \end{bmatrix}_I
\end{aligned} \tag{8.177}$$

Linearizing \mathbf{h}_2 , \mathbf{h}_3 and \mathbf{h}_4 , respectively

$$\mathbf{h}_2 = \mathbf{H}_{22} [\theta_x \ \theta_y \ \theta_z]_{t_i}^T + \mathbf{H}_{25} [q^1 \ q^2 \ \cdots \ q^n]_{t_i}^T + \mathbf{H}_{26} \tag{8.178}$$

$$\mathbf{h}_3 = \mathbf{H}_{35} [q^1 \ q^2 \ \cdots \ q^n]_{t_i}^T + \mathbf{H}_{36} \tag{8.179}$$

$$\mathbf{h}_4 = \mathbf{H}_{41} \begin{bmatrix} x_I \\ y_I \\ z_I \end{bmatrix}_{t_i} + \mathbf{H}_{45} \begin{bmatrix} q^1 \\ q^2 \\ \vdots \\ q^n \end{bmatrix}_{t_i} + \mathbf{H}_{46} \tag{8.180}$$

where

$$\begin{aligned}
 H_{22} &= C\bar{m} \int_0^l J_1(t_{i-1}) \bar{H} dx_2 \\
 H_{25} &= \left[\int_0^l \bar{m}(E_2 Y^1 + E_3 Z^1) dx_2 \quad \int_0^l \bar{m}(E_2 Y^2 + E_3 Z^2) dx_2 \quad \cdots \quad \int_0^l \bar{m}(E_2 Y^n + E_3 Z^n) dx_2 \right] \\
 H_{26} &= \int_0^l \bar{m} J_1(t_{i-1}) \bar{H} D_\theta dx_2 - \int_0^l \bar{m} [E_2 \nu_{t_{i-1}} + E_3 \omega_{t_{i-1}}] dx_2 \\
 H_{35} &= \left[\int_0^l \bar{m}(E_4 Y^1 + E_5 Z^1) dx_2 \quad \int_0^l \bar{m}(E_4 Y^2 + E_5 Z^2) dx_2 \quad \cdots \quad \int_0^l \bar{m}(E_4 Y^n + E_5 Z^n) dx_2 \right] \\
 H_{36} &= \int_0^l \bar{m} E_6 dx_2, \quad H_{41} = m A \tilde{r}_{IC}(t_{i-1}) \\
 H_{45} &= \left[\int_0^l E_7 \begin{bmatrix} 0 \\ Y^1 \\ Z^1 \end{bmatrix} dx_2 \quad \int_0^l E_7 \begin{bmatrix} 0 \\ Y^2 \\ Z^2 \end{bmatrix} dx_2 \quad \cdots \quad \int_0^l E_7 \begin{bmatrix} 0 \\ Y^n \\ Z^n \end{bmatrix} dx_2 \right] \\
 H_{46} &= -\frac{m \tilde{r}_I}{2} (t_{i-1}) \bar{A}(t_i) \begin{bmatrix} 1 \\ 0 \\ 0 \end{bmatrix} + m \tilde{r}_{IC}(t_{i-1}) (B_{r_I} - \ddot{r}_I(t_{i-1})) \\
 E_2 &= \begin{bmatrix} 2\nu & -x_2 & 0 \\ -x_2 & 0 & -w \\ 0 & -w & 2\nu \end{bmatrix}_{t_{i-1}}, \quad E_3 = \begin{bmatrix} 2w & 0 & -x_2 \\ 0 & 2w & -\nu \\ -x_2 & -\nu & 0 \end{bmatrix}_{t_{i-1}} \\
 E_4 &= \begin{bmatrix} \dot{w}_{t_{i-1}} - Cw_{t_{i-1}} \\ 0 \\ Cx_2 \end{bmatrix}, \quad E_5 = \begin{bmatrix} -\dot{\nu}_{t_{i-1}} + C\nu_{t_{i-1}} \\ -Cx_2 \\ 0 \end{bmatrix}, \quad E_6 = \begin{bmatrix} \nu_{t_{i-1}}(D_w - \dot{w}_{t_{i-1}}) + w_{t_{i-1}}(\dot{\nu}_{t_{i-1}} - D_\nu) \\ -x_2 D_w \\ x_2 D_\nu \end{bmatrix} \\
 E_7 &= -\frac{m \tilde{r}_I}{l} (t_{i-1}) \bar{A}(t_i) = -\frac{m}{l} \begin{bmatrix} 0 & -\ddot{z}_I & -\ddot{y}_I \\ \ddot{z}_I & 0 & -\ddot{x}_I \\ -\ddot{y}_I & \ddot{x}_I & 0 \end{bmatrix}_{t_{i-1}} \bar{A}(t_i), \quad \bar{H} = \begin{bmatrix} 1 & 0 & -\bar{s}_y \\ 0 & \bar{c}_x & \bar{s}_x \bar{c}_y \\ 0 & -\bar{s}_x & \bar{c}_x \bar{c}_y \end{bmatrix}
 \end{aligned}$$

\bar{s} and \bar{c} are determined by Equation (8.62).

Substituting Equations (8.178) to (8.180) into Equation (8.177) and rearranging yields

$$\begin{bmatrix} m_x(t_i) \\ m_y(t_i) \\ m_z(t_i) \end{bmatrix}_O = \mathbf{U}_{31} \begin{bmatrix} x_I \\ y_I \\ z_I \end{bmatrix}_{t_i} + \mathbf{U}_{32} \begin{bmatrix} \theta_x \\ \theta_y \\ \theta_z \end{bmatrix}_{t_i} + \begin{bmatrix} m_{x,I} \\ m_{y,I} \\ m_{z,I} \end{bmatrix}_{t_i} + \mathbf{U}_{34} \begin{bmatrix} q_{x,I} \\ q_{y,I} \\ q_{z,I} \end{bmatrix}_{t_i} + \mathbf{U}_{35} \begin{bmatrix} q^1 \\ q^2 \\ \vdots \\ q^n \end{bmatrix}_{t_i} + \mathbf{U}_{36} \quad (8.181)$$

where

$$\begin{aligned}
 \mathbf{U}_{31} &= \mathbf{H}_{41} + \bar{\mathbf{A}}\bar{\mathbf{r}}_{IO}\bar{\mathbf{A}}^T \mathbf{U}_{41}, \quad \mathbf{U}_{32} = \mathbf{C}\bar{\mathbf{A}}\mathbf{H}_{22} + \bar{\mathbf{A}}\bar{\mathbf{r}}_{IO}\bar{\mathbf{A}}^T \mathbf{U}_{42}, \quad \mathbf{U}_{34} = \bar{\mathbf{A}}\bar{\mathbf{r}}_{IO}\bar{\mathbf{A}}^T \\
 \mathbf{U}_{35} &= \mathbf{C}\bar{\mathbf{A}}(\mathbf{H}_{25} + \mathbf{H}_{35}) + \mathbf{H}_{45} + \bar{\mathbf{A}}\bar{\mathbf{r}}_{IO}\bar{\mathbf{A}}^T \mathbf{U}_{45} \\
 \mathbf{U}_{36} &= \mathbf{C}\bar{\mathbf{A}}(\mathbf{H}_{26} + \mathbf{H}_{36}) + \mathbf{D}_{G_I} + \mathbf{H}_{46} + \bar{\mathbf{A}}\bar{\mathbf{r}}_{IO}\bar{\mathbf{A}}^T \mathbf{U}_{46} - \bar{\mathbf{A}} \int_0^l \begin{bmatrix} \bar{m}_{2,x} \\ \bar{m}_{2,y} \\ \bar{m}_{2,z} \end{bmatrix} dx_2 - \bar{\mathbf{A}} \int_0^l \sum_j \bar{\mathbf{r}}_{lj} \begin{bmatrix} f_{2,x} \\ f_{2,y} \\ f_{2,z} \end{bmatrix} dx_2 \\
 \bar{\mathbf{A}} &= \begin{bmatrix} \bar{c}_y \bar{c}_z & \bar{s}_x \bar{s}_y \bar{c}_z - \bar{s}_z \bar{c}_x & \bar{c}_x \bar{s}_y \bar{c}_z + \bar{s}_z \bar{s}_x \\ \bar{c}_y \bar{s}_z & \bar{s}_x \bar{s}_y \bar{s}_z + \bar{c}_z \bar{c}_x & \bar{c}_x \bar{s}_y \bar{s}_z - \bar{c}_z \bar{s}_x \\ -\bar{s}_y & \bar{s}_x \bar{c}_y & \bar{c}_x \bar{c}_y \end{bmatrix}, \quad \bar{\mathbf{r}}_{IO} = \begin{bmatrix} 0 & -\bar{v}_{IO} & \bar{w}_{IO} \\ \bar{v}_{IO} & 0 & -l \\ -\bar{w}_{IO} & l & 0 \end{bmatrix}
 \end{aligned}$$

Substituting Equations (8.65) and (8.83) into Equation (8.167) and rearranging gives

$$\mathbf{r}_O = \mathbf{r}_I + \mathbf{U}_{12} \begin{bmatrix} \theta_x & \theta_y & \theta_z \end{bmatrix}_{t_i}^T + \mathbf{U}_{15} \begin{bmatrix} q^1 & q^2 & \cdots & q^n \end{bmatrix}_{t_i}^T + \mathbf{U}_{16} \quad (8.182)$$

where

$$\begin{aligned}
 \mathbf{U}_{12} &= \mathbf{A}(t_{i-1}) \begin{bmatrix} \tilde{\mathbf{T}}_1(t_{i-1}) \mathbf{l}_{IO} & \tilde{\mathbf{T}}_2(t_{i-1}) \mathbf{l}_{IO} & \tilde{\mathbf{T}}_3(t_{i-1}) \mathbf{l}_{IO} \end{bmatrix} \\
 \mathbf{U}_{15} &= \begin{bmatrix} \bar{\mathbf{A}}(t_i) \begin{bmatrix} 0 \\ Y^1(l) \\ Z^1(l) \end{bmatrix} & \bar{\mathbf{A}}(t_i) \begin{bmatrix} 0 \\ Y^2(l) \\ Z^2(l) \end{bmatrix} & \cdots & \bar{\mathbf{A}}(t_i) \begin{bmatrix} 0 \\ Y^n(l) \\ Z^n(l) \end{bmatrix} \end{bmatrix} \\
 \mathbf{U}_{16} &= \Phi(t_{i-1}) \mathbf{l}_{IO}
 \end{aligned}$$

$\Phi(t_{i-1})$ is determined by Equation (8.84), and \mathbf{T}_1 , \mathbf{T}_2 and \mathbf{T}_3 are determined by Equation (8.77).

Since the rotation angles of the beam at the input and output ends are equal in the floating frame, we obtain

$$\begin{bmatrix} \theta_x & \theta_y & \theta_z \end{bmatrix}_O^T = \begin{bmatrix} \mathbf{O}_{3 \times 3} & \mathbf{I}_3 & \mathbf{O}_{3 \times 3} & \mathbf{O}_{3 \times 3} & \mathbf{O}_{3 \times n_2} & \mathbf{O}_{3 \times n_3} & \mathbf{O}_{3 \times 1} \end{bmatrix} \mathbf{z}_I \quad (8.183)$$

The generalized coordinates are the same at an arbitrary point of the beam, which gives

$$\begin{bmatrix} q^1 & q^2 & \cdots & q^n \end{bmatrix}_O^T = \begin{bmatrix} \mathbf{O}_{n_2 \times 3} & \mathbf{O}_{n_2 \times 3} & \mathbf{O}_{n_2 \times 3} & \mathbf{O}_{n_2 \times 3} & \mathbf{I}_n & \mathbf{O}_{n_2 \times 1} \end{bmatrix} \mathbf{z}_I \quad (8.184)$$

From Equations (8.173), (8.181), (8.182), (8.183) and (8.184), the transfer equation of a Euler–Bernoulli beam with large spatial motion is obtained and denoted as

$$\mathbf{z}_O = \mathbf{U} \mathbf{z}_I \quad (8.185)$$

The transfer matrix is

$$\mathbf{U} = \begin{bmatrix} \mathbf{I}_3 & \mathbf{U}_{12} & \mathbf{O}_{3 \times 3} & \mathbf{O}_{3 \times 3} & \mathbf{U}_{15} & \mathbf{U}_{16} \\ \mathbf{O}_{3 \times 3} & \mathbf{I}_3 & \mathbf{O}_{3 \times 3} & \mathbf{O}_{3 \times 3} & \mathbf{O}_{3 \times 3} & \mathbf{O}_{3 \times 1} \\ \mathbf{U}_{31} & \mathbf{U}_{32} & \mathbf{I}_3 & \mathbf{U}_{34} & \mathbf{U}_{35} & \mathbf{U}_{36} \\ \mathbf{U}_{41} & \mathbf{U}_{42} & \mathbf{U}_{12} & \mathbf{I}_3 & \mathbf{U}_{45} & \mathbf{U}_{46} \\ \mathbf{O}_{n \times 3} & \mathbf{O}_{n \times 3} & \mathbf{O}_{n \times 3} & \mathbf{O}_{n \times 3} & \mathbf{I}_n & \mathbf{O}_{n \times 1} \\ \mathbf{O}_{1 \times 3} & \mathbf{O}_{1 \times 3} & \mathbf{O}_{1 \times 3} & \mathbf{O}_{1 \times 3} & \mathbf{O}_{1 \times n} & 1 \end{bmatrix} \quad (8.186)$$

The state vectors are

$$\mathbf{z}_I = [x, y, z, \theta_x, \theta_y, \theta_z, m_x, m_y, m_z, q_x, q_y, q_z, q^1, q^2, \dots, q^n, 1]^T$$

$$\mathbf{z}_O = [x, y, z, \theta_x, \theta_y, \theta_z, m_x, m_y, m_z, q_x, q_y, q_z, q^1, q^2, \dots, q^n, 1]^T$$

8.10 Transfer Matrices of Fixed Hinges Connected to a Beam with Large Spatial Motion

There are three kinds of fixed hinges connected to a beam with spatial motion: (1) the inboard body is rigid and the outboard body is flexible, (2) both the inboard and outboard bodies are flexible, and (3) the inboard body is flexible and the outboard body is rigid.

8.10.1 Transfer Matrix of a Fixed Hinge whose Inboard Body is a Rigid Body and whose Outboard Body is a Beam

For a transverse vibration beam fixed on the rigid body with fundamental motion, the position coordinates, orientation angles, internal forces and internal moments of fixed hinge are equal at its input and output ends. The generalized coordinates describing the deformation of the beam can be determined as follows.

The orthogonality of eigenvector functions in the theory of vibration yields

$$\int_0^l \bar{m} \begin{bmatrix} Y^j(x_2) \\ Z^j(x_2) \end{bmatrix} \begin{bmatrix} Y^k(x_2) \\ Z^k(x_2) \end{bmatrix} dx_2 = \begin{cases} 0, & j \neq k \\ d_j, & j = k \end{cases}, \quad \int_0^l EI \begin{bmatrix} Y^{j(2)}(x_2) \\ Z^{j(2)}(x_2) \end{bmatrix} \begin{bmatrix} Y^{k(2)}(x_2) \\ Z^{k(2)}(x_2) \end{bmatrix} dx_2 = \begin{cases} 0, & j \neq k \\ \Omega_j^2 d_j, & j = k \end{cases} \quad (8.187)$$

where Ω_k is the k th order natural frequency.

Using the modal analysis method to deal with transverse deformation in transverse vibration beam Equations (8.152) and (8.153), substituting Equations (8.146) and (8.171) into Equations (8.152) and (8.153) and linearizing, we obtain

$$\sum_{k=1}^n \begin{bmatrix} EI_{2z} {}^4 Y^k(x_2) \\ EI_{2y} {}^4 Z^k(x_2) \end{bmatrix} q^k(t) = \begin{bmatrix} f_{2y} - \frac{\partial \bar{m}_{2z}}{\partial x_2} \\ f_{2z} + \frac{\partial \bar{m}_{2y}}{\partial x_2} \end{bmatrix} - \bar{m} \begin{bmatrix} 0 & 1 & 0 \\ 0 & 0 & 1 \end{bmatrix} \mathbf{A}^T(t_i) \begin{bmatrix} \mathbf{B}_{\bar{r}} + \mathbf{A} \begin{bmatrix} x \\ y \\ z \end{bmatrix}_I (t_{i-1}) \end{bmatrix}$$

$$- \bar{m} \mathbf{A} \begin{bmatrix} 0 & 1 & 0 \\ 0 & 0 & 1 \end{bmatrix} \mathbf{A}^T(t_{i-1}) \begin{bmatrix} x \\ y \\ z \end{bmatrix}_I + \bar{m} \mathbf{A} \begin{bmatrix} 0 & 1 & 0 \\ 0 & 0 & 1 \end{bmatrix} \mathbf{A}^T(t_{i-1}) \begin{bmatrix} x \\ y \\ z \end{bmatrix}_I (t_{i-1}) - \bar{m} \mathbf{A} \sum_{k=1}^n \begin{bmatrix} Y^k(x_2) \\ Z^k(x_2) \end{bmatrix} q^k(t_i) \quad (8.188)$$

Multiplying both sides of Equation (8.188) by $\begin{bmatrix} Y^j(x_2) \\ Z^j(x_2) \end{bmatrix}$ and integrating along the axis direction of the beam gives

$$\begin{aligned}
\left(A + \Omega_j^2 \right) d_j q^j(t_i) = \int_0^l \begin{bmatrix} Y^j & Z^j \end{bmatrix} \begin{bmatrix} f_{2y} - \frac{\partial \bar{m}_{2,z}}{\partial x_2} \\ f_{2z} + \frac{\partial \bar{m}_{2,y}}{\partial x_2} \end{bmatrix} dx_2 - \bar{m} A \int_0^l \begin{bmatrix} 0 & Y^j & Z^j \end{bmatrix} A^T(t_{i-1}) dx_2 \begin{bmatrix} x \\ y \\ z \end{bmatrix}_I \\
- \bar{m} \int_0^l \begin{bmatrix} 0 & Y^j(x_2) & Z^j(x_2) \end{bmatrix} A^T(t_i) \begin{bmatrix} B_{\bar{r}} + A \begin{bmatrix} x_{t_{i-1}} \\ y_{t_{i-1}} \\ z_{t_{i-1}} \end{bmatrix}_I \end{bmatrix} dx_2 + \bar{m} A \int_0^l \begin{bmatrix} 0 & Y^j & Z^j \end{bmatrix} A^T(t_{i-1}) \begin{bmatrix} x_{t_{i-1}} \\ y_{t_{i-1}} \\ z_{t_{i-1}} \end{bmatrix}_I dx_2
\end{aligned} \quad (8.189)$$

yielding

$$- \bar{m} \int_0^l \begin{bmatrix} 0 & Y^j & Z^j \end{bmatrix} A^T(t_i) \left(B_{\bar{r}} + A \begin{bmatrix} x_{t_{i-1}} \\ y_{t_{i-1}} \\ z_{t_{i-1}} \end{bmatrix}_I \right) dx_2 = E_j + F_j \begin{bmatrix} \theta_x(t_i) \\ \theta_y(t_i) \\ \theta_z(t_i) \end{bmatrix} \quad (8.190)$$

where

$$\begin{aligned}
E_j &= -\bar{m} \int_0^l \begin{bmatrix} 0 & Y^j & Z^j \end{bmatrix} \Phi^T(t_{i-1}) \left(B_{\bar{r}} + A \begin{bmatrix} x_{t_{i-1}} \\ y_{t_{i-1}} \\ z_{t_{i-1}} \end{bmatrix}_I \right) dx_2 \\
F_j &= \bar{m} \int_0^l \begin{bmatrix} 0 & Y^j & Z^j \end{bmatrix} \left[\tilde{T}_1(t_{i-1}) A^T(t_{i-1}) \left(B_{\bar{r}} + A \begin{bmatrix} x_{t_{i-1}} \\ y_{t_{i-1}} \\ z_{t_{i-1}} \end{bmatrix}_I \right) \right. \\
&\quad \left. \tilde{T}_2(t_{i-1}) A^T(t_{i-1}) \left(B_{\bar{r}} + A \begin{bmatrix} x_{t_{i-1}} \\ y_{t_{i-1}} \\ z_{t_{i-1}} \end{bmatrix}_I \right), \tilde{T}_3(t_{i-1}) A^T(t_{i-1}) \left(B_{\bar{r}} + A \begin{bmatrix} x_{t_{i-1}} \\ y_{t_{i-1}} \\ z_{t_{i-1}} \end{bmatrix}_I \right) \right] dx_2
\end{aligned}$$

Substituting Equation (8.190) into Equation (8.189) and rearranging yields

$$q^j(t_i) = P_{1j} \begin{bmatrix} x \\ y \\ z \end{bmatrix}_I + P_{2j} \begin{bmatrix} \theta_x \\ \theta_y \\ \theta_z \end{bmatrix} + P_{5j} \quad (8.191)$$

where

$$\begin{aligned}
P_{1j} &= \frac{-\bar{m} A}{\left(A + \Omega_j^2 \right) d_j} \int_0^l \begin{bmatrix} 0 & Y^j & Z^j \end{bmatrix} A^T(t_{i-1}) dx_2, \quad P_{2j} = \frac{F_j}{\left(A + \Omega_j^2 \right) d_j} \\
P_{5j} &= \frac{1}{\left(A + \Omega_j^2 \right) d_j} \int_0^l \begin{bmatrix} Y^j & Z^j \end{bmatrix} \begin{bmatrix} f_{2y} - \frac{\partial \bar{m}_{2,z}}{\partial x_2} \\ f_{2z} + \frac{\partial \bar{m}_{2,y}}{\partial x_2} \end{bmatrix} dx_2 + \frac{E_j}{\left(A + \Omega_j^2 \right) d_j}
\end{aligned}$$

$$+ \frac{\bar{m}A}{(A + \bar{\Omega}_j^2)d_j} \int_0^l \begin{bmatrix} 0 & Y^j & Z^j \end{bmatrix} \mathbf{A}^T(t_{i-1}) \begin{bmatrix} x_{t_{i-1}} \\ y_{t_{i-1}} \\ z_{t_{i-1}} \end{bmatrix}_I dx_2$$

Hence, the transfer equation of a fixed hinge whose inboard body is rigid and whose outboard body is a beam is

$$\mathbf{z}_O = \mathbf{U} \mathbf{z}_I \quad (8.192)$$

The state vectors are

$$\begin{aligned} \mathbf{z}_I &= [x, y, z, \theta_x, \theta_y, \theta_z, m_x, m_y, m_z, q_x, q_y, q_z, 1]^T \\ \mathbf{z}_O &= [x, y, z, \theta_x, \theta_y, \theta_z, m_x, m_y, m_z, q_x, q_y, q_z, q^1, q^2, \dots, q^n, 1]^T \end{aligned}$$

The transfer matrix is

$$\mathbf{U} = \begin{bmatrix} \mathbf{I}_3 & \mathbf{O}_{3 \times 3} & \mathbf{O}_{3 \times 3} & \mathbf{O}_{3 \times 3} & \mathbf{O}_{3 \times 1} \\ \mathbf{O}_{3 \times 3} & \mathbf{I}_3 & \mathbf{O}_{3 \times 3} & \mathbf{O}_{3 \times 3} & \mathbf{O}_{3 \times 1} \\ \mathbf{O}_{3 \times 3} & \mathbf{O}_{3 \times 3} & \mathbf{I}_3 & \mathbf{O}_{3 \times 3} & \mathbf{O}_{3 \times 1} \\ \mathbf{O}_{3 \times 3} & \mathbf{O}_{3 \times 3} & \mathbf{O}_{3 \times 3} & \mathbf{I}_3 & \mathbf{O}_{3 \times 1} \\ \mathbf{U}_{51} & \mathbf{U}_{52} & \mathbf{O}_{n \times 3} & \mathbf{O}_{n \times 3} & \mathbf{U}_{55} \\ \mathbf{O}_{1 \times 3} & \mathbf{O}_{1 \times 3} & \mathbf{O}_{1 \times 3} & \mathbf{O}_{1 \times 3} & 1 \end{bmatrix} \quad (8.193)$$

where

$$\mathbf{U}_{51} = \begin{bmatrix} \mathbf{P}_{11} \\ \mathbf{P}_{12} \\ \vdots \\ \mathbf{P}_{1n} \end{bmatrix}, \mathbf{U}_{52} = \begin{bmatrix} \mathbf{P}_{21} \\ \mathbf{P}_{22} \\ \vdots \\ \mathbf{P}_{2n} \end{bmatrix}, \mathbf{U}_{55} = \begin{bmatrix} \mathbf{P}_{51} \\ \mathbf{P}_{52} \\ \vdots \\ \mathbf{P}_{5n} \end{bmatrix}$$

8.10.2 Transfer Matrix of a Fixed Hinge whose Inboard and Outboard Bodies are Beams

For a transverse vibration beam fixed on a moving beam, the position coordinates, internal forces and internal moment of the fixed hinge are equal at its input and output ends. The orientation angles and generalized coordinates describing the deformation of outboard beam can be determined as follows.

According to the derivation of the fixed hinge whose inboard body is a rigid body and whose outboard body is a beam in section 8.10.1 and the vibration equations of outboard beam, we obtain

$$\begin{bmatrix} q^1 \\ q^2 \\ \vdots \\ q^n \end{bmatrix}_O = \mathbf{U}_{51} \begin{bmatrix} x \\ y \\ z \end{bmatrix}_I + \mathbf{U}_{52} \begin{bmatrix} \theta_x \\ \theta_y \\ \theta_z \end{bmatrix}_O + \mathbf{U}_{56} \quad (8.194)$$

where \mathbf{U}_{56} is similar to \mathbf{U}_{55} in the transfer matrix of the fixed hinge whose inboard body is rigid and whose outboard body is a beam, and $[\theta_x \ \theta_y \ \theta_z]_O^T$ are the orientation angles of the body-fixed coordinate system of the outboard beam, which is determined by the state vector of the output end of the inboard beam.

The direction transformation matrices \mathbf{A}_O and \mathbf{A}_I have the following relation

$$\mathbf{A}_O = \mathbf{A}_I \mathbf{A}_d \quad (8.195)$$

where

$$\mathbf{A}_d = \begin{bmatrix} 1 & -\Delta\theta_z & \Delta\theta_y \\ \Delta\theta_z & 1 & 0 \\ -\Delta\theta_y & 0 & 1 \end{bmatrix}, \begin{bmatrix} \Delta\theta_y \\ \Delta\theta_z \end{bmatrix} = \begin{bmatrix} -\frac{\partial w}{\partial x_2} \\ \frac{\partial \nu}{\partial x_2} \end{bmatrix} = \sum_{k=1}^n \begin{bmatrix} -\frac{dZ^k(l)}{dx_2} \\ \frac{dY^k(l)}{dx_2} \end{bmatrix} q^k(t)$$

Y^k, Z^k, x_2, l and q^k are parameters of the inboard beam.

Then

$$\begin{bmatrix} \theta_x \\ \theta_y \\ \theta_z \end{bmatrix}_O = \begin{bmatrix} \theta_x \\ \theta_y \\ \theta_z \end{bmatrix}_I + \mathbf{U}_{25} \begin{bmatrix} q^1 \\ q^2 \\ \vdots \\ q^n \end{bmatrix} \quad (8.196)$$

where

$$\mathbf{P}_{5k} = \mathbf{H}^{-1} \begin{bmatrix} 0 & -\frac{dZ^k(l)}{dx_2} & \frac{dY^k(l)}{dx_2} \end{bmatrix}^T, \mathbf{H} = \begin{bmatrix} 1 & 0 & -s_y \\ 0 & c_x & s_x c_y \\ 0 & -s_x & c_x c_y \end{bmatrix}_I, \mathbf{U}_{25} = [P_{51} \ P_{52} \ \cdots \ P_{5n}]$$

Substituting Equation (8.196) into Equation (8.194) yields

$$\begin{bmatrix} q^1 \\ q^2 \\ \vdots \\ q^n \end{bmatrix}_O = \mathbf{U}_{51} \begin{bmatrix} x \\ y \\ z \end{bmatrix}_i + \mathbf{U}_{52} \begin{bmatrix} \theta_x \\ \theta_y \\ \theta_z \end{bmatrix}_I + \mathbf{U}_{52} \mathbf{U}_{25} \begin{bmatrix} q^1 \\ q^2 \\ \vdots \\ q^n \end{bmatrix}_I + \mathbf{U}_{56} \quad (8.197)$$

The transfer equation of the fixed hinge whose inboard and outboard bodies are beams becomes

$$\mathbf{z}_O = \mathbf{U} \mathbf{z}_I \quad (8.198)$$

The state vectors are

$$\mathbf{z}_I = [x, y, z, \theta_x, \theta_y, \theta_z, m_x, m_y, m_z, q_x, q_y, q_z, q^1, q^2, \dots, q^n, 1]^T$$

$$\mathbf{z}_O = [x, y, z, \theta_x, \theta_y, \theta_z, m_x, m_y, m_z, q_x, q_y, q_z, q^1, q^2, \dots, q^n, 1]^T$$

The transfer matrix is

$$U = \begin{bmatrix} I_3 & O_{3 \times 3} & O_{3 \times 3} & O_{3 \times 3} & O_{3 \times n} & O_{3 \times 1} \\ O_{3 \times 3} & I_3 & O_{3 \times 3} & O_{3 \times 3} & U_{25} & O_{3 \times 1} \\ O_{3 \times 3} & O_{3 \times 3} & I_3 & O_{3 \times 3} & O_{3 \times n} & O_{3 \times 1} \\ O_{3 \times 3} & O_{3 \times 3} & O_{3 \times 3} & I_3 & O_{3 \times n} & O_{3 \times 1} \\ U_{51} & U_{52} & O_{n \times 3} & O_{n \times 3} & U_{52} U_{25} & U_{56} \\ O_{1 \times 3} & O_{1 \times 3} & O_{1 \times 3} & O_{1 \times 3} & O_{1 \times n} & 1 \end{bmatrix} \quad (8.199)$$

8.10.3 Transfer Matrix of a Fixed Hinge whose Inboard Body is a Beam and whose Outboard Body is a Rigid Body

The derivation of the transfer matrix of a fixed hinge whose inboard body is a Euler–Bernoulli beam and whose outboard body is a rigid body is similar to that in section 8.5. By eliminating rows corresponding to the generalized coordinates in Equation (8.199), the transfer equation of the fixed hinge whose inboard body is a beam and whose outboard body is a rigid body can be obtained:

$$z_O = U z_I \quad (8.200)$$

The state vectors are

$$z_I = [x, y, z, \theta_x, \theta_y, \theta_z, m_x, m_y, m_z, q_x, q_y, q_z, q^1, q^2, \dots, q^n, 1]^T$$

$$z_O = [x, y, z, \theta_x, \theta_y, \theta_z, m_x, m_y, m_z, q_x, q_y, q_z, 1]^T$$

The transfer matrix is

$$U = \begin{bmatrix} I_3 & O_{3 \times 3} & O_{3 \times 3} & O_{3 \times 3} & O_{3 \times n} & O_{3 \times 1} \\ O_{3 \times 3} & I_3 & O_{3 \times 3} & O_{3 \times 3} & U_{25} & O_{3 \times 1} \\ O_{3 \times 3} & O_{3 \times 3} & I_3 & O_{3 \times 3} & O_{3 \times n} & O_{3 \times 1} \\ O_{3 \times 3} & O_{3 \times 3} & O_{3 \times 3} & I_3 & O_{3 \times n} & O_{3 \times 1} \\ O_{1 \times 3} & O_{1 \times 3} & O_{1 \times 3} & O_{1 \times 3} & O_{1 \times n} & 1 \end{bmatrix} \quad (8.201)$$

where the meaning of all elements is the same as in Equation (8.199).

8.11 Transfer Matrices of Smooth Hinges Connected to a Beam with Large Spatial Motion

There are four kinds of smooth hinges connected to a spatial beam: (1) both the outboard and inboard bodies are rigid bodies, (2) the outboard body is flexible and the inboard body is rigid, (3) both the outboard and inboard bodies are flexible, and (4) the outboard body is rigid and the

inboard body is flexible. Here, we introduce two kinds of transfer matrices of smooth hinges connected to a spatial beam: (1) the outboard body is a beam and (2) the outboard body is a rigid body.

8.11.1 Transfer Matrix of a Smooth Hinge whose Inboard Body is a Rigid Body and whose Outboard Body is a Beam

For a smooth hinge, the position coordinates, internal forces and internal moments of its input and output ends are equal. The generalized coordinates which are used to describe the deformation of a Euler–Bernoulli beam and orientation angles of the floating frame are described as follows.

Linearizing the vibration equations of the beam yields

$$\begin{bmatrix} q^1 \\ q^2 \\ \vdots \\ q^n \end{bmatrix}_O = \begin{bmatrix} \mathbf{P}_{11} \\ \mathbf{P}_{12} \\ \vdots \\ \mathbf{P}_{1n} \end{bmatrix} \begin{bmatrix} x \\ y \\ z \end{bmatrix}_I + \begin{bmatrix} \mathbf{P}_{21} \\ \mathbf{P}_{22} \\ \vdots \\ \mathbf{P}_{2n} \end{bmatrix} \begin{bmatrix} \theta_x \\ \theta_y \\ \theta_z \end{bmatrix}_O + \begin{bmatrix} \mathbf{P}_{51} \\ \mathbf{P}_{52} \\ \vdots \\ \mathbf{P}_{5n} \end{bmatrix} \quad (8.202)$$

where the meaning of \mathbf{P}_{ij} , ($i = 1, 2, 5, j = 1, 2, \dots, n$) is similar to that in Equation (8.191).

The moment of connection hinge at the output end of the beam is zero. From the rotational equations of the beam we obtain

$$\begin{bmatrix} m_x \\ m_y \\ m_z \end{bmatrix}_O = \mathbf{U}_{31} \begin{bmatrix} x \\ y \\ z \end{bmatrix}_I + \mathbf{U}_{32} \begin{bmatrix} \theta_x \\ \theta_y \\ \theta_z \end{bmatrix}_I + \begin{bmatrix} m_x \\ m_y \\ m_z \end{bmatrix}_I + \mathbf{U}_{34} \begin{bmatrix} q_x \\ q_y \\ q_z \end{bmatrix}_I + \mathbf{U}_{35} \begin{bmatrix} q^1 \\ q^2 \\ \vdots \\ q^n \end{bmatrix}_I + \mathbf{U}_{36} \quad (8.203)$$

where I is the input end of the outboard beam, which is also the output end of the smooth hinge. $\mathbf{U}_{3,1}$, $\mathbf{U}_{3,2}$, $\mathbf{U}_{3,4}$, $\mathbf{U}_{3,5}$ and $\mathbf{U}_{3,6}$ are submatrices of the transfer matrix of the flexible beam.

As $\begin{bmatrix} m_x & m_y & m_z \end{bmatrix}_O^T = \begin{bmatrix} m_x & m_y & m_z \end{bmatrix}_I^T = \mathbf{O}_{1 \times 3}$, this yields

$$\begin{bmatrix} 0 \\ 0 \\ 0 \end{bmatrix} = \mathbf{U}_{31} \begin{bmatrix} x \\ y \\ z \end{bmatrix}_O + \mathbf{U}_{32} \begin{bmatrix} \theta_x \\ \theta_y \\ \theta_z \end{bmatrix}_O + \mathbf{U}_{34} \begin{bmatrix} q_x \\ q_y \\ q_z \end{bmatrix}_O + \mathbf{U}_{35} \begin{bmatrix} q^1 \\ q^2 \\ \vdots \\ q^n \end{bmatrix}_O + \mathbf{U}_{36} \quad (8.204)$$

As the position coordinates and internal forces at the input and output ends are equal, combining Equations (8.202) and (8.203) gives

$$\begin{bmatrix} \theta_x & \theta_y & \theta_z & q^1 & q^2 & \cdots & q^n \end{bmatrix}_O^T = \begin{bmatrix} \mathbf{U}_{21} \\ \mathbf{U}_{51} \end{bmatrix} \begin{bmatrix} x \\ y \\ z \end{bmatrix}_I + \begin{bmatrix} \mathbf{U}_{24} \\ \mathbf{U}_{54} \end{bmatrix} \begin{bmatrix} q_x \\ q_y \\ q_z \end{bmatrix}_I + \begin{bmatrix} \mathbf{U}_{25} \\ \mathbf{U}_{55} \end{bmatrix} \quad (8.205)$$

where

$$\begin{bmatrix} \mathbf{U}_{21} \\ \mathbf{U}_{51} \end{bmatrix} = \begin{bmatrix} \mathbf{U}_{32} & \mathbf{U}_{35} \\ -\mathbf{P}_{21} & \mathbf{I}_{n \times 1} \\ -\mathbf{P}_{22} & \mathbf{I}_{n \times 1} \\ \vdots & \vdots \\ -\mathbf{P}_{2n} & \mathbf{I}_{n \times 1} \end{bmatrix}^{-1} \begin{bmatrix} \mathbf{U}_{31} \\ \mathbf{P}_{11} \\ \mathbf{P}_{12} \\ \vdots \\ \mathbf{P}_{1n} \end{bmatrix}, \quad \begin{bmatrix} \mathbf{U}_{24} \\ \mathbf{U}_{54} \end{bmatrix} = \begin{bmatrix} \mathbf{U}_{32} & \mathbf{U}_{35} \\ -\mathbf{P}_{21} & \mathbf{I}_{n \times 1} \\ -\mathbf{P}_{22} & \mathbf{I}_{n \times 1} \\ \vdots & \vdots \\ -\mathbf{P}_{2n} & \mathbf{I}_{n \times 1} \end{bmatrix}^{-1} \begin{bmatrix} -\mathbf{U}_{34} \\ \mathbf{O}_{n \times 3} \end{bmatrix},$$

$$\begin{bmatrix} \mathbf{U}_{25} \\ \mathbf{U}_{55} \end{bmatrix} = \begin{bmatrix} \mathbf{U}_{32} & \mathbf{U}_{35} \\ -\mathbf{P}_{21} & \mathbf{I}_{n \times 1} \\ -\mathbf{P}_{22} & \mathbf{I}_{n \times 1} \\ \vdots & \vdots \\ -\mathbf{P}_{2n} & \mathbf{I}_{n \times 1} \end{bmatrix}^{-1} \begin{bmatrix} -\mathbf{U}_{36} \\ \mathbf{P}_{51} \\ \mathbf{P}_{52} \\ \vdots \\ \mathbf{P}_{5n} \end{bmatrix}$$

The transfer equation of a smooth hinge whose inboard body is a rigid body and whose outboard body is a beam becomes

$$\mathbf{z}_O = \mathbf{U} \mathbf{z}_I \quad (8.206)$$

The state vectors are

$$\mathbf{z}_I = [x, y, z, \theta_x, \theta_y, \theta_z, m_x, m_y, m_z, q_x, q_y, q_z, 1]^T$$

$$\mathbf{z}_O = [x, y, z, \theta_x, \theta_y, \theta_z, m_x, m_y, m_z, q_x, q_y, q_z, q^1, q^2, \dots, q^n, 1]^T$$

The transfer matrix is

$$\mathbf{U} = \begin{bmatrix} \mathbf{I}_3 & \mathbf{O}_{3 \times 3} & \mathbf{O}_{3 \times 3} & \mathbf{O}_{3 \times 3} & \mathbf{O}_{3 \times 1} \\ \mathbf{U}_{21} & \mathbf{O}_{3 \times 3} & \mathbf{O}_{3 \times 3} & \mathbf{U}_{24} & \mathbf{U}_{25} \\ \mathbf{O}_{3 \times 3} & \mathbf{O}_{3 \times 3} & \mathbf{O}_{3 \times 3} & \mathbf{O}_{3 \times 3} & \mathbf{O}_{3 \times 1} \\ \mathbf{O}_{3 \times 3} & \mathbf{O}_{3 \times 3} & \mathbf{O}_{3 \times 3} & \mathbf{I}_3 & \mathbf{O}_{3 \times 1} \\ \mathbf{U}_{51} & \mathbf{O}_{n \times 3} & \mathbf{O}_{n \times 3} & \mathbf{U}_{54} & \mathbf{U}_{55} \\ \mathbf{O}_{1 \times 3} & \mathbf{O}_{1 \times 3} & \mathbf{O}_{1 \times 3} & \mathbf{O}_{1 \times 3} & 1 \end{bmatrix} \quad (8.207)$$

8.11.2 Transfer Matrix of a Smooth Hinge whose Inboard and Outboard Bodies are Beams

For smooth hinge whose inboard and outboard bodies are Euler–Bernoulli beams, its position coordinates, internal forces and internal moment at the input and output ends are equal. Similar to the smooth hinge whose inboard body is a rigid body and whose outboard body is a beam, the orientation angles of the floating frame and the generalized coordinates of deformation of the outboard beam of a smooth hinge whose inboard and outboard bodies are beams can be obtained from the vibration equation and the rotational equation of the outboard beam.

If the internal moment at the output end of the outboard beam is zero, the description is shown in Equations (8.202) and (8.205).

The transfer equation of a smooth hinge whose inboard and outboard bodies are beams yields

$$\mathbf{z}_O = \mathbf{U} \mathbf{z}_I \quad (8.208)$$

The state vectors are

$$\begin{aligned} \mathbf{z}_I &= [x, y, z, \theta_x, \theta_y, \theta_z, m_x, m_y, m_z, q_x, q_y, q_z, q^1, q^2, \dots, q^n, 1]^T \\ \mathbf{z}_O &= [x, y, z, \theta_x, \theta_y, \theta_z, m_x, m_y, m_z, q_x, q_y, q_z, q^1, q^2, \dots, q^n, 1]^T \end{aligned}$$

The transfer matrix is

$$\mathbf{U} = \begin{bmatrix} \mathbf{I}_3 & \mathbf{O}_{3 \times 3} & \mathbf{O}_{3 \times 3} & \mathbf{O}_{3 \times 3} & \mathbf{O}_{3 \times n} & \mathbf{O}_{3 \times 1} \\ \mathbf{U}_{21} & \mathbf{O}_{3 \times 3} & \mathbf{O}_{3 \times 3} & \mathbf{U}_{24} & \mathbf{O}_{3 \times n} & \mathbf{U}_{25} \\ \mathbf{O}_{3 \times 3} & \mathbf{O}_{3 \times 3} & \mathbf{O}_{3 \times 3} & \mathbf{O}_{3 \times 3} & \mathbf{O}_{3 \times n} & \mathbf{O}_{3 \times 1} \\ \mathbf{O}_{3 \times 3} & \mathbf{O}_{3 \times 3} & \mathbf{O}_{3 \times 3} & \mathbf{I}_3 & \mathbf{O}_{3 \times n} & \mathbf{O}_{3 \times 1} \\ \mathbf{U}_{51} & \mathbf{O}_{n \times 3} & \mathbf{O}_{n \times 3} & \mathbf{U}_{54} & \mathbf{O}_{n \times n} & \mathbf{O}_{n \times 1} \\ \mathbf{O}_{1 \times 3} & \mathbf{O}_{1 \times 3} & \mathbf{O}_{1 \times 3} & \mathbf{O}_{1 \times 3} & \mathbf{O}_{1 \times n} & 1 \end{bmatrix} \quad (8.209)$$

where the meaning of all elements is similar to that in Equation (8.207).

8.11.3 Transfer Matrix of a Smooth Hinge whose Inboard Body is a Beam and whose Outboard Body is a Rigid Body

The derivation of the transfer matrix of a smooth hinge whose inboard body is a beam and whose outboard body is a rigid body is the same as that in section 8.5, except that the rows corresponding to the generalized coordinates in Equation (8.209) are eliminated. Therefore, the transfer equation of a smooth hinge whose inboard body is a beam and whose outboard body is a rigid body yields

$$\mathbf{z}_O = \mathbf{U} \mathbf{z}_I \quad (8.210)$$

The state vectors are

$$\begin{aligned} \mathbf{z}_I &= [x, y, z, \theta_x, \theta_y, \theta_z, m_x, m_y, m_z, q_x, q_y, q_z, q^1, q^2, \dots, q^n, 1]^T \\ \mathbf{z}_O &= [x, y, z, \theta_x, \theta_y, \theta_z, m_x, m_y, m_z, q_x, q_y, q_z, 1]^T \end{aligned}$$

The transfer matrix is

$$\mathbf{U} = \begin{bmatrix} \mathbf{I}_3 & \mathbf{O}_{3 \times 3} & \mathbf{O}_{3 \times 3} & \mathbf{O}_{3 \times 3} & \mathbf{O}_{3 \times n} & \mathbf{O}_{3 \times 1} \\ \mathbf{U}_{21} & \mathbf{O}_{3 \times 3} & \mathbf{O}_{3 \times 3} & \mathbf{U}_{24} & \mathbf{O}_{3 \times n} & \mathbf{U}_{25} \\ \mathbf{O}_{3 \times 3} & \mathbf{O}_{3 \times 3} & \mathbf{O}_{3 \times 3} & \mathbf{O}_{3 \times 3} & \mathbf{O}_{3 \times n} & \mathbf{O}_{3 \times 1} \\ \mathbf{O}_{3 \times 3} & \mathbf{O}_{3 \times 3} & \mathbf{O}_{3 \times 3} & \mathbf{I}_3 & \mathbf{O}_{3 \times n} & \mathbf{O}_{3 \times 1} \\ \mathbf{O}_{1 \times 3} & \mathbf{O}_{1 \times 3} & \mathbf{O}_{1 \times 3} & \mathbf{O}_{1 \times 3} & \mathbf{O}_{1 \times n} & 1 \end{bmatrix} \quad (8.211)$$

where the meanings of all elements are the same as those in Equation (8.209).

8.12 Transfer Matrices of Spring Hinges Connected to a Beam with Large Spatial Motion

Here, an elastic hinge composed of a massless linear spring and a massless torsional spring, is considered. Let element $j + 1$ denote the spring hinge, and j and $j + 2$ denote its inboard and outboard bodies, respectively. According to the equilibrium of forces at the input and output ends of the spring, the following equations can be obtained

$$\begin{bmatrix} q_x \\ q_y \\ q_z \end{bmatrix}_{j,j+1} + \mathbf{K}(\mathbf{r}_{j+2,j+1} - \mathbf{r}_{j,j+1}) = \begin{bmatrix} 0 \\ 0 \\ 0 \end{bmatrix} \quad (8.212)$$

$$\mathbf{K} = \begin{bmatrix} K_x & 0 & 0 \\ 0 & K_y & 0 \\ 0 & 0 & K_z \end{bmatrix} \quad (8.213)$$

where \mathbf{K} is the stiffness coefficient matrix of the spring, and K_x , K_y and K_z are the coefficients of spring stiffness along the three axes of the inertia coordinate system.

Then

$$\mathbf{r}_{j+2,j+1} = \mathbf{r}_{j,j+1} - \mathbf{K}^{-1} [q_x \ q_y \ q_z]_{j,j+1}^T \quad (8.214)$$

For a torsional spring, that is

$$\mathbf{m}_I = \mathbf{K}' (\boldsymbol{\theta}'_{j+2,j+1} - \boldsymbol{\theta}'_{j,j+1}) \quad (8.215)$$

$$\mathbf{K}' = \begin{bmatrix} K'_x & 0 & 0 \\ 0 & K'_y & 0 \\ 0 & 0 & K'_z \end{bmatrix} \quad (8.216)$$

where \mathbf{K}' is the stiffness coefficient matrix of the torsional spring, and $\boldsymbol{\theta}'_{j,j+1}$ and $\boldsymbol{\theta}'_{j+2,j+1}$ are the orientation angles of the torsional spring at the input and output ends, respectively. K'_x , K'_y and K'_z are the stiffness coefficients of the torsional spring along the three axes of the inertial coordinate system.

The derivation of the transfer matrices of spring hinges connected to a Euler–Bernoulli beam with large spatial motion is discussed in three situations in the following sections.

8.12.1 Transfer Matrix of a Spring Hinge whose Inboard and Outboard Bodies are Beams

For a spring hinge whose inboard body j and outboard body $j + 2$ are beams moving in space, the transformation relation between the orientation angles of the inboard beam and the generalized coordinates describing the deformation of the outboard beam can be determined as follows.

The transformation matrices $\mathbf{A}_{j+1,I}$ and \mathbf{A}_j of the spring hinge at the input end and its inboard beam have the relation

$$\mathbf{A}_{j+1,I} = \mathbf{A}_j \mathbf{A}_{j,j+1} \quad (8.217)$$

where

$$\mathbf{A}_{j,j+1} = \begin{bmatrix} 1 & -\Delta\theta_{j,z} & \Delta\theta_{j,y} \\ \Delta\theta_{j,z} & 1 & 0 \\ -\Delta\theta_{j,y} & 0 & 1 \end{bmatrix}, \begin{bmatrix} \Delta\theta_{j,y} \\ \Delta\theta_{j,z} \end{bmatrix} = \begin{bmatrix} -\frac{\partial w_j}{\partial x_2} \\ \frac{\partial \nu_j}{\partial x_2} \end{bmatrix} = \sum_{k=1}^n \begin{bmatrix} -\frac{dZ_j^k(t_j)}{dx_2} \\ \frac{dY_j^k(t_j)}{dx_2} \end{bmatrix} q_j^k(t) \quad (8.218)$$

Y_j^k, Z_j^k, x_2, l_j and q_j^k are interrelated parameters of the inboard beam j .

$\mathbf{A}_{j+1,O}$ and \mathbf{A}_{j+2} are the transformation matrices of the spring hinge at the input end and its outboard beam, respectively. It has the relation

$$\mathbf{A}_{j+1,O} = \mathbf{A}_{j+2} \mathbf{A}_{j+2,j+1} \quad (8.219)$$

where

$$\mathbf{A}_{j+2,j+1} = \begin{bmatrix} 1 & -\Delta\theta_{j+2,z} & \Delta\theta_{j+2,y} \\ \Delta\theta_{j+2,z} & 1 & 0 \\ -\Delta\theta_{j+2,y} & 0 & 1 \end{bmatrix}, \begin{bmatrix} \Delta\theta_{j+2,y} \\ \Delta\theta_{j+2,z} \end{bmatrix} = \begin{bmatrix} -\frac{\partial w_{j+2}}{\partial x_2} \\ \frac{\partial \nu_{j+2}}{\partial x_2} \end{bmatrix} = \sum_{k=1}^n \begin{bmatrix} -\frac{dZ_{j+2}^k(0)}{dx_2} \\ \frac{dY_{j+2}^k(0)}{dx_2} \end{bmatrix} q_{j+2}^k(t) \quad (8.220)$$

$Y_{j+2}^k, Z_{j+2}^k, x_2$ and q_{j+2}^k are parameters of outboard beam $j+2$.

Linearizing Equations (8.217) and (8.219) yields

$$\begin{bmatrix} \theta_{x_{j+1,l}} \\ \theta_{y_{j+1,l}} \\ \theta_{z_{j+1,l}} \end{bmatrix} = \begin{bmatrix} \theta_x \\ \theta_y \\ \theta_z \end{bmatrix}_j + \mathbf{H}_j^{-1} \begin{bmatrix} 0 \\ \Delta\theta_{j,y} \\ \Delta\theta_{j,z} \end{bmatrix}, \begin{bmatrix} \theta_{x_{j+1,O}} \\ \theta_{y_{j+1,O}} \\ \theta_{z_{j+1,O}} \end{bmatrix} = \begin{bmatrix} \theta_x \\ \theta_y \\ \theta_z \end{bmatrix}_{j+2} + \mathbf{H}_{j+2}^{-1} \begin{bmatrix} 0 \\ \Delta\theta_{j+2,y} \\ \Delta\theta_{j+2,z} \end{bmatrix}, \quad (8.221)$$

where

$$\mathbf{H}_i = \begin{bmatrix} 1 & 0 & -s_y \\ 0 & c_x & c_y \\ 0 & -s_x & c_x c_y \end{bmatrix}_i \quad (i = j, j+2)$$

that is

$$\theta'_{j+2,j+1} = \begin{bmatrix} \theta_x \\ \theta_y \\ \theta_z \end{bmatrix}_{j+2} + \mathbf{H}_{j+2}^{-1} \begin{bmatrix} 0 \\ \Delta\theta_{j+2,y} \\ \Delta\theta_{j+2,z} \end{bmatrix}, \theta'_{j,j+1} = \begin{bmatrix} \theta_x \\ \theta_y \\ \theta_z \end{bmatrix}_j + \mathbf{H}_j^{-1} \begin{bmatrix} 0 \\ \Delta\theta_{j,y} \\ \Delta\theta_{j,z} \end{bmatrix} \quad (8.222)$$

Substituting Equations (8.217), (8.220) and (8.222) into Equation (8.215), we obtain

$$\begin{bmatrix} \theta_x \\ \theta_y \\ \theta_z \end{bmatrix}_{j+2} + \mathbf{L}_{j+2} \begin{bmatrix} q^1 \\ q^2 \\ \vdots \\ q^n \end{bmatrix}_{j+2} = \begin{bmatrix} \theta_x \\ \theta_y \\ \theta_z \end{bmatrix}_j + \mathbf{K}'^{-1} \mathbf{m}_l + \mathbf{L}_j \begin{bmatrix} q^1 \\ q^2 \\ \vdots \\ q^n \end{bmatrix}_j \quad (8.223)$$

where

$$L_{j+2} = H_{j+2}^{-1} \begin{bmatrix} 0 & 0 & \dots & 0 \\ -\frac{dZ_{j+2}^1(0)}{dx_2} & -\frac{dZ_{j+2}^2(0)}{dx_2} & \dots & -\frac{dZ_{j+2}^n(0)}{dx_2} \\ \frac{dY_{j+2}^1(0)}{dx_2} & \frac{dY_{j+2}^2(0)}{dx_2} & \dots & \frac{dY_{j+2}^n(0)}{dx_2} \end{bmatrix},$$

$$L_j = H_j^{-1} \begin{bmatrix} 0 & 0 & \dots & 0 \\ -\frac{dZ_j^1(l_j)}{dx_2} & -\frac{dZ_j^2(l_j)}{dx_2} & \dots & -\frac{dZ_j^n(l_j)}{dx_2} \\ \frac{dY_j^1(l_j)}{dx_2} & \frac{dY_j^2(l_j)}{dx_2} & \dots & \frac{dY_j^n(l_j)}{dx_2} \end{bmatrix}$$

Similar to Section 8.8.1, linearizing the equations of motion of the outboard beam $j+2$, we obtain

$$\begin{bmatrix} q^1 \\ q^2 \\ \vdots \\ q^n \end{bmatrix}_{j+2} = R_1 \begin{bmatrix} x \\ y \\ z \end{bmatrix}_{j+2,j+1} + R_2 \begin{bmatrix} \theta_x \\ \theta_y \\ \theta_z \end{bmatrix}_{j+2} + R_5 \quad (8.224)$$

where

$$R_1 = \begin{bmatrix} P_{11} \\ P_{12} \\ \vdots \\ P_{1n} \end{bmatrix}, \quad R_2 = \begin{bmatrix} P_{21} \\ P_{22} \\ \vdots \\ P_{2n} \end{bmatrix}, \quad R_5 = \begin{bmatrix} P_{51} \\ P_{52} \\ \vdots \\ P_{5n} \end{bmatrix}$$

The meaning of P_{ij} , ($i=1,2,5$ $j=1,2,\dots,n$) is similar to Equation (8.191).

According to Equations (8.214), (8.223) and (8.224), this yields

$$\begin{aligned} \begin{bmatrix} \theta_x & \theta_y & \theta_z & q^1 & q^2 & \dots & q^n \end{bmatrix}_{j+2,j+1}^T &= \begin{bmatrix} U_{21} \\ U_{51} \end{bmatrix} \begin{bmatrix} x \\ y \\ z \end{bmatrix}_{j,j+1} + \begin{bmatrix} U_{22} \\ U_{52} \end{bmatrix} \begin{bmatrix} \theta_x \\ \theta_y \\ \theta_z \end{bmatrix}_{j,j+1} \\ &+ \begin{bmatrix} U_{23} \\ U_{53} \end{bmatrix} m_{j,j+1} + \begin{bmatrix} U_{24} \\ U_{54} \end{bmatrix} \begin{bmatrix} q_x \\ q_y \\ q_z \end{bmatrix}_{j,j+1} + \begin{bmatrix} U_{25} \\ U_{55} \end{bmatrix} \begin{bmatrix} q^1 \\ q^2 \\ \vdots \\ q^n \end{bmatrix}_{j,j+1} + \begin{bmatrix} U_{26} \\ U_{56} \end{bmatrix} \end{aligned} \quad (8.225)$$

where the order of $\mathbf{U}_{2i}(i = 1, 2, 3, 4, 5, 6)$ is (3×3) and the order of $\mathbf{U}_{5i}(i = 1, 2, 3, 4, 5, 6)$ is $(n \times 3)$:

$$\begin{aligned} \begin{bmatrix} \mathbf{U}_{21} \\ \mathbf{U}_{51} \end{bmatrix} &= \begin{bmatrix} -\mathbf{R}_2 & \mathbf{I}_n \\ \mathbf{I}_3 & \mathbf{L}_{j+2} \end{bmatrix}^{-1} \begin{bmatrix} \mathbf{R}_1 \\ \mathbf{O}_{3 \times 3} \end{bmatrix}, \quad \begin{bmatrix} \mathbf{U}_{22} \\ \mathbf{U}_{52} \end{bmatrix} = \begin{bmatrix} -\mathbf{R}_2 & \mathbf{I}_n \\ \mathbf{I}_3 & \mathbf{L}_{j+2} \end{bmatrix}^{-1} \begin{bmatrix} \mathbf{O}_{n \times 3} \\ \mathbf{I}_3 \end{bmatrix} \\ \begin{bmatrix} \mathbf{U}_{23} \\ \mathbf{U}_{53} \end{bmatrix} &= \begin{bmatrix} -\mathbf{R}_2 & \mathbf{I}_n \\ \mathbf{I}_3 & \mathbf{L}_{j+2} \end{bmatrix}^{-1} \begin{bmatrix} \mathbf{O}_{n \times 3} \\ \mathbf{K}'^{-1} \end{bmatrix}, \quad \begin{bmatrix} \mathbf{U}_{24} \\ \mathbf{U}_{54} \end{bmatrix} = \begin{bmatrix} -\mathbf{R}_2 & \mathbf{I}_n \\ \mathbf{I}_3 & \mathbf{L}_{j+2} \end{bmatrix}^{-1} \begin{bmatrix} -\mathbf{R}_1 \mathbf{K}^{-1} \\ \mathbf{O}_{3 \times 3} \end{bmatrix} \\ \begin{bmatrix} \mathbf{U}_{25} \\ \mathbf{U}_{55} \end{bmatrix} &= \begin{bmatrix} -\mathbf{R}_2 & \mathbf{I}_n \\ \mathbf{I}_3 & \mathbf{L}_{j+2} \end{bmatrix}^{-1} \begin{bmatrix} \mathbf{O}_{n \times n} \\ \mathbf{L}_j \end{bmatrix}, \quad \begin{bmatrix} \mathbf{U}_{26} \\ \mathbf{U}_{56} \end{bmatrix} = \begin{bmatrix} -\mathbf{R}_2 & \mathbf{I}_n \\ \mathbf{I}_3 & \mathbf{L}_{j+2} \end{bmatrix}^{-1} \begin{bmatrix} \mathbf{R}_5 \\ \mathbf{O}_{3 \times 1} \end{bmatrix} \end{aligned}$$

According to Equations (8.214) and (8.225), the transfer equation of a spring hinge whose inboard and outboard bodies are beams moving in space is

$$\mathbf{z}_O = \mathbf{U} \mathbf{z}_I \quad (8.226)$$

The state vectors are

$$\mathbf{z}_I = [x, y, z, \theta_x, \theta_y, \theta_z, m_x, m_y, m_z, q_x, q_y, q_z, q^1, q^2, \dots, q^n, 1]^T$$

The transfer matrix is

$$\mathbf{U} = \begin{bmatrix} \mathbf{I}_3 & \mathbf{O}_{3 \times 3} & \mathbf{O}_{3 \times 3} & \mathbf{U}_{14} & \mathbf{O}_{3 \times n} & \mathbf{O}_{3 \times 1} \\ \mathbf{U}_{21} & \mathbf{U}_{22} & \mathbf{U}_{23} & \mathbf{U}_{24} & \mathbf{U}_{25} & \mathbf{U}_{26} \\ \mathbf{O}_{3 \times 3} & \mathbf{O}_{3 \times 3} & \mathbf{I}_3 & \mathbf{O}_{3 \times 3} & \mathbf{O}_{3 \times n} & \mathbf{O}_{3 \times 1} \\ \mathbf{O}_{3 \times 3} & \mathbf{O}_{3 \times 3} & \mathbf{O}_{3 \times 3} & \mathbf{I}_3 & \mathbf{O}_{3 \times n} & \mathbf{O}_{3 \times 1} \\ \mathbf{U}_{51} & \mathbf{U}_{52} & \mathbf{U}_{53} & \mathbf{U}_{54} & \mathbf{U}_{55} & \mathbf{U}_{56} \\ \mathbf{O}_{1 \times 3} & \mathbf{O}_{1 \times 3} & \mathbf{O}_{1 \times 3} & \mathbf{O}_{1 \times 3} & \mathbf{O}_{1 \times n} & 1 \end{bmatrix} \quad (8.227)$$

where $\mathbf{U}_{14} = -\mathbf{K}^{-1}$.

8.12.2 Transfer Matrix of a Spring Hinge whose Inboard Body is a Rigid Body and whose Outboard Body is a Beam

For a spring hinge whose inboard body is a rigid body and whose outboard body is a beam, the orientation angles $\theta'_{j,j+1}$ of the spring hinge at the input end are the orientation angles of its inboard rigid body. According to the derivation of the transfer matrix of a spring hinge whose inboard and outboard bodies are beams, the transfer matrix of a spring hinge whose inboard body is a rigid body and whose outboard body is a beam can be obtained by eliminating the columns corresponding to the generalized coordinates of the inboard beam in Equation (8.227). Therefore, the transfer equation of a spring hinge whose inboard body is a rigid body and whose outboard body is a beam is

$$\mathbf{z}_O = \mathbf{U} \mathbf{z}_I \quad (8.228)$$

The state vectors are

$$\begin{aligned} \mathbf{z}_I &= [x, y, z, \theta_x, \theta_y, \theta_z, m_x, m_y, m_z, q_x, q_y, q_z, 1]^T \\ \mathbf{z}_O &= [x, y, z, \theta_x, \theta_y, \theta_z, m_x, m_y, m_z, q_x, q_y, q_z, q^1, q^2, \dots, q^n, 1]^T \end{aligned}$$

The transfer matrix is

$$\mathbf{U} = \begin{bmatrix} \mathbf{I}_3 & \mathbf{O}_{3 \times 3} & \mathbf{O}_{3 \times 3} & \mathbf{U}_{14} & \mathbf{O}_{3 \times 1} \\ \mathbf{U}_{21} & \mathbf{U}_{22} & \mathbf{U}_{23} & \mathbf{U}_{24} & \mathbf{U}_{26} \\ \mathbf{O}_{3 \times 3} & \mathbf{O}_{3 \times 3} & \mathbf{I}_3 & \mathbf{O}_{3 \times 3} & \mathbf{O}_{3 \times 1} \\ \mathbf{O}_{3 \times 3} & \mathbf{O}_{3 \times 3} & \mathbf{O}_{3 \times 3} & \mathbf{I}_3 & \mathbf{O}_{3 \times 1} \\ \mathbf{U}_{51} & \mathbf{U}_{52} & \mathbf{U}_{53} & \mathbf{U}_{54} & \mathbf{U}_{56} \\ \mathbf{O}_{1 \times 3} & \mathbf{O}_{1 \times 3} & \mathbf{O}_{1 \times 3} & \mathbf{O}_{1 \times 3} & 1 \end{bmatrix} \quad (8.229)$$

where the meanings of all elements are the same as those in Equation (8.227).

8.12.3 Transfer Matrix of a Spring Hinge whose Inboard Body is a Beam and whose Outboard Body is a Rigid Body

For a spring hinge whose inboard body is a beam and whose outboard body is a rigid body, the orientation angles $\theta'_{j+2,j+1}$ of the spring hinge at the output end are exactly the orientation angles of its outboard rigid body. According to the derivation of the transfer matrix of a spring hinge whose inboard and outboard bodies are beams, let $\mathbf{L}_{j+2} = \mathbf{O}_{3 \times n}$, so from Equation (8.223) we obtain

$$\begin{bmatrix} \theta_x \\ \theta_y \\ \theta_z \end{bmatrix}_{j+2} = \begin{bmatrix} \theta_x \\ \theta_y \\ \theta_z \end{bmatrix}_j + \mathbf{K}'^{-1} \mathbf{m}_I + \mathbf{L}_j \begin{bmatrix} q^1 \\ q^2 \\ \vdots \\ q^n \end{bmatrix}_j \quad (8.230)$$

According to Equations (8.214) and (8.223), the transfer equation of a spring hinge whose inboard body is a Euler–Bernoulli beam and whose outboard body is a rigid body is

$$\mathbf{z}_O = \mathbf{U} \mathbf{z}_I \quad (8.231)$$

The state vectors are

$$\mathbf{z}_I = [x, y, z, \theta_x, \theta_y, \theta_z, m_x, m_y, m_z, q_x, q_y, q_z, q^1, q^2, \dots, q^n, 1]^T$$

$$\mathbf{z}_O = [x, y, z, \theta_x, \theta_y, \theta_z, m_x, m_y, m_z, q_x, q_y, q_z, 1]^T$$

The transfer matrix is

$$\mathbf{U} = \begin{bmatrix} \mathbf{I}_3 & \mathbf{O}_{3 \times 3} & \mathbf{O}_{3 \times 3} & \mathbf{U}_{14} & \mathbf{O}_{3 \times n} & \mathbf{O}_{3 \times 1} \\ \mathbf{O}_{3 \times 3} & \mathbf{I}_3 & \mathbf{K}'^{-1} & \mathbf{O}_{3 \times 3} & \mathbf{L}_j & \mathbf{O}_{3 \times 1} \\ \mathbf{O}_{3 \times 3} & \mathbf{O}_{3 \times 3} & \mathbf{I}_3 & \mathbf{O}_{3 \times 3} & \mathbf{O}_{3 \times n} & \mathbf{O}_{3 \times 1} \\ \mathbf{O}_{3 \times 3} & \mathbf{O}_{3 \times 3} & \mathbf{O}_{3 \times 3} & \mathbf{I}_3 & \mathbf{O}_{3 \times n} & \mathbf{O}_{3 \times 1} \\ \mathbf{O}_{1 \times 3} & \mathbf{O}_{1 \times 3} & \mathbf{O}_{1 \times 3} & \mathbf{O}_{1 \times 3} & \mathbf{O}_{1 \times n} & 1 \end{bmatrix} \quad (8.232)$$

where the meanings of \mathbf{U}_{14} , \mathbf{K}'^{-1} and \mathbf{L}_j are the same as in Equations (8.227) and (8.223).

8.13 Algorithm of the Discrete Time Transfer Matrix Method for Multi-flexible-body Systems

The algorithm for the computer solution of MRFS dynamics using the DTTMM for MRFSs can be described as follows:

- 1) Establish a floating coordinate system for each flexible element in the system, determine the numbers of generalized coordinates which describe the deformation of flexible elements, and determine the initial conditions and boundary conditions of the system. Let $i = 1$.
- 2) Compute the linearization coefficients A, B_z or \mathbf{B}_z, C, D_z or $\mathbf{D}_z, A, \Phi, T_1, T_2, T_3, \bar{s}, \bar{c}$ and so on for each element at time t_i by linearization approach, and determine the initial conditions of the generalized coordinates and the system parameters at time t_i .
- 3) Obtain the transfer matrix for each element and the overall transfer matrix of the system at time t_i .
- 4) Apply the boundary conditions and the overall transfer matrix to compute the unknown quantities of the boundary state vectors at time t_i .
- 5) Obtain the state vectors of all elements at time t_i by computing the transfer equations of each element successively.
- 6) Use the state vectors at time t_i to compute the position coordinates, the rotation angle and the generalized coordinates which describe the deformation of the flexible elements, then solve their first-order and second-order derivatives with respect to time.
- 7) Use the modal analysis method to solve the deformation of the flexible element at the investigated positions.
- 8) Let $i = i + 1$, use the computational results of the last step as the initial conditions and repeat all the above steps from step (2) until the time required for complete analysis.

8.14 Planar Multi-flexible-body System Dynamics

Example 8.1 A three-pendulum system moves in a plane composed of rigid body 2, beam 4 and rigid body 6, which are connected with smooth hinge, as shown in Figure 8.6. The system parameters are $EI = 2.22\text{N}\cdot\text{m}^2$, $m_2 = m_4 = m_6 = 1\text{kg}$, $l_2 = l_4 = l_6 = 1\text{m}$. Simulate the system dynamics under the effect of the gravity if the initial conditions are

$$\theta_2(0) = \theta_4(0) = \theta_6(0) = -\frac{\pi}{3} \text{ rad}, \quad \dot{\theta}_2(0) = \dot{\theta}_4(0) = \dot{\theta}_6(0) = 0 \text{ rad/s}.$$

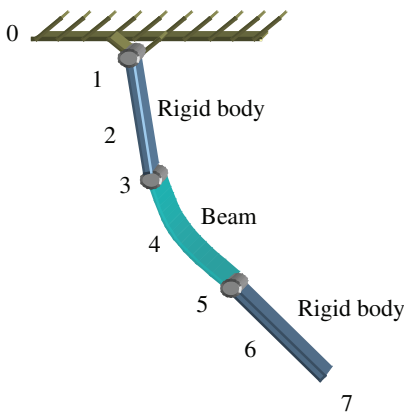


Figure 8.6 Three-pendulum model of a multi-rigid-flexible system.

Solution

The state vectors of the system are

$$\begin{cases} \mathbf{z}_{4,3} = [x, y, \theta, m, q_x, q_y, q^1, q^2, q^3, 1]^T_{4,3} \\ \mathbf{z}_{2,3} = [x, y, \theta, m, q_x, q_y, 1]^T_{2,3} \end{cases} \quad (8.233)$$

$$\begin{cases} \mathbf{z}_{6,5} = [x, y, \theta, m, q_x, q_y, 1]^T_{6,5} \\ \mathbf{z}_{4,5} = [x, y, \theta, m, q_x, q_y, q^1, q^2, q^3, 1]^T_{4,5} \end{cases} \quad (8.234)$$

The boundary conditions are

$$\begin{cases} \mathbf{z}_{2,1} = [0, 0, \theta, 0, q_x, q_y, 1]^T_{2,1} \\ \mathbf{z}_{6,7} = [x, y, \theta, 0, 0, 0, 1]^T_{6,7} \end{cases} \quad (8.235)$$

The overall transfer equation of system yields

$$\mathbf{z}_{6,7} = \mathbf{U}_6 \mathbf{U}_5 \mathbf{U}_4 \mathbf{U}_3 \mathbf{U}_2 \mathbf{z}_{2,1} = \mathbf{U} \mathbf{z}_{2,1} \quad (8.236)$$

where the transfer matrix of beam \mathbf{U}_4 is determined by Equation (8.90), and the transfer matrices \mathbf{U}_6 and \mathbf{U}_2 of the rigid bodies are determined by Equation (8.101). The transfer matrix \mathbf{U}_3 of a smooth hinge whose inboard body is a rigid body and whose outboard body is a beam is determined by Equation (8.101). The transfer matrix \mathbf{U}_5 of a smooth hinge whose inboard body is a beam and whose outboard body is a rigid body is determined by Equation (8.105).

For comparison with ordinary methods of multibody system dynamics, the global dynamic equations of the system using the Newton–Euler method are as follows:

$$\begin{aligned} & \ddot{\theta}_2(t) (J_{c2} + m_2 a_2^2 + m_4 l_2^2 + m_6 l_2^2) \\ & + \ddot{\theta}_4(t) \left\{ \left(m_6 + \frac{m_4}{2} \right) l_2 l_4 \cos[\theta_4(t) - \theta_2(t)] - m_4 l_2 \left[\sum_{k=1}^{\infty} \frac{1 - (-1)^k}{k\pi} q^k(t) \right] \sin[\theta_4(t) - \theta_2(t)] \right\} \\ & + \ddot{\theta}_6(t) m_6 l_2 a_6 \cos[\theta_6(t) - \theta_2(t)] + m_4 l_2 \left[\sum_{k=1}^{\infty} \frac{1 - (-1)^k}{k\pi} \ddot{q}^k(t) \right] \cos[\theta_4(t) - \theta_2(t)] \\ & = - (a_2 m_2 + l_2 m_4 + l_2 m_6) g \cos \theta_2(t) \\ & + \dot{\theta}_2^2(t) \left\{ \left(m_6 + \frac{m_4}{2} \right) l_2 l_4 \sin[\theta_4(t) - \theta_2(t)] + m_4 l_2 \left[\sum_{k=1}^{\infty} \frac{1 - (-1)^k}{k\pi} \dot{q}^k(t) \right] \cos[\theta_4(t) - \theta_2(t)] \right\} \\ & + \dot{\theta}_6^2(t) m_6 l_2 a_6 \sin[\theta_6(t) - \theta_2(t)] + 2 m_4 l_2 \dot{\theta}_4(t) \left[\sum_{k=1}^{\infty} \frac{1 - (-1)^k}{k\pi} \dot{q}^k(t) \right] \sin[\theta_4(t) - \theta_2(t)] \end{aligned} \quad (8.237)$$

$$\begin{aligned}
& \ddot{\theta}_2(t) \left\{ \left(m_6 + \frac{m_4}{2} \right) l_2 l_4 \cos[\theta_4(t) - \theta_2(t)] - m_4 l_2 \left[\sum_{k=1}^{\infty} \frac{1 - (-1)^k}{k\pi} q^k(t) \right] \sin[\theta_4(t) - \theta_2(t)] \right\} \\
& + \ddot{\theta}_4(t) \left[\left(m_6 + \frac{m_4}{3} \right) l_4^2 + \frac{m_4}{2} \sum_{k=1}^{\infty} q^k(t)^2 \right] + \ddot{\theta}_6(t) m_6 l_4 a_6 \cos[\theta_6(t) - \theta_4(t)] \\
& + m_4 l_4 \left[\sum_{k=1}^{\infty} \frac{(-1)^{k+1}}{k\pi} + \frac{[(-1)^{k+1} - 2] l_4}{(k\pi)^3} \right] \ddot{q}_k(t) = -m_4 \dot{\theta}_4(t) \left[\sum_{k=1}^{\infty} q^k(t) \dot{q}^k(t) \right] \\
& - \dot{\theta}_2^2(t) \left\{ \left(m_6 + \frac{m_4}{2} \right) l_2 l_4 \sin[\theta_4(t) - \theta_2(t)] + m_4 l_2 \left[\sum_{k=1}^{\infty} \frac{1 - (-1)^k}{k\pi} q^k(t) \right] \cos[\theta_4(t) - \theta_2(t)] \right\} \\
& + \dot{\theta}_6^2(t) m_6 l_4 a_6 \sin[\theta_6(t) - \theta_4(t)] - \left(\frac{m_4}{2} + m_4 \right) l_4 g \cos \theta_4(t)
\end{aligned} \tag{8.238}$$

$$\begin{aligned}
& m_6 l_2 a_6 \ddot{\theta}_2(t) \cos[\theta_6(t) - \theta_2(t)] + m_6 l_4 a_6 \ddot{\theta}_4(t) \cos[\theta_6(t) - \theta_4(t)] + (J_{c6} + m_6 a_6^2) \ddot{\theta}_6(t) \\
& = -m_6 a_6 l_2 \dot{\theta}_2^2(t) \sin[\theta_4(t) - \theta_2(t)] - m_6 l_4 a_6 \dot{\theta}_4^2(t) \sin[\theta_6(t) - \theta_4(t)] - m_6 a_6 g \cos \theta_6(t)
\end{aligned} \tag{8.239}$$

$$\begin{aligned}
& \frac{1 - (-1)^k}{k\pi} m_4 l_2 \cos[\theta_4(t) - \theta_2(t)] \ddot{\theta}_2(t) - \frac{(-1)^k}{k\pi} m_4 l_4 \ddot{\theta}_4(t) + \left(\rho I \frac{k^2 \pi^2}{2l_4} + \frac{m_4}{2} \right) \ddot{q}^k(t) \\
& = -\frac{1 - (-1)^k}{k\pi} m_4 g \cos \theta_4(t) + \dot{\theta}_4^2(t) q^k(t) \left(\frac{m_4}{2} + \rho I \frac{k^2 \pi^2}{2l_4} \right) \\
& - \frac{1 - (-1)^k}{k\pi} m_4 l_2 \sin[\theta_4(t) - \theta_2(t)] - EI \frac{k^4 \pi^4}{2l_4^3} q^k(t) \quad (k = 1, 2, 3, \dots, n)
\end{aligned} \tag{8.240}$$

The time history simulation of three planar pendulums of rigid and flexible bodies obtained using the DTTMM for multibody systems and the Newton–Euler method are shown in Figure 8.7. The results show that the computational results obtained by the two methods are in good agreement, which shows the validity and high computational efficiency of the DTTMM for the multibody system dynamics of multi-rigid-flexible-body systems.

Example 8.2 A dynamic model of a planar four-bar linkage, composed of rigid body 1, beam 3 and rigid body 5 connected with smooth hinges, is shown in Figure 8.8. The structural parameters of the system are

$$\begin{aligned}
\rho_1 = \rho_3 = \rho_5 &= 2.7 \times 10^3 \text{ kg/m}^3, \\
A_1 = A_3 = A_5 &= 4.0 \times 10^{-5} \text{ m}^2, EI = 0.931 \text{ N} \cdot \text{m}^2, l_3 = l_5 = 3l_1 = 30 \text{ cm}
\end{aligned}$$

The distance between hinges 0 and 6 is 40 cm. Rigid body 1 moves with angular velocity $\dot{\theta}_1 = 30 \text{ rad/s}$ rotating around smooth hinge 0. Simulate the system dynamics under the following initial conditions:

$$\theta_1(0) = 0 \text{ rad}, \quad \theta_3(0) = \frac{\pi}{3} \text{ rad}, \quad \theta_5(0) = -\frac{\pi}{3} \text{ rad}, \quad \dot{\theta}_3(0) = \dot{\theta}_5(0) = -10 \text{ rad/s},$$

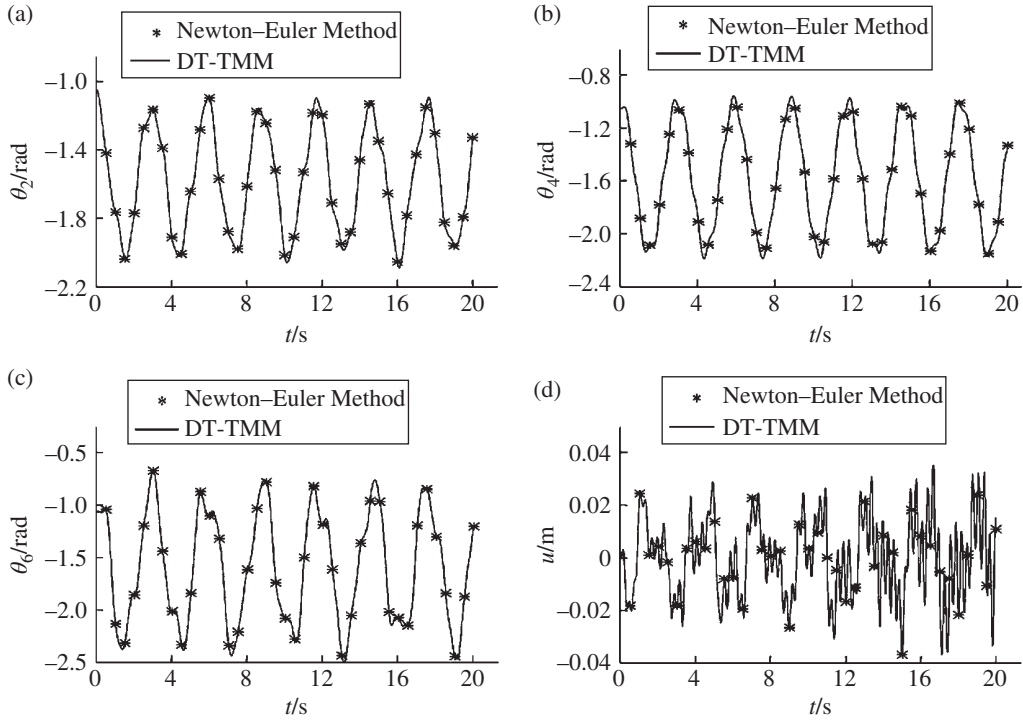


Figure 8.7 Time history of the dynamics of three pendulums moving in a plane: (a) orientation angle of rigid body 2, (b) orientation angle of the floating frame, (c) orientation angle of rigid body 6 and (d) deformation in the mid-point of the beam.

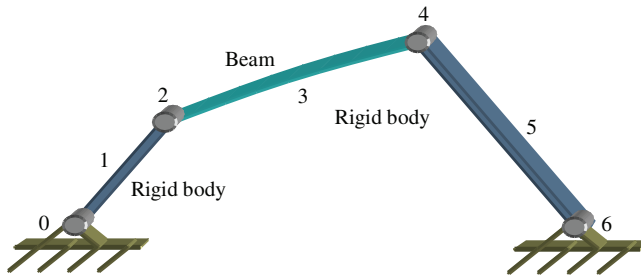


Figure 8.8 Dynamics model of a rigid-flexible four-bar linkage.

Solution

The state vectors of the system are

$$\begin{cases} \mathbf{z}_{3,2} = [x, y, \theta, m, q_x, q_y, q^1, q^2, q^3, 1]^T_{5,4} \\ \mathbf{z}_{1,2} = [x, y, \theta, m, q_x, q_y, 1]^T_{1,2} \end{cases} \quad (8.241)$$

$$\begin{cases} \mathbf{z}_{5,4} = [x, y, \theta, m, q_x, q_y, 1]_{5,4}^T \\ \mathbf{z}_{5,4} = [x, y, \theta, m, q_x, q_y, q^1, q^2, q^3, 1]_{5,4}^T \end{cases} \quad (8.242)$$

The boundary conditions are

$$\begin{cases} \mathbf{z}_{1,0} = [0, 0, \theta_1(t_i), m, q_x, q_y, 1]_{1,0}^T \\ \mathbf{z}_{5,6} = [x_{0,6}, 0, \theta, 0, q_x, q_y, 1]_{5,6}^T \end{cases} \quad (8.243)$$

The overall transfer equation of system becomes

$$\mathbf{z}_{5,6} = \mathbf{U}_5 \mathbf{U}_4 \mathbf{U}_3 \mathbf{U}_2 \mathbf{U}_1 \mathbf{z}_{1,0} \quad (8.244)$$

where \mathbf{U}_2 , \mathbf{U}_3 and \mathbf{U}_4 are expressed in Equations (8.101), (8.90) and (8.105), respectively. \mathbf{U}_1 and \mathbf{U}_5 are expressed in Equation (8.101).

The computational results obtained by the DTTMM for the multibody system and the Newton–Euler method are shown in Figure 8.9. These two methods show good agreement and validate the DTTMM for multibody system dynamics of multi-rigid-flexible-body systems.

8.15 Spatial Multi-flexible-body System Dynamics

Example 8.3 A dynamic model of three pendulums in a rigid-flexible-body system composed of rigid body 2, beam 4 and rigid body 6, which are connected with smooth hinges moving in space under the effect of the gravity, is shown in Figure 8.10. The structure parameters are $m_2 = m_6 = 1\text{kg}$, $\rho_4 = 3.3 \times 10^3 \text{kg/m}^3$, $m_4 = 1.32\text{kg}$ and $E_4 = 2.5 \times 10^{10} \text{N/m}^2$.

$$\begin{bmatrix} x \\ y \\ z \end{bmatrix}_{2,C} = \begin{bmatrix} x \\ y \\ z \end{bmatrix}_{4,C} = \begin{bmatrix} x \\ y \\ z \end{bmatrix}_{6,C} = \begin{bmatrix} 0.5 \\ 0.0 \\ 0.0 \end{bmatrix} \text{m}, \quad \begin{bmatrix} x \\ y \\ z \end{bmatrix}_{2,O} = \begin{bmatrix} x \\ y \\ z \end{bmatrix}_{4,O} = \begin{bmatrix} x \\ y \\ z \end{bmatrix}_{6,O} = \begin{bmatrix} 1.0 \\ 0.0 \\ 0.0 \end{bmatrix} \text{m}$$

$$\mathbf{J}_2 = \mathbf{J}_6 = \begin{bmatrix} \frac{1}{6} & 0 & 0 \\ 0 & \frac{5}{12} & 0 \\ 0 & 0 & \frac{5}{12} \end{bmatrix} \text{kg} \cdot \text{m}^2, \quad \mathbf{J}_4 = \begin{bmatrix} 8.8 \times 10^{-5} & 0 & 0 \\ 0 & 0.44 & 0 \\ 0 & 0 & 0.44 \end{bmatrix} \text{kg} \cdot \text{m}^2$$

Simulate the system dynamics under the following initial conditions:

$$\begin{bmatrix} \theta_x \\ \theta_y \\ \theta_z \end{bmatrix}_{2,1} = \begin{bmatrix} \theta_x \\ \theta_y \\ \theta_z \end{bmatrix}_{4,3} = \begin{bmatrix} \theta_x \\ \theta_y \\ \theta_z \end{bmatrix}_{6,5} = \begin{bmatrix} 0 \\ 0 \\ 0 \end{bmatrix} \text{rad}, \quad \begin{bmatrix} \dot{\theta}_x \\ \dot{\theta}_y \\ \dot{\theta}_z \end{bmatrix}_{2,1} = \begin{bmatrix} \dot{\theta}_x \\ \dot{\theta}_y \\ \dot{\theta}_z \end{bmatrix}_{4,3} = \begin{bmatrix} 0 \\ 0 \\ 0 \end{bmatrix} \text{rad/s}, \quad \begin{bmatrix} \dot{\theta}_x \\ \dot{\theta}_y \\ \dot{\theta}_z \end{bmatrix}_{6,5} = \begin{bmatrix} 0 \\ 0.1 \\ 0 \end{bmatrix} \text{rad/s}$$

Solution

The overall transfer equation of the system is

$$\mathbf{z}_{6,7} = \mathbf{U}_6 \mathbf{U}_5 \mathbf{U}_4 \mathbf{U}_3 \mathbf{U}_2 \mathbf{z}_{2,1} = \mathbf{U} \mathbf{z}_{2,1} \quad (8.245)$$

where \mathbf{U}_2 and \mathbf{U}_6 are expressed in Equation (8.174), \mathbf{U}_4 is expressed in Equation (8.186), \mathbf{U}_3 is expressed in Equation (8.207) and \mathbf{U}_5 is expressed in Equation (8.246).

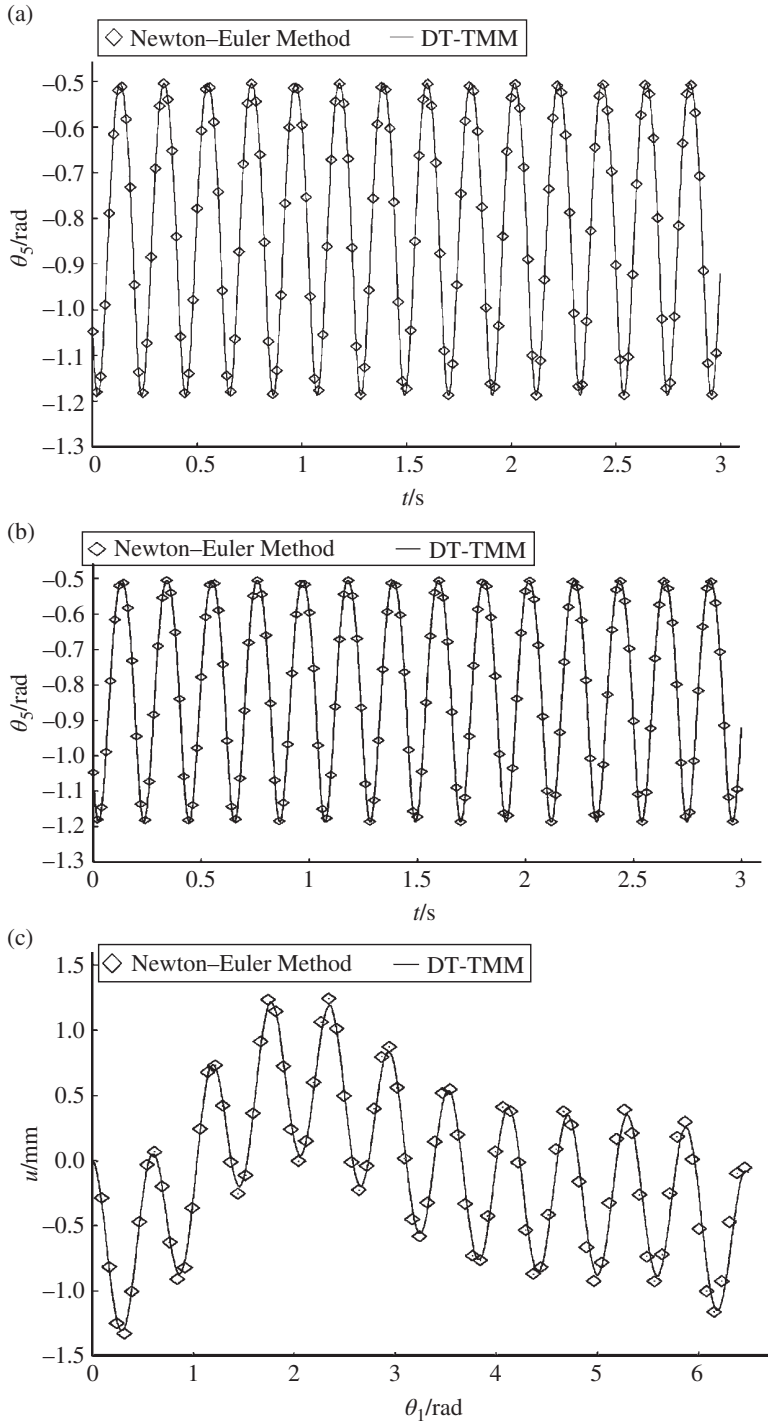


Figure 8.9 Time history of the dynamics of a rigid-flexible four-bar linkage moving in a plane: (a) orientation angle of rigid body 5, (b) orientation angle of beam 4 and (c) deformation in the mid-point of the beam 4.

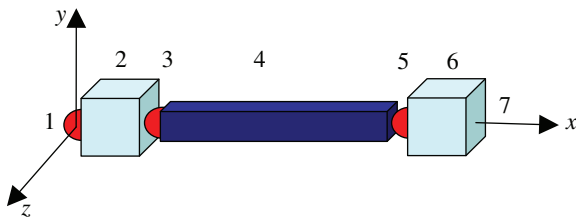


Figure 8.10 Model of a rigid-flexible-body system composed of three pendulums moving in space.

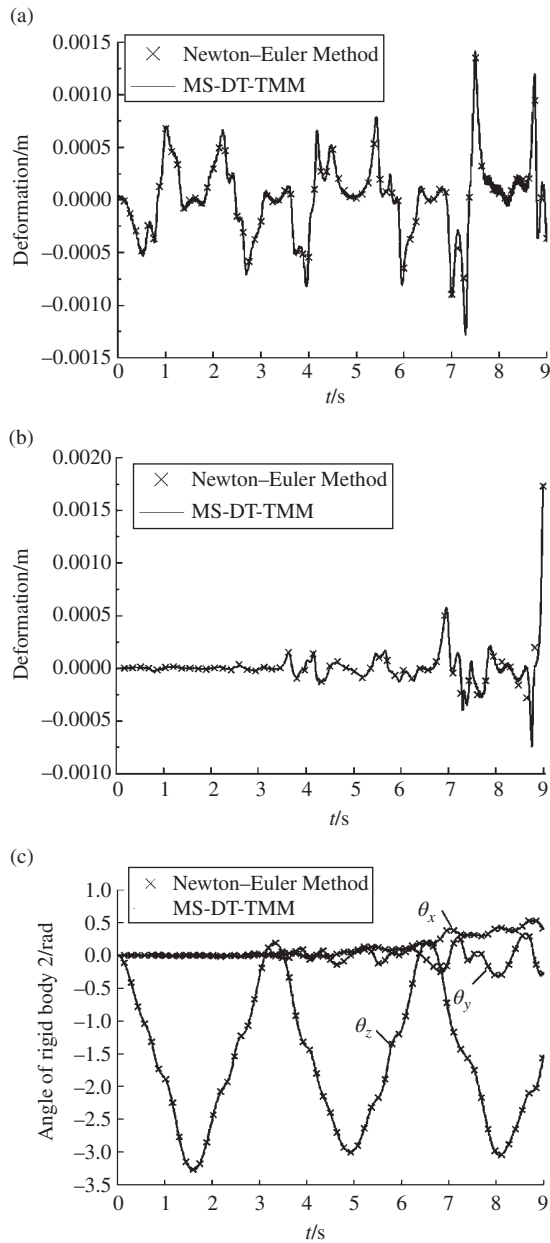


Figure 8.11 Time history of the dynamics of three pendulums moving in space: (a) deformation in the mid-point of beam 4, (b) deformation of beam 4 in z_2 , (c) angle of rigid body 2, (d) angle of floating frame of beam 4 and (e) angle of rigid body 6.

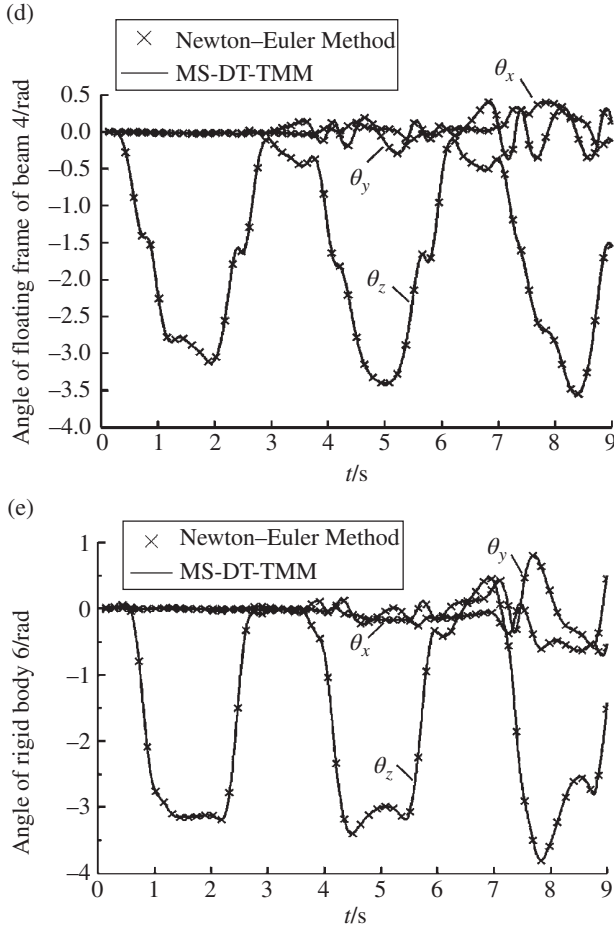


Figure 8.11 (Continued)

$$\mathbf{U}_5 = \begin{bmatrix} \mathbf{I}_3 & \mathbf{O}_{3 \times 3} & \mathbf{O}_{3 \times 3} & \mathbf{O}_{3 \times 3} & \mathbf{O}_{3 \times 3} & \mathbf{O}_{3 \times 3} & \mathbf{O}_{3 \times 1} \\ -\mathbf{U}_{3,2}^{-1} \mathbf{U}_{3,1} & \mathbf{O}_{3 \times 3} & \mathbf{O}_{3 \times 3} & -\mathbf{U}_{3,2}^{-1} \mathbf{U}_{3,4} & \mathbf{O}_{3 \times 3} & \mathbf{O}_{3 \times 3} & -\mathbf{U}_{3,2}^{-1} \mathbf{U}_{3,5} \\ \mathbf{O}_{3 \times 3} & \mathbf{O}_{3 \times 3} & \mathbf{O}_{3 \times 3} & \mathbf{O}_{3 \times 3} & \mathbf{O}_{3 \times 3} & \mathbf{O}_{3 \times 3} & \mathbf{O}_{3 \times 1} \\ \mathbf{O}_{3 \times 3} & \mathbf{O}_{3 \times 3} & \mathbf{O}_{3 \times 3} & \mathbf{I}_3 & \mathbf{O}_{3 \times 3} & \mathbf{O}_{3 \times 3} & \mathbf{O}_{3 \times 1} \\ \mathbf{O}_{1 \times 3} & \mathbf{O}_{1 \times 3} & \mathbf{O}_{1 \times 3} & \mathbf{O}_{1 \times 3} & \mathbf{O}_{1 \times 3} & \mathbf{O}_{1 \times 3} & 1 \end{bmatrix} \quad (8.246)$$

where $\mathbf{U}_{3,1}$, $\mathbf{U}_{3,2}$, $\mathbf{U}_{3,4}$ and $\mathbf{U}_{3,5}$ are submatrices of the transfer matrix \mathbf{U}_6 and similar to Equation (8.172).

The boundary conditions of the system are

$$\begin{cases} \mathbf{z}_{2,1} = [0, 0, 0, \theta_x, \theta_y, \theta_z, 0, 0, 0, q_x, q_y, q_z, 1]_{2,1}^T \\ \mathbf{z}_{6,7} = [x, y, z, \theta_x, \theta_y, \theta_z, 0, 0, 0, 0, 0, 0, 1]_{6,7}^T \end{cases} \quad (8.247)$$

The results of the system dynamics obtained using the DTTMM for a multibody system and the Newton–Euler method are shown in Figure 8.11. The results of the DTTMM for a multibody system are denoted by the solid line and the results of the Newton–Euler method are denoted by \times . It can be seen that the results obtained by two methods are in good agreement, which validates the DTTMM for multibody system dynamics of multi-rigid-flexible-body systems moving in space.

9

Transfer Matrix Method for Controlled Multibody Systems

9.1 Introduction

Research on the dynamics of multibody systems began more than 40 years ago and international commercial software based on a great many theories and methods for multibody systems has been developed. The transfer matrix method for multibody systems (MSTMM) does not need global dynamic equations of the system and has a lot of advantages, such as easy modeling, high programming stylization and high computational efficiency. In principle, the MSTMM can be combined with any other mechanics method, including all kinds of multibody system dynamics methods, the finite element method (FEM), the classic mechanics method and the analytical mechanics method, so that the advantages of different methods can be exploited. The MSTMM can be combined with all kinds of software to improve its computational speed. Precise performance prediction and effective controls of the multibody system are very important in control engineering problems, especially in fields such as the firing control of the launch system of high-performance weapons, spatial structure control and robots. Because the problems are complex and the computation speed for the multi-rigid-flexible-body system (MRFS) is too slow to satisfy the required response time for quick control, the dynamic models of multibody systems have to be simplified when dealing with those problems, and the model error needs to be compensated for through complex control design. The excessive simplification of the dynamic model usually results in difficulty when predicting the dynamic law of the system and the redundant high-frequency behavior of the system, and therefore the control precision of the system is deeply affected. For example, when the firing control system of the launch system of a modern weapon is designed, the launch system is modeled as a simple multi-rigid-body system, where the deformation vibration of the system is not considered, resulting in poor control precision and low sensitivity. The best way to solve this problem is to introduce the dynamic method of a controlled multibody system which describes the dynamic of an MRFS perfectly and also satisfies the demand for rapid computation speed for real-time control. The modeling of the multibody system and the controller are established synchronously and completely.

In this chapter, the following methods developed by the authors will be introduced: the mixed transfer matrix method for multibody systems and other multibody system dynamic methods [71, 72], the mixed MSTMM and the FEM [76], the finite segment discrete time MSTMM [81], the linear transfer matrix method (TMM) for controlled multibody systems [77], the discrete time TMM for controlled multibody systems [78] and the Riccati discrete time MSTMM [78, 80]. These methods make it easier to study the dynamics of multi-dimensional systems and complex structures by using the MSTMM.

9.2 Mixed Transfer Matrix Method for Multibody Systems

In this section, the mixed TMM for multibody systems and other multibody system dynamic methods [71, 72] developed by the authors is introduced. In this method, any multibody system can be decomposed into subsystems, and the connection relation among the subsystems can be regarded as the boundary of each subsystem, as if the other subsystems do not exist. We usually establish the “global” dynamic equations using the ordinary method of multibody system dynamics for some subsystems and the “overall” transfer equation using the MSTMM for other subsystems. The unknown state variables on these “boundary subsystems” are considered to be external forces in the subsystem handled by the ordinary dynamic method and the internal forces in the subsystem handled by the MSTMM. Combining the global dynamic equations (usually hybrid differential-algebra equations) with the overall transfer equations (algebra equations), the corresponding equations of the overall system can be assembled. Once all the global dynamic equations and the overall transfer equations of an MRFS are solved, the time history of the system dynamics can be obtained. It is an advantage of the method that each subsystem can adopt an optimum mathematic model and software.

The main steps for a numerical algorithm that can be used to solve MRFSs using the mixed MSTMM and other multibody system dynamics methods can be summarized as follows:

- 1) Give the system parameters and the initial state parameters etc.
- 2) Set the simulation step sequence number $i = 1$ (discrete time step).
- 3) According to the angular coordinates of a rigid body and their first- and second-order derivatives with respect to time at time t_{i-1} , calculate the coefficients for the step-by-step time integration method at time t_i and estimate the angular coordinates of a rigid body at time t_i . Take this as the initial value of the next iterative procedure.
- 4) Set the iterative variable $j = 1$.
- 5) Regard the motion state of a rigid body as the boundary condition of a flexible body and compute the dynamic response of a flexible body using the multibody system dynamic method.
- 6) Set the iterative variable for the angular coordinates of the rigid body $k = 1$.
- 7) Compute the transfer matrices of each body element and hinge element.
- 8) Assemble the overall transfer equations according to the structure of the system.
- 9) Regard the boundary conditions of the system and the motion state and force state of the subsystem boundary as the boundary conditions of the overall transfer equations. Solve the overall transfer equations to obtain the state variable of each element at time t_i .
- 10) Judge the convergence criterion. If the square sum of the errors of all angular coordinates of rigid bodies from the k th to the $(k - 1)$ th iterations is bigger than the required supposed precision value or the iterative loop does not reach the given iteration number, set $k = k + 1$ and return to (7).
- 11) Compute the end-point velocity, the acceleration of each element and the first- and second-order derivatives with respect to time of the rigid-body angular coordinates using the step-by-step time integration method.
- 12) Let $j = j + 1$. If j does not reach the required times, return to (5).
- 13) If the required simulation time has been reached, exit the program; if not, let $i = i + 1$ and return to (3).

The following two examples are given to validate the proposed method.

Example 9.1 A multibody system is composed of one reticulated lumped mass-spring system and four rigid bodies connected by smooth hinges, as shown in Figure 9.1. One end of the rigid body 1 is connected to the fixed point through the smooth hinge. The initial positions of this system are shown in Figure 9.1, and the initial velocities are zero. Determine the vertical-plane motion of the system under the effect of gravity using the mixed MSTMM and other multibody system dynamics methods.

Solution

This system is decomposed into five subsystems: body subsystem 1, reticulated lumped mass-spring subsystem 2, body subsystem 3, body subsystem 4 and body subsystem 5. The dynamic equations of reticulated lumped mass-spring subsystem 2 are obtained by the Newton–Euler method, and for bodies 1, 3, 4 and 5 the corresponding transfer equations can be assembled by the TMM for multibody systems. As shown in Figure 9.2, the reticulated lumped mass-spring subsystem 2 is a set of particles connected by springs. $m_{i,j}$ denotes the lumped mass and its mass in the i th row and j th column, $K_{i,(j,j+1)}$ denotes the spring and its elastic coefficient between the j th column and the $(j+1)$ th column in the i th row, $K_{(i,i+1),j}$ denotes the spring and its spring coefficient between the i th row and the $(i+1)$ th row in the j th column, and $\mathbf{r}(t) = [x_{i,j}(t), y_{i,j}(t)]^T$ denotes the position vector of particle $m_{i,j}$ at time t in the inertia coordinate system.

According to the force analysis of particles shown in Figure 9.3, the equations of motion of the set of lumped mass can be obtained

$$m_{i,j}\ddot{\mathbf{r}}_{i,j}(t) = \mathbf{F}_{i-1,j} + \mathbf{F}_{i+1,j} + \mathbf{F}_{i,j-1} + \mathbf{F}_{i,j+1} + \mathbf{F}_{i,j} \quad (i = 1, 2, \dots, 5; j = 1, 2, \dots, 5) \quad (a)$$

where $\mathbf{F}_{i-1,j}$, $\mathbf{F}_{i+1,j}$, $\mathbf{F}_{i,j-1}$ and $\mathbf{F}_{i,j+1}$ are the elastic forces of the springs, respectively, and $\mathbf{F}_{i,j}$ is the external force.

The initial conditions are

$$\mathbf{r}_{i,j}(0) = \begin{bmatrix} x_{i,j}(0) \\ y_{i,j}(0) \end{bmatrix} = \begin{bmatrix} x_{i,j,0} \\ y_{i,j,0} \end{bmatrix}, \quad \dot{\mathbf{r}}_{i,j}(0) = \begin{bmatrix} \dot{x}_{i,j}(0) \\ \dot{y}_{i,j}(0) \end{bmatrix} = \begin{bmatrix} 0 \\ 0 \end{bmatrix} \quad (b)$$

where $x_{i,j,0}$ and $y_{i,j,0}$ are the initial position coordinates of the lumped mass $m_{i,j}$.

For $i-1=0$, $i+1=6$, $j-1=0$ and $j+1=6$, the corresponding elastic forces of springs are zeros

$$\begin{aligned} \mathbf{F}_{0,j} &= \begin{bmatrix} 0 \\ 0 \end{bmatrix}, \quad \mathbf{F}_{6,j} = \begin{bmatrix} 0 \\ 0 \end{bmatrix} \quad (j = 1, 2, \dots, 5) \\ \mathbf{F}_{i,0} &= \begin{bmatrix} 0 \\ 0 \end{bmatrix}, \quad \mathbf{F}_{i,6} = \begin{bmatrix} 0 \\ 0 \end{bmatrix} \quad (i = 1, 2, \dots, 5) \end{aligned} \quad (c)$$

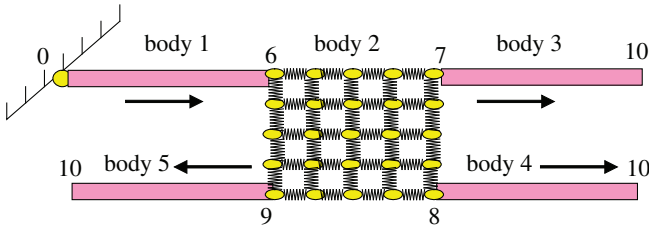


Figure 9.1 MRFS model with a reticulated particle-spring system.

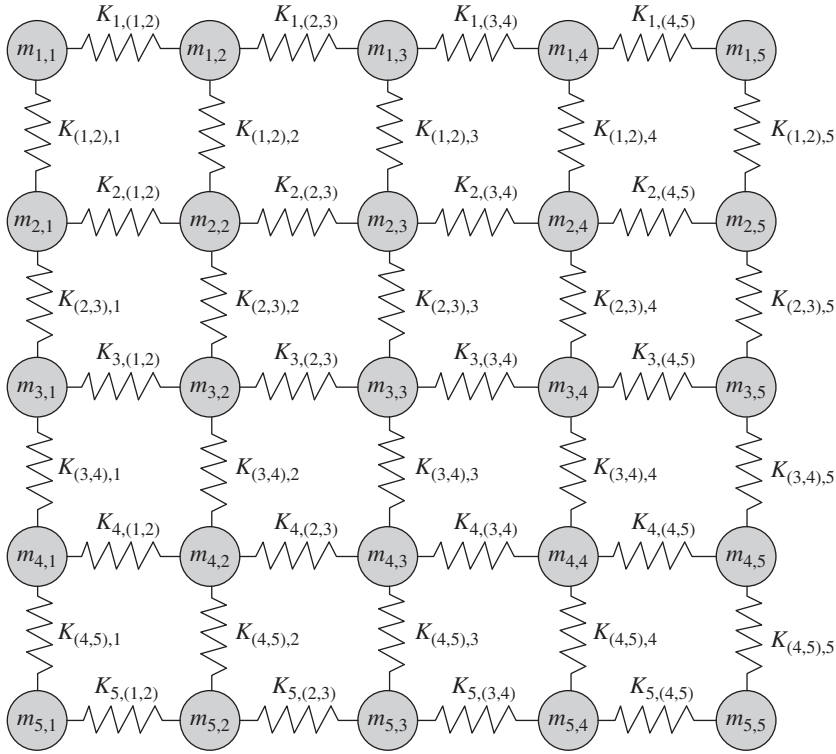


Figure 9.2 Reticulated lumped mass-spring system.

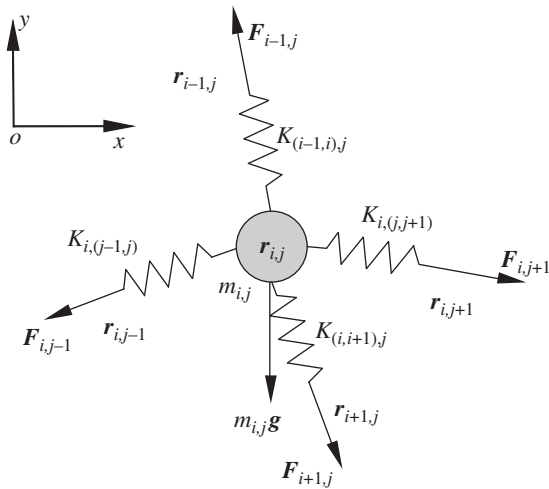


Figure 9.3 Force analysis of a lumped mass.

As an example, $F_{i-1,j}$ is used to show the computation procedure of the elastic force of the spring

$$F_{i-1,j} = -K_{(i-1,i),j} (|\mathbf{r}_{i-1,j} - \mathbf{r}_{i,j}| - |\mathbf{r}_{i-1,j} - \mathbf{r}_{i,j}|_{t=0}) \frac{\mathbf{r}_{i-1,j} - \mathbf{r}_{i,j}}{|\mathbf{r}_{i-1,j} - \mathbf{r}_{i,j}|} \quad (d)$$

Denoting $L_{(i-1,i),j}$ as the spring length at time t and $L_{(i-1,i),j,0}$ as the initial length of the spring gives

$$L_{(i-1,i),j} = |\mathbf{r}_{i-1,j} - \mathbf{r}_{i,j}| = \sqrt{(x_{i-1,j} - x_{i,j})^2 + (y_{i-1,j} - y_{i,j})^2} \quad (e)$$

$$L_{(i-1,i),j,0} = |\mathbf{r}_{i-1,j} - \mathbf{r}_{i,j}|_{t=0} = \sqrt{(x_{i-1,j,0} - x_{i,j,0})^2 + (y_{i-1,j,0} - y_{i,j,0})^2} \quad (f)$$

$$F_{i-1,j} = -K_{(i-1,i),j} \begin{bmatrix} (x_{i-1,j} - x_{i,j}) \\ (y_{i-1,j} - y_{i,j}) \end{bmatrix} \left(1 - \frac{L_{(i-1,i),j,0}}{L_{(i-1,i),j}} \right) \quad (g)$$

According to Equation (g), the elastic forces of the other springs can be obtained as follows:

$$\begin{aligned} F_{i+1,j} &= -K_{(i,i+1),j} \begin{bmatrix} (x_{i+1,j} - x_{i,j}) \\ (y_{i+1,j} - y_{i,j}) \end{bmatrix} \left(1 - \frac{L_{(i,i+1),j,0}}{L_{(i,i+1),j}} \right) \\ F_{i,j-1} &= -K_{i,(j-1),j} \begin{bmatrix} (x_{i,j-1} - x_{i,j}) \\ (y_{i,j-1} - y_{i,j}) \end{bmatrix} \left(1 - \frac{L_{i,(j-1),j,0}}{L_{i,(j-1),j}} \right) \\ F_{i,j+1} &= -K_{i,(j,j+1)} \begin{bmatrix} (x_{i,j+1} - x_{i,j}) \\ (y_{i,j+1} - y_{i,j}) \end{bmatrix} \left(1 - \frac{L_{i,(j,j+1),0}}{L_{i,(j,j+1)}} \right) \end{aligned} \quad (h)$$

The external forces $F_{i,j}$ acting on the lumped mass $m_{1,1}$, $m_{1,5}$, $m_{5,1}$ and $m_{5,5}$ can be written as

$$\begin{aligned} F_{1,1} &= \begin{bmatrix} q_{x1,6} \\ q_{y1,6} - m_{i,j}g \end{bmatrix}, \quad F_{1,5} = \begin{bmatrix} -q_{x3,7} \\ -q_{y3,7} - m_{i,j}g \end{bmatrix}, \\ F_{5,1} &= \begin{bmatrix} -q_{x4,8} \\ -q_{y4,8} - m_{i,j}g \end{bmatrix}, \quad F_{5,5} = \begin{bmatrix} -q_{x5,9} \\ -q_{y5,9} - m_{i,j}g \end{bmatrix} \end{aligned} \quad (i)$$

The external force acting on the other lumped mass can be written as

$$F_{i,j} = \begin{bmatrix} 0 \\ -m_{i,j}g \end{bmatrix} \quad (j)$$

The external forces acting on the “boundary” of the reticulated lumped mass-spring subsystem 2 include the interaction forces between bodies 1, 3, 4 and 5 and subsystem 2. These external forces are part of the state variables of the boundary state of subsystems 1, 3, 4 and 5.

The transfer equations of bodies 1, 3, 4 and 5 can be written as

$$\mathbf{z}_{1,6} = \mathbf{U}_1 \mathbf{z}_{1,10}, \quad \mathbf{z}_{3,10} = \mathbf{U}_3 \mathbf{z}_{3,7}, \quad \mathbf{z}_{4,10} = \mathbf{U}_4 \mathbf{z}_{4,8}, \quad \mathbf{z}_{5,10} = \mathbf{U}_5 \mathbf{z}_{5,9} \quad (k)$$

where \mathbf{U}_1 , \mathbf{U}_3 , \mathbf{U}_4 and \mathbf{U}_5 are the transfer matrices of bodies 1, 3, 4 and 5, respectively, and they are all the transfer matrices of a planar rigid body with one input and one output end, as shown in Equation (7.102). $\mathbf{z}_{1,0}$, $\mathbf{z}_{3,10}$, $\mathbf{z}_{4,10}$, $\mathbf{z}_{5,10}$ are the boundary state vectors of the system:

$$z_{1,0} = \begin{bmatrix} 0 \\ 0 \\ \theta \\ 0 \\ q_x \\ q_y \\ 1 \end{bmatrix}_{1,0}, \quad z_{3,10} = \begin{bmatrix} x \\ y \\ \theta \\ 0 \\ 0 \\ 0 \\ 1 \end{bmatrix}_{3,10}, \quad z_{4,10} = \begin{bmatrix} x \\ y \\ \theta \\ 0 \\ 0 \\ 0 \\ 1 \end{bmatrix}_{4,10}, \quad z_{5,10} = \begin{bmatrix} x \\ y \\ \theta \\ 0 \\ 0 \\ 0 \\ 1 \end{bmatrix}_{5,10} \quad (1)$$

$$z_{1,6} = \begin{bmatrix} x \\ y \\ \theta \\ 0 \\ q_x \\ q_y \\ 1 \end{bmatrix}_{1,6}, \quad z_{3,7} = \begin{bmatrix} 0 \\ 0 \\ \theta \\ 0 \\ q_x \\ q_y \\ 1 \end{bmatrix}_{3,7}, \quad z_{4,8} = \begin{bmatrix} 0 \\ 0 \\ \theta \\ 0 \\ q_x \\ q_y \\ 1 \end{bmatrix}_{4,8}, \quad z_{5,9} = \begin{bmatrix} 0 \\ 0 \\ \theta \\ 0 \\ q_x \\ q_y \\ 1 \end{bmatrix}_{5,9} \quad (m)$$

$z_{1,6}$, $z_{3,7}$, $z_{4,8}$ and $z_{5,9}$ are the boundary state vectors of the subsystems, and the state variables in these state vectors denote the internal forces that exist in the dynamic equations of the flexible body.

Substituting the boundary conditions into the transfer equations of the subsystem, the sum of the number of unknown variables in the independent algebra equations and the dynamic equations of the subsystem is equal to the number of equations. The system motion is determined by solving the simultaneous equations. The mass of each lumped mass is 0.04 kg and the elastic coefficient of each spring is 10 kN/m. Four rods are exactly the same, the mass center of each rod is its geometry center, the mass is 1 kg, the length is 1 m, each inertia moment with respect to the mass center is $1/12 \text{ kg} \cdot \text{m}^2$, the initial velocity of each rod is zero, and the initial position is shown in Figure 9.1. The results obtained by using the mixed MSTMM and other multibody system dynamics methods are shown in Figure 9.4. Figure 9.4h shows that the conservation of mechanical energy holds, which indicates that the method used in this section has high computation stability and computation accuracy.

Example 9.2 Replace the reticulated lumped mass-spring system shown in Example 9.1 by a flexible plate. The results obtained by the mixed MSTMM and the multibody system dynamics method are shown in Figure 9.5. In the computation process, the flexible plate is simplified as lumped masses, as shown in Figure 9.6. Figure 9.7 shows the positions of the system at time 0.5 s in Example 9.1 and in this example.

Example 9.3 An MRFS composed of rigid rods, springs and lumped mass is shown in Figure 9.8. One end of rigid body 2 is connected to fixed point through a smooth hinge. The system is horizontal and undeformed at the initial time, and the initial velocities are zero. Determine the vertical plane motion of the system under the effect of gravity using the mixed MSTMM and another multibody system dynamics method.

Solution

The MRFS is decomposed into three subsystems: the lumped mass-spring subsystem 4, body subsystem 2 and body subsystem 6. The lumped mass-spring subsystem 4 is computed by the Newton–Euler method, and bodies 2 and 6 can be computed by MSTMM.

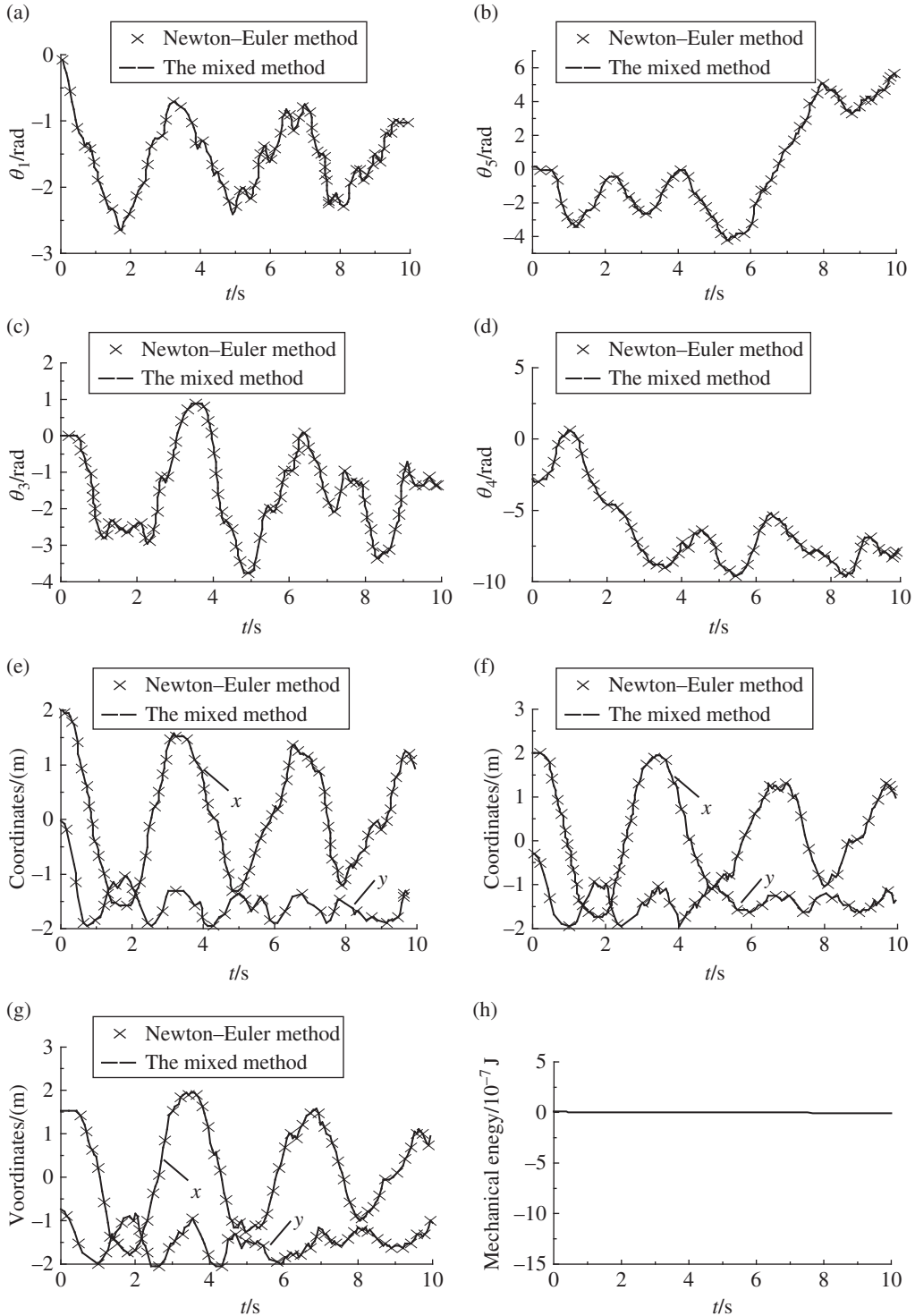


Figure 9.4 Dynamic simulation of a multibody system with a reticulated particle-spring system: (a) rotation angle of rigid body 1, (b) rotation angle of rigid body 5, (c) rotation angle of rigid body 3, (d) rotation angle of rigid body 4, (e) coordinates of particle 2, (f) coordinates of particle 17, (g) coordinates of particle 24 and (h) total mechanical energy of the system.

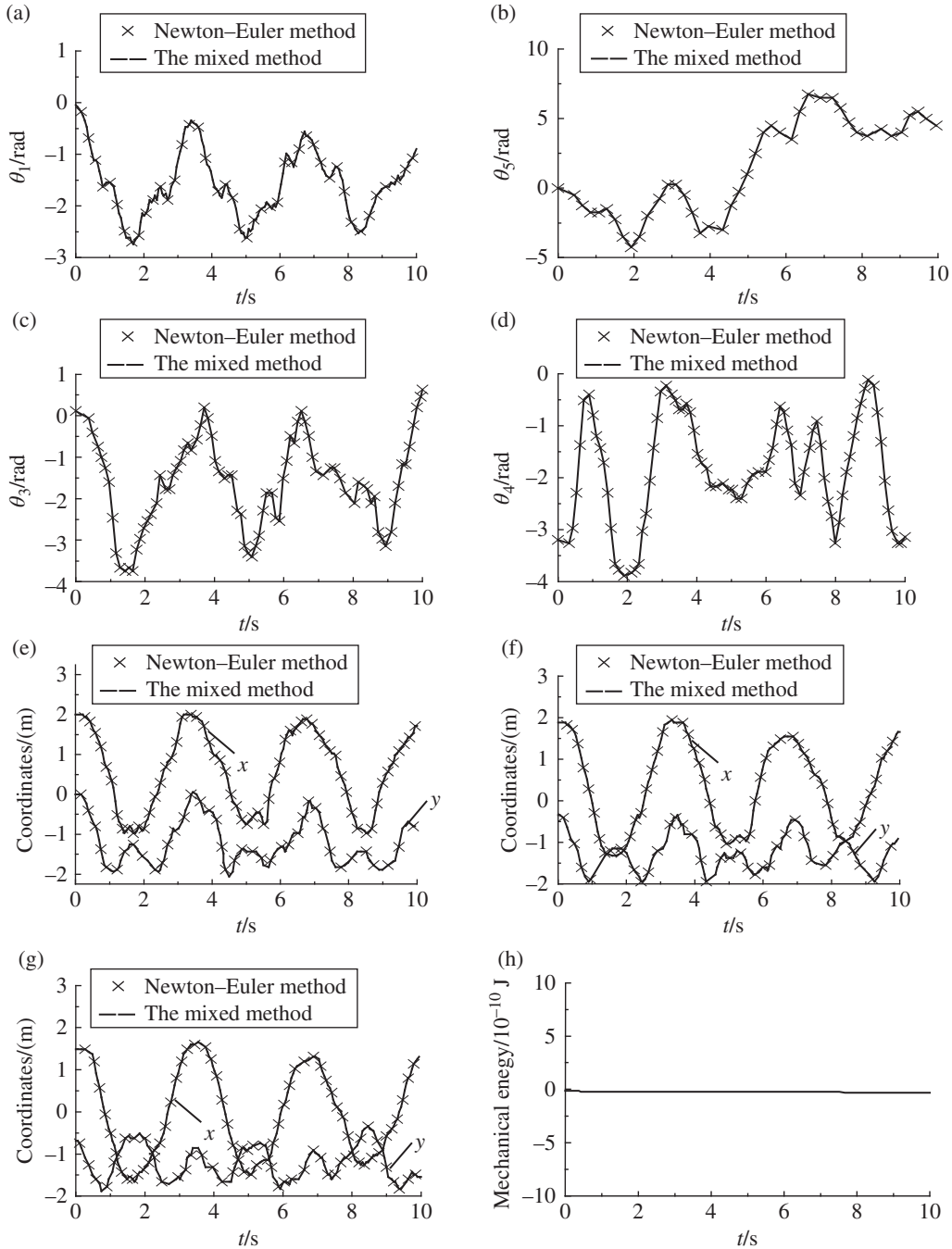


Figure 9.5 Dynamic simulation of a multibody system with a plate: (a) rotation angle of rigid body 1, (b) rotation angle of rigid body 5, (c) rotation angle of rigid body 3, (d) rotation angle of rigid body 4, (e) coordinates of particle 2, (f) coordinates of particle 17, (g) coordinates of particle 24 and (h) total mechanical energy of the system.

Figure 9.6 Equivalent flexible plate.

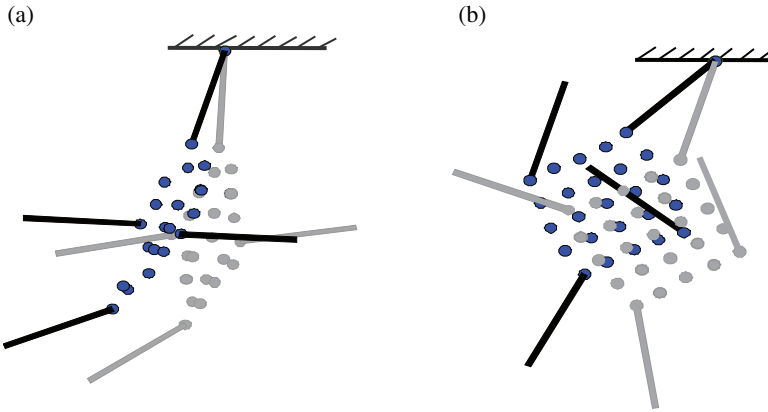
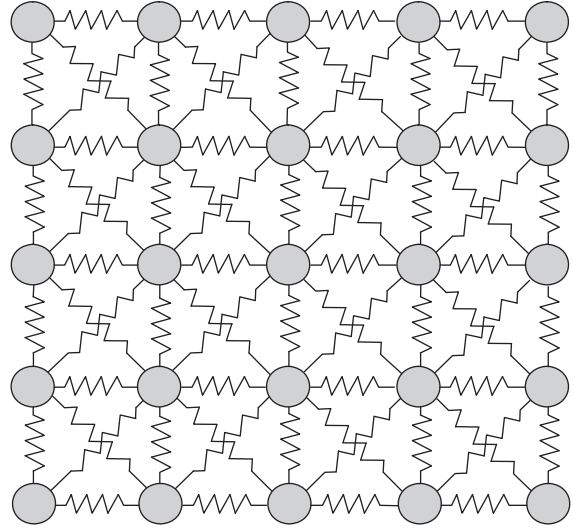


Figure 9.7 The positions of the system at 0.5 s in Examples 9.1 and 9.2: (a) system in Example 9.1 and (b) system in Example 9.2.

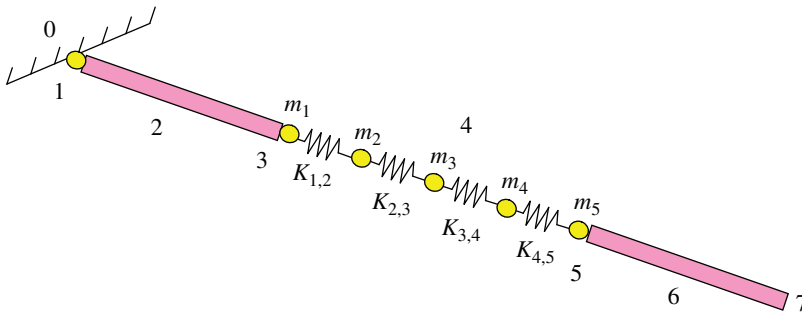


Figure 9.8 MRFS model.

Similarly to above example, the dynamic equations of lumped mass-spring subsystem 4 are

$$\begin{aligned}
 m_1 \begin{bmatrix} \ddot{x}_1(t) \\ \ddot{y}_1(t) \end{bmatrix} &= -K_{(1,2)} \begin{bmatrix} (x_2 - x_1) \\ (y_2 - y_1) \end{bmatrix} \left(1 - \frac{L_{(1,2),0}}{\sqrt{(x_2 - x_1)^2 + (y_2 - y_1)^2}} \right) + \begin{bmatrix} q_{x2,3} \\ q_{y2,3} - m_4 g \end{bmatrix} \\
 m_i \begin{bmatrix} \ddot{x}_i(t) \\ \ddot{y}_i(t) \end{bmatrix} &= -K_{(i-1,i)} \begin{bmatrix} (x_{i-1} - x_i) \\ (y_{i-1} - y_i) \end{bmatrix} \left(1 - \frac{L_{(i-1,i),0}}{\sqrt{(x_{i-1} - x_i)^2 + (y_{i-1} - y_i)^2}} \right) \\
 &\quad - K_{(i,i+1)} \begin{bmatrix} (x_{i+1} - x_i) \\ (y_{i+1} - y_i) \end{bmatrix} \left(1 - \frac{L_{(i,i+1),0}}{\sqrt{(x_{i+1} - x_i)^2 + (y_{i+1} - y_i)^2}} \right) + \begin{bmatrix} 0 \\ -m_i g \end{bmatrix} \quad (i = 2, 3, 4) \\
 m_5 \begin{bmatrix} \ddot{x}_5(t) \\ \ddot{y}_5(t) \end{bmatrix} &= -K_{(4,5)} \begin{bmatrix} (x_4 - x_5) \\ (y_4 - y_5) \end{bmatrix} \left(1 - \frac{L_{(4,5),0}}{\sqrt{(x_4 - x_5)^2 + (y_4 - y_5)^2}} \right) + \begin{bmatrix} -q_{x6,5} \\ -q_{y6,5} - m_4 g \end{bmatrix}
 \end{aligned} \tag{a}$$

where m_i is the mass of lumped mass i , $K_{(i,i+1)}$ is the elastic coefficient of the spring between the j th lumped mass and the $(j+1)$ th lumped mass, $L_{(i,i+1),0}$ is the initial length of spring $K_{(i,i+1)}$, and $x_i(t)$ and $y_i(t)$ are the position coordinates of lumped mass i in the inertia coordinate system at time t .

The initial conditions are

$$\begin{bmatrix} x_i(0) \\ y_i(0) \end{bmatrix} = \begin{bmatrix} x_{i,0} \\ y_{i,0} \end{bmatrix}, \quad \begin{bmatrix} \dot{x}_i(0) \\ \dot{y}_i(0) \end{bmatrix} = \begin{bmatrix} 0 \\ 0 \end{bmatrix} \tag{b}$$

The transfer equations of subsystem bodies 2 and 6 are obtained by MSTMM

$$\mathbf{z}_{2,3} = \mathbf{U}_2 \mathbf{z}_{2,1}, \quad \mathbf{z}_{6,7} = \mathbf{U}_6 \mathbf{z}_{6,5} \tag{c}$$

where \mathbf{U}_2 and \mathbf{U}_6 are the transfer matrices of subsystem bodies 2 and 6, respectively, as shown in Equation (7.101).

The boundary conditions of the system are

$$\mathbf{z}_{2,1} = [0, 0, \theta, 0, q_x, q_y, 1]_{2,1}^T, \quad \mathbf{z}_{6,7} = [x, y, \theta, 0, 0, 0, 1]_{6,7}^T \tag{d}$$

The boundary conditions of the subsystem are

$$\mathbf{z}_{2,3} = [x, y, \theta, 0, q_x, q_y, 1]_{2,3}^T, \quad \mathbf{z}_{6,5} = [x, y, \theta, 0, q_x, q_y, 1]_{6,5}^T \tag{e}$$

The mass of each lumped mass is 0.2 kg, the elastic coefficient of each spring is 10 kN/m, the mass center of each rigid body is the geometry center, and the mass is 1 kg. The length is 1 m. Each inertia moment with respect to the mass center is $1/12 \text{ kg} \cdot \text{m}^2$. The time history of the system is computed using the mixed method (the MSTMM and the Newton–Euler method) and the Newton–Euler method. The results are shown in Figure 9.9. In this figure, the numerical results obtained by the two methods show good agreement, which validates the efficiency of the mixed MSTMM and the Newton–Euler method for solving the dynamics of the MRFS.

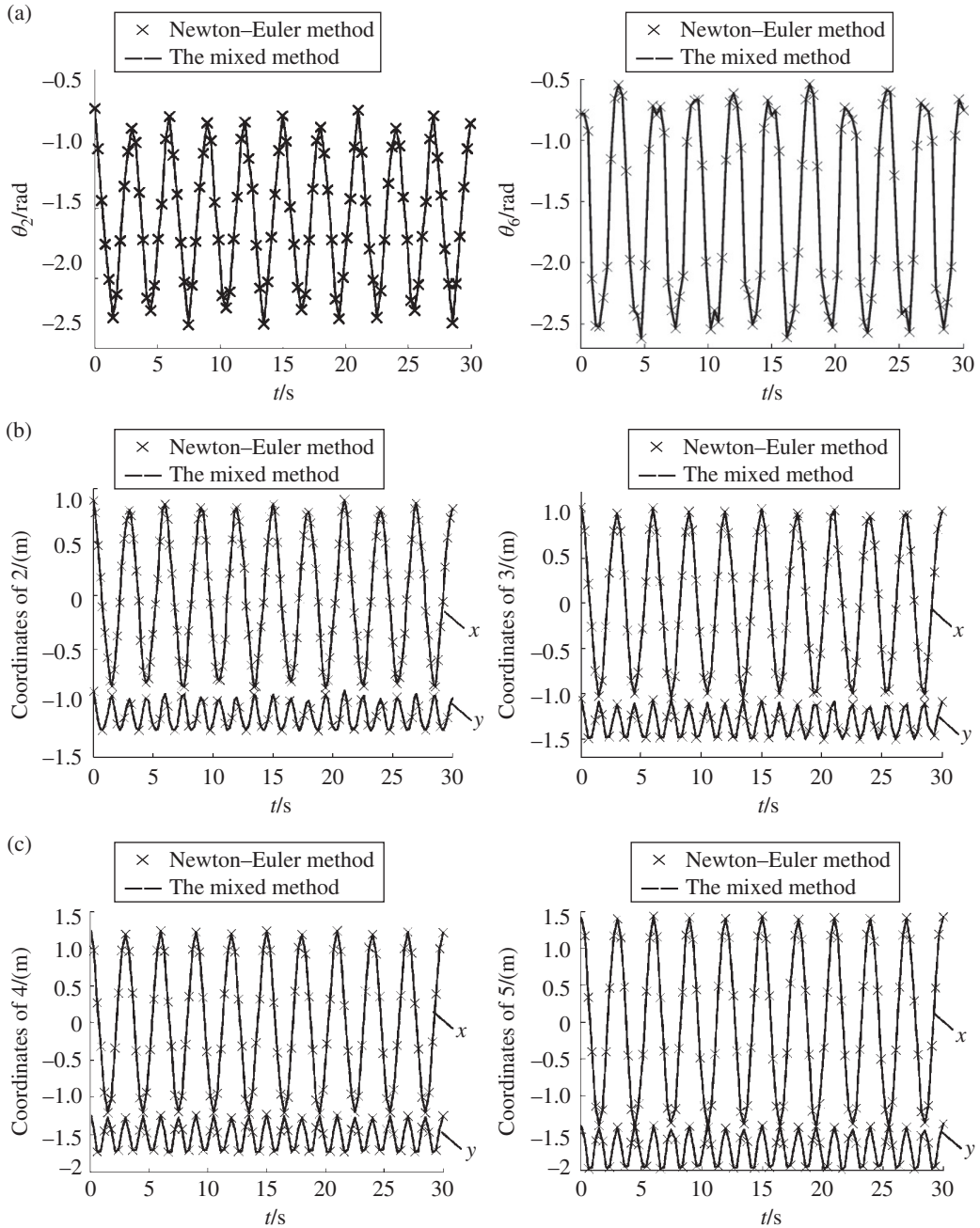


Figure 9.9 Time history of the dynamics of an MRFS: (a) time history of the rotations of rigid body 2 and rigid body 6, (b) coordinates of particle 2 and particle 3, and (c) coordinates of particle 4 and particle 5.

9.3 Finite Element Transfer Matrix Method for Multibody Systems

The dynamics of linear multibody systems are solved by combining the MSTMM and the FEM, and the FEM is “reconstructed” by the MSTMM, or the MSTMM is “reconstructed” by the FEM. The mixed MSTMM and the FEM [76] introduced in this section is different from the “reconstructed method” mentioned above. In the proposed method, the two independent methods are applied in different subsystems of the same multibody system, that is, the multibody system is divided into subsystems and each of these subsystems could be readily modeled by the MSTMM or the FEM. The overall transfer equation is obtained by the MSTMM, and the global dynamic equations of other two- or three-dimensional complex subsystems are obtained by the FEM. The subsequent processing method is the same as in section 9.2.

Example 9.4 As shown in Figure 9.10, the chain MRFS is composed of beam 1, smooth hinge 2, rigid rod 3, smooth hinge 4 and rigid rod 5. The left end of elastic rod 1 is fixed to the wall, and the right end of rod 5 is free. All the rods are initially placed in the horizontal position. Determine the dynamics of the system using the mixed MSTMM and the FEM.

Solution

The elastic rod 1 is regarded as subsystem 1 and computed by the FEM. Elements 2, 3, 4 and 5 are regarded as subsystem 2 and computed by the MSTMM.

Elastic rod 1 is regarded as an Euler–Bernoulli beam with only transverse deformation, the dynamic equation of beam 1 is established by the FEM, and the process is as follows.

As shown in Figure 9.11, the Euler–Bernoulli beam is divided into four elements, and the transverse displacement $v(x, t)$ of any point on the beam can be denoted as

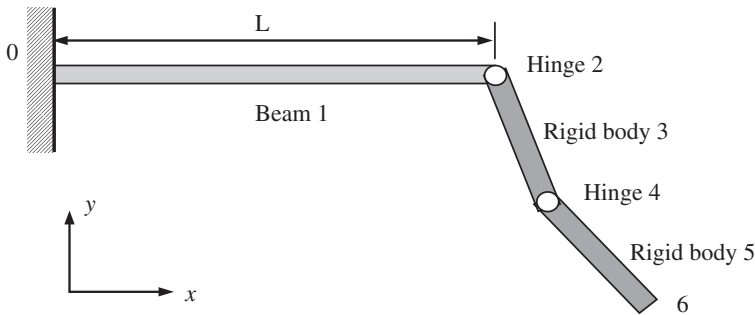


Figure 9.10 Chain MRFS.

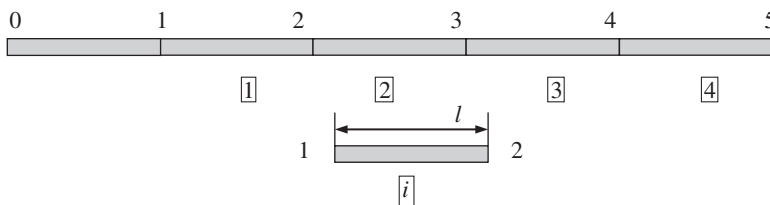


Figure 9.11 The element partition of beam 1.

$$v = \sum_{i=1}^4 \psi_i \delta_i \quad (a)$$

where ψ_i is the shape function and δ_i is the nodal coordinates.

Without loss of generality, δ_1 and δ_3 are regarded as the transverse deformations of nodes 1 and 2, respectively, $\delta_2 = \partial \delta_1 / \partial x$, $\delta_4 = \partial \delta_3 / \partial x$, thus ψ_i must satisfy the boundary conditions:

$$\begin{aligned} \psi_1(0) &= 1, \quad \psi_1'(0) = \psi_1'(l) = \psi_1''(l) = 0 \\ \psi_2'(0) &= 1, \quad \psi_2(0) = \psi_2(l) = \psi_2'(l) = 0 \\ \psi_3(l) &= 1, \quad \psi_3'(0) = \psi_3(0) = \psi_3'(l) = 0 \\ \psi_4'(l) &= 1, \quad \psi_4(0) = \psi_4(l) = \psi_4'(0) = 0 \end{aligned}$$

The strain energy and kinetic energy of a beam element are, respectively

$$\Pi^e = \frac{1}{2} \int_0^l EI \left(\frac{\partial^2 v}{\partial x^2} \right)^2 dx \quad (b)$$

$$T^e = \frac{1}{2} \int_0^l \bar{m} \left(\frac{\partial v}{\partial t} \right)^2 dx \quad (c)$$

where EI is bending stiffness, l is unit length and \bar{m} is the mass per unit length of the beam.

Let

$$v = c_1 + c_2 \frac{x}{l} + c_3 \left(\frac{x}{l} \right)^2 + c_4 \left(\frac{x}{l} \right)^3$$

According to the boundary conditions, we can obtain

$$\begin{aligned} \psi_1 &= 1 - 3 \left(\frac{x}{l} \right)^2 + 2 \left(\frac{x}{l} \right)^3, \quad \psi_2 = x - 2l \left(\frac{x}{l} \right)^2 + l \left(\frac{x}{l} \right)^3 \\ \psi_3 &= 3 \left(\frac{x}{l} \right)^2 - 2 \left(\frac{x}{l} \right)^3, \quad \psi_4 = -l \left(\frac{x}{l} \right)^2 + l \left(\frac{x}{l} \right)^3 \end{aligned}$$

Let

$$\boldsymbol{\delta} = [\delta_1, \delta_2, \delta_3, \delta_4]^T \quad (d)$$

Substituting Equation (a) into Equations (b) and (c)

$$\frac{\partial \Pi^e}{\partial \boldsymbol{\delta}} = \mathbf{k}^e \boldsymbol{\delta}, \quad \frac{\partial T^e}{\partial \boldsymbol{\delta}} = \mathbf{m}^e \boldsymbol{\delta}$$

the element stiffness matrix and element mass matrix can be obtained

$$k_{ij}^e = \int_0^l EI \psi_i'' \psi_j'' dx, \quad m_{ij}^e = \int_0^l \bar{m} \psi_i \psi_j dx$$

These equations can be expressed in matrix form as

$$\mathbf{k}^e = [k_{ij}^e] = \frac{EI}{l^3} \begin{bmatrix} 12 & 6l & -12 & 6l \\ 6l & 4l^2 & -6l & 2l^2 \\ -12 & -6l & 12 & -6l \\ 6l & 2l^2 & -6l & 4l^2 \end{bmatrix}, \quad \mathbf{m}^e = [m_{ij}^e] = \frac{\bar{m}l}{420} \begin{bmatrix} 156 & -22l & 54 & 13l \\ -22l & 4l^2 & -13l & -3l^2 \\ 54 & -6l & 156 & 22l \\ 13l & -3l^2 & 22l & 4l^2 \end{bmatrix} \quad (e)$$

The corresponding external force vector is

$$p_i^e = \int_0^l p(x_0, t) \psi_i dx$$

If we only consider the concentrated forces acting on the nodes, the node external force vector is

$$\mathbf{p}^e = [p_1^e, 0, p_2^e, 0]^T \quad (f)$$

Therefore, the dynamic equation of beam 1 is

$$\mathbf{M}\ddot{\boldsymbol{\delta}} + \mathbf{K}\boldsymbol{\delta} = \mathbf{P} \quad (g)$$

where

$$\mathbf{M} = \sum \mathbf{m}^e, \quad \mathbf{K} = \sum \mathbf{k}^e, \quad \mathbf{P} = \sum \mathbf{p}^e \quad (h)$$

When solving Equation (h), the element node displacement matrix is needed. For the partition mode shown in Figure 9.11, we can obtain

$$\begin{array}{c} 1 \quad \begin{bmatrix} 1 & 2 & 3 & 4 \end{bmatrix} \\ 2 \quad \begin{bmatrix} 2 & 3 & 4 & 5 \end{bmatrix} \\ \boxed{1} \quad \boxed{2} \quad \boxed{3} \quad \boxed{4} \end{array}$$

In this matrix, the row number and column number correspond to the element node number and element number, respectively. The matrix element is the global node number, denoted by \mathbf{B} . Let \mathbf{M} , \mathbf{K} and \mathbf{P} equal zero while computing, then the global stiffness matrix, global mass matrix and global external force vector can be obtained by the following loop:

DO I = 1, 5

$$k(2*\mathbf{B}(1, i) - 1:2*\mathbf{B}(1, i), 2*\mathbf{B}(1, i) - 1:2*\mathbf{B}(1, i)) = k(2*\mathbf{B}(1, i) - 1:2*\mathbf{B}(1, i), 2*\mathbf{B}(1, i) - 1:2*\mathbf{B}(1, i)) + kd(1:2, 1:2)$$

$$k(2*\mathbf{B}(1, i) - 1:2*\mathbf{B}(1, i), 2*\mathbf{B}(2, i) - 1:2*\mathbf{B}(2, i)) = k(2*\mathbf{B}(1, i) - 1:2*\mathbf{B}(1, i), 2*\mathbf{B}(2, i) - 1:2*\mathbf{B}(2, i)) + kd(1:2, 3:4)$$

$$k(2*\mathbf{B}(2, I) - 1:2*\mathbf{B}(2, I), 2*\mathbf{B}(1, I) - 1:2*\mathbf{B}(1, I)) = k(2*\mathbf{B}(2, I) - 1:2*\mathbf{B}(2, I), 2*\mathbf{B}(1, I) - 1:2*\mathbf{B}(1, I)) + kd(3:4, 1:2)$$

$$k(2*\mathbf{B}(2, I) - 1:2*\mathbf{B}(2, I), 2*\mathbf{B}(2, I) - 1:2*\mathbf{B}(2, I)) = k(2*\mathbf{B}(2, I) - 1:2*\mathbf{B}(2, I), 2*\mathbf{B}(2, I) - 1:2*\mathbf{B}(2, I)) + kd(3:4, 3:4)$$

$$m(2*\mathbf{B}(1, i) - 1:2*\mathbf{B}(1, i), 2*\mathbf{B}(1, i) - 1:2*\mathbf{B}(1, i)) = m(2*\mathbf{B}(1, i) - 1:2*\mathbf{B}(1, i), 2*\mathbf{B}(1, i) - 1:2*\mathbf{B}(1, i)) + md(1:2, 1:2)$$

$$m(2*\mathbf{B}(1, i) - 1:2*\mathbf{B}(1, i), 2*\mathbf{B}(2, i) - 1:2*\mathbf{B}(2, i)) = m(2*\mathbf{B}(1, i) - 1:2*\mathbf{B}(1, i), 2*\mathbf{B}(2, i) - 1:2*\mathbf{B}(2, i)) + md(1:2, 3:4)$$

$$m(2*\mathbf{B}(2, I) - 1:2*\mathbf{B}(2, I), 2*\mathbf{B}(1, I) - 1:2*\mathbf{B}(1, I)) = m(2*\mathbf{B}(2, I) - 1:2*\mathbf{B}(2, I), 2*\mathbf{B}(1, I) - 1:2*\mathbf{B}(1, I)) + md(3:4, 1:2)$$

$$m(2*\mathbf{B}(2, I) - 1:2*\mathbf{B}(2, I), 2*\mathbf{B}(2, I) - 1:2*\mathbf{B}(2, I)) = m(2*\mathbf{B}(2, I) - 1:2*\mathbf{B}(2, I), 2*\mathbf{B}(2, I) - 1:2*\mathbf{B}(2, I)) + md(3:4, 3:4)$$

$$p(2*\mathbf{b}(1, I) - 1:2*\mathbf{b}(1, I)) = p(2*\mathbf{b}(1, I) - 1:2*\mathbf{b}(1, I)) + pd(1:2)$$

$$p(2*\mathbf{b}(2, I) - 1:2*\mathbf{b}(2, I)) = p(2*\mathbf{b}(2, I) - 1:2*\mathbf{b}(2, I)) + pd(3:4)$$

ENDDO

Discretize Equation (g) using the Newmark- β method, thus

$$\mathbf{M}(\mathbf{A}\delta + \mathbf{B}\delta) + \mathbf{K}\delta = \mathbf{P} \Rightarrow (\mathbf{MA} + \mathbf{K})\delta = \mathbf{P} - \mathbf{MB}\delta \quad (\text{i})$$

For subsystem 2, the transfer equations of elements 3, 4 and 5 can be developed by the MSDTTMM

$$\mathbf{z}_{3,2} = \mathbf{U}_3 \mathbf{z}_{3,4}, \mathbf{z}_{3,4} = \mathbf{U}_4 \mathbf{z}_{5,4}, \mathbf{z}_{5,4} = \mathbf{U}_5 \mathbf{z}_{5,6} \quad (\text{j})$$

where \mathbf{U}_3 and \mathbf{U}_5 are the transfer matrices of elements 3 and 5, respectively, which are rigid bodies with one input and one output end moving in a plane, as shown in Equation (7.101). \mathbf{U}_4 is the transfer matrix of smooth hinge 4 moving in a plane which connects with the output ends of the rigid bodies and its internal torque is zero, as shown in Equation (7.230).

The overall transfer equation of the subsystem is

$$\mathbf{z}_{3,2} = \mathbf{U} \mathbf{z}_{5,6} \quad (\text{k})$$

The overall transfer matrix is

$$\mathbf{U} = \mathbf{U}_3 \mathbf{U}_4 \mathbf{U}_5 \quad (\text{l})$$

The smooth hinge 2 is the boundary of subsystem 2, that is

$$\mathbf{z}_{3,2} = [x, y, \theta, 0, q_x, q_y, 1]^T_{3,2} = [L, \delta_9, \theta_{3,2}, 0, q_{x3,2}, q_{y3,2}, 1]^T \quad (\text{m})$$

The boundary conditions of the system are

$$\mathbf{z}_{5,6} = [x, y, \theta, 0, 0, 0, 1]^T_{5,6}, \mathbf{z}_{1,0} = [0, 0, 0, m, q_x, q_y, 1]^T_{1,0} \quad (\text{n})$$

Combining Equation (i) with Equation (j), we can obtain 14 equations for subsystems 1 and 2 with 14 unknown variables in them: δ_j ($j = 3, 4, \dots, 10$), $\theta_{3,2}$, $q_{x,3,2}$, $q_{y,3,2}$, $x_{6,5}$, $y_{6,5}$ and $\theta_{6,5}$. Applying the external force and the initial conditions, the dynamic equations of the system can be solved.

The length of the homogeneous and elastic steel rod 1 is 1 m, and its cross-section is square with length 1 cm. The density of rod 1 is $7.8 \times 10^3 \text{ kg/m}^3$ and the Young's modulus is $E = 2.1 \times 10^{11} \text{ N/m}^2$. The configuration parameters of rigid rods 3 and 5 are the same, the mass is 1 kg, the length is 1 m, the mass center is the geometry center of the rod and the inertia moment with respect to the mass center is $E = 1/12 \text{ kg}\cdot\text{m}^2$. The initial angles of the two rigid bodies are both $\pi/3 \text{ rad}$ with respect to the horizontal line and the angular velocities are zero. The beam lies in the horizontal under the effect of gravity and its velocity is zero. The system dynamics are solved by the mixed method (MSTMM and FEM) and the Newton–Euler method, as shown in Figures 9.12–9.18. The transverse displacement of the connected point between rigid body 3 and the beam is given in Figure 9.12. The transverse displacements of nodes 1, 2 and 3 of the beam are given in Figures 9.13–9.15, respectively. The time histories of the angular motion of rigid bodies 3 and 5 are given in Figures 9.16 and 9.17, respectively. The time history of the interaction forces between rigid body 3 and beam 1 is illustrated in Figure 9.18.

Observation reveals that the results obtained by the mixed method (MTMM and FEM) and the Newton–Euler method are in good agreement, which validates the efficiency of the mixed MSTMM and the FEM for solving the dynamic response of the MRFS.

9.4 Finite Segment Transfer Matrix Method for Multibody Systems

This section introduces the *finite segment discrete time transfer matrix method for multibody systems* [81], which was developed by the authors. The beam is divided into finite rigid segments by the finite segment method, and the segments are connected by a torsional spring and a linear

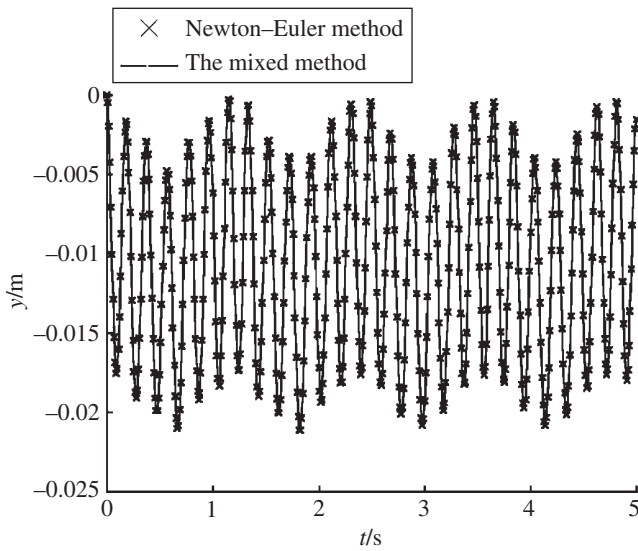


Figure 9.12 The transverse displacement of the connected point.

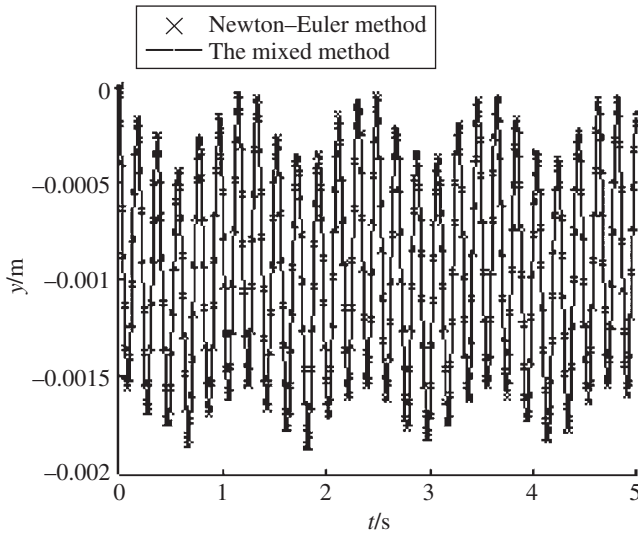


Figure 9.13 The transverse displacements of node 1 of the beam.

spring with a parallel damper. The inertia characteristic of the beam is described by a rigid segment, and the elasticity and damp characteristics are described by springs and dampers between the rigid segments, as shown in Figure 9.19. After being discretized by the finite segment method, the beam can be regarded as a chain-type MRS connected by springs and dampers. The finite segment model is similar to the continuous beam model, with an increase in the number of rigid segments.

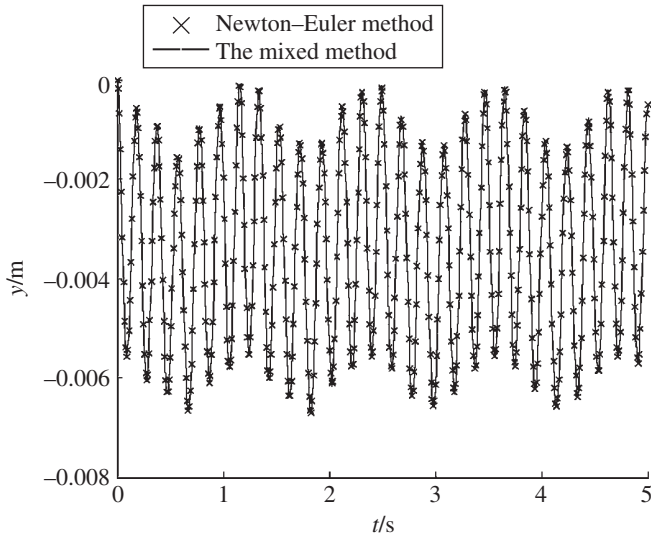


Figure 9.14 The transverse displacements of node 2 of the beam.

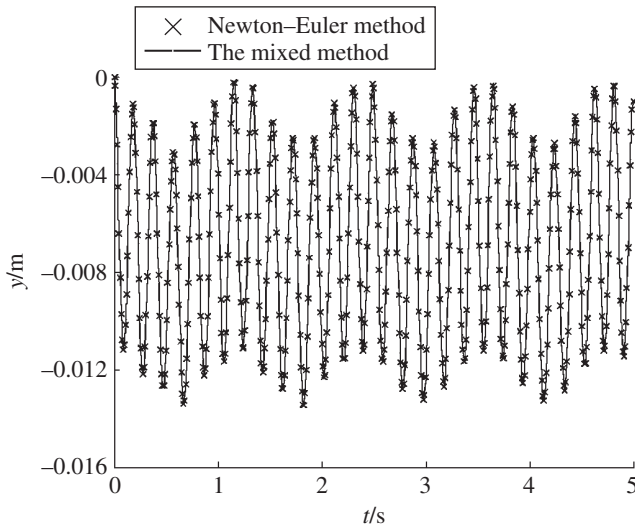


Figure 9.15 The transverse displacements of node 3 of the beam.

The stiffness coefficient of each spring connecting the segments can be determined as follows. The relation between the internal moment of the beam and the rotation angle generated by bending the beam can be obtained according to Euler–Bernoulli beam theory,

$$M = EI \frac{\partial \theta}{\partial x} \quad (9.1)$$

where M is the internal moment of the beam, EI is the bending stiffness and θ is the rotation angle generated by bending the beam.

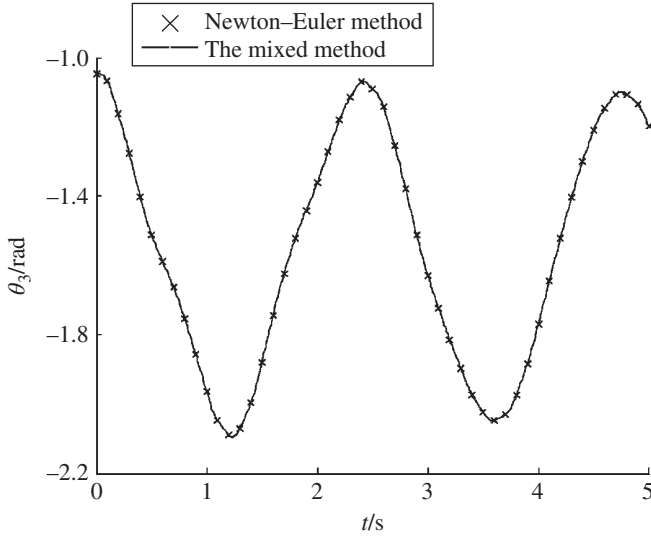


Figure 9.16 Time history of the azimuth angle of rigid body 3.

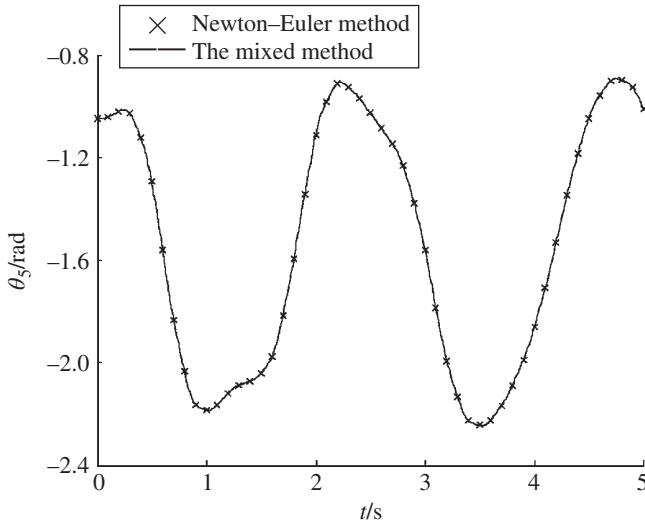


Figure 9.17 Time history of the azimuth angle of rigid body 5.

Substituting difference for differential, we obtain

$$M = \frac{EI_i}{l_i} \Delta \theta_i = K'_i \Delta \theta_i \quad (9.2)$$

where the subscript i denotes the i th finite segment, Δ denotes difference, K'_i is the torsional stiffness coefficient of a torsional spring with respect to the corresponding finite segment and l_i is the length of the finite segment.

The elasticity of the finite segment is regarded as two series torsional springs. For a homogeneous beam with uniform cross-section, it becomes

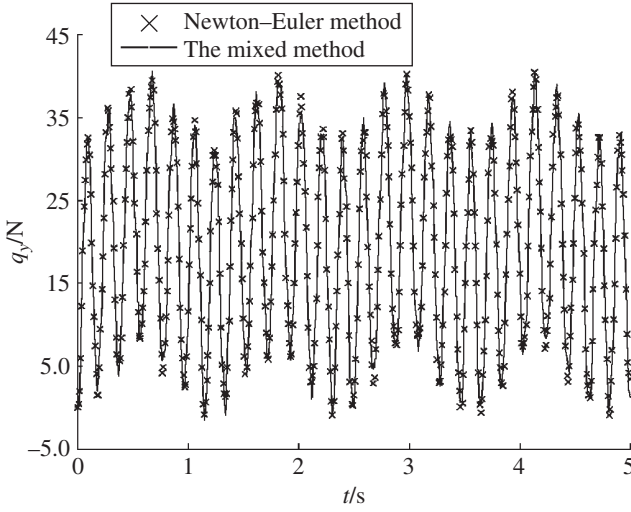


Figure 9.18 Time history of the interaction forces between rigid body 3 and beam 1.

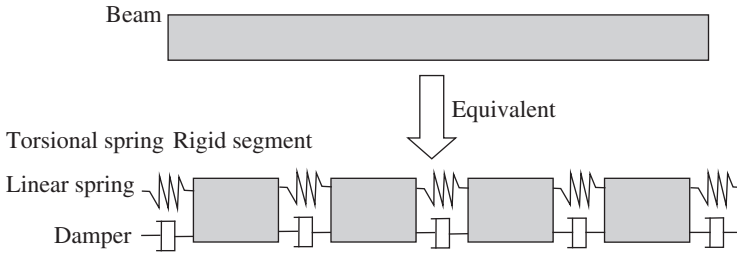


Figure 9.19 The finite segment model of a beam.

$$K'_{i,1} = K'_{i,2} = 2K'_i = 2\frac{EI_i}{l_i} \quad (9.3)$$

where $K'_{i,1}$ and $K'_{i,2}$ are the stiffness coefficients of two series torsional springs corresponding to K'_i .

According to the finite segment model, the torsional springs $K'_{i,2}$ and $K'_{i+1,1}$ are introduced for two rigid segments of the series. The torsional stiffness coefficient between two rigid segments is

$$K'_{i,i+1} = \frac{K'_{i,2} K'_{i+1,1}}{K'_{i,2} + K'_{i+1,1}} = \frac{2EI_i EI_{i+1}}{l_{i+1} EI_i + l_i EI_{i+1}} \quad (9.4)$$

The moment and rotation angle between the two rigid segments can be obtained from

$$m_{i,i+1} = K'_{i,i+1} (\theta_{i+1} - \theta_i) \quad (9.5)$$

where $m_{i,i+1}$ is the elastic moment between two rigid segments, and θ_{i+1} and θ_i are the orientation angles of the $(i+1)$ th rigid segment and the i th rigid segment, respectively.

Similarly, considering the torsion and compression deformation of the beam, we obtain

$$q_{i,i+1} = K_{i,i+1}(x_{i+1} - x_i) \quad (9.6)$$

where $q_{i,i+1}$ is the elastic force between rigid segments, namely the internal force between rigid segments, and x_{i+1} and x_i are the position coordinates of the hinge point of the $(i+1)$ th rigid segment and the i th rigid segment, respectively.

Similar to the above derivation, the elastic coefficient of the linear spring between two rigid segments is

$$K_{i,i+1} = \frac{2EA_iEA_{i+1}}{l_{i+1}EA_i + l_iEA_{i+1}} \quad (9.7)$$

where EA is the extensional rigidity coefficient.

Example 9.5 A plane-motion beam is mounted on a rotary base, as shown in Figure 9.20. The length of the beam is $l = 10\text{m}$, the cross-section area is $A = 4.601 \times 10^{-4}\text{m}^2$ and the Young's modulus is $E = 6.895 \times 10^{10}\text{N/m}^2$. The inertia moment of the cross-section area is $I = 2.031 \times 10^{-7}\text{m}^4$ and the density is $\rho = 2.767 \times 10^3\text{kg/m}^3$. The angular velocity of the rotary base is

$$\omega = \begin{cases} \frac{\Omega}{T} \left(t - \frac{T}{2\pi} \sin \frac{2\pi t}{T} \right) & (0 \leq t \leq T) \\ \Omega & (t > T) \end{cases} \quad (9.8)$$

where Ω is the steady-state angular velocity, $\Omega = 6\text{rad/s}$ and T is the accelerative time $T = 15\text{s}$. Solve the equations of motion and determine the driving force for the motion.

Solution

The flexible beam is divided into N rigid segments connected by the elastic hinge and damper hinge. According to the boundary conditions

$$\mathbf{z}_{0,1} = [0, 0, \theta, m, q_x, q_y, 1]_{0,1}^T \quad (9.9)$$

$$\mathbf{z}_{n,n+1} = [x, y, \theta, 0, 0, 0, 1]_{n,n+1}^T \quad (9.10)$$

and the overall transfer equation, the linear equation system about the unknown variables in state vector of the base motion, can be obtained

$$\begin{cases} u_{4,4}m + u_{4,5}q_x + u_{4,6}q_y = -u_{4,7} - u_{4,3}\theta \\ u_{5,4}m + u_{5,5}q_x + u_{5,6}q_y = -u_{5,7} - u_{5,3}\theta \\ u_{6,4}m + u_{6,5}q_x + u_{6,6}q_y = -u_{6,7} - u_{6,3}\theta \end{cases} \quad (9.11)$$

where θ is the rotation angle, obtained by integration of Equation (9.8), and $u_{i,j}$ is the element in the overall transfer matrix.

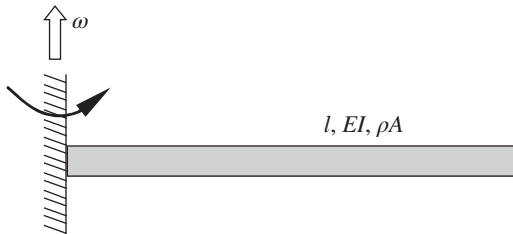


Figure 9.20 Plane-motion cantilever mounted on a rotary base.

The vector $[m, q_x, q_y]_{0,1}^T$ can be obtained by solving Equation (9.11), where $m_{0,1}$ is the required driving moment. The results of the system dynamics obtained by finite segment MSDTTMM are shown in Figures 9.21–9.23. The time history of driving moment which the system needs to realize the expected motion is shown in Figure 9.21. The time history of the transverse deformation and longitudinal deformation of the tip end of the beam are shown in Figures 9.22 and 9.23, respectively. The solid line denotes the computation results by the Kane method [250] and \diamond denotes the computation results by finite segment MSDTTMM. The results obtained by the two methods have good agreement. The computational speed of the finite segment MSDTTMM is much faster and it has higher computational efficiency.

For the converse problem, if the driving moment as shown in Figure 9.21 is known, we can determine the motion rule of the system. In this case, the state variable θ in the boundary condition (Equation (9.9)) will be treated as an unknown quantity. However, the state variable m may be considered as a known quantity. Solving the overall transfer equation, the motion rule

Figure 9.21 Time history of the driving moment.

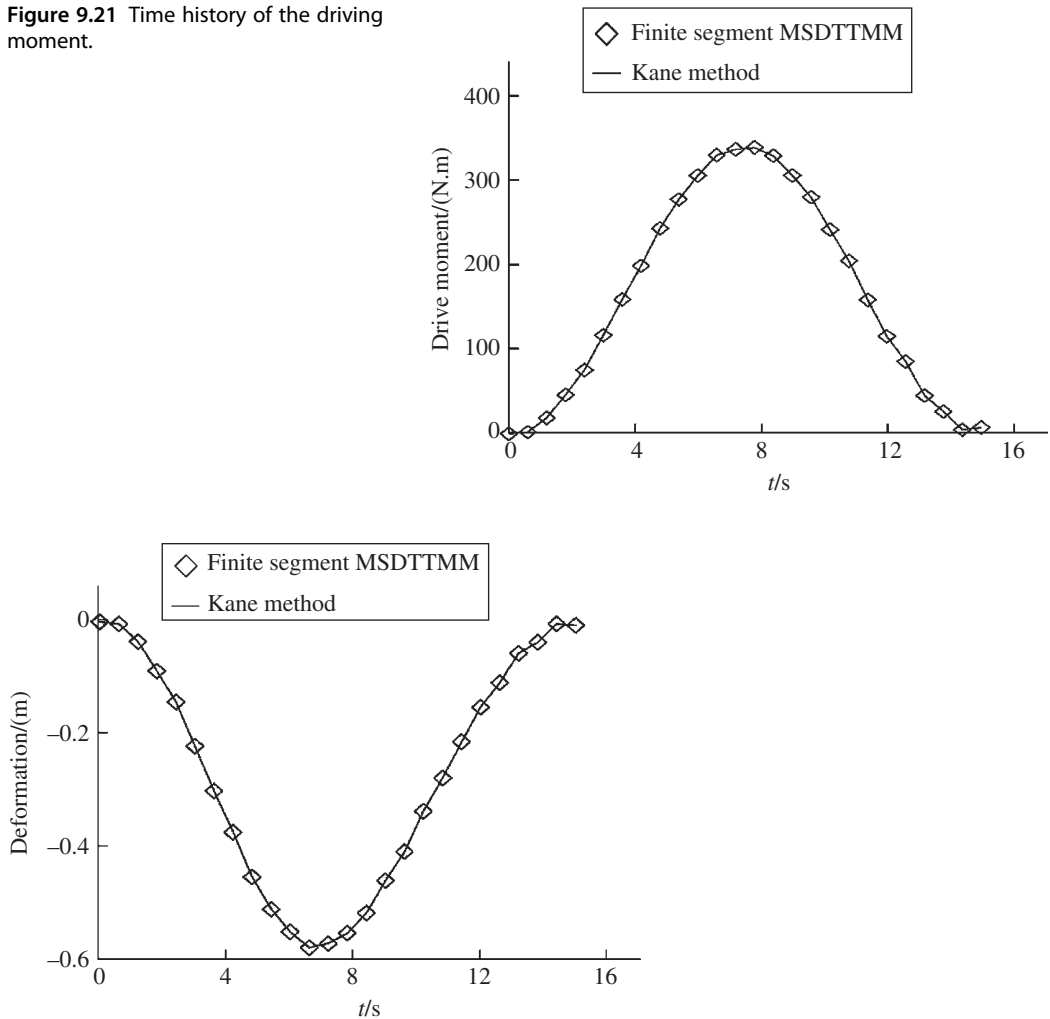


Figure 9.22 Time history of the transverse deformation of a tip end.

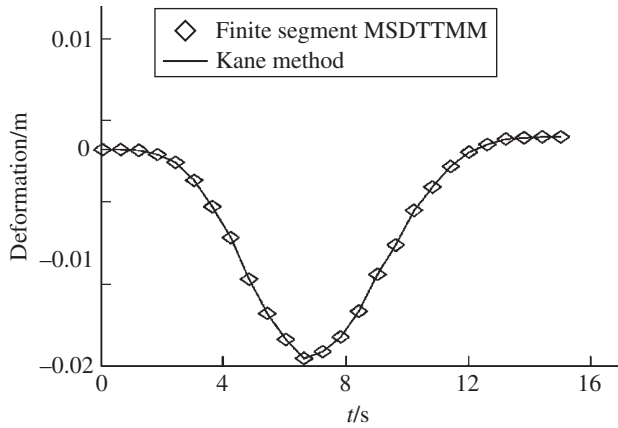


Figure 9.23 Time history of the longitudinal deformation of a tip end.

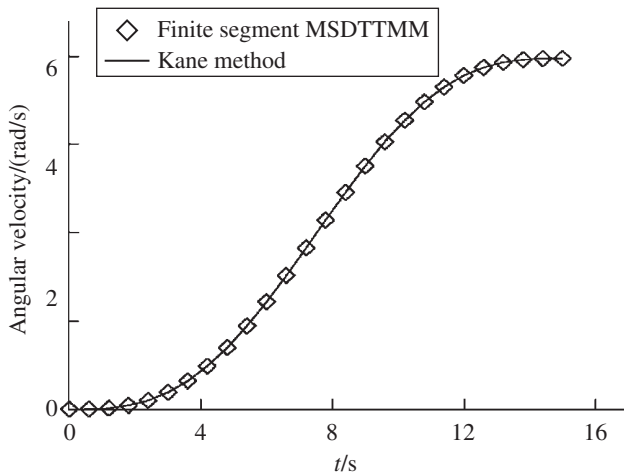


Figure 9.24 Time history of rotation angular velocity.

can be obtained. The computation results are shown in Figure 9.24. The solid line denotes the time history of the expected angular velocity, and \diamond represents the time history of angular velocity computed according to the driving moment, as shown in Figure 9.21.

The relation between computation time and numbers of segments (degrees of freedom) by finite segment MSDTTMM is shown in Figure 9.25. The computation time is proportional to the number of segments, while the computation time of the ordinary dynamic methods and the number of system degrees of freedom have an exponential relationship. This is the reason why the computing speed is faster by finite segment MSDTTMM than by other methods.

9.5 Transfer Matrix Method for Controlled Multibody Systems I

In reference [251], the control signal is regarded as the state variable of a state vector. The TMM is extended to control of a chain multibody system for modal analysis of the controlled multi-link mechanical arms. The computational method for the dynamics of a real-time controlled system, whose control force is related to the current system state, is introduced in this section.

Figure 9.25 Relation between computational time and number of segments.

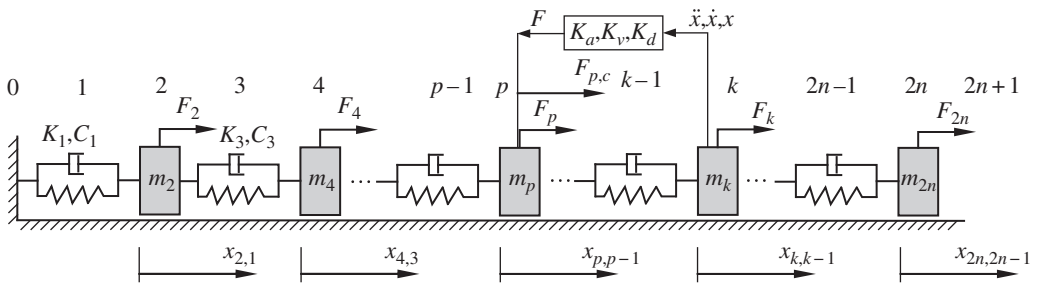
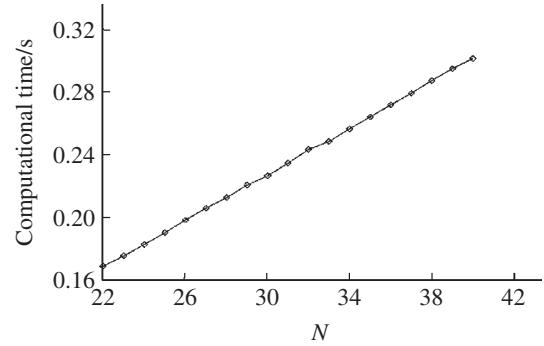


Figure 9.26 Dynamic model of a linear controlled multibody system.

By taking the control characteristic parameters of the system as special mechanical parameters and re-deriving the transfer matrices of controlled elements, there is no need to add the state variables corresponding to the control signal. The dynamics of controlled multibody systems can be studied by the MSTMM [77]. For a time-delay controlled multibody system, the control force can be denoted by the previous system state and regarded as an external force, and only the control forces in the terms of the external force column matrix of the MSTMM need to be considered. The dynamics of the controlled system can be solved using the same methods of the MSDTTMM.

9.5.1 Transfer Matrix Method for Linear Real-time Controlled Multibody Systems

9.5.1.1 Dynamic Model of Linear Controlled Multibody Systems

For the linear controlled multibody system shown in Figure 9.26, K_j and C_j ($j = 1, 3, \dots, 2n-1$) denote the elastic coefficient of the spring and viscous damping coefficient of element j , respectively. The *simple harmonic external force* with frequency Ω acting on lumped mass m_j ($j = 2, 4, \dots, 2n$) is

$$F_j = F_j^c \cos \Omega t + F_j^s \sin \Omega t \quad (9.12)$$

The sensor of the controlled system is fixed on lumped mass m_k and the real-time control force acting on the lumped mass m_p produced by the controller is

$$F_{p,c} = -K_a \ddot{x}_{k,k-1} - K_v \dot{x}_{k,k-1} - K_d x_{k,k-1} \quad (9.13)$$

9.5.1.2 Transfer Equation and Extended Transfer Matrix of Elements

According to the method given in Section 2.7, when the system is in steady-state motion, the motion of every lumped mass may be indicated by

$$x = \text{Re}(\bar{X}e^{i\Omega t}) \quad (9.14)$$

where $\bar{X} = X^r + iX^i$ is the complex amplitude of the steady-state forced vibration.

The complex amplitude of the simple-harmonic external force can be written as

$$\bar{F}_j = F_j^r + iF_j^i = F_j^c - iF_j^s \quad (9.15)$$

Substituting Equation (9.14) into Equation (9.13), the control force of the controlled element is

$$F_{p,c} = (K_a\Omega^2 - iK_v\Omega - K_d)\bar{X}_{k,k-1}e^{i\Omega t} \quad (9.16)$$

The complex amplitude of the control force is

$$\bar{F}_{p,c} = (K_a\Omega^2 - iK_v\Omega - K_d)\bar{X}_{k,k-1} \quad (9.17)$$

According to the geometrical relationship and the force balance condition of the two ends of the controlled lumped mass p , we can obtain

$$\begin{cases} \bar{X}_{p,p+1} = \bar{X}_{p,p-1} \\ \bar{Q}_{x,p,p+1} = m\Omega^2\bar{X}_{p,p-1} + \bar{Q}_{x,p,p-1} + \bar{F}_p + \bar{F}_{p,c} \end{cases} \quad (9.18)$$

Substituting Equation (9.17) into Equation (9.18), these equations can be written in the following matrix form

$$\begin{bmatrix} \bar{X} \\ \bar{Q}_x \\ 1 \end{bmatrix}_{p,p+1} = \begin{bmatrix} 1 & 0 & 0 \\ m_p\Omega^2 & 1 & \bar{F}_p \\ 0 & 0 & 1 \end{bmatrix} \begin{bmatrix} \bar{X} \\ \bar{Q}_x \\ 1 \end{bmatrix}_{p,p-1} + \begin{bmatrix} 0 & 0 & 0 \\ K_a\Omega^2 - iK_v\Omega - K_d & 0 & 0 \\ 0 & 0 & 0 \end{bmatrix} \begin{bmatrix} \bar{X} \\ \bar{Q}_x \\ 1 \end{bmatrix}_{k,k-1} \quad (9.19)$$

Thus, the transfer equation of the real-time controlled element p is

$$\hat{\hat{Z}}_{p,p+1} = \hat{\hat{U}}_p \hat{\hat{Z}}_{p,p-1} + \hat{\hat{U}}_{p,c} \hat{\hat{Z}}_{k,k-1} \quad (9.20)$$

The extended transfer equation of other elements without control is

$$\begin{aligned} \hat{\hat{Z}}_{j+1,j} &= \hat{\hat{U}}_j \hat{\hat{Z}}_{j-1,j} \quad (j = 1, 3, \dots, 2n-1) \\ \hat{\hat{Z}}_{j,j+1} &= \hat{\hat{U}}_j \hat{\hat{Z}}_{j,j-1} \quad (j = 2, 4, \dots, 2n) \quad (j \neq p) \end{aligned} \quad (9.21)$$

where

$$\begin{aligned} \hat{\hat{Z}} &= \begin{bmatrix} \bar{X} \\ \bar{Q}_x \\ 1 \end{bmatrix}, \quad \hat{\hat{U}}_j = \begin{bmatrix} 1 & -1/(K_j + iC_j\Omega) & 0 \\ 0 & 1 & 0 \\ 0 & 0 & 1 \end{bmatrix} \quad (j = 1, 3, \dots, 2n-1) \\ \hat{\hat{U}}_j &= \begin{bmatrix} 1 & 0 & 0 \\ m_j\Omega^2 & 1 & \bar{F}_j \\ 0 & 0 & 1 \end{bmatrix} \quad (j = 2, 4, \dots, 2n) \quad (j \neq p) \end{aligned} \quad (9.22)$$

9.5.1.3 Overall Transfer Equation and Overall Transfer Matrix

From Equations (9.20) and (9.21), we obtain

$$\begin{aligned}\hat{\bar{Z}}_{2n,2n+1} &= \hat{\bar{U}}_{2n} \hat{\bar{U}}_{2n-1} \cdots \hat{\bar{U}}_k \hat{\bar{Z}}_{k,k-1} \\ \hat{\bar{Z}}_{k,k-1} &= \hat{\bar{U}}_{k-1} \hat{\bar{U}}_{k-2} \cdots \hat{\bar{U}}_{p+1} \left(\hat{\bar{U}}_p \hat{\bar{U}}_{p-1} \cdots \hat{\bar{U}}_1 \hat{\bar{Z}}_{0,1} + \hat{\bar{U}}_{p,c} \hat{\bar{Z}}_{k,k-1} \right)\end{aligned}\quad (9.23)$$

The second formula of Equation (9.23) yields

$$\hat{\bar{Z}}_{k,k-1} = \left(I_3 - \hat{\bar{U}}_{k-1} \hat{\bar{U}}_{k-2} \cdots \hat{\bar{U}}_{p+1} \hat{\bar{U}}_{p,c} \right)^{-1} \hat{\bar{U}}_{k-1} \hat{\bar{U}}_{k-2} \cdots \hat{\bar{U}}_{p+1} \hat{\bar{U}}_p \hat{\bar{U}}_{p-1} \cdots \hat{\bar{U}}_1 \hat{\bar{Z}}_{0,1} \quad (9.24)$$

Substituting Equation (9.24) into the first formula of Equation (9.23), the overall transfer equation is obtained

$$\hat{\bar{Z}}_{2n,2n+1} = \hat{\bar{U}} \hat{\bar{Z}}_{0,1} \quad (9.25)$$

where the overall transfer matrix is

$$\hat{\bar{U}} = \hat{\bar{U}}_{2n} \hat{\bar{U}}_{2n-1} \cdots \hat{\bar{U}}_k \left(I_3 - \hat{\bar{U}}_{k-1} \hat{\bar{U}}_{k-2} \cdots \hat{\bar{U}}_{p+1} \hat{\bar{U}}_{p,c} \right)^{-1} \hat{\bar{U}}_{k-1} \hat{\bar{U}}_{k-2} \cdots \hat{\bar{U}}_{p+1} \hat{\bar{U}}_p \hat{\bar{U}}_{p-1} \cdots \hat{\bar{U}}_1 \quad (9.26)$$

9.5.1.4 Solving the Steady-state Motion of the System

The boundary conditions of the system are

$$\hat{\bar{Z}}_{2n,2n+1} = \begin{bmatrix} \bar{X} \\ 0 \\ 1 \end{bmatrix}_{2n,2n+1}, \quad \hat{\bar{Z}}_{0,1} = \begin{bmatrix} 0 \\ \bar{Q}_x \\ 1 \end{bmatrix} \quad (9.27)$$

Substituting Equation (9.27) into Equation (9.25) yields

$$\begin{bmatrix} \bar{X} \\ 0 \\ 1 \end{bmatrix}_{2n,2n+1} = \begin{bmatrix} u_{11} & u_{12} & u_{13} \\ u_{21} & u_{22} & u_{23} \\ 0 & 0 & 1 \end{bmatrix} \begin{bmatrix} 0 \\ \bar{Q}_x \\ 1 \end{bmatrix}_{0,1} \quad (9.28)$$

Solving Equation (9.28), the unknown state variables in the state vector of the system boundary can be obtained

$$\bar{Q}_{x0,1} = -\frac{u_{23}}{u_{22}}, \quad \bar{X}_{2n,2n+1} = -\frac{u_{23}u_{12}}{u_{22}} + u_{13} \quad (9.29)$$

By using Equation (9.21) in sequence and Equation (9.20), the state vectors at any point of the system can be determined. Therefore, the complex amplitude $\bar{X}_{j,j-1}$ ($j=2,4,\dots,2n$) of each lumped mass can be obtained. From Equation (9.14), the steady-state motion can be obtained

$$x_{j,j-1} = \operatorname{Re}(\bar{X}_{j,j-1} e^{i\Omega t}) = X_{j,j-1}^r \cos \Omega t - X_{j,j-1}^i \sin \Omega t \quad (9.30)$$

Example 9.6 For the linear controlled multibody system shown in Figure 9.27, let

$$\begin{cases} m_2 = 10.0 \text{ kg}, & m_4 = 3.0 \text{ kg}, & m_6 = 0.5 \text{ kg} \\ K_1 = 300 \text{ N/m}, & K_3 = 150 \text{ N/m}, & K_5 = 200 \text{ N/m} \\ C_1 = 2.5 \text{ N}\cdot\text{s/m}, & C_3 = 0.5 \text{ N}\cdot\text{s/m}, & C_5 = 0.1 \text{ N}\cdot\text{s/m} \\ F_4 = F_4^c \cos \Omega t + F_4^s \sin \Omega t, & \Omega = 8.0 \text{ rad/s}, & F_4^c = 4.0 \text{ N}, & F_4^s = 5.0 \text{ N} \end{cases}$$

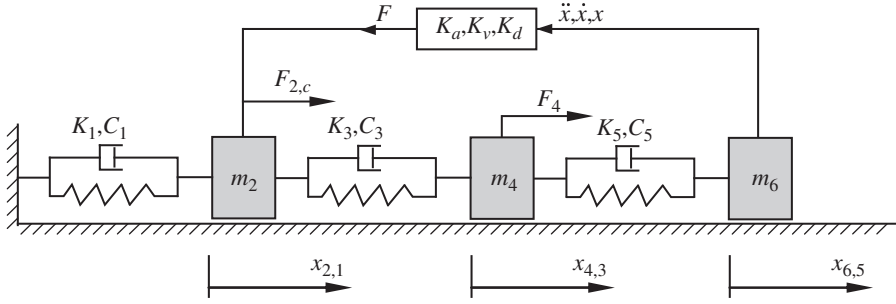


Figure 9.27 A linear multibody vibration system with a controlled loop.

The control signal comes from lumped mass 6. The control force acts on lumped mass 2, namely $F_{2,c} = -K_a \ddot{x}_{6,5} - K_v \dot{x}_{6,5} - K_d x_{6,5}$ with $K_a = 5.0 \text{ N}\cdot\text{s}^2/\text{m}$, $K_v = 0.0 \text{ N}\cdot\text{s}/\text{m}$ and $K_d = 0.0 \text{ N}/\text{m}$. Solve the steady-state response of the system using the multibody system dynamics method and the TMM for linear controlled multibody systems.

Solution

a) Multibody system dynamics method

The overall dynamic equation of the system is

$$M\ddot{X} + C\dot{X} + KX = f \quad (\text{a})$$

where

$$X = \begin{bmatrix} x_{2,1} \\ x_{4,3} \\ x_{6,5} \end{bmatrix}, f = \begin{bmatrix} 0 \\ F_4 \\ 0 \end{bmatrix}, M = \begin{bmatrix} m_2 & 0 & K_a \\ 0 & m_4 & 0 \\ 0 & 0 & m_6 \end{bmatrix}, C = \begin{bmatrix} C_1 + C_3 & -C_3 & K_v \\ -C_3 & C_3 + C_5 & -C_5 \\ 0 & -C_5 & C_5 \end{bmatrix},$$

$$K = \begin{bmatrix} K_1 + K_3 & -K_3 & K_d \\ -K_3 & K_3 + K_5 & -K_5 \\ 0 & -K_5 & K_5 \end{bmatrix}$$

Because the values of initial conditions will not affect the steady-state response of the system, they can be supposed to be zero

$$X|_{t=0} = \begin{bmatrix} x_{2,1} \\ x_{4,3} \\ x_{6,5} \end{bmatrix}_{t=0} = \begin{bmatrix} 0 \\ 0 \\ 0 \end{bmatrix}, \dot{X}|_{t=0} = \begin{bmatrix} \dot{x}_{2,1} \\ \dot{x}_{4,3} \\ \dot{x}_{6,5} \end{bmatrix}_{t=0} = \begin{bmatrix} 0 \\ 0 \\ 0 \end{bmatrix} \quad (\text{b})$$

b) TMM for linear controlled multibody systems

Substituting parameters into Equations (9.19) to (9.29), by matrix manipulation the steady-state motion of the system can be determined to be

$$X = \begin{bmatrix} x_{2,1} \\ x_{4,3} \\ x_{6,5} \end{bmatrix} = \begin{bmatrix} -0.0296 \cos \Omega t - 0.0434 \sin \Omega t \\ 0.0085 \cos \Omega t + 0.0169 \sin \Omega t \\ 0.0101 \cos \Omega t + 0.0202 \sin \Omega t \end{bmatrix} \quad (\text{c})$$

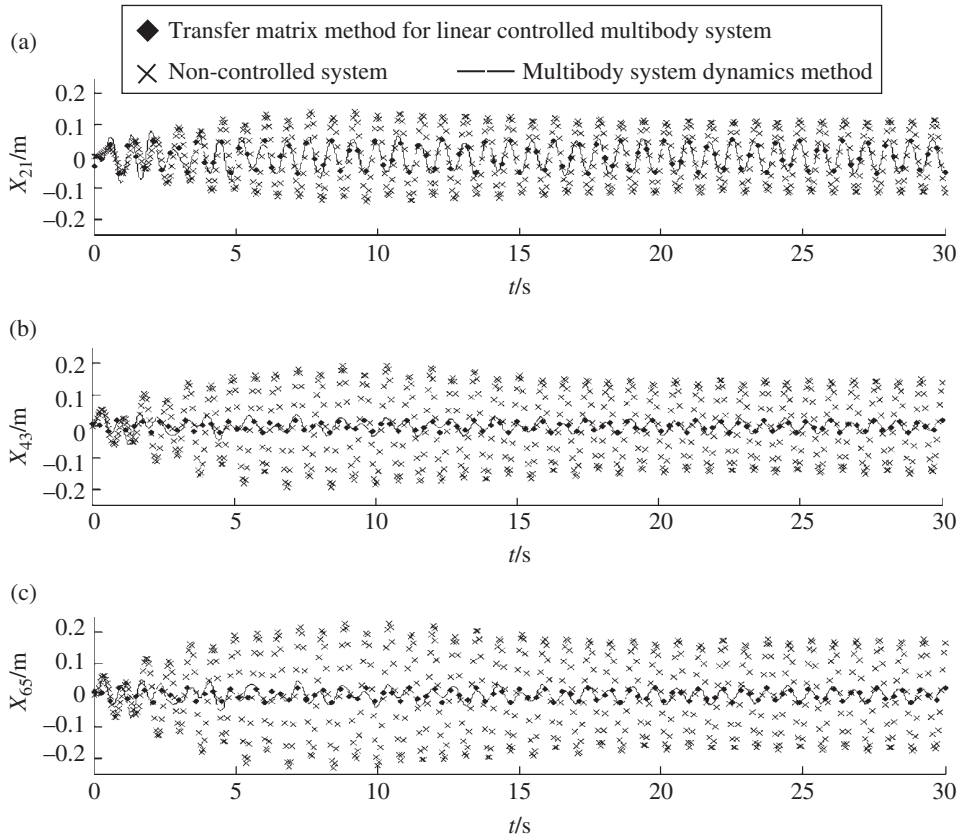


Figure 9.28 The computational results of system dynamics. (a) Time history of the location coordinate of lumped mass 2. (b) Time history of the location coordinate of lumped mass 4. (c) Time history of the location coordinate of lumped mass 6.

To illustrate the influence of the real-time control force on the motion of the system, the dynamics of the system with control ($K_a = 5.0$) and without control ($K_a = 0.0$) are computed by the TMM for linear controlled multibody systems and the multibody system dynamics method, respectively. The computation results are shown in Figure 9.28. The time history of the coordinate with control by the TMM for linear controlled multibody systems and the multibody system dynamics method are denoted by \blacklozenge and $—$, respectively. The time history of the coordinates without control by the multibody system dynamics method is denoted by \times .

The results obtained by the two methods are in good agreement, which validates the efficiency and accuracy of the TMM for a linear controlled multibody system for solving the dynamics of controlled multibody systems. After the implementation of control, the amplitude of the steady-state motion of the system is less than in the system without control.

It is convenient to obtain the frequency response of the linear controlled multibody system shown in Figure 9.27 using the TMM for a linear controlled multibody system, as shown in Figure 9.29. The amplitude and frequency characteristics of the system are changed because the controlled loop is considered, namely the vibration characteristics of the system are changed.

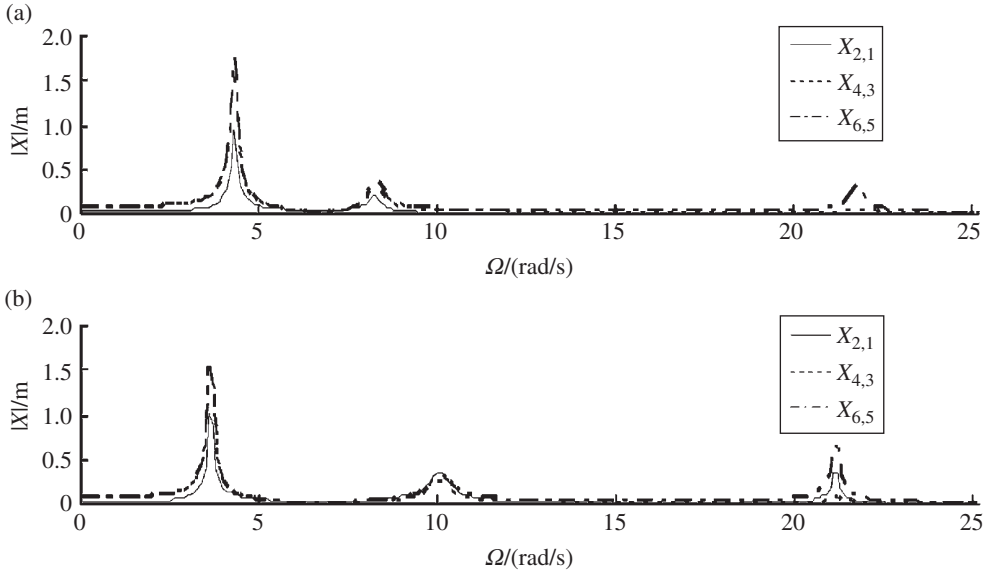


Figure 9.29 Frequency response for a linear controlled multibody system with a controlled loop. (a) Frequency response for $K_a = 0$. (b) Frequency response for $K_a = 5.0$.

Example 9.7 The linear controlled multibody system in Figure 9.30 is similar to that in Example 9.4. The control force acts on a spring hinge and damper hinge 3, and the parameters of the controller are different; all other parameters are the same as those in Example 9.4. The control signal comes from lumped mass 6, and the control force acts on the spring hinge and damper hinge 3, namely $F_{3,c} = -K_a \ddot{x}_{6,5} - K_v \dot{x}_{6,5} - K_d x_{6,5}$ with $K_a = 5.0 \text{ N}\cdot\text{s}^2/\text{m}$, $K_v = 5.0 \text{ N}\cdot\text{s}/\text{m}$ and $K_d = 5.0 \text{ N}/\text{m}$. Solve the steady-state response of the system using the multibody system dynamics method and the TMM for a linear controlled multibody system.

Solution

a) Multibody system dynamics method

The overall dynamic equation of the system is

$$M\ddot{X} + C\dot{X} + KX = f \quad (a)$$

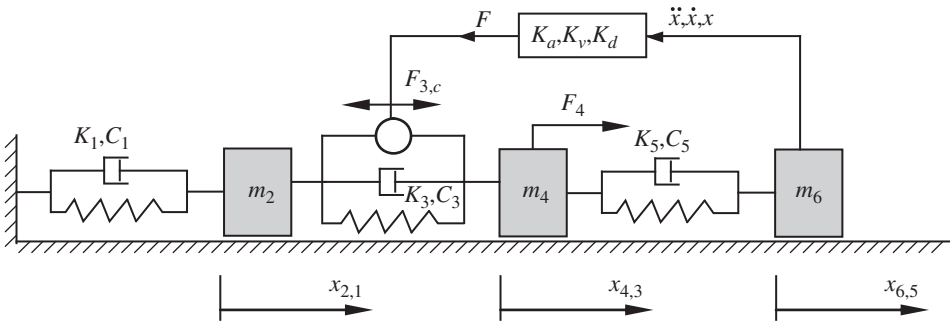


Figure 9.30 Linear controlled multibody system with a controlled loop.

where

$$X = \begin{bmatrix} x_{2,1} \\ x_{4,3} \\ x_{6,5} \end{bmatrix}, \quad f = \begin{bmatrix} 0 \\ F_4 \\ 0 \end{bmatrix}, \quad M = \begin{bmatrix} m_2 & 0 & -K_a \\ 0 & m_4 & K_a \\ 0 & 0 & m_6 \end{bmatrix},$$

$$C = \begin{bmatrix} C_1 + C_3 & -C_3 & -K_v \\ -C_3 & C_3 + C_5 & -C_5 + K_v \\ 0 & -C_5 & C_5 \end{bmatrix}, \quad K = \begin{bmatrix} K_1 + K_3 & -K_3 & -K_d \\ -K_3 & K_3 + K_5 & -K_5 + K_d \\ 0 & -K_5 & K_5 \end{bmatrix}$$

Since the initial conditions will not affect the steady-state response of the system, we select

$$X|_{t=0} = \begin{bmatrix} x_{2,1} \\ x_{4,3} \\ x_{6,5} \end{bmatrix}_{t=0} = \begin{bmatrix} 0 \\ 0 \\ 0 \end{bmatrix}, \quad \dot{X}|_{t=0} = \begin{bmatrix} \dot{x}_{2,1} \\ \dot{x}_{4,3} \\ \dot{x}_{6,5} \end{bmatrix}_{t=0} = \begin{bmatrix} 0 \\ 0 \\ 0 \end{bmatrix} \quad (b)$$

b) Transfer matrix method

The transfer equation of controlled element 3 is

$$\hat{\hat{Z}}_{4,3} = \hat{\hat{U}}_3 \hat{\hat{Z}}_{2,3} + \hat{\hat{U}}_{3,c} \hat{\hat{Z}}_{6,5} \quad (c)$$

where

$$\hat{\hat{Z}} = \begin{bmatrix} \bar{X} \\ \bar{Q}_x \\ 1 \end{bmatrix}, \quad \hat{\hat{U}}_3 = \begin{bmatrix} 1 & -1/(K_3 + iC_3\Omega) & 0 \\ 0 & 1 & 0 \\ 0 & 0 & 1 \end{bmatrix}, \quad \hat{\hat{U}}_{3,c} = \begin{bmatrix} (K_a\Omega^2 - iK_v\Omega - K_d)/(K_3 + iC_3\Omega) & 0 & 0 \\ 0 & 0 & 0 \\ 0 & 0 & 0 \end{bmatrix}$$

The transfer equations of the elements without control are

$$\begin{cases} \hat{\hat{Z}}_{2,1} = \hat{\hat{U}}_1 \hat{\hat{Z}}_{0,1}, & \hat{\hat{Z}}_{2,3} = \hat{\hat{U}}_2 \hat{\hat{Z}}_{2,1} \\ \hat{\hat{Z}}_{4,5} = \hat{\hat{U}}_4 \hat{\hat{Z}}_{4,3}, & \hat{\hat{Z}}_{6,5} = \hat{\hat{U}}_5 \hat{\hat{Z}}_{4,5}, & \hat{\hat{Z}}_{6,7} = \hat{\hat{U}}_6 \hat{\hat{Z}}_{6,5} \end{cases} \quad (d)$$

Then

$$\hat{\hat{Z}}_{6,5} = \left(I_3 - \hat{\hat{U}}_5 \hat{\hat{U}}_4 \hat{\hat{U}}_{3,c} \right)^{-1} \hat{\hat{U}}_5 \hat{\hat{U}}_4 \hat{\hat{U}}_3 \hat{\hat{U}}_2 \hat{\hat{U}}_1 \hat{\hat{Z}}_{0,1} \quad (e)$$

where the overall transfer equation is

$$\hat{\hat{Z}}_{6,7} = \hat{\hat{U}} \hat{\hat{Z}}_{0,1} \quad (f)$$

The overall transfer matrix is

$$\hat{\hat{U}} = \hat{\hat{U}}_6 \left(I_3 - \hat{\hat{U}}_5 \hat{\hat{U}}_4 \hat{\hat{U}}_{3,c} \right)^{-1} \hat{\hat{U}}_5 \hat{\hat{U}}_4 \hat{\hat{U}}_3 \hat{\hat{U}}_2 \hat{\hat{U}}_1 \quad (g)$$

Applying the boundary conditions and the given parameters, the steady-state response of the system is determined as

$$X = \begin{bmatrix} x_{2,1} \\ x_{4,3} \\ x_{6,5} \end{bmatrix} = \begin{bmatrix} -0.0076 \\ -0.0070 \\ -0.0084 \end{bmatrix} \cos \Omega t + \begin{bmatrix} -0.0094 \\ -0.0071 \\ -0.0085 \end{bmatrix} \sin \Omega t \quad (h)$$

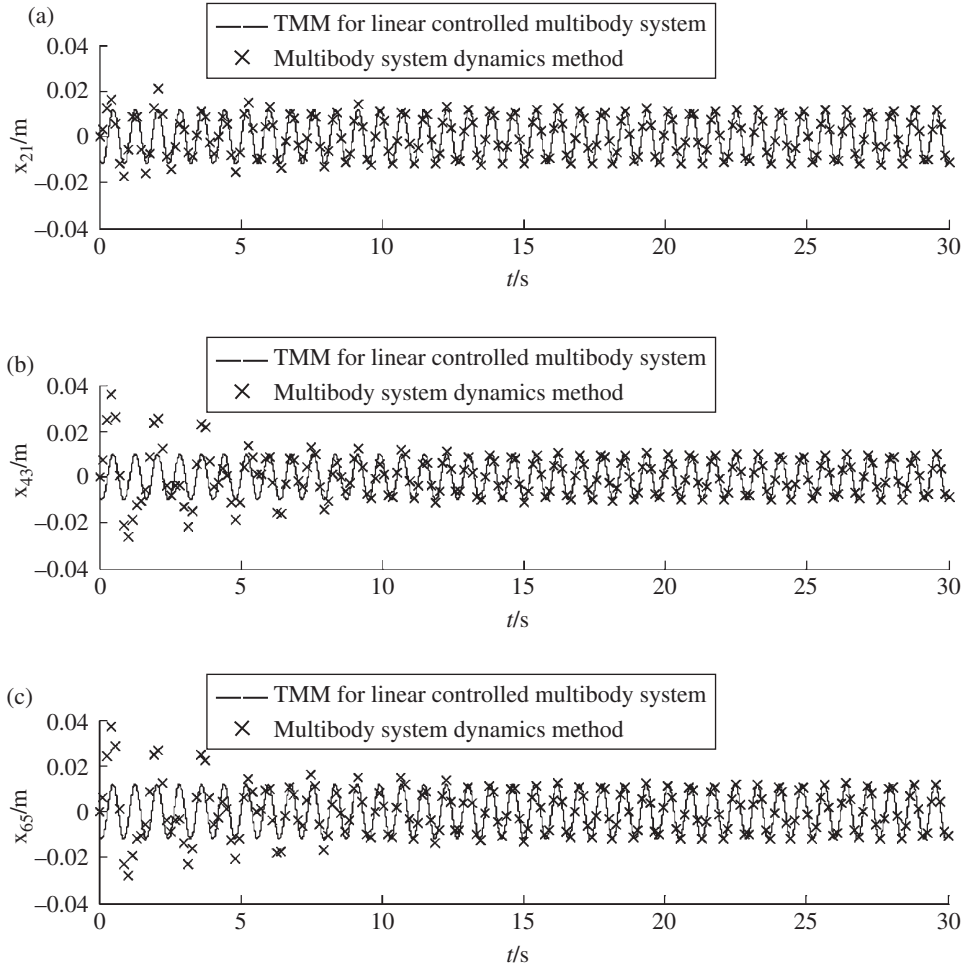


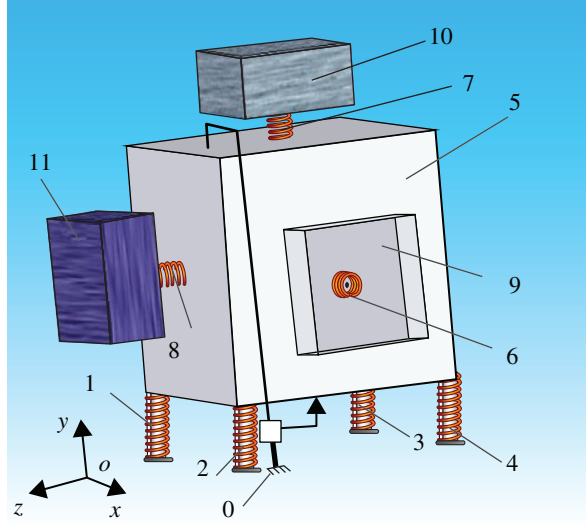
Figure 9.31 Time history of the dynamics of a system: (a) time history of the displacement of lumped mass 2, (b) time history of the displacement of lumped mass 4 and (c) time history of the displacement of lumped mass 6.

The steady-state response of the system is computed using the TMM for a linear controlled multibody system and the multibody system dynamics method, as shown in Figure 9.31. The results for the steady-state motion of the system obtained by the two methods are in good agreement, which validates the TMM of linear controlled multibody systems for solving the steady-state motion of controlled multibody systems.

Example 9.8 A controlled branch multibody system is shown in Figure 9.32. Elements 1, 2, 3 and 4 are spatial springs, element 5 is a rigid body, elements 6, 7 and 8 are torsional springs, and elements 9, 10 and 11 are rotors. Element 5 is a feedback element whose motion is controlled by its state variable feedback. The stiffnesses of springs 1, 2, 3 and 4 are

$$\begin{bmatrix} k_{x,1} \\ k_{y,1} \\ k_{z,1} \end{bmatrix} = \begin{bmatrix} 2000 \\ 3000 \\ 2000 \end{bmatrix} \text{ N/m}, \quad \begin{bmatrix} k_{x,2} \\ k_{y,2} \\ k_{z,2} \end{bmatrix} = \begin{bmatrix} 3000 \\ 2500 \\ 2000 \end{bmatrix} \text{ N/m}, \quad \begin{bmatrix} k_{x,3} \\ k_{y,3} \\ k_{z,3} \end{bmatrix} = \begin{bmatrix} 4000 \\ 2000 \\ 4500 \end{bmatrix} \text{ N/m}, \quad \begin{bmatrix} k_{x,4} \\ k_{y,4} \\ k_{z,4} \end{bmatrix} = \begin{bmatrix} 5000 \\ 3000 \\ 5000 \end{bmatrix} \text{ N/m}$$

Figure 9.32 Model of a branch multibody system.



The mass of element 5 is 2 kg, and the inertia moment with respect to the geometric center is

$$J_5 = \begin{bmatrix} 0.03 & 0 & 0 \\ 0 & 0.03 & 0 \\ 0 & 0 & 0.03 \end{bmatrix} \text{ kg} \cdot \text{m}^2$$

The mass of element 9 is 0.2 kg and the inertia moments of elements 9, 10 and 11 are all $0.0006 \text{ kg} \cdot \text{m}^2$. The torsional stiffnesses of elements 6, 7 and 8 are $k'_6 = 1500 \text{ N} \cdot \text{m}/\text{rad}$, $k'_7 = 1500 \text{ N} \cdot \text{m}/\text{rad}$ and $k'_8 = 1500 \text{ N} \cdot \text{m}/\text{rad}$, respectively. The coefficients of the proportional damping system are $\alpha = 0.025$ and $\beta = 0.05$. The external moment of elements 9, 10 and 11 are

$$M_x = 1.754 \sin(2\pi \times 37t) \text{ N} \cdot \text{m}, M_y = 1.754 \sin(2\pi \times 40t) \text{ N} \cdot \text{m}, M_z = 1.754 \sin(2\pi \times 43t) \text{ N} \cdot \text{m}$$

The angular displacement and angular acceleration are the feedback parameters, and the form of the control is

$$h_x = -k_{a_x} \ddot{\theta}_{x5,6} - k_{d_x} \dot{\theta}_{x5,6}, h_y = -k_{a_y} \ddot{\theta}_{y5,6} - k_{d_y} \dot{\theta}_{y5,6}, h_z = -k_{a_z} \ddot{\theta}_{z5,6} - k_{d_z} \dot{\theta}_{z5,6}$$

Solution

The state vectors of the connection point are defined as

$$\mathbf{Z}_{0,1} = [X, Y, Z, Q_x, Q_y, Q_z]_{0,1}^T \quad (9.31)$$

$$\mathbf{Z}_{5,6} = [X, Y, Z, \theta_x, \theta_y, \theta_z, M_x, M_y, M_z, Q_x, Q_y, Q_z]_{5,6}^T \quad (9.32)$$

$$\mathbf{Z}_{9,0} = [\theta_x, M_x]_{9,0}^T \quad (9.33)$$

$\mathbf{Z}_{0,2}, \mathbf{Z}_{0,3}, \mathbf{Z}_{0,4}, \mathbf{Z}_{5,1}, \mathbf{Z}_{5,2}, \mathbf{Z}_{5,3}, \mathbf{Z}_{5,4}$ and $\mathbf{Z}_{0,1}$ have the same forms, $\mathbf{Z}_{5,7}, \mathbf{Z}_{5,8}$ and $\mathbf{Z}_{5,6}$ have the same forms, and $\mathbf{Z}_{10,0}, \mathbf{Z}_{11,0}, \mathbf{Z}_{9,6}, \mathbf{Z}_{10,7}, \mathbf{Z}_{11,8}$ and $\mathbf{Z}_{9,0}$ have the same forms:

$$\mathbf{Z}_{0,1 \sim 4} = [X_{0,1}, Y_{0,1}, Z_{0,1}, Q_{x0,1}, Q_{y0,1}, Q_{z0,1}, \dots, Q_{x0,4}, Q_{y0,4}, Q_{z0,4}]^T \quad (9.34)$$

$$\mathbf{Z}_{5,6 \sim 8} = [X_{5,6}, Y_{5,6}, Z_{5,6}, \theta_{x5}, \theta_{y5}, \theta_{z5}, M_{x5,6}, M_{y5,6}, M_{z5,6}, \dots, Q_{x5,8}, Q_{y5,8}, Q_{z5,8}]^T \quad (9.35)$$

The overall transfer equation of the system is

$$\mathbf{U}_{\text{all}} \mathbf{Z}_{\text{all}} = \mathbf{0} \quad (9.36)$$

where

$$\mathbf{U}_{\text{all}} = \begin{bmatrix} \mathbf{U}_{11} & \mathbf{U}_{12} & \mathbf{0} & \mathbf{0} & \mathbf{0} \\ \mathbf{U}_{21} & \mathbf{U}_{22} & \mathbf{0} & \mathbf{0} & \mathbf{0} \\ \mathbf{0} & \mathbf{U}_6^{(1)} & -\mathbf{U}_6^{(2)} \mathbf{U}_9 & \mathbf{0} & \mathbf{0} \\ \mathbf{0} & \mathbf{U}_7^{(1)} & \mathbf{0} & -\mathbf{U}_7^{(2)} \mathbf{U}_{10} & \mathbf{0} \\ \mathbf{0} & \mathbf{U}_8^{(1)} & \mathbf{0} & \mathbf{0} & -\mathbf{U}_8^{(2)} \mathbf{U}_{11} \end{bmatrix} \quad (9.37)$$

$$\mathbf{U}_{11} = \mathbf{U}_{1 \sim 4}^{(1)} \mathbf{U}_{1 \sim 4} - \mathbf{U}_{1 \sim 4}^{(2)} \mathbf{U}_C, \mathbf{U}_{12} = \mathbf{U}_{1 \sim 4}^{(1)} \mathbf{U}_C, \mathbf{U}_{21} = -\mathbf{U}_{5,6 \sim 8}^{(2)} \mathbf{U}_{1 \sim 4}, \mathbf{U}_{22} = \mathbf{U}_{5,6 \sim 8}^{(1)} \mathbf{U}_{1 \sim 4} - \mathbf{U}_{5,6 \sim 8}^{(2)} \mathbf{U}_C$$

\mathbf{Z}_{all} is composed of the state vectors at the boundary points of the system and \mathbf{U}_{all} is the overall transfer matrix of the system with 24×54 dimension.

The detailed expressions of the components of the controlled element are

$$\mathbf{U}_C(7,4) = h_x, \mathbf{U}_C(8,5) = h_y, \mathbf{U}_C(9,6) = h_z$$

The control parameters are

$$k_{a_x} = 0.0002, k_{d_x} = 1000, k_{a_y} = 0.0003, k_{d_y} = 2000, k_{a_z} = 0.0004, k_{d_z} = 3000$$

The boundary conditions of the system are

$$X_{0,j} = 0, Y_{0,j} = 0, Z_{0,j} = 0, j = 1, \dots, 4$$

$$Q_{x5,j} = 0, Q_{y5,j} = 0, Q_{z5,j} = 0, j = 6, \dots, 8$$

$$M_{x5,7} = 0, M_{x5,8} = 0, M_{y5,6} = 0$$

$$M_{y5,8} = 0, M_{z5,6} = 0, M_{z5,7} = 0$$

$$M_{x9,0} = 0, M_{y10,0} = 0, M_{z11,0} = 0$$

Eliminating the zero elements in the state vector \mathbf{Z}_{all} yields the state vector $\bar{\mathbf{Z}}_{\text{all}}$, and deleting the rows in \mathbf{U}_{all} corresponding to the zero elements in \mathbf{Z}_{all} leads to the 24 order square matrix $\bar{\mathbf{U}}_{\text{all}}$:

$$\bar{\mathbf{U}}_{\text{all}} \bar{\mathbf{Z}}_{\text{all}} = \mathbf{0} \quad (9.38)$$

$\bar{\mathbf{U}}_{\text{all}}$ is related to the structure parameters of the system and the natural frequency ω_k . When the structure parameters of the system are determined, the value of the determinant of matrix $\bar{\mathbf{U}}_{\text{all}}$ corresponding to the eigenfrequency ω_k is zero, that is

$$\det \bar{\mathbf{U}}_{\text{all}} = 0 \quad (9.39)$$

Equation (9.39) is the eigenequation of the system. Solving the eigenequation, the eigenfrequency of the system ω_k can be obtained. Under the conditions of given normalization, solving $\bar{\mathbf{Z}}_{\text{all}}$ corresponding to the eigenfrequency ω_k , the state vectors $\mathbf{Z}_{0,1 \sim 4}$, $\mathbf{Z}_{5,6 \sim 8}$, $\mathbf{Z}_{9,0}$, $\mathbf{Z}_{10,0}$ and $\mathbf{Z}_{11,0}$ can be obtained. Then according to the body dynamic equations of elements, the dynamic response of the system is determined.

The responses of this system with or without control are computed by the TMM for linear controlled multibody systems and the Newton–Euler method, respectively. The results are shown in Figures 9.33–9.35. From the figures it can be seen that the results obtained by two methods are in good agreement. The steady-state vibration amplitude of the controlled system is smaller than that of the non-controlled system, which validates the capability of the TMM for linear controlled multibody systems to solve the dynamics problem of a controlled branch multibody system.

9.5.2 Transfer Matrix Method for Linear Delay Controlled Multibody Systems

A linear controlled multibody system is shown in Figure 9.26. If the system has a time delay τ and steady-state motion, the motion of a lumped mass can be denoted by

$$x = \operatorname{Re}(\bar{X} e^{i\Omega(t-\tau)}) \quad (9.40)$$

Figure 9.33 Time history of the angular velocity of element 5 around the x axis.

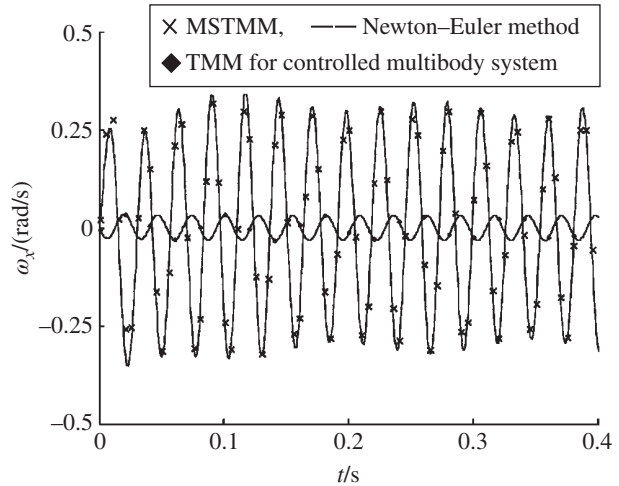
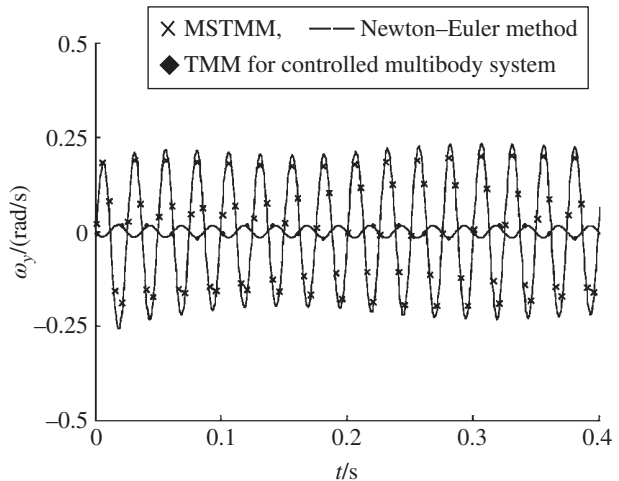


Figure 9.34 Time history of the angular velocity of element 5 around the y axis.



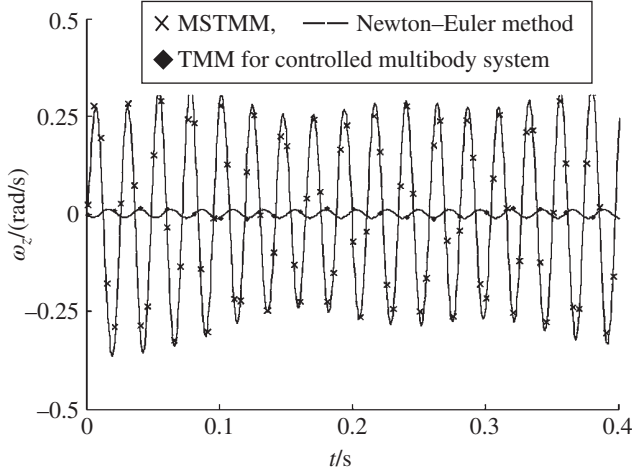


Figure 9.35 Time history of the angular velocity of element 5 around the z axis.

where $\bar{X} = X^r + iX^i$ is the complex amplitude of the steady-state forced vibration.

The control force is

$$F_{p,c} = -K_a \ddot{x}_{k,k-1}(t-\tau) - K_v \dot{x}_{k,k-1}(t-\tau) - K_d x_{k,k-1}(t-\tau) \quad (9.41)$$

Equation (9.41) can be written as

$$F_{p,c} = (K_a \Omega^2 - iK_v \Omega - K_d) \bar{X}_{k,k-1} e^{-i\Omega\tau} e^{i\Omega t} \quad (9.42)$$

The complex amplitude of the control force is

$$\bar{F}_{p,c} = (K_a \Omega^2 - iK_v \Omega - K_d) \bar{X}_{k,k-1} e^{-i\Omega\tau} \quad (9.43)$$

Taking the known control force $F_{p,c}$ of the current time into the transfer matrix of the controlled element, the transfer equation of the controlled element is

$$\begin{bmatrix} \bar{X} \\ \bar{Q}_x \\ 1 \end{bmatrix}_{p,p+1} = \begin{bmatrix} 1 & 0 & 0 \\ m_p \Omega^2 & 1 & F_p + F_{p,c} \\ 0 & 0 & 1 \end{bmatrix} \begin{bmatrix} \bar{X} \\ \bar{Q}_x \\ 1 \end{bmatrix}_{p,p-1} \quad (9.44)$$

namely

$$\hat{\bar{Z}}_{p,p+1} = \hat{\bar{U}}_{p,c} \hat{\bar{Z}}_{p,p-1} \quad (9.45)$$

The overall transfer matrix is

$$\hat{\bar{U}} = \hat{\bar{U}}_{2n} \hat{\bar{U}}_{2n-1} \cdots \hat{\bar{U}}_{p+1} \hat{\bar{U}}_{p,c} \hat{\bar{U}}_{p-1} \cdots \hat{\bar{U}}_1 \quad (9.46)$$

According to the boundary conditions of the system and the transfer relation, the complex amplitude of each lumped mass $\bar{X}_{j,j-1}$ ($j=2,4,\dots,2n$) can be obtained. The steady-state motion can be obtained from Equation (9.40):

$$x_{j,j-1} = \text{Re} \left(\bar{X}_{j,j-1} e^{i\Omega(t-\tau)} \right) = X_{j,j-1}^r \cos \Omega(t-\tau) - X_{j,j-1}^i \sin \Omega(t-\tau) \quad (9.47)$$

Example 9.9 For the linear controlled multibody system shown in Example 9.6, the time delay is 0.001 s. Solve the steady-state response of the system using the multibody system dynamics method and the TMM for linear controlled multibody systems.

$$X = \begin{bmatrix} x_{2,1} \\ x_{4,3} \\ x_{6,5} \end{bmatrix} = \begin{bmatrix} -0.0295 \cos \Omega t - 0.0434 \sin \Omega t \\ 0.0084 \cos \Omega t + 0.0170 \sin \Omega t \\ 0.0100 \cos \Omega t + 0.0202 \sin \Omega t \end{bmatrix}$$

The dynamics of this controlled system with time delay is solved by the TMM for linear controlled multibody systems and the controlled system Newton–Euler method, as shown in Figure 9.36. The computed results have good agreement, which validates the TMM for linear controlled multibody systems for solving the steady-state response of a controlled multibody system.

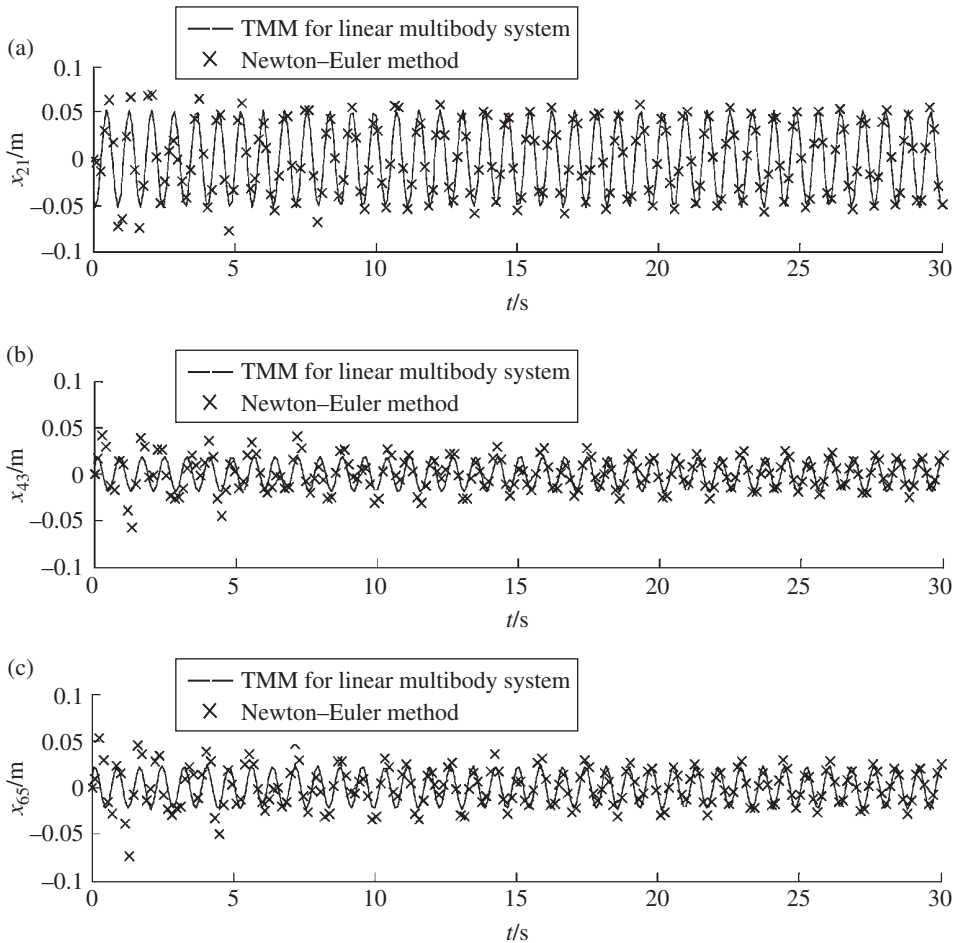


Figure 9.36 The time history of the motion of a controlled system with time delay: (a) time history of the displacement of lumped mass 2, (b) time history of the displacement of lumped mass 4 and (c) time history of the displacement of lumped mass 6.

9.6 Transfer Matrix Method for Controlled Multibody Systems II

In this section, using the system in Figure 9.37 as an example, the discrete time transfer matrix method (DTTMM) for controlled multibody systems [78], developed by the authors, is introduced.

9.6.1 Discrete Time Transfer Matrix Method of Real-time Controlled Multibody Systems

The DTTMM for multi-rigid-body systems was introduced in Chapter 7. The transfer equations of a lumped mass and a spring with longitudinal motion (see Figure 9.38) are obtained as follows

$$\mathbf{z}_{p,p-1} = \mathbf{U}_{p-1} \mathbf{z}_{p-2,p-1} \quad (9.48)$$

$$\mathbf{z}_{p,p+1} = \mathbf{U}_p \mathbf{z}_{p,p-1} \quad (9.49)$$

The state vector is

$$\mathbf{z} = [\mathbf{x}, \mathbf{q}, \mathbf{1}]^T \quad (9.50)$$

The transfer matrix of the spring is

$$\mathbf{U}_{p-1} = \begin{bmatrix} 1 & -1/(K_{p-1} + C_{p-1}C) & (C_{p-1}D_{xp-2,p-1} - C_{p-1}D_{xp,p-1} + K_{p-1}l_{p-1})/(K_{p-1} + C_{p-1}C) \\ 0 & 1 & 0 \\ 0 & 0 & 1 \end{bmatrix} \quad (9.51)$$

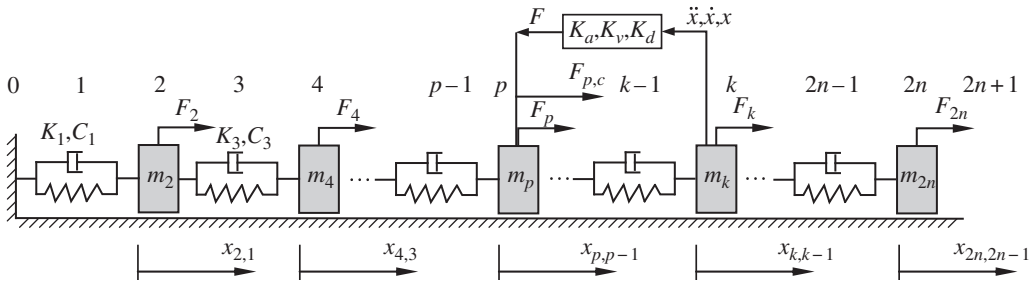


Figure 9.37 Controlled multibody system.

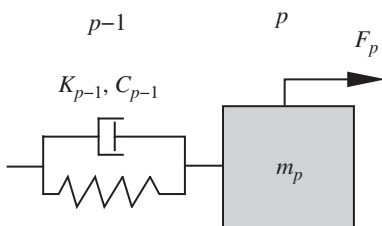


Figure 9.38 The subsystem composed of a spring and a lumped mass.

The transfer matrix of the lumped mass is

$$\mathbf{U}_p = \begin{bmatrix} 1 & 0 & 0 \\ -m_p A & 1 & -m_p B + F_p \\ 0 & 0 & 1 \end{bmatrix} \quad (9.52)$$

Linearizing the real-time control force as shown in Equation (9.13), this can be written as

$$F_{p,c} = -(K_a A + K_v C + K_d) x_{k,k-1} - K_a B_{x_{k,k-1}} - K_v D_{x_{k,k-1}} \quad (9.53)$$

From the geometry relation and the force equilibrium condition of element p , we have

$$\begin{cases} x_{p,p+1} = x_{p,p-1} \\ q_{xp,p+1} = m(Ax_{p,p-1} + B_{x_{p,p-1}}) + q_{xp,p-1} + F_{xp,p-1} + F_{p,c} \end{cases} \quad (9.54)$$

Substituting Equation (9.53) into Equation (9.54), the transfer equation of the controlled element p is

$$\mathbf{z}_{p,p+1} = \mathbf{U}_p \mathbf{z}_{p,p-1} + \mathbf{U}_{p,c} \mathbf{z}_{k,k-1} \quad (9.55)$$

where

$$\mathbf{U}_p = \begin{bmatrix} 1 & 0 & 0 \\ -m_p A & 1 & m_p B + F_p \\ 0 & 0 & 1 \end{bmatrix}, \quad \mathbf{U}_{p,c} = \begin{bmatrix} 0 & 0 & 0 \\ -(K_a A + K_v C + K_d) & 0 & -K_a B_{x_{k,k-1}} - K_v D_{x_{k,k-1}} \\ 0 & 0 & 0 \end{bmatrix} \quad (9.56)$$

From the system structure we can obtain

$$\begin{aligned} \mathbf{z}_{2n,2n+1} &= \mathbf{U}_{2n} \mathbf{U}_{2n-1} \cdots \mathbf{U}_k \mathbf{z}_{k,k-1} \\ \mathbf{z}_{k,k-1} &= \mathbf{U}_{k-1} \mathbf{U}_{k-2} \cdots \mathbf{U}_{p+1} (\mathbf{U}_p \mathbf{U}_{p-1} \cdots \mathbf{U}_1 \mathbf{z}_{0,1} + \mathbf{U}_{p,c} \mathbf{z}_{k,k-1}) \end{aligned} \quad (9.57)$$

From the second formula of Equation (9.57), we have

$$\mathbf{z}_{k,k-1} = (\mathbf{I}_3 - \mathbf{U}_{k-1} \mathbf{U}_{k-2} \cdots \mathbf{U}_{p+1} \mathbf{U}_{p,c})^{-1} \mathbf{U}_{k-1} \mathbf{U}_{k-2} \cdots \mathbf{U}_{p+1} \mathbf{U}_p \mathbf{U}_{p-1} \cdots \mathbf{U}_1 \mathbf{z}_{0,1} \quad (9.58)$$

Substituting Equation (9.58) into Equation (9.57), the overall transfer equation is

$$\mathbf{z}_{2n,2n+1} = \mathbf{U} \mathbf{z}_{0,1} \quad (9.59)$$

The overall transfer matrix is

$$\mathbf{U} = \mathbf{U}_{2n} \mathbf{U}_{2n-1} \cdots \mathbf{U}_k (\mathbf{I}_3 - \mathbf{U}_{k-1} \mathbf{U}_{k-2} \cdots \mathbf{U}_{p+1} \mathbf{U}_{p,c})^{-1} \mathbf{U}_{k-1} \mathbf{U}_{k-2} \cdots \mathbf{U}_{p+1} \mathbf{U}_p \mathbf{U}_{p-1} \cdots \mathbf{U}_1 \quad (9.60)$$

Substituting the boundary conditions $\mathbf{z}_{0,1} = [0, q, 1]_{0,1}^T$ and $\mathbf{z}_{2n,2n+1} = [x, 0, 1]_{2n,2n+1}^T$ into Equation (9.53) yields

$$\begin{bmatrix} x \\ 0 \\ 1 \end{bmatrix}_{2n,2n+1} = \begin{bmatrix} u_{11} & u_{12} & u_{13} \\ u_{21} & u_{22} & u_{23} \\ u_{31} & u_{32} & u_{33} \end{bmatrix} \begin{bmatrix} 0 \\ q \\ 1 \end{bmatrix}_{0,1} \quad (9.61)$$

Hence

$$q_{x0,1} = -\frac{u_{23}}{u_{22}}, \quad x_{2n,2n+1} = -\frac{u_{23}}{u_{22}} u_{12} + u_{13} \quad (9.62)$$

The state vector of each element in the system at any time can be solved using Equations (9.48) and (9.49) repeatedly, and Equation (9.55).

Example 9.10 Solve the dynamics of a controlled multibody system as shown in Example 9.6 using the DTTMM for controlled multibody systems.

The results obtained by the DTTMM for controlled multibody systems are shown in Figure 9.39. It can be seen that the motion amplitude of the controlled system is much smaller than that of the noncontrolled system.

The results obtained by the TMM for linear controlled multibody systems, the DTTMM for controlled multibody systems and the Newton–Euler method are shown in Figure 9.40, which validates the TMM for linear controlled multibody systems and the DTTMM for controlled multibody systems for solving the dynamics of real-time controlled multibody systems.

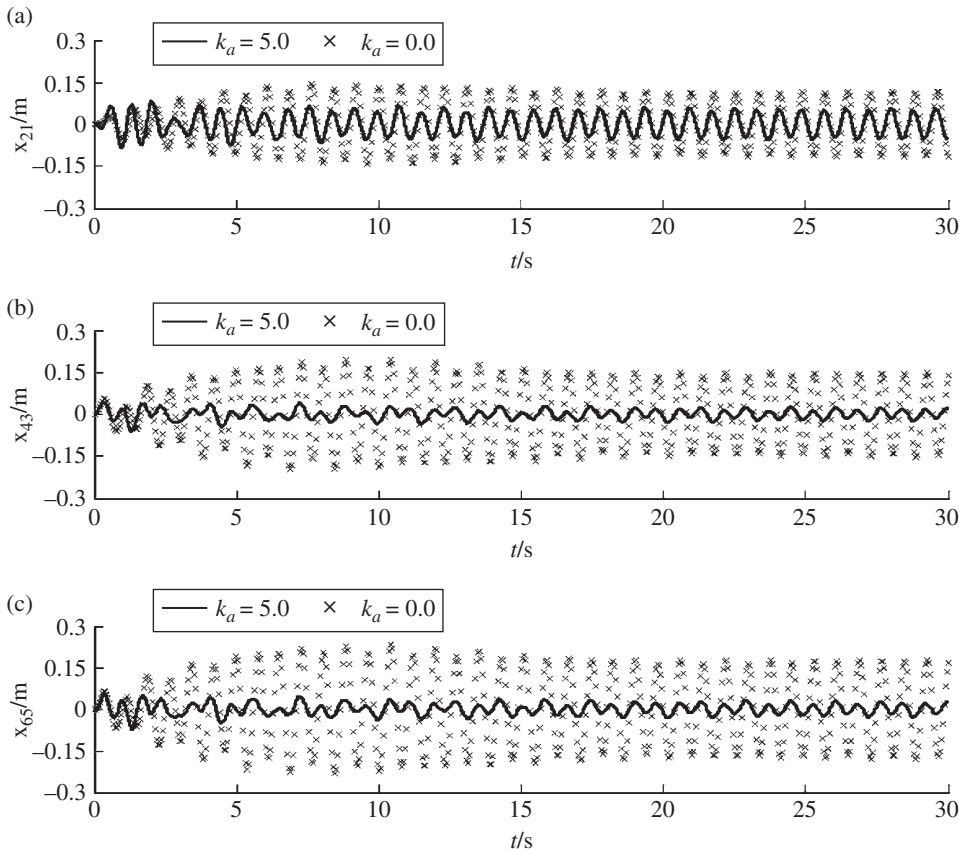


Figure 9.39 Time history of system motion with or without control: (a) time history of the displacement of lumped mass 2, (b) time history of the displacement of lumped mass 4 and (c) time history of the displacement of lumped mass 6.

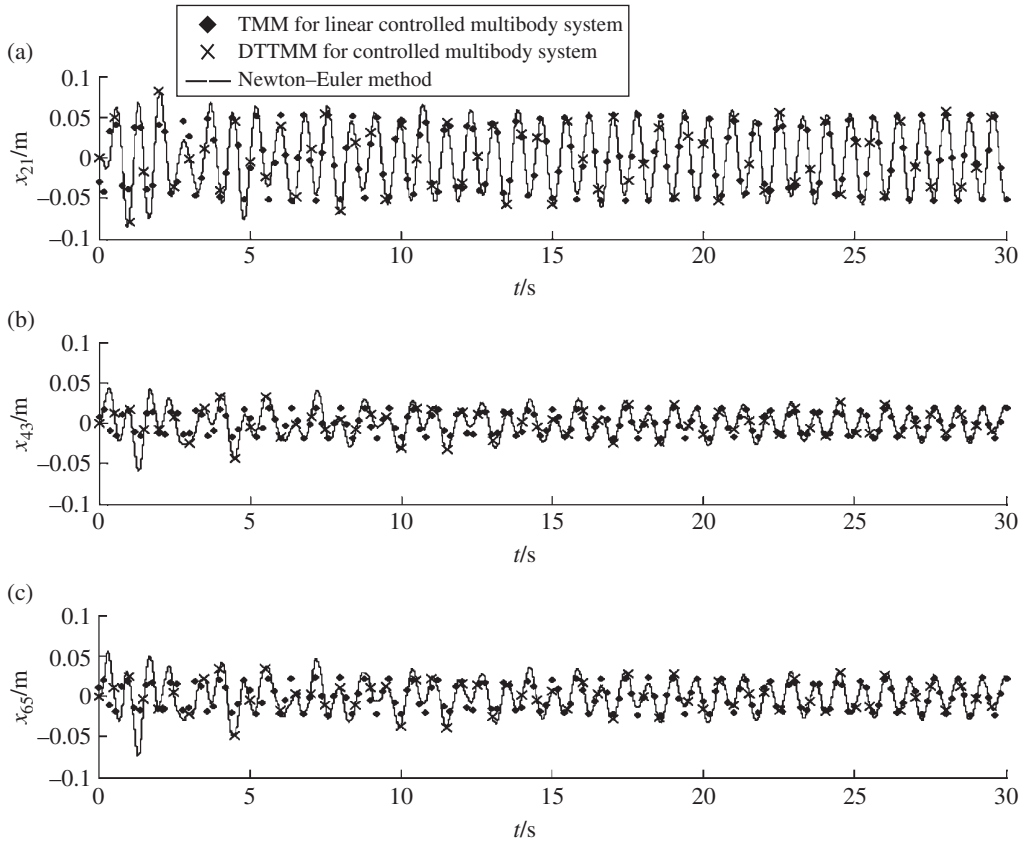


Figure 9.40 Time history of system motion: (a) time history of the displacement of lumped mass 2, (b) time history of the displacement of lumped mass 4 and (c) time history of the displacement of lumped mass 6.

Example 9.11 Solve the dynamics of the system in Example 9.7 using the TMM for linear controlled multibody systems, the DTTMM for controlled multibody systems and the Newton–Euler method.

The results obtained by the TMM for linear controlled multibody systems, the DTTMM for controlled multibody systems and the Newton–Euler method are shown in Figure 9.41. The results are in good agreement, which validates the TMM for linear controlled multibody systems and the DTTMM for controlled multibody systems.

Example 9.12 The controlled planar flexible mechanism manipulator system is composed of hub 1, rectangular cross-section beam 3 and fixed hinge 2 connected to elements 1 and 3, as shown in Figure 9.42a. The mass, radius of gyration and moment of inertia of hub 1 are $m_1 = 0.0568\text{kg}$, $r_1 = 0.1\text{m}$, $J_{c1} = 4.73 \times 10^{-5}\text{kg}\cdot\text{m}^2$, respectively. Hub 1 is driven by an electric motor and the expected time history of orientation angle is

$$\theta_1^d(t) = \begin{cases} \frac{\pi}{180} (50.0t^3 - 37.5t^4 + 7.5t^5) & 0 \leq t \leq 2 \\ 2\pi/9 & t \geq 2 \end{cases} \quad (9.63)$$

To detect and control the vibration of the rectangular cross-section beam, three pieces of piezoelectric ceramic (PZT) actuators/sensors are fixed onto its surface. The width and

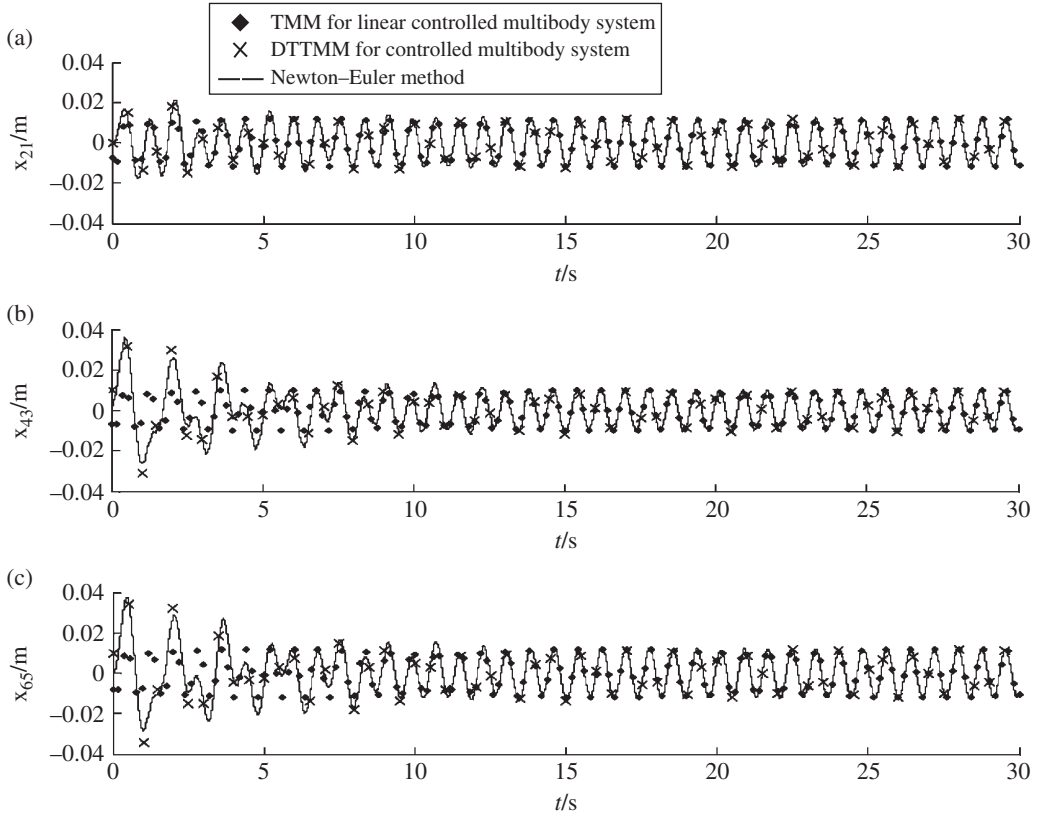


Figure 9.41 Time history of system motion: (a) time history of the displacement of lumped mass 2, (b) time history of the displacement of lumped mass 4 and (c) time history of the displacement of lumped mass 6.

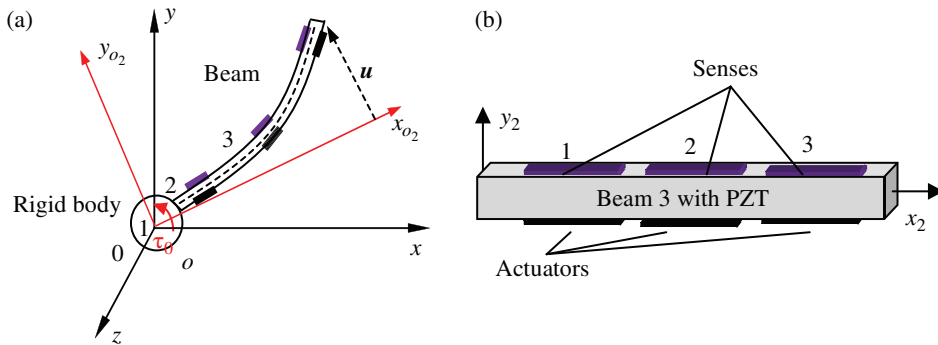


Figure 9.42 Model of a controlled planar flexible manipulator.

thickness of each PZT actuators/sensor are, respectively, the same as and much smaller than that of the beam. The positions of the PZT actuators/sensors on the corresponding flexible are $(0, 0.1)$, $(0.45, 0.55)$ and $(0.9, 1)$ in body-fixed reference coordinates. The structure parameters of flexible arm 3 are $EI_3 = 20.267 \text{ N} \cdot \text{m}^2$, $A_3 = 2.0 \text{ cm}^2$ and $l_3 = 1.0 \text{ m}$. The parameters of the PZT actuators/sensors are all the same, namely $E_a = 6.3 \times 10^{10} \text{ N/m}^2$, $l_a = 0.1 \text{ m}$,

$h_a = 0.4\text{mm}$ and $d_{31} = 110 \times 10^{-12}\text{mV}$. The PZT actuators/sensors are placed on flexible arm 3 as shown in Figure 9.42b.

The following assumptions are made for system modeling:

- 1) The thickness of the bond for each PZT actuator and the flexible arm is too thin to have a deep effect on dynamics of the system, thus is neglected.
- 2) The PZT actuators are rigidly bonded to the flexible arm.
- 3) The thickness of each PZT actuator is transparent, and their effects on the mass distribution and stiffness distribution of system are neglected. The flexible arm is considered to be a uniform cross-section Euler–Bernoulli beam.
- 4) The voltage of each PZT actuator is uniformly distributed. The polarization direction of each PZT is the same as the transverse vibration direction of the corresponding flexible arm. The trajectory tracking and active vibration control of the flexible arm are studied by combining the proportional-differential (PD) feedback control and the modal velocity feedback control.

The control moments acting on the hub rigid body and the driving voltage applied to the i th segmented PZT are, respectively

$$\tau_o(t) = -K_p[\theta_1(t) - \theta_1^d(t)] - K_v[\dot{\theta}_1(t) - \dot{\theta}_1^d(t)] - \sum_{i=1}^3 c_a V_i(t) \quad (9.64)$$

$$V_i(t) = -K_{ai} \frac{\partial \dot{u}}{\partial x_2} \Big|_{x_{i,1}^a}^{x_{i,2}^a} = -K_{ai} [{}^1s_1 {}^1s_2 \cdots {}^1s_n] \Big|_{x_{i,1}^a}^{x_{i,2}^a} [\dot{q}^1, \dot{q}^2, \dots, \dot{q}^n]^T \quad (9.65)$$

where $\theta_1^d(t)$ and $\dot{\theta}_1^d$ are the desired angle and angular velocity of hub rigid body 1, respectively, θ_1 and $\dot{\theta}_1$ are the actual angle and angular velocity, respectively, K_p and K_v are the proportion gain and velocity gain, respectively, $\tau_o(t)$ is the control moment for drive motor, K_{ai} is the gain coefficient of the i th segmented PZT actuator, V_i is the driving voltage applied to the i th segmented PZT actuator, u is the transverse deformation of the flexible arm, $Y^k(x_2)$ is the k th ($k = 1, 2, \dots, n$) model function of the flexible arm, and ${}^1s_k = \partial Y^k(x_2)/\partial x_2$. $\left(x_{i,1}^a, x_{i,2}^a\right)$ is the position coordinate of each PZT on the corresponding flexible arm in the body-fixed reference coordinate system.

Considering only the control moment on the rigid body related to its feedback state, the transfer matrix of the controlled rigid body vibrating in a plane is

$$\mathbf{U} = \begin{bmatrix} 1 & 0 & -y_{IO}(t_{i-1}) & 0 & 0 & 0 & b_1 G_1 - b_2 G_2 \\ 0 & 1 & x_{IO}(t_{i-1}) & 0 & 0 & 0 & b_1 G_2 + b_2 G_1 \\ 0 & 0 & 1 & 0 & 0 & 0 & 0 \\ u_{41} & u_{42} & u_{43} & 1 & u_{45} & u_{46} & u_{47} \\ -mA & 0 & mA y_{IC}(t_{i-1}) & 0 & 1 & 0 & u_{57} \\ 0 & -mA & -mA x_{IC}(t_{i-1}) & 0 & 0 & 1 & u_{67} \\ 0 & 0 & 0 & 0 & 0 & 0 & 1 \end{bmatrix} \quad (9.66)$$

where

$$\begin{aligned} u_{43} &= -mA x_{IC}(t_{i-1}) x_{IO} - mA y_{IC}(t_{i-1}) y_{IO} + J_I A + K_p + K_v C \\ u_{47} &= -m_C + u_{67} x_{IO} - u_{57} y_{IO} + J_I B + (m B_{y_I} - f_{y,C}) x_{IC} + (f_{x,C} - m B_{x_I}) y_{IC} \\ &\quad - K_p \theta_1^d(t) - K_v \dot{\theta}_1^d(t) + K_v D_\theta \end{aligned}$$

u_{41} , u_{42} , u_{45} , u_{46} , u_{57} and u_{67} are the same as in Equation (7.101).

Using Equations (9.66) to (9.68), and considering the control moment of the PZT actuators, the transfer matrix of the controlled piezoelectric beam vibrating in a plane is

$$U = \begin{bmatrix} 1 & 0 & u_{1,3} & 0 & 0 & 0 & u_{1,6+1} & \cdots & u_{1,6+n} & u_{1,6+n+1} \\ 0 & 1 & u_{2,3} & 0 & 0 & 0 & u_{2,6+1} & \cdots & u_{2,6+n} & u_{2,6+n+1} \\ 0 & 0 & 1 & 0 & 0 & 0 & 0 & \cdots & 0 & 0 \\ u_{4,1} & u_{4,2} & u_{4,3} & 1 & u_{4,5} & u_{4,6} & u_{4,6+1} & \cdots & u_{4,6+n} & u_{4,6+n+1} \\ u_{5,1} & 0 & u_{5,3} & 0 & 1 & 0 & u_{5,6+1} & \cdots & u_{5,6+n} & u_{5,6+n+1} \\ 0 & u_{6,2} & u_{6,3} & 0 & 0 & 1 & u_{6,6+1} & \cdots & u_{6,6+n} & u_{6,6+n+1} \\ 0 & 0 & 0 & 0 & 0 & 0 & 1 & \cdots & 0 & 0 \\ \vdots & \vdots & \vdots & \vdots & \vdots & \vdots & \vdots & \ddots & \vdots & \vdots \\ 0 & 0 & 0 & 0 & 0 & 0 & 0 & \cdots & 1 & 0 \\ 0 & 0 & 0 & 0 & 0 & 0 & 0 & \cdots & 0 & 1 \end{bmatrix} \quad (9.67)$$

where

$$\begin{aligned} u_{1,3} &= -l_3 s - c \sum_{k=1}^n Y_O^k q_{t_{i-1}}^k, u_{1,6+k} = -s Y_O^k (k=1, \dots, n), \\ u_{1,6+n+1} &= l_3(c + \theta s) + c \sum_{k=1}^n Y_O^k q_{t_{i-1}}^k \theta_{t_{i-1}}, u_{2,3} = l_3 c - s \sum_{k=1}^n Y_O^k q_{t_{i-1}}^k, u_{2,6+k} = c Y_O^k \\ & (k=1, \dots, n) \\ u_{2,6+n+1} &= l_3(s - \theta c) + s \sum_{k=1}^n Y_O^k q_{t_{i-1}}^k \theta_{t_{i-1}}, u_{4,j} = l_3 \zeta_{1,j} + \xi_j \quad (j=1, 2, 3) \\ u_{4,5} &= -l_3 \bar{s}, u_{4,6} = l_3 \bar{c}, u_{4,6+k} = \xi_{6+k} - \sum_{i=1}^3 c_a K_{ai} l_{ai}^{-1} s_k \Big|_{x_{i,1}^a}^{x_{i,2}^a} C + l_3 \zeta_{1,6+k} (k=1, \dots, n) \\ u_{4,6+n+1} &= l_3 \zeta_{1,6+n+1} + \xi_{6+n+1} - \int_0^{l_3} x_2 f_{2,y}(x_2, t) dx_2 - \int_0^{l_3} m'(x_2, t) dx_2 + \sum_{k=1}^n \sum_{i=1}^3 c_a K_{ai} l_{ai}^{-1} s_k \Big|_{x_{i,1}^a}^{x_{i,2}^a} D_{q^k} \\ u_{5,1} &= -m A, u_{5,j} = \bar{c} \zeta_{2,j} - \bar{s} \zeta_{1,j} \quad (j=3, 6+1, \dots, 6+n, 6+n+1) \\ u_{6,2} &= -m A, u_{6,j} = \bar{s} \zeta_{2,j} + \bar{c} \zeta_{1,j} \quad (j=3, 6+1, \dots, 6+n, 6+n+1) \\ \xi_1 &= -\left(m \bar{c} \sum_{k=1}^n s_k^0 q_{t_{i-1}}^k + \frac{l_3}{2} m \bar{s} \right) A, \xi_2 = \left(\frac{l_3}{2} m \bar{c} - \bar{m} \bar{s} \sum_{k=1}^n s_k^0 q_{t_{i-1}}^k \right) A \\ \xi_3 &= \bar{m} \sum_{k=1}^n \sum_{j=1}^n s_{k,j}^0 [2C q^k(t_{i-1}) \dot{q}^j(t_{i-1}) + A q^k(t_{i-1}) q^j(t_{i-1})] + m \frac{l_3^2}{3} A \\ \xi_{6+k} &= \bar{m} \sum_{j=1}^n s_{k,j}^0 \left(2\dot{\theta}_{t_{i-1}} \dot{q}_{t_{i-1}}^j + 2C \dot{\theta}_{t_{i-1}} q_{t_{i-1}}^j + 2\ddot{\theta}_{t_{i-1}} q_{t_{i-1}}^j \right) + \bar{m} \sum_{k=1}^n s_k^1 A - \bar{m} (\bar{s} s_k^0 \ddot{y}_{O_2, t_{i-1}} + \bar{c} s_k^0 \ddot{x}_{O_2, t_{i-1}}) \\ & (k=1, \dots, n) \\ \xi_{6+n+1} &= 2\bar{m} \sum_{k=1}^n \sum_{j=1}^n s_{k,j}^0 \left[D_{\theta} q_{t_{i-1}}^k q_{t_{i-1}}^j + \dot{\theta}_{t_{i-1}} q_{t_{i-1}}^k D_{q^j} - 2\dot{\theta}(t_{i-1}) q_{t_{i-1}}^k q_{t_{i-1}}^j \right] + \bar{m} \sum_{k=1}^n s_k^1 B_{q^k} \\ & + \bar{m} \sum_{k=1}^n \sum_{j=1}^n s_{k,j}^0 \left[B_{\theta} q_{t_{i-1}}^k q_{t_{i-1}}^j - 2\ddot{\theta}(t_{i-1}) q_{t_{i-1}}^k q_{t_{i-1}}^j \right] + \frac{l_3}{2} m \left(\bar{c} B_{y_{O_2}} - \bar{s} B_{x_{O_2}} \right) + m \frac{l_3^2}{3} B_{\theta} \\ & - \bar{m} \sum_{k=1}^n s_k^0 \left[\bar{s} \left(q_{t_{i-1}}^k B_{y_{O_2}} - q_{t_{i-1}}^k \ddot{y}_{O_2, t_{i-1}} \right) + \bar{c} \left(q_{t_{i-1}}^k B_{x_{O_2}} - q_{t_{i-1}}^k \ddot{x}_{O_2, t_{i-1}} \right) \right] \end{aligned}$$

$$\begin{aligned}
\zeta_{1,1} &= m\bar{s}A, \zeta_{1,2} = -m\bar{c}A, \zeta_{1,3} = 2\bar{m}C\dot{\theta}_{t_{i-1}} \sum_{k=1}^n s_k^0 q_{t_{i-1}}^k - \frac{ml_3}{2}A, \zeta_{1,6+k} = \bar{m}(\dot{\theta}_{t_{i-1}}^2 - A)s_k^0 \\
\zeta_{1,6+n+1} &= \int_0^{l_3} f_{2,y}(x_2, t) dx_2 + m\bar{s}B_{x_{O_2}} - m\bar{c}B_{y_{O_2}} - \frac{ml_3}{2}B_\theta + 2\bar{m}D_\theta \dot{\theta}_{t_{i-1}} \sum_{k=1}^n s_k^0 q_{t_{i-1}}^k \\
&\quad - 2\bar{m}\dot{\theta}_{t_{i-1}}^2 \sum_{k=1}^n s_k^0 q_{t_{i-1}}^k - \bar{m} \sum_{k=1}^n s_k^0 B_{q^k} + \bar{m} \sum_{k=1}^n s_k^0 [\ddot{\theta}_{t_{i-1}}^2 q_{t_{i-1}}^k + 2\dot{\theta}_{t_{i-1}} \ddot{\theta}_{t_{i-1}} \dot{q}_{t_{i-1}}^k] \Delta T^2 \\
\zeta_{2,1} &= -m\bar{c}A, \zeta_{2,2} = -m\bar{s}A, \zeta_{2,3} = \bar{m} \left(l_3^2 C \dot{\theta}_{t_{i-1}} + A \sum_{k=1}^n s_k^0 q_{t_{i-1}}^k + 2C \sum_{k=1}^n s_k^0 \dot{q}_{t_{i-1}}^k \right) \\
\zeta_{2,6+k} &= \bar{m} (2\dot{\theta}_{t_{i-1}} C + \ddot{\theta}_{t_{i-1}}) s_k^0 \quad (k=1, 2, \dots, n) \\
\zeta_{2,6+n+1} &= \int_0^{l_3} f_{2,x}(x_2, t) dx_2 + 2\bar{m}\dot{\theta}_{t_{i-1}} \sum_{k=1}^n s_k^0 D_{q^k} + 2\bar{m}D_\theta \sum_{k=1}^n s_k^0 \dot{q}_{t_{i-1}}^k - 2\bar{m}\dot{\theta}_{t_{i-1}} \sum_{k=1}^n s_k^0 \dot{q}_{t_{i-1}}^k \\
&\quad + \bar{m}B_\theta \sum_{k=1}^n s_k^0 q_{t_{i-1}}^k - \bar{m}\ddot{\theta}_{t_{i-1}} \sum_{k=1}^n s_k^0 q_{t_{i-1}}^k + \frac{ml_3}{2} (2D_\theta \dot{\theta}_{t_{i-1}} - \dot{\theta}_{t_{i-1}}^2 + \ddot{\theta}_{t_{i-1}} \Delta T^2) \\
&\quad - m\bar{s}B_{y_{O_2}} - m\bar{c}B_{x_{O_2}} + 2\bar{m}\ddot{\theta}_{t_{i-1}} \Delta T^2 \sum_{k=1}^n s_k^0 \ddot{q}_{t_{i-1}}^k \\
Y_O^k &= Y^k(l_3), s_k^0 = \int_0^{l_3} Y^k(x_2) dx_2, s_{k,k}^0 = \int_0^{l_3} Y^k(x_2) Y^k(x_2) dx_2, s_k^1 = \int_0^{l_3} Y^k(x_2) x_2 dx_2 \\
c_a &= \frac{1}{2} d_{31} E_a b (t_a + 2t_b), H(x) = \begin{cases} 1 & x \geq 0 \\ 0 & x < 0 \end{cases}, m = \bar{m}l_3
\end{aligned}$$

b and t_b are the width and thickness of the flexible arm, respectively. t_a is the thickness of the segmented PZT actuator.

For the fixed hinge whose inboard body is a rigid body and whose outboard body is a piezoelectric beam with large planar motion the position coordinates, orientation angles, internal moments and internal forces of the rigid body's input and output are equal. The transfer relation between the generalized coordinates describing the deformation of the outboard flexible body and the input end of the fixed hinge only needs to be determined. The dynamics equation of the transverse vibration of the beam is given by Equation (8.91) and the highest order of the mode shapes is chosen to be 3. The distributed moments of the PZT actuators and the control equation of the PZT actuators should be taken into consideration when we deduce the transfer equation of the beam. The state vectors of the fixed hinge whose input end is a rigid body and output end is a piezoelectric beam with large planar motion are defined as

$$\begin{aligned}
z_O &= [x, y, \theta, m, q_x, q_y, q^1, q^2, q^3, 1]^T \\
z_I &= [x, y, \theta, m, q_x, q_y, 1]^T
\end{aligned} \tag{9.68}$$

The transfer equation is

$$z_O = \mathbf{U} z_I \tag{9.69}$$

The transfer matrix is

$$\mathbf{U} = \begin{bmatrix} 1 & 0 & 0 & 0 & 0 & 0 & 0 \\ 0 & 1 & 0 & 0 & 0 & 0 & 0 \\ 0 & 0 & 1 & 0 & 0 & 0 & 0 \\ 0 & 0 & 0 & 1 & 0 & 0 & 0 \\ 0 & 0 & 0 & 0 & 1 & 0 & 0 \\ 0 & 0 & 0 & 0 & 0 & 1 & 0 \\ \Delta_{11}/\Delta & \Delta_{12}/\Delta & \Delta_{13}/\Delta & 0 & 0 & 0 & \Delta_{14}/\Delta \\ \Delta_{21}/\Delta & \Delta_{22}/\Delta & \Delta_{23}/\Delta & 0 & 0 & 0 & \Delta_{24}/\Delta \\ \Delta_{31}/\Delta & \Delta_{32}/\Delta & \Delta_{33}/\Delta & 0 & 0 & 0 & \Delta_{34}/\Delta \\ 0 & 0 & 0 & 0 & 0 & 0 & 1 \end{bmatrix} \quad (9.70)$$

where

$$\Delta = \begin{vmatrix} A_{11} & A_{12} & A_{13} \\ A_{21} & A_{22} & A_{23} \\ A_{31} & A_{32} & A_{33} \end{vmatrix}, \Delta_{1i} = \begin{vmatrix} B_{1i} & A_{12} & A_{13} \\ B_{2i} & A_{22} & A_{23} \\ B_{3i} & A_{32} & A_{33} \end{vmatrix}, \Delta_{2i} = \begin{vmatrix} A_{11} & B_{1i} & A_{13} \\ A_{21} & B_{2i} & A_{23} \\ A_{31} & B_{3i} & A_{33} \end{vmatrix}, \Delta_{3i} = \begin{vmatrix} A_{11} & A_{12} & B_{1i} \\ A_{21} & A_{22} & B_{2i} \\ A_{31} & A_{32} & B_{3i} \end{vmatrix} \quad (i = 1, 2, 3, 4)$$

$$A_{k',k} = -\bar{m}s_{k,k'}\dot{\theta}_{t_{i-1}}^2 - \sum_{i=1}^M c_a K_{ai} \int_{x_{1,i}^a}^{x_{2,i}^a} Y^{k'}(x_2) dx_2 {}^1s_k \Big|_{x_{1,i}^a}^{x_{2,i}^a} C \quad (k = 1, 2, 3, \quad k' \neq k)$$

$$A_{k',k'} = {}^4s_{k,k'}EI - {}^2s_{k,k'}\rho IA + \bar{m}s_{k,k'}A - \bar{m}s_{k,k'}\dot{\theta}_{t_{i-1}}^2 - \sum_{i=1}^M c_a K_{ai} \int_{x_{1,i}^a}^{x_{2,i}^a} Y^{k'}(x_2) dx_2 {}^1s_k \Big|_{x_{1,i}^a}^{x_{2,i}^a} C$$

$$B_{k',1} = \bar{m}\bar{s}s_{k'}^0 A, B_{k',2} = -\bar{m}\bar{c}s_{k'}^0 A, B_{k',3} = -\bar{m} \left(s_{k'}^1 A - 2Cs_{k',k'}q_{t_{i-1}}^k \dot{\theta}_{t_{i-1}} \right)$$

$$B_{k',5+n} = \int_0^{l_3} Y^{k'}(x_2) f(x_2, t) dx_2 - \int_0^{l_3} Y^{k'}(x_2) \frac{\partial}{\partial x_2} m'(x_2, t) dx_2 + \rho I^2 s_{k',k'} B_{q^{k'}} \\ - \bar{m} \left\{ s_{k',k'} B_{q^{k'}} - s_{k',k'} \left[2q_{t_{i-1}}^{k'} \dot{\theta}_{t_{i-1}} D_\theta - 2q^{k'}(t_{i-1}) \dot{\theta}_{t_{i-1}}^2 \right] + s_{k'}^1 B_\theta + \bar{c}s_{k'}^0 B_{y_{O_2}} - \bar{s}s_{k'}^0 B_{x_{O_2}} \right\} \quad (k' = 1, 2, 3)$$

For compound control by the PD controller and modal velocity feedback control based on PZT actuators, the transfer matrix $\mathbf{U}_{1'}$ of the control element is

$$\mathbf{U}_{1'} = (\mathbf{I} - \mathbf{U}_1^3 \mathbf{U}_2)^{-1} \quad (9.71)$$

where \mathbf{U}_1^3 is the feedback parameter matrix related to the feedback parameter from feedback beam 3 to hub 1.

For the modal velocity feedback control, we have

$$\mathbf{U}_1^3 = - \sum_{i=1}^M c_a K_{ai} \begin{bmatrix} \mathbf{O}_{3 \times 6} & \mathbf{O}_{3 \times n} & 0 \\ \mathbf{O}_{1 \times 6} & C^1 s_1 \Big|_{x_{i,1}^a}^{x_{i,2}^a} & \cdots & C^1 s_n \Big|_{x_{i,1}^a}^{x_{i,2}^a} & \sum_{k=1}^n D_{q^k} {}^1s_k \Big|_{x_{i,1}^a}^{x_{i,2}^a} \\ \mathbf{O}_{3 \times 6} & \mathbf{O}_{3 \times n} & 0 \end{bmatrix} \quad (9.72)$$

According to the DTTMM for controlled multibody systems, the state vectors of the system are

$$\begin{aligned}
 \mathbf{z}_{3,4} &= [x, y, \theta, m, q_x, q_y, q^1, q^2, q^3, 1]_{3,4}^T \\
 \mathbf{z}_{3,2} &= [x, y, \theta, m, q_x, q_y, q^1, q^2, q^3, 1]_{3,2}^T \\
 \mathbf{z}_{1',2} &= [x, y, \theta, m, q_x, q_y, 1]_{1',2}^T \\
 \mathbf{z}_{1,1'} &= [x, y, \theta, m, q_x, q_y, 1]_{1,1'}^T \\
 \mathbf{z}_{1,0} &= [x, y, \theta, m, q_x, q_y, 1]_{1,0}^T
 \end{aligned} \tag{9.73}$$

The boundary conditions are

$$\begin{aligned}
 \mathbf{z}_{1,0} &= [0, 0, \theta_1(t_i), 0, q_x, q_y, 1]_{1,0}^T \\
 \mathbf{z}_{3,4} &= [x, y, \theta, 0, 0, 0, q^1, q^2, q^3, 1]_{3,4}^T
 \end{aligned} \tag{9.74}$$

The overall transfer equation is

$$\mathbf{z}_{3,4} = \mathbf{U}_3 \mathbf{U}_2 \mathbf{U}_{1'} \mathbf{U}_1 \mathbf{z}_{1,0} \tag{9.75}$$

where \mathbf{U}_3 , \mathbf{U}_2 , \mathbf{U}_1 and $\mathbf{U}_{1'}$ are determined by Equations (9.67), (9.70), (9.66) and (9.71), respectively.

The dynamics of the controlled flexible manipulator system calculated by the DTTMM for controlled multibody systems are shown in Figure 9.43. The time history of the expected orientation angle of the body-fixed reference system of flexible arm 3 is shown in Figure 9.43a. The time history of the transverse deformation at the tip of arm 3 with and without PZT active control is shown in Figure 9.43b. The driving voltage applied to segmented PZT 1 is shown in Figure 9.43c. The simulation results show that the orientation angle of the flexible manipulator and expected track have good agreement. The transverse deformation at the tip of the arm decreases quickly. This validates the DTTMM for controlled multibody systems for the solution of the trajectory tracking of the flexible manipulator and active control of vibration.

Example 9.13 The system shown in Figure 9.44 is composed of a rigid body with one input and one output end and a spatial elastic hinge, and the effect of damping is not considered. Solve the dynamic response of the system under an external force acting on the rigid body.

The state vector of the input end of element 1 is defined as

$$\mathbf{z}_{0,1} = [x, y, z, \theta_x, \theta_y, \theta_z, m_x, m_y, m_z, q_x, q_y, q_z, 1]_{0,1}^T \tag{9.76}$$

The state vector of the output end of feedback element 2 is defined as

$$\mathbf{z}_{2,3} = [x, y, z, \theta_x, \theta_y, \theta_z, m_x, m_y, m_z, q_x, q_y, q_z, 1]_{2,3}^T \tag{9.77}$$

The transfer matrix of the control element is

$$\mathbf{U}_C = \begin{bmatrix} \mathbf{O}_{8 \times 5} & \mathbf{O}_{8 \times 1} & \mathbf{O}_{8 \times 6} & \mathbf{O}_{8 \times 1} \\ \mathbf{O}_{1 \times 5} & H_z & \mathbf{O}_{1 \times 6} & H_{z1} \\ \mathbf{O}_{4 \times 5} & \mathbf{O}_{4 \times 1} & \mathbf{O}_{4 \times 6} & \mathbf{O}_{4 \times 1} \end{bmatrix} \tag{9.78}$$

where $H_z = -K_a A - K_v C - K_d$, $H_{z1} = -K_a B_{\theta_z} - K_v D_{\theta_z}$

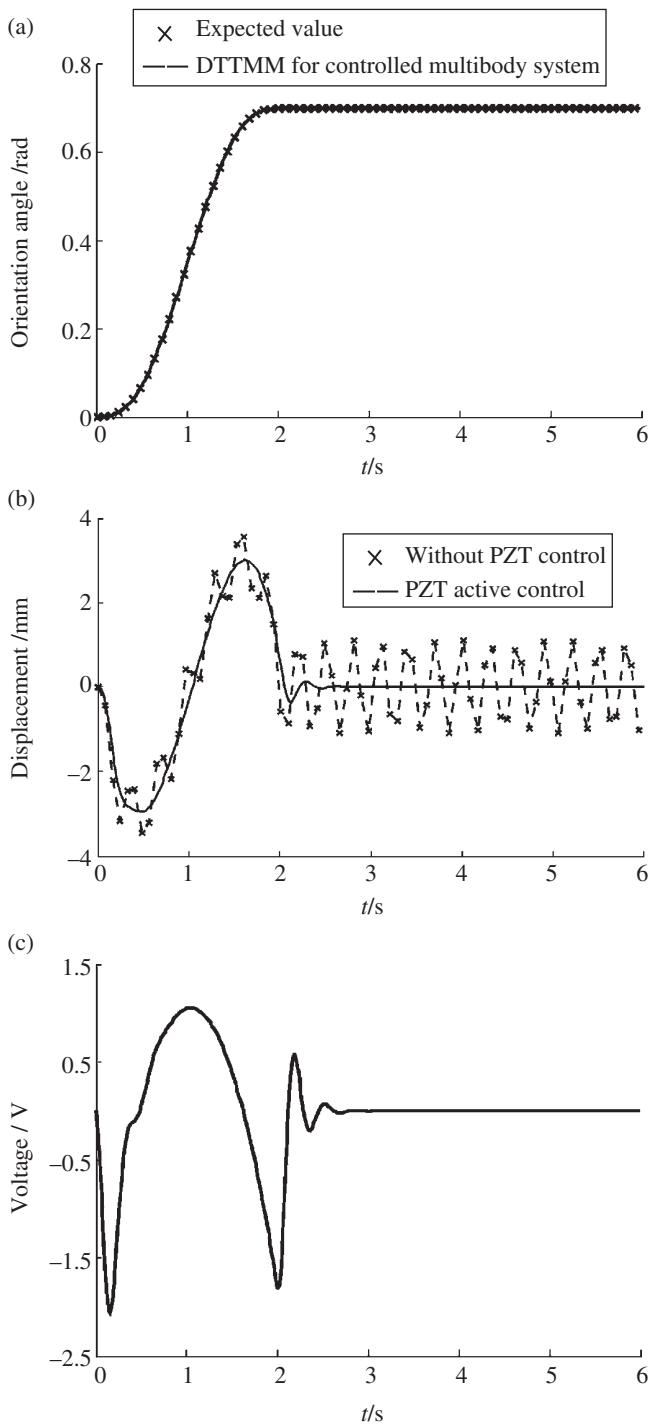
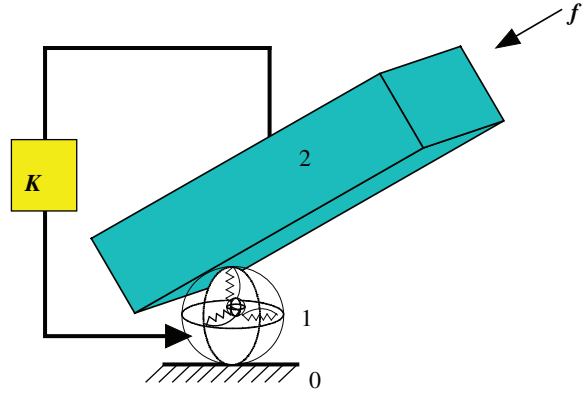


Figure 9.43 Dynamics of a controlled flexible manipulator system: (a) time history of the orientation angle of a flexible arm, (b) time history of the transverse deformation at the tip of the arm and (c) time history of the driven voltage applied to segmented PZT 1.

Figure 9.44 Multibody system composing of a rigid body and an elastic hinge moving in space.



The control parameters are

$$K_a = 0.0 \text{ N}\cdot\text{s}^2/\text{m}, K_v = 700000.0 \text{ N}\cdot\text{s}/\text{m}, K_d = 80000.0 \text{ N}/\text{m}$$

The transfer relation of control is

$$\begin{aligned} z_{2,1} &= \mathbf{U}_1 z_{0,1} + \mathbf{U}_C z_{2,3} \\ z_{2,3} &= \mathbf{U}_2 \mathbf{H}_\alpha z_{2,1} \end{aligned} \quad (9.79)$$

The overall transfer matrix is

$$z_{2,3} = (\mathbf{I} - \mathbf{U}_2 \mathbf{H}_\alpha \mathbf{U}_C)^{-1} \mathbf{U}_2 \mathbf{H}_\alpha \mathbf{U}_1 z_{0,1} \quad (9.80)$$

where \mathbf{U}_1 is the transfer matrix of the spatial elastic hinge and \mathbf{U}_2 is the transfer matrix of the rigid body moving in space. \mathbf{H}_α is the coordinate transformation matrix around the z axis.

The boundary conditions are $x_{0,1} = 0$, $y_{0,1} = 0$, $z_{0,1} = 0$, $\theta_{x0,1} = 0$, $\theta_{y0,1} = 0$, $\theta_{z0,1} = 0$, $m_{x2,3} = 0$, $m_{y2,3} = 0$, $m_{z2,3} = 0$, $q_{x2,3} = 0$, $q_{y2,3} = 0$ and $q_{z2,3} = 0$.

The dynamics of the controlled multibody system are simulated by the DTTMM for controlled multibody systems and the Newton–Euler method. The simulation results are shown in Figure 9.45. From Figure 9.45, it can be seen that the system vibrates with equal amplitude under an external force without control, and the system motion attenuates to the equilibrium balancing position under feedback control. The results obtained by the two methods are in good agreement, which validates the DTTMM for controlled multibody systems for solving the dynamics of controlled multibody systems.

9.6.2 Discrete Time Transfer Matrix Method for Controlled Multibody Systems with Time Delay

For a controlled system with time delay, the control force in Equation (9.13) with time delay can be described as the function of the former motion parameters $x_{k,k-1}$, $\dot{x}_{k,k-1}$ and $\ddot{x}_{k,k-1}$ as follows

$$F_{p,c} = -K_a \ddot{x}_{k,k-1}(t-\tau) - K_v \dot{x}_{k,k-1}(t-\tau) - K_d x_{k,k-1}(t-\tau) \quad (9.81)$$

where τ is the time delay.

For the controlled system with time delay, substituting Equation (9.81) into Equation (9.54) and replacing u_{23} of the control transfer matrix by the known control force $F_{p,c}$ in current time yields

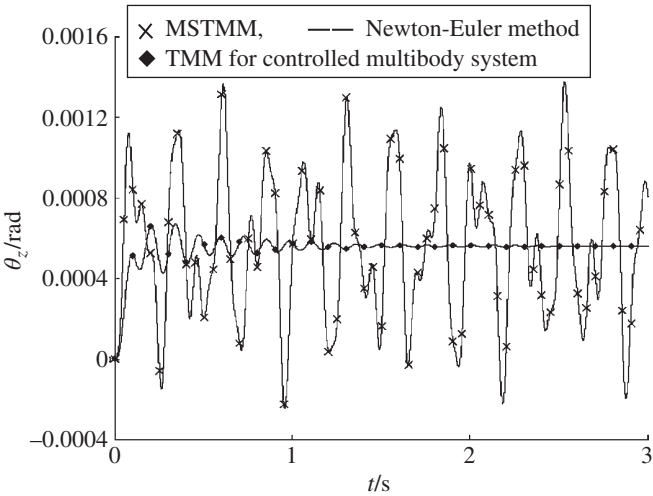


Figure 9.45 Time history of the angle of a rigid body around the z axis.

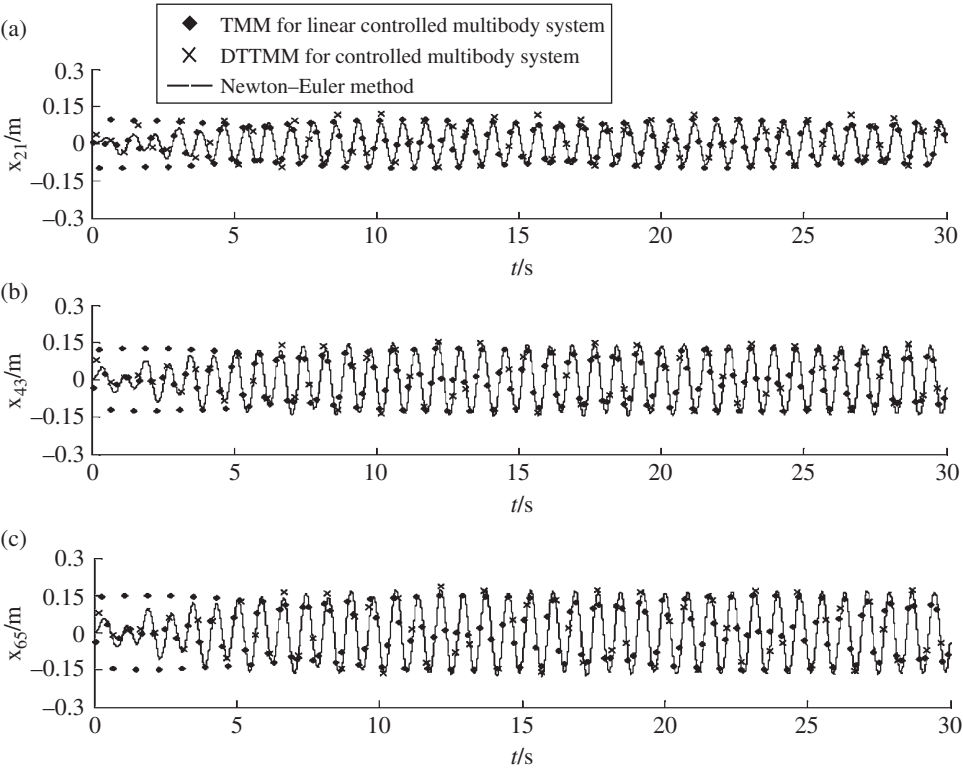


Figure 9.46 Time history of system motion: (a) time history of the displacement of lumped mass 2, (b) time history of the displacement of lumped mass 4 and (c) time history of the displacement of lumped mass 6.

$$\mathbf{U}_{p,c} = \begin{bmatrix} 0 & 0 & 0 \\ 0 & 0 & -K_a \ddot{x}_{k,k-1} - K_v \dot{x}_{k,k-1} - K_d x_{k,k-1} \\ 0 & 0 & 0 \end{bmatrix} \quad (9.82)$$

For the controlled system with time delay, the current control force is the function of the former force and can be regarded as an external force. The elements of $\mathbf{U}_{p,c}$ are all known functions of the previous time step, and Equation (9.60) can be written as

$$\mathbf{U} = \mathbf{U}_{2n} \mathbf{U}_{2n-1} \cdots \mathbf{U}_{p+1} (\mathbf{U}_p + \mathbf{U}_{p,c}) \mathbf{U}_{p-1} \cdots \mathbf{U}_1 \quad (9.83)$$

Applying the boundary conditions of the system and using Equations (9.48) and (9.49) repeatedly, the state vectors of each element at any time can be obtained.

Example 9.14 In Example 9.7, the control signals $\ddot{x}_{6,5}$, $\dot{x}_{6,5}$ and $x_{6,5}$ are the functions of motion parameters in the previous time (0.001 s), namely there is time delay 0.001 s. $K_a = 0.1 \text{ N}\cdot\text{s}^2/\text{m}$, $K_v = 1.0 \text{ N}\cdot\text{s}/\text{m}$ and $K_d = 30.0 \text{ N}/\text{m}$. The numerical results of the dynamics of controlled multibody systems with time delay and controlled multibody systems with real-time are obtained by the DTTMM for controlled multibody systems, the TMM for linear controlled multibody systems and the Newton–Euler method, as shown in Figure 9.46.

Comparing the results in Figures 9.41 and 9.46, and it can be seen that the three methods show the validity of solving the dynamics of controlled multibody systems by the TMM of linear controlled multibody systems and the DTTMM of controlled multibody systems.

10

Derivation and Computation of Transfer Matrices

10.1 Introduction

Generally speaking, all kinds of dynamics problems of multibody systems (MSs) can be easily solved using the transfer matrix method for multibody systems (MSTMM) once the transfer matrices of elements are obtained. The library of transfer matrices of various kinds of elements related to MSs is listed in Chapter 15. Those transfer matrices which are not included in the transfer matrix library can be derived by using the methods introduced in this book. The transfer matrices of elements can mainly be derived from differential equations of motion, from solving an n -order differential equation, from n first-order differential equations and from the stiffness matrix. The transfer matrices of discrete elements such as rigid bodies, lumped masses, springs and rotary springs whose dynamic equations are expressed by *ordinary differential equations*, can be directly derived from differential equations of motion with simple substitution and rewriting of the dynamic equations of elements. The transfer matrices of continuous elements such as elastic beams, rods, shafts, plates, etc., whose dynamic equations are expressed by *partial differential equations*, can be derived by solving partial differential equations, which is primarily done by solving the n -order ordinary differential equations after substitution, or by solving n first-order differential equations. For continuous elements (including one-, two- and three-dimensional problems), the transfer matrices can be obtained directly from *stiffness matrices* after dividing the continuous elements into small pieces according to the specified input and output ends (points, lines or planes). This provides a new train of thought to solve problems of complex system dynamics combining the finite element method (FEM) and the MSTMM.

Generally speaking, the MSTMM belongs to precise computation methods in terms of the exactness of the transfer equations and satisfaction with boundary conditions. The high efficiency of numerical computation is one of the most important characteristics of the MSTMM. However, during the process of the computation of higher-order modal eigenvalues, because of the large numerical difference for different transfer matrix elements, larger computational error may occur, with small numbers submerged by large numbers. This case is similar to the numerical “ill-condition” in computing structural dynamics with a large stiffness gradient using the FEM. However, it is much easier for the MSTMM than the FEM to overcome such problems.

The general derivation method of transfer matrices is introduced in this chapter. The numerical computational problems related to the transfer matrix and their solution procedures are discussed in detail, such as how to obtain the inverse matrix directly by using the MSTMM according to the natural characteristics of a mechanical system to avoid numerical errors in

Table 10.1 Comparing transfer matrices in different situations

Situation		Lumped mass		Spring	
		Transfer matrix	Characteristics	Transfer matrix	Characteristics
Free vibration	Undamped	$\begin{bmatrix} 1 & 0 \\ m\omega^2 & 1 \end{bmatrix}$	ω is the natural frequency of the system, eigenvalue $\lambda = i\omega$	$\begin{bmatrix} 1 & -\frac{1}{K} \\ 0 & 1 \end{bmatrix}$	The transfer matrix has the same form of damped free vibration with the damping coefficient $C = 0$
	Damped	$\begin{bmatrix} 1 & 0 \\ -m\lambda^2 & 1 \end{bmatrix}$	The same form as undamped free vibration, transfer matrix is obtained by substituting $-\lambda^2$ for ω^2	$\begin{bmatrix} 1 & -\frac{1}{K + C\lambda} \\ 0 & 1 \end{bmatrix}$	The same form as undamped free vibration is obtained by substituting $K + C\lambda$ for K
Forced vibration	Undamped	$\begin{bmatrix} 1 & 0 & 0 \\ m\Omega^2 & 1 & F \\ 0 & 0 & 1 \end{bmatrix}$	The principal part has the same form as the transfer matrix of undamped free vibration; Ω is the excitation frequency	$\begin{bmatrix} 1 & -\frac{1}{K} & 0 \\ 0 & 1 & 0 \\ 0 & 0 & 1 \end{bmatrix}$	The principal part has the same form as the transfer matrix of undamped free vibration
	Damped	$\begin{bmatrix} 1 & 0 & 0 \\ m\Omega^2 & 1 & \bar{F} \\ 0 & 0 & 1 \end{bmatrix}$	The principal part has the same form as the transfer matrix of undamped free vibration; Ω is the excitation frequency	$\begin{bmatrix} 1 & -\frac{1}{K + iC\Omega} & 0 \\ 0 & 1 & 0 \\ 0 & 0 & 1 \end{bmatrix}$	The principal part has the same form as the transfer matrix of undamped free vibration, substituting $K + iC\Omega$ for K

computing the inverse matrix, and how to improve the algorithm for solving eigenvalues to avoid overflow when computing eigenvalues. Finally, the Riccati transfer matrix method, obtained by combining the Riccati transformation and the MSTMM, is introduced to reduce the computational cumulative error and increase the computing speed.

The computational method of transfer matrices mainly relates to the multiplication of transfer matrices, the improved algorithm for the *eigenvalue problem*, the *chessboard rule*, and the Riccati MSTMM, etc. Comparing the forms of the transfer matrices of lumped masses and springs in a spring–mass system under different situations, as shown in Table 10.1, both the principal parts of the transfer matrices of damped systems and the extended transfer matrices of forced vibration systems can be obtained by transforming the transfer matrices of elements in *undamped free vibration*.

In this chapter, the derivation method of the transfer matrices of elements in undamped free vibration systems is discussed first, then ways of obtaining transfer matrices in other situations are introduced. For extended transfer matrices of *forced vibration systems* we introduce how to derive the block matrix f .

10.2 Derivation from Dynamics Equations

The transfer matrices of lumped masses, springs, dampers, etc. are derived in Chapter 2. The derivation of the transfer matrices of rigid bodies and rotary springs is introduced in this section to outline the idea of deriving the transfer matrices of discrete elements by their *dynamics equations*.

10.2.1 Transfer Matrix of a Rigid Body

The transfer matrix of a rigid body consists of its geometrical equations and dynamics equations.

10.2.1.1 Rigid Body Vibrating in a Plane

A rigid body with one input end and one output end vibrating in a plane is shown in Figure 10.1, where m is the mass. In a body-fixed coordinate system, the inboard end I is the origin, J_I is the moment of inertia of the rigid body with respect to the point I , the coordinates of the outboard end O are (b_1, b_2) and the coordinates of the mass center C are (c_{c1}, c_{c2}) .

In the inertial coordinate system Ixy , the rotation angles of the outboard end O and the inboard end I of a rigid body are the same, that is, $\theta_{z,O} = \theta_{z,I}$. The relations between the displacements of output end O and input end I are

$$\begin{cases} x_O = x_I - b_2 \sin \theta_{z,I} - b_1 (1 - \cos \theta_{z,I}) \\ y_O = y_I + b_1 \sin \theta_{z,I} - b_2 (1 - \cos \theta_{z,I}) \end{cases} \quad (10.1)$$

For a small rotation angle $|\theta_{z,I}| \ll 1$, $\sin \theta_{z,I} \approx \theta_{z,I}$ and $\cos \theta_{z,I} \approx 1$, hence

$$x_O = x_I - b_2 \theta_{z,I}, \quad y_O = y_I + b_1 \theta_{z,I} \quad \theta_{z,I} = \theta_{z,O} \quad (10.2)$$

For a free vibration system, we can obtain the dynamics equations based on the motion theorem of mass center and the absolute moment of momentum theorem with respect to a moving point. After a linearization, we obtain

$$\begin{cases} q_{x,I} - q_{x,O} = m \ddot{x}_C = m(\ddot{x}_I - c_{c2} \ddot{\theta}_{z,I}) \\ q_{y,I} - q_{y,O} = m \ddot{y}_C = m(\ddot{y}_I - c_{c1} \ddot{\theta}_{z,I}) \\ J_I \ddot{\theta}_{z,I} = m_{z,O} - m_{z,I} + b_2 q_{x,O} - b_1 q_{y,O} - m c_{c1} \ddot{y}_I + m c_{c2} \ddot{x}_I \end{cases} \quad (10.3)$$

Rearranging Equation (10.3), we obtain

$$\begin{cases} q_{x,O} = q_{x,I} - m \ddot{x}_I + m c_{c2} \ddot{\theta}_{z,I} \\ q_{y,O} = q_{y,I} - m \ddot{y}_I - m c_{c1} \ddot{\theta}_{z,I} \\ m_{z,O} = m_{z,I} + m(b_2 - c_{c2}) \ddot{x}_I - m(b_1 - c_{c1}) \ddot{y}_I \\ \quad + [J_I - m(b_2 c_{c2} + b_1 c_{c1})] \ddot{\theta}_{z,I} - b_2 q_{x,I} + b_1 q_{y,I} \end{cases} \quad (10.4)$$

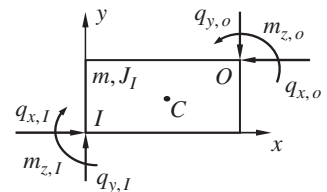
Defining the state vectors of inboard end I and outboard end O in physical coordinates as

$$z_I = [x, y, \theta_z, m_z, q_x, q_y]^T_I, \quad z_O = [x, y, \theta_z, m_z, q_x, q_y]^T_O \quad (10.5)$$

for free vibration systems we have

$$z_I = Z_I e^{i\omega t}, \quad z_O = Z_O e^{i\omega t} \quad (10.6)$$

Figure 10.1 A rigid body with a single input end and a single output end vibrating in a plane.



where ω is the eigenfrequency of the system, and \mathbf{Z}_I and \mathbf{Z}_O are the state vectors of inboard end I and outboard end O in modal coordinates, respectively

$$\mathbf{Z}_I = [X, Y, \Theta_z, M_z, Q_x, Q_y]_I^T, \quad \mathbf{Z}_O = [X, Y, \Theta_z, M_z, Q_x, Q_y]_O^T \quad (10.7)$$

Combining Equation (10.2) with Equation (10.4) and using Equations (10.6) and (10.7), we obtain

$$\begin{cases} X_O = X_I - b_2 \Theta_{z,I} \\ Y_O = Y_I + b_1 \Theta_{z,I} \\ \Theta_{z,O} = \Theta_{z,I} \\ M_{z,O} = M_{z,I} - m\omega^2(b_2 - c_{c2})X_I + m\omega^2(b_1 - c_{c1})Y_I \\ \quad - \omega^2[J_I - m(b_2 c_{c2} + b_1 c_{c1})]\Theta_{z,I} - b_2 Q_{x,I} + b_1 Q_{y,I} \\ Q_{x,O} = Q_{x,I} + m\omega^2 X_I - m\omega^2 c_{c2} \Theta_{z,I} \\ Q_{y,O} = Q_{y,I} + m\omega^2 Y_I + m\omega^2 c_{c1} \Theta_{z,I} \end{cases} \quad (10.8)$$

Writing Equation (10.8) in matrix form yields

$$\mathbf{Z}_O = \mathbf{U} \mathbf{Z}_I \quad (10.9)$$

where

$$\mathbf{U} = \begin{bmatrix} 1 & 0 & -b_2 & 0 & 0 & 0 \\ 0 & 1 & b_1 & 0 & 0 & 0 \\ 0 & 0 & 1 & 0 & 0 & 0 \\ -m\omega^2(b_2 - c_{c2}) & m\omega^2(b_1 - c_{c1}) & -\omega^2[J_I - m(b_2 c_{c2} + b_1 c_{c1})] & 1 & -b_2 & b_1 \\ m\omega^2 & 0 & -m\omega^2 c_{c2} & 0 & 1 & 0 \\ 0 & m\omega^2 & m\omega^2 c_{c1} & 0 & 0 & 1 \end{bmatrix} \quad (10.10)$$

\mathbf{U} is the transfer matrix of a rigid body with one input end and one output end vibrating in a plane.

10.2.1.2 Rigid Body Vibrating in Space

A rigid body with mass m and one input end and one output end vibrates in space, as shown in Figure 10.2. In the body-fixed coordinate system, the inboard end I is the origin, J_I is the inertia moment matrix of the rigid body with respect to point I , the coordinates of the outboard end

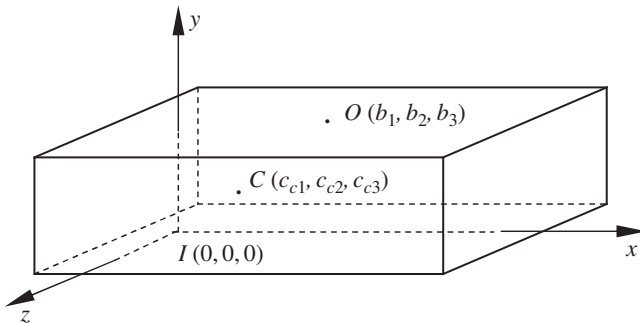


Figure 10.2 A rigid body with one input end and one output end vibrating in space.

O are (b_1, b_2, b_3) and the coordinates of the mass center C are (c_{c1}, c_{c2}, c_{c3}) . The rotation angles of inboard end I and output end O are the same, that is

$$\begin{bmatrix} \theta_x \\ \theta_y \\ \theta_z \end{bmatrix}_O = \begin{bmatrix} \theta_x \\ \theta_y \\ \theta_z \end{bmatrix}_I \quad (10.11)$$

The displacements of the outboard end O of a spatial rigid body with small vibration can be described by the displacements and the angular displacements of the inboard end I

$$\begin{bmatrix} x \\ y \\ z \end{bmatrix}_O = \begin{bmatrix} x \\ y \\ z \end{bmatrix}_I - \tilde{\mathbf{l}}_{IO} \begin{bmatrix} \theta_x \\ \theta_y \\ \theta_z \end{bmatrix}_I \quad (10.12)$$

where

$$\tilde{\mathbf{l}}_{IO} = \begin{bmatrix} 0 & -b_3 & b_2 \\ b_3 & 0 & -b_1 \\ -b_2 & b_1 & 0 \end{bmatrix} \quad (10.13)$$

This is the *cross-product matrix* of the displacement vector pointing from inboard end I to outboard end O .

For free vibration, the equation of translation motion is obtained from Newton's second law of motion

$$m \begin{bmatrix} \ddot{x} \\ \ddot{y} \\ \ddot{z} \end{bmatrix}_C = \begin{bmatrix} q_x \\ q_y \\ q_z \end{bmatrix}_I - \begin{bmatrix} q_x \\ q_y \\ q_z \end{bmatrix}_O \quad (10.14)$$

where

$$m \begin{bmatrix} x \\ y \\ z \end{bmatrix}_C = \begin{bmatrix} x \\ y \\ z \end{bmatrix}_I - \tilde{\mathbf{l}}_{IC} \begin{bmatrix} \theta_x \\ \theta_y \\ \theta_z \end{bmatrix}_I \quad (10.15)$$

$[q_x, q_y, q_z]_I^T$ and $[q_x, q_y, q_z]_O^T$ are the internal forces of inboard end I and outboard end O , respectively. \mathbf{l}_{IC} is the cross-product matrix of the displacement vector pointing from point I to mass center C .

Substituting Equation (10.15) into Equation (10.14), we obtain

$$\begin{bmatrix} q_x \\ q_y \\ q_z \end{bmatrix}_O = \begin{bmatrix} q_x \\ q_y \\ q_z \end{bmatrix}_I - m \begin{bmatrix} \ddot{x} \\ \ddot{y} \\ \ddot{z} \end{bmatrix}_I + m \tilde{\mathbf{l}}_{IC} \begin{bmatrix} \ddot{\theta}_x \\ \ddot{\theta}_y \\ \ddot{\theta}_z \end{bmatrix}_I \quad (10.16)$$

Considering the theorem of absolute moment of momentum with respect to a moving point, noticing small angular vibrations and ignoring higher order terms, the rotation equation is obtained as

$$\begin{bmatrix} m_x \\ m_y \\ m_z \end{bmatrix}_O = \begin{bmatrix} m_x \\ m_y \\ m_z \end{bmatrix}_I + (J_I + m \tilde{\mathbf{l}}_{IO} \tilde{\mathbf{l}}_{IC}) \begin{bmatrix} \ddot{\theta}_x \\ \ddot{\theta}_y \\ \ddot{\theta}_z \end{bmatrix}_I + \tilde{\mathbf{l}}_{IO} \begin{bmatrix} q_x \\ q_y \\ q_z \end{bmatrix}_I + m (\tilde{\mathbf{l}}_{IC} - \tilde{\mathbf{l}}_{IO}) \begin{bmatrix} \ddot{x} \\ \ddot{y} \\ \ddot{z} \end{bmatrix}_I \quad (10.17)$$

Define the state vectors of inboard end I and outboard end O in physical coordinates as

$$\begin{cases} \mathbf{z}_I = [x, y, z, \theta_x, \theta_y, \theta_z, m_x, m_y, m_z, q_x, q_y, q_z]_I^T \\ \mathbf{z}_O = [x, y, z, \theta_x, \theta_y, \theta_z, m_x, m_y, m_z, q_x, q_y, q_z]_O^T \end{cases}$$

Then their corresponding state vectors in modal coordinates are

$$\begin{cases} \mathbf{Z}_I = [X, Y, Z, \Theta_x, \Theta_y, \Theta_z, M_x, M_y, M_z, Q_x, Q_y, Q_z]_I^T \\ \mathbf{Z}_O = [X, Y, Z, \Theta_x, \Theta_y, \Theta_z, M_x, M_y, M_z, Q_x, Q_y, Q_z]_O^T \end{cases}$$

Combining Equations (10.11), (10.12) and (10.16), and considering Equation (10.6), the transfer equation of a rigid body vibrating in space is

$$\mathbf{Z}_O = \mathbf{U} \mathbf{Z}_I \quad (10.18)$$

where

$$\mathbf{U} = \begin{bmatrix} \mathbf{I}_3 & -\tilde{\mathbf{l}}_{IO} & \mathbf{O}_{3 \times 3} & \mathbf{O}_{3 \times 3} \\ \mathbf{O}_{3 \times 3} & \mathbf{I}_3 & \mathbf{O}_{3 \times 3} & \mathbf{O}_{3 \times 3} \\ m\omega^2 \tilde{\mathbf{l}}_{CO} & -\omega^2 (m \tilde{\mathbf{l}}_{IO} \tilde{\mathbf{l}}_{IC} + \mathbf{J}_I) & \mathbf{I}_3 & \tilde{\mathbf{l}}_{IO} \\ m\omega^2 \mathbf{I}_3 & -m\omega^2 \tilde{\mathbf{l}}_{IC} & \mathbf{O}_{3 \times 3} & \mathbf{I}_3 \end{bmatrix} \quad (10.19)$$

$$\tilde{\mathbf{l}}_{CO} = \begin{bmatrix} 0 & c_{c3} - b_3 & b_2 - c_{c2} \\ b_3 - c_{c3} & 0 & c_{c1} - b_1 \\ c_{c2} - b_2 & b_1 - c_{c1} & 0 \end{bmatrix} = \tilde{\mathbf{l}}_{IO} - \tilde{\mathbf{l}}_{IC}, \quad \mathbf{J}_I = \begin{bmatrix} J_x & -J_{xy} & -J_{xz} \\ -J_{xy} & J_y & -J_{yz} \\ -J_{xz} & -J_{yz} & J_z \end{bmatrix}$$

\mathbf{U} is the transfer matrix of a rigid body vibrating in space with one input and one output end, m is the mass of the rigid body, \mathbf{J}_I is the inertia moment matrix of the rigid body in the body-fixed coordinate system and ω is the natural frequency of the MS.

There are twelve variables in the state vector of a rigid body vibrating in space, which includes the six variables in the state vector of the planar vibration and six additional variables in rows 3, 4, 5, 7, 8 and 12.

Thus, the transfer matrix of a rigid body vibrating in a plane (Equation (10.10)) is a special example of the transfer matrix of a rigid body vibrating in space (Equation (10.19)) after deleting the third, fourth, fifth, seventh, eighth and twelfth rows and the third, fourth, fifth, seventh, eighth and twelfth columns in Equation (10.19). Only spatial motions of elements will be discussed in the following deduction of the transfer matrices of elements, and the planar motion is considered as a special case of spatial motion.

When simple harmonic excitation force \mathbf{F} and excitation moment \mathbf{M} act on point D (d_1, d_2, d_3) and point E (e_1, e_2, e_3) of the rigid body with frequency Ω all extended transfer matrices can be denoted in the following form no matter the system with or without damping

$$\hat{\mathbf{U}} = \begin{bmatrix} \mathbf{U} & \mathbf{f} \\ \mathbf{0} & \mathbf{1} \end{bmatrix} \quad (10.20)$$

The expression of the partitioned matrix $\mathbf{U} = \mathbf{U}(\Omega)$ is the same as Equation (10.19), and the expression of the partitioned matrix \mathbf{f} is as follows.

The first six of the twelve variables of \mathbf{f} are all zeros. In the undamped system, \mathbf{q}_I is substituted by $\mathbf{F} + \mathbf{q}_I$ in Equation (10.16). Thus, the last three variables of \mathbf{f} are the three components of \mathbf{F} on the three coordinates axes, that is, $[F_x, F_y, F_z]^T$.

The original \mathbf{q}_I is substituted by $\mathbf{F} + \mathbf{q}_I$ in Equation (10.17), and the original \mathbf{m}_O is substituted by $\mathbf{M} + \mathbf{l}_{ID} \times \mathbf{F} + \mathbf{m}_O$ at the same time. Hence, the seventh, eighth and ninth variables of \mathbf{f} are the components of $-\mathbf{M} - \mathbf{l}_{ID} \times \mathbf{F} + \mathbf{l}_{IO} \times \mathbf{F} = -\mathbf{M} + \mathbf{l}_{DO} \times \mathbf{F}$ on the three coordinate axes. The expression of the partitioned matrix \mathbf{f} is

$$\mathbf{f} = \begin{bmatrix} \mathbf{0}_3 \\ \mathbf{0}_3 \\ -\mathbf{M} + \tilde{\mathbf{l}}_{DO} \mathbf{F} \\ \mathbf{F} \end{bmatrix} \quad (10.21)$$

In the damped system, the expression of the partitioned matrix \mathbf{f} is

$$\mathbf{f} = \begin{bmatrix} \mathbf{0}_3 \\ \mathbf{0}_3 \\ -\bar{\mathbf{M}} + \tilde{\mathbf{l}}_{DO} \bar{\mathbf{F}} \\ \bar{\mathbf{F}} \end{bmatrix} \quad (10.22)$$

10.2.1.3 The Transfer Matrix of a Rigid Body with N Input Ends and L Output Ends

For the rigid body with N input ends and L output ends shown in Figure 10.3, the state vectors are defined as

$$\begin{cases} \mathbf{Z}_I = [X_{I_1}, Y_{I_1}, Z_{I_1}, \theta_{x, I_1}, \theta_{y, I_1}, \theta_{z, I_1}, M_{x, I_1}, M_{y, I_1}, M_{z, I_1}, Q_{x, I_1}, Q_{y, I_1}, Q_{z, I_1}, \dots, \\ \quad M_{x, I_N}, M_{y, I_N}, M_{z, I_N}, Q_{x, I_N}, Q_{y, I_N}, Q_{z, I_N}]^T \\ \mathbf{Z}_O = [X_{O_1}, Y_{O_1}, Z_{O_1}, \theta_{x, O_1}, \theta_{y, O_1}, \theta_{z, O_1}, M_{x, O_1}, M_{y, O_1}, M_{z, O_1}, Q_{x, O_1}, Q_{y, O_1}, Q_{z, O_1}, \dots, \\ \quad M_{x, O_L}, M_{y, O_L}, M_{z, O_L}, Q_{x, O_L}, Q_{y, O_L}, Q_{z, O_L}]^T \end{cases} \quad (10.23)$$

Similar to Equation (10.11), we obtain

$$\begin{bmatrix} \theta_x \\ \theta_y \\ \theta_z \end{bmatrix}_{O_1} = \begin{bmatrix} \theta_x \\ \theta_y \\ \theta_z \end{bmatrix}_{I_1} \quad (10.24)$$

Similar to Equation (10.12), this yields

$$\begin{bmatrix} x \\ y \\ z \end{bmatrix}_{O_1} = \begin{bmatrix} x \\ y \\ z \end{bmatrix}_{I_1} - \tilde{\mathbf{l}}_{I_1 O_1} \begin{bmatrix} \theta_x \\ \theta_y \\ \theta_z \end{bmatrix}_{I_1} \quad (10.25)$$

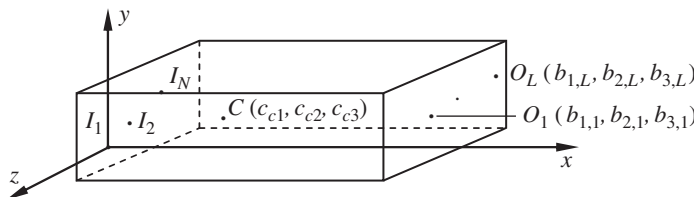


Figure 10.3 A rigid body with N input ends and L output ends.

Similar to Equation (10.16), but with \mathbf{q}_O not substituted by \mathbf{q}_b , the translational equation is

$$\sum_{l=1}^L \begin{bmatrix} q_x \\ q_y \\ q_z \end{bmatrix}_{O_l} = \sum_{n=1}^N \begin{bmatrix} q_x \\ q_y \\ q_z \end{bmatrix}_{I_n} - m \begin{bmatrix} \ddot{x} \\ \ddot{y} \\ \ddot{z} \end{bmatrix}_{I_1} + m \tilde{\mathbf{l}}_{I_1 C} \begin{bmatrix} \ddot{\theta}_x \\ \ddot{\theta}_y \\ \ddot{\theta}_z \end{bmatrix}_{I_1} \quad (10.26)$$

Similar to Equation (10.17), the rotational equation is

$$\sum_{l=1}^L \left(\begin{bmatrix} m_x \\ m_y \\ m_z \end{bmatrix}_{O_l} - \tilde{\mathbf{l}}_{I_1 O_l} \begin{bmatrix} q_x \\ q_y \\ q_z \end{bmatrix}_{O_l} \right) = \sum_{n=1}^N \left(\begin{bmatrix} m_x \\ m_y \\ m_z \end{bmatrix}_{I_n} - \tilde{\mathbf{l}}_{I_1 I_n} \begin{bmatrix} q_x \\ q_y \\ q_z \end{bmatrix}_{I_n} \right) + J_{I_1} \begin{bmatrix} \ddot{\theta}_x \\ \ddot{\theta}_y \\ \ddot{\theta}_z \end{bmatrix}_{I_1} + m \tilde{\mathbf{l}}_{I_1 C} \begin{bmatrix} \ddot{x} \\ \ddot{y} \\ \ddot{z} \end{bmatrix}_{I_1} \quad (10.27)$$

Combining Equations (10.24), (10.25), (10.26) and (10.27), and considering Equation (10.6), the transfer equation of a rigid body vibrating in space with N input ends and L output ends is

$$\mathbf{U}_O \mathbf{Z}_O = \mathbf{U}_I \mathbf{Z}_I \quad (10.28)$$

where

$$\mathbf{U}_O = \begin{bmatrix} \mathbf{I}_3 & \mathbf{O}_{3 \times 3} & \mathbf{O}_{3 \times 3} & \mathbf{O}_{3 \times 3} & \mathbf{O}_{3 \times 3} & \mathbf{O}_{3 \times 3} & \cdots & \cdots & \mathbf{O}_{3 \times 3} & \mathbf{O}_{3 \times 3} \\ \mathbf{O}_{3 \times 3} & \mathbf{I}_3 & \mathbf{O}_{3 \times 3} & \mathbf{O}_{3 \times 3} & \mathbf{O}_{3 \times 3} & \mathbf{O}_{3 \times 3} & \cdots & \cdots & \mathbf{O}_{3 \times 3} & \mathbf{O}_{3 \times 3} \\ \mathbf{O}_{3 \times 3} & \mathbf{O}_{3 \times 3} & \mathbf{I}_3 & -\tilde{\mathbf{l}}_{I_1 O_1} & \mathbf{I}_3 & -\tilde{\mathbf{l}}_{I_1 O_2} & \cdots & \cdots & \mathbf{I}_3 & -\tilde{\mathbf{l}}_{I_1 O_n} \\ \mathbf{O}_{3 \times 3} & \mathbf{O}_{3 \times 3} & \mathbf{O}_{3 \times 3} & \mathbf{I}_3 & \mathbf{O}_{3 \times 3} & \mathbf{I}_3 & \cdots & \cdots & \mathbf{O}_{3 \times 3} & \mathbf{I}_3 \end{bmatrix}$$

$$\mathbf{U}_I = \begin{bmatrix} \mathbf{I}_3 & -\tilde{\mathbf{l}}_{I_1 O_1} & \mathbf{O}_{3 \times 3} & \mathbf{O}_{3 \times 3} & \mathbf{O}_{3 \times 3} & \mathbf{O}_{3 \times 3} & \cdots & \cdots & \mathbf{O}_{3 \times 3} & \mathbf{O}_{3 \times 3} \\ \mathbf{O}_{3 \times 3} & \mathbf{I}_3 & \mathbf{O}_{3 \times 3} & \mathbf{O}_{3 \times 3} & \mathbf{O}_{3 \times 3} & \mathbf{O}_{3 \times 3} & \cdots & \cdots & \mathbf{O}_{3 \times 3} & \mathbf{O}_{3 \times 3} \\ -m\omega^2 \tilde{\mathbf{l}}_{I_1 C} & -\omega^2 J_{I_1} & \mathbf{I}_3 & -\tilde{\mathbf{l}}_{I_1 I_1} & \mathbf{I}_3 & -\tilde{\mathbf{l}}_{I_1 I_2} & \cdots & \cdots & \mathbf{I}_3 & -\tilde{\mathbf{l}}_{I_1 I_l} \\ m\omega^2 \mathbf{I}_3 & m\omega^2 \tilde{\mathbf{l}}_{I_1 C}^T & \mathbf{O}_{3 \times 3} & \mathbf{I}_3 & \mathbf{O}_{3 \times 3} & \mathbf{I}_3 & \cdots & \cdots & \mathbf{O}_{3 \times 3} & \mathbf{I}_3 \end{bmatrix} \quad (10.29)$$

10.2.1.4 Rigid Body with Multiple Input Ends and One Output End

A rigid body with N input ends and one output end whose mass is m is shown in Figure 10.4. In the body-fixed coordinate system with the origin at the inboard end I_1 , J_{I_1} is the matrix of the inertia moment of the rigid body with respect to point I_1 . The coordinates of the inboard ends $I_n (n = 1, 2, \dots, N)$, the outboard end O and the mass center C are denoted as $(a_{1,n}, a_{2,n}, a_{3,n})$,

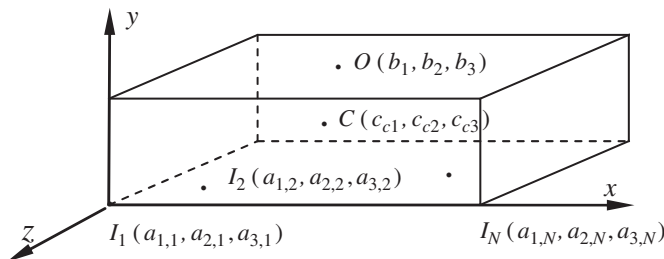


Figure 10.4 A rigid body with N input ends and one output end.

(b_1, b_2, b_3) and (c_{c1}, c_{c2}, c_{c3}) , respectively. The state vectors of the inboard ends and the outboard end are defined as

$$\begin{cases} \mathbf{Z}_I = [X_{I_1}, Y_{I_1}, Z_{I_1}, \theta_{x, I_1}, \theta_{y, I_1}, \theta_{z, I_1}, M_{x, I_1}, M_{y, I_1}, M_{z, I_1}, Q_{x, I_1}, Q_{y, I_1}, Q_{z, I_1}, \dots, \\ \quad M_{x, I_N}, M_{y, I_N}, M_{z, I_N}, Q_{x, I_N}, Q_{y, I_N}, Q_{z, I_N}]^T \\ \mathbf{Z}_O = [X, Y, Z, \theta_x, \theta_y, \theta_z, M_x, M_y, M_z, Q_x, Q_y, Q_z]^T_O \end{cases} \quad (10.30)$$

Using a similar method to that in section 10.2.1.3, the transfer equation of a rigid body with multiple input ends and one output end can be expressed as

$$\mathbf{Z}_O = \mathbf{U} \mathbf{Z}_I \quad (10.31)$$

The transfer matrix of a rigid body with multiple input ends and one output end is

$$\mathbf{U} = \begin{bmatrix} \mathbf{I}_3 & -\tilde{\mathbf{l}}_{I_1 O} & \mathbf{O}_{3 \times 3} & \mathbf{O}_{3 \times 3} & \cdots & \mathbf{O}_{3 \times 3} & \mathbf{O}_{3 \times 3} \\ \mathbf{O}_{3 \times 3} & \mathbf{I}_3 & \mathbf{O}_{3 \times 3} & \mathbf{O}_{3 \times 3} & \cdots & \mathbf{O}_{3 \times 3} & \mathbf{O}_{3 \times 3} \\ m\omega^2 \tilde{\mathbf{l}}_{CO} & -\omega^2 (m\tilde{\mathbf{l}}_{I_1 O} \tilde{\mathbf{l}}_{I_1 C} + \mathbf{J}_{I_1}) & \mathbf{I}_3 & -\tilde{\mathbf{l}}_{I_1 O} & \cdots & \mathbf{I}_3 & \tilde{\mathbf{l}}_{NO} \\ m\omega^2 \mathbf{I}_3 & -m\omega^2 \tilde{\mathbf{l}}_{I_1 C} & \mathbf{O}_{3 \times 3} & \mathbf{I}_3 & \cdots & \mathbf{O}_{3 \times 3} & \mathbf{I}_3 \end{bmatrix} \quad (10.32)$$

It is obvious that the first twelve columns of Equation (10.32) are the same as the term on the right-hand side of Equation (10.19), which is the transfer matrix of a rigid body with one input end and one output end.

The forming rule of the extended transfer matrix for forced vibrations is the same as the forming rule of the extended transfer matrix for a rigid body with a single input end and a single output end. The expressions of the partitioned matrix \mathbf{f} are also the same as the expressions of a rigid body with one input end and one output end.

10.2.1.5 Rigid Body with One Input End and Multiple Output Ends

A rigid body with one input end and L output ends whose mass is m is shown in Figure 10.5. In the body-fixed coordinate system with the origin at the inboard end I , \mathbf{J}_{I_1} is the matrix of the inertia moment of the rigid body with respect to point I . The coordinates of the outboard ends $O_l (l=1, 2, \dots, L)$ and the mass center C are denoted as $(b_{1,l}, b_{2,l}, b_{3,l})$ and (c_{c1}, c_{c2}, c_{c3}) , respectively. The state vectors are defined as

$$\begin{cases} \mathbf{Z}_I = [X, Y, Z, \theta_x, \theta_y, \theta_z, M_x, M_y, M_z, Q_x, Q_y, Q_z]^T_I \\ \mathbf{Z}_O = [X_{O_1}, Y_{O_1}, Z_{O_1}, \theta_{x, O_1}, \theta_{y, O_1}, \theta_{z, O_1}, M_{x, O_1}, M_{y, O_1}, M_{z, O_1}, Q_{x, O_1}, Q_{y, O_1}, Q_{z, O_1}, \\ \quad \dots, M_{x, O_L}, M_{y, O_L}, M_{z, O_L}, Q_{x, O_L}, Q_{y, O_L}, Q_{z, O_L}]^T \end{cases} \quad (10.33)$$

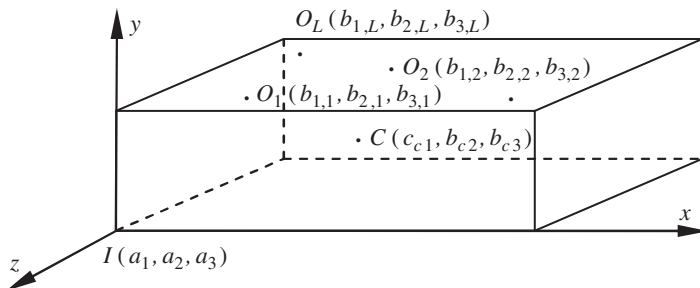


Figure 10.5 A rigid body with one input end and L output ends.

Similar to the method used in section 10.2.1.3, the transfer equation of a rigid body with one input end and multiple output ends can be expressed as

$$\mathbf{U}\mathbf{Z}_O = \mathbf{Z}_I \quad (10.34)$$

and the transfer matrix of a rigid body with one input end and multiple output ends is

$$\mathbf{U} = \begin{bmatrix} \mathbf{I}_3 & -\tilde{\mathbf{l}}_{IO_1} & \mathbf{O}_{3 \times 3} & \mathbf{O}_{3 \times 3} & \cdots & \mathbf{O}_{3 \times 3} & \mathbf{O}_{3 \times 3} \\ \mathbf{O}_{3 \times 3} & \mathbf{I}_3 & \mathbf{O}_{3 \times 3} & \mathbf{O}_{3 \times 3} & \cdots & \mathbf{O}_{3 \times 3} & \mathbf{O}_{3 \times 3} \\ m\omega^2\tilde{\mathbf{l}}_{IC} & \omega^2(m\tilde{\mathbf{l}}_{IC}\tilde{\mathbf{l}}_{IO_1} + \mathbf{J}_I) & \mathbf{I}_3 & -\tilde{\mathbf{l}}_{IO_1} & \cdots & \mathbf{I}_3 & -\tilde{\mathbf{l}}_{IO_L} \\ -m\omega^2\mathbf{I}_3 & m\omega^2\tilde{\mathbf{l}}_{O_1C} & \mathbf{O}_{3 \times 3} & \mathbf{I}_3 & \cdots & \mathbf{O}_{3 \times 3} & \mathbf{I}_3 \end{bmatrix} \quad (10.35)$$

It should be noticed that the transfer matrix is written on the side of the outboard end. The expression for the partitioned matrix of the expanded transfer matrix \mathbf{f} for forced vibration is

$$\mathbf{f} = \begin{bmatrix} \mathbf{0}_3 \\ \mathbf{0}_3 \\ \mathbf{M} - \tilde{\mathbf{l}}_{DI}\mathbf{F} \\ -\mathbf{F} \end{bmatrix} \quad \text{or} \quad \mathbf{f} = \begin{bmatrix} \mathbf{0}_3 \\ \mathbf{0}_3 \\ \bar{\mathbf{M}} - \tilde{\mathbf{l}}_{DI}\bar{\mathbf{F}} \\ -\bar{\mathbf{F}} \end{bmatrix} \quad (10.36)$$

10.2.2 Transfer Matrix of Rotary Spring

A massless planar rotary spring with stiffness K' is shown in Figure 10.6. The moment on the input end of the rotary spring is equal to that on the output end, that is

$$m_{z,O} = m_{z,I} = K'_z(\theta_{z,O} - \theta_{z,I}) \quad (10.37)$$

Define the state vectors of the input and output ends as follows

$$\mathbf{z}_I = \begin{bmatrix} \theta_z \\ m_z \end{bmatrix}_I, \quad \mathbf{z}_O = \begin{bmatrix} \theta_z \\ m_z \end{bmatrix}_O$$

Equation (10.37) can then be expressed as the transfer equation of the planar rotary spring

$$\mathbf{z}_O = \mathbf{U}\mathbf{z}_I$$

where

$$\mathbf{U} = \begin{bmatrix} 1 & \frac{1}{K'_z} \\ 0 & 1 \end{bmatrix} \quad (10.38)$$

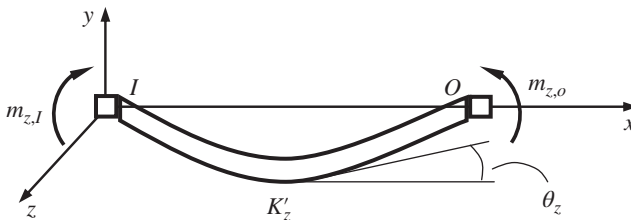


Figure 10.6 Planar rotary spring K'_z .

is the transfer matrix of the planar rotary spring.

For a spatial rotary spring with three directions, as shown in Figure 10.7, the state vectors of the input and output ends are defined as

$$\begin{cases} \mathbf{Z}_I = [\theta_x, \theta_y, \theta_z, M_x, M_y, M_z]^T_I \\ \mathbf{Z}_O = [\theta_x, \theta_y, \theta_z, M_x, M_y, M_z]^T_O \end{cases}$$

The transfer equation and the transfer matrix of the spatial rotary spring can be deduced as

$$\mathbf{Z}_O = \mathbf{U} \mathbf{Z}_I$$

and

$$\mathbf{U} = \begin{bmatrix} \mathbf{I}_3 & \mathbf{U}_{12} \\ \mathbf{O}_{3 \times 3} & \mathbf{I}_3 \end{bmatrix}, \quad \mathbf{U}_{12} = \begin{bmatrix} \frac{1}{K'_x} & 0 & 0 \\ 0 & \frac{1}{K'_y} & 0 \\ 0 & 0 & \frac{1}{K'_z} \end{bmatrix} \quad (10.39)$$

where K'_x, K'_y and K'_z are the stiffnesses of the rotary spring in directions x, y and z , respectively.

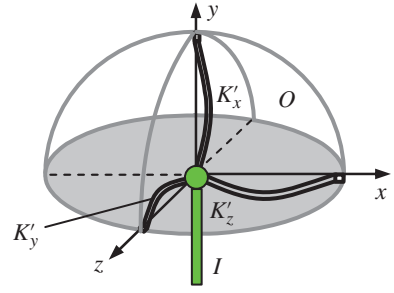


Figure 10.7 Spatial rotary spring with three directions.

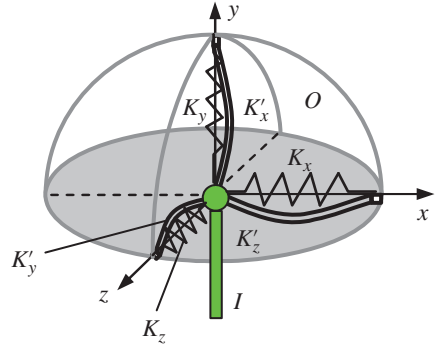


Figure 10.8 Spatial elastic hinge.

10.2.3 Transfer Matrix of a Spatial Elastic Hinge

A spatial elastic hinge, as shown in Figure 10.8, is composed of longitudinal springs and rotary springs in three directions. The state vectors of the input and output ends are defined as

$$\begin{cases} \mathbf{Z}_I = [X, Y, Z, \theta_x, \theta_y, \theta_z, M_x, M_y, M_z, Q_x, Q_y, Q_z]^T_I \\ \mathbf{Z}_O = [X, Y, Z, \theta_x, \theta_y, \theta_z, M_x, M_y, M_z, Q_x, Q_y, Q_z]^T_O \end{cases}$$

The transfer matrix of the spatial elastic hinge can be deduced as

$$\mathbf{U} = \begin{bmatrix} \mathbf{I}_3 & \mathbf{O}_{3 \times 3} & \mathbf{O}_{3 \times 3} & \mathbf{U}_{14} \\ \mathbf{O}_{3 \times 3} & \mathbf{I}_3 & \mathbf{U}_{23} & \mathbf{O}_{3 \times 3} \\ \mathbf{O}_{3 \times 3} & \mathbf{O}_{3 \times 3} & \mathbf{I}_3 & \mathbf{O}_{3 \times 3} \\ \mathbf{O}_{3 \times 3} & \mathbf{O}_{3 \times 3} & \mathbf{O}_{3 \times 3} & \mathbf{I}_3 \end{bmatrix} \quad (10.40)$$

$$\mathbf{U}_{14} = \begin{bmatrix} -\frac{1}{K_x} & 0 & 0 \\ 0 & -\frac{1}{K_y} & 0 \\ 0 & 0 & -\frac{1}{K_z} \end{bmatrix}, \quad \mathbf{U}_{23} = \begin{bmatrix} \frac{1}{K'_x} & 0 & 0 \\ 0 & \frac{1}{K'_y} & 0 \\ 0 & 0 & \frac{1}{K'_z} \end{bmatrix}$$

where K_x, K_y, K_z and K'_x, K'_y, K'_z are the stiffnesses of the longitudinal springs and the rotary springs in directions x, y and z , respectively.

10.2.4 Transfer Matrix of a Lumped Mass Vibrating in Space

The geometric relation between the input and output ends for a lumped mass vibrating in space is

$$\begin{bmatrix} x \\ y \\ z \end{bmatrix}_O = \begin{bmatrix} x \\ y \\ z \end{bmatrix}_I$$

The dynamics equation of a lumped mass vibrating in space is

$$m \begin{bmatrix} \ddot{x} \\ \ddot{y} \\ \ddot{z} \end{bmatrix}_I = \begin{bmatrix} q_x \\ q_y \\ q_z \end{bmatrix}_I - \begin{bmatrix} q_x \\ q_y \\ q_z \end{bmatrix}_O$$

where m is the mass of the particle.

In modal coordinates the state vectors of a lumped mass vibrating in space are defined as

$$\begin{cases} \mathbf{Z}_I = [X, Y, Z, Q_x, Q_y, Q_z]_I^T \\ \mathbf{Z}_O = [X, Y, Z, Q_x, Q_y, Q_z]_O^T \end{cases}$$

Considering Equation (10.6), the transfer equation of a lumped mass vibrating in space is

$$\mathbf{Z}_O = \mathbf{U} \mathbf{Z}_I$$

The transfer matrix of the lumped mass vibrating in space is

$$\mathbf{U} = \begin{bmatrix} \mathbf{I}_3 & \mathbf{O}_{3 \times 3} \\ \mathbf{U}_{21} & \mathbf{I}_3 \end{bmatrix}, \quad \mathbf{U}_{21} = \begin{bmatrix} m\omega^2 & 0 & 0 \\ 0 & m\omega^2 & 0 \\ 0 & 0 & m\omega^2 \end{bmatrix} \quad (10.41)$$

10.3 Derivation from an n th-order Differential Equation

We can also derive the transfer matrix by solving the dynamics equation of a continuous element represented by an n th order differential equation. In this section the transfer matrices of a torsional vibrating shaft, a Timoshenko beam, an Euler–Bernoulli beam and a longitudinal vibrating rod are derived in this way.

10.3.1 Transfer Matrix of an Elastic Shaft with Torsional Vibration

An elastic shaft is shown in Figure 10.9, where l is length, ρ is material density, J_p is polar moment of inertia of the cross-section and GJ_p is torsional stiffness. The free torsional vibration equation of the elastic shaft is

$$GJ_p \frac{\partial^2 \theta_x}{\partial x^2} - \rho J_p \frac{\partial^2 \theta_x}{\partial t^2} = 0 \quad (10.42)$$

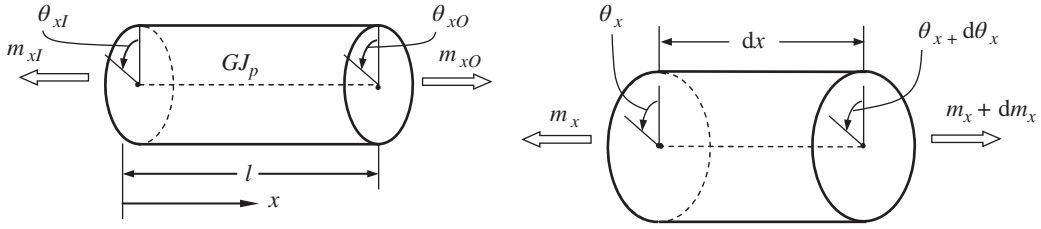


Figure 10.9 Elastic shaft with torsional vibration.

Let $\theta_x(x, t) = \Theta_x(x) e^{i\omega t}$ and substitute this into Equation (10.42) to yield

$$\frac{d^2 \Theta_x}{dx^2} + \frac{\rho J_p \omega^2}{G J_p} \Theta_x = 0 \quad (10.43)$$

The general solution of Equation (10.43) is

$$\Theta_x = A_1 \sin \gamma x + A_2 \cos \gamma x \quad (0 \leq x \leq l) \quad (10.44a)$$

where $\gamma^2 = \frac{\rho J_p \omega^2}{G J_p} = \frac{\rho \omega^2}{G}$ and A_1 and A_2 are arbitrary constants.

According to the Mechanics of Materials, this yields

$$M_x = G J_p \frac{d\Theta_x}{dx} = \gamma G J_p A_1 \cos \gamma x - \gamma G J_p A_2 \sin \gamma x \quad (10.44b)$$

Combining Equations (10.44a) and (10.44b) yields

$$\begin{bmatrix} \Theta_x \\ M_x \end{bmatrix} = \begin{bmatrix} \sin \gamma x & \cos \gamma x \\ \gamma G J_p \cos \gamma x & -\gamma G J_p \sin \gamma x \end{bmatrix} \begin{bmatrix} A_1 \\ A_2 \end{bmatrix} \quad (10.45)$$

For the input end I , $x = 0$, $\Theta_x = \Theta_{xl}$ and $M_x = M_{xl}$, we obtain

$$\begin{bmatrix} 0 & 1 \\ \gamma G J_p & 0 \end{bmatrix} \begin{bmatrix} A_1 \\ A_2 \end{bmatrix} = \begin{bmatrix} \Theta_x \\ M_x \end{bmatrix}_I$$

So $A_2 = \Theta_{xl}$ and $A_1 = \frac{1}{\gamma G J_p} M_{xl}$.

From Equation (10.45), considering $x = l$ for output end O , the transfer equation of the elastic shaft is

$$\begin{bmatrix} \Theta_x \\ M_x \end{bmatrix}_O = \begin{bmatrix} \cos \gamma l & \frac{1}{\gamma G J_p} \sin \gamma l \\ -\gamma G J_p \sin \gamma l & \cos \gamma l \end{bmatrix} \begin{bmatrix} \Theta_x \\ M_x \end{bmatrix}_I \quad (10.46a)$$

and the transfer matrix of the elastic shaft is

$$\mathbf{U}_{x=l} = \begin{bmatrix} \cos \gamma l & \frac{1}{\gamma G J_p} \sin \gamma l \\ -\gamma G J_p \sin \gamma l & \cos \gamma l \end{bmatrix} \quad (10.46b)$$

If the mass of the shaft can be ignored, that is, $\rho \rightarrow 0$, then $\gamma \rightarrow 0$ and Equation (10.46b) becomes Equation (10.22), which is the transfer matrix of a massless shaft.

10.3.2 Transfer Matrix of a Timoshenko Beam

A Timoshenko beam is shown in Figure 10.10. Its length, line density and cross-section area are l , \bar{m} and A , respectively. The polar inertia moment of the cross-section with respect to the axial line passing through the mass center and perpendicular to the x - y plane is I_z , and the radius of gyration is ρ_z .

The shear deformation and the bending moment have to be considered in a Timoshenko beam. The dip angle of the neutral axis of the beam is $\partial y / \partial x$. The rotary angle of the cross-section due to the bending moment is θ_z . The angle of the neutral axis due to the shear force is $\partial y / \partial x$, but the angle of the cross-section has not changed. The angle between the cross-section's perpendicular and neutral axis is $(-\partial y / \partial x + \theta_z)$. The relation between the angle and the shear force is

$$q_y = GA_s \left(-\frac{\partial y}{\partial x} + \theta_z \right) \quad \text{or} \quad \frac{\partial y}{\partial x} = \theta_z - \frac{q_y}{GA_s} \quad (10.47a)$$

where $GA_s = GA/\kappa_s$ is the shear stiffness and κ_s is the shape factor determined by the shape of the cross-section.

The relation between bending moment and the angle θ_z is

$$m_z = EI_z \frac{\partial \theta_z}{\partial x} \quad \text{or} \quad \frac{\partial \theta_z}{\partial x} = \frac{m_z}{EI_z} \quad (10.47b)$$

From force analysis, we find

$$\frac{\partial m_z}{\partial x} = q_y + \bar{m} \rho_z^2 \frac{\partial^2 \theta_z}{\partial t^2} \quad (10.47c)$$

$$\frac{\partial q_y}{\partial x} = -\bar{m} \frac{\partial^2 y}{\partial t^2} \quad (10.47d)$$

Taking the partial derivative of Equation (10.47a) with respect to x and substituting it together with Equation (10.47b) into Equation (10.47d) yields

$$-\frac{\partial^2 y}{\partial x^2} + \frac{\bar{m}}{GA_s} \frac{\partial^2 y}{\partial t^2} + \frac{m_z}{EI_z} = 0 \quad (10.48)$$

The second-order partial derivative of Equation (10.48) with respect to x is

$$-\frac{\partial^4 y}{\partial x^4} + \frac{\bar{m}}{GA_s} \frac{\partial^4 y}{\partial t^2 \partial x^2} + \frac{1}{EI_z} \frac{\partial^2 m_z}{\partial x^2} = 0 \quad (10.49)$$

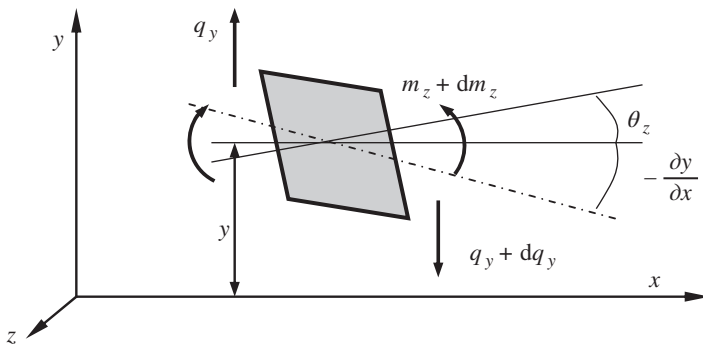


Figure 10.10 Infinitesimal part of a Timoshenko beam.

Substituting the partial derivative of Equation (10.47c) with respect to x into Equation (10.49) and using Equations (10.47b), (10.47d) and (10.48) to eliminate q_y , θ_z and m_z yields

$$\frac{\partial^4 y}{\partial x^4} + \frac{\bar{m}}{EI_z} \frac{\partial^2 y}{\partial t^2} - \frac{\bar{m} \rho_z^2}{EI_z} \frac{\partial^4 y}{\partial x^2 \partial t^2} + \frac{\bar{m}}{GA_s} \left(\frac{\bar{m} \rho_z^2}{EI_z} \frac{\partial^4 y}{\partial t^4} - \frac{\partial^4 y}{\partial x^2 \partial t^2} \right) = 0 \quad (10.50)$$

Equation (10.50) is the transverse vibration equation of a Timoshenko beam. The displacement of free vibration can be expressed as

$$y(x, t) = Y(x) e^{i\omega t} \quad (10.51)$$

Substituting Equation (10.51) into Equation (10.50) and eliminating the parameter t yields

$$\frac{d^4 Y}{dx^4} + \frac{\bar{m} \omega^2}{EI_z} \left(\frac{EI_z}{GA_s} + \rho_z^2 \right) \frac{d^2 Y}{dx^2} - \frac{\bar{m} \omega^2}{EI_z} \left(1 - \frac{\bar{m} \rho_z^2 \omega^2}{GA_s} \right) Y = 0 \quad (10.52)$$

The general solution of Equation (10.52) is

$$Y(x) = A_1 \cosh \lambda_1 x + A_2 \sinh \lambda_1 x + A_3 \cosh \lambda_2 x + A_4 \sinh \lambda_2 x \quad (10.53)$$

where

$$\lambda_{1,2} = \sqrt{\sqrt{\beta^4 + \frac{1}{4}(\sigma - \tau)^2} \mp \frac{1}{2}(\sigma + \tau)}, \quad \sigma = \frac{\bar{m} \omega^2}{GA_s}, \quad \tau = \frac{\bar{m} \rho_z^2 \omega^2}{EI_z}, \quad \beta^4 = \frac{\bar{m} \omega^2}{EI_z}$$

$$\lambda_2^2 - \lambda_1^2 = \sigma + \tau, \quad \lambda_1^2 \lambda_2^2 = \beta^4 - \sigma \tau$$

Considering $\mathbf{z} = \mathbf{Z} e^{i\omega t}$ and using Equations (10.47a) to (10.47d), we obtain

$$\begin{cases} \frac{dY}{dx} = \Theta_z - \frac{Q_y}{GA_s} \\ \frac{d\Theta_z}{dx} = \frac{M_z}{EI_z} \\ \frac{dM_z}{dx} = Q_y - \bar{m} \rho_z^2 \omega^2 \Theta_z \\ \frac{dQ_y}{dx} = \omega^2 \bar{m} Y \end{cases} \quad \text{or} \quad \begin{cases} \Theta_z = \frac{dY}{dx} - \frac{Q_y}{GA_s} \\ M_z = EI_z \frac{d\Theta_z}{dx} \\ Q_y = \frac{dM_z}{dx} + \bar{m} \rho_z^2 \omega^2 \Theta_z \end{cases} \quad (10.54)$$

From Equations (10.53) and (10.54), we obtain

$$\begin{bmatrix} Y \\ \Theta_z \\ M_z \\ Q_y \end{bmatrix}_x = \begin{bmatrix} \cosh \lambda_1 x & \sinh \lambda_1 x & \cos \lambda_2 x & \sin \lambda_2 x \\ \frac{\sigma + \lambda_1^2}{\lambda_1} \sinh \lambda_1 x & \frac{\sigma + \lambda_1^2}{\lambda_1} \cosh \lambda_1 x & \frac{\sigma - \lambda_2^2}{\lambda_2} \sin \lambda_2 x & -\frac{\sigma - \lambda_2^2}{\lambda_2} \cos \lambda_2 x \\ C_1 \cosh \lambda_1 x & C_1 \sinh \lambda_1 x & C_2 \cos \lambda_2 x & C_2 \sin \lambda_2 x \\ \frac{\bar{m} \omega^2}{\lambda_1} \sinh \lambda_1 x & \frac{\bar{m} \omega^2}{\lambda_1} \cosh \lambda_1 x & \frac{\bar{m} \omega^2}{\lambda_2} \sin \lambda_2 x & -\frac{\bar{m} \omega^2}{\lambda_2} \cos \lambda_2 x \end{bmatrix} \begin{bmatrix} A_1 \\ A_2 \\ A_3 \\ A_4 \end{bmatrix} \quad (10.55)$$

where

$$C_1 = EI_z (\sigma + \lambda_1^2), \quad C_2 = EI_z (\sigma - \lambda_2^2)$$

Thus, Equation (10.55) can be written as

$$\mathbf{Z}(x) = \mathbf{B}(x) \mathbf{a}$$

$$\mathbf{a} = [A_1, A_2, A_3, A_4]^T$$

When $x = 0$, namely for the input point I of a beam, we have

$$\mathbf{Z}(0) = \mathbf{B}(0)\mathbf{a} = \mathbf{Z}_I = [Y, \Theta_z, M_z, Q_y]_I^T \quad (10.56)$$

$$\mathbf{B}(0) = \begin{bmatrix} 1 & 0 & 1 & 0 \\ 0 & \frac{\sigma + \lambda_1^2}{\lambda_1} & 0 & -\frac{\sigma - \lambda_2^2}{\lambda_2} \\ EI_z(\sigma + \lambda_1^2) & 0 & EI_z(\sigma - \lambda_2^2) & 0 \\ 0 & \frac{\bar{m}\omega^2}{\lambda_1} & 0 & -\frac{\bar{m}\omega^2}{\lambda_2} \end{bmatrix} \quad (10.57)$$

that is

$$\mathbf{a} = \mathbf{B}^{-1}(0)\mathbf{Z}_I \quad (10.58)$$

therefore

$$\mathbf{Z}(x) = \mathbf{B}(x)\mathbf{B}^{-1}(0)\mathbf{Z}_I \quad (10.59)$$

For the output end O of a beam, $x = l$, we have

$$\mathbf{Z}(l) = \mathbf{B}(l)\mathbf{B}^{-1}(0)\mathbf{Z}_I$$

Thus, the transfer matrix of a Timoshenko beam is

$$\mathbf{U} = \mathbf{B}(l)\mathbf{B}^{-1}(0) = \frac{1}{\lambda_1^2 + \lambda_2^2} \begin{bmatrix} a_{11} & a_{12} & a_{13} & a_{14} \\ a_{21} & a_{22} & a_{23} & a_{24} \\ a_{31} & a_{32} & a_{33} & a_{34} \\ a_{41} & a_{42} & a_{43} & a_{44} \end{bmatrix} \quad (10.60)$$

where

$$\begin{aligned} a_{11} &= -(\sigma - \lambda_2^2)\cosh \lambda_1 l + (\sigma + \lambda_1^2)\cos \lambda_2 l, \quad a_{12} = \lambda_1 \sinh \lambda_1 l + \lambda_2 \sin \lambda_2 l \\ a_{21} &= -(\sigma - \lambda_2^2)(\sigma + \lambda_1^2) \left(\frac{\sin \lambda_1 l}{\lambda_1} - \frac{\sin \lambda_2 l}{\lambda_2} \right), \quad a_{22} = (\sigma + \lambda_1^2)\cosh \lambda_1 l - (\sigma - \lambda_2^2)\cos \lambda_2 l \\ a_{31} &= -EI_z(\sigma - \lambda_2^2)(\sigma + \lambda_1^2)(\cos \lambda_1 l - \cos \lambda_2 l) \\ a_{32} &= EI_z[\lambda_1(\sigma + \lambda_1^2)\sinh \lambda_1 l + \lambda_2(\sigma - \lambda_2^2)\sin \lambda_1 l] \\ a_{41} &= -\frac{\bar{m}\omega^2(\sigma - \lambda_2^2)}{\lambda_1}\sin \lambda_1 l + \frac{\bar{m}\omega^2(\sigma + \lambda_1^2)}{\lambda_2}\sin \lambda_2 l, \quad a_{42} = \bar{m}\omega^2(\cos \lambda_1 l - \cos \lambda_2 l) \\ a_{13} &= \frac{1}{EI_z}(\cosh \lambda_1 l - \cos \lambda_2 l), \quad a_{14} = -\frac{\lambda_1(\sigma - \lambda_2^2)}{\bar{m}\omega^2}\sin \lambda_1 l - \frac{\lambda_2(\sigma + \lambda_1^2)}{\bar{m}\omega^2}\sin \lambda_2 l \\ a_{23} &= \frac{\sigma + \lambda_1^2}{EI_z\lambda_1}\sinh \lambda_1 l - \frac{(\sigma - \lambda_2^2)}{EI_z\lambda_2}\sinh \lambda_2 l, \quad a_{24} = -\frac{(\sigma - \lambda_2^2)(\sigma + \lambda_1^2)}{\bar{m}\omega^2}(\cosh \lambda_1 l - \cos \lambda_2 l) \\ a_{33} &= (\sigma + \lambda_1^2)\cosh \lambda_1 l - (\sigma - \lambda_2^2)\cos \lambda_2 l, \quad a_{34} = -\frac{EI_z(\sigma - \lambda_2^2)(\sigma + \lambda_1^2)}{\bar{m}\omega^2}(\lambda_1 \sinh \lambda_1 l + \lambda_2 \sin \lambda_2 l) \\ a_{43} &= \frac{\bar{m}\omega^2}{EI_z} \left(\frac{\sinh \lambda_1 l}{\lambda_1} - \frac{\sin \lambda_2 l}{\lambda_2} \right), \quad a_{44} = -(\sigma - \lambda_2^2)\cosh \lambda_1 l + (\sigma + \lambda_1^2)\cosh \lambda_2 l \end{aligned}$$

Example 10.1 Derive the transfer matrix of a Euler–Bernoulli beam.

Solution

The transverse free-vibration differential equation of a Euler–Bernoulli beam is

$$EI \frac{\partial^4 y}{\partial x^4} + \bar{m} \frac{\partial^2 y}{\partial t^2} = 0 \quad (a)$$

where EI is the bending stiffness of the beam and \bar{m} is the mass density per unit length.

Let $y(x, t) = Y(x)e^{i\omega t}$ and substitute this into Equation (a) to obtain

$$\frac{\partial^4 Y(x)}{\partial x^4} - \frac{\bar{m}\omega^2}{EI} Y(x) = 0 \quad (b)$$

The general solution is

$$Y(x) = A_1 \cosh \lambda x + A_2 \sinh \lambda x + A_3 \cos \lambda x + A_4 \sin \lambda x \quad (c)$$

where $\lambda = \sqrt[4]{\bar{m}\omega^2/(EI)}$.

Similar to Equation (10.54), for a Euler–Bernoulli beam we have

$$\Theta_z = \frac{dY}{dx}, \quad M_z = EI \frac{d\Theta_z}{dx}, \quad Q_y = \frac{dM_z}{dx} \quad (d)$$

and thus

$$\begin{bmatrix} Y \\ \Theta_z \\ M_z \\ Q_y \end{bmatrix}_x = \begin{bmatrix} \cosh \lambda x & \sinh \lambda x & \cos \lambda x & \sin \lambda x \\ \lambda \sinh \lambda x & \lambda \cosh \lambda x & -\lambda \sin \lambda x & \lambda \cos \lambda x \\ EI \lambda^2 \cosh \lambda x & EI \lambda^2 \sinh \lambda x & -EI \lambda^2 \cos \lambda x & -EI \lambda^2 \sin \lambda x \\ EI \lambda^3 \sinh \lambda x & EI \lambda^3 \cosh \lambda x & EI \lambda^3 \sin \lambda x & -EI \lambda^3 \cos \lambda x \end{bmatrix} \begin{bmatrix} A_1 \\ A_2 \\ A_3 \\ A_4 \end{bmatrix} \quad (e)$$

that is, $\mathbf{Z}(x) = \mathbf{B}(x)\mathbf{a}$ and $\mathbf{a} = [A_1, A_2, A_3, A_4]^T$.

If $x = 0$ in $\mathbf{B}(x)$, we obtain

$$\mathbf{B}(0) = \begin{bmatrix} 1 & 0 & 1 & 0 \\ 0 & \lambda & 0 & \lambda \\ EI \lambda^2 & 0 & -EI \lambda^2 & 0 \\ 0 & EI \lambda^3 & 0 & -EI \lambda^3 \end{bmatrix}$$

therefore the transfer matrix of the Euler–Bernoulli beam is

$$\mathbf{U} = \mathbf{B}(l)\mathbf{B}^{-1}(0) = \begin{bmatrix} S(\lambda l) & \frac{T(\lambda l)}{\lambda} & \frac{U(\lambda l)}{EI \lambda^2} & \frac{V(\lambda l)}{EI \lambda^3} \\ \lambda V(\lambda l) & S(\lambda l) & \frac{T(\lambda l)}{EI \lambda} & \frac{U(\lambda l)}{EI \lambda^2} \\ EI \lambda^2 U(\lambda l) & EI \lambda V(\lambda l) & S(\lambda l) & \frac{T(\lambda l)}{\lambda} \\ EI \lambda^3 T(\lambda l) & EI \lambda^2 U(\lambda l) & \lambda V(\lambda l) & S(\lambda l) \end{bmatrix} \quad (10.61)$$

where $S(x)$, $T(x)$, $U(x)$ and $V(x)$ are the *Kрылов functions* [235]:

$$\begin{cases} S(x) = \frac{\cosh x + \cos x}{2}, & T(x) = \frac{\sinh x + \sin x}{2} \\ U(x) = \frac{\cosh x - \cos x}{2}, & V(x) = \frac{\sinh x - \sin x}{2} \end{cases} \quad (10.62)$$

10.3.3 Steps to Derive the Transfer Matrix

As shown in section 10.3.2, a partial differential equation of a continuous element can be disassembled into an n th order ordinary differential equation independent in space and time by separating the variables.

Once the general solution of the n th order ordinary differential equation has been obtained for one variable, the correlative n constants are determined by the boundary conditions, and then the transfer matrix of the continuous element can be derived. The general approach to deriving the transfer matrix of a continuous element can be summarized as follows.

First, develop the n th order differential equation of motion for an infinitesimal continuous element and write out the general solution, for example

$$Z_1(x) = A_1 B_{11}(x) + A_2 B_{12}(x) + \cdots + A_n B_{1n}(x)$$

where $B_{1i}(x) (i = 1, 2, \dots, n)$ are n linearly independent solutions and $A_j (j = 1, 2, \dots, n)$ are constants.

Second, based on the constitutive relation of the continuous element, the other state variables in the state vector can be obtained from the general solution. Write the general solution of the full state matrix form as

$$\mathbf{Z}(x) = \mathbf{B}(x)\mathbf{a} \quad (10.63)$$

where

$$\mathbf{Z}(x) = \begin{bmatrix} Z_1(x) \\ Z_2(x) \\ \vdots \\ Z_n(x) \end{bmatrix}, \quad \mathbf{a} = \begin{bmatrix} A_1 \\ A_2 \\ \vdots \\ A_n \end{bmatrix}, \quad \mathbf{B}(x) = \begin{bmatrix} B_{11}(x) & B_{12}(x) & \cdots & B_{1n}(x) \\ B_{21}(x) & B_{22}(x) & \cdots & B_{2n}(x) \\ \vdots & \vdots & \ddots & \vdots \\ B_{n1}(x) & B_{n2}(x) & \cdots & B_{nn}(x) \end{bmatrix}$$

The matrix $\mathbf{B}(x)$ is the system's fundamental solution matrix.

Using the state vector of the input end, the unknown constant \mathbf{a} is eliminated, that is

$$\mathbf{Z}_I = \mathbf{Z}(0) = \mathbf{B}(0)\mathbf{a} \Rightarrow \mathbf{a} = \mathbf{B}^{-1}(0)\mathbf{Z}_I$$

Finally, substitute \mathbf{a} into Equation (10.63) and the transfer equation can be obtained

$$\mathbf{Z}(x) = \mathbf{B}(x)\mathbf{B}^{-1}(0)\mathbf{Z}_I \quad (10.64)$$

where the transfer matrix is

$$\mathbf{U}_x = \mathbf{B}(x)\mathbf{B}^{-1}(0) \quad (10.65)$$

In particular, for the output end we obtain

$$\mathbf{Z}_O = \mathbf{U}\mathbf{Z}_I, \quad \mathbf{U} = \mathbf{U}_{x=l} = \mathbf{B}(l)\mathbf{B}^{-1}(0)$$

Example 10.2 The force analysis for infinitesimal segment dx_1 of a uniform rod with length l is shown in Figure 10.11, where \bar{m} is the mass density, EA is the tensile stiffness, $x(x_1, t)$ is the longitudinal displacement of the cross-section with distance x_1 from the input end and $p(x_1, t)$ is the external distributed force. Find the transfer matrix of the longitudinal vibration rod.

Solution

It can be proved that the dynamics equation of the longitudinal vibration of a straight uniform rod is

$$\bar{m} \frac{\partial^2 x}{\partial t^2} - EA \frac{\partial^2 x}{\partial x_1^2} = p(x_1, t) \quad (a)$$

and its free vibration equation is

$$\bar{m} \frac{\partial^2 x}{\partial t^2} - EA \frac{\partial^2 x}{\partial x_1^2} = 0 \quad (b)$$

Let $x(x_1, t) = X(x_1)e^{i\omega t}$ and substitute this into Equation (b)

$$\frac{d^2 X(x_1)}{dx_1^2} + \frac{\bar{m}\omega^2}{EA} X(x_1) = 0 \quad (c)$$

The general solution of Equation (c) is

$$X(x_1) = A_1 \cos \beta x_1 + A_2 \sin \beta x_1 \quad (0 \leq x_1 \leq l) \quad (d)$$

where $\beta = \sqrt{\bar{m}\omega^2/(EA)}$, and A_1 and A_2 are arbitrary constants.

According to the Mechanics of Materials, we have

$$Q_x(x_1) = -EA \frac{dX(x_1)}{dx_1} = A_1 \beta EA \sin \beta x_1 - A_2 \beta EA \cos \beta x_1 \quad (e)$$

Combining Equations (d) and (e) yields

$$\begin{bmatrix} X(x_1) \\ Q_x(x_1) \end{bmatrix} = \begin{bmatrix} \cos \beta x_1 & \sin \beta x_1 \\ \beta EA \sin \beta x_1 & -\beta EA \cos \beta x_1 \end{bmatrix} \begin{bmatrix} A_1 \\ A_2 \end{bmatrix} \quad (f)$$

that is, $\mathbf{Z}(x_1) = \mathbf{B}(x_1)\mathbf{a}$ where $\mathbf{a} = [A_1, A_2]^T$.

If $x_1 = 0$ in Equation (f) this yields

$$\begin{bmatrix} X \\ Q_x \end{bmatrix}_I = \begin{bmatrix} 1 & 0 \\ 0 & -\beta EA \end{bmatrix} \begin{bmatrix} A_1 \\ A_2 \end{bmatrix} \quad (g)$$

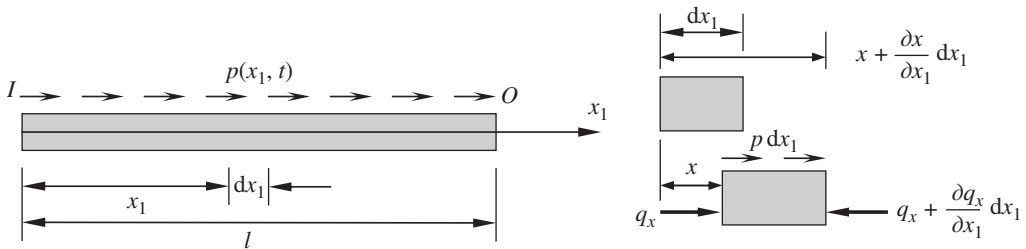


Figure 10.11 Free-body diagram of the longitudinal vibration of a straight rod.

so the transfer matrix of the longitudinal vibration of a straight uniform rod is

$$\begin{aligned} \mathbf{U}_{x_1} = \mathbf{B}(x_1)\mathbf{B}^{-1}(0) &= \begin{bmatrix} \cos \beta x_1 & \sin \beta x_1 \\ \beta EA \sin \beta x_1 & -\beta EA \cos \beta x_1 \end{bmatrix} \begin{bmatrix} 1 & 0 \\ 0 & -\beta EA \end{bmatrix}^{-1} \\ &= \begin{bmatrix} \cos \beta x_1 & -\frac{1}{\beta EA} \sin \beta x_1 \\ \beta EA \sin \beta x_1 & \cos \beta x_1 \end{bmatrix} \end{aligned} \quad (10.66)$$

The derivation of an extended transfer matrix of a continuous element is similar to that for its transfer matrix of free vibration. The principal part of the former has the same form as the latter. The main difference is that only the general solution of the high-order homogeneous differential equation is used for the former, while both of the general and the particular solutions are essential for the latter.

The partitioned matrix \mathbf{f} in the extended transfer matrix for a continuous element is more complex than that for a discrete element. Usually it is difficult to write out directly because it depends not only on the particular solution corresponding to the nonhomogeneous term, but also on the general solution of the homogeneous differential equation. To understand this easily, the following examples are given.

Example 10.3 Let the external distributed force $p(x_1, t) = p(x_1)\cos\Omega t$ in Example 10.2. Find the extended transfer matrix of the longitudinal vibration of the straight uniform rod.

Solution

It can be proved that the vibration equation of the straight uniform rod is

$$\bar{m} \frac{\partial^2 x}{\partial t^2} - EA \frac{\partial^2 x}{\partial x_1^2} = P(x_1)\cos\Omega t \quad (a)$$

Let $x(x_1, t) = \text{Re}[X(x_1)e^{i\Omega t}]$ and substitute this into Equation (a) to obtain

$$X''(x_1) + \frac{\bar{m}\Omega^2}{EA}X(x_1) = -\frac{1}{EA}P(x_1) \quad (b)$$

The solution is

$$X(x_1) = A_1 \cos \beta x_1 + A_2 \sin \beta x_1 + X^*(x_1) \quad (0 \leq x_1 \leq l) \quad (c)$$

where $\beta = \sqrt{\bar{m}\Omega^2/(EA)}$, A_1 and A_2 are arbitrary constants, and $X^*(x_1)$ is the particular solution corresponding to the nonhomogeneous term.

Based on Hooke's law we obtain

$$Q_x(x_1) = -EA \frac{dX(x_1)}{dx_1} = A_1 \beta EA \sin \beta x_1 - A_2 \beta EA \cos \beta x_1 - EAX'^*(x_1) \quad (d)$$

Using Equations (c) and (d) we obtain

$$\begin{bmatrix} X(x_1) \\ Q_x(x_1) \end{bmatrix} = \begin{bmatrix} \cos \beta x_1 & \sin \beta x_1 \\ \beta EA \sin \beta x_1 & -\beta EA \cos \beta x_1 \end{bmatrix} \begin{bmatrix} A_1 \\ A_2 \end{bmatrix} + \begin{bmatrix} X^*(x_1) \\ -EAX'^*(x_1) \end{bmatrix} \quad (e)$$

Let $x_1 = 0$ in Equation (e), then we obtain

$$\begin{bmatrix} X \\ Q_x \end{bmatrix}_I = \begin{bmatrix} 1 & 0 \\ 0 & -\beta EA \end{bmatrix} \begin{bmatrix} A_1 \\ A_2 \end{bmatrix} + \begin{bmatrix} X^*(0) \\ -EAX'^*(0) \end{bmatrix} \quad (f)$$

that is

$$\begin{bmatrix} A_1 \\ A_2 \end{bmatrix} = \begin{bmatrix} 1 & 0 \\ 0 & -\beta EA \end{bmatrix}^{-1} \begin{bmatrix} X \\ Q_x \end{bmatrix}_I - \begin{bmatrix} 1 & 0 \\ 0 & -\beta EA \end{bmatrix}^{-1} \begin{bmatrix} X^*(0) \\ -EAX'^*(0) \end{bmatrix} \quad (g)$$

Using the result of matrix multiplication in Example 10.2 and substituting Equation (g) into Equation (e), the extended transfer matrix can be written as

$$\begin{bmatrix} X(x_1) \\ Q_x(x_1) \\ 1 \end{bmatrix} = \begin{bmatrix} \mathbf{U} & \mathbf{f} \\ \mathbf{0} & 1 \end{bmatrix} \begin{bmatrix} X \\ Q_x \\ 1 \end{bmatrix}_I \quad (h)$$

where $\mathbf{U} = \mathbf{U}(\Omega)$ has the same form as the transfer matrix of free vibration of the straight uniform rod in Example 10.2, and

$$\mathbf{f} = \begin{bmatrix} -X^*(0)\cos \beta x_1 - \frac{1}{\beta}X'^*(0)\sin \beta x_1 + X^*(x_1) \\ -\beta EAX^*(0)\sin \beta x_1 + EAX'^*(0)\cos \beta x_1 - EAX'^*(x_1) \end{bmatrix} \quad (10.67)$$

Expressions of \mathbf{f} for a straight uniform rod for various distributed loads are listed in Table 10.2.

Table 10.2 Expressions of \mathbf{f} of a straight uniform rod for various distributed loads

Load form	The expressions of the particular solution $X^*(x_1)$	The expressions of \mathbf{f}
$P \cos \Omega t$	$X^*(x_1) = -\frac{P}{\bar{m}\Omega^2}$	$\mathbf{f} = \begin{bmatrix} -\frac{P}{\bar{m}\Omega^2}(1 - \cos \beta x_1) \\ \frac{P}{\beta} \sin \beta x_1 \end{bmatrix}$
$\frac{x_1}{l} P \cos \Omega t$	$X^*(x_1) = -\frac{P}{\bar{m}\Omega^2} \frac{x_1}{l}$	$\mathbf{f} = \begin{bmatrix} -\frac{P}{\bar{m}\Omega^2 l} \left(x_1 - \frac{\sin \beta x_1}{\beta} \right) \\ -\frac{P}{\beta^2 l} (1 - \cos \beta x_1) \end{bmatrix}$
$\frac{x_1^2}{l^2} P \cos \Omega t$	$X^*(x_1) = -\frac{P}{\bar{m}\Omega^2 l^2} \left(x_1^2 - \frac{2}{\beta^2} \right)$	$\mathbf{f} = \begin{bmatrix} -\frac{P}{\bar{m}\Omega^2 l^2} \left[x_1^2 + \frac{2(\cos \beta x_1 - 1)}{\beta^2} \right] \\ -\frac{2P}{\beta^2 l^2} \left(x_1 - \frac{\sin \beta x_1}{\beta} \right) \end{bmatrix}$

10.4 Derivation from n First-order Differential Equations

There are many kinds of methods to derive the transfer matrix through system matrix A . Cayley–Hamilton theory is introduced in this book to derive the transfer matrix.

The homogeneous differential equation composed of n first-order differential equations with constant coefficients is

$$\frac{dZ}{ds} = AZ \quad (10.68)$$

Its general solution is

$$Z(s) = e^{As} Z(0) = U(s)Z(0) \quad (10.69)$$

where $Z(0)$ is the initial state vector, $Z(0)$ is the state vector of the input end Z_I if the parameter s expresses the x coordinate, and $U(s) = e^{As}$ is the transfer matrix, which can be expressed in the infinite series

$$U(s) = e^{As} = I + As + \frac{1}{2!}(As)^2 + \frac{1}{3!}(As)^3 + \frac{1}{4!}(As)^4 + \cdots = \sum_{k=0}^{\infty} \frac{(As)^k}{k!} \quad (10.70)$$

The transfer matrix $U(s)$ can be computed using Equation (10.70) directly under some conditions, but Cayley–Hamilton theory is usually used for the computation. Assuming the characteristic polynomial of A is

$$\varphi(a) = \det(aI - A) \quad (10.71)$$

from Cayley–Hamilton theory we obtain

$$\phi(A) = 0 \quad (10.72)$$

As a result, A^n, A^{n+1}, \dots can be linearly expressed by $A^{n-1}, A^{n-2}, \dots, I$, that is

$$U(s) = e^{As} = C_0 I + C_1 A + C_2 A^2 + \cdots + C_{n-1} A^{n-1} \quad (10.73)$$

If all the roots of $\varphi(a) = 0$ are single roots, and the eigenvector corresponding to eigenvalue a_i is v_i , we obtain

$$\begin{cases} A^m v_i = a_i^m v_i \\ \left[I + As + \frac{(As)^2}{2!} + \cdots + \frac{(As)^k}{k!} + \cdots \right] v_i = (C_0 I + C_1 A + \cdots + C_{n-1} A^{n-1}) v_i \end{cases}$$

which yields

$$\left[1 + a_i s + \frac{(a_i s)^2}{2!} + \cdots + \frac{(a_i s)^k}{k!} + \cdots \right] v_i = (C_0 + C_1 a_i + \cdots + C_{n-1} a_i^{n-1}) v_i$$

Thus eigenvalue a_i satisfies

$$e^{a_i s} = C_0 + C_1 a_i + \cdots + C_{n-1} a_i^{n-1} \quad (i = 1, 2, \dots, n) \quad (10.74)$$

The unknown values $C_0, C_1, C_2, \dots, C_{n-1}$ are obtained by solving these n equations, and the transfer matrix can then be computed by Equation (10.73).

The transfer matrix of the Euler–Bernoulli beam is derived in the following to explain the procedure. The differential equation of the Euler–Bernoulli beam can be obtained by letting $GA_s \rightarrow \infty$, $\rho_z \rightarrow 0$ in Equation (10.54)

$$\frac{d}{dx} \begin{bmatrix} Y \\ \Theta_z \\ M_z \\ Q_y \end{bmatrix} = \begin{bmatrix} 0 & 1 & 0 & 0 \\ 0 & 0 & \frac{1}{EI_z} & 0 \\ 0 & 0 & 0 & 1 \\ \bar{m}\omega^2 & 0 & 0 & 0 \end{bmatrix} \begin{bmatrix} Y \\ \Theta_z \\ M_z \\ Q_y \end{bmatrix} \quad (10.75)$$

The characteristic equation is

$$\det(a\mathbf{I} - \mathbf{A}) = \begin{vmatrix} a & -1 & 0 & 0 \\ 0 & a & -\frac{1}{EI_z} & 0 \\ 0 & 0 & a & -1 \\ -\bar{m}\omega^2 & 0 & 0 & a \end{vmatrix} = a^4 - \lambda^4 = 0 \quad (10.76)$$

where $\lambda^4 = \frac{\bar{m}\omega^2}{EI_z}$, and the eigenvalues $\lambda, -\lambda, i\lambda$ and $i\lambda$ of \mathbf{A} are all single roots.

According to Equation (10.73) it follows that

$$\mathbf{U}_x = e^{Ax} = C_0\mathbf{I} + C_1\mathbf{A} + C_2\mathbf{A}^2 + C_3\mathbf{A}^3$$

\mathbf{A} is substituted by its eigenvalue in the above equations to yield

$$\begin{cases} e^{\lambda x} = C_0 + C_1\lambda + C_2\lambda^2 + C_3\lambda^3 \\ e^{-\lambda x} = C_0 - C_1\lambda + C_2\lambda^2 + C_3\lambda^3 \\ e^{i\lambda x} = C_0 + iC_1\lambda - C_2\lambda^2 - iC_3\lambda^3 \\ e^{-i\lambda x} = C_0 - iC_1\lambda - C_2\lambda^2 + iC_3\lambda^3 \end{cases}$$

Obtaining the expressions C_0 , C_1 , C_2 and C_3 from these equations and using Equation (10.62), the transfer matrix is given by

$$\mathbf{U}_x = \begin{bmatrix} S(\lambda x) & \frac{T(\lambda x)}{\lambda} & \frac{U(\lambda x)}{EI_z\lambda^2} & \frac{V(\lambda x)}{EI_z\lambda^3} \\ \lambda V(\lambda x) & S(\lambda x) & \frac{T(\lambda x)}{EI_z\lambda} & \frac{U(\lambda x)}{EI_z\lambda^2} \\ EI_z\lambda^2 U(\lambda x) & EI_z\lambda V(\lambda x) & S(\lambda x) & \frac{T(\lambda x)}{\lambda} \\ EI_z\lambda^3 T(\lambda x) & EI_z\lambda^2 U(\lambda x) & \lambda V(\lambda x) & S(\lambda x) \end{bmatrix} \quad (10.77)$$

If the steady-state vibration equations of a continuous element subjected to a harmonic external force are composed of n first-order partial differential equations, they can be transformed into n first-order nonhomogeneous differential equations with first-order constant coefficients by modal transformation

$$\frac{d\mathbf{Z}}{dx} = \mathbf{AZ} + \mathbf{F}(x) \quad (10.78)$$

where $\mathbf{F}(x)$ is the column matrix of the external force.

The solution of these equations can be written as

$$\mathbf{Z}(x) = e^{Ax}\mathbf{Z}(0) + e^{Ax} \int_0^x e^{-As}\mathbf{F}(s)ds = \mathbf{U}(x)\mathbf{Z}(0) + \mathbf{U}(x) \int_0^x \mathbf{U}(-s)\mathbf{F}(s)ds \quad (10.79a)$$

or

$$\mathbf{Z}(x) = e^{Ax}\mathbf{Z}(0) + \int_0^x e^{-A(x-s)}\mathbf{F}(s)ds = \mathbf{U}(x)\mathbf{Z}(0) + \int_0^x \mathbf{U}(x-s)\mathbf{F}(s)ds \quad (10.79b)$$

denoting

$$\mathbf{f} = \mathbf{U}(x) \int_0^x \mathbf{U}(-s)\mathbf{F}(s)ds \quad \text{or} \quad \mathbf{f} = \int_0^x \mathbf{U}(x-s)\mathbf{F}(s)ds \quad (10.80)$$

Then Equation (10.79) becomes

$$\hat{\mathbf{Z}}(x) = \begin{bmatrix} \mathbf{Z}(x) \\ 1 \end{bmatrix} = \begin{bmatrix} \mathbf{U}(x) & \mathbf{f} \\ 0 & 1 \end{bmatrix} \begin{bmatrix} \mathbf{Z}(0) \\ 1 \end{bmatrix} = \hat{\mathbf{U}}_x \hat{\mathbf{Z}}(0) \quad (10.81)$$

$\mathbf{U}(x)$ has the same form as $\mathbf{U}(s)$ in Equations (10.70) and (10.73). By finding the expressions for \mathbf{f} , the extended transfer matrix of the continuous element subjected to a harmonic external force can be derived. This is illustrated in the following.

Example 10.4 Derive the extended transfer matrix of a transverse vibrating Euler–Bernoulli beam.

Solution

Under distributed external force $p(x,t) = P(x)\cos\Omega t$ and distributed external moment $m(x,t) = M(x)\cos\Omega t$, the vibration equation of the Euler–Bernoulli beam is

$$\frac{\partial y}{\partial x} = \theta_z, \quad \frac{\partial \theta_z}{\partial x} = \frac{m_z}{EI_z}, \quad \frac{\partial m_z}{\partial x} = q_y - m(x,t), \quad \frac{\partial q_y}{\partial x} = -\bar{m} \frac{\partial^2 y}{\partial t^2} + p(x,t) \quad (a)$$

Let

$$\mathbf{z}(x,t) = [y(x,t), \theta_z(x,t), m_z(x,t), q_y(x,t)]^T, \quad \mathbf{Z}(x) = [Y(x), \Theta_z(x), M_z(x), Q_y(x)]^T$$

$$\mathbf{z}(x,t) = \text{Re}[\mathbf{Z}(x)e^{i\Omega t}]$$

and note that

$$p(x,t) = \text{Re}[P(x)e^{i\Omega t}], \quad m(x,t) = \text{Re}[M(x)e^{i\Omega t}]$$

Substituting this into Equation (a) yields

$$\frac{d\mathbf{Z}(x)}{dx} = A\mathbf{Z}(x) + \mathbf{F}(x) \quad (b)$$

where

$$A = \begin{bmatrix} 0 & 1 & 0 & 0 \\ 0 & 0 & \frac{1}{EI_z} & 0 \\ 0 & 0 & 0 & 1 \\ \bar{m}\Omega^2 & 0 & 0 & 0 \end{bmatrix}, \quad \mathbf{F}(x) = \begin{bmatrix} 0 \\ 0 \\ -M(x) \\ P(x) \end{bmatrix} \quad (c)$$

Based on the above equation and Equations (10.79) and (10.81), the main part $\mathbf{U}(x)$ of the extended transfer matrix of a Euler–Bernoulli beam vibrating transversely can be obtained by replacing $\lambda = \sqrt{\bar{m}\omega^2/(EI_z)}$ in Equation (10.77) by $\lambda = \sqrt{\bar{m}\Omega^2/(EI_z)}$. The partitioned matrix \mathbf{f} can be obtained from Equation (10.80):

$$\mathbf{f} = \begin{bmatrix} S(\lambda x) & \frac{T(\lambda x)}{\lambda} & \frac{U(\lambda x)}{EI_z \lambda^2} & \frac{V(\lambda x)}{EI_z \lambda^3} \\ \lambda V(\lambda x) & S(\lambda x) & \frac{T(\lambda x)}{EI_z \lambda} & \frac{U(\lambda x)}{EI_z \lambda^2} \\ EI_z \lambda^2 U(\lambda x) & EI_z \lambda V(\lambda x) & S(\lambda x) & \frac{T(\lambda x)}{\lambda} \\ EI_z \lambda^3 T(\lambda x) & EI_z \lambda^2 U(\lambda x) & \lambda V(\lambda x) & S(\lambda x) \end{bmatrix} \int_0^x \begin{bmatrix} \frac{V(-\lambda s)}{EI_z \lambda^3} P(s) - \frac{V(-\lambda s)}{EI_z \lambda^2} M(s) \\ \frac{U(-\lambda s)}{EI_z \lambda^2} P(s) - \frac{T(-\lambda s)}{EI_z \lambda^2} M(s) \\ \frac{T(-\lambda s)}{\lambda} P(s) - S(-\lambda s) M(s) \\ S(-\lambda s) P(s) - \lambda V(-\lambda s) M(s) \end{bmatrix} ds \quad (d)$$

For $p(x, t) = P \cos \Omega t$, $m(x, t) = M \cos \Omega t$, \mathbf{f} is

$$\mathbf{f} = \begin{bmatrix} \frac{S(\lambda x) - 1}{EI_z \lambda^4} \\ \frac{V(\lambda x)}{EI_z \lambda^3} \\ \frac{U(\lambda x)}{\lambda^2} \\ \frac{T(\lambda x)}{\lambda} \end{bmatrix} P + \begin{bmatrix} -\frac{V(\lambda x)}{EI_z \lambda^3} \\ -\frac{U(\lambda x)}{EI_z \lambda^2} \\ -\frac{T(-\lambda x)}{\lambda} \\ 1 - S(\lambda x) \end{bmatrix} M \quad (e)$$

10.5 Derivation from Stiffness Matrices

When the stiffness matrix between input end I and output end O of an element has been obtained by the finite element method or other methods, the corresponding transfer matrix can be computed by the following method, which is usually used for deriving the transfer matrices of complicated structures.

Assuming the displacements and forces of the state variables in points I and O are $\mathbf{d}_I, \mathbf{f}_I, \mathbf{d}_O$ and \mathbf{f}_O , respectively, then the stiffness matrix can be presented as

$$\begin{bmatrix} \mathbf{f}_I \\ \mathbf{f}_O \end{bmatrix} = \begin{bmatrix} \mathbf{A} & \mathbf{B} \\ \mathbf{C} & \mathbf{D} \end{bmatrix} \begin{bmatrix} \mathbf{d}_I \\ \mathbf{d}_O \end{bmatrix} \quad (10.82)$$

where \mathbf{A} , \mathbf{B} , \mathbf{C} , and \mathbf{D} are the partitioned matrices of the stiffness matrix.

Expressing \mathbf{d}_O and \mathbf{f}_O by using \mathbf{d}_I and \mathbf{f}_I in Equation (10.82), we obtain

$$\begin{bmatrix} \mathbf{d} \\ \mathbf{f} \end{bmatrix}_O = \begin{bmatrix} -\mathbf{B}^{-1}\mathbf{A} & \mathbf{B}^{-1} \\ \mathbf{C} - \mathbf{D}\mathbf{B}^{-1}\mathbf{A} & \mathbf{D}\mathbf{B}^{-1} \end{bmatrix} \begin{bmatrix} \mathbf{d} \\ \mathbf{f} \end{bmatrix}_I \quad (10.83)$$

thus the transfer matrix is

$$\mathbf{U} = \begin{bmatrix} -\mathbf{B}^{-1}\mathbf{A} & \mathbf{B}^{-1} \\ \mathbf{C} - \mathbf{D}\mathbf{B}^{-1}\mathbf{A} & \mathbf{D}\mathbf{B}^{-1} \end{bmatrix} \quad (10.84)$$

Example 10.5 Determine the transfer matrix of a massless uniform beam.

Solution

According to the Mechanics of Materials, the stiffness matrix of a beam can be expressed as

$$\begin{bmatrix} m_{zl} \\ q_{zl} \\ m_{zo} \\ q_{zo} \end{bmatrix} = \begin{bmatrix} -\frac{6EI}{l^2} & -\frac{4EI}{l^2} & \frac{6EI}{l^2} & -\frac{2EI}{l^2} \\ \frac{12EI}{l^2} & \frac{6EI}{l^2} & -\frac{12EI}{l^2} & \frac{6EI}{l^2} \\ \frac{6EI}{l^2} & \frac{2EI}{l} & -\frac{6EI}{l^2} & \frac{4EI}{l} \\ \frac{12EI}{l^3} & \frac{6EI}{l^2} & -\frac{12EI}{l^3} & \frac{6EI}{l^2} \end{bmatrix} \begin{bmatrix} y_l \\ \theta_{zl} \\ y_o \\ \theta_{zo} \end{bmatrix} \quad (a)$$

Comparing with Equation (10.82), we find

$$A = \begin{bmatrix} -\frac{6EI}{l^2} & -\frac{4EI}{l} \\ \frac{12EI}{l^3} & \frac{6EI}{l^2} \end{bmatrix}, B = \begin{bmatrix} \frac{6EI}{l^2} & -\frac{2EI}{l} \\ -\frac{12EI}{l^3} & \frac{6EI}{l^2} \end{bmatrix}, C = \begin{bmatrix} \frac{6EI}{l^2} & \frac{2EI}{l} \\ \frac{12EI}{l^3} & \frac{6EI}{l^2} \end{bmatrix}, D = \begin{bmatrix} -\frac{6EI}{l^2} & \frac{4EI}{l} \\ -\frac{12EI}{l^3} & \frac{6EI}{l^2} \end{bmatrix} \quad (b)$$

In addition

$$B^{-1} = \begin{bmatrix} \frac{l^2}{2EI} & \frac{l^2}{6EI} \\ \frac{l}{EI} & \frac{l^2}{2EI} \end{bmatrix} \quad (c)$$

Substituting this into Equation (10.84) and noticing that

$$d = \begin{bmatrix} y \\ \theta_z \end{bmatrix}, f = \begin{bmatrix} m_z \\ q_y \end{bmatrix} \quad (d)$$

then the transfer matrix of a massless uniform beam is

$$U = \begin{bmatrix} 1 & l & \frac{l^2}{2EI} & \frac{l^3}{6EI} \\ 0 & 1 & \frac{l}{EI} & \frac{l^2}{2EI} \\ 0 & 0 & 1 & l \\ 0 & 0 & 0 & 1 \end{bmatrix} \quad (e)$$

10.6 Computational Method of the Transfer Matrix

In this section, the problems involved in improving the matrix computation efficiency in the MSTMM will be discussed.

10.6.1 Multiplication of Transfer Matrices

The multiplication of transfer matrices is in sequence, and generally does not satisfy the commutative law. For the transfer matrix of “point elements”, such as lumped mass, elastic hinge etc., the multiplications satisfy the commutative law. This is because the dynamics characteristics of

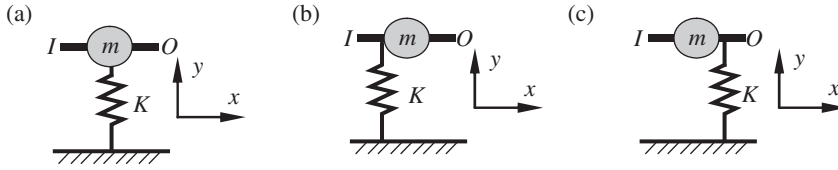


Figure 10.12 A spring and a lumped mass vibrating transversely: (a) a normal mass-spring system, (b) the spring is connected to the input end of the mass and (c) the spring is connected to the output end of the mass.

the system do not change even when the positions of the adjacent “point elements” of the MS are changed.

For example, as shown in Figure 10.12a, the state vector of the spring and lumped mass vibrating in the direction of the y axis is $\mathbf{Z} = [Y, Q_y]^T$. The transfer matrices of the spring and lumped mass are, respectively

$$\mathbf{U}_K = \begin{bmatrix} 1 & 0 \\ -K & 1 \end{bmatrix}, \quad \mathbf{U}_m = \begin{bmatrix} 1 & 0 \\ m\omega^2 & 1 \end{bmatrix}$$

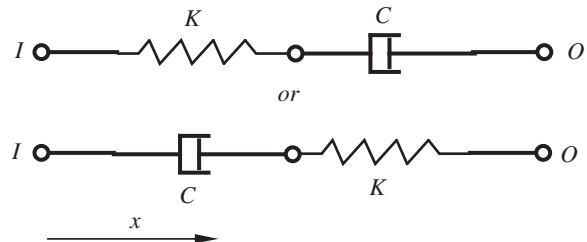
The product of the transfer matrices of the two elements does not change whether the spring is connecting with the input end or the output end of the lumped mass, as shown in Figures 10.12b and 10.12c, respectively. For example

$$\begin{aligned} \mathbf{U}_K \mathbf{U}_m &= \begin{bmatrix} 1 & 0 \\ -K & 1 \end{bmatrix} \begin{bmatrix} 1 & 0 \\ m\omega^2 & 1 \end{bmatrix} = \begin{bmatrix} 1 & 0 \\ m\omega^2 - K & 1 \end{bmatrix} \\ \mathbf{U}_m \mathbf{U}_K &= \begin{bmatrix} 1 & 0 \\ m\omega^2 & 1 \end{bmatrix} \begin{bmatrix} 1 & 0 \\ -K & 1 \end{bmatrix} = \begin{bmatrix} 1 & 0 \\ m\omega^2 - K & 1 \end{bmatrix} \end{aligned}$$

Another example is shown in Figure 10.13, where a longitudinal vibration spring is in series with a damper, with the state vector $\mathbf{Z} = [X, Q_x]^T$. The product of the transfer matrices of the two elements does not change at all, whether the spring is connecting with the input end or the output end of the damper. For example

$$\begin{aligned} \hat{\mathbf{U}}_C \hat{\mathbf{U}}_K &= \begin{bmatrix} 1 & -1/(iC\Omega) & 0 \\ 0 & 1 & 0 \\ 0 & 0 & 1 \end{bmatrix} \begin{bmatrix} 1 & -1/K & 0 \\ 0 & 1 & 0 \\ 0 & 0 & 1 \end{bmatrix} = \begin{bmatrix} 1 & -1/K - 1/(iC\Omega) & 0 \\ 0 & 1 & 0 \\ 0 & 0 & 1 \end{bmatrix} \\ \hat{\mathbf{U}}_K \hat{\mathbf{U}}_C &= \begin{bmatrix} 1 & -1/K & 0 \\ 0 & 1 & 0 \\ 0 & 0 & 1 \end{bmatrix} \begin{bmatrix} 1 & -1/(iC\Omega) & 0 \\ 0 & 1 & 0 \\ 0 & 0 & 1 \end{bmatrix} = \begin{bmatrix} 1 & -1/K - 1/(iC\Omega) & 0 \\ 0 & 1 & 0 \\ 0 & 0 & 1 \end{bmatrix} \end{aligned}$$

Figure 10.13 A spring and a damper in series.



10.6.2 Multiplication of Complex Transfer Matrices

A complex state vector and a complex transfer matrix can be decomposed into a real part and an imaginary part noted by the superscripts r and i , respectively, that is

$$\begin{cases} \bar{\mathbf{Z}} = \mathbf{Z}^r + i\mathbf{Z}^i \\ \bar{\mathbf{U}} = \mathbf{U}^r + i\mathbf{U}^i \end{cases} \quad (10.85)$$

The transfer equation of the element then is expressed as

$$\begin{bmatrix} \mathbf{Z}^r \\ \mathbf{Z}^i \end{bmatrix}_O = \begin{bmatrix} \mathbf{U}^r & -\mathbf{U}^i \\ \mathbf{U}^i & \mathbf{U}^r \end{bmatrix} \begin{bmatrix} \mathbf{Z}^r \\ \mathbf{Z}^i \end{bmatrix}_I \quad (10.86)$$

The complex extended state vector can be written as

$$\hat{\mathbf{Z}} = \begin{bmatrix} \mathbf{Z}^r \\ \mathbf{Z}^i \\ 1 \end{bmatrix} \quad (10.87)$$

The complex extended transfer equation of the element is

$$\begin{bmatrix} \mathbf{Z}^r \\ \mathbf{Z}^i \\ 1 \end{bmatrix}_O = \begin{bmatrix} \mathbf{U}^r & -\mathbf{U}^i & \mathbf{Z}^r \\ \mathbf{Z}^i & \mathbf{Z}^r & \mathbf{Z}^i \\ \mathbf{0} & \mathbf{0} & 1 \end{bmatrix} \begin{bmatrix} \mathbf{Z}^r \\ \mathbf{Z}^i \\ 1 \end{bmatrix}_I \quad (10.88)$$

The overall transfer matrix of a chain system is

$$\mathbf{U} = \mathbf{U}_n \mathbf{U}_{n-1} \cdots \mathbf{U}_2 \mathbf{U}_1 \text{ or } \hat{\mathbf{U}} = \hat{\mathbf{U}}_n \hat{\mathbf{U}}_{n-1} \cdots \hat{\mathbf{U}}_2 \hat{\mathbf{U}}_1 \quad (10.89)$$

Because of

$$\begin{bmatrix} \mathbf{A} & -\mathbf{B} \\ \mathbf{B} & \mathbf{A} \end{bmatrix} \begin{bmatrix} \mathbf{C} & -\mathbf{D} \\ \mathbf{D} & \mathbf{C} \end{bmatrix} = \begin{bmatrix} \mathbf{AC} - \mathbf{BD} & -(\mathbf{AD} + \mathbf{BC}) \\ \mathbf{AD} + \mathbf{BC} & \mathbf{AC} - \mathbf{BD} \end{bmatrix} = \begin{bmatrix} \mathbf{E} & -\mathbf{F} \\ \mathbf{F} & \mathbf{E} \end{bmatrix} \quad (10.90)$$

it can be proved that

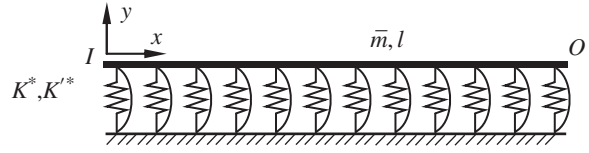
$$\mathbf{U} = \begin{bmatrix} \mathbf{U}^r & -\mathbf{U}^i \\ \mathbf{U}^i & \mathbf{U}^r \end{bmatrix}, \hat{\mathbf{U}} = \begin{bmatrix} \mathbf{U}^r & -\mathbf{U}^i & \mathbf{f}^r \\ \mathbf{U}^i & \mathbf{U}^r & \mathbf{f}^i \\ \mathbf{0} & \mathbf{0} & 1 \end{bmatrix} \quad (10.91)$$

If the product of the complex transfer matrices is decomposed into a real part and an imaginary part based on above characteristics of the multiplication of a complex transfer matrix, only half of their elements are necessary for the product of transfer matrices. Hence, half of the computational work can be saved.

10.6.3 Merging Basic Elements into a Composite Element

To improve computational efficiency, some basic elements of a system can be merged. For example, beams, lumped masses and springs can be assembled into one component regarded as the basic element of the system.

Figure 10.14 A transverse vibration homogeneous rigid body with elastic foundation.



A transverse vibration homogeneous rigid body with uniform cross-section and elastic foundation, as shown in Figure 10.14, has the following state vector

$$\mathbf{Z} = [Y, \Theta_z, M_z, Q_y]^T$$

The transfer matrix is

$$\mathbf{U} = \begin{bmatrix} 1 & l & 0 & 0 \\ 0 & l & 0 & 0 \\ \frac{l^2(\bar{m}\omega^2 - K^*)}{2} & \frac{l^2(\bar{m}\omega^2 - K^*)}{6} + l(K'^* - r^2\bar{m}\omega^2) & 1 & l \\ l(\bar{m}\omega^2 - K^*) & \frac{l^2(\bar{m}\omega^2 - K^*)}{2} & 0 & 1 \end{bmatrix}$$

where l is the length of the rigid body, \bar{m} is the mass per unit length, K^* is the Winkler (elastic) foundation modulus, K'^* is the rotary foundation modulus and r is the gyration radius of the cross-section about the z axis.

If there is no elastic foundation, then $K^* = K'^* = 0$. For this kind of elastic foundation where only linear elasticity is considered and the rotary elasticity is neglected, $K'^* = 0$. If only rotary elasticity is considered and the linear elasticity is neglected, $K^* = 0$.

10.6.4 Dimensionless Transfer Matrix

For easy processing, improving computational precision and avoiding computational overflow, the state vector and the transfer matrix can be made dimensionless and all matrix elements given a magnitude of 1.

For example, the transfer equation of a massless elastic beam is

$$\begin{bmatrix} Y \\ \Theta_z \\ M_z \\ Q_y \end{bmatrix}_O = \begin{bmatrix} 1 & l & \frac{l^2}{2EI} & \frac{l^3}{6EI} \\ 0 & 1 & \frac{l}{EI} & \frac{l^2}{2EI} \\ 0 & 0 & 1 & l \\ 0 & 0 & 0 & 1 \end{bmatrix} \begin{bmatrix} Y \\ \Theta_z \\ M_z \\ Q_y \end{bmatrix}_I$$

By transforming the state vectors, we obtain

$$\begin{bmatrix} Y \\ l\Theta_z \\ \frac{l^2}{EI}M_z \\ \frac{l^3}{EI}Q_y \end{bmatrix}_O = \begin{bmatrix} 1 & 1 & \frac{1}{2} & \frac{1}{6} \\ 0 & 1 & 1 & \frac{1}{2} \\ 0 & 0 & 1 & 1 \\ 0 & 0 & 0 & 1 \end{bmatrix} \begin{bmatrix} Y \\ l\Theta_z \\ \frac{l^2}{EI}M_z \\ \frac{l^3}{EI}Q_y \end{bmatrix}_I$$

All the elements of the transfer matrix are dimensionless, and the differences between their magnitudes are not too great.

10.7 Improved Algorithm for Eigenvalue Problems

The form of the real characteristics equation of the MSTMM is

$$D(\omega) = |\mathbf{U}(\omega)| = 0 \quad (10.92)$$

where $D(\omega)$ is the characteristic determinant with order N that varies with ω .

By triangularization of matrix \mathbf{U} , the value of $D(\omega)$ is

$$D(\omega) = \prod_{i=1}^N d_{ii}(\omega) \quad (10.93)$$

where $d_{ii}(\omega)$ is the diagonal element of the triangularized matrix $\mathbf{U}(\omega)$.

For two different variables ω_a and ω_b we have

$$D(\omega_a) \cdot D(\omega_b) < 0 \quad (10.94)$$

There is at least one root ω in the interval (ω_a, ω_b) satisfying Equation (10.92). If the secant method is used for solving Equation (10.92), the approximate value ω_c of ω can be acquired using $D(\omega_a)$ and $D(\omega_b)$:

$$\omega_c = \omega_a + \frac{\omega_b - \omega_a}{1 - D(\omega_b)/D(\omega_a)} \quad (10.95)$$

Because of the limitation of the expression range of the floating-point number in computers, when computing the value of the characteristics determinant directly using Equation (10.95), the numerical value will overflow because the absolute value of the determinant is either too large or too small, which leads to a failure in the solution. The method of solving this problem used in the reference [252] is introduced in the following. Let

$$a_{jj}(\omega) = d_{jj}(\omega) \frac{|d_{jj}(\omega)|^{1/k}}{|d_{jj}(\omega)|} \quad (10.96)$$

$$A(\omega) = \prod_{j=1}^N a_{jj}(\omega) \quad (10.97)$$

It is notable from Equations (10.96) and (10.97) that the variation range of the absolute value of $A(\omega)$ is much smaller than the variation range of the absolute value of $D(\omega)$ if $k > 1.0$.

Sometimes some absolute values of $a_{jj}(\omega)$ are very small and sometimes they are very large. The small absolute values, as well as the large ones, emerge successively, resulting in an overflow phenomenon when computing $A(\omega)$ in the natural sequence.

This problem can be solved by adjusting the computational sequence of Equation (10.97) as follows. First, the largest absolute value and the smallest absolute value are multiplied, then the next largest absolute value and the next smallest value are multiplied.

If we can make a *combination* of the expression of $A(\omega)$ and the secant method given in Equation (10.95), then the overflow problem could be solved in an efficient way.

Using Equations (10.93), (10.95), (10.96) and (10.97) yields

$$\omega_c = \omega_a + \frac{\omega_b - \omega_a}{1 - R} \quad (10.98)$$

where

$$R = \frac{A(\omega_b)}{A(\omega_a)} \cdot \left| \frac{A(\omega_b)}{A(\omega_a)} \right|^{k-1} \quad (10.99)$$

Equation (10.98) remains the approximative characterization of Equation (10.95). According to Equations (10.96) and (10.97), if the value of k is large enough, the overflow problem is completely avoided while solving Equation (10.92) by using Equation (10.98).

The ω_c obtained by computing Equation (10.98) will equal to ω_b or ω_a when $|\omega_b - \omega_a|$ is huge or $|R|$ is huge or tiny. In this situation, let $\omega_c = (\omega_a + \omega_b)/2$.

When $A(\omega_c) \cdot D(\omega_a) < 0$, the procedure is continued in the interval between the points ω_c and ω_a . When $A(\omega_c) \cdot D(\omega_b) < 0$, the procedure is continued in the interval between the points ω_c and ω_b .

The form of the complex characteristic equation of the MSTMM is

$$D(\lambda) = 0 \quad (10.100)$$

where the values of the characteristic variable λ and the characteristic determinant $D(\lambda)$ are all complex numbers.

After triangularization, the value of $D(\lambda)$ is

$$D(\lambda) = \prod_{j=1}^N d_{jj}(\lambda) \quad (10.101)$$

To solve Equation (10.100) using the tangent method, take a point λ_1 on the complex plane as the starting point for finding roots and the approximate solution of λ can be expressed as

$$\lambda^* = \lambda_1 + \frac{h}{1 - D(\lambda_1 + h)/D(\lambda_1)} \quad (10.102)$$

where h is the derivative step.

The numerical overflow will still be a problem if we compute the value of the characteristic determinant $D(\lambda)$ directly using Equation (10.101), so we let

$$a_{jj}(\lambda) = d_{jj}(\lambda)^{1/k}, \quad A(\lambda) = \prod_{j=1}^N a_{jj}(\lambda) \quad (10.103)$$

Using Equations (10.101) to (10.103), we obtain

$$\lambda^* = \lambda_1 + \frac{h}{1 - [A(\lambda_1 + h)/A(\lambda_1)]^k} \quad (10.104)$$

It is notable from Equations (10.101) and (10.103) that the region of modulus variation of $A(\lambda)$ is far less than that of $D(\lambda)$ if $k > 10$. Consequently, the numerical overflow problem can be avoided when solving Equation (10.100) using Equation (10.104) and the value of k is large enough.

Example 10.6 Analyze and compare the real and complex eigenvalues of the rotor-bearing crankcase system of an engine [252] using the secant method directly and the improved method, respectively.

Solution

Using the improved secant method, taking $k = 10$, the eigenvalue $\omega = 1171.21\text{Hz}$ can be obtained by only three iterations in the interval $\omega_a = 1000\text{Hz}$, $\omega_b = 1200\text{Hz}$, and the precision of the eigenvalue is 10^{-5} .

The largest absolute value of $A(\omega)$ is only 8.72×10^8 . When solving the same problem using the secant method directly, the largest absolute value of $D(\omega)$ is 7.86×10^{36} and the overflow

problem occurs. If the node number is reduced from 108 to 32, that is, the degrees of freedom of the system are reduced to about 30% of the original, the overflow problem will be eliminated.

The result of the simple model obtained by the secant method is $\omega = 1247.51\text{Hz}$, and the computational error relative to the result obtained by the original model is 6.5%.

Computing the complex eigenvalues using the improved method and taking still $k = 10$, a pair of conjugate complex eigenvalues of the system $\lambda = -5.7 \pm i2024.1$ is found by five approximations starting from point $\lambda_1 = 0 + i0$. Using the secant method directly, the overflow problem will appear at the start point.

If the simple model is used, the eigenvalue $\lambda = -5.1 \pm i2182.6$ corresponding to the former result is obtained and the relative error between the two results is 7.8%.

The largest absolute value of $A(\lambda)$ is 6.16×10^5 when using the improved method, while the largest absolute value of $D(\lambda)$ is up to 8.72×10^{31} if the tangent method and the simple model are used.

10.8 Properties of the Inverse Matrix of a Transfer Matrix

Some properties of the inverse matrix of transfer matrices will be introduced in this section. The solution of the inverse matrix of a transfer matrix will be simple and easy in some situations if these properties are used.

10.8.1 Chessboard Rule

The *chessboard rule* [37] is a very simple method for solving the inverse matrix of a transfer matrix. For example, the elements of system matrix A are put in a chessboard in sequence, as shown in Figure 10.15. The matrix that has all nonzero elements in the black squares of the chessboard is called the black chessboard matrix and the matrix that has all nonzero elements in the white squares is called the white chessboard matrix. For example, system matrix A in Equation (10.75), with all its nonzero elements on black squares, is a black chessboard matrix.

Generally speaking, for a black chessboard matrix, its even order will become a white chessboard matrix, and its odd order is still a black chessboard; while for a white chessboard matrix, both of its even and odd orders are always white chessboard matrices. These identities can be used for checking numerical computations.

0	1	0	0		
0	0	$\frac{1}{EI_z}$	0		...
0	0	0	1		
$\bar{m}\omega^2$	0	0	0		...
⋮		⋮		⋮	⋱

Figure 10.15 Chessboard.

It can be seen from observing Equation (10.70) and using these identities that coefficient matrices with even order s are all white chessboard matrices, and coefficient matrices with odd order s are all black chessboard matrices.

Because of

$$e^{As}e^{A(-s)} = e^{A(-s)}e^{As} = \mathbf{I} \quad (10.105)$$

the inverse matrix can be obtained just by adding a minus sign to s in Equation (10.70), so the inverse matrix of e^{As} is $e^{A(-s)}$. Since only terms with an odd order need to change sign, the sign of functions in the black chessboard squares only needs to be changed in the final matrix. This rule of obtaining the inverse matrix is called the chessboard rule.

Example 10.7 Find the transfer matrix of a Euler–Bernoulli beam and its inverse transfer matrix.

Solution

Expand the transfer matrix of Equation (10.75) according to Equation (10.70) and suppose the general expression of the transfer matrix \mathbf{U} is

$$\mathbf{U}(x) = e^{Ax} = \begin{bmatrix} u_{11} & u_{12} & u_{13} & u_{14} \\ u_{21} & u_{22} & u_{23} & u_{24} \\ u_{31} & u_{32} & u_{33} & u_{34} \\ u_{41} & u_{42} & u_{43} & u_{44} \end{bmatrix} \quad (a)$$

The general expansion term of u_{11} is $\frac{(\lambda x)^{4n}}{(4n)!}$ ($n = 0, 1, 2, \dots$), namely the general term of $S(\lambda x)$

$$u_{11} = \sum_{n=0}^{\infty} \frac{1}{\lambda} \frac{(\lambda x)^{4n}}{(4n)!} = S(\lambda x) \quad (b)$$

where

$$\lambda^4 = \frac{\bar{m}\omega^2}{EI_z}$$

If

$$\begin{cases} u_{12} = \sum_{n=0}^{\infty} \frac{1}{\lambda} \frac{(\lambda x)^{1+4n}}{(1+4n)!} = \frac{1}{\lambda} T(\lambda x) \\ u_{32} = \sum_{n=0}^{\infty} EI_z \lambda \frac{(\lambda x)^{n+3}}{(n+3)!} = EI_z \lambda V(\lambda x) \\ \vdots \end{cases} \quad (c)$$

then

$$e^{Ax} = \begin{bmatrix} S(\lambda x) & \frac{T(\lambda x)}{\lambda} & \frac{U(\lambda x)}{EI_z \lambda^2} & \frac{V(\lambda x)}{EI_z \lambda^3} \\ \lambda V(\lambda x) & S(\lambda x) & \frac{T(\lambda x)}{EI_z \lambda} & \frac{U(\lambda x)}{EI_z \lambda^2} \\ EI_z \lambda^2 U(\lambda x) & EI_z \lambda V(\lambda x) & S(\lambda x) & \frac{T(\lambda x)}{\lambda} \\ EI_z \lambda^3 T(\lambda x) & EI_z \lambda^2 U(\lambda x) & \lambda V(\lambda x) & S(\lambda x) \end{bmatrix} \quad (d)$$

By changing the sign of the function in the black chessboard, its inverse matrix can be obtained as

$$e^{A(-x)} = \begin{bmatrix} S(\lambda x) & -\frac{T(\lambda x)}{\lambda} & \frac{U(\lambda x)}{EI_z \lambda^2} & -\frac{V(\lambda x)}{EI_z \lambda^3} \\ -\lambda V(\lambda x) & S(\lambda x) & -\frac{T(\lambda x)}{EI_z \lambda} & \frac{U(\lambda x)}{EI_z \lambda^2} \\ EI_z \lambda^2 U(\lambda x) & -EI_z \lambda V(\lambda x) & S(\lambda x) & -\frac{T(\lambda x)}{\lambda} \\ -EI_z \lambda^3 T(\lambda x) & EI_z \lambda^2 U(\lambda x) & -\lambda V(\lambda x) & S(\lambda x) \end{bmatrix} \quad (e)$$

The same result can be achieved by changing the sign of the independent variable of the function in the matrix according to $e^{A(-x)}$. However, according to the chessboard rule these characteristics are acquired before the computation finishes.

10.8.2 Inverse Matrix of the Transfer Matrix of a Symmetrical Object

A symmetrical object is an object that has uniform distribution with the same boundary conditions at its two ends. The inverse matrix of the transfer matrix of a symmetrical object has remarkable characteristics. Arranging the state vector by the usual order and using the chessboard rule, the inverse matrix of the transfer matrix of a symmetrical object can be obtained by changing the signs of all the black chessboard squares.

A fourth-order transfer matrix is used as an illustration, but it can be easily extended to the general situation, for example the transfer equation is

$$\begin{bmatrix} Y(x) \\ Y'(x) \\ Y''(x) \\ Y'''(x) \end{bmatrix}_O = \begin{bmatrix} u_{11} & u_{12} & u_{13} & u_{14} \\ u_{21} & u_{22} & u_{23} & u_{24} \\ u_{31} & u_{32} & u_{33} & u_{34} \\ u_{41} & u_{42} & u_{43} & u_{44} \end{bmatrix} \begin{bmatrix} Y(x) \\ Y'(x) \\ Y''(x) \\ Y'''(x) \end{bmatrix}_I \quad (10.106)$$

or

$$\mathbf{Z}_O(x) = \mathbf{U}(x) \mathbf{Z}_I(x)$$

where the superscript denotes differentiation with respect to x .

When \mathbf{U} is nonsingular, we obtain

$$\mathbf{Z}_I(x) = \mathbf{U}^{-1}(x) \mathbf{Z}_O(x) \quad (10.107)$$

where \mathbf{U}^{-1} is a transfer matrix in the inverse direction.

For the symmetrical object, the distinction in the transfer matrices is no more than the transfer direction. Suppose $s = -x$, then

$$\frac{d}{ds} = -\frac{d}{dx}, \quad \frac{d^2}{ds^2} = \frac{d^2}{dx^2}, \quad \frac{d^3}{ds^3} = -\frac{d^3}{dx^3} \quad (10.108)$$

and

$$\mathbf{Z}_I(-s) = \mathbf{U}^{-1}(-s) \mathbf{Z}_O(-s) \quad (10.109)$$

where $\mathbf{Z}_I(x)$ and $\mathbf{Z}_O(-s)$ are the expressions of the state vector at the same point in the two coordinates, respectively, and $\mathbf{Z}_O(-s)$ is similar to $\mathbf{Z}_O(x)$.

The sign convention is the same for $Y(x)$ whether transferring in the positive or negative direction, but the sign of the second and the fourth elements of the state vector is changed, therefore

$$\begin{bmatrix} Y(x) \\ -Y'(x) \\ Y''(x) \\ -Y'''(x) \end{bmatrix}_I = \mathbf{U}^{-1}(x) \begin{bmatrix} Y(x) \\ -Y'(x) \\ Y''(x) \\ -Y'''(x) \end{bmatrix}_O \quad (10.110)$$

The sign of the second and fourth elements of the state vector of the input end and the output end in Equation (10.110) can be transferred to the transfer matrix. Letting the state vector keep its form and comparing with Equation (10.107), the inverse matrix $\mathbf{U}^{-1}(x)$ can be obtained only by changing the sign of the elements in the black chessboard of $\mathbf{U}(x)$, that is

$$\mathbf{U}^{-1}(x) = \begin{bmatrix} u_{11} & -u_{12} & u_{13} & -u_{14} \\ -u_{21} & u_{22} & -u_{23} & u_{24} \\ u_{31} & -u_{32} & u_{33} & -u_{34} \\ -u_{41} & u_{42} & -u_{43} & u_{44} \end{bmatrix} \quad (10.111)$$

Taking the Euler–Bernoulli beam as an object, the transfer equation is

$$\begin{bmatrix} Y \\ \theta_z \\ M_z \\ Q_y \end{bmatrix}_x = \begin{bmatrix} S(\lambda x) & \frac{T(\lambda x)}{\lambda} & \frac{U(\lambda x)}{EI_z \lambda^2} & \frac{V(\lambda x)}{EI_z \lambda^3} \\ \lambda V(\lambda x) & S(\lambda x) & \frac{T(\lambda x)}{EI_z \lambda} & \frac{U(\lambda x)}{EI_z \lambda^2} \\ EI_z \lambda^2 U(\lambda x) & EI_z \lambda V(\lambda x) & S(\lambda x) & \frac{T(\lambda x)}{\lambda} \\ EI_z \lambda^3 T(\lambda x) & EI_z \lambda^2 U(\lambda x) & \lambda V(\lambda x) & S(\lambda x) \end{bmatrix} \begin{bmatrix} Y \\ \theta_z \\ M_z \\ Q_y \end{bmatrix}_I \quad (10.112)$$

The positive directions of the state variables of an element are shown in Figure 10.16. It can be easily seen that when the transfer direction is inverted, the positive directions of Y and M_z will not be changed, only the positive directions of θ_z and Q_y are changed.

The inverse transfer matrix can therefore be obtained by changing the sign of the elements in the black chessboard in the transfer matrix according to Equation (10.111). The result is the

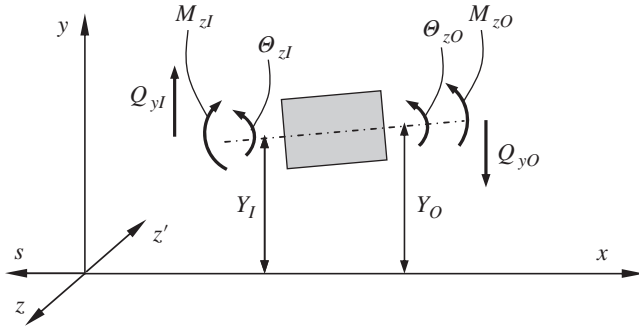


Figure 10.16 The positive directions of the state variables of a Euler–Bernoulli beam.

same as in Example 10.7. In fact, it can be verified that the determinant of the transfer matrix of a Euler–Bernoulli beam is always equal to 1, that is

$$\det \begin{bmatrix} S(\lambda x) & \frac{T(\lambda x)}{\lambda} & \frac{U(\lambda x)}{EI_z \lambda^2} & \frac{V(\lambda x)}{EI_z \lambda^3} \\ \lambda V(\lambda x) & S(\lambda x) & \frac{T(\lambda x)}{EI_z \lambda} & \frac{U(\lambda x)}{EI_z \lambda^2} \\ EI_z \lambda^2 U(\lambda x) & EI_z \lambda V(\lambda x) & S(\lambda x) & \frac{T(\lambda x)}{\lambda} \\ EI_z \lambda^3 T(\lambda x) & EI_z \lambda^2 U(\lambda x) & \lambda V(\lambda x) & S(\lambda x) \end{bmatrix} = \cos^2 \lambda x + \sin^2 \lambda x = 1$$

To summarize:

- 1) The distinction between the inverse matrix of a transfer matrix and the original matrix for symmetrical objects is only the sign.
- 2) If the state vector is arrayed in a certain order, the inverse matrix will satisfy the chessboard rule obtained by changing the signs of the elements in the black squares of the transfer matrix. It will be simple to find the inverse matrix of a transfer matrix using these properties.

10.8.3 Conditions of the Symmetrical Object

The condition of the symmetrical object is closely correlated to the symmetry criterion of the dynamics system [253]. The characteristics of those objects such as linear acoustic filter, vibration isolator, medium wave filter etc. can all be decided by two state variables for a one-dimensional system, which are commonly pressure and velocity of sound for an acoustic filter, force and velocity for mechanical systems, and voltage and current for electric systems. All of these system characteristics can be decided by linear ordinary differential equations with a common similar constant coefficient. The concept of the symmetry of a system is correlated to the one-dimensional passive system. Some characteristics of the 2×2 -dimension transfer matrix of a one-dimensional symmetrical mechanical system [254] was obtained by Snowdon using the fact that the position of the input and output ends in the geometric symmetrical system can be exchanged. This concept can be extended to an active system with an arbitrary number of state vectors. These characteristics need the transfer matrix to be equal to its inverse matrix, and the general relations among the parameters of transfer matrix are obtained.

If the positive direction of the state vector defined is independent of the direction of the observed system, as shown in Figure 10.17, the transfer equation of the passive system is still written as

$$\mathbf{Z}_O = \mathbf{U} \mathbf{Z}_I \quad (10.113)$$

Premultiplying Equation (10.113) by \mathbf{U}^{-1} yields

$$\mathbf{Z}_I = \mathbf{U}^{-1} \mathbf{Z}_O$$

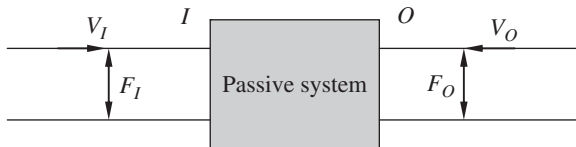


Figure 10.17 A state vector defined symmetrically.

The transfer matrix in the reverse transfer direction will not change for a symmetrical system, that is

$$\mathbf{Z}_I = \mathbf{U}\mathbf{Z}_O$$

Therefore, the symmetry needs

$$\mathbf{U} = \mathbf{U}^{-1} \quad \text{or} \quad \mathbf{U}\mathbf{U} = \mathbf{I} \quad (10.114)$$

that is, the inverse matrix of the transfer matrix is equal to the transfer matrix, or the square of the transfer matrix is the unit matrix. This is called the general criterion for the symmetry of the transfer matrix. If the dimension of the transfer matrix is $n \times n$, then Equation (10.114) could be expanded as

$$\sum_{j=1}^n u_{ij}u_{jk} = \begin{cases} 0 & i \neq k \\ 1 & i = k \end{cases} \quad (10.115)$$

In other words, the i th row and the k th column are orthogonal. Taking the determinant of Equation (10.114), we get

$$|\mathbf{U}^2| = 1$$

that is

$$\Delta = |\mathbf{U}| = \pm 1 \quad (10.116)$$

Therefore, the determinant of the transfer matrix for a symmetrical system must equal +1 or -1.

For an explanation, take the second-order transfer matrix

$$\mathbf{U} = \begin{bmatrix} u_{11} & u_{12} \\ u_{21} & u_{22} \end{bmatrix} \quad (10.117)$$

as an example, and from Equation (10.115), we obtain

$$\begin{cases} u_{11}^2 + u_{12}u_{21} = 1 \\ u_{11}u_{12} + u_{12}u_{22} = 0 \\ u_{21}u_{11} + u_{22}u_{21} = 0 \\ u_{21}u_{12} + u_{22}^2 = 1 \end{cases}$$

that is

$$u_{22} = -u_{11} \quad (10.118)$$

Hence, the value of the determinant is

$$\Delta = u_{11}u_{22} - u_{12}u_{21} = -u_{11}^2 - u_{12}u_{21} = -1 \quad (10.119)$$

The determinant of the second-order transfer matrix of a symmetrical system is equal to -1.

If the system is symmetrical, but the directions of the state variables defined are asymmetrical, the sign of one row (column) or several rows (columns) of the transfer matrix will be changed in Equation (10.113).

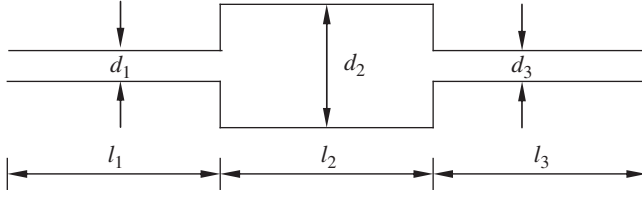


Figure 10.18 An acoustics low pass filter.

Example 10.8 Symmetry problem for an acoustics filter system.

An acoustics filter system with uniform cross-section, as shown in Figure 10.18, defines the state vector symmetrically and yields the transfer equation of the acoustics filter [255]:

$$\begin{bmatrix} F \\ V \end{bmatrix}_O = e^{-iK_C M l} \begin{bmatrix} \cos K_C l & -iY \sin K_C l \\ \frac{i}{Y} \sin K_C l & -\cos K_C l \end{bmatrix} \begin{bmatrix} F \\ V \end{bmatrix}_I \quad (a)$$

where the elements of the state vector are the pressure F and the mass-velocity V . l is the length, $Y = a/S$ is the characteristic impedance, a is the wave velocity in the quiescence medium, S is the section area, $K_C = K/(1 - M^2)$ is the transmitted wave number, K is the number of waves, M is the Mach number of incoming inflow and i is the imaginary unit.

For the quiescence medium, $M = 0$, $K_C = K$ and the transfer matrix in Equation (a) is simplified as

$$\begin{bmatrix} \cos Kl & -iY \sin Kl \\ \frac{i}{Y} \sin Kl & -\cos Kl \end{bmatrix} \quad (b)$$

It is obviously

$$u_{22} = -u_{11}, \quad \Delta = -1 \quad (c)$$

Therefore, the acoustics filter with uniform cross-section is symmetrical for a quiescence medium in geometry and in function.

For the transfer matrix in Equation (a), when $M \neq 0$ we have

$$u_{22} = -u_{11}, \quad \Delta = e^{-2K_C M l} \neq \pm 1 \quad (d)$$

Therefore, the acoustics filter with uniform cross-section is not symmetrical for a flowing medium in function even though it is symmetrical in geometry. This is because the incoming flow is not reversible.

For the acoustics low-pass filter system shown in Figure 10.18, it can be proved easily using transfer matrices that Equation (10.116) will be satisfied if $d_1 = d_3$, $l_1 = l_3$, $M_1 = M_2 = M_3 = 0$. Therefore, the geometric of the system is certainly not a sufficient condition for the symmetry of acoustic's dynamics. To satisfy the symmetry, the velocity of incoming flow has to be zero.

Example 10.9 Symmetry problem for the dynamic of a trumpet.

Consider the exponential curve-shaped trumpet with static medium, as shown between lines 2 and 3 in Figure 10.19, for which the transfer equation is [256, 257]

$$\begin{bmatrix} p_3 \\ v_3 \end{bmatrix} = \begin{bmatrix} e^{k_0 l} \left(\cos K' l - \frac{k_0}{K'} \sin K' l \right) & iY_3 e^{k_0 l} \frac{K}{K'} \sin K' l \\ \frac{i}{Y_3} e^{-k_0 l} \frac{K' - ik_0}{K} \left(1 + i \frac{k_0}{K'} \right) \sin K' l & e^{-k_0 l} \left(\cos K' l + \frac{k_0}{K'} \sin K' l \right) \end{bmatrix} \begin{bmatrix} p_2 \\ v_2 \end{bmatrix} \quad (10.120)$$

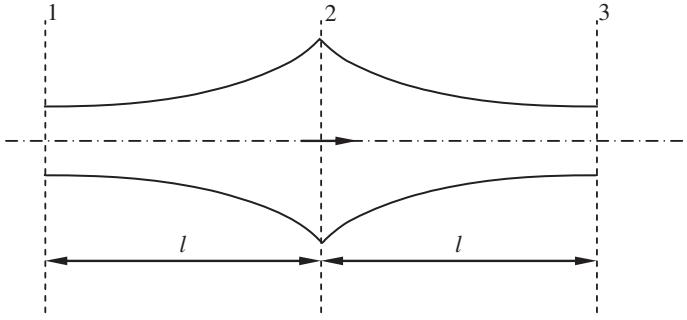


Figure 10.19 Two identical exponential curve-shaped trumpets joined back to back.

where p and v are sound pressure and mass velocity, $K' = \sqrt{K^2 - k_0^2}$, k_0 is the exponent expand constant and Y_3 is the characteristic impedance in section 3 of the pipe.

Obviously, since the system is geometrically asymmetrical, the transfer matrix is also asymmetrical.

If the same two exponential curve-shaped trumpets are connected back-to-back, as shown in Figure 10.19, and then substituting k_0 and Y_3 by $-k_0$ and Y_2 in Equation (10.120), respectively, the transfer matrix of the mirror image trumpet will not be changed. Multiplying the two transfer matrices and noticing that $Y_2 = Y_3 e^{2k_0 l}$, the overall transfer equation is

$$\begin{bmatrix} p_3 \\ v_3 \end{bmatrix} = \begin{bmatrix} \cos 2K'l - \frac{2k_0^2}{K'^2} \sin^2 K'l & iY_2 \frac{K}{K'} \left(\sin 2K'l - \frac{2k_0}{K'} \sin^2 K'l \right) \\ \frac{i}{Y_2 K'} \left(\sin 2K'l + \frac{2k_0}{K'} \sin^2 K'l \right) & \cos 2K'l - \frac{2k_0^2}{K'^2} \sin^2 K'l \end{bmatrix} \begin{bmatrix} p_1 \\ v_1 \end{bmatrix} \quad (10.121)$$

where the transfer matrix satisfies the symmetry condition and the system as a whole is symmetrical even through all elements of the system are asymmetrical.

Example 10.10 Symmetry problem for the dynamic of a beam.

According to the convention for the positive direction, as shown in Figure 10.20, symmetrically define the elements in the state vector of the Euler–Bernoulli beam. The transfer matrix of the Euler–Bernoulli beam is

$$\begin{bmatrix} Y \\ \Theta_z \\ M_z \\ Q_y \end{bmatrix} = \begin{bmatrix} S(\lambda x) & -\frac{T(\lambda x)}{\lambda} & \frac{U(\lambda x)}{EI_z \lambda^2} & -\frac{V(\lambda x)}{EI_z \lambda^3} \\ \lambda V(\lambda x) & -S(\lambda x) & \frac{T(\lambda x)}{EI_z \lambda} & -\frac{U(\lambda x)}{EI_z \lambda^2} \\ EI_z \lambda^2 U(\lambda x) & -EI_z \lambda V(\lambda x) & S(\lambda x) & -\frac{T(\lambda x)}{\lambda} \\ EI_z \lambda^3 T(\lambda x) & -EI_z \lambda^2 U(\lambda x) & \lambda V(\lambda x) & -S(\lambda x) \end{bmatrix} \begin{bmatrix} Y \\ -\Theta_z \\ M_z \\ -Q_y \end{bmatrix}_I \quad (10.122)$$

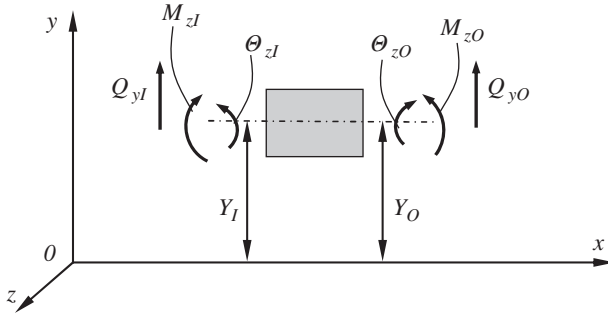


Figure 10.20 The direction of the state variable of a Euler–Bernoulli beam.

The transfer matrix is

$$\mathbf{U} = \begin{bmatrix} S(\lambda x) & -\frac{T(\lambda x)}{\lambda} & \frac{U(\lambda x)}{EI_z \lambda^2} & -\frac{V(\lambda x)}{EI_z \lambda^3} \\ \lambda V(\lambda x) & -S(\lambda x) & \frac{T(\lambda x)}{EI_z \lambda} & -\frac{U(\lambda x)}{EI_z \lambda^2} \\ EI_z \lambda^2 U(\lambda x) & -EI_z \lambda V(\lambda x) & S(\lambda x) & -\frac{T(\lambda x)}{\lambda} \\ EI_z \lambda^3 T(\lambda x) & -EI_z \lambda^2 U(\lambda x) & \lambda V(\lambda x) & -S(\lambda x) \end{bmatrix}$$

It is easy to prove that the transfer matrix satisfies the general symmetry criterion, that is

$$\mathbf{U} = \mathbf{U}^{-1}, \quad \mathbf{U}\mathbf{U} = \mathbf{I}$$

Nevertheless, the transfer matrix of a Timoshenko beam, that is, Equation (10.60), generally does not satisfy the symmetry criterion. Even the state vector is redefined according to the convention for the positive direction, as shown in Figure 10.20. The transfer matrix of the Timoshenko beam still does not satisfy the symmetry criterion. This is another example where the symmetry in geometry is not enough for the function symmetry.

The reason for the asymmetry is that accurate elastic theory is applied in the approximate theory of the Timoshenko beam. Therefore, in contrast to the Euler–Bernoulli beam, the Timoshenko beam is a multi-crunodes elastic system, and its characteristics are described by the wave numbers λ_1 and λ_2 , rather than the single wave number λ . It is impossible to completely describe multi-crunodes characteristics using a one-dimension system criterion.

In summary:

- 1) The symmetrical system is not only symmetrical in geometry, but also has the same transfer matrices observed from the two ends of the system.
- 2) The transfer matrix of a symmetrical system is involution and its characteristics are described by Equation (10.114) or Equation (10.116). The determinant of the transfer matrix of a symmetrical system is always +1 or –1, whether or not the direction of the state variable is defined symmetrically or standardized.
- 3) The uniform acoustics filter is only symmetrical for the quiescence medium, the uniqueness of the one-way transmission of the incoming flow breaks the symmetry in function; the uniform Euler–Bernoulli beam is symmetrical, but the uniform Timoshenko beam is not generally symmetrical.

10.9 Riccati Transfer Matrix Method for Multibody Systems

The difficulty of numerical computation appears occasionally when using the MSTMM to compute the responses and eigenvalues of a system. The Riccati MSTMM, which combines Riccati transformation and the MSTMM, is an effective method of overcoming numerical problems. While keeping the main advantage of the MSTMM, the Riccati MSTMM decreases accumulated error and improves computation stability and precision as well as efficiency. The computational time of the discrete time transfer matrix method for multibody systems (MSDTTMM) is proportional to the number of elements in general. To transfer in space, the dynamic equations of each element are linearized in a time domain by the MSDTTMM, and the space transmission and time iteration are considered in the analysis of its numerical characteristics. When the number of elements is large, we have to perform matrix multiplication many times to obtain the overall transfer matrix of the system, and the computational errors increase with the times of the matrix multiplication, sometimes leading to computational interruption [36, 38, 258]. The computational accuracy of the MSDTTMM can be improved by the predictor–corrector method, adopting the high-precision multistep method and the iterative operation method [67].

Generally speaking, when using the transfer matrix method (TMM) to compute the natural frequency of a system, there are two difficulties.

- 1) With increasing frequency and stiffness, the differences between element values in a transfer matrix become large. The numerical problems may be caused by multiplication of the transfer matrices such as the addition or subtraction of a large number and a small number, or the multiplication of two large numbers or two small numbers. This may result in a decrease in computational accuracy and even interruption of the computation. Pestel [36] and Yan Li [252] put forward a modified transfer matrix method and the Delta transfer matrix method to overcome the computational difficulty of transfer matrices. Loewy [259] tried to overcome computational difficulty by using the double precision number, but failed. Pei Ming Hu [260] improved computational accuracy by increasing the word length of a computer, but the cost of computational time increases.
- 2) When the overall transfer matrix of a system is obtained by multiplying the transfer matrices of elements, truncation errors will be caused by every multiplication. If the system is too large, with an increase in the number of elements, the accumulated errors caused by truncation errors can interrupt the computation. Horner [218] put forward the Riccati TMM. In the theory of differential equation, we can convert a two-point boundary value problem to an initial value problem to improve the numerical stability. The Riccati TMM takes the boundary conditions as the transfer initial value, resulting in the reduction of the matrix orders and the conversion of a two-point boundary value problem into an initial value problem. It maintains the advantages of traditional TMM, and at the same time improves numerical stability. Dokanish [223] put forward the *finite element transfer matrix method* to solve the planar frame vibration problem by combining the FEM and the TMM. Ohga [226] used a combined finite element transfer matrix method to analysis the transient response of plates. Huiyu Xue [227] and Yuhua Chen [261] put forward the *Riccati finite element transfer matrix method* by improving the finite element transfer matrix method.

In this section, the Riccati TMM and the Riccati MSDTTMM [79, 80], which were developed by the authors, are introduced. By using these methods the computational stability of the MSDTTMM can be improved. Taking the chain multibody system composed of many rigid bodies connected with rotary springs as an example, the dynamics of the chain multi-rigid-body

system with up to 100,000 degrees of freedom is solved successfully. This indicates that it is valid to solve the dynamic problem of super-large-scale multibody systems by the Riccati MSDTTMM.

10.9.1 Riccati Transfer Matrix Method for Multibody Systems

Usually, there is a relation between the state vector of the input and output ends of element i as follows

$$\mathbf{Z}_{O,i} = \mathbf{U}_i \mathbf{Z}_{I,i} + \mathbf{f}_i \quad (10.123)$$

where \mathbf{Z} is a state vector with m order, \mathbf{U} is a transfer matrix with $m \times m$ order and \mathbf{f} is load column matrix with m order.

The computing model used in the Riccati MSTMM is the same as in the MSTMM. If each state vector of the system contains m elements, namely the state variables (m is even), then Equation (10.123) can be partitioned as follows

$$\begin{bmatrix} \mathbf{Z}_a \\ \mathbf{Z}_b \end{bmatrix}_{O,i} = \begin{bmatrix} \mathbf{T}_{11} & \mathbf{T}_{12} \\ \mathbf{T}_{21} & \mathbf{T}_{22} \end{bmatrix}_i \begin{bmatrix} \mathbf{Z}_a \\ \mathbf{Z}_b \end{bmatrix}_{I,i} + \begin{bmatrix} \mathbf{f}_a \\ \mathbf{f}_b \end{bmatrix}_i \quad (10.124)$$

where \mathbf{Z}_a contains $m/2$ elements which are zeros in the state vector at the input end of the system, \mathbf{Z}_b contains the other unknown $m/2$ state variables of the system input state vector, \mathbf{T}_{11} , \mathbf{T}_{12} , \mathbf{T}_{21} and \mathbf{T}_{22} are the partitioned matrices by rearranging the elements of the transfer matrix \mathbf{U} , \mathbf{f}_a is the column matrix composed of column matrix $m/2$ elements of the load column matrix \mathbf{f} corresponding to \mathbf{Z}_a , while \mathbf{f}_b is the column matrix composed of $m/2$ elements of the load column matrix \mathbf{f} corresponding to \mathbf{Z}_b .

The following *Riccati transformation* is introduced

$$\mathbf{Z}_{aI,i} = \mathbf{S}_i \mathbf{Z}_{bI,i} + \mathbf{e}_i \quad (10.125)$$

The state variables \mathbf{Z}_a and \mathbf{Z}_b are related by Equation (10.125). \mathbf{S}_i is called the Riccati transfer matrix of junction $P_{I,i}$ which is the undetermined $(m/2) \times (m/2)$ order matrix, and \mathbf{e}_i is a column matrix related to load. Spreading Equation (10.124) gives

$$\mathbf{Z}_{aO,i} = \mathbf{T}_{11i} \mathbf{Z}_{aI,i} + \mathbf{T}_{12i} \mathbf{Z}_{bI,i} + \mathbf{f}_{ai} \quad (10.126)$$

$$\mathbf{Z}_{bO,i} = \mathbf{T}_{21i} \mathbf{Z}_{aI,i} + \mathbf{T}_{22i} \mathbf{Z}_{bI,i} + \mathbf{f}_{bi} \quad (10.127)$$

Substituting Equation (10.125) into Equation (10.127) gives

$$\mathbf{Z}_{bI,i} = (\mathbf{T}_{21i} \mathbf{S}_i + \mathbf{T}_{22i})^{-1} \mathbf{Z}_{bO,i} - (\mathbf{T}_{21i} \mathbf{S}_i + \mathbf{T}_{22i})^{-1} (\mathbf{T}_{21i} \mathbf{e}_i + \mathbf{f}_{bi}) \quad (10.128)$$

Using Equations (10.125) and (10.128) to cancel out the $\mathbf{Z}_{aI,i}$ and $\mathbf{Z}_{bI,i}$ in Equation (10.126), one obtains

$$\begin{aligned} \mathbf{Z}_{aO,i} = & (\mathbf{T}_{11i} \mathbf{S}_i + \mathbf{T}_{12i}) (\mathbf{T}_{21i} \mathbf{S}_i + \mathbf{T}_{22i})^{-1} \mathbf{Z}_{bO,i} \\ & + \mathbf{T}_{11i} \mathbf{e}_i + \mathbf{f}_{ai} - (\mathbf{T}_{11i} \mathbf{S}_i + \mathbf{T}_{12i}) (\mathbf{T}_{21i} \mathbf{S}_i + \mathbf{T}_{22i})^{-1} (\mathbf{T}_{21i} \mathbf{e}_i + \mathbf{f}_{bi}) \end{aligned} \quad (10.129)$$

Equation (10.129) can be written as follows

$$\mathbf{Z}_{aO,i} = \mathbf{S}_{i+1} \mathbf{Z}_{bO,i} + \mathbf{e}_{i+1} \quad (10.130)$$

where

$$\mathbf{S}_{i+1} = (\mathbf{T}_{11i}\mathbf{S}_i + \mathbf{T}_{12i})(\mathbf{T}_{21i}\mathbf{S}_i + \mathbf{T}_{22i})^{-1} \quad (10.131)$$

$$\mathbf{e}_{i+1} = \mathbf{T}_{11i}\mathbf{e}_i + \mathbf{f}_{ai} - \mathbf{S}_{i+1}(\mathbf{T}_{21i}\mathbf{e}_i + \mathbf{f}_{bi}) \quad (10.132)$$

Equations (10.131) and (10.132) are general recurrence equations of \mathbf{S}_i and \mathbf{e}_i . It can be shown that $\mathbf{Z}_{al,1} = \mathbf{0}$, $\mathbf{Z}_{bl,1} \neq \mathbf{0}$ from the boundary conditions of the system input (suppose the number of the first element of the system is 1, then the system input end is $P_{l,1}$). This is substituted into Equation (10.125), making the initial conditions of Equations (10.131) and (10.132)

$$\mathbf{S}_1 = \mathbf{0}, \quad \mathbf{e}_1 = \mathbf{0} \quad (10.133)$$

For chain MS, using Equations (10.133), (10.131) and (10.132), \mathbf{S}_i and \mathbf{e}_i of the whole system can be computed, including \mathbf{S}_{n+1} and \mathbf{e}_{n+1} of the system output end. For the output end $P_{O,0}$ of the system composed of n elements, using Equation (10.130) we obtain

$$\mathbf{Z}_{aO,0} = \mathbf{S}_{n+1}\mathbf{Z}_{bO,0} + \mathbf{e}_{n+1} \quad (10.134)$$

Obviously, $\mathbf{Z}_{aO,0}$ and $\mathbf{Z}_{bO,0}$ contain all m elements of a state vector at the output end of the system, where $m/2$ elements are known and equal to zero. For the steady-state vibration and static load, Equation (10.134) is a nonhomogeneous linear equation which contains $m/2$ unknown quantities. Substituting the boundary conditions of the output end of the system into Equation (10.134), the unknown elements in the state vector of the output end of the system can be solved.

For the eigenvalue problem, Equation (10.134) is a system of homogeneous equations which are composed of $m/2$ equations. Substituting the boundary conditions of the output end of the system into Equation (10.134), if the system has a nontrivial solution, the determinant of the homogeneous equations must be zero. Consequently, the frequency equation of the system can be derived and the eigenfrequencies are easily evaluated.

The state vector of the output end of the system can be obtained by solving Equation (10.134) with a given eigenfrequency. Either for a steady-state vibration problem or a static load problem, as well as for an eigenvalue problem, the state vector $\mathbf{Z}_{O,0}$ of the output end, namely $\mathbf{Z}_{aO,0}$ and $\mathbf{Z}_{bO,0}$, can be obtained by solving Equation (10.134). Hence, it can be seen that Equation (10.134) is similar to the overall transfer equation in the general MSTMM.

Combining Equations (10.128) and (10.125)

$$\begin{cases} \mathbf{Z}_{bl,i} = (\mathbf{T}_{21i}\mathbf{S}_i + \mathbf{T}_{22i})^{-1}\mathbf{Z}_{bO,i} - (\mathbf{T}_{21i}\mathbf{S}_i + \mathbf{T}_{22i})^{-1}(\mathbf{T}_{21i}\mathbf{e}_i + \mathbf{f}_{bi}) \\ \mathbf{Z}_{al,i} = \mathbf{S}_i\mathbf{Z}_{bl,i} + \mathbf{e}_i \end{cases} \quad (10.135)$$

After the state vector of the output end of system is obtained, the state vector of all junction points of the system can be computed successively according to Equation (10.135). In fact, the transfer in both forward and backward directions is equivalent to the Gauss elimination method.

10.9.2 Algorithm of the Riccati Transfer Matrix Method for Multibody Systems

- 1) Develop the transfer equation and the transfer matrix of every element of the system.
- 2) According to the boundary conditions of the input end of the system, that is, $\mathbf{Z}_{al,1} = \mathbf{0}$ and $\mathbf{Z}_{bl,1} = \mathbf{0}$, obtain the initial condition $\mathbf{S}_1 = \mathbf{e}_1 = \mathbf{0}$.
- 3) Compute \mathbf{S}_i and \mathbf{e}_i of each connection point individually from the input end to the output end by using Equations (10.131) and (10.132), and save all intermediate values of \mathbf{S}_i and \mathbf{e}_i .
- 4) For the output end $P_{O,0}$ of system, use Equation (10.134).

Table 10.3 The comparison of the Riccati MSTMM and the MSTMM

	Properties	Riccati MSTMM	MSTMM
Computational time	Eigenvalue problem	$n^3/2$	n^3
	Static-state or steady-state response	$n^3/2 + n^2$	$n^3 + n^2$
Storage requirements	Eigenvalue problem	$n^2/2$	n^2
	Static-state or steady-state response	$n^2/2 + n$	$n^2 + n$

- 5) Using the boundary conditions in the output end of the system, determine the condition which \mathbf{S}_{n+1} should satisfy. For the eigenvalue problem, Equation (10.134) is homogeneous linear equations. After the characteristic equation and the eigenfrequencies have been derived, solve Equation (10.134); for the steady-state vibration and static load problem, Equation (10.134) is non-homogeneous and can be solved directly.
- 6) Determine the state vector of every joint by inverse recursion individually from the output end to the input end of the system using Equation (10.135), after the state vector of the output end is obtained.

10.9.3 Efficiency of the Riccati Transfer Matrix Method for Multibody Systems

The comparison of the Riccati MSTMM and the MSTMM in computational time and storage requirements is shown in Table 10.3, which shows that the computational speed of the Riccati MSTMM is twice as fast as the MSTMM while the storage requirement of the Riccati MSTMM is only half that of the MSTMM.

In the MSTMM the overall transfer matrix of the system is determined by successively multiplying the matrix \mathbf{U} with m order; in the Riccati MSTMM \mathbf{S}_{n+1} is determined by the recursion of matrix \mathbf{S}_i with $m/2$ order.

The two-point boundary value of differential equations becomes an initial value problem in the theory of differential equations by Riccati transformation, and the numerical stability is improved.

The computational stability of the MSTMM is increased by introducing Riccati transformation in the MSTMM. This effect becomes more obvious with the increase in modal order in the computation of the eigenvalue problem.

10.9.4 Example of the Riccati Transfer Matrix Method for Multibody Systems

Example 10.11 Solve the eigenfrequencies, eigenvectors and steady-state response of the system with two degrees of freedom shown in Figure 10.21 using the Riccati MSTMM, where $\Omega = \sqrt{3K/m}$.

Solution

The state vectors $\mathbf{Z}_{1,0}$, $\mathbf{Z}_{2,1}$, $\mathbf{Z}_{2,3}$, $\mathbf{Z}_{4,3}$, $\mathbf{Z}_{4,5}$ and $\mathbf{Z}_{5,0}$ are defined as $\mathbf{Z} = [\mathbf{X}, \mathbf{Q}_x]^T$ and the boundary conditions are

$$\mathbf{Z}_{1,0} = [0, \mathbf{Q}_x]_{1,0}^T, \quad \mathbf{Z}_{5,0} = [0, \mathbf{Q}_x]_{5,0}^T \quad (\text{a})$$

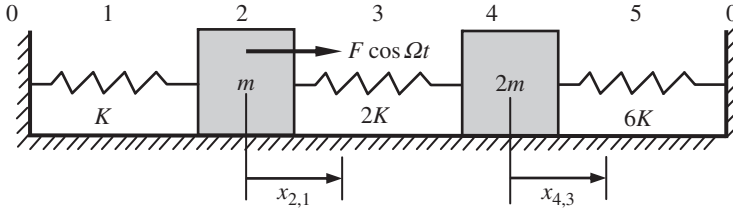


Figure 10.21 A spring-mass system with two degrees of freedom.

The transfer equations of every element can be written in the form of Equation (10.124) as follows

$$\begin{aligned}
 \begin{bmatrix} X \\ Q_x \end{bmatrix}_{2,1} &= \begin{bmatrix} 1 & -1/K \\ 0 & 1 \end{bmatrix} \begin{bmatrix} 0 \\ Q_x \end{bmatrix}_{1,0} + \begin{bmatrix} 0 \\ 0 \end{bmatrix}, & \begin{bmatrix} X \\ Q_x \end{bmatrix}_{2,3} &= \begin{bmatrix} 1 & 0 \\ m\omega^2 & 1 \end{bmatrix} \begin{bmatrix} X \\ Q_x \end{bmatrix}_{2,1} + \begin{bmatrix} 0 \\ F \end{bmatrix} \\
 \begin{bmatrix} X \\ Q_x \end{bmatrix}_{4,3} &= \begin{bmatrix} 1 & -1/(2K) \\ 0 & 1 \end{bmatrix} \begin{bmatrix} X \\ Q_x \end{bmatrix}_{2,3} + \begin{bmatrix} 0 \\ 0 \end{bmatrix}, & \begin{bmatrix} X \\ Q_x \end{bmatrix}_{4,5} &= \begin{bmatrix} 1 & 0 \\ 2m\omega^2 & 1 \end{bmatrix} \begin{bmatrix} X \\ Q_x \end{bmatrix}_{4,3} + \begin{bmatrix} 0 \\ 0 \end{bmatrix} \\
 \begin{bmatrix} 0 \\ Q_x \end{bmatrix}_{5,0} &= \begin{bmatrix} 1 & -1/(6K) \\ 0 & 1 \end{bmatrix} \begin{bmatrix} X \\ Q_x \end{bmatrix}_{4,5} + \begin{bmatrix} 0 \\ 0 \end{bmatrix}
 \end{aligned} \tag{b}$$

The transfer equations of the five elements can be partitioned according to Equation (10.124), and the partitioned matrices of the transfer matrices of every element are shown in Table 10.4.

Using Equations (10.133), (10.131) and (10.132), we obtain

$$\begin{aligned}
 S_1 &= 0, & S_2 &= -\frac{1}{K}, & S_3 &= \frac{1}{m\omega^2 - K}, & S_4 &= \frac{3K - m\omega^2}{2K(m\omega^2 - K)} \\
 S_5 &= -\frac{3K - m\omega^2}{2(m^2\omega^4 - 4Km\omega^2 + K^2)}, & S_6 &= -\frac{m^2\omega^4 - 7Km\omega^2 + 10K^2}{6K(m^2\omega^4 - 4Km\omega^2 + K^2)}
 \end{aligned} \tag{c}$$

From the boundary condition and Equation (10.134), namely

$$Z_{a0,0} = S_{n+1} Z_{b0,0} \quad (n = 5)$$

we obtain

$$0 = X_{5,0} = S_6 Q_{x5,0} \tag{d}$$

Table 10.4 The partitioned matrices of the transfer matrices of every element

i	1	2	3	4	5
$T_{11,i}$	1	1	1	1	1
$T_{12,i}$	$-\frac{1}{K}$	0	$-\frac{1}{2K}$	0	$-\frac{1}{6K}$
$T_{21,i}$	0	$m\omega^2$	0	$2m\omega^2$	0
$T_{22,i}$	1	1	1	1	1
$f_{a,i}$	0	0	0	0	0
$f_{b,i}$	0	F	0	0	0

Therefore, the characteristic equation of the system is

$$S_6 = -\frac{m^2\omega^4 - 7Km\omega^2 + 10K^2}{6K(m^2\omega^4 - 4Km\omega^2 + K^2)} = 0 \quad (e)$$

and the eigenfrequencies can be obtained by solving Equation (e)

$$\omega_1 = \sqrt{\frac{2K}{m}}, \quad \omega_2 = \sqrt{\frac{5K}{m}} \quad (f)$$

For $\omega_1 = \sqrt{\frac{2K}{m}}$ or $\omega_2 = \sqrt{\frac{5K}{m}}$, let $Q_{x1,0} = 1$, and we obtain the first- and second-order eigenvectors as follows

$$\begin{bmatrix} X_{2,1}^1 \\ X_{4,3}^1 \end{bmatrix} = \frac{1}{K} \begin{bmatrix} -1 \\ -1/2 \end{bmatrix}, \quad \begin{bmatrix} X_{2,1}^2 \\ X_{4,3}^2 \end{bmatrix} = \frac{1}{K} \begin{bmatrix} -1 \\ 1 \end{bmatrix} \quad (g)$$

To solve the steady-state response of the system, let $\omega = \Omega = \sqrt{3K/m}$ in the above formulas, using Equations (10.133), (10.131) and (10.132) to obtain

$$\begin{cases} S_1 = 0, & S_2 = -\frac{1}{K}, & S_3 = \frac{1}{2K} \\ S_4 = 0, & S_5 = 0, & S_6 = -\frac{1}{6K} \end{cases}, \quad \begin{cases} e_1 = 0, & e_2 = 0, & e_3 = -\frac{F}{2K}, \\ e_4 = -\frac{F}{2K}, & e_5 = -\frac{F}{2K}, & e_6 = -\frac{F}{2K} \end{cases} \quad (h)$$

From the boundary conditions and Equation (10.134), we obtain

$$0 = X_{5,0} = S_6 Q_{x5,0} + e_6 = -\frac{1}{6K} Q_{x5,0} - \frac{F}{2K} \quad (i)$$

that is

$$Q_{x5,0} = -3F \quad (j)$$

According to Equation (10.135), we can compute successively as follows

$$\begin{aligned} \begin{bmatrix} X_{5,0} \\ Q_{x5,0} \end{bmatrix} &= \begin{bmatrix} 0 \\ -3F \end{bmatrix}, \quad \begin{bmatrix} X_{4,5} \\ Q_{x4,5} \end{bmatrix} = \begin{bmatrix} -\frac{F}{2K} \\ -3F \end{bmatrix}, \quad \begin{bmatrix} X_{4,3} \\ Q_{x4,3} \end{bmatrix} = \begin{bmatrix} -\frac{F}{2K} \\ 0 \end{bmatrix} \\ \begin{bmatrix} X_{2,3} \\ Q_{x2,3} \end{bmatrix} &= \begin{bmatrix} -\frac{F}{2K} \\ 0 \end{bmatrix}, \quad \begin{bmatrix} X_{2,1} \\ Q_{x2,1} \end{bmatrix} = \begin{bmatrix} -\frac{F}{2K} \\ \frac{F}{2} \end{bmatrix}, \quad \begin{bmatrix} X_{1,0} \\ Q_{x1,0} \end{bmatrix} = \begin{bmatrix} 0 \\ \frac{F}{2} \end{bmatrix} \end{aligned} \quad (k)$$

The steady-state response of the system is

$$\begin{aligned} z_{1,0} &= \begin{bmatrix} 0 \\ \frac{F}{2} \end{bmatrix} \cos \Omega t, \quad z_{2,1} = \begin{bmatrix} -\frac{F}{2K} \\ \frac{F}{2} \end{bmatrix} \cos \Omega t, \quad z_{2,3} = \begin{bmatrix} -\frac{F}{2K} \\ 0 \end{bmatrix} \cos \Omega t \\ z_{4,3} &= \begin{bmatrix} -\frac{F}{2K} \\ 0 \end{bmatrix} \cos \Omega t, \quad z_{4,5} = \begin{bmatrix} -\frac{F}{2K} \\ -3F \end{bmatrix} \cos \Omega t, \quad z_{5,0} = \begin{bmatrix} 0 \\ -3F \end{bmatrix} \cos t \end{aligned} \quad (l)$$

It can be seen from this example that both the matrix order involved and the memory demanded of the MSTMM are decreased by 50% to solve the eigenfrequencies, eigenvectors and the steady-state responses of the system when using the Riccati MSTMM. Hence, the computational efficiency and accuracy of the MSTMM are increased greatly. This is very important in research into complex MRFS dynamics, especially for computing the high-order eigenfrequencies of huge MRFSs.

10.9.5 Recursion Formula of the Riccati Distrete Time Transfer Matrix Method for Multibody Systems

The overall transfer equation of the chain system is

$$\mathbf{z}_O = \mathbf{U}_{\text{all}} \mathbf{z}_I \quad (10.136)$$

The overall transfer matrix \mathbf{U}_{all} is obtained by multiplying the transfer matrices of elements \mathbf{U}_i in turn as follows

$$\mathbf{U}_{\text{all}} = \prod_{i=1}^n \mathbf{U}_i \quad (10.137)$$

where \mathbf{z}_I and \mathbf{z}_O are the boundary state vectors of the chain system, respectively, and n is the number of all elements in the system.

With the increase in the element number n in the system, the accumulated error increases because of the successive multiplication of the transfer matrix \mathbf{U}_i in Equation (10.137), and this may cause the computation difficulty. The numerical stability problem [38] caused by the accumulated error can be overcome effectively by the Riccati TMM for multibody systems. Generally speaking, in the boundary state vectors \mathbf{z}_I and \mathbf{z}_O in Equation (10.136), half of the elements are known state variables and the other half are unknown state variables. The state variables in the state vector \mathbf{z} can be rearranged again and partitioned as follows

$$\mathbf{z} = [\mathbf{z}_a^T, \mathbf{z}_b^T, 1]^T \quad (10.138)$$

where \mathbf{z}_a is composed of the known state variables in the state vector \mathbf{z}_I of the system input, while \mathbf{z}_b is composed of the unknown state vectors.

According to Equation (10.138), the transfer equation of element i can be written as

$$\begin{bmatrix} \mathbf{z}_a \\ \mathbf{z}_b \end{bmatrix}_{O,i} = \begin{bmatrix} \mathbf{T}_{11} & \mathbf{T}_{12} \\ \mathbf{T}_{21} & \mathbf{T}_{22} \end{bmatrix}_i \begin{bmatrix} \mathbf{z}_a \\ \mathbf{z}_b \end{bmatrix}_{I,i} + \begin{bmatrix} \mathbf{f}_a \\ \mathbf{f}_b \end{bmatrix}_i \quad (10.139)$$

where \mathbf{T}_{11} , \mathbf{T}_{12} , \mathbf{T}_{21} and \mathbf{T}_{22} are the submatrices of the transfer matrix \mathbf{U} after rearrangement and \mathbf{f}_a and \mathbf{f}_b are rearranged by the elements of the column corresponding to the external force item.

Introducing the Riccati transform [218] we get

$$\mathbf{z}_{aI,i} = \mathbf{S}_i \mathbf{z}_{bI,i} + \mathbf{e}_i \quad (10.140)$$

Substituting Equation (10.140) into Equation (10.139) gives

$$\mathbf{z}_{bO,i} = (\mathbf{T}_{21i} \mathbf{S}_i + \mathbf{T}_{22i}) \mathbf{z}_{bI,i} + \mathbf{T}_{21i} \mathbf{e}_i + \mathbf{f}_{bi} \quad (10.141)$$

then

$$\mathbf{z}_{bI,i} = (\mathbf{T}_{21i} \mathbf{S}_i + \mathbf{T}_{22i})^{-1} \mathbf{z}_{bO,i} - (\mathbf{T}_{21i} \mathbf{S}_i + \mathbf{T}_{22i})^{-1} (\mathbf{T}_{21i} \mathbf{e}_i + \mathbf{f}_{bi}) \quad (10.142)$$

Let

$$\mathbf{P}_i = (\mathbf{T}_{21i} \mathbf{S}_i + \mathbf{T}_{22i})^{-1} \quad (10.143)$$

$$\mathbf{Q}_i = -\mathbf{P}_i (\mathbf{T}_{21i} \mathbf{e}_i + \mathbf{f}_{bi}) \quad (10.144)$$

Equation (10.142) can be written as

$$\mathbf{z}_{bI,i} = \mathbf{P}_i \mathbf{z}_{bO,i} + \mathbf{Q}_i \quad (10.145)$$

Substituting Equations (10.140) and (10.145) into Equation (10.139) yields

$$\mathbf{z}_{aO,i} = \mathbf{T}_{11i} [\mathbf{S}_i (\mathbf{P}_i \mathbf{z}_{bO,i} + \mathbf{Q}_i) + \mathbf{e}_i] + \mathbf{T}_{12i} (\mathbf{P}_i \mathbf{z}_{bO,i} + \mathbf{Q}_i) + \mathbf{f}_{ai} \quad (10.146)$$

Substituting Equation (10.144) into Equation (10.146) yields

$$\mathbf{z}_{aO,i} = (\mathbf{T}_{11i} \mathbf{S}_i + \mathbf{T}_{12i}) \mathbf{P}_i \mathbf{z}_{bO,i} + \mathbf{T}_{11i} \mathbf{e}_i + \mathbf{f}_{ai} - (\mathbf{T}_{11i} \mathbf{S}_i + \mathbf{T}_{12i}) \mathbf{P}_i (\mathbf{T}_{21i} \mathbf{e}_i + \mathbf{f}_{bi}) \quad (10.147)$$

Comparing Equations (10.140) and (10.147), the recursion formulas [262, 263] can be obtained as follows

$$\mathbf{S}_{i+1} = (\mathbf{T}_{11i} \mathbf{S}_i + \mathbf{T}_{12i}) \mathbf{P}_i \quad (10.148)$$

$$\mathbf{e}_{i+1} = \mathbf{T}_{11i} \mathbf{e}_i + \mathbf{f}_{ai} - \mathbf{S}_{i+1} (\mathbf{T}_{21i} \mathbf{e}_i + \mathbf{f}_{bi}) \quad (10.149)$$

Equation (10.95) can be written as

$$\mathbf{z}_{aO,i} = \mathbf{S}_{i+1} \mathbf{z}_{bO,i} + \mathbf{e}_{i+1} \quad (10.150)$$

To reduce the computational time, comparing Equations (10.149) and (10.144), we define the variables again as follows

$$\mathbf{Q}_i = -(\mathbf{T}_{21i} \mathbf{e}_i + \mathbf{f}_{bi}) \quad (10.151)$$

Then Equations (10.145) and (10.149) can be written as

$$\mathbf{z}_{bI,i} = \mathbf{P}_i \mathbf{z}_{bO,i} + \mathbf{P}_i \mathbf{Q}_i \quad (10.152)$$

$$\mathbf{e}_{i+1} = \mathbf{T}_{11i} \mathbf{e}_i + \mathbf{f}_{ai} + \mathbf{S}_{i+1} \mathbf{Q}_i \quad (10.153)$$

Compared with Equations (10.144), (10.145) and (10.149), if we take Equations (10.151), (10.152) and (10.153) as the recursion formulas, we can save one matrix multiplication and one matrix addition. Equations (10.148) and (10.153) are the Riccati transfer formulas used in the Riccati MSDTTMM.

10.9.6 Algorithm Analysis of the Riccati Distrete Time Transfer Matrix Method for Multibody Systems

Before the recursion computation using Equations (10.148) and (10.153), \mathbf{S} and \mathbf{e} must be given on the boundary. According to Equation (10.140) and applying the boundary conditions of the input end of the system, we obtain $\mathbf{z}_{aI,1} = \mathbf{0}$, $\mathbf{z}_{bI,1} \neq \mathbf{0}$ (suppose that the first element of the system is numbered 1, and the input end of the system is denoted by $P_{I,1}$). It follows that

$$\mathbf{S}_1 = \mathbf{0}, \quad \mathbf{e}_1 = \mathbf{0} \quad (10.154)$$

From Equation (10.154), using Equations (10.148) and (10.153) repeatedly, we can get \mathbf{S}_i and \mathbf{e}_i for any connected point. Finally, \mathbf{S}_{n+1} and \mathbf{e}_{n+1} with respect to the output end of system are obtained. Substituting this into Equation (10.50) we obtain

$$\mathbf{z}_{aO,n} = \mathbf{S}_{n+1} \mathbf{z}_{bO,n} + \mathbf{e}_{n+1} \quad (10.155)$$

Obviously, Equation (10.155) is the algebra equation composed of the state vectors of the output of the system. Generally, in the boundary state vector \mathbf{z}_O half the elements are known variables and the others are unknown variables. Solving the algebra equation in Equation (10.155), we can get the unknown variables in the state vector of \mathbf{z}_O , the output of the system. Then, using

Equations (10.152) and (10.140), we can obtain \mathbf{z}_b and \mathbf{z}_a of any connected point. Under the following two conditions the computation steps can be reduced further.

- 1) If the boundary conditions of the output of system are $\mathbf{z}_{bO,n} = \mathbf{0}$, Equation (10.155) can be written simply as

$$\mathbf{z}_{aO,n} = \mathbf{e}_{n+1} \quad (10.156)$$

that is, $\mathbf{z}_{aO,n}$ or $\mathbf{z}_{bO,n}$ can be computed directly and there is no need to solve Equation (10.155).

- 2) For the system with $\mathbf{z}_b = [x, y, \theta_z]^T$, once the motion of the system is solved, the system dynamics analysis can proceed directly and it is not necessary to solve the internal force and internal moment by Equation (10.140).

10.9.7 Computational Steps of the Riccati Discrete Time Transfer Matrix Method for Multibody Systems

When deducing the transfer matrix of an element, the linearization method and many numerical integral approximation methods will cause some errors. If the velocity and acceleration are approximated by the Newmark- β method, there is a second-order truncation error $o(\Delta T^2)$ in the adopted numerical method. The round-off error, caused by the word length of the computer, is a function of this and its control is related to the computer system adopted. To control the round-off errors, correction methods should be applied in the algorithm for the dynamic analysis.

The computational steps of the Riccati MSDTTMM are as follows:

- 1) Let time subscript $i = 1$.
- 2) Let iteration subscript $k = 1$.
- 3) According to the initial condition, compute the transfer matrices of all elements at time t_i .
- 4) According to Equation (10.154), using Equations (10.148), (10.153), (10.143) and (10.151), compute \mathbf{S}_i , \mathbf{e}_i , \mathbf{P}_i and \mathbf{Q}_i in every joint point.
- 5) According to the boundary condition of the output end of the system, compute the unknown elements of the system output state vector using Equation (10.155).
- 6) Using Equations (10.152) and (10.140), compute the dynamic responses of the system at time t_i including $x(t_{i,k})$, $y(t_{i,k})$ and $\theta_z(t_{i,k})$, etc.
- 7) If $\theta_z(t_{i,k}) - \theta_z(t_{i,k-1})$ does not meet the required precision, substitute $\theta_z(t_{i,k})$ into the following equation for modifying g_1 and g_2 ,

$$g_1 = \cos \theta_z(t_{i,k}), g_2 = \sin \theta_z(t_{i,k}) \quad (10.157)$$

Let $k = k + 1$ and return to step (3) until $\theta_z(t_{i,k}) - \theta_z(t_{i,k-1})$ satisfies the required precision.

- 8) According to the geometry relation, correct $x(t_i)$ and $y(t_i)$ using $\theta_z(t_i)$. Let $i = i + 1$, and using the dynamic responses of the system as the initial values, return to step (2) until the time required for complete analysis.

Here, we only deal with trigonometric functions at the current time expressed by the function of the values in the previous time steps. For example, using the computed values of $x(t_i)$, $y(t_i)$ and $\theta_z(t_i)$ in each connected point at time t_i , by a similar equation we can obtain $\dot{x}(t_i)$, $\dot{y}(t_i)$ and $\dot{\theta}_z(t_i)$ approximately, then substitute them into the dynamic equations of the element to correct $\ddot{x}(t_i)$, $\ddot{y}(t_i)$ and $\ddot{\theta}_z(t_i)$, respectively.

10.9.8 Example for Super-large Multibody System Dynamics

Example 10.12 In Example 9.5, as shown in Figure 9.20, the beam moving in a plane can be regarded as a chain multibody system composed of many rigid bodies connected with rotating springs. Solve the motion of the system and obtain the driving force needed for this motion.

Solution

The beam is divided into 40 rigid segments and the time step is $\Delta T = 2 \times 10^{-3}$ s. The dynamics of the system are solved by the Riccati discrete time TMM for multibody systems, the discrete time transfer method for multibody systems and the Newton–Euler method. The results of the driving moment and transverse deformation of the beam at the free end computed by the three methods are presented in Figures 10.22 and 10.23. These figures shown that the results obtained by these methods are nearly the same.

In this example, with the increase in the number of rigid segments, the physical model of a multi-rigid-body system is closer to the original flexible system, and it can validate the effective of any kind of dynamic method for a super-large multibody system. This also indicates that the Riccati MSDTTMM still works even when the number of rigid segments is more than 100,000 while the time step is $\Delta T = 5 \times 10^{-4}$ s. When the number of rigid segments is 40 and the time step is $\Delta T = 1 \times 10^{-4}$ s, the Riccati MSDTTMM can ensure the right computation results.

Using the Gauss–Jordan elimination method with complete pivoting to solve the inverse matrices [264], the computational times on a computer with an AMD-1.2GHz CPU are compared (Table 10.5). One can see clearly that the Riccati MSDTTMM is better than the other two methods in both computational speed and computational stability. As the computational stability is improved, the stability of the recursion computation is improved. If the number of elements in multibody system is large, using the intermediate variables in the improved Riccati transformation for the computation can obviously reduce the computational time. When the number of rigid segments is larger than 1000, computational time can be reduced by 20% using the proposed method.

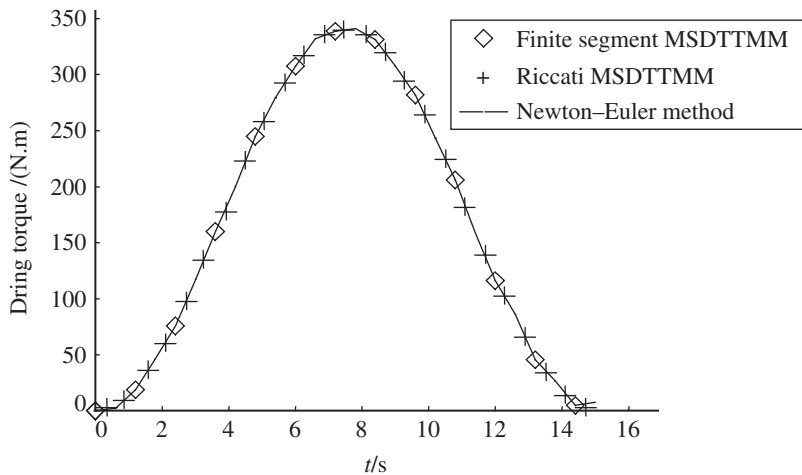


Figure 10.22 Time history of a driving torque.

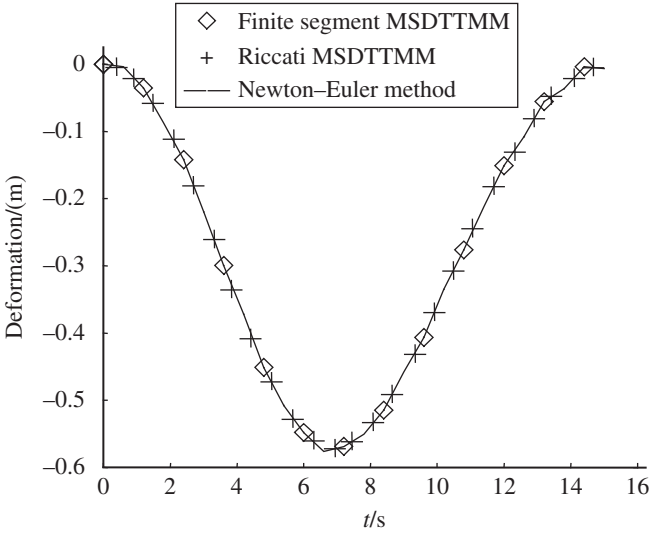


Figure 10.23 Time history of the transverse deformation of a beam at the free end.

Table 10.5 Comparison of the computational time of different segments and different time steps

$\Delta T/s$	Number of segments	Computational time		Relative saved time $\frac{T_3 - T_2}{T_2} \times 100\%$
		Original Riccati transformation T_2/s	Improved Riccati transformation T_3/s	
0.002	40	2.663	2.453	-7.89
0.002	60	3.945	3.726	-5.55
0.002	80	5.358	5.118	-4.48
0.002	100	6.960	6.429	-7.63
0.001	40	5.107	4.977	-2.55
0.00075	40	6.790	6.599	-2.81
0.0005	40	10.115	9.874	-2.38
0.00025	40	20.249	19.659	-2.91
0.0001	40	50.282	48.630	-3.29
0.0005	1000	596.108	468.694	-21.37
0.0005	10000	5978.346	4866.348	-18.60
0.0005	100000	60914.521	49420.204	-18.87

10.9.9 The Characteristics of the Riccati Distrete Time Transfer Matrix Method for Multibody Systems

Comparing the MSDTTMM and the ordinary multibody system dynamic methods, the Riccati MSDTTMM has the following characteristics

- 1) For a super-large system with more than 100,000 degrees of freedom, the order of the system matrix using ordinary dynamic methods for a multibody system is more than 200,000, the

order of the system matrix using MS-DT-TMM is six and the order of the system matrix using the Riccati MSDTTMM is only three. The order of the matrix is reduced greatly, and computational time is saved along with computational workload.

- 2) The computation results indicate that the difficulty of the transfer in space can be overcome by using the Riccati MSDTTMM. Even when the general MSDTTMM fails due to a large number of elements, the Riccati MSDTTMM still works and could give the right results.
- 3) We can choose more suitable intermediate Riccati variables by improving the Riccati transformation to save computational time under the conditions that the required memory space does not increase and computational accuracy is not decreased.

10.10 Stability of the Transfer Matrix Method for Multibody Systems

10.10.1 Error Analysis of the Transfer Matrix Method for Multibody Systems

For numerical computation, the computational errors in the process of integration or iteration come from two aspects: the truncation error and the round-off error. The truncation error is caused by the method itself, and it can be estimated in general, but the round-off error is caused and accumulated with complexity. When the integration step length is larger, the truncation error is relative bigger, and when the integration step length is smaller, the round-off error becomes bigger relatively because of error accumulation. For the time-varying system, in the step-by-step computation if there is an error which includes the truncation error and round-off error in one step, this can cause an error in all steps in the following computation. Sometimes the computational error is increased sharply with an increase in the time step, and this causes the roots of the equation to disappear, resulting in computational instability. In the computation process of the dynamic problems of the time-varying system, we therefore must forecast the influence of various errors reasonably to ensure computational stability and precision.

In the MSDTTMM, the main factor that affects computational precision is the truncation error. When using the MSDTTMM for dynamic analysis, the high-order terms of the angular coordinate differences and angular velocity differences between the adjacent time instants are neglected in the linearization of dynamic equations and the building of the transfer matrices. The high-order terms of the angle coordinates and angular velocities are taken as the linear functions of the first-order term, and the trigonometric functions at the current time step are linearized by second-order Taylor expansion. These can bring the truncation error and round-off error for the angle coordinates and the related high-order items.

The MSDTTMM utilizes the concept of step-by-step time integration when taking velocity and acceleration as the linear functions of the displacement. The rapidity of convergence and the computational stability are directly related to the step-by-step time integration method. For the various step-by-step time integration methods of linear acceleration discussed in section 7.3, the $O(\Delta t^2)$ in the computation process is omitted, resulting in the high-order round-off error. The acceleration has second-order precision $O(\Delta t^2)$, the velocity has third-order precision $O(\Delta t^3)$, and the displacement has fourth-order precision $O(\Delta t^4)$.

10.10.2 Methods to Improve Computational Accuracy and Stability

10.10.2.1 Choice of Time Step

Because of the sensitivity of the time step in the numerical integration process when choosing a difference scheme, a reasonable time step should be chosen to ensure computational stability and avoid a larger accumulated error caused by a large number of computational steps.

10.10.2.2 The Step-by-step Integration Method and its Parameters

For the For–Euler method, the Newmark- β method and the Wilson- θ method, the linearization coefficients are computed only by the known quantities, and the initial conditions are determined easily. The formulas of the For–Euler method are simpler, but computational accuracy is lower. The linearization coefficients are computed by the three previous time steps in the Houbolt method, consequently computational accuracy is higher. For some problems, the step-by-step integration method and its parameters should be chosen according to the required computational accuracy.

10.10.2.3 Iterative Computation Loop Algorithm

The iteration algorithm of angular coordinates can be designed to improve the computational accuracy and stability. The iterative computational loop for dynamic analysis of a multibody system by the MSDTTMM is described as follows.

- 1) Decide the system parameters, the initial condition, the parameters of the step-by-step time integral method and other computation parameters.
- 2) Set the serial number of the simulation step $i = 1$ (i refers to the serial number of discrete time).
- 3) According to the motion parameters and their first- and second-order derivatives with respect to time at time instant t_{i-1} , compute the coefficients of the step-by-step time integration method and set the initial values at time instant t_i .
- 4) Set the loop variable $k = 1$.
- 5) Compute the transfer matrices of each element at time instant t_i .
- 6) Solve the overall transfer equations and element transfer equations to obtain the state vectors of each connection point at time t_i .
- 7) Determine the convergence criterion. If the sum of the square of the difference between the motion parameters of the k th and $(k - 1)$ th iteration is bigger than the given admissible value of precision or the number of iteration loops is smaller than the given maximal iteration number, let $k = k + 1$, and return to (5). Otherwise go to the next step.
- 8) Adopting the step-by-step time integration method, obtain the current velocity and acceleration of each connection point.
- 9) When the simulation time is reached, stop the program. Otherwise let $i = i + 1$ and return to (3).

10.10.2.4 Riccati MSDTTMM

Adding Riccati transformation into the MSDTTMM, the method of the Riccati MSDTTMM was developed. Besides the advantages of the ordinary MSDTTMM, the operations of the matrix addition and multiplication are further reduced, and the accumulated error in the computation can also be minimized effectively. Hence, not only can the computational accuracy and stability of the MSDTTMM be improved, but the computational efficiency can also be greatly improved.

10.10.3 Influence of Parameters Chosen on Computational Stability

To illustrate the influence of the parameters chosen for the step-by-step time integration method on computational stability, the stability conditions are discussed for the example solved by the Newmark- β method. Assume that the accumulated errors are $\Delta\xi(t_i)$, $\Delta\xi(t_{i+1})$ and $\Delta\xi(t_{i+2})$ at time instants t_i , t_{i+1} and t_{i+2} , respectively. Use the equation $\ddot{\xi} + \omega^2\xi = 0$ to check the computation stability, then

$$\begin{aligned}
 \Delta\xi(t_{i+2}) &= \Delta\xi(t_{i+1}) + \Delta\dot{\xi}(t_{i+1})\Delta T + \left(\frac{1}{2} - \beta\right)\Delta\ddot{\xi}(t_{i+1})\Delta T^2 + \beta\Delta T^2\Delta\ddot{\xi}(t_{i+2}) \\
 &= \Delta\xi(t_{i+1}) + [\Delta\dot{\xi}(t_i) + (1-\gamma)\Delta\ddot{\xi}(t_i)\Delta T + \gamma\Delta\ddot{\xi}(t_{i+1})\Delta T]\Delta T \\
 &\quad - \omega^2\left(\frac{1}{2} - \beta\right)\Delta\xi(t_{i+1})\Delta T^2 - \omega^2\beta\Delta\xi(t_{i+2})\Delta T^2 \\
 &= \Delta\xi(t_{i+1}) + \Delta\dot{\xi}(t_i)\Delta T - \omega^2(1-\gamma)\Delta\xi(t_i)\Delta T^2 \\
 &\quad - \omega^2\left(\frac{1}{2} - \beta\right)\Delta\xi(t_{i+1})\Delta T^2 - \omega^2\beta\Delta\xi(t_{i+2})\Delta T^2
 \end{aligned} \tag{10.158}$$

It follows that

$$\begin{aligned}
 (1 + \beta\Delta T^2\omega^2)\Delta\xi(t_{i+2}) &= \left[1 - \left(\frac{1}{2} - \beta\right)\omega^2\Delta T^2\right]\Delta\xi(t_{i+1}) \\
 &\quad + [\Delta\dot{\xi}(t_i)\Delta T - \omega^2(1-\gamma)\Delta\xi(t_i)\Delta T^2 - \gamma\omega^2\Delta T^2\Delta\dot{\xi}(t_{i+1})]
 \end{aligned} \tag{10.159}$$

Similarly, we have

$$(1 + \beta\Delta T^2\omega^2)\Delta\xi(t_{i+1}) = \left[1 - \left(\frac{1}{2} - \beta\right)\omega^2\Delta T^2\right]\Delta\xi(t_i) + \Delta\dot{\xi}(t_i)\Delta T \tag{10.160}$$

so

$$\begin{aligned}
 (1 + \beta\Delta T^2\omega^2)[\Delta\xi(t_{i+2}) - \Delta\xi(t_{i+1})] &= \left[1 - \left(\frac{1}{2} - \beta\right)\omega^2\Delta T^2\right][\Delta\xi(t_{i+1}) - \Delta\xi(t_i)] \\
 &\quad - \omega^2(1-\gamma)\Delta\xi(t_i)\Delta T^2 - \gamma\omega^2\Delta T^2\Delta\dot{\xi}(t_{i+1})
 \end{aligned} \tag{10.161}$$

$$\begin{aligned}
 (1 + \beta\Delta T^2\omega^2)\Delta\xi(t_{i+2}) &+ \left[-2 + \left(\frac{1}{2} - 2\beta + \gamma\right)\omega^2\Delta T^2\right]\Delta\xi(t_{i+1}) \\
 &+ \left[1 + \left(\frac{1}{2} + \beta - \gamma\right)\omega^2\Delta T^2\right]\Delta\xi(t_i) = 0
 \end{aligned} \tag{10.162}$$

Let

$$\frac{\Delta\xi(t_{i+2})}{\Delta\xi(t_{i+1})} = \frac{\Delta\xi(t_{i+1})}{\Delta\xi(t_i)} = \lambda$$

Hence

$$(1 + \beta\Delta T^2\omega^2)\lambda^2 + \left[-2 + \left(\frac{1}{2} - 2\beta + \gamma\right)\omega^2\Delta T^2\right]\lambda + \left[1 + \left(\frac{1}{2} + \beta - \gamma\right)\omega^2\Delta T^2\right] = 0 \tag{10.163}$$

The necessary and sufficient condition of computation stability is $|\lambda| \leq 1$. Use complex linear fractional translation to change the interior region of the unit circle $|\lambda| \leq 1$ into the left half plane $\text{Re}(W) \leq 0$ that is

$$W = \frac{\lambda - 1}{\lambda + 1} \quad (10.164)$$

Hence

$$\lambda = \frac{W + 1}{1 - W} \quad (10.165)$$

Substituting Equation (10.165) into Equation (10.163) gives

$$\begin{aligned} (1 + \beta \Delta T^2 \omega^2)(W + 1)^2 + \left[-2 + \left(\frac{1}{2} - 2\beta + \gamma \right) \omega^2 \Delta T^2 \right] (1 - W^2) \\ + \left[1 + \left(\frac{1}{2} + \beta - \gamma \right) \omega^2 \Delta T^2 \right] (1 - W)^2 = 0 \end{aligned} \quad (10.166)$$

namely

$$[4 + (4\beta - 2\gamma)\omega^2 \Delta T^2] W^2 + (2\gamma - 1)\Delta T^2 \omega^2 W + \Delta T^2 \omega^2 = 0 \quad (10.167)$$

The necessary and sufficient condition of $|\lambda| \leq 1$ is $\text{Re}(W) \leq 0$. The necessary and sufficient conditions of the real part root of Equation (10.167) being smaller than or equal to zero are

$$\begin{cases} 4 + (4\beta - 2\gamma)\omega^2 \Delta T^2 \geq 0 \\ (2\gamma - 1)\Delta T^2 \omega^2 \geq 0 \\ \Delta T^2 \omega^2 \geq 0 \end{cases} \quad (10.168)$$

Hence

$$\gamma \geq \frac{1}{2}, \quad \beta \geq \frac{\gamma}{2} \quad (10.169)$$

Therefore, for linear systems, the stability conditions of the Newmark- β method are $\gamma \geq \frac{1}{2}, \beta \geq \frac{\gamma}{2}$. The stability conditions are not related to ΔT . It is unconditionally stable. If $\gamma \geq \frac{1}{2}$ is satisfied, but $\beta \geq \frac{\gamma}{2}$ is not satisfied, to ensure computational stability, let $4 + (4\beta - 2\gamma)\omega^2 \Delta T^2 \geq 0$ by choosing a suitable ΔT . If $\gamma > \frac{1}{2}$ and $\beta > \frac{\gamma}{2}$, then $|\lambda| < 1$, which means that there exists artificial damping.

Example 10.13 Solve the dynamic response of the following system by the Newmark- β method and analyze the influence of the parameters chosen on the computation stability.

$$\begin{cases} \ddot{x} + 4x = 0 \\ x(0) = 1, \quad \dot{x}(0) = 0 \end{cases}$$

Solution

The analytical solution of the system is $x = \cos 2t$. The response of the system in the first 20 seconds is computed with three groups of chosen parameters: (1) $\gamma = 0.9, \beta = 0.45$, (2) $\gamma = 0.5, \beta = 0.25$ and (3) $\gamma = 0.2, \beta = 0.1$. The computation results are shown in Figure 10.24, where

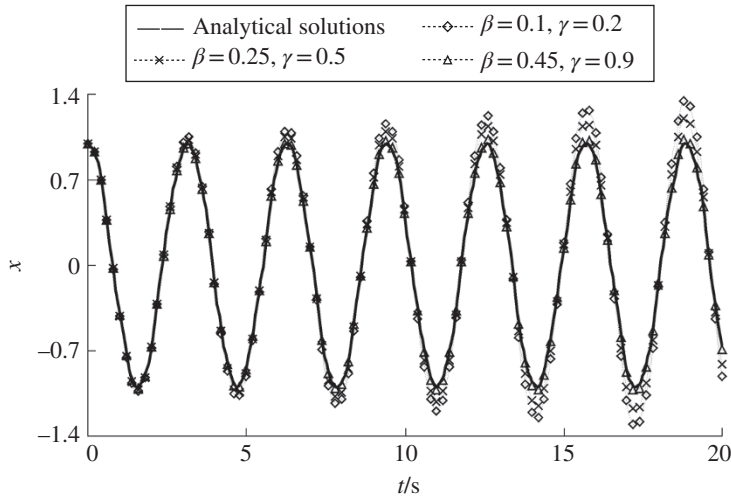


Figure 10.24 Analytical results and computation results by the Newmark- β method.

the solid line refers to the analytical result and \triangle , \times and \diamond represent the results obtained using group (1), (2) and (3) parameters, respectively. We find that choosing parameters $\gamma = 0.9$ and $\beta = 0.45$ ensures computational precision and computational stability, while the choice of parameters $\gamma = 0.5$, $\beta = 0.25$ or $\gamma = 0.2$, $\beta = 0.1$ results in larger computation error and instability. The computation results show that the parameters chosen for the step-by-step time integral method have a direct influence on numerical computational precision and stability.

11

Theorem to Deduce the Overall Transfer Equation Automatically

11.1 Introduction

The transfer matrix method for multibody systems (MSTMM) provides a new idea, a simple and efficient method of studying complex multibody system dynamics (MSD) that differs from all previous ways. The MSTMM can be applied widely to the dynamics of complex multibody systems with various topologies, such as chain multibody systems, tree multibody systems, closed-loop multibody systems, general multibody systems etc. In principle, as long as the transfer matrix of the element is obtained, various MSD problems could be solved with ease. Applying the MSTMM, according to the topology figure of the system dynamics model and the automatic deduction theorem of the overall transfer equation, with the transfer matrix of each element in a system the overall transfer equation and overall transfer matrix of the system would be deduced manually or by computer. Then with the substitution of the system boundary condition into the overall transfer equation of the system, the overall transfer equation of the system and the transfer equation of the element can be solved.

For general MSD methods, the global dynamics equation of the system should be established again if there is any change in the elements. However, the same kinds of elements (elements with the same input end number and motion mode) share the same transfer matrix in various multibody systems. Therefore, the same transfer matrix expression can be used without making any changes once the transfer matrix of one element has been deduced. Such an important characteristic of the element transfer matrix makes the transfer matrix method of MSD easy to learn and convenient to use. In addition, after the increase or decrease in elements, the overall transfer equation of the new system can be obtained by adding (multiplying) or deleting the element transfer matrix at a corresponding position and there is no need for re-deduction.

11.2 Topology Figure of Multibody Systems

Any complex MSD model is composed of various body elements and hinge elements. To make a clear and intuitive description of the transfer relationship and transfer direction between the state vectors of every element in the MSD model, new concepts concerning the topology figure of the MSTMM dynamics model are proposed. The topology figure of the dynamics model of multibody systems is a new graphic representation for the state vector relationship, sequence number of position, sequence number of boundary and transfer direction between body elements and hinge elements, and a concise means for MSD study. The given instruction uses the tree MSD model topology figure shown in Figure 11.1 as an example. The dynamics model

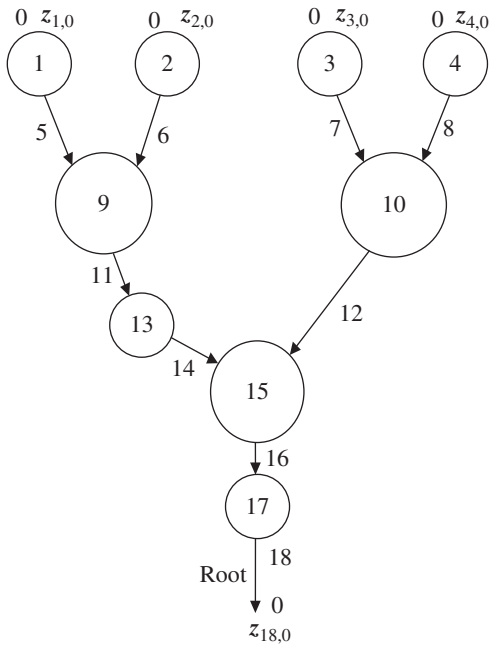


Figure 11.1 Topology figure of a dynamics model of a tree multibody system.

topology figure intuitively describes the transfer relationship and transfer direction of the state vector of each element, which is very important for the automatic deduction of the overall transfer equation of a multibody system by handwriting or by computer.

Besides the sign conventions introduced in Chapter 1, the following sign conventions are used in the topology figures:

- 1) A circle \circ denotes a body element and the number inside this circle is the sequence number of the body element.
- 2) An arrow \rightarrow denotes a hinge element and the transfer direction of state vectors, and the number beside the arrow is the sequence number of the hinge element.
- 3) If a body has more than two connection ends with other elements, then one of the connection ends will be regarded as the output end of this body and the other connection ends will be considered as the input ends. As a special case, if a body has only two connection ends, then it will be treated as a single-input-single-output body.
- 4) For a nonboundary end, the subscripts i and j ($i, j \neq 0$) in the state vector $\mathbf{z}_{i,j}$ of the end denote the sequence numbers of the adjacent body element and hinge element, respectively. For a boundary end, the second subscript j in the state vector $\mathbf{z}_{i,j}$ will be replaced by 0, namely we replace $\mathbf{z}_{i,j}$ by $\mathbf{z}_{i,0}$. In other words, the second subscript 0 denotes a boundary end and the first subscript i in the state vector $\mathbf{z}_{i,0}$ of the boundary end is the sequence number of the element involved.
- 5) In a multibody system, only one boundary end is considered as the root, and the state vector of the root is noted as $\mathbf{z}_{i,0}$, where i is the sequence number of the root element, while all the other boundary ends are considered as the tips, and the state vectors of the tips are denoted as $\mathbf{z}_{j,0}$, where j is the sequence number of the tip element. The transfer directions of a system are always from its tips to the root.
- 6) The subscript i in transfer matrix \mathbf{U}_i denotes the sequence number of element i . The subscript $(i-k)$ in the transfer matrix \mathbf{U}_{i-k} and the partitioned matrix \mathbf{U}_{i-k} means from element

i to element k . \mathbf{U}_{i-k} and \mathbf{U}_{i-k} mean the successive multiplication of the transfer matrices of all elements in the transfer path from the element i to element k of the system.

11.3 Automatic Deduction of the Overall Transfer Equation of a Closed-loop System

For the topology figure of the dynamics model of an arbitrary closed-loop multibody system composed of n elements (including body elements and hinge elements), after “cutting” at the junction of body element n and hinge element 1, the original closed-loop system becomes a chain system, as shown in Figure 11.3. Setting the two cutting points generated by cutting as the boundary ends of state vectors $\mathbf{z}_{1,0}$ and $\mathbf{z}_{n,0}$, then the original closed-loop system in Figure 11.2 is transformed into the chain system with equal state vectors $\mathbf{z}_{1,0}$ and $\mathbf{z}_{n,0}$.

Hence, the transfer equation of a closed-loop system can be treated as a chain system. It can be automatically deduced that

$$\mathbf{z}_{n,0} = \mathbf{U}_{1-n} \mathbf{z}_{1,0} \quad (11.1)$$

where

$$\mathbf{U}_{1-n} = \mathbf{U}_n \mathbf{U}_{n-1} \dots \mathbf{U}_2 \mathbf{U}_1 \quad (11.2)$$

Note that the state vectors of the cutting points are equal, that is

$$\mathbf{z}_{n,0} = \mathbf{z}_{1,0} \quad (11.3)$$

therefore the overall transfer matrix of a chain system can be deduced automatically by handwriting or by computer

$$\mathbf{U}_{\text{all}} \mathbf{z}_{1,0} = 0 \quad (11.4)$$

where

$$\mathbf{U}_{\text{all}} = [-\mathbf{I} \mathbf{U}_{1-n}] \mathbf{U}_{\text{all}} = (\mathbf{I} - \mathbf{U}_{1-n}) \quad (11.5)$$

11.4 Automatic Deduction of the Overall Transfer Equation of a Tree System

For a body element with more than two endpoints, one endpoint is regarded as the output end while the others are considered as input ends. The transfer equation ought to contain the geometric relation between the first input end and the output end and the dynamics equations

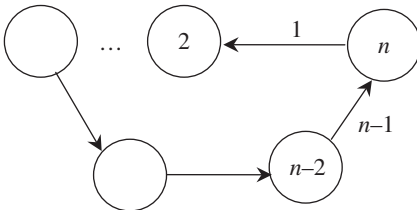


Figure 11.2 Topology figure of a closed-loop system.

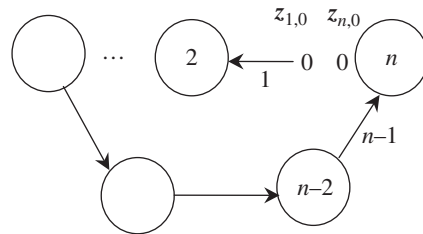


Figure 11.3 Topology figure of closed-loop system after cutting hinge n .

governing the motion of the element. It can be proved that the transfer equation of the rigid body j with L input ends can be written as

$$\mathbf{z}_{j,O} = \mathbf{U}_j \mathbf{z}_{j,I_1} + \mathbf{U}_{j,I_2} \mathbf{z}_{j,I_2} + \dots + \mathbf{U}_{j,I_L} \mathbf{z}_{j,I_L} \quad (11.6)$$

where subscript j is the sequence number of the body element, O represents the output end, while I_1, I_2, \dots , and I_L denote the first, the second, ..., and the L th input ends, respectively, $\mathbf{z}_{j,O}$ and \mathbf{z}_{j,I_k} ($k = 2, 3, 4, \dots, L$) are the state vector of output end and the k th input end of the body element, respectively, \mathbf{U}_j is the transfer matrix of element j with only one input end and one output end, and \mathbf{U}_{j,I_k} is the matrix to extract internal force and internal moment from \mathbf{z}_{j,I_k} , called the force extraction matrix.

It can be proved that for the geometric relation between the first input end I_1 and the k th output end I_k of the element with L input ends and one output end, the geometric equation is

$$\mathbf{H}_j \mathbf{z}_{j,I_1} = \mathbf{H}_{j,I_k} \mathbf{z}_{j,I_k} \quad (k = 2, 3, 4, \dots, L) \quad (11.7)$$

where \mathbf{H}_j is the constant matrix to extract the position coordinates and rotation angles from state vector \mathbf{z}_{j,I_1} , called the position extraction matrix in this book. \mathbf{H}_{j,I_k} is associated with the relative position of the first input end and the k th input end of body j , called the position incidence matrix in this book.

According to the transfer equation and geometric equation of the element, the automatic deduction of the system overall transfer equation can easily be obtained. For the topology figure of the system dynamics model shown in Figure 11.1, joint points $P_{9,5}, P_{10,7}, P_{15,14}$ and $P_{9,6}, P_{10,8}, P_{15,12}$ are the first and second input ends of body elements 9, 10 and 15, respectively. According to Equation (11.6), the relation between the state vectors and transfer equations of each element are depicted in Figure 11.4.

The equation describing the relations among the state vectors of each boundary end shown in Figure 11.4 can be easily deduced, and is known as the system overall transfer equation.

$$\begin{aligned} \mathbf{z}_{18,0} &= \mathbf{U}_{18} \mathbf{z}_{17,18} = \mathbf{U}_{18} \mathbf{U}_{17} \mathbf{U}_{16} \mathbf{z}_{15,16} = \mathbf{U}_{18} \mathbf{U}_{17} \mathbf{U}_{16} \mathbf{U}_{15} \mathbf{z}_{15,14} + \mathbf{U}_{18} \mathbf{U}_{17} \mathbf{U}_{16} \mathbf{U}_{15,12} \mathbf{z}_{15,12} \\ &= \mathbf{U}_{18} \mathbf{U}_{17} \mathbf{U}_{16} \mathbf{U}_{15} \mathbf{U}_{14} \mathbf{U}_{13} \mathbf{U}_{11} \mathbf{z}_{9,11} + \mathbf{U}_{18} \mathbf{U}_{17} \mathbf{U}_{16} \mathbf{U}_{15,12} \mathbf{U}_{12} \mathbf{z}_{10,12} \\ &= \mathbf{U}_{18} \mathbf{U}_{17} \mathbf{U}_{16} \mathbf{U}_{15} \mathbf{U}_{14} \mathbf{U}_{13} \mathbf{U}_{11} \mathbf{U}_9 \mathbf{z}_{9,5} + \mathbf{U}_{18} \mathbf{U}_{17} \mathbf{U}_{16} \mathbf{U}_{15} \mathbf{U}_{14} \mathbf{U}_{13} \mathbf{U}_{11} \mathbf{U}_{9,6} \mathbf{z}_{9,6} \\ &\quad + \mathbf{U}_{18} \mathbf{U}_{17} \mathbf{U}_{16} \mathbf{U}_{15,12} \mathbf{U}_{12} \mathbf{U}_{10} \mathbf{z}_{10,7} + \mathbf{U}_{18} \mathbf{U}_{17} \mathbf{U}_{16} \mathbf{U}_{15,12} \mathbf{U}_{12} \mathbf{U}_{10,8} \mathbf{z}_{10,8} \\ &= \mathbf{U}_{18} \mathbf{U}_{17} \mathbf{U}_{16} \mathbf{U}_{15} \mathbf{U}_{14} \mathbf{U}_{13} \mathbf{U}_{11} \mathbf{U}_9 \mathbf{U}_5 \mathbf{U}_1 \mathbf{z}_{1,0} + \mathbf{U}_{18} \mathbf{U}_{17} \mathbf{U}_{16} \mathbf{U}_{15} \mathbf{U}_{14} \mathbf{U}_{13} \mathbf{U}_{11} \mathbf{U}_{9,6} \mathbf{U}_6 \mathbf{U}_2 \mathbf{z}_{2,0} \\ &\quad + \mathbf{U}_{18} \mathbf{U}_{17} \mathbf{U}_{16} \mathbf{U}_{15,12} \mathbf{U}_{12} \mathbf{U}_{10} \mathbf{U}_7 \mathbf{U}_3 \mathbf{z}_{3,0} + \mathbf{U}_{18} \mathbf{U}_{17} \mathbf{U}_{16} \mathbf{U}_{15,12} \mathbf{U}_{12} \mathbf{U}_{10,8} \mathbf{U}_8 \mathbf{U}_4 \mathbf{z}_{4,0} \\ &= \mathbf{T}_{1-18} \mathbf{z}_{1,0} + \mathbf{T}_{2-18} \mathbf{z}_{2,0} + \mathbf{T}_{3-18} \mathbf{z}_{3,0} + \mathbf{T}_{4-18} \mathbf{z}_{4,0} \end{aligned} \quad (11.8)$$

where

$$\begin{cases} \mathbf{T}_{1-18} = \mathbf{U}_{18} \mathbf{U}_{17} \mathbf{U}_{16} \mathbf{U}_{15} \mathbf{U}_{14} \mathbf{U}_{13} \mathbf{U}_{11} \mathbf{U}_9 \mathbf{U}_5 \mathbf{U}_1 \\ \mathbf{T}_{2-18} = \mathbf{U}_{18} \mathbf{U}_{17} \mathbf{U}_{16} \mathbf{U}_{15} \mathbf{U}_{14} \mathbf{U}_{13} \mathbf{U}_{11} \mathbf{U}_{9,6} \mathbf{U}_6 \mathbf{U}_2 \\ \mathbf{T}_{3-18} = \mathbf{U}_{18} \mathbf{U}_{17} \mathbf{U}_{16} \mathbf{U}_{15,12} \mathbf{U}_{12} \mathbf{U}_{10} \mathbf{U}_7 \mathbf{U}_3 \\ \mathbf{T}_{4-18} = \mathbf{U}_{18} \mathbf{U}_{17} \mathbf{U}_{16} \mathbf{U}_{15,12} \mathbf{U}_{12} \mathbf{U}_{10,8} \mathbf{U}_8 \mathbf{U}_4 \end{cases} \quad (11.9)$$

According to Equation (11.7), the geometric equation of body element 9 is

$$\mathbf{H}_9 \mathbf{z}_{9,5} = \mathbf{H}_{9,6} \mathbf{z}_{9,6} \quad (11.10)$$

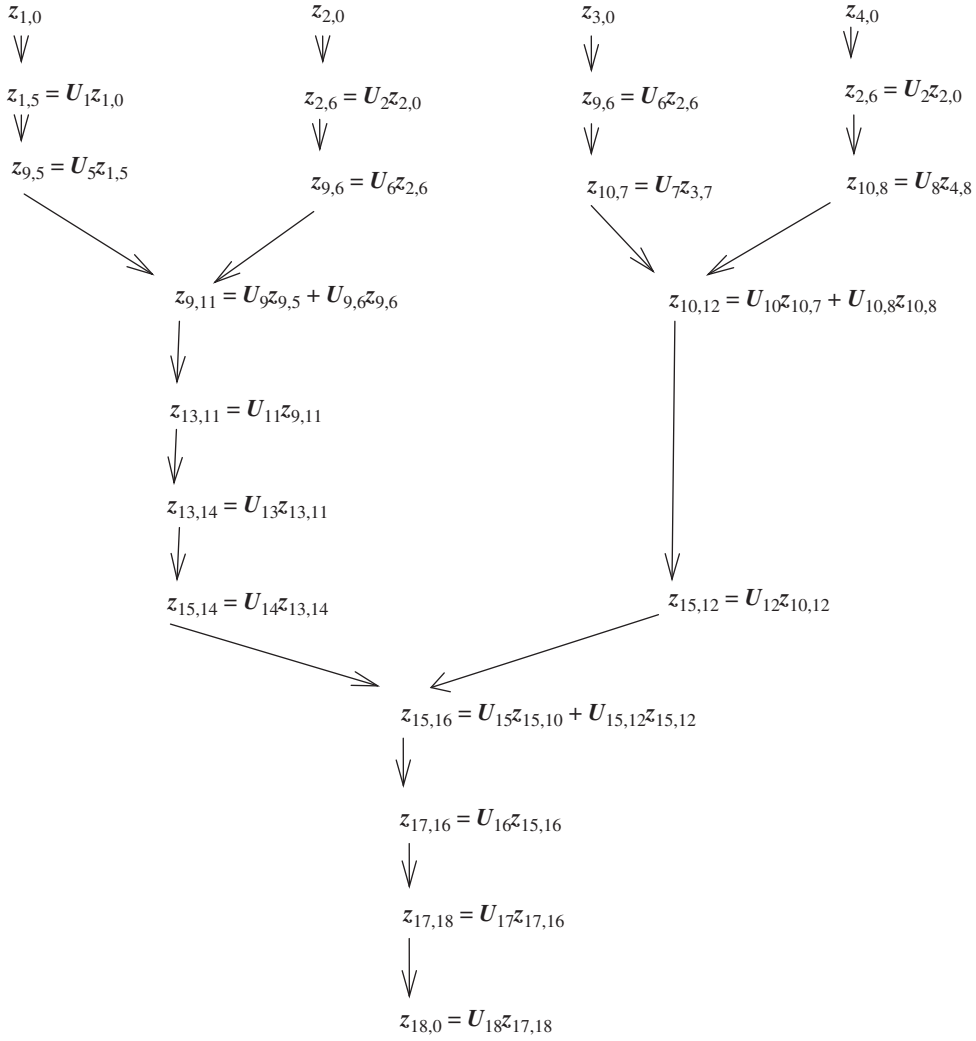


Figure 11.4 A system topology structure described by state vectors and transfer equations.

where \mathbf{H}_9 and $\mathbf{H}_{9,6}$ are the position extraction matrix and position incidence matrix of rigid body 9.

Applying the system topology structure described by state vectors and transfer equations shown in Figure 11.4, the state vectors $z_{9,5}$ and $z_{9,6}$ are written as

$$z_{9,5} = \mathbf{U}_5 \mathbf{U}_1 z_{1,0} \quad (11.11)$$

$$z_{9,6} = \mathbf{U}_6 \mathbf{U}_2 z_{2,0} \quad (11.12)$$

Substituting Equations (11.11) and (11.12) into Equation (11.10), we obtain

$$-\mathbf{H}_9 \mathbf{U}_5 \mathbf{U}_1 z_{1,0} + \mathbf{H}_{9,6} \mathbf{U}_6 \mathbf{U}_2 z_{2,0} = \mathbf{0} \quad (11.13)$$

Equation (11.13) can be written as

$$\mathbf{G}_{1-9} z_{1,0} + \mathbf{G}_{2-9} z_{2,0} = \mathbf{0} \quad (11.14)$$

where

$$\begin{cases} \mathbf{G}_{1-9} = -\mathbf{H}_9 \mathbf{U}_5 \mathbf{U}_1 \\ \mathbf{G}_{2-9} = \mathbf{H}_{9,6} \mathbf{U}_6 \mathbf{U}_2 \end{cases} \quad (11.15)$$

In the same manner, the geometric equations of body elements 10 and 15 can be deduced

$$\mathbf{G}_{3-10} \mathbf{z}_{3,0} + \mathbf{G}_{4-10} \mathbf{z}_{4,0} = \mathbf{0} \quad (11.16)$$

$$\mathbf{G}_{1-15} \mathbf{z}_{1,0} + \mathbf{G}_{2-15} \mathbf{z}_{2,0} + \mathbf{G}_{3-15} \mathbf{z}_{3,0} + \mathbf{G}_{4-15} \mathbf{z}_{4,0} = \mathbf{0} \quad (11.17)$$

where

$$\begin{cases} \mathbf{G}_{3-10} = -\mathbf{H}_{10} \mathbf{U}_7 \mathbf{U}_3 \\ \mathbf{G}_{4-10} = \mathbf{H}_{10,8} \mathbf{U}_8 \mathbf{U}_4 \end{cases} \begin{cases} \mathbf{G}_{1-15} = -\mathbf{H}_{15} \mathbf{U}_{14} \mathbf{U}_{13} \mathbf{U}_{11} \mathbf{U}_9 \mathbf{U}_5 \mathbf{U}_1 \\ \mathbf{G}_{2-15} = -\mathbf{H}_{15} \mathbf{U}_{14} \mathbf{U}_{13} \mathbf{U}_{11} \mathbf{U}_{9,6} \mathbf{U}_6 \mathbf{U}_2 \\ \mathbf{G}_{3-15} = \mathbf{H}_{15,12} \mathbf{U}_{12} \mathbf{U}_{10} \mathbf{U}_7 \mathbf{U}_3 \\ \mathbf{G}_{4-15} = \mathbf{H}_{15,12} \mathbf{U}_{12} \mathbf{U}_{10,8} \mathbf{U}_8 \mathbf{U}_4 \end{cases} \quad (11.18)$$

After combining the main transfer equation and the geometric equations of all relevant elements in Equations (11.8), (11.14), (11.16) and (11.17), the overall transfer equation of the system can be obtained:

$$\mathbf{U}_{\text{all}} \mathbf{z}_{\text{all}} = \mathbf{0} \quad (11.19)$$

where

$$\mathbf{z}_{\text{all}} = [\mathbf{z}_{18,0}^T \quad \mathbf{z}_{1,0}^T \quad \mathbf{z}_{2,0}^T \quad \mathbf{z}_{3,0}^T \quad \mathbf{z}_{4,0}^T]^T \quad (11.20)$$

$$\mathbf{U}_{\text{all}} = \begin{bmatrix} -\mathbf{I} & \mathbf{T}_{1-18} & \mathbf{T}_{2-18} & \mathbf{T}_{3-18} & \mathbf{T}_{4-18} \\ \mathbf{O} & \mathbf{G}_{1-9} & \mathbf{G}_{2-9} & \mathbf{O} & \mathbf{O} \\ \mathbf{O} & \mathbf{O} & \mathbf{O} & \mathbf{G}_{3-10} & \mathbf{G}_{4-10} \\ \mathbf{O} & \mathbf{G}_{1-15} & \mathbf{G}_{2-15} & \mathbf{G}_{3-15} & \mathbf{G}_{4-15} \end{bmatrix} \quad (11.21)$$

We can rewrite Equations (11.20) and (11.21) as

$$\mathbf{z}_{\text{all}} = [\mathbf{z}_{\text{root}}^T \quad \mathbf{z}_{\text{tip}}^T]^T \quad (11.22)$$

$$\mathbf{U}_{\text{all}} = \begin{bmatrix} -\mathbf{I} & \mathbf{T} \\ \mathbf{O} & \mathbf{G} \end{bmatrix} \quad (11.23)$$

where

$$\mathbf{z}_{\text{root}} = \mathbf{z}_{18,0} \quad (11.24)$$

$$\mathbf{z}_{\text{tip}} = [\mathbf{z}_{1,0}^T \quad \mathbf{z}_{2,0}^T \quad \mathbf{z}_{3,0}^T \quad \mathbf{z}_{4,0}^T]^T \quad (11.25)$$

$$\mathbf{T} = [\mathbf{T}_{1-18} \quad \mathbf{T}_{2-18} \quad \mathbf{T}_{3-18} \quad \mathbf{T}_{4-18}] \quad (11.26)$$

$$\mathbf{G} = \begin{bmatrix} \mathbf{G}_{1-9} & \mathbf{G}_{2-9} & \mathbf{O} & \mathbf{O} \\ \mathbf{O} & \mathbf{O} & \mathbf{G}_{3-10} & \mathbf{G}_{4-10} \\ \mathbf{G}_{1-15} & \mathbf{G}_{2-15} & \mathbf{G}_{3-15} & \mathbf{G}_{4-15} \end{bmatrix} \quad (11.27)$$

The overall transfer Equation (11.19) of the tree system includes the main transfer Equation (11.8) and geometric Equations (11.14), (11.16) and (11.17), where \mathbf{I} is the identity

matrix, and the coefficient matrices of all the state vectors in the first column are zero matrices, with the exception of the first row of the overall transfer matrix. In this book, the state vector \mathbf{z}_{all} (see Equation (11.20)) is defined as the state vector of the system boundary, while the coefficient matrix \mathbf{U}_{all} (see Equations (11.21) or (11.23)) is defined as the overall transfer matrix of system. The coefficient matrix \mathbf{T} (see Equation (11.26)) is defined as main transfer equation coefficient matrix, and the coefficient matrix \mathbf{G} (see Equation (11.27)) is defined as the geometric equation coefficient matrix.

From Equation (11.9), the coefficient matrix of the system boundary state vector of the tree system main transfer equation corresponds to the first row in the overall transfer matrix (see Equation (11.23)), the coefficient matrix of the root state vector is a minus identity matrix and the structure of coefficient matrix \mathbf{T} of the branch state vector has the following regular pattern: the transfer matrix (like \mathbf{T}_{1-18} and \mathbf{T}_{3-18}) from the branch, through the first input end of the multiple input element, to root is equal to the successive multiplication of transfer matrices of all elements along this route, in which the transfer matrix of the involved element with multiple input ends is the transfer matrix of the element with one input (the first input end) and one output (output end). The transfer matrix (\mathbf{T}_{2-18} and \mathbf{T}_{4-18}) is equal to the successive multiplication of transfer matrices of all elements, in which the related transfer matrix of the element with multiple input ends is the force extraction matrix of the corresponding input end of the element.

For the geometric equations of the tree system, the regular pattern of the coefficient matrices of the branch state vectors could be concluded from Equations (11.15) and (11.18). If a branch terminates at the first input end of a multiple-input element, then the corresponding coefficient (e.g. \mathbf{G}_{1-9} , \mathbf{G}_{1-15} and \mathbf{G}_{3-10}) is obtained by successive multiplication of the transfer matrices of all elements along this path and by a final premultiplication of the corresponding negative position extraction matrix. Likewise, if a branch terminates at a nonfirst input end of a multiple-input element, then the corresponding coefficient (e.g. \mathbf{G}_{2-9} , \mathbf{G}_{2-15} , \mathbf{G}_{3-15} , \mathbf{G}_{4-10} and \mathbf{G}_{4-15}) is obtained by successive multiplication of the transfer matrices of all elements along this path and by a final premultiplication of the corresponding positive position extraction matrix. The state vector coefficient matrices of branch are zero matrices if there is no transfer route between the branch and the input end of the element with multiple input ends.

11.5 Automatic Deduction of the Overall Transfer Equation of a General System

As shown in Figure 11.5, a general multibody system is regarded as a system composed of a tree subsystem and some closed-loop subsystems. After cutting at the junction between body 2 and hinge 19, a couple of new boundaries with equivalent state vectors, signed as $\mathbf{z}_{2,0}$ and $\mathbf{z}_{19,0}$, are generated at the cutting point, as shown in Figure 11.6. The former nontree system has changed to a tree system with two new boundary state vectors $\mathbf{z}_{2,0}$ and $\mathbf{z}_{19,0}$ at the cutting point. Thus, according to section 11.4, the overall transfer equation of a general system composed of closed-loop subsystems and tree subsystems can be derived manually or by computer.

It should be noted that both $\mathbf{z}_{2,0}$ and $\mathbf{z}_{19,0}$ are the input ends of some elements (here the input ends of elements 2 and 19, respectively), therefore the internal forces and internal moments in $\mathbf{z}_{2,0}$ and $\mathbf{z}_{19,0}$ are equal in magnitude and opposite in direction according to sign conventions, that is

$$\mathbf{z}_{19,0} = \mathbf{C}\mathbf{z}_{2,0} \quad (11.28)$$

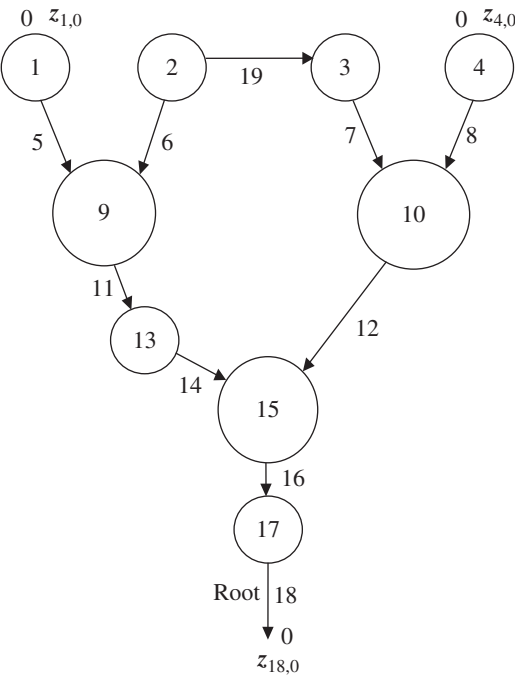


Figure 11.5 Topology figure of a nontree system.

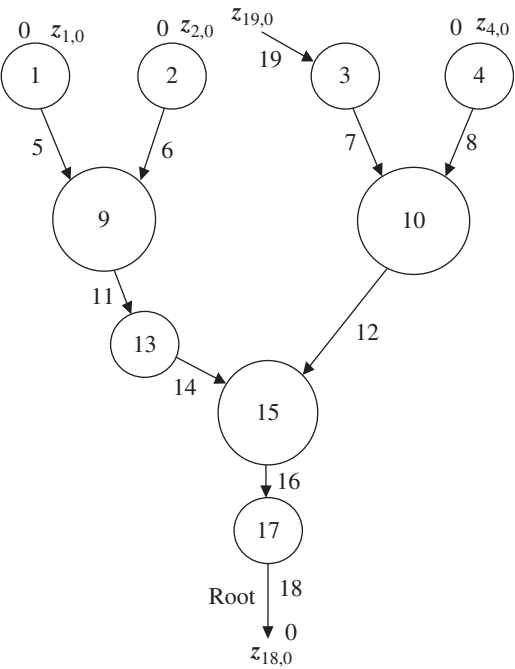


Figure 11.6 Topology figure of a tree system generated by a nontree system after cutting hinge 19.

where

$$C = \begin{bmatrix} I_n & O_n & O_{n \times 1} \\ O_n & -I_n & O_{n \times 1} \\ O_{1 \times n} & O_{1 \times n} & 1 \end{bmatrix} \quad (11.29)$$

is the cutting point sign convention matrix in this book, where n is equal to 3 or 6 for planar motion or spatial motion, respectively.

For tree systems, taking the relation expression of $\mathbf{z}_{2,0}$ and $\mathbf{z}_{19,0}$, namely Equation (11.28), into account, the overall transfer equation of a general multibody system, as shown in Figure 11.6, with closed-loop subsystems can be derived automatically by handwriting or by computer,

$$\mathbf{U}_{\text{all}} \mathbf{z}_{\text{all}} = \mathbf{0} \quad (11.30)$$

where

$$\mathbf{U}_{\text{all}} = \begin{bmatrix} -I & T_{1-18} & T_{2-18} & T_{19-18} & T_{4-18} \\ O & G_{1-9} & G_{2-9} & O & O \\ O & O & O & G_{19-10} & G_{4-10} \\ O & G_{1-15} & G_{2-15} & G_{19-15} & G_{4-15} \\ O & O & C & -I & O \end{bmatrix}, \mathbf{z}_{\text{all}} = \begin{bmatrix} \mathbf{z}_{18,0} \\ \mathbf{z}_{1,0} \\ \mathbf{z}_{2,0} \\ \mathbf{z}_{19,0} \\ \mathbf{z}_{4,0} \end{bmatrix} \quad (11.31)$$

Considering that $\mathbf{z}_{19,0}$ can be described by $\mathbf{z}_{2,0}$ using Equation (11.28), the overall transfer equation, the overall transfer matrix and the system boundary state vector of the general system can be written as

$$\mathbf{U}_{\text{all}} \mathbf{z}_{\text{all}} = \mathbf{0} \quad (11.32)$$

where

$$\mathbf{z}_{\text{all}} = [\mathbf{z}_{18,0}^T \quad \mathbf{z}_{1,0}^T \quad \mathbf{z}_{2,0}^T \quad \mathbf{z}_{4,0}^T]^T \quad (11.33)$$

$$\mathbf{U}_{\text{all}} = \begin{bmatrix} -I & T_{1-18} & T_{2-18} + T_{19-18}C & T_{4-18} \\ O & G_{1-9} & G_{2-9} & O \\ O & O & G_{19-10}C & G_{4-10} \\ O & G_{1-15} & G_{2-15} + G_{19-15}C & G_{4-15} \end{bmatrix} \quad (11.34)$$

$$\begin{cases} T_{1-18} = U_{18}U_{17}U_{16}U_{15}U_{14}U_{13}U_{11}U_9U_5U_1 \\ T_{2-18} = U_{18}U_{17}U_{16}U_{15}U_{14}U_{13}U_{11}U_{9,6}U_6U_2 \\ T_{19-18} = U_{18}U_{17}U_{16}U_{15,12}U_{12}U_{10}U_7U_3U_{19} \\ T_{4-18} = U_{18}U_{17}U_{16}U_{15,12}U_{12}U_{10,8}U_8U_4 \end{cases} \quad (11.35)$$

$$\begin{cases} G_{1-9} = -H_9U_5U_1 \\ G_{2-9} = H_{9,6}U_6U_2 \end{cases}, \begin{cases} G_{19-10} = -H_{10}U_7U_3U_{19} \\ G_{4-10} = H_{10,8}U_8U_4 \end{cases} \quad (11.36)$$

$$\begin{cases} G_{1-15} = -H_{15}U_{14}U_{13}U_{11}U_9U_5U_1 \\ G_{2-15} = -H_{15}U_{14}U_{13}U_{11}U_{9,6}U_6U_2 \\ G_{19-15} = H_{15,12}U_{12}U_{10}U_7U_3U_{19} \\ G_{4-15} = H_{15,12}U_{12}U_{10,8}U_8U_4 \end{cases} \quad (11.37)$$

Equations (11.32) to (11.34) show that as long as the state vectors of each pair of cutting points are the same and comply with sign conventions, the forms of the overall transfer equation, the main transfer equation and the geometric equation of a general system that consists of closed-loop subsystems and a tree subsystem are identical as those of the tree system developed by cutting the closed-loop subsystem. In this book, the original system boundary state vectors and all the body element end state vectors at the cutting point are defined as augmented boundary state vectors.

11.6 Automatic Deduction Theorem of the Overall Transfer Equation

Owing to the deduction process introduced in sections 11.3–11.5, the following characteristics of the multibody system transfer equation are found, by which the automatic deduction theorem of the overall transfer equation of closed-loop systems, tree systems and general systems can be developed.

- a) The state vector involved in the overall transfer equation, \mathbf{z}_{all} , is referred to as the system boundary state vector. The coefficient matrix of the system boundary state vector is the overall transfer matrix \mathbf{U}_{all} of the system.
- b) For tree systems the overall transfer equation includes the main transfer equation and geometric equations. The coefficient matrix of the system boundary state vector in the main transfer equation corresponds to the first row of the overall transfer matrix, in which the coefficient matrix of the root state vector is the minus identity matrix. The coefficient matrix of the main transfer equation, that is, the coefficient matrix \mathbf{T} of the branch state vector, has a structure with the following rules: the coefficient matrix of each branch state vector is the successive multiplication of the transfer matrices of all the elements from branch to root along the transfer route.

As for the geometric equations of the tree system, if a branch terminates at the first input end of a multiple-input element, then the corresponding coefficient is obtained by successive multiplication of the transfer matrices of all elements along this path and by a final premultiplication of the corresponding negative position extraction matrix. Likewise, if a branch terminates at a nonfirst input end of a multiple-input element, then the corresponding coefficient is obtained by successive multiplication of the transfer matrices of all elements along this path and by a final premultiplication of the corresponding positive position extraction matrix.

- c) For a chain system, any chain system can be regarded as a special case of a tree system which has only two boundaries. No geometric equations are involved for a chain system. In addition, the automatic deduction theorem (b) of the overall transfer equation for tree systems is also valid for chain systems.
- d) For a closed-loop system, by cutting the loop into a chain the original system can be regarded as a chain system. The automatic deduction theorem (b) of the overall transfer equation for tree systems is also valid for closed-loop systems.
- e) For a general system composed of a tree subsystem and a closed-loop subsystem, by cutting off the closed loops, the original system can be changed to a tree system with the boundary ends corresponding to the cutting points. Therefore, the forms of the overall transfer equation, the main transfer equation and the geometric equation in general systems with closed-loop subsystems and tree subsystems are the same as in tree systems formed by cutting the closed-loop subsystems.

The above automatic deduction theorem of the overall transfer equation of multibody systems applies for a variety of MRSs, chain multi-rigid-flexible-body systems (MRFSSs), closed-loop MRFSSs, tree MRFSSs and general MRFSSs in which a body element with more than two ends is assumed to be a rigid body, and has laid a foundation for building large-scale MSD software with high computing speed.

11.7 Numerical Example of Closed-loop System Dynamics

11.7.1 Vibration Characteristics of a Closed-loop Multibody System

For a closed-loop MRFSS, the sequence number of the first element is the same as that of the end element, thus it can be regarded as a chain system if the system is “cut” at a connection point. The multibody dynamic problems of closed-loop systems can be studied using the MSTMM.

For example, Figure 11.7 shows a closed-loop system composed of three lumped masses and three springs. A connection point can be defined as the input end of the system, and at the same time it is the output end of the system. Each element is numbered successively along the loop. The transfer direction can be defined arbitrarily. The following discussion is based on the sequence numbers shown in Figure 11.7.

The state vectors $\mathbf{Z}_{6,1}$, $\mathbf{Z}_{2,1}$, $\mathbf{Z}_{2,3}$, $\mathbf{Z}_{4,3}$, $\mathbf{Z}_{4,5}$ and $\mathbf{Z}_{6,5}$ are defined as $\mathbf{Z} = [X, \dot{Q}_x]^T$. The transfer equations are

$$\begin{cases} \mathbf{Z}_{2,1} = \mathbf{U}_1 \mathbf{Z}_{6,1}, & \mathbf{Z}_{2,3} = \mathbf{U}_2 \mathbf{Z}_{2,1}, & \mathbf{Z}_{4,3} = \mathbf{U}_3 \mathbf{Z}_{2,3} \\ \mathbf{Z}_{4,5} = \mathbf{U}_4 \mathbf{Z}_{4,3}, & \mathbf{Z}_{6,5} = \mathbf{U}_5 \mathbf{Z}_{4,5}, & \mathbf{Z}_{6,1} = \mathbf{U}_6 \mathbf{Z}_{6,5} \end{cases} \quad (11.38)$$

The transfer matrices have already been given in Equations (2.13) and (2.19), and thus are omitted here. According to Equation (11.38), we obtain

$$\mathbf{Z}_{6,1} = \mathbf{U}_6 \mathbf{U}_5 \mathbf{U}_4 \mathbf{U}_3 \mathbf{U}_2 \mathbf{U}_1 \mathbf{Z}_{6,1} \quad (11.39)$$

Equation (11.39) is the overall transfer equation of the system, which can be written as

$$(\mathbf{U}_6 \mathbf{U}_5 \mathbf{U}_4 \mathbf{U}_3 \mathbf{U}_2 \mathbf{U}_1 - \mathbf{I}_2) \mathbf{Z}_{6,1} = \mathbf{0} \text{ or } \mathbf{U}_{\text{all}} \mathbf{Z}_{\text{all}} = \mathbf{0} \quad (11.40)$$

The elements of $\mathbf{Z}_{6,1}$ are all unknown because $\mathbf{Z}_{6,1}$ is not the state vector at the boundary point but the state vector at the connection point, that is

$$\bar{\mathbf{U}}_{\text{all}} = \mathbf{U}_{\text{all}} = \mathbf{U}_6 \mathbf{U}_5 \mathbf{U}_4 \mathbf{U}_3 \mathbf{U}_2 \mathbf{U}_1 - \mathbf{I}_2, \quad \bar{\mathbf{Z}}_{\text{all}} = \mathbf{Z}_{\text{all}} = \mathbf{Z}_{6,1} \quad (11.41)$$

Therefore, the characteristic equation is obtained as

$$\Delta = |\bar{\mathbf{U}}_{\text{all}}| = 0 \quad (11.42)$$

The closed-loop MRFSS shown in Figure 11.8 is composed of four elastic beams and four rigid bodies. The transverse and longitudinal vibrations of the beams are considered in a plane. The

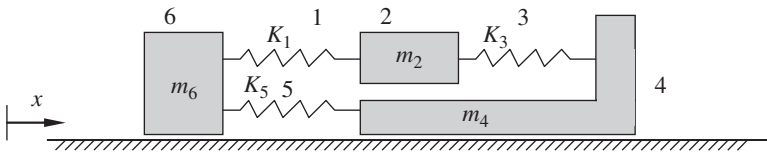


Figure 11.7 A closed-loop system composed of lumped masses and springs.

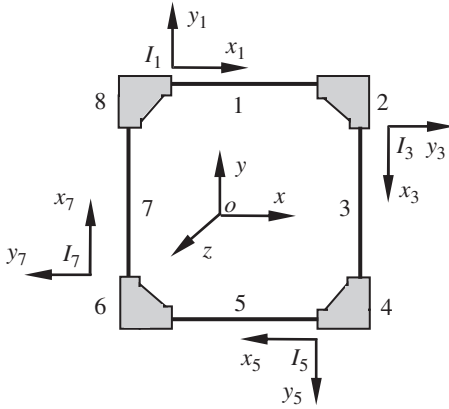


Figure 11.8 A closed-loop system of a multi-rigid-flexible-body.

sequence number of each element is shown. The state vectors $\mathbf{Z}_{8,1}$, \mathbf{Z}_{x_1} , $\mathbf{Z}_{2,1}$, $\mathbf{Z}_{2,3}$, \mathbf{Z}_{x_3} , $\mathbf{Z}_{4,3}$, $\mathbf{Z}_{4,5}$, \mathbf{Z}_{x_5} , $\mathbf{Z}_{6,5}$, $\mathbf{Z}_{6,7}$, \mathbf{Z}_{x_7} and $\mathbf{Z}_{8,7}$ are defined in the form of $\mathbf{Z} = [X, Y, \theta_z, M_z, Q_x, Q_y]^T$, where $\mathbf{Z}_{8,1}$, \mathbf{Z}_{x_1} and $\mathbf{Z}_{2,1}$ are defined in the coordinate system $I_1x_1y_1$, $\mathbf{Z}_{2,3}$, \mathbf{Z}_{x_3} and $\mathbf{Z}_{4,3}$ are defined in the coordinate system $I_3x_3y_3$, $\mathbf{Z}_{4,5}$, \mathbf{Z}_{x_5} and $\mathbf{Z}_{6,5}$ are defined in the coordinate system $I_5x_5y_5$, and $\mathbf{Z}_{6,7}$, \mathbf{Z}_{x_7} and $\mathbf{Z}_{8,7}$ are defined in the coordinate system $I_7x_7y_7$.

The transfer equation of element 1 in the coordinate system $I_1x_1y_1$ is

$$\mathbf{Z}_{2,1} = \mathbf{U}_1 \mathbf{Z}_{8,1} \quad (11.43)$$

where \mathbf{U}_1 is the transfer matrix of beam 1.

The state vectors $\mathbf{Z}_{2,1}$ at the input end and $\mathbf{Z}_{2,3}$ at the output end of rigid body 2 are defined in the two different coordinate systems $I_1x_1y_1$ and $I_3x_3y_3$, respectively. The orientation discrepancy of the two coordinate systems is 90° . As a result, a coordinates transformation has to be made in the transfer equation of rigid body 2, that is

$$\mathbf{Z}_{2,3} = \mathbf{H} \mathbf{U}_2 \mathbf{Z}_{2,1} \quad (11.44)$$

where

$$\mathbf{H} = \begin{bmatrix} \mathbf{H}_{1,1} & \mathbf{O}_{3 \times 3} \\ \mathbf{O}_{3 \times 3} & \mathbf{H}_{2,2} \end{bmatrix}, \quad \mathbf{H}_{1,1} = \begin{bmatrix} 0 & -1 & 0 \\ 1 & 0 & 0 \\ 0 & 0 & 1 \end{bmatrix}, \quad \mathbf{H}_{2,2} = \begin{bmatrix} 1 & 0 & 0 \\ 0 & 0 & -1 \\ 0 & 1 & 0 \end{bmatrix}$$

\mathbf{U}_2 is the transfer matrix of rigid body 2 and \mathbf{H} is the coordinate transformation matrix.

Similarly, we can obtain

$$\begin{cases} \mathbf{Z}_{4,3} = \mathbf{U}_3 \mathbf{Z}_{2,3}, & \mathbf{Z}_{4,5} = \mathbf{H} \mathbf{U}_4 \mathbf{Z}_{4,3} \\ \mathbf{Z}_{6,5} = \mathbf{U}_5 \mathbf{Z}_{4,5}, & \mathbf{Z}_{6,7} = \mathbf{H} \mathbf{U}_6 \mathbf{Z}_{6,5} \\ \mathbf{Z}_{8,7} = \mathbf{U}_7 \mathbf{Z}_{6,7}, & \mathbf{Z}_{8,1} = \mathbf{H} \mathbf{U}_8 \mathbf{Z}_{8,7} \end{cases} \quad (11.45)$$

According to Equations (11.43) to (11.45), the overall transfer equation is obtained

$$\mathbf{Z}_{8,1} = \mathbf{H} \mathbf{U}_8 \mathbf{U}_7 \mathbf{H} \mathbf{U}_6 \mathbf{U}_5 \mathbf{H} \mathbf{U}_4 \mathbf{U}_3 \mathbf{H} \mathbf{U}_2 \mathbf{U}_1 \mathbf{Z}_{8,1}$$

that is

$$(\mathbf{H} \mathbf{U}_8 \mathbf{U}_7 \mathbf{H} \mathbf{U}_6 \mathbf{U}_5 \mathbf{H} \mathbf{U}_4 \mathbf{U}_3 \mathbf{H} \mathbf{U}_2 \mathbf{U}_1 - \mathbf{I}_6) \mathbf{Z}_{8,1} = \mathbf{0} \quad (11.46)$$

The characteristic equation is

$$|\mathbf{H} \mathbf{U}_8 \mathbf{U}_7 \mathbf{H} \mathbf{U}_6 \mathbf{U}_5 \mathbf{H} \mathbf{U}_4 \mathbf{U}_3 \mathbf{H} \mathbf{U}_2 \mathbf{U}_1 - \mathbf{I}_6| = 0 \quad (11.47)$$

The natural frequencies $\omega_k (k=1,2,\dots)$ of the system can be determined by solving Equation (11.47), and $\mathbf{Z}_{8,1}$ is obtained by Equation (11.46). The state vectors at each point can be evaluated by the transfer equations of every element. Since the state vectors are not defined in the same coordinate system, they must be transformed to the common coordinate system $oxyz$ when computing the mode shapes by the state vectors. Because the orientation of $I_1x_1y_1$ is the same as the orientation of $oxyz$, $\mathbf{Z}_{8,1}$, \mathbf{Z}_{x_1} and $\mathbf{Z}_{2,1}$ need not be transformed. The others need to be transformed according to the following relations:

$$\begin{cases} \mathbf{Z}_{2,3}, \mathbf{Z}_{x_3}, \mathbf{Z}_{4,3} \Rightarrow \mathbf{H}^{-1}\mathbf{Z}_{2,3}, \mathbf{H}^{-1}\mathbf{Z}_{x_3}, \mathbf{H}^{-1}\mathbf{Z}_{4,3} \\ \mathbf{Z}_{4,5}, \mathbf{Z}_{x_5}, \mathbf{Z}_{6,5} \Rightarrow (\mathbf{H}^{-1})^2\mathbf{Z}_{4,5}, (\mathbf{H}^{-1})^2\mathbf{Z}_{x_5}, (\mathbf{H}^{-1})^2\mathbf{Z}_{6,5} \\ \mathbf{Z}_{6,7}, \mathbf{Z}_{x_7}, \mathbf{Z}_{8,7} \Rightarrow (\mathbf{H}^{-1})^3\mathbf{Z}_{6,7}, (\mathbf{H}^{-1})^3\mathbf{Z}_{x_7}, (\mathbf{H}^{-1})^3\mathbf{Z}_{8,7} \end{cases}$$

where

$$\mathbf{H}^{-1} = \begin{bmatrix} \mathbf{H}_{1,1}^{-1} & \mathbf{O}_{3 \times 3} \\ \mathbf{O}_{3 \times 3} & \mathbf{H}_{2,2}^{-1} \end{bmatrix}, \quad \mathbf{H}_{1,1}^{-1} = \begin{bmatrix} 0 & 1 & 0 \\ -1 & 0 & 0 \\ 0 & 0 & 1 \end{bmatrix}, \quad \mathbf{H}_{2,2}^{-1} = \begin{bmatrix} 1 & 0 & 0 \\ 0 & 0 & 1 \\ 0 & -1 & 0 \end{bmatrix}$$

Example 11.1 For the system shown in Figure 11.8, only transverse vibrations perpendicular to the plane are considered and vibrations in the plane are neglected. Derive the overall transfer equation and the characteristic equation.

Solution

The coordinates and sequence numbers of the elements are set by the similarity method as before, and the state vectors are defined in the form of $\mathbf{Z} = [Z, \Theta_x, \Theta_y, M_x, M_y, Q_z]^T$ according to the difference of motion. The transfer equations are still

$$\begin{cases} \mathbf{Z}_{2,1} = \mathbf{U}_1\mathbf{Z}_{8,1}, \quad \mathbf{Z}_{2,3} = \mathbf{H}\mathbf{U}_2\mathbf{Z}_{2,1} \\ \mathbf{Z}_{4,3} = \mathbf{U}_3\mathbf{Z}_{2,3}, \quad \mathbf{Z}_{4,5} = \mathbf{H}\mathbf{U}_4\mathbf{Z}_{4,3} \\ \mathbf{Z}_{6,5} = \mathbf{U}_5\mathbf{Z}_{4,5}, \quad \mathbf{Z}_{6,7} = \mathbf{H}\mathbf{U}_6\mathbf{Z}_{6,5} \\ \mathbf{Z}_{8,7} = \mathbf{U}_7\mathbf{Z}_{6,7}, \quad \mathbf{Z}_{8,1} = \mathbf{H}\mathbf{U}_8\mathbf{Z}_{8,7} \end{cases} \quad (11.48)$$

but the transfer matrices and coordinate transformation matrices mentioned above are different. According to Chapter 2 and the form of current state vectors, the transfer equations of elements can be obtained

$$\mathbf{U}_i = \begin{bmatrix} S(\lambda_z x_i) & 0 & -\frac{T(\lambda_z x_i)}{\lambda_z} & 0 & -\frac{U(\lambda_z x_i)}{EI_i \lambda_z^2} & \frac{V(\lambda_z x_i)}{EI_i \lambda_z^3} \\ 0 & u_{22} & 0 & u_{24} & 0 & 0 \\ -\lambda_z V(\lambda_z x_i) & 0 & S(\lambda_z x_i) & 0 & \frac{T(\lambda_z x_i)}{EI_i \lambda_z} & -\frac{U(\lambda_z x_i)}{EI_i \lambda_z^2} \\ 0 & u_{42} & 0 & u_{44} & 0 & 0 \\ -EI_i \lambda_z^2 U(\lambda_z x_i) & 0 & EI_i \lambda_z V(\lambda_z x_i) & 0 & S(\lambda_z x_i) & -\frac{T(\lambda_z x_i)}{\lambda_z} \\ EI_i \lambda_z^3 T(\lambda_z x_i) & 0 & -EI_i \lambda_z^2 U(\lambda_z x_i) & 0 & -\lambda_z V(\lambda_z x_i) & S(\lambda_z x_i) \end{bmatrix}_{x_i = l_i} \quad (i = 1, 3, 5, 7) \quad (11.49)$$

where

$$\begin{aligned}
 u_{22} = u_{44} = \cos \gamma_{\theta_x} x_i, u_{24} = \frac{\sin \gamma_{\theta_x} x_i}{\gamma_{\theta_x} (GJ_p)_i}, u_{42} = -\gamma_{\theta_x} (GJ_p)_i \sin \gamma_{\theta_x} x_i \\
 \gamma_{\theta_x} = \sqrt{(\rho J_p)_i \omega^2 / (GJ_p)_i}, \lambda_z = \sqrt[4]{\bar{m}_i \omega^2 / (EI_i)} \\
 \mathbf{U}_i = \begin{bmatrix} 1 & b_2 & -b_1 & 0 & 0 & 0 \\ 0 & 1 & 0 & 0 & 0 & 0 \\ 0 & 0 & 1 & 0 & 0 & 0 \\ m_i \omega^2 (b_2 - c_{c2}) & u_{42} & u_{43} & 1 & 0 & b_2 \\ -m_i \omega^2 (b_1 - c_{c1}) & u_{52} & u_{53} & 0 & 1 & -b_1 \\ m_i \omega^2 & m_i \omega^2 c_{c2} & -m_i \omega^2 c_{c1} & 0 & 0 & 1 \end{bmatrix} \quad (i = 2, 4, 6, 8) \quad (11.50)
 \end{aligned}$$

where

$$\begin{aligned}
 u_{42} = -\omega^2 [J_{i,x} - m_i (b_2 c_{c2} + b_3 c_{c3})], u_{43} = -\omega^2 (J_{i,xy} + m_i b_2 c_{c1}) \\
 u_{52} = -\omega^2 (J_{i,xy} + m_i b_1 c_{c2}), u_{53} = -\omega^2 [J_{i,y} - m_i (b_3 c_{c3} + b_1 c_{c1})] \\
 \mathbf{H} = \begin{bmatrix} \mathbf{H}_{1,1} & \mathbf{O}_{3 \times 3} \\ \mathbf{O}_{3 \times 3} & \mathbf{H}_{2,2} \end{bmatrix}, \mathbf{H}_{1,1} = \begin{bmatrix} 1 & 0 & 0 \\ 0 & 0 & -1 \\ 0 & 1 & 0 \end{bmatrix}, \mathbf{H}_{2,2} = \begin{bmatrix} 0 & -1 & 0 \\ 1 & 0 & 0 \\ 0 & 0 & 1 \end{bmatrix} \quad (11.51)
 \end{aligned}$$

Comparing Equation (11.48) with Equation (11.45), if only the transverse vibration perpendicular to the plane is considered, the expression of the overall transfer equation and characteristic equation are the same as the expressions of Equations (11.46) and (11.47).

11.7.2 Dynamics of a Closed-Loop Multibody System

The closed-loop multibody system shown in Figure 11.9 can be regarded as a chain system with the same input and output state vectors. Hence

$$\mathbf{z}_{n,1} = \mathbf{U} \mathbf{z}_{n,1} \quad (11.52)$$

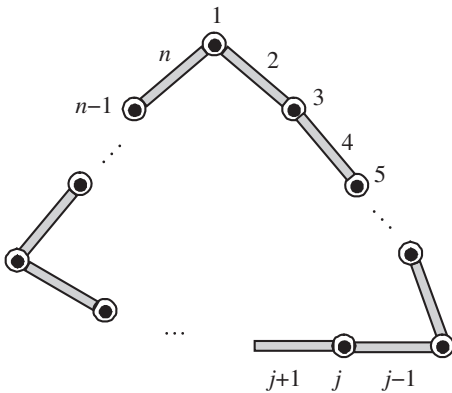
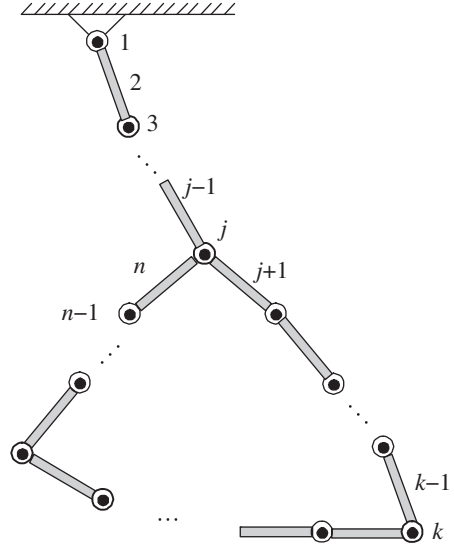


Figure 11.9 A closed-loop multibody system.

Figure 11.10 A multibody system with a closed-loop structure.



where

$$\mathbf{U} = \mathbf{U}_n \mathbf{U}_{n-1} \cdots \mathbf{U}_j \cdots \mathbf{U}_3 \mathbf{U}_2 \mathbf{U}_1 \quad (11.53)$$

The overall transfer equation of the system is

$$(\mathbf{U} - \mathbf{I}) \mathbf{z}_{n,1} = \mathbf{0} \quad (11.54)$$

and the overall transfer matrix of the system is

$$\mathbf{U}_{\text{all}} = \mathbf{U} - \mathbf{I} \quad (11.55)$$

It can be seen that the solution process of a closed-loop multibody system using the MSDTTMM is as easy as for a chain multibody system.

For the closed-loop multibody system shown in Figure 11.10, we obtain

$$\begin{cases} \mathbf{z}_{j-1,j} = \mathbf{U}_I \mathbf{z}_{2,1} \\ \mathbf{z}_{n,j} = \mathbf{U}_{II} \mathbf{z}_{j+1,j} \end{cases} \quad (11.56)$$

where

$$\begin{cases} \mathbf{U}_I = \mathbf{U}_{j-1} \mathbf{U}_{j-2} \cdots \mathbf{U}_3 \mathbf{U}_2 \mathbf{U}_1 \\ \mathbf{U}_{II} = \mathbf{U}_n \mathbf{U}_{n-1} \cdots \mathbf{U}_{j+1} \end{cases} \quad (11.57)$$

The boundary conditions are

$$\begin{cases} \mathbf{z}_{2,1} = [0, 0, \theta, 0, q_x, q_y, 1]^T_{2,1} \\ \mathbf{z}_{j+1,j} = [x, y, \theta, 0, q_x, q_y, 1]^T_{j+1,j} \end{cases} \quad (11.58)$$

If element j is a smooth hinge, according to the continuous condition of position coordinate and the equilibrium of forces, we can obtain

$$\begin{cases} \mathbf{z}_{j-1,j}(1) = \mathbf{z}_{j+1,j}(1) = \mathbf{z}_{n,j}(1) \\ \mathbf{z}_{j-1,j}(2) = \mathbf{z}_{j+1,j}(2) = \mathbf{z}_{n,j}(2) \\ \mathbf{z}_{j-1,j}(5) - \mathbf{z}_{j+1,j}(5) + \mathbf{z}_{n,j}(5) = 0 \\ \mathbf{z}_{j-1,j}(6) - \mathbf{z}_{j+1,j}(6) + \mathbf{z}_{n,j}(6) = 0 \\ \mathbf{z}_{j-1,j}(4) = \mathbf{z}_{n,j}(4) = 0 \end{cases} \quad (11.59)$$

Hence,

$$\begin{cases} \mathbf{U}_{b1} \mathbf{U}_I \mathbf{z}_{2,1} = \mathbf{U}_{b1} \mathbf{z}_{j+1,j} - \mathbf{U}_{b1} \mathbf{U}_{II} \mathbf{z}_{j+1,j} \\ \mathbf{U}_{b2} \mathbf{U}_I \mathbf{z}_{2,1} = \mathbf{U}_{b2} \mathbf{z}_{j+1,j} = \mathbf{U}_{b2} \mathbf{U}_{II} \mathbf{z}_{j+1,j} \\ \mathbf{U}_{b3} \mathbf{U}_I \mathbf{z}_{2,1} = \mathbf{0} \\ \mathbf{U}_{b3} \mathbf{U}_{II} \mathbf{z}_{j+1,j} = \mathbf{0} \end{cases} \quad (11.60)$$

The overall transfer equation of the system is

$$\mathbf{U}_{all} \begin{bmatrix} \mathbf{z}_{2,1}^T & \mathbf{z}_{j+1,j}^T \end{bmatrix}^T = \mathbf{0} \quad (11.61)$$

The overall transfer matrix of the system is

$$\mathbf{U}_{all} = \begin{bmatrix} \mathbf{U}_{b1} \mathbf{U}_I & -\mathbf{U}_{b1} (\mathbf{I}_7 - \mathbf{U}_{II}) \\ \mathbf{U}_{b2} \mathbf{U}_I & -\mathbf{U}_{b2} \\ \mathbf{O}_{2 \times 7} & \mathbf{U}_{b2} (\mathbf{I}_7 - \mathbf{U}_{II}) \\ \mathbf{U}_{b3} \mathbf{U}_I & \mathbf{O}_{1 \times 7} \\ \mathbf{O}_{1 \times 7} & \mathbf{U}_{b3} \mathbf{U}_{II} \end{bmatrix} \quad (11.62)$$

Example 11.2 In this example, we solve the dynamics of the multi-rigid-body system with closed-loop structure under the effect of gravity, as shown in Figure 11.11. The length of bar 10 is $\sqrt{3}\text{m}$, bars 2, 4, 6 and 8 are all 1 m and the mass centers are the geometrical centers of each bar. The moment of inertia of bar 4 with respect to the input is $\sqrt{3}\text{kg}\cdot\text{m}^2$, the others are $1/3\text{kg}\cdot\text{m}^2$. The initial velocities of the five bars are zeros and the initial angles of the bars are $-\pi/3$, $-\pi/3$, $-\pi/3$, $-\pi$ and $\pi/2$.

Solution

The overall transfer equation of the system can be obtained using the MSDTTMM:

$$\mathbf{U}_{all} \begin{bmatrix} \mathbf{z}_{2,1}^T & \mathbf{z}_{4,3}^T \end{bmatrix}^T = \mathbf{0} \quad (11.63)$$

The overall transfer matrix of the system is

$$\mathbf{U}_{all} = \begin{bmatrix} \mathbf{U}_{b1} \mathbf{U}_I & \mathbf{U}_{b1} (\mathbf{I}_7 - \mathbf{U}_{II}) \\ \mathbf{U}_{b2} \mathbf{U}_I & -\mathbf{U}_{b2} \\ \mathbf{O}_{2 \times 7} & \mathbf{U}_{b2} (\mathbf{I}_7 - \mathbf{U}_{II}) \\ \mathbf{U}_{b3} \mathbf{U}_I & \mathbf{O}_{1 \times 7} \\ \mathbf{O}_{1 \times 7} & \mathbf{U}_{b3} \mathbf{U}_{II} \end{bmatrix} \quad (11.64)$$

The dynamics of the multibody system are computed using the MSDTTMM and the Newton–Euler method. The computational results for the two methods are shown in Figure 11.12 and are in good agreement.

Example 11.3 A tree MRFS moving in a plane, as shown in Figure 11.13, consists of two fixed hinges 2 and 4, two elastic hinges 6 and 7, three rigid bodies 1, 5 and 8, and one uniform beam element 3, with three boundary ends. The simulation parameters are $m_1 = m_5 = m_8 = 7.8 \text{ kg}$, $J_{C,1} = J_{C,5} = J_{C,8} = 0.013 \text{ kg}\cdot\text{m}^2$, $l_3 = 3 \text{ m}$, $EA_3 = 1000 \text{ N}$, $\bar{m}_3 = 0.78 \text{ kg/m}$, $El_3 = 166.67 \text{ N}\cdot\text{m}^2$, $K_{x,6} = K_{x,7} = 1000 \text{ N/m}$, $K_{y,6} = K_{y,7} = 500 \text{ N/m}$ and $K'_6 = K'_7 = 150 \text{ N}\cdot\text{m/rad}$.

Solution

According to the theorem to deduce the overall transfer equation of a multibody system automatically, the topology figure of the system can be found as shown in Figure 11.14, and the overall transfer equation of the system can be deduced automatically and denoted as

$$\mathbf{U}_{\text{all}} \mathbf{z}_{\text{all}} = \mathbf{0} \quad (0.62)$$

where the overall transfer matrix is

$$\mathbf{U}_{\text{all}} = \begin{bmatrix} -\mathbf{I} & \mathbf{T}_{6-1} & \mathbf{T}_{8-1} \\ \mathbf{O} & \mathbf{G}_{6-5} & \mathbf{G}_{8-5} \end{bmatrix} \quad (0.63)$$

The state vectors of all the boundary ends are

$$\mathbf{z}_{\text{all}} = \begin{bmatrix} \mathbf{z}_{1,0} \\ \mathbf{z}_{6,0} \\ \mathbf{z}_{8,0} \end{bmatrix} \quad (0.64)$$

According to the proposed sign conventions, we know that

$$\mathbf{T}_{6-1} = \mathbf{U}_1 \mathbf{U}_2 \mathbf{U}_3 \mathbf{U}_4 \mathbf{U}_5 \mathbf{U}_6 \quad (0.65)$$

$$\mathbf{T}_{8-1} = \mathbf{U}_1 \mathbf{U}_2 \mathbf{U}_3 \mathbf{U}_4 \mathbf{U}_{5,7} \mathbf{U}_7 \mathbf{U}_8$$

$$\mathbf{G}_{6-5} = -\mathbf{H}_5 \mathbf{U}_6 \quad (0.66)$$

$$\mathbf{G}_{8-5} = \mathbf{H}_{5,7} \mathbf{U}_7 \mathbf{U}_8$$

$\mathbf{z}_{1,0}$ is state vector of the root, $\mathbf{z}_{6,0}$ and $\mathbf{z}_{8,0}$ are the state vectors of the tips, and $\mathbf{U}_1, \mathbf{U}_2, \mathbf{U}_3, \mathbf{U}_4, \mathbf{U}_5, \mathbf{U}_{5,7}, \mathbf{U}_6, \mathbf{U}_7$ and \mathbf{U}_8 are the transfer matrices of body 1, fixed hinge 2, uniform beam 3, fixed hinge 4, body 5, elastic hinge 6, elastic hinge 7 and body 8, respectively.

The boundary conditions of the system are

$$\begin{aligned} \mathbf{z}_{1,0} &= [\ddot{x} \ \ddot{y} \ \ddot{\theta}_z \ 0 \ 0 \ 0 \ 1]^T_{1,0} \\ \mathbf{z}_{6,0} &= [0 \ 0 \ 0 \ m_z \ q_x \ q_y \ 1]^T_{6,0} \\ \mathbf{z}_{8,0} &= [\ddot{x} \ \ddot{y} \ \ddot{\theta}_z \ 0 \ 0 \ 0 \ 1]^T_{8,0} \end{aligned} \quad (0.67)$$

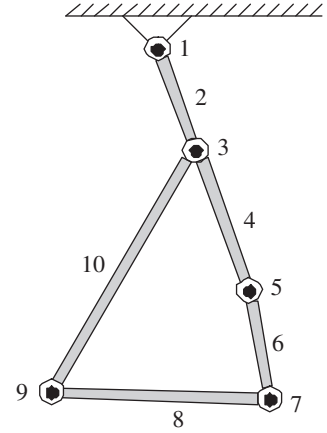


Figure 11.11 A multi-rigid-body system with a closed-loop structure.

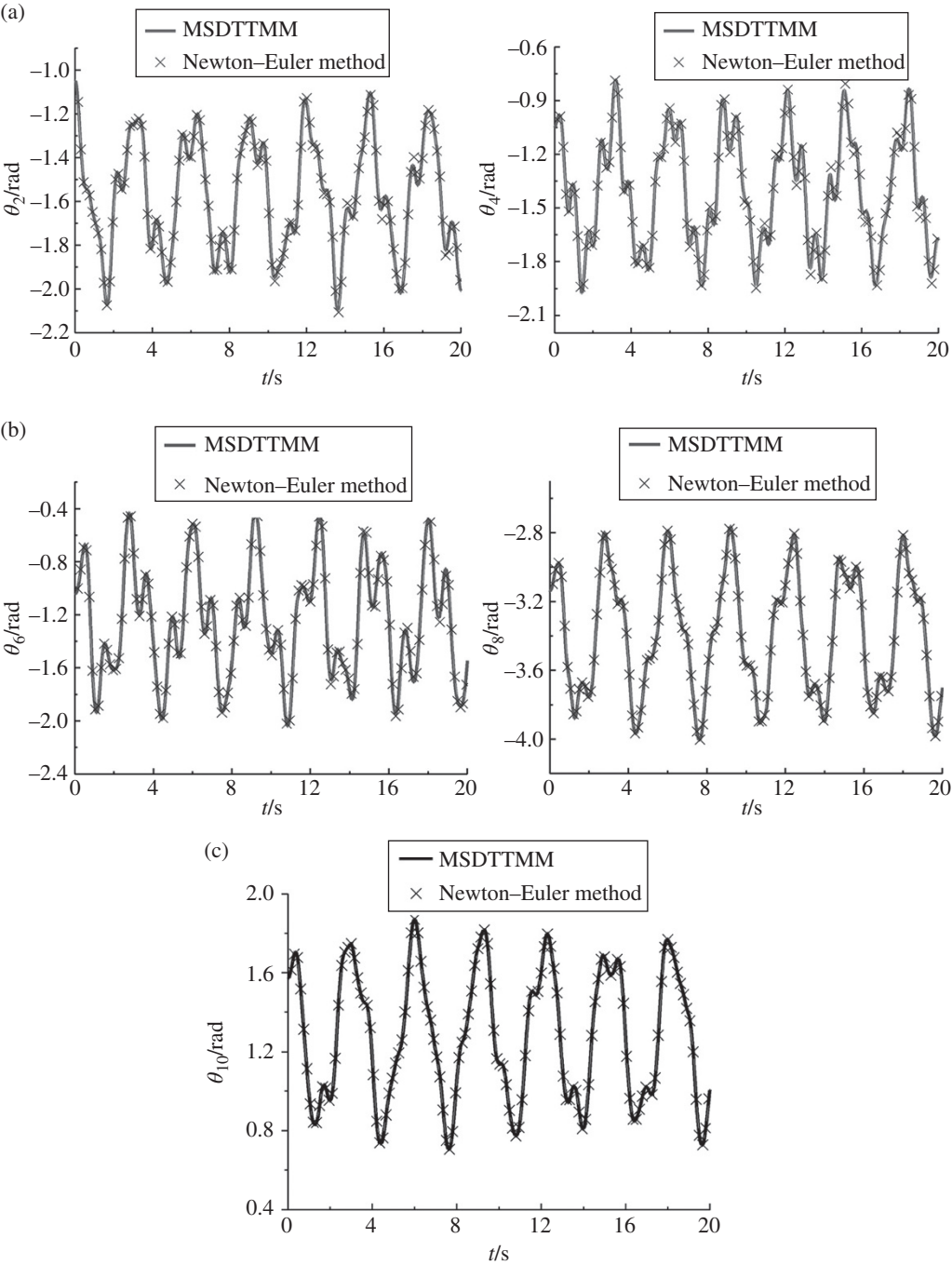


Figure 11.12 Time history of orientation angles of closed-loop multibody systems: (a) computational results of the time history of the orientation angles of rigid body 2 and rigid body 4, (b) computational results of the time history of the orientation angles of rigid body 6 and rigid body 8 and (c) computational results of the time history of the orientation angle of rigid body 10.

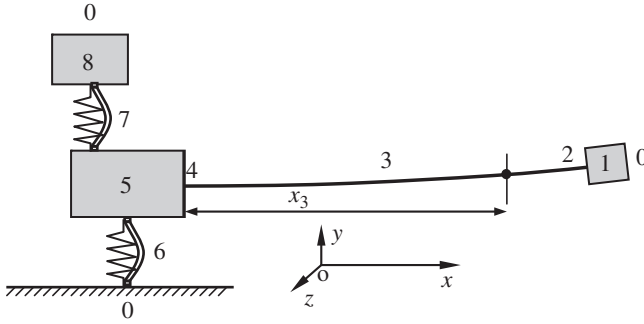


Figure 11.13 Tree MRFS.

The system experiences a step upward force at the mass center of body element 1 at time instant zero while the initial displacement and velocity of the whole system are zero. The computational results of the system dynamics obtained by the proposed method and by the Newton–Euler method are shown in Figure 11.15. It can be seen that the computational results obtained by these two methods are in good agreement.

11.8 Numerical Example of Tree System Dynamics

11.8.1 Vibration Characteristics of Tree Systems

For a branched MRFS, the MSTMM is very effective. To study the dynamic problems of a branched MRFS, the solution steps are the same as for the chain system. For each connection point, the geometric equations and the equilibrium equations need to be formulated according to the geometric relations and equilibrium conditions, respectively.

11.8.1.1 Another Form of Characteristic Equation

If the number of elements in a chain system is n , the overall transfer equation of the system is

$$\mathbf{Z}_{n,0} = \mathbf{U}\mathbf{Z}_{1,0} \quad (11.68)$$

which can be written as

$$\mathbf{U}\mathbf{Z}_{1,0} - \mathbf{Z}_{n,0} = \mathbf{0} \quad (11.69)$$

Let $\mathbf{Z}_{\text{all}} = \begin{bmatrix} \mathbf{Z}_{1,0}^T & \mathbf{Z}_{n,0}^T \end{bmatrix}^T$ and $\mathbf{U}_{\text{all}} = [\mathbf{U} \quad -\mathbf{I}]$. Then Equation (11.69) turns into

$$\mathbf{U}_{\text{all}}\mathbf{Z}_{\text{all}} = \mathbf{0} \quad (11.70)$$

\mathbf{Z}_{all} is composed of $\mathbf{Z}_{1,0}$ and $\mathbf{Z}_{n,0}$, which are both state vectors at the boundary of the system, and half of the elements in \mathbf{Z}_{all} are zeros according to the boundary conditions. We delete the null elements of \mathbf{Z}_{all} and define the column vector composed of the remainder as $\bar{\mathbf{Z}}_{\text{all}}$. At the

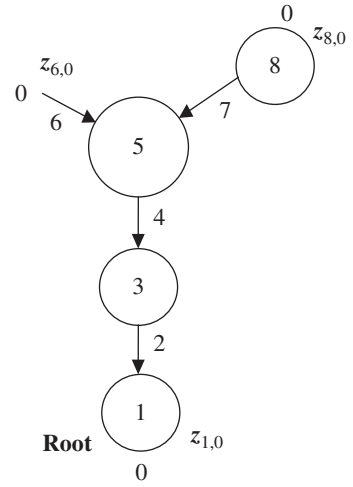


Figure 11.14 Topology figure of the tree MRFS.

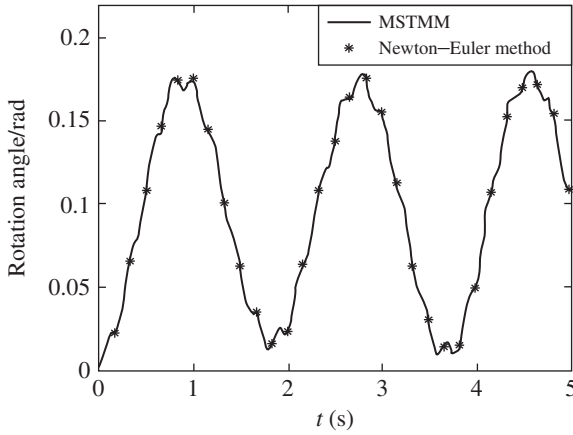


Figure 11.15 Computational results of the angle of the right end of the beam.

same time we delete the corresponding columns of \mathbf{U}_{all} and define the remainder as $\bar{\mathbf{U}}_{\text{all}}$, which is a square matrix, thus

$$\bar{\mathbf{U}}_{\text{all}} \bar{\mathbf{Z}}_{\text{all}} = \mathbf{0} \quad (11.71)$$

$\bar{\mathbf{Z}}_{\text{all}}$ is composed of the unknown elements. If the homogeneous equation has a nonzero solutions, there must be

$$\Delta = |\bar{\mathbf{U}}_{\text{all}}| = 0 \quad (11.72)$$

Equation (11.72) is another form of the characteristic equation. It can be proved that the equation has the same solutions as the characteristic equation $|\mathbf{U}'| = 0$ obtained from $\mathbf{U}' \mathbf{Z}'_{1,0} = \mathbf{0}$ in the chain system, but the order number of $\bar{\mathbf{U}}_{\text{all}}$ is higher than that of \mathbf{U}' . We can obtain \mathbf{U}' in the chain system. For other complex systems, we cannot obtain \mathbf{U}' , only $\bar{\mathbf{U}}_{\text{all}}$.

11.8.1.2 Characteristic Equation of a Tree System

The branched MRFS in Figure 11.16 is composed of two elastic hinges, two rigid bodies and a beam with a uniform cross-section vibrating in a plane. It also has three boundary points. The right-hand side of the beam is defined as the output end of the system, and the other two boundary points are input ends. Let the point connected with the ground be the first input end, and the other point be the second input end.

The sequence numbers of the elements are shown in Figure 11.16, and the system is composed of five elements, that is, $n = 5$, in two transfer directions. The elements are numbered 5, 4, 3 and 2 sequentially along the direction from the output end to the second input end. The elastic hinge between element 4 and the ground is numbered 1, the boundaries at both input ends are

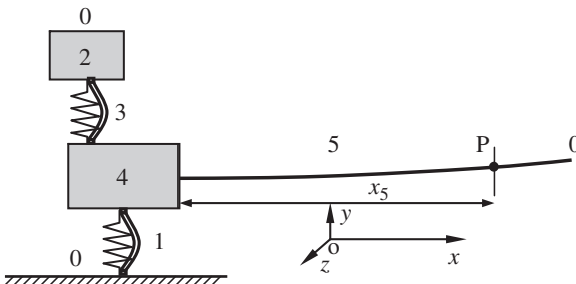


Figure 11.16 A branched MRFS.

numbered 0 and the boundary at the output end is numbered $n + 1 = 6$. The state vectors $\mathbf{Z}_{1,0}$, $\mathbf{Z}_{4,1}$, $\mathbf{Z}_{2,0}$, $\mathbf{Z}_{2,3}$, $\mathbf{Z}_{4,3}$, $\mathbf{Z}_{4,5}$, \mathbf{Z}_{x_5} and $\mathbf{Z}_{5,0}$ are defined in the form of $\mathbf{Z} = [X, Y, \Theta_z, M_z, Q_x, Q_y]^T$, therefore the transfer equations are

$$\mathbf{Z}_{4,1} = \mathbf{U}_1 \mathbf{Z}_{1,0}, \quad \mathbf{Z}_{2,3} = \mathbf{U}_2 \mathbf{Z}_{2,0}, \quad \mathbf{Z}_{4,3} = \mathbf{U}_3 \mathbf{Z}_{2,3} = \mathbf{U}_3 \mathbf{U}_2 \mathbf{Z}_{2,0}, \quad \mathbf{Z}_{5,0} = \mathbf{U}_5 \mathbf{Z}_{4,5} \quad (11.73)$$

where \mathbf{U}_1 and \mathbf{U}_3 are the transfer matrices of the planar elastic hinges, \mathbf{U}_2 is the transfer matrix of the rigid body with one input end and one output end, and \mathbf{U}_5 is the transfer matrix of a beam with transverse and longitudinal vibrations.

$$\mathbf{U}_i = \begin{bmatrix} \mathbf{I}_3 & \mathbf{U}_{1,2} \\ \mathbf{O}_{3 \times 3} & \mathbf{I}_3 \end{bmatrix}, \quad \mathbf{U}_{1,2} = \begin{bmatrix} 0 & -\frac{1}{K_{x,i}} & 0 \\ 0 & 0 & -\frac{1}{K_{y,i}} \\ \frac{1}{K'_{z,i}} & 0 & 0 \end{bmatrix}, \quad (i = 1, 3) \quad (11.74)$$

$$\mathbf{U}_2 = \begin{bmatrix} 1 & 0 & -b_2 & 0 & 0 & 0 \\ 0 & 1 & b_1 & 0 & 0 & 0 \\ 0 & 0 & 1 & 0 & 0 & 0 \\ -m_2 \omega^2 (b_2 - c_{c2}) & m_2 \omega^2 (b_1 - c_{c1}) & -\omega^2 [J_i - m_2 (b_2 c_{c2} + b_1 c_{c1})] & 1 & -b_2 & b_1 \\ m_2 \omega^2 & 0 & -m_2 \omega^2 c_{c2} & 0 & 1 & 0 \\ 0 & m_2 \omega^2 & m_2 \omega^2 c_{c1} & 0 & 0 & 1 \end{bmatrix} \quad (11.75)$$

$$\mathbf{U}_5 = \begin{bmatrix} u_{11} & 0 & 0 & 0 & u_{15} & 0 \\ 0 & S(\lambda_y x_5) & \frac{T(\lambda_y x_5)}{\lambda_y} & \frac{U(\lambda_y x_5)}{EI_5 \lambda_y^2} & 0 & \frac{V(\lambda_y x_5)}{EI_5 \lambda_y^3} \\ 0 & \lambda_y V(\lambda_y x_5) & S(\lambda_y x_5) & \frac{T(\lambda_y x_5)}{EI_5 \lambda_y} & 0 & \frac{U(\lambda_y x_5)}{EI_5 \lambda_y^2} \\ 0 & EI_5 \lambda_y^2 U(\lambda_y x_5) & EI_5 \lambda_y V(\lambda_y x_5) & S(\lambda_y x_5) & 0 & \frac{T(\lambda_y x_5)}{\lambda_y} \\ u_{51} & 0 & 0 & 0 & u_{55} & 0 \\ 0 & EI_5 \lambda_y^3 T(\lambda_y x_5) & EI_5 \lambda_y^2 U(\lambda_y x_5) & \lambda_y V(\lambda_y x_5) & 0 & S(\lambda_y x_5) \end{bmatrix}_{x_5 = l_5} \quad (11.76)$$

$$u_{11} = u_{55} = \cos \beta_x x_5, \quad u_{15} = \frac{-\sin \beta_x x_5}{\beta_x EA_5}, \quad u_{51} = \beta_x EA_5 \sin \beta_x x_5$$

Here (b_1, b_2) and (c_{c1}, c_{c2}) are the position coordinates of the output end and mass center, respectively, in the body-fixed coordinate system in which the input end is the origin, $\beta_x = \sqrt{\bar{m}_5 \omega^2 / (EA_5)}$ and $\lambda_y = \sqrt[4]{\bar{m}_5 \omega^2 / (EI_5)}$.

Element 4 is a rigid body with two input ends and one output end, and the state vectors are $\mathbf{Z}_{4,1}$ and $\mathbf{Z}_{4,3}$ at the two input ends. The state vector $\mathbf{Z}_{l,4}$ at the input end is defined as

$$\mathbf{Z}_{l,4} = [X_{4,1}, Y_{4,1}, \Theta_{z4,1}, M_{z4,1}, Q_{x4,1}, Q_{y4,1}, M_{z4,3}, Q_{x4,3}, Q_{y4,3}]^T = \mathbf{E}_1 \mathbf{Z}_{4,1} + \mathbf{E}_2 \mathbf{Z}_{4,3} \quad (11.77)$$

where

$$E_1 = \begin{bmatrix} I_6 \\ O_{3 \times 6} \end{bmatrix}, \quad E_2 = \begin{bmatrix} O_{6 \times 3} & O_{6 \times 3} \\ O_{3 \times 3} & I_3 \end{bmatrix}$$

Therefore, the transfer equation of element 4 is

$$Z_{4,5} = U_4 Z_{I,4} \quad (11.78)$$

$$U_4 = \begin{bmatrix} 1 & 0 & -b_2 & 0 & 0 & 0 & 0 & 0 & 0 \\ 0 & 1 & b_1 & 0 & 0 & 0 & 0 & 0 & 0 \\ 0 & 0 & 1 & 0 & 0 & 0 & 0 & 0 & 0 \\ u_{41} & u_{42} & u_{43} & 1 & -b_2 & b_1 & 1 & -(b_2 - a_{2,2}) & b_1 - a_{1,2} \\ m_4 \omega^2 & 0 & -m_4 \omega^2 c_{c2} & 0 & 1 & 0 & 0 & 1 & 0 \\ 0 & m_4 \omega^2 & m_4 \omega^2 c_{c1} & 0 & 0 & 1 & 0 & 0 & 1 \end{bmatrix} \quad (11.79)$$

where (b_1, b_2) and (c_{c1}, c_{c2}) are the position coordinates of the output end and the mass center of rigid body 4 in the body-fixed coordinate system, respectively, and the first input end is the origin of the body-fixed coordinate system. $(a_{1,2}, a_{2,2})$ are the position coordinates of the second input end of rigid body 4 in the body-fixed coordinate system, and the detailed expressions of u_{41} , u_{42} and u_{43} are $u_{41} = -m_4 \omega^2 (b_2 - c_{c2})$, $u_{42} = m_4 \omega^2 (b_1 - c_{c1})$ and $u_{43} = -\omega^2 [J_4 - m_4 (b_2 c_{c2} + b_1 c_{c1})]$, respectively.

According to Equations (11.73), (11.74) and (11.78), we have

$$Z_{5,0} = U_5 Z_{4,5} = U_5 U_4 Z_{I,4} = U_5 U_4 (E_1 Z_{4,1} + E_2 Z_{4,3}) = U_5 U_4 (E_1 U_1 Z_{1,0} + E_2 U_3 U_2 Z_{2,0})$$

that is

$$U_5 U_4 E_1 U_1 Z_{1,0} + U_5 U_4 E_2 U_3 U_2 Z_{2,0} - Z_{5,0} = 0 \quad (11.80)$$

In addition, there are relations between the three elements denoting the displacement in $Z_{4,3}$ and $Z_{4,1}$, that is

$$E_3 Z_{4,3} = E_4 Z_{4,1} \quad (11.81)$$

where

$$E_3 = \begin{bmatrix} I_3 & O_{3 \times 3} \end{bmatrix}, \quad E_4 = \begin{bmatrix} 1 & 0 & -a_{2,2} \\ 0 & 1 & a_{1,2} & O_{3 \times 3} \\ 0 & 0 & 1 \end{bmatrix}$$

therefore

$$E_4 U_1 Z_{1,0} - E_3 U_3 U_2 Z_{2,0} = 0 \quad (11.82)$$

Combining Equations (11.80) and (11.82) yields

$$U_{\text{all}} Z_{\text{all}} = 0$$

where

$$U_{\text{all}} = \begin{bmatrix} U_5 U_4 E_1 U_1 & U_5 U_4 E_2 U_3 U_2 & -I_6 \\ E_4 U_1 & -E_3 U_3 U_2 & O_{3 \times 6} \end{bmatrix}_{9 \times 18}, \quad Z_{\text{all}} = \begin{bmatrix} Z_{0,1} \\ Z_{2,0} \\ Z_{5,6} \end{bmatrix}_{18 \times 1} \quad (11.83)$$

According to the boundary conditions

$$\begin{cases} \mathbf{Z}_{1,0} = [0, 0, 0, M_z, Q_x, Q_y]^T_{1,0} \\ \mathbf{Z}_{2,0} = [X, Y, \theta_z, 0, 0, 0]^T_{2,0} \\ \mathbf{Z}_{5,0} = [X, Y, \theta_z, 0, 0, 0]^T_{5,0} \end{cases} \quad (11.84)$$

The 1st, 2nd, 3rd, 10th, 11th, 12th, 16th, 17th and 18th elements of \mathbf{Z}_{all} are zero. These null elements are deleted from \mathbf{Z}_{all} and the corresponding columns are deleted from \mathbf{U}_{all} , therefore

$$\bar{\mathbf{U}}_{\text{all}} \bar{\mathbf{Z}}_{\text{all}} = \mathbf{0} \quad (11.85)$$

$9 \times 9 \quad 9 \times 1$

The characteristic equation is

$$\Delta = |\bar{\mathbf{U}}_{\text{all}}| = 0 \quad (11.86)$$

11.8.1.3 Mode Shapes of Tree Systems

The natural frequencies $\omega_k (k=1,2,\dots)$ of the system can be obtained by solving Equation (11.86). For each ω_k the corresponding boundary state vectors $\mathbf{Z}_{1,0}$, $\mathbf{Z}_{2,0}$ and $\mathbf{Z}_{5,0}$ can be determined by solving Equation (11.85). Consequently, the state vectors of the other connection points can be evaluated, and the state vectors at arbitrary positions of the beam can be computed from the transfer equation $\mathbf{Z}_{x_5} = \mathbf{U}_{x_5} \mathbf{Z}_{4,5}$. Thus, the mode shape of the system is acquired. When solving the vibration characteristics of the tree system, the method is the same as that of the chain system, and both have the same procedure.

Example 11.4 As shown in Figure 11.16, the rigid bodies 2 and 4 have the same form with width $b = 0.1\text{m}$ and height $h = 0.1\text{m}$. The input end $P_{2,0}$ of rigid body 2 is located at the middle of its upper surface, therefore $(b_1, b_2)_2 = (0, -h)$, $(c_{c1}, c_{c2})_2 = (0, -h/2)$ and $J_2 = m_2(b^2 + 4h^2)/12$. The first input end of rigid body 4 is $P_{1,4}$, and it is located in the middle of its bottom surface. The output end $P_{4,5}$ is in the middle of the right-hand side, hence $(c_{c1}, c_{c2})_4 = (0, h/2)$, $(b_1, b_2)_4 = (b/2, h/2)$ and $J_4 = m_4(b^2 + 4h^2)/12$, and the second input is $P_{3,4}$ on the top left corner so $(a_{1,2}, a_{2,2})_4 = (-b/2, h)$. Let $K_{x,1} = K_{x,3} = 1000 \text{ N/m}$, $K_{y,1} = K_{y,3} = 500 \text{ N/m}$, $l_5 = 3 \text{ m}$, $EA_5 = 1000 \text{ N}$, $\bar{m}_5 = 0.78 \text{ kg/m}$, $K'_1 = K'_3 = 150 \text{ N}\cdot\text{m/rad}$, $EI_5 = 166.67 \text{ N}\cdot\text{m}^2$ and $m_2 = m_4 = 7.8 \text{ kg}$. Find the vibration characteristics of the system and plot the mode shapes.

Solution

Substituting these parameters into Equations (11.73) to (11.86), the vibration characteristics of the system can be obtained. The first eight natural frequencies are shown in Table 11.1 and the corresponding mode shapes are shown in Figure 11.17.

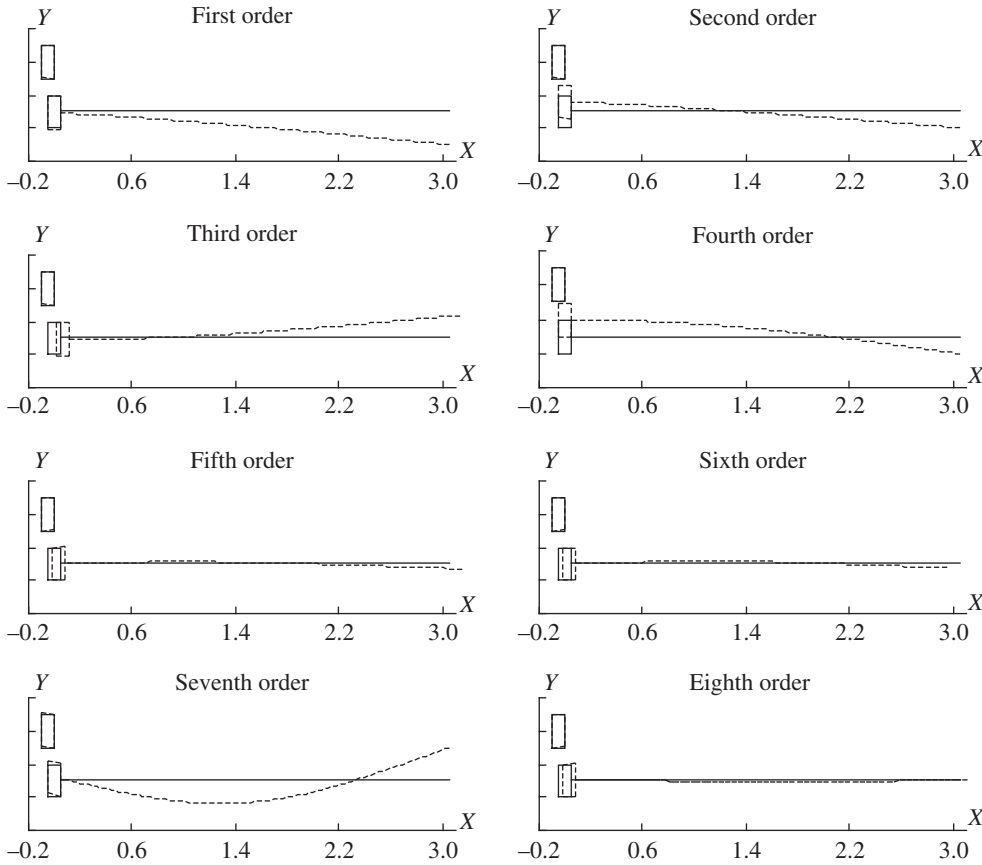
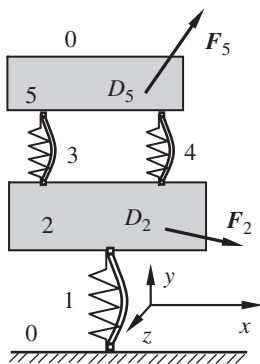
11.8.2 Dynamics of Tree Multibody Systems

11.8.2.1 Solve the Steady-state Response of an MRFS under Harmonic Excitation using the Extended MSTMM

Some simple chain systems were discussed in Chapter 2. The general systems will be studied using this method in the following.

Table 11.1 Computational results of natural frequencies

Mode k	1	2	3	4	5	6	7	8
$\omega_k/(\text{rad/s})$	3.423	4.965	6.649	12.614	15.105	22.818	28.109	57.056


Figure 11.17 Mode shapes.

Figure 11.18 Planar MRFS composed of two rigid bodies and three elastic hinges.

The planar MRFS shown in Figure 11.18 is composed of two rigid bodies and three elastic hinges. The elastic hinges have viscous damping with coefficients $C_{x,i}$, $C_{y,i}$ and $C'_{z,i}$ ($j = 1, 3, 4$), respectively, along the x and y directions as well as rotation about the z direction. Two rigid bodies are excited to harmonic forces acting on points D_2 and D_5 :

$$\mathbf{F}_2 = \mathbf{F}_2^c \cos \Omega t + \mathbf{F}_2^s \sin \Omega t, \mathbf{F}_5 = \mathbf{F}_5^c \cos \Omega t + \mathbf{F}_5^s \sin \Omega t \quad (11.87)$$

$$\mathbf{F}_2^c = \begin{bmatrix} F_{x,2}^c \\ F_{y,2}^c \end{bmatrix}, \mathbf{F}_2^s = \begin{bmatrix} F_{x,2}^s \\ F_{y,2}^s \end{bmatrix}, \mathbf{F}_5^c = \begin{bmatrix} F_{x,5}^c \\ F_{y,5}^c \end{bmatrix}, \mathbf{F}_5^s = \begin{bmatrix} F_{x,5}^s \\ F_{y,5}^s \end{bmatrix} \quad (11.88)$$

The external force is expressed in the complex form $\bar{F} = F^r + iF^i$, then

$$F = F^c \cos \Omega t + F^s \sin \Omega t = \operatorname{Re}(\bar{F} e^{i\Omega t}) = F^r \cos \Omega t - F^i \sin \Omega t$$

therefore

$$F^r = F^c, \quad F^i = -F^s$$

namely

$$\bar{F}_2 = F_2^c - iF_2^s, \quad \bar{F}_5 = F_5^c - iF_5^s \quad (11.89)$$

The extended state vectors $\hat{Z}_{1,0}, \hat{Z}_{2,1}, \hat{Z}_{2,3}, \hat{Z}_{2,4}, \hat{Z}_{5,3}, \hat{Z}_{5,4}$ and $\hat{Z}_{5,0}$ are defined as

$$\hat{Z} = \left[X^r, Y^r, \Theta_z^r, M_z^r, Q_x^r, Q_y^r, X^i, Y^i, \Theta_z^i, M_z^i, Q_x^i, Q_y^i, 1 \right]^T \quad (11.90)$$

The state vectors $\hat{Z}_{O,2}$ and $\hat{Z}_{I,5}$ are

$$\hat{Z}_{O,2} = E_1 \hat{Z}_{2,3} + E_2 \hat{Z}_{2,4}, \quad \hat{Z}_{I,5} = E_1 \hat{Z}_{5,3} + E_2 \hat{Z}_{5,4} \quad (11.91)$$

where

$$E_1 = \begin{bmatrix} I_6 & O_{6 \times 6} & O_{6 \times 1} \\ O_{3 \times 6} & O_{3 \times 6} & O_{3 \times 1} \\ O_{6 \times 6} & I_6 & O_{6 \times 1} \\ O_{4 \times 6} & O_{4 \times 6} & O_{4 \times 1} \end{bmatrix}, \quad E_2 = \begin{bmatrix} O_{6 \times 3} & O_{6 \times 3} & O_{6 \times 3} & O_{6 \times 4} \\ O_{3 \times 3} & I_3 & O_{3 \times 3} & O_{3 \times 4} \\ O_{6 \times 3} & O_{6 \times 3} & O_{6 \times 3} & O_{6 \times 4} \\ O_{4 \times 3} & O_{4 \times 3} & O_{4 \times 3} & I_4 \end{bmatrix}$$

The extended transfer equation of each element is

$$\begin{cases} \hat{Z}_{2,1} = \hat{U}_1 \hat{Z}_{1,0}, & \hat{Z}_{2,1} = \hat{U}_2 \hat{Z}_{O,2} \\ \hat{Z}_{5,3} = \hat{U}_3 \hat{Z}_{2,3}, & \hat{Z}_{5,4} = \hat{U}_4 \hat{Z}_{2,4}, \quad \hat{Z}_{5,0} = \hat{U}_5 \hat{Z}_{I,5} \end{cases} \quad (11.92)$$

where \hat{U}_1, \hat{U}_3 and \hat{U}_4 are the extended transfer matrices of hinges 1, 3 and 4, respectively. \hat{U}_2 is the extended transfer matrix of a rigid body with one input and two output ends, \hat{U}_5 is the extended transfer matrix of a rigid body with two input ends and one output end

$$\hat{U}_j = \begin{bmatrix} U^r & -U^i & O_{6 \times 1} \\ U^j & U^r & O_{6 \times 1} \\ O_{1 \times 6} & O_{1 \times 6} & 1 \end{bmatrix} \quad (j = 1, 3, 4) \quad (11.93)$$

$$U^r = \begin{bmatrix} I_3 & U_{1,2}^r \\ O_{3 \times 3} & I_3 \end{bmatrix}, \quad U^i = \begin{bmatrix} O_{3 \times 3} & U_{1,2}^i \\ O_{3 \times 3} & O_{3 \times 3} \end{bmatrix}$$

$$U_{1,2}^r = \begin{bmatrix} 0 & \frac{-K_{x,j}}{K_{x,j}^2 + C_{x,j}^2 \Omega^2} & 0 \\ 0 & 0 & \frac{-K_{y,j}}{K_{y,j}^2 + C_{y,j}^2 \Omega^2} \\ \frac{K'_{z,j}}{K_{z,j}^2 + C_{z,j}^2 \Omega^2} & 0 & 0 \end{bmatrix}$$

$$u_{1,2}^j = \begin{bmatrix} 0 & \frac{C_{x,j}\Omega}{K_{x,j}^2 + C_{x,j}^2\Omega^2} & 0 \\ 0 & 0 & \frac{C_{y,j}\Omega}{K_{y,j}^2 + C_{y,j}^2\Omega^2} \\ -\frac{C_{z,j}'\Omega}{K_{z,j}'^2 + C_{z,j}'^2\Omega^2} & 0 & 0 \end{bmatrix}$$

$$\hat{u}_2 = \begin{bmatrix} u^r & o_{6 \times 9} & f^r \\ o_{6 \times 9} & u^r & f^i \\ o_{1 \times 9} & o_{1 \times 9} & 1 \end{bmatrix} \quad (11.94)$$

$$u^r = \begin{bmatrix} 1 & 0 & b_{2,1} & 0 & 0 & 0 & 0 & 0 & 0 \\ 0 & 1 & -b_{1,1} & 0 & 0 & 0 & 0 & 0 & 0 \\ 0 & 0 & 1 & 0 & 0 & 0 & 0 & 0 & 0 \\ -m_2\Omega^2 c_{c2} & m_2\Omega^2 c_{c1} & u_{4,3} & 1 & b_{2,1} & -b_{1,1} & 1 & b_{2,2} & -b_{1,2} \\ -m_2\Omega^2 & 0 & m_2\Omega^2(c_{c2} - b_{2,1}) & 0 & 1 & 0 & 0 & 1 & 0 \\ 0 & -m_2\Omega^2 & -m_2\Omega^2(c_{c1} - b_{1,1}) & 0 & 0 & 1 & 0 & 0 & 1 \end{bmatrix}$$

$$f^r = \begin{bmatrix} o_3 \\ M_{z,2}^c - d_2 F_{x,2}^c + d_1 F_{y,2}^c \\ -F_{x,2}^c \\ -F_{y,2}^c \end{bmatrix}, \quad f^i = \begin{bmatrix} o_3 \\ -M_{z,2}^s + d_2 F_{x,2}^s - d_1 F_{y,2}^s \\ F_{x,2}^s \\ F_{y,2}^s \end{bmatrix}$$

where $u_{4,3} = \Omega^2 [j_2 - m_2(c_{c2}b_{2,1} + c_{c1}b_{1,1})]$ and (d_1, d_2) denotes the coordinates of point D_2 in the body-fixed coordinate system of rigid body 2.

$$\hat{u}_5 = \begin{bmatrix} u^r & o_{6 \times 9} & f^r \\ o_{6 \times 9} & u^r & f^i \\ o_{1 \times 9} & o_{1 \times 9} & 1 \end{bmatrix} \quad (11.95)$$

$$u^r = \begin{bmatrix} 1 & 0 & -b_2 & 0 & 0 & 0 & 0 & 0 & 0 \\ 0 & 1 & b_1 & 0 & 0 & 0 & 0 & 0 & 0 \\ 0 & 0 & 1 & 0 & 0 & 0 & 0 & 0 & 0 \\ u_{4,1} & u_{4,2} & u_{4,3} & 1 & -b_2 & b_1 & 1 & -(b_2 - a_{2,2}) & b_1 - a_{1,2} \\ m_5\Omega^2 & 0 & -m_5\Omega^2 c_{c2} & 0 & 1 & 0 & 0 & 1 & 0 \\ 0 & m_5\Omega^2 & m_5\Omega^2 c_{c1} & 0 & 0 & 1 & 0 & 0 & 1 \end{bmatrix}$$

$$\mathbf{f}^r = \begin{bmatrix} \mathbf{0}_3 \\ -M_{z,5}^c - (b_2 - d_2)F_{x,5}^c + (b_1 - d_1)F_{y,5}^c \\ F_{x,5}^c \\ F_{y,5}^c \end{bmatrix}, \quad \mathbf{f}^i = \begin{bmatrix} \mathbf{0}_3 \\ M_{z,5}^s + (b_2 - d_2)F_{x,5}^s - (b_1 - d_1)F_{y,5}^s \\ -F_{x,5}^s \\ -F_{y,5}^s \end{bmatrix}$$

where $u_{4,1} = -m_5\Omega^2(b_2 - c_{e2})$, $u_{4,2} = m_5\Omega^2(b_1 - c_{e1})$ and $u_{4,3} = -\Omega^2[J_5 - m_5(b_2c_{e2} + b_1c_{e1})]$, and (d_1, d_2) denotes the coordinates of point D_5 in the body-fixed coordinate system of rigid body 5.

According to Equation (11.83),

$$\begin{aligned} \hat{\mathbf{U}}_1\hat{\mathbf{Z}}_{1,0} - \hat{\mathbf{U}}_2\mathbf{E}_1\hat{\mathbf{Z}}_{2,3} - \hat{\mathbf{U}}_2\mathbf{E}_2\hat{\mathbf{Z}}_{2,4} &= \mathbf{0}_{13} \\ \hat{\mathbf{U}}_5\mathbf{E}_1\hat{\mathbf{U}}_3\hat{\mathbf{Z}}_{2,3} + \hat{\mathbf{U}}_5\mathbf{E}_2\hat{\mathbf{U}}_4\hat{\mathbf{Z}}_{2,4} - \hat{\mathbf{Z}}_{5,0} &= \mathbf{0}_{13} \end{aligned} \quad (11.96)$$

According to the geometrical relationship between different ends of body 2, we have

$$\mathbf{E}_4\hat{\mathbf{Z}}_{2,4} = \mathbf{E}_3\hat{\mathbf{Z}}_{2,3} \quad (11.97)$$

where

$$\begin{aligned} \mathbf{E}_4 &= \begin{bmatrix} \mathbf{I}_3 & \mathbf{O}_{3 \times 3} & \mathbf{O}_{3 \times 3} & \mathbf{O}_{3 \times 4} \\ \mathbf{O}_{3 \times 3} & \mathbf{O}_{3 \times 3} & \mathbf{I}_3 & \mathbf{O}_{3 \times 4} \end{bmatrix} \\ \mathbf{E}_3 &= \begin{bmatrix} \mathbf{E}_{1,1} & \mathbf{O}_{3 \times 3} & \mathbf{O}_{3 \times 3} & \mathbf{O}_{3 \times 4} \\ \mathbf{O}_{3 \times 3} & \mathbf{O}_{3 \times 3} & \mathbf{E}_{1,1} & \mathbf{O}_{3 \times 4} \end{bmatrix}, \quad \mathbf{E}_{1,1} = \begin{bmatrix} 1 & 0 & -(b_{2,2} - b_{2,1}) \\ 0 & 1 & b_{1,2} - b_{1,1} \\ 0 & 0 & 1 \end{bmatrix} \end{aligned}$$

Similarly, we obtain

$$\mathbf{E}_4\hat{\mathbf{Z}}_{4,5} = \mathbf{E}_5\hat{\mathbf{Z}}_{3,5} \quad (11.98)$$

where

$$\mathbf{E}_5 = \begin{bmatrix} \mathbf{E}_{1,1} & \mathbf{O}_{3 \times 3} & \mathbf{O}_{3 \times 3} & \mathbf{O}_{3 \times 4} \\ \mathbf{O}_{3 \times 3} & \mathbf{O}_{3 \times 3} & \mathbf{E}_{1,1} & \mathbf{O}_{3 \times 4} \end{bmatrix}, \quad \mathbf{E}_{1,1} = \begin{bmatrix} 1 & 0 & -a_{2,2} \\ 0 & 1 & a_{1,2} \\ 0 & 0 & 1 \end{bmatrix}$$

Substituting the part transfer equations of Equation (11.92) into Equation (11.98) yields

$$\mathbf{E}_3\hat{\mathbf{Z}}_{2,3} - \mathbf{E}_4\hat{\mathbf{Z}}_{2,4} = \mathbf{0}_6, \quad \mathbf{E}_5\hat{\mathbf{U}}_3\hat{\mathbf{Z}}_{2,3} - \mathbf{E}_4\hat{\mathbf{U}}_4\hat{\mathbf{Z}}_{2,4} = \mathbf{0}_6 \quad (11.99)$$

Combining Equation (11.96) with Equation (11.99) and rewriting in the form of a matrix

$$\begin{bmatrix} \hat{\mathbf{U}}_1 & \mathbf{O}_{13 \times 13} & -\hat{\mathbf{U}}_2\mathbf{E}_1 & -\hat{\mathbf{U}}_2\mathbf{E}_2 \\ \mathbf{O}_{13 \times 13} & -\mathbf{I}_{13} & \hat{\mathbf{U}}_5\mathbf{E}_1\hat{\mathbf{U}}_3 & \hat{\mathbf{U}}_5\mathbf{E}_2\hat{\mathbf{U}}_4 \\ \mathbf{O}_{6 \times 13} & \mathbf{O}_{6 \times 13} & \mathbf{E}_3 & -\mathbf{E}_4 \\ \mathbf{O}_{6 \times 13} & \mathbf{O}_{6 \times 13} & \mathbf{E}_5\hat{\mathbf{U}}_3 & -\mathbf{E}_4\hat{\mathbf{U}}_4 \end{bmatrix} \begin{bmatrix} \hat{\mathbf{Z}}_{1,0} \\ \hat{\mathbf{Z}}_{5,0} \\ \hat{\mathbf{Z}}_{2,3} \\ \hat{\mathbf{Z}}_{2,4} \end{bmatrix} = \mathbf{0}, \text{ namely } \mathbf{U}_{\text{all}} \mathbf{Z}_{\text{all}} = \mathbf{0} \quad (11.100)$$

$38 \times 52 \quad 52 \times 1$

According to boundary conditions, we obtain

$$\begin{cases} \hat{\mathbf{Z}}_{1,0} = [0, 0, 0, M_z^r, Q_x^r, Q_y^r, 0, 0, 0, M_z^i, Q_x^i, Q_y^i, 1]^T_{1,0} \\ \hat{\mathbf{Z}}_{5,0} = [X^r, Y^r, \theta_z^r, 0, 0, 0, X^i, Y^i, \theta_z^i, 0, 0, 0, 1]^T_{5,0} \end{cases} \quad (11.101)$$

Thus, the 1st, 2nd, 3rd, 7th, 8th, 9th, 17th, 18th, 19th, 23rd, 24th and 25th variables in \mathbf{Z}_{all} are all zero, meanwhile the 13th, 26th, 39th and 52nd variables are equal to 1. These known elements are removed from \mathbf{Z}_{all} , and the columns corresponding to each zero element are removed from \mathbf{U}_{all} . Move the columns corresponding to all nonzero elements to the right-hand side of the equation and cancel the 13th and 26th rows in Equation (11.100). Then

$$\hat{\mathbf{U}}_{\text{all}} \hat{\mathbf{Z}}_{\text{all}} = -\mathbf{f} \quad (11.102)$$

$36 \times 36 \quad 36 \times 1$

where

$$\mathbf{f} = \begin{bmatrix} u_{1,13} + u_{1,26} + u_{1,39} + u_{1,52} \\ u_{2,13} + u_{2,26} + u_{2,39} + u_{2,52} \\ \vdots \\ u_{38,13} + u_{38,26} + u_{38,39} + u_{38,52} \end{bmatrix}$$

and $u_{i,j}$ is the variable in the i th row and j th column in \mathbf{U}_{all} .

With the inverse of $\hat{\mathbf{U}}_{\text{all}}$, Equation (11.102) becomes

$$\hat{\mathbf{Z}}_{\text{all}} = -\hat{\mathbf{U}}_{\text{all}}^{-1} \mathbf{f} \quad (11.103)$$

Then the unknown state variables in \mathbf{Z}_{all} are obtained. $X_{2,1}^r, Y_{2,1}^r, \Theta_{z2,1}^r, X_{2,1}^i, Y_{2,1}^i, \Theta_{z2,1}^i$ and $X_{5,3}^r, Y_{5,3}^r, \Theta_{z5,3}^r, X_{5,3}^i, Y_{5,3}^i, \Theta_{z5,3}^i$ can be determined using transfer equations of elements. With $\bar{X} = X^r + iX^i$, this becomes

$$x = \text{Re}(\bar{X}e^{i\Omega t}) = X^r \cos \Omega t - X^i \sin \Omega t$$

therefore the steady-state response of the system is obtained

$$\mathbf{v} = \begin{bmatrix} x_{2,1} \\ y_{2,1} \\ \theta_{z2,1} \\ x_{5,3} \\ y_{5,3} \\ \theta_{z5,3} \end{bmatrix} = \begin{bmatrix} X_{2,1}^r \\ Y_{2,1}^r \\ \Theta_{z2,1}^r \\ X_{5,3}^r \\ Y_{5,3}^r \\ \Theta_{z5,3}^r \end{bmatrix} \cos \Omega t - \begin{bmatrix} X_{2,1}^i \\ Y_{2,1}^i \\ \Theta_{z2,1}^i \\ X_{5,3}^i \\ Y_{5,3}^i \\ \Theta_{z5,3}^i \end{bmatrix} \sin \Omega t$$

The exact value of a particular solution is obtained using the MSTMM in the above example, and the computational effort is greatly reduced.

Example 11.5 For the system shown in Figure 11.18, set

$$\left\{ \begin{array}{l} m_2 = 7.8\text{kg} \\ J_2 = 0.052\text{kg}\cdot\text{m}^2 \\ (a_{1,1}, a_{2,1})_2 = (0\text{m}, 0\text{m}) \\ (b_{1,1}, b_{2,1})_2 = (-0.05\text{m}, 0.1\text{m}) \\ (b_{1,2}, b_{2,2})_2 = (0.05\text{m}, 0.1\text{m}) \\ (c_{c1}, c_{c2})_2 = (0\text{m}, 0.05\text{m}) \end{array} \right\}, \quad \left\{ \begin{array}{l} m_5 = 7.8\text{kg} \\ J_5 = 0.1349\text{kg}\cdot\text{m}^2 \\ (a_{1,1}, a_{2,1})_5 = (0\text{m}, 0\text{m}) \\ (a_{1,2}, a_{2,2})_5 = (0.1\text{m}, 0\text{m}) \\ (b_1, b_2)_5 = (0.05\text{m}, 0.2\text{m}) \\ (c_{c1}, c_{c2})_5 = (0.05\text{m}, 0.1\text{m}) \end{array} \right\}$$

$$\begin{cases} K_{x,1} = 1000\text{N/m} \\ K_{y,1} = 500\text{N/m} \\ K'_{z,1} = 150\text{N}\cdot\text{m/rad} \end{cases}, \begin{cases} K_{x,3} = 800\text{N/m} \\ K_{y,3} = 400\text{N/m} \\ K'_{z,3} = 100\text{N}\cdot\text{m/rad} \end{cases}, \begin{cases} K_{x,4} = 800\text{N/m} \\ K_{y,4} = 400\text{N/m} \\ K'_{z,4} = 100\text{N}\cdot\text{m/rad} \end{cases}$$

$$\begin{cases} C_{x,1} = 4\text{kg/s} \\ C_{y,1} = 5\text{kg/s} \\ C'_{z,1} = 2\text{N}\cdot\text{m}\cdot\text{s/rad} \end{cases}, \begin{cases} C_{x,3} = 10\text{kg/s} \\ C_{y,3} = 6\text{kg/s} \\ C'_{z,3} = 2\text{N}\cdot\text{m}\cdot\text{s/rad} \end{cases}, \begin{cases} C_{x,4} = 5\text{kg/s} \\ C_{y,4} = 4\text{kg/s} \\ C'_{z,4} = 2\text{N}\cdot\text{m}\cdot\text{s/rad} \end{cases}$$

$$\mathbf{F}_2 = \begin{bmatrix} 10 \\ 0 \end{bmatrix} \cos 10t + \begin{bmatrix} -5 \\ 0 \end{bmatrix} \sin 10t, \quad \mathbf{F}_5 = \begin{bmatrix} 20 \\ 20 \end{bmatrix} \cos 20t + \begin{bmatrix} 8 \\ 8 \end{bmatrix} \sin 20t$$

Solve the steady-state responses of the system using the extended MSTMM.

Solution

It can be seen from the expressions of \mathbf{F}_2 and \mathbf{F}_5 that $\Omega_1 = 10\text{rad/s}$, $\Omega_2 = 20\text{rad/s}$ and $\Omega_1 \neq \Omega_2$. Solve the steady-state responses \mathbf{v}_1 and \mathbf{v}_2 of the system under the excitation of \mathbf{F}_2 and \mathbf{F}_5 , respectively. The steady-state response of the system is obtained by the superposition of \mathbf{v}_1 and \mathbf{v}_2 .

$$\mathbf{v} = \mathbf{v}_1 + \mathbf{v}_2 = \begin{bmatrix} -0.04830 \\ 0.00421 \\ 0.01467 \\ -0.10729 \\ 0.02296 \\ 0.06256 \end{bmatrix} \cos 10t + \begin{bmatrix} 0.03033 \\ -0.00202 \\ -0.01867 \\ 0.05539 \\ 0.02794 \\ -0.03248 \end{bmatrix} \sin 10t + \begin{bmatrix} 0.00030 \\ 0.00018 \\ 0.00331 \\ -0.01098 \\ -0.00942 \\ 0.01175 \end{bmatrix} \cos 20t + \begin{bmatrix} -0.00026 \\ -0.00010 \\ 0.00007 \\ -0.00300 \\ -0.00316 \\ 0.00435 \end{bmatrix} \sin 20t$$

The computational results of the time history of displacement of $P_{5,6}$ along x and y are shown in Figure 11.19.

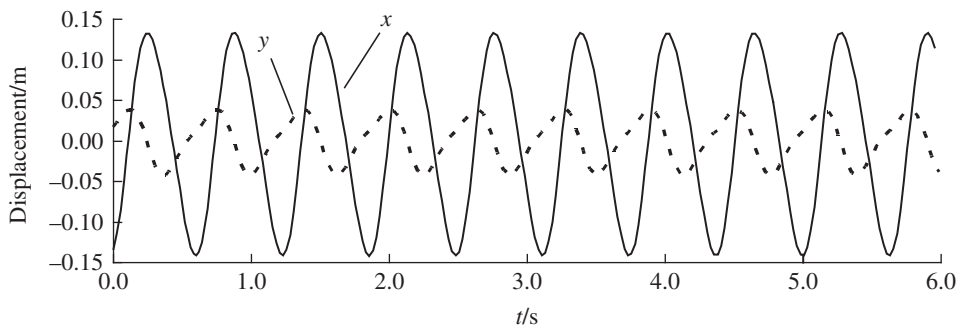


Figure 11.19 Time history of displacement of $P_{5,6}$ along x and y .

11.8.2.2 Static Response of a Multibody System

Example 11.6 The planar frame construction shown in Figure 11.20 is composed of seven rods, and the mass of each rod is neglected. The frame is under the distributed load $P_4(x)$ and the concentrated loads F_6 and F_7 . Solve the static deflection of this structure.

Solution

Obviously, both ends of rod 3 are simply supported, and there is only tensile force or pressure acting on rod 3. For the other rods, there is not only tensile force or pressure, but also shearing force and the bending moment acting on them. In the coordinate system oxy , the state vectors are defined as $\hat{z}_{2,1}$, $\hat{z}_{2,3}$, $\hat{z}_{4,3}$, $\hat{z}_{4,5}$, $\hat{z}_{6,5}$ and $\hat{z}_{6,7}$. The state vectors $\hat{z}_{1,0}$, $\hat{z}_{1,2}$, $\hat{z}_{3,0}$, $\hat{z}_{3,2}$, $\hat{z}_{5,0}$, $\hat{z}_{5,4}$, $\hat{z}_{7,0}$ and $\hat{z}_{7,6}$ are defined separately in the coordinate system $I_i x_i y_i (i = 1, 3, 5, 7)$ as follows,

$$\hat{z} = [x, y, \theta_z, m_z, q_x, q_y, 1]^T \quad (11.104)$$

The extended transfer equations of all elements are

$$\begin{cases} \hat{z}_{2,3} = \hat{U}_2 \hat{z}_{2,1}, & \hat{z}_{4,5} = \hat{U}_4 \hat{z}_{4,3}, & \hat{z}_{6,7} = \hat{U}_6 \hat{z}_{6,5} \\ \hat{z}_{1,2} = \hat{U}_1 \hat{z}_{1,0}, & \hat{z}_{3,2} = \hat{U}_3 \hat{z}_{3,0}, & \hat{z}_{5,4} = \hat{U}_5 \hat{z}_{5,0}, & \hat{z}_{7,6} = \hat{U}_7 \hat{z}_{7,0} \end{cases} \quad (11.105)$$

where U_1, U_2, \dots, U_7 are the transfer matrices of each elastic rod, respectively

$$\hat{U}_i = \begin{bmatrix} 1 & 0 & 0 & 0 & -\frac{x_i}{EA_i} & 0 & 0 \\ 0 & 1 & x_i & \frac{x_i^2}{2EI_i} & 0 & \frac{x_i^3}{6EI_i} & 0 \\ 0 & 0 & 1 & \frac{x_i}{EI_i} & 0 & \frac{x_i^2}{2EI_i} & 0 \\ 0 & 0 & 0 & 1 & 0 & x_i & 0 \\ 0 & 0 & 0 & 0 & 1 & 0 & 0 \\ 0 & 0 & 0 & 0 & 0 & 1 & 0 \\ 0 & 0 & 0 & 0 & 0 & 0 & 1 \end{bmatrix}_{x_i=l_i} \quad (i = 1, 2, 3, 5) \quad (11.106)$$

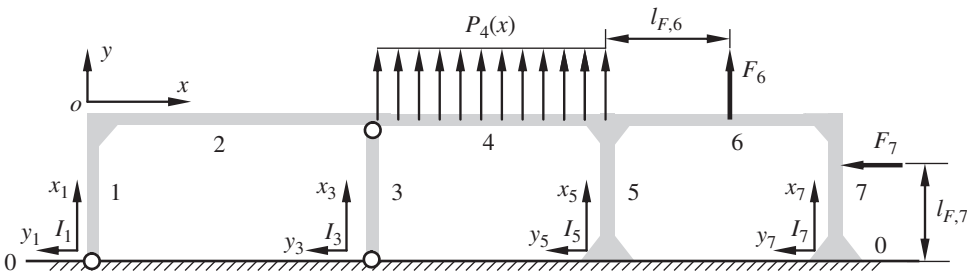


Figure 11.20 A planar frame structure.

$$\hat{\mathbf{U}}_4 = \begin{bmatrix} 1 & 0 & 0 & 0 & -\frac{x_4}{EA_4} & 0 & 0 \\ 0 & 1 & x_4 & \frac{x_4^2}{2EI_4} & 0 & \frac{x_4^3}{6EI_4} & \frac{P_4 x_4^4}{24EI_4} \\ 0 & 0 & 1 & \frac{x_4}{EI_4} & 0 & \frac{x_4^2}{2EI_4} & \frac{P_4 x_4^3}{6EI_4} \\ 0 & 0 & 0 & 1 & 0 & x_4 & \frac{P_4 x_4^2}{2} \\ 0 & 0 & 0 & 0 & 1 & 0 & 0 \\ 0 & 0 & 0 & 0 & 0 & 1 & P_4 x_4 \\ 0 & 0 & 0 & 0 & 0 & 0 & 1 \end{bmatrix}_{x_4 = l_4} \quad (11.107)$$

$$\hat{\mathbf{U}}_i = \begin{bmatrix} 1 & 0 & 0 & 0 & -\frac{l_i}{EA_i} & 0 & 0 \\ 0 & 1 & l_i & \frac{l_i^2}{2EI_i} & 0 & \frac{l_i^3}{6EI_i} & \frac{\langle l_i - l_{F,i} \rangle^3}{6EI_i} F_i \\ 0 & 0 & 1 & \frac{l_i}{EI_i} & 0 & \frac{l_i^2}{2EI_i} & \frac{\langle l_i - l_{F,i} \rangle^2}{2EI_i} F_i \\ 0 & 0 & 0 & 1 & 0 & l_i & \langle l_i - l_{F,i} \rangle F_i \\ 0 & 0 & 0 & 0 & 1 & 0 & 0 \\ 0 & 0 & 0 & 0 & 0 & 1 & F_i \\ 0 & 0 & 0 & 0 & 0 & 0 & 1 \end{bmatrix} \quad (i = 6, 7) \quad (11.108)$$

$$\langle l_i - l_{F,i} \rangle = \begin{cases} 0 & (l_i < l_{F,i}) \\ l_i - l_{F,i} & (l_i \geq l_{F,i}) \end{cases}$$

EA_i is the tensile stiffness, EI_i is the bending stiffness and l_i is the length of each segment of the total beam.

At the connection point $P_{1,2}$, according to the connection and the coordinate transformation, we obtain

$$\hat{\mathbf{z}}_{2,1} = \mathbf{E}_1 \hat{\mathbf{z}}_{1,2} \quad (11.109)$$

where

$$\mathbf{E}_1 = \begin{bmatrix} 0 & -1 & 0 & 0 & 0 & 0 & 0 \\ 1 & 0 & 0 & 0 & 0 & 0 & 0 \\ 0 & 0 & 1 & 0 & 0 & 0 & 0 \\ 0 & 0 & 0 & 1 & 0 & 0 & 0 \\ 0 & 0 & 0 & 0 & 0 & -1 & 0 \\ 0 & 0 & 0 & 0 & 1 & 0 & 0 \\ 0 & 0 & 0 & 0 & 0 & 0 & 1 \end{bmatrix}$$

At the connection point $P_{2,4}$, according to the connection and the coordinate transformation, we obtain

$$\begin{cases} \hat{\mathbf{z}}_{4,3} = \hat{\mathbf{z}}_{2,3} + \mathbf{E}_2 \hat{\mathbf{z}}_{3,2} \\ \mathbf{E}_3 \hat{\mathbf{z}}_{2,3} = \mathbf{E}_4 \hat{\mathbf{z}}_{3,2} \end{cases} \quad (11.110)$$

where

$$E_2 = \begin{bmatrix} 0 & 0 & 0 & 0 & 0 & 0 & 0 \\ 0 & 0 & 0 & 0 & 0 & 0 & 0 \\ 0 & 0 & 0 & 0 & 0 & 0 & 0 \\ 0 & 0 & 0 & 0 & 0 & 0 & 0 \\ 0 & 0 & 0 & 0 & 0 & -1 & 0 \\ 0 & 0 & 0 & 0 & 1 & 0 & 0 \\ 0 & 0 & 0 & 0 & 0 & 0 & 0 \end{bmatrix}$$

$$E_3 = \begin{bmatrix} 1 & 0 & 0 & 0 & 0 & 0 & 0 \\ 0 & 1 & 0 & 0 & 0 & 0 & 0 \\ 0 & 0 & 1 & 0 & 0 & 0 & 0 \end{bmatrix}, \quad E_4 = \begin{bmatrix} 0 & -1 & 0 & 0 & 0 & 0 & 0 \\ 1 & 0 & 0 & 0 & 0 & 0 & 0 \\ 0 & 0 & 1 & 0 & 0 & 0 & 0 \end{bmatrix}$$

At the connection point $P_{4,6}$, according to the connection and the coordinate transformation, we similarly obtain

$$\begin{cases} \hat{\mathbf{z}}_{6,5} = E_5 \hat{\mathbf{z}}_{4,5} + E_6 \hat{\mathbf{z}}_{5,4} \\ E_3 \hat{\mathbf{z}}_{4,5} = E_4 \hat{\mathbf{z}}_{5,4} \end{cases} \quad (11.111)$$

where

$$E_5 = \begin{bmatrix} 1 & 0 & 0 & 0 & 0 & 0 & 0 \\ 0 & 1 & 0 & 0 & 0 & 0 & 0 \\ 0 & 0 & 1 & 0 & 0 & 0 & 0 \\ 0 & 0 & 0 & 1 & 0 & 0 & 0 \\ 0 & 0 & 0 & 0 & 1 & 0 & 0 \\ 0 & 0 & 0 & 0 & 0 & 1 & 0 \\ 0 & 0 & 0 & 0 & 0 & 0 & 1 \end{bmatrix}, \quad E_6 = \begin{bmatrix} 0 & 0 & 0 & 0 & 0 & 0 & 0 \\ 0 & 0 & 0 & 0 & 0 & 0 & 0 \\ 0 & 0 & 0 & 0 & 0 & 0 & 0 \\ 0 & 0 & 0 & 1 & 0 & 0 & 0 \\ 0 & 0 & 0 & 0 & 0 & -1 & 0 \\ 0 & 0 & 0 & 0 & 1 & 0 & 0 \\ 0 & 0 & 0 & 0 & 0 & 0 & 0 \end{bmatrix}$$

At connection point $P_{6,7}$, according to the connection and the coordinate transformation, we obtain

$$\hat{\mathbf{z}}_{6,7} = E_1 \hat{\mathbf{z}}_{7,6} \quad (11.112)$$

According to Equations (11.105), (11.109), (11.110), (11.111) and (11.112), it follows that

$$\mathbf{U}_{\text{all}} \mathbf{z}_{\text{all}} = \mathbf{0}_{13} \quad (11.113)$$

$\begin{smallmatrix} 13 \times 28 & 28 \times 1 \end{smallmatrix}$

where

$$\mathbf{U}_{\text{all}} = \begin{bmatrix} \hat{\mathbf{U}}_6 E_5 \hat{\mathbf{U}}_4 \hat{\mathbf{U}}_2 E_1 \hat{\mathbf{U}}_1 & \hat{\mathbf{U}}_6 E_5 \hat{\mathbf{U}}_4 E_2 \hat{\mathbf{U}}_3 & \hat{\mathbf{U}}_6 E_6 \hat{\mathbf{U}}_5 & -E_1 \hat{\mathbf{U}}_7 \\ E_3 \hat{\mathbf{U}}_2 E_1 \hat{\mathbf{U}}_1 & -E_4 \hat{\mathbf{U}}_3 & \mathbf{O}_{3 \times 7} & \mathbf{O}_{3 \times 7} \\ E_3 \hat{\mathbf{U}}_4 \hat{\mathbf{U}}_2 E_1 \hat{\mathbf{U}}_1 & E_3 \hat{\mathbf{U}}_4 E_2 \hat{\mathbf{U}}_3 & -E_4 \hat{\mathbf{U}}_5 & \mathbf{O}_{3 \times 7} \end{bmatrix}, \quad \mathbf{z}_{\text{all}} = \begin{bmatrix} \hat{\mathbf{z}}_{1,0} \\ \hat{\mathbf{z}}_{3,0} \\ \hat{\mathbf{z}}_{5,0} \\ \hat{\mathbf{z}}_{7,0} \end{bmatrix}$$

According to the boundary conditions, we obtain

$$\begin{cases} \hat{\mathbf{z}}_{1,0} = [0, 0, \theta_z, 0, q_x, q_y, 1]_{1,0}^T \\ \hat{\mathbf{z}}_{3,0} = [0, 0, \theta_z, 0, q_x, q_y, 1]_{3,0}^T \\ \hat{\mathbf{z}}_{5,0} = [0, 0, 0, m_z, q_x, q_y, 1]_{5,0}^T \\ \hat{\mathbf{z}}_{7,0} = [0, 0, 0, m_z, q_x, q_y, 1]_{7,0}^T \end{cases} \quad (11.114)$$

Therefore, the 1st, 2nd, 4th, 8th, 9th, 11th, 15th, 16th, 17th, 22nd, 23rd and 24th variables of \mathbf{z}_{all} are zero. The 7th, 14th, 21st and 28th variables of \mathbf{z}_{all} are equal to 1. Removing these known variables from \mathbf{z}_{all} , getting rid of the column vector corresponding to each zero element in \mathbf{z}_{all} from \mathbf{U}_{all} , moving the column vector corresponding to each known nonzero element in \mathbf{z}_{all} to the right-hand side of equation, and removing the 7th column vector from Equation (11.113), we obtain

$$\hat{\mathbf{U}}_{\text{all}} \hat{\mathbf{z}}_{\text{all}} = -\mathbf{f} \quad (11.115)$$

$12 \times 12 \quad 12 \times 1$

where

$$\mathbf{f} = \begin{bmatrix} u_{1,7} + u_{1,14} + u_{1,21} + u_{1,28} \\ u_{2,7} + u_{2,14} + u_{2,21} + u_{2,28} \\ \vdots \\ u_{13,7} + u_{13,14} + u_{13,21} + u_{13,28} \end{bmatrix}$$

$u_{i,j}$ is the variable in the i th row and the j th column of \mathbf{U}_{all} .

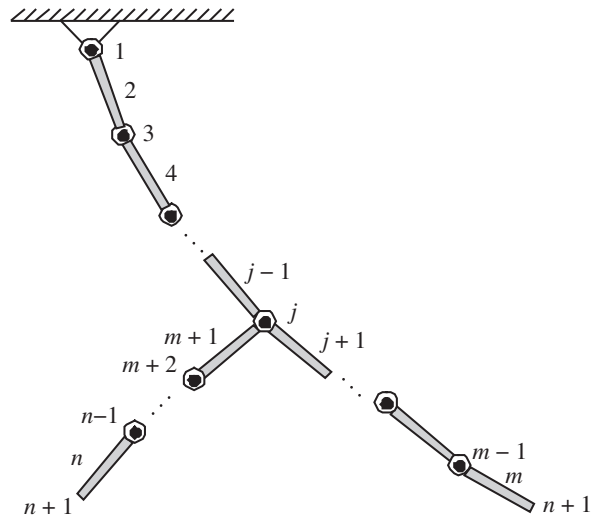
Solving the inhomogeneous equations Equation (11.115), it follows that

$$\hat{\mathbf{z}}_{\text{all}} = -\hat{\mathbf{U}}_{\text{all}}^{-1} \mathbf{f} \quad (11.116)$$

Thus, the unknown state vectors $\hat{\mathbf{z}}_{1,0}$, $\hat{\mathbf{z}}_{3,0}$, $\hat{\mathbf{z}}_{5,0}$ and $\hat{\mathbf{z}}_{7,0}$ in \mathbf{z}_{all} are obtained, and the state vector of an arbitrary connection point can be evaluated using the transfer equation of the element, therefore the static deflection of the system is obtained.

For the branched multibody system shown in Figure 11.21, the transfer equations of each element can be derived. The branched multibody system can be regarded as several multi-chain subsystems, so the transfer equations are

Figure 11.21 A multibody system with a branched topology structure.



$$\begin{cases} \mathbf{z}_{j-1,j} = \mathbf{U}_I \mathbf{z}_{2,1} \\ \mathbf{z}_{m,n+1} = \mathbf{U}_{II} \mathbf{z}_{j+1,j} \\ \mathbf{z}_{m+1,j} = \mathbf{U}_{III} \mathbf{z}_{n,n+1} \end{cases} \quad (11.117)$$

where

$$\begin{cases} \mathbf{U}_I = \mathbf{U}_{j-1} \mathbf{U}_{j-2} \cdots \mathbf{U}_3 \mathbf{U}_2 \\ \mathbf{U}_{II} = \mathbf{U}_m \mathbf{U}_{m-1} \cdots \mathbf{U}_{j+1} \\ \mathbf{U}_{III} = \mathbf{U}_{m+1} \mathbf{U}_{m+2} \cdots \mathbf{U}_n \end{cases} \quad (11.118)$$

If the branched point is a smooth hinge, using the continuous condition of position and the force equilibrium the following relationship among the state vectors $\mathbf{z}_{j-1,j}$, $\mathbf{z}_{j+1,j}$ and $\mathbf{z}_{m+1,j}$ is obtained

$$\begin{cases} \mathbf{z}_{j-1,j}(1) = \mathbf{z}_{j+1,j}(1) = \mathbf{z}_{m+1,j}(1) \\ \mathbf{z}_{j-1,j}(2) = \mathbf{z}_{j+1,j}(2) = \mathbf{z}_{m+1,j}(2) \\ \mathbf{z}_{j-1,j}(5) - \mathbf{z}_{j+1,j}(5) - \mathbf{z}_{m+1,j}(5) = 0 \\ \mathbf{z}_{j-1,j}(6) - \mathbf{z}_{j+1,j}(6) - \mathbf{z}_{m+1,j}(6) = 0 \\ \mathbf{z}_{j-1,j}(4) = \mathbf{z}_{j+1,j}(4) = \mathbf{z}_{m+1,j}(4) = 0 \end{cases} \quad (11.119)$$

where $\mathbf{z}(i)$ denotes the i th state variable in the state vector \mathbf{z} .

The boundary conditions are

$$\begin{cases} \mathbf{z}_{2,1}(1) = \mathbf{z}_{2,1}(2) = \mathbf{z}_{2,1}(4) = 0 \\ \mathbf{z}_{m,n+1}(4) = \mathbf{z}_{m,n+1}(5) = \mathbf{z}_{m,n+1}(6) = 0 \\ \mathbf{z}_{n,n+1}(4) = \mathbf{z}_{n,n+1}(5) = \mathbf{z}_{n,n+1}(6) = 0 \end{cases} \quad (11.120)$$

Define

$$\mathbf{U}_{b1} = [\mathbf{O}_{2 \times 4} \quad \mathbf{I}_2 \quad \mathbf{O}_{2 \times 1}] \quad , \quad \mathbf{U}_{b2} = [\mathbf{I}_2 \quad \mathbf{O}_{2 \times 5}] \quad , \quad \mathbf{U}_{b3} = [\mathbf{O}_{1 \times 3} \quad 1 \quad \mathbf{O}_{1 \times 3}] \quad (11.121)$$

According to the continuous condition of position and the force equilibrium of the smooth hinge, for smooth hinge j we obtain

$$\begin{cases} \mathbf{U}_{b1} \mathbf{U}_I \mathbf{z}_{2,1} = \mathbf{U}_{b1} \mathbf{U}_{II}^{-1} \mathbf{z}_{m,n+1} + \mathbf{U}_{b1} \mathbf{U}_{III} \mathbf{z}_{n,n+1} \\ \mathbf{U}_{b2} \mathbf{U}_I \mathbf{z}_{2,1} = \mathbf{U}_{b2} \mathbf{U}_{II}^{-1} \mathbf{z}_{m,n+1} = \mathbf{U}_{b2} \mathbf{U}_{III} \mathbf{z}_{n,n+1} \\ \mathbf{U}_{b3} \mathbf{U}_I \mathbf{z}_{2,1} = \mathbf{0} \\ \mathbf{U}_{b3} \mathbf{U}_{II}^{-1} \mathbf{z}_{m,n+1} = \mathbf{0} \\ \mathbf{U}_{b3} \mathbf{U}_{III} \mathbf{z}_{n,n+1} = \mathbf{0} \end{cases} \quad (11.122)$$

The overall transfer equation of the system can be obtained

$$\mathbf{U}_{\text{all}} \begin{bmatrix} \mathbf{z}_{2,1}^T & \mathbf{z}_{m,n+1}^T & \mathbf{z}_{n,n+1}^T \end{bmatrix}^T = \mathbf{0} \quad (11.123)$$

The overall transfer matrix is

$$\mathbf{U}_{all} = \begin{bmatrix} \mathbf{U}_{b1}\mathbf{U}_I & -\mathbf{U}_{b1}\mathbf{U}_{II}^{-1} & -\mathbf{U}_{b1}\mathbf{U}_{III} \\ \mathbf{O}_{2 \times 7} & \mathbf{U}_{b2}\mathbf{U}_{II}^{-1} & -\mathbf{U}_{b2}\mathbf{U}_{III} \\ \mathbf{U}_{b2}\mathbf{U}_I & -\mathbf{U}_{b2}\mathbf{U}_{II}^{-1} & \mathbf{O}_{2 \times 7} \\ \mathbf{U}_{b3}\mathbf{U}_I & \mathbf{O}_{1 \times 7} & \mathbf{O}_{1 \times 7} \\ \mathbf{O}_{1 \times 7} & \mathbf{U}_{b3}\mathbf{U}_{II}^{-1} & \mathbf{O}_{1 \times 7} \\ \mathbf{O}_{1 \times 7} & \mathbf{O}_{1 \times 7} & \mathbf{U}_{b3}\mathbf{U}_{III} \end{bmatrix} \quad (11.124)$$

When the overall transfer equation and the overall transfer matrix have been obtained, the dynamics of the branched multibody system can be computed using the same method as for the chain multibody system.

Example 11.7 The dynamics model of four rigid pendulums connected by smooth hinges is shown in Figure 11.22. The four bars are the same. The mass center is at the geometrical center. The mass is 1 kg and the length is 1 m. The moment of inertia with respect to the mass center is $1/12 \text{ kg} \cdot \text{m}^2$. The initial velocities of all bars are zero. The initial rotation angles of bars 2, 4, 6 and 7 are $-\pi/3$, $-\pi/3$, $-\pi/3$ and $-2\pi/3$, respectively. Compute the dynamics of this system under the effect of gravity.

Solution

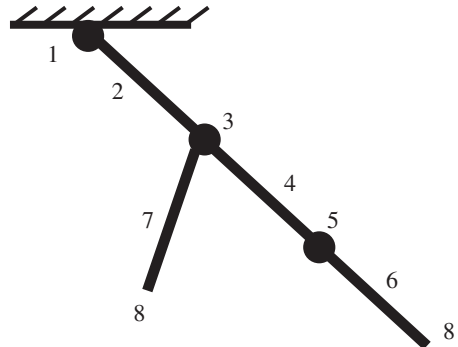
According to the analysis method of branched systems discussed above, the overall transfer equation of the system can be obtained using the MSDTTMM as

$$\mathbf{U}_{all} \begin{bmatrix} \mathbf{z}_{2,1}^T & \mathbf{z}_{6,8}^T & \mathbf{z}_{7,8}^T \end{bmatrix}^T = \mathbf{0} \quad (11.125)$$

The overall transfer matrix of the system is

$$\mathbf{U}_{all} = \begin{bmatrix} \mathbf{U}_{b1}\mathbf{U}_I & -\mathbf{U}_{b1}\mathbf{U}_{II}^{-1} & -\mathbf{U}_{b1}\mathbf{U}_{III} \\ \mathbf{O}_{2 \times 7} & \mathbf{U}_{b2}\mathbf{U}_{II}^{-1} & -\mathbf{U}_{b2}\mathbf{U}_{III} \\ \mathbf{U}_{b2}\mathbf{U}_I & -\mathbf{U}_{b2}\mathbf{U}_{II}^{-1} & \mathbf{O}_{2 \times 7} \\ \mathbf{U}_{b3}\mathbf{U}_I & \mathbf{O}_{1 \times 7} & \mathbf{O}_{1 \times 7} \\ \mathbf{O}_{1 \times 7} & \mathbf{U}_{b3}\mathbf{U}_{II}^{-1} & \mathbf{O}_{1 \times 7} \\ \mathbf{O}_{1 \times 7} & \mathbf{O}_{1 \times 7} & \mathbf{U}_{b3}\mathbf{U}_{III} \end{bmatrix} \quad (11.126)$$

Figure 11.22 Dynamics model of a branched multi-rigid-body system.



where

$$\begin{cases} \mathbf{U}_I = \mathbf{U}_2 \\ \mathbf{U}_{II} = \mathbf{U}_6 \mathbf{U}_5 \mathbf{U}_4 \\ \mathbf{U}_{III} = \mathbf{U}_7 \end{cases} \quad (11.127)$$

The boundary conditions are

$$\begin{cases} \mathbf{z}_{2,1} = [0, 0, \theta, 0, q_x, q_y, 1]_{2,1}^T \\ \mathbf{z}_{6,8} = [x, y, \theta, 0, 0, 0, 1]_{6,8}^T \\ \mathbf{z}_{7,8} = [x, y, \theta, 0, 0, 0, 1]_{7,8}^T \end{cases} \quad (11.128)$$

The dynamics of the multibody system is computed using the MSDTTMM and the Newton–Euler method. The computational results of both methods have good agreement, as shown in Figure 11.23, which validates the proposed method.

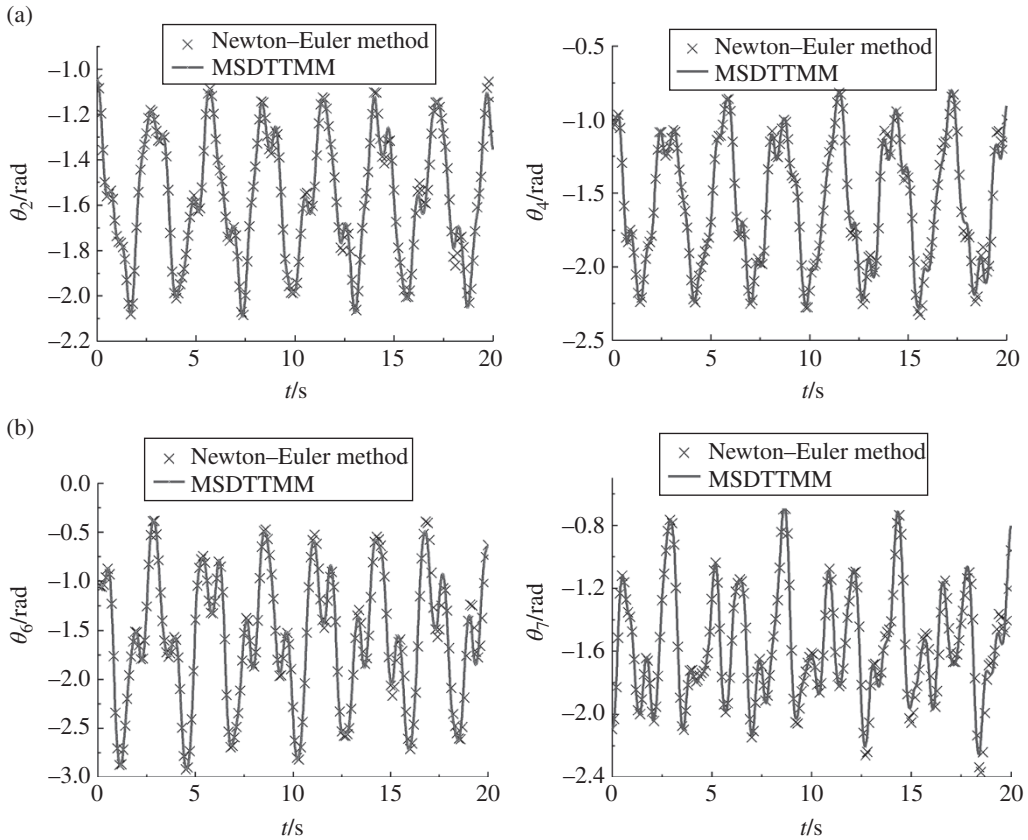


Figure 11.23 Simulation results of a branched multibody system moving in a plane: (a) computational results of the time history of the orientation angles of rigid body 2 and rigid body 4, and (b) computational results of the time history of the orientation angles of rigid body 6 and rigid body 7.

Example 11.8 A multi-rigid-body system moving in a plane with one input and many output ends is shown in Figure 11.24. The mass of each rigid body is 1 kg, the length from the input to the output is 1 m and the rigid body with multiple points is a triangular plate. The moment of inertia of each body with respect to its mass center is $1/12 \text{ kg} \cdot \text{m}^2$. The initial velocities of all bars are zero, and the initial rotation angles of bars 2, 6, 8 and 10 are $-\pi$. Solve the motion of the system under the effect of gravity.

Solution

According to the MSDTTMM, the overall transfer equation of the system is

$$\mathbf{U}_{\text{all}} \begin{bmatrix} \mathbf{z}_{2,1}^T & \mathbf{z}_{8,11}^T & \mathbf{z}_{10,11}^T \end{bmatrix}^T = \mathbf{0} \quad (11.129)$$

The overall transfer matrix of the system is

$$\mathbf{U}_{\text{all}} = \mathbf{U}_4 \begin{bmatrix} \mathbf{U}_I & & \\ & \mathbf{U}_{II}^{-1} & \\ & & \mathbf{U}_{III}^{-1} \end{bmatrix} \quad (11.130)$$

where

$$\begin{cases} \mathbf{U}_I = \mathbf{U}_3 \mathbf{U}_2 \\ \mathbf{U}_{II} = \mathbf{U}_8 \mathbf{U}_7 \mathbf{U}_6 \mathbf{U}_5 \\ \mathbf{U}_{III} = \mathbf{U}_{10} \mathbf{U}_9 \end{cases} \quad (11.131)$$

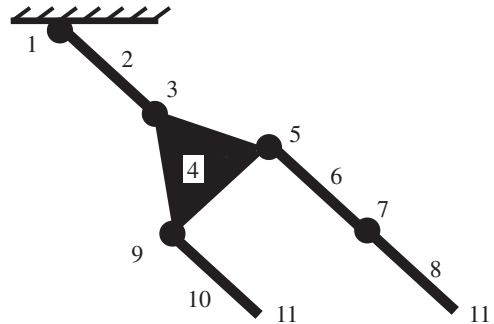
$$\begin{cases} \mathbf{z}_{4,3} = \mathbf{U}_1 \mathbf{z}_{2,1} \\ \mathbf{z}_{8,11} = \mathbf{U}_{II} \mathbf{z}_{4,5} \\ \mathbf{z}_{10,11} = \mathbf{U}_{III} \mathbf{z}_{4,9} \\ \mathbf{U}_4 \begin{bmatrix} \mathbf{z}_{4,3}^T & \mathbf{z}_{4,5}^T & \mathbf{z}_{4,9}^T \end{bmatrix}^T = \mathbf{0} \end{cases} \quad (11.132)$$

\mathbf{U}_4 is the transfer matrix of a rigid body with one input end and two output ends.

The boundary conditions are

$$\begin{cases} \mathbf{z}_{2,1} = [0, 0, \theta, 0, q_x, q_y, 1]^T_{2,1} \\ \mathbf{z}_{8,11} = [x, y, \theta, 0, 0, 0, 1]^T_{8,11} \\ \mathbf{z}_{10,11} = [x, y, \theta, 0, 0, 0, 1]^T_{10,11} \end{cases} \quad (11.133)$$

Figure 11.24 Multi-rigid-body system with one input and multi-output ends moving in a plane.



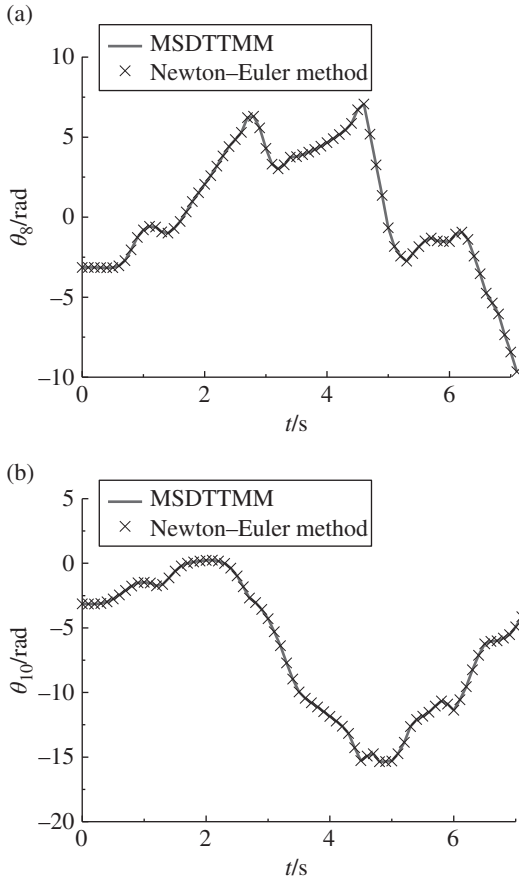


Figure 11.25 Time history of the orientation angles of a multi-rigid-body system with one input and multi-output ends moving in a plane: (a) orientation angle of rigid body 8 and (b) orientation angle of rigid body 10.

The computational results of the dynamics of the multibody system using the MSDTTMM and the Newton-Euler method are shown in Figure 11.25. The computational results of both methods are in good agreement, which validates the proposed method.

11.9 Numerical Example of Multi-level System Dynamics

A system is comparative of the principal system, as shown in Figure 11.26. A multi-level MRFS or multi-layer system has several layers superposed, and each branch is a subsystem connected with the adjacent subsystems.

Assuming the state vectors at each layer are $\mathbf{Z}_1, \mathbf{Z}_2, \dots, \mathbf{Z}_m$, respectively, the state vector of a whole column is

$$\mathbf{z} = [\mathbf{z}_1^T, \mathbf{z}_2^T, \dots, \mathbf{z}_m^T]^T \quad (11.134)$$

If the transfer matrices of each layer are $\mathbf{U}_1, \mathbf{U}_2, \dots, \mathbf{U}_m$, the transfer equation of a whole column is

$$\begin{bmatrix} \mathbf{Z}_1 \\ \mathbf{Z}_2 \\ \vdots \\ \mathbf{Z}_m \end{bmatrix}_i = \begin{bmatrix} \mathbf{U}_1 & \mathbf{O} & \cdots & \mathbf{O} \\ \mathbf{O} & \mathbf{U}_2 & \cdots & \mathbf{O} \\ \vdots & \vdots & \ddots & \vdots \\ \mathbf{O} & \mathbf{O} & \cdots & \mathbf{U}_m \end{bmatrix} \begin{bmatrix} \mathbf{Z}_1 \\ \mathbf{Z}_2 \\ \vdots \\ \mathbf{Z}_m \end{bmatrix}_{i-1} \quad (11.135)$$

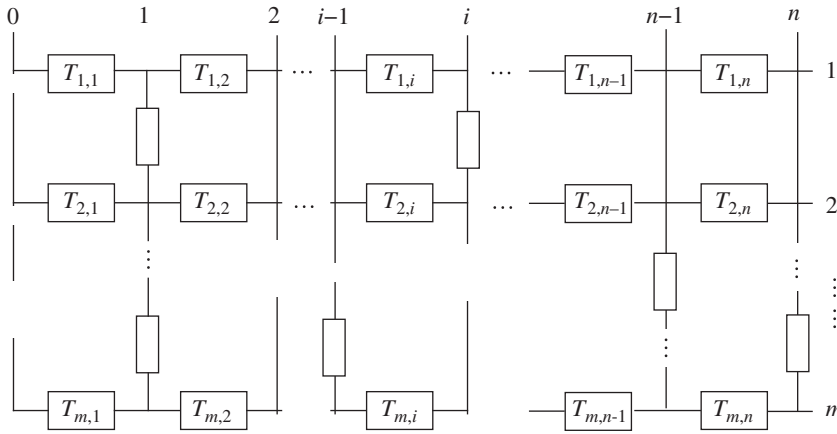
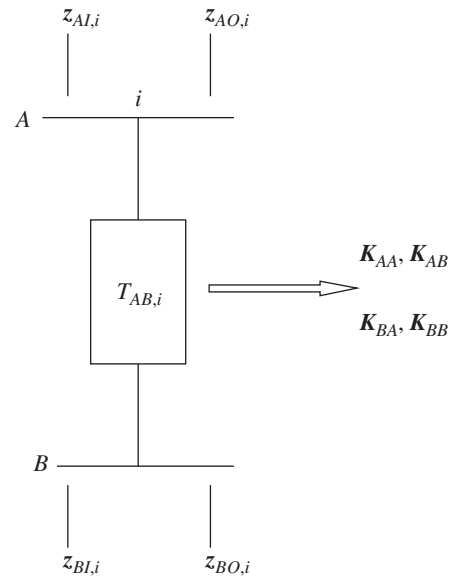


Figure 11.26 Multi-level MRFS.

Figure 11.27 Subsystem of a two-level system.



In the subsystem, the transfer matrix at a certain point is introduced by a simple basic example of a two-level system as follows.

For the two-level system AB shown in Figure 11.27, the transfer equation related to layers A and B is

$$\begin{bmatrix} d_A \\ f_A \\ d_B \\ f_B \end{bmatrix}_{O,i} = \begin{bmatrix} I & O & O & O \\ K_{AA} & I & K_{AB} & O \\ O & O & I & O \\ K_{BA} & 0 & K_{BB} & I \end{bmatrix}_i \begin{bmatrix} d_A \\ f_A \\ d_B \\ f_B \end{bmatrix}_{I,i} \quad (11.136)$$

where the vectors \mathbf{d} and \mathbf{f} denote displacements and forces, respectively, and subscripts I and O denote the input and output ends, respectively. Furthermore, subscripts A and B denote the corresponding quantities on layers A and B , respectively. \mathbf{K}_{AA} , \mathbf{K}_{AB} , \mathbf{K}_{BA} and \mathbf{K}_{BB} are the elastic matrices, and the computational method is as follows.

11.9.1 Derivation of an Elastic Matrix from the Stiffness Matrix of a Subsystem

The stiffness matrix of a subsystem can be given in the coordinates of a subsystem, that is

$$\begin{bmatrix} \hat{\mathbf{f}}_A \\ \hat{\mathbf{f}}_B \end{bmatrix} = \begin{bmatrix} \mathbf{K}_{11} & \mathbf{K}_{12} \\ \mathbf{K}_{21} & \mathbf{K}_{22} \end{bmatrix} \begin{bmatrix} \hat{\mathbf{d}}_A \\ \hat{\mathbf{d}}_B \end{bmatrix} \quad (11.137)$$

The elastic matrix of Equation (11.105) is obtained as follows

$$\begin{cases} \mathbf{K}_{AA} = \mathbf{G}_2 \mathbf{K}_{11} \mathbf{G}_1 \\ \mathbf{K}_{AB} = \mathbf{G}_2 \mathbf{K}_{12} \mathbf{G}_3 \\ \mathbf{K}_{BA} = \mathbf{G}_4 \mathbf{K}_{21} \mathbf{G}_1 \\ \mathbf{K}_{BB} = \mathbf{G}_4 \mathbf{K}_{22} \mathbf{G}_3 \end{cases} \quad (11.138)$$

where \mathbf{G}_1 , \mathbf{G}_2 , \mathbf{G}_3 and \mathbf{G}_4 are coordinate transformation matrices.

11.9.2 Derivation of an Elastic Matrix from the Transfer Matrix of a Subsystem

The transfer equation of the subsystem is

$$\begin{bmatrix} \hat{\mathbf{d}}_A \\ \hat{\mathbf{f}}_A \end{bmatrix} = \begin{bmatrix} \mathbf{C}_1 & \mathbf{C}_2 \\ \mathbf{C}_3 & \mathbf{C}_4 \end{bmatrix} \begin{bmatrix} \hat{\mathbf{d}}_B \\ \hat{\mathbf{f}}_B \end{bmatrix} \quad (11.139)$$

Solving it, we obtain

$$\hat{\mathbf{f}}_B = \mathbf{C}_2^{-1} \hat{\mathbf{d}}_A - \mathbf{C}_2^{-1} \mathbf{C}_1 \hat{\mathbf{d}}_B \quad (11.140)$$

$$\hat{\mathbf{f}}_A = \mathbf{C}_4 \mathbf{C}_2^{-1} \hat{\mathbf{d}}_A + (\mathbf{C}_3 - \mathbf{C}_4 \mathbf{C}_2^{-1} \mathbf{C}_1) \hat{\mathbf{d}}_B \quad (11.141)$$

The coordinate transformation from the subsystem to the principal system yields

$$\begin{bmatrix} \hat{\mathbf{d}}_A \\ \hat{\mathbf{f}}_A \end{bmatrix} = \begin{bmatrix} \mathbf{G}_1 & \mathbf{O} \\ \mathbf{O} & \mathbf{G}_2^{-1} \end{bmatrix} \begin{bmatrix} \mathbf{d}_A \\ \mathbf{f}_A \end{bmatrix}, \quad \begin{bmatrix} \hat{\mathbf{d}}_B \\ \hat{\mathbf{f}}_B \end{bmatrix} = \begin{bmatrix} \mathbf{G}_3 & \mathbf{O} \\ \mathbf{O} & \mathbf{G}_4^{-1} \end{bmatrix} \begin{bmatrix} \mathbf{d}_B \\ \mathbf{f}_B \end{bmatrix} \quad (11.142)$$

From the equations above, the forces at layers A and B are expressed by their displacement in the principle system

$$\begin{bmatrix} \mathbf{f}_A \\ \mathbf{f}_B \end{bmatrix} = \begin{bmatrix} \mathbf{G}_2 \mathbf{C}_4 \mathbf{C}_2^{-1} \mathbf{G}_1 & \mathbf{G}_2 (\mathbf{C}_3 - \mathbf{C}_4 \mathbf{C}_2^{-1} \mathbf{C}_1) \mathbf{G}_3 \\ \mathbf{G}_4 \mathbf{C}_2^{-1} \mathbf{G}_1 & -\mathbf{G}_4 \mathbf{C}_2^{-1} \mathbf{C}_1 \mathbf{G}_3 \end{bmatrix} \begin{bmatrix} \mathbf{d}_A \\ \mathbf{d}_B \end{bmatrix} \quad (11.143)$$

therefore the transfer equation is

$$\begin{bmatrix} \mathbf{d}_A \\ \mathbf{d}_B \\ \mathbf{f}_B \\ \mathbf{f}_A \end{bmatrix}_O = \begin{bmatrix} \mathbf{I} & \mathbf{O} & \mathbf{O} & \mathbf{O} \\ \mathbf{O} & \mathbf{I} & \mathbf{O} & \mathbf{O} \\ \mathbf{G}_4 \mathbf{C}_2^{-1} \mathbf{G}_1 & -\mathbf{G}_4 \mathbf{C}_2^{-1} \mathbf{C}_1 \mathbf{G}_3 & \mathbf{I} & \mathbf{O} \\ \mathbf{G}_2 \mathbf{C}_4 \mathbf{C}_2^{-1} \mathbf{G}_1 & \mathbf{G}_2 (\mathbf{C}_3 - \mathbf{C}_4 \mathbf{C}_2^{-1} \mathbf{C}_1) \mathbf{G}_3 & \mathbf{O} & \mathbf{I} \end{bmatrix} \begin{bmatrix} \mathbf{d}_A \\ \mathbf{d}_B \\ \mathbf{f}_B \\ \mathbf{f}_A \end{bmatrix}_I \quad (11.144)$$

According to the expanded transfer matrix

$$\begin{bmatrix} \hat{\mathbf{d}}_A \\ \hat{\mathbf{f}}_A \\ 1 \end{bmatrix} = \begin{bmatrix} \mathbf{C}_1 & \mathbf{C}_2 & \hat{\mathbf{r}}_d \\ \mathbf{C}_3 & \mathbf{C}_4 & \hat{\mathbf{r}}_f \\ \mathbf{O} & \mathbf{O} & 1 \end{bmatrix} \begin{bmatrix} \hat{\mathbf{d}}_B \\ \hat{\mathbf{f}}_B \\ 1 \end{bmatrix} \quad (11.145)$$

After transforming the coordinate, the expanded transfer equation of the subsystem is obtained

$$\begin{bmatrix} \mathbf{d}_A \\ \mathbf{d}_B \\ \mathbf{f}_B \\ \mathbf{f}_A \\ 1 \end{bmatrix}_O = \begin{bmatrix} \mathbf{I} & \mathbf{O} & \mathbf{O} & \mathbf{O} & \mathbf{O} \\ \mathbf{O} & \mathbf{I} & \mathbf{O} & \mathbf{O} & \mathbf{O} \\ \mathbf{G}_4 \mathbf{C}_2^{-1} \mathbf{G}_1 & -\mathbf{G}_4 \mathbf{C}_2^{-1} \mathbf{C}_1 \mathbf{G}_3 & \mathbf{I} & \mathbf{O} & -\mathbf{G}_4 \mathbf{C}_2^{-1} \hat{\mathbf{r}}_d \\ \mathbf{G}_2 \mathbf{C}_4 \mathbf{C}_2^{-1} \mathbf{G}_1 & \mathbf{G}_2 (\mathbf{C}_3 - \mathbf{C}_4 \mathbf{C}_2^{-1} \mathbf{C}_1) \mathbf{G}_3 & \mathbf{O} & \mathbf{I} & -\mathbf{G}_2 \mathbf{C}_4 \mathbf{C}_2^{-1} \hat{\mathbf{r}}_d + \mathbf{G}_2 \hat{\mathbf{r}}_f \\ \mathbf{O} & \mathbf{O} & \mathbf{O} & \mathbf{O} & 1 \end{bmatrix} \begin{bmatrix} \mathbf{d}_A \\ \mathbf{d}_B \\ \mathbf{f}_B \\ \mathbf{f}_A \\ 1 \end{bmatrix}_I \quad (11.146)$$

11.9.3 Two-level Parallel System with Nonvertical Connection

As shown in Figure 11.28, the two-level parallel system is connected in a slanted direction by the subsystem. It is assumed that the connection of nodes *A* and *B* is a stiffness connection. The displacement is continuous, but the internal force is discontinuous. In local coordinates of the subsystem, the state vectors of the ends of nodes *A* and *B* have the following relations

$$\begin{bmatrix} \hat{\mathbf{d}}_A \\ \hat{\mathbf{f}}_A \end{bmatrix} = \begin{bmatrix} \hat{\mathbf{C}}_1 & \hat{\mathbf{C}}_2 \\ \hat{\mathbf{C}}_3 & \hat{\mathbf{C}}_4 \end{bmatrix} \begin{bmatrix} \hat{\mathbf{d}}_B \\ \hat{\mathbf{f}}_B \end{bmatrix} \quad (11.147)$$

where $\hat{\mathbf{d}}$ and $\hat{\mathbf{f}}$ express the displacement and internal force of vectors in local coordinates, respectively.

In the whole coordinate belong to the principal systems I and II, the increment of internal force at nodes *A* and *B* can be expressed by their displacements

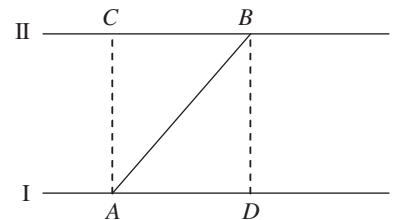
$$\begin{bmatrix} \Delta \mathbf{f}_B \\ \Delta \mathbf{f}_A \end{bmatrix} = \begin{bmatrix} \mathbf{G}_4 \hat{\mathbf{C}}_2^{-1} \mathbf{G}_1 & -\mathbf{G}_4 \hat{\mathbf{C}}_2^{-1} \hat{\mathbf{C}}_1 \mathbf{G}_3 \\ \mathbf{G}_2 \hat{\mathbf{C}}_4 \hat{\mathbf{C}}_2^{-1} \mathbf{G}_1 & \mathbf{G}_2 (\hat{\mathbf{C}}_3 - \hat{\mathbf{C}}_4 \hat{\mathbf{C}}_2^{-1} \hat{\mathbf{C}}_1) \mathbf{G}_3 \end{bmatrix} \begin{bmatrix} \mathbf{d}_A \\ \mathbf{d}_B \end{bmatrix} \quad (11.148)$$

where \mathbf{G}_1 , \mathbf{G}_2 , \mathbf{G}_3 and \mathbf{G}_4 are the transformation matrices of the displacements and the internal forces at nodes *A* and *B* from the local coordinate system to the principal coordinate system.

The transfer equation from *C* to *B* in principal system II is

$$\mathbf{Z}_B = \begin{bmatrix} \bar{\mathbf{C}}_1 & \bar{\mathbf{C}}_2 \\ \bar{\mathbf{C}}_3 & \bar{\mathbf{C}}_4 \end{bmatrix} \mathbf{Z}_C \quad (11.149)$$

Figure 11.28 Two-level parallel system with nonvertical connection.



therefore

$$\mathbf{d}_B = \bar{\mathbf{C}}_1 \mathbf{d}_C + \bar{\mathbf{C}}_2 \mathbf{f}_C \quad (11.150)$$

Substituting Equation (11.150) into Equation (11.149) yields

$$\begin{bmatrix} \Delta \mathbf{f}_B \\ \Delta \mathbf{f}_A \end{bmatrix} = \begin{bmatrix} \mathbf{G}_4 \hat{\mathbf{C}}_2^{-1} \mathbf{G}_1 & -\mathbf{G}_4 \hat{\mathbf{C}}_2^{-1} \hat{\mathbf{C}}_1 \mathbf{G}_3 \bar{\mathbf{C}}_1 & -\mathbf{G}_4 \hat{\mathbf{C}}_2^{-1} \hat{\mathbf{C}}_1 \mathbf{G}_3 \bar{\mathbf{C}}_2 \\ \mathbf{G}_2 \hat{\mathbf{C}}_4 \hat{\mathbf{C}}_2^{-1} \mathbf{G}_1 & \mathbf{G}_2 (\hat{\mathbf{C}}_3 - \hat{\mathbf{C}}_4 \hat{\mathbf{C}}_2^{-1} \hat{\mathbf{C}}_1) \mathbf{G}_3 \bar{\mathbf{C}}_1 & \mathbf{G}_2 (\hat{\mathbf{C}}_3 - \hat{\mathbf{C}}_4 \hat{\mathbf{C}}_2^{-1} \hat{\mathbf{C}}_1) \mathbf{G}_3 \bar{\mathbf{C}}_2 \end{bmatrix} \begin{bmatrix} \mathbf{d}_A \\ \mathbf{d}_C \\ \mathbf{f}_C \end{bmatrix} \quad (11.151)$$

Considering the continuity of displacements and internal forces without subsystem AB , the transfer equation of principal systems I and II can be obtained at section AC as

$$\begin{bmatrix} \mathbf{d}_I \\ \mathbf{d}_{II} \\ \mathbf{f}_{II} \\ \mathbf{f}_I \end{bmatrix}_O = \begin{bmatrix} \mathbf{I} & \mathbf{O} & \mathbf{O} & \mathbf{O} \\ \mathbf{O} & \mathbf{I} & \mathbf{O} & \mathbf{O} \\ \mathbf{O} & \mathbf{O} & \mathbf{I} & \mathbf{O} \\ \mathbf{G}_2 \hat{\mathbf{C}}_4 \hat{\mathbf{C}}_2^{-1} \mathbf{G}_1 & \mathbf{G}_2 (\hat{\mathbf{C}}_3 - \hat{\mathbf{C}}_4 \hat{\mathbf{C}}_2^{-1} \hat{\mathbf{C}}_1) \mathbf{G}_3 \bar{\mathbf{C}}_1 & \mathbf{G}_2 (\hat{\mathbf{C}}_3 - \hat{\mathbf{C}}_4 \hat{\mathbf{C}}_2^{-1} \hat{\mathbf{C}}_1) \mathbf{G}_3 \bar{\mathbf{C}}_2 & \mathbf{I} \end{bmatrix} \begin{bmatrix} \mathbf{d}_I \\ \mathbf{d}_{II} \\ \mathbf{f}_{II} \\ \mathbf{f}_I \end{bmatrix}_I \quad (11.152)$$

Similarly, the transfer equation of principal systems I and II at section BD is

$$\begin{bmatrix} \mathbf{d}_I \\ \mathbf{d}_{II} \\ \mathbf{f}_{II} \\ \mathbf{f}_I \end{bmatrix}_O = \begin{bmatrix} \mathbf{I} & \mathbf{O} & \mathbf{O} & \mathbf{O} \\ \mathbf{O} & \mathbf{I} & \mathbf{O} & \mathbf{O} \\ \mathbf{G}_4 \hat{\mathbf{C}}_2^{-1} \mathbf{G}_1 \mathbf{C}'_1 & -\mathbf{G}_4 \hat{\mathbf{C}}_2^{-1} \hat{\mathbf{C}}_1 \mathbf{G}_3 & \mathbf{I} & \mathbf{G}_4 \hat{\mathbf{C}}_2 \mathbf{G}_1 \mathbf{C}'_2 \\ \mathbf{O} & \mathbf{O} & \mathbf{O} & \mathbf{I} \end{bmatrix} \begin{bmatrix} \mathbf{d}_I \\ \mathbf{d}_{II} \\ \mathbf{f}_{II} \\ \mathbf{f}_I \end{bmatrix}_I \quad (11.153)$$

where \mathbf{C}'_1 and \mathbf{C}'_2 are submatrices of the transfer matrices in principal system I from D to A .

11.10 Numerical Example of General System Dynamics

11.10.1 Vibration Characteristics of a Hybrid Multibody System with a Branched and Closed-loop System

A hybrid MRFS with a branched and closed-loop system only needs to build geometric relation equations and equilibrium equations according to the displacement geometric conditions and equilibrium conditions in each connection point, respectively, and the other steps of the solution are the same as those in the chain system. The MSTMM can expediently solve the dynamic problems of the hybrid MRFS with a branched and closed-loop system.

Figure 11.29 shows a hybrid MRFS with a branched and closed-loop system vibrating in a plane. The elements 1, 3, 4 and 6 are planar elastic hinges, elements 2, 5 and 7 are rigid bodies, and element 8 is an elastic beam. The sequence number of the elements is shown in Figure 11.29. The free end of the beam is defined as the output end of system. The connection point between element 1 and the ground is defined as the first input end of system, and the free end of element 5 is defined as the second input end of the system.

The state vectors $\mathbf{Z}_{1,0}$, $\mathbf{Z}_{2,1}$, $\mathbf{Z}_{2,3}$, $\mathbf{Z}_{2,4}$, $\mathbf{Z}_{5,0}$, $\mathbf{Z}_{5,6}$, $\mathbf{Z}_{7,3}$, $\mathbf{Z}_{7,4}$, $\mathbf{Z}_{7,6}$, $\mathbf{Z}_{7,8}$, \mathbf{Z}_{x_8} and $\mathbf{Z}_{8,0}$ can be defined in the form of $\mathbf{Z} = [X, Y, \theta_z, M_z, Q_x, Q_y]^T$.

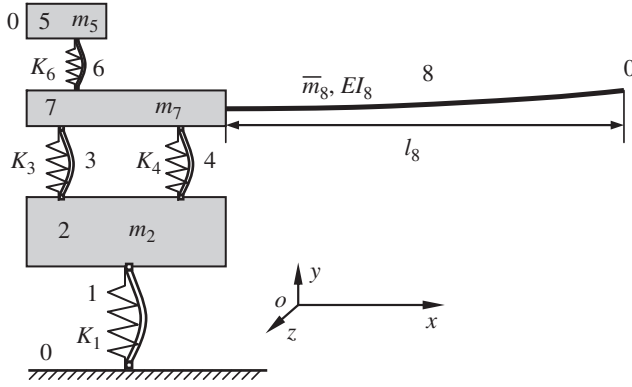


Figure 11.29 A hybrid MRFS with a branched and closed-loop system.

Element 7 is a rigid body with three input ends and one output end. Its three state vectors at the input ends are $Z_{7,3}$, $Z_{7,4}$ and $Z_{7,6}$. The state vector $Z_{I,7}$ at the input end is defined as

$$Z_{I,7} = E_1 Z_{7,3} + E_2 Z_{7,4} + E_3 Z_{7,6} \quad (11.154)$$

where

$$E_1 = \begin{bmatrix} I_6 \\ O_{6 \times 6} \end{bmatrix}, \quad E_2 = \begin{bmatrix} O_{6 \times 3} & O_{6 \times 3} \\ O_{3 \times 3} & I_3 \\ O_{3 \times 3} & O_{3 \times 3} \end{bmatrix}, \quad E_3 = \begin{bmatrix} O_{9 \times 3} & O_{9 \times 3} \\ O_{3 \times 3} & I_3 \end{bmatrix}$$

The transfer equation is

$$Z_{7,8} = U_7 Z_{I,7} \quad (11.155)$$

The transfer matrix is

$$U_7 = \begin{bmatrix} 1 & 0 & -b_2 & 0 & 0 & 0 & 0 & 0 & 0 & 0 & 0 & 0 \\ 0 & 1 & b_1 & 0 & 0 & 0 & 0 & 0 & 0 & 0 & 0 & 0 \\ 0 & 0 & 1 & 0 & 0 & 0 & 0 & 0 & 0 & 0 & 0 & 0 \\ u_{4,1} & u_{4,2} & u_{4,3} & 1 & -b_2 & b_1 & 1 & u_{4,8} & u_{4,9} & 1 & u_{4,11} & u_{4,12} \\ m_7 \omega^2 & 0 & -m_7 \omega^2 c_{c2} & 0 & 1 & 0 & 0 & 1 & 0 & 0 & 1 & 0 \\ 0 & m_7 \omega^2 & m_7 \omega^2 c_{c1} & 0 & 0 & 1 & 0 & 0 & 1 & 0 & 0 & 1 \end{bmatrix}$$

where

$$u_{4,1} = -m_7 \omega^2 (b_2 - c_{c2}), \quad u_{4,2} = m_7 \omega^2 (b_1 - c_{c1}), \quad u_{4,3} = -\omega^2 [J_7 - m_7 (b_2 c_{c2} + b_1 c_{c1})] \\ u_{4,8} = -(b_2 - a_{2,2}), \quad u_{4,9} = b_1 - a_{1,2}, \quad u_{4,11} = -(b_2 - a_{2,3}), \quad u_{4,12} = b_1 - a_{1,3}$$

(b_1, b_2) and (c_{c1}, c_{c2}) are the position coordinates of the output end and the mass center of rigid body 7, respectively, in the body-fixed coordinate system in which the first input end is the origin. $(a_{1,2}, a_{2,2})$ and $(a_{1,3}, a_{2,3})$ are the position coordinates of the second and third input ends, respectively, of rigid body 7 in the body-fixed coordinate system.

Element 2 is a rigid body with one input end and two output ends, and its two state vectors at the output ends are $\mathbf{Z}_{2,3}$ and $\mathbf{Z}_{2,4}$. The state vector $\mathbf{Z}_{O,2}$ of the output end is defined as

$$\mathbf{Z}_{O,2} = \mathbf{E}_4 \mathbf{Z}_{2,3} + \mathbf{E}_5 \mathbf{Z}_{2,4} \quad (11.156)$$

where

$$\mathbf{E}_4 = \begin{bmatrix} \mathbf{I}_6 \\ \mathbf{O}_{3 \times 6} \end{bmatrix}, \quad \mathbf{E}_5 = \begin{bmatrix} \mathbf{O}_{6 \times 3} & \mathbf{O}_{6 \times 3} \\ \mathbf{O}_{3 \times 3} & \mathbf{I}_3 \end{bmatrix}$$

The transfer equation is

$$\mathbf{U}_2 \mathbf{Z}_{O,2} = \mathbf{Z}_{2,1} \quad (11.157)$$

The transfer matrix is

$$\mathbf{U}_2 = \begin{bmatrix} 1 & 0 & b_{2,1} & 0 & 0 & 0 & 0 & 0 & 0 \\ 0 & 1 & -b_{1,1} & 0 & 0 & 0 & 0 & 0 & 0 \\ 0 & 0 & 1 & 0 & 0 & 0 & 0 & 0 & 0 \\ -m_2 \omega^2 c_{c2} & m_2 \omega^2 c_{c1} & u_{43} & 1 & b_{2,1} & -b_{1,1} & 1 & b_{2,2} & -b_{1,2} \\ -m_2 \omega^2 & 0 & m_2 \omega^2 (c_{c2} - b_{2,1}) & 0 & 1 & 0 & 0 & 1 & 0 \\ 0 & -m_2 \omega^2 & -m_2 \omega^2 (c_{c1} - b_{1,1}) & 0 & 0 & 1 & 0 & 0 & 1 \end{bmatrix}$$

where

$$u_{43} = \omega^2 [J_2 - m_2 (c_{c2} b_{2,1} + c_{c1} b_{1,1})]$$

$(b_{1,1}, b_{2,1})$ and $(b_{1,2}, b_{2,2})$ are the position coordinates of the two output ends of rigid body 2 in the body-fixed coordinate system, whose input end is the origin.

The transfer equations of the other elements are

$$\begin{cases} \mathbf{Z}_{2,1} = \mathbf{U}_1 \mathbf{Z}_{1,0} \\ \mathbf{Z}_{7,3} = \mathbf{U}_3 \mathbf{Z}_{2,3}, \quad \mathbf{Z}_{7,4} = \mathbf{U}_4 \mathbf{Z}_{2,4}, \quad \mathbf{Z}_{5,6} = \mathbf{U}_5 \mathbf{Z}_{5,0} \\ \mathbf{Z}_{7,6} = \mathbf{U}_6 \mathbf{Z}_{5,6}, \quad \mathbf{Z}_{8,0} = \mathbf{U}_8 \mathbf{Z}_{7,8} \end{cases} \quad (11.158)$$

where \mathbf{U}_1 , \mathbf{U}_3 , \mathbf{U}_4 and \mathbf{U}_6 are the transfer matrices of hinges 1, 3, 4 and 6, respectively, \mathbf{U}_5 is the transfer matrix of a rigid body with one input and one output end, and \mathbf{U}_8 is the transfer matrix of the beam.

According to Equations (11.155), (11.157) and (11.158), we obtain

$$\begin{cases} \mathbf{U}_1 \mathbf{Z}_{1,0} - \mathbf{U}_2 \mathbf{E}_4 \mathbf{Z}_{2,3} - \mathbf{U}_2 \mathbf{E}_5 \mathbf{Z}_{2,4} = \mathbf{0}_6 \\ \mathbf{U}_8 \mathbf{U}_7 \mathbf{E}_1 \mathbf{U}_3 \mathbf{Z}_{2,3} + \mathbf{U}_8 \mathbf{U}_7 \mathbf{E}_2 \mathbf{U}_4 \mathbf{Z}_{2,4} + \mathbf{U}_8 \mathbf{U}_7 \mathbf{E}_3 \mathbf{U}_6 \mathbf{U}_5 \mathbf{Z}_{5,0} - \mathbf{Z}_{8,0} = \mathbf{0}_6 \end{cases} \quad (11.159)$$

$\mathbf{Z}_{2,3}$ and $\mathbf{Z}_{2,4}$ are both state vectors of rigid body 2, where the six elements denoting displacement are linear correlative

$$\mathbf{E}_6 \mathbf{Z}_{2,4} - \mathbf{E}_7 \mathbf{Z}_{2,3} = \mathbf{0}_3 \quad (11.160)$$

where

$$\mathbf{E}_6 = [\mathbf{I}_3, \mathbf{O}_{3 \times 3}], \quad \mathbf{E}_7 = \begin{bmatrix} 1 & 0 & -(b_{2,2} - b_{2,1}) \\ 0 & 1 & b_{1,2} - b_{1,1} & \mathbf{O}_{3 \times 3} \\ 0 & 0 & 1 \end{bmatrix}$$

Similarly, both $\mathbf{Z}_{7,4}$ and $\mathbf{Z}_{7,6}$ are state vectors of rigid body 7. The dependent displacements can be expressed linearly by three independent displacements in state vector $\mathbf{Z}_{7,3}$ at the first input end of element 7

$$\mathbf{E}_6 \mathbf{Z}_{7,4} = \mathbf{E}_8 \mathbf{Z}_{7,3}, \quad \mathbf{E}_6 \mathbf{Z}_{7,6} = \mathbf{E}_9 \mathbf{Z}_{7,3} \quad (11.161)$$

where

$$\mathbf{E}_8 = \begin{bmatrix} 1 & 0 & -a_{2,2} \\ 0 & 1 & a_{1,2} & \mathbf{O}_{3 \times 3} \\ 0 & 0 & 1 \end{bmatrix}, \quad \mathbf{E}_9 = \begin{bmatrix} 1 & 0 & -a_{2,3} \\ 0 & 1 & a_{1,3} & \mathbf{O}_{3 \times 3} \\ 0 & 0 & 1 \end{bmatrix}$$

In the body-fixed coordinate system, $(a_{1,2}, a_{2,2})$ and $(a_{1,3}, a_{2,3})$ are the position coordinates of the second and third input ends of rigid body 7.

According to Equations (11.158) and (11.161), we obtain

$$\begin{cases} \mathbf{E}_6 \mathbf{U}_4 \mathbf{Z}_{2,4} - \mathbf{E}_8 \mathbf{U}_3 \mathbf{Z}_{2,3} = \mathbf{0}_3 \\ \mathbf{E}_6 \mathbf{U}_6 \mathbf{U}_5 \mathbf{Z}_{5,0} - \mathbf{E}_9 \mathbf{U}_3 \mathbf{Z}_{2,3} = \mathbf{0}_3 \end{cases} \quad (11.162)$$

Combining Equations (11.159), (11.160) and (11.162), the matrix form is

$$\mathbf{U}_{\text{all}} \mathbf{Z}_{\text{all}} = \mathbf{0}$$

where

$$\mathbf{U}_{\text{all}} = \begin{bmatrix} \mathbf{U}_1 & \mathbf{O}_{6 \times 6} & \mathbf{O}_{6 \times 6} & -\mathbf{U}_2 \mathbf{E}_4 & -\mathbf{U}_2 \mathbf{E}_5 \\ \mathbf{O}_{6 \times 6} & \mathbf{U}_8 \mathbf{U}_7 \mathbf{E}_3 \mathbf{U}_6 \mathbf{U}_5 & -\mathbf{I}_6 & \mathbf{U}_8 \mathbf{U}_7 \mathbf{E}_1 \mathbf{U}_3 & \mathbf{U}_8 \mathbf{U}_7 \mathbf{E}_2 \mathbf{U}_4 \\ \mathbf{O}_{3 \times 6} & \mathbf{O}_{3 \times 6} & \mathbf{O}_{3 \times 6} & -\mathbf{E}_7 & \mathbf{E}_6 \\ \mathbf{O}_{3 \times 6} & \mathbf{O}_{3 \times 6} & \mathbf{O}_{3 \times 6} & -\mathbf{E}_8 \mathbf{U}_3 & \mathbf{E}_6 \mathbf{U}_4 \\ \mathbf{O}_{3 \times 6} & \mathbf{E}_6 \mathbf{U}_6 \mathbf{U}_5 & \mathbf{O}_{3 \times 6} & -\mathbf{E}_9 \mathbf{U}_3 & \mathbf{O}_{3 \times 6} \end{bmatrix}, \quad \mathbf{Z}_{\text{all}} = \begin{bmatrix} \mathbf{Z}_{1,0} \\ \mathbf{Z}_{5,0} \\ \mathbf{Z}_{8,0} \\ \mathbf{Z}_{2,3} \\ \mathbf{Z}_{2,4} \end{bmatrix} \quad (11.163)$$

According to the boundary conditions, we obtain

$$\begin{cases} \mathbf{Z}_{1,0} = [0, 0, 0, M_z, Q_x, Q_y]^T_{1,0} \\ \mathbf{Z}_{5,0} = [X, Y, \theta_z, 0, 0, 0]^T_{5,0} \\ \mathbf{Z}_{8,0} = [X, Y, \theta_z, 0, 0, 0]^T_{8,0} \end{cases} \quad (11.164)$$

therefore elements 1, 2, 3, 10, 11, 12, 16, 17 and 18 in \mathbf{Z}_{all} are zeros. These null elements are deleted from \mathbf{Z}_{all} , and the corresponding columns are deleted from \mathbf{U}_{all} . We obtain $\bar{\mathbf{U}}_{\text{all}} \bar{\mathbf{Z}}_{\text{all}} = \mathbf{0}_{21}$, and the characteristic equation is $\Delta = |\bar{\mathbf{U}}_{\text{all}}| = 0$.

It is important to note that both the state vectors at connection points $\mathbf{Z}_{2,3}$ and $\mathbf{Z}_{2,4}$ are contained in $\bar{\mathbf{Z}}_{\text{all}}$. This is different from the case where $\bar{\mathbf{Z}}_{\text{all}}$ contains only state vectors at the boundary points, as mentioned before. This is caused by the closed loop in the system. The overall transfer equation of a closed-loop system does not contain state vectors at any boundary points, but only contains state vectors at the interior connection points.

The state vectors at interior connection points may linearly depend on the state vectors at the boundary points, but from knowledge of linear algebra this does not affect the solution of the characteristic equation and $\bar{\mathbf{U}}_{\text{all}} \bar{\mathbf{Z}}_{\text{all}} = \mathbf{0}$. In this system, $\mathbf{Z}_{2,3}$ and $\mathbf{Z}_{2,4}$ of Equation (11.163) can be substituted by $\mathbf{Z}_{0,2}$. Consequently, the order of the overall transfer equation and the overall

transfer matrix can be decreased to three. We can even make $Z_{2,3}$ and $Z_{2,4}$ disappear in \bar{Z}_{all} by skillful transformation, which will greatly decrease the order of the overall transfer equation and the overall transfer matrix. The details are discussed below.

The transformation relation from $Z_{2,3}$ and $Z_{2,4}$ to $Z_{O,2}$ is established in Equation (11.157), while the transformation relations from $Z_{O,2}$ to $Z_{2,3}$ and $Z_{2,4}$ are transformed as follows

$$Z_{2,3} = E_{10}Z_{O,2}, \quad Z_{2,4} = E_{11}Z_{O,2} \quad (11.165)$$

where

$$E_{10} = [I_6 \quad O_{6 \times 3}], \quad E_{11} = \begin{bmatrix} E_7 & O_{3 \times 3} \\ O_{3 \times 3} & O_{3 \times 3} & I_3 \end{bmatrix} \quad (11.166)$$

Equation (11.165) can be substituted into Equations (11.159) and (11.162), and the matrix form written as

$$U_{\text{all}}Z_{\text{all}} = 0$$

where

$$U_{\text{all}} = \begin{bmatrix} U_1 & O_{6 \times 6} & O_{6 \times 6} & -U_2 \\ O_{6 \times 6} & U_8 U_7 E_3 U_6 U_5 & -I_6 & U_8 U_7 (E_1 U_3 E_{10} + E_2 U_4 E_{11}) \\ O_{3 \times 6} & O_{3 \times 6} & O_{3 \times 6} & -E_8 U_3 E_{10} + E_6 U_4 E_{11} \\ O_{3 \times 6} & E_6 U_6 U_5 & O_{3 \times 6} & -E_9 U_3 E_{10} \end{bmatrix}, \quad Z_{\text{all}} = \begin{bmatrix} Z_{1,0} \\ Z_{5,0} \\ Z_{8,0} \\ Z_{O,2} \end{bmatrix} \quad (11.167)$$

Thus, we can obtain $\bar{U}_{\text{all}18 \times 18} \bar{Z}_{\text{all}18 \times 1} = 0_{18}$. There are only 18 unknown elements in \bar{Z}_{all} and three less than before, so the order of \bar{U}_{all} is correspondingly reduced by three.

If Equation (11.159) is rewritten as

$$\begin{cases} U_2 E_4 Z_{2,3} + U_2 E_5 Z_{2,4} = U_1 Z_{1,0} \\ U_8 U_7 E_1 U_3 Z_{2,3} + U_8 U_7 E_2 U_4 Z_{2,4} = Z_{8,0} - U_8 U_7 E_3 U_6 U_5 Z_{5,0} \end{cases}$$

that is

$$\begin{bmatrix} U_2 E_4 & U_2 E_5 \\ U_8 U_7 E_1 U_3 & U_8 U_7 E_2 U_4 \end{bmatrix} \begin{bmatrix} Z_{2,3} \\ Z_{2,4} \end{bmatrix} = \begin{bmatrix} U_1 & O_{6 \times 6} & O_{6 \times 6} \\ O_{6 \times 6} & -U_8 U_7 E_3 U_6 U_5 & I_6 \end{bmatrix} \begin{bmatrix} Z_{1,0} \\ Z_{5,0} \\ Z_{8,0} \end{bmatrix} \quad (11.168)$$

we obtain

$$\begin{bmatrix} Z_{2,3} \\ Z_{2,4} \end{bmatrix} = \begin{bmatrix} U_2 E_4 & U_2 E_5 \\ U_8 U_7 E_1 U_3 & U_8 U_7 E_2 U_4 \end{bmatrix}^{-1} \begin{bmatrix} U_1 & O_{6 \times 6} & O_{6 \times 6} \\ O_{6 \times 6} & -U_8 U_7 E_3 U_6 U_5 & I_6 \end{bmatrix} \begin{bmatrix} Z_{1,0} \\ Z_{5,0} \\ Z_{8,0} \end{bmatrix} \quad (11.169)$$

We can define

$$\begin{bmatrix} E_{12} & E_{13} & E_{14} \\ E_{15} & E_{16} & E_{17} \end{bmatrix} = \begin{bmatrix} U_2 E_4 & U_2 E_5 \\ U_8 U_7 E_1 U_3 & U_8 U_7 E_2 U_4 \end{bmatrix}^{-1} \begin{bmatrix} U_1 & O_{6 \times 6} & O_{6 \times 6} \\ O_{6 \times 6} & -U_8 U_7 E_3 U_6 U_5 & I_6 \end{bmatrix} \quad (11.170)$$

then

$$\begin{cases} Z_{2,3} = E_{12}Z_{1,0} + E_{13}Z_{5,0} + E_{14}Z_{8,0} \\ Z_{2,4} = E_{15}Z_{1,0} + E_{16}Z_{5,0} + E_{17}Z_{8,0} \end{cases} \quad (11.171)$$

Substituting Equation (11.171) into Equations (11.160) and (11.162), and writing them in matrix form gives

$$\mathbf{U}_{\text{all}} \mathbf{Z}_{\text{all}} = \mathbf{0}$$

where

$$\mathbf{U}_{\text{all}} = \begin{bmatrix} E_6 E_{15} - E_7 E_{12} & E_6 E_{16} - E_7 E_{13} & E_6 E_{17} - E_7 E_{14} \\ E_6 U_4 E_{15} - E_8 U_3 E_{12} & E_6 U_4 E_{16} - E_8 U_3 E_{13} & E_6 U_4 E_{17} - E_8 U_3 E_{14} \\ -E_9 U_3 E_{12} & E_6 U_6 U_5 - E_9 U_3 E_{13} & -E_9 U_3 E_{14} \end{bmatrix}, \quad \mathbf{Z}_{\text{all}} = \begin{bmatrix} Z_{1,0} \\ Z_{5,0} \\ Z_{8,0} \end{bmatrix} \quad (11.172)$$

Thus, there are only nine unknown elements in $\bar{\mathbf{Z}}_{\text{all}}$. Correspondingly, $\bar{\mathbf{U}}_{\text{all}}$ is a square matrix with order 9, and its order is greatly reduced.

Example 11.9 A spatial vibration system composed of four pillars and four beams is shown in Figure 11.30. The base of pillars is fixed to the ground, and the other ends are welded with beams. Derive the overall transfer equation and the characteristic equation considering the transverse, longitudinal and torsional vibrations of the pillars and beams.

Solution

First, find the transfer routes and the coordinate systems for each transfer route. The closed loop along with the four beams is defined as the principal transfer route, and the four pillars are defined as branched transfer routes from the ground to the main transfer route. For convenience the welded connections at the four corners are regarded as four small rigid bodies, and all are fixed to the pillars and beams. Thus, the system includes 12 elements in all. The coordinate systems and sequence numbers of each element are shown in Figure 11.30.

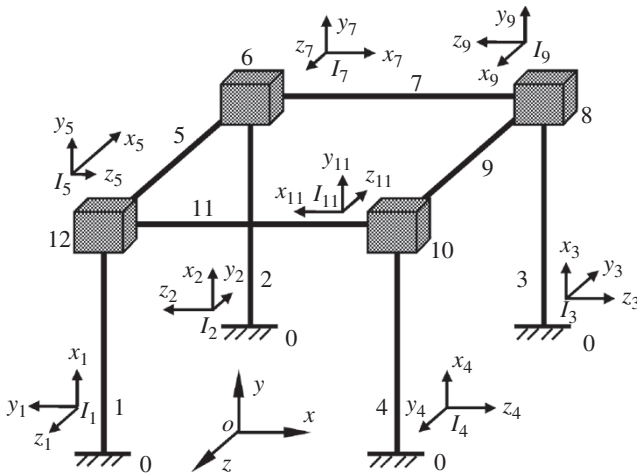


Figure 11.30 A MRFS composed of elastic beams and rigid bodies.

The state vectors $Z_{1,0}, Z_{2,0}, Z_{3,0}, Z_{4,0}, Z_{6,2}, Z_{6,5}, Z_{6,7}, Z_{8,3}, Z_{8,7}, Z_{8,9}, Z_{10,4}, Z_{10,9}, Z_{10,11}, Z_{12,1}, Z_{12,5}$ and $Z_{12,11}$ are defined in different coordinate systems (see Figure 4.18) in the form of $Z = [X, Y, Z, \theta_x, \theta_y, \theta_z, M_x, M_y, M_z, Q_x, Q_y, Q_z]^T$. Elements 6, 8, 10 and 12 are all rigid bodies with two input ends and one output end. The state vectors are defined as follows

$$\begin{cases} Z_{I,6} = E_1 Z_{6,5} + E_2 Z_{6,2} & (\text{in } I_7 x_7 y_7 z_7) \\ Z_{I,8} = E_1 Z_{8,7} + E_2 Z_{8,3} & (\text{in } I_9 x_9 y_9 z_9) \\ Z_{I,10} = E_1 Z_{10,9} + E_2 Z_{10,4} & (\text{in } I_{11} x_{11} y_{11} z_{11}) \\ Z_{I,12} = E_1 Z_{12,11} + E_2 Z_{12,1} & (\text{in } I_5 x_5 y_5 z_5) \end{cases} \quad (11.173)$$

where

$$E_1 = \begin{bmatrix} E_{1,1} & O_{3 \times 3} & O_{3 \times 3} & O_{3 \times 3} \\ O_{3 \times 3} & E_{1,1} & O_{3 \times 3} & O_{3 \times 3} \\ O_{3 \times 3} & O_{3 \times 3} & E_{1,1} & O_{3 \times 3} \\ O_{3 \times 3} & O_{3 \times 3} & O_{3 \times 3} & E_{1,1} \\ O_{6 \times 3} & O_{6 \times 3} & O_{6 \times 3} & O_{6 \times 3} \end{bmatrix}, \quad E_{1,1} = \begin{bmatrix} 0 & 0 & 1 \\ 0 & 1 & 0 \\ -1 & 0 & 0 \end{bmatrix}$$

$$E_2 = \begin{bmatrix} O_{12 \times 6} & O_{12 \times 3} & O_{12 \times 3} \\ O_{3 \times 6} & E_{2,2} & O_{3 \times 3} \\ O_{3 \times 6} & O_{3 \times 3} & E_{2,2} \end{bmatrix}, \quad E_{2,2} = \begin{bmatrix} 0 & 0 & -1 \\ 1 & 0 & 0 \\ 0 & -1 & 0 \end{bmatrix}$$

The transfer equations of the elements are

$$\begin{cases} Z_{12,1} = U_1 Z_{1,0} \\ Z_{6,2} = U_2 Z_{2,0} \\ Z_{8,3} = U_3 Z_{3,0} \\ Z_{10,4} = U_4 Z_{4,0} \end{cases}, \quad \begin{cases} Z_{6,5} = U_5 Z_{12,5} \\ Z_{8,7} = U_7 Z_{6,7} \\ Z_{10,9} = U_9 Z_{8,9} \\ Z_{12,11} = U_{11} Z_{10,11} \end{cases}, \quad \begin{cases} Z_{6,7} = U_6 Z_{I,6} \\ Z_{8,9} = U_8 Z_{I,8} \\ Z_{10,11} = U_{10} Z_{I,10} \\ Z_{12,5} = U_{12} Z_{I,12} \end{cases} \quad (11.174)$$

where $U_1, U_2, U_3, U_4, U_5, U_7, U_9$ and U_{11} are the transfer matrices of the beams and U_6, U_8, U_{10} and U_{12} are the transfer matrices of rigid bodies with two input ends and one output end.

From Equation (11.174) we obtain

$$\begin{cases} Z_{12,5} = U_{12}(E_1 U_{11} Z_{10,11} + E_2 U_1 Z_{1,0}) \\ Z_{10,11} = U_{10}(E_1 U_9 Z_{8,9} + E_2 U_4 Z_{4,0}) \\ Z_{8,9} = U_8(E_1 U_7 Z_{6,7} + E_2 U_3 Z_{3,0}) \\ Z_{6,7} = U_6(E_1 U_5 Z_{12,5} + E_2 U_2 Z_{2,0}) \end{cases} \quad (11.175)$$

The relations of Equation (11.175) may be summarized as

$$U_{12} E_2 U_1 Z_{1,0} + U_{6-12} E_2 U_2 Z_{2,0} + U_{8-12} E_2 U_3 Z_{3,0} + U_{10-12} E_2 U_4 Z_{4,0} + (U_{6-12} E_1 U_5 - I_{12}) Z_{12,5} = \mathbf{0}_{12} \quad (11.176)$$

where

$$\begin{cases} \mathbf{U}_{10-12} = \mathbf{U}_{12}\mathbf{E}_1\mathbf{U}_{11}\mathbf{U}_{10} \\ \mathbf{U}_{8-12} = \mathbf{U}_{12}\mathbf{E}_1\mathbf{U}_{11}\mathbf{U}_{10}\mathbf{E}_1\mathbf{U}_9\mathbf{U}_8 \\ \mathbf{U}_{6-12} = \mathbf{U}_{12}\mathbf{E}_1\mathbf{U}_{11}\mathbf{U}_{10}\mathbf{E}_1\mathbf{U}_9\mathbf{U}_8\mathbf{E}_1\mathbf{U}_7\mathbf{U}_6 \end{cases}$$

For rigid body 6, there are geometric relations

$$[\mathbf{I}_6 \quad \mathbf{O}_{6 \times 12}] \mathbf{Z}_{I,6} = \begin{bmatrix} \mathbf{E}_{1,1} & \mathbf{O}_{3 \times 3} & \mathbf{O}_{6 \times 6} \\ \mathbf{O}_{3 \times 3} & \mathbf{E}_{1,1} & \mathbf{O}_{6 \times 6} \end{bmatrix} \mathbf{Z}_{6,5} = \begin{bmatrix} \mathbf{I}_3 & -\tilde{\mathbf{l}}_{P_{6,5}P_{6,2}} \\ \mathbf{O}_{3 \times 3} & \mathbf{I}_3 \end{bmatrix} \begin{bmatrix} \mathbf{E}_{2,2} & \mathbf{O}_{3 \times 3} & \mathbf{O}_{6 \times 6} \\ \mathbf{O}_{3 \times 3} & \mathbf{E}_{2,2} & \mathbf{O}_{6 \times 6} \end{bmatrix} \mathbf{Z}_{6,2}$$

Similar geometric relations can be obtained for rigid bodies 8, 10 and 12. Combining all the equations yields

$$\begin{cases} \mathbf{E}_3 \mathbf{Z}_{6,5} = \mathbf{E}_{4(i=6)} \mathbf{Z}_{6,2} \\ \mathbf{E}_3 \mathbf{Z}_{8,7} = \mathbf{E}_{4(i=8)} \mathbf{Z}_{8,3} \\ \mathbf{E}_3 \mathbf{Z}_{10,9} = \mathbf{E}_{4(i=10)} \mathbf{Z}_{10,4} \\ \mathbf{E}_3 \mathbf{Z}_{12,11} = \mathbf{E}_{4(i=12)} \mathbf{Z}_{12,1} \end{cases} \quad (11.177)$$

where

$$\mathbf{E}_3 = \begin{bmatrix} \mathbf{E}_{1,1} & \mathbf{O}_{3 \times 3} & \mathbf{O}_{6 \times 6} \\ \mathbf{O}_{3 \times 3} & \mathbf{E}_{1,1} & \mathbf{O}_{6 \times 6} \end{bmatrix}, \quad \mathbf{E}_{4(i)} = \begin{bmatrix} \mathbf{I}_3 & -\tilde{\mathbf{l}}_{I_1 I_2, i} \\ \mathbf{O}_{3 \times 3} & \mathbf{I}_3 \end{bmatrix} \begin{bmatrix} \mathbf{E}_{2,2} & \mathbf{O}_{3 \times 3} & \mathbf{O}_{6 \times 6} \\ \mathbf{O}_{3 \times 3} & \mathbf{E}_{2,2} & \mathbf{O}_{6 \times 6} \end{bmatrix}$$

I_1 and I_2 represent the first and second input ends, respectively, that is, I_1 represents $P_{6,5}$, $P_{8,7}$, $P_{10,9}$ and $P_{12,11}$, and I_2 represents $P_{6,2}$, $P_{8,3}$, $P_{10,4}$ and $P_{12,5}$.

Substituting Equations (11.173)–(11.175) into Equation (11.177) we obtain

$$\begin{cases} -\mathbf{E}_{4(i=6)} \mathbf{U}_2 \mathbf{Z}_{2,0} + \mathbf{E}_3 \mathbf{U}_5 \mathbf{Z}_{12,5} = \mathbf{0}_6 \\ \mathbf{E}_3 \mathbf{U}_7 \mathbf{U}_6 \mathbf{E}_2 \mathbf{U}_2 \mathbf{Z}_{2,0} - \mathbf{E}_{4(i=8)} \mathbf{U}_3 \mathbf{Z}_{3,0} + \mathbf{E}_3 \mathbf{U}_7 \mathbf{U}_6 \mathbf{E}_1 \mathbf{U}_5 \mathbf{Z}_{12,5} = \mathbf{0}_6 \\ \mathbf{U}_{6-9} \mathbf{E}_2 \mathbf{U}_2 \mathbf{Z}_{2,0} + \mathbf{E}_3 \mathbf{U}_9 \mathbf{U}_8 \mathbf{E}_2 \mathbf{U}_3 \mathbf{Z}_{3,0} - \mathbf{E}_{4(i=10)} \mathbf{U}_4 \mathbf{Z}_{4,0} + \mathbf{U}_{6-9} \mathbf{E}_1 \mathbf{U}_5 \mathbf{Z}_{12,5} = \mathbf{0}_6 \\ -\mathbf{E}_{4(i=12)} \mathbf{U}_1 \mathbf{Z}_{1,0} + \mathbf{U}_{6-11} \mathbf{E}_2 \mathbf{U}_2 \mathbf{Z}_{2,0} + \mathbf{U}_{8-11} \mathbf{E}_2 \mathbf{U}_3 \mathbf{Z}_{3,0} \\ + \mathbf{E}_3 \mathbf{U}_{11} \mathbf{U}_{10} \mathbf{E}_2 \mathbf{U}_4 \mathbf{Z}_{4,0} + \mathbf{U}_{6-11} \mathbf{E}_1 \mathbf{U}_5 \mathbf{Z}_{12,5} = \mathbf{0}_6 \end{cases} \quad (11.178)$$

where

$$\begin{cases} \mathbf{U}_{6-9} = \mathbf{E}_3 \mathbf{U}_9 \mathbf{U}_8 \mathbf{E}_1 \mathbf{U}_7 \mathbf{U}_6 \\ \mathbf{U}_{6-11} = \mathbf{E}_3 \mathbf{U}_{11} \mathbf{U}_{10} \mathbf{E}_1 \mathbf{U}_9 \mathbf{U}_8 \mathbf{E}_1 \mathbf{U}_7 \mathbf{U}_6 \\ \mathbf{U}_{8-11} = \mathbf{E}_3 \mathbf{U}_{11} \mathbf{U}_{10} \mathbf{E}_1 \mathbf{U}_9 \mathbf{U}_8 \end{cases}$$

Combining Equation (11.176) with Equation (11.178), and writing them in matrix form, the overall transfer equation is

$$\mathbf{U}_{\text{all}} \mathbf{Z}_{\text{all}} = \mathbf{0}$$

where

$$\mathbf{Z}_{\text{all}} = \left[\mathbf{Z}_{1,0}^T, \mathbf{Z}_{2,0}^T, \mathbf{Z}_{3,0}^T, \mathbf{Z}_{4,0}^T, \mathbf{Z}_{12,5}^T \right]^T$$

$$\mathbf{U}_{\text{all}} = \begin{bmatrix} \mathbf{U}_{12}\mathbf{E}_2\mathbf{U}_1 & \mathbf{U}_{6-12}\mathbf{E}_2\mathbf{U}_2 & \mathbf{U}_{8-12}\mathbf{E}_2\mathbf{U}_3 & \mathbf{U}_{10-12}\mathbf{E}_2\mathbf{U}_4 & \mathbf{U}_{6-12}\mathbf{E}_1\mathbf{U}_5 - \mathbf{I}_{12} \\ \mathbf{O}_{6 \times 12} & -\mathbf{E}_{4(i=6)}\mathbf{U}_2 & \mathbf{O}_{6 \times 12} & \mathbf{O}_{6 \times 12} & \mathbf{E}_3\mathbf{U}_5 \\ \mathbf{O}_{6 \times 12} & \mathbf{E}_3\mathbf{U}_7\mathbf{U}_6\mathbf{E}_2\mathbf{U}_2 & -\mathbf{E}_{4(i=8)}\mathbf{U}_3 & \mathbf{O}_{6 \times 12} & \mathbf{E}_3\mathbf{U}_7\mathbf{U}_6\mathbf{E}_1\mathbf{U}_5 \\ \mathbf{O}_{6 \times 12} & \mathbf{U}_{6-9}\mathbf{E}_2\mathbf{U}_2 & \mathbf{E}_3\mathbf{U}_9\mathbf{U}_8\mathbf{E}_2\mathbf{U}_3 & -\mathbf{E}_{4(i=10)}\mathbf{U}_4 & \mathbf{U}_{6-9}\mathbf{E}_1\mathbf{U}_5 \\ -\mathbf{E}_{4(i=12)}\mathbf{U}_1 & \mathbf{U}_{6-11}\mathbf{E}_2\mathbf{U}_2 & \mathbf{U}_{8-11}\mathbf{E}_2\mathbf{U}_3 & \mathbf{E}_3\mathbf{U}_{11}\mathbf{U}_{10}\mathbf{E}_2\mathbf{U}_4 & \mathbf{U}_{6-11}\mathbf{E}_1\mathbf{U}_5 \end{bmatrix}$$

(11.179)

From the boundary conditions we obtain

$$\begin{cases} \mathbf{Z}_{1,0} = [0, 0, 0, 0, 0, 0, M_x, M_y, M_z, Q_x, Q_y, Q_z]_{1,0}^T \\ \mathbf{Z}_{2,0} = [0, 0, 0, 0, 0, 0, M_x, M_y, M_z, Q_x, Q_y, Q_z]_{2,0}^T \\ \mathbf{Z}_{3,0} = [0, 0, 0, 0, 0, 0, M_x, M_y, M_z, Q_x, Q_y, Q_z]_{3,0}^T \\ \mathbf{Z}_{4,0} = [0, 0, 0, 0, 0, 0, M_x, M_y, M_z, Q_x, Q_y, Q_z]_{4,0}^T \end{cases} \quad (11.180)$$

The 24 elements in \mathbf{Z}_{all} , that is, elements 1–6, 13–18, 25–30 and 37–42, are therefore zero. These null elements are deleted from \mathbf{Z}_{all} and the corresponding columns are deleted from \mathbf{U}_{all} , finally resulting in $\bar{\mathbf{U}}_{\text{all}}\bar{\mathbf{Z}}_{\text{all}} = \mathbf{0}_{36}$. The characteristic equation is obtained as $\Delta = |\bar{\mathbf{U}}_{\text{all}}| = 0$. We can reduce the number of the order by eliminating $\mathbf{Z}_{12,5}$ from \mathbf{Z}_{all} using the method described earlier. The process is as follows.

Rewriting Equation (11.176) as

$$(\mathbf{I}_{12} - \mathbf{U}_{6-12}\mathbf{E}_1\mathbf{U}_5)\mathbf{Z}_{12,5} = \mathbf{U}_{12}\mathbf{E}_2\mathbf{U}_1\mathbf{Z}_{1,0} + \mathbf{U}_{6-12}\mathbf{E}_2\mathbf{U}_2\mathbf{Z}_{2,0} + \mathbf{U}_{8-12}\mathbf{E}_2\mathbf{U}_3\mathbf{Z}_{3,0} + \mathbf{U}_{10-12}\mathbf{E}_2\mathbf{U}_4\mathbf{Z}_{4,0}$$

yields

$$\mathbf{Z}_{12,5} = (\mathbf{I}_{12} - \mathbf{U}_{6-12}\mathbf{E}_1\mathbf{U}_5)^{-1}(\mathbf{U}_{12}\mathbf{E}_2\mathbf{U}_1\mathbf{Z}_{1,0} + \mathbf{U}_{6-12}\mathbf{E}_2\mathbf{U}_2\mathbf{Z}_{2,0} + \mathbf{U}_{8-12}\mathbf{E}_2\mathbf{U}_3\mathbf{Z}_{3,0} + \mathbf{U}_{10-12}\mathbf{E}_2\mathbf{U}_4\mathbf{Z}_{4,0})$$

We then define

$$\mathbf{Z}_{12,5} = \mathbf{E}_5\mathbf{Z}_{1,0} + \mathbf{E}_6\mathbf{Z}_{2,0} + \mathbf{E}_7\mathbf{Z}_{3,0} + \mathbf{E}_8\mathbf{Z}_{4,0} \quad (11.181)$$

Substituting Equation (11.181) into Equation (11.179) yields

$$\mathbf{U}_{\text{all}}\mathbf{z}_{\text{all}} = \mathbf{0}$$

$$\mathbf{U}_{\text{all}} = \begin{bmatrix} \mathbf{E}_3\mathbf{U}_5\mathbf{E}_5 & \mathbf{E}_3\mathbf{U}_5\mathbf{E}_6 - \mathbf{E}_{4(i=6)}\mathbf{U}_2 \\ \mathbf{E}_3\mathbf{U}_7\mathbf{U}_6\mathbf{E}_1\mathbf{U}_5\mathbf{E}_5 & \mathbf{E}_3\mathbf{U}_7\mathbf{U}_6(\mathbf{E}_1\mathbf{U}_5\mathbf{E}_6 + \mathbf{E}_2\mathbf{U}_2) \\ \mathbf{U}_{6-9}\mathbf{E}_1\mathbf{U}_5\mathbf{E}_5 & \mathbf{U}_{6-9}(\mathbf{E}_1\mathbf{U}_5\mathbf{E}_6 + \mathbf{E}_2\mathbf{U}_2) \\ \mathbf{U}_{6-11}\mathbf{E}_1\mathbf{U}_5\mathbf{E}_5 - \mathbf{E}_{4(i=12)}\mathbf{U}_1 & \mathbf{U}_{6-11}(\mathbf{E}_1\mathbf{U}_5\mathbf{E}_6 + \mathbf{E}_2\mathbf{U}_2) \\ \mathbf{E}_3\mathbf{U}_5\mathbf{E}_7 & \mathbf{E}_3\mathbf{U}_5\mathbf{E}_8 \\ \mathbf{E}_3\mathbf{U}_7\mathbf{U}_6\mathbf{E}_1\mathbf{U}_5\mathbf{E}_7 - \mathbf{E}_{4(i=8)}\mathbf{U}_3 & \mathbf{E}_3\mathbf{U}_7\mathbf{U}_6\mathbf{E}_1\mathbf{U}_5\mathbf{E}_8 \\ \mathbf{U}_{6-9}\mathbf{E}_1\mathbf{U}_5\mathbf{E}_7 + \mathbf{E}_3\mathbf{U}_9\mathbf{U}_8\mathbf{E}_2\mathbf{U}_3 & \mathbf{U}_{6-9}\mathbf{E}_1\mathbf{U}_5\mathbf{E}_8 - \mathbf{E}_{4(i=10)}\mathbf{U}_4 \\ \mathbf{U}_{6-11}\mathbf{E}_1\mathbf{U}_5\mathbf{E}_7 + \mathbf{U}_{8-11}\mathbf{E}_2\mathbf{U}_3 & \mathbf{U}_{6-11}\mathbf{E}_1\mathbf{U}_5\mathbf{E}_8 + \mathbf{E}_3\mathbf{U}_{11}\mathbf{U}_{10}\mathbf{E}_2\mathbf{U}_4 \end{bmatrix} \quad (11.182)$$

where

$$\mathbf{Z}_{\text{all}} = \left[\mathbf{Z}_{1,0}^T, \mathbf{Z}_{2,0}^T, \mathbf{Z}_{3,0}^T, \mathbf{Z}_{4,0}^T \right]^T$$

$$\mathbf{U}_{\text{all}} = \begin{bmatrix} E_3 U_5 E_5 & E_3 U_5 E_6 - E_{4(i=6)} U_2 \\ E_3 U_7 U_6 E_1 U_5 E_5 & E_3 U_7 U_6 (E_1 U_5 E_6 + E_2 U_2) \\ U_{6-9} E_1 U_5 E_5 & U_{6-9} (E_1 U_5 E_6 + E_2 U_2) \\ U_{6-11} E_1 U_5 E_5 - E_{4(i=12)} U_1 & U_{6-11} (E_1 U_5 E_6 + E_2 U_2) \\ E_3 U_5 E_7 & E_3 U_5 E_8 \\ E_3 U_7 U_6 E_1 U_5 E_7 - E_{4(i=8)} U_3 & E_3 U_7 U_6 E_1 U_5 E_8 \\ U_{6-9} E_1 U_5 E_7 + E_3 U_9 U_8 E_2 U_3 & U_{6-9} E_1 U_5 E_8 - E_{4(i=10)} U_4 \\ U_{6-11} E_1 U_5 E_7 + U_{8-11} E_2 U_3 & U_{6-11} E_1 U_5 E_8 + E_3 U_{11} U_{10} E_2 U_4 \end{bmatrix} \quad (11.183)$$

Thus, $\bar{\mathbf{Z}}_{\text{all}}$ only contains 24 unknown elements, and therefore the order of $\bar{\mathbf{U}}_{\text{all}}$ is reduced from 36 to 24.

11.10.2 Dynamics of a Network Multibody System

Example 11.10 A network multibody system is shown in Figure 11.31. All the hinges are smooth hinges and all the bars are the same. The mass centers are the geometrical centers, and the mass is 1 kg. The length of each bar is 1 m and the moment of inertia with respect to one end is $1/3 \text{ kg}\cdot\text{m}^2$. The initial velocities of the bars are zeros, and the initial angular coordinates are $-\pi/3$, $-2\pi/3$, $2\pi/3$, $\pi/3$, 0 and π . Solve the plumed motion of the system under the effect of gravity.

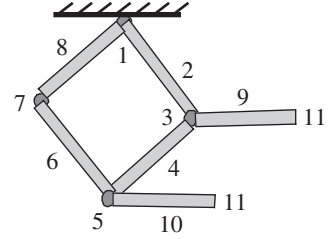


Figure 11.31 A multibody system with a network structure.

Solution

The transfer equations of the subsystem are

$$\begin{aligned} \mathbf{z}_{2,3} &= \mathbf{U}_2 \mathbf{z}_{2,1}, \quad \mathbf{z}_{9,11} = \mathbf{U}_9 \mathbf{z}_{9,3}, \quad \mathbf{z}_{4,5} = \mathbf{U}_4 \mathbf{z}_{4,3} \\ \mathbf{z}_{10,11} &= \mathbf{U}_{10} \mathbf{z}_{10,5}, \quad \mathbf{z}_{8,1} = \mathbf{U}_8 \mathbf{U}_7 \mathbf{U}_6 \mathbf{z}_{6,5} \end{aligned} \quad (11.184)$$

Let $\mathbf{U}_8 \mathbf{U}_7 \mathbf{U}_6 = \mathbf{U}_I$, then

$$\mathbf{z}_{8,1} = \mathbf{U}_I \mathbf{z}_{6,5} \quad (11.185)$$

According to the continuous condition of the position coordinates and the equilibrium of forces, we obtain

$$\begin{aligned} \mathbf{U}_{b_1} \mathbf{U}_2 \mathbf{z}_{2,1} &= \mathbf{U}_{b_1} \mathbf{U}_9^{-1} \mathbf{z}_{9,11} + \mathbf{U}_{b_1} \mathbf{z}_{4,3}, \quad \mathbf{U}_{b_2} \mathbf{U}_2 \mathbf{z}_{2,1} = \mathbf{U}_{b_2} \mathbf{U}_9^{-1} \mathbf{z}_{9,11} = \mathbf{U}_{b_2} \mathbf{z}_{4,3} \\ \mathbf{U}_{b_1} \mathbf{U}_I^{-1} \mathbf{z}_{8,1} &= -\mathbf{U}_{b_1} \mathbf{U}_{10}^{-1} \mathbf{z}_{10,11} + \mathbf{U}_{b_1} \mathbf{U}_4 \mathbf{z}_{4,3}, \quad \mathbf{U}_{b_2} \mathbf{U}_I^{-1} \mathbf{z}_{8,1} = \mathbf{U}_{b_2} \mathbf{U}_{10}^{-1} \mathbf{z}_{10,11} = \mathbf{U}_{b_2} \mathbf{U}_4 \mathbf{z}_{4,3} \\ \mathbf{U}_{b_3} \mathbf{U}_9^{-1} \mathbf{z}_{9,11} &= \mathbf{0}, \quad \mathbf{U}_{b_3} \mathbf{U}_2 \mathbf{z}_{2,1} = \mathbf{0}, \quad \mathbf{U}_{b_3} \mathbf{U}_4 \mathbf{z}_{4,3} = \mathbf{0}, \quad \mathbf{U}_{b_3} \mathbf{U}_{10}^{-1} \mathbf{z}_{10,11} = \mathbf{0}, \quad \mathbf{U}_{b_3} \mathbf{U}_I^{-1} \mathbf{z}_{8,1} = \mathbf{0} \end{aligned} \quad (11.186)$$

The overall transfer equation of the system is

$$\mathbf{U}_{\text{all}} \begin{bmatrix} \mathbf{z}_{2,1}^T & \mathbf{z}_{4,3}^T & \mathbf{z}_{8,1}^T & \mathbf{z}_{9,11}^T & \mathbf{z}_{10,11}^T \end{bmatrix}^T = \mathbf{0} \quad (11.187)$$

The overall transfer matrix is

$$\mathbf{U}_{\text{all}} = \begin{bmatrix} \mathbf{U}_{b_1} \mathbf{U}_2 & -\mathbf{U}_{b_1} & \mathbf{0} & -\mathbf{U}_{b_1} \mathbf{U}_9^{-1} & \mathbf{0} \\ \mathbf{0} & -\mathbf{U}_{b_1} \mathbf{U}_4 & \mathbf{U}_{b_1} \mathbf{U}_I^{-1} & \mathbf{0} & \mathbf{U}_{b_1} \mathbf{U}_{10}^{-1} \\ \mathbf{U}_{b_2} \mathbf{U}_2 & -\mathbf{U}_{b_2} & \mathbf{0} & \mathbf{0} & \mathbf{0} \\ \mathbf{U}_{b_2} \mathbf{U}_2 & \mathbf{0} & \mathbf{0} & -\mathbf{U}_{b_2} \mathbf{U}_9^{-1} & \mathbf{0} \\ \mathbf{0} & \mathbf{U}_{b_2} \mathbf{U}_4 & -\mathbf{U}_{b_2} \mathbf{U}_I^{-1} & \mathbf{0} & \mathbf{0} \\ \mathbf{0} & \mathbf{U}_{b_2} \mathbf{U}_4 & \mathbf{0} & \mathbf{0} & -\mathbf{U}_{b_2} \mathbf{U}_{10}^{-1} \\ \mathbf{U}_{b_3} \mathbf{U}_2 & \mathbf{0} & \mathbf{0} & \mathbf{0} & \mathbf{0} \\ \mathbf{0} & \mathbf{U}_{b_3} \mathbf{U}_4 & \mathbf{0} & \mathbf{0} & \mathbf{0} \\ \mathbf{0} & \mathbf{0} & \mathbf{U}_{b_3} \mathbf{U}_I^{-1} & \mathbf{0} & \mathbf{0} \\ \mathbf{0} & \mathbf{0} & \mathbf{0} & \mathbf{U}_{b_3} \mathbf{U}_9^{-1} & \mathbf{0} \\ \mathbf{0} & \mathbf{0} & \mathbf{0} & \mathbf{0} & \mathbf{U}_{b_3} \mathbf{U}_{10}^{-1} \end{bmatrix} \quad (11.188)$$

The boundary conditions are

$$\begin{cases} \mathbf{z}_{2,1} = [0, 0, \theta, 0, q_x, q_y, 1]^T_{2,1} \\ \mathbf{z}_{4,3} = [x, y, \theta, 0, q_x, q_y, 1]^T_{4,3} \\ \mathbf{z}_{8,1} = [0, 0, \theta, 0, q_x, q_y, 1]^T_{8,1} \\ \mathbf{z}_{9,11} = [x, y, \theta, 0, 0, 0, 1]^T_{9,11} \\ \mathbf{z}_{10,11} = [x, y, \theta, 0, 0, 0, 1]^T_{10,11} \end{cases} \quad (11.189)$$

The dynamics of the multibody system are computed using the MSDTTMM and an analytical mechanics method, and the computational results as shown in Figure 11.32. The dashed line denotes the results obtained by the analytical mechanics method, and the solid line denotes the results obtained by the MSDTTMM. The computational results of both methods are in good agreement.

11.10.3 Dynamics of General Multibody System

A general multi-rigid-body system containing a close loop moving in a plane is shown in Figure 11.33. The planar rigid bodies (numbered 1, 3, 5, 7, 9, 11 and 13) are connected by pin hinges (numbered 2, 4, 6, 8, 10, 12 and 14), and rigid body 1 is connected with the ground by a smooth pin. Each rigid body has the identical dynamics parameters

$$m = 1 \text{ kg} \quad J_C = \frac{1}{6} \text{ kg} \cdot \text{m}^2.$$

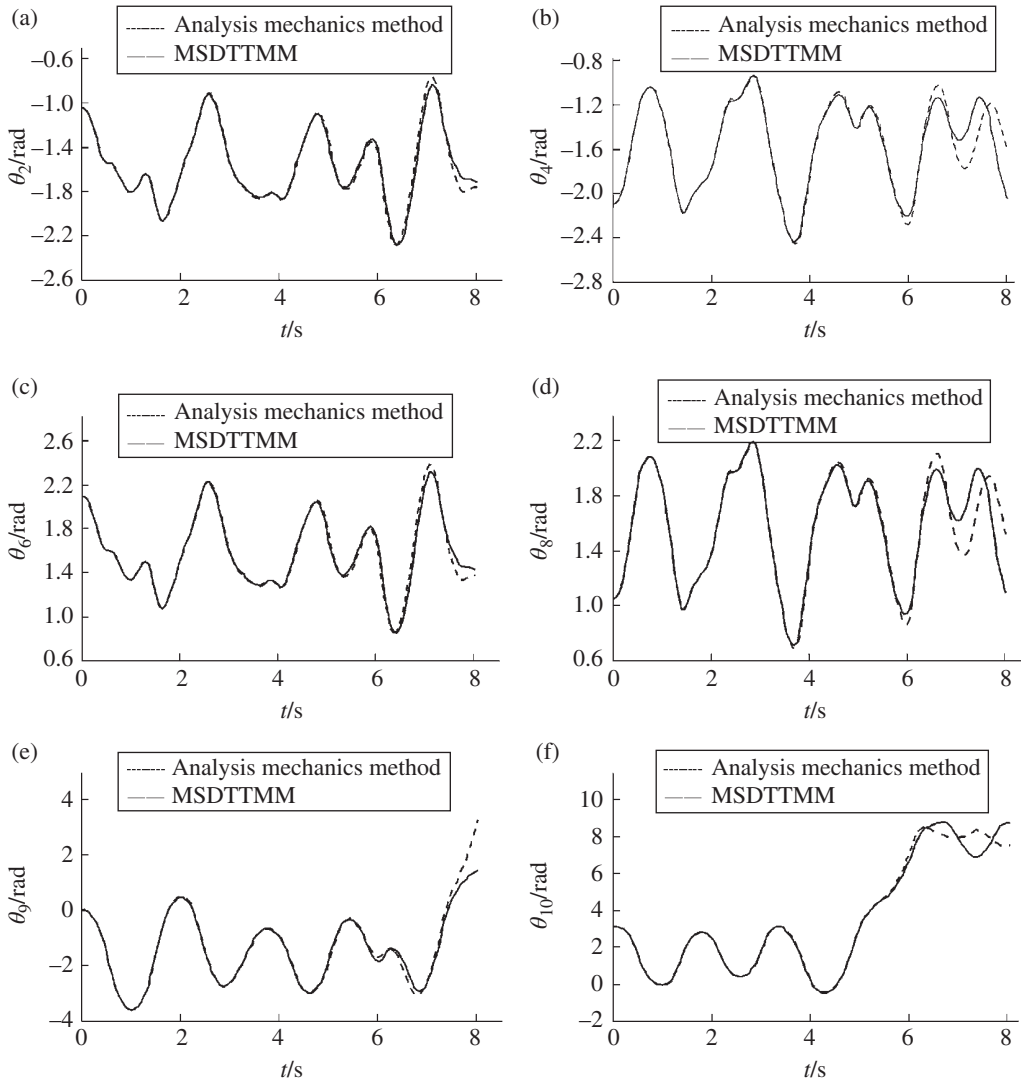


Figure 11.32 Time history of the orientation angles of each rigid body in a multibody system with a network structure: (a) orientation angle of rigid body 2, (b) orientation angle of rigid body 4, (c) orientation angle of rigid body 6, (d) orientation angle of rigid body 8, (e) orientation angle of rigid body 9 and (f) orientation angle of rigid body 10.

By “cutting” at the junction of body 9 and hinge 14, and following the proposed theorem, the topology figure of the system can be drawn, as shown in Figure 11.34. The overall transfer equation of the system can be derived automatically as

$$\mathbf{U}_{\text{all}} \mathbf{z}_{\text{all}} = \mathbf{0} \quad (11.190)$$

where the overall transfer matrix takes the form

$$\mathbf{U}_{\text{all}} = \begin{bmatrix} -\mathbf{I} & \mathbf{T}_{9-1} & \mathbf{T}_{14-1} \\ \mathbf{O} & \mathbf{G}_{9-3} & \mathbf{G}_{14-3} \\ \mathbf{O} & \mathbf{C} & -\mathbf{I} \end{bmatrix} \quad (11.191)$$

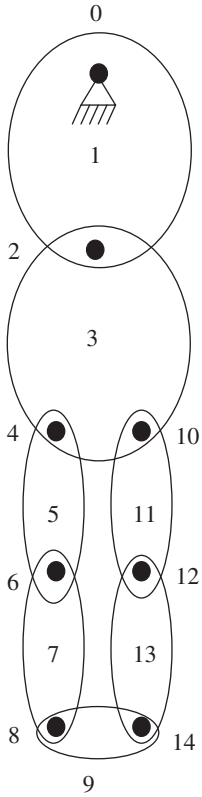


Figure 11.33 A general system moving in a plane.

The state vectors of all the boundary ends are

$$\mathbf{z}_{all} = \begin{bmatrix} \mathbf{z}_{1,0} \\ \mathbf{z}_{9,0} \\ \mathbf{z}_{14,0} \end{bmatrix} \quad (11.192)$$

According to the proposed sign conventions, we obtain

$$\mathbf{T}_{9-1} = \mathbf{U}_1 \mathbf{U}_2 \mathbf{U}_3 \mathbf{U}_4 \mathbf{U}_5 \mathbf{U}_6 \mathbf{U}_7 \mathbf{U}_8 \mathbf{U}_9 \quad (11.193)$$

$$\mathbf{T}_{14-1} = \mathbf{U}_1 \mathbf{U}_2 \mathbf{U}_{3,10} \mathbf{U}_{10} \mathbf{U}_{11} \mathbf{U}_{12} \mathbf{U}_{13} \mathbf{U}_{14}$$

$$\mathbf{G}_{9-3} = -\mathbf{H}_3 \mathbf{U}_4 \mathbf{U}_5 \mathbf{U}_6 \mathbf{U}_7 \mathbf{U}_8 \mathbf{U}_9 \quad (11.194)$$

$$\mathbf{G}_{14-3} = \mathbf{H}_{3,10} \mathbf{U}_{10} \mathbf{U}_{11} \mathbf{U}_{12} \mathbf{U}_{13} \mathbf{U}_{14}$$

$\mathbf{z}_{1,0}$ is the state vector of the root, $\mathbf{z}_{9,0}$ and $\mathbf{z}_{14,0}$ are the state vectors of the tips that emerge after the cutting. $\mathbf{U}_1, \mathbf{U}_3, \mathbf{U}_{3,10}, \mathbf{U}_5, \mathbf{U}_7, \mathbf{U}_9, \mathbf{U}_{11}$ and \mathbf{U}_{13} are the transfer matrices of the corresponding planar rigid bodies. $\mathbf{U}_2, \mathbf{U}_4, \mathbf{U}_6, \mathbf{U}_8, \mathbf{U}_{10}, \mathbf{U}_{12}$ and \mathbf{U}_{14} are the transfer matrices of the corresponding planar pin hinges.

The boundary conditions of the system are

$$\mathbf{z}_{1,0} = [0 \ 0 \ \ddot{\theta}_z \ 0 \ q_x \ q_y \ 1]^T_{1,0} \quad (11.195)$$

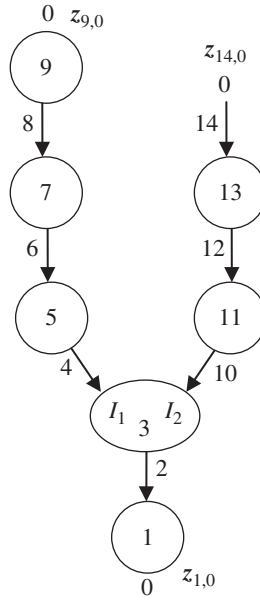


Figure 11.34 Topology figure of the general system moving in a plane.

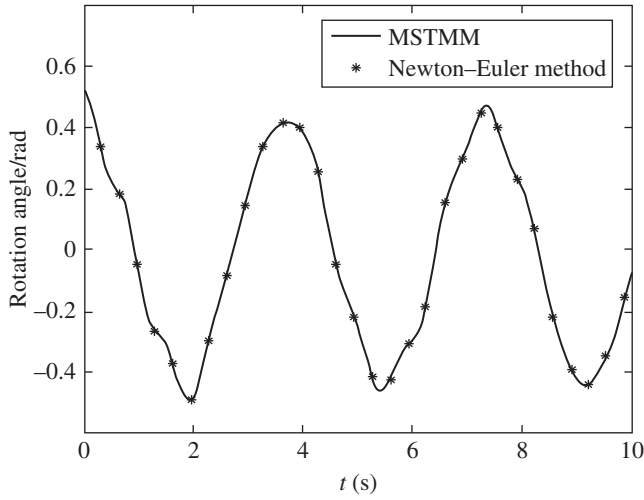


Figure 11.35 Computational results of the angle of rigid body 1.

The initial angle of the rigid body 1 is $\pi/6$ rad and the relative angles of the pin hinges (numbered 2, 4, 6, 8, 10, 12 and 14) are all zero. The system moves from rest under the effect of gravity. The computational results of the system dynamics are obtained by the proposed method and by the Newton–Euler method. The time history of the angle of rigid body 1 is given in Figure 11.35, which shows that the computational results obtained by the two methods are in good agreement.

Part IV

Applications of the Transfer Matrix Method for Multibody Systems

This part (Chapters 12–15) introduces some important engineering applications to solve international hotspot problems in the weapons field using the transfer matrix method for multibody systems (MSTMM) and the library of transfer matrices. The application of the linear MSTMM to the launch dynamics of a multiple launch rocket system (MLRS) is introduced in Chapter 12, the application of linear MSTMM to the launch dynamics of self-propelled artillery is introduced in Chapter 13 and the application of the discrete time transfer matrix method for multibody systems (MSDTTMM) to the launch dynamics of shipboard launch systems is introduced in Chapter 14. The library of transfer matrices for linear and nonlinear multibody systems is given in Chapter 15.

Based on the MSTMM, the theory and technology of the launch dynamics of a multibody system and its numerical simulation system have been established by the authors, including the launch dynamics of MLRSs [87–101], self-propelled artillery [102–111], shipboard guns [112, 113] and super high-firing frequency weapons [114]. They have been used to study fuze mechanism dynamics [115, 116] and spacecraft dynamics [117], and to improve the firing precision of missiles [118]. A new theoretical computing and test evaluating method for the firing dispersion of weapons has also been developed [110–127]. The first equipment and test technology for simulating the rotation, nutation and precession of projectiles with high spin speed has been demonstrated [128–130], as has the equipment and test technology for measuring the pose of projectiles moving in a gun tube and the initial disturbance of large caliber projectiles [131]. These theories of launch dynamics and simulation results of systems based on the MSTMM have been proved by a series of tests and have played a very important role in weapon design, research, test and assessment. These theories of launch dynamics and the simulation results of systems based on the MSTMM are important tools to improve and evaluate the performance of weapon systems such as firing dispersion, and for which there are 22 important key engineering projects, including 12 aspects of the National High-Tech Project, which have been solved and have produced an economic benefit of more than a hundred million yuan. The established technology for reducing the number of rockets consumed by MLRS firing dispersion tests decreases the consumption by 50–86% compared with the general test method in firing dispersion tests for many kinds of MLRSs, which has achieved the highest level in the world. The technology for improving the firing dispersion makes the firing dispersion of many MLRSs achieve the international leading level. These engineering results indicate the powerful function of the MSTMM.

12

Dynamics of Multiple Launch Rocket Systems

12.1 Introduction

As a practical example in important engineering applications of the linear MSTMM, this chapter solves the difficult problem in launch dynamics of MLRSs using the MSTMM.

MLRSs with 40 launch tubes are the best equipped among MLRSs in the world today, for example the Russian BM-21 type MLRS, shown in Figure 12.1. The number of launchers for an MLRS may be just a few or up to 40, and all the rockets can be launched in one volley in a few seconds, forming a glomerate assaulting strike. As a powerful oppressive weapon in modern war, MLRSs have received enormous attention from every powerful military country for their high speed, high power, violent firepower, long range, high mobility, ability to generate high-density firepower in a short time, and many other tactical advantages. With the changing features of modern war and the development of new technologies, the status and function of MLRSs are more and more important. How can their firing precision be predicted? How can dynamic performance be guaranteed by dynamic design? How can rocket consumption in MLRS testing be decreased while still guaranteeing the quality of the test? To address these problems in the development, production and testing of MLRSs, it is necessary to solve the theory and technology issues that influence them. These issues have been given attention at home and abroad, for example the computation of vibration characteristics, the orthogonality of eigenvectors and the exact analysis of the dynamic response. Prediction of the launch dynamics of MLRSs requires an understanding of the acting forces, motion law and control processes during the launching of MLRSs and provides tools for scientific evaluation and improving the performance of MLRSs. The MSTMM is a powerful tool for studying the launch dynamics of MLRSs. The function of MLRS launch dynamics is that through studying the theory, simulation and testing of launch and flight dynamics of MLRSs from the point of view of a weapons system, and optimizing the total parameters of the system, it provides method and means for the dynamic design and performance evaluation of weapons. By studying the acting force and motion law of MLRSs under various disturbance factors, searching the computational method, measurement means and influence factors of initial disturbance and dynamic performance, establishing the quantitative relation between the total parameters of weapons and the initial disturbance and dynamic performance, and providing methods and technology means for the dynamic design and scientific evaluation of MLRS, the dynamic performance and combat ability of weapons can be improved, and the corresponding research period can be shortened. Improving production efficiency, decreasing rocket consumption in tests and increasing economic benefit can be realized by further decreasing the ball firing test.

From the viewpoint of large system dynamics, including rockets, guns, propellants and the launch environment, the theory of MLRS launch dynamics is established in this chapter based



Figure 12.1 An MLRS with 40 launch tubes (Russia).

on the MSTMM, where the process of MLRSs from ignition to the level point is studied. The difficult computation problem of the vibration characteristics of a multi-rigid-flexible-body system (MRFS) for MLRSs is solved. The vibration characteristics of MLRSs and their variation with a change in the number of rockets on the launching equipment are obtained conveniently using the MSTMM. The exact analysis for the dynamic response of an MRFS for an MLRS is realized using the orthogonality theory of augmented eigenvectors established by authors, and the quantitative relation between the system performance of MLRSs and the firing sequence and firing interval is achieved. The two great practical applications of MLRS launch dynamics based on the MSTMM are also introduced in this chapter [87–101].

- 1) A new test technology for MLRSs, with low rocket consumption under equivalent initial disturbance, is established, which solves the difficult problem for strong military countries of decreasing rocket consumption in MLRS tests. This technology has been used in the approval tests of several MLRSs in the National High-Tech Project, with rocket consumption being decreased by 50–86%.
- 2) The launch technology for MLRSs with low initial disturbance and high firing precision is established, which improves the firing precision and combat ability of several MLRSs of the National High-Tech Project.

12.2 Launch Dynamics Model of the System and its Topology

MLRSs are used in almost all branches of the armed services, and the carrier vehicle can be an airplane, warship, ground vehicle and so on. In this chapter, an MLRS with 40 launch tubes carried by a ground vehicle is taken as an example to sketch the procedure of the study of the dynamics of the MLRS. This version is most often used, while the structures of the MLRS mounted on the other kinds of carrier vehicles are relatively much simpler than this case and their dynamics could be researched in a similar way. Firing precision includes firing accuracy and firing dispersion. The firing accuracy can be indicated from the deviation between the center of projectile scattering and the aiming point, which is determined by the characteristics of the

weapon system itself, and can be corrected theoretically through many firings. The firing dispersion is used to express the scattering degree of projectiles with respect to the center of projectile scattering, and is usually denoted by E . The disturbance factors of rocket motion are divided into two kinds, random and deterministic. Random factors cannot be predefined, for example wind, initial disturbance, thrust malalignment, mass distribution unbalance, the deviation of the firing interval, the randomness of the MLRS vibration characteristics and so on. Deterministic factors can be predefined, for example the average deviation of air temperature and pressure, the weight deviation of the rocket, the loading position of the rocket, the firing sequence and so on. The influence of deterministic disturbance factors can be eliminated through ballistic correction theory [133], but the influence of random disturbance factors cannot be eliminated. The study of the change in initial disturbance and trajectory caused by various factors can provide a theoretic foundation and technology tool to evaluate and control firing precision.

The launch and free flight process of a rocket from firing and flying to impacting the target is divided into four phases.

- 1) Locking phase: from the moment the rocket engine is fired to the moment the rocket begins to move. In this period, the rocket gun begins to move under the action of rocket propulsion, but it can only move longitudinally relative to the launch tube because of the locking mechanism.
- 2) Moving in the launch tube: from the moment the rocket begins to move when it breaks loose from the locking mechanism under the action of rocket propulsion to the moment the rear bourrelet of the rocket leaves the launch tube. During this period, the motion of the rocket is restricted by the launch tube, leading to the mutual influence between the vibration of the rocket launcher and rocket motion. This, in addition to the gap between the bourrelet of rocket and launch tube, makes the rocket motion in launch tube very complex.
- 3) Power phase: from the moment that the rear bourrelet of the rocket leaves the muzzle of the launch tube to the time that the fuel of the rocket engine burns out. In this period, the motion of the rocket is accelerated and the speed usually reaches a maximum when the fuel of the rocket engine burns out.
- 4) Power-off phase: from the moment that the fuel of the rocket engine burns out to the time that the rocket impacts the target, in which the rocket moves further with inertia due to its kinetic energy. Aerodynamics and gravity decrease the rocket velocity gradually during the climb phase, but the rocket velocity may increase during the fall phase.

Strictly speaking, the components of MLRSs are nonlinear elastic bodies in the launch process, and the dynamics model of a weapons system is a complex nonlinear elastic system with large rocket motion. Such engineering problems with complex models are impossible to solve even using today's highly developed computation technology and mechanic theory, and in fact it is not necessary to regard them as complete elastic body models in engineering problems. As with most mechanism systems, the principle of engineering modeling is to simplify the model as much as possible and reduce the computation scale under the precondition of satisfying the engineering precision. That is to say, if the precision meets the engineering requirement, the component should be regarded as a simple lumped mass or rigid body. The component must be regarded as an elastic body if the precision does not meet the requirement when it is regarded as a lumped mass or rigid body, for example if it has been validated by tests that the stiffness of the MLRS launch tube has an obvious influence on its firing dispersion [249].

The components of MLRSs can be regarded as a lumped mass, rigid body, elastic beam, rotary spring, spring, damper and other mechanics elements according to their natural properties. The

launch dynamics model of MLRSs with 40 launch tubes that is most often used around the world today is shown in Figure 12.2. The pitching part defined here does not include the fired rockets and the launch tube that loads the launching rocket, the gyration part defined here does not include the pitching part, the vehicle chassis excluding the wheels is called the vehicle, the trail of the launch tube excluding the newly launched rocket is called the launch tube trail, and each of these is regarded as a rigid body with 6 degrees of freedom (DOFs). The six wheels are regarded as a lumped mass with 3 DOFs. The launch tube defined here does not include the newly launched rocket (omitting the launch tube trail), and is regarded as an elastic beam moving in space. The action between the launch tube and the pitching part, between the elevating mechanism and the equilibrator, the elastic and damping effect of the gyration part and the pitching part, the action of the gyration mechanism, the elastic and damping effect of the vehicle, the elastic and damping action between the vehicle and the wheels, the elastic and damping effect of the wheels and the action of the ground, and the connection between the cradle and the launch tube are modeled with three-dimensional rotary springs and parallel dampers (representing relative angle motion) and three-dimensional linear springs and parallel dampers (representing relative linear motion), respectively.

The main body of the rocket is regarded as a rigid body, its elastic effect is modeled with the elastic contact action between its three bourrelets and the launch tube, rocket weight, thrust, thrust malalignment angle, linear thrust malalignment, contact force between bourrelet and launch tube, mass eccentricity and dynamic unbalance are considered, the propulsion of the rocket engine is treated as a random asymmetric external force, and the thrust effect of the gas ejected from the rocket engine on the rocket gun is treated as an external force.

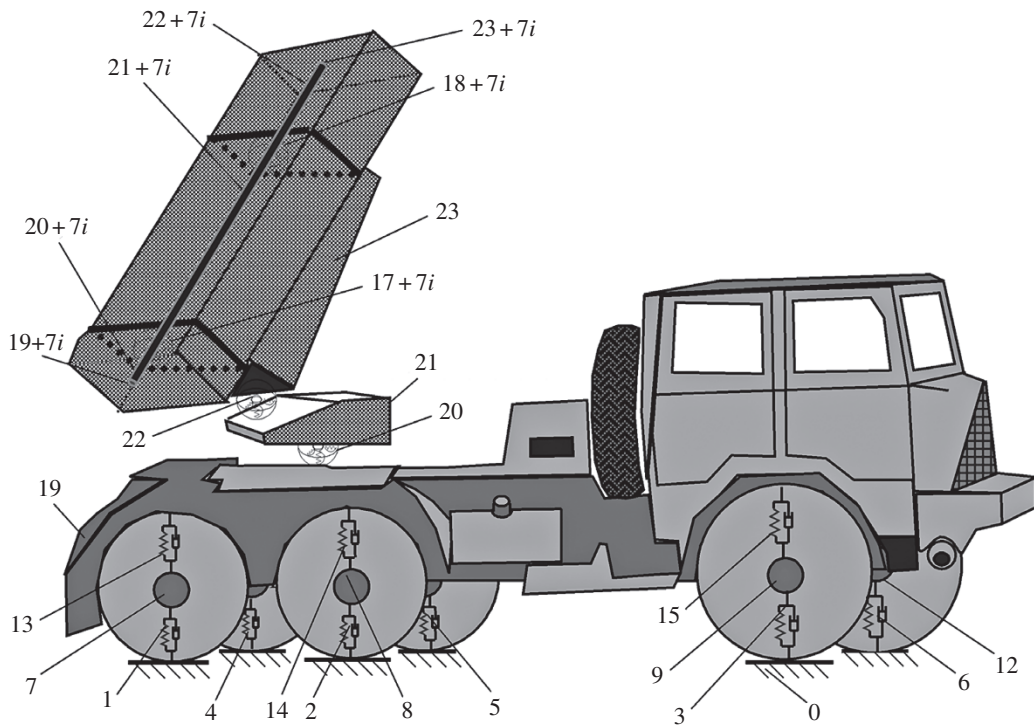


Figure 12.2 Launch dynamics model of an MLRS with 40 launch tubes.

The various deterministic and random factors, such as elastic deformation, interaction and total parameters of the components of the rocket gun, collision between rocket and tube, jet flow impact force, rocket-tube clearance, mass distribution unbalance of the rocket, and asymmetric propulsion distribution during the launch process, are considered, so the launch dynamics model can approximate the real physical system, which roundly reflects the influence of these factors on vibration characteristics, dynamic response, initial disturbance, rocket flight and firing dispersion of the MLRS from the point of view of the whole system.

According to the principle of uniform numbering of body and joints in the MSTMM, the ground boundary is numbered 0, the six pairs of parallel springs and dampers connecting the wheels and the ground are numbered 1, 2, 3, 4, 5 and 6, the six wheels are numbered 7, 8, 9, 10, 11 and 12, the six pairs of parallel springs and dampers connecting the wheels and the vehicle are numbered 13, 14, 15, 16, 17 and 18, the vehicle, the revolving part and the elevating part are numbered 19, 21, 23, respectively, the action of the traversing mechanism and the connection between elements 19 and 21, the action of the elevating mechanism and the equilibrator and the parallel rotary spring, spring and damper between elements 21 and 23 are numbered 20 and 22, respectively, the two sets of parallel rotary springs, tension springs and dampers between the cradle and the i th launch tube are numbered $17 + 7i$ and $18 + 7i$, respectively, the rear free boundary of the i th launch tube is numbered $19 + 7i$, the i th launch tube trail is numbered $20 + 7i$, the part between the front and rear bearing frames of the i th launch tube is numbered $21 + 7i$, the front part of the front bearing frame of the i th launch tube is numbered $22 + 7i$, and the front free boundary of the i th launch tube is numbered $23 + 7i$. Therefore, the launch dynamics model of MLRS is a MRFS which is composed of 44 rigid bodies, 40 elastic bodies and 6 lumped masses, and connected with various springs, rotary springs and dampers under the action of ground support, jet flow and coupling between rocket and launch tube.

In nature, the dynamics model of an MLRS is a nonlinear time-varying system, whose nonlinear and time-varying characteristics mainly come from three aspects:

- 1) the nonlinear contact force between the rocket and tube caused by the rocket motion in the launch tube, the rocket-tube clearance and the collision between the rocket and the tube
- 2) the variance of contact stiffness between the ground and the wheels along with the variance of the total rocket number in the cradle
- 3) the variance of the mass distribution of the MLRS caused by the variance of the total rocket number in the cradle and the position variance of the rocket motion in the launch tube during the launch process.

For these nonlinear factors the solutions are:

- 1) the nonlinear contact forces caused by the rocket motion in the launch tube, the rocket-tube clearance and the collision between the rocket and the guider are treated as "forcing forces", that is, their influence on the dynamic response of the MLRS is considered, but their influence on the vibration characteristics of the MLRS is not considered
- 2) the nonlinear contact stiffness between the ground and the wheels is expressed with subsection linear functions, that is, the value of contact stiffness is different along with the variance of the total rocket number in the cradle, which is decided by calculation and the static test result
- 3) the variance of the total rocket number in the cradle will lead to a change in the vibration characteristics of the MLRS, and we can take this effect into account in this way: the variance of the total rocket number results in different mass and mass distribution of the elevating part, thus leading to different vibration characteristics.

Thus, the MLRS can be regarded as linear time-invariant system during the firing round of every rocket. There are two reasons for the treatment methods: one is that there isn't any strict computation method in theory for the vibration characteristics of a general linear time-variant system at present; the other is that the result of the treatment method can meet the requirement of engineering precision because the mass of one rocket is only 1.5–4.0% of the elevating parts of the MLRS with 40 launch tubes, and the variance of natural frequency is very small between two near rocket rounds which have been validated by theory and test so it does not need to consider the variance of the system mode caused by the position variance of the rocket in the launch tube. The correctness of treating a nonlinear time-variant system as a piecewise linear time-invariant system has been proved by many test results and such treatment has high engineering precision.

12.3 State Vector, Transfer Equation and Transfer Matrix

12.3.1 State Vector

For the launch dynamics model of the MLRS shown in Figure 12.2, noting the sign convention, according to the MSTMM, the state vectors of the connection point of the MLRS are defined as follows:

$$\mathbf{Z}_{0,1\sim6} = [X_{0,1}, Y_{0,1}, Z_{0,1}, Q_{x\ 0,1}, Q_{y\ 0,1}, Q_{z\ 0,1}, X_{0,2}, Y_{0,2}, Z_{0,2}, Q_{x\ 0,2}, Q_{y\ 0,2}, Q_{z\ 0,2}, \dots, X_{0,6}, Y_{0,6}, Z_{0,6}, Q_{x\ 0,6}, Q_{y\ 0,6}, Q_{z\ 0,6}]^T \quad (12.1)$$

$$\mathbf{Z}_{7\sim12,1\sim6} = [X_{7,1}, Y_{7,1}, Z_{7,1}, Q_{x\ 7,1}, Q_{y\ 7,1}, Q_{z\ 7,1}, X_{8,2}, Y_{8,2}, Z_{8,2}, Q_{x\ 8,2}, Q_{y\ 8,2}, Q_{z\ 8,2}, \dots, X_{12,6}, Y_{12,6}, Z_{12,6}, Q_{x\ 12,6}, Q_{y\ 12,6}, Q_{z\ 12,6}]^T \quad (12.2)$$

$$\mathbf{Z}_{7\sim12,13\sim18} = [X_{7,13}, Y_{7,13}, Z_{7,13}, Q_{x\ 7,13}, Q_{y\ 7,13}, Q_{z\ 7,13}, X_{8,14}, Y_{8,14}, Z_{8,14}, Q_{x\ 8,14}, Q_{y\ 8,14}, Q_{z\ 8,14}, \dots, X_{12,18}, Y_{12,18}, Z_{12,18}, Q_{x\ 12,18}, Q_{y\ 12,18}, Q_{z\ 12,18}]^T \quad (12.3)$$

$$\mathbf{Z}_{19,13\sim18} = [X_{19,13}, Y_{19,13}, Z_{19,13}, \theta_{x\ 19,13}, \theta_{y\ 19,13}, \theta_{z\ 19,13}, Q_{x\ 19,13}, Q_{y\ 19,13}, Q_{z\ 19,13}, Q_{x\ 19,14}, Q_{y\ 19,14}, Q_{z\ 19,14}, \dots, Q_{x\ 19,18}, Q_{y\ 19,18}, Q_{z\ 19,18}]^T \quad (12.4)$$

$$\mathbf{Z}_{19,20} = [X, Y, Z, \theta_x, \theta_y, \theta_z, M_x, M_y, M_z, Q_x, Q_y, Q_z]_{19,20}^T \quad (12.5)$$

$$\begin{aligned} \mathbf{Z}_{23,17+7i\sim18+7i} &= [X_{23,17+7i}, Y_{23,17+7i}, Z_{23,17+7i}, \theta_{x\ 23,17+7i}, \theta_{y\ 23,17+7i}, \theta_{z\ 23,17+7i}, \\ &\quad M_{x\ 23,17+7i}, M_{y\ 23,17+7i}, M_{z\ 23,17+7i}, Q_{x\ 23,17+7i}, Q_{y\ 23,17+7i}, Q_{z\ 23,17+7i}, \\ &\quad M_{x\ 23,18+7i}, M_{y\ 23,18+7i}, M_{z\ 23,18+7i}, Q_{x\ 23,18+7i}, Q_{y\ 23,18+7i}, Q_{z\ 23,18+7i}]^T \end{aligned} \quad (12.6)$$

The form of $\mathbf{Z}_{21,22}$, $\mathbf{Z}_{23,22}$, $\mathbf{Z}_{20+7i,19+7i}$, $\mathbf{Z}_{20+7i,17+7i}$, $\mathbf{Z}_{21+7i,17+7i}$, $\mathbf{Z}_{21+7i,18+7i}$, $\mathbf{Z}_{22+7i,18+7i}$, and $\mathbf{Z}_{22+7i,23+7i}$ is similar to $\mathbf{Z}_{19,20}$, the subscripts denote the sequence number of bodies and joints at the connection point, and i is the sequence number of the launch tube.

12.3.2 Transfer Matrix and the Transfer Equation of a Component in the MLRS

12.3.2.1 From Ground to Wheels (axes)

According to the transfer equation of a spatial spring, the transfer equation from contact points between the wheels and the ground ($0, 1 \sim 6$) to the wheel (axle) points ($7 \sim 12, 1 \sim 6$) can be obtained:

$$\underset{36 \times 1}{Z_{7 \sim 12, 1 \sim 6}} = \underset{36 \times 36}{U_{1 \sim 6}} \underset{36 \times 1}{Z_{0, 1 \sim 6}} \quad (12.7)$$

$U_{1 \sim 6}$ is the transfer matrix from the ground to the wheels (axes):

$$\underset{36 \times 36}{U_{1 \sim 6}} = \begin{bmatrix} U_1 & & & & & \\ & U_2 & & & & \\ & & U_3 & & & \\ & & & U_4 & & \\ & & & & U_5 & \\ & & & & & U_6 \end{bmatrix} \quad (12.8)$$

where $U_i (i = 1, 2, \dots, 6)$ is the transfer matrix of the spatial spring.

12.3.2.2 Wheels (axes)

According to the transfer equation of a lumped mass with spatial vibration, the transfer equation of the wheels (axes) from every axis point ($7 \sim 12, 1 \sim 6$) to point ($7 \sim 12, 13 \sim 18$) can be obtained:

$$\underset{36 \times 1}{Z_{7 \sim 12, 13 \sim 18}} = \underset{36 \times 36}{U_{7 \sim 12}} \underset{36 \times 1}{Z_{7 \sim 12, 1 \sim 6}} \quad (12.9)$$

$U_{7 \sim 12}$ is the transfer matrix of the wheels (axes):

$$\underset{36 \times 36}{U_{7 \sim 12}} = \begin{bmatrix} U_7 & & & & & \\ & U_8 & & & & \\ & & U_9 & & & \\ & & & U_{10} & & \\ & & & & U_{11} & \\ & & & & & U_{12} \end{bmatrix} \quad (12.10)$$

where $U_i (i = 7, 8, \dots, 12)$ is the transfer matrix of a lumped mass with spatial vibration.

12.3.2.3 From Wheels (axes) to Vehicle

According to the geometric and mechanic relation between the wheel (axes) points ($7 \sim 12, 13 \sim 18$) and the vehicle points ($19, 13 \sim 18$), the transfer equations from the wheel (axes) points ($7 \sim 12, 13 \sim 18$) to the vehicle points ($19, 13 \sim 18$) can be obtained:

$$\underset{24 \times 1}{Z_{19, 13 \sim 18}} = \underset{24 \times 36}{U_{13 \sim 18}} \underset{36 \times 1}{Z_{7 \sim 12, 13 \sim 18}} \quad (12.11)$$

$$\underset{12 \times 24}{U_{13 \sim 18}}^{(1)} \underset{24 \times 1}{Z_{19, 13 \sim 18}} = \underset{12 \times 36}{U_{13 \sim 18}}^{(2)} \underset{36 \times 1}{Z_{7 \sim 12, 13 \sim 18}} \quad (12.12)$$

where

$$\begin{aligned}
 \mathbf{U}_{13 \sim 18}^{24 \times 36} &= \begin{bmatrix} \mathbf{U}_{11} & \mathbf{O}_{3 \times 6} & \mathbf{O}_{3 \times 6} & \mathbf{O}_{3 \times 6} & \mathbf{O}_{3 \times 6} & \mathbf{O}_{3 \times 6} \\ \mathbf{U}_{21} & \mathbf{O}_{3 \times 6} & \mathbf{U}_{23} & \mathbf{U}_{24} & \mathbf{O}_{3 \times 6} & \mathbf{O}_{3 \times 6} \\ \mathbf{U}_{31} & \mathbf{O}_{3 \times 6} & \mathbf{O}_{3 \times 6} & \mathbf{O}_{3 \times 6} & \mathbf{O}_{3 \times 6} & \mathbf{O}_{3 \times 6} \\ & \mathbf{U}_{42} & \mathbf{O}_{3 \times 6} & \mathbf{O}_{3 \times 6} & \mathbf{O}_{3 \times 6} & \mathbf{O}_{3 \times 6} \\ & & \mathbf{U}_{53} & \mathbf{O}_{3 \times 6} & \mathbf{O}_{3 \times 6} & \mathbf{O}_{3 \times 6} \\ & & & \mathbf{U}_{64} & \mathbf{O}_{3 \times 6} & \mathbf{O}_{3 \times 6} \\ & \mathbf{O} & & & \mathbf{U}_{75} & \mathbf{O}_{3 \times 6} \\ & & & & & \mathbf{U}_{86} \end{bmatrix} \quad (12.13) \\
 \mathbf{U}_{11} &= \begin{bmatrix} 1 & 0 & 0 & -\frac{1}{K_{x \ 13}} & 0 & 0 \\ 0 & 1 & 0 & 0 & -\frac{1}{K_{y \ 13}} & 0 \\ 0 & 0 & 1 & 0 & 0 & -\frac{1}{K_{z \ 13}} \end{bmatrix}, \mathbf{U}_{21} = \begin{bmatrix} 0 & \frac{1}{a_{3,4}} & 0 & 0 & -\frac{1}{a_{3,4}K_{y \ 13}} & 0 \\ -\frac{1}{a_{3,4}} & 0 & 0 & \frac{1}{a_{3,4}K_{x \ 13}} & 0 & 0 \\ 0 & -\frac{1}{a_{1,3}} & 0 & 0 & \frac{1}{a_{1,3}K_{y \ 13}} & 0 \end{bmatrix} \\
 \mathbf{U}_{23} &= \begin{bmatrix} 0 & 0 & 0 & 0 & 0 & 0 \\ 0 & 0 & 0 & 0 & 0 & 0 \\ 0 & \frac{1}{a_{1,3}} & 0 & 0 & \frac{-1}{a_{1,3}K_{y \ 15}} & 0 \end{bmatrix}, \mathbf{U}_{24} = \begin{bmatrix} 0 & -\frac{1}{a_{3,4}} & 0 & 0 & \frac{1}{a_{3,4}K_{y \ 16}} & 0 \\ \frac{1}{a_{3,4}} & 0 & 0 & -\frac{1}{a_{3,4}K_{x \ 16}} & 0 & 0 \\ 0 & 0 & 0 & 0 & 0 & 0 \end{bmatrix} \\
 \mathbf{U}_{ij} &= \begin{bmatrix} 0 & 0 & 0 & 1 & 0 & 0 \\ 0 & 0 & 0 & 0 & 1 & 0 \\ 0 & 0 & 0 & 0 & 0 & 1 \end{bmatrix} \quad (i = 3, 4, 5, 6, 7, 8; \ j = i - 2) \\
 \mathbf{U}_{13 \sim 18}^{(1)}_{12 \times 24} &= \begin{bmatrix} \mathbf{U}_{11} & \mathbf{O}_{3 \times 18} \\ \mathbf{U}_{21} & \mathbf{O}_{2 \times 18} \\ \mathbf{U}_{31} & \mathbf{O}_{1 \times 18} \\ \mathbf{U}_{41} & \mathbf{O}_{3 \times 18} \\ \mathbf{U}_{51} & \mathbf{O}_{3 \times 18} \end{bmatrix} \quad (12.14) \\
 \mathbf{U}_{11} &= \begin{bmatrix} 1 & 0 & 0 & 0 & 0 & 0 \\ 0 & 1 & 0 & 0 & 0 & a_{1,2} \\ 0 & 0 & 1 & 0 & -a_{1,2} & 0 \end{bmatrix}, \mathbf{U}_{41} = \begin{bmatrix} 1 & 0 & 0 & 0 & a_{3,4} & 0 \\ 0 & 1 & 0 & -a_{3,4} & 0 & a_{1,2} \\ 0 & 0 & 1 & 0 & -a_{1,2} & 0 \end{bmatrix} \\
 \mathbf{U}_{31} &= [0 \ 0 \ 1 \ 0 \ -a_{1,4} \ 0], \mathbf{U}_{21} = \begin{bmatrix} 1 & 0 & 0 & 0 & 0 & 0 \\ 0 & 0 & 1 & 0 & -a_{1,3} & 0 \end{bmatrix} \\
 \mathbf{U}_{51} &= \begin{bmatrix} 1 & 0 & 0 & 0 & a_{3,4} & 0 \\ 0 & 1 & 0 & -a_{3,4} & 0 & a_{1,3} \\ 0 & 0 & 1 & 0 & -a_{1,3} & 0 \end{bmatrix}
 \end{aligned}$$

$$\begin{aligned}
 \mathbf{U}_{13 \sim 18}^{(2)} = \begin{bmatrix} \mathbf{O}_{3 \times 6} & \mathbf{U}_{12} & & & & \\ \mathbf{O}_{2 \times 6} & & \mathbf{U}_{23} & & & \mathbf{O} \\ \mathbf{O}_{1 \times 6} & & & \mathbf{U}_{34} & & \\ \mathbf{O}_{3 \times 6} & \mathbf{O} & & & \mathbf{U}_{45} & \\ \mathbf{O}_{3 \times 6} & & & & & \mathbf{U}_{56} \end{bmatrix} \quad (12.15) \\
 \mathbf{U}_{12} = \begin{bmatrix} 1 & 0 & 0 & -\frac{1}{K_{x14}} & 0 & 0 \\ 0 & 1 & 0 & 0 & -\frac{1}{K_{y14}} & 0 \\ 0 & 0 & 1 & 0 & 0 & -\frac{1}{K_{z14}} \end{bmatrix}, \mathbf{U}_{23} = \begin{bmatrix} 1 & 0 & 0 & -\frac{1}{K_{x15}} & 0 & 0 \\ 0 & 0 & 1 & 0 & 0 & -\frac{1}{K_{z15}} \end{bmatrix} \\
 \mathbf{U}_{34} = \begin{bmatrix} 0 & 0 & 1 & 0 & 0 & -\frac{1}{K_{z16}} \end{bmatrix} \\
 \mathbf{U}_{45} = \begin{bmatrix} 1 & 0 & 0 & -\frac{1}{K_{x17}} & 0 & 0 \\ 0 & 1 & 0 & 0 & -\frac{1}{K_{y17}} & 0 \\ 0 & 0 & 1 & 0 & 0 & -\frac{1}{K_{z17}} \end{bmatrix}, \mathbf{U}_{56} = \begin{bmatrix} 1 & 0 & 0 & -\frac{1}{K_{x18}} & 0 & 0 \\ 0 & 1 & 0 & 0 & -\frac{1}{K_{y18}} & 0 \\ 0 & 0 & 1 & 0 & 0 & -\frac{1}{K_{z18}} \end{bmatrix}
 \end{aligned}$$

$(a_{1,2}, a_{2,2}, a_{3,2})$, $(a_{1,3}, a_{2,3}, a_{3,3})$, $(a_{1,4}, a_{2,4}, a_{3,4})$, $(a_{1,5}, a_{2,5}, a_{3,5})$, and $(a_{1,6}, a_{2,6}, a_{3,6})$ are the coordinates of points (19, 14), (19, 15), (19, 16), (19, 17), and (19, 18) at the coordinate system whose origin is fixed on the first input end of body 19.

12.3.2.4 Vehicle

A vehicle is a rigid body with six inputs and one output. According to the transfer equation of a rigid body, the transfer equation from the vehicle points (19, 13 ~ 18) to (19, 20) can be obtained:

$$\mathbf{Z}_{19,20} = \mathbf{U}_{19} \mathbf{Z}_{19,13 \sim 18} \quad (12.16)$$

$\begin{matrix} 12 \times 1 & 12 \times 24 & 24 \times 1 \end{matrix}$

where \mathbf{U}_{19} is the transfer matrix of a rigid body (vehicle) with six input ends and one output end (see Equation (3.25)).

12.3.2.5 Traversing Mechanism and Elevating Mechanism

The actions of traversing and elevating mechanisms are equivalent to the actions of rotary springs and springs. According to the transfer matrices of spatial springs and rotary springs, the transfer equations from the traversing mechanism point (19, 20) to point (21, 20) and from the elevating mechanism point (21, 22) to point (23, 22) can be obtained as, respectively,

$$\mathbf{Z}_{21,20} = \mathbf{H}_\alpha \mathbf{U}_{20} \mathbf{Z}_{19,20} \quad (12.17)$$

$\begin{matrix} 12 \times 1 & 12 \times 12 & 12 \times 12 & 12 \times 1 \end{matrix}$

$$\mathbf{Z}_{23,22} = \mathbf{H}_\theta \mathbf{U}_{22} \mathbf{Z}_{21,22} \quad (12.18)$$

$\begin{matrix} 12 \times 1 & 12 \times 12 & 12 \times 12 & 12 \times 1 \end{matrix}$

where \mathbf{U}_{20} and \mathbf{U}_{22} are the corresponding transfer matrices of the elastic joints, respectively (see Equation (3.36)), and \mathbf{H}_α and \mathbf{H}_θ are the corresponding coordinate transformation matrices with angles of azimuth α and departure angle θ , respectively.

12.3.2.6 Gyration Part

A gyration part is a rigid body with one input end and one output end. According to the transfer equation of a rigid body, the transfer equation of the gyration part can be obtained:

$$\mathbf{Z}_{21,22} = \mathbf{U}_{21} \mathbf{Z}_{21,20} \quad (12.19)$$

$12 \times 1 \quad 12 \times 12 \quad 12 \times 1$

where \mathbf{U}_{21} is the transfer matrix of a rigid body (gyration part) with one input end and one output end (see Equation (3.19)).

12.3.2.7 Pitching Part

A pitching part is a rigid body with one input end and two output ends. According to the transfer equation of a rigid body, the transfer equation of the pitching part can be obtained:

$$\mathbf{Z}_{23,22} = \mathbf{U}_{23} \mathbf{Z}_{23,17+7i \sim 18+7i} \quad (12.20)$$

$12 \times 1 \quad 12 \times 18 \quad 18 \times 1$

where \mathbf{U}_{23} is the transfer matrix of a rigid body (pitching part) with one input end and two output ends.

12.3.2.8 The i th Launch Tube Trail (to rear bearing)

Similar to the gyration part, the transfer equation of the i th launch tube rear end point $(20+7i, 19+7i)$ to point $(20+7i, 17+7i)$ can be obtained:

$$\mathbf{Z}_{20+7i, 17+7i} = \mathbf{U}_{20+7i} \mathbf{Z}_{20+7i, 19+7i} \quad (12.21)$$

$12 \times 1 \quad 12 \times 12 \quad 12 \times 1$

where \mathbf{U}_{20+7i} is the transfer matrix of a rigid body (the i th launch tube trail) with one input end and one output end.

12.3.2.9 Transfer Matrix of a Connection Point from the Pitching Part to the i th Launch Tube

The i th launch tube is connected to the pitching part through two points $(21+7i, 17+7i)$ and $(22+7i, 18+7i)$, forming a loop between the pitching part and the launch tube. Using the geometric relation and the force equilibrium between point $(20+7i, 17+7i)$ and point $(21+7i, 17+7i)$, we obtain

$$\mathbf{Z}_{21+7i, 17+7i} = \mathbf{Z}_{20+7i, 17+7i} + [0, 0, 0, 0, 0, 0, M_x, M_y, M_z, Q_x, Q_y, Q_z]_{23, 17+7i}^T \quad (12.22)$$

Equation (12.22) can be written as

$$\mathbf{Z}_{21+7i, 17+7i} = \mathbf{Z}_{20+7i, 17+7i} + \mathbf{U}_{17+7i} \mathbf{Z}_{23, 17+7i \sim 18+7i} \quad (12.23)$$

where

$$\mathbf{U}_{17+7i} = \begin{bmatrix} \mathbf{O}_{6 \times 6} & \mathbf{O}_{6 \times 6} & \mathbf{O}_{6 \times 6} \\ \mathbf{O}_{6 \times 6} & \mathbf{I}_6 & \mathbf{O}_{6 \times 6} \end{bmatrix} \quad (12.24)$$

Similarly, using the geometric relation and the force equilibrium between point $(21+7i, 18+7i)$ and point $(22+7i, 18+7i)$, we obtain

$$\mathbf{Z}_{22+7i, 18+7i} = \mathbf{Z}_{21+7i, 18+7i} + \mathbf{U}_{18+7i} \mathbf{Z}_{23, 17+7i \sim 18+7i} \quad (12.25)$$

where

$$\mathbf{u}_{18+7i} = \begin{bmatrix} \mathbf{O}_{6 \times 6} & \mathbf{O}_{6 \times 6} & \mathbf{O}_{6 \times 6} \\ \mathbf{O}_{6 \times 6} & \mathbf{O}_{6 \times 6} & \mathbf{I}_6 \end{bmatrix} \quad (12.26)$$

The displacement (including angular displacement) relation between points $(23, 17+7i)$ and $(20+7i, 17+7i)$ is

$$\begin{aligned} \mathbf{u}_{17+7i}^{(1)} \mathbf{Z}_{23, 17+7i \sim 18+7i} &= [X, Y, Z, \boldsymbol{\theta}_x, \boldsymbol{\theta}_y, \boldsymbol{\theta}_z]^T_{20+7i, 17+7i} \\ &= \mathbf{u}_{17+7i}^{(2)} \mathbf{Z}_{20+7i, 17+7i} = \mathbf{u}_{17+7i}^{(2)} \mathbf{U}_{20+7i} \mathbf{Z}_{20+7i, 19+7i} \end{aligned} \quad (12.27)$$

where

$$\begin{aligned} \mathbf{u}_{17+7i}^{(1)} &= \begin{bmatrix} \mathbf{I}_3 & \mathbf{O}_{3 \times 3} & \mathbf{O}_{3 \times 3} & \mathbf{u}_{14} & \mathbf{O}_{3 \times 3} & \mathbf{O}_{3 \times 3} \\ \mathbf{O}_{3 \times 3} & \mathbf{I}_3 & \mathbf{u}_{23} & \mathbf{O}_{3 \times 3} & \mathbf{O}_{3 \times 3} & \mathbf{O}_{3 \times 3} \end{bmatrix} \\ \mathbf{u}_{14} &= \begin{bmatrix} -\frac{1}{K_x'_{17+7i}} & 0 & 0 \\ 0 & -\frac{1}{K_y'_{17+7i}} & 0 \\ 0 & 0 & -\frac{1}{K_z'_{17+7i}} \end{bmatrix}, \mathbf{u}_{23} = \begin{bmatrix} \frac{1}{K_x'_{17+7i}} & 0 & 0 \\ 0 & \frac{1}{K_y'_{17+7i}} & 0 \\ 0 & 0 & \frac{1}{K_z'_{17+7i}} \end{bmatrix} \end{aligned} \quad (12.28)$$

The displacement (including angular displacement) relation between points $(23, 18+7i)$ and $(21+7i, 18+7i)$ is

$$\mathbf{u}_{18+7i}^{(1)} \mathbf{Z}_{23, 17+7i \sim 18+7i} = [X, Y, Z, \boldsymbol{\theta}_x, \boldsymbol{\theta}_y, \boldsymbol{\theta}_z]^T_{21+7i, 18+7i} = \mathbf{u}_{18+7i}^{(2)} \mathbf{Z}_{21+7i, 18+7i} \quad (12.29)$$

namely

$$\left(\mathbf{u}_{18+7i}^{(1)} - \mathbf{u}_{18+7i}^{(2)} \mathbf{u}_{21+7i} \mathbf{u}_{17+7i} \right) \mathbf{Z}_{23, 17+7i \sim 18+7i} = \mathbf{u}_{18+7i}^{(2)} \mathbf{u}_{21+7i} \mathbf{u}_{20+7i} \mathbf{Z}_{20+7i, 19+7i} \quad (12.30)$$

where

$$\mathbf{u}_{18+7i}^{(1)} = \begin{bmatrix} \mathbf{I}_3 & \tilde{\mathbf{t}}_{(23, 17+7i)(23, 18+7i)}^T & \mathbf{O}_{3 \times 3} & \mathbf{O}_{3 \times 3} & \mathbf{O}_{3 \times 3} & \mathbf{u}_{16} \\ \mathbf{O}_{3 \times 3} & \mathbf{I}_3 & \mathbf{O}_{3 \times 3} & \mathbf{O}_{3 \times 3} & \mathbf{u}_{25} & \mathbf{O}_{3 \times 3} \end{bmatrix} \quad (12.31)$$

$$\mathbf{u}_{16} = \begin{bmatrix} -\frac{1}{K_x'_{18+7i}} & 0 & 0 \\ 0 & -\frac{1}{K_y'_{18+7i}} & 0 \\ 0 & 0 & -\frac{1}{K_z'_{18+7i}} \end{bmatrix}, \mathbf{u}_{25} = \begin{bmatrix} \frac{1}{K_x'_{18+7i}} & 0 & 0 \\ 0 & \frac{1}{K_y'_{18+7i}} & 0 \\ 0 & 0 & \frac{1}{K_z'_{18+7i}} \end{bmatrix}$$

$$\mathbf{u}_{17+7i}^{(2)} = \mathbf{u}_{18+7i}^{(2)} = [\mathbf{I}_6 \quad \mathbf{O}_{6 \times 6}] \quad (12.32)$$

12.3.2.10 The i th Launch Tube

The i th launch tube in which the moving rocket is located is regarded as a transversely vibrating elastic beam, and its longitudinal and torsional deformation are neglected. The transfer

equations from point $(21 + 7i, 17 + 7i)$ to point $(21 + 7i, 18 + 7i)$ and from point $(22 + 7i, 18 + 7i)$ to point $(22 + 7i, 23 + 7i)$ at the i th launch tube are, respectively,

$$\mathbf{Z}_{21+7i, 18+7i}^{12 \times 1} = \mathbf{U}_{21+7i}^{12 \times 12} \mathbf{Z}_{21+7i, 17+7i}^{12 \times 1} \quad (12.33)$$

$$\mathbf{Z}_{22+7i, 23+7i}^{12 \times 1} = \mathbf{U}_{22+7i}^{12 \times 12} \mathbf{Z}_{22+7i, 18+7i}^{12 \times 1} \quad (12.34)$$

where \mathbf{U}_{21+7i} and \mathbf{U}_{22+7i} are the transfer matrices of transversely vibrating elastic beams without considering longitudinal and torsional deformation (see Equations (11.41) and (11.42)).

12.4 Overall Transfer Equation of the System

12.4.1 Transfer Equations from Ground (0, 1-6) to Pitching Part (23, 17 + 7i ~ 18 + 7i)

According to the transfer equations (12.7), (12.9), (12.11), (12.16), (12.17), (12.19), (12.18) and (12.20), the transfer equation from the ground to the pitching part can be obtained:

$$\mathbf{U}_{22-1 \sim 6} \mathbf{Z}_{0, 1 \sim 6} - \mathbf{U}_{23} \mathbf{Z}_{23, 17+7i \sim 18+7i} = \mathbf{0} \quad (12.35)$$

where

$$\mathbf{U}_{22-1 \sim 6} = \mathbf{H}_\theta \mathbf{U}_{22} \mathbf{U}_{21} \mathbf{H}_\alpha \mathbf{U}_{20} \mathbf{U}_{19} \mathbf{U}_{13 \sim 18} \mathbf{U}_{7 \sim 12} \mathbf{U}_{1 \sim 6} \quad (12.36)$$

12.4.2 Transfer Equation from Ground (0, 1 ~ 6) to Vehicle (7, 7 ~ 12)

According to the transfer equations (12.7), (12.9), (12.11) and (12.12), the transfer equation from point (0, 1 ~ 6) to point (19, 13 ~ 18) can be obtained:

$$\mathbf{U}_{7 \sim 12-1 \sim 6} \mathbf{Z}_{0, 1 \sim 6} = \mathbf{0} \quad (12.37)$$

where

$$\mathbf{U}_{7 \sim 12-1 \sim 6} = \left(\mathbf{U}_{13 \sim 18}^{(1)} \mathbf{U}_{13 \sim 18} - \mathbf{U}_{13 \sim 18}^{(2)} \right) \mathbf{U}_{7 \sim 12} \mathbf{U}_{1 \sim 6} \quad (12.38)$$

12.4.3 Transfer Equation from Launch Tube Trail (20 + 7i, 19 + 7i) to Launch Tube Muzzle (22 + 7i, 23 + 7i)

According to the transfer equations (12.21), (12.23), (12.33), (12.25) and (12.34), the transfer equation from point $(20 + 7i, 19 + 7i)$ to point $(22 + 7i, 23 + 7i)$ can be obtained:

$$\mathbf{U}_{22+7i \sim 23} \mathbf{Z}_{23, 17+7i \sim 18+7i} + \mathbf{U}_{22+7i \sim 20+7i} \mathbf{Z}_{20+7i, 19+7i} - \mathbf{Z}_{22+7i, 23+7i} = \mathbf{0} \quad (12.39)$$

where

$$\begin{cases} \mathbf{U}_{22+7i \sim 23} = \mathbf{U}_{22+7i} (\mathbf{U}_{18+7i} + \mathbf{U}_{21+7i} \mathbf{U}_{17+7i}) \\ \mathbf{U}_{22+7i \sim 20+7i} = \mathbf{U}_{22+7i} \mathbf{U}_{21+7i} \mathbf{U}_{20+7i} \end{cases} \quad (12.40)$$

12.4.4 Transfer Equation from Point (23, 18 + 7i) to Point (20 + 7i, 18 + 7i)

According to the transfer equations (12.21), (12.23), (12.33) and (12.29), we obtain

$$- \mathbf{U}_{21+7i \sim 23} \mathbf{Z}_{23, 17+7i \sim 18+7i} + \mathbf{U}_{21+7i \sim 20+7i} \mathbf{Z}_{20+7i, 19+7i} = \mathbf{0} \quad (12.41)$$

where

$$\begin{cases} \mathbf{U}_{21+7i \sim 23} = \left(\mathbf{U}_{18+7i}^{(1)} - \mathbf{U}_{18+7i}^{(2)} \mathbf{U}_{21+7i} \mathbf{U}_{17+7i} \right) \\ \mathbf{U}_{21+7i \sim 20+7i} = \mathbf{U}_{18+7i}^{(2)} \mathbf{U}_{21+7i} \mathbf{U}_{20+7i} \end{cases} \quad (12.42)$$

12.4.5 Transfer Equation from Point (23, 17 + 7i) to Point (20 + 7i, 17 + 7i)

According to the transfer equations (12.21) and (12.27), we obtain

$$- \mathbf{U}_{17+7i}^{(1)} \mathbf{Z}_{23, 17+7i \sim 18+7i} + \mathbf{U}_{17+7i}^{(2)} \mathbf{U}_{20+7i} \mathbf{Z}_{20+7i, 19+7i} = \mathbf{0} \quad (12.43)$$

According to Equations (12.39) and (12.43), we obtain

$$\begin{bmatrix} \mathbf{U}_{22+7i \sim 23} \\ \mathbf{U}_{17+7i}^{(1)} \end{bmatrix} \mathbf{Z}_{23, 17+7i \sim 18+7i} = \begin{bmatrix} -\mathbf{U}_{22+7i \sim 20+7i} & \mathbf{I}_{12} \\ \mathbf{U}_{17+7i}^{(2)} \mathbf{U}_{20+7i} & \mathbf{O}_{6 \times 12} \end{bmatrix} \begin{bmatrix} \mathbf{Z}_{20+7i, 19+7i} \\ \mathbf{Z}_{22+7i, 23+7i} \end{bmatrix} \quad (12.44)$$

$$\mathbf{Z}_{23, 17+7i \sim 18+7i} = \begin{bmatrix} \mathbf{U}_{22+7i \sim 23} \\ \mathbf{U}_{17+7i}^{(1)} \end{bmatrix}^{-1} \begin{bmatrix} -\mathbf{U}_{22+7i \sim 20+7i} & \mathbf{I}_{12} \\ \mathbf{U}_{17+7i}^{(2)} \mathbf{U}_{20+7i} & \mathbf{O}_{6 \times 12} \end{bmatrix} \begin{bmatrix} \mathbf{Z}_{20+7i, 19+7i} \\ \mathbf{Z}_{22+7i, 23+7i} \end{bmatrix} \quad (12.45)$$

Let

$$\begin{bmatrix} \mathbf{U}_{22+7i \sim 23} \\ \mathbf{U}_{17+7i}^{(1)} \end{bmatrix}^{-1} \begin{bmatrix} -\mathbf{U}_{22+7i \sim 20+7i} & \mathbf{I}_{12} \\ \mathbf{U}_{17+7i}^{(2)} \mathbf{U}_{20+7i} & \mathbf{O}_{6 \times 12} \end{bmatrix} = [\mathbf{U}_{23 \sim 20+7i} \quad \mathbf{U}_{23 \sim 22+7i}] \quad (12.46)$$

then

$$\mathbf{Z}_{23, 17+7i \sim 18+7i} = \mathbf{U}_{23 \sim 20+7i} \mathbf{Z}_{20+7i, 19+7i} + \mathbf{U}_{23 \sim 22+7i} \mathbf{Z}_{22+7i, 23+7i} \quad (12.47)$$

Substituting this into Equation (12.35) yields

$$\mathbf{U}_{22-1 \sim 6} \mathbf{Z}_{0, 1 \sim 6} - \mathbf{U}_{23} \mathbf{U}_{23 \sim 20+7i} \mathbf{Z}_{20+7i, 19+7i} - \mathbf{U}_{23} \mathbf{U}_{23 \sim 22+7i} \mathbf{Z}_{22+7i, 23+7i} = \mathbf{0} \quad (12.48)$$

Substituting this into Equation (12.41), it follows that

$$(\mathbf{U}_{21+7i \sim 20+7i} - \mathbf{U}_{21+7i \sim 23} \mathbf{U}_{23 \sim 20+7i}) \mathbf{Z}_{20+7i, 19+7i} - \mathbf{U}_{21+7i \sim 23} \mathbf{U}_{23 \sim 22+7i} \mathbf{Z}_{22+7i, 23+7i} = \mathbf{0} \quad (12.49)$$

12.4.6 Overall Transfer Equation and Transfer Matrix of MLRS

According to Equations (12.37), (12.48) and (12.49), the overall transfer equation of MLRS can be obtained:

$$\mathbf{U}_{\text{all}} \mathbf{Z}_{\text{all}} = \mathbf{0} \quad (12.50)$$

where

$$\mathbf{Z}_{\text{all}} = \begin{bmatrix} \mathbf{Z}_{0, 1 \sim 6}^T & \mathbf{Z}_{20+7i, 19+7i}^T & \mathbf{Z}_{22+7i, 23+7i}^T \end{bmatrix}^T \quad (12.51)$$

$$\mathbf{U}_{\text{all}} = \begin{bmatrix} \mathbf{U}_{22-1 \sim 6} & -\mathbf{U}_{23}\mathbf{U}_{23 \sim 20+7i} & -\mathbf{U}_{23}\mathbf{U}_{23 \sim 22+7i} \\ \mathbf{U}_{7 \sim 12-1 \sim 6} & \mathbf{O}_{12 \times 12} & \mathbf{O}_{12 \times 12} \\ \mathbf{O}_{6 \times 36} & \mathbf{U}_{21+7i \sim 20+7i} - \mathbf{U}_{21+7i \sim 23}\mathbf{U}_{23 \sim 20+7i} & -\mathbf{U}_{21+7i \sim 23}\mathbf{U}_{23 \sim 22+7i} \end{bmatrix} \quad (12.52)$$

\mathbf{Z}_{all} is composed of state vectors at the boundary points of the system and \mathbf{U}_{all} is the overall transfer matrix of the MLRS, a 30×60 matrix.

12.5 Vibration Characteristics of the System

The string firing of the MLRS means its vibration characteristics greatly influence the dynamic performance and firing precision, and the matching relation between firing frequency and vibration frequency has great influence on the dynamic performance, so it is necessary in dynamic design to compute the vibration characteristics of the MLRS and its change with a firing sequence at high speed. Because the total mass of the rocket is bigger than that of the launch tube, the mass of the rocket has a big influence on the vibration characteristics of the MLRS, which makes the vibration characteristics of the system different at every rocket round, so a large error will occur if the influence of the rocket mass on the vibration characteristics is not considered. In order to scientifically evaluate or ensure good dynamic performance and firing precision, the vibration characteristics of the MLRS must be expressed exactly and computed quickly, the quantitative relation between the total parameters of the MLRS and the vibration characteristics must be set up, and the vibration frequency distribution adjusted through altering the total parameters, which makes the vibration frequency match the firing frequency and improves firing precision. After the eigenvalues of the MLRS have been obtained, the dynamic response of the MLRS can be computed using the orthogonality of augmented eigenvectors.

Theory and test have proved that the firing sequence of the MLRS greatly influences the firing dispersion because different firing sequences can result in different vibration characteristics, different initial disturbance and different firing dispersion. The difficulty in solving the problem of quickly computing the vibration characteristics of the MLRS is the problems of too much computation work and computation error due to the “illness” when using the common mechanics method to compute the vibration characteristics of the MRFS. The “illness” in computing the vibration characteristics of the MRFS and the problem of quick computing are solved using the MSTMM. For example, for the MLRS with 40 launch tubes mentioned above, in order to ascertain the best firing precision by adjusting the firing sequence and the firing interval, only the optional schemes for firing sequence will reach $40!$ which is a surprisingly large number. It is first necessary to compute the vibration characteristics of every scheme when choosing the firing sequence and the firing interval, so quickly computing the vibration characteristics of the MLRS is an important precondition to realize practical engineering dynamic design. In fact, it is these important and urgent engineering requirements that have led to the MSTMM being rapidly developed.

12.5.1 Characteristic Equation of the System

It can be seen from Equation (12.51) that \mathbf{Z}_{all} is composed of the state vectors at the boundary points of the system, including ground points $(0, 1 \sim 6)$, launch tube trail point $(20 + 7i, 19 + 7i)$ and launch tube muzzle $(22 + 7i, 23 + 7i)$. Half of the elements of the state vector at the boundary points are determined by the boundary condition. There are 36 elements in total in $\mathbf{Z}_{0,1 \sim 6}$,

including the displacement and force in three directions at six contact points between six wheels and the ground, where 18 elements representing displacement are zero. Getting rid of these zeros, $\mathbf{Z}_{0,1\sim6}$ can be written as

$$\bar{\mathbf{Z}}_{0,1\sim6} = [Q_{x\ 0,1}, Q_{y\ 0,1}, Q_{z\ 0,1}, \dots, Q_{x\ 0,6}, Q_{y\ 0,6}, Q_{z\ 0,6}]^T \quad (12.53)$$

The state vectors $\mathbf{Z}_{20+7i,19+7i}$ and $\mathbf{Z}_{22+7i,23+7i}$ of point $(20+7i,19+7i)$ and point $(22+7i,23+7i)$ include linear displacement, angular displacement, force and moment in three directions of corresponding points, and within the 12 elements involved in the state vector of each point, six of them (forces and displacements) are zeros. Getting rid of these zeros, we obtain

$$\bar{\mathbf{Z}}_{20+7i,19+7i} = [X, Y, Z, \theta_x, \theta_y, \theta_z]_{20+7i,19+7i}^T \quad (12.54)$$

$$\bar{\mathbf{Z}}_{22+7i,23+7i} = [X, Y, Z, \theta_x, \theta_y, \theta_z]_{22+7i,23+7i}^T \quad (12.55)$$

Getting rid of these 30 zeros from \mathbf{Z}_{all} , a new state vector can be obtained:

$$\bar{\mathbf{Z}}_{\text{all}} = [\bar{\mathbf{Z}}_{0,1\sim6}^T, \bar{\mathbf{Z}}_{20+7i,19+7i}^T, \bar{\mathbf{Z}}_{22+7i,23+7i}^T]^T \quad (12.56)$$

Getting rid of columns 1, 2, 3, 7, 8, 9, 13, 14, 15, 19, 20, 21, 25, 26, 27, 31, 32, 33, 43, 44, 45, 46, 47, 48, 55, 56, 57, 58, 59, 60 in \mathbf{U}_{all} , a square matrix $\bar{\mathbf{U}}_{\text{all}}$ with 30 orders can be obtained. Then Equation (12.50) is written as

$$\bar{\mathbf{U}}_{\text{all}} \bar{\mathbf{Z}}_{\text{all}} = \mathbf{0} \quad (12.57)$$

or

$$\bar{\mathbf{U}}_{\text{all}} [\bar{\mathbf{Z}}_{0,1\sim6}^T, \bar{\mathbf{Z}}_{20+7i,19+7i}^T, \bar{\mathbf{Z}}_{22+7i,23+7i}^T]^T = \mathbf{0} \quad (12.58)$$

It can be seen from the derivation process that both $\bar{\mathbf{U}}_{\text{all}}$ and \mathbf{U}_{all} are only relative to the total parameters of the system and the natural frequency ω_k ($k = 1, 2, 3, \dots$). When the total parameters of the system are determined, the determinant of matrix $\bar{\mathbf{U}}_{\text{all}}$ corresponding to the natural frequency ω_k is zero and Equation (12.58) must have a nontrivial solution, namely

$$\det \bar{\mathbf{U}}_{\text{all}} = 0 \quad (12.59)$$

Equation (12.59) is the eigenequation of the MLRS. Solving Equation (12.59), the eigenfrequency ω_k ($k = 1, 2, 3, \dots$) of the MLRS can be obtained. After the eigenfrequency ω_k ($k = 1, 2, 3, \dots$) of the MLRS is obtained, under the defined normalized condition (such as letting the maximal absolute value of the 30 elements of $\bar{\mathbf{Z}}_{\text{all}}$ to be 1), solving Equation (12.58), $\bar{\mathbf{Z}}_{\text{all}}$ and \mathbf{Z}_{all} corresponding to ω_k can be obtained, namely the state vectors $\mathbf{Z}_{0,1\sim6}$, $\mathbf{Z}_{20+7i,19+7i}$ and $\mathbf{Z}_{22+7i,23+7i}$ corresponding to ω_k can be obtained. All state vectors (such as $\mathbf{Z}_{7\sim12,13\sim18}$, $\mathbf{Z}_{19,13\sim18}$, $\mathbf{Z}_{19,20}$, $\mathbf{Z}_{21,20}$, $\mathbf{Z}_{21,22}$, $\mathbf{Z}_{21+7i,17+7i}$, $\mathbf{Z}_{20+7i,17+7i}$, $\mathbf{Z}_{22+7i,18+7i}$, $\mathbf{Z}_{21+7i,18+7i}$, $\mathbf{Z}_{22+7i,23+7i}$, and so on) at every connection joint and any point at the beam corresponding to ω_k can be obtained through the transfer equation of each element.

12.5.2 Vibration Characteristics of the System

Substituting the corresponding parameters into the characteristic equation and solving it, the natural frequency of the MLRS in any case can be obtained. The state vectors corresponding to natural frequency ω_k ($k = 1, 2, 3, \dots$) at any point of the MLRS can be obtained through the transfer equation of the system.

The quantitative relation between the vibration characteristics of the MLRS and the total parameters of the system is established. By changing the total parameters of the system, the vibration characteristics can be modified easily. The order of the transfer matrix and the eigenequation of the MLRS all are very low, which ensures the high-speed computation of the vibration characteristics.

12.6 Dynamics Response of the System

In this section, the body dynamics equations of the MRFs for the MLRS are established, augmented eigenvectors which automatically satisfy orthogonality are constructed, and the way to exactly analyze the dynamics response of the multibody system for the MLRS is paved.

12.6.1 Body Dynamics Equations of the System

The body dynamics equation of single body element j ($j = 7, 8, 9, 10, 11, 12, 19, 21, 23, 20 + 7i, 21 + 7i, 22 + 7i$) is

$$M_j v_{j,tt} + C_j v_{j,t} + K_j v_j = f_j \quad (12.60)$$

The body dynamics equation of every element is rearranged and assembled according to their sequence number, and so the body dynamics equation of the MLRS can be obtained:

$$M v_{tt} + C v_t + K v = f \quad (12.61)$$

where

$$M = \begin{bmatrix} M_{j_1} & & & \\ & M_{j_2} & & \\ & & \ddots & \\ & & & M_{j_n} \end{bmatrix}, K = \begin{bmatrix} K_{j_1} & & & \\ & K_{j_2} & & \\ & & \ddots & \\ & & & K_{j_n} \end{bmatrix}, v = \begin{bmatrix} v_{j_1} \\ v_{j_2} \\ \vdots \\ v_{j_n} \end{bmatrix}, f = \begin{bmatrix} f_{j_1} \\ f_{j_2} \\ \vdots \\ f_{j_n} \end{bmatrix} \quad (12.62)$$

v is the column matrix of system displacement coordinates, M and K are augmented operators, C is the damping augmented operator, f is a column matrix of external force, and j_1, j_2, \dots, j_n are the sequence numbers of the body element.

For proportional damping we have

$$C = \alpha M + \beta K \quad (12.63)$$

where α and β are constant.

12.6.2 Orthogonality of Augmented Eigenvectors of the System

Let

$$v = \sum_{k=1}^{\infty} V^k q^k(t) \quad (12.64)$$

where k is mode rank, $q(t)$ is the generalized coordinate, and V is the augmented eigenvector of the MLRS.

The parameter matrices M_j , K_j , v_j , and f_j of the body elements and the augmented eigenvector V of the system are introduced in the following.

12.6.2.1 Six Wheels (Element $j = 7, 8, \dots, 12$)

For six wheels, from Equation (5.7) we obtain

$$M_j = \begin{bmatrix} m_j & 0 & 0 \\ 0 & m_j & 0 \\ 0 & 0 & m_j \end{bmatrix}, K_j = (-D^3|_{I,j} + D^3|_{O,j})I_3, v_j = \begin{bmatrix} x_{j,j-6} \\ y_{j,j-6} \\ z_{j,j-6} \end{bmatrix}, f_j = \begin{bmatrix} f_{xC,j} \\ f_{yC,j} \\ f_{zC,j} \end{bmatrix} \quad (12.65)$$

where m_j is the mass of the wheel and $[f_{xC,j}, f_{yC,j}, f_{zC,j}]^T$ is the column matrix of external force acting on the wheel.

For convenience, this is denoted as

$$M_{7 \sim 12} = \begin{bmatrix} M_7 & & \\ & M_8 & \\ & & \ddots \\ & & & M_{12} \end{bmatrix}, K_{7 \sim 12} = \begin{bmatrix} K_7 & & \\ & K_8 & \\ & & \ddots \\ & & & K_{12} \end{bmatrix}, v_{7 \sim 12} = \begin{bmatrix} v_7 \\ v_8 \\ \vdots \\ v_{12} \end{bmatrix}, f_{7 \sim 12} = \begin{bmatrix} f_7 \\ f_8 \\ \vdots \\ f_{12} \end{bmatrix} \quad (12.66)$$

12.6.2.2 Vehicle, Gyration Parts, Pitching Parts and Launch Tube Trail

(Element $j = 19, 21, 23, 20 + 7i$)

For the vehicle, gyration parts, pitching parts and launch tube trail, we obtain

$$M_j = \begin{bmatrix} m_j I_{3 \times 3} & m_j \tilde{I}_{I_1 C, j}^T \\ m_j \tilde{I}_{I_1 C, j} & I_{I_1, j} \end{bmatrix}, v_j = \begin{bmatrix} x_{I_1, j} \\ y_{I_1, j} \\ z_{I_1, j} \\ \theta_{xI_1, j} \\ \theta_{yI_1, j} \\ \theta_{zI_1, j} \end{bmatrix}, f_j = \begin{bmatrix} \begin{pmatrix} f_{xC,j} \\ f_{yC,j} \\ f_{zC,j} \end{pmatrix} \\ \begin{pmatrix} m_{xC,j} \\ m_{yC,j} \\ m_{zC,j} \end{pmatrix} + \tilde{I}_{I_1 C} \begin{pmatrix} f_{xC,j} \\ f_{yC,j} \\ f_{zC,j} \end{pmatrix} \end{bmatrix}$$

$$K_j = \begin{bmatrix} -\sum_{n=1}^N D^3|_{I_n, j} I_3 + \sum_{l=1}^L D^3|_{O_l, j} I_3 & \mathbf{O}_{3 \times 3} \\ -\sum_{n=2}^N \tilde{I}_{I_1 I_n, j} D^3|_{I_n, j} I_3 + \sum_{l=1}^L \tilde{I}_{I_1 O_l, j} D^3|_{O_l, j} I_3 & \sum_{n=1}^N D^1|_{I_n, j} I_3 - \sum_{l=1}^L D^1|_{O_l, j} I_3 \end{bmatrix} \quad (12.67)$$

where m_j is the mass of rigid body j , C is the mass center, I_{I_1} is the moment of inertia matrix about the first input end I_1 , $[m_{xC,j}, m_{yC,j}, m_{zC,j}]^T$ is the column matrix of external moment coordinates acting on the rigid body, $[f_{xC,j}, f_{yC,j}, f_{zC,j}]^T$ is the column matrix of external force acting on the rigid body, I_n is the n th input point, and O_l is the l th output end.

12.6.2.3 Launch Tube (Element $j = 21 + 7i, 22 + 7i$)

For the launch tube, if the longitudinal and torsional deformations are neglected, we obtain

$$\begin{aligned}
 \mathbf{M}_j &= \begin{bmatrix} m_j & 0 & 0 & 0 \\ 0 & J_{j,x} & 0 & 0 \\ 0 & 0 & \bar{m}_j & 0 \\ 0 & 0 & 0 & \bar{m}_j \end{bmatrix}, \quad \mathbf{v}_j = \begin{bmatrix} x_{L,j} \\ \theta_{xL,j} \\ y(x_j, t) \\ z(x_j, t) \end{bmatrix}, \quad \mathbf{f}_j = \begin{bmatrix} \int_0^{l_j} f_x(x_j, t) dx_j \\ \int_0^{l_j} m_x(x_j, t) dx_j \\ f_y(x_j, t) - \frac{\partial m_z(x_j, t)}{\partial x_j} \\ f_z(x_j, t) + \frac{\partial m_y(x_j, t)}{\partial x_j} \end{bmatrix} \\
 \mathbf{K}_j &= \begin{bmatrix} -D^3|_{L,j} + D^3|_{O,j} & 0 & 0 & 0 \\ 0 & D^1|_{L,j} - D^1|_{O,j} & 0 & 0 \\ 0 & 0 & EI_z \frac{\partial^4}{\partial x_j^4} & 0 \\ 0 & 0 & 0 & EI_y \frac{\partial^4}{\partial x_j^4} \end{bmatrix}
 \end{aligned} \tag{12.68}$$

where x_j are the coordinates of the point on elastic beam j , l_j is the length of beam j , \bar{m}_j is the mass per unit length of beam j , EI is bending stiffness, m_j is the total mass of beam j , $m_j = \bar{m}_j l_j$ and $J_{j,x}$ is the moment of inertia with respect to the axis of beam j .

So we obtain

$$\begin{aligned}
 \mathbf{M} &= \begin{bmatrix} \mathbf{M}_{7 \sim 12} & & & & & \\ & \mathbf{M}_{19} & & & & \\ & & \mathbf{M}_{21} & & & \\ & & & \mathbf{M}_{23} & & \\ & & & & \mathbf{M}_{20+7i} & \\ & & & & & \mathbf{M}_{21+7i} \\ & & & & & & \mathbf{M}_{22+7i} \end{bmatrix}, \quad \mathbf{v} = \begin{bmatrix} \mathbf{v}_{7 \sim 12} \\ \mathbf{v}_{19} \\ \mathbf{v}_{21} \\ \mathbf{v}_{23} \\ \mathbf{v}_{20+7i} \\ \mathbf{v}_{21+7i} \\ \mathbf{v}_{22+7i} \end{bmatrix} \\
 \mathbf{K} &= \begin{bmatrix} \mathbf{K}_{7 \sim 12} & & & & & \\ & \mathbf{K}_{19} & & & & \\ & & \mathbf{K}_{21} & & & \\ & & & \mathbf{K}_{23} & & \\ & & & & \mathbf{K}_{20+7i} & \\ & & & & & \mathbf{K}_{21+7i} \\ & & & & & & \mathbf{K}_{22+7i} \end{bmatrix}, \quad \mathbf{f} = \begin{bmatrix} \mathbf{f}_{7 \sim 12} \\ \mathbf{f}_{19} \\ \mathbf{f}_{21} \\ \mathbf{f}_{23} \\ \mathbf{f}_{20+7i} \\ \mathbf{f}_{21+7i} \\ \mathbf{f}_{22+7i} \end{bmatrix}
 \end{aligned} \tag{12.69}$$

The augmented eigenvector V of the MLRS is

$$V = [V_{7 \sim 12}^T, V_{19}^T, V_{21}^T, V_{23}^T, V_{20+7i}^T, V_{21+7i}^T, V_{22+7i}^T]^T \quad (12.70)$$

where

$$\begin{aligned} V_{7 \sim 12} &= [X_{7,1}, Y_{7,1}, Z_{7,1}, X_{8,2}, Y_{8,2}, Z_{8,2}, \dots, X_{12,6}, Y_{12,6}, Z_{12,6}]^T \\ V_{19} &= [X, Y, Z, \theta_x, \theta_y, \theta_z]_{19,13}^T \\ V_{21} &= [X, Y, Z, \theta_x, \theta_y, \theta_z]_{21,20}^T \\ V_{23} &= [X, Y, Z, \theta_x, \theta_y, \theta_z]_{23,22}^T \\ V_{20+7i} &= [X, Y, Z, \theta_x, \theta_y, \theta_z]_{20+7i,0}^T \\ V_{21+7i} &= [X_{I,21+7i}, \theta_{xI,21+7i}, Y(x_{21+7i}), Z(x_{21+7i})]_{21+7i}^T \\ V_{22+7i} &= [X_{I,22+7i}, \theta_{xI,22+7i}, Y(x_{22+7i}), Z(x_{22+7i})]_{22+7i}^T \end{aligned} \quad (12.71)$$

From the orthogonality of the augmented eigenvectors of the multibody system established in this book, we obtain

$$\langle MV^k, V^p \rangle = \delta_{k,p} M_p, \quad \langle KV^k, V^p \rangle = \delta_{k,p} \omega_p^2 M_p \quad (12.72)$$

where $\omega_p (p=1,2,\dots)$ is the natural frequency of the system and M_p is the p th rank mode mass.

It is then possible to solve the dynamic responses of the MLRS once the following problems have been solved: calculating eigenvalues, constructing and verifying the orthogonality of the augmented eigenvectors, and establishing the launch dynamics equation of the MLRS. Some ways are offered here to calculate and analyze dynamics performance and the quantitative relation between dynamics performance and the total parameters of system, and the basis for decreasing rocket consumption in the MLRS test and improving the weapon performance is provided. As the multi-uninterrupted firing weapon, the initial conditions of each firing and its vibration characteristics of corresponding system are different, and attention should be given to this when analyzing the dynamics response.

12.6.3 Dynamics Response of the System

Substituting Equations (12.64) and (12.63) into Equation (12.61), we obtain

$$\sum_{k=1}^{\infty} MV^k \ddot{q}^k(t) + \sum_{k=1}^{\infty} (\alpha MV^k + \beta KV^k) \dot{q}^k(t) + \sum_{k=1}^{\infty} KV^k q^k(t) = f \quad (12.74)$$

Finding the inner products of $V^p (p=1,2,3,\dots)$ and the terms on both sides of Equation (12.74), we obtain

$$\ddot{q}^p(t) + (\alpha + \beta \omega_p^2) \dot{q}^p(t) + \omega_p^2 q^p(t) = \frac{\langle f, V^p \rangle}{M_p} \quad (p=1,2,\dots) \quad (12.75)$$

So $q^p(t) (p=1,2,\dots)$ can be obtained by substituting the column matrix of external force f and step-by-step integration of the above equation, using the Equation (12.64), gives the exact analysis of the dynamics response and high-speed computation of the MRFS for the MLRS. This is an

exact analysis because the difficult problem of orthogonality of eigenvectors of the MRFS for the MLRS is solved by the MSTMM, and it is a high-speed computation because the problem of computation of eigenvalues and the dynamics response of the MRFS for the MLRS is also solved by the MSTMM, which ensures that the order of the involved matrix is low all the time, which cannot be achieved by other methods.

12.6.4 Initial Value of Each Firing for the System

For the MLRS, the condition of the rocket launcher is changed with each rocket being fired, that is, when t is changed from t_{i-1}^- to t_{i-1}^+ , the relative positions of point $(23, 17 + 7i)$, point $(23, 18 + 7i)$, point $(21 + 7i, 17 + 7i)$, point $(22 + 7i, 18 + 7i)$, and point $(22 + 7i, 23 + 7i)$ are also changed. The mass, relative position of mass center, and inertial matrix of body 23 are changed, as are the eigenfrequency and eigenvector of the system. In this case, it is wrong to regard the numerical value of the response at time t_{i-1}^- as that of time t_{i-1}^+ directly. It is necessary to convert the response at time t_{i-1}^- into the initial value of the dynamics response relative to the new balance position, and to deduce the system generalized coordinates in the new mode of the system from the initial value. Superscript i shows the sequence number of the rocket fired, superscript $+$ means after firing, while superscript $-$ means before firing. Supposing the initial value of the system is known before firing the $(i-1)$ th rocket, that is to say, the initial value at time t_{i-1}^- is known. How to determine the initial values of $\mathbf{v}(x_1, t_{i-1}^+)$ and $\mathbf{v}_t(x_1, t_{i-1}^+)$ corresponding to the balance position when the system contains $(40-i)$ rockets is as follows. The detailed calculation method can be seen in reference [1].

The weight of the rocket being fired is considered in the launch dynamics equations, and its action affecting the rocket launcher is embodied by contact force. The initial conditions of the dynamics response of the MLRS are displacement \mathbf{v} and velocity \mathbf{v}_t when one rocket is fired, and the eigenvector, balance position and dynamics response relative to the balance position of the system excluding the fired rocket. Although the balance positions of the system in every firing are different, they are all static; the difference in the orientation angles of two neighboring balance positions caused by the weight of each rocket is small. So for two neighboring balance positions, the projections $\mathbf{v}_t^i(I, t_{i-1}^+)$ and $\mathbf{v}_t^{i-1}(I, t_{i-1}^+)$ of system velocity in the corresponding coordinate system can be regarded as being the same, where I is a point fixed on body 7, ..., 12, 19, 21 or 23. In interval (t_{i-1}^+, t_i^+) , the corresponding launch tube and rocket can be regarded as parts of body 23, so linear the displacement and angular displacement of every point at bodies $20 + 7(i+1)$, $21 + 7(i+1)$ and $22 + 7(i+1)$ are determined by the rigid body motion of body 23.

12.6.4.1 Initial Value of the First Rocket Being Fired

When the first rocket is fired, the other 39 rockets are contained in the system and the initial value relative to the balance position is

$$\begin{cases} \mathbf{v}^1(I, 0^+) = \mathbf{v}^0(I, 0^-) - \Delta \mathbf{v}_{1-0}(I) \\ \mathbf{v}_t^1(I, 0^+) \approx \mathbf{v}_t^0(I, 0^-) = 0 \end{cases} \quad (12.76)$$

where $\mathbf{v}^i(I, t)$ is the displacement of point I at the moment of t relative to the balance position of the system when the launch tube contains $(40-i)$ rockets, $\Delta \mathbf{v}_{i-j}(I)$ represents the difference between the displacement relative to the balance position of the system when the launch tube contains $(40-i)$ rockets and that when launch tube contains $(40-j)$ rockets.

When the first rocket is fired, the system initial value relative to the balance position of the system with a full load is

$$\begin{cases} \mathbf{v}^0(I, 0^+) = \mathbf{v}^1(I, 0^+) + \Delta \mathbf{v}_{1-0}(I) = 0 \\ \mathbf{v}_t^0(I, 0^+) \approx \mathbf{v}_t^1(I, 0^+) = 0 \end{cases} \quad (12.77)$$

12.6.4.2 Initial Value of the Second Rocket Being Fired

When the second rocket is fired, the other 38 rockets are contained in the system. The mode shape of the system, the balance position and the dynamics response $\mathbf{v}^2(I, t) = \sum_{k=1}^{\infty} \mathbf{V}^{k,2}(I) q^{k,2}(t)$ are all relative to the balance position of the system with 38 rockets, namely

$$\begin{cases} \mathbf{v}^2(I, t_1^+) = \mathbf{v}^1(I, t_1^-) - \Delta \mathbf{v}_{2-1}(I) \\ \mathbf{v}_t^2(I, t_1^+) \approx \mathbf{v}_t^1(I, t_1^-) \end{cases} \quad (12.78)$$

When the second rocket is fired, the system initial value relative to the balance position of the full-load system is

$$\begin{cases} \mathbf{v}^0(I, t_1^+) = \mathbf{v}^2(I, t_1^+) + \Delta \mathbf{v}_{2-1}(I) + \Delta \mathbf{v}_{1-0}(I) \\ \mathbf{v}_t^0(I, t_1^+) \approx \mathbf{v}_t^2(I, t_1^+) \end{cases} \quad (12.79)$$

12.6.4.3 Initial Value of the i th Rocket Being Fired

When the i th rocket is fired, there are $(40-i)$ rockets contained in the system. The mode shape of the system, the balance position and the response $\mathbf{v}^i(I, t) = \sum_{k=1}^{\infty} \mathbf{V}^{k,i}(I) q^{k,i}(t)$ are all relative to the balance position of the system containing $(40-i)$ rockets, namely

$$\begin{cases} \mathbf{v}^i(I, t_{i-1}^+) = \mathbf{v}^{i-1}(I, t_{i-1}^-) - \Delta \mathbf{v}_{i-(i-1)}(I) \\ \mathbf{v}_t^i(I, t_{i-1}^+) \approx \mathbf{v}_t^{i-1}(I, t_{i-1}^-) \end{cases} \quad (12.80)$$

When the i th rocket is fired, the initial value of the system relative to the balance position of the full-load system is

$$\begin{cases} \mathbf{v}^0(I, t_{i-1}^+) = \mathbf{v}^i(I, t_{i-1}^+) + \Delta \mathbf{v}_{i-0}(I) \\ \mathbf{v}_t^0(I, t_{i-1}^+) \approx \mathbf{v}_t^i(I, t_{i-1}^+) \end{cases} \quad (12.81)$$

where

$$\Delta \mathbf{v}_{i-0}(I) = \Delta \mathbf{v}_{i-(i-1)}(I) + \Delta \mathbf{v}_{(i-1)-(i-2)}(I) + \cdots + \Delta \mathbf{v}_{2-1}(I) + \Delta \mathbf{v}_{1-0}(I) \quad (12.82)$$

The initial values of each rocket are determined as shown above, including the values relative to the corresponding balance position and the balance position of the full-load system. These values are used to calculate the dynamics response of the system at every period. Finally, these dynamics responses of the system represented in their local equilibrium positions will be converted to the corresponding values represented in the initial (full-load) equilibrium position.

12.6.5 Solving the Dynamics Response of the System

After the first rocket is fired, from the initial conditions we obtain

$$q^k(0^+) = \frac{\langle M\mathbf{v}(x_1, 0^+), \mathbf{V}^k \rangle}{M_k}, \quad \dot{q}^k(0^+) = \frac{\langle M\mathbf{v}_t(x_1, 0^+), \mathbf{V}^k \rangle}{M_k} \quad (12.83)$$

Solving Equations (12.74) and (12.75) and taking notice of Equation (12.83), $q^k(t)$, $\dot{q}^k(t)$ ($k=1,2,3,\dots$) in interval $(t_0, t_1]$, the dynamic response of the system, the rocket motion in the launch tube and the initial disturbance can be obtained.

According to this calculation, $q^k(t_1^-)$, $\dot{q}^k(t_1^-)$ ($k=1,2,3,\dots$), displacement $\mathbf{v}(x_1, t_1^-)$ and velocity $\mathbf{v}_t(x_1, t_1^-)$ at time t_1^- can also be obtained. Using Equation (12.78), displacement $\mathbf{v}(x_1, t_1^+)$ and velocity $\mathbf{v}_t(x_1, t_1^+)$ relative to the balance position of the system at time t_1^+ (38 rockets are contained in the system) can be obtained. Similar to determining $q^k(0^+)$ and $\dot{q}^k(0^+)$ ($k=1,2,\dots$), $q^k(t_1^+)$ and $\dot{q}^k(t_1^+)$ ($k=1,2,\dots$) after the firing of the second rocket can be obtained. Using the augmented eigenvector \mathbf{V}^k corresponding to interval $(t_1, t_2]$, using Equations (12.73) and (12.75), $q^k(t)$, $\dot{q}^k(t)$ ($k=1,2,3,\dots$) in interval $(t_1, t_2]$, the dynamics response of the system, the parameters of rocket motion in the launch tube, and the initial disturbance can be obtained. Proceeding with this, the dynamics response of the system during the whole firing process can be obtained as follows:

$$\mathbf{v}^0(x_1, t) = \begin{cases} \sum_{k=1}^{\infty} \mathbf{V}^k q^k(t) + \Delta \mathbf{v}_{1-0} & t \in [t_0, t_1] \\ \sum_{k=1}^{\infty} \mathbf{V}^k q^k(t) + \Delta \mathbf{v}_{2-0} & t \in (t_1, t_2] \\ \vdots \\ \sum_{k=1}^{\infty} \mathbf{V}^k q^k(t) + \Delta \mathbf{v}_{n-0} & t \in (t_{n-1}, t_n] \end{cases} \quad (12.84)$$

12.7 Launch Dynamics Equation and Forces Acting on the System

12.7.1 Coordinate Systems

The o_1xyz coordinate system (translational coordinate system): The origin o_1 is attached to the geometric center of the rocket projectile at the initial position of the rocket, the x axis is directed toward the launch tube muzzle and along the tangent of the launch tube axis, the y axis is directed along the vertical plane and perpendicular to the x axis, and the z axis completes the triad, so the direction of every coordinate axis is then fixed. The system is mostly used to determine the basis of the orientation of the rocket, as shown in Figure 12.3.

The $o_o x_o y_o z_o$ coordinate system (rocket launcher coordinate system): The origin o_o is the crosspoint of the cross-section of the rocket at the mass center and launch tube axis. The x_o axis is directed toward the launch tube muzzle and along the tangent of the launch tube, the y_o axis is directed along the vertical plane and perpendicular to the x_o axis, and the z_o axis completes the triad. The system is used to determine the basis of the orientation of the rocket relative to the launch tube.

Figure 12.3 Translational coordinate system and inertial coordinate system.

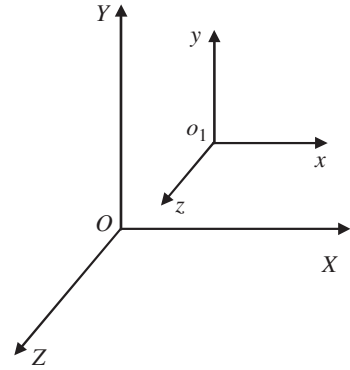


Figure 12.4 Rocket axis coordinate system and translational coordinate system.

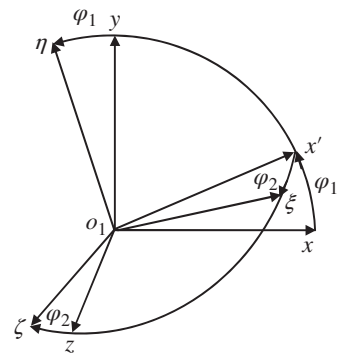
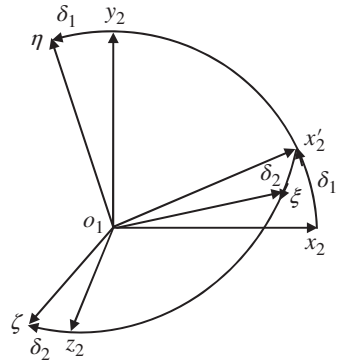


Figure 12.5 Rocket axis coordinate system and velocity coordinate system.



The $o_1\xi\eta\zeta$ coordinate system (rocket projectile coordinate system): The origin o_1 is attached to the geometric center of rocket projectile, the ξ axis is directed toward the head of the rocket and along the geometric longitudinal axis of the rocket, the η axis is directed along the vertical plane and perpendicular to the ξ axis, and the ζ axis completes the triad. As shown in Figure 12.4, the system is used to determine the orientation of the rocket axis.

The $o_1x_2y_2z_2$ coordinate system (velocity coordinate system): The origin o_1 is attached to the geometric center of the rocket projectile, the x_2 axis is directed toward the velocity of the geometric center of the rocket, the y_2 axis is directed along the vertical plane and perpendicular to

the x_2 axis, and the z_2 axis completes the triad. As shown in Figure 12.5, the system is used to determine the translation of the rocket.

12.7.2 Forces Analysis of the Launching Process

Forces on the MLRS include weight, the mechanic interactive forces among the components and between the MLRS launcher and the ground, the projectile-launcher action force, the thrust of the engine, the impact force of the jet flow and so on. Mechanic interactive forces among components and between the MLRS launcher and the ground may be equivalent to the corresponding spring and damping forces of elastic joints with damping, which are all internal forces of the system. In solving the launch dynamics of the MLRS using the MSTMM, the supporting forces of the ground are included in the system dynamic model as internal forces, and these internal forces are all considered in the state vector and need not be expressed with intricate external forces. These are also features of solving the launch dynamics of the MLRS by the MSTMM.

The static balance position of the system is regarded as the basis of system displacement, where the rockets fired and being fired are not included in the system. In this way, the function of system weight (including all components and the rocket not fired) in dynamics equations is offset by that of the static deformation of system components, so in the chosen coordinate system the action related to the weight of the system and the static deformation need not be considered, which greatly simplifies the forces analyzed and the dynamics solved for the MLRS. The large impact force on the rocket launcher [265] is made by the rocket exhaust, which causes vibration of the rocket launcher. The initial disturbance of the subsequently fired rocket is affected, and the firing dispersion of the MLRS is also affected. The forces between the rocket and the launch tube are a pair of acting forces and counterforces. The kinetic equation of the rocket launcher and the vibration equation of the rocket launcher couple together, via the interaction force between bourrelet and launch tube, as well as the interaction force between the guide button and the guide trough. These forces include the normal collision force and the tangential friction force between the bourrelet and the launch tube, and between the guide button and the guide trough. That the weight of the fired rocket affects the rocket launcher is demonstrated by the contact force between the rocket and the launcher. The thrust of the engine and the impingement force of the rocket exhaust on the firing equipment can be calculated theoretically or measured by testing.

The forces acting on the rocket in the launch tube include weight, the thrust of the engine, air resistance, as well as the force between the launch tube and the guide button, and the contact force between the bourrelet and the launch tube. The expressions are given in reference [1].

12.7.3 The Launch Dynamics Equation of the Rocket

As launch dynamics is very complex, the launch dynamics of a multibody system such as an MLRS with high temperature, high pressure, short time and violent change cannot be solved using the usual kinds of research methods. In the research field and the expansive literature of launch dynamics at home and abroad, the model of launch dynamics has had to be simplified again and again, so the differences between the model and the reality are so great that the resulting level of error is large. In launch dynamics research an assumption is always made by the researcher that the rear bourrelet center moves along the bore axis as this simplifies the research problem. In 1984, the general differential equation of motion of a projectile in a bore was developed by Marting, an American expert in weapon dynamics [266]. To overcome the shortcomings of the Marting's equation, a uniform launch dynamics equation of a rocket suitable for all kinds of motion has been established by the authors. Not only are the factors considered more

general and closer to reality than those of Marting's model, but also the form of the differential equation of motion is more concise than that of Marting's equation. In the model of launch dynamics, the rocket weight, thrust, thrust misalignment angle, linear thrust misalignment, rocket-tube clearance, contact force between bourrelet and launch tube, mass eccentricity, and dynamic unbalance are all considered. The translational and rotational equations are established in the rocket launcher coordinate system $o_o x_o y_o z_o$ and the rocket axis system $o_1 \xi \eta \zeta$, respectively [1].

The general dynamics equations of an asymmetric rocket in the launch tube are

$$\begin{aligned}
 \ddot{x}'_{oc} &= \frac{F_p}{m} - \ddot{x}'_o - g \sin \theta_1 \cos \psi_2^I - \frac{(\sin \alpha + \mu \cos \alpha) C \ddot{\gamma}}{(\cos \alpha - \mu \sin \alpha) m r_b} + \frac{F_x^{sf}}{m} + \frac{F_{2x}^{sf}}{m} \\
 \ddot{y}'_{oc} &= -\ddot{y}'_o - g \cos \theta_1 + \frac{F_{2y}^{sf}}{m} - \frac{C \ddot{\gamma}}{m r_b} \sin(\gamma + \gamma_0) + \frac{F_y^{sf}}{m} + \frac{F_p}{m} (\delta_1^I + \beta_{p_\eta}) \\
 \ddot{z}'_{oc} &= -\ddot{z}'_o + \frac{F_{2z}^{sf}}{m} + \frac{C \ddot{\gamma}}{m r_b} \cos(\gamma + \gamma_0) + \frac{F_z^{sf}}{m} + \frac{F_p}{m} (\delta_2^I + \beta_{p_\zeta}) + g \sin \theta_1 \sin \psi_2^I \\
 \dot{\gamma} &= \frac{\tan \alpha}{r_b} v_p \\
 \ddot{\delta}_1^I &= -\frac{C}{A} \dot{\gamma} (\dot{\psi}_2^I + \dot{\delta}_2^I) + \left(1 - \frac{C}{A}\right) (\dot{\gamma}^2 \beta_{D_\eta} + \ddot{\gamma} \beta_{D_\zeta}) - \frac{C \ddot{\gamma}}{A} \delta_2^I + \frac{m L_{m_\eta}}{A} \left(a_p + \frac{\partial^2 \ddot{x}'_0}{\partial t^2}\right) \\
 &\quad + \frac{C \ddot{\gamma}}{A} \left\{ \frac{\sin \alpha + \mu \cos \alpha}{\cos \alpha - \mu \sin \alpha} [\cos(\gamma + \gamma_0) - \delta_1^I l_R] + \frac{l_R}{r_b} \sin(\gamma + \gamma_0) \right\} \\
 &\quad - \frac{l_R}{A} F_{2y}^{sf} + \frac{l_1}{A} F_y^{sf} - \frac{F_p L_\eta}{A} - \ddot{\psi}_1^I \\
 \ddot{\delta}_2^I &= \frac{C}{A} \dot{\gamma} (\dot{\psi}_1^I + \dot{\delta}_1^I) + \left(1 - \frac{C}{A}\right) (\dot{\gamma}^2 \beta_{D_\zeta} - \ddot{\gamma} \beta_{D_\eta}) + \frac{C \ddot{\gamma}}{A} \delta_1^I + \frac{m L_{m_\zeta}}{A} \left(a_p + \frac{\partial^2 \ddot{x}'_0}{\partial t^2}\right) \\
 &\quad + \frac{C \ddot{\gamma}}{A} \left\{ \frac{\sin \alpha + \mu \cos \alpha}{\cos \alpha - \mu \sin \alpha} [\sin(\gamma + \gamma_0) - \delta_2^I l_R] - \frac{l_R}{r_b} \cos(\gamma + \gamma_0) \right\} \\
 &\quad - \frac{l_R}{A} F_{2z}^{sf} + \frac{l_1}{A} F_z^{sf} - \frac{F_p L_\zeta}{A} - \ddot{\psi}_2^I
 \end{aligned} \tag{12.73}$$

where

$$\begin{aligned}
 \ddot{y}'_o &= \sum_{k=1}^{\infty} Y^k(x_p) \ddot{q}^k(t) - 2v_p \sum_{k=1}^{\infty} Y'^k(x_p) \dot{q}^k(t) - v_p^2 \sum_{k=1}^{\infty} Y''^k(x_p) q^k(t) + \frac{\partial^2 \ddot{x}'_0}{\partial t^2} \sum_{k=1}^{\infty} Y'^k(x_p) q^k(t) \\
 \ddot{z}'_o &= \sum_{k=1}^{\infty} Z^k(x_p) \ddot{q}^k(t) - 2v_p \sum_{k=1}^{\infty} Z'^k(x_p) \dot{q}^k(t) - v_p^2 \sum_{k=1}^{\infty} Z''^k(x_p) q^k(t) + \frac{\partial^2 \ddot{x}'_0}{\partial t^2} \sum_{k=1}^{\infty} Z'^k(x_p) q^k(t) \\
 L_{m_\eta} &= L_{m_1} \cos \gamma - L_{m_2} \sin \gamma, \quad L_{m_\zeta} = L_{m_1} \sin \gamma + L_{m_2} \cos \gamma \\
 L_\eta &= L_1 \cos \gamma - L_2 \sin \gamma, \quad L_\zeta = L_1 \sin \gamma + L_2 \cos \gamma \\
 \beta_{D_\eta} &= \beta_{D_1} \cos \gamma - \beta_{D_2} \sin \gamma, \quad \beta_{D_\zeta} = \beta_{D_1} \sin \gamma + \beta_{D_2} \cos \gamma \\
 \beta_{p_\eta} &= \beta_{p_1} \cos \gamma - \beta_{p_2} \sin \gamma, \quad \beta_{p_\zeta} = \beta_{p_1} \sin \gamma + \beta_{p_2} \cos \gamma \\
 y'_{oo} &= y'_{oc} - L_{m_\eta} - l_R \delta_1^I, \quad z'_{oo} = z'_{oc} - L_{m_\zeta} - l_R \delta_2^I
 \end{aligned}$$

\ddot{x}'_{oc} , \ddot{y}'_{oc} and \ddot{z}'_{oc} are the longitudinal, vertical and sidewise accelerations, respectively, of the mass center of the rocket projectile in the rocket launcher coordinate system $o_o x_o y_o z_o$, \ddot{x}'_o , \ddot{y}'_o and \ddot{z}'_o are the projections in the rocket launcher coordinate system $o_o x_o y_o z_o$ of acceleration of the mass center of the rocket launch tube with respect to the ground coordinate system, F_p is thrust, μ is the frictional coefficient between the guide button and the launch tube, m is the mass of the rocket, θ_1 is the departure angle of the rocket launcher, γ is the roll angle of the rocket, γ_0 is the initial orientation angle of the guide slot, g is the acceleration due to gravity, a_p is the axial acceleration at the origin point o_o of the rocket launcher coordinate system $o_o x_o y_o z_o$ for launching the tube, F_{2y}^{sf} and F_{2z}^{sf} are the vertical and sidewise components of the contact force F_2^{sf} between the rear bourrelet and the launch tube, respectively, and F_y^{sf} and F_z^{sf} are the vertical and sidewise components of the contact force F^{sf} between the front bourrelet and the launch tube, respectively. δ_1^l and δ_2^l are the vertical and sidewise components of the bracket angle between the projectile spin axis and the tangent of the launch tube axis, β_{p_η} and β_{p_ζ} are the projections of thrust malalignment angle β_p in axes η and ζ of the rocket axis coordinate system $o_1 \xi \eta \zeta$, respectively, α is the twist angle of the guide flute, r_b is the neutral circular radius of the guide button, ψ_1^l and ψ_2^l are the vertical and sideways components of the bracket angle between the tangent of the launch tube axes and the aiming line, respectively, A is the transverse moment of inertia of the rocket, C is the polar moment of inertia, β_{D_η} and β_{D_ζ} are the projections of dynamic unbalance angle β_D in axes η and ζ of the rocket axis coordinate system $o_1 \xi \eta \zeta$, respectively, L_{m_η} and L_{m_ζ} are the projections of mass eccentricity L_m in axes η and ζ of the rocket axis coordinate system $o_1 \xi \eta \zeta$, respectively, L_η and L_ζ are the projections of thrust malalignment L in axes η and ζ of the rocket axis coordinate system $o_1 \xi \eta \zeta$, respectively, l_R is the distance between the mass center of the rocket and the rear bourrelet, and l_1 is the distance between the mass center of the rocket and the front bourrelet.

12.8 Dynamics Simulation of the System and its Test Verifying

On the basis of the launch dynamics of the MLRS based on the MSTMM, the 6-DOF rigid-body ballistics model [267, 268] is adopted, the influence of the aerodynamic force of the rocket, mass, mass eccentricity, dynamic unbalance, propellant mass, thrust, linear thrust malalignment, thrust malalignment angle, gusts of wind, and other random factors relevant to flight process are considered synthetically, and the flight dynamics model and the dynamics equation of the MLRS are established, although they are omitted here and can be seen in reference [1]. Combining with the launch and flight dynamics of the MLRS, the dynamic performance of the weapon system from ignition in the rocket engine to the rocket impacting the ground in the MLRS can be studied. The firing and flying process of the MLRS is influenced by many random factors, including the random change in the parameters of the rocket, launcher and propellant, the randomness of the application environment (weather condition, ground condition etc.) and the handling process (personnel technical diathesis, handling error ect.), and so on. There are two main ways of handling firing and flying dynamics problems for the MLRS: the deterministic model, where the random factors of the firing and flying process are not considered, and the random model, where the random factors of the firing and flying process are considered. The deterministic model handles system problems in isolation, so it is difficult to obtain satisfying analysis results for the firing and flying process for the MLRS. By starting from the view of a system of rocket, launcher, propellant and circumstance, and studying the firing and flying process by applying the random model, the essence of the launch process can be revealed, and the

regular pattern of the launch dynamics can be found. The Monte Carlo method is an efficient way to solve the random model.

Random simulation is a numerical method of finding the approximate solution of mathematical, physical, engineering and other problems by simulation and statistical tests. It studies the dynamic process and characteristics of the simulated system by numerical experiment. The core of launch dynamics simulation is the random-firing and flying-dynamics equation, which is based on the MSTMM established by the author. The detailed processes are as follows. Based on the statistical characteristics (such as the mean value and mean-square deviation) of a random variable (such as rocket mass, mass eccentricity, dynamics unbalance, propellant mass, thrust, linear thrust malalignment, thrust malalignment angle, firing interval, rocket-tube clearance, bending property, gust wind, and so on), generate the corresponding random variable sequence by using the random simulation principle. Then, regard the launch dynamics equations as deterministic equations and carry out several times of certain computation. For each of the certain computations, the random variables are assigned with a set of certain values chosen from the random variable sequence. The statistical characteristics of corresponding parameters in the random firing and flying dynamics process can be obtained by computing these results. According to the eigenequations, the augmented eigenvector and its orthogonality conditions, the launch dynamics and ballistics equations, the random launch dynamics simulation system of the MLRS based on the MSTMM is established and can be used to study the influence of random or nonrandom factors on firing dispersion. The simulation results are validated by vibration characteristics, dynamic response, and the ballistic and firing dispersion of the MLRS, which also validate the theory and simulation system of the MLRS based on the MSTMM.

12.8.1 Composition, Flow and Functions of the Simulation System

The launch dynamics simulation system of the MLRS based on the MSTMM is as follows:

- 1) General control module: This module is used to mobilize all function modules, simulate the launch dynamics, carry out the statistical analysis and output the results.
- 2) Random number module: This module produces the random number for other the function modules according to the statistical characteristics of the random parameter, which are prescribed by a specified distribution.
- 3) Weapon vibration characteristics module: This module is used to simulate the eigenfrequency, eigenvector, damping ratio and so on.
- 4) Interior ballistics module: This module is used to simulate the thrust and interior ballistics with the random number obtained in (2) as one part of the basic parameter.
- 5) Impingement force of the rocket exhaust module: This module is used to simulate the impingement force of the rocket exhaust.
- 6) Weapon dynamic characteristics of the firing process module: This module is used to simulate projectile and barrel motion, projectile-barrel interaction, and the initial disturbance of the rocket according to the data obtained in (2), (3), (4) and (5).
- 7) Exterior ballistics module: This module is used to simulate the ballistics data of the rocket projectile and hitting point scattering according to the data obtained in (2), (4) and (6).
- 8) Statistical analysis module: This module is used to deal with the simulation results statistically.
- 9) Correlation analysis module: This module is used to analyze correlation among all kinds of factors, the dynamic performance of the MLRS and the firing accuracy according to the data obtained in (2), (6) and (7), to offer the primary influence factors of dynamic performance of

the MLRS and the firing accuracy, and to provide the basis for the general parameter dynamic design of the MLRS.

- 10) Result output module: This module is used to output simulation results in the form of character, curve and figure etc.

The simulation flow of the launch dynamics of the MLRS based on the MSTMM is shown in Figure 12.6.

The functions of the launch dynamics simulation system based on the MSTMM are:

- 1) Simulation of the vibration characteristics of the MLRS and its variance caused by the variance of the total rocket number in the launcher.
- 2) Simulation of the dynamic response of the MLRS (including displacement, velocity, acceleration, angular displacement, angular velocity, angular acceleration etc.).
- 3) Simulation of the initial disturbance of the rocket (including initial swing angle, initial swing velocity, muzzle rotation angle, rotation angular velocity, displacement, velocity, and other motion parameters).
- 4) Simulation of exterior ballistics and firing precision of the MLRS (including exterior ballistics data, ballistics parameters of burning phase end, flight time, points of fall, firing accuracy, firing dispersion, etc.).

12.8.2 Simulation Results of the Dynamics Response of the System

The firing sequence and the loading position of a MLRS with 40 launch tubes are shown in Figure 12.7. The loading position of every rocket is denoted with a dual (n_1, n_2) , where n_1 shows

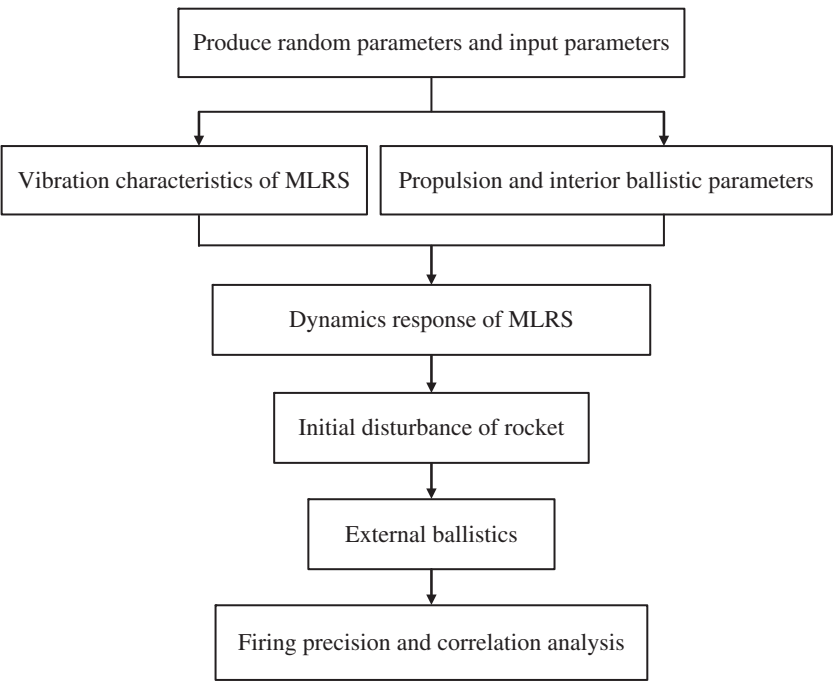


Figure 12.6 Simulation flow of the launch dynamics of an MLRS based on the MSTMM.

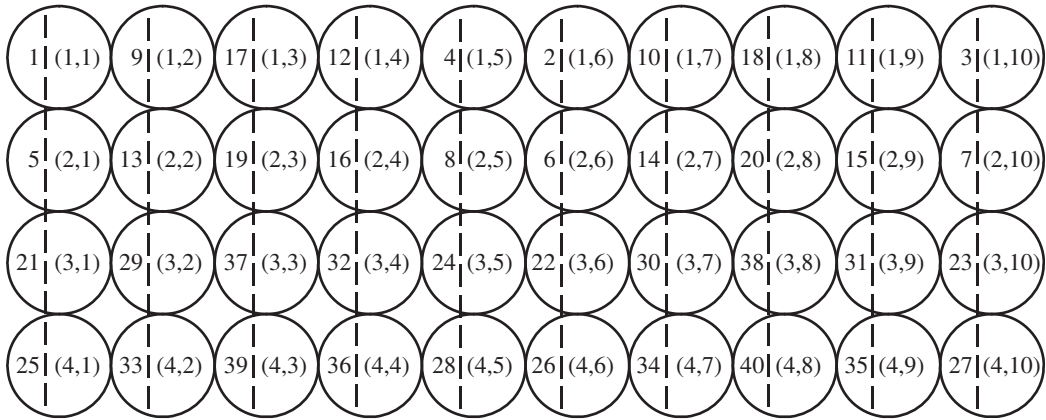


Figure 12.7 Firing sequence and loading position of an MLRS with 40 launch tubes.

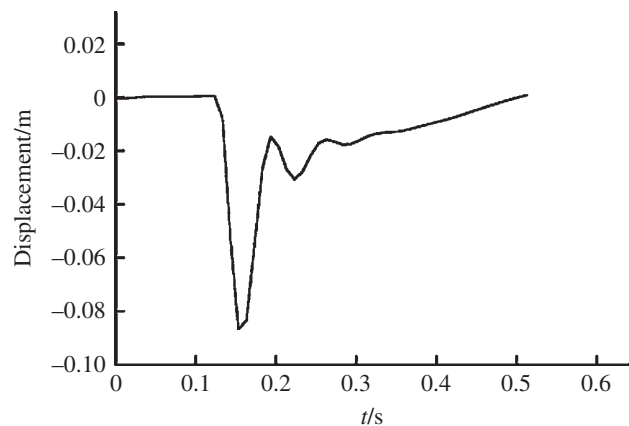
the row number with 1, 2, 3 and 4 from up to down, while n_2 shows column number with 1, 2... 10 from left to right. In the figure, each circle represents a launch tube, the nearside number inside the circle represents the firing sequence of a 40-rocket salvo, and the dextral number inside the circle represents the loading position of the rockets. For example, the loading position of the 26th rocket in the firing sequence is represented by (4, 6).

Using the launch dynamics simulation system of the MLRS based on the MSTMM, the launch dynamic simulation results of a MLRS with 40 launch tubes and rockets in the process of firing are obtained as follows.

12.8.2.1 Simulation Results of the Launch Dynamics of a MLRS with Single Firing

The numerical simulation of an MLRS with 40 launch tubes single firing was carried out. Some of the simulation results of the launch tube vibration during single tube firing are shown in Figures 12.8–12.17. The time histories of the motion and the impact forces of the rocket are illustrated in Figures 12.18–12.27.

Figure 12.8 Muzzle displacement in the x direction.



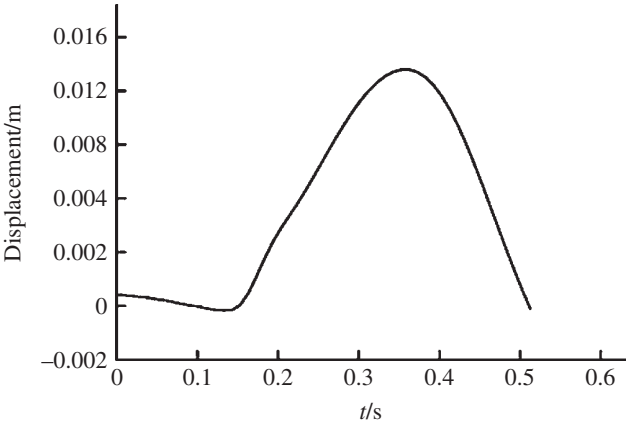


Figure 12.9 Muzzle displacement in the y direction.

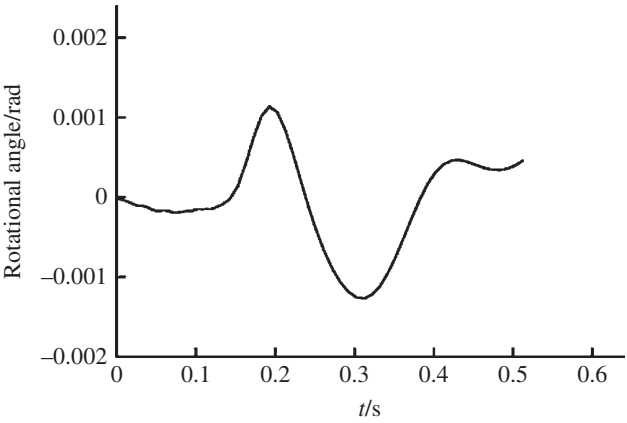


Figure 12.10 Muzzle rotational angle in the x direction.

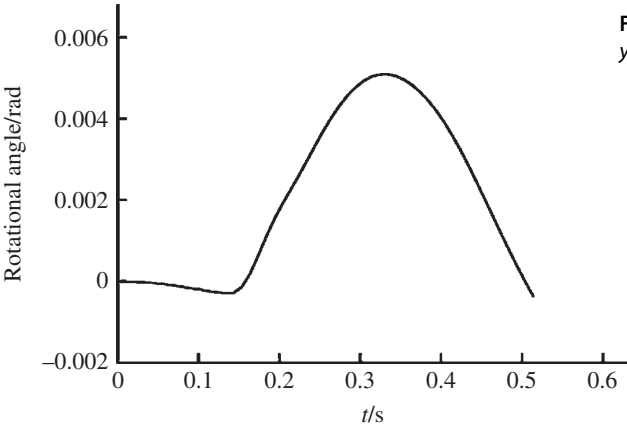


Figure 12.11 Muzzle rotational angle in the y direction.

Figure 12.12 Muzzle velocity in the z direction.

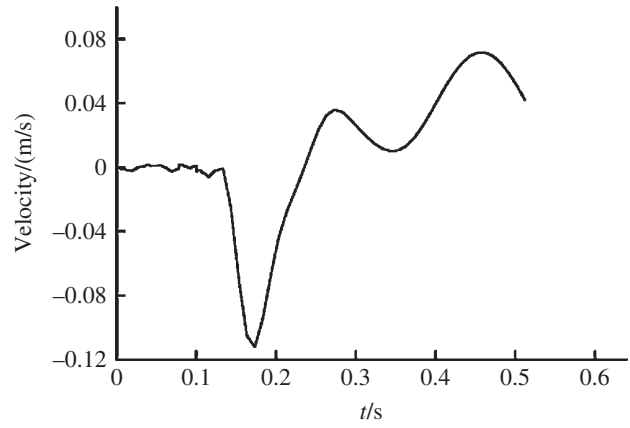


Figure 12.13 Muzzle velocity in the x direction.

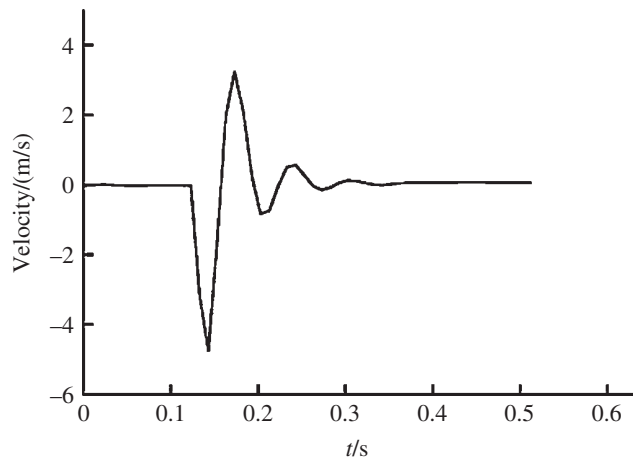
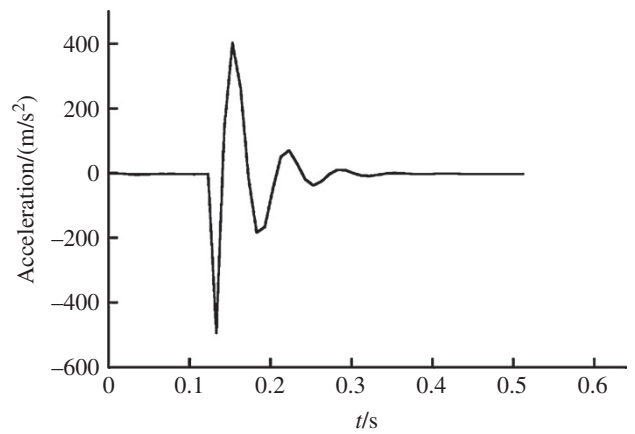


Figure 12.14 Muzzle acceleration in the x direction.



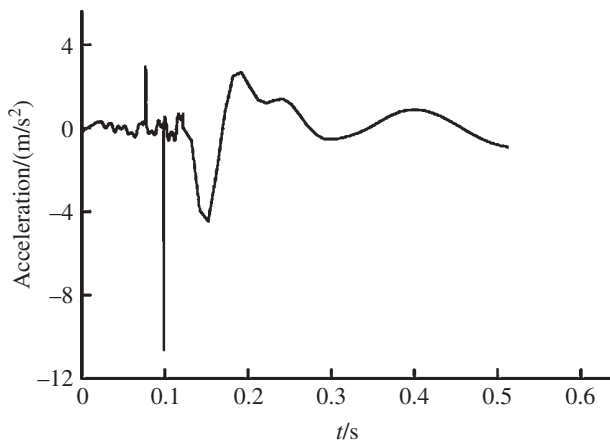


Figure 12.15 Muzzle acceleration in the z direction.

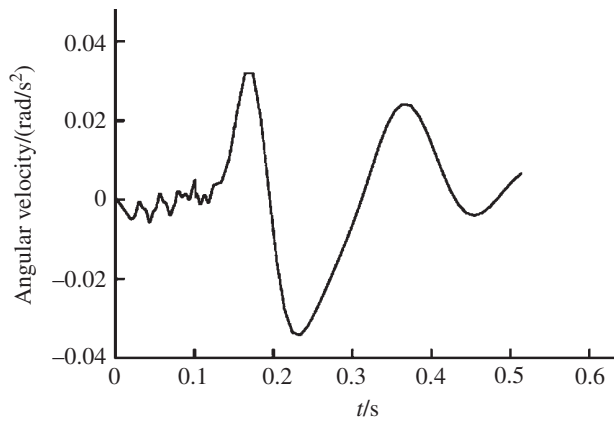


Figure 12.16 Muzzle angular velocity in the x direction.

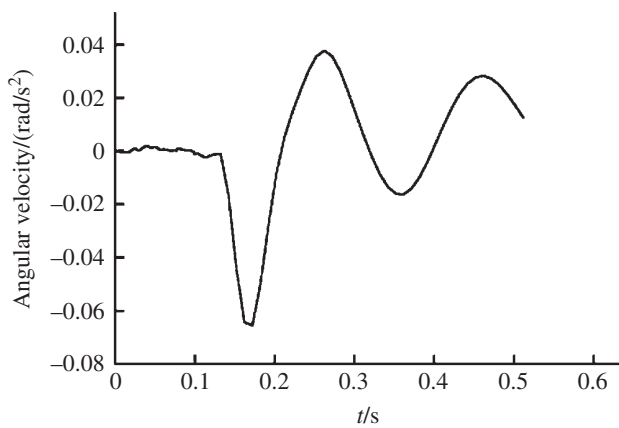


Figure 12.17 Muzzle angular velocity in the y direction.

Figure 12.18 Lognitudinal displacement of the rocket.

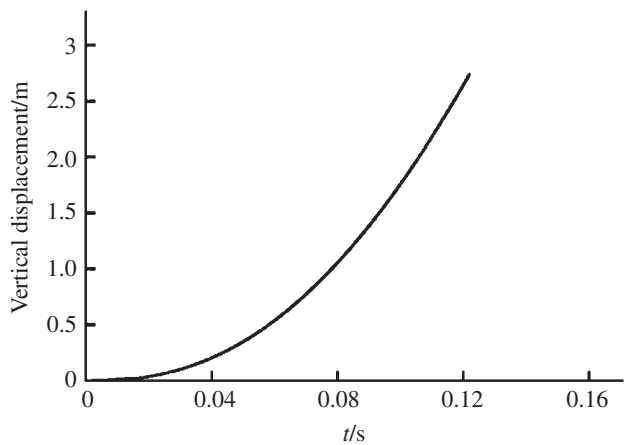


Figure 12.19 Lognitudinal velocity of the rocket.

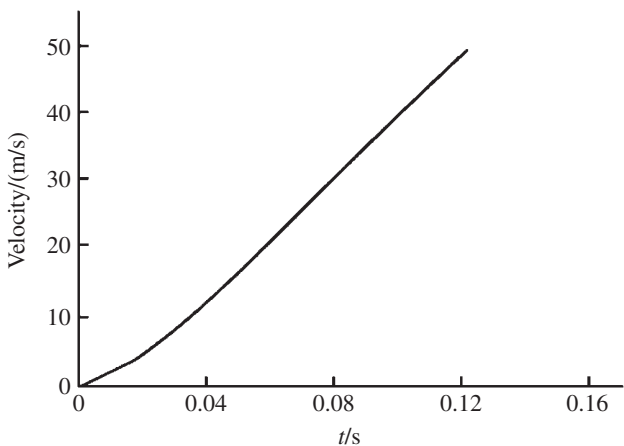
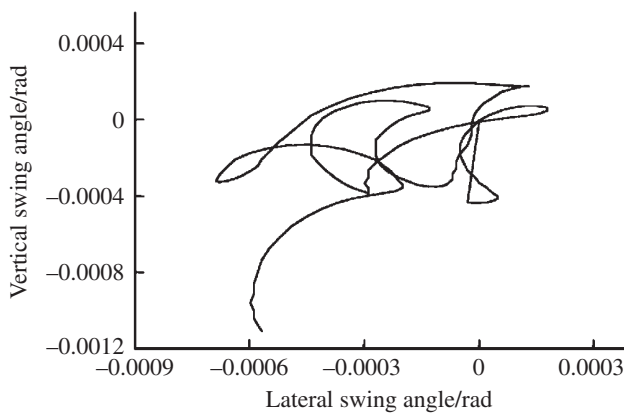


Figure 12.20 Swing-angle track of the rocket.



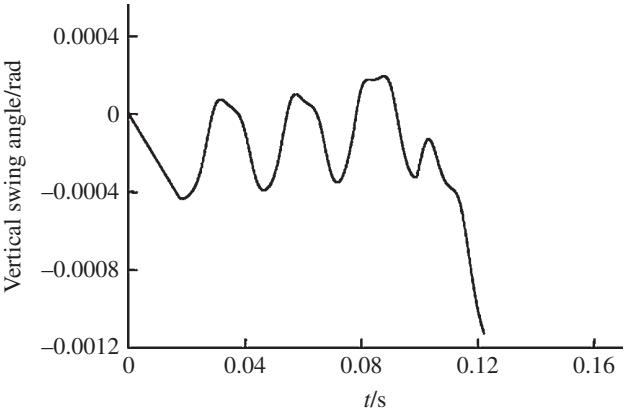


Figure 12.21 Vertical swing angle of the rocket.

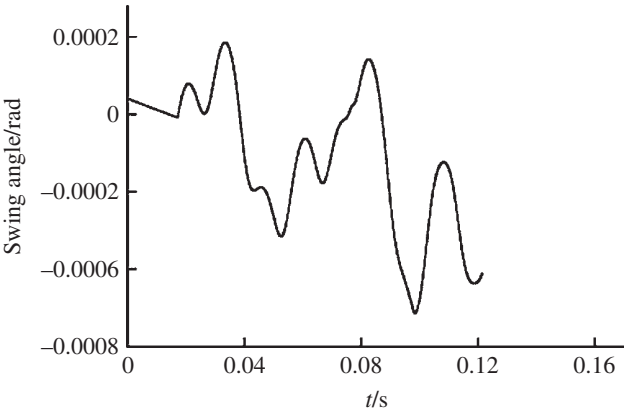


Figure 12.22 Lateral swing angle of the rocket.

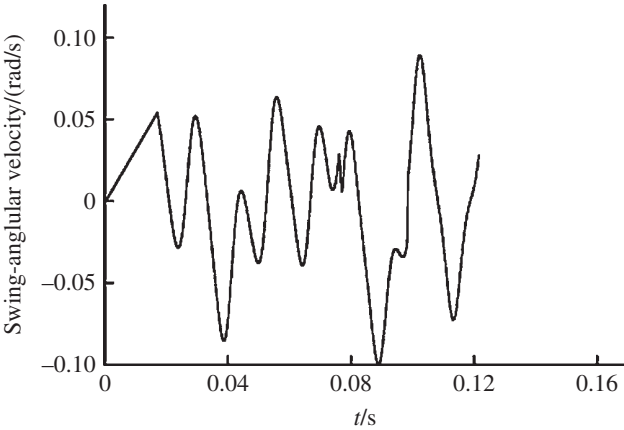


Figure 12.23 Lateral swing angular velocity of the rocket.

Figure 12.24 Vertical swing angular velocity of the rocket.

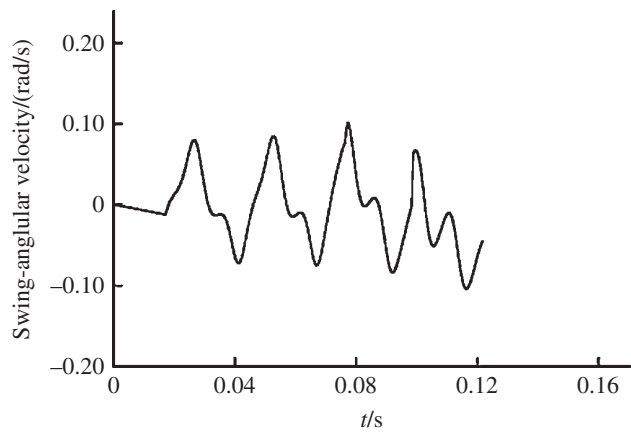


Figure 12.25 Rotational angular velocity of the rocket.

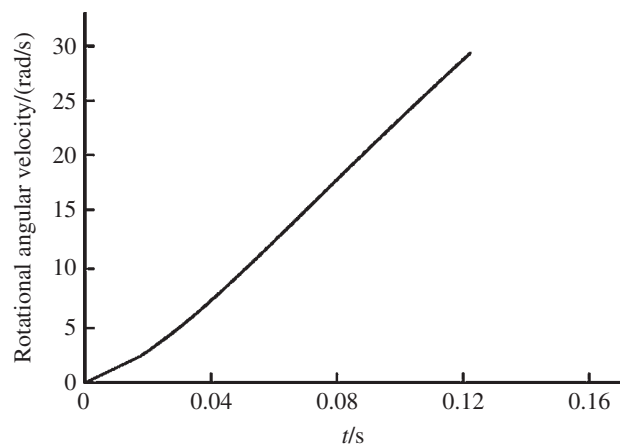
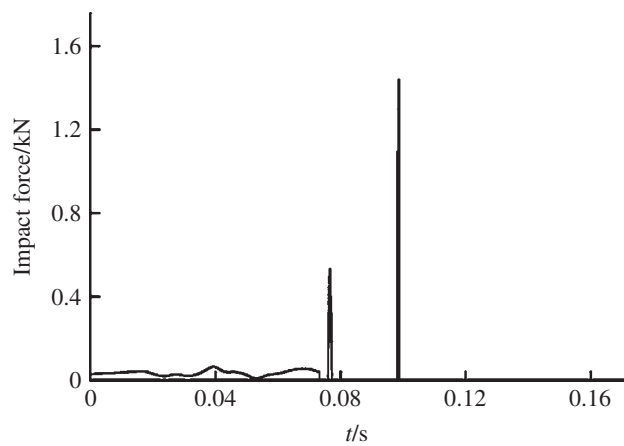


Figure 12.26 Impact force of the forward bourrelet.



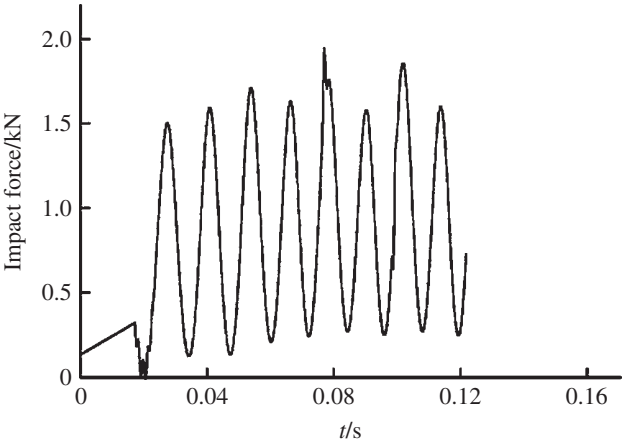


Figure 12.27 Impact force of the aft bourrelet.

12.8.2.2 Simulation Results of the Launch Dynamics of a MLRS with a 40-rocket Salvo

The numerical simulation for an MLRS with a 40-rocket salvo was carried out. Some of the numerical simulation results are shown in Figures 12.28–12.43.

12.8.3 Simulation Result of the Initial Disturbance of the Rocket

The initial disturbance of an MLRS with 40 launch tubes is simulated by the launch dynamics simulation system of the MLRS based on the MSTMM. Some of the numerical simulation results are shown in Table 12.1.

12.8.4 Simulation and Test Validation of the Vibration Characteristics of the System

The simulation results and the mode test results of the first 14 eigenfrequencies of an MLRS with 40 launch tubes under the condition of full-load and non-load are shown in Tables 12.2 and 12.3, respectively. The comparison indicates that they have good agreement, and the simulation results are validated by a modal test.

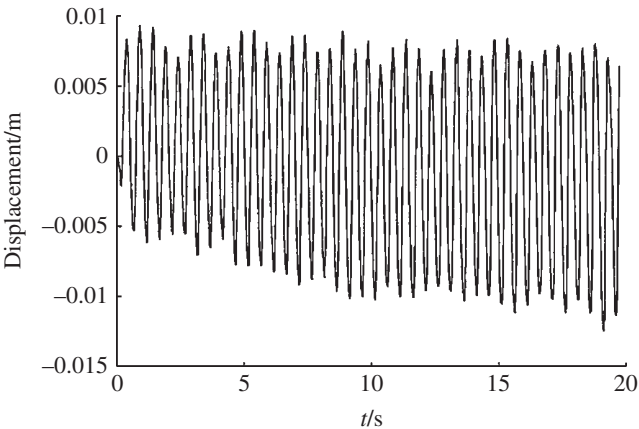


Figure 12.28 Muzzle displacement in the x direction.

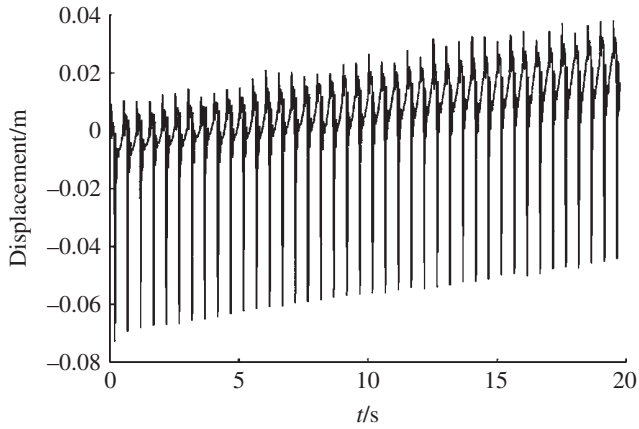


Figure 12.29 Muzzle displacement in the y direction.

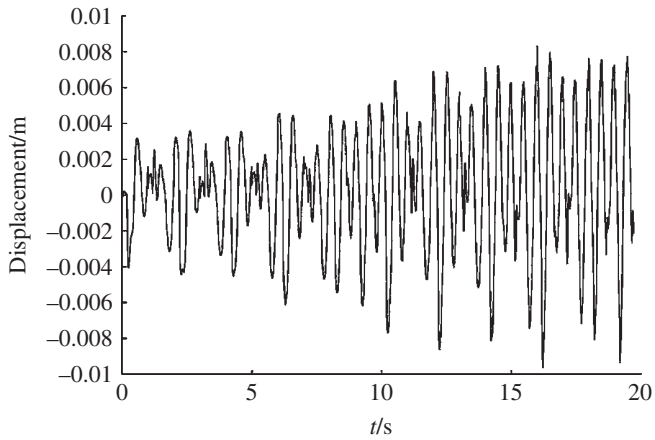


Figure 12.30 Muzzle displacement in the z direction.

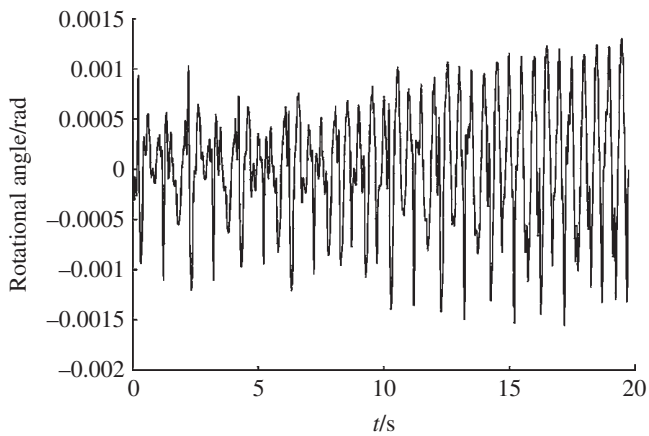


Figure 12.31 Muzzle rotational angle in the x direction.

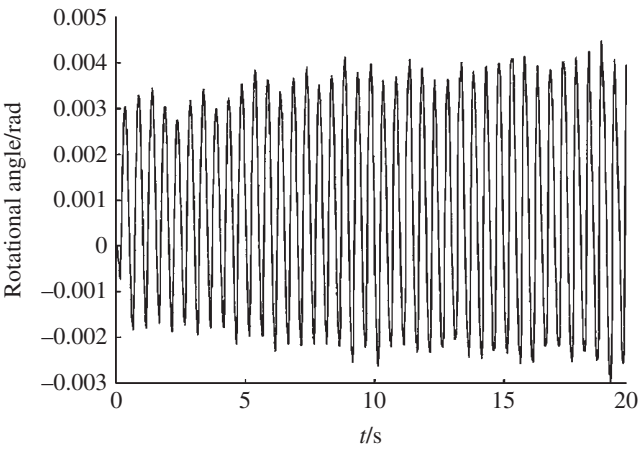


Figure 12.32 Muzzle rotational angle in the y direction.

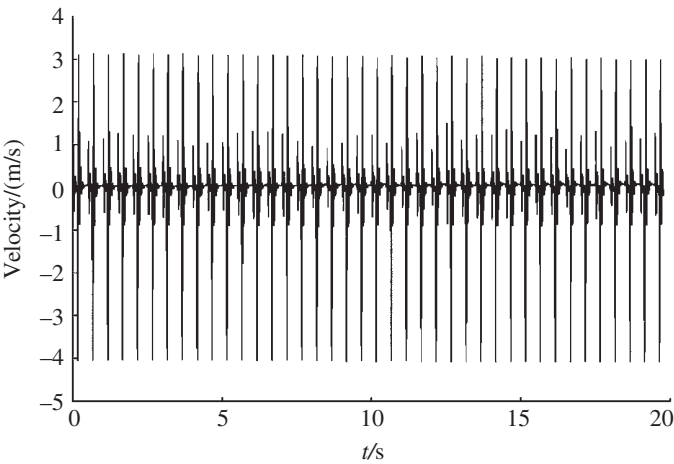


Figure 12.33 Muzzle velocity in the x direction.

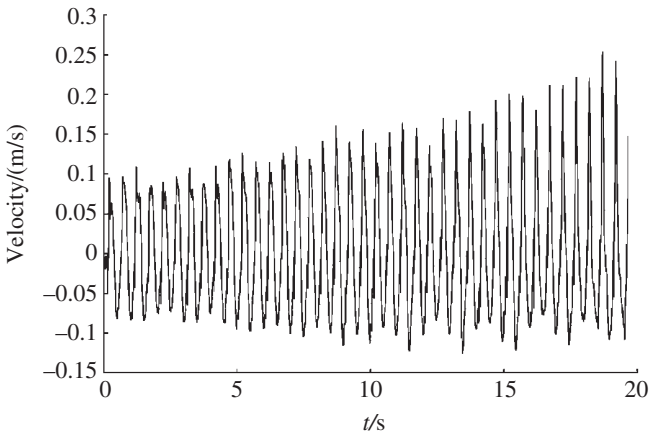


Figure 12.34 Muzzle velocity in the y direction.

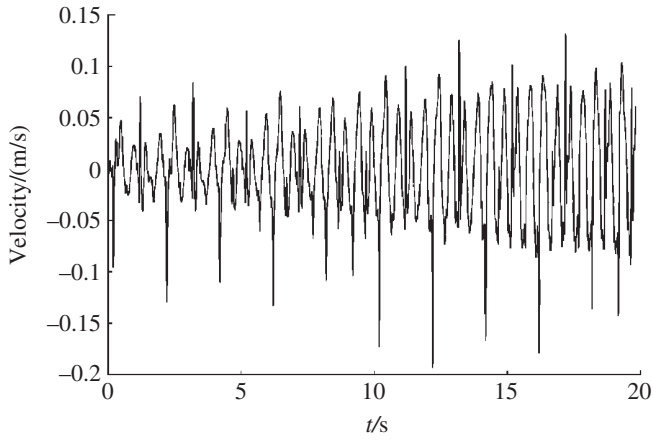


Figure 12.35 Muzzle velocity in the z direction.

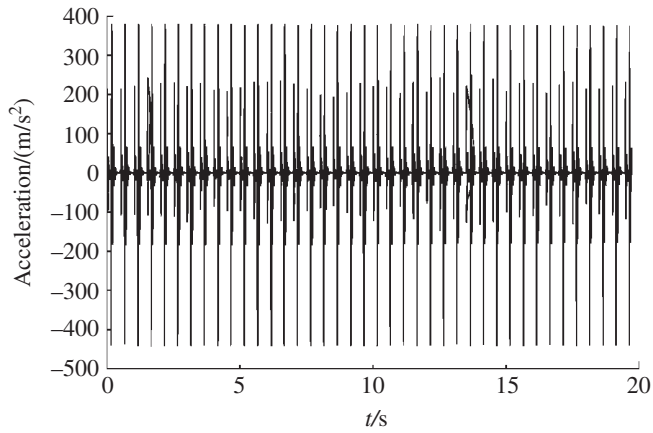


Figure 12.36 Muzzle acceleration in the x direction.

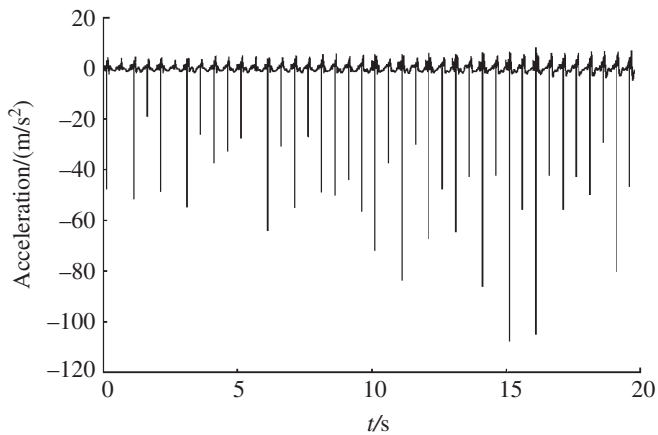


Figure 12.37 Muzzle acceleration in the y direction.

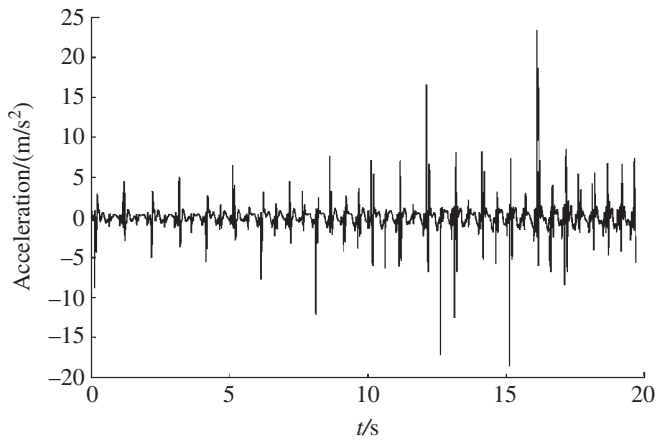


Figure 12.38 Muzzle acceleration in the z direction.

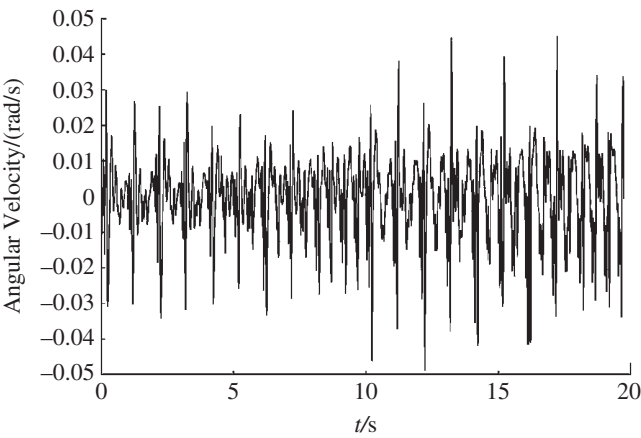


Figure 12.39 Muzzle angular velocity in the x direction.

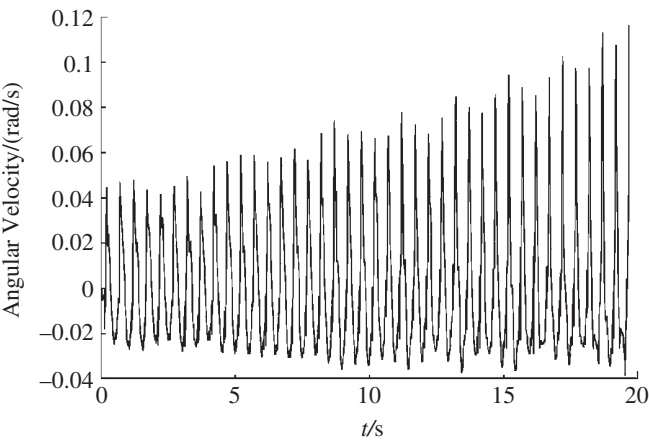


Figure 12.40 Muzzle angular velocity in the y direction.

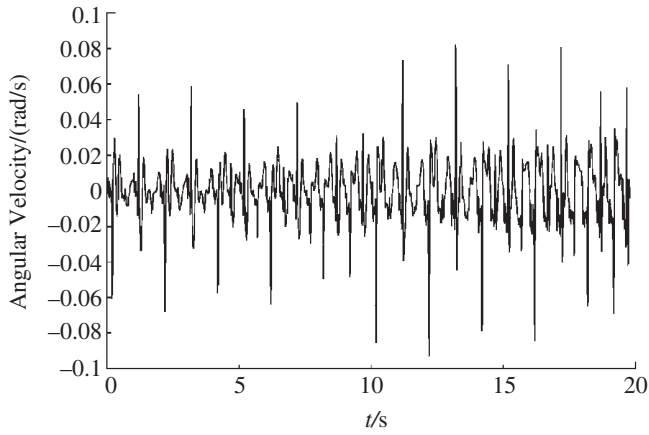


Figure 12.41 Muzzle angular velocity in the z direction.

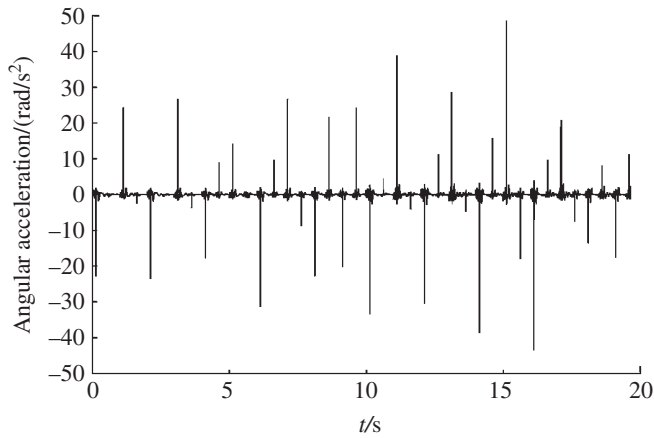


Figure 12.42 Muzzle angular acceleration in the x direction.

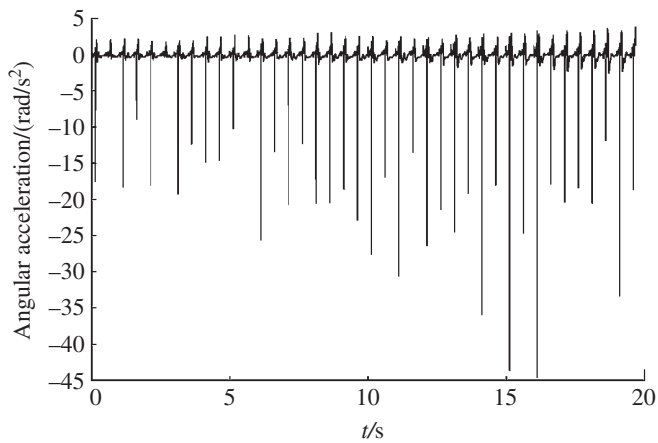


Figure 12.43 Muzzle angular acceleration in the y direction.

Table 12.1 Simulation results of initial disturbance of rocket

	Swing angle		Swing angular velocity		Yaw angle	
	φ_a/rad	φ_2/rad	$\dot{\varphi}_a/(\text{rad/s})$	$\dot{\varphi}_2/(\text{rad/s})$	ψ_1/rad	ψ_2/rad
Mean value	0.866	-2.03×10^{-5}	-0.102	-5.07×10^{-3}	-4.19×10^{-3}	-9.45×10^{-4}
Mean square	4.96×10^{-5}	5.61×10^{-5}	3.03×10^{-3}	2.40×10^{-3}	6.27×10^{-5}	6.04×10^{-5}

Table 12.2 Comparison of simulation and modal test results of eigenfrequencies under the condition of full-load

Mode, k	$\omega_k/(\text{rad/s})$			Mode, k	$\omega_k/(\text{rad/s})$		
	Compute	Test	Relative error/%		Compute	Test	Relative error/%
1	8.61	8.67	-0.69	8	52.77	50.27	4.97
2	10.40	10.99	-5.37	9	57.43	56.23	2.13
3	19.33	18.98	1.84	10	60.39	64.34	-6.14
4	26.67	26.51	0.60	11	66.05	67.61	-2.31
5	28.93	29.59	-2.23	12	80.06	79.73	0.41
6	31.99	32.86	-2.65	13	97.86	97.89	-0.03
7	36.82	—	—	14	105.62	105.81	-0.18

Table 12.3 Comparison of simulation and modal test results of eigenfrequencies under the condition of non-load

Mode, k	$\omega_k/(\text{rad/s})$			Mode, k	$\omega_k/(\text{rad/s})$		
	Compute	Test	Relative error/%		Compute	Test	Relative error/%
1	10.72	10.93	-1.92	8	41.37	37.51	10.29
2	13.03	12.32	5.76	9	50.30	50.20	0.20
3	17.88	—	—	10	58.74	55.54	5.76
4	23.56	24.44	-3.60	11	75.68	71.94	5.20
5	26.27	25.01	5.04	12	90.98	92.05	-1.16
6	27.17	29.97	-9.34	13	98.13	97.45	0.70
7	31.75	34.49	-7.94	14	108.75	110.65	-1.72

12.8.5 Simulation and Test Validation of the Vibration of the System

The simulation results and test results for the vehicle response of an MLRS with a salvo of 40 launch tubes are shown in Figure 12.44 (departure angle is 50° , azimuth angle is 45°) and the simulation results and test results of the vehicle response when firing 16 rounds with the B scheme are shown in Figure 12.45. It is obvious that the simulation and test results have good agreement. The simulation results are validated by the tests.

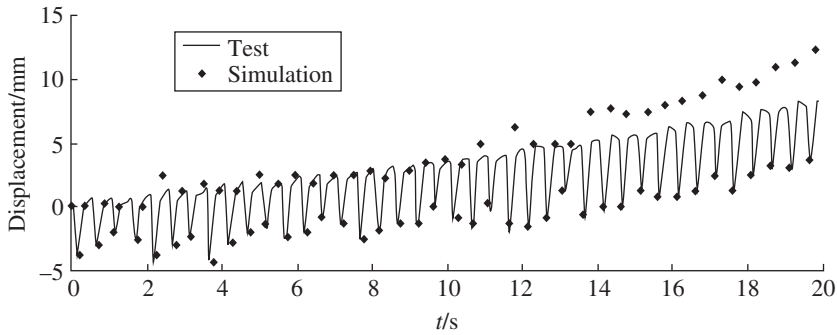


Figure 12.44 Simulation and test results of the vertical displacement of a vehicle when salvo firing.

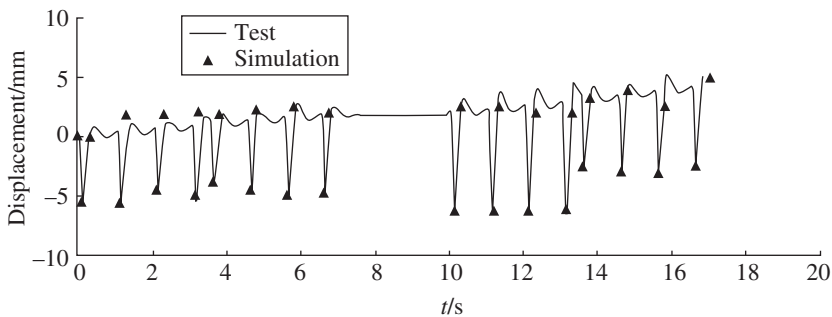


Figure 12.45 Simulation and test results of the vertical displacement of a vehicle with B scheme.

12.8.6 Simulation and Test Verifying of Firing Dispersion

The simulation and test results for firing dispersion at a certain range of an MLRS with 40 launch tubes are shown in Table 12.4 and show good agreement. The simulation results are also validated by the tests.

12.9 Low Rocket Consumption Technique for the System Test

The question of whether or not the weapon performance fulfils the tactical-technical criteria must be answered by a shooting test when the weapon is approved to be used. In test for firing dispersion, generally three groups of firing test are carried out under each of the conditions of

Table 12.4 Simulation and test results of firing dispersion

	E_x/m	E_z/m
Simulation	73.7	222.0
Test	73.3	208.9

high, low and normal temperature, and the number of firing rounds of each group for firing of the MLRS is “the number in one salvo”, that is to say, it is necessary to fire nine groups for a full-load salvo test. Taking the Russian BM-21 type MLRS with 40 launch tubes as an example, one salvo needs 40 rockets, thus at least 360 rockets will be consumed to assess its firing dispersion at maximum range. For another Russian MLRS with 12 launch tubes, one salvo needs 12 rockets, thus 108 rockets will be consumed to assess its firing dispersion at maximum range. As a result a lot of ammunition and a vast test budget are required to check the dispersion at maximum range.

In this section, for a whole system, including rocket, gun, propellant and environment, using the theory of MLRS launch dynamics based on the MSTMM, a totally new programmed firing dispersion test technology that substitutes a non-full charge loading test for a full charge loading test is introduced, which greatly reduces the rocket consumption in the MLRS test. Many tests show that the rocket consumption for the firing dispersion of the MLRS of several National High-Tech Projects is decreased by 50–86% compared to the usual methods, and is the lowest level in the world.

12.9.1 Principle of Decreasing Rocket Consumption in MLRS Tests

12.9.1.1 Launch Dynamic Principle of Decreasing Rocket Consumption in MLRS Tests

The grouping test method is usually used in testing the firing dispersion of MLRSs. Its advantages are as follows:

- 1) By grouping the rockets in the test, the firing time for the same number of rockets is relative short for each group, which reduces the influence of gusts of wind, temperature and other factors on firing dispersion, so the firing dispersion of the weapon system is more accurately and objectively reflected.
- 2) Using a limited number of firing rounds, the error in the dispersion test caused by operation, settling guns and other factors can be eliminated or greatly reduced by taking an average value after each grouped test.

The National Military Standard regulates that the dispersion test for an MLRS should use the grouping test method [269].

Decreasing rocket consumption in the MLRS test means that, using this new theory and technology, the rocket consumption in an MLRS test is much less than with the current test scheme when evaluating and checking MLRSs under the precondition of ensuring checking accuracy. The method of decreasing the rounds used in each group should be adopted to decrease rocket consumption in MLRS testing under the precondition that the quality of the test is guaranteed.

The theory of launch dynamic and firing tests shows that there are three main factors that influence the firing dispersion of MLRSs: (i) the initial disturbance of the rocket, (ii) factors of the rocket itself (such as mass, mass eccentricity, dynamic unbalance, propellant mass, thrust malalignment and so on) and (iii) the meteorological conditions (such as wind). The influences of the vibration characteristics of the MLRS, the performance of the MLRS, the loading scheme of the rockets and the firing sequence on firing dispersion are embodied in the initial disturbance of the rocket. For single-round firing, only factors of the rocket itself and the firing dispersion influence the factors of rockets and gusts of wind, thus seven rounds in each group are capable of giving sufficiently precise results according to the engineering precision demand. For the same MLRS, the firing dispersion of a full-load salvo or seven rounds of string firing in one go is different from that of single-round firing. However, when rockets have stable performance, the influence of factors of the rocket itself including weight, diameter, mass eccentricity, dynamic unbalance, thrust malalignment, etc.) on the firing dispersion in every group for these two

conditions (a full-load salvo and seven rounds of string firing in one go) is not large. Therefore, for the same MLRS, the main reason for a large difference in firing dispersion between a full-load salvo and nonfull-load string firing is the difference in initial disturbance for these two situations. This viewpoint has been validated by firing tests for MLRSs over many years.

Applying the theory and technology of launch dynamics based on the MSTMM, and optimizing the total parameters of the MLRS, the vibration characteristics of the MLRS, the dynamic response, the trajectory and the dispersion can be realized according to the scheduled distribution law under different firing schemes. The nonfull-charge loading test scheme can then be found whose firing dispersion is the same as that of the full-charge loading test. A firing dispersion test in which the nonfull-charge loading test is substituted for a full-charge loading test can be done. The rocket number (seven, for example) of nonfull-charge loading must assure the demand for assessing the influence of factors of rocket itself on firing dispersion. So, the replacement of the dispersion test of full-charge loading by nonfull-charge loading should be carried out based on the fact that there is no distinct difference between the two estimating values of firing dispersion of the MLRS under the two cases. This is the basic principle of decreasing the rocket consumption in the MLRS test via the theory and technology of launch dynamics.

12.9.1.2 Statistics Principle of Decreasing Rocket Consumption in the MLRS Test

The impact coordinates are random variables and are usually considered to have a normal distribution. The distance coordinate of the impact point is given by x and the transverse coordinate by z . Both these show normal distribution and are independent from each other, so the situation can be explained by discussing only distance x . The probability $p_E(n)$ is called the confidence level of the estimated value \bar{x} located in interval $[\mu - 0.6745\hat{\sigma}_{\bar{x}}, \mu + 0.6745\hat{\sigma}_{\bar{x}}]$. For different DOFs $\nu = n - 1$ (where n is the number of test rounds), the probability is $p_E(n)$ and the value $p_E(n)/p_E(\infty)$ is found from the computation where $p_E(\infty)$ is the confidence level of estimated value \bar{x} located in interval $[\mu - 0.6745\hat{\sigma}_{\bar{x}}, \mu + 0.6745\hat{\sigma}_{\bar{x}}]$ when testing infinite rounds and $p_E(n)/p_E(\infty)$ denotes the confidence level of replacing the estimated value \bar{x}_∞ of infinite rounds by estimated value \bar{x}_n of n rounds. The confidence levels of the estimation of the mean and its variation tendency along with the number of test rounds are shown in Table 12.5 and Figure 12.46.

It can be seen from Table 12.5 and Figure 12.46 that when the number of test rounds bigger than seven, the confidence level increases very slowly and at the same time the confidence level reaches then exceeds 94.8% of that of the infinite rounds test. Therefore, for the same batch of ammunition with steady performance and single-round firing with a launch tube, only seven rounds are needed to describe the influence of random factors of the rocket itself on the mean value of the coordinates of the points of fall.

When estimating firing dispersion, we usually suppose that it is a random variable with normal distribution. E is the system firing dispersion and its estimated value is \hat{E} , where $E = 0.6745\sigma$ and $\hat{E} = 0.6745\hat{\sigma}$. The probabilities (confidence level) of the estimated value $\hat{\sigma}$ of the standard

Table 12.5 Confidence level of estimation for mean along with test rounds ($t_\alpha = 0.6745$)

n	3	4	5	6	7	8	9	10	40	∞
$p_E(n)$	0.429	0.450	0.461	0.469	0.474	0.477	0.480	0.482	0.496	0.50
$\frac{p_E(n)}{p_E(\infty)}$	0.858	0.900	0.922	0.938	0.948	0.954	0.960	0.964	0.992	1

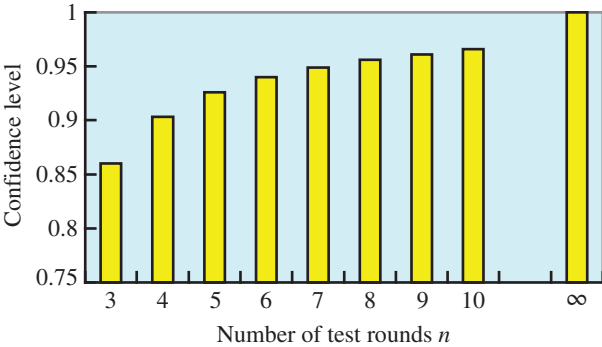


Figure 12.46 Histogram of change in $p_E(n)/p_E(\infty)$ along with test rounds.

deviation located in interval $(\sigma - 0.5\sigma, \sigma + 0.5\sigma)$ are shown in Table 12.6 and Figure 12.47 for $\lambda = 50\%$. This is also the probability (confidence level) of the estimated value \hat{E} of the dispersion located in interval $(E - 0.5E, E + 0.5E)$. The probability (confidence level) of the estimated value \hat{E} located in interval $(E - 0.5E, E + 0.5E)$ is therefore 91.7% for seven test rounds with a launch tube. Table 12.6 and Figure 12.47 show that when the number of test rounds is more than seven, confidence level increases slowly as number of test rounds increases.

Taking both of these factors into account, firing seven rounds is the routine method for the firing dispersion test of a weapon with a single launch tube for the same batch of ammunition with steady performance, the basis being that the corresponding confidence level of the estimated value of the firing dispersion can reach 91.7%. For an MLRS with 40 launch tubes, if the number of test rounds is bigger than seven in one group the confidence level of the estimated value of the firing dispersion should reach 91.7%. If the influence of factors such as coupling between the rocket and the gun on firing dispersion is considered, it is necessary to optimize the loading position, firing sequence and firing interval when searching the test scheme, substituting the nonfull-charge loading test for the full-charge loading test.

Table 12.6 Confidence level of estimation for mean square deviation along with test rounds

<i>n</i>	3	4	5	6	7	8	9	10	40	∞
Confidence level	0.682	0.779	0.842	0.886	0.917	0.938	0.954	0.966	0.999	1

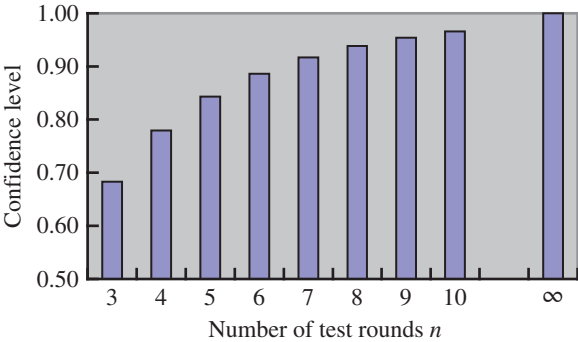


Figure 12.47 Confidence level of estimation for mean square deviation along with test rounds.

12.9.2 Programming Technology of Substituting Nonfull Loading for Full Loading

A difficult engineering problem that urgently needs to be solved is how to optimize and design a system that includes random and discrete variables at the same time because the existing theories and methods of optimization design cannot do this. Because of the low efficiency of optimization design for discrete variables and the sample effect of mathematical statistics which results in huge computational work, it is difficult to determine the optimal solution for the global area. Compared with the case of continuous variables, the optimization design of discrete variables has many different characteristics, such as the discontinuity of the variable, the discontinuity of the feasible area space (feasible area becomes feasible assemblage), the undifferentiability of the function, the nonapplicability of the Kuhn–Tucker condition and so on. These features make the optimization design for discrete variables different to that for continuous variables. Not only is the selection method for the chosen design variable different, but the judgement condition of optimization is also different. To address this problem, a totally new method for optimization design, random integer programming, has been developed by the authors. In this method, the continuity, discrete, randomness and hypothesis tests of design variables are considered, with the aim of first ascertaining the necessary solution space and then solving the optimal solution. Thus, the difficult problem, namely that optimization design for discrete variables based on statistics cannot be used in large engineering due to its low computation efficiency, is overcome. The engineering optimization problem of decreasing rocket consumption in the firing dispersion test of an MLRS is also solved using this method. This method has been verified and further details can be found in reference [1].

The general approach to decreasing rocket consumption in the firing dispersion test of an MLRS is to take the MLRS system as research background, synthetically apply the new theory and technology of launch dynamics based on the MSTMM, adjust the loading position, firing sequence and firing interval of the nonfull-loading scheme, and search the nonfull-loading scheme whose firing dispersion is same as that of the original 40-rocket full-loading scheme. In this way rocket consumption in the MLRS test can be greatly decreased as long as the test quality is assured.

The detailed procedure to decrease rocket consumption in the firing dispersion test of the MLRS is to apply the newest study results for the launch dynamics based on the MSTMM, along launch scheme → initial disturbance of rocket → dispersion of the MLRS, taking the theory of launch dynamics of the MLRS as the foundation, the launch dynamics simulation system as the core, the random integer programming [1] as a tool, using the same firing dispersions for two systems as the constraint condition, taking the minimum rocket consumption as the target, by mean of adjusting loading position, firing sequence and firing interval, through plenty of computation and optimization, getting a new test scheme, and inspecting whether the estimated values of firing dispersion for the two schemes are distinctly different with statistical methods. Thus, the new test scheme substituting full loading with non-full loading for dispersion test of MLRS can be found. The programmed technology for decreasing rocket consumption in the MLRS test by substituting full loading with nonfull loading is shown in Figure 12.48. The steps involved are as follows:

- 1) Select the applicable launch dynamics model of the MLRS from the library of models and determine the statistical property (such as mean and standard deviation) of the correlated parameters according to measured parameters.
- 2) Using the launch dynamic simulation system of the MLRS based on the MSTMM, carry out simulations for the firing dispersion of the MLRS.
- 3) Optimize the test scheme, substituting full loading with nonfull loading for dispersion of the MLRS using random integer programming.

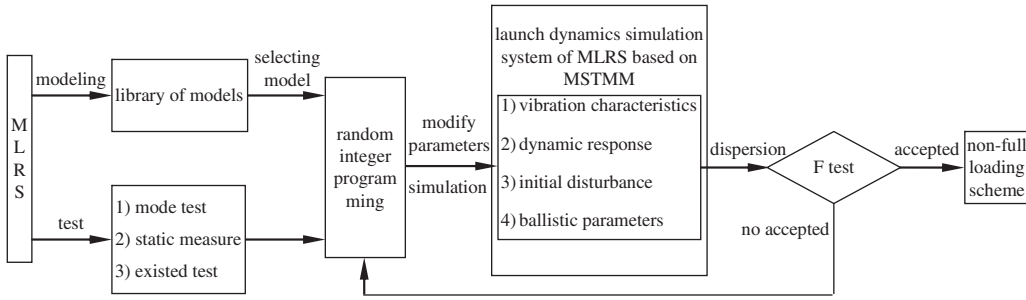


Figure 12.48 Programming technology with low rocket consumption in an MLRS test.

12.9.3 Optimization of a Nonfull-load Firing Scheme and Test Verifying

When determining a nonfull-loading MLRS system A_1 to simulate the firing dispersion of a full-loading salvo, random integer programming is used to optimize the firing dispersion test scheme of the MLRS. The factors that influence the dispersion of the MLRS are divided into two types, one is decided by the inherent mechanics characteristics of the rocket-launcher system and the other is decided by various random factors. The main influence of the inherent mechanics characteristics of a rocket-launcher system on firing dispersion is the change in the initial disturbance of the rocket due to the difference in rocket-launcher vibration produced by the mass and stiffness of the rocket launcher, firing sequence, interval of the rocket, rocket exhaust and so on.

The main influence of various random factors is the change in rocket ballistics caused by the randomness of parameters such as rocket-tube clearance, dynamic unbalance, mass eccentricity, thrust malalignment and firing interval. For the same batch of rockets, with steady performance and the same rocket launcher, the statistical properties of various random parameters are steady, their influence on firing dispersion is rather slight, but the variance of the inherent mechanics characteristics of the MLRS (including loading position, firing sequence, and so on) is main factor that influences the variance of the firing dispersion. The influence of these factors on firing dispersion must be fully considered when determining a test scheme. The firing dispersion E_A of the MLRS is a multivariable function that has the following form:

$$E_A = f(\mathbf{B}, \mathbf{X}, \mathbf{T}, \mathbf{C}) \quad (12.85)$$

where \mathbf{B} is a constant structure parameter of the system which influences firing dispersion, \mathbf{X} is the rocket loading position vector (x_1, x_2, \dots, x_n) , x_i is an integer variable equal to 0 or 1, and \mathbf{T} is the mean of firing interval \mathbf{t} .

Let $\mathbf{t} = \mathbf{T} + \boldsymbol{\tau}$, $M(\mathbf{t}) = \mathbf{T}$, $D(\mathbf{t}) = D(\boldsymbol{\tau})$, and $M(\boldsymbol{\tau}) = 0$. The random part $\boldsymbol{\tau}$ of the firing interval \mathbf{t} is considered in \mathbf{C} , where \mathbf{C} is a random vector that influences the firing dispersion (such as mass of rocket, thrust, thrust malalignment, dynamic unbalance, mass eccentricity, propellant mass, the random part of firing interval, or weather condition). Because the influence of random vector \mathbf{C} and constant structure parameter \mathbf{B} on the firing dispersion E_A of full-load salvo system A_0 and nonfull-load system A_1 is steady, \mathbf{X} and \mathbf{T} are the main factors causing a difference in the firing dispersion between the two systems. \mathbf{X} and \mathbf{T} are the main design variables when determining the nonfull-loading system, and the influence of various random factors on system firing

dispersion and the discontinuity of X must be considered at the same time. The following discrete variable mathematical programming problem based on statistics is constructed:

$$\begin{aligned} \min \quad & y = \sum_{i=1}^n x_i \\ \text{s.t.} \quad & H_0 : E_{A_1} = E_{A_0} \\ & y \geq 7 \end{aligned} \quad (12.86)$$

where y is the target function, x_i is the loading position function of the rocket for the MLRS with 40 launch tubes, $i = 1, 2, \dots, 40$, where x_i is an integer equal to 0 or 1, $x_i = 0$ means there is no loading rocket in the i th position of the launch tube and $x_i = 1$ means a rocket is loaded in the i th launch tube. $H_0 : E_{A_1} = E_{A_0}$ is a hypothesis test of the firing dispersion of the full-load salvo system A_0 and the target system A_1 .

On the foundation of the launch dynamics of the MLRS based on the MSTMM, using the method of random integer programming [1], the nonfull-load system A_1 is obtained with an estimated value of firing dispersion that is not distinctly different from that of the full-load salvo system A_0 , so the firing test scheme substituting full-load salvo with nonfull-load is obtained:

- 1) number of rounds in each group: 7
- 2) firing interval: 0.5 ± 0.05 s
- 3) loading position and firing sequence: 1 (2,6), 2 (3,6), 3 (4,5), 4 (1,7), 5 (2,4), 6 (2,7), 7 (3,4).

In Figure 12.49 each circle represents a launch tube, the number on the left of each circle represents the original firing sequence in a 40-round salvo, and the number on the right of each circle represents the new firing sequence in the seven-round string firing scheme. The serial numbers of the launch tube corresponding to the seven-round string firing scheme are 6, 22, 28, 10, 16, 14, and 32.

According to the static measure results for the rocket (including rocket weight, mass eccentricity, eccentricity position, bourrelet diameter and so on), using the established simulation system, the firing dispersions of the seven-round string firing scheme and the original 40-round salvo are numerically simulated. The variance trends for firing dispersion along with the number of firing groups for the seven-round string firing scheme and the original 40-round salvo scheme are shown in Figure 12.50, and the critical values of the F test is shown at the same time. It can be seen from the predicted results that the variation tendencies of the firing dispersions of the two

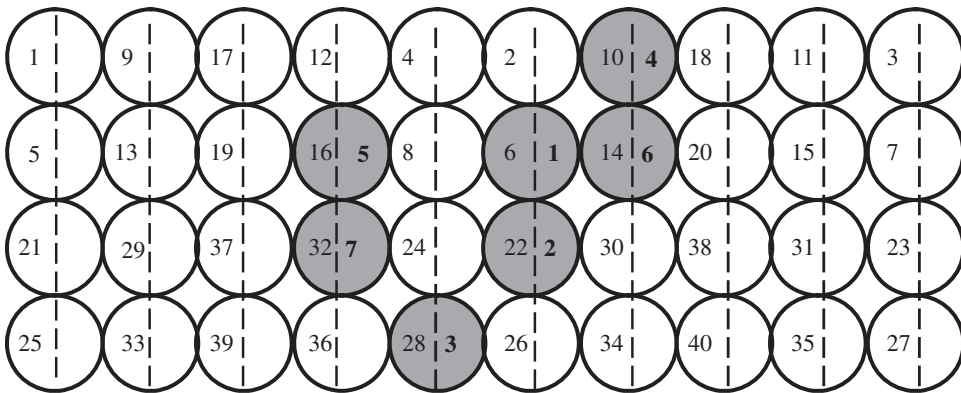


Figure 12.49 Test scheme of nonfull loading with seven rounds.

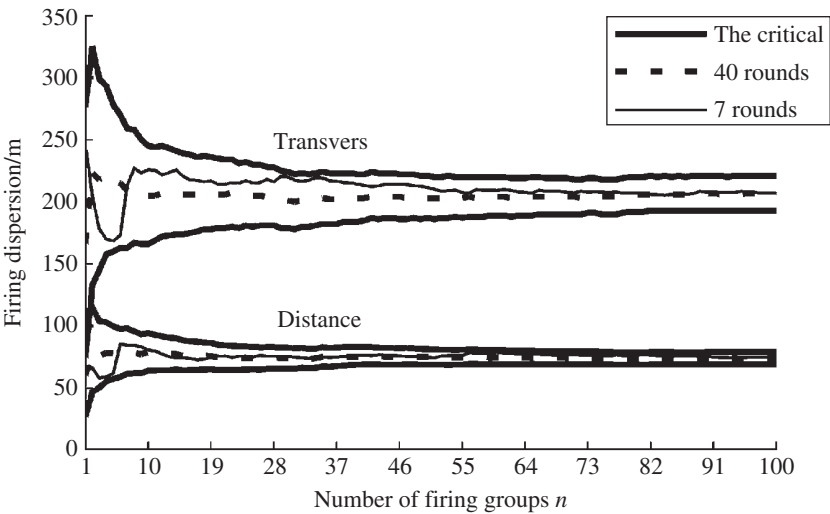


Figure 12.50 The variance trends for firing dispersion along with the number of firing groups for the seven-round string firing scheme and the original 40-round salvo scheme, as well as the critical values of the F test.

schemes share the same pattern as the number of the test groups increases, and the firing dispersions always meet the requirement of the F test, which shows that the two schemes have the same firing dispersion. In order to verify the correctness of the seven-round string firing scheme, special dispersion contrast tests for both the seven-round string firing scheme and the 40-round salvo scheme are completed. The test results prove that the seven-round string firing scheme is correct and the test technology for the firing dispersion of the MLRS substituting full-charge loading with nonfull-charge loading is effective. The simulation and test results for the firing dispersion of the seven-round string firing scheme and the 40-round salvo are shown in Table 12.7 and are in good agreement. The F test shows that there are no distinct differences between the test results for the seven-round string firing scheme and the 40-round salvo when $\alpha = 0.1$, so the system firing dispersions of the two launch schemes are the same, which validates the seven-round optimization test scheme.

The following conclusions can be drawn from the test results:

- 1) The simulation results are validated by the test, and the launch dynamics theory of the MLRS based on the MSTMM is also validated.
- 2) The test results for the firing dispersion of the seven-round firing scheme and the 40-round salvo are same, so the seven-round optimization test scheme is validated, which shows that

Table 12.7 Simulation and test results of firing dispersion of seven rounds of firing and 40-round salvo

	Launch scheme	E_x/m	E_z/m
Simulation	40-round salvo	74.1	207.1
	Seven rounds of string firing	74.8	206.8
Test	40-round salvo	73.3	208.9
	Seven rounds of string firing	80.2	198.0

the technology for decreasing rocket consumption in the MLRS test is right and that the rocket consumption in the firing dispersion test of the MLRS is decreased by 82.5% compared to the common method.

The difficult problem of decreasing rocket consumption in the MLRS test was solved by the test technology. Under the precondition of ensuring test quality, the test budget greatly decreases when the firing dispersion test of the MLRS of the full-loading salvo is substituted with the nonfull-loading scheme, and such a substitution has good operability and can be easily applied in engineering practice.

12.10 High Launch Precision Technique for the System

Precise striking is one of the main goals for modern weapons, and the firing dispersion of weapons is given great attention by all countries. In this section, the MLRS firing technology established by authors of high precision and little initial disturbance using the theory of multibody system launch dynamics based on the MSTMM is introduced. Real firing tests have shown that the firing precision and firing dispersion of several MLRSs in the National High-Tech Project are greatly improved, the corresponding research period is short, and the cost of the research is low.

12.10.1 Technique for Improving the Firing Dispersion of the System

A lot of research for improving the firing dispersion of the MLRS has carried out by rocket experts all over the world. The concept of passive control [270–272] for improving firing dispersion was first put forward by John E. Cochran. The basic idea is that the ballistic difference caused by the initial disturbance of the rocket could be counteracted by the ballistic difference caused by thrust malalignment, dynamics unbalance and mass eccentricity by a thorough study of the amplitude frequency and phase frequency response function of the launch equipment. The main purpose of passive control is to improve the firing dispersion, mainly by reducing the angular velocity dispersion of the deflection angle at the end of the power period. No outside energy source is needed, the control is realized only by using the feedback of rocket launch system itself and the control sources are rocket's own random factors. Although passive control looks tempting in theory, the model is very simple, which is very important in reality because it lacks a way of establishing the quantitative relation between the total parameters of the MLRS and its dynamic performance. This means it is difficult to reach the goal of reducing initial disturbance through adjusting the total parameters of the MLRS, and so far there has been no practical application of this result. It is, however, an important way of using simple control to improve the firing accuracy of the MLRS, for example a rocket with simple control has been used in the Russian PC30 CMEП4 MLRS and the US M270 MLRS, and is being developed in Italy, Britain and other countries to improve the firing accuracy of the MLRS. The cost of a rocket with simple control is several times higher than that of an ordinary rocket. The search continues around the world for a new method of improving the firing accuracy of the MLRS.

The firing technology of an MLRS with high precision has been established by the authors using the theory and method of MSTMM launch dynamics. The main features of this technology are as follows:

- 1) Through optimizing the parameters of the rocket-launcher system (such as firing sequence and firing interval) the initial disturbance can be reduced.

- 2) Using the concept of equivalent initial disturbance, through the design of the parameters of the rocket-launcher system, the initial disturbance of the rocket counteracts the equivalent initial disturbance caused by its own deficiency (mass eccentricity, dynamics unbalance, thrust malalignment and other factors). In addition, the ballistic difference caused by the initial disturbance of the rocket is counteracted by the ballistic difference caused by its own deficiency.
- 3) The integration soft/hard module of launch dynamics is installed on a rocket launcher to control the initial disturbance of the rocket by controlling the motion of the launch tube of the MLRS. This greatly reduces the cost of improving the firing precision of noncontrol MLRSs compared to using simple control. This method and its application in improving the firing dispersion of an MLRS by reducing the initial disturbance due to optimizing the firing sequence and firing interval are discussed in this section.

The MLRS is a kind of string-firing weapon, and its firing sequence and firing interval have a very big influence on its dynamic performance. It has been shown that different firing sequences and different total system parameters will lead to different vibration characteristics and different initial conditions for each rocket fired, resulting in different initial disturbance of the rocket. The matching relation between the firing frequency and the natural frequency also largely influences dynamic performance, and a reasonable firing interval is very important to ensure and improve firing dispersion. Therefore, the goal of improving the firing dispersion of the MLRS through reasonable adjustment of the firing sequence and firing interval can be achieved.

12.10.2 Random Combinatorial Optimization for Firing Dispersion

How can we optimize the firing sequence and firing interval to ensure the highest firing dispersion of the MLRS? For an MLRS with n launch tubes, there are $n!$ kinds of firing sequences. To obtain the optimum solution for the whole area, all kinds of firing sequences must be scanned one by one. If a group of calculations is taken as one scan, the total computation time is about 1.2 quadrillion years using a PIV-3.2G computer, which is not feasible. In addition, the theory and algorithm of global optimization is not as advanced as that of local optimization, so the analysis condition similar to the condition “gradient is zero and the second derivative matrix is orthogonality” of the local minima point has not yet been achieved, that is to say, it there is not an affirmative method of judging whether or not a local minima point is a global minima point. Even the filling function method, a kind of global optimization algorithm proposed in recent years, can only solve an optimization problem whose target function is analytical expression of continuous variables and whose constructed filling function is an analytical function about target function and optimization variables, which is useless for an optimization problem about discrete variables. Because it is difficult to find an optimal solution of global area, many approximation algorithms have been constructed, including the greed method, the local scanning method and the incomplete enumeration method. These methods behave better in seeking preferable solutions. Based on these methods, focused on the essence of the problem, the arithmetic of random combinatorial optimization is constructed, in which a random combination is adopted in each optimization and every combination is forbidden to repeat the former. Thus, the local optimal solution can be searched and the firing dispersion of the original system is improved to meet engineering requirements.

In order to find the local optimal solution, a constraint condition for the firing sequence is first decided according to the research results of MLRS launch dynamics. The firing sequence (from far to near) is symmetrical about the center of the launcher, and the rocket nearest to the center of the launcher is fired at last. Next, a random firing sequence is produced, which must satisfy the

constraint conditions, and the firing dispersion is simulated corresponding to the firing sequence combination and estimated using the maximum entropy method. Lastly, the hypothesis test is applied to judge whether or not the firing dispersion is higher than that of original firing sequence. After many random combinatorial optimizations, the firing sequence corresponding to a high firing dispersion can be obtained. In fact, the key to improve the firing dispersion via the optimization of the firing sequence is that the firing dispersion of the MLRS corresponding to different firing sequences can be simulated exactly, and the optimization of the firing sequence is merely a combinatorial optimization problem of mathematics. The flow-chart for random combinatorial optimization is shown in Figure 12.51.

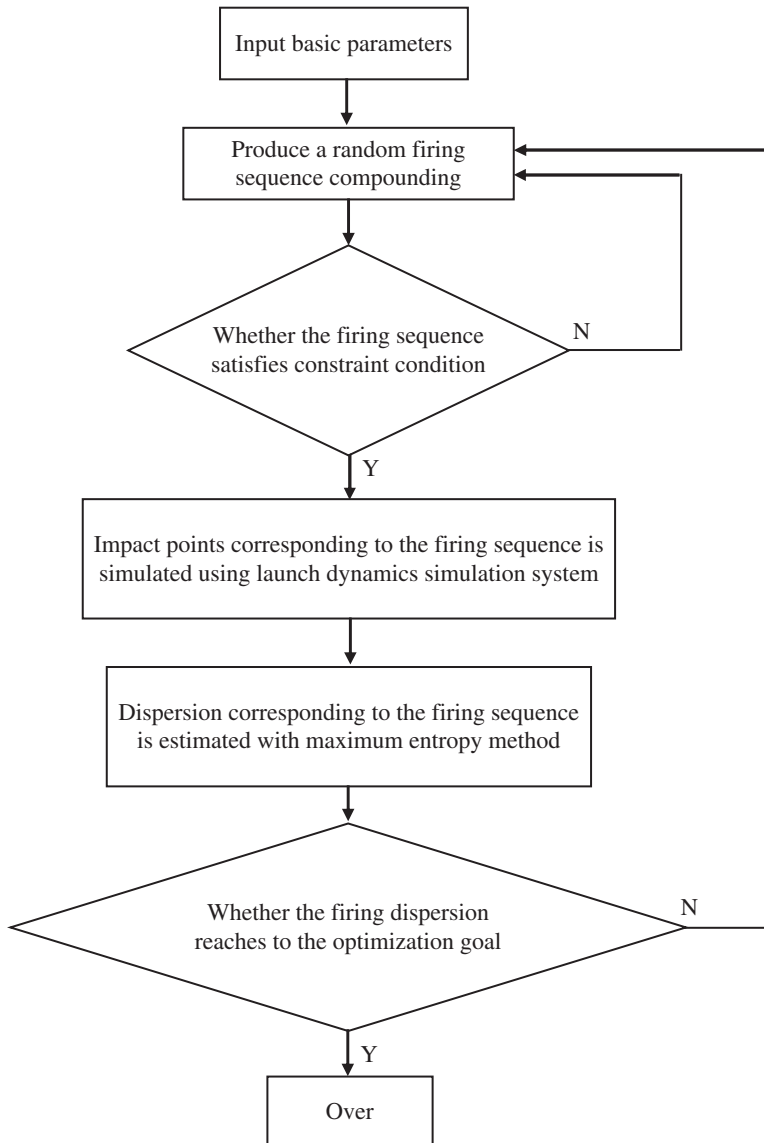


Figure 12.51 Flow of random combinatorial optimization.

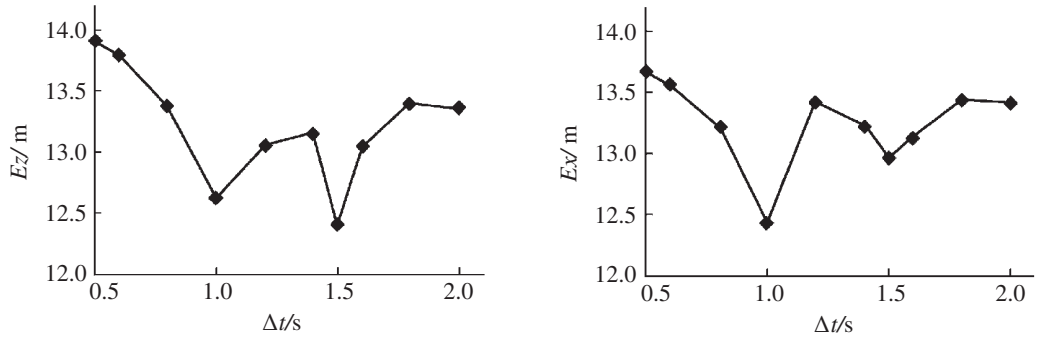


Figure 12.52 Relations between firing interval and firing dispersion.

12.10.3 High Firing Dispersion Scheme and its Test Verification

Taking the launch dynamics simulation system of the MLRS to be a platform based on the MSTMM, the influences of various factors on firing dispersion, such as rocket, launcher, propellant and environment, are all taken into consideration, and the firing sequence and firing interval of the optimization firing scheme are obtained using random combinatorial optimization. The simulation results for the corresponding relation between firing interval and firing dispersion for an MLRS are shown in Figure 12.52, from which it can be seen that a reasonable firing interval for the weapon system is 1.0 s.

Many test results have indicated that firing dispersion is improved more than four times by the optimization scheme relative to the original firing sequence and firing interval.

13

Dynamics of Self-propelled Launch Systems

13.1 Introduction

The launch process affects the characteristics of weapon systems in many ways, especially the firing precision. The influence of artillery characteristics on the scattering of projectiles can only be evaluated by the initial disturbances of the projectiles as a result of the launching process. The interaction between projectile and artillery during the launch process must be fully considered and the initial disturbance must be accurately computed when analyzing and computing the weapon system. How to solve the difficult problem of self-propelled artillery is a practical example of the important engineering applications of the linear transfer matrix method for multibody system (MSTMM) introduced in this chapter [106–111]. Self-propelled artillery weapon systems, which are widely equipped all over the world, are chosen as our study object in this chapter. Using MSTMM, self-propelled artillery is regarded as a multi-rigid-flexible-body system (MRFS). The natural vibration characteristics of the system are computed first, then the body dynamic equations of the system are established and the augmented eigenvector and its orthogonality are constructed, and finally the dynamic response and initial disturbance of the projectile are solved. The simulation system for the launch dynamics of self-propelled artillery is also formed, which provides an important tool for the dynamic design to improve the firing precision and other aspects of weapon performance.

13.2 Dynamics Model of the System and its Topology

The launch process of a projectile refers to the whole process from the moment that the primer is fired to the end of the period during which the projectile is affected by the gas that ejects from the gun muzzle. The movements of the artillery and the projectile are very complex during the launch process because of the complex structure of the self-propelled artillery and the extreme environment, such as high temperature, high pressure and high speed. The complexity of the launch process is shown in four interactions: between the projectile and the artillery, between the transverse motion and the longitudinal motion, between the rigid body and the flexible body, and between the space coordinates and the time coordinates for the motion parameters. The launch dynamics model of self-propelled artillery is a very complex mechanics multibody system connected in certain modes that contain many rigid bodies and flexible bodies with large motion.

13.2.1 Dynamic Model of a Self-propelled Launch System

The M109A6 155-mm type self-propelled artillery (USA) is shown in Figure 13.1. The main components of self-propelled artillery are the muzzle device, barrel (including an evacuator), gun breech, recoil and counterrecoil mechanism, cradle, pitching mechanism, equilibrator, turret, traversing mechanism, chassis (artillery bogie), torsion bar, balance elbow, shock absorber, track chain and road wheel. According to the motion state of each component, the firepower system of self-propelled artillery can be divided into recoil, lifting, turning, sprung, walking and so on. The recoil part contains the muzzle device, barrel, gun breech, recoil and counterrecoil mechanism. The lifting part contains the total recoil part, cradle and the elements moving with cradle, which include the elevating mechanism, equilibrator and so on. The turning part contains the total lifting part, turret and the elements moving with turret, which include the traversing mechanism and so on. The walking part, which contains track chain and road wheels, is used to support the weight of self-propelled artillery and drive the self-propelled artillery to run smoothly. The sprung part is used to connect the chassis to the walking part, which contains the torsion bar, balance elbow and shock absorber.

The components of self-propelled artillery are arranged from bottom to top in sequence, that is, road wheels, chassis without road wheels (simplified called hull, including carriage and sprung part), traversing mechanism, turning parts which do not contain the lifting part (the revolving part), elevating mechanism and equilibrator, lifting part without recoil part (the pitching part), gun breech, barrel and muzzle brake. Self-propelled artillery can thus be divided into 12 road wheels, barrel (partitioned into six segments), hull, revolving parts, pitching part, gun breech and muzzle brake. The launch dynamic model of self-propelled artillery is shown in Figure 13.2. The road wheels are regarded as lumped masses. The hull, revolving part, pitching part, gun breech and muzzle brake are regarded as rigid bodies. The barrel is divided into six segments and each is regarded as a beam with equal sectional area. Therefore, the whole structure contains 12 lumped masses, 6 elastic beams and 5 rigid bodies. The ground that supports the self-propelled artillery is regarded as an infinity rigid body. The elastic and damping effects of each road wheel, the interaction between the ground and each road wheel, and the connection between each road wheel and the hull are modeled as springs and dampers in three directions.



Figure 13.1 M109A6 type 155 mm self-propelled artillery (USA).

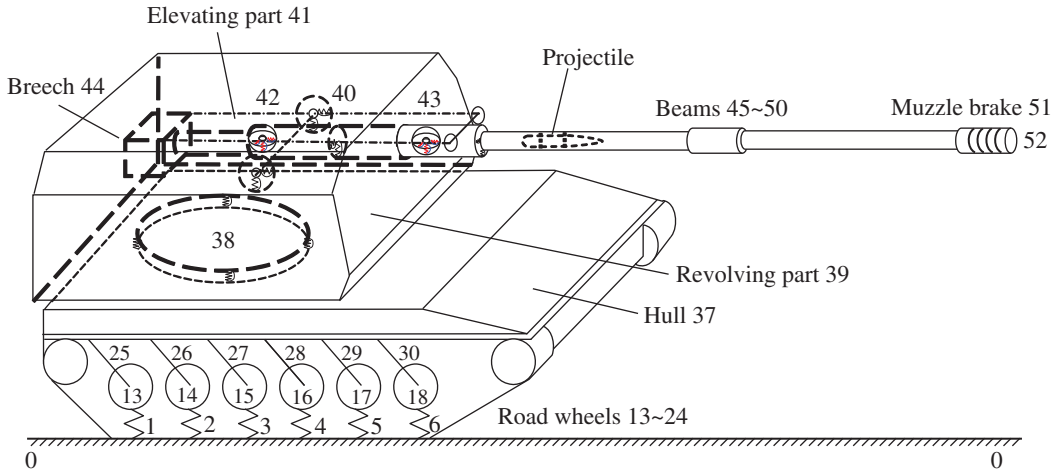


Figure 13.2 Launch dynamic model of self-propelled artillery.

The effect of the traversing mechanism associated with the elastic and damping effects of the hull, the effect of the elevating mechanism and equilibrator associated with the elastic and damping effects between the revolving and pitching parts, and the interaction between the barrel and the pitching part are modeled as springs and rotary springs accompanying dampers which can represent relative linear motion and relative angle motion in three directions at the same time. The connections between barrel and gun breech, the connection between the barrel and the muzzle brake, and the connection between each segment of the barrel are regarded as fixed connections. The masses of the traversing mechanism, the elevating mechanism and the equilibrator are divided into the pitching part, the revolving part and the hull, respectively. The launch dynamics model of self-propelled artillery is therefore an MRFS composed of 23 bodies and 28 joints.

Each element is numbered, and there are $23 + 28 = 51$ elements in all, so $n = 51$. The system has three boundaries: ground, gun breech and muzzle. The ground is regarded as the first input end, the gun breech is the second input end and the muzzle is the output end, therefore the muzzle boundary is numbered $n + 1 = 52$. Both the ground boundary and the gun breech boundary are numbered 0. The other elements are numbered in sequence, as shown in Figure 13.2. All the interaction forces and moments between barrel and pitching part, pitching part and revolving part, revolving part and hull, hull and road wheels, road wheels and the ground during the launch process are regarded as internal forces. To deal with vibration characteristics easily, the recoil resistance between the barrel and the pitching part produced by the recoil and counterrecoil mechanism is decomposed into two parts, the external force and the internal force, and the internal force is proportional to the relative displacement between the barrel and the pitching part. All the forces acting on the barrel by the projectile and propellant gas, and acting on the muzzle brake by the propellant gas are regarded as external forces of self-propelled artillery.

13.2.2 Launch Dynamic Model of a Projectile

Because of the complexity of the problem, the launch dynamic model of a projectile moving in a gun tube has to be simplified. As a result of the derivation from the actual models, the mathematical modal of a projectile moving in a gun tube reported in the literature on launch dynamics often results in large computation errors. In the past, the hypothesis “the center of the

rotating band moves along the axes of the gun tube” was proposed to simplify the problem. To address the deficiency of past research, this hypothesis has been abandoned by the authors. The main body of a projectile is regarded as a rigid body and the elastic effect of the projectile is equal to the elastic effect of the rotating band and bourrelet. Almost all factors are considered, including the dynamic unbalance, mass eccentricity, gravity, pressure of propellant gas, resistance acted on the head of projectile by air, rotating band/bore contact force, bourrelet/bore contact force and corresponding moment.

13.2.3 Dynamic Model of Interior Ballistics Two-phase Flow

The configuration of ammunition for self-propelled artillery is shown in Figure 13.3. It is a separated cartridge with a metal cartridge case. Its charge includes granular propellant and a metal central ignition tube. When the cartridge primer is fired, the gas jet of the primer ejects into the ignition tube. Then the ignition powder in the central ignition tube is ignited systematically, and the burning gas produced makes the pressure and temperature of the gas in the ignition tube rise continually. When the pressure is high enough to break the ignition holes on the ignition tube, the ignition gas flows into the propellant bed, which is ignited, and the increase in propellant burning gas makes the pressure in the chamber rise sharply. When the pressure at the end of the projectile is high enough the projectile begins to move. Subsequently, the propellant grains and burning gas flow into the barrel. During the ignition process and burning propagation in the chamber, gas flow is stopped due to the existence of solid propellant grain, causing a gradient of speed and pressure. The asymmetric distribution of propellant grains occurs due to the mutual action between the gas phase and the solid phase. The propellant bed moves to the end of the projectile due to the pressure difference in the chamber, then stacks and collides. At the same time, various waves are reflected at the end of the projectile, resulting in an inverted pressure gradient that forces the propellant bed to move back toward the breech. There is mutual movement and action between the solid phase and the gas phase before the propellant is finished burning, which forms a complex two-phase flow movement in the gun tube.

To deal with this problem, one-dimensional grids and the one-dimensional two-phase flow model are adopted in the main charge and in the central ignition tube, respectively. Between these two areas mass, momentum and energy are exchanged. Interphase drag, interphase heat transfer, the ignition process of the solid phase, the stress between solid propellant grains, the engraving of the projectile, the resistance of the projectile moving in the gun tube and other factors are considered. The basic hypotheses are:

- 1) The main charge is regarded as a continuous medium.
- 2) In the ignition tube only gas flows, solid grains do not flow and only gas can spurt out from the ignition holes on the ignition tube.

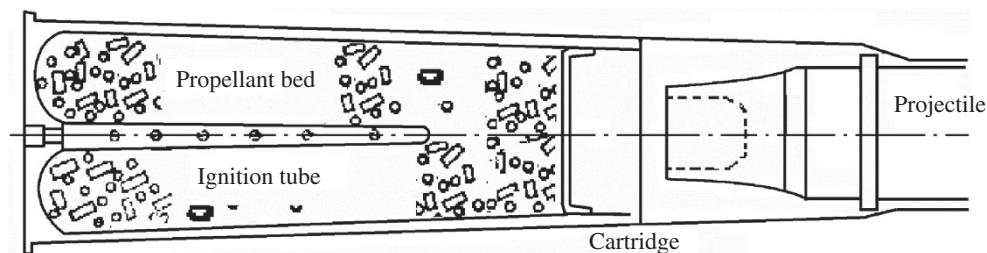


Figure 13.3 Configuration of propellant charge for large caliber self-propelled artillery.

- 3) Both flows in the gun tube and the ignition tube are one-dimensional, and the state parameters in the same section are constant.
- 4) There is only a gas phase and a solid phase in the gun tube, and the solid phase cannot be compressed.
- 5) Combustion of propellant obeys the geometric burning law and the exponential law of burning rate.
- 6) Burning gas obeys the Nobel–Abel gas state equation.
- 7) The viscosity of the gas is omitted, as is the heat lost from the wall of the gun tube.

13.3 State Vector, Transfer Equation and Transfer Matrix

13.3.1 State Vector

According to the launch dynamic model of self-propelled artillery and the sequence number of each element, there are 49 connection points ($P_{i,i-12}$, $P_{i,i+12}$ ($i = 13, 14, \dots, 24$), $P_{37,i}$ ($i = 25, 26, \dots, 36$), $P_{37,38}$, $P_{39,38}$, $P_{39,40}$, $P_{41,40}$, $P_{41,42}$, $P_{41,43}$, $P_{44,45}$, $P_{45,46}$, $P_{46,47}$, $P_{47,48}$, $P_{48,49}$, $P_{49,50}$ and $P_{51,50}$) and 14 boundary points ($P_{0,i}$ ($i = 1, 2, \dots, 12$), $P_{44,0}$, $P_{51,52}$), therefore 63 state vectors are defined as follows

$$\mathbf{Z}_{0,i} = [X, Y, Z, Q_x, Q_y, Q_z]_{0,i}^T \quad (i = 1, 2, \dots, 12) \quad (13.1)$$

$$\mathbf{Z}_{37,38} = [X, Y, Z, \theta_x, \theta_y, \theta_z, M_x, M_y, M_z, Q_x, Q_y, Q_z]_{37,38}^T \quad (13.2)$$

The form of $\mathbf{Z}_{i,i-12}$, $\mathbf{Z}_{i,i+12}$ ($i = 13, 14, \dots, 24$) and $\mathbf{Z}_{37,i}$ ($i = 25, 26, \dots, 36$) is similar to Equation (13.1), and the form of $\mathbf{Z}_{39,38}$, $\mathbf{Z}_{39,40}$, $\mathbf{Z}_{41,40}$, $\mathbf{Z}_{41,42}$, $\mathbf{Z}_{41,43}$, $\mathbf{Z}_{44,45}$, $\mathbf{Z}_{45,46}$, $\mathbf{Z}_{46,47}$, $\mathbf{Z}_{47,48}$, $\mathbf{Z}_{48,49}$, $\mathbf{Z}_{49,50}$, $\mathbf{Z}_{51,50}$, $\mathbf{Z}_{44,0}$ and $\mathbf{Z}_{51,52}$ is similar to $\mathbf{Z}_{37,38}$.

To simplify the deduction procedures, we introduce several intermediate state vectors according to the launch dynamic model of the self-propelled artillery

$$\mathbf{Z}_{0,1 \sim 12} = \begin{bmatrix} \mathbf{Z}_{0,1} \\ \mathbf{Z}_{0,2} \\ \vdots \\ \mathbf{Z}_{0,12} \end{bmatrix}, \mathbf{Z}_{13 \sim 24, 1 \sim 12} = \begin{bmatrix} \mathbf{Z}_{1,13} \\ \mathbf{Z}_{2,14} \\ \vdots \\ \mathbf{Z}_{12,24} \end{bmatrix}, \mathbf{Z}_{13 \sim 24, 25 \sim 36} = \begin{bmatrix} \mathbf{Z}_{13,25} \\ \mathbf{Z}_{14,26} \\ \vdots \\ \mathbf{Z}_{24,36} \end{bmatrix}, \mathbf{Z}_{37,25 \sim 36} = \begin{bmatrix} \mathbf{Z}_{37,25} \\ \mathbf{Z}_{37,26} \\ \vdots \\ \mathbf{Z}_{37,36} \end{bmatrix} \quad (13.3)$$

$$\mathbf{Z}_{I,37} = [X_{37,25}, Y_{37,25}, Z_{37,25}, \theta_{x37,25}, \theta_{y37,25}, \theta_{z37,25}, Q_{x37,25}, Q_{y37,25}, Q_{z37,25}, Q_{x37,26}, Q_{y37,26}, Q_{z37,26}, \dots, Q_{x37,36}, Q_{y37,36}, Q_{z37,36}]^T \quad (13.4)$$

$$\mathbf{Z}_{O,41} = [X_{41,42}, Y_{41,42}, Z_{41,42}, \theta_{x41,42}, \theta_{y41,42}, \theta_{z41,42}, M_{x41,42}, M_{y41,42}, M_{z41,42}, Q_{x41,42}, Q_{y41,42}, Q_{z41,42}, M_{x41,43}, M_{y41,43}, M_{z41,43}, Q_{x41,43}, Q_{y41,43}, Q_{z41,43}]^T \quad (13.5)$$

namely

$$\mathbf{Z}_{O,41} = \mathbf{E}_1 \mathbf{Z}_{41,42} + \mathbf{E}_2 \mathbf{Z}_{41,43}$$

where

$$\mathbf{E}_1 = \begin{bmatrix} \mathbf{I}_{12} \\ \mathbf{O}_{6 \times 12} \end{bmatrix}, \mathbf{E}_2 = \begin{bmatrix} \mathbf{O}_{12 \times 6} & \mathbf{O}_{12 \times 6} \\ \mathbf{O}_{6 \times 6} & \mathbf{I}_6 \end{bmatrix} \quad (13.6)$$

or

$$\mathbf{Z}_{41,42} = \mathbf{E}_3 \mathbf{Z}_{O,41}, \quad \mathbf{Z}_{41,43} = \mathbf{E}_4 \mathbf{Z}_{O,41} \quad (13.7)$$

where

$$\mathbf{E}_3 = [\mathbf{I}_{12} \quad \mathbf{O}_{12 \times 6}], \quad \mathbf{E}_4 = \begin{bmatrix} \mathbf{I}_3 & -\tilde{l}_{p_{41,42} p_{41,43}} & \mathbf{O}_{3 \times 6} & \mathbf{O}_{3 \times 6} \\ \mathbf{O}_{3 \times 3} & \mathbf{I}_3 & \mathbf{O}_{3 \times 6} & \mathbf{O}_{3 \times 6} \\ \mathbf{O}_{6 \times 3} & \mathbf{O}_{6 \times 3} & \mathbf{O}_{6 \times 6} & \mathbf{I}_6 \end{bmatrix} \quad (13.8)$$

13.3.2 Transfer Equations of Elements

13.3.2.1 From Ground to Road Wheels (Elements 1–12)

The elements $i (i = 1, 2, \dots, 12)$ are those from the ground to the road wheels. According to the transfer matrix of a three-dimensional spring (Equation (11.3)), the transfer matrices \mathbf{U}_i can be obtained and the transfer equations of element i are

$$\mathbf{Z}_{i+12,i} = \mathbf{U}_i \mathbf{Z}_{0,i} \quad (i = 1, 2, \dots, 12) \quad (13.9)$$

$6 \times 1 \quad 6 \times 6 \quad 6 \times 1$

By means of Equation (13.3), these 12 equations can be written as

$$\mathbf{Z}_{13 \sim 24, 1 \sim 12} = \mathbf{U}_{1 \sim 12} \mathbf{Z}_{0, 1 \sim 12} \quad (13.10)$$

$72 \times 1 \quad 72 \times 72 \quad 72 \times 1$

where

$$\mathbf{U}_{1 \sim 12} = \begin{bmatrix} \mathbf{U}_1 & \mathbf{O}_{6 \times 6} & \mathbf{O}_{6 \times 6} \\ \mathbf{O}_{6 \times 6} & \mathbf{U}_2 & \mathbf{O}_{6 \times 6} \\ & & \ddots \\ \mathbf{O}_{6 \times 6} & \mathbf{O}_{6 \times 6} & \mathbf{O}_{6 \times 6} \\ \mathbf{O}_{6 \times 6} & \mathbf{O}_{6 \times 6} & \mathbf{U}_{12} \end{bmatrix} \quad (13.11)$$

13.3.2.2 Road Wheels (Elements 13–24)

According to the transfer matrix of a lumped mass vibrating in three-dimensional space, the transfer matrices \mathbf{U}_i can be obtained, and the transfer equations of elements $i (i = 13, 14, \dots, 24)$ for the road wheels are

$$\mathbf{Z}_{i,i+12} = \mathbf{U}_i \mathbf{Z}_{i,i-12} \quad (i = 13, 14, \dots, 24) \quad (13.12)$$

$6 \times 1 \quad 6 \times 6 \quad 6 \times 1$

By means of Equation (13.3), these 12 equations can be written as

$$\mathbf{Z}_{13 \sim 24, 25 \sim 36} = \mathbf{U}_{13 \sim 24} \mathbf{Z}_{13 \sim 24, 1 \sim 12} \quad (13.13)$$

$72 \times 1 \quad 72 \times 72 \quad 72 \times 1$

where

$$\mathbf{U}_{13 \sim 24} = \begin{bmatrix} \mathbf{U}_{13} & \mathbf{O}_{6 \times 6} & \mathbf{O}_{6 \times 6} \\ \mathbf{O}_{6 \times 6} & \mathbf{U}_{14} & \mathbf{O}_{6 \times 6} \\ & & \ddots \\ \mathbf{O}_{6 \times 6} & \mathbf{O}_{6 \times 6} & \mathbf{O}_{6 \times 6} \\ \mathbf{O}_{6 \times 6} & \mathbf{O}_{6 \times 6} & \mathbf{U}_{24} \end{bmatrix} \quad (13.14)$$

13.3.2.3 From Road Wheels to Hull (Elements 25–36)

Similar to section 13.3.2.1, the transfer equations of elements $i (i = 25, 26, \dots, 36)$ from the road wheels to the hull are

$$\mathbf{Z}_{37,i} = \mathbf{U}_i \mathbf{Z}_{i-12,i} \quad (i = 25, 26, \dots, 36) \quad (13.15)$$

$6 \times 1 \quad 6 \times 6 \quad 6 \times 1$

By means of Equation (13.3), these 12 transfer equations can be written as

$$\mathbf{Z}_{37,25 \sim 36} = \mathbf{U}_{25 \sim 36} \mathbf{Z}_{13 \sim 24,25 \sim 36} \quad (13.16)$$

$72 \times 1 \quad 72 \times 72 \quad 72 \times 1$

where

$$\mathbf{U}_{25 \sim 36} = \begin{bmatrix} \mathbf{U}_{25} & \mathbf{O}_{6 \times 6} & \mathbf{O}_{6 \times 6} \\ \mathbf{O}_{6 \times 6} & \mathbf{U}_{26} & \mathbf{O}_{6 \times 6} \\ & & \ddots \\ \mathbf{O}_{6 \times 6} & \mathbf{O}_{6 \times 6} & \mathbf{O}_{6 \times 6} \\ \mathbf{O}_{6 \times 6} & \mathbf{O}_{6 \times 6} & \mathbf{U}_{36} \end{bmatrix} \quad (13.17)$$

According to the form of $\mathbf{Z}_{I,37}$ in Equation (13.4), the 72 equations in Equation (13.16) can be divided into two parts. The first part is

$$\mathbf{Z}_{I,37} = \mathbf{E}_5 \mathbf{Z}_{37,25 \sim 36} = \mathbf{E}_5 \mathbf{U}_{25 \sim 36} \mathbf{Z}_{13 \sim 24,25 \sim 36} \quad (13.18)$$

$42 \times 1 \quad 42 \times 72 \quad 72 \times 1 \quad 42 \times 72 \quad 72 \times 72 \quad 72 \times 1$

where

$$\mathbf{E}_5 = \begin{bmatrix} \mathbf{E}_{1,1} & \mathbf{O}_{3 \times 6} & \mathbf{O}_{3 \times 18} & \mathbf{O}_{3 \times 6} & \mathbf{O}_{3 \times 6} & \mathbf{O}_{3 \times 24} & \mathbf{O}_{3 \times 6} \\ \mathbf{E}_{2,1} & \mathbf{O}_{3 \times 6} & \mathbf{O}_{3 \times 18} & \mathbf{E}_{2,6} & \mathbf{E}_{2,7} & \mathbf{O}_{3 \times 24} & \mathbf{O}_{3 \times 6} \\ \mathbf{E}_{3,1} & & & & & & \\ & \mathbf{E}_{4,2} & & & & & \\ & & \ddots & & & & \\ & & & \mathbf{E}_{8,6} & & & \\ & & & & \mathbf{E}_{9,7} & & \\ & & & & & \ddots & \\ & & & & & & \mathbf{E}_{14,12} \end{bmatrix} \quad (13.19)$$

$$\mathbf{E}_{1,1} = [\mathbf{I}_3 \quad \mathbf{O}_{3 \times 3}], \quad \mathbf{E}_{2+i,i} = [\mathbf{O}_{3 \times 3} \quad \mathbf{I}_3] \quad (i = 1, 2, \dots, 12)$$

$$\mathbf{E}_{2,1} = \begin{bmatrix} 0 & 1/a_{3,7} & 0 & 0 & 0 & 0 \\ -1/a_{3,7} & 0 & 0 & 0 & 0 & 0 \\ 0 & -1/a_{1,6} & 0 & 0 & 0 & 0 \end{bmatrix}$$

$$\mathbf{E}_{2,6} = \begin{bmatrix} 0 & 0 & 0 & 0 & 0 & 0 \\ 0 & 0 & 0 & 0 & 0 & 0 \\ 0 & 1/a_{1,6} & 0 & 0 & 0 & 0 \end{bmatrix}, \quad \mathbf{E}_{2,7} = \begin{bmatrix} 0 & -1/a_{3,7} & 0 & 0 & 0 & 0 \\ 1/a_{3,7} & 0 & 0 & 0 & 0 & 0 \\ 0 & 0 & 0 & 0 & 0 & 0 \end{bmatrix}$$

$(a_{1,6}, a_{2,6}, a_{3,6})$ and $(a_{1,7}, a_{2,7}, a_{3,7})$ are the coordinates of $P_{37,31}$ and $P_{37,32}$ at the body coordinate system fixed on body 37.

At point $P_{37,i}(i = 26, 27, \dots, 36)$ we have

$$[X, Y, Z]_{P_{37,i}}^T = \begin{bmatrix} I_3 & -\tilde{l}_{P_{37,25}P_{37,i}} & O_{3 \times 36} \end{bmatrix} Z_{I,37} = \begin{bmatrix} I_3 & O_{3 \times 3} \end{bmatrix} Z_{37,i} = \begin{bmatrix} I_3 & O_{3 \times 3} \end{bmatrix} U_i Z_{i-12,i}$$

namely

$$\begin{bmatrix} I_3 & O_{3 \times 3} \end{bmatrix} U_i Z_{i-12,i} = \begin{bmatrix} I_3 & -\tilde{l}_{P_{37,25}P_{37,i}} & O_{3 \times 36} \end{bmatrix} Z_{I,37}, \quad (i = 26, 27, \dots, 36) \quad (13.20)$$

There are 33 equations in Equation (13.20), and the 14th, 16th and 17th equations are already used in Equation (13.18). After removing these three equations, the other 30 equations are the second part of the 72 equations in Equation (13.16), that is

$$E_6 U_{25 \sim 36} Z_{13 \sim 24, 25 \sim 36} = E_7 Z_{I,37} \quad (13.21)$$

where

$$E_6 = \begin{bmatrix} O_{3 \times 6} & E_{1,2} & O_{3 \times 12} & O_{3 \times 6} & O_{3 \times 6} & O_{3 \times 6} & O_{3 \times 6} & O_{3 \times 6} & O_{3 \times 18} & O_{3 \times 6} \\ O_{6 \times 6} & & \ddots & & & & & & & \\ O_{3 \times 6} & & & E_{4,5} & & & & & & \\ O_{2 \times 6} & & & & E_{5,6} & & & & & \\ O_{1 \times 6} & & & & & E_{6,7} & & & & \\ O_{3 \times 6} & & & & & & E_{7,8} & & & \\ O_{9 \times 6} & & & & & & & \ddots & & \\ O_{3 \times 6} & & & & & & & & E_{11,12} \end{bmatrix} \quad (13.22)$$

$$E_{i-1,i} = \begin{bmatrix} I_3 & O_{3 \times 3} \end{bmatrix} \quad (i = 2, 3, 4, 5, 8, 9, 10, 11, 12)$$

$$E_{5,6} = \begin{bmatrix} 1 & 0 & 0 & 0 & 0 & 0 \\ 0 & 0 & 1 & 0 & 0 & 0 \end{bmatrix}, \quad E_{6,7} = \begin{bmatrix} 0 & 0 & 1 & 0 & 0 & 0 \end{bmatrix}$$

$$E_7 = \begin{bmatrix} I_3 & -\tilde{l}_{P_{37,25}P_{37,26}} & O_{3 \times 36} \\ \vdots & \vdots & O_{6 \times 36} \\ I_3 & -\tilde{l}_{P_{37,25}P_{37,29}} & O_{3 \times 36} \\ E_{6,1} & E_{6,2} & O_{2 \times 36} \\ E_{7,1} & E_{7,2} & O_{1 \times 36} \\ I_3 & -\tilde{l}_{P_{37,25}P_{37,32}} & O_{3 \times 36} \\ \vdots & \vdots & O_{9 \times 36} \\ I_3 & -\tilde{l}_{P_{37,25}P_{37,36}} & O_{3 \times 36} \end{bmatrix} \quad (13.23)$$

$$E_{6,1} = \begin{bmatrix} 1 & 0 & 0 \\ 0 & 0 & 1 \end{bmatrix}, \quad E_{6,2} = \begin{bmatrix} 0 & a_{3,6} & -a_{2,6} \\ a_{2,6} & -a_{1,6} & 0 \end{bmatrix}$$

$$E_{7,1} = \begin{bmatrix} 0 & 0 & 1 \end{bmatrix}, \quad E_{7,2} = \begin{bmatrix} a_{2,7} & -a_{1,7} & 0 \end{bmatrix}$$

13.3.2.4 Hull (Element 37)

The hull is regarded as a rigid body with 12 input ends and one output end. According to the transfer matrix of a rigid body with N input ends and one output end (Equation (11.18)), the transfer matrix \mathbf{U}_{37} can be obtained, and the transfer equation of element 37 for the hull is

$$\mathbf{Z}_{37,38} = \mathbf{U}_{37} \mathbf{E}_8 \mathbf{Z}_{I,37} \quad (13.24)$$

$12 \times 1 \quad 12 \times 7878 \times 42 \quad 42 \times 1$

where

$$\mathbf{E}_8 = \begin{bmatrix} \mathbf{I}_6 & \mathbf{O}_{6 \times 3} & & \\ \mathbf{O}_{6 \times 6} & \mathbf{E}_{2,2} & & \\ & & \mathbf{E}_{3,3} & \\ & & & \ddots \\ & & & & \mathbf{E}_{13,13} \end{bmatrix}, \quad \mathbf{E}_{1+i,1+i} = \begin{bmatrix} \mathbf{O}_{3 \times 3} \\ \mathbf{I}_3 \end{bmatrix} \quad (i = 1, 2, \dots, 12), \quad (13.25)$$

13.3.2.5 From Hull to Revolving Part (Element 38)

According to the transfer matrix of a spatial elastic joint, the transfer matrix \mathbf{U}_{38} of element 38 from the hull to the revolving part can be obtained. Considering the coordinate transform of the angle α between the hull and the revolving part, the transfer equation is

$$\mathbf{Z}_{39,38} = \mathbf{H}_\alpha \mathbf{U}_{38} \mathbf{Z}_{37,38} \quad (13.26)$$

where

$$\mathbf{H}_\alpha = \begin{bmatrix} \mathbf{H}_{1,1} & & & \\ & \mathbf{H}_{2,2} & & \\ & & \mathbf{H}_{3,3} & \\ & & & \mathbf{H}_{4,4} \end{bmatrix}, \quad \mathbf{H}_{i,i} = \begin{bmatrix} \cos \alpha & 0 & -\sin \alpha \\ 0 & 1 & 0 \\ \sin \alpha & 0 & \cos \alpha \end{bmatrix} \quad (i = 1, 2, 3, 4), \quad (13.27)$$

\mathbf{H}_α is the coordinate transform matrix corresponding to angle α .

13.3.2.6 Revolving Part (Element 39)

According to the transfer matrix of a rigid body with one input end and one output end, the transfer matrix \mathbf{U}_{39} can be obtained, and the transfer equation of the revolving part is

$$\mathbf{Z}_{39,40} = \mathbf{U}_{39} \mathbf{Z}_{39,38} \quad (13.28)$$

13.3.2.7 From Revolving Part to Pitching Part (Element 40)

Similar to section 13.3.2.5, the transfer equation from the revolving part to the pitching part is

$$\mathbf{Z}_{41,40} = \mathbf{H}_\theta \mathbf{U}_{40} \mathbf{Z}_{39,40} \quad (13.29)$$

where

$$\mathbf{H}_\theta = \begin{bmatrix} \mathbf{H}_{1,1} & & & \\ & \mathbf{H}_{2,2} & & \\ & & \mathbf{H}_{3,3} & \\ & & & \mathbf{H}_{4,4} \end{bmatrix}, \quad \mathbf{H}_{i,i} = \begin{bmatrix} \cos \theta & \sin \theta & 0 \\ -\sin \theta & \cos \theta & 0 \\ 0 & 0 & 1 \end{bmatrix} \quad (i = 1, 2, 3, 4), \quad (13.30)$$

\mathbf{U}_{40} is the transfer matrix from the revolving part to the pitching part and \mathbf{H}_θ is the coordinate transform matrix corresponding to the departure angle θ .

13.3.2.8 Pitching Part (Element 41)

The pitching part is regarded as a rigid body with one input end and two output ends. According to the transfer matrix of a rigid body with one input end and L output ends, the transfer matrix \mathbf{U}_{41} can be obtained, and the transfer equation of the pitching part is

$$\mathbf{Z}_{41,40} = \mathbf{U}_{41} \mathbf{Z}_{O,41} \quad (13.31)$$

13.3.2.9 Gun Breech and Muzzle Brake (Elements 44 and 51)

According to the transfer matrix of a rigid body with one input end and one output end, both the transfer matrix \mathbf{U}_{44} of the gun breech and the transfer matrix \mathbf{U}_{51} of the muzzle brake can be obtained. Their transfer equations are

$$\mathbf{Z}_{44,45} = \mathbf{U}_{44} \mathbf{Z}_{44,0} \quad (13.32)$$

$$\mathbf{Z}_{51,52} = \mathbf{U}_{51} \mathbf{Z}_{51,50} \quad (13.33)$$

13.3.2.10 Barrel (Six Elastic Beams, Elements 45–50)

According to the transfer matrix of a spatial vibrating beam, the transfer matrices \mathbf{U}_{45} , \mathbf{U}_{46} , \mathbf{U}_{47} , \mathbf{U}_{48} , \mathbf{U}_{49} and \mathbf{U}_{50} of six elastic beams can be determined, and the corresponding transfer equations are, respectively

$$\mathbf{Z}_{45,46} = \mathbf{U}_{45} \mathbf{Z}_{44,45} + \mathbf{E}_9 \mathbf{U}_{42} \mathbf{Z}_{41,42} \quad (13.34)$$

$$\mathbf{Z}_{46,47} = \mathbf{U}_{46} \mathbf{Z}_{45,46} + \mathbf{E}_9 \mathbf{U}_{43} \mathbf{Z}_{41,43} \quad (13.35)$$

$$\mathbf{Z}_{47,48} = \mathbf{U}_{47} \mathbf{Z}_{46,47} \quad (13.36)$$

$$\mathbf{Z}_{48,49} = \mathbf{U}_{48} \mathbf{Z}_{47,48} \quad (13.37)$$

$$\mathbf{Z}_{49,50} = \mathbf{U}_{49} \mathbf{Z}_{48,49} \quad (13.38)$$

$$\mathbf{Z}_{51,50} = \mathbf{U}_{50} \mathbf{Z}_{49,50} \quad (13.39)$$

where

$$\mathbf{E}_9 = \begin{bmatrix} \mathbf{O}_{6 \times 6} & \mathbf{O}_{6 \times 6} \\ \mathbf{O}_{6 \times 6} & \mathbf{I}_6 \end{bmatrix} \quad (13.40)$$

\mathbf{U}_{42} and \mathbf{U}_{43} are the transfer matrices of elements 42 and 43, respectively, which can be obtained through the transfer matrix of a spatial elastic joint.

At points $P_{45,46}$ and $P_{46,47}$, according to the geometric relation, we have

$$[X, Y, Z, \theta_x, \theta_y, \theta_z]_{45,46}^T = [\mathbf{I}_6 \quad \mathbf{O}_{6 \times 6}] \mathbf{U}_{45} \mathbf{Z}_{44,45} = [\mathbf{I}_6 \quad \mathbf{O}_{6 \times 6}] \mathbf{U}_{42} \mathbf{Z}_{41,42} \quad (13.41)$$

$$[X, Y, Z, \theta_x, \theta_y, \theta_z]_{46,47}^T = [\mathbf{I}_6 \quad \mathbf{O}_{6 \times 6}] \mathbf{U}_{46} \mathbf{Z}_{45,46} = [\mathbf{I}_6 \quad \mathbf{O}_{6 \times 6}] \mathbf{U}_{43} \mathbf{Z}_{41,43} \quad (13.42)$$

Let $\mathbf{E}_{10} = [\mathbf{I}_6 \quad \mathbf{O}_{6 \times 6}]$, and substituting Equation (13.7) into Equations (13.41) and (13.42), we obtain

$$\mathbf{E}_{10} \mathbf{U}_{45} \mathbf{Z}_{44,45} = \mathbf{E}_{10} \mathbf{U}_{42} \mathbf{E}_3 \mathbf{Z}_{O,41} \quad (13.43)$$

$$\mathbf{E}_{10} \mathbf{U}_{46} \mathbf{Z}_{45,46} = \mathbf{E}_{10} \mathbf{U}_{43} \mathbf{E}_4 \mathbf{Z}_{O,41} \quad (13.44)$$

13.4 Overall Transfer Equation of the System

Substituting Equations (13.7), (13.31), (13.32) and (13.34)–(13.39) into Equation (13.33), we obtain

$$\mathbf{Z}_{51,52} = \mathbf{U}_{51}\mathbf{U}_{50}\mathbf{U}_{49}\mathbf{U}_{48}\mathbf{U}_{47}[\mathbf{U}_{46}\mathbf{U}_{45}\mathbf{U}_{44}\mathbf{Z}_{44,0} + (\mathbf{U}_{46}\mathbf{E}_9\mathbf{U}_{42}\mathbf{E}_3 + \mathbf{E}_9\mathbf{U}_{43}\mathbf{E}_4)\mathbf{Z}_{0,41}]$$

Let

$$\mathbf{E}_{11} = (\mathbf{U}_{46}\mathbf{E}_9\mathbf{U}_{42}\mathbf{E}_3 + \mathbf{E}_9\mathbf{U}_{43}\mathbf{E}_4)^{-1}(\mathbf{U}_{51}\mathbf{U}_{50}\mathbf{U}_{49}\mathbf{U}_{48}\mathbf{U}_{47})^{-1}$$

$$\mathbf{E}_{12} = -(\mathbf{U}_{46}\mathbf{E}_9\mathbf{U}_{42}\mathbf{E}_3 + \mathbf{E}_9\mathbf{U}_{43}\mathbf{E}_4)^{-1}\mathbf{U}_{46}\mathbf{U}_{45}\mathbf{U}_{44}$$

Then

$$\mathbf{Z}_{0,41} = \mathbf{E}_{11}\mathbf{Z}_{51,52} + \mathbf{E}_{12}\mathbf{Z}_{44,0} \quad (13.45)$$

Substituting Equations (13.10), (13.13), (13.18), (13.24), (13.26), (13.28), (13.29) and (13.45) into Equation (13.31), substituting Equations (13.10), (13.13) and (13.18) into Equation (13.21), substituting Equations (13.32) and (13.45) into Equation (13.43), and substituting Equations (13.7), (13.32), (13.34) and (13.45) into Equation (13.44), we obtain

$$\begin{bmatrix} \mathbf{U}_{1,1} & \mathbf{U}_{1,2} & \mathbf{U}_{1,3} \\ \mathbf{U}_{2,1} & \mathbf{O}_{30 \times 12} & \mathbf{O}_{30 \times 12} \\ \mathbf{O}_{6 \times 72} & \mathbf{U}_{3,2} & \mathbf{U}_{3,3} \\ \mathbf{O}_{6 \times 72} & \mathbf{U}_{4,2} & \mathbf{U}_{4,3} \end{bmatrix} \begin{bmatrix} \mathbf{Z}_{0,1 \sim 12} \\ \mathbf{Z}_{44,0} \\ \mathbf{Z}_{51,52} \end{bmatrix} = \mathbf{0}, \text{ namely, } \mathbf{U}_{\text{all}}\mathbf{Z}_{\text{all}} = \mathbf{0} \quad (13.46)$$

where

$$\begin{cases} \mathbf{U}_{1,1} = \mathbf{H}_\theta \mathbf{U}_{40} \mathbf{U}_{39} \mathbf{H}_\alpha \mathbf{U}_{38} \mathbf{U}_{37} \mathbf{E}_8 \mathbf{E}_5 \mathbf{U}_{25 \sim 36} \mathbf{U}_{13 \sim 24} \mathbf{U}_{1 \sim 12} \\ \mathbf{U}_{1,2} = -\mathbf{U}_{41} \mathbf{E}_{12} \\ \mathbf{U}_{1,3} = -\mathbf{U}_{41} \mathbf{E}_{11} \\ \mathbf{U}_{2,1} = (\mathbf{E}_6 - \mathbf{E}_7 \mathbf{E}_5) \mathbf{U}_{25 \sim 36} \mathbf{U}_{13 \sim 24} \mathbf{U}_{1 \sim 12} \\ \mathbf{U}_{3,2} = \mathbf{E}_{10} (\mathbf{U}_{45} \mathbf{U}_{44} - \mathbf{U}_{42} \mathbf{E}_3 \mathbf{E}_{12}) \\ \mathbf{U}_{3,3} = -\mathbf{E}_{10} \mathbf{U}_{42} \mathbf{E}_3 \mathbf{E}_{11} \\ \mathbf{U}_{4,2} = \mathbf{E}_{10} (\mathbf{U}_{46} \mathbf{U}_{45} \mathbf{U}_{44} - \mathbf{U}_{43} \mathbf{E}_4 \mathbf{E}_{12} + \mathbf{U}_{46} \mathbf{E}_9 \mathbf{U}_{42} \mathbf{E}_3 \mathbf{E}_{12}) \\ \mathbf{U}_{4,3} = \mathbf{E}_{10} \mathbf{U}_{46} \mathbf{E}_9 \mathbf{U}_{42} \mathbf{E}_3 \mathbf{E}_{11} - \mathbf{E}_{10} \mathbf{U}_{43} \mathbf{E}_4 \mathbf{E}_{11} \end{cases} \quad (13.47)$$

Equation (13.46) is the overall transfer equation of a self-propelled artillery system and \mathbf{U}_{all} is the overall transfer matrix of the system.

13.5 Vibration Characteristics of the System

It is important in the launch dynamics of self-propelled artillery to compute the natural vibration characteristics exactly. There are two important features of the natural vibration characteristics of self-propelled artillery: (1) the performance of self-propelled artillery can be improved by adjusting the distribution of the natural frequencies of self-propelled artillery and (2) they can provide indispensable modal parameters for analyzing the dynamic response of

self-propelled artillery with the modal method. The workload involved in computing the vibration characteristics of self-propelled artillery with the transfer matrix method of multibody system is small, the computation speed is fast and the computation precision is high.

13.5.1 Eigenequation of a Self-propelled Launch System

In Equation (13.46), \mathbf{Z}_{all} is composed of the state vectors ($\mathbf{Z}_{0,1\sim 12}$, $\mathbf{Z}_{44,0}$, $\mathbf{Z}_{51,52}$) at system boundary points. Half of the elements of the state vector at a boundary point are determined by the boundary conditions. For self-propelled artillery, each state vector $\mathbf{Z}_{0,i}$ ($i = 1, 2, \dots, 12$) between the 12 road wheels and the ground contains six elements, that is, the displacements and forces in three directions each, in which the three elements representing the displacement are always equal to 0. Thus, 36 elements of the 72 elements of $\mathbf{Z}_{0,1\sim 12}$ are 0. Let the symbol $\bar{\mathbf{Z}}_{0,1\sim 12}$ represent the state vector that only includes the remnant elements after these 0 elements have been removed from $\mathbf{Z}_{0,1\sim 12}$; it therefore has 36 elements. $\mathbf{Z}_{44,0}$ is the state vector at the boundary points of the gun breech and $\mathbf{Z}_{51,52}$ is the state vector at the boundary points at the muzzle. Each of these contains 12 elements, including displacements, angle displacements, forces and moments in three directions each. Both the gun breech and muzzle are free of boundaries, therefore the six elements representing the forces and moments are always equal to 0. In the same way, let $\bar{\mathbf{Z}}_{44,0}$ and $\bar{\mathbf{Z}}_{51,52}$ represent the remnants after these 0 elements are removed from $\mathbf{Z}_{44,0}$ and $\mathbf{Z}_{51,52}$, respectively, and each of them has six elements. In this case, there are 48 elements always equal to 0 in \mathbf{Z}_{all} . Removing them from \mathbf{Z}_{all} leads to a new state vector $\bar{\mathbf{Z}}_{\text{all}}$, which has 48 elements, that is

$$\bar{\mathbf{Z}}_{\text{all}} = [\bar{\mathbf{Z}}_{0,1\sim 12}^T, \bar{\mathbf{Z}}_{44,0}^T, \bar{\mathbf{Z}}_{51,52}^T]^T \quad (13.48)$$

Deleting columns 1–3, 7–9, 13–15, 19–21, 25–27, 31–33, 37–39, 43–45, 49–51, 55–57, 61–63, 67–69, 79–84 and 91–96 in \mathbf{U}_{all} , a new matrix $\bar{\mathbf{U}}_{\text{all}}$ with 48 orders can be obtained. Equation (13.46) can be written as

$$\bar{\mathbf{U}}_{\text{all}} \bar{\mathbf{Z}}_{\text{all}} = \mathbf{0} \quad (13.49)$$

The elements of \mathbf{U}_{all} and $\bar{\mathbf{U}}_{\text{all}}$ are only decided by the total parameters and eigenfrequencies of the system. When the total parameters are determined, Equation (13.49) should have a nontrivial solution for any eigenvalue of the system. Here, the determinant of $\bar{\mathbf{U}}_{\text{all}}$ should be zero

$$\det(\bar{\mathbf{U}}_{\text{all}}) = 0 \quad (13.50)$$

Solving Equation (13.50), the eigenfrequencies of self-propelled artillery, ω_k ($k = 1, 2, \dots$), can be obtained. The state vector $\bar{\mathbf{Z}}_{\text{all}}^k$ corresponding to ω_k can be evaluated by solving Equation (13.49). Of course, $\mathbf{Z}_{\text{all}}^k$ is also obtained, that is, the state vectors $\mathbf{Z}_{0,1\sim 12}$, $\mathbf{Z}_{44,0}$ and $\mathbf{Z}_{51,52}$ corresponding to ω_k are obtained. Based on these state vectors at the system boundary, through the transfer equation of each element one by one, all the state vectors in the system, including each connection point and an arbitrary point on the beam (gun tube), can be obtained. Thus, the vibration characteristics of self-propelled artillery are obtained, which include the eigenfrequencies ω_k ($k = 1, 2, \dots$) and the eigenvectors corresponding to each ω_k , and the datum of eigenvectors are included in the elements of all state vectors of the system, which can be obtained by selecting them from state vectors.

13.6 Dynamic Response of the System

13.6.1 Body Dynamic Equation of a Body Element and its Parameter Matrix

The body dynamic equations of the system can be obtained by combining the body dynamic equations of the elements

$$\mathbf{M}_i \mathbf{v}_{i,tt} + \mathbf{C}_i \mathbf{v}_{i,t} + \mathbf{K}_i \mathbf{v}_i = \mathbf{f}_i \quad (i = 13, 14, \dots, 24, 37, 39, 41, 44, \dots, 51) \quad (13.51)$$

In this section, the body dynamic equations of self-propelled artillery are established, and the augmented eigenvector of self-propelled artillery, which automatically satisfies the orthogonality, is introduced.

Let the static equilibrium position of the artillery system before firing be the reference position. The force and the moment of the gravity acting on each element of the artillery system will not appear in the corresponding dynamic equation because they have been counteracted by the elastic force and the elastic moment produced by the static deformation of the corresponding spring and rotary spring. All the displacements and angle displacements involved in the elastic forces and elastic moments are measured from the static equilibrium position. This treatment not only leads to concise dynamic equations, but is also in good agreement with the real method of measuring the dynamic response of artillery in which the static equilibrium position of the artillery system is the benchmark.

13.6.1.1 Road Wheels (Elements 13–24)

A road wheel is a lumped mass with spatial vibration, and the parameter matrices of the road wheel i ($i = 13, 14, \dots, 24$) are

$$\mathbf{M}_i = \begin{bmatrix} m_i & & \\ & m_i & \\ & & m_i \end{bmatrix}, \mathbf{v}_i = \begin{bmatrix} x_{i,i-12} \\ y_{i,i-12} \\ z_{i,i-12} \end{bmatrix}, \mathbf{f}_i = \begin{bmatrix} F_{x,i} \\ F_{y,i} \\ F_{z,i} \end{bmatrix} \quad (13.52)$$

$$\mathbf{K}_i = \left(-D^3|_{L,i} + D^3|_{O,i} \right) \mathbf{I}_3, \mathbf{C}_i = \left(-d^3|_{L,i} + d^3|_{O,i} \right) \mathbf{I}_3, \quad (i = 13, 14, \dots, 24)$$

where m_i , \mathbf{v}_i and \mathbf{f}_i are the mass of road wheel i , the coordinates of the column matrix of linear displacement with respect to the static equilibrium position and the coordinates of the column matrix of external force, respectively.

13.6.1.2 Hull, Revolving Part, Pitching Part, Gun Breech, Muzzle Brake (Elements 37, 39, 41, 44 and 51)

The hull, revolving part, pitching part, gun breech and muzzle brake are all rigid bodies, and the parameter matrices of elements 37, 39, 41, 44 and 51 are

$$\mathbf{M}_i = \begin{bmatrix} m_i \mathbf{I}_3 & -m_i \tilde{\mathbf{l}}_{L_1 C, i} \\ m_i \tilde{\mathbf{l}}_{L_1 C, i} & J_{L_1, i} \end{bmatrix}, \mathbf{v}_i = \begin{bmatrix} \mathbf{r}_{L_1, i} \\ \boldsymbol{\theta}_{L_1, i} \end{bmatrix}, \mathbf{f}_i = \begin{bmatrix} \mathbf{F}_i \\ \mathbf{m}_i + \tilde{\mathbf{l}}_{L_1 D, i} \mathbf{F}_i \end{bmatrix}$$

$$\begin{aligned}
\mathbf{K}_i &= \begin{bmatrix} -\sum_{n=1}^N \mathbf{I}_3 \mathbf{D}^3|_{I_{n,i}} + \sum_{l=1}^L \mathbf{I}_3 \mathbf{D}^3|_{O_{l,i}} & \mathbf{O}_{3 \times 3} \\ -\sum_{n=2}^N \tilde{\mathbf{I}}_{I_1 I_{n,i}} \mathbf{D}^3|_{I_{n,i}} + \sum_{l=1}^L \tilde{\mathbf{I}}_{I_1 O_{l,i}} \mathbf{D}^3|_{O_{l,i}} & \sum_{n=1}^N \mathbf{I}_3 \mathbf{D}^1|_{I_{n,i}} - \sum_{l=1}^L \mathbf{I}_3 \mathbf{D}^1|_{O_{l,i}} \end{bmatrix} \\
\mathbf{C}_i &= \begin{bmatrix} -\sum_{n=1}^N \mathbf{I}_3 \mathbf{d}^3|_{I_{n,i}} + \sum_{l=1}^L \mathbf{I}_3 \mathbf{d}^3|_{O_{l,i}} & \mathbf{O}_{3 \times 3} \\ -\sum_{n=2}^N \tilde{\mathbf{I}}_{I_1 I_{n,i}} \mathbf{d}^3|_{I_{n,i}} + \sum_{l=1}^L \tilde{\mathbf{I}}_{I_1 O_{l,i}} \mathbf{d}^3|_{O_{l,i}} & \sum_{n=1}^N \mathbf{I}_3 \mathbf{d}^1|_{I_{n,i}} - \sum_{l=1}^L \mathbf{I}_3 \mathbf{d}^1|_{O_{l,i}} \end{bmatrix} \quad (i = 37, 39, 41, 44, 51)
\end{aligned} \quad (13.53)$$

where m_i is the mass of the rigid body i , I_1 represents the first input end of the rigid body and C is the mass center of the rigid body. D represents the action point of external force, $J_{I_1,i}$ is the inertia moment matrix of rigid body i with respect to the first input end and $r_{I_1,i}$ is the linear displacement of the first input end with respect to equilibrium position. $\theta_{I_1,i}$ is the angle displacement of rigid body i , F_i and m_i are column matrices of external force and external moment, and N and L are the total number of input and output ends, respectively.

13.6.1.3 Barrel (Elements 45, 46, 47, 48, 49 and 50)

If the longitudinal and torsional deformations are neglected, that is, both longitudinal and rotation motion are rigid in the direction of the x axis of the beam, the parameter matrices of the six segments of the barrels numbered 45, 46, 47, 48, 49 and 50 are

$$\begin{aligned}
\mathbf{M}_i &= \begin{bmatrix} m_i \\ J_{i,x} \\ \bar{m}_i \\ \bar{m}_i \end{bmatrix}, \quad \mathbf{v}_i = \begin{bmatrix} x_{I,i} \\ \theta_{xI,i} \\ y(x_i, t) \\ z(x_i, t) \end{bmatrix}, \quad \mathbf{f}_i(x_i, t) = \begin{bmatrix} \int_0^{l_i} f_x(x_i, t) dx_i \\ \int_0^{l_i} m_x(x_i, t) dx_i \\ f_y(x_i, t) - \frac{\partial m_z(x_i, t)}{\partial x_i} \\ f_z(x_i, t) + \frac{\partial m_y(x_i, t)}{\partial x_i} \end{bmatrix} \\
\mathbf{K}_i &= \begin{bmatrix} -\mathbf{D}^3|_{I,i} + \mathbf{D}^3|_{O,i} & & & \\ & \mathbf{D}^1|_{I,i} - \mathbf{D}^1|_{O,i} & & \\ & & EI_{z,i} \frac{\partial^4}{\partial x_i^4} & \\ & & & EI_{y,i} \frac{\partial^4}{\partial x_i^4} \end{bmatrix} \\
\mathbf{C}_i &= \begin{bmatrix} -\mathbf{d}^3|_{I,i} + \mathbf{d}^3|_{O,i} & & & \\ & \mathbf{d}^1|_{I,i} - \mathbf{d}^1|_{O,i} & & \\ & & \bar{C}_{z,i} \frac{\partial^4}{\partial x_i^4} & \\ & & & \bar{C}_{y,i} \frac{\partial^4}{\partial x_i^4} \end{bmatrix} \quad (0 \leq x_i \leq l_i) \quad (i = 45, 46, \dots, 50)
\end{aligned} \quad (13.54)$$

where x_i are the coordinates of the point on beam i , l_i is the length of beam i , \bar{m}_i is the linear density of beam i , EI is bending stiffness, m_i is the total mass, $m_i = \bar{m}_i l_i$, and $J_{i,x}$ is the moment of inertia with respect to the axis of beam i .

13.6.2 Body Dynamic Equations and the Augmented Eigenvector of the System

After the body dynamic equations of all body elements have been written according to the sequence number, the body dynamic equation of self-propelled artillery can be written as follows:

$$M\mathbf{v}_{tt} + C\mathbf{v}_t + K\mathbf{v} = \mathbf{f} \quad (13.55)$$

where

$$M = \begin{bmatrix} M_{13} & & & & \\ & M_{14} & & & \\ & & \ddots & & \\ & & & M_i & \\ & & & & \ddots \\ & & & & & M_{51} \end{bmatrix}, \quad \mathbf{v} = \begin{bmatrix} v_{13} \\ v_{14} \\ \vdots \\ v_i \\ \vdots \\ v_{51} \end{bmatrix}, \quad \mathbf{f} = \begin{bmatrix} f_{13} \\ f_{14} \\ \vdots \\ f_i \\ \vdots \\ f_{51} \end{bmatrix} \quad (13.56)$$

$$K = \begin{bmatrix} K_{13} & & & & \\ & K_{14} & & & \\ & & \ddots & & \\ & & & K_i & \\ & & & & \ddots \\ & & & & & K_{51} \end{bmatrix}, \quad C = \begin{bmatrix} C_{13} & & & & \\ & C_{14} & & & \\ & & \ddots & & \\ & & & C_i & \\ & & & & \ddots \\ & & & & & C_{51} \end{bmatrix} \quad (13.57)$$

where \mathbf{v} is the displacement column matrix of the system, M and K are augmented operators, and C is the damping augmented operator. \mathbf{f} is the column matrix of external force and i is the sequence number of each body element.

Let

$$\mathbf{v} = \sum_{k=1}^{\infty} \mathbf{V}^k q^k(t) \quad (13.58)$$

Where

$$\mathbf{V} = [\mathbf{V}_{13}^T, \mathbf{V}_{14}^T, \dots, \mathbf{V}_i^T, \dots, \mathbf{V}_{51}^T]^T \quad (13.59)$$

$$\begin{cases} \mathbf{V}_i = [X, Y, Z]_{i,i-12}^T \quad (i = 13, 14, \dots, 24) \\ \mathbf{V}_{37} = [X, Y, Z, \theta_x, \theta_y, \theta_z]_{37,25}^T \\ \mathbf{V}_{39} = [X, Y, Z, \theta_x, \theta_y, \theta_z]_{39,38}^T \\ \mathbf{V}_{41} = [X, Y, Z, \theta_x, \theta_y, \theta_z]_{41,40}^T \\ \mathbf{V}_{44} = [X, Y, Z, \theta_x, \theta_y, \theta_z]_{44,0}^T \\ \mathbf{V}_i = [X_{Li}, \theta_{xLi}, Y(x_i), Z(x_i)]^T \quad (i = 45, 46, \dots, 50) \\ \mathbf{V}_{51} = [X, Y, Z, \theta_x, \theta_y, \theta_z]_{51,50}^T \end{cases} \quad (13.60)$$

where k is mode rank, $q(t)$ is generalized coordinates and V is the augmented eigenvector of self-propelled artillery.

According to the MSTMM, the augmented eigenvector V satisfies the orthogonality automatically

$$\langle MV^k, V^p \rangle = \delta_{k,p} M_p, \quad \langle KV^k, V^p \rangle = \delta_{k,p} \omega_p^2 M_p \quad (13.61)$$

where $\omega_p (p=1, 2, \dots)$ is the eigenfrequency of the system and M_p is the modal mass of the p th rank.

For proportional damping, the damping augmented operator C is

$$C = \alpha M + \beta K \quad (13.62)$$

where α and β are constant.

13.6.3 Validation of an Augmented Eigenvector Automatically Satisfying Orthogonality

13.6.3.1 V is Symmetric about Augmented Operator M

Because $M_i (i=13, 14, \dots, 24, 37, 39, 41, 44, 45, 46, \dots, 50, 51)$ are all real symmetric matrices, it is known from Equation (13.56) that M is also a real symmetric matrix, indicating that $M^T = M$

$$\langle MV^k, V^p \rangle = (MV^k)^T V^p = (V^k)^T M^T V^p = (V^k)^T M V^p = \langle V^k, M V^p \rangle \quad (13.63)$$

Thus, V is symmetric about augmented operator M .

13.6.3.2 V is Symmetric about Augmented Operator K

The following equations hold for the dynamics of the self-propelled artillery weapon system:

$$\begin{aligned} \langle KV^k, V^p \rangle &= \sum_i \langle K_i V_i^k, V_i^p \rangle \quad (i=13 \sim 24, 37, 39, 41, 44, 45 \sim 50, 51) \\ &\langle K_{13 \sim 24} V_{13 \sim 24}^k, V_{13 \sim 24}^p \rangle \\ &= \sum_{i=13 \sim 24} \langle -Q_{i,i-12}^k + Q_{i,i+12}^k, R_{i,i-12}^p \rangle = \sum_{i=13 \sim 24} \left[(-Q_{i,i-12}^k)^T R_{i,i-12}^p + (Q_{i,i+12}^k)^T R_{i,i+12}^p \right] \\ &\langle K_{37} V_{37}^k, V_{37}^p \rangle \\ &= \langle -\sum_{i=25}^{36} Q_{37,i}^k + Q_{37,38}^k, R_{37,25}^p \rangle + \langle -M_{37,38}^k - \sum_{i=25}^{36} \tilde{l}_{P_{37,25}P_{37,i}} Q_{37,i}^k + \tilde{l}_{P_{37,25}P_{37,38}} Q_{37,38}^k, \theta_{37,25}^p \rangle \\ &= -\sum_{i=25}^{36} \left[(Q_{37,i}^k)^T R_{37,25}^p \right] + (Q_{37,38}^k)^T R_{37,25}^p - (M_{37,38}^k)^T \theta_{37,25}^p \\ &\quad + \sum_{i=25}^{36} \left[(Q_{37,i}^k)^T \tilde{l}_{P_{37,25}P_{37,i}} \theta_{37,25}^p \right] - (Q_{37,38}^k)^T \tilde{l}_{P_{37,25}P_{37,38}} \theta_{37,25}^p \\ &= -\sum_{i=25}^{36} \left[(Q_{37,i}^k)^T R_{37,i}^p \right] + (Q_{37,38}^k)^T R_{37,38}^p - (M_{37,38}^k)^T \theta_{37,38}^p \end{aligned}$$

$$\begin{aligned}
& \langle K_{39} V_{39}^k, V_{39}^p \rangle \\
&= \langle -Q_{39,38}^k + Q_{39,40}^k, R_{39,38}^p \rangle + \langle M_{39,38}^k - M_{39,40}^k + \tilde{l}_{P_{39,38}P_{39,40}} Q_{39,40}^k, \theta_{39,38}^p \rangle \\
&= - (Q_{39,38}^k)^T R_{39,38}^p + (Q_{39,40}^k)^T R_{39,38}^p \\
&\quad + (M_{39,38}^k)^T \theta_{39,38}^p - (M_{39,40}^k)^T \theta_{39,38}^p - (Q_{39,40}^k)^T \tilde{l}_{P_{39,38}P_{39,40}} \theta_{39,38}^p \\
&= - (Q_{39,38}^k)^T R_{39,38}^p + (Q_{39,40}^k)^T R_{39,40}^p + (M_{39,38}^k)^T \theta_{39,38}^p - (M_{39,40}^k)^T \theta_{39,40}^p \\
&\langle K_{41} V_{41}^k, V_{41}^p \rangle \\
&= \langle -Q_{41,40}^k + Q_{41,42}^k + Q_{41,43}^k, R_{41,40}^p \rangle \\
&\quad + \langle M_{41,40}^k - M_{41,42}^k - M_{41,43}^k + \tilde{l}_{P_{41,40}P_{41,42}} Q_{41,42}^k + \tilde{l}_{P_{41,40}P_{41,43}} Q_{41,43}^k, \theta_{41,40}^p \rangle \\
&= - (Q_{41,40}^k)^T R_{41,40}^p + (Q_{41,42}^k)^T R_{41,42}^p + (Q_{41,43}^k)^T R_{41,43}^p \\
&\quad + (M_{41,40}^k)^T \theta_{41,40}^p - (M_{41,42}^k)^T \theta_{41,42}^p - (M_{41,43}^k)^T \theta_{41,43}^p \\
&\langle K_{44} V_{44}^k, V_{44}^p \rangle \\
&= \langle -Q_{44,0}^k + Q_{44,45}^k, R_{44,0}^p \rangle + \langle M_{44,0}^k - M_{44,45}^k + \tilde{l}_{P_{44,0}P_{44,45}} Q_{44,45}^k, \theta_{44,0}^p \rangle \\
&= - (Q_{44,0}^k)^T R_{44,0}^p + (Q_{44,45}^k)^T R_{44,45}^p + (M_{44,0}^k)^T \theta_{44,0}^p - (M_{44,45}^k)^T \theta_{44,45}^p \\
&\quad \langle K_{45 \sim 50} V_{45 \sim 50}^k, V_{45 \sim 50}^p \rangle \\
&= - (Q_{44,45}^k)^T R_{44,45}^p - (Q_{46,42}^k)^T R_{46,42}^p - (Q_{47,43}^k)^T R_{47,43}^p + (Q_{51,50}^k)^T R_{51,50}^p \\
&\quad + (M_{44,45}^k)^T \theta_{44,45}^p + (M_{46,42}^k)^T \theta_{46,42}^p + (M_{47,43}^k)^T \theta_{47,43}^p - (M_{51,50}^k)^T \theta_{51,50}^p \\
&\quad + \sum_{i=45 \sim 50} EI_{z,i} \int_{P_{i-1,i}}^{P_{i+1,i}} \frac{d^2 Y^k(x_i)}{dx_i^2} \frac{d^2 Y^p(x_i)}{dx_i^2} dx_i + \sum_{i=45 \sim 50} EI_{y,i} \int_{P_{i-1,i}}^{P_{i+1,i}} \frac{d^2 Z^k(x_i)}{dx_i^2} \frac{d^2 Z^p(x_i)}{dx_i^2} dx_i \\
&\langle K_{51} V_{51}^k, V_{51}^p \rangle \\
&= \langle -Q_{51,50}^k + Q_{51,52}^k, R_{51,50}^p \rangle + \langle M_{51,50}^k - M_{51,52}^k + \tilde{l}_{P_{51,50}P_{51,52}} Q_{51,52}^k, \theta_{51,50}^p \rangle \\
&= - (Q_{51,50}^k)^T R_{51,50}^p + (Q_{51,52}^k)^T R_{51,52}^p + (M_{51,50}^k)^T \theta_{51,50}^p - (M_{51,52}^k)^T \theta_{51,52}^p
\end{aligned} \tag{13.64}$$

Note that the force and moment at both sides of the joint are equal and the boundary conditions are as follows:

$$\begin{cases} R_{0,i}^p = 0 & (i = 1, 2, \dots, 12; \quad p = 1, 2, \dots) \\ Q_{44,0}^k = 0, \quad M_{44,0}^k = 0 & (k = 1, 2, \dots) \\ Q_{51,52}^k = 0, \quad M_{51,52}^k = 0 & (k = 1, 2, \dots) \end{cases} \tag{13.65}$$

Hence

$$\begin{aligned}
& \langle KV^k, V^p \rangle \\
&= \sum_{i=1 \sim 12} \left[-(\mathbf{Q}_{0,i}^k)^T (\mathbf{R}_{i+12,i}^p - \mathbf{R}_{0,i}^p) \right] - \sum_{i=25 \sim 36} \left[(\mathbf{Q}_{i-12,i}^k)^T (\mathbf{R}_{37,i}^p - \mathbf{R}_{i-12,i}^p) \right] \\
&\quad - (\mathbf{Q}_{37,38}^k)^T (\mathbf{R}_{39,38}^p - \mathbf{R}_{37,38}^p) + (\mathbf{M}_{37,38}^k)^T (\boldsymbol{\Theta}_{39,38}^p - \boldsymbol{\Theta}_{37,38}^p) \\
&\quad - (\mathbf{Q}_{39,40}^k)^T (\mathbf{R}_{41,40}^p - \mathbf{R}_{39,40}^p) + (\mathbf{M}_{39,40}^k)^T (\boldsymbol{\Theta}_{41,40}^p - \boldsymbol{\Theta}_{39,40}^p) \\
&\quad - (\mathbf{Q}_{41,42}^k)^T (\mathbf{R}_{46,42}^p - \mathbf{R}_{41,42}^p) + (\mathbf{M}_{41,42}^k)^T (\boldsymbol{\Theta}_{46,42}^p - \boldsymbol{\Theta}_{41,42}^p) \\
&\quad - (\mathbf{Q}_{41,43}^k)^T (\mathbf{R}_{47,43}^p - \mathbf{R}_{41,43}^p) + (\mathbf{M}_{41,43}^k)^T (\boldsymbol{\Theta}_{47,43}^p - \boldsymbol{\Theta}_{41,43}^p) \\
&\quad + \sum_{i=45 \sim 50} EL_{z,i} \int_{P_{i-1,i}}^{P_{i+1,i}} \frac{d^2 Y^k(x_i)}{dx_i^2} \frac{d^2 Y^p(x_i)}{dx_i^2} dx_i + \sum_{i=45 \sim 50} EL_{y,i} \int_{P_{i-1,i}}^{P_{i+1,i}} \frac{d^2 Z^k(x_i)}{dx_i^2} \frac{d^2 Z^p(x_i)}{dx_i^2} dx_i
\end{aligned}$$

Let

$$[K_i] = \begin{bmatrix} K_{x,i} & 0 & 0 \\ 0 & K_{y,i} & 0 \\ 0 & 0 & K_{z,i} \end{bmatrix}, \quad [K'_i] = \begin{bmatrix} K'_{x,i} & 0 & 0 \\ 0 & K'_{y,i} & 0 \\ 0 & 0 & K'_{z,i} \end{bmatrix} \quad (13.66)$$

There are relations between both sides of joint i in the following

$$\mathbf{R}_{O,i} = \mathbf{R}_{L,i} - [K_i]^{-1} \mathbf{Q}_{L,i}, \quad \boldsymbol{\Theta}_{O,i} = \boldsymbol{\Theta}_{L,i} + [K'_i]^{-1} \mathbf{M}_{L,i} \quad (13.67)$$

namely

$$\mathbf{R}_{O,i} - \mathbf{R}_{L,i} = -[K_i]^{-1} \mathbf{Q}_{L,i}, \quad \boldsymbol{\Theta}_{O,i} - \boldsymbol{\Theta}_{L,i} = [K'_i]^{-1} \mathbf{M}_{L,i} \quad (13.68)$$

Thus, if both the departure angle and the azimuth angle are 0, that is, $\alpha = \theta = 0$, then

$$\begin{aligned}
\langle KV^k, V^p \rangle &= \sum_{i=1 \sim 12} \left[(\mathbf{Q}_{0,i}^k)^T [K_i]^{-1} \mathbf{Q}_{0,i}^p \right] + \sum_{i=25 \sim 36} \left[(\mathbf{Q}_{i-12,i}^k)^T [K_i]^{-1} \mathbf{Q}_{i-12,i}^p \right] \\
&\quad + (\mathbf{Q}_{37,38}^k)^T [K_{38}]^{-1} \mathbf{Q}_{37,38}^p + (\mathbf{M}_{37,38}^k)^T [K'_{38}]^{-1} \mathbf{M}_{37,38}^p \\
&\quad + (\mathbf{Q}_{39,40}^k)^T [K_{40}]^{-1} \mathbf{Q}_{39,40}^p + (\mathbf{M}_{39,40}^k)^T [K'_{40}]^{-1} \mathbf{M}_{39,40}^p \\
&\quad + (\mathbf{Q}_{41,42}^k)^T [K_{42}]^{-1} \mathbf{Q}_{41,42}^p + (\mathbf{M}_{41,42}^k)^T [K'_{42}]^{-1} \mathbf{M}_{41,42}^p \\
&\quad + (\mathbf{Q}_{41,43}^k)^T [K_{43}]^{-1} \mathbf{Q}_{41,43}^p + (\mathbf{M}_{41,43}^k)^T [K'_{43}]^{-1} \mathbf{M}_{41,43}^p \\
&\quad + \sum_{i=45 \sim 50} EL_{z,i} \int_{P_{i-1,i}}^{P_{i+1,i}} \frac{d^2 Y^k(x_i)}{dx_i^2} \frac{d^2 Y^p(x_i)}{dx_i^2} dx_i + \sum_{i=45 \sim 50} EL_{y,i} \int_{P_{i-1,i}}^{P_{i+1,i}} \frac{d^2 Z^k(x_i)}{dx_i^2} \frac{d^2 Z^p(x_i)}{dx_i^2} dx_i
\end{aligned}$$

Considering the symmetry of matrices $[K]$ and $[K']$, k and p on the right-hand side of the above equation are exchangeable, so we have an equation as follows:

$$\langle KV^k, V^p \rangle = \langle KV^p, V^k \rangle = \langle V^k, KV^p \rangle \quad (13.69)$$

Thus, when $\alpha = \theta = 0$, V is symmetric about augmented operator K . If the departure angle and the azimuth angle are not 0, taking the term $-(Q_{39,38}^k)^T R_{39,38}^p + (Q_{37,38}^k)^T R_{37,38}^p$ as an example, $\alpha \neq 0$ results in $Q_{39,38}^k \neq Q_{37,38}^k$ and $R_{39,38}^p \neq R_{37,38}^p - [K_{38}]^{-1} Q_{37,38}^p$, but

$$Q_{39,38}^k = H_\alpha Q_{37,38}^k, \quad R_{39,38}^p = H_\alpha (R_{37,38}^p - [K_{38}]^{-1} Q_{37,38}^p)$$

Considering $H_\alpha^T = H_\alpha^{-1}$, we have

$$\begin{aligned} -(Q_{39,38}^k)^T R_{39,38}^p + (Q_{37,38}^k)^T R_{37,38}^p &= (Q_{37,38}^k)^T R_{37,38}^p - (H_\alpha Q_{37,38}^k)^T H_\alpha (R_{37,38}^p - [K_{38}]^{-1} Q_{37,38}^p) \\ &= (Q_{37,38}^k)^T R_{37,38}^p - (Q_{37,38}^k)^T (R_{37,38}^p - [K_{38}]^{-1} Q_{37,38}^p) \\ &= (Q_{37,38}^k)^T [K_{38}]^{-1} Q_{37,38}^p \end{aligned}$$

Obviously, even if $\alpha \neq 0$ and $\theta \neq 0$, Equation (13.69) still is valid.

In conclusion, V is symmetric about augmented operators M and K . It is validated that the augmented eigenvector of self-propelled artillery automatically satisfies the orthogonality.

13.6.4 Dynamic Response of the System

Substituting Equations (13.58) and (13.62) into Equation (13.55) gives

$$\sum_{k=1}^{\infty} M V^k \ddot{q}^k(t) + \sum_{k=1}^{\infty} (\alpha M V^k + \beta K V^k) \dot{q}^k(t) + \sum_{k=1}^{\infty} K V^k q^k(t) = f \quad (13.106)$$

Taking the inner product to V^p ($p = 1, 2, 3, \dots$) for both sides of Equation (13.106) yields

$$\ddot{q}^p(t) + (\alpha + \beta \omega_p^2) \dot{q}^p(t) + \omega_p^2 q^p(t) = \frac{\langle f, V^p \rangle}{M_p} \quad (p = 1, 2, \dots) \quad (13.107)$$

Substituting the column matrix of external force f into Equation (13.107), we can obtain $q^p(t)$ ($p = 1, 2, \dots$) by integration, and then the dynamic response of self-propelled artillery can be obtained through Equation (13.58).

Combining the generalized coordinate equations of self-propelled artillery (Equation (13.107)), the launch dynamic equation of the projectile (Equation (13.70)) and the dynamic equations of interior ballistic two-phase flow (Equations (13.73)–(13.105)), the launch dynamic equations of self-propelled artillery can be determined. For the same moment, using the MacCormack format, the dynamic equations of interior ballistic two-phase flow are solved, then, using the Runge–Kutta method, the body dynamic equations, as well as the launch dynamic equation of the projectile, are solved. After that, the dynamic parameters, including the dynamic response of the artillery and projectile motion in the gun tube, can be obtained. These are required to design, research and test for self-propelled artillery.

13.7 Launch Dynamic Equations and Forces Analysis

The launch dynamic equations of a self-propelled artillery system include the body dynamic equations of self-propelled artillery, the launch dynamic equations of the projectile and the interior ballistic equation. The body dynamic equations of self-propelled artillery were presented in

section 13.4. Other dynamic equations are introduced in this section. The two-phase flow dynamic model is adopted for interior ballistics.

13.7.1 Launch Dynamic Equation of a Projectile

The relevant coordinate systems are defined. The gun coordinate system $O_3x'_0y'_0z'_0$ is used to determine the orientation of the projectile with respect to the gun tube. The origin O_3 is the intersection point between the axis of the gun tube and its vertical plane passing the mass center of the projectile, the x'_0 axis is directed toward the muzzle along the tangent of gun tube axis at O_3 , the y' axis is in the plumb plane vertical with x'_0 axis and points up, and the z'_0 axis is determined by the right-hand law.

The projectile axis coordinate system $O_1\xi'\eta'\zeta'$ is used to determine the orientation of the projectile axis. The origin O_1 is the geometrical center of the projectile (the intersection point between the cross-section passing the mass center of the projectile and its geometrical longitudinal axis), the ξ' axis is directed toward the head of the projectile along its geometrical longitudinal axis, the η' axis is in the plumb plane vertical with ξ' axis and points up, and the ζ' axis is determined by the right-hand law.

The motion of the projectile mass center is described in the gun coordinate system $O_3x'_0y'_0z'_0$ and the rotational motion of the projectile is described in the projectile axis coordinate system. It can be proved that the launch dynamic equations of a nonsymmetric projectile are [132]

$$\begin{aligned}
 a_p &= \frac{F_{O_3x'_0}}{m_q} - \frac{\partial^2 X'}{\partial t^2} \\
 \ddot{y}'_{O_3C} &= \frac{F_{O_3y'_0}}{m_q} - \ddot{y}'_{O_3} \\
 \ddot{z}'_{O_3C} &= \frac{F_{O_3z'_0}}{m_q} - \ddot{z}'_{O_3} \\
 \ddot{\delta}_1^I &= \frac{M_{O_1\xi'}}{A} + \left(1 - \frac{C}{A}\right) \left(\beta_{D_{\xi'}} \ddot{\gamma} + \beta_{D_{\eta'}} \dot{\gamma}^2\right) - \frac{C}{A} (\dot{\psi}_2^I + \dot{\delta}_2^I) \dot{\gamma} + \frac{L_{m_{\eta'}} (a_p + \partial^2 X' / \partial t^2)}{A} - \ddot{\psi}_1^I \\
 \ddot{\delta}_2^I &= -\frac{M_{O_1\eta'}}{A} - \left(1 - \frac{C}{A}\right) \left(\beta_{D_{\eta'}} \ddot{\gamma} - \beta_{D_{\xi'}} \dot{\gamma}^2\right) + \frac{C}{A} (\dot{\psi}_1^I + \dot{\delta}_1^I) \dot{\gamma} + \frac{L_{m_{\xi'}} (a_p + \partial^2 X' / \partial t^2)}{A} - \ddot{\psi}_2^I
 \end{aligned} \tag{13.70}$$

where

$$\begin{cases} \beta_{D_{\eta'}} = \beta_{D_1} \cos \gamma - \beta_{D_2} \sin \gamma \\ \beta_{D_{\xi'}} = \beta_{D_1} \sin \gamma + \beta_{D_2} \cos \gamma \end{cases}, \quad \begin{cases} L_{m_{\eta'}} = L_{m_1} \cos \gamma - L_{m_2} \sin \gamma \\ L_{m_{\xi'}} = L_{m_1} \sin \gamma + L_{m_2} \cos \gamma \end{cases}, \tag{13.71}$$

a_p is the component of the acceleration of the projectile mass center along the gun axis with respect to the gun coordinate system $O_3x'_0y'_0z'_0$. m_q is the mass of the projectile. X' is the recoil displacement of the gun. y_{O_3C} and z_{O_3C} are the vertical and lateral components of the projectile centroid displacement with respect to the gun coordinate system $O_3x'_0y'_0z'_0$. y_{O_3} and z_{O_3} are the vertical and lateral components of displacement of O_3 . $F_{O_3x'_0}$, $F_{O_3y'_0}$ and $F_{O_3z'_0}$ are the components of the force acting on the projectile along three coordinate axes at $O_3x'_0y'_0z'_0$. $M_{O_1\xi'}$ and $M_{O_1\eta'}$ are the components of external moment along the ξ' and η' axes, respectively. C is the polar moment of inertia of the projectile. A is the equatorial moment of inertia of the projectile. γ is the spinning

angle of the projectile. δ_1^I is the angle between the x'_0 axis and the projection of the projectile polar axis ξ' on plane $x'_0O_3y'_0$ and is positive when the ξ' axis is upside to the x'_0 axis. δ_2^I is the angle between the projectile polar axis ξ' and the plane $x'_0O_3y'_0$ and is positive when the ξ' axis is on the right of $x'_0O_3y'_0$. ψ_1^I is the angle between the x' axis and the projection of the x'_0 axis on plane $x'O_3y'$ and is positive when the x'_0 axis is upside to the x' axis. ψ_2^I is the angle between the x'_0 axis and plane $x'O_3y'$ and is positive when the x'_0 axis is on the right of $x'O_3y'$. $L_{m_{\eta'}}$ and $L_{m_{\xi'}}$ are projections of mass eccentricity along the η' and ξ' axes in projectile axis coordinate system $O_1\xi'\eta'\zeta'$, respectively. L_{m_1} and L_{m_2} are components of mass eccentricity in the coordinate system fixed on the projectile. $\beta_{D_{\eta'}}$ and $\beta_{D_{\xi'}}$ are projections of the dynamic unbalance along the η' and ξ' axes of projectile axis coordinate system $O_1\xi'\eta'\zeta'$. β_{D_1} and β_{D_2} are the components of dynamic unbalance in the coordinate system fixed on the projectile.

The piecewise rifling is expressed by

$$\gamma = \begin{cases} \frac{2 \tan \alpha_0}{d_0} x_q + \frac{k_\alpha}{d_0} x_q^2 & (x_q < l_\alpha) \\ \frac{2 \tan \alpha_g}{d_0} x_q - \frac{k_\alpha}{d_0} l_\alpha^2 & (x_q \geq l_\alpha) \end{cases} \quad (13.72)$$

where α is the twist angle of rifling, l_α is the position of the switch point between uniform and increasing twist rifling, $k_\alpha = (\tan \alpha_g - \tan \alpha_0)/l_\alpha$, α_g is the twist angle of rifling at the muzzle and α_0 is the initial twist angle of rifling.

13.7.2 Dynamic Equations of Interior Ballistic Two-phase Flow

According to the dynamic model of interior ballistic two-phase flow and basic hypotheses, basic equations of the main charge and central ignition tube are established using one-dimensional gridding.

13.7.2.1 Basic Equations of Two-phase Flow Dynamics for the Main Charge

Basic equations of the two-phase flow dynamics for the main charge founded in Eulerian coordinates include the conservation equations of gas phase mass, gas phase momentum, gas phase energy, solid phase mass and solid phase momentum, namely

$$\begin{aligned} \frac{\partial A \phi \rho_g}{\partial t} + \frac{\partial A \phi \rho_g u_g}{\partial x} &= A \dot{m}_c + A \dot{m}_{\text{ign}} \\ \frac{\partial A \phi \rho_g u_g}{\partial t} + \frac{\partial A \phi \rho_g u_g^2}{\partial x} + A \phi \frac{\partial P}{\partial x} &= -AD + A \dot{m}_c u_p \\ \frac{\partial A \phi \rho_g (e_g + u_g^2/2)}{\partial t} + \frac{\partial A \phi \rho_g u_g (e_g + u_g^2/2)}{\partial x} + \frac{\partial A \phi u_g P}{\partial x} + P \frac{\partial A \phi}{\partial t} &= A \dot{m}_c H_c + A \dot{m}_{\text{ign}} H_{\text{ign}} - AD u_p - A Q_s \\ \frac{\partial A(1-\phi) \rho_p}{\partial t} + \frac{\partial A(1-\phi) \rho_p u_p}{\partial x} &= -A \dot{m}_c \\ \frac{\partial A(1-\phi) \rho_p u_p}{\partial t} + \frac{\partial A(1-\phi) \rho_p u_p^2}{\partial x} + A(1-\phi) \frac{\partial P}{\partial x} &= AD - A \dot{m}_c u_p - A(1-\phi) \frac{\partial R_p}{\partial x} \end{aligned} \quad (13.73)$$

where A is the cross-section area of the gun tube, ϕ is the porosity and ρ_g is the gas phase density. u_g is the gas phase velocity, \dot{m}_c is the mass production rate of gas per unit bulk and \dot{m}_{ign} is the mass flux of the gas source in the total bulk of a grid in the chamber. D is the drag force between two phases, P is the gas pressure and u_p is the solid phase velocity. e_g is the internal energy of gas, H_c is the enthalpy per unit mass released by propellant burning and H_{ign} is the enthalpy per unit mass brought by influent gas. Q_s is the heat transfer between two phases and R_p is the stress within propellant grains.

In addition

$$e_g = RT/(\gamma - 1) \quad (13.74)$$

$$H_c = e_\Delta + u_p^2/2 + P/\rho_p \quad (13.75)$$

$$e_\Delta = f_p/(\gamma - 1) \quad (13.76)$$

$$H_{\text{ign}} = e_{\text{ig}} + P_{\text{ig}}/\rho_{\text{ig}} + u_{\text{ig}}^2/2 \quad (13.77)$$

where R is the gas constant, T is the gas temperature, γ is the gas adiabatic exponent and f_p is the propellant force.

13.7.2.2 Basic Equations Group for the Central Ignition Tube

The basic equations for the central ignition tube founded in Eulerian coordinates include the conservation equations of gas phase mass, gas phase momentum and gas phase energy, namely

$$\begin{aligned} \frac{\partial A_{\text{ig}} \phi_{\text{ig}} \rho_{\text{ig}}}{\partial t} + \frac{\partial A_{\text{ig}} \phi_{\text{ig}} \rho_{\text{ig}} u_{\text{ig}}}{\partial x} &= A_{\text{ig}} \dot{m}_{\text{ig}} - A_{\text{ig}} \dot{m}_{\text{ign}} \\ \frac{\partial A_{\text{ig}} \phi_{\text{ig}} \rho_{\text{ig}} u_{\text{ig}}}{\partial t} + \frac{\partial A_{\text{ig}} \phi_{\text{ig}} \rho_{\text{ig}} u_{\text{ig}}^2}{\partial x} + A_{\text{ig}} \phi_{\text{ig}} \frac{\partial P_{\text{ig}}}{\partial x} &= 0 \\ \frac{\partial A_{\text{ig}} \phi_{\text{ig}} \rho_{\text{ig}} \left(e_{\text{ig}} + \frac{u_{\text{ig}}^2}{2} \right)}{\partial t} + \frac{\partial A_{\text{ig}} \phi_{\text{ig}} \rho_{\text{ig}} u_{\text{ig}} \left(e_{\text{ig}} + \frac{u_{\text{ig}}^2}{2} \right)}{\partial x} + \frac{\partial A_{\text{ig}} \phi_{\text{ig}} u_{\text{ig}} P_{\text{ig}}}{\partial x} \\ + P_{\text{ig}} \frac{\partial A_{\text{ig}} \phi_{\text{ig}}}{\partial t} &= A_{\text{ig}} \dot{m}_{\text{ig}} H_{\text{ig}} - A_{\text{ig}} \dot{m}_{\text{ign}} H_{\text{ign}} \end{aligned} \quad (13.78)$$

where A_{ig} is the cross-section area of the central ignition tube, ϕ_{ig} is the porosity in the ignition tube and ρ_{ig} is the gas phase density in the ignition tube. u_{ig} is the gas phase velocity, \dot{m}_{ig} is the mass production rate per unit bulk produced by the ignition powder and \dot{m}_{ign} is the mass flux out of the ignition tube. P_{ig} is the gas pressure in the ignition tube, e_{ig} is the internal energy of the ignition gas, H_{ig} is the enthalpy released by ignition powder burning and H_{ign} is the enthalpy flowing out from the ignition tube. This yields

$$H_{\text{ig}} = \frac{f_{\text{ig}}}{\gamma_{\text{ig}} - 1} + \frac{P_{\text{ig}}}{\rho_{p, \text{ig}}} \quad (13.79)$$

$$H_{\text{ign}} = e_{\text{ig}} + \frac{P_{\text{ig}}}{\rho_{\text{ig}}} + \frac{u_{\text{ig}}^2}{2} \quad (13.80)$$

$$e_{\text{ig}} = \frac{R_{\text{ig}} T_{\text{ig}}}{\gamma_{\text{ig}} - 1} \quad (13.81)$$

$$R_{ig} = \frac{f_{ig}}{T_{1,ig}} \quad (13.82)$$

where R_{ig} is the ignition gas constant, γ_{ig} is the adiabatic exponent of the ignition gas, T_{ig} is the ignition gas temperature, f_{ig} is the propellant force of the ignition powder and $T_{1,ig}$ is the explosion temperature of the ignition powder.

13.7.2.3 Auxiliary Equations

1) Nobel–Abel gas state equation

$$P \left(\frac{1}{\rho_g} - \alpha \right) = RT \quad (13.83)$$

where α is the covolume of propellant gas, P is the gas pressure, ρ_g is the gas density, R is the gas constant and T is the gas temperature.

2) Mass production rate of gas

$$\dot{m}_c = \frac{(1-\phi)\rho_p}{1-\psi} \frac{d\psi}{dt} \quad (13.84)$$

where ρ_p is the solid density, which is constant, and ψ is the relative burnt bulk of propellant.

The combustion of propellant obeys the geometric burning law

$$\psi = \begin{cases} \chi Z(1 + \lambda Z + \mu Z^2) & (Z \leq 1) \\ \chi_s Z(1 + \lambda_s Z) & (1 < Z \leq Z_k) \end{cases} \quad (13.85)$$

$$\frac{d\psi}{dt} = \begin{cases} \chi(1 + 2\lambda Z + 3\mu Z^2) \frac{dZ}{dt} & (Z \leq 1) \\ \chi_s(1 + 2\lambda_s Z) \frac{dZ}{dt} & (1 < Z \leq Z_k) \end{cases} \quad (13.86)$$

where χ , λ , μ , χ_s and λ_s are the characteristic quantities of propellant grain form and Z is the relative burnt thickness.

Burning rate obeys the exponential law, that is

$$\frac{dZ}{dt} = \frac{u_1 p^\nu}{e_1} \quad (Z \leq Z_k) \quad (13.87)$$

where e_1 is half of the propellant web size, and u_1 and ν are the coefficient and exponent of burning rate, respectively.

3) Anderson formula for the drag force between two phases [273]

$$D = C_f \rho_g \frac{1-\phi}{\phi d_p} (u_g - u_p) |u_g - u_p| \quad (13.88)$$

where

$$d_p = \left(\frac{3}{2} D_p^2 L_p \right)^{1/3} \quad (13.89)$$

$$C_f = \begin{cases} c_{fz} & (\phi \leq \phi_0) \\ c_{fz} \left(\frac{1-\phi}{1-\phi_0} \cdot \frac{\phi_0}{\phi} \right)^{0.21} & (\phi \leq 0.97) \\ 0.45 & (\phi > 0.97) \end{cases} \quad (13.90)$$

$$c_{fz} = \begin{cases} 0.31(\lg Re) - 2.55 \lg Re + 6.33 & (Re \leq 20000) \\ 1.10 & (Re > 20000) \end{cases} \quad (13.91)$$

$$Re = \frac{d_p \rho_g |u_g - u_p|}{\mu_g} \quad (13.92)$$

$$\mu_g = c_1 \sqrt{T^3} / (c_2 + T) \quad (13.93)$$

where d_p is the equivalent diameter of the propellant grain, D_p and L_p are the diameter and length of the propellant grain, ϕ_0 is the critical porosity of the propellant with free loading, Re is the Reynolds number of gas motion calculated with the characteristic size that is the equivalent diameter d_p , μ_g is the viscosity coefficient, $c_1 = 1.546 \times 10^{-6} \text{Pa} \cdot \text{s}$ and $c_2 = 240.9 \text{K}$.

4) Formula for stress within propellant grains [273]

Stress R_p is calculated through the following formula according to porosity ϕ

$$R_p = \begin{cases} \frac{298.8}{1-\phi} \left(\frac{\phi_0 - \phi}{1-\phi_0} \right)^{1.48} \text{ (MPa)} & (\phi < \phi_0) \\ 0 & (\phi > \phi_0) \end{cases} \quad (13.94)$$

5) Formula for heat transfer between two phases

Heat transfers from gas to solid, and the quantity of heat exchange per unit bulk is

$$Q_s = A_p h_t (T - T_{ps}) \quad (13.95)$$

where A_p is the surface area of the propellant grain, T_{ps} is the surface temperature and h_t is the coefficient of heat interchange. It should be noted that

$$h_t = h_p + h_{re} \quad (13.96)$$

$$T_{ps}(t + \Delta t) = T_{ps}(t) + \frac{2\sqrt{a_p}}{k_p \sqrt{\pi}} h_t (T - T_{ps}) \left[(t + \Delta t)^{0.5} - t^{0.5} \right] \quad (13.97)$$

where a_p is the coefficient of temperature conductivity of the propellant, k_p is the coefficient of heat conductivity of the propellant, and h_p and h_{re} are the coefficients of convection heat transfer and radiative heat interchange, respectively. Note that

$$h_p = N_{up} k_g / d_p \quad (13.98)$$

$$k_g = c_3 \sqrt{T^3} / (c_4 + T) \quad (13.99)$$

$$N_{up} = 0.4 Re^{2/3} \cdot Pr^{1/3} \quad (13.100)$$

$$h_{re} = c_5 (T + T_{ps}) (T^2 + T_{ps}^2) \quad (13.101)$$

where k_g is the coefficient of the heat conductivity of the gas, N_{up} is the Nusselt number and Pr is Planck's constant. Commonly, $Pr = 0.7$, $c_3 = 3.53 \times 10^{-3} \text{W}/(\text{m} \cdot \text{s} \cdot \text{K})$, $c_4 = 648.42 \text{K}$, $c_5 = \varepsilon_p \sigma_0$, ε_p is the superficial blackness $\varepsilon_p = 1$, σ_0 is the Stefan-Boltzmann constant and $\sigma_0 = 4.9 \times 10^{-8} \text{cal}/(\text{m}^2 \cdot \text{h})$.

6) Formula for the mass flux of jet ejected from the primer

When the primer is fired, it produces hot gas and jet into the first grid of the ignition tube, and the jet can be regarded as the “source” of the grid. Because \dot{m}_{ign} has been defined as “the mass flux out of the ignition tube in the total bulk of a grid” in Equation (13.78), the mass flux of the source is defined in the total bulk of the grid

$$\dot{m}_{\text{ign},1} = -\frac{\dot{m}_b}{A_{\text{ig}} \cdot \Delta x_{\text{ig}}} \quad (13.102)$$

where \dot{m}_b is the mass flux of the jet form primer.

Taking a primer as an example, the test result of the mass flux of jet [273] is

$$\dot{m}_b = \begin{cases} 5.19t^2 + 1.74t & \leq (t \leq 0.663 \text{ ms}) \\ -0.0845t^3 - 4.725t^2 + 11.74t - 2.53 & (0.663 < t \leq 1.547 \text{ ms}) \\ -2.958t + 8.576 & \leq (1.547 < t \leq 2.431 \text{ ms}) \\ 2.0115 \times 10^3 e^{-2.95t} 1.547 & (t > 2.431 \text{ ms}) \end{cases} \quad (13.103)$$

7) Formula for the mass flux of the ignition hole

The ignition gas out of the ignition tube from the ignition hole is regarded as the “source” in a grid, and the mass flux of excurrent gas is

$$\dot{m}_{\text{ign}} = \frac{n_{\text{ig}} \cdot \dot{m}_{\text{out}}}{A_{\text{ig}} \cdot \Delta x_{\text{ig}}} \quad (13.104)$$

$$\dot{m}_{\text{out}} = \begin{cases} \eta S_k \phi_{\text{ig}} \rho_{\text{ig}} \sqrt{\frac{2\gamma_{\text{ig}}}{\gamma_{\text{ig}} - 1} R_{\text{ig}} T_{\text{ig}} \left[\left(\frac{P_{\text{out}}}{P_{\text{ig}}} \right)^{\frac{2}{\gamma_{\text{ig}}}} - \left(\frac{P_{\text{out}}}{P_{\text{ig}}} \right)^{\frac{\gamma_{\text{ig}} + 1}{\gamma_{\text{ig}}}} \right]} & \frac{P_{\text{out}}}{P_{\text{ig}}} > \left(\frac{2}{\gamma_{\text{ig}} + 1} \right)^{\frac{\gamma_{\text{ig}}}{\gamma_{\text{ig}} - 1}} \\ \eta S_k \phi_{\text{ig}} \rho_{\text{ig}} \sqrt{\frac{2\gamma_{\text{ig}}}{\gamma_{\text{ig}} - 1} \left(\frac{2}{\gamma_{\text{ig}} + 1} \right)^{\frac{2}{\gamma_{\text{ig}} - 1}} R_{\text{ig}} T_{\text{ig}}} & \frac{P_{\text{out}}}{P_{\text{ig}}} \leq \left(\frac{2}{\gamma_{\text{ig}} + 1} \right)^{\frac{\gamma_{\text{ig}}}{\gamma_{\text{ig}} - 1}} \end{cases} \quad (13.105)$$

where n_{ig} is the total number of ignition holes in one grid (when ignition holes are not broken $n_{\text{ig}} = 0$), \dot{m}_{out} is the mass flux of the ignition hole, η is the flux coefficient, S_k is the area of the ignition hole and P_{out} is the pressure out of the ignition tube.

13.7.3 Analysis for the Force Acting on a Self-propelled Launch System

During the launch process, the forces acting on self-propelled artillery are mainly the interaction forces between the gun barrel and the pitching part, the pitching part and the revolving part, the revolving part and the hull, the hull and the road wheels, and the road wheels and the ground. All these forces and moments are regarded as the internal forces of the system. The recoil resistance produced by the recoil and counterrecoil mechanism is decomposed into two parts: the internal force and the external force. The internal force is proportional to the relative displacement between the barrel and the pitching part. The force of the propellant gas, the Bourdon force, the force acting on the barrel by the projectile and the tensile force of the pedrail are external forces.

The forces acting on the projectile in the gun tube are very complex and include gravity, the pressure of the propellant gas, the air resistance acting on the head of the projectile, the contact force between the rotating band and the wall of the gun tube, the contact force between the bourrelet and the wall of the gun tube, and the corresponding moment.

The forces acting on the projectile are described in the form of column matrices in gun coordinate system $O_3x'_0y'_0z'_0$, and the corresponding moments acting on the projectile are described in the form of column matrices in projectile axis coordinate system $O_1\xi'\eta'\zeta'$. The detailed analysis processes and expressions of all the forces can be found in reference [132]. All external forces acting on the artillery are expressed in the corresponding inertia coordinate which corresponds to each element, and the column matrix f_i of external forces in the body dynamic equation of each element can be evaluated. The column matrix f of the external forces of the system is obtained according to the form of Equation (13.57). The computation methods of the force acting on the artillery by the propellant gas, the Burdon force and the force acting on the barrel by the projectile, the force acting on the barrel and pitching part by the recoil and counterrecoil mechanism, and the tensile force of the pedrail can be found in references [132], and [274–277], respectively.

13.8 Dynamics Simulation of the System and its Test Verifying

13.8.1 Launch Dynamics Simulation System of Self-Propelled Artillery

The launch dynamics simulation system of self-propelled artillery is based on the MSTMM. The program for computing the launch dynamics of self-propelled artillery is written in FORTRAN. The launch process of self-propelled artillery with the initial disturbance is simulated under the condition of 0° departure angle and 0° azimuth angle. The vibration characteristics, the interior ballistic, the motion of the projectile in the gun tube and the dynamic response of artillery are computed. Some tests have been carried out and their results verify the simulation system. Some results of simulation and testing are given below.

13.8.2 Simulation and Test Verifying for Vibration Characteristics

Natural vibration characteristics of self-propelled artillery are simulated using the MSTMM according to the 0° departure angle and 0° azimuth angle. The modal parameters and the vibration characteristics are obtained via the experimental modal analysis of self-propelled artillery. The simulation and test results of eigenfrequencies for the first 16 ranks are given in Table 13.1 and it can be seen that the simulation results are in good agreement with the test results.

Some of simulation results of mode shapes are shown in Figures 13.4–13.7, in which the abscissas denote the sequence numbers of points, and the corresponding relation between the position of the point and the sequence number is shown in Table 13.2. The first rank mode represents the recoil motion of the barrel, and the second one represents the horizontal revolving motions of the turret, cradle and barrel. The third mode represents the pitching motions of the cradle and barrel, and the 16th mode represents the transverse motion of the barrel and complex motions of other elements. The low rank mode shapes do not represent the transverse elastic deformation of the barrel and such transverse elastic deformation can only be observed in higher rank mode shapes.

Table 13.1 Simulation and test results of eigenfrequencies

Mode rank, k	$\omega_k/(\text{rad/s})$		Relative error/%	Mode rank, k	$\omega_k/(\text{rad/s})$		Relative error/%
	Simulation	Test			Simulation	Test	
1	3.02	—	—	9	87.7	82.1	6.82
2	15.2	15.5	-1.94	10	94.5	—	—
3	18.5	18.7	-1.07	11	101.1	105.5	-4.17
4	28.9	29.9	-3.34	12	—	128.4	—
5	44.3	42.2	4.98	13	141.3	136.3	3.67
6	46.5	49.8	-6.63	14	215.1	202.9	6.01
7	64.9	—	—	15	226.6	229.2	-1.13
8	75.6	—	—	16	243.4	244.4	-0.41

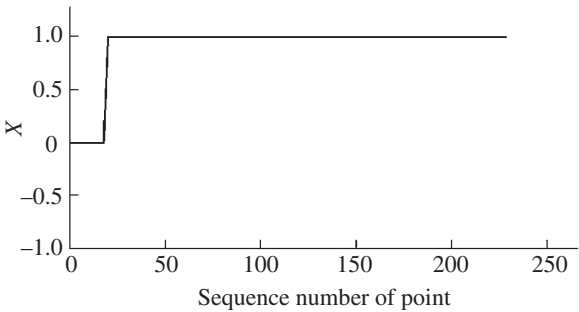


Figure 13.4 The first mode shape in the x direction.

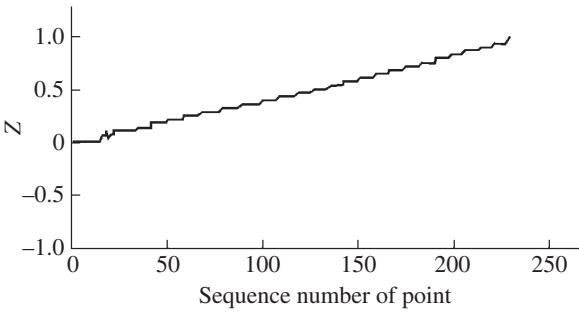


Figure 13.5 The second mode shape in the z direction.

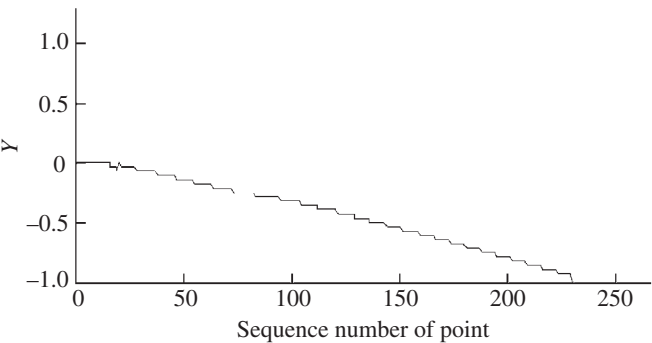


Figure 13.6 The third mode shape in the y direction.

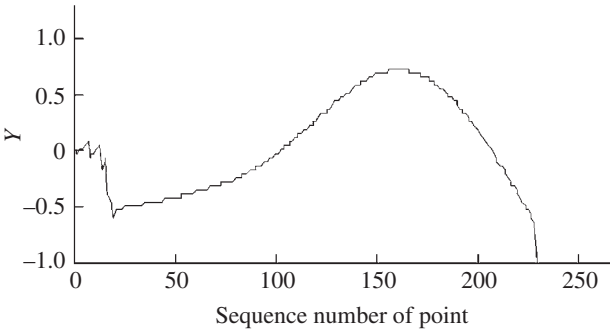


Figure 13.7 The 16th mode shape in the y direction.

Table 13.2 Corresponding relation between the position of point and the sequence number

Sequence number	1	2–13		14	15	16	17	18
Position	Ground	$P_{13,1}, P_{14,2}, \dots, P_{24,12}$		$P_{37,25}$	$P_{37,38}$	$P_{39,38}$	$P_{39,40}$	$P_{41,40}$
Sequence number	19	20	21	22–29	30	31–68		69
Position	$P_{41,42}$	$P_{44,0}$	$P_{44,45}$	Element 45 (beam 1)	$P_{45,46}$	Element 46 (beam 2)		$P_{46,47}$
Sequence number	70–104		105–126	127–148		149–229		230
Position	Element 47 (beam 3)		Element 48 (beam 4)	Element 49 (beam 5)		Element 50 (beam 6)		$P_{51,52}$

13.8.3 Simulation and Test Verifying for Interior Ballistic Two-phase Flow Dynamics

Simulation results of interior ballistic two-phase flow dynamics and some experiment results are shown in Figures 13.8–13.12. These results play an important role in interior ballistic design.

The simulation and test results of the time-history of the breech pressure are shown in Figure 13.8, and the simulation and test results of interior ballistic performances are shown in Table 13.3. The simulation and test results have good agreement, which demonstrates the accuracy of the simulation system. The simulation results of gas pressure distribution behind

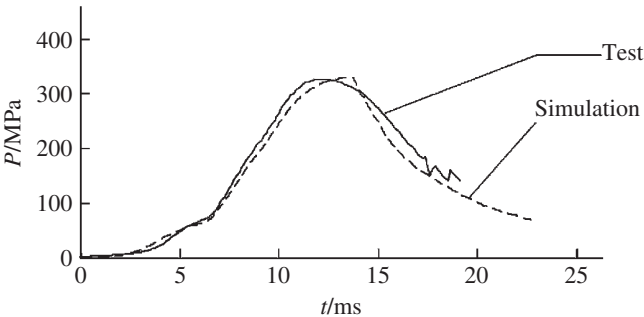


Figure 13.8 Simulation and test results of breech pressure vs time.

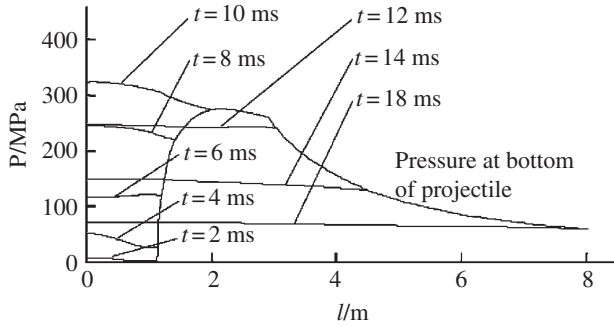


Figure 13.9 Gas pressure distribution.

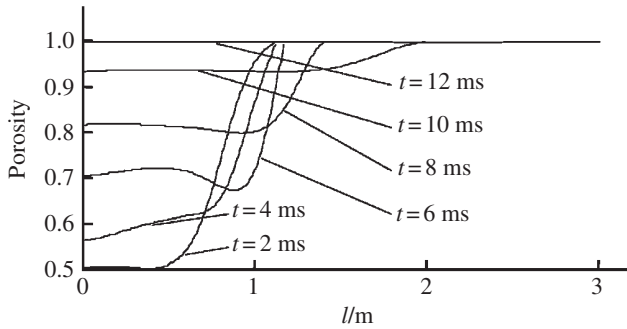


Figure 13.10 Porosity distribution.

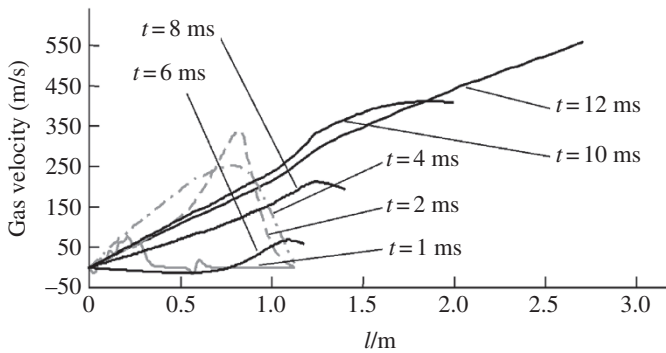


Figure 13.11 Gas velocity distribution.

the projectile and its change over time are shown in Figure 13.9. The simulation results of porosity distribution behind the projectile and its change over time are shown in Figure 13.10. The simulation results of gas velocity distribution behind the projectile and its change over time are shown in Figure 13.11. The simulation results of solid velocity distribution behind the projectile and its change over time are shown in Figure 13.12.

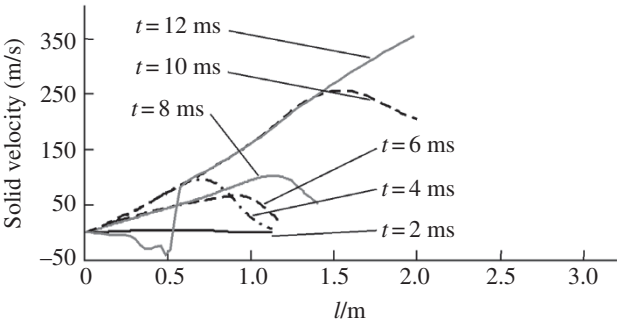


Figure 13.12 Solid velocity distribution.

Table 13.3 Simulation and test results of interior ballistic performances

	Maximal pressure at breech/MPa	Muzzle velocity of projectile/(m/s)
Simulation	330.6	928.2
Test	327.4	931.0

13.8.4 Simulation and Test Verifying for the Dynamic Response of the System

The simulation results of the dynamic response of self-propelled artillery and some test results are shown in Figures 13.13–13.16. These results are an important foundation for the design and performance evaluation of artillery. Time-history simulations of the resultant force acting on the

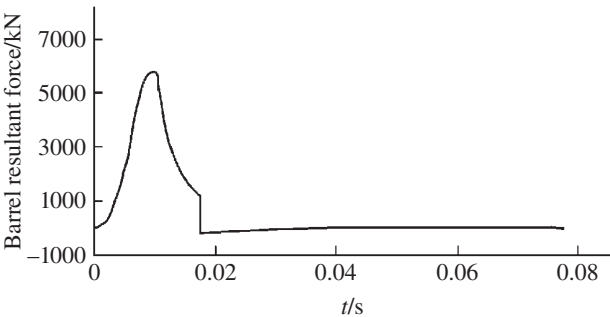


Figure 13.13 Resultant force of barrel.

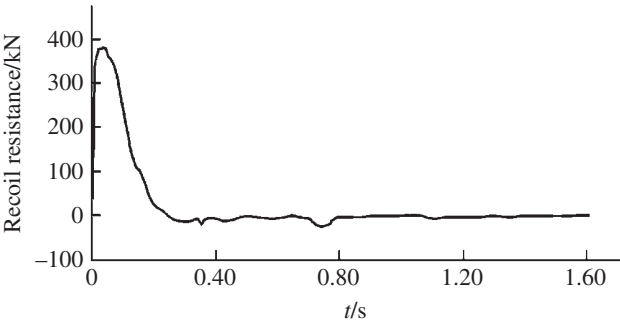


Figure 13.14 Recoil resistance.

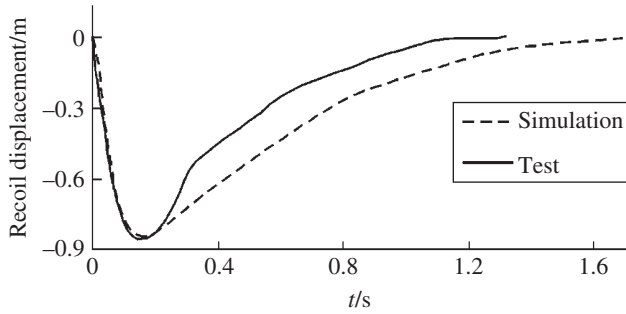


Figure 13.15 Recoil displacement.

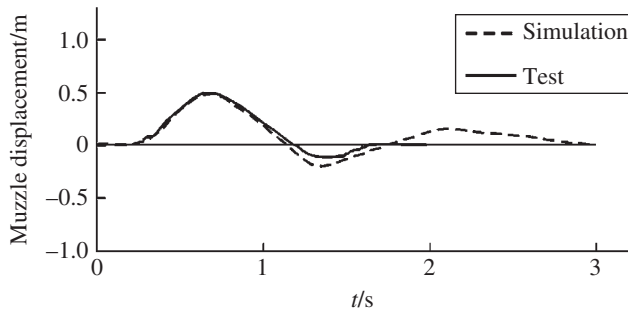


Figure 13.16 Muzzle displacement.

barrel, recoil resistances, recoil and muzzle displacements with their test results are presented in Figures 13.13–13.16. Some simulation and test results are in good agreement.

13.8.5 Simulation and Test Verifying for Projectile Launch Dynamics

The simulation results of the launch dynamics of projectiles are shown in Figure 13.17–13.26. These results provide a necessary ballistic environment for design and failure diagnosis of the mechanism carried by the projectile, such as fuze, and provide an important foundation for performance evaluation and design improvement of the projectile.

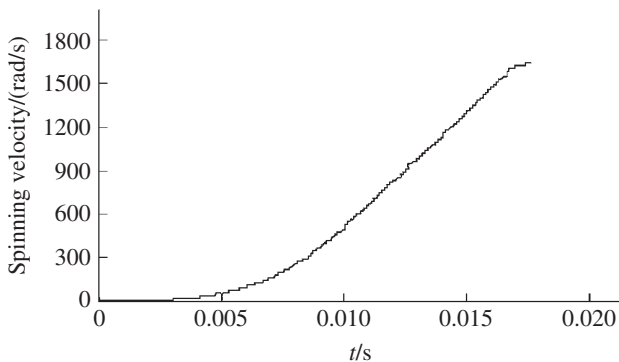


Figure 13.17 Spinning velocity of a projectile.

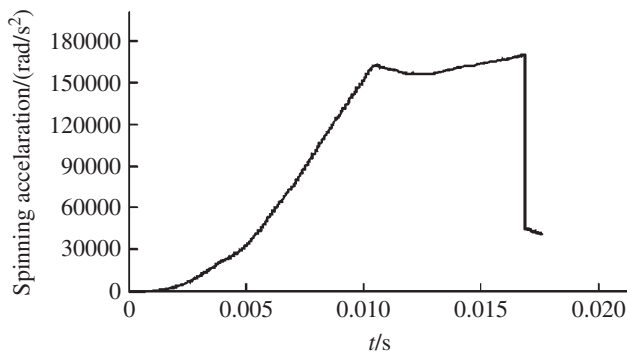


Figure 13.18 Spinning acceleration of a projectile.

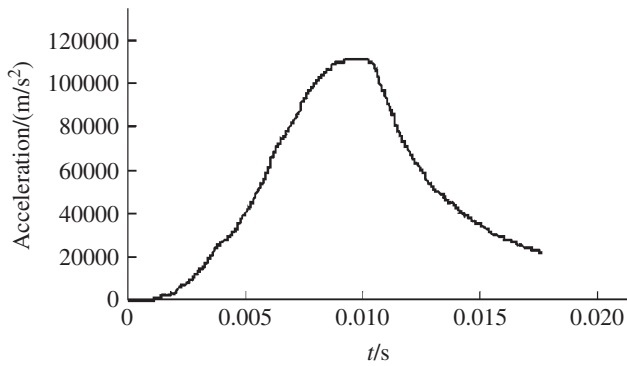


Figure 13.19 Acceleration of a projectile.

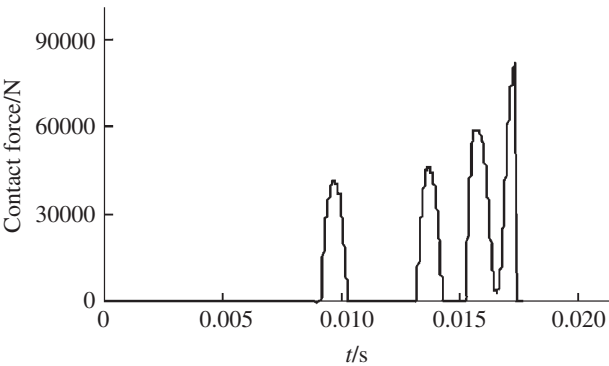
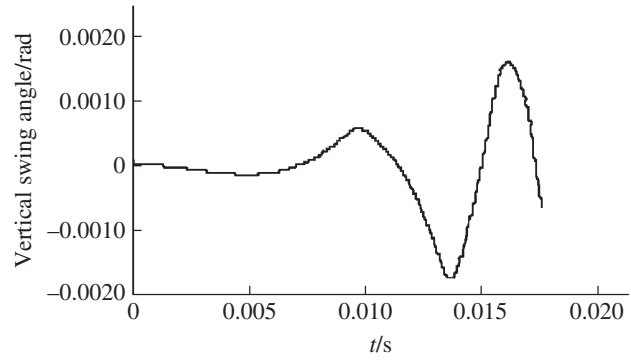
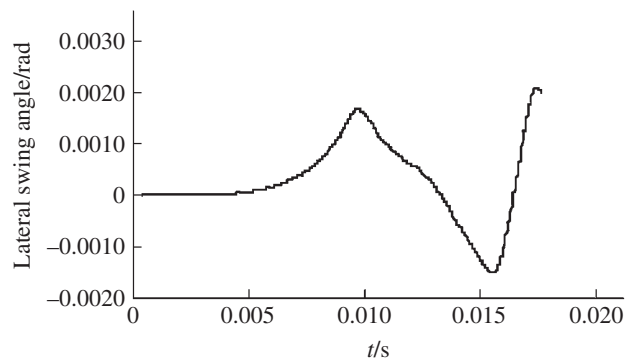
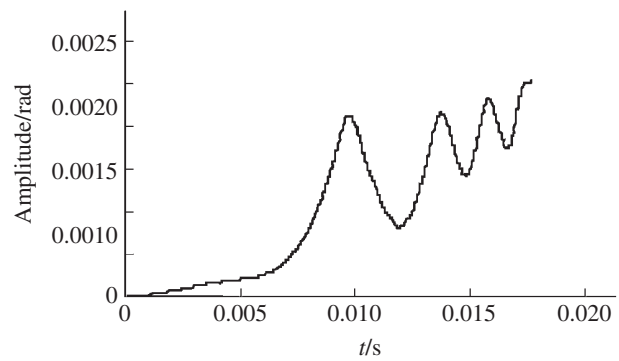
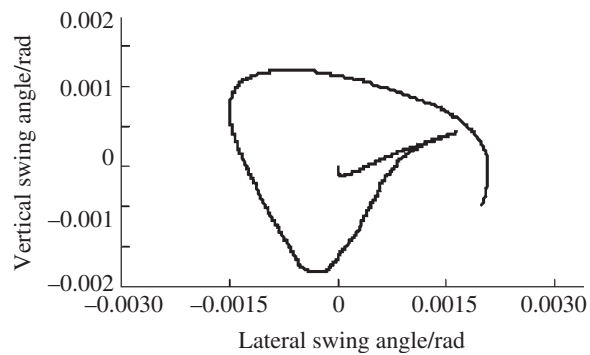


Figure 13.20 Contact force of a front bourrelet.

The simulation results of the time-history of projectile spinning velocity, spinning and longitudinal accelerations are shown in Figures 13.17–13.19. The simulation results of the contact force between the front bourrelet and the wall of the gun tube are shown in Figure 13.20. The time-history results of the vertical and lateral swing angle of the projectile are illustrated

Figure 13.21 Vertical swing angle.**Figure 13.22** Lateral swing angle.**Figure 13.23** Amplitude swing angle.**Figure 13.24** Track of swing angle.

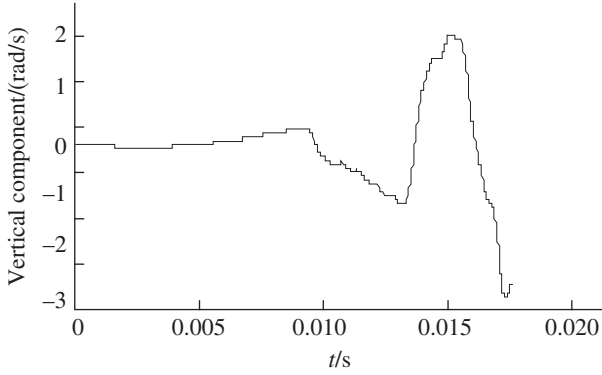


Figure 13.25 Vertical swing angular velocity.

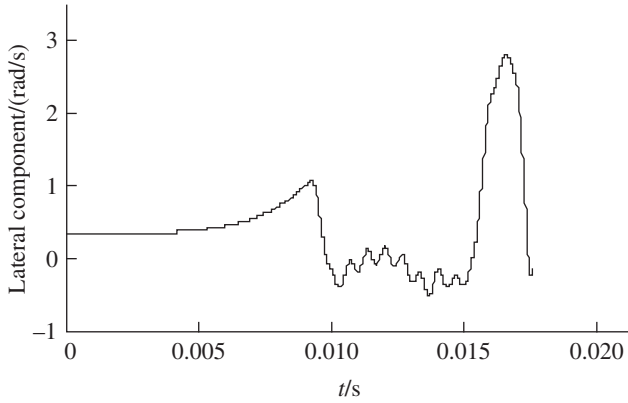


Figure 13.26 Lateral swing angular velocity.

in Figures 13.21 and 13.22. The time-history result of the amplitude swing angle of the projectile is illustrated in Figure 13.23. The simulation result of the track of the swing angle of the projectile axis is shown in Figure 13.24. The simulation results of the vertical and lateral swing angular velocities of the projectile are shown in Figures 13.25 and 13.26.

13.8.6 Computation of the Initial Disturbance of the Projectile

The initial disturbance of the projectile includes the initial deflection angle Ψ , the initial swing angle Φ , the initial attack angle Δ and the angular velocity $\dot{\Psi}$, $\dot{\Phi}$, $\dot{\Delta}$ at the end time of the launch period. It also includes the initial coordinates, initial velocity, initial spinning angle and initial spinning velocity. When the projectile leaves the muzzle, the initial deflection angle Ψ when projectile begins to fly is the angle between the speed vector of the projectile mass center and the line of sight, that is

$$\begin{cases} \psi_{01} = \frac{\dot{y}'_{O_3C,g} + \dot{y}'_{O_3,g}}{v_g} \\ \psi_{02} = \frac{\dot{z}'_{O_3C,g} + \dot{z}'_{O_3,g}}{v_g} \end{cases} \quad (13.108)$$

where $\dot{y}'_{O_3,g}$ and $\dot{z}'_{O_3,g}$ are the vertical and lateral components of the muzzle speed, respectively, when the projectile is just flying off from the muzzle. At the same moment $\dot{y}'_{O_3C,g}$ and $\dot{z}'_{O_3C,g}$ are the vertical and lateral components, respectively, of the projectile mass center speed relative to the barrel axis and v_g is the axial component of projectile speed relative to the gun tube.

If we differentiate Equation (13.108) with respect to time, the initial deflection angular velocity of projectile flight $\dot{\Psi}$ can be obtained:

$$\begin{cases} \dot{\psi}_{01} = \frac{(\ddot{y}'_{O_3C,g} + \ddot{y}'_{O_3,g})v_g - a_g(\dot{y}'_{O_3C,g} + \dot{y}'_{O_3,g})}{v_g^2} \\ \dot{\psi}_{02} = \frac{(\ddot{z}'_{O_3C,g} + \ddot{z}'_{O_3,g})v_g - a_g(\dot{z}'_{O_3C,g} + \dot{z}'_{O_3,g})}{v_g^2} \end{cases} \quad (13.109)$$

where $\ddot{y}'_{O_3,g}$ and $\ddot{z}'_{O_3,g}$ are the vertical and lateral components of the muzzle acceleration, respectively, $\ddot{y}'_{O_3C,g}$ and $\ddot{z}'_{O_3C,g}$ are the vertical and lateral components of the acceleration of the center of mass of the projectile relative to the barrel axis and a_g is the axial component of acceleration of the center of mass of the projectile relative to the gun tube.

The initial swing angle of projectile Φ is the angle between the projectile axis and the line of sight at the moment the projectile flies off the muzzle, that is

$$\begin{cases} \varphi_{01} = \delta_{01}^l + \psi_{01}^l \\ \varphi_{02} = \delta_{02}^l + \psi_{02}^l \end{cases}, \quad \begin{cases} \dot{\varphi}_{01} = \dot{\delta}_{01}^l + \dot{\psi}_{01}^l \\ \dot{\varphi}_{02} = \dot{\delta}_{02}^l + \dot{\psi}_{02}^l \end{cases} \quad (13.110)$$

where δ_{01}^l and δ_{02}^l are the vertical and lateral components of the angle between the projectile axis and the tangent of the barrel axis of the muzzle while the projectile is just flying off the muzzle. ψ_{01}^l and ψ_{02}^l are the vertical and lateral components of the angle between the tangent of the barrel axis at the muzzle and the line of sight at the same moment. These variables and their first partial derivatives with respect to time can be obtained after the projectile motion and artillery dynamic response are obtained through solving the launch dynamic equations of the system.

The initial attack angle and its angular velocity when the projectile flies off the muzzle is

$$\begin{cases} \delta_{01} = \varphi_{01} - \psi_{01} \\ \delta_{02} = \varphi_{02} - \psi_{02} \end{cases}, \quad \begin{cases} \dot{\delta}_{01} = \dot{\varphi}_{01} - \dot{\psi}_{01} \\ \dot{\delta}_{02} = \dot{\varphi}_{02} - \dot{\psi}_{02} \end{cases} \quad (13.111)$$

The simulation results of the initial disturbance of a round of projectiles are shown in Table 13.4.

Table 13.4 Simulation results of initial disturbance of projectile

Initial disturbance	Vertical component	Lateral component
Deflection angle/(10^{-3} rad)	-0.2193	-0.0621
Swing angle/(10^{-3} rad)	-0.5071	1.9894
Swing angle velocity/(rad/s)	-2.5851	-0.5468

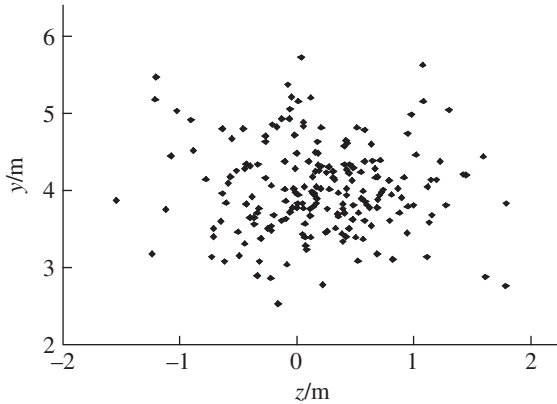


Figure 13.27 Simulation result of target impact dispersion.

13.8.7 Simulation Result and Test Verifying for Firing Dispersion

Using the six degrees of freedom rigid body ballistic model and considering the effects on the flight process of the projectile produced by random factors such as the deviation of projectile mass, mass eccentricity, dynamic unbalance and wind synthetically, the flight dynamic equation of the projectile is established. On the basis of the launch dynamics of self-propelled artillery based on the MSTMM, the simulation system for launch and flight dynamics is established and the simulations for launch and flight dynamics are achieved. Using Monte Carlo simulation technology and taking account of random variables such as the mass of the projectile, the mass of the propellant, the burning rate, the gap between the projectile and the barrel, the moment of inertia of the projectile, mass eccentricity, dynamic unbalance and wind speed, many simulation times for launch and flight dynamics are obtained, as well as the simulation results for the firing dispersion of a self-propelled artillery system.

According to the static measurement data in the firing dispersion test of self-propelled artillery, using the method mentioned above, the vertical target dispersion and ground dispersion can be simulated. These results can be used to discuss the influence of random factors on firing dispersion, and to analyze the measures for improving the firing dispersion of weapon systems. The simulation is carried out by adopting the same parameters of the experiment, such as the mean values and the variances of the mass eccentricity, dynamic unbalance, projectile/barrel clearance and propellant mass, etc. 200 and 100 rounds are simulated to evaluate the vertical target dispersion at 1000 m, and the ground dispersion at a maximum range of the self-propelled artillery, respectively. The simulation result of target impact dispersion is shown in Figure 13.27. The simulation results of target impact dispersion and firing dispersion are in good agreement with the test results (the detailed data are omitted), which shows that the theory of launch dynamics based on MSTMM can provide important technology support to improve the firing precision and other dynamic performance for self-propelled artillery.

14

Dynamics of Shipboard Launch Systems

14.1 Introduction

Shipboard launch systems are essential ship-borne weapons because of their rapid reaction, high firing rate, large allowance of ammunition, strong continuous fighting ability, difficult-to-intercept projectiles and high economic efficiency. These advantages make shipboard launch systems high-efficiency weapons against marine and aerial targets, as well as targets on land. Shipboard launch systems are powerful in modern warfare and many destroyers are equipped with 127-mm or 130-mm shipboard launch systems. Any launch system can be regarded as a nonlinear, time-variant multi-rigid-flexible-body system. The nonlinear and time-variant characteristics of shipboard launch systems include the time-variant mass distribution and stiffness distribution caused by the large motion of the gun body and the projectile during the launching process, and collisions induced by the projectile–barrel gap.

In this chapter, we utilize discrete time transfer matrix method for multi-rigid-flexible-body systems to solve some important problems in the launch dynamics of shipboard launch systems [112, 113].

14.2 Dynamics Model of Shipboard Launch Systems

Shipboard launch systems are usually fixed on the deck of the ship, as shown in Figure 14.1. The Russian AK-176 shipboard launch system is shown in Figure 14.2. Shipboard launch systems include a gun tube, breech, anti-recoil devices, cradle, elevating mechanism, equilibrator, casemate, traversing mechanism, chassis, ramming mechanism, feeding mechanism, projectile hoist, barrette, ship body and so on. The launch dynamic model of a shipboard launch system is shown in Figure 14.3. The shipboard launch system can be cut at various connection points because of its component nature and divided into a number of mechanical parts. The ship's body and barrette form rigid body 2. The revolving part, not including the tipping part, is rigid body 4. The tipping part, not including the recoiling part, is rigid body 6. The breech and the part of a gun tube that slides on the cradle form rigid body 8. The part of the gun barrel that runs out of the cradle is an elastic beam, numbered 10. The anti-recoil devices between the gun tube and the cradle are modeled as the massless sliding joint 7 and the spring-damper between 8 and 6, and the mass of anti-recoil devices is assigned to rigid bodies 8 and 6. The combination of the elevating mechanism and the equilibrator is regarded as the viscoelastic hinge 5 that joins 6 and 4. The masses of elevating mechanism and the equilibrator are merged into

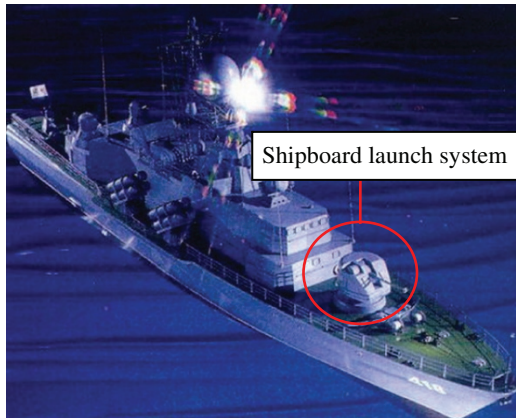


Figure 14.1 Russian Lightning class warship and AK-176 shipboard launch system.

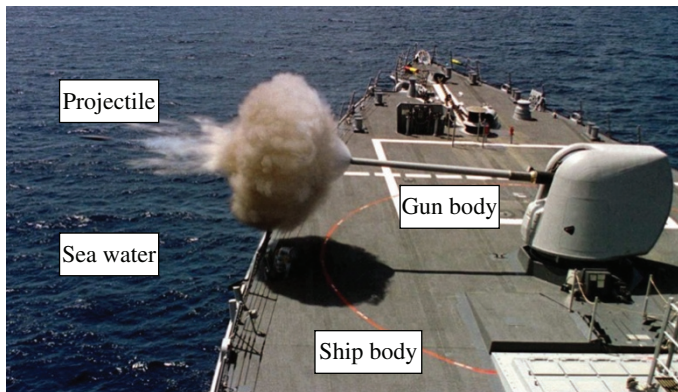


Figure 14.2 Russia AK-176 shipboard launch system.

rigid bodies 6 and 4 in the theoretical analysis. The traversing mechanism is modeled by the viscoelastic joint 3 that connects bodies 4 and 2, whose mass is merged into rigid bodies 4 and 2. The interactive force of the seawater on the ship's body is equivalent to the distributed-elastic-damping joint 1 [278]. Rigid body 8 and beam 10 are connected by a fixed joint 9. The parts below the seawater and the muzzle are regarded as the system boundaries and numbered 0 and 11, respectively. The launch dynamics model of a shipboard launch system has therefore developed as a nonlinear, time-variant multi-rigid-flexible-body system which moves under a powder gas drive. This system is composed of four rigid bodies and one elastic beam connected by a distributing elastic spring-damping joint, two elastic joints, one sliding joint and one fixed joint.

When the projectile is moving in the gun tube, the main body of the projectile is regarded as a rigid body, and its elasticity effect is equivalent to the contacting elasticity between the rotating band, the bourrelet and the tube bore wall account. The factors of mass eccentricity and dynamic unbalance of the projectile, and the force between the projectile-barrel and the powder gas thrust must be considered. Classical interior ballistic modeling has been used in the analysis.

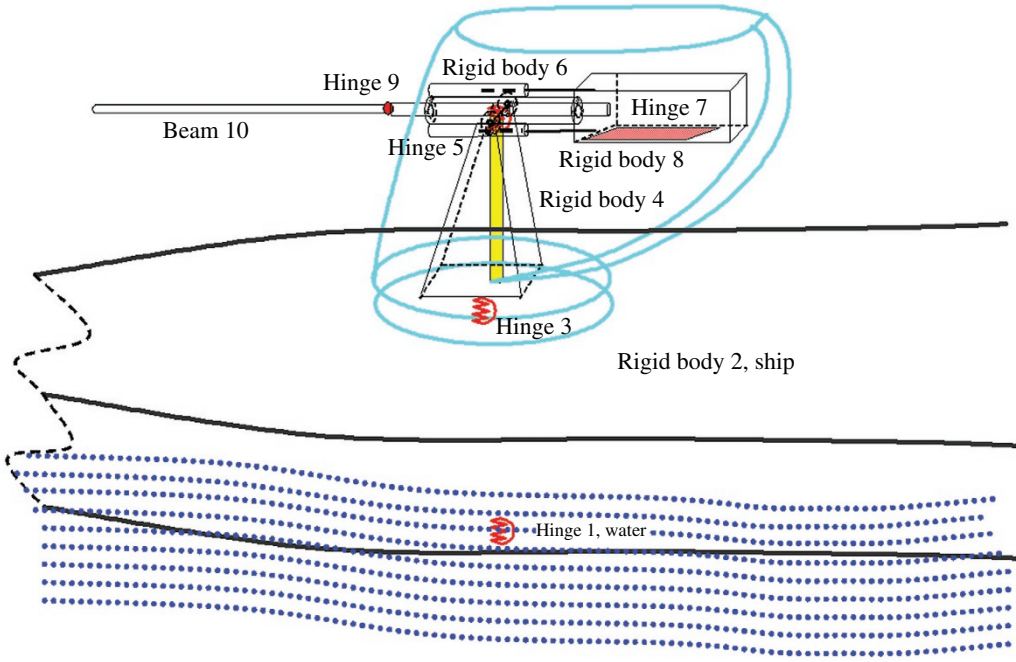


Figure 14.3 Launch dynamic model of a shipboard launch system.

14.3 State Vector, Transfer Equation and Transfer Matrix

Some state vectors, transfer equations and transfer matrices involved in the discrete time transfer matrix method for multibody systems (MSDTTMM) were introduced in Chapters 7 and 8. In this section, besides the above content, the special transfer matrices involved in the launch dynamics of shipboard launch systems will be introduced.

14.3.1 Distributed-Elastic-damping Foundation Equivalent to the Seawater

When the ship undergoes translational motion, the effect of seawater on the ship along the vertical orientation can be regarded as distributed elastic springs and dampers, but in the horizontal orientation there is only a damping effect. Likewise, only the damping effect is considered when the ship rotates around the vertical orientation. The effect of seawater on the ship can be modeled as the distributing spring and damper in the motion of ship rolling and pitching. Assuming that K_y^* is the distributing elastic coefficient of vertical orientation, and $K_x'^*$ and $K_z'^*$ are distributing rotational elastic coefficients, we obtain

$$\begin{aligned}
 -q_{y,O} &= \int_0^{l_x} \int_0^{l_z} [(y_O - y_I) + (\theta_{z,O} - \theta_{z,I})x - (\theta_{x,O} - \theta_{x,I})z] K_y^* dz dx \\
 &= (y_O - y_I) l_x l_z K_y^* + \frac{1}{2} (\theta_{z,O} - \theta_{z,I}) l_x^2 l_z K_y^* - \frac{1}{2} (\theta_{x,O} - \theta_{x,I}) l_x l_z^2 K_y^*
 \end{aligned} \tag{14.1}$$

$$m_{z,O} = \int_0^{l_x} (\theta_{z,O} - \theta_{z,I}) K_z'^* dx = (\theta_{z,O} - \theta_{z,I}) K_z'^* l_x \tag{14.2}$$

$$m_{x,O} = \int_0^{l_z} (\theta_{x,O} - \theta_{x,I}) K_x'^* dz = (\theta_{x,O} - \theta_{x,I}) K_x'^* l_z \quad (14.3)$$

where l_x and l_z are the length and width of the ship's bottom, respectively.

Considering the effect of damping, combining Equations (7.223), (14.2) and (14.3) yields

$$K'^* \left(\begin{bmatrix} \theta_x l_z \\ 0 \\ \theta_z l_x \end{bmatrix}_O - \begin{bmatrix} \theta_x l_z \\ 0 \\ \theta_z l_x \end{bmatrix}_I \right) + C'^* A_O H_O (C \theta_O + D \theta_O) - C'^* A_I H_I (C \theta_I + D \theta_I) - \begin{bmatrix} m_x \\ m_y \\ m_z \end{bmatrix}_I = \begin{bmatrix} 0 \\ 0 \\ 0 \end{bmatrix} \quad (14.4)$$

Rewriting the above equation gives

$$[\theta_x, \theta_y, \theta_z]_O^T = [O_{3 \times 3} \quad U_{22} \quad U_{23} \quad O_{3 \times 3} \quad U_{25}] z_I \quad (14.5)$$

where

$$U_{22} = N_O^{-1} N_I, \quad U_{23} = N_O^{-1}, \quad U_{25} = C'^* N_O^{-1} [A_I H_I D \theta_I - A_O H_O D \theta_O]$$

$$N_O = C'^* A_O H_O C + \begin{bmatrix} l_z K_x'^* & 0 & 0 \\ 0 & 0 & 0 \\ 0 & 0 & l_x K_z'^* \end{bmatrix}, \quad N_I = C'^* A_I H_I C + \begin{bmatrix} l_z K_x'^* & 0 & 0 \\ 0 & 0 & 0 \\ 0 & 0 & l_x K_z'^* \end{bmatrix}$$

Combining Equations (14.1), (14.4) and (8.221) gives

$$q_I + C^* C r_O + C^* D r_O - C^* C r_I - C^* D r_I + l_x l_z K_y^* \begin{bmatrix} 0 \\ y_O - y_I + \frac{1}{2} l_x (\theta_{z,O} - \theta_{z,I}) - \frac{1}{2} l_z (\theta_{x,O} - \theta_{x,I}) \\ 0 \end{bmatrix} = 0 \quad (14.6)$$

Rearranging this yields

$$[x, y, z]_O^T = [U_{11} \quad U_{12} \quad U_{13} \quad U_{14} \quad U_{15}] z_I \quad (14.7)$$

where

$$U_{11} = P_O^{-1} P_I, \quad U_{12} = P_O^{-1} P_\theta, \quad U_{13} = P_O^{-1} P_m, \quad U_{14} = -P_O^{-1}, \quad U_{15} = P_O^{-1} P_5$$

$$P_O = C^* C + \begin{bmatrix} 0 & 0 & 0 \\ 0 & l_x l_z K_y^* & 0 \\ 0 & 0 & 0 \end{bmatrix}, \quad P_I = C^* C + \begin{bmatrix} 0 & 0 & 0 \\ 0 & l_x l_z K_y^* & 0 \\ 0 & 0 & 0 \end{bmatrix}$$

$$P_\theta = \begin{bmatrix} 0, & \frac{1}{2} l_z l_x K_y^*, & 0 \end{bmatrix}^T \{ l_z [(u_{4,4} - 1) \quad u_{4,5} \quad u_{4,6}] - l_x [u_{6,4} \quad u_{6,5} \quad (u_{6,6} - 1)] \}$$

$$P_m = \begin{bmatrix} 0, & \frac{1}{2} l_z l_x K_y^*, & 0 \end{bmatrix}^T \{ l_z [u_{4,7} \quad u_{4,8} \quad u_{4,9}] - l_x [u_{6,7} \quad u_{6,8} \quad u_{6,9}] \}$$

$$P_5 = \begin{bmatrix} 0, & \frac{1}{2} l_z l_x K_y^*, & 0 \end{bmatrix}^T (l_z u_{4,13} - l_x u_{6,13}) - C^* D r_O + C^* D r_I$$

Thus the transfer equation of the distributed-elastic-damping foundation is

$$\mathbf{z}_O = \mathbf{U} \mathbf{z}_I \quad (14.8)$$

The state vectors are

$$\begin{cases} \mathbf{z}_I = [x, y, z, \theta_x, \theta_y, \theta_z, m_x, m_y, m_z, q_x, q_y, q_z, 1]_I^T \\ \mathbf{z}_O = [x, y, z, \theta_x, \theta_y, \theta_z, m_x, m_y, m_z, q_x, q_y, q_z, 1]_O^T \end{cases}$$

The transfer matrix is

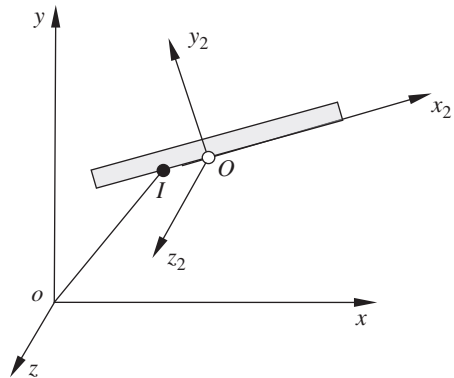
$$\mathbf{U} = \begin{bmatrix} \mathbf{U}_{11} & \mathbf{U}_{12} & \mathbf{U}_{13} & \mathbf{U}_{14} & \mathbf{U}_{15} \\ \mathbf{O}_{3 \times 3} & \mathbf{U}_{22} & \mathbf{U}_{23} & \mathbf{O}_{3 \times 3} & \mathbf{U}_{25} \\ \mathbf{O}_{3 \times 3} & \mathbf{O}_{3 \times 3} & \mathbf{I}_3 & \mathbf{O}_{3 \times 3} & \mathbf{O}_{3 \times 1} \\ \mathbf{O}_{3 \times 3} & \mathbf{O}_{3 \times 3} & \mathbf{O}_{3 \times 3} & \mathbf{I}_3 & \mathbf{O}_{3 \times 1} \\ \mathbf{O}_{1 \times 3} & \mathbf{O}_{1 \times 3} & \mathbf{O}_{1 \times 3} & \mathbf{O}_{1 \times 3} & 1 \end{bmatrix} \quad (14.9)$$

14.3.2 Sliding Joints

The gun tube moves on the cradle and mainly slides along the cradle axis under the action of anti-recoil devices and the resultant interaction force between the gun tube and the projectile during the launching process. If the connection constraint between the gun tube and the cradle is regarded as a sliding joint, the action of the anti-recoil devices is regarded as an external force and external moment between the gun tube and the cradle. The object shown in Figure 14.4 is a part of the gun tube. The interaction from the gun tube to the cradle is concentrated at point I and the interaction from the cradle to the gun tube is concentrated at point O . The input end I of the sliding joint is fixed on the cradle and the output end O of the sliding joint is fixed on the gun tube. We assume that points O and I coincide at the initial time and slide against each other. Let $Ox_2y_2z_2$ be the body-fixed coordinate system of the gun tube. Since the two rigid bodies only have relative linear motion along the x_2 axis, the rotation angles of these two bodies are equal. The projections of the position vectors of the input and output ends on the y_2 and z_2 axes are equal. Thus, we have

$$\theta_{j,I} = \theta_{j,O} \quad (j = x, y, z) \quad (14.10)$$

Figure 14.4 Model of a sliding hinge.



$$\begin{cases} y_{2,I} = y_{2,O} \\ z_{2,I} = z_{2,O} \end{cases} \quad (14.11)$$

If the friction and damping are eliminated we obtain

$$\begin{cases} q_{x_2,I} = q_{x_2,O} = 0 \\ q_{y_2,I} = q_{y_2,O} \\ q_{z_2,I} = q_{z_2,O} \end{cases} \quad (14.12)$$

$$\begin{bmatrix} m_x \\ m_y \\ m_z \end{bmatrix}_O = \begin{bmatrix} m_x \\ m_y \\ m_z \end{bmatrix}_I + (\tilde{\mathbf{r}}_O - \tilde{\mathbf{r}}_I) \begin{bmatrix} q_x \\ q_y \\ q_z \end{bmatrix}_I \quad (14.13)$$

The position coordinates of output end O and input end I in the inertia coordinate system are

$$\mathbf{r}_O = [x, y, z]_O^T, \quad \mathbf{r}_I = [x, y, z]_I^T$$

From Equations (14.12) and (14.13) we obtain

$$[q_x, q_y, q_z]_O^T = [q_x, q_y, q_z]_I^T \quad (14.14)$$

$$[a_{11} \ a_{21} \ a_{31}] [q_x, q_y, q_z]_I^T = 0 \quad (14.15)$$

Projecting Equation (14.11) onto the inertia coordinate system yields

$$\begin{bmatrix} a_{12} & a_{22} & a_{32} \\ a_{13} & a_{23} & a_{33} \end{bmatrix} \begin{bmatrix} x \\ y \\ z \end{bmatrix}_I = \begin{bmatrix} a_{12} & a_{22} & a_{32} \\ a_{13} & a_{23} & a_{33} \end{bmatrix} \begin{bmatrix} x \\ y \\ z \end{bmatrix}_O \quad (14.16)$$

where (a_{11}, a_{21}, a_{31}) , (a_{12}, a_{22}, a_{32}) and (a_{13}, a_{23}, a_{33}) are elements of the transformation matrix \mathbf{A} from the body-fixed coordinate system to the inertia coordinate system of the gun tube.

Let $\mathbf{r}' = \mathbf{r}_O - \mathbf{r}_I$, then from Equation (14.13) we obtain

$$\begin{bmatrix} m_x \\ m_y \\ m_z \end{bmatrix}_O = \begin{bmatrix} m_x \\ m_y \\ m_z \end{bmatrix}_I + \tilde{\mathbf{r}}' \begin{bmatrix} q_x \\ q_y \\ q_z \end{bmatrix}_I \approx \begin{bmatrix} m_x \\ m_y \\ m_z \end{bmatrix}_I + \left[\tilde{\mathbf{r}}'(t_{i-1}) + \dot{\tilde{\mathbf{r}}}'(t_{i-1})\Delta T + \frac{1}{2}\ddot{\tilde{\mathbf{r}}}'(t_{i-1})\Delta T^2 \right] \begin{bmatrix} q_x \\ q_y \\ q_z \end{bmatrix}_I \quad (14.17)$$

Combining Equation (14.10) and Equations (14.14) to (14.17), and expressing the transformation matrix as the known function of previous time step, the transfer matrix of the sliding joint is

$$\begin{bmatrix} \mathbf{U}_1^{(1)} & \mathbf{U}_1^{(2)} \end{bmatrix} \begin{bmatrix} \mathbf{z}_I \\ \mathbf{z}_O \end{bmatrix} = \mathbf{0} \quad (14.18)$$

where

$$\begin{cases} \mathbf{z}_I = [x, y, z, \theta_x, \theta_y, \theta_z, m_x, m_y, m_z, q_x, q_y, q_z, 1]^T_I \\ \mathbf{z}_O = [x, y, z, \theta_x, \theta_y, \theta_z, m_x, m_y, m_z, q_x, q_y, q_z, 1]^T_O \end{cases}$$

$$\mathbf{U}_1^{(1)} = \begin{bmatrix} \mathbf{O}_{3 \times 3} & \mathbf{I}_3 & \mathbf{O}_{3 \times 3} & \mathbf{O}_{3 \times 3} & \mathbf{O}_{3 \times 1} \\ \mathbf{O}_{3 \times 3} & \mathbf{O}_{3 \times 3} & \mathbf{O}_{3 \times 3} & \mathbf{I}_3 & \mathbf{O}_{3 \times 1} \\ \mathbf{O}_{1 \times 3} & \mathbf{O}_{1 \times 3} & \mathbf{O}_{1 \times 3} & \mathbf{U}_{34}^{(1)} & 0 \\ \mathbf{U}_{41}^{(1)} & \mathbf{O}_{2 \times 3} & \mathbf{O}_{2 \times 3} & \mathbf{O}_{2 \times 3} & \mathbf{O}_{2 \times 1} \\ \mathbf{O}_{3 \times 3} & \mathbf{O}_{3 \times 3} & \mathbf{I}_3 & \mathbf{U}_{54}^{(1)} & \mathbf{O}_{3 \times 1} \end{bmatrix}, \quad \mathbf{U}_1^{(2)} = \begin{bmatrix} \mathbf{O}_{3 \times 3} & -\mathbf{I}_3 & \mathbf{O}_{3 \times 3} & \mathbf{O}_{3 \times 3} & \mathbf{O}_{3 \times 1} \\ \mathbf{O}_{3 \times 3} & \mathbf{O}_{3 \times 3} & \mathbf{O}_{3 \times 3} & -\mathbf{I}_3 & \mathbf{O}_{3 \times 1} \\ \mathbf{O}_{1 \times 3} & \mathbf{O}_{1 \times 3} & \mathbf{O}_{1 \times 3} & \mathbf{O}_{1 \times 3} & 0 \\ \mathbf{U}_{41}^{(2)} & \mathbf{O}_{2 \times 3} & \mathbf{O}_{2 \times 3} & \mathbf{O}_{2 \times 3} & \mathbf{O}_{2 \times 1} \\ \mathbf{O}_{3 \times 3} & \mathbf{O}_{3 \times 3} & -\mathbf{I}_3 & \mathbf{O}_{3 \times 3} & \mathbf{O}_{3 \times 1} \end{bmatrix}$$

$$\mathbf{U}_{34}^{(1)} = [a_{11} \ a_{21} \ a_{31}], \mathbf{U}_{41}^{(1)} = -\mathbf{U}_{41}^{(2)} = \begin{bmatrix} a_{12} & a_{22} & a_{32} \\ a_{13} & a_{23} & a_{33} \end{bmatrix}, \mathbf{U}_{54}^{(1)} = \tilde{\mathbf{r}}(t_{i-1}) + \dot{\tilde{\mathbf{r}}}'(t_{i-1})\Delta T + \frac{1}{2}\ddot{\tilde{\mathbf{r}}}'(t_{i-1})\Delta T^2$$

(14.19)

The elements of the transformation matrix $a_{kj}(k, j = 1, 2, 3)$ are known as the functions of the previous time step.

14.4 Overall Transfer Equation of the System

According to the dynamic model of shipboard launch systems, the ship's body and barbette 2 are regarded as rigid bodies under the action of distributing the basic elastic and damping effect. The revolving part, except for the tipping part, is regarded as rigid body 4, which has one input end and one output end. The tipping part, except for the recoil part, is regarded as rigid body 6, which has one input end and one output end. The breech and the gun tube slide on the cradle are regarded as rigid body 8, which has one input end and one output end. The remaining part of the gun tube is regarded as beam 10. The action of seawater on shipboard is equivalent to the distributed elastic damping joints 1, 3, and 5, 7 is a smooth elastic damping composite joint which can be regarded as an elastic damping joint and a prismatic joint in series, whereas 9 is a fixed joint connecting the rigid body and the beam.

According to the launch dynamic model of the shipboard launch system, each element state vector of the system can be defined. $\mathbf{z}_{8,7}$ is the output end state vector of joint 7, which is located at a fixed point on the gun tube in contact with the cradle at the initial time.

The transfer matrix for distributing the basic elastic damping joint yields

$$\mathbf{z}_{0,1} = \mathbf{U}_1 \mathbf{z}_{2,1} \tag{14.20}$$

From the transfer matrix equation of a rigid body with one input end and one output end, the transfer equations for the ship's body, revolving body, cradle and breech can be obtained:

$$\mathbf{z}_{2,1} = \mathbf{U}_2 \mathbf{z}_{2,3} \tag{14.21}$$

$$\mathbf{z}_{4,3} = \mathbf{U}_4 \mathbf{z}_{4,5} \tag{14.22}$$

$$\mathbf{z}_{6,7} = \mathbf{U}_6 \mathbf{z}_{6,5} \quad (14.23)$$

$$\mathbf{z}_{8,9} = \mathbf{U}_8 \mathbf{z}_{8,7} \quad (14.24)$$

According to the transfer equation of an elastic damping joint, the transfer equations of elastic damping joints 3, 5 and 7 can be obtained:

$$\mathbf{z}_{2,3} = \mathbf{U}_3 \mathbf{z}_{4,3} \quad (14.25)$$

$$\mathbf{z}_{4,5} = \mathbf{U}_5 \mathbf{z}_{6,5} \quad (14.26)$$

$$\mathbf{z}_{6,7} = \mathbf{U}_7 \mathbf{z}'_{8,7} \quad (14.27)$$

According to the transfer matrix Equation (14.18) of a sliding joint, the transfer equation can be obtained:

$$\begin{bmatrix} \mathbf{U}_7^{(1)} & \mathbf{U}_7^{(2)} \end{bmatrix} \begin{bmatrix} \mathbf{z}'_{8,7} \\ \mathbf{z}_{8,7} \end{bmatrix} = \mathbf{0} \quad (14.28)$$

The transfer matrix Equation (8.193) of a fixed joint from a rigid body to a beam yields the transfer equation from rigid body 8 to flexible gun tube 10, that is

$$\mathbf{z}_{10,9} = \mathbf{U}_9 \mathbf{z}_{8,9} \quad (14.29)$$

According to the transfer matrix Equation (8.186) of a beam, the transfer equation of a flexible tube is

$$\mathbf{z}_{10,11} = \mathbf{U}_{10} \mathbf{z}_{10,9} \quad (14.30)$$

We obtain from the connection relationship of the shipboard launch system model:

$$\mathbf{z}_{0,1} = \mathbf{U}_1 \mathbf{U}_2 \mathbf{U}_3 \mathbf{U}_4 \mathbf{U}_5 \mathbf{U}_6 \mathbf{U}_7 \mathbf{z}'_{8,7} \quad (14.31)$$

$$\mathbf{z}_{10,11} = \mathbf{U}_{10} \mathbf{U}_9 \mathbf{U}_8 \mathbf{z}_{8,7} \quad (14.32)$$

Combining Equations (14.67), (14.70) and (14.71), the transfer equation of the shipboard launch system is

$$\mathbf{U}_{\text{all}} \mathbf{z}_{\text{all}} = \mathbf{0} \quad (14.33)$$

where

$$\mathbf{z}_{\text{all}} = \begin{bmatrix} \mathbf{z}_{0,1}^T, & \mathbf{z}'_{8,7}^T, & \mathbf{z}_{8,7}^T, & \mathbf{z}_{10,11}^T \end{bmatrix}^T \quad (14.34)$$

The overall transfer matrix of the shipboard launch system is

$$\mathbf{U}_{\text{all}} = \begin{bmatrix} -\mathbf{I}_{13} & \mathbf{U}_1 \mathbf{U}_2 \mathbf{U}_3 \mathbf{U}_4 \mathbf{U}_5 \mathbf{U}_6 \mathbf{U}_7 & \mathbf{O}_{13 \times 13} & \mathbf{O}_{13 \times (13+2n)} \\ \mathbf{O}_{(13+2n) \times 13} & \mathbf{O}_{(13+2n) \times 13} & \mathbf{U}_{10} \mathbf{U}_9 \mathbf{U}_8 & -\mathbf{I}_{13+2n} \\ \mathbf{O}_{12 \times 13} & \mathbf{U}_7^{(1)} & \mathbf{U}_7^{(2)} & \mathbf{O}_{12 \times (13+2n)} \end{bmatrix} \quad (14.35)$$

In conclusion, the overall transfer matrix of the shipboard launch system is obtained by combining the transfer matrices of the elements of the shipboard launch system. The process of establishing the overall transfer matrix of a system by using the transfer matrices of elements is just like the process of assembling the shipboard launch system by its parts. This is a simple and highly stable process.

14.5 Launch Dynamics Equation and Forces of the System

14.5.1 Force Analysis of the Shipboard Launch System

Only the external force is analyzed using the MSDTTMM. During the firing process, apart from the force of the projectile acting on the gun tube, the external force acting on the shipboard launch system involves total resistance to recoil, the powder gas's force acting on the gun tube and the projectile's force acting on the artillery. The interaction forces, such as the force between the cradle and the rotating body, the force between the rotating body and the ship's body etc., are internal forces, internal moments and the corresponding damping forces. The expressions of the force and moment are made simple by using the MSDTTMM.

The recoil resistance force F_R is

$$F_R = F_{\Phi h} + F_f + F + F_T - m_h g \sin \theta_1 \quad (14.36)$$

where $F_{\Phi h}$ is the recoil brake force, F_f is the recuperator force and F is the friction force of the sealing device. F_T is the friction force of the cradle guiderail, m_h is the mass of the recoiling parts and θ_1 is the setting departure angle.

The resultant force of the recoil brake and recuperator can be expressed as

$$F_{\Phi h} + F_f = \begin{cases} \left(\frac{k_1 (A_0 - A_p)^3}{2 a_x^2} + \frac{k_2 A_{fj}^3}{2 A_1^2} \right) \rho \dot{s}^2 + A_f P_{f0} \left(\frac{w_0}{w_0 + s A_f} \right)^n & (\dot{s} < 0) \\ - \frac{k_2 A_{fj}^3}{2 a_f^2} \rho \dot{s}^2 + A_f P_{f0} \left(\frac{w_0}{w_0 + s A_f} \right)^n & (\dot{s} > 0, \lambda + s \leq L_p) \\ - \left(\frac{k_{1f} A_{of}^3}{2 a_x^2} + \frac{k_{2f} (A_{fj} + a_f)^3}{2 a_f^2} \right) \rho \dot{s}^2 + A_f P_{f0} \left(\frac{w_0}{w_0 + s A_f} \right)^n & (\dot{s} > 0, \lambda + s > L_p) \end{cases} \quad (14.37)$$

where s is the recoil distance, \dot{s} is the recoil velocity and $A_0 = (D_T^2 - d_T^2)\pi/4$ is the working area of the recoil brake piston. D_T is the inner diameter of the recoil cylinder and d_T is the outer diameter of the recoil rod. $A_p = d_p^2\pi/4$ is the area of the throttling ring (d_p is the inner diameter of the throttling ring) and $A_{fj} = d_{fj}^2\pi/4$ is the working area of the return throttling device (d_{fj} is the inner diameter of the recoil rod). A_1 is the smallest cross-section area of the branch and $a_x = A_p - A_x$ is the area of the liquid orifice corresponding to an arbitrary cross-section of the throttling rod ($A_x = d_x^2\pi/4$ is an arbitrary cross-section area of the throttling rod and d_x is an arbitrary cross-section diameter of the throttling rod). k_1 is the coefficient of mainstream liquid resistance and k_2 is the coefficient of a branch liquid resistance. ρ is the liquid density, k_{1f} is the coefficient of recuperating hydraulic pressure resistance and k_{2f} is the coefficient of the hydraulic pressure resistance of the return throttling device. $A_{of} = \pi(D_T^2 - d_p^2)/4$ is the working area of the recoil brake piston while recuperating, a_f is the area of the hole of the return throttling device and P_{f0} is the initial gas pressure in the recuperator. A_f is the working area of the recuperator piston, w_0 is the initial gas volume in the recuperator, n is the polytrophic exponent and $\lambda = s|_{\dot{s}=0}$ is the recoiling length, $L_p = \lambda d_T^2/D_T^2$.

The two friction forces are

$$F = \nu m_h g \quad (14.38)$$

$$F_T = \mu m_h g \cos \theta_1 \quad (14.39)$$

where ν is the sealing device friction coefficient and μ is the cradle guide-rail friction coefficient.

When a projectile moves in the gun tube, the powder gas's resultant force F_{pt} acting on the gun tube is made up of two parts: the breech pressure F_t and the axial component F_{2M} of pressure on the chamber slope, that is

$$F_{pt} = F_t - F_{2M} \quad (14.40)$$

where

$$F_t = P_t A_t, \quad F_{2M} = P_t (A_t - A)$$

A_t is the area of the breech end, A is the cross-section area of the rifled gun bore and P_t is the breech pressure.

The resultant force in the bore at the beginning of the gun ulterior period (the after-effect period) is

$$F_g = \frac{1}{\phi} \left(1 + \frac{\omega}{2m} \right) A P_g \quad (14.41)$$

where P_g is the mean pressure of powder gas in the bore at the beginning of the gun ulterior period, ω is the main charge mass, m is the projectile mass and ϕ_1 is the coefficient of secondary work.

In the gun ulterior period, the process of powder gas outflow from the gun bore can be regarded as an ejection process of a semi-closed round-piped vessel with uniform cross-section. If there is no muzzle brake, the resultant force in the bore during the ulterior period is

$$F_{pt} = F_g e^{-b(t-t_g)} \quad (t_g < t \leq t_k) \quad (14.42)$$

$$b = \frac{(\beta - 0.5)\omega v_g}{A(P_g - P_R)}$$

where b is the decay factor, t_g is the time when the projectile flies out of the muzzle, t_k is the termination time of the gun ulterior period, P_R is the mean pressure of the powder gas in the gun bore at the end of the ulterior period, v_g is the muzzle speed of the projectile and β is the coefficient of the powder gas effect.

When the pressure of the powder gas in the gun tube falls to $P_R = 0.176 \text{ MPa}$, the gas exhaust ulterior period reaches its end. We have

$$P_R = P_g e^{-b(t_k - t_g)} = P_g e^{-b\tau}$$

that is

$$\tau = \frac{1}{b} \ln \frac{P_g}{P_R} \quad (14.43)$$

The formula for the resultant force in the bore F_{pt} is

$$F_{pt} = \begin{cases} A P_t & (0 \leq t \leq t_g) \\ F_g e^{-b(t-t_g)} & (t_g < t \leq t_g + \tau) \end{cases} \quad (14.44)$$

The interaction forces between the projectile and the gun tube includes the contact force of the rotating band and the front bourrelet, and these are introduced in the following.

14.5.1.1 Engraving Force to Gun Tube

The value of the engraving resistance from the projectile to the gun tube $f_{j,x}^c$ is equal to the engraving resistance F_j^c acting on the projectile, and its direction is along the tangential direction of bore axis pointing at muzzle. We have

$$f_{j,x}^c = -F_{j,O_3x'_0}^c \delta[x_1 - (x_p - l_R)] = \sigma_n A_n (\mu_n \cos \phi + \sin \phi) \delta[x_1 - (x_p - l_R)] \quad (14.45)$$

where

$$\delta[x_1 - (x_p - l_R)] = \begin{cases} 0 & (x_1 \neq x_p - l_R) \\ \infty & (x_1 = x_p - l_R) \end{cases} \quad (14.46)$$

$$\int_0^\infty \delta[x_1 - (x_p - l_R)] dx_1 = 1 \quad (0 < x_1 < \infty) \quad (14.47)$$

where x_1 is the coordinate of an arbitrary point in the bore wall on the x axis in the gun tube coordinate system, x_p is the coordinate of the projectile center of mass on the x axis in the gun tube coordinate system and l_R is the distance between the center of the rotating band and the projectile center of mass. $(x_p - l_R)$ is the distance between the breech end and the center of the rotating band or the coordinate of the center of the rotating band on the x axis in the gun tube coordinate system, and $\delta[x_1 - (x_p - l_R)]$ is the Dirac function.

14.5.1.2 Driving Side Force and Moment to the Gun Tube

Under the action of the driving side force, the driving resistance F_d^c and moment $C\ddot{\gamma}$ act on the projectile. Therefore, the driving side force $f_{d,x}^c$ and moment $m_{d,x}^c$ of the projectile to the gun tube are

$$f_{d,x}^c = -F_{d,O_3x'_0}^c \delta[x_1 - (x_p - l_R)] = \frac{2C\ddot{\gamma}(\mu_\tau \cos \alpha + \sin \alpha)}{(\cos \alpha - \mu_\tau \sin \alpha)d_0} \delta[x_1 - (x_p - l_R)] \quad (14.48)$$

$$m_{d,x}^c = -C\ddot{\gamma} \cdot \delta[x_1 - (x_p - l_R)] \quad (14.49)$$

where C is the polar inertia moment of the projectile and $\ddot{\gamma}$ is the angular velocity of the projectile.

14.5.1.3 Elastic Force and Moment between the Rotating Band and the Gun Tube

The applied forces caused by the elasticity and friction between the rotating band and the gun tube are

$$\begin{cases} f_{t,x}^c = K_b \mu_\tau \sqrt{\left(y'_{O_3O}\right)^2 + \left(z'_{O_3O}\right)^2} \cos \alpha \delta[x_1 - (x_p - l_R)] \\ f_{t,y}^c = K_b \left(y'_{O_3O} - z'_{O_3O} \mu_\tau \sin \alpha\right) \delta[x_1 - (x_p - l_R)] \\ f_{t,z}^c = K_b \left(z'_{O_3O} + y'_{O_3O} \mu_\tau \sin \alpha\right) \delta[x_1 - (x_p - l_R)] \end{cases} \quad (14.50)$$

According to the Winkler elastic basic model, the elastic basic moment and the friction moment of the rotating band to the gun tube are

$$\begin{cases} m_{t,x}^c = 0 \\ m_{t,y}^c = \left[K_b r_b \mu_\tau z'_{O_3O} \cos \alpha - K_b h^2 (-\delta_2^l + \delta_1^l \mu_\tau \sin \alpha) / 12 \right] \delta [x_1 - (x_p - l_R)] \\ m_{t,z}^c = \left[-K_b r_b \mu_\tau y'_{O_3O} \cos \alpha + K_b h^2 (\delta_1^l + \delta_2^l \mu_\tau \sin \alpha) / 12 \right] \delta [x_1 - (x_p - l_R)] \end{cases} \quad (14.51)$$

14.5.1.4 Effect of Front Bourrelet on the Gun Tube

The applied forces of the gun tube acting on the front bourrelet are

$$\begin{cases} f_x^s = \mu_1 F^s \cos \alpha \cdot \delta [x_1 - (x_p + l_1)] \\ f_y^s = F^s \left(-y'_{O_3O_2} + \mu_1 z'_{O_3O_2} \sin \alpha \right) / r_{O_3O_2} \delta [x_1 - (x_p + l_1)] \\ f_z^s = F^s \left(-z'_{O_3O_2} - \mu_1 y'_{O_3O_2} \sin \alpha \right) / r_{O_3O_2} \delta [x_1 - (x_p + l_1)] \end{cases} \quad (14.52)$$

where l_1 is the distance from the projectile center of mass to the front plane of the front bourrelet and $r_{O_3O_2}$ is the radial displacement of O_2 relative to the bore axis.

For a curved tube, the inner surface of the gun bore does not have axial symmetry, that is, the up-down surface areas of the gun bore neutral plane will not equal each other any more. When the gun bore is filled with high-pressure gas, the gas pressure makes the gun tube straight. This phenomenon is called the Bourdon effect and the force produced by the Bourdon effect is called the Bourdon force. The gun tube is not straight before firing. The Bourdon effect in a curving tube occurs when high-pressure gas fills the gun tube, therefore the gun tube is loaded by the Bourdon force during the firing process.

The Bourdon force that is vertical to the axis of the gun tube is the distribution force acting on the gun tube behind the projectile, and it relates to the gas pressure in the gun bore, inner diameter and curvature of the gun tube. The formula of the Bourdon force acting on unit length is

$$\begin{cases} \bar{f}_y^B = -\pi r_b^2 \frac{\partial^2 y}{\partial x_1^2} P_{x_1} H(x_p - l_R - x_1) \\ \bar{f}_z^B = -\pi r_b^2 \frac{\partial^2 z}{\partial x_1^2} P_{x_1} H(x_p - l_R - x_1) \end{cases} \quad (14.53)$$

$$H(x_p - l_R - x_1) = \begin{cases} 1 & (0 \leq x_1 < x_p - l_R) \\ 0 & (x_1 \geq x_p - l_R) \end{cases} \quad (14.54)$$

where x_1 is the distance from an arbitrary point in the chamber to the breech end, P_{x_1} is the gas pressure at x_1 , and $\partial^2 y / \partial x_1^2$ and $\partial^2 z / \partial x_1^2$ are the curvatures of the gun tube at x_1 . r_b is the inner diameter of the gun tube, $H(x_p - l_R - x_1)$ is the Heaviside function and x_p is the distance from the breech end to the projectile center of mass. l_R is the distance from the center of the rotating band to the projectile center of mass, thus $(x_p - l_R)$ is the distance from the breech end to the center of the rotating band.

14.5.2 Force Analysis of the Projectile

In general, the rotating band is made of material that has good tractility. After launch ignition, the projectile makes the rotating band distort to embed into the rifling continually under high temperature and high-pressure powder gas. The rifling here means “the cutting of spiral grooves on the inside of the barrel of the gun tube”. Generally, the process from ignition to the rotating band being completely embedded into the rifling is called the engraving process. The force status between the rotating band and the gun tube is complex during the engraving process. After the rotating band is embedded into the rifling, the twist angle of the rifling brings the driving side force between the rotating band and the rifling. Under the action of this force, projectile motion is affected by a rotating moment around the bore axis and the driving resistance force, which stops the projectile moving forward. When relative displacement arises between the centers of the rotating band and the bore axis because of the elasticity of the rotating band, the projectile is affected by elastic resilience. The rotating band and the gun bore are contacted via surfaces. When the geometry symmetric axis $o_1\xi$ of the projectile and the bore axis o_0x_0 deviate from each other, a basic restoring moment arises between the rotating band and the gun bore. During the launching process, some forces and moments between the rotating band and the gun bore have to be considered, that is, the engraving force and its moment, and the driving side force and its moment.

14.5.2.1 Engraving Resistance and its Moment

Engraving resistance can prevent a projectile moving forward and such a force is induced by the plasticity deformation of the rotating band when the rotating band embeds the rifling. It is expressed by F_j^c and is related to the stress σ_n of the rotating band groove, the engraving contact area A_n , the coefficient of friction μ_n and the forcing cone angle ϕ , while it points at the breech along the bore axis. The matrix form of F_j^c in the gun tube coordinate system $o_0x_0y_0z_0$ is

$$\begin{bmatrix} F_{j,o_0x_0}^c \\ F_{j,o_0y_0}^c \\ F_{j,o_0z_0}^c \end{bmatrix} = \begin{bmatrix} -\sigma_n A_n (\mu_n \cos \phi + \sin \phi) \\ 0 \\ 0 \end{bmatrix} \quad (14.55)$$

where A_n is the engraving contact area.

When engraving happens, the motion speed of the rotating band is not very high, therefore the coefficient of friction can be replaced by the static coefficient of friction. In general, the static coefficient of friction of copper to steel is $\mu_n = 0.36-0.53$. The stress σ_n of the rotating band groove can be computed with the following formula:

$$\sigma_n = \frac{\sigma_s (1 - \xi/\sqrt{3})}{\sqrt{(1 + 3\mu^2) - 2\xi/\sqrt{3}}} \quad (14.56)$$

For a copper rotating band, let $\xi = 0$ and $\mu = \sqrt{3}/3$, thus $\sigma_n = \sigma_s/\sqrt{2}$ and $\sigma_n = \sigma_s/\sqrt{2}$.

The expression for the engraving resistance moment M_{j,o_1}^c in the body-fixed coordinate system $o_1\xi\eta\zeta$ is

$$\begin{bmatrix} M_{j,o_0x_0}^c \\ M_{j,o_0y_0}^c \\ M_{j,o_0z_0}^c \end{bmatrix} = \begin{bmatrix} 0 \\ l_R \delta_2^I \sigma_n A_n (\mu_n \cos \phi + \sin \phi) \\ -l_R \delta_1^I \sigma_n A_n (\mu_n \cos \phi + \sin \phi) \end{bmatrix} \quad (14.57)$$

where l_R is the distance from the center of the rotating band to the geometry center.

14.5.2.2 Driving Side Force and its Moment

After the projectile was engraved into the rifling, under the action of the powder gas pressure and the driving side force of the rifling, the projectile moves straight along the bore axis and rotates at the same time. There are some contact and friction forces between the driving side of each rifling and the rotating band. Integrating this contact force along the gun bore axial direction integral yields a total resultant force, denoted by N_t . Its effect can be divided into two parts, one is a driving resistance force F_d^c , which prevents the projectile moving forward, the other is a moment $C\ddot{\gamma}$, which makes the projectile spin in the bore axis.

It can be verified that

$$N_t = \frac{2C\ddot{\gamma}}{(\cos\alpha - \mu_\tau \sin\alpha)d_0} \quad (14.58)$$

where α is the twist angle of the rifling and μ_τ is the sliding coefficient of friction between the rotating band and the rifling.

The sliding coefficient of friction μ_τ between the copper rotating band and the rifling adopts a combing formula, that is

$$\mu_\tau = \begin{cases} 0.4 & (0 \leq \sigma_n u_q < 0.714) \\ 0.6017 - 0.315(\sigma_n u_q) + 0.0447(\sigma_n u_q)^2 & (0.714 \leq \sigma_n u_q < 2.143) \\ 0.223 - 0.04946(\sigma_n u_q) + 0.00348(\sigma_n u_q)^2 & (2.143 \leq \sigma_n u_q < 4.286) \\ 0.1408 - 0.01844(\sigma_n u_q) + 0.00071(\sigma_n u_q)^2 & (4.286 \leq \sigma_n u_q < 12.888) \\ 0.021 & (12.888 \leq \sigma_n u_q) \end{cases} \quad (14.59)$$

where the unit of $\sigma_n u_q$ is GPa·m/s.

For a rifled gun, the twist angle of the gun tube rifling is a function of the projectile travel distance x_q . For the combined twist rifling whose first part is increasing twist rifling and second part is uniform twist rifling, we have

$$\alpha = \begin{cases} \arctan(\tan\alpha_0 + k_\alpha x_q) & (x < l_\alpha) \\ \alpha_g & (x \geq l_\alpha) \end{cases} \quad (14.60)$$

where l_α is the position of the switch point of uniform twist rifling and increasing twist rifling, α_0 is the initial twist angle of the rifling, α_g is the twist angle of the muzzle rifling and $k_\alpha = (\tan\alpha_g - \tan\alpha_0)/l_\alpha$.

From Equation (14.44), the relationship between the spin angle of the projectile and the displacement of the projectile x_q is

$$\gamma = \begin{cases} \frac{2\tan\alpha_0}{d_0}x_q + \frac{k_\alpha}{d_0}x_q^2 & (x_q < l_\alpha) \\ \frac{2\tan\alpha_g}{d_0}x_q - \frac{k_\alpha}{d_0}l_\alpha^2 & (x_q \geq l_\alpha) \end{cases} \quad (14.61)$$

Differentiating Equation (14.45) yields

$$\dot{\gamma} = \begin{cases} \frac{2\tan\alpha_0}{d_0}u_q + \frac{2k_\alpha}{d_0}x_q u_q & (x_q < l_\alpha) \\ \frac{2\tan\alpha_g}{d_0}u_q & (x_q \geq l_\alpha) \end{cases}, \quad \ddot{\gamma} = \begin{cases} \frac{2\tan\alpha_0}{d_0}a_q + \frac{2k_\alpha}{d_0}(u_q^2 + x_q a_q) & (x_q < l_\alpha) \\ \frac{2\tan\alpha_g}{d_0}a_q & (x_q \geq l_\alpha) \end{cases} \quad (14.62)$$

where u_q and a_q are the longitudinal velocity and longitudinal acceleration of the projectile relative to the gun bore, respectively.

The driving resistance force F_d^c in the gun tube coordinate system $O_3x'_0y'_0z'_0$ can be written in matrix form

$$\begin{bmatrix} F_{d,O_3x'_0}^c \\ F_{d,O_3y'_0}^c \\ F_{d,O_3z'_0}^c \end{bmatrix} = \begin{bmatrix} -N_t(\mu_\tau \cos \alpha + \sin \alpha) \\ 0 \\ 0 \end{bmatrix} = \frac{-2C\ddot{\gamma}(\mu_\tau \cos \alpha + \sin \alpha)}{(\cos \alpha - \mu_\tau \sin \alpha)d_0} \begin{bmatrix} 1 \\ 0 \\ 0 \end{bmatrix} \quad (14.63)$$

The driving resistance moment M_{d,O_1}^c in the body-fixed coordinate system $O_1\xi'\eta'\zeta'$ can also be written in matrix form

$$\begin{bmatrix} M_{d,O_1\xi'}^c \\ M_{d,O_1\eta'}^c \\ M_{d,O_1\zeta'}^c \end{bmatrix} = C\ddot{\gamma} \begin{bmatrix} 1 \\ -\delta_1^I \\ -\delta_2^I \end{bmatrix} + \frac{2C\ddot{\gamma}(\mu_\tau \cos \alpha + \sin \alpha)}{(\cos \alpha - \mu_\tau \sin \alpha)d_0} \begin{bmatrix} 0 \\ l_R\delta_2^I \\ -l_R\delta_1^I \end{bmatrix} \quad (14.64)$$

14.5.3 Launch Dynamics Equation of a Projectile

In the 1980s, the general motion differential equation of a projectile in a gun tube was developed by Marting, which brought research into projectile motion in a gun tube into a new phase. One weakness of Marting's model is that it does not consider the dynamic unbalance of the projectile and dealing with the mass eccentricity of the projectile is not reasonable enough, but these two factors are very important in the study of launch dynamics. To address this, the authors made an essential improvement to Marting's model and developed a uniform form of the dynamics equation of nonsymmetrical projectile motion in a gun tube and the ulterior period.

Considering the effect of the weight of the projectile in the bore, the contact force between the rotating band and gun bore, the air pressure of the powder gas and the contact force between the bourrelet and the gun tube and the corresponding moment, the dynamic equations of a nonsymmetrical projectile undergoing general motion in an increasingly twisted rifling gun tube are

$$\begin{aligned} a_p &= \frac{P_b S_b}{m \varphi_3} - \frac{\partial^2 x'}{\partial t^2} \\ \ddot{y}'_{oc} &= -g \cos \theta_1 - \frac{K}{m}(y'_{oo} - \mu z'_{oo} \sin \alpha) + \frac{F_y^{sf}}{m} - \ddot{y}'_o \\ \ddot{z}'_{oc} &= \frac{-K}{m}(z'_{oo} + \mu y'_{oo} \sin \alpha) + \frac{F_z^{sf}}{m} - \ddot{z}'_o \\ \ddot{\delta}_1^I &= -\frac{C}{A}\dot{\gamma}(\dot{\psi}_2^I + \dot{\delta}_2^I) + \left(1 - \frac{C}{A}\right)(\dot{\gamma}^2 \beta_{D_\eta} + \ddot{\gamma} \beta_{D_\xi}) - \frac{C\ddot{\gamma}}{A}\delta_2^I + \frac{P_b S_b}{A \varphi_3} y'_{oc} - \frac{K h^2}{12A}(\delta_1^I - \delta_2^I \mu \sin \alpha) \\ &\quad + \frac{K(l_R + r_b \mu)}{A} y'_{oo} - \frac{K l_R \mu \sin \alpha}{A} z'_{oo} + \frac{l_1}{A} F_y^{sf} - \ddot{\psi}_1^I \\ \ddot{\delta}_2^I &= \frac{C}{A}\dot{\gamma}(\dot{\psi}_1^I + \dot{\delta}_1^I) + \left(1 - \frac{C}{A}\right)(\dot{\gamma}^2 \beta_{D_\xi} - \ddot{\gamma} \beta_{D_\eta}) + \frac{C\ddot{\gamma}}{A}\delta_1^I + \frac{P_b S_b}{A \varphi_3} z'_{oc} - \frac{K h^2}{12A}(\delta_2^I + \delta_1^I \mu \sin \alpha) \\ &\quad + \frac{K(l_R + r_b \mu)}{A} z'_{oo} + \frac{K}{A} l_R \mu y'_{oo} \sin \alpha + \frac{l_1}{A} F_z^{sf} - \ddot{\psi}_2^I \end{aligned}$$

$$\gamma = \frac{\tan \alpha}{r_b} x + \frac{k_\alpha}{2r_b} x^2 + \gamma_0 \quad (14.65)$$

where y'_{oc} and z'_{oc} are the vertical and lateral displacements of the center of mass of the projectile relative to the gun tube coordinate system $O_3x'_oy'_oz'_o$, respectively. $a_p = \ddot{x}'_{O_3}$ is the acceleration of the center of mass of the projectile relative to the gun tube, δ_1^I and δ_2^I are the pitch and revolution angles, respectively, formed by the misalignment of the tangent line of tube and projectile axes, and γ is the rotation angle of the projectile in the gun tube. P_b is the pressure of the projectile base, S_b is the area of the projectile base and m is the mass of the projectile. φ_3 is the coefficient of second work, θ_1 is the setting fire angle of the artillery and g is the acceleration due to gravity. $K = \pi r_b k h$ is the equivalence stiffness coefficient when the projectile contacts the bore wall, h is the width of the rotating band and r_b is the radius of the projectile bourrelet. μ is the coefficient of friction between the rotating band and the bore wall, α is the rifling twist angle and A is the equator rotation inertia of the projectile. C is the polar inertia moment, l_R is the distance from the centroid to the center of the rotating band and l_1 is the distance from the center of mass of the projectile to the front plane of the bourrelet. $\partial^2 x' / \partial t^2$ is the recoiling acceleration of the gun tube and x is the distance from the rotating band to the beginning of the rifling in the equation of the spin angle. The dynamic unbalance of the projectile is $\beta_D = \beta_{D_1} + i\beta_{D_2}$, where $\beta_{D_\eta} = \beta_{D_1} \cos \gamma - \beta_{D_2} \sin \gamma$ is the projection of the dynamic unbalance on the η axis of the body-fixed coordinate system and $\beta_{D_\xi} = \beta_{D_1} \sin \gamma + \beta_{D_2} \cos \gamma$ is the projection of the dynamic unbalance on the ξ axis of the body-fixed coordinate system. The mass eccentricity of the projectile is $L_m = L_{m_1} + iL_{m_2}$, where $L_{m_\eta} = L_{m_1} \cos \gamma - L_{m_2} \sin \gamma$ is the projection of the mass eccentricity on the η axis of the body-fixed coordinate system and $L_{m_\xi} = L_{m_1} \sin \gamma + L_{m_2} \cos \gamma$ is the projection of the mass eccentricity on the ξ axis of the body-fixed coordinate system. y'_o and z'_o are the vertical and lateral displacements of the center of mass of the projectile relative to the aiming line, respectively, and $\psi_1^I = \partial y'_o / \partial x$ and $\psi_2^I = \partial z'_o / \partial x$ are the vertical and lateral components of the angle between the tangent of the tube axis and the line of sight. Differentiating twice with respect to time yields

$$\begin{aligned} \dot{y}'_o &= \frac{d y'_o}{dt} = \frac{\partial y'_o}{\partial t} + \frac{\partial y'_o}{\partial x} v_p, \quad \ddot{y}'_o = \frac{d^2 y'_o}{dt^2} = \frac{\partial^2 y'_o}{\partial t^2} + 2 \frac{\partial^2 y'_o}{\partial x \partial t} v_p + \frac{\partial^2 y'_o}{\partial x^2} v_p^2 + \frac{\partial y'_o}{\partial x} a_p \\ \dot{z}'_o &= \frac{d z'_o}{dt} = \frac{\partial z'_o}{\partial t} + \frac{\partial z'_o}{\partial x} v_p, \quad \ddot{z}'_o = \frac{d^2 z'_o}{dt^2} = \frac{\partial^2 z'_o}{\partial t^2} + 2 \frac{\partial^2 z'_o}{\partial x \partial t} v_p + \frac{\partial^2 z'_o}{\partial x^2} v_p^2 + \frac{\partial z'_o}{\partial x} a_p \\ \dot{\psi}_1^I &= \frac{d \psi_1^I}{dt} = \frac{\partial^2 y'_o}{\partial x \partial t} + \frac{\partial^2 y'_o}{\partial x^2} v_p, \quad \ddot{\psi}_1^I = \frac{d^2 \psi_1^I}{dt^2} = \frac{\partial^3 y'_o}{\partial x \partial t^2} + 2 \frac{\partial^3 y'_o}{\partial x^2 \partial t} v_p + \frac{\partial^3 y'_o}{\partial x^3} v_p^2 + \frac{\partial^2 y'_o}{\partial x^2} a_p \\ \dot{\psi}_2^I &= \frac{d \psi_2^I}{dt} = \frac{\partial^2 z'_o}{\partial x \partial t} + \frac{\partial^2 z'_o}{\partial x^2} v_p, \quad \ddot{\psi}_2^I = \frac{d^2 \psi_2^I}{dt^2} = \frac{\partial^3 z'_o}{\partial x \partial t^2} + 2 \frac{\partial^3 z'_o}{\partial x^2 \partial t} v_p + \frac{\partial^3 z'_o}{\partial x^3} v_p^2 + \frac{\partial^2 z'_o}{\partial x^2} a_p \end{aligned} \quad (14.66)$$

y'_{oo} and z'_{oo} are the vertical and lateral displacements of the center of the rotating band relative to the gun tube coordinate system $O_3x'_oy'_oz'_o$, respectively, that is

$$\begin{cases} y'_{oo} = y'_{oc} - L_{m_\eta} - l_R \delta_1^I \\ z'_{oo} = z'_{oc} - L_{m_\xi} - l_R \delta_2^I \end{cases} \quad (14.67)$$

F^{sf} is the contact force between the bourrelet and the bore, including collision and friction forces, that is

$$F^{sf} = -F^s(1 + i\mu_1 \sin \alpha)e^{i\beta_3} \quad (14.68)$$

where

$$\begin{cases} F_y^{sf} = -F^s(\cos \beta_3 - \mu_1 \sin \alpha \sin \beta_3) \\ F_z^{sf} = -F^s(\sin \beta_3 + \mu_1 \sin \alpha \cos \beta_3) \end{cases} \quad (14.69)$$

$$\beta_3 = \arctan \left[(z'_{oc} - L_{m_\zeta} + l_1 \delta_2^l) / (y'_{oc} - L_{m_\eta} + l_1 \delta_1^l) \right]$$

$$F^s = (b\dot{r}_{02} + K_1)(r_{02} - E)$$

μ_1 is the coefficient of friction between the bourrelet and the bore.

14.5.4 Equations of Classical Interior Ballistics

Classical interior ballistics theory has been used widely and can satisfy engineering requirements in many respects because it is a simple model on a small computational scale. The basic assumptions of classical interior ballistics are:

- 1) The propellant bed burns at the same time and the initial pressure is the ignition pressure.
- 2) The firing gas keeps the same components, and the physical and chemical performance parameters are all constant.
- 3) Propellant burning obeys geometric burning law and exponential burning rate law, and the firing gas obeys the Nobel–Abel equation.
- 4) The gas pressure in the gun tube obeys the Lagrange assumption.

The equations of interior ballistics are

$$\begin{aligned} \frac{dl}{dt} &= v \\ \frac{dv}{dt} &= \frac{SP}{\varphi m} \\ \frac{dZ}{dt} &= \frac{u_1}{e_1} P^\nu \\ SP(l_\psi + l) &= f\omega\psi - (\gamma - 1)\varphi m v^2 / 2 \\ l_\psi &= l_0 \left[1 - \Delta(1 - \psi)/\rho_p - \alpha\Delta\psi \right] \\ \psi &= \begin{cases} \chi Z(1 + \lambda Z + \mu Z^2) & (Z \leq 1) \\ \chi_s Z(1 + \lambda_s Z) & (1 < Z \leq Z_k) \end{cases} \end{aligned} \quad (14.70)$$

where l is the projectile travel distance, v is the velocity of the projectile and S is the area of the projectile base. m is the mass of the projectile, φ is the coefficient of second work and Z is the relative burning thickness of the propellant. e_1 , u_1 and ν are half thickness, burning rate coefficient and burning rate exponent of propellant, respectively. P is the average pressure in the gun tube, ψ is the relative burning volume of the propellant and l_ψ is the chamber volume-to-bore area ratio. ω is the charge mass, l_0 is the length of the powder chamber and α is the volume of powder gas. Δ is the loading density and ρ_p is the propellant solid density. χ , λ , μ , χ_s and λ_s are the

shape characteristic parameters of the powder, while γ is the adiabatic exponent of the powder gas.

The pressure of the projectile base P_b is

$$P_b = \frac{P}{1 + \frac{\omega}{3\varphi_1 m}} \quad (14.71)$$

$$\Delta = \frac{\omega}{W_0} \quad (14.72)$$

where W_0 is the chamber volume, φ_1 is the coefficient of resistance and $\varphi_1 = \varphi - \omega/(3m)$.

The distribution of gas pressure in the gun tube is

$$P_{x_1} = P_b \left[1 + \frac{\omega}{2\varphi_1 m} \left(1 - \frac{x_1^2}{L^2} \right) \right] \quad (14.73)$$

The breech pressure is

$$P_t = P_b \left(1 + \frac{\omega}{2\varphi_1 m} \right) \quad (14.74)$$

14.6 Solution of Shipboard Launch System Motion

Substituting the system boundary conditions

$$\begin{cases} \mathbf{z}_{0,1} = [0, 0, 0, 0, 0, 0, m_x, m_y, m_z, q_x, q_y, q_z, 1]_{0,1}^T \\ \mathbf{z}_{10,11} = [x, y, z, \theta_x, \theta_y, \theta_z, 0, 0, 0, 0, 0, 0, q^1, q^2, \dots, q^n, 1]_{10,11}^T \end{cases}$$

into Equation (14.33), the motion of the shipboard launch system can be obtained. Thus, Equation (14.33) can be rewritten as

$$\bar{\mathbf{U}}_{\text{all}} \bar{\mathbf{z}}_{\text{all}} = -\mathbf{f} \quad (14.75)$$

where $\bar{\mathbf{z}}_{\text{all}}$ is the residue column matrix after removing the zero state variables and 1 from the overall boundary state vector \mathbf{z}_{all} , and $\bar{\mathbf{U}}_{\text{all}}$ is a matrix with $(36 + 2n)$ order obtained from \mathbf{U}_{all} after the columns 1–6, 13, 26, 39, 46–51 and $52 + 2n$, and rows 13 and $26 + 2n$ have been deleted. \mathbf{f} is a column matrix obtained from adding columns 13, 26, 39 and $52 + 2n$ of \mathbf{U}_{all} and then deleting rows 13 and $26 + 2n$.

Thus, the matrix order involved in solving the dynamics of a complex shipboard launch MRFS by the MSTMM is low. The order of the transfer matrix of the system is $36 + 2n$, but the degrees of freedom of a discrete system in a hybrid system are 24. The matrix order is much smaller than the matrix order $[2 \times (30 + 2n)]$ obtained by ordinary methods, therefore the computational efficiency is very high.

$\bar{\mathbf{z}}_{\text{all}}$ is obtained by solving the linear algebraic Equations (14.75), consequently \mathbf{z}_{all} is determined. The state vectors of any of the connection points can be determined by using the transfer equations of the elements, and the system motion can be obtained.

The algorithm for solving the motion of a shipboard launch system is as follows:

- 1) Confirm the initial conditions and boundary conditions of the system: let $i = 1$.
- 2) Obtain the values of A, B_z, C, D_z, \dots on the various element joints using the linearization method.

- 3) Let the motion parameters of the system at time t_i be the initial values, then the motion parameters of the projectile, the resultant force of the gun bore and the applied force of the projectile barrel are solved from the equations of the launch dynamics of the projectile (Equation (14.49)) and equations of interior ballistics (Equation (14.54)), and the resistance to recoil is solved from Equation (14.20).
- 4) Compute the transfer matrix of the element and the overall transfer equation of the system by regarding the resultant force of the gun bore, the applied force of projectile-barrel and the resistance to recoil as external forces.
- 5) Compute the unknown quantities of the boundary state vectors using boundary conditions and the overall transfer equation of the system.
- 6) Compute the state vectors of the connection point at time t_{i+1} using the transfer equations of the elements.
- 7) Compute the position coordinates and attitude angles, and the corresponding velocities and accelerations using the state vector at t_{i+1} .
- 8) Let $i = i + 1$, treat the computational result of step (7) as the initial conditions, and return to step (2) until the time required for complete analysis.

In conclusion, it is simple, efficient and highly programmable to solve the dynamics response of a complex shipboard launch the MRFS by using the MSDTTMM.

14.7 Dynamics Simulation of the System and its Test Verifying

14.7.1 Launch Dynamics Simulation System for a Shipboard Launch System

The numerical simulation system of the launch dynamics of the shipboard launch system is established based on the MSDTTMM. The launch dynamics process of a large-caliber shipboard launch system with zero angle of elevation and zero angle of azimuth is numerically simulated. The vibration characteristics, rule of motion and initial disturbance of the projectile in the gun bore and the dynamic response of artillery are obtained. A related experiment is used to verify the simulation results. Some computation and experiment results are as follows.

14.7.2 Dynamics Simulation and Test Verifying for a Shipboard Launch System

The simulation results of the dynamic response of a shipboard launch system obtained by the launch dynamics simulation system for shipboard launch systems, as well as the corresponding experiment results, are shown in Figures 14.5–14.12. The simulation results for the muzzle position coordinate along the x axis are shown in Figure 14.5 and the simulation results for the time-history of resistance to recoil are shown in Figure 14.6. Figures 14.7 and 14.8 show the simulation results of the time-history of the muzzle position coordinate along the y and z axes, respectively. Figures 14.9 and 14.10 show the time history of the muzzle speed along the y and z axes, respectively. Figures 14.11 and 14.12 are plots of the simulation and experiment results for the lateral and vertical deflection angles of the muzzle. These figures show that the numerical simulation of launch dynamics for the shipboard launch system is in good agreement with the experiment results.

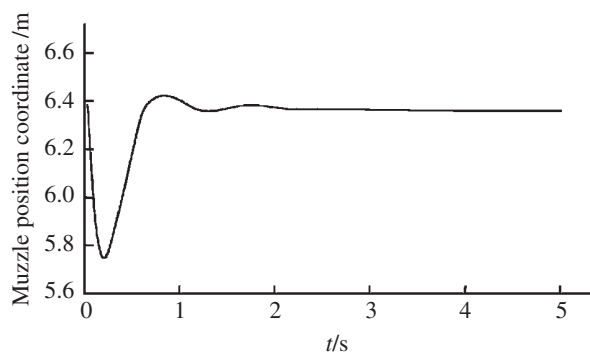


Figure 14.5 Muzzle position coordinate along the x axis.

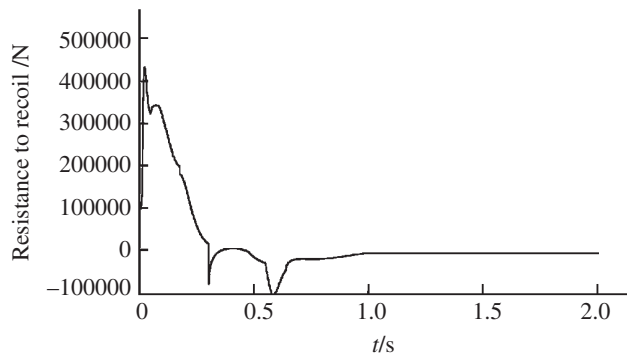


Figure 14.6 Time history of recoil.

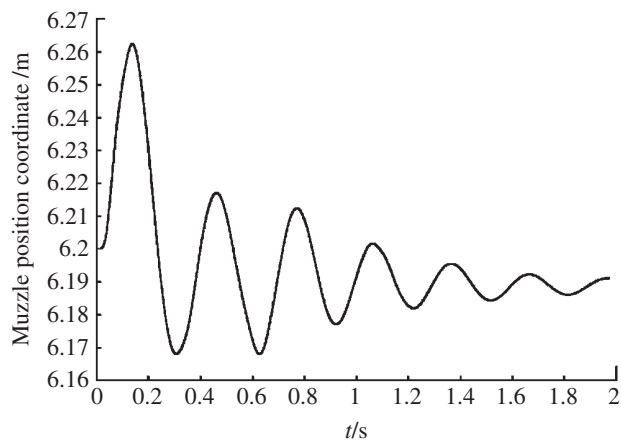


Figure 14.7 Muzzle position coordinate along the y axis.

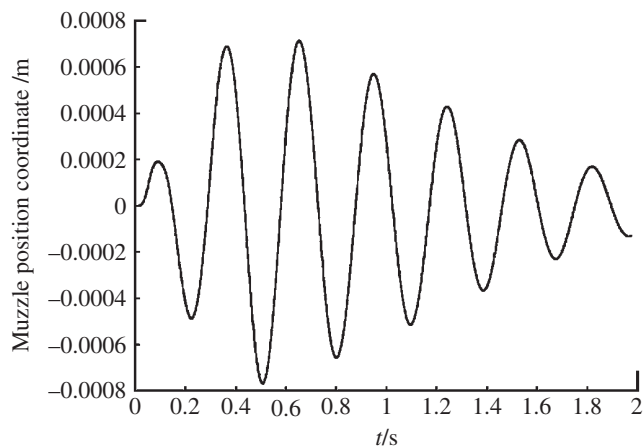


Figure 14.8 Muzzle position coordinate along the z axis.

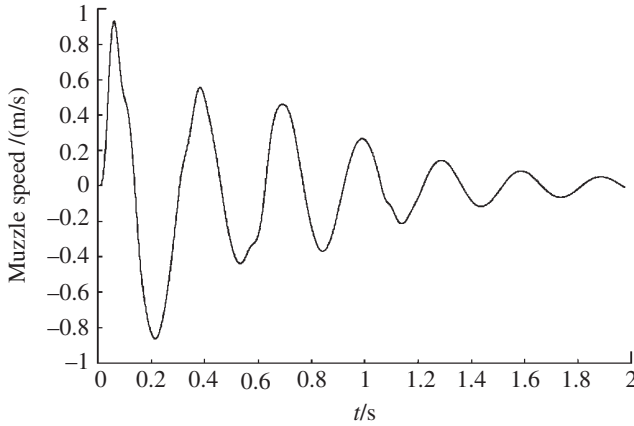
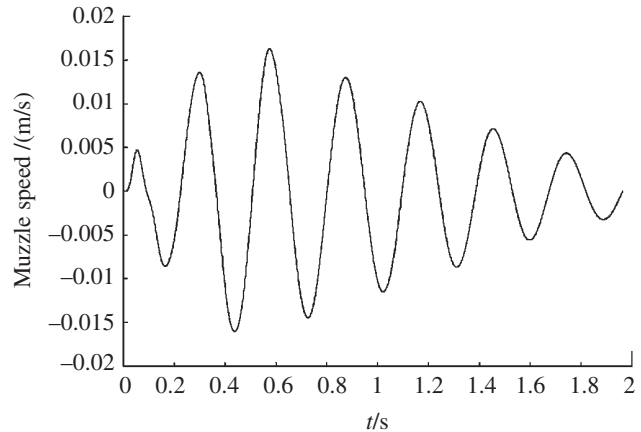


Figure 14.9 Muzzle speed along the y axis.

Figure 14.10 Muzzle speed along the z axis.



14.7.3 Launch Dynamic Simulation Result for a Projectile

The launch dynamic simulation results for a projectile obtained using the numerical simulation system of the launch dynamics of the shipboard launch system are shown in Figures 14.13–14.24. These figures show the time histories of the longitudinal displacement (Figure 14.13), the longitudinal velocity (Figure 14.14), the longitudinal acceleration (Figure 14.15) and the transverse displacement of the projectile (Figure 14.16), the collision force of the projectile-barrel (Figure 14.17), the transverse speed of the mass centre of the projectile (Figure 14.18), and the lateral and vertical swing angles of the projectile axis (Figures 14.19 and 14.20, respectively). The lateral and vertical swing angular speeds of the projectile axis are shown in Figures 14.21 and 14.22, respectively. The time histories of the yaw angle and the mass center trajectory of the projectile are presented in Figures 14.23 and 14.24, respectively.

14.7.4 Simulation and Test Verifying of Eigenfrequencies

The vibration characteristics of a large-caliber shipboard launch system when the angle of elevation and the angle of azimuth are both zero are numerically simulated using the launch

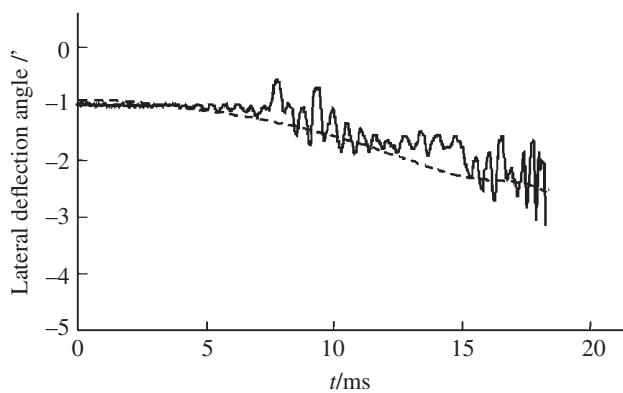


Figure 14.11 Simulation and experiment results of the lateral deflection angle of the muzzle.

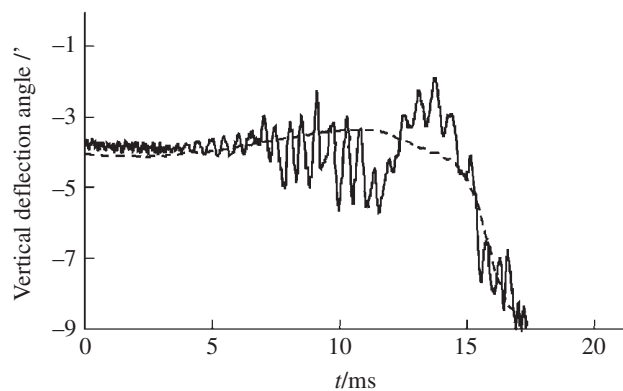


Figure 14.12 Simulation and experiment results of the vertical deflection angle of the muzzle.

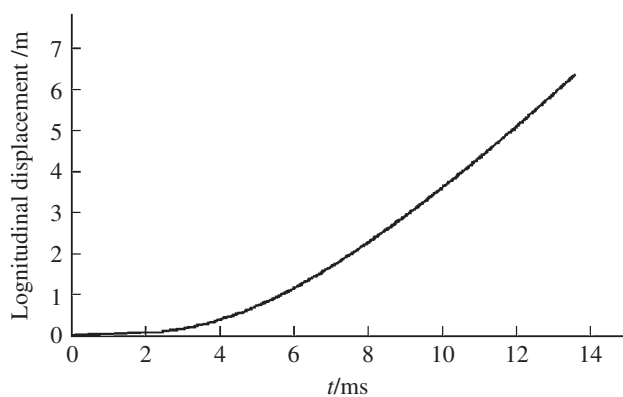


Figure 14.13 Longitudinal displacement.

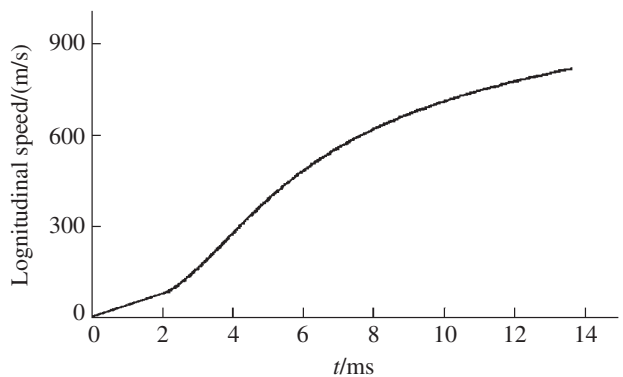


Figure 14.14 Longitudinal velocity.

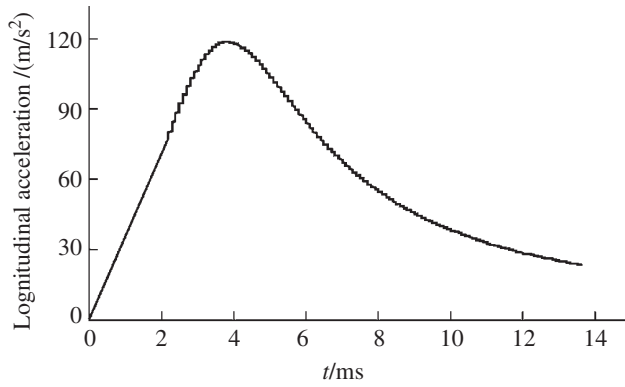


Figure 14.15 Longitudinal acceleration.

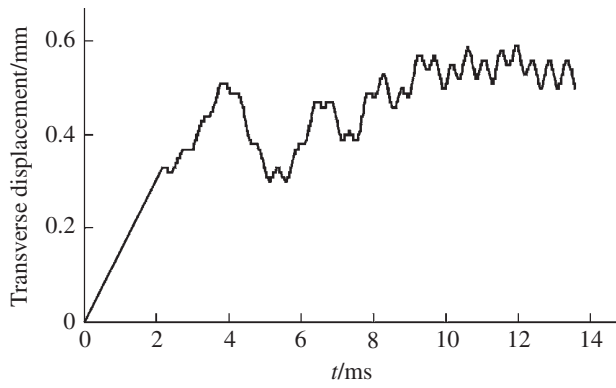


Figure 14.16 Transverse displacement.

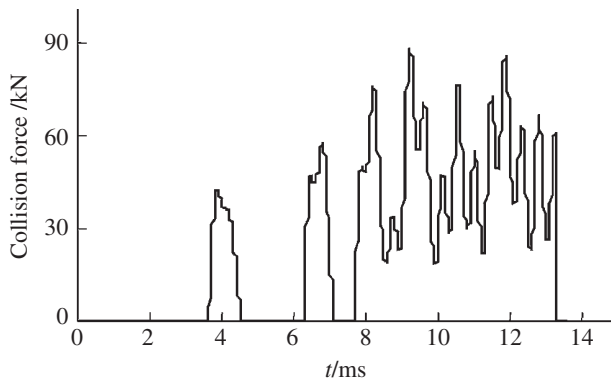


Figure 14.17 Collision force of the projectile-barrel.

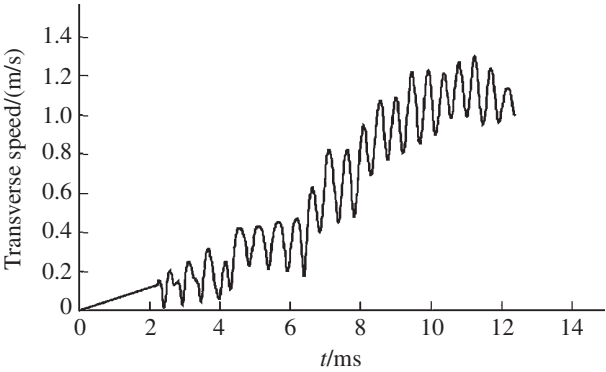


Figure 14.18 Transverse velocity of the center of mass of the projectile.

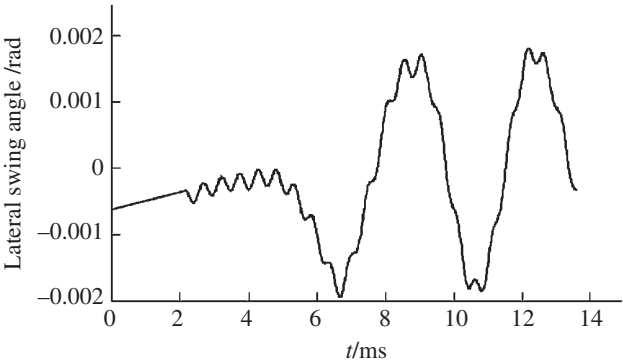


Figure 14.19 Lateral swing angle of the projectile axis.

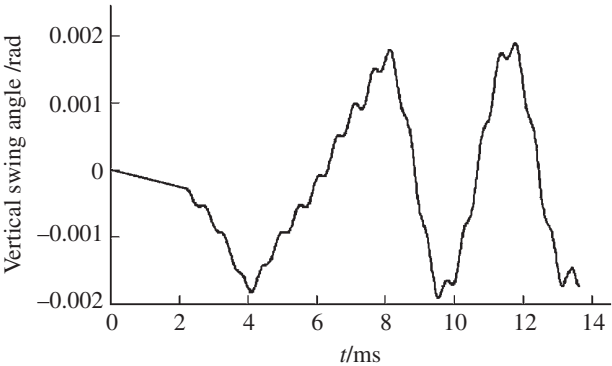


Figure 14.20 Vertical swing angle of the projectile axis.

Figure 14.21 Lateral swing angular velocity.

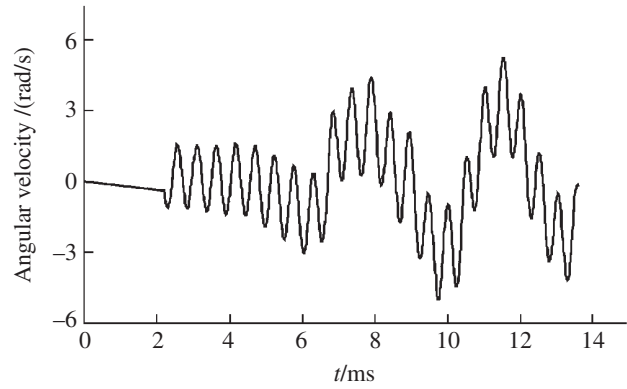


Figure 14.22 Vertical swing angular velocity.

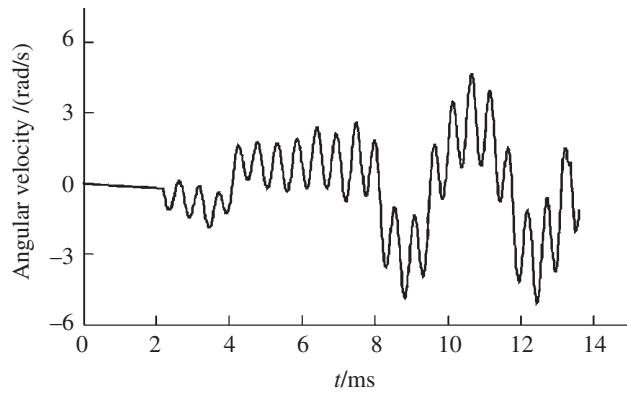
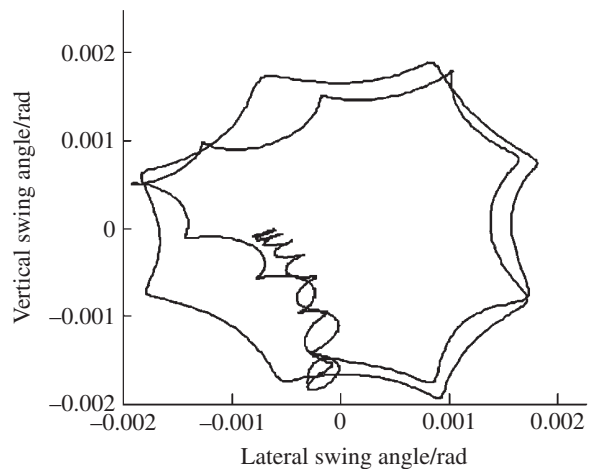


Figure 14.23 Track of yaw angle of the projectile axis.



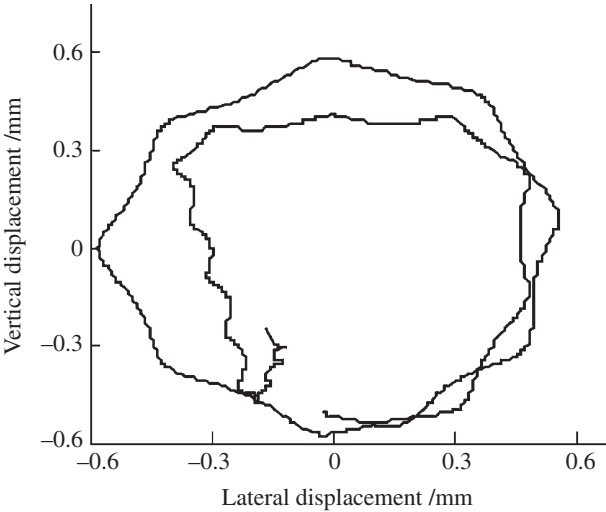


Figure 14.24 Track of the center of mass of the projectile.

Table 14.1 Simulation and experiment results of eigenfrequencies

Modal order, k	$\omega_k/(\text{rad/s})$		Relative error/%	Modal order, k	$\omega_k/(\text{rad/s})$		Relative error/%
	Simulation	Experiment			Simulation	Experiment	
1	6.3	6.26	1.27	9	26.9	—	—
2	7.6	—	—	10	32.1	—	—
3	11.3	11.24	0.85	11	34.6	36.86	-6.13
4	11.4	11.25	1.7	12	38.8	41.12	-5.49
5	15.5	—	—	13	43.4	42.41	2.33
6	18.9	—	—	14	64.0	60.51	5.89
7	20.7	21.32	-2.61	15	65.1	67.77	-3.92
8	26.1	—	—	16	74.4	74.35	0.08

dynamics numerical simulation system for a shipboard launch system. A modal experiment is carried out, and the modal parameters of the shipboard launch system are obtained. The simulation and experiment results of the first 16 order eigenfrequencies are shown in Table 14.1. It can be seen that the numerical simulations and the experiment results are in good agreement, which validates the simulation results.

15

Transfer Matrix Library for Multibody Systems

15.1 Introduction

Applying transfer matrix method for multibody systems (MSTMM) to solve the eigenvalue problem of linear time-invariant multibody systems, steady-state response and the dynamics problem of general multibody systems requires the transfer matrices of elements to be gathered into the overall transfer matrix of the system. From the boundary conditions of the system, we can easily compute the dynamics of the system by solving the overall transfer equation and the transfer equation of each element. The transfer matrix of each element has an important feature, that is, the element has the same transfer matrix even in a different system if it has the same connection relationship and motion mode. This feature makes the solution process of multibody system dynamics very simple and convenient. Once the transfer matrix of a certain element has been derived, it can be used for the same kind of elements in different multibody systems.

The transfer matrices of various elements [279–452] are listed in this chapter so readers can check them when they are needed. If the transfer matrix of a new element is not found in this chapter, readers can derive the corresponding transfer matrix using the proposed methods in Chapters 5, 6, 7, 8 and 10, and add it to the transfer matrix library. The transfer matrix library can be used to solve the dynamics problems of various complex multibody systems, including chain multibody systems, branch multibody systems, closed-loop multibody systems, network multibody systems and controlled multibody systems, for example the eigenvalue problem of linear multibody systems, the steady-state response of linear multibody systems, the steady-state response of nonlinear multibody systems, the dynamics of multi-rigid-body systems (MRSs), the dynamics of multi-rigid-flexible-body systems (MRFs) and the dynamics of controlled systems. The library of transfer matrices for multibody systems provides an important tool for setting up dynamic simulation software with powerful functions and high computational speed. This is an important research branch in this field. Readers and experts in other fields are welcome to cooperate in this area by supplying the transfer matrices of new elements in research and engineering which are not listed in this library. The authors will continue to provide the transfer matrices of new elements, and add bricks and tiles to the development of the transfer matrix library for multibody systems, the MSTMM and MBD.

15.2 Springs

Different kinds of springs are shown in Figure 15.1.

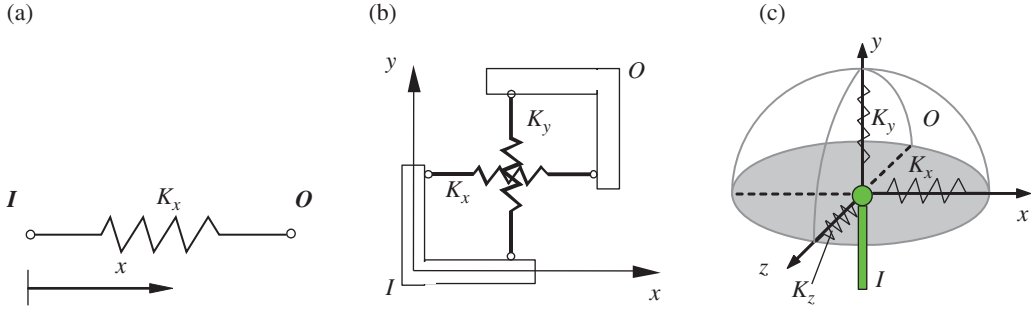


Figure 15.1 Springs for longitudinal vibrations: (a) one-dimensional, (b) two-dimensional and (c) three-dimensional.

15.2.1 One-dimensional Longitudinal Vibration

The state vector is

$$\mathbf{Z} = [X, Q_x]^T$$

The transfer matrix is

$$\mathbf{U} = \begin{bmatrix} 1 & -\frac{1}{K_x} \\ 0 & 1 \end{bmatrix} \quad (15.1)$$

where K_x is the stiffness of the spring.

15.2.2 Longitudinal Vibration in Plane

The state vector is

$$\mathbf{Z} = [X, Y, Q_x, Q_y]^T$$

The transfer matrix is

$$\mathbf{U} = \begin{bmatrix} 1 & 0 & -\frac{1}{K_x} & 0 \\ 0 & 1 & 0 & -\frac{1}{K_y} \\ 0 & 0 & 1 & 0 \\ 0 & 0 & 0 & 1 \end{bmatrix} \quad (15.2)$$

where K_x and K_y are the stiffnesses of the springs in the x and y directions, respectively.

15.2.3 Longitudinal Vibration in Space

The state vector is

$$\mathbf{Z} = [X, Y, Z, Q_x, Q_y, Q_z]^T$$

The transfer matrix is

$$U = \begin{bmatrix} I_3 & K \\ O_{3 \times 3} & I_3 \end{bmatrix}, \quad K = \begin{bmatrix} -\frac{1}{K_x} & 0 & 0 \\ 0 & -\frac{1}{K_y} & 0 \\ 0 & 0 & -\frac{1}{K_z} \end{bmatrix} \quad (15.3)$$

where K_x , K_y and K_z are the stiffnesses of the springs in the x , y and z directions, respectively.

15.3 Rotary Springs

Different kinds of rotary springs are shown in Figure 15.2.

15.3.1 One-dimensional Torsional Vibration

The state vector is

$$Z = [\theta_z, M_z]^T$$

The transfer matrix is

$$U = \begin{bmatrix} 1 & \frac{1}{K'_z} \\ 0 & 1 \end{bmatrix} \quad (15.4)$$

where K'_z is the torsional stiffness of the rotary spring.

15.3.2 Torsional Vibration in Plane

The state vector is

$$Z = [\theta_x, \theta_z, M_x, M_z]^T$$

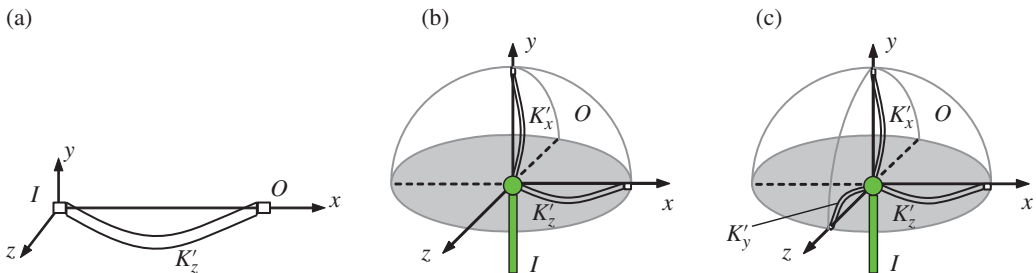


Figure 15.2 Rotary springs of torsion vibration: (a) one-dimensional, (b) two-dimensional and (c) three-dimensional.

The transfer matrix is

$$\mathbf{U} = \begin{bmatrix} 1 & 0 & 1/K'_x & 0 \\ 0 & 1 & 0 & 1/K'_z \\ 0 & 0 & 1 & 0 \\ 0 & 0 & 0 & 1 \end{bmatrix} \quad (15.5)$$

where K'_x and K'_z are the torsional stiffnesses of the rotary springs about the x and z directions, respectively.

15.3.3 Torsional Vibration in Space

The state vector is

$$\mathbf{Z} = [\theta_x, \theta_y, \theta_z, M_x, M_y, M_z]^T$$

The transfer matrix is

$$\mathbf{U} = \begin{bmatrix} \mathbf{I}_3 & \mathbf{K}' \\ \mathbf{O}_{3 \times 3} & \mathbf{I}_3 \end{bmatrix}, \quad \mathbf{K}' = \begin{bmatrix} \frac{1}{K'_x} & 0 & 0 \\ 0 & \frac{1}{K'_y} & 0 \\ 0 & 0 & \frac{1}{K'_z} \end{bmatrix} \quad (15.6)$$

where K'_x, K'_y and K'_z are the torsional stiffnesses of the rotary springs about the x, y and z axes, respectively.

15.4 Elastic Hinges

Different of elastic hinges are shown in Figure 15.3.

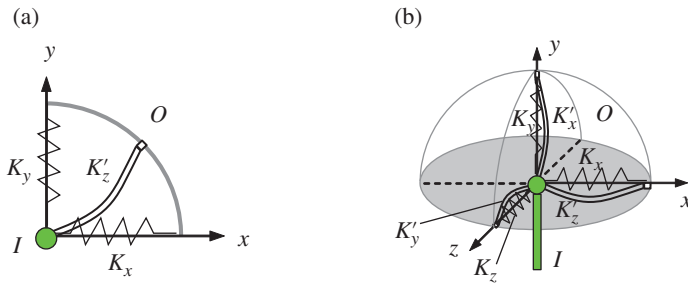


Figure 15.3 Elastic hinges: (a) planar elastic hinge and (b) spacial elastic hinge.

15.4.1 The Planar Elastic Hinge

The state vector is

$$\mathbf{Z} = [\theta_x, \theta_y, \theta_z, M_x, M_y, M_z]^T$$

The transfer matrix is

$$\mathbf{U} = \begin{bmatrix} \mathbf{I}_3 & \mathbf{U}_{1,2} \\ \mathbf{O}_{3 \times 3} & \mathbf{I}_3 \end{bmatrix}, \quad \mathbf{U}_{1,2} = \begin{bmatrix} 0 & -\frac{1}{K_x} & 0 \\ 0 & 0 & -\frac{1}{K_y} \\ \frac{1}{K'_z} & 0 & 0 \end{bmatrix} \quad (15.7)$$

where K_x and K_y are the stiffness of the springs in the x and y directions, respectively, and K'_z is the torsional stiffness of the rotary spring in the z direction.

15.4.2 The Spatial Elastic Hinge

The state vector is

$$\mathbf{Z} = [X, Y, Z, \theta_x, \theta_y, \theta_z, M_x, M_y, M_z, Q_x, Q_y, Q_z]^T$$

The transfer matrix is

$$\mathbf{U} = \begin{bmatrix} \mathbf{I}_3 & \mathbf{O}_{3 \times 3} & \mathbf{O}_{3 \times 3} & \mathbf{K} \\ \mathbf{O}_{3 \times 3} & \mathbf{I}_3 & \mathbf{K}' & \mathbf{O}_{3 \times 3} \\ \mathbf{O}_{3 \times 3} & \mathbf{O}_{3 \times 3} & \mathbf{I}_3 & \mathbf{O}_{3 \times 3} \\ \mathbf{O}_{3 \times 3} & \mathbf{O}_{3 \times 3} & \mathbf{O}_{3 \times 3} & \mathbf{I}_3 \end{bmatrix} \quad (15.8)$$

where

$$\mathbf{K} = \begin{bmatrix} -\frac{1}{K_x} & 0 & 0 \\ 0 & -\frac{1}{K_y} & 0 \\ 0 & 0 & -\frac{1}{K_z} \end{bmatrix}, \quad \mathbf{K}' = \begin{bmatrix} \frac{1}{K'_x} & 0 & 0 \\ 0 & \frac{1}{K'_y} & 0 \\ 0 & 0 & \frac{1}{K'_z} \end{bmatrix}$$

where K_x, K_y and K_z are the stiffnesses of the springs in the x, y and z directions, respectively, and K'_x, K'_y and K'_z are the torsional stiffness of the rotary springs about the x, y and z axes, respectively.

15.5 Lumped Mass Vibrating in a Longitudinal Direction

15.5.1 Lumped Mass with Longitudinal Vibration

The state vector is

$$\mathbf{Z} = [X, Q_x]^T$$

The transfer matrix is

$$\mathbf{U} = \begin{bmatrix} 1 & 0 \\ m\omega^2 & 1 \end{bmatrix} \quad (15.9)$$

where m is the mass of the lumped mass and ω is the eigenfrequency.

15.5.2 Lumped Mass with Longitudinal Vibration in a Plane

The state vector is

$$\mathbf{Z} = [X, Y, Q_x, Q_y]^T$$

The transfer matrix is

$$\mathbf{U} = \begin{bmatrix} 1 & 0 & 0 & 0 \\ 0 & 1 & 0 & 0 \\ m\omega^2 & 0 & 1 & 0 \\ 0 & m\omega^2 & 0 & 1 \end{bmatrix} \quad (15.10)$$

15.5.3 Lumped Mass with Longitudinal Vibration in Space

The state vector is

$$\mathbf{Z} = [X, Y, Z, Q_x, Q_y, Q_z]^T$$

The transfer matrix is

$$\mathbf{U} = \begin{bmatrix} \mathbf{I}_3 & \mathbf{O}_{3 \times 3} \\ \mathbf{U}_{2,1} & \mathbf{I}_3 \end{bmatrix}, \quad \mathbf{U}_{2,1} = \begin{bmatrix} m\omega^2 & 0 & 0 \\ 0 & m\omega^2 & 0 \\ 0 & 0 & m\omega^2 \end{bmatrix} \quad (15.11)$$

15.6 Vibration of Rigid Bodies

15.6.1 Planar Vibration of a Rigid Body with One Input End and One Output End

The state vector is

$$\mathbf{Z} = [X, Y, \Theta_z, M_z, Q_x, Q_y]^T$$

The transfer matrix is

$$\mathbf{U} = \begin{bmatrix} 1 & 0 & -b_2 & 0 & 0 & 0 \\ 0 & 1 & b_1 & 0 & 0 & 0 \\ 0 & 0 & 1 & 0 & 0 & 0 \\ -m\omega^2(b_2 - c_{c2}) & m\omega^2(b_1 - c_{c1}) & -\omega^2[J_I - m(b_2 c_{c2} + b_1 c_{c1})] & 1 & -b_2 & b_1 \\ m\omega^2 & 0 & -m\omega^2 c_{c2} & 0 & 1 & 0 \\ 0 & m\omega^2 & m\omega^2 c_{c1} & 0 & 0 & 1 \end{bmatrix} \quad (15.12)$$

where ω is the eigenfrequency, m is the mass of the rigid body and J_I is the moment of inertia with respect to point I . (b_1, b_2) are the position coordinates of the output end O and (c_{c1}, c_{c2}) are the position coordinates of the mass center C .

If only the transverse displacement and torsional vibration of the rigid body are considered, the longitudinal displacement can be neglected and the state vector is defined as

$$\mathbf{Z} = [Y, \Theta_z, M_z, Q_y]^T$$

The transfer matrix is

$$\mathbf{U} = \begin{bmatrix} 1 & b_1 & 0 & 0 \\ 0 & 1 & 0 & 0 \\ m\omega^2(b_1 - c_{c1}) & -\omega^2(J_I - mb_1c_{c1}) & 1 & b_1 \\ m\omega^2 & m\omega^2c_{c1} & 0 & 1 \end{bmatrix} \quad (15.13)$$

15.6.2 Spatial Vibration of a Rigid Body with One Input End and One Output End

The state vector is

$$\mathbf{Z} = [X, Y, Z, \Theta_x, \Theta_y, \Theta_z, M_x, M_y, M_z, Q_x, Q_y, Q_z]^T$$

The transfer matrix is

$$\mathbf{U} = \begin{bmatrix} \mathbf{I}_3 & -\tilde{\mathbf{l}}_{IO} & \mathbf{O}_{3 \times 3} & \mathbf{O}_{3 \times 3} \\ \mathbf{O}_{3 \times 3} & \mathbf{I}_3 & \mathbf{O}_{3 \times 3} & \mathbf{O}_{3 \times 3} \\ m\omega^2\tilde{\mathbf{l}}_{CO} & -\omega^2(m\tilde{\mathbf{l}}_{IO}\tilde{\mathbf{l}}_{IC} + \mathbf{I}_I) & \mathbf{I}_3 & \tilde{\mathbf{l}}_{IO} \\ m\omega^2\mathbf{I}_3 & -m\omega^2\tilde{\mathbf{l}}_{IC} & \mathbf{O}_{3 \times 3} & \mathbf{I}_3 \end{bmatrix} \quad (15.14)$$

where

$$\mathbf{J}_I = \begin{bmatrix} J_x & -J_{xy} & -J_{xz} \\ -J_{xy} & J_y & -J_{yz} \\ -J_{xz} & -J_{yz} & J_z \end{bmatrix}, \tilde{\mathbf{l}}_{IO} = \begin{bmatrix} 0 & -b_3 & b_2 \\ b_3 & 0 & -b_1 \\ -b_2 & b_1 & 0 \end{bmatrix}, \tilde{\mathbf{l}}_{IC} = \begin{bmatrix} 0 & -c_{c3} & c_{c2} \\ c_{c3} & 0 & -c_{c1} \\ -c_{c2} & c_{c1} & 0 \end{bmatrix}, \tilde{\mathbf{l}}_{CO} = \tilde{\mathbf{l}}_{IO} - \tilde{\mathbf{l}}_{IC}$$

which is decomposed in a body-fixed coordinate system with origin the input end I , \mathbf{J}_I is the inertia matrix with respect to point I , (b_1, b_2, b_3) are the position coordinates of the output end O and (c_{c1}, c_{c2}, c_{c3}) are the position coordinates of the mass center C .

The state vector is defined as

$$\mathbf{Z} = [Z, \Theta_x, \Theta_y, M_x, M_y, Q_z]^T$$

The corresponding transfer matrix is

$$\mathbf{U} = \begin{bmatrix} 1 & b_2 & -b_1 & 0 & 0 & 0 \\ 0 & 1 & 0 & 0 & 0 & 0 \\ 0 & 0 & 1 & 0 & 0 & 0 \\ m\omega^2(b_2 - c_{c2}) & u_{4,2} & u_{4,3} & 1 & 0 & b_2 \\ -m\omega^2(b_1 - c_{c1}) & u_{5,2} & u_{5,3} & 0 & 1 & -b_1 \\ m\omega^2 & m\omega^2c_{c2} & -m\omega^2c_{c1} & 0 & 0 & 1 \end{bmatrix} \quad (15.15)$$

where

$$\begin{aligned} u_{4,2} &= -\omega^2 [J_{I,x} - m(b_2 c_{c2} + b_3 c_{c3})], & u_{4,3} &= -\omega^2 (J_{I,xy} + mb_2 c_{c1}) \\ u_{5,2} &= -\omega^2 (J_{I,xy} + mb_1 c_{c2}), & u_{5,3} &= -\omega^2 [J_{I,y} - m(b_3 c_{c3} + b_1 c_{c1})] \end{aligned}$$

15.6.3 Spatial Vibration of a Rigid Body with N Input Ends and L Output Ends

The state vectors are

$$\begin{aligned} \mathbf{Z}_I &= [X_{I_1}, Y_{I_1}, Z_{I_1}, \theta_{x,I_1}, \theta_{y,I_1}, \theta_{z,I_1}, M_{x,I_1}, M_{y,I_1}, M_{z,I_1}, Q_{x,I_1}, Q_{y,I_1}, Q_{z,I_1}, \\ &\quad \dots, M_{x,I_N}, M_{y,I_N}, M_{z,I_N}, Q_{x,I_N}, Q_{y,I_N}, Q_{z,I_N}]^T \\ \mathbf{Z}_O &= [X_{O_1}, Y_{O_1}, Z_{O_1}, \theta_{x,O_1}, \theta_{y,O_1}, \theta_{z,O_1}, M_{x,O_1}, M_{y,O_1}, M_{z,O_1}, Q_{x,O_1}, Q_{y,O_1}, Q_{z,O_1}, \\ &\quad \dots, M_{x,O_L}, M_{y,O_L}, M_{z,O_L}, Q_{x,O_L}, Q_{y,O_L}, Q_{z,O_L}]^T \end{aligned}$$

The transfer equation is

$$\mathbf{U}_O \mathbf{Z}_O = \mathbf{U}_I \mathbf{Z}_I \quad (15.16)$$

The transfer matrices are

$$\begin{aligned} \mathbf{U}_O &= \begin{bmatrix} \mathbf{I}_3 & \mathbf{O}_{3 \times 3} & \mathbf{O}_{3 \times 3} & \mathbf{O}_{3 \times 3} & \mathbf{O}_{3 \times 3} & \mathbf{O}_{3 \times 3} & \cdots & \mathbf{O}_{3 \times 3} & \mathbf{O}_{3 \times 3} \\ \mathbf{O}_{3 \times 3} & \mathbf{I}_3 & \mathbf{O}_{3 \times 3} & \mathbf{O}_{3 \times 3} & \mathbf{O}_{3 \times 3} & \mathbf{O}_{3 \times 3} & \cdots & \mathbf{O}_{3 \times 3} & \mathbf{O}_{3 \times 3} \\ \mathbf{O}_{3 \times 3} & \mathbf{O}_{3 \times 3} & \mathbf{I}_3 & -\tilde{\mathbf{l}}_{I_1 O_1} & \mathbf{I}_3 & -\tilde{\mathbf{l}}_{I_1 O_2} & \cdots & \mathbf{I}_3 & -\tilde{\mathbf{l}}_{I_1 O_n} \\ \mathbf{O}_{3 \times 3} & \mathbf{O}_{3 \times 3} & \mathbf{O}_{3 \times 3} & \mathbf{I}_3 & \mathbf{O}_{3 \times 3} & \mathbf{I}_3 & \cdots & \mathbf{O}_{3 \times 3} & \mathbf{I}_3 \end{bmatrix} \\ \mathbf{U}_I &= \begin{bmatrix} \mathbf{I}_3 & -\tilde{\mathbf{l}}_{I_1 O_1} & \mathbf{O}_{3 \times 3} & \mathbf{O}_{3 \times 3} & \mathbf{O}_{3 \times 3} & \mathbf{O}_{3 \times 3} & \cdots & \mathbf{O}_{3 \times 3} & \mathbf{O}_{3 \times 3} \\ \mathbf{O}_{3 \times 3} & \mathbf{I}_3 & \mathbf{O}_{3 \times 3} & \mathbf{O}_{3 \times 3} & \mathbf{O}_{3 \times 3} & \mathbf{O}_{3 \times 3} & \cdots & \mathbf{O}_{3 \times 3} & \mathbf{O}_{3 \times 3} \\ -m\omega^2 \tilde{\mathbf{l}}_{I_1 C}^T & -\omega^2 \mathbf{J}_{I_1} & \mathbf{I}_3 & -\tilde{\mathbf{l}}_{I_1 I_1} & \mathbf{I}_3 & -\tilde{\mathbf{l}}_{I_1 I_2} & \cdots & \mathbf{I}_3 & -\tilde{\mathbf{l}}_{I_1 I_L} \\ m\omega^2 \mathbf{I}_3 & m\omega^2 \tilde{\mathbf{l}}_{I_1 C}^T & \mathbf{O}_{3 \times 3} & \mathbf{I}_3 & \mathbf{O}_{3 \times 3} & \mathbf{I}_3 & \cdots & \mathbf{O}_{3 \times 3} & \mathbf{I}_3 \end{bmatrix} \end{aligned} \quad (15.17)$$

The related structural parameters are described in the body-fixed coordinate system whose origin is the first input end I_1 .

15.6.4 Spatial Vibration of a Rigid Body with N Input Ends and One Output End

The state vectors are

$$\begin{aligned} \mathbf{Z}_I &= [X_{I_1}, Y_{I_1}, Z_{I_1}, \theta_{x,I_1}, \theta_{y,I_1}, \theta_{z,I_1}, M_{x,I_1}, M_{y,I_1}, M_{z,I_1}, Q_{x,I_1}, Q_{y,I_1}, Q_{z,I_1}, \\ &\quad M_{x,I_2}, M_{y,I_2}, M_{z,I_2}, Q_{x,I_2}, Q_{y,I_2}, Q_{z,I_2}, \dots, M_{x,I_N}, M_{y,I_N}, M_{z,I_N}, Q_{x,I_N}, Q_{y,I_N}, Q_{z,I_N}]^T \\ \mathbf{Z}_O &= [X, Y, Z, \theta_x, \theta_y, \theta_z, M_x, M_y, M_z, Q_x, Q_y, Q_z]^T_O \end{aligned}$$

The transfer equation is

$$\mathbf{Z}_O = \mathbf{U} \mathbf{Z}_I$$

The transfer matrix is

$$U = \begin{bmatrix} I_3 & -\tilde{I}_{I_1 O} & O_{3 \times 3} & O_{3 \times 3} & \cdots & O_{3 \times 3} & O_{3 \times 3} \\ O_{3 \times 3} & I_3 & O_{3 \times 3} & O_{3 \times 3} & \cdots & O_{3 \times 3} & O_{3 \times 3} \\ m\omega^2 \tilde{I}_{CO} & -\omega^2 \left(m\tilde{I}_{I_1 O} \tilde{I}_{I_1 C} + J_{I_1} \right) & I_3 & \tilde{I}_{I_1 O} & \cdots & I_3 & \tilde{I}_{I_N O} \\ m\omega^2 I_3 & -m\omega^2 \tilde{I}_{I_1 C} & O_{3 \times 3} & I_3 & \cdots & O_{3 \times 3} & I_3 \end{bmatrix} \quad (15.18)$$

where $I_n(a_{1,n}, a_{2,n}, a_{3,n})$ ($n = 1, 2, \dots, N$) is the n th input end. The related structural parameters are described in the body-fixed coordinate system whose origin is the first input end I_1 and J_{I_1} is the inertia matrix with respect to I_1 .

15.6.5 Spatial Vibration of a Rigid Body with One Input End and L Output Ends

The state vectors are

$$\begin{aligned} Z_I &= [X, Y, Z, \theta_x, \theta_y, \theta_z, M_x, M_y, M_z, Q_x, Q_y, Q_z]_I^T \\ Z_O &= [X_{O_1}, Y_{O_1}, Z_{O_1}, \theta_{x,O_1}, \theta_{y,O_1}, \theta_{z,O_1}, M_{x,O_1}, M_{y,O_1}, M_{z,O_1}, Q_{x,O_1}, Q_{y,O_1}, Q_{z,O_1}, \\ &\quad M_{x,O_2}, M_{y,O_2}, M_{z,O_2}, Q_{x,O_2}, Q_{y,O_2}, Q_{z,O_2}, \dots, M_{x,O_L}, M_{y,O_L}, M_{z,O_L}, Q_{x,O_L}, Q_{y,O_L}, Q_{z,O_L}]^T \end{aligned}$$

The transfer matrix is

$$U = \begin{bmatrix} I_3 & \tilde{I}_{IO_1} & O_{3 \times 3} & O_{3 \times 3} & \cdots & O_{3 \times 3} & O_{3 \times 3} \\ O_{3 \times 3} & I_3 & O_{3 \times 3} & O_{3 \times 3} & \cdots & O_{3 \times 3} & O_{3 \times 3} \\ m\omega^2 \tilde{I}_{IC} & \omega^2 \left(m\tilde{I}_{IC} \tilde{I}_{IO_1} + J_I \right) & I_3 & -\tilde{I}_{IO_1} & \cdots & I_3 & -\tilde{I}_{IO_L} \\ -m\omega^2 I_3 & m\omega^2 \tilde{I}_{O_1 C} & O_{3 \times 3} & I_3 & \cdots & O_{3 \times 3} & I_3 \end{bmatrix} \quad (15.19)$$

where $O_l(b_{1,l}, b_{2,l}, b_{3,l})$ ($l = 1, 2, \dots, L$) is the l th output end. The related structural parameters are described in the body-fixed coordinate system whose origin is located at input end I . It should be noted that the transfer equation in this case is $Z_I = UZ_O$.

15.7 Beam with Transverse Vibration

The state vector is

$$Z = [Y, \theta_z, M_z, Q_y]^T$$

15.7.1 Euler-Bernoulli Beam with Transverse Vibration

The transfer matrix is

$$U = \begin{bmatrix} S(\lambda x) & \frac{T(\lambda x)}{\lambda} & \frac{U(\lambda x)}{EI\lambda^2} & \frac{V(\lambda x)}{EI\lambda^3} \\ \lambda V(\lambda x) & S(\lambda x) & \frac{T(\lambda x)}{EI\lambda} & \frac{U(\lambda x)}{EI\lambda^2} \\ EI\lambda^2 U(\lambda x) & EI\lambda V(\lambda x) & S(\lambda x) & \frac{T(\lambda x)}{\lambda} \\ EI\lambda^3 T(\lambda x) & EI\lambda^2 U(\lambda x) & \lambda V(\lambda x) & S(\lambda x) \end{bmatrix}, \quad (0 < x \leq l) \quad (15.20)$$

where S , V , U and T are the Крылов functions:

$$S(\lambda x) = \frac{\cosh \lambda x + \cos \lambda x}{2}, \quad T(\lambda x) = \frac{\sinh \lambda x + \sin \lambda x}{2}$$

$$U(\lambda x) = \frac{\cosh \lambda x - \cos \lambda x}{2}, \quad V(\lambda x) = \frac{\sinh \lambda x - \sin \lambda x}{2}$$

where l is the length of the beam, $\lambda = \sqrt{\bar{m}\omega^2/(EI)}$, EI is the bending stiffness of the beam and \bar{m} is the line mass density of the beam.

15.7.2 Timoshenko Beam with Transverse Vibration

The transfer matrix is

$$\mathbf{U} = \frac{1}{\lambda_1^2 + \lambda_2^2} \begin{bmatrix} a_{11} & a_{12} & a_{13} & a_{14} \\ a_{21} & a_{22} & a_{23} & a_{24} \\ a_{31} & a_{32} & a_{33} & a_{34} \\ a_{41} & a_{42} & a_{43} & a_{44} \end{bmatrix} \quad (0 < x \leq l) \quad (15.21)$$

where

$$\lambda_{1,2} = \sqrt{\sqrt{\beta^4 + \frac{1}{4}(\sigma - \tau)^2} \mp \frac{1}{2}(\sigma + \tau)}, \quad \sigma = \frac{\bar{m}\omega^2}{GA_s}, \quad \tau = \frac{\bar{m}\rho_z^2\omega^2}{EI_z}, \quad \beta^4 = \frac{\bar{m}\omega^2}{EI_z},$$

$$a_{11} = -(\sigma - \lambda_2^2) \cosh \lambda_1 l + (\sigma + \lambda_1^2) \cos \lambda_2 l, \quad a_{12} = \lambda_1 \sinh \lambda_1 l + \lambda_2 \sin \lambda_2 l,$$

$$a_{21} = -(\sigma - \lambda_2^2)(\sigma + \lambda_1^2) \left(\frac{\sinh \lambda_1 l}{\lambda_1} - \frac{\sin \lambda_2 l}{\lambda_2} \right), \quad a_{22} = (\sigma + \lambda_1^2) \cosh \lambda_1 l - (\sigma - \lambda_2^2) \cos \lambda_2 l,$$

$$a_{31} = -EI_z(\sigma - \lambda_2^2)(\sigma + \lambda_1^2)(\cosh \lambda_1 l - \cos \lambda_2 l),$$

$$a_{32} = EI_z[\lambda_1(\sigma + \lambda_1^2) \sinh \lambda_1 l + \lambda_2(\sigma - \lambda_2^2) \sin \lambda_2 l],$$

$$a_{41} = -\frac{\bar{m}\omega^2(\sigma - \lambda_2^2)}{\lambda_1} \sinh \lambda_1 l + \frac{\bar{m}\omega^2(\sigma + \lambda_1^2)}{\lambda_2} \sin \lambda_2 l, \quad a_{42} = \bar{m}\omega^2(\cosh \lambda_1 l - \cos \lambda_2 l),$$

$$a_{13} = \frac{1}{EI_z}(\cosh \lambda_1 l - \cos \lambda_2 l), \quad a_{14} = -\frac{\lambda_1(\sigma - \lambda_2^2)}{\bar{m}\omega^2} \sinh \lambda_1 l - \frac{\lambda_2(\sigma + \lambda_1^2)}{\bar{m}\omega^2} \sin \lambda_2 l,$$

$$a_{23} = \frac{\sigma + \lambda_1^2}{EI_z \lambda_1} \sinh \lambda_1 l - \frac{(\sigma - \lambda_2^2)}{EI_z \lambda_2} \sin \lambda_2 l, \quad a_{24} = -\frac{(\sigma - \lambda_2^2)(\sigma + \lambda_1^2)}{\bar{m}\omega^2}(\cosh \lambda_1 l - \cos \lambda_2 l),$$

$$a_{33} = (\sigma + \lambda_1^2) \cosh \lambda_1 l - (\sigma - \lambda_2^2) \cos \lambda_2 l,$$

$$a_{34} = -\frac{EI_z(\sigma - \lambda_2^2)(\sigma + \lambda_1^2)}{\bar{m}\omega^2}(\lambda_1 \sinh \lambda_1 l + \lambda_2 \sin \lambda_2 l),$$

$$a_{43} = \frac{\bar{m}\omega^2}{EI_z} \left(\frac{\sinh \lambda_1 l}{\lambda_1} - \frac{\sin \lambda_2 l}{\lambda_2} \right), \quad a_{44} = -(\sigma - \lambda_2^2) \cosh \lambda_1 l + (\sigma + \lambda_1^2) \cos \lambda_2 l$$

where l is the length of the beam, EI is the bending stiffness of the beam and \bar{m} is the line mass density of the beam. A is the cross-section area, I_z is the moment of inertia of the cross-section with respect to the neutral line and ρ_z is the gyration radius of the cross-section with respect to the neutral line. $GA_s = GA/\kappa_s$ is the shear stiffness and κ_s is the shape factor determined by the shape of the cross-section.

15.7.3 Massless Euler–Bernoulli Beam with Transverse Vibration

The transfer matrix is

$$\mathbf{U} = \begin{bmatrix} 1 & x & \frac{x^2}{2EI} & \frac{x^3}{6EI} \\ 0 & 1 & \frac{x}{EI} & \frac{x^2}{2EI} \\ 0 & 0 & 1 & x \\ 0 & 0 & 0 & 1 \end{bmatrix} \quad (0 < x \leq l) \quad (15.22)$$

Considering the influence of shear deformation, the transfer matrix of the massless Euler–Bernoulli beam with transverse vibration is

$$\mathbf{U} = \begin{bmatrix} 1 & x & \frac{x^2}{2EI} & \frac{x^3}{6EI} - \frac{x}{GA_s} \\ 0 & 1 & \frac{x}{EI} & \frac{x^2}{2EI} \\ 0 & 0 & 1 & x \\ 0 & 0 & 0 & 1 \end{bmatrix} \quad (0 < x \leq l) \quad (15.23)$$

15.7.4 Massless Euler–Bernoulli Beam with Axial Load and Shear Deformation

The transfer matrix is

$$\mathbf{U} = \begin{bmatrix} 1 & \frac{\sinh \lambda x}{\lambda} & -\frac{1 - \cosh \lambda x}{d_1 EI} & -\frac{\lambda x - \sinh \lambda x}{6 \lambda EI} - \frac{x}{GA_s} \\ 0 & \cosh \lambda x & \frac{\sinh \lambda x}{\lambda EI} & -\frac{1 - \cosh \lambda x}{d_1 EI} \\ 0 & \frac{d_1 EI \sinh \lambda x}{\lambda} & \cosh \lambda x & \frac{\sinh \lambda x}{\lambda} \\ 0 & 0 & 0 & 1 \end{bmatrix} \quad (0 < x \leq l) \quad (15.24)$$

where for the axial compressive force P , $\lambda = \sqrt{P/(EI)}$ and $d_1 = -\lambda^2$. For the axial tensile force P , $\lambda = \sqrt{-P/(EI)}$ and $d_1 = \lambda^2$.

15.7.5 Massless Euler–Bernoulli Beam with Elastic Foundation

The transfer matrix is

$$\mathbf{U} = \begin{bmatrix} e_1 & e_2 & e_3/(EI) & e_4/(EI) \\ -\lambda e_4 & e_1 & e_2/(EI) & e_3/(EI) \\ -\lambda EI e_3 & -\lambda EI e_4 & e_1 & e_2 \\ -\lambda EI e_2 & -\lambda EI e_3 & -\lambda e_4 & e_1 \end{bmatrix} \quad (0 < x \leq l) \quad (15.25)$$

where

$$\begin{aligned} e_1 &= \cosh \beta x \cos \beta x, & e_2 &= \frac{1}{2\beta} (\cosh \beta x \sin \beta x + \sinh \beta x \cos \beta x) \\ e_3 &= \frac{1}{2\beta^2} \sinh \beta x \sin \beta x, & e_4 &= \frac{1}{4\beta^3} (\cosh \beta x \sin \beta x - \sinh \beta x \cos \beta x) \end{aligned}$$

where $z \lambda = k^*/(EI)$, k^* is the Winckler (elastic) modulus of the foundation and $\beta^4 = \lambda/4$.

15.7.6 Massless Transverse Vibrational Euler–Bernoulli Beam with Elastic Foundation

The massless transverse vibrational Euler–Bernoulli beam with elastic foundation is shown in Figure 15.4.

The transfer matrix is

$$\mathbf{U} = \begin{bmatrix} 1 & l & 0 & 0 \\ 0 & 1 & 0 & 0 \\ \frac{l^2(\bar{m}\omega^2 - K^*)}{2} & \frac{l^2(\bar{m}\omega^2 - K^*)}{6} + l(K'^* - r^2\bar{m}\omega^2) & 1 & l \\ l(\bar{m}\omega^2 - K^*) & \frac{l^2(\bar{m}\omega^2 - K^*)}{2} & 0 & 1 \end{bmatrix} \quad (15.26)$$

where K^* is the Winckler (elastic) modulus of the foundation, K'^* is the rotational (elastic) modulus of the foundation and r is the gyration radius of the cross-section about the z axis.

15.7.7 Flexible Point Support

Different kinds of flexible point supports are shown in Figure 15.5.

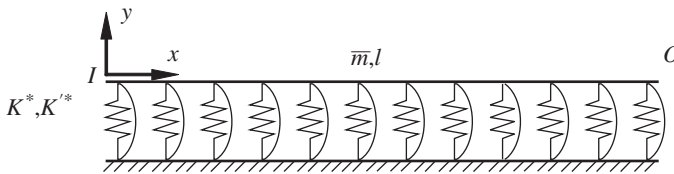


Figure 15.4 A transverse vibrational rigid beam with elastic foundation.

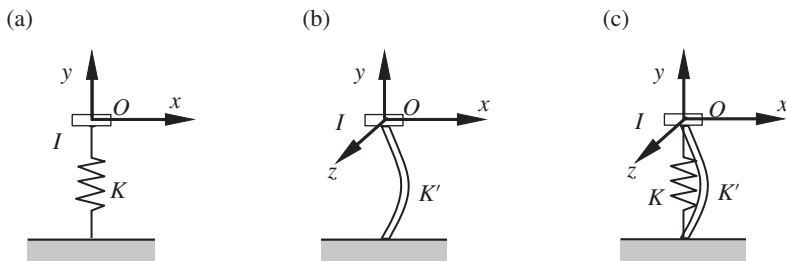


Figure 15.5 Elastic point support: (a) spring, (b) rotary spring and (c) elastic hinge.

The transfer matrices of the flexible points supported by spring, rotary spring and elastic hinges are

$$\mathbf{U} = \begin{bmatrix} 1 & 0 & 0 & 0 \\ 0 & 1 & 0 & 0 \\ 0 & 0 & 1 & 0 \\ -K & 0 & 0 & 1 \end{bmatrix}, \quad \mathbf{U} = \begin{bmatrix} 1 & 0 & 0 & 0 \\ 0 & 1 & 0 & 0 \\ 0 & K' & 1 & 0 \\ 0 & 0 & 0 & 1 \end{bmatrix}, \quad \mathbf{U} = \begin{bmatrix} 1 & 0 & 0 & 0 \\ 0 & 1 & 0 & 0 \\ 0 & K' & 1 & 0 \\ -K & 0 & 0 & 1 \end{bmatrix} \quad (15.27)$$

where K is the translational stiffness of the support and K' is the torsional stiffness.

If there is a lumped mass at the support point, the rotary inertia of the lumped mass is considered. Then the corresponding transfer matrix is

$$\mathbf{U} = \begin{bmatrix} 1 & 0 & 0 & 0 \\ 0 & 1 & 0 & 0 \\ 0 & K' - J\omega^2 & 1 & 0 \\ -K + m\omega^2 & 0 & 0 & 1 \end{bmatrix} \quad (15.28)$$

where m is the mass of the lumped mass and J is the moment of inertia of the lumped mass.

15.7.8 Nonuniform Cross-section Euler–Bernoulli Beam with Axial Compressive Force

A nonuniform cross-section Euler–Bernoulli beam with axial compressive force is shown in Figure 15.6.

The transfer matrix is

$$\mathbf{U} = \begin{bmatrix} 1 & -\frac{\sqrt{c_1}d_2d_8}{\beta c_2} & \frac{d_2d_8d_{10}}{\sqrt{c_1}P} - d_{11} & \frac{\sqrt{c_1}d_2d_8}{\beta c_2P} + \frac{l}{P} \\ 0 & \sqrt{\frac{c_1}{d_2}}\left(d_7 - \frac{1}{2}\frac{d_8}{\beta}\right) & \frac{c_2}{\sqrt{c_1}d_1P}\left(\frac{d_{12}}{2} + \frac{d_{13}}{d_7} + \frac{d_8d_{10}}{2}\right) & \frac{1}{P}\left(1 - \frac{\sqrt{c_1}d_9}{d_2} + \frac{\sqrt{c_1}d_8}{2\beta d_2}\right) \\ 0 & -\frac{P\sqrt{c_1}d_1d_8}{\beta c_2} & \sqrt{\frac{d_1}{c_1}}\left(\frac{d_3}{d_5} + d_8d_{10}\right) & \frac{\sqrt{c_1}d_1d_8}{\beta c_2} \\ 0 & 0 & 0 & 1 \end{bmatrix} \quad (15.29)$$

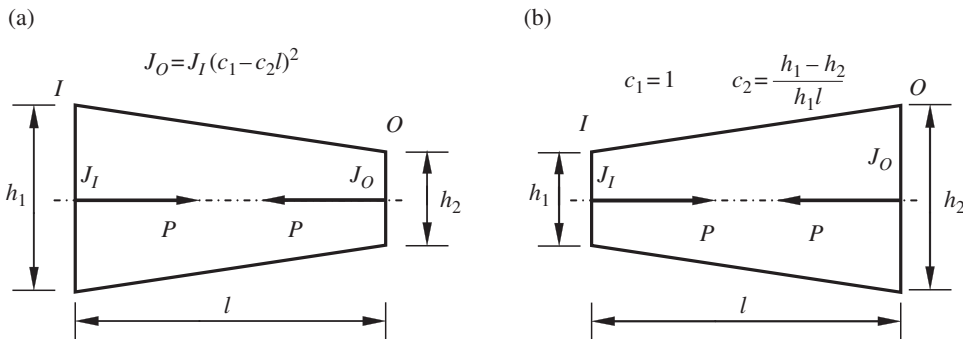


Figure 15.6 Nonuniform cross-section Euler–Bernoulli beam with axial compressive force. (a) The output end is thinner than the input end. (b) The output end is thicker than the input end.

where

$$\beta^2 = \frac{P}{c_2^2 EI_I} - \frac{1}{4}$$

$$d_1 = c_1 - c_2 l, \quad d_2 = \sqrt{d_1}, \quad d_3 = \sin(\beta l_n d_1), \quad d_4 = \cos(\beta l_n d_1), \quad d_5 = \sin(\beta l_n c_1)$$

$$d_6 = \cos(\beta l_n c_1), \quad d_7 = \tan(\beta l_n c_1), \quad d_8 = d_4 d_5 - d_3 d_6, \quad d_9 = d_3 d_5 + d_4 d_6$$

$$d_{10} = \frac{1}{2\beta} + \frac{1}{d_7}, \quad d_{11} = \frac{1 - d_2 d_3 / (\sqrt{c_1} d_5)}{P}, \quad d_{12} = \frac{d_3}{d_5} - d_9, \quad d_{13} = \frac{d_4}{d_6} - d_9$$

15.8 Shaft with Torsional Vibration

The state vector is

$$\mathbf{Z} = [\Theta_x, M_x]^T$$

15.8.1 Torsional Vibration of an Elastic Shaft with Uniform Cross-section

The transfer matrix is

$$\mathbf{U} = \begin{bmatrix} \cos \gamma x & \frac{\sin \gamma x}{\gamma G J_p} \\ -\gamma G J_p \sin \gamma x & \cos \gamma x \end{bmatrix} \quad (0 < x \leq l) \quad (15.30)$$

where l is the length of the shaft, $\gamma^2 = \rho J_p \omega^2 / (G J_p) = \rho \omega^2 / G$ and ρ is the mass density of the shaft. J_p is the polar inertia of the cross-section of the shaft and $G J_p$ is the torsional stiffness of the shaft.

15.8.2 Torsional Vibration of a Massless Elastic Shaft with Uniform Cross-section

The transfer matrix is

$$\mathbf{U} = \begin{bmatrix} 1 & \frac{x}{G J_p} \\ 0 & 1 \end{bmatrix} \quad (0 < x \leq l) \quad (15.31)$$

15.8.3 Massless Torsional Vibrational Elastic Shaft with Elastic Foundation and Uniform Cross-section

The transfer matrix is

$$\mathbf{U} = \begin{bmatrix} \cosh \gamma x & \frac{\sinh \gamma x}{\gamma G J_p} \\ \gamma G J_p \sinh \gamma x & \cosh \gamma x \end{bmatrix} \quad (0 < x \leq l) \quad (15.32)$$

where $\gamma^2 = \frac{K_t}{G J_p}$ and K_t is the elastic modulus of the foundation.

15.8.4 Torsional Vibration of a Rigid Shaft with Elastic Foundation

The transfer matrix is

$$\mathbf{U} = \begin{bmatrix} 1 & 0 \\ l(K_t - \rho J_p \omega^2) & 1 \end{bmatrix} \quad (0 < x \leq l) \quad (15.33)$$

15.8.5 Torsional Vibration of an Elastic Shaft with Elastic Foundation and Uniform Cross-section

The transfer matrix is

$$\mathbf{U} = \begin{bmatrix} \cos \gamma x & \frac{\sin \gamma x}{\gamma G J_p} \\ -\gamma G J_p \sin \gamma x & \cos \gamma x \end{bmatrix} \quad (0 < x \leq l) \quad (15.34)$$

where $\gamma^2 = \frac{\rho J_p \omega^2 - K_t}{G J_p}$. If $\gamma^2 < 0$, $\gamma^2 = \frac{K_t - \rho J_p \omega^2}{G J_p}$ and Equation (15.32) are used.

15.8.6 Flexible Point Support of a Lumped Mass on a Torsional Vibrational Shaft

The transfer matrix is

$$\mathbf{U} = \begin{bmatrix} 1 & 0 \\ K'_b - J \omega^2 & 1 \end{bmatrix} \quad (15.35)$$

where K'_b is the torsional stiffness of the flexible point support and J is the moment of inertia of the lumped mass.

15.9 Rod with Longitudinal Vibration

The state vector is

$$\mathbf{Z} = [X, Q_x]^T$$

15.9.1 Longitudinal Vibration of an Elastic Rod with Uniform Cross-section

The transfer matrix is

$$\mathbf{U} = \begin{bmatrix} \cos \beta x_1 & -\frac{\sin \beta x_1}{\beta EA} \\ \beta EA \sin \beta x_1 & \cos \beta x_1 \end{bmatrix} \quad (0 \leq x \leq l) \quad (15.36)$$

where l is the length of the rod, EA is the tensile stiffness, $\beta = \sqrt{\frac{\bar{m} \omega^2}{EA}}$ and \bar{m} is the mass per unit length.

15.9.2 Longitudinal Vibration of a Massless Elastic Rod with Uniform Cross-section

The transfer matrix is

$$\mathbf{U} = \begin{bmatrix} 1 & -\frac{x_1}{EA} \\ 0 & 1 \end{bmatrix} \quad (0 \leq x \leq l) \quad (15.37)$$

15.9.3 Flexible Point Support of a Lumped Mass on a Translational Vibrational Rod

The transfer matrix is

$$\mathbf{U} = \begin{bmatrix} 1 & 0 \\ -K_b + m\omega^2 & 1 \end{bmatrix} \quad (15.38)$$

where K_b is the elastic coefficient of the flexible point support and m is the mass of the lumped mass.

15.10 Euler–Bernoulli Beam

15.10.1 Euler–Bernoulli Beam Vibrating Longitudinally in the x Direction and Transversely in the y Direction

The state vector is

$$\mathbf{Z} = [X, Y, \Theta_z, M_z, Q_x, Q_y]^T$$

The transfer matrix is

$$\mathbf{U} = \begin{bmatrix} \cos\beta_x x_1 & 0 & 0 & 0 & \frac{-\sin\beta_x x_1}{\beta_x EA} & 0 \\ 0 & S(\lambda_y x_1) & \frac{T(\lambda_y x_1)}{\lambda_y} & \frac{U(\lambda_y x_1)}{EI_z \lambda_y^2} & 0 & \frac{V(\lambda_y x_1)}{EI_z \lambda_y^3} \\ 0 & \lambda_y V(\lambda_y x_1) & S(\lambda_y x_1) & \frac{T(\lambda_y x_1)}{EI_z \lambda_y} & 0 & \frac{U(\lambda_y x_1)}{EI_z \lambda_y^2} \\ 0 & EI_z \lambda_y^2 U(\lambda_y x_1) & EI_z \lambda_y V(\lambda_y x_1) & S(\lambda_y x_1) & 0 & \frac{T(\lambda_y x_1)}{\lambda_y} \\ \beta_x EA \sin\beta_x x_1 & 0 & 0 & 0 & \cos\beta_x x_1 & 0 \\ 0 & EI_z \lambda_y^3 T(\lambda_y x_1) & EI_z \lambda_y^2 U(\lambda_y x_1) & \lambda_y V(\lambda_y x_1) & 0 & S(\lambda_y x_1) \end{bmatrix} \quad (15.39)$$

where $0 \leq x_1 \leq l$, $\beta_x = \sqrt{\bar{m}\omega^2/(EA)}$ and $\lambda_y = \sqrt[4]{\bar{m}\omega^2/(EI_z)}$.

15.10.2 Euler–Bernoulli Beam Vibrating Torsionally about the x Axis and Transversely in the z Direction

The state vector is

$$\mathbf{Z} = [Z, \Theta_x, \Theta_y, M_x, M_y, Q_z]^T$$

The transfer matrix is

$$\mathbf{U} = \begin{bmatrix} S(\lambda_z x_1) & 0 & \frac{T(\lambda_z x_1)}{\lambda_z} & 0 & \frac{U(\lambda_z x_1)}{EI_y \lambda_z^2} & \frac{V(\lambda_z x_1)}{EI_y \lambda_z^3} \\ 0 & \cos \gamma_{\theta_x} x_1 & 0 & \frac{\sin \gamma_{\theta_x} x_1}{\gamma_{\theta_x} (GJ_p)} & 0 & 0 \\ \lambda_z V(\lambda_z x_1) & 0 & S(\lambda_z x_1) & 0 & \frac{T(\lambda_z x_1)}{EI_y \lambda_z} & \frac{U(\lambda_z x_1)}{EI_y \lambda_z^2} \\ 0 & -\gamma_{\theta_x} (GJ_p) \sin \gamma_{\theta_x} x_1 & 0 & \cos \gamma_{\theta_x} x_1 & 0 & 0 \\ EI_y \lambda_z^2 U(\lambda_z x_1) & 0 & EI_y \lambda_z V(\lambda_z x_1) & 0 & S(\lambda_z x_1) & \frac{T(\lambda_z x_1)}{\lambda_z} \\ EI_y \lambda_z^3 T(\lambda_z x_1) & 0 & EI_y \lambda_z^2 U(\lambda_z x_1) & 0 & \lambda_z V(\lambda_z x_1) & S(\lambda_z x_1) \end{bmatrix} \quad (15.40)$$

where $0 \leq x_1 \leq l$, $\gamma_{\theta_x} = \sqrt{(\rho J_p) \omega^2 / (GJ_p)}$ and $\lambda_z = \sqrt[4]{m \omega^2 / (EI_y)}$.

15.10.3 Euler–Bernoulli Beam Vibrating Torsionally about the x Axis, Longitudinally in the x Direction and Transversely in the y and z Directions

The state vector is

$$\mathbf{Z} = [X, Y, Z, \Theta_x, \Theta_y, \Theta_z, M_x, M_y, M_z, Q_x, Q_y, Q_z]^T$$

The transfer matrix is

$$\mathbf{U} = \begin{bmatrix} u_{1,1} & 0 & 0 & 0 & 0 & 0 & 0 & 0 & 0 & u_{1,10} & 0 & 0 \\ 0 & u_{2,2} & 0 & 0 & 0 & u_{2,6} & 0 & 0 & u_{2,9} & 0 & u_{2,11} & 0 \\ 0 & 0 & u_{3,3} & 0 & u_{3,5} & 0 & 0 & u_{3,8} & 0 & 0 & 0 & u_{3,12} \\ 0 & 0 & 0 & u_{4,4} & 0 & 0 & u_{4,7} & 0 & 0 & 0 & 0 & 0 \\ 0 & 0 & u_{5,3} & 0 & u_{5,5} & 0 & 0 & u_{5,8} & 0 & 0 & 0 & u_{5,12} \\ 0 & u_{6,2} & 0 & 0 & 0 & u_{6,6} & 0 & 0 & u_{6,9} & 0 & u_{6,11} & 0 \\ 0 & 0 & 0 & u_{7,4} & 0 & 0 & u_{7,7} & 0 & 0 & 0 & 0 & 0 \\ 0 & 0 & u_{8,3} & 0 & u_{8,5} & 0 & 0 & u_{8,8} & 0 & 0 & 0 & u_{8,12} \\ 0 & u_{9,2} & 0 & 0 & 0 & u_{9,6} & 0 & 0 & u_{9,9} & 0 & u_{9,11} & 0 \\ u_{10,1} & 0 & 0 & 0 & 0 & 0 & 0 & 0 & 0 & u_{10,10} & 0 & 0 \\ 0 & u_{11,2} & 0 & 0 & 0 & u_{11,6} & 0 & 0 & u_{11,9} & 0 & u_{11,11} & 0 \\ 0 & 0 & u_{12,3} & 0 & u_{12,5} & 0 & 0 & u_{12,8} & 0 & 0 & 0 & u_{12,12} \end{bmatrix} \quad (15.41)$$

where

$$\begin{aligned}
 u_{1,1} &= u_{10,10} = \cos \beta_x x_i, \quad u_{1,10} = \frac{-\sin \beta_x x_i}{\beta_x E A_i}, \quad u_{10,1} = \beta_x E A_i \sin \beta_x x_i \\
 u_{4,4} &= u_{7,7} = \cos \gamma_{\theta_x} x_i, \quad u_{4,7} = \frac{\sin \gamma_{\theta_x} x_i}{\gamma_{\theta_x} (G J_p)_i}, \quad u_{7,4} = -\gamma_{\theta_x} (G J_p)_i \sin \gamma_{\theta_x} x_i \\
 u_{2,2} &= u_{6,6} = u_{9,9} = u_{11,11} = S(\lambda_y x_i), \quad u_{3,3} = u_{5,5} = u_{8,8} = u_{12,12} = S(\lambda_z x_i) \\
 u_{2,6} &= u_{9,11} = \frac{T(\lambda_y x_i)}{\lambda_y}, \quad u_{2,9} = u_{6,11} = \frac{U(\lambda_y x_i)}{E I_{z,i} \lambda_y^2}, \quad u_{2,11} = \frac{V(\lambda_y x_i)}{E I_{z,i} \lambda_y^3}, \quad u_{5,8} = \frac{T(\lambda_z x_i)}{E I_{y,i} \lambda_z} \\
 u_{3,5} &= u_{8,12} = \frac{-T(\lambda_z x_i)}{\lambda_z}, \quad u_{3,8} = u_{5,12} = \frac{-U(\lambda_z x_i)}{E I_{y,i} \lambda_z^2}, \quad u_{3,12} = \frac{V(\lambda_z x_i)}{E I_{y,i} \lambda_z^3}, \quad u_{6,9} = \frac{T(\lambda_y x_i)}{E I_{z,i} \lambda_y} \\
 u_{5,3} &= u_{12,8} = -\lambda_z V(\lambda_z x_i), \quad u_{6,2} = u_{11,9} = \lambda_y V(\lambda_y x_i), \quad u_{8,3} = u_{12,5} = -E I_{y,i} \lambda_z^2 U(\lambda_z x_i) \\
 u_{8,5} &= E I_{y,i} \lambda_z V(\lambda_z x_i), \quad u_{9,2} = u_{11,6} = E I_{z,i} \lambda_y^2 U(\lambda_y x_i) \\
 u_{9,6} &= E I_{z,i} \lambda_y V(\lambda_y x_i), \quad u_{11,2} = E I_{z,i} \lambda_y^3 T(\lambda_y x_i), \quad u_{12,3} = E I_{y,i} \lambda_z^3 T(\lambda_z x_i) \\
 \beta_x &= \sqrt{\bar{m}_i \omega^2 / (E A_i)}, \quad \lambda_y = \sqrt[4]{\bar{m}_i \omega^2 / (E I_{z,i})}, \quad \lambda_z = \sqrt[4]{\bar{m}_i \omega^2 / (E I_{y,i})} \\
 \gamma_{\theta_x} &= \sqrt{(\rho J_p)_i \omega^2 / (G J_p)_i} \quad 0 \leq x_i \leq l_i.
 \end{aligned}$$

If the longitudinal motion in the x direction and the rotation about x axis are regarded as rigid motion, then

$$\begin{aligned}
 u_{1,1} &= u_{10,10} = 1, \quad u_{1,10} = 0, \quad u_{10,1} = m_i \omega^2 \\
 u_{4,4} &= u_{7,7} = 1, \quad u_{4,7} = 0, \quad u_{7,4} = -J_x \omega^2
 \end{aligned} \tag{15.42}$$

15.11 Rectangular Plate

15.11.1 Dynamic Equations of an Anisotropic Rectangle Plate

For an orthogonal anisotropic rectangle plate, as shown in Figure 15.7, the basic equations of the bending motion [38] are

$$\begin{aligned}
 \frac{\partial w}{\partial x} &= -\theta \\
 \frac{\partial \theta}{\partial x} &= \mu_y \frac{\partial^2 w}{\partial y^2} + \frac{M_x}{D_x} + \frac{M_{Tx}}{D_x} \\
 \frac{\partial M_x}{\partial x} &= -4D_{xy} \frac{\partial^2 \theta}{\partial y^2} + Q_x \\
 \frac{\partial Q_x}{\partial x} &= D_y \left(1 - \mu_x \mu_y \right) \frac{\partial^4 w}{\partial y^4} + \left(P_y - \mu_y P_x \right) \frac{\partial^2 w}{\partial y^2} - \frac{1}{D_x} \left(P_x + \mu_x D_y \frac{\partial^2}{\partial y^2} \right) M_x \\
 &\quad + K w + \rho \frac{\partial^2 w}{\partial t^2} - \frac{1}{D_x} \left(P_x + \mu_x D_y \frac{\partial^2}{\partial y^2} \right) M_{Tx} + \frac{\partial^2 M_{Ty}}{\partial y^2} - p(x, y, t)
 \end{aligned} \tag{15.43}$$

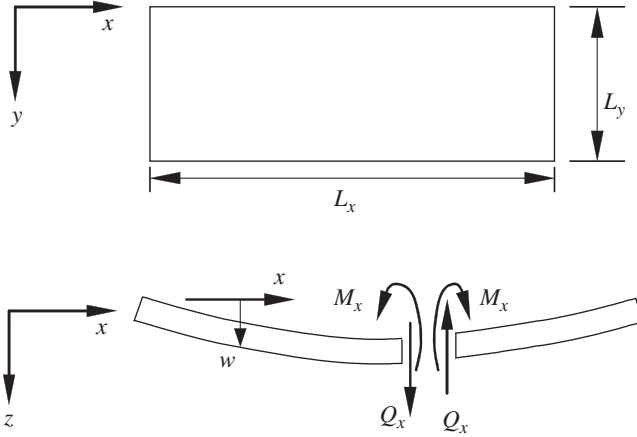


Figure 15.7 Positive deflection, internal bending moment and shearing force.

where

$$D_x = \frac{E_x h^3}{12(1 - \mu_x \mu_y)}, \quad D_y = \frac{E_y h^3}{12(1 - \mu_x \mu_y)}, \quad D_{xy} = \frac{G h^3}{12} \quad (15.44)$$

$$\begin{cases} M_y = -D_y \left(\frac{\partial^2 w}{\partial y^2} + \mu_x \frac{\partial^2 w}{\partial x^2} \right) - M_{Ty} \\ M_{xy} = 2D_{xy} \frac{\partial^2 w}{\partial x \partial y} = -M_{yx} \\ Q_y = \frac{\partial M_y}{\partial y} - 2D_{xy} \left(\frac{\partial^3 w}{\partial x^2 \partial y} + \frac{\partial^3 w}{\partial x \partial y^2} \right) \end{cases} \quad (15.45)$$

$$\begin{cases} M_{Tx} = \int_{-h/2}^{+h/2} \frac{E_x (\alpha_x + \mu_y \alpha_y)}{1 - \mu_x \mu_y} \Delta T z dz \\ M_{Ty} = \int_{-h/2}^{+h/2} \frac{E_y (\alpha_y + \mu_x \alpha_x)}{1 - \mu_x \mu_y} \Delta T z dz \end{cases} \quad (15.46)$$

P_x and P_y are the planar pressure, w is the transverse deflection, D_x , D_y and D_{xy} are the flexural stiffness, and μ_x and μ_y are the Poisson's ratios with respect to the x and y axes, respectively. ρ is the mass density, K is the elastic modulus of the foundation and p is the distributed transversely loading intensity. E_x and E_y are the material elastic moduli with respect to the x and y axes, respectively. G is the shear elastic modulus of the material, h is the thickness of the plate and ΔT is the temperature variation. α_x and α_y are the heat expansion coefficients with respect to the x and y axes, respectively. M_x and M_y are the bending moments, M_{yx} and M_{xy} are torsional moments, and Q_x and Q_y are the shear forces.

Equation (15.43) can be written as

$$D_x \frac{\partial^4 w}{\partial x^4} + 2B \frac{\partial^4 w}{\partial x^2 \partial y^2} + D_y \frac{\partial^4 w}{\partial y^4} + P_x \frac{\partial^2 w}{\partial x^2} + P_y \frac{\partial^2 w}{\partial y^2} + Kw + \rho \frac{\partial^2 w}{\partial t^2} = p - \left(\frac{\partial^2 M_{Tx}}{\partial x^2} + \frac{\partial^2 M_{Ty}}{\partial y^2} \right) \quad (15.47)$$

where $B = (D_x\mu_y + D_y\mu_x + 4D_{xy})/2$.

If the pressures P_x and P_y are replaced by $-P_x$ and $-P_y$, then Equation (15.43) and Equation (15.47) are valid for the case with a tensile force.

If the proposed plate is simply supported on both sides of $y = 0$ and $y = L_y$, the variables w , θ , M_x and Q_x can be expanded in Fourier series. Deleting the variable y in Equation (15.46) yields

$$\left\{ \begin{array}{l} w(x, y, t) = \sum_{m=1}^{\infty} w_m(x, t) \sin \frac{m\pi y}{L_y} \\ \theta(x, y, t) = \sum_{m=1}^{\infty} \theta_m(x, t) \sin \frac{m\pi y}{L_y} \\ M_x(x, y, t) = \sum_{m=1}^{\infty} M_{xm}(x, t) \sin \frac{m\pi y}{L_y} \\ Q_x(x, y, t) = \sum_{m=1}^{\infty} Q_{xm}(x, t) \sin \frac{m\pi y}{L_y} \end{array} \right. \quad (15.48)$$

The mechanical load and heat load can be expanded as follows

$$\left\{ \begin{array}{l} p(x, y, t) = \sum_{m=1}^{\infty} p_m(x, t) \sin \frac{m\pi y}{L_y} \\ M_{Tx}(x, y, t) = \sum_{m=1}^{\infty} M_{Txm}(x, t) \sin \frac{m\pi y}{L_y} \\ M_{Ty}(x, y, t) = \sum_{m=1}^{\infty} M_{Tym}(x, t) \sin \frac{m\pi y}{L_y} \end{array} \right. \quad (15.49)$$

therefore

$$\left\{ \begin{array}{l} p_m(x, t) = \frac{2}{L_y} \int_0^{L_y} p(x, y, t) \sin \frac{m\pi y}{L_y} dy \\ M_{Txm}(x, t) = \frac{2}{L_y} \int_0^{L_y} M_{Tx}(x, y, t) \sin \frac{m\pi y}{L_y} dy \\ M_{Tym}(x, t) = \frac{2}{L_y} \int_0^{L_y} M_{Ty}(x, y, t) \sin \frac{m\pi y}{L_y} dy \end{array} \right. \quad (15.50)$$

Substituting Equations (15.49) and (15.50) into Equations (15.43) and (15.52) gives

$$\begin{aligned} \frac{\partial w_m}{\partial x} &= -\theta_m \\ \frac{\partial \theta_m}{\partial x} &= -\mu_y \left(\frac{m\pi}{L_y} \right)^2 w_m + \frac{M_{xm}}{D_x} + \frac{M_{Txm}}{D_x} \\ \frac{\partial M_{xm}}{\partial x} &= 4D_{xy} \left(\frac{m\pi}{L_y} \right)^2 \theta_m + Q_{xm} \end{aligned}$$

$$\begin{aligned}
\frac{\partial Q_x}{\partial x} = & \left[D_y (1 - \mu_x \mu_y) \left(\frac{m\pi}{L_y} \right)^4 - (P_y - \mu_y P_x) \left(\frac{m\pi}{L_y} \right)^2 + K \right] w_m \\
& + \left[-\frac{P_x}{D_x} + \frac{D_y}{D_x} \mu_x \left(\frac{m\pi}{L_y} \right)^2 \right] M_{xm} + \rho \frac{\partial^2 w_m}{\partial t^2} \\
& - \frac{1}{D_x} \left[P_x - \mu_x D_y \left(\frac{m\pi}{L_y} \right)^2 \right] M_{Txm} - \left(\frac{m\pi}{L_y} \right)^2 M_{Tym} - p_m(x, t).
\end{aligned} \tag{15.51}$$

The state vector is defined as

$$\mathbf{Z}_m(y) = [w_m, \theta_m, M_{xm}, Q_{xm}]^T \tag{15.52}$$

The corresponding transfer matrix can be obtained as follows.

15.11.2 Massless Isotropic Rectangle Plate

The transfer matrix is

$$\mathbf{U}_x = \begin{bmatrix} -\frac{\beta(1-\mu)}{2}xs + c & u_{12} & -\frac{xs}{2D\beta} & -\frac{1}{2D\beta^2}\left(\frac{s}{\beta} - xc\right) \\ u_{21} & \frac{\beta(1-\mu)}{2}xs + c & \frac{1}{2D}\left(\frac{s}{\beta} + xc\right) & \frac{xs}{2D\beta} \\ \frac{D\beta^3(1-\mu)^2}{2}xs & u_{32} & \frac{\beta(1-\mu)}{2}xs + c & u_{34} \\ u_{41} & -\frac{D\beta^3(1-\mu)^2}{2}xs & u_{43} & -\frac{\beta(1-\mu)}{2}xs + c \end{bmatrix} \tag{15.53}$$

where $\beta = m\pi/L_y$, $s = \sinh\beta x$ and $c = \cosh\beta x$, and

$$\begin{aligned}
u_{12} &= -\frac{1}{2} \left[(1+\mu)\frac{s}{\beta} + (1-\mu)xc \right], \quad u_{21} = -\frac{\beta^2}{2} \left[(1+\mu)\frac{s}{\beta} - (1-\mu)xc \right] \\
u_{32} &= \frac{D\beta^2}{2} \left[\left(3 - 2\mu - \mu^2 \right) \frac{s}{\beta} + (1-\mu)^2 xc \right], \quad u_{34} = \frac{1}{2} \left[(1+\mu)\frac{s}{\beta} + (1-\mu)xc \right] \\
u_{41} &= \frac{D\beta^4}{2} \left[\left(3 - 2\mu - \mu^2 \right) \frac{s}{\beta} - (1-\mu)^2 xc \right], \quad u_{43} = \frac{\beta^2}{2} \left[(1+\mu)\frac{s}{\beta} - (1-\mu)xc \right]
\end{aligned}$$

15.11.3 Isotropic Rectangle Plate with Axial Force

The transfer matrix is

$$\mathbf{U}_x = \begin{bmatrix} \frac{1}{g}(\eta_1 c + \eta_2 C) & -\frac{1}{g} \left(\frac{\eta_2 s}{a} + \frac{\eta_1 S}{b} \right) & -\frac{1}{gD}(c - C) & -\frac{1}{gD} \left(\frac{s}{a} - \frac{S}{b} \right) \\ -\frac{1}{g}(\eta_1 as - \eta_2 bS) & \frac{1}{g}(\eta_1 c + \eta_2 C) & \frac{1}{gD}(as + bS) & \frac{1}{gD}(c - C) \\ -\frac{D}{g}\eta_1 \eta_2 (c - C) & \frac{D}{g} \left(\frac{\eta_2^2 s}{a} - \frac{\eta_1^2 S}{b} \right) & \frac{1}{g}(\eta_1 c + \eta_2 C) & \frac{1}{g} \left(\frac{\eta_2 s}{a} + \frac{\eta_1 S}{b} \right) \\ \frac{D}{g}(\eta_1^2 as + \eta_2^2 bS) & \frac{D}{g}\eta_1 \eta_2 (c - C) & \frac{1}{g}(\eta_1 as - \eta_2 bS) & \frac{1}{g}(\eta_1 c + \eta_2 C) \end{bmatrix} \tag{15.54}$$

where $s = \sinh ax$, $S = \sin bx$, $c = \cosh ax$ and $C = \cos bx$.

For the plate with free vibration

$$a^2 = \sqrt{\frac{\rho}{D}}\omega + \left(\frac{m\pi}{L_y}\right)^2, \quad b^2 = \sqrt{\frac{\rho}{D}}\omega - \left(\frac{m\pi}{L_y}\right)^2, \quad g = 2\sqrt{\frac{\rho}{D}}\omega$$

$$\eta_1 = \sqrt{\frac{\rho}{D}}\omega - (1-\mu)\left(\frac{m\pi}{L_y}\right)^2, \quad \eta_2 = \sqrt{\frac{\rho}{D}}\omega + (1-\mu)\left(\frac{m\pi}{L_y}\right)^2$$

For the plate under the planar pressure $P_y \neq 0$ and $P_x = 0$, we get

$$a^2 = \frac{m\pi}{L_y}\sqrt{\frac{P_y}{D}} + \left(\frac{m\pi}{L_y}\right)^2, \quad b^2 = \frac{m\pi}{L_y}\sqrt{\frac{P_y}{D}} - \left(\frac{m\pi}{L_y}\right)^2, \quad g = 2\frac{m\pi}{L_y}\sqrt{\frac{P_y}{D}}$$

$$\eta_1 = \frac{m\pi}{L_y}\sqrt{\frac{P_y}{D}} - (1-\mu)\left(\frac{m\pi}{L_y}\right)^2, \quad \eta_2 = \frac{m\pi}{L_y}\sqrt{\frac{P_y}{D}} + (1-\mu)\left(\frac{m\pi}{L_y}\right)^2$$

15.11.4 General Rectangle Plate

The transfer matrix is

$$\mathbf{U}_x = \begin{bmatrix} e_1 + (\zeta + \alpha_1)e_3 & -e_2 - (\zeta + \alpha_2)e_4 & -e_3/D_x & -e_4/D_x \\ -e_0 - (\zeta + \alpha_1)e_2 & e_1 + (\zeta + \alpha_2)e_3 & e_2/D_x & e_3/D_x \\ D_x[\lambda + \alpha_1(\zeta + \alpha_1)]e_3 & u_{32} & e_1 - \alpha_1e_3 & e_2 - \alpha_1e_4 \\ u_{41} & -D_x[\lambda + \alpha_2(\zeta + \alpha_2)]e_3 & e_0 - \alpha_2e_2 & e_1 - \alpha_2e_3 \end{bmatrix} \quad (15.55)$$

where

$$u_{32} = D_x[e_0 - (\alpha_1 - \zeta - \alpha_2)e_2 - \alpha_1(\zeta + \alpha_2)e_4]$$

$$u_{41} = D_x[(\lambda + \alpha_1\alpha_2 + \alpha_1\zeta)e_2 - \lambda(\alpha_2 - \alpha_1)e_4]$$

P_x and P_y are the pressures, if the planar force is tensile, P_x and P_y should be replaced by $-P_x$ and $-P_y$, and e_0, e_1, e_2, e_3 and e_4 are shown in Table 15.1.

A, B, C, D, g, a and b in Table 15.1 are shown in Table 15.2.

For the orthogonal anisotropic plate

$$\lambda = \frac{1}{D_x} \left[K - \rho\omega^2 + D_y \left(\frac{m\pi}{L_y} \right)^4 - P_y \left(\frac{m\pi}{L_y} \right)^2 \right], \quad \zeta = \frac{1}{D_x} \left[P_x - 2B \left(\frac{m\pi}{L_y} \right)^2 \right]$$

$$B = (D_x\mu_y + D_y\mu_x + 4D_{xy})/2, \quad \alpha_1 = \mu_y \left(\frac{m\pi}{L_y} \right)^2, \quad \alpha_2 = \left(\frac{4D_{yx}}{D_x} + \mu_y \right) \left(\frac{m\pi}{L_y} \right)^2$$

For the isotropic plate

$$\lambda = \frac{1}{D} \left[K - \rho\omega^2 + D \left(\frac{m\pi}{L_y} \right)^4 - P_y \left(\frac{m\pi}{L_y} \right)^2 \right], \quad \zeta = \frac{1}{D} \left[P_x - 2D \left(\frac{m\pi}{L_y} \right)^2 \right]$$

$$\alpha_1 = \mu \left(\frac{m\pi}{L_y} \right)^2, \quad \alpha_2 = (2-\mu) \left(\frac{m\pi}{L_y} \right)^2$$

Table 15.1 The expression of e_0, e_1, e_2, e_3 and e_4

		$\lambda > 0$			
	$\lambda < 0$	$\lambda = 0$	$\lambda = \zeta^2/4$	$\lambda < \zeta^2/4$	$\lambda > \zeta^2/4$
e_0	$\frac{1}{g}(a^3C - b^3D)$	$-\zeta B$	$-\frac{\zeta}{4}(3C + Ax)$	$-\frac{1}{g}(b^3D - a^3C)$	$-\lambda e_4 - \zeta e_2$
e_1	$\frac{1}{g}(a^2A + b^2B)$	A	$\frac{1}{2}(2A - Bx)$	$\frac{1}{g}(b^2B - a^2A)$	$AB - \frac{b^2 - a^2}{2ab}CD$
e_2	$\frac{1}{g}(aC + bD)$	B	$\frac{1}{2}(C + Ax)$	$\frac{1}{2}(bD - aC)$	$\frac{1}{2ab}(aAD + bBC)$
e_3	$\frac{1}{g}(A - B)$	$\frac{1}{\zeta}(1 - A)$	$\frac{Cx}{2}$	$\pm \frac{1}{g}(A - B)$	$\frac{1}{2ab}CD$
	$\frac{1}{g}\left(\frac{C}{a} - \frac{D}{b}\right)$	$\frac{1}{\zeta}(x - B)$	$\frac{1}{\zeta}(C - Ax)$	$\pm \frac{1}{g}\left(\frac{C}{a} - \frac{D}{b}\right)$	$\frac{1}{2(a^2 + b^2)}\left(\frac{AD}{b} - \frac{BC}{a}\right)$
				+ is fit for $\zeta > 0$ - is fit for $\zeta < 0$	
				+ is fit for $\zeta > 0$ - is fit for $\zeta < 0$	

Table 15.2 The expression of A, B, C, D, g, a and b

$\lambda < 0$	$\lambda = 0$	$\lambda > 0$		
		$\lambda = \zeta^2/4$	$\lambda < \zeta^2/4$	$\lambda > \zeta^2/4$
$A = \cosh ax$ $B = \cos bx$ $C = \sinh ax$ $D = \sin bx$ $g = a^2 + b^2$ $a^2 = \sqrt{\beta^4 + \frac{\zeta^2}{4}} - \frac{\zeta}{2}$ $b^2 = \sqrt{\beta^4 + \frac{\zeta^2}{4}} + \frac{\zeta}{2}$ $\beta^4 = -\lambda$	$\zeta > 0$ $\alpha^2 = \zeta$ $A = \cos ax$ $B = \frac{\sin ax}{\alpha}$	$\zeta > 0$ $\beta^2 = \zeta/2$ $A = \cos \beta x$ $B = \beta \sin \beta x$ $C = \frac{\sin \beta x}{\beta}$	$\zeta > 0$ $A = \cos ax, B = \cos bx$ $C = \sin ax, D = \sin bx$ $g = b^2 - a^2$ $a^2 = \zeta/2 - \sqrt{\zeta^2/4 - \lambda}$ $b^2 = \zeta/2 + \sqrt{\zeta^2/4 - \lambda}$	$A = \cosh ax$ $B = \cos bx$ $C = \sinh ax$ $D = \sin bx$ $a^2 = \frac{\sqrt{\lambda}}{2} - \frac{\zeta}{4}$ $b^2 = \frac{\sqrt{\lambda}}{2} + \frac{\zeta}{4}$
	$\zeta < 0$ $\alpha^2 = -\zeta$ $A = \cosh ax$ $B = \frac{\sinh ax}{\alpha}$	$\zeta < 0$ $\beta^2 = \zeta/2$ $A = \cosh \beta x$ $B = -\beta \sinh \beta x$ $C = \frac{\sinh \beta x}{\beta}$	$\zeta < 0$ $A = \cosh ax, B = \cosh bx$ $C = \sinh ax, D = \sinh bx$ $g = b^2 - a^2$ $a^2 = -\zeta/2 + \sqrt{\zeta^2/4 - \lambda}$ $b^2 = -\zeta/2 - \sqrt{\zeta^2/4 - \lambda}$	

15.12 Disk

15.12.1 Dynamic Equations of a Disk

As shown in Figure 15.8, the disk acts on a symmetrical load. Its basic dynamic equations of flexural motion are

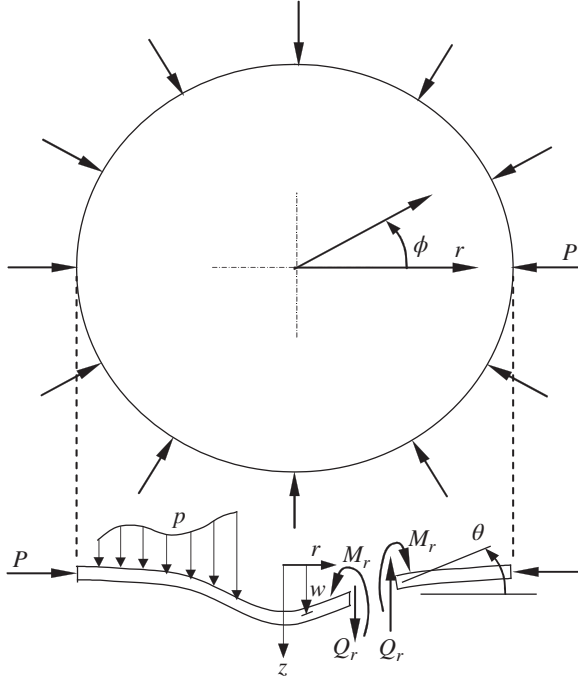


Figure 15.8 Positive deflection, slope, bending moment and shearing force.

$$\begin{aligned}
 \frac{\partial w}{\partial r} &= -\theta \\
 \frac{\partial \theta}{\partial r} &= \frac{M_r}{D_r} + \mu_\phi \left(\frac{1}{r^2} \frac{\partial^2 w}{\partial \phi^2} - \frac{\theta}{r} \right) + \frac{M_{Tr}}{D_r} \\
 \frac{\partial M_r}{\partial r} &= - \left(1 - \frac{\mu_r D_\phi}{D_r} \right) \frac{M_r}{r} + Q_r - [D_\phi (1 - \mu_r \mu_\phi) + 4D_{r\phi}] \frac{1}{r^3} \frac{\partial^2 w}{\partial \phi^2} \\
 &\quad - P_r \theta + \frac{D_\phi (1 - \mu_r \mu_\phi)}{r^2} \theta - \frac{4D_{r\phi}}{r^2} \frac{\partial^2 \theta}{\partial \phi^2} - \frac{1}{r} \left(M_{T\phi} - \frac{\mu_r D_\phi}{D_r} M_{Tr} \right) + \rho i_\phi^2 \frac{\partial^2 \theta}{\partial t^2} \\
 \frac{\partial Q_r}{\partial r} &= - \frac{Q_r}{r} - \frac{\mu_r D_\phi}{r^2 D_r} \frac{\partial^2 M_r}{\partial \phi^2} + \frac{D_\phi (1 - \mu_r \mu_\phi)}{r^4} \frac{\partial^4 w}{\partial \phi^4} - \frac{4D_{r\phi}}{r^4} \frac{\partial^2 w}{\partial \phi^2} \\
 &\quad - [D_\phi (1 - \mu_r \mu_\phi) + 4D_{r\phi}] \frac{1}{r^3} \frac{\partial^2 \theta}{\partial \phi^2} + \frac{1}{r^2} \frac{\partial}{\partial \phi} \left(P_\phi \frac{\partial w}{\partial \phi} \right) \\
 &\quad + \frac{1}{r^2} \left(\frac{\partial^2 M_{T\phi}}{\partial \phi^2} - \frac{\mu_r D_\phi}{D_r} \frac{\partial^2 M_{Tr}}{\partial \phi^2} \right) + Kw - \rho \frac{i_r^2}{r^2} \frac{\partial^4 w}{\partial t^2 \partial \phi^2} + \rho \frac{\partial^2 w}{\partial t^2} - p(r, \phi, t)
 \end{aligned} \tag{15.56}$$

where

$$D_r = \frac{E_r h^3}{12(1 - \mu_r \mu_\phi)}, \quad D_\phi = \frac{E_\phi h^3}{12(1 - \mu_r \mu_\phi)}, \quad D_{r\phi} = \frac{G h^3}{12} \tag{15.57}$$

$$\begin{cases} M_{Tr} = \int_{-h/2}^{+h/2} \frac{E_r(\alpha_r + \mu_\phi \alpha_\phi)}{1 - \mu_r \mu_\phi} \Delta T z dz \\ M_{T\phi} = \int_{-h/2}^{+h/2} \frac{E_\phi(\alpha_\phi + \mu_r \alpha_r)}{1 - \mu_r \mu_\phi} \Delta T z dz \end{cases} \quad (15.58)$$

$$\begin{cases} M_\phi = -D_\phi \left(\frac{1}{r} \frac{\partial w}{\partial r} + \frac{1}{r^2} \frac{\partial^2 w}{\partial \phi^2} + \mu_r \frac{\partial^2 w}{\partial r^2} \right) - M_{T\phi} \\ M_{r\phi} = M_{\phi r} = 2D_{r\phi} \left(\frac{1}{r} \frac{\partial^2 w}{\partial r \partial \phi} - \frac{1}{r^2} \frac{\partial w}{\partial \phi} \right) \end{cases} \quad (15.59)$$

P_r and P_ϕ are the planar pressures, w is the transverse deflection and D_r , D_ϕ and $D_{r\phi}$ are the bending stiffnesses. μ_r and μ_ϕ are the Poisson's ratios with respect to the r and ϕ directions, respectively. ρ is the mass density, and i_r and i_ϕ are the rotational gyration radius around the axial and tangent directions, respectively. K is the elastic modulus of the foundation, p is the distributed transverse loading intensity, and E_r and E_ϕ are the material elastic modulus with respect to the direction of r and ϕ . G is the material shear elastic modulus, h is the thickness of the plate and ΔT is the temperature variation. α_r and α_ϕ are the heat expansion coefficients with respect to the direction of r and ϕ . M_r and M_ϕ are the bending moments, and $M_{r\phi}$ and $M_{\phi r}$ are the torsional moments.

If an isotropic disk only vibrates transversely, Equation (15.56) is usually written as the fourth-order basic equation:

$$D\nabla^4 w + \frac{\partial}{\partial r} \left(P_r \frac{\partial w}{\partial r} \right) - \frac{P_r}{r} \frac{\partial w}{\partial r} + \frac{1}{r^2} \frac{\partial^2}{\partial \phi^2} \left(P_\phi \frac{\partial w}{\partial \phi} \right) + Kw + \rho \frac{\partial^2 w}{\partial t^2} = p(x, y, t) \nabla^2 M_T \quad (15.60)$$

where

$$\nabla^2 = \frac{\partial^2}{\partial r^2} + \frac{1}{r} \frac{\partial}{\partial r} + \frac{1}{r^2} \frac{\partial^2}{\partial \phi^2}, \quad M_T = \int_{-h/2}^{+h/2} E\alpha(1-\mu)\Delta T z dz, \quad \nabla^4 = (\nabla^2)^2.$$

If the pressures P_x and P_y are replaced by $-P_x$ and $-P_y$, then Equation (15.56) or Equation (15.60) is also valid for tensile forces.

The variables w , θ , M_r and Q_r can be expanded in Fourier series as follows

$$\begin{cases} w(r, \phi, t) = \sum_{m=0}^{\infty} [w_m^c(r, t) \cos m\phi + w_m^s(r, t) \sin m\phi] \\ \theta(r, \phi, t) = \sum_{m=0}^{\infty} [\theta_m^c(r, t) \cos m\phi + \theta_m^s(r, t) \sin m\phi] \\ M_r(r, \phi, t) = \sum_{m=0}^{\infty} [M_{rm}^c(r, t) \cos m\phi + M_{rm}^s(r, t) \sin m\phi] \\ Q_r(r, \phi, t) = \sum_{m=0}^{\infty} [Q_{rm}^c(r, t) \cos m\phi + Q_{rm}^s(r, t) \sin m\phi] \end{cases} \quad (15.61)$$

$$w(r, t) = w_0^c(r, t), \quad \theta(r, t) = \theta_0^c(r, t), \quad M_r(r, t) = M_{r0}^c(r, t), \quad Q_r(r, t) = Q_{r0}^c(r, t) \quad (15.62)$$

For a symmetrical motion ($m=0$), Equation (15.61) can be further simplified:

$$w(r, t) = w_0^c(r, t), \quad \theta(r, t) = \theta_0^c(r, t), \quad M_r(r, t) = M_{r0}^c(r, t), \quad Q_r(r, t) = Q_{r0}^c(r, t) \quad (15.62)$$

The mechanical load and heat load are expanded as follows:

$$\begin{cases} p(r, \phi, t) = \sum_{m=0}^{\infty} [p_m^c(r, t) \cos m\phi + p_m^s(r, t) \sin m\phi] \\ M_T(r, \phi, t) = \sum_{m=0}^{\infty} [M_{Tm}^c(r, t) \cos m\phi + M_{Tm}^s(r, t) \sin m\phi] \end{cases} \quad (15.63)$$

Substituting Equations (15.61) and (15.63) into Equation (15.56) yields

$$\begin{cases} \frac{\partial w_m^j}{\partial r} = -\theta_m^j \\ \frac{\partial \theta_m^j}{\partial r} = \frac{M_{rm}^j}{D_r} - \frac{\mu_\phi}{r} \theta_m^j - \frac{\mu_\phi m^2}{r^2} w_m^j + \frac{M_{Trm}^j}{D_r} \\ \frac{\partial M_{rm}^j}{\partial r} = - \left(1 - \frac{\mu_r D_\phi}{D_r} \right) \frac{M_{rm}^j}{r} + Q_{rm}^j + [D_\phi (1 - \mu_r \mu_\phi) + 4D_{r\phi}] \frac{m^2}{r^3} w_m^j \\ \quad + \left[D_\phi (1 - \mu_r \mu_\phi) \frac{1}{r^2} + 4D_{r\phi} \frac{m^2}{r^2} - P_r \right] \theta_m^j - \frac{1}{r} \left(M_{T\phi m}^j - \frac{\mu_r D_\phi}{D_r} M_{Trm}^j \right) + \rho i_\phi^2 \frac{\partial^2 \theta_m^j}{\partial t^2} \\ \frac{\partial Q_{rm}^j}{\partial r} = - \frac{Q_{rm}^j}{r} - \frac{\mu_r D_\phi m^2}{r^2 D_r} M_{rm}^j + \frac{1}{r^4} [D_\phi (1 - \mu_r \mu_\phi) m^4 + 4D_{r\phi} m^2] w_m^j \\ \quad + [D_\phi (1 - \mu_r \mu_\phi) + 4D_{r\phi}] \frac{m^2}{r^3} \theta_m^j + \frac{P_\phi m^2}{r^2} w_m^j - \frac{m^2}{r^2} \left(M_{T\phi m}^j - \frac{\mu_r D_\phi}{D_r} M_{Trm}^j \right) \\ \quad + K w_m^j + \frac{m^2 \rho i_r^2}{r^2} \frac{\partial^2 w_m^j}{\partial t^2} + \rho \frac{\partial^2 w_m^j}{\partial t^2} - p_m^j(r, t) \end{cases} \quad (15.64)$$

where $j = c$ or $j = s$.

The state vector is defined as

$$\mathbf{Z}_m(y) = [w_m^j, \theta_m^j, M_{rm}^j, Q_{rm}^j]^T \quad (15.65)$$

The corresponding transfer matrix can be obtained as follows.

15.12.2 Massless Isotropic Disk

The transfer matrix is

1) $m = 0$

$$\mathbf{U}_r = \begin{bmatrix} 1 & 0 & -\frac{r^2}{2D(1+\mu)} & 0 \\ 0 & 0 & \frac{r}{D(1+\mu)} & 0 \\ 0 & 0 & 1 & 0 \\ 0 & 0 & 0 & 0 \end{bmatrix} \quad (15.66a)$$

2) $m = 1$

$$\mathbf{U}_r = \begin{bmatrix} 0 & -r & 0 & -\frac{r^3}{2D(3+\mu)} \\ 0 & 1 & 0 & \frac{3r^2}{2D(3+\mu)} \\ 0 & 0 & 0 & r \\ 0 & 0 & 0 & 1 \end{bmatrix} \quad (15.66b)$$

3) $m \geq 2$

$$\mathbf{U}_r = \begin{bmatrix} r^m & r^{m+2} & 0 & 0 \\ -mr^{m-1} & -(m+2)r^{m+1} & 0 & 0 \\ -Dm(m-1)(1-\mu)r^{m-2} & -D(1+m)(m+2-\mu m+2\mu)r^m & 0 & 0 \\ Dm^2(m-1)(1-\mu)r^{m-3} & Dm(1+m)[m(1-\mu)-4]r^{m-1} & 0 & 0 \end{bmatrix} \quad (15.66c)$$

15.12.3 Massless Rigid Disk

The transfer matrix is

1) $m = 0$

$$\mathbf{U}_r = \begin{bmatrix} 1 & 0 & 0 & 0 \\ 0 & 0 & 0 & 0 \\ 0 & 0 & 1 & 0 \\ 0 & 0 & 0 & 0 \end{bmatrix} \quad (15.67a)$$

2) $m = 1$

$$\mathbf{U}_r = \begin{bmatrix} 0 & -r & 0 & 0 \\ 0 & 1 & 0 & 0 \\ 0 & 0 & 0 & r \\ 0 & 0 & 0 & 1 \end{bmatrix} \quad (15.67b)$$

3) $m \geq 2$

$$\mathbf{U}_r \equiv \mathbf{O} \quad (15.67c)$$

15.12.4 Massless Disk with a Rigid Support at its Center

The transfer matrix is

1) $m = 0$

$$\mathbf{U}_r = \begin{bmatrix} -\frac{r^2}{8\pi D}(\ln r - 1) & \frac{r^2}{4} & 0 & 0 \\ \frac{r}{4\pi D}\left(\ln r - \frac{1}{2}\right) & -\frac{r}{2} & 0 & 0 \\ \frac{r}{4\pi}\left[(1+\mu)\ln r + \frac{1-\mu}{2}\right] & -\frac{D}{2}(1+\mu) & 0 & 0 \\ \frac{1}{2\pi r} & 0 & 0 & 0 \end{bmatrix} \quad (15.68)$$

2) $m > 0$

The transfer matrix can be obtained from Equation (15.66b) or Equation (15.66c).

15.12.5 Massless Disk with Planar Symmetrical Pressure P_r

The transfer matrix is

$$\mathbf{U}_r = \begin{bmatrix} 1 & 0 & \frac{J_0(\alpha r) - 1}{D\alpha^2} & 0 \\ 0 & 0 & \frac{J_1(\alpha r)}{D\alpha} & 0 \\ 0 & 0 & J_0(\alpha r) - \frac{(1-\mu)J_1(\alpha r)}{D\alpha} & 0 \\ 0 & 0 & 0 & 0 \end{bmatrix} \quad (15.69)$$

where $J_0(\alpha r)$ and $J_1(\alpha r)$ are the Bessel functions and $\alpha^2 = P/D$.

15.12.6 Symmetrical Disk

The transfer matrix is

$$\mathbf{U}_r = \begin{bmatrix} \frac{J_0(\alpha r) + I_0(\alpha r)}{2} & 0 & \frac{J_0(\alpha r) - I_0(\alpha r)}{2D\alpha^2} & 0 \\ \alpha \frac{J_1(\alpha r) - I_1(\alpha r)}{2} & 0 & \frac{J_1(\alpha r) + I_1(\alpha r)}{2D\alpha} & 0 \\ u_{31} & 0 & u_{33} & 0 \\ -D\alpha^3 \frac{J_1(\alpha r) + I_1(\alpha r)}{2} & 0 & -\alpha \frac{J_1(\alpha r) - I_1(\alpha r)}{2} & 0 \end{bmatrix} \quad (15.70)$$

where

$$\alpha^2 = \sqrt{\omega^2 P/D}$$

$$u_{31} = D\alpha \left(\frac{\alpha[J_0(\alpha r) - I_0(\alpha r)]}{2} - \frac{(1-\mu)[J_1(\alpha r) - I_1(\alpha r)]}{2r} \right)$$

$$u_{33} = \frac{J_0(\alpha r) + I_0(\alpha r)}{2} - \frac{(1-\mu)[J_1(\alpha r) + I_1(\alpha r)]}{2\alpha r}$$

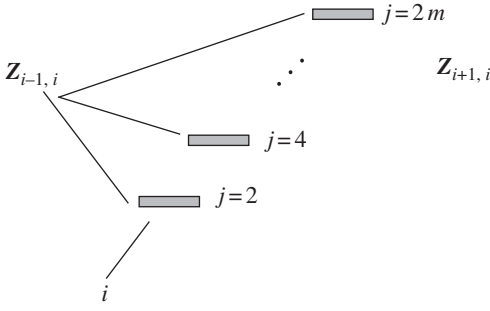


Figure 15.9 The beam strips in a two-dimensional plate.

15.13 Strip Element of a Two-dimensional Thin Plate

15.13.1 Massless Beam Strip

The beam strip i in a two-dimensional plate, as shown in Figure 15.9, comprises m massless elastic beams. The state vectors of its input and output ends are defined as

$$\mathbf{Z}_{i-1,i} = \left[\mathbf{Z}_{(i-1,i),2}^T, \mathbf{Z}_{(i-1,i),4}^T, \dots, \mathbf{Z}_{(i-1,i),2m}^T \right]^T \quad (15.71)$$

$$\mathbf{Z}_{i+1,i} = \left[\mathbf{Z}_{(i+1,i),2}^T, \mathbf{Z}_{(i+1,i),4}^T, \dots, \mathbf{Z}_{(i+1,i),2m}^T \right]^T \quad (15.72)$$

where

$$\mathbf{Z}_{(i-1,i),j} = \left[Z, \theta_x, \theta_y, M_x, M_y, Q_z \right]_{(i-1,i),j}^T \quad (15.73)$$

$$\mathbf{Z}_{(i+1,i),j} = \left[Z, \theta_x, \theta_y, M_x, M_y, Q_z \right]_{(i+1,i),j}^T \quad (15.74)$$

The sequence number of the row of beam element (i,j) is denoted by index $j, j = 2, 4, \dots, 2m$.

The transfer equation of the beam strip i is

$$\mathbf{Z}_{i+1,i} = \mathbf{U}_i \mathbf{Z}_{i-1,i} \quad (15.75)$$

The transfer matrix is

$$\mathbf{U}_i = \begin{bmatrix} \mathbf{U}_{i,2} & & & \\ & \mathbf{U}_{i,4} & & \\ & & \ddots & \\ & & & \mathbf{U}_{i,2m} \end{bmatrix} \quad (15.76)$$

where

$$\mathbf{U}_{i,j} = \begin{bmatrix} 1 & 0 & -x & 0 & -\frac{x^2}{2EI_{i,j}} & \frac{x^3}{6EI_{i,j}} \\ 0 & 1 & 0 & \frac{x}{(GJ_p)_{i,j}} & 0 & 0 \\ 0 & 0 & 1 & 0 & \frac{x}{EI_{i,j}} & -\frac{x^2}{2EI_{i,j}} \\ 0 & 0 & 0 & 1 & 0 & 0 \\ 0 & 0 & 0 & 0 & 1 & -x \\ 0 & 0 & 0 & 0 & 0 & 1 \end{bmatrix}_{x=l_{i,j}} \quad (15.77)$$

$\mathbf{U}_{i,j}$ ($j = 2, 4, 6, \dots, 2m$) is the transfer matrix of single beam element (i, j) , and EI_{ij} , l_{ij} and $(GJ_p)_{ij}$ are the bending stiffness, length and torsional stiffness of the beam element (i, j) , respectively.

15.13.2 Lumped Mass Strip

The lumped mass strip i in a two-dimensional plate, as shown in Figure 15.10, comprises m lumped masses and $m + 1$ massless beams. The state vectors of its input and output ends are defined as

$$\mathbf{Z}_{i,i-1} = \begin{bmatrix} \mathbf{Z}_{(i,i-1),2}^T & \mathbf{Z}_{(i,i-1),4}^T & \cdots & \mathbf{Z}_{(i,i-1),2m}^T \end{bmatrix}^T \quad (15.78)$$

$$\mathbf{Z}_{i,i+1} = \begin{bmatrix} \mathbf{Z}_{(i,i+1),2}^T & \mathbf{Z}_{(i,i+1),4}^T & \cdots & \mathbf{Z}_{(i,i+1),2m}^T \end{bmatrix}^T \quad (15.79)$$

where

$$\mathbf{Z}_{(i,i-1),j} = [Z, \theta_x, \theta_y, M_x, M_y, Q_z]_{(i,i-1),j}^T \quad (15.80)$$

$$\mathbf{Z}_{(i,i+1),j} = [Z, \theta_x, \theta_y, M_x, M_y, Q_z]_{(i,i+1),j}^T \quad (15.81)$$

The sequence number of the row of lumped mass element (i, j) is denoted by index j .

The transfer equation of the lumped mass strip i is

$$\mathbf{Z}_{i,i+1} = \mathbf{U}_i \mathbf{Z}_{i,i-1} \quad (15.82)$$

The transfer matrix is

$$\mathbf{U}_i = \begin{bmatrix} \mathbf{U}_{i,2,0} & \mathbf{U}_{i,2,+2} & & & & \\ \mathbf{U}_{i,4,-2} & \mathbf{U}_{i,4,0} & \mathbf{U}_{i,4,+2} & & & \\ & \mathbf{U}_{i,6,-2} & \mathbf{U}_{i,6,0} & \mathbf{U}_{i,6,+2} & & \\ & & \ddots & \ddots & \ddots & \\ & & & \mathbf{U}_{i,2m-2,-2} & \mathbf{U}_{i,2m-2,0} & \mathbf{U}_{i,2m-2,+2} \\ & & & & \mathbf{U}_{i,2m,-2} & \mathbf{U}_{i,2m,0} \end{bmatrix} \quad (15.83)$$

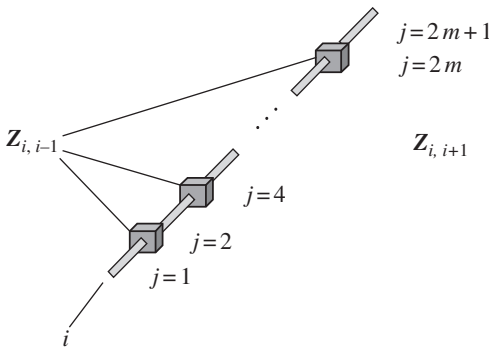


Figure 15.10 The lumped mass strips in a two-dimensional plate.

where

$$\mathbf{u}_{i,j,-2} = \begin{bmatrix} \mathbf{O}_{3 \times 3} & \mathbf{O}_{3 \times 3} \\ \mathbf{u}_{-2,2,1} & \mathbf{O}_{3 \times 3} \end{bmatrix}, \quad \mathbf{u}_{-2,2,1} = \begin{bmatrix} \frac{6EI_{i,j-1}}{l_{i,j-1}^2} & \frac{2EI_{i,j-1}}{l_{i,j-1}} & 0 \\ 0 & 0 & -\frac{(GJ_p)_{i,j-1}}{l_{i,j-1}} \\ \frac{12EI_{i,j-1}}{l_{i,j-1}^3} & \frac{6EI_{i,j-1}}{l_{i,j-1}^2} & 0 \end{bmatrix} \quad (j = 4, 6, \dots, 2m) \quad (15.84)$$

$$\mathbf{u}_{i,j,0} = \begin{bmatrix} \mathbf{I}_3 & \mathbf{O}_{3 \times 3} \\ \mathbf{u}_{0,2,1} & \mathbf{I}_3 \end{bmatrix}, \quad (j = 2, 4, 6, \dots, 2m-2, 2m) \quad (15.85)$$

$$\begin{aligned} \mathbf{u}_{i,j,+2} &= \begin{bmatrix} \mathbf{O}_{3 \times 3} & \mathbf{O}_{3 \times 3} \\ \mathbf{u}_{+2,2,1} & \mathbf{O}_{3 \times 3} \end{bmatrix}, \quad \mathbf{u}_{+2,2,1} \\ &= \begin{bmatrix} -\frac{6EI_{i,j+1}}{l_{i,j+1}^2} & \frac{2EI_{i,j+1}}{l_{i,j+1}} & 0 \\ 0 & 0 & -\frac{(GJ_p)_{i,j+1}}{l_{i,j+1}} \\ \frac{12EI_{i,j+1}}{l_{i,j+1}^3} & -\frac{6EI_{i,j+1}}{l_{i,j+1}^2} & 0 \end{bmatrix} \quad (j = 2, 4, \dots, 2m-2) \quad (15.86) \\ \mathbf{u}_{0,2,1} &= \begin{bmatrix} -\frac{6EI_{i,j-1}}{l_{i,j-1}^2} + \frac{6EI_{i,j+1}}{l_{i,j+1}^2} & \frac{4EI_{i,j-1}}{l_{i,j-1}} + \frac{4EI_{i,j+1}}{l_{i,j+1}} - J_{xi,j}\omega^2 & 0 \\ 0 & 0 & \frac{(GJ_p)_{i,j-1}}{l_{i,j-1}} + \frac{(GJ_p)_{i,j+1}}{l_{i,j+1}} - J_{yi,j}\omega^2 \\ m_{i,j}\omega^2 - \frac{12EI_{i,j-1}}{l_{i,j-1}^3} - \frac{12EI_{i,j+1}}{l_{i,j+1}^3} & \frac{6EI_{i,j-1}}{l_{i,j-1}^2} - \frac{6EI_{i,j+1}}{l_{i,j+1}^2} & 0 \end{bmatrix} \\ &\quad (j = 4, 6, \dots, 2m-2) \quad (15.87) \end{aligned}$$

If the beam element (i, j) has a simply supported boundary, when $j = 2$ and $j = 2m$, we obtain

$$\mathbf{u}_{0,2,1} = \begin{bmatrix} -\frac{3EI_{i,j-1}}{l_{i,j-1}^2} + \frac{6EI_{i,j+1}}{l_{i,j+1}^2} & \frac{3EI_{i,j-1}}{l_{i,j-1}} + \frac{4EI_{i,j+1}}{l_{i,j+1}} - J_{xi,j}\omega^2 & 0 \\ 0 & 0 & \frac{(GJ_p)_{i,j-1}}{l_{i,j-1}} + \frac{(GJ_p)_{i,j+1}}{l_{i,j+1}} - J_{yi,j}\omega^2 \\ m_{i,j}\omega^2 - \frac{3EI_{i,j-1}}{l_{i,j-1}^3} - \frac{12EI_{i,j+1}}{l_{i,j+1}^3} & \frac{3EI_{i,j-1}}{l_{i,j-1}^2} - \frac{6EI_{i,j+1}}{l_{i,j+1}^2} & 0 \end{bmatrix} \quad (j = 2) \quad (15.88)$$

$$\mathbf{U}_{0,2,1} = \begin{bmatrix} -\frac{6EI_{i,j-1}}{l_{i,j-1}^2} + \frac{3EI_{i,j+1}}{l_{i,j+1}^2} & \frac{4EI_{i,j-1}}{l_{i,j-1}} + \frac{3EI_{i,j+1}}{l_{i,j+1}} - J_{xi,j}\omega^2 & 0 \\ 0 & 0 & \frac{(GJ_p)_{i,j-1}}{l_{i,j-1}} + \frac{(GJ_p)_{i,j+1}}{l_{i,j+1}} - J_{yi,j}\omega^2 \\ m_{i,j}\omega^2 - \frac{12EI_{i,j-1}}{l_{i,j-1}^3} - \frac{3EI_{i,j+1}}{l_{i,j+1}^3} & \frac{6EI_{i,j-1}}{l_{i,j-1}^2} - \frac{3EI_{i,j+1}}{l_{i,j+1}^2} & 0 \end{bmatrix} \quad (j=2m) \quad (15.89)$$

If the beam element (i, j) has a fixed boundary, when $j = 2$ and $j = 2m$, $\mathbf{U}_{0,2,1}$ in Equation (15.86) can be determined by Equation (15.87).

If the beam element (i, j) has a free boundary, when $j = 2$ and $j = 2m$,

$$\mathbf{U}_{0,2,1} = \begin{bmatrix} \frac{6EI_{i,j+1}}{l_{i,j+1}^2} & \frac{4EI_{i,j+1}}{l_{i,j+1}} - J_{xi,j}\omega^2 & 0 \\ 0 & 0 & \frac{(GJ_p)_{i,j+1}}{l_{i,j+1}} - J_{yi,j}\omega^2 \\ m_{i,j}\omega^2 - \frac{12EI_{i,j+1}}{l_{i,j+1}^3} & -\frac{6EI_{i,j+1}}{l_{i,j+1}^2} & 0 \end{bmatrix} \quad (j=2) \quad (15.90)$$

$$\mathbf{U}_{0,2,1} = \begin{bmatrix} -\frac{6EI_{i,j-1}}{l_{i,j-1}^2} & \frac{4EI_{i,j-1}}{l_{i,j-1}} - J_{xi,j}\omega^2 & 0 \\ 0 & 0 & \frac{(GJ_p)_{i,j-1}}{l_{i,j-1}} - J_{yi,j}\omega^2 \\ m_{i,j}\omega^2 - \frac{12EI_{i,j-1}}{l_{i,j-1}^3} & \frac{6EI_{i,j-1}}{l_{i,j-1}^2} & 0 \end{bmatrix} \quad (j=2m) \quad (15.91)$$

15.14 Thick-walled Cylinder

15.14.1 Dynamic Equations of a Thick-walled Cylinder

As shown in Figure 15.11, the basic equations [38] for the radial motion of a thick-walled cylinder are

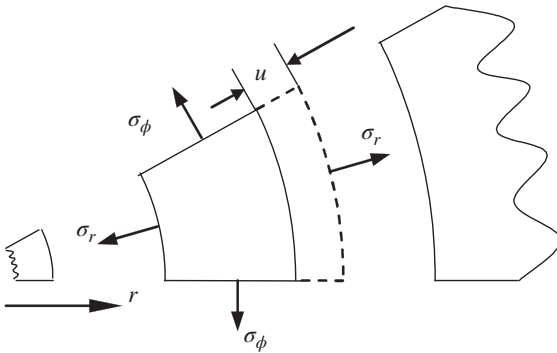


Figure 15.11 Positive radial displacement and stress.

$$\begin{aligned}\frac{\partial u}{\partial r} &= -\frac{\lambda}{r(\lambda + 2G)}u + \frac{1}{\lambda + 2G}\sigma_r + \frac{3\lambda + 2G}{\lambda + 2G}\alpha\Delta T \\ \frac{\partial \sigma_r}{\partial r} &= \frac{4G}{r^2}\frac{G + \lambda}{\lambda + 2G}u - \frac{1}{r}\frac{2G}{\lambda + 2G}\sigma_r + \rho\frac{\partial^2 u}{\partial t^2} - \frac{1}{r}\frac{2G(3\lambda + 2G)}{\lambda + 2G}\alpha\Delta T - p_r(r, t)\end{aligned}\quad (15.92)$$

where

$$G = \frac{E}{2(1 + \mu)}, \quad \lambda = \frac{E\mu}{2(1 - \mu^2)} \quad (15.93)$$

r and ϕ are the radial coordinate and the circumferential coordinate. u is the radial displacement, σ_r is the radial stress, σ_ϕ is the shear stress, p_r is the distributed radial loading intensity, ρ is the mass density, α is the heat expansion coefficient, ΔT is the temperature variation, G is the material shear elastic modulus, λ is the Reynolds coefficient, E is the material elastic modulus and μ is the material Poisson's ratio.

The state vector is defined as

$$\mathbf{Z}(r) = [u, \sigma_r]^T \quad (15.94)$$

The corresponding transfer matrix can be obtained as follows.

15.14.2 Massless Isotropic Cylinder

The transfer matrix is

$$\mathbf{U}_r = \begin{bmatrix} \frac{1}{1-\mu} \left(\frac{G\mu}{\lambda} \frac{r}{a_k} + \frac{a_k}{2r} \right) & \frac{\mu}{2(1-\mu)\lambda} \frac{r^2 - a_k^2}{r} \\ \frac{G}{1-\mu} \frac{r^2 - a_k^2}{a_k r^2} & \frac{1}{1-\mu} \left[\frac{1}{2} + \frac{G\mu}{\lambda} \left(\frac{a_k}{r} \right)^2 \right] \end{bmatrix} \quad (15.95)$$

where a_k is the radial coordinate of the inner surface of the cylinder.

15.14.3 Massless Isotropic Cylinder without a Center Hole

The transfer matrix is

$$\mathbf{U}_r = \begin{bmatrix} 0 & \frac{\mu r}{\lambda} \\ 0 & 1 \end{bmatrix} \quad (15.96)$$

15.14.4 Isotropic Cylinder

The transfer matrix is

$$\mathbf{U}_r = \begin{bmatrix} \frac{1}{e_1} [e_3(a_k)J_\gamma(\beta r) - e_2(a_k)y_\gamma(\beta r)] & \frac{1}{e_1} [J_\gamma(\beta a_k)y_\gamma(\beta r) - y_\gamma(\beta a_k)J_\gamma(\beta r)] \\ \frac{1}{e_1} [e_3(a_k)e_2(r) - e_2(a_k)e_3(r)] & \frac{1}{e_1} [J_\gamma(\beta a_k)e_3(r) - y_\gamma(\beta a_k)e_2(r)] \end{bmatrix} \quad (15.97)$$

where

$$\gamma = 1, \quad \beta^2 = \frac{\rho\omega^2}{\lambda + 2G}, \quad e_1 = e_3(a_k)J_1(\beta a_k) - e_2(a_k)y_1(\beta a_k)$$

$$e_2(r) = \frac{\lambda + 2G}{r} \left[\frac{2(\lambda + G)}{\lambda + 2G} J_1(\beta r) - \beta r J_2(\beta r) \right], \quad e_3(r) = \frac{\lambda + 2G}{r} \left[\frac{2(\lambda + G)}{\lambda + 2G} y_1(\beta r) - \beta r y_2(\beta r) \right]$$

$J_\gamma(\beta r)$ and $y_\gamma(\beta r)$ are the first type and second type of Bessel functions with λ , respectively.

15.14.5 Isotropic Cylinder without a Center Hole

The transfer matrix is

$$\mathbf{U}_r = \begin{bmatrix} 0 & \frac{J_1(\beta r)}{(\lambda + G)\beta} \\ 0 & \frac{\lambda + 2G}{(\lambda + G)\beta} \left[\frac{2(\lambda + G)}{\lambda + 2G} J_1(\beta r) - \beta r J_2(\beta r) \right] \end{bmatrix} \quad (15.98)$$

where $\beta = \sqrt{\rho\omega^2/(\lambda + 2G)}$ and $J_1(\beta r)$, $J_2(\beta r)$ are the first kind Bessel functions.

15.15 Thin-walled Cylinder

15.15.1 Dynamic Equations of a Thin-walled Cylinder

As shown in Figure 15.12, the basic equations [38] for the radial motion and flexural displacement of a thin-walled cylinder are

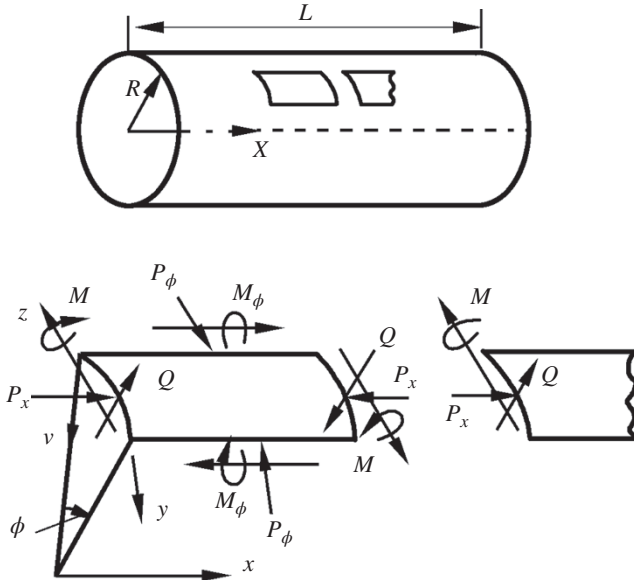


Figure 15.12 Positive deflection, internal moment and internal force.

$$\begin{aligned}
\frac{\partial v}{\partial x} &= -\theta + \frac{Q}{D_Q} \\
\frac{\partial \theta}{\partial x} &= \frac{M + M_{Tx}}{D_x} \\
\frac{\partial M}{\partial x} &= Q - P_x \theta + \rho r_y^2 \frac{\partial^2 \theta}{\partial t^2} - c(x, t) \\
\frac{\partial Q}{\partial x} &= \frac{K_\phi (1 - \mu_x \mu_\phi)}{R^2} v + \rho \frac{\partial^2 \theta}{\partial t^2} - p(x, t) \\
&\quad + \frac{1}{R} \left[\frac{\mu_x K_\phi}{K_x} (P_x + P_{Tx}) - P_{T\phi} \right]
\end{aligned} \tag{15.99}$$

where x and ϕ are the axial coordinate and the circumferential coordinate, v is the radial displacement, θ is the rotational angle of the displacement course, R is the radius of the cylinder, M is the axial moment per unit circumferential length, Q is the shear force per unit circumferential length, D_Q is the shear stiffness, K_x and K_ϕ are the extension stiffnesses, D_x and D_ϕ are the flexural stiffnesses, p and c are the distributed loading intensities, ρ is the mass density, μ_x and μ_ϕ are the Poisson ratios of the material, r_y is the gyration radius of the cross-section around the y axis, P_x is the axial pressure, and P_{Tx} and $P_{T\phi}$ are the temperature effect forces.

For an isotropic homogeneous material

$$\begin{aligned}
\mu_x &= \mu_\phi = \mu \\
D_x &= D_\phi = D = \frac{Eh^3}{12(1-\mu^2)}, \quad K_x = K_\phi = K = \frac{Eh^3}{12(1-\mu^2)} \\
P_{Tx} &= P_{T\phi} = -\frac{1}{1-\mu} \int_h E\alpha \Delta T dz, \quad M_{Tx} = \frac{1}{1-\mu} \int_h E\alpha \Delta T z dz
\end{aligned}$$

where α is the heat expansion coefficient, ΔT is the temperature variation and E is the material elastic modulus.

The state vector is defined as

$$\mathbf{Z}(x) = [v, \theta, M, Q]^T \tag{15.100}$$

The corresponding transfer matrix can be obtained as follows.

15.15.2 Massless Thin-walled Cylinder with Shear Deformation

The transfer matrix is

$$\mathbf{U}_x = \begin{bmatrix} 1 & -x & -\frac{x^2}{2D_x} & -\frac{x^3}{3D_x} + \frac{x}{D_Q} \\ 0 & 1 & \frac{x}{D_x} & \frac{x^2}{2D_x} \\ 0 & 0 & 1 & x \\ 0 & 0 & 0 & 1 \end{bmatrix} \tag{15.101}$$

Table 15.3 The expression of e_0, e_1, e_2, e_3 and e_4

	$\lambda < 0$	$\lambda = 0, \lambda - \zeta\eta = 0$		$\lambda = 0, \lambda - \zeta\eta = 0$		
		$\zeta = \eta = 0$	$\zeta \neq 0, \eta = 0$	$\lambda - \zeta\eta = \frac{1}{4}(\zeta - \eta)^2$	$\lambda - \zeta\eta < \frac{1}{4}(\zeta - \eta)^2, \zeta - \eta \neq 0$	$\lambda - \zeta\eta > \frac{1}{4}(\zeta - \eta)^2$
e_0	$\frac{1}{g}(a^3C - b^3D)$	0	$-\zeta B$	$-\frac{\xi - \eta}{4}(3C + Ax)$	$-\frac{1}{g}(b^3D - a^3C)$	$-(\lambda - \zeta\eta)e_4 - (\zeta - \eta)e_2$
e_1	$\frac{1}{g}(a^2A + b^2B)$	1	A	$\frac{1}{2}(2A - Bx)$	$\frac{P}{g}(b^2B - a^2A)$	$AB - \frac{b^2 - a^2}{2ab}CD$
e_2	$\frac{1}{g}(aC + bD)$	x	B	$\frac{1}{2}(C + Ax)$	$\frac{P}{2}(bD - aC)$	$\frac{1}{2ab}(aAD + bBC)$
e_3	$\frac{1}{g}(A - B)$	$\frac{x^2}{2}$	$\frac{1}{\zeta}(1 - A)$	$\frac{Cx}{2}$	$\frac{1}{g}(A - B)$	$\frac{1}{2ab}CD$
e_4	$\frac{1}{g}\left(\frac{C}{a} - \frac{D}{b}\right)$	$\frac{x^3}{6}$	$\frac{1}{\zeta}(x - B)$	$\frac{1}{\zeta}(C - Ax)$	$\frac{1}{g}\left(\frac{C}{a} - \frac{D}{b}\right)$	$\frac{1}{2(a^2 + b^2)}\left(\frac{AD}{b} - \frac{BC}{a}\right)$

15.15.3 General Thin-walled Cylinder

The transfer matrix is

$$\mathbf{U}_x = \begin{bmatrix} e_1 + \zeta e_3 & -e_2 & -\frac{e_3}{D_x} & -\frac{e_4}{D_x} + \frac{e_2 + \zeta e_4}{D_Q} \\ \lambda e_4 & e_1 - \eta e_3 & \frac{e_2 - \eta e_4}{D_x} & \frac{e_3}{D_x} \\ \lambda D_x e_3 & D_x(e_0 - \eta e_2) & e_1 - \eta e_3 & e_2 \\ \lambda D_x(e_2 + \zeta e_4) & -\lambda D_x e_3 & -\lambda e_4 & e_1 + \zeta e_3 \end{bmatrix} \quad (15.102)$$

where

$$\lambda = \frac{\frac{Eh}{R^2} - \rho\omega^2}{D_x}, \quad \eta = \frac{\frac{Eh}{R^2} - \rho\omega^2}{D_Q}, \quad \zeta = \frac{P_x + \rho r_y^2 \omega^2}{D_x}$$

e_0, e_1, e_2, e_3 and e_4 are shown in Table 15.3.

A, B, C, D, g, a and b in Table 15.3 are shown in Table 15.4.

15.16 Coordinate Transformation Matrix

For convenient study, the inertial coordinate system describing the motion of each element may have different orientations. For instance, elements i and $i + 1$ are adjacent elements in a system. There is an angle between the coordinate system of element i and coordinate system $i + 1$, and the angle is denoted as ϕ . The state vector of the output end of element i described in the

Table 15.4 The expression of A, B, C, D, g, a and b

$\lambda < 0$	$\lambda = 0, \lambda - \zeta\eta = 0$	$\lambda = 0, \lambda - \zeta\eta = 0$		
		$\lambda - \zeta\eta = \frac{1}{4}(\zeta - \eta)^2$	$\lambda - \zeta\eta < \frac{1}{4}(\zeta - \eta)^2, \zeta - \eta \neq 0$	$\lambda - \zeta\eta > \frac{1}{4}(\zeta - \eta)^2$
$A = \cosh ax, B = \cos bx$ $C = \sinh ax, D = \sin bx$ $g = a^2 + b^2$ $a^2 = \sqrt{\beta^4 + \frac{(\zeta + \eta)^2}{4}} - \frac{\zeta - \eta}{2}$ $b^2 = \sqrt{\beta^4 + \frac{(\zeta + \eta)^2}{4}} + \frac{\zeta - \eta}{2}$ $\beta^4 = -\lambda$	$\zeta > 0$ $\alpha^2 = \zeta$ $A = \cos ax$ $B = \frac{\sin ax}{\alpha}$	$\zeta - \eta > 0$ $\beta^2 = (\zeta - \eta)/2$ $A = \cos \beta x$ $B = \beta \sin \beta x$ $C = \frac{\sin \beta x}{\beta}$	$\zeta - \eta > 0$ $g = b^2 - a^2, P = 1$ $A = \cos ax, B = \cos bx$ $C = \sin ax, D = \sin bx$ $a^2 = (\zeta - \eta)/2 - \sqrt{(\zeta + \eta)^2/4 - \lambda}$ $b^2 = (\zeta - \eta)/2 + \sqrt{(\zeta + \eta)^2/4 - \lambda}$	$A = \cosh ax$ $B = \cos bx$ $C = \sinh ax$ $D = \sin bx$ $a^2 = \frac{1}{2}\sqrt{\lambda - \zeta\eta} - \frac{\zeta - \eta}{4}$ $b^2 = \frac{1}{2}\sqrt{\lambda - \zeta\eta} + \frac{\zeta - \eta}{4}$
	$\zeta < 0$ $\alpha^2 = -\zeta$ $A = \cosh ax$ $B = \frac{\sinh ax}{\alpha}$	$\zeta - \eta < 0$ $\beta^2 = -(\zeta - \eta)/2$ $A = \cosh \beta x$ $B = -\beta \sinh \beta x$ $C = \frac{\sinh \beta x}{\beta}$	$\zeta - \eta < 0$ $g = a^2 - b^2, P = -1$ $A = \cosh ax, B = \cosh bx$ $C = \sinh ax, D = \sinh bx$ $a^2 = -(\zeta - \eta)/2 + \sqrt{(\zeta + \eta)^2/4 - \lambda}$ $b^2 = -(\zeta - \eta)/2 - \sqrt{(\zeta + \eta)^2/4 - \lambda}$	

coordinates of element i is $\mathbf{Z}_{O,i} = \mathbf{U}_i \mathbf{Z}_{I,i}$, and the state vector of the input end of element $i + 1$ described in the coordinates of element $i + 1$ is $\mathbf{Z}_{I,i+1}$. The state vector $\mathbf{Z}_{i+1,i}$ is often described in the coordinates of element $i + 1$, that is, $\mathbf{Z}_{i+1,i} = \mathbf{Z}_{I,i+1}$. However, $\mathbf{Z}_{O,i}$ and $\mathbf{Z}_{i+1,i}$ are also the same state vectors, but are described in different coordinate systems. The relation between them is

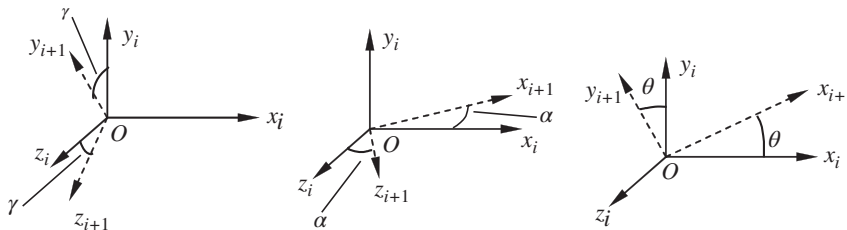
$$\mathbf{Z}_{i+1,i} = \mathbf{H}_\phi \mathbf{Z}_{O,i} \quad (15.103)$$

where \mathbf{H}_ϕ is the coordinate transformation matrix corresponding to the angle ϕ between the two coordinates.

When spatial motion is studied, the state vector is defined as

$$\mathbf{Z} = [X, Y, Z, \theta_x, \theta_y, \theta_z, M_x, M_y, M_z, Q_x, Q_y, Q_z]^T$$

The three types of coordinate transform matrix that could be used are shown in Figure 15.13.

**Figure 15.13** Coordinate transformation in space.

1) Rotation about the x axis with angle γ

$$\mathbf{H}_\gamma = \begin{bmatrix} \mathbf{H}_{1,1} & & & \\ & \mathbf{H}_{2,2} & & \\ & & \mathbf{H}_{3,3} & \\ & & & \mathbf{H}_{4,4} \end{bmatrix} \quad (15.104)$$

where

$$\mathbf{H}_{j,j} = \begin{bmatrix} 1 & 0 & 0 \\ 0 & \cos \gamma & \sin \gamma \\ 0 & -\sin \gamma & \cos \gamma \end{bmatrix} \quad (j = 1, 2, 3, 4)$$

2) Rotation about the y axis with angle α

$$\mathbf{H}_\alpha = \begin{bmatrix} \mathbf{H}_{1,1} & & & \\ & \mathbf{H}_{2,2} & & \\ & & \mathbf{H}_{3,3} & \\ & & & \mathbf{H}_{4,4} \end{bmatrix} \quad (15.105)$$

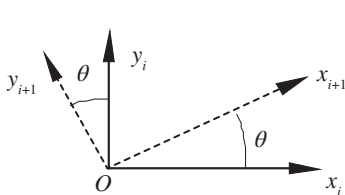
where

$$\mathbf{H}_{j,j} = \begin{bmatrix} \cos \alpha & 0 & -\sin \alpha \\ 0 & 1 & 0 \\ \sin \alpha & 0 & \cos \alpha \end{bmatrix} \quad (j = 1, 2, 3, 4)$$

3) Rotation about the z axis with angle θ

$$\mathbf{H}_\theta = \begin{bmatrix} \mathbf{H}_{1,1} & & & \\ & \mathbf{H}_{2,2} & & \\ & & \mathbf{H}_{3,3} & \\ & & & \mathbf{H}_{4,4} \end{bmatrix} \quad (15.106)$$

where



$$\mathbf{H}_{j,j} = \begin{bmatrix} \cos \theta & \sin \theta & 0 \\ -\sin \theta & \cos \theta & 0 \\ 0 & 0 & 1 \end{bmatrix} \quad (j = 1, 2, 3, 4)$$

If planar motion is studied, as shown in Figure 15.14, the state vector can be defined as

Figure 15.14 Coordinate transformation in a plane.

$$\mathbf{Z} = [X, Y, \theta_z, M_z, Q_x, Q_y]^T$$

The coordinate transformation matrix is

$$H_\theta = \begin{bmatrix} \cos\theta & \sin\theta & 0 & 0 & 0 & 0 \\ -\sin\theta & \cos\theta & 0 & 0 & 0 & 0 \\ 0 & 0 & 1 & 0 & 0 & 0 \\ 0 & 0 & 0 & \cos\theta & \sin\theta & 0 \\ 0 & 0 & 0 & -\sin\theta & \cos\theta & 0 \end{bmatrix} \quad (15.107)$$

If the form of the state vector is

$$\mathbf{Z} = [Z, \theta_x, \theta_y, M_x, M_y, Q_z]^T$$

the coordinate transformation matrix is

$$H_\theta = \begin{bmatrix} 1 & 0 & 0 & 0 & 0 & 0 \\ 0 & \cos\theta & \sin\theta & 0 & 0 & 0 \\ 0 & -\sin\theta & \cos\theta & 0 & 0 & 0 \\ 0 & 0 & 0 & \cos\theta & \sin\theta & 0 \\ 0 & 0 & 0 & -\sin\theta & \cos\theta & 0 \\ 0 & 0 & 0 & 0 & 0 & 1 \end{bmatrix} \quad (15.108)$$

15.17 Linearization and State Vectors

15.17.1 Linearization

1) Linearization of velocity (angular velocity) and acceleration (angular acceleration) leads to

$$\ddot{\mathbf{z}}(t_i) = \mathbf{A}(t_{i-1})\mathbf{z}(t_i) + \mathbf{B}_z(t_{i-1}), \dot{\mathbf{z}}(t_i) = \mathbf{C}(t_{i-1})\mathbf{z}(t_i) + \mathbf{D}_z(t_{i-1})$$

According to the different numerical integration methods, the choices of $\mathbf{A}(t_{i-1})$, $\mathbf{B}_z(t_{i-1})$, $\mathbf{C}(t_{i-1})$ and $\mathbf{D}_z(t_{i-1})$ are shown in Table 7.2.

2) Linearization of nonlinear functions

See Table 7.3.

3) Linearization of the coordinate transformation matrix

The direction cosine matrix may be given as rotations about the spatially fixed three axes x - y - z . Thus the angular velocity vector in the body-fixed reference system is

$$\boldsymbol{\omega} = [\mathbf{T}_1 \quad \mathbf{T}_2 \quad \mathbf{T}_3] [\dot{\theta}_x, \dot{\theta}_y, \dot{\theta}_z]^T$$

The linearization of the direction cosine matrix is

$$\mathbf{A}(t_i) = \mathbf{A}(t_{i-1})\tilde{\mathbf{T}}_1(t_{i-1})\theta_x(t_i) + \mathbf{A}(t_{i-1})\tilde{\mathbf{T}}_2(t_{i-1})\theta_y(t_i) + \mathbf{A}(t_{i-1})\tilde{\mathbf{T}}_3(t_{i-1})\theta_z(t_i) + \boldsymbol{\Phi}(t_{i-1}) \quad (15.109)$$

where

$$\begin{aligned} \Phi(t_{i-1}) = \mathbf{A}(t_{i-1}) & \left\{ \mathbf{I} - \tilde{\mathbf{T}}_1(t_{i-1})\theta_x(t_{i-1}) - \tilde{\mathbf{T}}_2(t_{i-1})\theta_y(t_{i-1}) - \tilde{\mathbf{T}}_3(t_{i-1})\theta_z(t_{i-1}) \right. \\ & + \left[\frac{1}{2}\tilde{\mathbf{T}}_1^2(t_{i-1})\dot{\theta}_x^2(t_{i-1}) + \frac{1}{2}\tilde{\mathbf{T}}_2^2(t_{i-1})\dot{\theta}_y^2(t_{i-1}) + \frac{1}{2}\tilde{\mathbf{T}}_3^2(t_{i-1})\dot{\theta}_z^2(t_{i-1}) + \tilde{\mathbf{T}}_2(t_{i-1})\tilde{\mathbf{T}}_1(t_{i-1})\dot{\theta}_y(t_{i-1})\dot{\theta}_x(t_{i-1}) \right. \\ & \left. \left. + \tilde{\mathbf{T}}_3(t_{i-1})\tilde{\mathbf{T}}_2(t_{i-1})\dot{\theta}_z(t_{i-1})\dot{\theta}_y(t_{i-1}) + \tilde{\mathbf{T}}_3(t_{i-1})\tilde{\mathbf{T}}_1(t_{i-1})\dot{\theta}_z(t_{i-1})\dot{\theta}_x(t_{i-1}) \right] \Delta T^2 \right\} \end{aligned} \quad (15.110)$$

15.17.2 State Vectors

1) Planar rigid body

$$\mathbf{z} = [x, y, \theta, m, q_x, q_y, 1]^T \quad (15.111)$$

2) Spatial rigid body

$$\mathbf{z} = [x, y, z, \theta_x, \theta_y, \theta_z, m_x, m_y, m_z, q_x, q_y, q_z, 1]^T \quad (15.112)$$

3) Planar beam

$$\mathbf{z} = [x, y, \theta, m, q_x, q_y, q^1, q^2, \dots, q^n, 1]^T \quad (15.113)$$

4) Spatial beam

$$\mathbf{z} = [x, y, z, \theta_x, \theta_y, \theta_z, m_x, m_y, m_z, q_x, q_y, q_z, q^1, q^2, \dots, q^n, 1]^T \quad (15.114)$$

15.18 Spring and Damper Hinges Connected to Rigid Bodies

15.18.1 Spring Hinge whose Inboard and Outboard Bodies are Planar Rigid Bodies

Neglecting the mass and the initial length of the spring, the constitutive relationships of the nonlinear spring hinge are

$$\begin{cases} \mathbf{q} = K_1 \Delta \mathbf{l} + K_2 \Delta \mathbf{l}^3 \\ m_l = K'_1(\theta_O - \theta_l) + K'_2(\theta_O - \theta_l)^3 \end{cases}$$

where $|\Delta \mathbf{l}| = \sqrt{(x_O - x_l)^2 + (y_O - y_l)^2}$ is a variable quantity of the length of the spring and \mathbf{q} is the elastic force. K_1 and K_2 are the longitudinal stiffness coefficients of the nonlinear translational spring, and K'_1 and K'_2 are the torsional stiffness coefficients of the nonlinear rotational spring.

The transfer matrix is

$$\mathbf{U} = \begin{bmatrix} 1 & 0 & 0 & 0 & \frac{\Delta_{11}}{\Delta} & \frac{\Delta_{12}}{\Delta} & \frac{\Delta_{13}}{\Delta} \\ 0 & 1 & 0 & 0 & \frac{\Delta_{21}}{\Delta} & \frac{\Delta_{22}}{\Delta} & \frac{\Delta_{23}}{\Delta} \\ 0 & 0 & 1 & u_{34} & 0 & 0 & u_{37} \\ 0 & 0 & 0 & 1 & 0 & 0 & 0 \\ 0 & 0 & 0 & 0 & 1 & 0 & 0 \\ 0 & 0 & 0 & 0 & 0 & 1 & 0 \\ 0 & 0 & 0 & 0 & 0 & 0 & 1 \end{bmatrix} \quad (15.115)$$

where

$$\Delta = \begin{vmatrix} a_1 & a_2 \\ b_1 & b_2 \end{vmatrix}$$

$$\Delta_{11} = \begin{vmatrix} -1 & a_2 \\ 0 & b_2 \end{vmatrix}, \Delta_{12} = \begin{vmatrix} 0 & a_2 \\ -1 & b_2 \end{vmatrix}, \Delta_{13} = \begin{vmatrix} -a_3 & a_2 \\ -b_3 & b_2 \end{vmatrix}$$

$$\Delta_{21} = \begin{vmatrix} a_1 & -1 \\ b_1 & 0 \end{vmatrix}, \Delta_{22} = \begin{vmatrix} a_1 & 0 \\ b_1 & -1 \end{vmatrix}, \Delta_{23} = \begin{vmatrix} a_1 & -a_3 \\ b_1 & -b_3 \end{vmatrix}$$

$$u_{34} = \frac{1}{K'_1 + 3 K'_2 [\theta_O(t_{i-1}) - \theta_I(t_{i-1})]^2}$$

$$u_{37} = - \frac{K'_2 \left\{ 3 [\dot{\theta}_O(t_{i-1}) - \dot{\theta}_I(t_{i-1})]^2 [\theta_O(t_{i-1}) - \theta_I(t_{i-1})] \Delta T^2 - 2 [\theta_O(t_{i-1}) - \theta_I(t_{i-1})]^3 \right\}}{K'_1 + 3 K'_2 [\theta_O(t_{i-1}) - \theta_I(t_{i-1})]^2}$$

a_1, a_2, a_3, b_1, b_2 and b_3 are the linearization coefficients, as shown in Equation (8.199).

15.18.2 Damper Hinge whose Inboard and Outboard Bodies are Planar Rigid Bodies

For a viscous damper hinge whose inboard body and outboard body are planar rigid bodies, the damper force and damper torques are

$$q_x = -C_d(\dot{x}_O - \dot{x}_I), q_y = -C_d(\dot{y}_O - \dot{y}_I), m = C'_d(\dot{\theta}_O - \dot{\theta}_I)$$

where C_d and C'_d are the translational and rotary damper coefficients of dampers.

The transfer matrix is

$$\mathbf{U} = \begin{bmatrix} 1 & 0 & 0 & 0 & u_{15} & 0 & u_{17} \\ 0 & 1 & 0 & 0 & 0 & u_{26} & u_{27} \\ 0 & 0 & 1 & u_{34} & 0 & 0 & u_{37} \\ 0 & 0 & 0 & 1 & 0 & 0 & 0 \\ 0 & 0 & 0 & 0 & 1 & 0 & 0 \\ 0 & 0 & 0 & 0 & 0 & 1 & 0 \\ 0 & 0 & 0 & 0 & 0 & 0 & 1 \end{bmatrix} \quad (15.116)$$

where

$$u_{15} = -\frac{1}{C_d C}, \quad u_{26} = -\frac{1}{C_d C}, \quad u_{34} = \frac{1}{C'_d C},$$

$$u_{17} = \frac{D_{x_I} - D_{x_O}}{C}, \quad u_{27} = \frac{D_{y_I} - D_{y_O}}{C}, \quad u_{37} = -\frac{D_{\theta_I} - D_{\theta_O}}{C}$$

$C, D_{x_I}, D_{x_O}, D_{y_I}, D_{y_O}, D_{\theta_I}$ and D_{θ_O} are the linearization coefficients.

15.18.3 Spring and Damper Hinge whose Inboard and Outboard Bodies are Spatial Rigid Bodies

The transfer matrix is

$$\mathbf{U} = \begin{bmatrix} \mathbf{I}_3 & \mathbf{O}_{3 \times 3} & \mathbf{O}_{3 \times 3} & \mathbf{U}_{14} & \mathbf{U}_{15} \\ \mathbf{O}_{3 \times 3} & \mathbf{U}_{22} & \mathbf{U}_{23} & \mathbf{O}_{3 \times 3} & \mathbf{U}_{25} \\ \mathbf{O}_{3 \times 3} & \mathbf{O}_{3 \times 3} & \mathbf{O}_{3 \times 3} & \mathbf{O}_{3 \times 3} & \mathbf{O}_{3 \times 1} \\ \mathbf{O}_{3 \times 3} & \mathbf{O}_{3 \times 3} & \mathbf{O}_{3 \times 3} & \mathbf{I}_3 & \mathbf{O}_{3 \times 1} \\ \mathbf{O}_{1 \times 3} & \mathbf{O}_{3 \times 1} & \mathbf{O}_{3 \times 1} & \mathbf{O}_{3 \times 1} & 1 \end{bmatrix} \quad (15.117)$$

where

$$\begin{aligned} \mathbf{U}_{14} &= -(\mathbf{K} + \mathbf{C}_d \mathbf{C})^{-1} \\ \mathbf{U}_{15} &= -(\mathbf{K} + \mathbf{C}_d \mathbf{C})^{-1} \mathbf{C}_d (\mathbf{D}_{r_l} - \mathbf{D}_{r_o}) \\ \mathbf{U}_{22} &= (\mathbf{K}' + \mathbf{C}_d' \mathbf{A}_O \mathbf{H}_O \mathbf{C})^{-1} (\mathbf{K}' + \mathbf{C}_d' \mathbf{A}_I \mathbf{H}_I \mathbf{C}) \\ \mathbf{U}_{23} &= (\mathbf{K}' + \mathbf{C}_d' \mathbf{A}_O \mathbf{H}_O \mathbf{C})^{-1} \\ \mathbf{U}_{25} &= (\mathbf{K}' + \mathbf{C}_d' \mathbf{A}_O \mathbf{H}_O \mathbf{C})^{-1} \mathbf{C}_d' (\mathbf{A}_I \mathbf{H}_I \mathbf{D}_{\theta_l} - \mathbf{A}_O \mathbf{H}_O \mathbf{D}_{\theta_o}) \end{aligned}$$

15.19 Smooth Hinges Connected to Rigid Bodies

The transfer matrix of a smooth pin hinge whose outboard body also has a smooth pin hinge at its output is given as follows. The transfer matrix of a smooth pin hinge whose outboard hinge is neither a smooth ball-and-socket hinge nor a dummy hinge can be derived the method given in section 7.6.3.

15.19.1 Smooth Pin Hinge whose Inboard and Outboard Bodies are Planar Rigid Bodies

The transfer matrix is

$$\mathbf{U} = \begin{bmatrix} 1 & 0 & 0 & 0 & 0 & 0 & 0 \\ 0 & 1 & 0 & 0 & 0 & 0 & 0 \\ -\frac{u_{41}}{u_{43}} & -\frac{u_{42}}{u_{43}} & 0 & 0 & -\frac{u_{45}}{u_{43}} & -\frac{u_{46}}{u_{43}} & -\frac{u_{47}}{u_{43}} \\ 0 & 0 & 0 & 0 & 0 & 0 & 0 \\ 0 & 0 & 0 & 0 & 1 & 0 & 0 \\ 0 & 0 & 0 & 0 & 0 & 1 & 0 \\ 0 & 0 & 0 & 0 & 0 & 0 & 1 \end{bmatrix} \quad (15.118)$$

where $u_{41}, u_{42}, u_{43}, u_{45}, u_{46}$ and u_{47} are elements of the transfer matrix of the outboard rigid body.

15.19.2 Smooth Ball-and-socket Hinge whose Inboard and Outboard Bodies are Spatial Rigid Bodies

The transfer matrix is

$$\mathbf{U} = \begin{bmatrix} \mathbf{I}_3 & \mathbf{O}_{3 \times 3} & \mathbf{O}_{3 \times 3} & \mathbf{O}_{3 \times 3} & \mathbf{O}_{3 \times 1} \\ -\mathbf{U}_{32}^{-1}\mathbf{U}_{31} & \mathbf{O}_{3 \times 3} & \mathbf{O}_{3 \times 3} & -\mathbf{U}_{32}^{-1}\mathbf{U}_{34} & -\mathbf{U}_{32}^{-1}\mathbf{U}_{35} \\ \mathbf{O}_{3 \times 3} & \mathbf{O}_{3 \times 3} & \mathbf{O}_{3 \times 3} & \mathbf{O}_{3 \times 3} & \mathbf{O}_{3 \times 1} \\ \mathbf{O}_{3 \times 3} & \mathbf{O}_{3 \times 3} & \mathbf{O}_{3 \times 3} & \mathbf{I}_3 & \mathbf{O}_{3 \times 1} \\ \mathbf{O}_{1 \times 3} & \mathbf{O}_{1 \times 3} & \mathbf{O}_{1 \times 3} & \mathbf{O}_{1 \times 3} & 1 \end{bmatrix} \quad (15.119)$$

where \mathbf{U}_{31} , \mathbf{U}_{32} , \mathbf{U}_{34} and \mathbf{U}_{35} are elements of the transfer matrix of the outboard rigid body.

15.20 Rigid Bodies Moving in a Plane

15.20.1 Rigid Body with One Input End and One Output End Moving in a Plane

The transfer matrix is

$$\mathbf{U} = \begin{bmatrix} 1 & 0 & -y_{IO}(t_{i-1}) & 0 & 0 & 0 & b_1G_1 - b_2G_2 \\ 0 & 1 & x_{IO}(t_{i-1}) & 0 & 0 & 0 & b_1G_2 + b_2G_1 \\ 0 & 0 & 1 & 0 & 0 & 0 & 0 \\ u_{41} & u_{42} & u_{43} & 1 & u_{45} & u_{46} & u_{47} \\ -mA & 0 & mA y_{IC}(t_{i-1}) & 0 & 1 & 0 & u_{57} \\ 0 & -mA & -mA x_{IC}(t_{i-1}) & 0 & 0 & 1 & u_{67} \\ 0 & 0 & 0 & 0 & 0 & 0 & 1 \end{bmatrix} \quad (15.120)$$

where

$$\begin{aligned} u_{41} &= mA(y_{IO} - y_{IC}), \quad u_{42} = -mA(x_{IO} - x_{IC}), \quad u_{45} = -y_{IO}, \quad u_{46} = x_{IO} \\ u_{43} &= -mA x_{IC}(t_{i-1})x_{IO} - mA y_{IC}(t_{i-1})y_{IO} + J_I A \\ u_{47} &= -m_C + u_{67}x_{IO} - u_{57}y_{IO} + J_I B_\theta + (mB_{y_I} - f_{y,C})x_{IC} + (f_{x,C} - mB_{x_I})y_{IC} \\ u_{57} &= f_{x,C} - mA(c_{c1}G_1 - c_{c2}G_2) - mB_{x_C}, \quad u_{67} = f_{y,C} - mA(c_{c1}G_2 + c_{c2}G_1) - mB_{y_C} \\ x_{IC}(t_{i-1}) &= (c_{c1}c_I - c_{c2}s_I)|_{t_{i-1}}, \quad y_{IC}(t_{i-1}) = (c_{c1}s_I + c_{c2}c_I)|_{t_{i-1}} \\ x_{IO}(t_{i-1}) &= (b_1c_I - b_2s_I)|_{t_{i-1}}, \quad y_{IO}(t_{i-1}) = (b_1s_I + b_2c_I)|_{t_{i-1}} \\ x_{IC} &= c_{c1}c_I - c_{c2}s_I \approx c_{c1}g_1 - c_{c2}g_2, \quad y_{IC} = c_{c1}s_I + c_{c2}c_I \approx c_{c1}g_2 + c_{c2}g_1 \\ x_{IO} &= b_1c_I - b_2s_I \approx b_1g_1 - b_2g_2, \quad y_{IO} = b_1s_I + b_2c_I \approx b_1g_2 + b_2g_1 \end{aligned}$$

15.20.2 Planar Rigid Body with Multiple Input and Multiple Output Ends

The state vector is

$$\mathbf{z} = \left[\mathbf{z}_{I_1}^T, \mathbf{z}_{I_2}^T, \dots, \mathbf{z}_{I_n}^T, \mathbf{z}_{O_1}^T, \mathbf{z}_{O_2}^T, \dots, \mathbf{z}_{O_{n'}}^T \right]^T \quad (15.121)$$

The transfer equation is

$$\mathbf{U}\mathbf{z} = \mathbf{0}_{3n+3n'} \quad (15.122)$$

The transfer matrix is

$$\mathbf{U} = \begin{bmatrix} \mathbf{U}_{I_2 I_1} & \mathbf{U}_{I_1} & \mathbf{O}_{3 \times 7} & \cdots & \mathbf{O}_{3 \times 7} & \mathbf{O}_{3 \times 7} & \mathbf{O}_{3 \times 7} & \cdots & \mathbf{O}_{3 \times 7} \\ \mathbf{U}_{I_3 I_1} & \mathbf{O}_{3 \times 7} & \mathbf{U}_{I_1} & \cdots & \mathbf{O}_{3 \times 7} & \mathbf{O}_{3 \times 7} & \mathbf{O}_{3 \times 7} & \cdots & \mathbf{O}_{3 \times 7} \\ \vdots & \vdots & \vdots & \ddots & \vdots & \vdots & \vdots & & \vdots \\ \mathbf{U}_{I_n I_1} & \mathbf{O}_{3 \times 7} & \mathbf{O}_{3 \times 7} & \cdots & \mathbf{U}_{I_1} & \mathbf{O}_{3 \times 7} & \mathbf{O}_{3 \times 7} & \cdots & \mathbf{O}_{3 \times 7} \\ \mathbf{U}_{O_1 I_1} & \mathbf{O}_{3 \times 7} & \mathbf{O}_{3 \times 7} & \cdots & \mathbf{O}_{3 \times 7} & \mathbf{U}_{I_1} & \mathbf{O}_{3 \times 7} & \cdots & \mathbf{O}_{3 \times 7} \\ \mathbf{U}_{O_2 I_1} & \mathbf{O}_{3 \times 7} & \mathbf{O}_{3 \times 7} & \cdots & \mathbf{O}_{3 \times 7} & \mathbf{O}_{3 \times 7} & \mathbf{U}_{I_1} & \cdots & \mathbf{O}_{3 \times 7} \\ \vdots & \vdots & \vdots & & \vdots & \vdots & \vdots & \ddots & \vdots \\ \mathbf{U}_{O_{n'} I_1} & \mathbf{O}_{3 \times 7} & \mathbf{O}_{3 \times 7} & \cdots & \mathbf{O}_{3 \times 7} & \mathbf{O}_{3 \times 7} & \mathbf{O}_{3 \times 7} & \cdots & \mathbf{U}_{I_1} \\ \mathbf{U}_{I_1}^4 & \mathbf{U}_{I_2}^4 & \mathbf{U}_{I_3}^4 & \cdots & \mathbf{U}_{I_n}^4 & \mathbf{U}_{O_1}^4 & \mathbf{U}_{O_2}^4 & \cdots & \mathbf{U}_{O_{n'}}^4 \end{bmatrix} \quad (15.123)$$

Where

$$\mathbf{U}_{I_j I_1} = \begin{bmatrix} 1 & 0 & -y_{I_1 I_j}(t_{i-1}) & 0 & 0 & 0 & a_{1,j}G_1 - a_{2,j}G_2 \\ 0 & 1 & x_{I_1 I_j}(t_{i-1}) & 0 & 0 & 0 & a_{1,j}G_2 + a_{2,j}G_1 \\ 0 & 0 & 1 & 0 & 0 & 0 & 0 \end{bmatrix}_{I_j} \quad (j = 2, 3, \dots, n)$$

$$\mathbf{U}_{I_1} = [-\mathbf{I}_3 \quad \mathbf{O}_{3 \times 4}]$$

$$\mathbf{U}_{O_j I_1} = \begin{bmatrix} 1 & 0 & -y_{I_1 O_j}(t_{i-1}) & 0 & 0 & 0 & b_{1,j}G_1 - b_{2,j}G_2 \\ 0 & 1 & x_{I_1 O_j}(t_{i-1}) & 0 & 0 & 0 & b_{1,j}G_2 + b_{2,j}G_1 \\ 0 & 0 & 1 & 0 & 0 & 0 & 0 \end{bmatrix} \quad (j = 1, 2, \dots, n')$$

$$\mathbf{U}_{I_1}^4 = \begin{bmatrix} -m y_{I_1 C} A & m x_{I_1 C} A & J_{I_1} A & 1 & 0 & 0 & u_{47, I_1} \\ -m A & 0 & m A y_{I_1 C}(t_{i-1}) & 0 & 1 & 0 & u_{57, I_1} \\ 0 & -m A & -m A x_{I_1 C}(t_{i-1}) & 0 & 0 & 1 & u_{67, I_1} \end{bmatrix}$$

$$u_{47, I_1} = -m_C + J_{I_1} B_\theta + (m B_{y_{I_1}} - f_{y, C}) x_{I_1, C} - (m B_{x_{I_1}} - f_{x, C}) y_{I_1, C}$$

$$u_{57, I_1} = f_{x, C} - m A (c_{c1} G_1 - c_{c2} G_2) - m B_{x_C}$$

$$u_{67, I_1} = f_{y, C} - m A (c_{c1} G_2 + c_{c2} G_1) - m B_{y_C}$$

$$\mathbf{U}_{I_j}^4 = \begin{bmatrix} 0 & 0 & 0 & 1 & y_{I_1 I_j} & -x_{I_1 I_j} & 0 \\ 0 & 0 & 0 & 0 & 1 & 0 & 0 \\ 0 & 0 & 0 & 0 & 0 & 1 & 0 \end{bmatrix} \quad (j = 2, 3, \dots, n)$$

$$\mathbf{U}_{O_j}^4 = - \begin{bmatrix} 0 & 0 & 0 & 1 & y_{I_1 O_j} & -x_{I_1 O_j} & 0 \\ 0 & 0 & 0 & 0 & 1 & 0 & 0 \\ 0 & 0 & 0 & 0 & 0 & 1 & 0 \end{bmatrix} \quad (j = 1, 2, \dots, n')$$

15.20.3 Planar Rigid Body with Multiple Input Ends and One Output End

The state vector is

$$\mathbf{z} = \left[\mathbf{z}_{I_1}^T, \mathbf{z}_{I_2}^T, \dots, \mathbf{z}_{I_n}^T, \mathbf{z}_{O_1}^T \right]^T \quad (15.124)$$

The transfer equation is

$$\mathbf{U}\mathbf{z} = \mathbf{0}_{3n+3} \quad (15.125)$$

The transfer matrix is

$$\mathbf{U} = \begin{bmatrix} \mathbf{U}_{I_2 I_1} & \mathbf{U}_{I_1} & \mathbf{O}_{3 \times 7} & \cdots & \mathbf{O}_{3 \times 7} & \mathbf{O}_{3 \times 7} \\ \mathbf{U}_{I_3 I_1} & \mathbf{O}_{3 \times 7} & \mathbf{U}_{I_1} & \cdots & \mathbf{O}_{3 \times 7} & \mathbf{O}_{3 \times 7} \\ \vdots & \vdots & \vdots & \ddots & \vdots & \vdots \\ \mathbf{U}_{I_n I_1} & \mathbf{O}_{3 \times 7} & \mathbf{O}_{3 \times 7} & \cdots & \mathbf{U}_{I_1} & \mathbf{O}_{3 \times 7} \\ \mathbf{U}_{O_1 I_1} & \mathbf{O}_{3 \times 7} & \mathbf{O}_{3 \times 7} & \cdots & \mathbf{O}_{3 \times 7} & \mathbf{U}_{I_1} \\ \mathbf{U}_{I_1}^4 & \mathbf{U}_{I_2}^4 & \mathbf{U}_{I_3}^4 & \cdots & \mathbf{U}_{I_n}^4 & \mathbf{U}_{O_1}^4 \end{bmatrix} \quad (15.126)$$

where the submatrices are the same as in Equation (15.102).

15.20.4 Planar Rigid Body with One Input End and Multiple Output Ends

The state vector is

$$\mathbf{z} = \left[\mathbf{z}_{I_1}^T, \mathbf{z}_{O_1}^T, \mathbf{z}_{O_2}^T, \dots, \mathbf{z}_{O_{n'}}^T \right]^T \quad (15.127)$$

The transfer equation is

$$\mathbf{U}\mathbf{z} = \mathbf{0}_{2n'+4} \quad (15.128)$$

The transfer matrix is

$$\mathbf{U} = \begin{bmatrix} \mathbf{U}_{O_1 I_1} & \mathbf{U}_{I_1} & \mathbf{O}_{3 \times 7} & \cdots & \mathbf{O}_{3 \times 7} \\ \mathbf{U}_{O_2 I_1} & \mathbf{O}_{3 \times 7} & \mathbf{U}_{I_1} & \cdots & \mathbf{O}_{3 \times 7} \\ \vdots & \vdots & \vdots & \ddots & \vdots \\ \mathbf{U}_{O_{n'} I_1} & \mathbf{O}_{3 \times 7} & \mathbf{O}_{3 \times 7} & \cdots & \mathbf{U}_{I_1} \\ \mathbf{U}_{I_1}^4 & \mathbf{U}_{O_1}^4 & \mathbf{U}_{O_2}^4 & \cdots & \mathbf{U}_{O_{n'}}^4 \end{bmatrix} \quad (15.129)$$

where the submatrices are the same as those in Equation (15.123).

15.21 Spatial Rigid Bodies with Large Motion and Various Connections

15.21.1 Spatial Rigid Body with One Input End and One Output End

The transfer equation is

$$\mathbf{z}_O = \mathbf{U}\mathbf{z}_I \quad (15.130)$$

The transfer matrix is

$$U = \begin{bmatrix} I_3 & \Psi_{IO} & O_{3 \times 3} & O_{3 \times 3} & \Phi(t_{i-1})l_{IO} \\ O_{3 \times 3} & I_3 & O_{3 \times 3} & O_{3 \times 3} & O_{3 \times 1} \\ U_{31} & U_{32} & I_3 & U_{34} & U_{35} \\ -mA I_3 & -mA \Psi_{IC} & O_{3 \times 3} & I_3 & U_{45} \\ O_{1 \times 3} & O_{1 \times 3} & O_{1 \times 3} & O_{1 \times 3} & 1 \end{bmatrix} \quad (15.131)$$

where

$$\begin{aligned} U_{31} &= mA(\tilde{r}_{IC} - \tilde{r}_{IO}), \quad U_{32} = \kappa_4 - mA\tilde{r}_{IO}\Psi_{IC}, \quad U_{34} = \tilde{r}_{IO} \\ U_{35} &= \kappa_5 - \begin{bmatrix} m_x \\ m_y \\ m_z \end{bmatrix}_C + \tilde{r}_{IC} \left(mB_{r_I} - \begin{bmatrix} f_x \\ f_y \\ f_z \end{bmatrix}_C \right) + \tilde{r}_{IO}U_{45} \\ U_{45} &= \begin{bmatrix} f_x, f_y, f_z \end{bmatrix}_C^T - mA\Phi(t_{i-1})l_{IC} - mB_{r_C} \\ \Psi_{IO} &= A(t_{i-1})[\tilde{T}_1(t_{i-1})l_{IO} \quad \tilde{T}_2(t_{i-1})l_{IO} \quad \tilde{T}_3(t_{i-1})l_{IO}] \\ \kappa_4 &= AJHA + (H_1\kappa_1 + H_2\kappa_2)C \\ \kappa_5 &= AJHB_{\theta_I} + (H_1\kappa_1 + H_2\kappa_2)\kappa_3 + H_1 \begin{bmatrix} \ddot{\theta}_x^2 \\ \ddot{\theta}_y^2 \\ \ddot{\theta}_z^2 \end{bmatrix} \Delta T^2 + H_2 \begin{bmatrix} \ddot{\theta}_x \ddot{\theta}_y \\ \ddot{\theta}_y \ddot{\theta}_z \\ \ddot{\theta}_z \ddot{\theta}_x \end{bmatrix} \Delta T^2 \\ \kappa_1 &= 2 \begin{bmatrix} \dot{\theta}_x & 0 & 0 \\ 0 & \dot{\theta}_y & 0 \\ 0 & 0 & \dot{\theta}_z \end{bmatrix}_{t_{i-1}}, \quad \kappa_2 = \begin{bmatrix} \dot{\theta}_y & \dot{\theta}_x & 0 \\ 0 & \dot{\theta}_z & \dot{\theta}_y \\ \dot{\theta}_z & 0 & \dot{\theta}_x \end{bmatrix}_{t_{i-1}}, \quad \kappa_3 = D_{\theta_I} - \frac{1}{2}\dot{\theta}(t_{i-1}) \\ H_1 &= A[\tilde{T}_1JT_1 \quad \tilde{T}_2JT_2 \quad \tilde{T}_3JT_3] \\ H_2 &= A[JT_{12} + \tilde{T}_1JT_2 + \tilde{T}_2JT_1 \quad JT_{23} + \tilde{T}_2JT_3 + \tilde{T}_3JT_2 \quad JT_{13} + \tilde{T}_1JT_3 + \tilde{T}_3JT_1] \\ T_1 &= \begin{bmatrix} 1 \\ 0 \\ 0 \end{bmatrix}, \quad T_2 = \begin{bmatrix} 0 \\ c_x \\ -s_x \end{bmatrix}, \quad T_3 = \begin{bmatrix} -s_y \\ s_x c_y \\ c_x c_y \end{bmatrix} \end{aligned}$$

15.21.2 Spatial Rigid Body with Multiple Input and Multiple Output Ends

The state vector is

$$z = [z_{I_1}^T, z_{I_2}^T, \dots, z_{I_n}^T, z_{O_1}^T, z_{O_2}^T, \dots, z_{O_m}^T]^T \quad (15.132)$$

The transfer equation is

$$Uz = 0_{6n+6m} \quad (15.133)$$

The transfer matrix is

$$\mathbf{U} = \begin{bmatrix} \mathbf{U}_{I_2 I_1} & \mathbf{U}_{I_1} & \mathbf{O}_{6 \times 13} & \cdots & \mathbf{O}_{6 \times 13} & \mathbf{O}_{6 \times 13} & \mathbf{O}_{6 \times 13} & \cdots & \mathbf{O}_{6 \times 13} \\ \mathbf{U}_{I_3 I_1} & \mathbf{O}_{6 \times 13} & \mathbf{U}_{I_1} & \cdots & \mathbf{O}_{6 \times 13} & \mathbf{O}_{6 \times 13} & \mathbf{O}_{6 \times 13} & \cdots & \mathbf{O}_{6 \times 13} \\ \vdots & \vdots & \vdots & \ddots & \vdots & \vdots & \vdots & & \vdots \\ \mathbf{U}_{I_n I_1} & \mathbf{O}_{6 \times 13} & \mathbf{O}_{6 \times 13} & \cdots & \mathbf{U}_{I_1} & \mathbf{O}_{6 \times 13} & \mathbf{O}_{6 \times 13} & \cdots & \mathbf{O}_{6 \times 13} \\ \mathbf{U}_{O_1 I_1} & \mathbf{O}_{6 \times 13} & \mathbf{O}_{6 \times 13} & \cdots & \mathbf{O}_{6 \times 13} & \mathbf{U}_{I_1 O_1} & \mathbf{O}_{6 \times 13} & \cdots & \mathbf{O}_{6 \times 13} \\ \mathbf{U}_{O_2 I_1} & \mathbf{O}_{6 \times 13} & \mathbf{O}_{6 \times 13} & \cdots & \mathbf{O}_{6 \times 13} & \mathbf{O}_{6 \times 13} & \mathbf{U}_{I_1} & \cdots & \mathbf{O}_{6 \times 13} \\ \vdots & \vdots & \vdots & & \vdots & \vdots & \vdots & \ddots & \vdots \\ \mathbf{U}_{O_m I_1} & \mathbf{O}_{6 \times 13} & \mathbf{O}_{6 \times 13} & \cdots & \mathbf{O}_{6 \times 13} & \mathbf{O}_{6 \times 13} & \mathbf{O}_{6 \times 13} & \cdots & \mathbf{U}_{I_1} \\ \mathbf{U}_{I_1}^4 & \mathbf{U}_{I_2}^4 & \mathbf{U}_{I_3}^4 & \cdots & \mathbf{U}_{I_n}^4 & \mathbf{U}_{O_1}^4 & \mathbf{U}_{O_2}^4 & \cdots & \mathbf{U}_{O_m}^4 \end{bmatrix} \quad (15.134)$$

where

$$\begin{aligned} \mathbf{U}_{I_1} &= [-\mathbf{I}_6 \quad \mathbf{O}_{6 \times 7}] \\ \mathbf{U}_{O_j I_1} &= \begin{bmatrix} \mathbf{I}_3 & \boldsymbol{\Psi}_{I_1 O_j} & \mathbf{O}_{3 \times 3} & \mathbf{O}_{3 \times 3} & \boldsymbol{\Phi}(t_{i-1}) \mathbf{l}_{I_1 O_j} \\ \mathbf{O}_{3 \times 3} & \mathbf{I}_3 & \mathbf{O}_{3 \times 3} & \mathbf{O}_{3 \times 3} & \mathbf{O}_{3 \times 1} \end{bmatrix} \quad (j = 1, 2, \dots, m) \\ \mathbf{U}_{I_j I_1} &= \begin{bmatrix} \mathbf{I}_3 & \boldsymbol{\Psi}_{I_1 I_j} & \mathbf{O}_{3 \times 3} & \mathbf{O}_{3 \times 3} & \boldsymbol{\Phi}(t_{i-1}) \mathbf{l}_{I_1 I_j} \\ \mathbf{O}_{3 \times 3} & \mathbf{I}_3 & \mathbf{O}_{3 \times 3} & \mathbf{O}_{3 \times 3} & \mathbf{O}_{3 \times 1} \end{bmatrix} \quad (j = 2, 3, \dots, n) \\ \mathbf{U}_{I_1}^4 &= \begin{bmatrix} m \mathbf{A} \tilde{\mathbf{r}}_{I_1 C} & \boldsymbol{\kappa}_4 & \mathbf{I}_3 & \mathbf{O}_{3 \times 3} & -m_C + \boldsymbol{\kappa}_5 - \tilde{\mathbf{r}}_{I_1 C} (\mathbf{f}_C - m \mathbf{B}_{r_{I_1}}) \\ -m \mathbf{A} \mathbf{I}_3 & -m \mathbf{A} \boldsymbol{\Psi}_{I_1 C} & \mathbf{O}_{3 \times 3} & \mathbf{I}_3 & -m \mathbf{A} \boldsymbol{\Phi}(t_{i-1}) \mathbf{l}_{I_1 C} + (\mathbf{f}_C - m \mathbf{B}_{r_C}) \end{bmatrix} \\ \mathbf{U}_{I_j}^4 &= \begin{bmatrix} \mathbf{O}_{3 \times 3} & \mathbf{O}_{3 \times 3} & \mathbf{I}_3 & -\tilde{\mathbf{r}}_{I_1 I_j} & \mathbf{O}_{3 \times 1} \\ \mathbf{O}_{3 \times 3} & \mathbf{O}_{3 \times 3} & \mathbf{O}_{3 \times 3} & \mathbf{I}_3 & \mathbf{O}_{3 \times 1} \end{bmatrix} \quad (j = 2, 3, \dots, n) \\ \mathbf{U}_{O_j}^4 &= \begin{bmatrix} \mathbf{O}_{3 \times 3} & \mathbf{O}_{3 \times 3} & -\mathbf{I}_3 & \tilde{\mathbf{r}}_{I_1 O_j} & \mathbf{O}_{3 \times 1} \\ \mathbf{O}_{3 \times 3} & \mathbf{O}_{3 \times 3} & \mathbf{O}_{3 \times 3} & -\mathbf{I}_3 & \mathbf{O}_{3 \times 1} \end{bmatrix} \quad (j = 1, 2, \dots, m) \\ \mathbf{r}_{I_1 C} &= \mathbf{A} \mathbf{l}_{I_1 C}, \mathbf{r}_{I_1 I_j} = \mathbf{A} \mathbf{l}_{I_1 I_j} \quad (j = 1, 2, \dots, n), \mathbf{r}_{I_1 O_j} = \mathbf{A} \mathbf{l}_{I_1 O_j} \quad (j = 1, 2, \dots, m) \\ \boldsymbol{\Psi}_{I_1 O_j} &= \mathbf{A}(t_{i-1}) \left[\tilde{\mathbf{T}}_1(t_{i-1}) \mathbf{l}_{I_1 O_j} \quad \tilde{\mathbf{T}}_2(t_{i-1}) \mathbf{l}_{I_1 O_j} \quad \tilde{\mathbf{T}}_3(t_{i-1}) \mathbf{l}_{I_1 O_j} \right] \\ \boldsymbol{\Psi}_{I_1 I_j} &= \mathbf{A}(t_{i-1}) \left[\tilde{\mathbf{T}}_1(t_{i-1}) \mathbf{l}_{I_1 I_j} \quad \tilde{\mathbf{T}}_2(t_{i-1}) \mathbf{l}_{I_1 I_j} \quad \tilde{\mathbf{T}}_3(t_{i-1}) \mathbf{l}_{I_1 I_j} \right] \\ \boldsymbol{\Psi}_{I_1 C} &= \mathbf{A}(t_{i-1}) \left[\tilde{\mathbf{T}}_1(t_{i-1}) \mathbf{l}_{I_1 C} \quad \tilde{\mathbf{T}}_2(t_{i-1}) \mathbf{l}_{I_1 C} \quad \tilde{\mathbf{T}}_3(t_{i-1}) \mathbf{l}_{I_1 C} \right] \end{aligned}$$

$\boldsymbol{\Phi}(t_{i-1})$ is determined by Equation (7.84), $\mathbf{T}_1, \mathbf{T}_2$ and \mathbf{T}_3 are determined by Equation (7.77), and m is the mass of the rigid body. \mathbf{f}_C is an external force acting on the mass center of the rigid body.

15.21.3 Spatial Rigid Body with Multiple Input Ends and One Output End

The state vector is

$$\mathbf{z} = \left[\mathbf{z}_{I_1}^T, \mathbf{z}_{I_2}^T, \dots, \mathbf{z}_{I_n}^T, \mathbf{z}_{O_1}^T \right]^T \quad (15.135)$$

The transfer equation is

$$\mathbf{U}\mathbf{z} = \mathbf{0}_{6n+6} \quad (15.136)$$

The transfer matrix is

$$\mathbf{U} = \begin{bmatrix} \mathbf{U}_{I_2 I_1} & \mathbf{U}_{I_1} & \mathbf{O}_{6 \times 13} & \cdots & \mathbf{O}_{6 \times 13} & \mathbf{O}_{6 \times 13} \\ \mathbf{U}_{I_3 I_1} & \mathbf{O}_{6 \times 13} & \mathbf{U}_{I_1} & \cdots & \mathbf{O}_{6 \times 13} & \mathbf{O}_{6 \times 13} \\ \vdots & \vdots & \vdots & \ddots & \vdots & \vdots \\ \mathbf{U}_{I_n I_1} & \mathbf{O}_{6 \times 13} & \mathbf{O}_{6 \times 13} & \cdots & \mathbf{U}_{I_1} & \mathbf{O}_{6 \times 13} \\ \mathbf{U}_{O_1 I_1} & \mathbf{O}_{6 \times 13} & \mathbf{O}_{6 \times 13} & \cdots & \mathbf{O}_{6 \times 13} & \mathbf{U}_{I_1} \\ \mathbf{U}_{I_1}^4 & \mathbf{U}_{I_2}^4 & \mathbf{U}_{I_3}^4 & \cdots & \mathbf{U}_{I_n}^4 & \mathbf{U}_{O_1}^4 \end{bmatrix} \quad (15.137)$$

where the submatrices are the same as in Equation (15.134).

15.21.4 Spatial Rigid Body with One Input End and Multiple Output Ends

The state vector is

$$\mathbf{z} = \left[\mathbf{z}_{I_1}^T, \mathbf{z}_{O_1}^T, \mathbf{z}_{O_2}^T, \cdots, \mathbf{z}_{O_m}^T \right]^T \quad (15.138)$$

The transfer equation is

$$\mathbf{U}\mathbf{z} = \mathbf{0}_{6m+6} \quad (15.139)$$

The transfer matrix is

$$\mathbf{U} = \begin{bmatrix} \mathbf{U}_{O_1 I_1} & \mathbf{U}_{I_1} & \mathbf{O}_{6 \times 13} & \cdots & \mathbf{O}_{6 \times 13} \\ \mathbf{U}_{O_2 I_1} & \mathbf{O}_{6 \times 13} & \mathbf{U}_{I_1} & \cdots & \mathbf{O}_{6 \times 13} \\ \vdots & \vdots & \vdots & \ddots & \vdots \\ \mathbf{U}_{O_m I_1} & \mathbf{O}_{6 \times 13} & \mathbf{O}_{6 \times 13} & \cdots & \mathbf{U}_{I_1} \\ \mathbf{U}_{I_1}^4 & \mathbf{U}_{O_1}^4 & \mathbf{U}_{O_2}^4 & \cdots & \mathbf{U}_{O_m}^4 \end{bmatrix} \quad (15.140)$$

where the submatrices are the same as in Equation (15.134).

15.22 Planar Beam with Large Motion

The state vector is

$$\mathbf{z}(x, t) = [x, y, \theta, m, q_x, q_y, q^1, q^2, q^3, 1]^T \quad (15.141)$$

The transfer equation is

$$\mathbf{z}(l, t) = \mathbf{U}\mathbf{z}(0, t) \quad (15.142)$$

The transfer matrix is

$$\mathbf{U} = \begin{bmatrix} 1 & 0 & u_{1,3} & 0 & 0 & 0 & 0 & 0 & 0 & u_{1,10} \\ 0 & 1 & u_{2,3} & 0 & 0 & 0 & 0 & 0 & 0 & u_{2,10} \\ 0 & 0 & 1 & 0 & 0 & 0 & 0 & 0 & 0 & 0 \\ u_{4,1} & u_{4,2} & u_{4,3} & 1 & u_{4,5} & u_{4,6} & u_{4,7} & u_{4,8} & u_{4,9} & u_{4,10} \\ u_{5,1} & 0 & u_{5,3} & 0 & 1 & 0 & u_{5,7} & 0 & u_{5,9} & u_{5,10} \\ 0 & u_{6,2} & u_{6,3} & 0 & 0 & 1 & u_{6,7} & 0 & u_{6,9} & u_{6,10} \\ 0 & 0 & 0 & 0 & 0 & 0 & 1 & 0 & 0 & 0 \\ 0 & 0 & 0 & 0 & 0 & 0 & 0 & 1 & 0 & 0 \\ 0 & 0 & 0 & 0 & 0 & 0 & 0 & 0 & 1 & 0 \\ 0 & 0 & 0 & 0 & 0 & 0 & 0 & 0 & 0 & 1 \end{bmatrix} \quad (15.143)$$

where

$$\begin{aligned} u_{1,3} &= -ls, \quad u_{1,10} = l(c + \theta s), \quad u_{2,3} = lc, \quad u_{2,10} = l(s - \theta c) \\ u_{4,j} &= l\zeta_{1,j} + \xi_j \quad (j = 1, 2, 3, 7, 9) \\ u_{4,5} &= -l\bar{s}, \quad u_{4,6} = l\bar{c}, \quad u_{4,8} = \xi_8 \\ u_{4,10} &= l\zeta_{1,10} + \xi_{10} - \int_0^l x_2 f_{2,y}(x_2, t) dx_2 - \int_0^l m'(x_2, t) dx_2 \\ u_{5,1} &= -mA, \quad u_{5,j} = \bar{c}\zeta_{2,j} - \bar{s}\zeta_{1,j} \quad (j = 3, 7, 9, 10) \\ u_{6,2} &= -mA, \quad u_{6,j} = \bar{s}\zeta_{2,j} + \bar{c}\zeta_{1,j} \quad (j = 3, 7, 9, 10) \\ \zeta_{1,1} &= m\bar{s}A, \quad \zeta_{1,2} = -m\bar{c}A, \quad \zeta_{1,3} = m \left\{ -\frac{lA}{2} + \frac{4C}{\pi} \left[\dot{\theta} \left(q^1 + \frac{1}{3}q^3 \right) \right]_{t_{i-1}} \right\} \\ \zeta_{2,1} &= -m\bar{c}A, \quad \zeta_{2,2} = -m\bar{s}A, \quad \zeta_{2,3} = m \left[\frac{2A}{\pi} \left(q^1 + \frac{1}{3}q^3 \right)_{t_{i-1}} + \frac{4C}{\pi} \left(\dot{q}^1 + \frac{1}{3}\dot{q}^3 \right)_{t_{i-1}} + lC\dot{\theta}_{t_{i-1}} \right] \\ \zeta_{1,7} &= \frac{2m}{\pi} \left(-A + \dot{\theta}_{t_{i-1}}^2 \right), \quad \zeta_{2,7} = \frac{2m}{\pi} (\ddot{\theta}_{t_{i-1}} + 2C\dot{\theta}_{t_{i-1}}), \quad \zeta_{1,9} = \frac{1}{3}\zeta_{1,7}, \quad \zeta_{2,9} = \frac{1}{3}\zeta_{2,7} \\ \zeta_{1,10} &= -\frac{2m}{\pi} \left(B_{q^1} + \frac{1}{3}B_{q^3} \right) - \frac{ml}{2}B_\theta + \frac{4mD_\theta}{\pi} \left[\dot{\theta} \left(q^1 + \frac{1}{3}q^3 \right) \right]_{t_{i-1}} - \frac{4m}{\pi} \left[\dot{\theta}^2 \left(q^1 + \frac{1}{3}q^3 \right) \right]_{t_{i-1}} \\ &\quad - m\bar{c}B_{y_{O_2}} + m\bar{s}B_{x_{O_2}} + \int_0^l f_{2,y}(x_2, t) dx_2 \\ \zeta_{2,10} &= \frac{2m}{\pi} B_\theta \left(q^1 + \frac{1}{3}q^3 \right)_{t_{i-1}} - \frac{2m}{\pi} \ddot{\theta}_{t_{i-1}} \left(q^1 + \frac{1}{3}q^3 \right)_{t_{i-1}} + \frac{4mD_\theta}{\pi} \left(\dot{q}^1 + \frac{1}{3}\dot{q}^3 \right)_{t_{i-1}} \\ &\quad + \frac{4m}{\pi} \dot{\theta}_{t_{i-1}} \left(D_{q^1} + \frac{1}{3}D_{q^3} \right) - \frac{4m}{\pi} \dot{\theta}_{t_{i-1}} \left(\dot{q}^1 + \frac{1}{3}\dot{q}^3 \right)_{t_{i-1}} + ml\dot{\theta}_{t_{i-1}} \left(D_\theta - \frac{\dot{\theta}_{t_{i-1}}}{2} \right) \\ &\quad - m\bar{s}B_{y_{O_2}} - m\bar{c}B_{x_{O_2}} + \int_0^l f_{2,x}(x_2, t) dx_2 \end{aligned}$$

$$\begin{aligned}
\xi_1 &= mA \left[-\frac{l\bar{s}}{2} - \frac{2\bar{c}}{\pi} \left(q^1 + \frac{1}{3}q^3 \right) \right]_{t_{i-1}} \\
\xi_2 &= mA \left[\frac{l\bar{c}}{2} - \frac{2\bar{s}}{\pi} \left(q^1 + \frac{1}{3}q^3 \right) \right]_{t_{i-1}} \\
\xi_3 &= m \left[\left(\dot{q}^1 \dot{q}^1 + q^2 \dot{q}^2 + q^3 \dot{q}^3 \right)_{t_{i-1}} C + \frac{A}{2} \left(q^1 q^1 + q^2 q^2 + q^3 q^3 \right)_{t_{i-1}} + \frac{A}{3} l^2 \right] \\
\xi_7 &= m \left\{ \left[\dot{\theta}(\dot{q}^1 + q^1 C) + \ddot{\theta} q^1 \right]_{t_{i-1}} + \frac{lA}{\pi} - \frac{2}{\pi} (\bar{s} \ddot{y}_{O_2} + \bar{c} \ddot{x}_{O_2})_{t_{i-1}} \right\} \\
\xi_8 &= m \left\{ \left[\dot{\theta}(\dot{q}^2 + q^2 C) + \ddot{\theta} q^2 \right]_{t_{i-1}} - \frac{lA}{2\pi} \right\} \\
\xi_9 &= m \left\{ \left[\dot{\theta}(\dot{q}^3 + q^3 C) + \ddot{\theta} q^3 \right]_{t_{i-1}} + \frac{lA}{3\pi} - \frac{2}{3\pi} (\bar{s} \ddot{y}_{O_2} + \bar{c} \ddot{x}_{O_2})_{t_{i-1}} \right\} \\
\xi_{10} &= m \left(q^1 \dot{q}^1 + q^2 \dot{q}^2 + q^3 \dot{q}^3 \right)_{t_{i-1}} (D_\theta - 2\dot{\theta}_{t_{i-1}}) + m \dot{\theta}_{t_{i-1}} (q^1 D_{q^1} + q^2 D_{q^2} + q^3 D_{q^3})_{t_{i-1}} \\
&\quad + m \left(q^1 q^1 + q^2 q^2 + q^3 q^3 \right)_{t_{i-1}} \left(\frac{B_\theta}{2} - \ddot{\theta}_{t_{i-1}} \right) + \frac{ml^2}{3} B_\theta + \frac{ml}{\pi} \left(B_{q^1} - \frac{B_{q^2}}{2} + \frac{B_{q^3}}{3} \right) \\
&\quad + \frac{ml}{2} (\bar{c} B_{y_{O_2}} - \bar{s} B_{x_{O_2}}) \\
&\quad - \frac{2m}{\pi} \bar{s} \left(q^1 + \frac{1}{3}q^3 \right)_{t_{i-1}} (B_{y_{O_2}} - \ddot{y}_{O_2})_{t_{i-1}} - \frac{2m}{\pi} \bar{c} \left(q^1 + \frac{1}{3}q^3 \right)_{t_{i-1}} (B_{x_{O_2}} - \ddot{x}_{O_2})_{t_{i-1}}
\end{aligned}$$

$f_{2,x}$ and $f_{2,y}$ are distributing external forces with respect to the body-fixed coordinate system, and m' is the distributed external torque acting on the beam. \bar{s} and \bar{c} are determined by Equation (7.62).

15.23 Spatial Beam with Large Motion

The state vector is

$$\mathbf{z} = [x, y, z, \theta_x, \theta_y, \theta_z, m_x, m_y, m_z, q_x, q_y, q_z, q^1, q^2, \dots, q^n, 1]^T \quad (15.144)$$

The transfer equation is

$$\mathbf{z}_O = \mathbf{U} \mathbf{z}_I \quad (15.145)$$

The transfer matrix is

$$\mathbf{U} = \begin{bmatrix} \mathbf{I}_3 & \mathbf{U}_{12} & \mathbf{O}_{3 \times 3} & \mathbf{O}_{3 \times 3} & \mathbf{U}_{15} & \mathbf{U}_{16} \\ \mathbf{O}_{3 \times 3} & \mathbf{I}_3 & \mathbf{O}_{3 \times 3} & \mathbf{O}_{3 \times 3} & \mathbf{O}_{3 \times 3} & \mathbf{O}_{3 \times 1} \\ \mathbf{U}_{31} & \mathbf{U}_{32} & \mathbf{I}_3 & \mathbf{U}_{34} & \mathbf{U}_{35} & \mathbf{U}_{36} \\ \mathbf{U}_{41} & \mathbf{U}_{42} & \mathbf{U}_{12} & \mathbf{I}_3 & \mathbf{U}_{45} & \mathbf{U}_{46} \\ \mathbf{O}_{n \times 3} & \mathbf{O}_{n \times 3} & \mathbf{O}_{n \times 3} & \mathbf{O}_{n \times 3} & \mathbf{I}_n & \mathbf{O}_{n \times 1} \\ \mathbf{O}_{1 \times 3} & \mathbf{O}_{1 \times 3} & \mathbf{O}_{1 \times 3} & \mathbf{O}_{1 \times 3} & \mathbf{O}_{1 \times n} & 1 \end{bmatrix} \quad (15.146)$$

where

$$\begin{aligned}
\mathbf{U}_{12} &= \mathbf{A}(t_{i-1}) \begin{bmatrix} \tilde{\mathbf{T}}_1(t_{i-1}) \mathbf{l}_{IO} & \tilde{\mathbf{T}}_2(t_{i-1}) \mathbf{l}_{IO} & \tilde{\mathbf{T}}_3(t_{i-1}) \mathbf{l}_{IO} \end{bmatrix} \\
\mathbf{U}_{15} &= \begin{bmatrix} \bar{\mathbf{A}}(t_i) \begin{bmatrix} 0 \\ Y^1(l) \\ Z^1(l) \end{bmatrix} & \bar{\mathbf{A}}(t_i) \begin{bmatrix} 0 \\ Y^2(l) \\ Z^2(l) \end{bmatrix} & \cdots & \bar{\mathbf{A}}(t_i) \begin{bmatrix} 0 \\ Y^{n_2}(l) \\ Z^{n_2}(l) \end{bmatrix} \end{bmatrix} \\
\mathbf{U}_{16} &= \Phi(t_{i-1}) \mathbf{l}_{IO} \\
\mathbf{U}_{31} &= \mathbf{H}_{41} + \bar{\mathbf{A}} \tilde{\mathbf{r}}_{IO} \bar{\mathbf{A}}^T \mathbf{U}_{41}, \mathbf{U}_{32} = C \bar{\mathbf{A}} \mathbf{H}_{22} + \bar{\mathbf{A}} \tilde{\mathbf{r}}_{IO} \bar{\mathbf{A}}^T \mathbf{U}_{42}, \mathbf{U}_{34} = \bar{\mathbf{A}} \tilde{\mathbf{r}}_{IO} \bar{\mathbf{A}}^T, \\
\mathbf{U}_{35} &= C \bar{\mathbf{A}} (\mathbf{H}_{25} + \mathbf{H}_{35}) + \mathbf{H}_{45} + \bar{\mathbf{A}} \tilde{\mathbf{r}}_{IO} \bar{\mathbf{A}}^T \mathbf{U}_{45} \\
\mathbf{U}_{36} &= C \bar{\mathbf{A}} (\mathbf{H}_{26} + \mathbf{H}_{36}) + \mathbf{D}_{G_I} + \mathbf{H}_{46} + \bar{\mathbf{A}} \tilde{\mathbf{r}}_{IO} \bar{\mathbf{A}}^T \mathbf{U}_{46} - \bar{\mathbf{A}} \int_0^l \begin{bmatrix} \bar{m}_x \\ \bar{m}_y \\ \bar{m}_z \end{bmatrix} dx_2 - \bar{\mathbf{A}} \int_0^l \sum_j \tilde{\mathbf{r}}_{Ij} \begin{bmatrix} f_x \\ f_y \\ f_z \end{bmatrix} dx_2 \\
\bar{\mathbf{A}} &= \begin{bmatrix} \bar{c}_y \bar{c}_z & \bar{s}_x \bar{s}_y \bar{c}_z - \bar{s}_z \bar{c}_x & \bar{c}_x \bar{s}_y \bar{c}_z + \bar{s}_z \bar{s}_x \\ \bar{c}_y \bar{s}_z & \bar{s}_x \bar{s}_y \bar{s}_z + \bar{c}_z \bar{c}_x & \bar{c}_x \bar{s}_y \bar{s}_z - \bar{c}_z \bar{s}_x \\ -\bar{s}_y & \bar{s}_x \bar{c}_y & \bar{c}_x \bar{c}_y \end{bmatrix}, \tilde{\mathbf{r}}_{IO} = \begin{bmatrix} 0 & -\bar{\nu}_{IO} & \bar{w}_{IO} \\ \bar{\nu}_{IO} & 0 & -l \\ -\bar{w}_{IO} & l & 0 \end{bmatrix} \\
\mathbf{H}_{22} &= C \bar{m} \int_0^l \mathbf{J}_1(t_{i-1}) \bar{\mathbf{H}} dx_2 \\
\mathbf{H}_{25} &= \left[\int_0^l \bar{m} (\mathbf{E}_2 Y^1 + \mathbf{E}_3 Z^1) dx_2 \quad \int_0^l \bar{m} (\mathbf{E}_2 Y^2 + \mathbf{E}_3 Z^2) dx_2 \quad \cdots \quad \int_0^l \bar{m} (\mathbf{E}_2 Y^n + \mathbf{E}_3 Z^n) dx_2 \right] \\
\mathbf{H}_{26} &= \int_0^l \bar{m} \mathbf{J}_1(t_{i-1}) \bar{\mathbf{H}} \mathbf{D}_\theta dx_2 - \int_0^l \bar{m} [\mathbf{E}_2 \nu_{t_{i-1}} + \mathbf{E}_3 \omega_{t_{i-1}}] dx_2 \\
\mathbf{H}_{35} &= \left[\int_0^l \bar{m} (\mathbf{E}_4 Y^1 + \mathbf{E}_5 Z^1) dx_2 \quad \int_0^l \bar{m} (\mathbf{E}_4 Y^2 + \mathbf{E}_5 Z^2) dx_2 \quad \cdots \quad \int_0^l \bar{m} (\mathbf{E}_4 Y^n + \mathbf{E}_5 Z^n) dx_2 \right] \\
\mathbf{H}_{36} &= \int_0^l \bar{m} \mathbf{E}_6 dx_2, \mathbf{H}_{41} = m \bar{\mathbf{A}} \tilde{\mathbf{r}}_{IC}(t_{i-1}) \\
\mathbf{H}_{45} &= \begin{bmatrix} \int_0^l \mathbf{E}_7 \begin{bmatrix} 0 \\ Y^1 \\ Z^1 \end{bmatrix} dx_2 & \int_0^l \mathbf{E}_7 \begin{bmatrix} 0 \\ Y^2 \\ Z^2 \end{bmatrix} dx_2 & \cdots & \int_0^l \mathbf{E}_7 \begin{bmatrix} 0 \\ Y^n \\ Z^n \end{bmatrix} dx_2 \end{bmatrix} \\
\mathbf{H}_{46} &= -\frac{ml}{2} \tilde{\mathbf{r}}_I(t_{i-1}) \bar{\mathbf{A}}(t_i) \begin{bmatrix} 1 \\ 0 \\ 0 \end{bmatrix} + m \tilde{\mathbf{r}}_{IC}(t_{i-1}) (\mathbf{B}_{r_I} - \ddot{\mathbf{r}}_I(t_{i-1})) \\
\bar{\mathbf{H}} &= \begin{bmatrix} 1 & 0 & -\bar{s}_y \\ 0 & \bar{c}_x & \bar{s}_x \bar{c}_y \\ 0 & -\bar{s}_x & \bar{c}_x \bar{c}_y \end{bmatrix}, \mathbf{E}_2 = \begin{bmatrix} 2\nu & -x_2 & 0 \\ -x_2 & 0 & -w \\ 0 & -w & 2\nu \end{bmatrix}_{t_{i-1}}, \boldsymbol{\omega}_{t_{i-1}}, \mathbf{E}_3 = \begin{bmatrix} 2w & 0 & -x_2 \\ 0 & 2w & -\nu \\ -x_2 & -\nu & 0 \end{bmatrix}_{t_{i-1}} \boldsymbol{\omega}_{t_{i-1}}
\end{aligned}$$

$$\begin{aligned}
E_4 &= \begin{bmatrix} \dot{w}_{t_{i-1}} - Cw_{t_{i-1}} \\ 0 \\ Cx_2 \end{bmatrix}, E_5 = \begin{bmatrix} -\dot{v}_{t_{i-1}} + Cv_{t_{i-1}} \\ -Cx_2 \\ 0 \end{bmatrix}, E_6 = \begin{bmatrix} v_{t_{i-1}}(D_w - \dot{w}_{t_{i-1}}) + w_{t_{i-1}}(\dot{v}_{t_{i-1}} - D_v) \\ -x_2 D_w \\ x_2 D_v \end{bmatrix} \\
E_7 &= -\frac{m}{l} \tilde{r}_I(t_{i-1}) \bar{A}(t_i) = -\frac{m}{l} \begin{bmatrix} 0 & -\ddot{z}_I & -\ddot{y}_I \\ \ddot{z}_I & 0 & -\ddot{x}_I \\ -\ddot{y}_I & \ddot{x}_I & 0 \end{bmatrix}_{t_{i-1}} \bar{A}(t_i) \\
U_{41} &= -mAI_3, U_{42} = -\bar{m}AA(t_{i-1}) \left[\tilde{T}_1 \int_0^l \begin{bmatrix} x_2 \\ v \\ w \end{bmatrix} dx_2 \quad \tilde{T}_2 \int_0^l \begin{bmatrix} x_2 \\ v \\ w \end{bmatrix} dx_2 \quad \tilde{T}_3 \int_0^l \begin{bmatrix} x_2 \\ v \\ w \end{bmatrix} dx_2 \right]_{t_{i-1}} \\
U_{45} &= -\bar{m}AA(t_{i-1}) \left[\int_0^l \begin{bmatrix} 0 \\ Y^1(x_2) \\ Z^1(x_2) \end{bmatrix} dx_2 \quad \int_0^l \begin{bmatrix} 0 \\ Y^2(x_2) \\ Z^2(x_2) \end{bmatrix} dx_2 \quad \cdots \quad \int_0^l \begin{bmatrix} 0 \\ Y^n(x_2) \\ Z^n(x_2) \end{bmatrix} dx_2 \right] \\
U_{46} &= \int_0^l \begin{bmatrix} f_x \\ f_y \\ f_z \end{bmatrix} dx_2 - mB_{r_I} - \bar{m}A\Phi(t_{i-1}) \int_0^l \begin{bmatrix} x_2 \\ v \\ w \end{bmatrix}_{t_{i-1}} dx_2 + \bar{m}AA(t_{i-1}) \int_0^l \begin{bmatrix} 0 \\ v \\ w \end{bmatrix}_{t_{i-1}} dx_2 - \bar{m} \int_0^l B_{r_i, o_2} dx_2
\end{aligned}$$

$\Phi(t_{i-1})$ is determined by Equation (7.84), T_1, T_2 and T_3 are determined by Equation (7.77), A is the coordinate transform matrix, EI, l and \bar{m} are the bending stiffness, length and line density of the beam, respectively, $Y^k(x_2)$ and $Z^k(x_2)$ are the eigenvectors of outboard beam, and \bar{s} and \bar{c} are determined by Equation (7.62).

15.24 Fixed Hinges Connected to a Planar Beam with Large Motion

15.24.1 Fixed Hinge whose Inboard Body is a Rigid Body and whose Outboard Body is a Euler–Bernoulli Beam Moving in a Plane

The state vectors are

$$\begin{aligned}
z_I &= [x, y, \theta, m, q_x, q_y, 1]^T \\
z_O &= [x, y, \theta, m, q_x, q_y, q^1, q^2, \dots, q^n, 1]^T
\end{aligned} \tag{15.147}$$

The transfer equation is

$$z_O = Uz_I \tag{15.148}$$

The transfer matrix is

$$U = \begin{bmatrix} I_3 & O_{3 \times 3} & O_{3 \times 1} \\ O_{3 \times 3} & I_3 & O_{3 \times 1} \\ M^{-1}N_1 & O_{3 \times 3} & M^{-1}N_3 \\ O_{1 \times 3} & O_{1 \times 3} & 1 \end{bmatrix} \tag{15.149}$$

where all elements are the same as in Equation (8.135).

15.24.2 Fixed Hinge whose Inboard and Outboard Bodies are Euler–Bernoulli Beams Moving in a Plane

The state vectors are

$$\begin{aligned} \mathbf{z}_I &= [x, y, \theta, m, q_x, q_y, q^1, q^2, \dots, q^n, 1]^T \\ \mathbf{z}_O &= [x, y, \theta, m, q_x, q_y, q^1, q^2, \dots, q^n, 1]^T \end{aligned} \quad (15.150)$$

The transfer equation is

$$\mathbf{z}_O = \mathbf{U} \mathbf{z}_I \quad (15.151)$$

The transfer matrix is

$$\mathbf{U} = \begin{bmatrix} \mathbf{I}_3 & \mathbf{O}_{3 \times 3} & \mathbf{U}_{13} & \mathbf{O}_{3 \times 1} \\ \mathbf{O}_{3 \times 3} & \mathbf{I}_3 & \mathbf{O}_{3 \times n} & \mathbf{O}_{3 \times 1} \\ \mathbf{M}^{-1} \mathbf{N}_1 & \mathbf{O}_{n_O \times 3} & \mathbf{M}^{-1} \mathbf{N}_2 & \mathbf{M}^{-1} \mathbf{N}_3 \\ \mathbf{O}_{1 \times 3} & \mathbf{O}_{1 \times 3} & \mathbf{O}_{1 \times n} & 1 \end{bmatrix} \quad (15.152)$$

where

$$\mathbf{M} = \begin{bmatrix} m_{11} & m_{12} & \cdots & m_{1n} \\ m_{21} & m_{22} & \cdots & m_{2n} \\ \vdots & & \ddots & \vdots \\ m_{n1} & m_{n2} & \cdots & m_{nn} \end{bmatrix}, \quad \mathbf{N}_1 = \begin{bmatrix} n_{11} & n_{12} & n_{13} \\ n_{21} & n_{22} & n_{23} \\ \vdots & \vdots & \vdots \\ n_{n1} & n_{n2} & n_{n3} \end{bmatrix}, \quad \mathbf{N}_2 = \begin{bmatrix} n_{14} & n_{15} & \cdots & n_{1(n+3)} \\ n_{24} & n_{25} & \cdots & n_{2(n+3)} \\ \vdots & & \ddots & \vdots \\ n_{n4} & n_{n5} & \cdots & n_{n(n+3)} \end{bmatrix}$$

$$\mathbf{N}_3 = [n_{1(n+4)} \quad n_{2(n+4)} \quad \cdots \quad n_{n(n+4)}]^T$$

$$m_{k'k} = {}^4s_{k,k'} EI - {}^2s_{k,k'} \rho I A + \bar{m} s_{k,k'} A - \bar{m} s_{k,k'} \dot{\theta}_{O,t_{i-1}}^2$$

$$n_{k'1} = \bar{m} \bar{c} s_{k'}^0 A, \quad n_{k'2} = -\bar{m} \bar{s} \bar{s}_{k'}^0 A, \quad n_{k'3} = -\bar{m} \left(s_{k'}^1 A - 2C \sum_{k=1}^n s_{k,k'} q_{t_{i-1}}^k \dot{\theta}_{O,t_{i-1}} \right)$$

$$n_{k'(j+3)} = -\bar{m} \left(s_{k'}^1 A - 2C \sum_{k=1}^n s_{k,k'} q_{t_{i-1}}^k \dot{\theta}_{O,t_{i-1}} \right) \partial \frac{Y_I^j(l_2)}{\partial x_2}$$

$$\begin{aligned} n_{k'(n_I+3+1)} &= \int_0^l Y^{k'}(x_2) f(x_2, t) dx_2 - \int_0^l Y^{k'}(x_2) \frac{\partial}{\partial x_2} m'(x_2, t) dx_2 + \rho I \sum_{k=1}^n s_{k,k'} B_{q^k} \\ &\quad - \bar{m} \left\{ \sum_{k=1}^n s_{k,k'} B_{q^k} - \sum_{k=1}^n s_{k,k'} \left[2q_{t_{i-1}}^k \dot{\theta}_{O,t_{i-1}} D_{\theta_O} - 2q^k(t_{i-1}) \dot{\theta}_{O,t_{i-1}}^2 \right] + s_{k'}^1 B_{\theta_O} \right. \\ &\quad \left. + \bar{s} \bar{s}_{k'}^0 B_{y_{O_2}} - \bar{c} \bar{s}_{k'}^0 B_{x_{O_2}} \right\} \quad (k, k', j = 1, 2, \dots, n) \end{aligned}$$

$$\mathbf{U}_{13} = \begin{bmatrix} 0 & \cdots & 0 \\ 0 & \cdots & 0 \\ \frac{\partial Y_I^1(l_2)}{\partial x_2} & \cdots & \frac{\partial Y_I^n(l_2)}{\partial x_2} \end{bmatrix}$$

θ_O is the orientation angle of the output end of the fixed hinge, that is, the orientation angle of the body-fixed coordinate system of its outboard beam. Y_I^k is the eigenvector of the inboard beam. The n is the highest order of the modes of the beam connected with the fixed hinge. The other elements are the parameters of the outboard beam, and their meanings are the same as in Equation (8.116).

15.24.3 Fixed Hinge whose Inboard Body is a Euler–Bernoulli Beam and whose Outboard Body is a Rigid Body Moving in a Plane

The state vectors are

$$\begin{aligned} \mathbf{z}_I &= [x, y, \theta, m, q_x, q_y, q^1, q^2, \dots, q^n, 1]^T \\ \mathbf{z}_O &= [x, y, \theta, m, q_x, q_y, 1]^T \end{aligned} \quad (15.153)$$

The transfer equation is

$$\mathbf{z}_O = \mathbf{U} \mathbf{z}_I \quad (15.154)$$

The transfer matrix is

$$\mathbf{U} = \begin{bmatrix} \mathbf{I}_3 & \mathbf{O}_{3 \times 3} & \mathbf{U}_{13} & \mathbf{O}_{3 \times 1} \\ \mathbf{O}_{3 \times 3} & \mathbf{I}_3 & \mathbf{O}_{3 \times n} & \mathbf{O}_{3 \times 1} \\ \mathbf{O}_{1 \times 3} & \mathbf{O}_{1 \times 3} & \mathbf{O}_{1 \times n} & 1 \end{bmatrix} \quad (15.155)$$

where the meanings of all the elements are the same as in Equation (8.135).

15.25 Fixed Hinges Connected to a Spatial Beam with Large Motion

15.25.1 Fixed Hinge whose Inboard Body is a Rigid Body and whose Outboard Body is a Beam Moving in Space

The state vectors are

$$\begin{aligned} \mathbf{z}_I &= [x, y, z, \theta_x, \theta_y, \theta_z, m_x, m_y, m_z, q_x, q_y, q_z, 1]^T \\ \mathbf{z}_O &= [x, y, z, \theta_x, \theta_y, \theta_z, m_x, m_y, m_z, q_x, q_y, q_z, q^1, q^2, \dots, q^n, 1]^T \end{aligned} \quad (15.156)$$

The transfer equation is

$$\mathbf{z}_O = \mathbf{U} \mathbf{z}_I \quad (15.157)$$

The transfer matrix is

$$\mathbf{U} = \begin{bmatrix} \mathbf{I}_3 & \mathbf{O}_{3 \times 3} & \mathbf{O}_{3 \times 3} & \mathbf{O}_{3 \times 3} & \mathbf{O}_{3 \times 1} \\ \mathbf{O}_{3 \times 3} & \mathbf{I}_3 & \mathbf{O}_{3 \times 3} & \mathbf{O}_{3 \times 3} & \mathbf{O}_{3 \times 1} \\ \mathbf{O}_{3 \times 3} & \mathbf{O}_{3 \times 3} & \mathbf{I}_3 & \mathbf{O}_{3 \times 3} & \mathbf{O}_{3 \times 1} \\ \mathbf{O}_{3 \times 3} & \mathbf{O}_{3 \times 3} & \mathbf{O}_{3 \times 3} & \mathbf{I}_3 & \mathbf{O}_{3 \times 1} \\ \mathbf{U}_{51} & \mathbf{U}_{52} & \mathbf{O}_{n \times 3} & \mathbf{O}_{n \times 3} & \mathbf{U}_{55} \\ \mathbf{O}_{1 \times 3} & \mathbf{O}_{1 \times 3} & \mathbf{O}_{1 \times 3} & \mathbf{O}_{1 \times 3} & 1 \end{bmatrix} \quad (15.158)$$

where

$$\begin{aligned}
 \mathbf{U}_{51} &= \begin{bmatrix} \mathbf{P}_{11} \\ \mathbf{P}_{12} \\ \vdots \\ \mathbf{P}_{1n} \end{bmatrix}, \mathbf{U}_{52} = \begin{bmatrix} \mathbf{P}_{21} \\ \mathbf{P}_{22} \\ \vdots \\ \mathbf{P}_{2n} \end{bmatrix}, \mathbf{U}_{55} = \begin{bmatrix} P_{51} \\ P_{52} \\ \vdots \\ P_{5n} \end{bmatrix} \\
 \mathbf{P}_{1j} &= \frac{-\bar{m}A}{(A + \Omega_j^2)d_j} \int_0^l \begin{bmatrix} 0 & Y^j & Z^j \end{bmatrix} \mathbf{A}^T(t_{i-1}) dx_2, \quad \mathbf{P}_{2j} = \frac{\mathbf{F}_j}{(A + \Omega_j^2)d_j}, \\
 \mathbf{P}_{5j} &= \frac{1}{(A + \Omega_j^2)d_j} \int_0^l \begin{bmatrix} Y^j & Z^j \end{bmatrix} \mathbf{A}^T \begin{bmatrix} f_{2y} - \frac{\partial \bar{m}_{2z}}{\partial x_2} \\ f_{2z} + \frac{\partial \bar{m}_{2y}}{\partial x_2} \end{bmatrix} dx_2 + \frac{\mathbf{E}_j}{(A + \Omega_j^2)d_j} \\
 &\quad + \frac{\bar{m}A}{(A + \Omega_j^2)d_j} \int_0^l \begin{bmatrix} 0 & Y^j & Z^j \end{bmatrix} \mathbf{A}^T(t_{i-1}) \begin{bmatrix} x_{t_{i-1}} \\ y_{t_{i-1}} \\ z_{t_{i-1}} \end{bmatrix}_I dx_2 \\
 \mathbf{E}_j &= -\bar{m} \int_0^l \begin{bmatrix} 0 & Y^j & Z^j \end{bmatrix} \Phi^T(t_{i-1}) \left(\mathbf{B}_{\bar{r}} + A \begin{bmatrix} x_{t_{i-1}} \\ y_{t_{i-1}} \\ z_{t_{i-1}} \end{bmatrix}_I \right) dx_2 \\
 \mathbf{F}_j &= \bar{m} \int_0^l \begin{bmatrix} 0 & Y^j & Z^j \end{bmatrix} \left[\tilde{\mathbf{T}}_1(t_{i-1})\mathbf{R}, \tilde{\mathbf{T}}_2(t_{i-1})\mathbf{R}, \tilde{\mathbf{T}}_3(t_{i-1})\mathbf{R} \right] dx_2 \\
 \mathbf{R} &= \mathbf{A}^T(t_{i-1}) \left(\mathbf{B}_{\bar{r}} + A \begin{bmatrix} x_{t_{i-1}} \\ y_{t_{i-1}} \\ z_{t_{i-1}} \end{bmatrix}_I \right) \\
 \int_0^l \bar{m} \begin{bmatrix} Y^j(x_2) \\ Z^j(x_2) \end{bmatrix} \cdot \begin{bmatrix} Y^k(x_2) \\ Z^k(x_2) \end{bmatrix} dx_2 &= \begin{cases} 0 & j \neq k \\ d_j & j = k \end{cases}, \int_0^l EI \begin{bmatrix} Y^{j(2)}(x_2) \\ Z^{j(2)}(x_2) \end{bmatrix} \cdot \begin{bmatrix} Y^{k(2)}(x_2) \\ Z^{k(2)}(x_2) \end{bmatrix} dx_2 = \begin{cases} 0 & j \neq k \\ \Omega_j^2 d_j & j = k \end{cases}
 \end{aligned}$$

Ω_k is the k th natural frequency, $\Phi(t_{i-1})$ is determined by Equation (7.84), $\mathbf{T}_1, \mathbf{T}_2$ and \mathbf{T}_3 are determined by Equation (7.77), and A is the coordinate transform matrix. EI , l and \bar{m} are the bending stiffness, length and mass per unit length of the beam, respectively. \bar{m}_{2z} and \bar{m}_{2y} (f_{2z} and f_{2y}) are distributing external torques (forces) with respect to the body-fixed coordinate system. $Y^j(x_2)$ and $Z^j(x_2)$ are the eigenvectors of the outboard beam.

15.25.2 Fixed Hinge whose Inboard and Outboard Bodies are Euler–Bernoulli Beams Moving in Space

The state vectors are

$$\begin{aligned}
 \mathbf{z}_I &= [x, y, z, \theta_x, \theta_y, \theta_z, m_x, m_y, m_z, q_x, q_y, q_z, q^1, q^2, \dots, q^n, 1]^T \\
 \mathbf{z}_O &= [x, y, z, \theta_x, \theta_y, \theta_z, m_x, m_y, m_z, q_x, q_y, q_z, q^1, q^2, \dots, q^n, 1]^T
 \end{aligned} \tag{15.159}$$

The transfer equation is

$$\mathbf{z}_O = \mathbf{U} \mathbf{z}_I \quad (15.160)$$

The transfer matrix is

$$\mathbf{U} = \begin{bmatrix} \mathbf{I}_3 & \mathbf{O}_{3 \times 3} & \mathbf{O}_{3 \times 3} & \mathbf{O}_{3 \times 3} & \mathbf{O}_{3 \times n} & \mathbf{O}_{3 \times 1} \\ \mathbf{O}_{3 \times 3} & \mathbf{I}_3 & \mathbf{O}_{3 \times 3} & \mathbf{O}_{3 \times 3} & \mathbf{U}_{25} & \mathbf{O}_{3 \times 1} \\ \mathbf{O}_{3 \times 3} & \mathbf{O}_{3 \times 3} & \mathbf{I}_3 & \mathbf{O}_{3 \times 3} & \mathbf{O}_{3 \times n} & \mathbf{O}_{3 \times 1} \\ \mathbf{O}_{3 \times 3} & \mathbf{O}_{3 \times 3} & \mathbf{O}_{3 \times 3} & \mathbf{I}_3 & \mathbf{O}_{3 \times n} & \mathbf{O}_{3 \times 1} \\ \mathbf{U}_{51} & \mathbf{U}_{52} & \mathbf{O}_{n \times 3} & \mathbf{O}_{n \times 3} & \mathbf{U}_{52} \mathbf{U}_{25} & \mathbf{U}_{56} \\ \mathbf{O}_{1 \times 3} & \mathbf{O}_{1 \times 3} & \mathbf{O}_{1 \times 3} & \mathbf{O}_{1 \times 3} & \mathbf{O}_{1 \times n} & 1 \end{bmatrix} \quad (15.161)$$

where

$$\mathbf{U}_{25} = [P_{51} \ P_{52} \ \cdots \ P_{5n}], \ P_{5k} = \mathbf{H}^{-1} \begin{bmatrix} 0 & -\frac{dZ^k(l)}{dx_2} & \frac{dY^k(l)}{dx_2} \end{bmatrix}^T, \ \mathbf{H} = \begin{bmatrix} 1 & 0 & -s_y \\ 0 & c_x & s_x c_y \\ 0 & -s_x & c_x c_x \end{bmatrix}_I$$

$$\mathbf{U}_{51} = \begin{bmatrix} \mathbf{P}_{11} \\ \mathbf{P}_{12} \\ \vdots \\ \mathbf{P}_{1n} \end{bmatrix}, \ \mathbf{U}_{52} = \begin{bmatrix} \mathbf{P}_{21} \\ \mathbf{P}_{22} \\ \vdots \\ \mathbf{P}_{2n} \end{bmatrix}, \ \mathbf{U}_{56} = \begin{bmatrix} P_{51} \\ P_{52} \\ \vdots \\ P_{5n} \end{bmatrix}$$

$$\mathbf{P}_{1j} = \frac{-\bar{m}A}{(A + \Omega_j^2)d_j} \int_0^l [0 \ Y^j \ Z^j] \mathbf{A}^T(t_{i-1}) dx_2, \ \mathbf{P}_{2j} = \frac{\mathbf{F}_j}{(A + \Omega_j^2)d_j}$$

$$P_{5j} = \frac{1}{(A + \Omega_j^2)d_j} \int_0^l [Y^j \ Z^j] \begin{bmatrix} f_{2y} - \frac{\partial \bar{m}_{2z}}{\partial x_2} \\ f_{2z} + \frac{\partial \bar{m}_{2y}}{\partial x_2} \end{bmatrix} dx_2 + \frac{\mathbf{E}_j}{(A + \Omega_j^2)d_j}$$

$$+ \frac{\bar{m}A}{(A + \Omega_j^2)d_j} \int_0^l [0 \ Y^j \ Z^j] \mathbf{A}^T(t_{i-1}) \begin{bmatrix} x_{t_{i-1}} \\ y_{t_{i-1}} \\ z_{t_{i-1}} \end{bmatrix}_I dx_2$$

$$\mathbf{E}_j = -\bar{m} \int_0^l [0 \ Y^j \ Z^j] \boldsymbol{\Phi}^T(t_{i-1}) \left(\mathbf{B}_F + A \begin{bmatrix} x_{t_{i-1}} \\ y_{t_{i-1}} \\ z_{t_{i-1}} \end{bmatrix}_I \right) dx_2$$

$$\mathbf{F}_j = \bar{m} \int_0^l [0 \ Y^j \ Z^j] [\tilde{\mathbf{T}}_1(t_{i-1})\mathbf{R}, \ \tilde{\mathbf{T}}_2(t_{i-1})\mathbf{R}, \ \tilde{\mathbf{T}}_3(t_{i-1})\mathbf{R}] dx_2$$

$$\mathbf{R} = \mathbf{A}^T(t_{i-1}) \left(\mathbf{B}_F + A \begin{bmatrix} x_{t_{i-1}} \\ y_{t_{i-1}} \\ z_{t_{i-1}} \end{bmatrix}_I \right)$$

$$\int_0^l \bar{m} \begin{bmatrix} Y^j(x_2) \\ Z^j(x_2) \end{bmatrix} \cdot \begin{bmatrix} Y^k(x_2) \\ Z^k(x_2) \end{bmatrix} dx_2 = \begin{cases} 0 & j \neq k \\ d_j & j = k \end{cases}, \quad \int_0^l EI \begin{bmatrix} Y^{j(2)}(x_2) \\ Z^{j(2)}(x_2) \end{bmatrix} \cdot \begin{bmatrix} Y^{k(2)}(x_2) \\ Z^{k(2)}(x_2) \end{bmatrix} dx_2 = \begin{cases} 0 & j \neq k \\ \Omega_j^2 d_j & j = k \end{cases}$$

Ω_k is the k th natural frequency, $\Phi(t_{i-1})$ is determined by Equation (7.84), T_1, T_2 and T_3 are determined by Equation (7.77), and A is the coordinate transform matrix. EI , l and \bar{m} are the bending stiffness, length and mass per unit length of the beam, respectively. $Y^j(x_2)$ and $Z^j(x_2)$ are the eigenvectors of the outboard beam. f_{2z} and f_{2y} (\bar{m}_{2z} and \bar{m}_{2y}) are distributing external forces (torques) with respect to the body-fixed coordinate system.

15.25.3 Fixed Hinge whose Inboard Body is a Euler–Bernoulli Beam and whose Outboard Body is a Rigid Body Moving in Space

Deleting the row elements corresponding to generalized coordinates in Equation (15.161), the transfer equation and transfer matrix of a fixed hinge whose inboard body is a beam and whose outboard body is a rigid body moving in space can be obtained.

The state vectors are

$$\begin{aligned} \mathbf{z}_I &= [x, y, z, \theta_x, \theta_y, \theta_z, m_x, m_y, m_z, q_x, q_y, q_z, q^1, q^2, \dots, q^n, 1]^T \\ \mathbf{z}_O &= [x, y, z, \theta_x, \theta_y, \theta_z, m_x, m_y, m_z, q_x, q_y, q_z, 1]^T \end{aligned} \quad (15.162)$$

The transfer equation is

$$\mathbf{z}_O = \mathbf{U} \mathbf{z}_I \quad (15.163)$$

The transfer matrix is

$$\mathbf{U} = \begin{bmatrix} \mathbf{I}_3 & \mathbf{O}_{3 \times 3} & \mathbf{O}_{3 \times 3} & \mathbf{O}_{3 \times 3} & \mathbf{O}_{3 \times n} & \mathbf{O}_{3 \times 1} \\ \mathbf{O}_{3 \times 3} & \mathbf{I}_3 & \mathbf{O}_{3 \times 3} & \mathbf{O}_{3 \times 3} & \mathbf{U}_{25} & \mathbf{O}_{3 \times 1} \\ \mathbf{O}_{3 \times 3} & \mathbf{O}_{3 \times 3} & \mathbf{I}_3 & \mathbf{O}_{3 \times 3} & \mathbf{O}_{3 \times n} & \mathbf{O}_{3 \times 1} \\ \mathbf{O}_{3 \times 3} & \mathbf{O}_{3 \times 3} & \mathbf{O}_{3 \times 3} & \mathbf{I}_3 & \mathbf{O}_{3 \times n} & \mathbf{O}_{3 \times 1} \\ \mathbf{O}_{1 \times 3} & \mathbf{O}_{1 \times 3} & \mathbf{O}_{1 \times 3} & \mathbf{O}_{1 \times 3} & \mathbf{O}_{1 \times n} & 1 \end{bmatrix} \quad (15.164)$$

where the meanings of all the elements are the same as in Equation (15.161).

15.26 Smooth Hinges Connected to a Beam with Large Planar Motion

15.26.1 Smooth Hinge whose Inboard and Outboard Bodies are Euler–Bernoulli Beams Moving in a Plane

The state vectors are

$$\begin{aligned} \mathbf{z}_I &= [x, y, \theta, m, q_x, q_y, q^1, q^2, q^3, 1]^T \\ \mathbf{z}_O &= [x, y, \theta, m, q_x, q_y, q^1, q^2, q^3, 1]^T \end{aligned} \quad (15.165)$$

The transfer equation is

$$\mathbf{z}_O = \mathbf{U} \mathbf{z}_I \quad (15.166)$$

The transfer matrix is

$$U = \begin{bmatrix} 1 & 0 & 0 & 0 & 0 & 0 & 0 & 0 & 0 & 0 \\ 0 & 1 & 0 & 0 & 0 & 0 & 0 & 0 & 0 & 0 \\ \Delta_{41}/\Delta & \Delta_{42}/\Delta & 0 & 0 & \Delta_{43}/\Delta & \Delta_{44}/\Delta & 0 & 0 & 0 & \Delta_{45}/\Delta \\ 0 & 0 & 0 & 0 & 0 & 0 & 0 & 0 & 0 & 0 \\ 0 & 0 & 0 & 0 & 1 & 0 & 0 & 0 & 0 & 0 \\ 0 & 0 & 0 & 0 & 0 & 1 & 0 & 0 & 0 & 0 \\ \Delta_{11}/\Delta & \Delta_{12}/\Delta & 0 & 0 & \Delta_{13}/\Delta & \Delta_{14}/\Delta & 0 & 0 & 0 & \Delta_{15}/\Delta \\ \Delta_{21}/\Delta & \Delta_{22}/\Delta & 0 & 0 & \Delta_{23}/\Delta & \Delta_{24}/\Delta & 0 & 0 & 0 & \Delta_{25}/\Delta \\ \Delta_{31}/\Delta & \Delta_{32}/\Delta & 0 & 0 & \Delta_{33}/\Delta & \Delta_{34}/\Delta & 0 & 0 & 0 & \Delta_{35}/\Delta \\ 0 & 0 & 0 & 0 & 0 & 0 & 0 & 0 & 0 & 1 \end{bmatrix} \quad (15.167)$$

where

$$\Delta = \begin{bmatrix} D_{11} & & D_{14} \\ & D_{22} & D_{24} \\ & & D_{33} & D_{34} \\ D_{41} & D_{42} & D_{43} & D_{44} \end{bmatrix}$$

$$\left\{ \begin{array}{l} \Delta_{1j} = \begin{bmatrix} H_{1i} & & D_{14} \\ H_{2i} & D_{22} & D_{24} \\ H_{3i} & & D_{33} & D_{34} \\ H_{4i} & D_{42} & D_{43} & D_{44} \end{bmatrix}, \quad \Delta_{2j} = \begin{bmatrix} D_{11} & H_{1i} & D_{14} \\ & H_{2i} & D_{24} \\ & H_{3i} & D_{33} & D_{34} \\ D_{41} & H_{4i} & D_{43} & D_{44} \end{bmatrix} \\ \Delta_{3j} = \begin{bmatrix} D_{11} & & H_{1i} & D_{14} \\ & D_{22} & H_{2i} & D_{24} \\ & & H_{3i} & D_{34} \\ D_{41} & D_{42} & H_{4i} & D_{44} \end{bmatrix}, \quad \Delta_{4j} = \begin{bmatrix} D_{11} & & & H_{1i} \\ & D_{22} & & H_{2i} \\ & & D_{33} & H_{3i} \\ D_{41} & D_{42} & D_{43} & H_{4i} \end{bmatrix} \end{array} \right. \quad (j = 1, 2, 3, 4, 5)$$

$$D_{kk} = \frac{l}{2} \left[EI \frac{k^4 \pi^4}{l^4} - \bar{m} \dot{\theta}^2(t_{i-1}) \right] + \frac{l}{2} \left(\rho I \frac{k^2 \pi^2}{l^2} + \bar{m} \right) A \quad (k = 1, 2, 3)$$

$$D_{k4} = (-1)^{k-1} \bar{m} \frac{l^2}{k\pi} A - \bar{m} l \dot{\theta}(t_{i-1}) q^k(t_{i-1}) C \quad (k = 1, 2, 3)$$

$$D_{41} = u_{4,7}, \quad D_{42} = u_{4,8}, \quad D_{43} = u_{4,9}, \quad D_{44} = u_{4,3}$$

$$H_{k1} = \left[1 - (-1)^k \right] \bar{m} \frac{l}{k\pi} \bar{s} A, \quad H_{k2} = - \left[1 - (-1)^k \right] \bar{m} \frac{l}{k\pi} \bar{c} A$$

$$H_{k5} = \int_0^l \left[f_{2,y}(x_2, t) - \frac{\partial}{\partial x_2} m'(x_2, t) \right] \sin \frac{k\pi x_2}{l} dx_2 - \frac{l}{2} \left(\bar{m} + \rho I \frac{k^2 \pi^2}{l^2} \right) B_{q^k} - \bar{m} l \dot{\theta}^2(t_{i-1}) q^k(t_{i-1})$$

$$- (-1)^{k-1} \frac{\bar{m} l^2}{k\pi} B_{\theta} - \left[1 - (-1)^k \right] \frac{\bar{m} l}{k\pi} \left(\bar{c} B_{y_{02}} - \bar{s} B_{x_{02}} \right) + \bar{m} l \dot{\theta}(t_{i-1}) q^k(t_{i-1}) D_{\theta}$$

$$H_{41} = -u_{4,1}, \quad H_{42} = -u_{4,2}, \quad H_{43} = -u_{4,5}, \quad H_{44} = -u_{4,6}, \quad H_{45} = -u_{4,10}$$

$u_{4,1}, u_{4,2}, \dots, u_{4,10}$ are the elements of the transfer matrix of the outboard beam. EI is the bending stiffness of the beam, \bar{m} is the mass per unit length of the beam and l is the length of the beam. $f_{2,y}(x_2, t)$ are the distributed external forces acted on the beam in the y_2 direction and m' is the distributed external torque acted on the beam. \bar{s} and \bar{c} are determined by Equation (7.62).

15.26.2 Smooth Hinge whose Inboard Body is a Rigid Body and whose Outboard Body is a Euler–Bernoulli Beam Moving in a Plane

The state vectors are

$$\begin{aligned} \mathbf{z}_I &= [x, y, \theta, m, q_x, q_y, 1]^T \\ \mathbf{z}_O &= [x, y, \theta, m, q_x, q_y, q^1, q^2, q^3, 1]^T \end{aligned} \quad (15.168)$$

The transfer equation is

$$\mathbf{z}_O = \mathbf{U} \mathbf{z}_I \quad (15.169)$$

The transfer matrix is

$$\mathbf{U} = \begin{bmatrix} 1 & 0 & 0 & 0 & 0 & 0 & 0 \\ 0 & 1 & 0 & 0 & 0 & 0 & 0 \\ \Delta_{41}/\Delta & \Delta_{42}/\Delta & 0 & 0 & \Delta_{43}/\Delta & \Delta_{44}/\Delta & \Delta_{45}/\Delta \\ 0 & 0 & 0 & 0 & 0 & 0 & 0 \\ 0 & 0 & 0 & 0 & 1 & 0 & 0 \\ 0 & 0 & 0 & 0 & 0 & 1 & 0 \\ \Delta_{11}/\Delta & \Delta_{12}/\Delta & 0 & 0 & \Delta_{13}/\Delta & \Delta_{14}/\Delta & \Delta_{15}/\Delta \\ \Delta_{21}/\Delta & \Delta_{22}/\Delta & 0 & 0 & \Delta_{23}/\Delta & \Delta_{24}/\Delta & \Delta_{25}/\Delta \\ \Delta_{31}/\Delta & \Delta_{32}/\Delta & 0 & 0 & \Delta_{33}/\Delta & \Delta_{34}/\Delta & \Delta_{35}/\Delta \\ 0 & 0 & 0 & 0 & 0 & 0 & 1 \end{bmatrix} \quad (15.170)$$

where the meanings of all the elements are the same as in Equation (15.167).

15.26.3 Smooth Pin Hinge whose Inboard Body is a Euler–Bernoulli Beam and whose Outboard Body is a Rigid Body Moving in a Plane

The state vectors are

$$\begin{aligned} \mathbf{z}_I &= [x, y, \theta, m, q_x, q_y, q^1, q^2, q^3, 1]^T \\ \mathbf{z}_O &= [x, y, \theta, m, q_x, q_y, 1]^T \end{aligned} \quad (15.171)$$

The transfer equation is

$$\mathbf{z}_O = \mathbf{U} \mathbf{z}_I \quad (15.172)$$

The transfer matrix is

$$\mathbf{U} = \begin{bmatrix} 1 & 0 & 0 & 0 & 0 & 0 & 0 & 0 & 0 \\ 0 & 1 & 0 & 0 & 0 & 0 & 0 & 0 & 0 \\ -\frac{u_{4,1}}{u_{4,3}} & -\frac{u_{4,2}}{u_{4,3}} & 0 & 0 & -\frac{u_{4,5}}{u_{4,3}} & -\frac{u_{4,6}}{u_{4,3}} & 0 & 0 & -\frac{u_{4,7}}{u_{4,3}} \\ 0 & 0 & 0 & 0 & 0 & 0 & 0 & 0 & 0 \\ 0 & 0 & 0 & 0 & 0 & 0 & 0 & 0 & 0 \\ 0 & 0 & 0 & 0 & 0 & 1 & 0 & 0 & 0 \\ 0 & 0 & 0 & 0 & 0 & 0 & 0 & 0 & 0 \end{bmatrix} \quad (15.173)$$

where the meanings of all the elements are the same as in Equation (7.219).

15.27 Smooth Hinges Connected to a Beam with Large Spatial Motion

15.27.1 Smooth Ball-and-socket Hinge whose Inboard Body is a Rigid Body and whose Outboard Body is a Euler–Bernoulli Beam Moving in Space

The state vectors are

$$\begin{aligned} \mathbf{z}_I &= [x, y, z, \theta_x, \theta_y, \theta_z, m_x, m_y, m_z, q_x, q_y, q_z, 1]^T \\ \mathbf{z}_O &= [x, y, z, \theta_x, \theta_y, \theta_z, m_x, m_y, m_z, q_x, q_y, q_z, q^1, q^2, \dots, q^n, 1]^T \end{aligned} \quad (15.174)$$

The transfer equation is

$$\mathbf{z}_O = \mathbf{U} \mathbf{z}_I \quad (15.175)$$

The transfer matrix is

$$\mathbf{U} = \begin{bmatrix} \mathbf{I}_3 & \mathbf{O}_{3 \times 3} & \mathbf{O}_{3 \times 3} & \mathbf{O}_{3 \times 3} & \mathbf{O}_{3 \times 1} \\ \mathbf{U}_{21} & \mathbf{O}_{3 \times 3} & \mathbf{O}_{3 \times 3} & \mathbf{U}_{24} & \mathbf{U}_{25} \\ \mathbf{O}_{3 \times 3} & \mathbf{O}_{3 \times 3} & \mathbf{O}_{3 \times 3} & \mathbf{O}_{3 \times 3} & \mathbf{O}_{3 \times 1} \\ \mathbf{O}_{3 \times 3} & \mathbf{O}_{3 \times 3} & \mathbf{O}_{3 \times 3} & \mathbf{I}_3 & \mathbf{O}_{3 \times 1} \\ \mathbf{U}_{51} & \mathbf{O}_{n \times 3} & \mathbf{O}_{n \times 3} & \mathbf{U}_{54} & \mathbf{U}_{55} \\ \mathbf{O}_{1 \times 3} & \mathbf{O}_{1 \times 3} & \mathbf{O}_{1 \times 3} & \mathbf{O}_{1 \times 3} & 1 \end{bmatrix} \quad (15.176)$$

where

$$\begin{bmatrix} \mathbf{U}_{21} \\ \mathbf{U}_{51} \end{bmatrix} = \begin{bmatrix} \mathbf{U}_{32} & \mathbf{U}_{35} \\ -\mathbf{P}_{21} & \mathbf{I}_{n \times 1} \\ -\mathbf{P}_{22} & \mathbf{I}_{n \times 1} \\ \vdots & \vdots \\ -\mathbf{P}_{2n} & \mathbf{I}_{n \times 1} \end{bmatrix}^{-1} \begin{bmatrix} \mathbf{U}_{31} \\ \mathbf{P}_{11} \\ \mathbf{P}_{12} \\ \vdots \\ \mathbf{P}_{1n} \end{bmatrix}, \quad \begin{bmatrix} \mathbf{U}_{24} \\ \mathbf{U}_{54} \end{bmatrix} = \begin{bmatrix} \mathbf{U}_{32} & \mathbf{U}_{35} \\ -\mathbf{P}_{21} & \mathbf{I}_{n \times 1} \\ -\mathbf{P}_{22} & \mathbf{I}_{n \times 1} \\ \vdots & \vdots \\ -\mathbf{P}_{2n} & \mathbf{I}_{n \times 1} \end{bmatrix}^{-1} \begin{bmatrix} -\mathbf{U}_{34} \\ \mathbf{O}_{n \times 3} \end{bmatrix},$$

$$\begin{bmatrix} \mathbf{U}_{25} \\ \mathbf{U}_{55} \end{bmatrix} = \begin{bmatrix} \mathbf{U}_{32} & \mathbf{U}_{35} \\ -\mathbf{P}_{21} & \mathbf{I}_{n \times 1} \\ -\mathbf{P}_{22} & \mathbf{I}_{n \times 1} \\ \vdots & \vdots \\ -\mathbf{P}_{2n} & \mathbf{I}_{n \times 1} \end{bmatrix}^{-1} \begin{bmatrix} -\mathbf{U}_{36} \\ \mathbf{P}_{51} \\ \mathbf{P}_{52} \\ \vdots \\ \mathbf{P}_{5n} \end{bmatrix}$$

$$\mathbf{P}_{2j} = \frac{\mathbf{F}_j}{(A + \Omega_j^2)d_j}$$

$$\begin{aligned}
\mathbf{P}_{5j} = & \frac{1}{(A + \Omega_j^2)d_j} \int_0^l [\mathbf{Y}^j \quad \mathbf{Z}^j] \begin{bmatrix} f_{2y} - \frac{\partial \bar{m}_{2z}}{\partial x_2} \\ f_{2z} + \frac{\partial \bar{m}_{2y}}{\partial x_2} \end{bmatrix} dx_2 + \frac{\mathbf{E}_j}{(A + \Omega_j^2)d_j} \\
& + \frac{\bar{m}A}{(A + \Omega_j^2)d_j} \int_0^l [0 \quad \mathbf{Y}^j \quad \mathbf{Z}^j] \mathbf{A}^T(t_{i-1}) \begin{bmatrix} x \\ y \\ z \end{bmatrix}_I (t_{i-1}) dx_2 \\
\mathbf{E}_j = & -\bar{m} \int_0^l [0 \quad \mathbf{Y}^j \quad \mathbf{Z}^j] \boldsymbol{\Phi}^T(t_{i-1}) \left[\mathbf{B}_{\bar{r}} + A \begin{bmatrix} x \\ y \\ z \end{bmatrix}_I (t_{i-1}) \right] dx_2 \\
\mathbf{F}_j = & \bar{m} \int_0^l [0 \quad \mathbf{Y}^j \quad \mathbf{Z}^j] [\tilde{\mathbf{T}}_1(t_{i-1})\mathbf{R}, \tilde{\mathbf{T}}_2(t_{i-1})\mathbf{R}, \tilde{\mathbf{T}}_3(t_{i-1})\mathbf{R}] dx_2 \\
\mathbf{R} = & \mathbf{A}^T(t_{i-1}) \left(\mathbf{B}_{\bar{r}} + A \begin{bmatrix} x_{t_{i-1}} \\ y_{t_{i-1}} \\ z_{t_{i-1}} \end{bmatrix}_I \right) \\
\int_0^l \rho U_i U_k dx = & \begin{cases} 0 & i \neq k \\ d_j & i = k \end{cases}, \quad \int_0^l EI U_{i,xx} U_{k,xx} dx = \begin{cases} 0 & i \neq k \\ \Omega_j^2 d_j & i = k \end{cases}
\end{aligned}$$

Ω_k is the k th natural frequency, $\boldsymbol{\Phi}(t_{i-1})$ is determined by Equation (7.84), $\mathbf{T}_1, \mathbf{T}_2$ and \mathbf{T}_3 are determined by Equation (7.77) and \mathbf{A} is the coordinate transform matrix. l and \bar{m} are the length and mass per unit length of the beam, respectively. $\mathbf{Y}^j(x_2)$ and $\mathbf{Z}^j(x_2)$ are the eigenvectors of the outboard beam. f_{2z} and f_{2y} (\bar{m}_{2z} and \bar{m}_{2y}) are distributing external forces (torques) with respect to the body-fixed coordinate system.

15.27.2 Smooth Ball-and-socket Hinge whose Inboard and Outboard Bodies are Euler-Bernoulli Beams Moving in Space

The state vectors are

$$\begin{aligned}
\mathbf{z}_I &= [x, y, z, \theta_x, \theta_y, \theta_z, m_x, m_y, m_z, q_x, q_y, q_z, q^1, q^2, \dots, q^n, 1]^T \\
\mathbf{z}_O &= [x, y, z, \theta_x, \theta_y, \theta_z, m_x, m_y, m_z, q_x, q_y, q_z, q^1, q^2, \dots, q^n, 1]^T
\end{aligned} \tag{15.177}$$

The transfer equation is

$$\mathbf{z}_O = \mathbf{U} \mathbf{z}_I \quad (15.178)$$

The transfer matrix is

$$\mathbf{U} = \begin{bmatrix} \mathbf{I}_3 & \mathbf{O}_{3 \times 3} & \mathbf{O}_{3 \times 3} & \mathbf{O}_{3 \times 3} & \mathbf{O}_{3 \times n} & \mathbf{O}_{3 \times 1} \\ \mathbf{U}_{21} & \mathbf{O}_{3 \times 3} & \mathbf{O}_{3 \times 3} & \mathbf{U}_{24} & \mathbf{O}_{3 \times n} & \mathbf{U}_{25} \\ \mathbf{O}_{3 \times 3} & \mathbf{O}_{3 \times 3} & \mathbf{O}_{3 \times 3} & \mathbf{O}_{3 \times 3} & \mathbf{O}_{3 \times n} & \mathbf{O}_{3 \times 1} \\ \mathbf{O}_{3 \times 3} & \mathbf{O}_{3 \times 3} & \mathbf{O}_{3 \times 3} & \mathbf{I}_3 & \mathbf{O}_{3 \times n} & \mathbf{O}_{3 \times 1} \\ \mathbf{U}_{51} & \mathbf{O}_{n \times 3} & \mathbf{O}_{n \times 3} & \mathbf{U}_{54} & \mathbf{O}_{n \times n} & \mathbf{O}_{n \times 1} \\ \mathbf{O}_{1 \times 3} & \mathbf{O}_{1 \times 3} & \mathbf{O}_{1 \times 3} & \mathbf{O}_{1 \times 3} & \mathbf{O}_{1 \times n} & 1 \end{bmatrix} \quad (15.179)$$

where the meanings of all the elements are the same as in Equation (15.176).

15.27.3 Smooth Ball-and-socket Hinge whose Inboard Body is a Euler–Bernoulli Beam and whose Outboard Body is a Rigid Body Moving in Space

The state vectors are

$$\begin{aligned} \mathbf{z}_I &= [x, y, z, \theta_x, \theta_y, \theta_z, m_x, m_y, m_z, q_x, q_y, q_z, q^1, q^2, \dots, q^n, 1]^T \\ \mathbf{z}_O &= [x, y, z, \theta_x, \theta_y, \theta_z, m_x, m_y, m_z, q_x, q_y, q_z, 1]^T \end{aligned} \quad (15.180)$$

The transfer equation is

$$\mathbf{z}_O = \mathbf{U} \mathbf{z}_I \quad (15.181)$$

The transfer matrix is

$$\mathbf{U} = \begin{bmatrix} \mathbf{I}_3 & \mathbf{O}_{3 \times 3} & \mathbf{O}_{3 \times 3} & \mathbf{O}_{3 \times 3} & \mathbf{O}_{3 \times n} & \mathbf{O}_{3 \times 1} \\ \mathbf{U}_{21} & \mathbf{O}_{3 \times 3} & \mathbf{O}_{3 \times 3} & \mathbf{U}_{24} & \mathbf{O}_{3 \times n} & \mathbf{U}_{25} \\ \mathbf{O}_{3 \times 3} & \mathbf{O}_{3 \times 3} & \mathbf{O}_{3 \times 3} & \mathbf{O}_{3 \times 3} & \mathbf{O}_{3 \times n} & \mathbf{O}_{3 \times 1} \\ \mathbf{O}_{3 \times 3} & \mathbf{O}_{3 \times 3} & \mathbf{O}_{3 \times 3} & \mathbf{I}_3 & \mathbf{O}_{3 \times n} & \mathbf{O}_{3 \times 1} \\ \mathbf{O}_{1 \times 3} & \mathbf{O}_{1 \times 3} & \mathbf{O}_{1 \times 3} & \mathbf{O}_{1 \times 3} & \mathbf{O}_{1 \times n} & 1 \end{bmatrix} \quad (15.182)$$

where the meanings of all the elements are the same as in Equation (15.176).

15.28 Elastic Hinges Connected to a Beam with Large Planar Motion

15.28.1 Elastic Hinge whose Inboard and Outboard Bodies are Beams Moving in a Plane

The state vectors are

$$\begin{aligned} \mathbf{z}_I &= [x, y, \theta, m, q_x, q_y, q^1, q^2, \dots, q^n, 1]^T \\ \mathbf{z}_O &= [x, y, \theta, m, q_x, q_y, q^1, q^2, \dots, q^n, 1]^T \end{aligned} \quad (15.183)$$

The transfer equation is

$$\mathbf{z}_O = \mathbf{U} \mathbf{z}_I \quad (15.184)$$

The transfer matrix is

$$\mathbf{U} = \begin{bmatrix} 1 & 0 & 0 & 0 & \frac{\Delta_{11}}{\Delta} & \frac{\Delta_{12}}{\Delta} & 0 & 0 & \cdots & 0 & \frac{\Delta_{13}}{\Delta} \\ 0 & 1 & 0 & 0 & \frac{\Delta_{21}}{\Delta} & \frac{\Delta_{22}}{\Delta} & 0 & 0 & \cdots & 0 & \frac{\Delta_{23}}{\Delta} \\ \frac{\Delta'_{n+1,1}}{\Delta'} & \frac{\Delta'_{n+1,2}}{\Delta'} & \frac{\Delta'_{n+1,3}}{\Delta'} & \frac{\Delta'_{n+1,4}}{\Delta'} & 0 & 0 & \frac{\Delta'_{n+1,4+1}}{\Delta'} & \frac{\Delta'_{n+1,4+2}}{\Delta'} & \cdots & \frac{\Delta'_{n+1,4+n}}{\Delta'} & \frac{\Delta'_{n+1,5+n}}{\Delta'} \\ 0 & 0 & 0 & 1 & 0 & 0 & 0 & 0 & \cdots & 0 & 0 \\ 0 & 0 & 0 & 0 & 1 & 0 & 0 & 0 & \cdots & 0 & 0 \\ 0 & 0 & 0 & 0 & 0 & 1 & 0 & 0 & \cdots & 0 & 0 \\ \frac{\Delta'_{1,1}}{\Delta'} & \frac{\Delta'_{1,2}}{\Delta'} & \frac{\Delta'_{1,3}}{\Delta'} & \frac{\Delta'_{1,4}}{\Delta'} & 0 & 0 & \frac{\Delta'_{1,4+1}}{\Delta'} & \frac{\Delta'_{1,4+2}}{\Delta'} & \cdots & \frac{\Delta'_{1,4+n}}{\Delta'} & \frac{\Delta'_{1,5+n}}{\Delta'} \\ \frac{\Delta'_{2,1}}{\Delta'} & \frac{\Delta'_{2,2}}{\Delta'} & \frac{\Delta'_{2,3}}{\Delta'} & \frac{\Delta'_{2,4}}{\Delta'} & 0 & 0 & \frac{\Delta'_{2,4+1}}{\Delta'} & \frac{\Delta'_{2,4+2}}{\Delta'} & \cdots & \frac{\Delta'_{2,4+n}}{\Delta'} & \frac{\Delta'_{2,5+n}}{\Delta'} \\ \vdots & \vdots & \vdots & \vdots & \vdots & \vdots & \vdots & \vdots & \ddots & \vdots & \vdots \\ \frac{\Delta'_{n,1}}{\Delta'} & \frac{\Delta'_{n,2}}{\Delta'} & \frac{\Delta'_{n,3}}{\Delta'} & \frac{\Delta'_{n,4}}{\Delta'} & 0 & 0 & \frac{\Delta'_{n,4+1}}{\Delta'} & \frac{\Delta'_{n,4+2}}{\Delta'} & \cdots & \frac{\Delta'_{n,4+n}}{\Delta'} & \frac{\Delta'_{n,5+n}}{\Delta'} \\ 0 & 0 & 0 & 0 & 0 & 0 & 0 & 0 & \cdots & 0 & 1 \end{bmatrix} \quad (15.185)$$

where

$$\Delta = \begin{vmatrix} a_1 & a_2 \\ b_1 & b_2 \end{vmatrix}$$

$$\Delta_{11} = \begin{vmatrix} -1 & a_2 \\ 0 & b_2 \end{vmatrix}, \quad \Delta_{12} = \begin{vmatrix} 0 & a_2 \\ -1 & b_2 \end{vmatrix}, \quad \Delta_{13} = \begin{vmatrix} -a_3 & a_2 \\ -b_3 & b_2 \end{vmatrix}$$

$$\Delta_{21} = \begin{vmatrix} a_1 & -1 \\ b_1 & 0 \end{vmatrix}, \quad \Delta_{22} = \begin{vmatrix} a_1 & 0 \\ b_1 & -1 \end{vmatrix}, \quad \Delta_{23} = \begin{vmatrix} a_1 & -a_3 \\ b_1 & -b_3 \end{vmatrix}$$

$$\Delta' = \begin{vmatrix} A_{1,1} & A_{1,2} & \cdots & A_{1,n} & A_{1,n+1} \\ A_{2,1} & A_{2,2} & \cdots & A_{2,n} & A_{2,n+1} \\ \vdots & \vdots & \ddots & \vdots & \vdots \\ A_{n,1} & A_{n,2} & \cdots & A_{n,n} & A_{n,n+1} \\ A_{n+1,1} & A_{n+1,2} & \cdots & A_{n+1,n} & A_{n+1,n+1} \end{vmatrix}$$

$$\Delta'_{k,i} = \begin{vmatrix} A_{1,1} & \cdots & A_{1,k-1} & B_{1,i} & A_{1,k+1} & \cdots & A_{1,n+1} \\ A_{2,1} & \cdots & A_{2,k-1} & B_{2,i} & A_{2,k+1} & \cdots & A_{2,n+1} \\ \vdots & \ddots & \vdots & \vdots & \vdots & \ddots & \vdots \\ A_{n,1} & \cdots & A_{n,k-1} & B_{n,i} & A_{n,k+1} & \cdots & A_{n,n+1} \\ A_{n+1,1} & \cdots & A_{n+1,k-1} & B_{n+1,i} & A_{n+1,k+1} & \cdots & A_{n+1,n+1} \end{vmatrix} \quad \begin{pmatrix} k=1,2,\dots,n+1 \\ i=1,2,\dots,n+5 \end{pmatrix}$$

For example

$$\Delta'_{1,i} = \begin{vmatrix} B_{1,i} & A_{1,2} & \cdots & A_{1,n} & A_{1,n+1} \\ B_{2,i} & A_{2,2} & \cdots & A_{2,n} & A_{2,n+1} \\ \vdots & \vdots & \ddots & \vdots & \vdots \\ B_{n,i} & A_{n,2} & \cdots & A_{n,n} & A_{n,n+1} \\ B_{n+1,i} & A_{n+1,2} & \cdots & A_{n+1,n} & A_{n+1,n+1} \end{vmatrix}, \Delta'_{2,i} = \begin{vmatrix} A_{1,1} & B_{1,i} & \cdots & A_{1,n} & A_{1,n+1} \\ A_{2,1} & B_{2,i} & \cdots & A_{2,n} & A_{2,n+1} \\ \vdots & \vdots & \ddots & \vdots & \vdots \\ A_{n,1} & B_{n,i} & \cdots & A_{n,n} & A_{n,n+1} \\ A_{n+1,1} & B_{n+1,i} & \cdots & A_{n+1,n} & A_{n+1,n+1} \end{vmatrix}$$

$$A_{k',k} = {}^4s_{k,k'}EI - {}^2s_{k,k'}\rho IA_{q^k} + \bar{m}s_{k,k'}A_{q^k} - \bar{m}\dot{\theta}_{t_{i-1}}^2 \quad (k=1,2,\dots,n)$$

$$A_{k',n+1} = \bar{m} \left(s_{k'}^1 A_{\theta} - 2C_{\theta} \sum_{k=1}^n s_{k,k'} q_{t_{i-1}}^k \dot{\theta}_{t_{i-1}} \right)$$

$$B_{k',1} = -\bar{m}\bar{c}s_{k'}^0 A_{x_{O_2}}, \quad B_{k',2} = \bar{m}\bar{s}s_{k'}^0 A_{y_{O_2}}, \quad B_{k',k} = 0 \quad (k=3,4,\dots,4+n)$$

$$B_{k',5+n} = \int_0^l Y^{k'}(x_2) f_{2,y}(x_2, t) dx_2 - \int_0^l Y^{k'}(x_2) \frac{\partial}{\partial x_2} m'(x_2, t) dx_2 + \rho I \sum_{k=1}^n {}^2s_{k,k'} B_{q^k} - \bar{m} \left\{ \sum_{k=1}^n s_{k,k'} B_{q^k} - \sum_{k=1}^n s_{k,k'} \left[2q_{t_{i-1}}^k \dot{\theta}_{t_{i-1}} D_{\theta} - 2q^k(t_{i-1}) \dot{\theta}_{t_{i-1}}^2 \right] + s_{k'}^1 B_{\theta} + \bar{s}s_{k'}^0 B_{y_{O_2}} - \bar{c}s_{k'}^0 B_{x_{O_2}} \right\}$$

$$A_{n+1,k} = {}^1Y_O^k \quad (k=1,2,\dots,n), \quad A_{n+1,n+1} = 1$$

$$B_{n+1,1} = 0, \quad B_{n+1,2} = 0, \quad B_{n+1,3} = 1, \quad B_{n+1,4} = \lambda_1, \quad B_{n+1,5+n} = -\lambda_2$$

$$B_{n+1,4+k} = {}^1Y_I^k \quad (k=1,2,\dots,n)$$

$$\lambda_1 = \frac{1}{K'_1 + 3K'_2 (\theta'_O - \theta'_I)_{t_{i-1}}^2}, \quad \lambda_2 = \frac{K'_2 \left[3 \left(\dot{\theta}'_O - \dot{\theta}'_I \right)_{t_{i-1}}^2 (\theta'_O - \theta'_I)_{t_{i-1}} \Delta T^2 - 2 (\theta'_O - \theta'_I)_{t_{i-1}}^3 \right]}{K'_1 + 3K'_2 (\theta'_O - \theta'_I)_{t_{i-1}}^2}$$

$$a_1 = K_1 + 3K_2 [x_O(t_{i-1}) - x_I(t_{i-1})]^2 + K_2 [y_O(t_{i-1}) - y_I(t_{i-1})]^2$$

$$a_2 = 2K_2 [y_O(t_{i-1}) - y_I(t_{i-1})] [x_O(t_{i-1}) - x_I(t_{i-1})]$$

$$a_3 = K_2 \left\{ -2[x_O(t_{i-1}) - x_I(t_{i-1})]^3 + 3[\dot{x}_O(t_{i-1}) - \dot{x}_I(t_{i-1})]^2 [x_O(t_{i-1}) - x_I(t_{i-1})] \Delta T^2 + [\dot{y}_O(t_{i-1}) - \dot{y}_I(t_{i-1})]^2 [x_O(t_{i-1}) - x_I(t_{i-1})] \Delta T^2 - 2[y_O(t_{i-1}) - y_I(t_{i-1})]^2 [x_O(t_{i-1}) - x_I(t_{i-1})] + 2[\dot{y}_O(t_{i-1}) - \dot{y}_I(t_{i-1})] [\dot{x}_O(t_{i-1}) - \dot{x}_I(t_{i-1})] [y_O(t_{i-1}) - y_I(t_{i-1})] \Delta T^2 \right\}$$

$$b_1 = 2K_2 [y_O(t_{i-1}) - y_I(t_{i-1})] [x_O(t_{i-1}) - x_I(t_{i-1})]$$

$$b_2 = K_1 + K_2 [x_O(t_{i-1}) - x_I(t_{i-1})]^2 + 3K_2 [y_O(t_{i-1}) - y_I(t_{i-1})]^2$$

$$\begin{aligned}
b_3 = & K_2 \{ -2[y_O(t_{i-1}) - y_I(t_{i-1})]^3 + 3[\dot{y}_O(t_{i-1}) - \dot{y}_I(t_{i-1})]^2[y_O(t_{i-1}) - y_I(t_{i-1})]\Delta T^2 \\
& + [\dot{x}_O(t_{i-1}) - \dot{x}_I(t_{i-1})]^2[y_O(t_{i-1}) - y_I(t_{i-1})]\Delta T^2 \\
& - 2[x_O(t_{i-1}) - x_I(t_{i-1})]^2[y_O(t_{i-1}) - y_I(t_{i-1})] \\
& + 2[\dot{y}_O(t_{i-1}) - \dot{y}_I(t_{i-1})][\dot{x}_O(t_{i-1}) - \dot{x}_I(t_{i-1})][x_O(t_{i-1}) - x_I(t_{i-1})]\Delta T^2 \} \\
{}^4s_{k,k'} = & \int_0^l \frac{dY^{k(4)}}{dx_2^{(4)}} Y^{k'}(x_2) dx_2, \quad {}^2s_{k,k'} = \int_0^l \frac{dY^{k(2)}}{dx_2^{(2)}} Y^{k'}(x_2) dx_2, \quad {}^1Y = \frac{dY^k(x_2)}{dx_2} \\
s_k^0 = & \int_0^l Y^k(x_2) dx_2, \quad s_{k,k'} = \int_0^l Y^k(x_2) Y^{k'}(x_2) dx_2, \quad s_k^1 = \int_0^l Y^k(x_2) x_2 dx_2
\end{aligned}$$

K_1 and K_2 are the stiffness coefficients of the nonlinear spring, K'_1 and K'_2 are the torsional stiffness coefficients of the nonlinear rotary spring. l is the length of the beam. \bar{m} is the mass per unit length of the beam, $f_{2,y}$ is the distributed external force acted on the beam in the y_2 direction and m' is the distributed external torque acted on the beam. $Y^k(x_2)$ is the eigenvector of the outboard beam, Y_I^k is the eigenvector of the inboard beam, θ'_I and θ'_O are determined by Equation (8.109), and \bar{s} and \bar{c} are determined by Equation (7.62).

15.28.2 Elastic Hinge whose Inboard Body is a Rigid Body and whose Outboard Body is a Euler–Bernoulli Beam Moving in a Plane

The state vectors are

$$\begin{aligned}
\mathbf{z}_I &= [x, y, \theta, m, q_x, q_y, 1]^T \\
\mathbf{z}_O &= [x, y, \theta, m, q_x, q_y, q^1, q^2, \dots, q^n, 1]^T
\end{aligned} \tag{15.186}$$

The transfer equation is

$$\mathbf{z}_O = \mathbf{U} \mathbf{z}_I \tag{15.187}$$

The transfer matrix is

$$\mathbf{U} = \begin{bmatrix}
1 & 0 & 0 & 0 & \Delta_{11}/\Delta & \Delta_{12}/\Delta & \Delta_{13}/\Delta \\
0 & 1 & 0 & 0 & \Delta_{21}/\Delta & \Delta_{22}/\Delta & \Delta_{23}/\Delta \\
\frac{\Delta'_{n+1,1}}{\Delta'} & \frac{\Delta'_{n+1,2}}{\Delta'} & \frac{\Delta'_{n+1,3}}{\Delta'} & \frac{\Delta'_{n+1,4}}{\Delta'} & 0 & 0 & \frac{\Delta'_{n+1,5+n}}{\Delta'} \\
0 & 0 & 0 & 1 & 0 & 0 & 0 \\
0 & 0 & 0 & 0 & 1 & 0 & 0 \\
0 & 0 & 0 & 0 & 0 & 1 & 0 \\
\frac{\Delta'_{1,1}}{\Delta'} & \frac{\Delta'_{1,2}}{\Delta'} & \frac{\Delta'_{1,3}}{\Delta'} & \frac{\Delta'_{1,4}}{\Delta'} & 0 & 0 & \frac{\Delta'_{1,5+n}}{\Delta'} \\
\frac{\Delta'_{2,1}}{\Delta'} & \frac{\Delta'_{2,2}}{\Delta'} & \frac{\Delta'_{2,3}}{\Delta'} & \frac{\Delta'_{2,4}}{\Delta'} & 0 & 0 & \frac{\Delta'_{2,5+n}}{\Delta'} \\
\vdots & \vdots & \vdots & \vdots & \vdots & \vdots & \vdots \\
\frac{\Delta'_{n,1}}{\Delta'} & \frac{\Delta'_{n,2}}{\Delta'} & \frac{\Delta'_{n,3}}{\Delta'} & \frac{\Delta'_{n,4}}{\Delta'} & 0 & 0 & \frac{\Delta'_{n,5+n}}{\Delta'} \\
0 & 0 & 0 & 0 & 0 & 0 & 0
\end{bmatrix} \tag{15.188}$$

where the meanings of all the elements are the same as in Equation (15.185). In the computation $B_{n+1,k+4} = 0$ ($k = 1, 2, \dots, n$) should be used.

15.28.3 Elastic Hinge whose Inboard Body is a Euler–Bernoulli Beam and whose Outboard Body is a Rigid Body Moving in a Plane

The state vectors are

$$\begin{aligned} \mathbf{z}_I &= [x, y, \theta, m, q_x, q_y, q^1, q^2, \dots, q^n, 1]^T \\ \mathbf{z}_O &= [x, y, \theta, m, q_x, q_y, 1]^T \end{aligned} \quad (15.189)$$

The transfer equation is

$$\mathbf{z}_O = \mathbf{U} \mathbf{z}_I \quad (15.190)$$

The transfer matrix is

$$\mathbf{U} = \begin{bmatrix} 1 & 0 & 0 & 0 & \Delta_{11}/\Delta & \Delta_{12}/\Delta & 0 & 0 & \dots & 0 & \Delta_{13}/\Delta \\ 0 & 1 & 0 & 0 & \Delta_{21}/\Delta & \Delta_{22}/\Delta & 0 & 0 & \dots & 0 & \Delta_{23}/\Delta \\ 0 & 0 & 1 & \lambda_1 & 0 & 0 & {}^1Y^1(x_2) & {}^1Y^2(x_2) & \dots & {}^1Y^n(x_2) & -\lambda_2 \\ 0 & 0 & 0 & 1 & 0 & 0 & 0 & 0 & \dots & 0 & 0 \\ 0 & 0 & 0 & 0 & 1 & 0 & 0 & 0 & \dots & 0 & 0 \\ 0 & 0 & 0 & 0 & 0 & 1 & 0 & 0 & \dots & 0 & 0 \\ 0 & 0 & 0 & 0 & 0 & 0 & 0 & 0 & \dots & 0 & 1 \end{bmatrix} \quad (15.191)$$

where ${}^1Y^k = \frac{dY^k(x_2)}{dx_2}$ and the meanings of all the other elements are the same as in Equation (15.185).

15.29 Elastic Hinges Connected to a Beam Moving in Space

15.29.1 Elastic Hinge whose Inboard and Outboard Bodies are Euler–Bernoulli Beams Moving in Space

The state vectors are

$$\begin{aligned} \mathbf{z}_I &= [x, y, z, \theta_x, \theta_y, \theta_z, m_x, m_y, m_z, q_x, q_y, q_z, q^1, q^2, \dots, q^n, 1]^T \\ \mathbf{z}_O &= [x, y, z, \theta_x, \theta_y, \theta_z, m_x, m_y, m_z, q_x, q_y, q_z, q^1, q^2, \dots, q^n, 1]^T \end{aligned} \quad (15.192)$$

The transfer equation is

$$\mathbf{z}_O = \mathbf{U} \mathbf{z}_I \quad (15.193)$$

The transfer matrix is

$$U = \begin{bmatrix} I_3 & O_{3 \times 3} & O_{3 \times 3} & U_{14} & O_{3 \times n} & O_{3 \times 1} \\ U_{21} & U_{22} & U_{23} & U_{24} & U_{25} & U_{26} \\ O_{3 \times 3} & O_{3 \times 3} & I_3 & O_{3 \times 3} & O_{3 \times n} & O_{3 \times 1} \\ O_{3 \times 3} & O_{3 \times 3} & O_{3 \times 3} & I_3 & O_{3 \times n} & O_{3 \times 1} \\ U_{51} & U_{52} & U_{53} & U_{54} & U_{55} & U_{56} \\ O_{1 \times 3} & O_{1 \times 3} & O_{1 \times 3} & O_{1 \times 3} & O_{1 \times n} & 1 \end{bmatrix} \quad (15.194)$$

where $U_{2i} (i = 1, 2, 3, 4, 5, 6)$ is a (3×3) matrix and $U_{5i} (i = 1, 2, 3, 4, 5, 6)$ is a $(n \times 3)$ matrix.

$$\begin{aligned} \begin{bmatrix} U_{21} \\ U_{51} \end{bmatrix} &= \begin{bmatrix} -R_2 & I_n \\ I_3 & L_{j+2} \end{bmatrix}^{-1} \begin{bmatrix} R_1 \\ O_{3 \times 3} \end{bmatrix}, \quad \begin{bmatrix} U_{22} \\ U_{52} \end{bmatrix} = \begin{bmatrix} -R_2 & I_n \\ I_3 & L_{j+2} \end{bmatrix}^{-1} \begin{bmatrix} O_{n \times 3} \\ I_3 \end{bmatrix} \\ \begin{bmatrix} U_{23} \\ U_{53} \end{bmatrix} &= \begin{bmatrix} -R_2 & I_n \\ I_3 & L_{j+2} \end{bmatrix}^{-1} \begin{bmatrix} O_{n \times 3} \\ K'^{-1} \end{bmatrix}, \quad \begin{bmatrix} U_{24} \\ U_{54} \end{bmatrix} = \begin{bmatrix} -R_2 & I_n \\ I_3 & L_{j+2} \end{bmatrix}^{-1} \begin{bmatrix} -R_1 K^{-1} \\ O_{3 \times 3} \end{bmatrix} \\ \begin{bmatrix} U_{25} \\ U_{55} \end{bmatrix} &= \begin{bmatrix} -R_2 & I_n \\ I_3 & L_{j+2} \end{bmatrix}^{-1} \begin{bmatrix} O_{n \times n} \\ L_j \end{bmatrix}, \quad \begin{bmatrix} U_{26} \\ U_{56} \end{bmatrix} = \begin{bmatrix} -R_2 & I_n \\ I_3 & L_{j+2} \end{bmatrix}^{-1} \begin{bmatrix} R_5 \\ O_{3 \times 1} \end{bmatrix} \\ U_{14} = -K^{-1}, \quad R_1 &= \begin{bmatrix} P_{11} \\ P_{12} \\ \vdots \\ P_{1n} \end{bmatrix}, \quad R_2 = \begin{bmatrix} P_{21} \\ P_{22} \\ \vdots \\ P_{2n} \end{bmatrix}, \quad R_5 = \begin{bmatrix} P_{51} \\ P_{52} \\ \vdots \\ P_{5n} \end{bmatrix}, \quad H_i = \begin{bmatrix} 1 & 0 & -s_y \\ 0 & c_x & c_y \\ 0 & -s_x & c_x c_y \end{bmatrix}_i \quad (i = j, j+2) \\ L_{j+2} &= H_{j+2}^{-1} \begin{bmatrix} 0 & 0 & \dots & 0 \\ -\frac{dZ_{j+2}^1(0)}{dx_2} & -\frac{dZ_{j+2}^2(0)}{dx_2} & \dots & -\frac{dZ_{j+2}^n(0)}{dx_2} \\ \frac{dY_{j+2}^1(0)}{dx_2} & \frac{dY_{j+2}^2(0)}{dx_2} & \dots & \frac{dY_{j+2}^n(0)}{dx_2} \end{bmatrix}, \\ L_j &= H_j^{-1} \begin{bmatrix} 0 & 0 & \dots & 0 \\ -\frac{dZ_j^1(l_j)}{dx_2} & -\frac{dZ_j^2(l_j)}{dx_2} & \dots & -\frac{dZ_j^n(l_j)}{dx_2} \\ \frac{dY_j^1(l_j)}{dx_2} & \frac{dY_j^2(l_j)}{dx_2} & \dots & \frac{dY_j^n(l_j)}{dx_2} \end{bmatrix} \\ K' &= \begin{bmatrix} K'_x & 0 & 0 \\ 0 & K'_y & 0 \\ 0 & 0 & K'_z \end{bmatrix}, \quad K = \begin{bmatrix} K_x & 0 & 0 \\ 0 & K_y & 0 \\ 0 & 0 & K_z \end{bmatrix} \end{aligned}$$

$P_{ij} (i = 1, 2, 5 \ j = 1, 2, \dots, n)$ have the same meaning as in Equation (8.191). K' is the torsional stiffness of the rotary springs, K is the stiffness of the springs, and K_x, K_y and K_z and

K'_x , K'_y and K'_z are the stiffness coefficients of the linear springs and the torsional stiffness coefficients of the rotary springs, respectively.

15.29.2 Elastic Hinge whose Inboard Body is a Rigid Body and whose Outboard Body is a Euler–Bernoulli Beam Moving in Space

The state vectors are

$$\begin{aligned} \mathbf{z}_I &= [x, y, z, \theta_x, \theta_y, \theta_z, m_x, m_y, m_z, q_x, q_y, q_z, 1]^T \\ \mathbf{z}_O &= [x, y, z, \theta_x, \theta_y, \theta_z, m_x, m_y, m_z, q_x, q_y, q_z, q^1, q^2, \dots, q^n, 1]^T \end{aligned} \quad (15.195)$$

The transfer equation is

$$\mathbf{z}_O = \mathbf{U} \mathbf{z}_I \quad (15.196)$$

The transfer matrix is

$$\mathbf{U} = \begin{bmatrix} \mathbf{I}_3 & \mathbf{O}_{3 \times 3} & \mathbf{O}_{3 \times 3} & \mathbf{U}_{14} & \mathbf{O}_{3 \times 1} \\ \mathbf{U}_{21} & \mathbf{U}_{22} & \mathbf{U}_{23} & \mathbf{U}_{24} & \mathbf{U}_{26} \\ \mathbf{O}_{3 \times 3} & \mathbf{O}_{3 \times 3} & \mathbf{I}_3 & \mathbf{O}_{3 \times 3} & \mathbf{O}_{3 \times 1} \\ \mathbf{O}_{3 \times 3} & \mathbf{O}_{3 \times 3} & \mathbf{O}_{3 \times 3} & \mathbf{I}_3 & \mathbf{O}_{3 \times 1} \\ \mathbf{U}_{51} & \mathbf{U}_{52} & \mathbf{U}_{53} & \mathbf{U}_{54} & \mathbf{U}_{56} \\ \mathbf{O}_{1 \times 3} & \mathbf{O}_{1 \times 3} & \mathbf{O}_{1 \times 3} & \mathbf{O}_{1 \times 3} & 1 \end{bmatrix} \quad (15.197)$$

where the meanings of all the elements are the same as in Equation (15.194).

15.29.3 Elastic Hinge whose Inboard Body is a Euler–Bernoulli Beam and whose Outboard Body is a Rigid Body Moving in Space

The state vectors are

$$\begin{aligned} \mathbf{z}_I &= [x, y, z, \theta_x, \theta_y, \theta_z, m_x, m_y, m_z, q_x, q_y, q_z, q^1, q^2, \dots, q^n, 1]^T \\ \mathbf{z}_O &= [x, y, z, \theta_x, \theta_y, \theta_z, m_x, m_y, m_z, q_x, q_y, q_z, 1]^T \end{aligned} \quad (15.198)$$

The transfer equation is

$$\mathbf{z}_O = \mathbf{U} \mathbf{z}_I \quad (15.199)$$

The transfer matrix is

$$\mathbf{U} = \begin{bmatrix} \mathbf{I}_3 & \mathbf{O}_{3 \times 3} & \mathbf{O}_{3 \times 3} & \mathbf{U}_{14} & \mathbf{O}_{3 \times n} & \mathbf{O}_{3 \times 1} \\ \mathbf{O}_{3 \times 3} & \mathbf{I}_3 & \mathbf{K}'^{-1} & \mathbf{O}_{3 \times 3} & \mathbf{L}_j & \mathbf{O}_{3 \times 1} \\ \mathbf{O}_{3 \times 3} & \mathbf{O}_{3 \times 3} & \mathbf{I}_3 & \mathbf{O}_{3 \times 3} & \mathbf{O}_{3 \times n} & \mathbf{O}_{3 \times 1} \\ \mathbf{O}_{3 \times 3} & \mathbf{O}_{3 \times 3} & \mathbf{O}_{3 \times 3} & \mathbf{I}_3 & \mathbf{O}_{3 \times n} & \mathbf{O}_{3 \times 1} \\ \mathbf{O}_{1 \times 3} & \mathbf{O}_{1 \times 3} & \mathbf{O}_{1 \times 3} & \mathbf{O}_{1 \times 3} & \mathbf{O}_{1 \times n} & 1 \end{bmatrix} \quad (15.200)$$

where the meaning of \mathbf{U}_{14} is the same as in Equation (9.227) and the meanings of \mathbf{K}'^{-1} and \mathbf{L}_j are the same as in Equation (9.223).

15.30 Controlled Elements of a Linear System

15.30.1 Vibration System under Real-time Control

The controlled vibration system is shown in Figure 15.15. The system is mounted on the lumped mass k , where the controlled force acting on the displacement, velocity and acceleration of lumped mass k is

$$F_{p,c} = -K_a \ddot{x}_{k,k-1} - K_v \dot{x}_{k,k-1} - K_d x_{k,k-1} \quad (15.201)$$

The transfer equation of the lumped mass k under real-time control can be obtained as

$$\hat{\mathbf{Z}}_{p,p+1} = \hat{\mathbf{U}}_p \hat{\mathbf{Z}}_{p,p-1} + \hat{\mathbf{U}}_{p,c} \hat{\mathbf{Z}}_{k,k-1} \quad (15.202)$$

where

$$\hat{\mathbf{Z}} = \begin{bmatrix} \bar{X} \\ \bar{Q}_x \\ 1 \end{bmatrix}, \quad \hat{\mathbf{U}}_p = \begin{bmatrix} 1 & 0 & 0 \\ m_p \Omega^2 & 1 & \bar{F}_p \\ 0 & 0 & 1 \end{bmatrix}, \quad \hat{\mathbf{U}}_{p,c} = \begin{bmatrix} 0 & 0 & 0 \\ K_a \Omega^2 - iK_v \Omega - K_d & 0 & 0 \\ 0 & 0 & 0 \end{bmatrix} \quad (15.203)$$

m_p is the mass of the lumped mass p . F_p is a simple harmonic external force acting on the lumped mass p with frequency Ω .

15.30.2 Controlled Branched System

A controlled branched system is shown in Figure 9.32. The state vectors of each connection point are

$$\mathbf{Z}_{0,1} = [X_{0,1}, Y_{0,1}, Z_{0,1}, Q_{x0,1}, Q_{y0,1}, Q_{z0,1}]^T \quad (15.204)$$

$$\mathbf{Z}_{5,6} = [X_{5,6}, Y_{5,6}, Z_{5,6}, \Theta_{x5}, \Theta_{y5}, \Theta_{z5}, M_{x5,6}, M_{y5,6}, M_{z5,6}, Q_{x5,6}, Q_{y5,6}, Q_{z5,6}]^T \quad (15.205)$$

$$\mathbf{Z}_{9,0} = [\Theta_9, M_9]^T \quad (15.206)$$

$\mathbf{Z}_{0,2}, \mathbf{Z}_{0,3}, \mathbf{Z}_{0,4}, \mathbf{Z}_{5,1}, \mathbf{Z}_{5,2}, \mathbf{Z}_{5,3}$ and $\mathbf{Z}_{5,4}$ have the same form as $\mathbf{Z}_{0,1}$, $\mathbf{Z}_{5,7}$ and $\mathbf{Z}_{5,8}$ have the same form as $\mathbf{Z}_{5,6}$, and $\mathbf{Z}_{10,0}, \mathbf{Z}_{11,0}, \mathbf{Z}_{9,6}, \mathbf{Z}_{10,7}$ and $\mathbf{Z}_{11,8}$ have the same form as $\mathbf{Z}_{9,0}$.

$$\mathbf{Z}_{0,1 \sim 4} = [X_{0,1}, Y_{0,1}, Z_{0,1}, Q_{x0,1}, Q_{y0,1}, Q_{z0,1}, \dots, Q_{x0,4}, Q_{y0,4}, Q_{z0,4}]^T \quad (15.207)$$

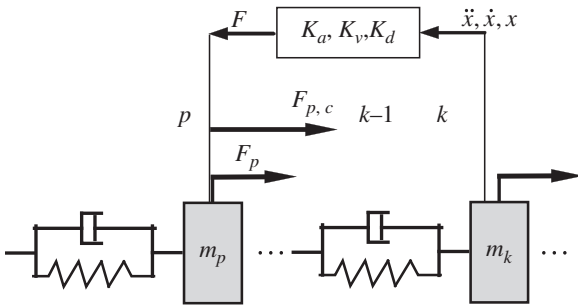


Figure 15.15 Vibration system under real-time control.

$$\mathbf{Z}_{5,6\sim 8} = [X_{5,6}, Y_{5,6}, Z_{5,6}, \boldsymbol{\theta}_{x5}, \boldsymbol{\theta}_{y5}, \boldsymbol{\theta}_{z5}, M_{x5,6}, M_{y5,6}, M_{z5,6}, \dots, Q_{x5,8}, Q_{y5,8}, Q_{z5,8}]^T \quad (15.208)$$

The overall transfer equation is

$$\mathbf{U}_{\text{all}} \mathbf{Z}_{\text{all}} = \mathbf{0} \quad (15.209)$$

The state vector is

$$\mathbf{Z}_{\text{all}} = [\mathbf{Z}_{0,1\sim 4}^T, \mathbf{Z}_{5,6\sim 8}^T, \mathbf{Z}_{9,0}^T, \mathbf{Z}_{10,0}^T, \mathbf{Z}_{11,0}^T]^T$$

The transfer matrix is

$$\mathbf{U}_{\text{all}} = \begin{bmatrix} \mathbf{U}_{11} & \mathbf{U}_{12} & \mathbf{0} & \mathbf{0} & \mathbf{0} \\ \mathbf{U}_{21} & \mathbf{U}_{22} & \mathbf{0} & \mathbf{0} & \mathbf{0} \\ \mathbf{0} & \mathbf{u}_6^{(1)} & -\mathbf{u}_6^{(2)} \mathbf{u}_9 & \mathbf{0} & \mathbf{0} \\ \mathbf{0} & \mathbf{u}_7^{(1)} & \mathbf{0} & -\mathbf{u}_7^{(2)} \mathbf{u}_{10} & \mathbf{0} \\ \mathbf{0} & \mathbf{u}_8^{(1)} & \mathbf{0} & \mathbf{0} & -\mathbf{u}_8^{(2)} \mathbf{u}_{11} \end{bmatrix} \quad (15.210)$$

where

$$\mathbf{U}_{11} = \mathbf{u}_{1\sim 4}^{(1)} \mathbf{u}_{1\sim 4} - \mathbf{u}_{1\sim 4}^{(2)}, \mathbf{U}_{12} = \mathbf{u}_{1\sim 4}^{(1)} \mathbf{U}_C, \mathbf{U}_{21} = -\mathbf{u}_{5,6\sim 8}^{(2)} \mathbf{u}_{1\sim 4}, \mathbf{U}_{22} = \mathbf{u}_{5,6\sim 8}^{(1)} - \mathbf{u}_{5,6\sim 8}^{(2)} \mathbf{U}_C$$

15.31 Controlled Elements of a General Time-variable System

15.31.1 Vibration System under Real-time Control

For the controlled vibration system shown in Figure 15.15, linearizing Equation (15.201) yields

$$F_{p,c} = -(K_a A + K_v C + K_d) x_{k,k-1} - K_a B_{x_{k,k-1}} - K_v D_{x_{k,k-1}} \quad (15.211)$$

The transfer equation of the controlled lumped mass p is

$$\mathbf{z}_{p,p+1} = \mathbf{U}_p \mathbf{z}_{p,p-1} + \mathbf{U}_{p,c} \mathbf{z}_{k,k-1} \quad (15.212)$$

where

$$\mathbf{z} = [x, q, 1]^T \quad (15.213)$$

$$\mathbf{U}_p = \begin{bmatrix} 1 & 0 & 0 \\ -m_p A & 1 & m_p B + F_p \\ 0 & 0 & 1 \end{bmatrix}, \quad \mathbf{U}_{p,c} = \begin{bmatrix} 0 & 0 & 0 \\ -(K_a A + K_v C + K_d) & 0 & -K_a B_{x_{k,k-1}} - K_v D_{x_{k,k-1}} \\ 0 & 0 & 0 \end{bmatrix} \quad (15.214)$$

m_p is the mass of the lumped mass p . F_p is the external force acting on the lumped mass p .

For the delay controlled system, the control force can be seen as an external force related to the previous time motion state. By adding the control force into the external force submatrix of the corresponding transfer matrix, the controlled system can be considered as a system

without control. The control force $F_{p,c}$ in Equation (15.201) is a function of the motion quantities $x_{k,k+1}$, $\dot{x}_{k,k+1}$ and $\ddot{x}_{k,k+1}$:

$$F_{p,c} = -K_a \ddot{x}_{k,k-1}(t-\tau) - K_v \dot{x}_{k,k-1}(t-\tau) - K_d x_{k,k-1}(t-\tau) \quad (15.215)$$

where τ is the delay time. Adding the control force $F_{p,c}$ into the element u_{23} of the transfer matrix of the element p , we obtain

$$\mathbf{U}_{p,c} = \begin{bmatrix} 0 & 0 & 0 \\ 0 & 0 & -K_a \ddot{x}_{k,k-1} - K_v \dot{x}_{k,k-1} - K_d x_{k,k-1} \\ 0 & 0 & 0 \end{bmatrix} \quad (15.216)$$

15.31.2 Controlled Flexible Manipulator System

The controlled planar flexible manipulator system assembled by hub 1 and flexible arm 3, featuring surface-bonded piezoceramics and piezofilms, is shown in Figure 9.42a. $m_1, r_1, J_{c1}, \theta_1^d(t)$ and $\dot{\theta}_1^d$ are the mass, gyration radius, moment of inertia, desired orientation angle and desired orientation angular velocity of the hub 1, respectively. θ_1 and $\dot{\theta}_1$ are the actual orientation angle and actual angular velocity, respectively. EL_3, A_3, l_3, b and t_b are the bending stiffness, cross-section area, length, width and thickness of flexible arm 3, respectively. E_a, l_a, t_a and d_{31} are the piezoelectric elastic modulus, length, thickness and strain constant of the segmented piezoelectric ceramic (PZT) actuator. K_p and K_v are the proportional gain coefficient and velocity gain coefficient of the servomotors, respectively. $\tau_0(t)$ is the control torque of the motor, K_{ai} is the gain coefficient of the segmented PZT actuator, V_i is the driven voltage applied to segmented PZT actuator i and u is the deformation of the flexible arm. $Y^k(x_2)$ is the k th generalized eigenvector describing the deformation of the flexible arm. ${}^1s_k = \partial Y^k(x_2)/\partial x_2$, $(x_{i,1}^a, x_{i,2}^a)$ is the position of each piezofilm sensor/PZT on the corresponding flexible arm in the body-fixed reference frames. Adopting the proportional-differential (PD) controller and modal velocity feedback control on the PZT actuators, the transfer matrices of the rigid body and beam under control are derived as follows.

Considering only the control moment related to its feedback state, the transfer matrix of the rigid body under control can be obtained as

$$\mathbf{U} = \begin{bmatrix} 1 & 0 & -y_{IO}(t_{i-1}) & 0 & 0 & 0 & b_1 G_1 - b_2 G_2 \\ 0 & 1 & x_{IO}(t_{i-1}) & 0 & 0 & 0 & b_1 G_2 + b_2 G_1 \\ 0 & 0 & 1 & 0 & 0 & 0 & 0 \\ u_{41} & u_{42} & u_{43} & 1 & u_{45} & u_{46} & u_{47} \\ -mA & 0 & mA y_{IC}(t_{i-1}) & 0 & 1 & 0 & u_{57} \\ 0 & -mA & -mA x_{IC}(t_{i-1}) & 0 & 0 & 1 & u_{67} \\ 0 & 0 & 0 & 0 & 0 & 0 & 1 \end{bmatrix} \quad (15.217)$$

where

$$\begin{aligned} u_{43} &= -mA x_{IC}(t_{i-1}) x_{IO} - mA y_{IC}(t_{i-1}) y_{IO} + J_1 A + K_p + K_v C, \\ u_{47} &= -m_C + u_{67} x_{IO} - u_{57} y_{IO} + J_1 B_\theta + (m B_{y_i} - f_{y,C}) x_{IC} + (f_{x,C} - m B_{x_i}) y_{IC} \\ &\quad - K_p \theta_1^d(t) - K_v \dot{\theta}_1^d(t) + K_v D_\theta \end{aligned}$$

The meanings of $u_{41}, u_{42}, u_{45}, u_{46}, u_{57}$ and u_{67} are the same as in Equation (7.101).

Considering the control moment of the PZT actuators, the transfer matrix of the beam under control is

$$U = \begin{bmatrix} 1 & 0 & u_{1,3} & 0 & 0 & 0 & u_{1,6+1} & \cdots & u_{1,6+n} & u_{1,6+n+1} \\ 0 & 1 & u_{2,3} & 0 & 0 & 0 & u_{2,6+1} & \cdots & u_{2,6+n} & u_{2,6+n+1} \\ 0 & 0 & 1 & 0 & 0 & 0 & 0 & \ddots & 0 & 0 \\ u_{4,1} & u_{4,2} & u_{4,3} & 1 & u_{4,5} & u_{4,6} & u_{4,6+1} & \cdots & u_{4,6+n} & u_{4,6+n+1} \\ u_{5,1} & 0 & u_{5,3} & 0 & 1 & 0 & u_{5,6+1} & \cdots & u_{5,6+n} & u_{5,6+n+1} \\ 0 & u_{6,2} & u_{6,3} & 0 & 0 & 1 & u_{6,6+1} & \cdots & u_{6,6+n} & u_{6,6+n+1} \\ 0 & 0 & 0 & 0 & 0 & 0 & 1 & \cdots & 0 & 0 \\ \vdots & \vdots & \vdots & \vdots & \vdots & \vdots & \vdots & \ddots & \vdots & \vdots \\ 0 & 0 & 0 & 0 & 0 & 0 & 0 & \cdots & 1 & 0 \\ 0 & 0 & 0 & 0 & 0 & 0 & 0 & \cdots & 0 & 1 \end{bmatrix} \quad (15.218)$$

Where

$$\begin{aligned} u_{1,3} &= -l_3 s - c \sum_{k=1}^n Y_O^k q_{t_{i-1}}^k, u_{1,6+k} = -s Y_O^k (k=1, \cdots, n), u_{1,6+n+1} = l_3(c + \theta s) + c \sum_{k=1}^n Y_O^k q_{t_{i-1}}^k \theta_{t_{i-1}} \\ u_{2,3} &= l_3 c - s \sum_{k=1}^n Y_O^k q_{t_{i-1}}^k, u_{2,6+k} = c Y_O^k (k=1, \cdots, n), u_{2,6+n+1} = l_3(s - \theta c) + s \sum_{k=1}^n Y_O^k q_{t_{i-1}}^k \theta_{t_{i-1}} \\ u_{4,j} &= l_3 \zeta_{1,j} + \xi_j \quad (j=1, 2, 3), u_{4,5} = -l_3 \bar{s}, u_{4,6} = l_3 \bar{c} \\ u_{4,6+k} &= \xi_{6+k} - \sum_{i=1}^3 c_a K_{ai} l_{ai}^{-1} s_k \Big|_{x_{i,1}^a}^{x_{i,2}^a} C + l_3 \zeta_{1,6+k} \quad (k=1, \cdots, n) \\ u_{4,6+n+1} &= l_3 \zeta_{1,6+n+1} + \xi_{6+n+1} - \int_0^{l_3} x_2 f_{2,y}(x_2, t) dx_2 - \int_0^{l_3} m'(x_2, t) dx_2 \\ &\quad + \sum_{k=1}^n \sum_{i=1}^3 c_a K_{ai} l_{ai}^{-1} s_k \Big|_{x_{i,1}^a}^{x_{i,2}^a} D q^k \\ u_{5,1} &= -m A, u_{5,j} = \bar{c} \zeta_{2,j} - \bar{s} \zeta_{1,j} \quad (j=3, 6+1, \cdots, 6+n+1) \\ u_{6,2} &= -m A, u_{6,j} = \bar{s} \zeta_{2,j} + \bar{c} \zeta_{1,j} \quad (j=3, 6+1, \cdots, 6+n+1) \\ \xi_1 &= - \left(m \bar{c} \sum_{k=1}^n s_k^0 q_{t_{i-1}}^k + \frac{l_3}{2} m \bar{s} \right) A, \xi_2 = \left(\frac{l_3}{2} m \bar{c} - \bar{m} \bar{s} \sum_{k=1}^n s_k^0 q_{t_{i-1}}^k \right) A \\ \xi_3 &= \bar{m} \sum_{k=1}^n \sum_{j=1}^n s_{k,j}^0 [2C q^k(t_{i-1}) \dot{q}^j(t_{i-1}) + A q^k(t_{i-1}) q^j(t_{i-1})] + m \frac{l_3^2}{3} A \\ \xi_{6+k} &= \bar{m} \sum_{j=1}^n s_{k,j}^0 \left(2\dot{\theta}_{t_{i-1}} \dot{q}_{t_{i-1}}^j + 2C \dot{\theta}_{t_{i-1}} q_{t_{i-1}}^j + 2\ddot{\theta}_{t_{i-1}} q_{t_{i-1}}^j \right) + \bar{m} \sum_{k=1}^n s_k^1 A - \bar{m} (\bar{s} s_k^0 \ddot{y}_{O_2, t_{i-1}} + \bar{c} s_k^0 \ddot{x}_{O_2, t_{i-1}}) \\ \xi_{6+n+1} &= 2\bar{m} \sum_{k=1}^n \sum_{j=1}^n s_{k,j}^0 \left[D \theta q_{t_{i-1}}^k \dot{q}_{t_{i-1}}^j + \dot{\theta}_{t_{i-1}} q_{t_{i-1}}^k D q^j - 2\dot{\theta}(t_{i-1}) q_{t_{i-1}}^k q_{t_{i-1}}^j \right] + \bar{m} \sum_{k=1}^n s_k^1 B_{q^k} \\ &\quad + \bar{m} \sum_{k=1}^n \sum_{j=1}^n s_{k,j}^0 \left[B_{\theta} q_{t_{i-1}}^k \dot{q}_{t_{i-1}}^j - 2\ddot{\theta}(t_{i-1}) q_{t_{i-1}}^k q_{t_{i-1}}^j \right] + \frac{l_3}{2} m \left(\bar{c} B_{y_{O_2}} - \bar{s} B_{x_{O_2}} \right) + m \frac{l_3^2}{3} B_{\theta} \\ &\quad - \bar{m} \sum_{k=1}^n s_k^0 \left[\bar{s} \left(q_{t_{i-1}}^k B_{y_{O_2}} - q_{t_{i-1}}^k \ddot{y}_{O_2, t_{i-1}} \right) + \bar{c} \left(q_{t_{i-1}}^k B_{x_{O_2}} - q_{t_{i-1}}^k \ddot{x}_{O_2, t_{i-1}} \right) \right] \end{aligned}$$

$$\begin{aligned}
\zeta_{1,1} &= m\bar{s}A, \zeta_{1,2} = -m\bar{c}A, \zeta_{1,3} = 2\bar{m}C\dot{\theta}_{t_{i-1}} \sum_{k=1}^n s_k^0 q_{t_{i-1}}^k - \frac{ml_3}{2}A, \zeta_{1,6+k} = \bar{m}(\dot{\theta}_{t_{i-1}}^2 - A)s_k^0 \\
\zeta_{1,6+n+1} &= \int_0^{l_3} f_{2,y}(x_2, t)dx_2 + m\bar{s}B_{x_{O_2}} - m\bar{c}B_{y_{O_2}} - \frac{ml_3}{2}B_\theta + 2\bar{m}D_\theta\dot{\theta}_{t_{i-1}} \sum_{k=1}^n s_k^0 q_{t_{i-1}}^k \\
&\quad - 2\bar{m}\dot{\theta}_{t_{i-1}}^2 \sum_{k=1}^n s_k^0 q_{t_{i-1}}^k - \bar{m} \sum_{k=1}^n s_k^0 B_{q^k} + \bar{m} \sum_{k=1}^n s_k^0 [\ddot{\theta}_{t_{i-1}}^2 q_{t_{i-1}}^k + 2\dot{\theta}_{t_{i-1}}\ddot{\theta}_{t_{i-1}}\dot{q}_{t_{i-1}}^k] \Delta T^2 \\
\zeta_{2,1} &= -m\bar{c}A, \zeta_{2,2} = -m\bar{s}A, \zeta_{2,3} = \bar{m} \left(l_3^2 C\dot{\theta}_{t_{i-1}} + A \sum_{k=1}^n s_k^0 q_{t_{i-1}}^k + 2C \sum_{k=1}^n s_k^0 \dot{q}_{t_{i-1}}^k \right) \\
\zeta_{2,6+k} &= \bar{m}(2\dot{\theta}_{t_{i-1}}C + \ddot{\theta}_{t_{i-1}})s_k^0, (k=1, 2, \dots, n) \\
\zeta_{2,6+n+1} &= \int_0^{l_3} f_{2,x}(x_2, t)dx_2 + 2\bar{m}\dot{\theta}_{t_{i-1}} \sum_{k=1}^n s_k^0 D_{q^k} + 2\bar{m}D_\theta \sum_{k=1}^n s_k^0 \dot{q}_{t_{i-1}}^k - 2\bar{m}\dot{\theta}_{t_{i-1}} \sum_{k=1}^n s_k^0 \dot{q}_{t_{i-1}}^k \\
&\quad + \bar{m}B_\theta \sum_{k=1}^n s_k^0 q_{t_{i-1}}^k - \bar{m}\ddot{\theta}_{t_{i-1}} \sum_{k=1}^n s_k^0 q_{t_{i-1}}^k + \frac{ml_3}{2} \left(2D_\theta\dot{\theta}_{t_{i-1}} - \dot{\theta}_{t_{i-1}}^2 + \ddot{\theta}_{t_{i-1}}^2 \Delta T^2 \right) \\
&\quad - m\bar{s}B_{y_{O_2}} - m\bar{c}B_{x_{O_2}} + 2\bar{m}\ddot{\theta}_{t_{i-1}} \Delta T^2 \sum_{k=1}^n s_k^0 \ddot{q}_{t_{i-1}}^k \\
Y_O^k &= Y^k(l_3), s_k^0 = \int_0^{l_3} Y^k(x_2)dx_2, s_{k,k}^0 = \int_0^{l_3} Y^k(x_2)Y^k(x_2)dx_2, s_k^1 = \int_0^{l_3} Y^k(x_2)x_2dx_2 \\
c_a &= \frac{1}{2}d_{31}E_ab(t_a + 2t_b), H(x) = \begin{cases} 1 & x \geq 0 \\ 0 & x < 0 \end{cases}, m = \bar{m}l_3
\end{aligned} \tag{15.219}$$

Considering the distributed moment of the PZT actuators, combining the control equation of PZT actuators and the numerical integration procedure, if the highest order of the modes considered is $n=3$, then the state vectors of the fixed hinge connected to the beam under control can be defined as

$$\begin{cases} \mathbf{z}_O = [x, y, \theta, m, q_x, q_y, q^1, q^2, q^3, 1]^T \\ \mathbf{z}_I = [x, y, \theta, m, q_x, q_y, 1]^T \end{cases} \tag{15.220}$$

The transfer equation is

$$\mathbf{z}_O = \mathbf{U}\mathbf{z}_I \tag{15.221}$$

The transfer matrix is

$$\mathbf{U} = \begin{bmatrix} 1 & 0 & 0 & 0 & 0 & 0 & 0 \\ 0 & 1 & 0 & 0 & 0 & 0 & 0 \\ 0 & 0 & 1 & 0 & 0 & 0 & 0 \\ 0 & 0 & 0 & 1 & 0 & 0 & 0 \\ 0 & 0 & 0 & 0 & 1 & 0 & 0 \\ 0 & 0 & 0 & 0 & 0 & 1 & 0 \\ \Delta_{11}/\Delta & \Delta_{12}/\Delta & \Delta_{13}/\Delta & 0 & 0 & 0 & \Delta_{14}/\Delta \\ \Delta_{21}/\Delta & \Delta_{22}/\Delta & \Delta_{23}/\Delta & 0 & 0 & 0 & \Delta_{24}/\Delta \\ \Delta_{31}/\Delta & \Delta_{32}/\Delta & \Delta_{33}/\Delta & 0 & 0 & 0 & \Delta_{34}/\Delta \\ 0 & 0 & 0 & 0 & 0 & 0 & 1 \end{bmatrix} \tag{15.222}$$

where

$$\Delta = \begin{bmatrix} A_{11} & A_{12} & A_{13} \\ A_{21} & A_{22} & A_{23} \\ A_{31} & A_{32} & A_{33} \end{bmatrix}, \quad \Delta_{1i} = \begin{bmatrix} B_{1i} & A_{12} & A_{13} \\ B_{2i} & A_{22} & A_{23} \\ B_{3i} & A_{32} & A_{33} \end{bmatrix}, \quad \Delta_{2i} = \begin{bmatrix} A_{11} & B_{1i} & A_{13} \\ A_{21} & B_{2i} & A_{23} \\ A_{31} & B_{3i} & A_{33} \end{bmatrix},$$

$$\Delta_{3i} = \begin{bmatrix} A_{11} & A_{12} & B_{1i} \\ A_{21} & A_{22} & B_{2i} \\ A_{31} & A_{32} & B_{3i} \end{bmatrix} \quad (i = 1, 2, 3, 4)$$

$$A_{k',k} = -\bar{m}s_{k,k'}\dot{\theta}_{t_{i-1}}^2 - \sum_{i=1}^M c_a K_{ai} \int_{x_{1,i}^a}^{x_{2,i}^a} Y^{k'}(x_2) dx_2^1 s_k \Big|_{x_{1,i}^a}^{x_{2,i}^a} C \quad (k = 1, 2, 3, \quad k' \neq k)$$

$$A_{k',k'} = {}^4s_{k,k'}EI - {}^2s_{k,k'}\rho IA + \bar{m}s_{k,k'}A - \bar{m}s_{k,k'}\dot{\theta}_{t_{i-1}}^2 - \sum_{i=1}^M c_a K_{ai} \int_{x_{1,i}^a}^{x_{2,i}^a} Y^{k'}(x_2) dx_2^1 s_k \Big|_{x_{1,i}^a}^{x_{2,i}^a} C$$

$$B_{k',1} = \bar{m}\bar{s}s_{k',1}^0 A, B_{k',2} = -\bar{m}\bar{c}s_{k',2}^0 A, B_{k',3} = -\bar{m} \left(s_{k',3}^1 A - 2Cs_{k',k'}q_{t_{i-1}}^k \dot{\theta}_{t_{i-1}} \right)$$

$$B_{k',5+n} = \int_0^{l_3} Y^{k'}(x_2) f(x_2, t) dx_2 - \int_0^{l_3} Y^{k'}(x_2) \frac{\partial}{\partial x_2} m'(x_2, t) dx_2 + \rho l^2 s_{k',k'} B_{q^{k'}} \\ - \bar{m} \left\{ s_{k',k'} B_{q^{k'}} - s_{k',k'} \left[2q_{t_{i-1}}^{k'} \dot{\theta}_{t_{i-1}} D_\theta - 2q^{k'}(t_{i-1}) \dot{\theta}_{t_{i-1}}^2 \right] + s_{k',k'}^1 B_\theta + \bar{c}s_{k',k'}^0 B_{y_{O_2}} - \bar{s}s_{k',k'}^0 B_{x_{O_2}} \right\} \\ (k' = 1, 2, 3)$$

Adopting the PD controller and modal velocity feedback control on the PZT actuators, the transfer matrix $\mathbf{U}_{1'}$ of the equivalent control element is

$$\mathbf{U}_{1'} = (\mathbf{I} - \mathbf{U}_1^3 \mathbf{U}_2)^{-1} \quad (15.223)$$

where \mathbf{U}_1^3 is the feedback parameter matrix related to the feedback from beam 3 to hub 1. For the modal velocity feedback control, that is

$$\mathbf{U}_1^3 = - \sum_{i=1}^M c_a K_{ai} \begin{bmatrix} \mathbf{O}_{3 \times 6} & \mathbf{O}_{3 \times n} & 0 \\ \mathbf{O}_{1 \times 6} & C^1 s_1 \Big|_{x_{i,1}^a}^{x_{i,2}^a} \dots C^1 s_n \Big|_{x_{i,1}^a}^{x_{i,2}^a} \sum_{k=1}^n D_{q^k}^1 s_k \Big|_{x_{i,1}^a}^{x_{i,2}^a} \\ \mathbf{O}_{3 \times 6} & \mathbf{O}_{3 \times n} & 0 \end{bmatrix} \quad (15.224)$$

Appendix I

Rotation Formula Around an Axis

Consider that A is a right-handed inertia coordinate system with unit orthogonal bases \mathbf{i}, \mathbf{j} and \mathbf{k} , and B is a right-handed body-fixed coordinate system with unit orthogonal bases $\mathbf{i}_1, \mathbf{j}_1$ and \mathbf{k}_1 . \mathbf{a} is any vector fixed in A and \mathbf{b} is a vector fixed in B and equal to \mathbf{a} prior to the motion of B in A . λ is a unit vector whose orientation relative to both A and B remains unaltered throughout the motion, and the radian measure θ is the angle when B rotates relative to A . Let $\mathbf{EF} = \mathbf{a}$ and $\mathbf{GH} = \mathbf{b}$, as shown in Figure AI.1.

The plane π_1 contains point E and is perpendicular to vector λ , and point O_1 is the intersection point of π_1 and the line including λ . The plane π_2 contains point F and is perpendicular to vector λ , and O_2 is the intersection point of π_2 and the line including λ . Then the point G is in π_1 and H is in π_2 :

$$|\mathbf{O}_1\mathbf{E}_1| = |\mathbf{O}_1\mathbf{G}|, \quad \angle \mathbf{EO}_1\mathbf{G} = \theta \quad (\text{A.1})$$

$$|\mathbf{O}_2\mathbf{F}| = |\mathbf{O}_2\mathbf{H}|, \quad \angle \mathbf{FO}_2\mathbf{H} = \theta \quad (\text{A.2})$$

We find a point \mathbf{E}_1 in plane π_1 that makes

$$\mathbf{O}_1\mathbf{E}_1 \perp \mathbf{O}_1\mathbf{E} \quad (\text{A.3})$$

and

$$|\mathbf{O}_1\mathbf{E}_1| = |\mathbf{O}_1\mathbf{E}| \quad (\text{A.4})$$

hold, where the three pairwise perpendicular vectors λ , $\mathbf{O}_1\mathbf{E}_1$ and $\mathbf{O}_1\mathbf{E}$ form a right-handed system.

Then

$$\mathbf{O}_1\mathbf{G} = \mathbf{O}_1\mathbf{E} \cos \theta + \mathbf{O}_1\mathbf{E}_1 \sin \theta = \mathbf{O}_1\mathbf{E} \cos \theta + \lambda \times \mathbf{O}_1\mathbf{E} \sin \theta \quad (\text{A.5})$$

Similarly

$$\mathbf{O}_2\mathbf{H} = \mathbf{O}_2\mathbf{F} \cos \theta + \lambda \times \mathbf{O}_2\mathbf{F} \sin \theta \quad (\text{A.6})$$

Thus, we get

$$\begin{aligned} \mathbf{GH} &= \mathbf{GO}_1 + \mathbf{O}_1\mathbf{O}_2 + \mathbf{O}_2\mathbf{H} \\ &= -\mathbf{O}_1\mathbf{E} \cos \theta - \lambda \times \mathbf{O}_1\mathbf{E} \sin \theta + \mathbf{O}_1\mathbf{O}_2 + \mathbf{O}_2\mathbf{F} \cos \theta + \lambda \times \mathbf{O}_2\mathbf{F} \sin \theta \\ &= (\mathbf{EO}_1 + \mathbf{O}_1\mathbf{O}_2 + \mathbf{O}_2\mathbf{F} - \mathbf{O}_1\mathbf{O}_2) \cos \theta + \lambda \times (\mathbf{EO}_1 + \mathbf{O}_1\mathbf{O}_2 + \mathbf{O}_2\mathbf{F} - \mathbf{O}_1\mathbf{O}_2) \sin \theta + \mathbf{O}_1\mathbf{O}_2 \\ &= \mathbf{a} \cos \theta - \mathbf{O}_1\mathbf{O}_2 \cos \theta + \mathbf{O}_1\mathbf{O}_2 + \lambda \times \mathbf{a} \sin \theta \\ &= \mathbf{a} \cos \theta - \mathbf{a} \times \lambda \sin \theta + \mathbf{O}_1\mathbf{O}_2 (1 - \cos \theta) \end{aligned} \quad (\text{A.7})$$

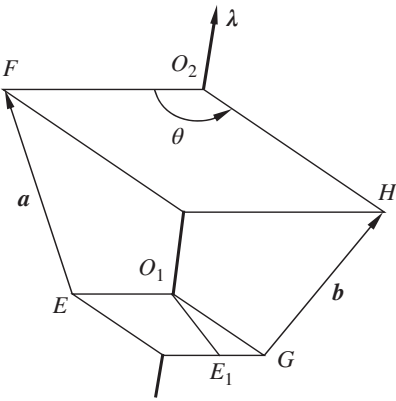


Figure AI.1 A inertia system rotating angle θ around λ .

so

$$\mathbf{b} = \mathbf{a} \cos \theta - \mathbf{a} \times \boldsymbol{\lambda} \sin \theta + (\mathbf{a} \cdot \boldsymbol{\lambda}) \boldsymbol{\lambda} (1 - \cos \theta) \tag{A.8}$$

Appendix II

Orientation of a Body-fixed Coordinate System

The orientation of a body-fixed coordinate system can be obtained by rotating the inertia coordinate system in space three times.

II.1 First Rotation

If the bases before rotation are $(\mathbf{i}, \mathbf{j}, \mathbf{k})$, the bases after rotation are $(\mathbf{i}_1, \mathbf{j}_1, \mathbf{k}_1)$, the rotation axis is \mathbf{i} , and the rotation angle is θ_1 , substituting $\mathbf{b} = \mathbf{i}_1$, $\mathbf{a} = \mathbf{i}$ and $\lambda = \mathbf{i}$ into Equation (A.8) gives

$$\mathbf{i}_1 = \mathbf{i}c_1 - (\mathbf{i} \times \mathbf{i})s_1 + \mathbf{i}(1 - c_1) = \mathbf{i} \quad (\text{A.9})$$

where $c_1 = \cos\theta_1$, $s_1 = \sin\theta_1$, and similarly hereinafter.

Substituting $\mathbf{b} = \mathbf{j}_1$, $\mathbf{a} = \mathbf{j}$ and $\lambda = \mathbf{i}$ into Equation (A.8), we get

$$\mathbf{j}_1 = \mathbf{j}c_1 - (\mathbf{j} \times \mathbf{i})s_1 + (\mathbf{j} \cdot \mathbf{i})\mathbf{i}(1 - c_1) = c_1\mathbf{j} + s_1\mathbf{k} \quad (\text{A.10})$$

Substituting $\mathbf{b} = \mathbf{k}_1$, $\mathbf{a} = \mathbf{k}$, and $\lambda = \mathbf{i}$ into Equation (A.8), we get

$$\mathbf{k}_1 = \mathbf{k}c_1 - (\mathbf{k} \times \mathbf{i})s_1 + (\mathbf{k} \cdot \mathbf{i})\mathbf{i}(1 - c_1) = c_1\mathbf{k} - s_1\mathbf{j} \quad (\text{A.11})$$

So

$$(\mathbf{i} \ \mathbf{j} \ \mathbf{k}) = (\mathbf{i}_1 \ \mathbf{j}_1 \ \mathbf{k}_1) \begin{bmatrix} 1 & 0 & 0 \\ 0 & c_1 & s_1 \\ 0 & -s_1 & c_1 \end{bmatrix} \quad (\text{A.12})$$

$$(\mathbf{i}_1 \ \mathbf{j}_1 \ \mathbf{k}_1) = (\mathbf{i} \ \mathbf{j} \ \mathbf{k}) \begin{bmatrix} 1 & 0 & 0 \\ 0 & c_1 & -s_1 \\ 0 & s_1 & c_1 \end{bmatrix} \quad (\text{A.13})$$

II.2 Second Rotation

The bases before rotation are $(\mathbf{i}_1, \mathbf{j}_1, \mathbf{k}_1)$, the bases after rotation are $(\mathbf{i}_2, \mathbf{j}_2, \mathbf{k}_2)$, the rotation axis is $\mathbf{j} = c_1\mathbf{j}_1 - s_1\mathbf{k}_1 = \lambda$, and the rotation angle is θ_2 . Similar to Equation (A.9), substituting these parameters into Equation (A.8), and considering

$$\begin{vmatrix} \mathbf{i}_1 & \mathbf{j}_1 & \mathbf{k}_1 \\ 1 & 0 & 0 \\ 0 & c_1 & -s_1 \end{vmatrix} = (0 \quad s_1 \quad c_1), \quad \begin{vmatrix} \mathbf{i}_1 & \mathbf{j}_1 & \mathbf{k}_1 \\ 0 & 1 & 0 \\ 0 & c_1 & -s_1 \end{vmatrix} = (-s_1 \quad 0 \quad 0), \quad \begin{vmatrix} \mathbf{i}_1 & \mathbf{j}_1 & \mathbf{k}_1 \\ 0 & 0 & 1 \\ 0 & c_1 & -s_1 \end{vmatrix} = (-c_1 \quad 0 \quad 0)$$

we get

$$\begin{cases} \mathbf{i}_2 = \mathbf{i}_1 c_2 - (\mathbf{i}_1 \times \boldsymbol{\lambda}) s_2 + (\mathbf{i}_1 \cdot \boldsymbol{\lambda}) \boldsymbol{\lambda} (1 - c_2) = \mathbf{i}_1 c_2 - \mathbf{j}_1 s_1 s_2 - \mathbf{k}_1 c_1 s_2 \\ \mathbf{j}_2 = \mathbf{j}_1 c_2 - (\mathbf{j}_1 \times \boldsymbol{\lambda}) s_2 + (\mathbf{j}_1 \cdot \boldsymbol{\lambda}) \boldsymbol{\lambda} (1 - c_2) = \mathbf{i}_1 s_1 s_2 + \mathbf{j}_1 [1 - (1 - c_2) s_1^2] - \mathbf{k}_1 s_1 c_2 (1 - c_2) \\ \mathbf{k}_2 = \mathbf{k}_1 c_2 - (\mathbf{k}_1 \times \boldsymbol{\lambda}) s_2 + (\mathbf{k}_1 \cdot \boldsymbol{\lambda}) \boldsymbol{\lambda} (1 - c_2) = \mathbf{i}_1 c_1 s_2 - \mathbf{j}_1 s_1 c_2 (1 - c_2) + \mathbf{k}_1 [c_2 + (1 - c_2) s_1^2] \end{cases} \quad (\text{A.14})$$

namely

$$\begin{aligned} (\mathbf{i}_2 \quad \mathbf{j}_2 \quad \mathbf{k}_2) &= (\mathbf{i}_1 \quad \mathbf{j}_1 \quad \mathbf{k}_1) \begin{bmatrix} c_2 & s_1 s_2 & c_1 s_2 \\ -s_1 s_2 & 1 - (1 - c_2) s_1^2 & -s_1 c_2 (1 - c_2) \\ -c_1 s_2 & -s_1 c_2 (1 - c_2) & c_2 + (1 - c_2) s_1^2 \end{bmatrix} \\ &= (\mathbf{i} \quad \mathbf{j} \quad \mathbf{k}) \begin{bmatrix} 1 & 0 & 0 \\ 0 & c_1 & -s_1 \\ 0 & s_1 & c_1 \end{bmatrix} \begin{bmatrix} c_2 & s_1 s_2 & c_1 s_2 \\ -s_1 s_2 & c_1^2 + c_2 s_1^2 & -s_1 c_2 (1 - c_2) \\ -c_1 s_2 & -s_1 c_2 (1 - c_2) & c_2 c_1^2 + s_1^2 \end{bmatrix} = (\mathbf{i} \quad \mathbf{j} \quad \mathbf{k}) \begin{bmatrix} c_2 & s_1 s_2 & c_1 s_2 \\ 0 & c_1 & -s_1 \\ -s_2 & s_1 c_2 & c_1 c_2 \end{bmatrix} \end{aligned} \quad (\text{A.15})$$

$$(\mathbf{i} \quad \mathbf{j} \quad \mathbf{k}) = (\mathbf{i}_2 \quad \mathbf{j}_2 \quad \mathbf{k}_2) \begin{bmatrix} c_2 & 0 & -s_2 \\ s_1 s_2 & c_1 & s_1 c_2 \\ c_1 s_2 & -s_1 & c_1 c_2 \end{bmatrix} \quad (\text{A.16})$$

II.3 Third Rotation

The bases before rotation are $(\mathbf{i}_2, \mathbf{j}_2, \mathbf{k}_2)$, the bases after rotation are $(\mathbf{i}_3, \mathbf{j}_3, \mathbf{k}_3)$, the rotation axis is $\mathbf{k} = -s_2 \mathbf{i}_2 + s_1 c_2 \mathbf{j}_2 + c_1 c_2 \mathbf{k}_2 = \boldsymbol{\lambda}$ and the rotation angle is θ_3 . Similar to Equation (A.9), substituting these parameters into Equation (A.8) and considering

$$\begin{aligned} \begin{vmatrix} \mathbf{i}_2 & \mathbf{j}_2 & \mathbf{k}_2 \\ 1 & 0 & 0 \\ -s_2 & s_1 c_2 & c_1 c_2 \end{vmatrix} &= (0 \quad c_1 c_2 \quad s_1 c_2) \\ \begin{vmatrix} \mathbf{i}_2 & \mathbf{j}_2 & \mathbf{k}_2 \\ 0 & 1 & 0 \\ -s_2 & s_1 c_2 & c_1 c_2 \end{vmatrix} &= (c_1 c_2 \quad 0 \quad s_2) \\ \begin{vmatrix} \mathbf{i}_2 & \mathbf{j}_2 & \mathbf{k}_2 \\ 0 & 0 & 1 \\ -s_2 & s_1 c_2 & c_1 c_2 \end{vmatrix} &= (-s_1 c_2 \quad -s_2 \quad 0) \end{aligned}$$

we get

$$\left\{ \begin{array}{l} \mathbf{i}_3 = \mathbf{i}_2 c_3 - (\mathbf{i}_2 \times \boldsymbol{\lambda}) s_3 + (\mathbf{i}_2 \cdot \boldsymbol{\lambda}) \boldsymbol{\lambda} (1 - c_3) \\ \quad = \mathbf{i}_2 (c_3 + s_2^2 - c_3 s_2^2) + \mathbf{j}_2 (c_1 c_2 s_3 - s_1 s_2 c_2 + s_1 s_2 c_2 c_3) + \mathbf{k}_2 (-s_1 c_2 s_3 - c_1 s_2 c_2 + c_1 s_2 c_2 c_3) \\ \mathbf{j}_3 = \mathbf{j}_2 c_3 - (\mathbf{j}_2 \times \boldsymbol{\lambda}) s_3 + (\mathbf{j}_2 \cdot \boldsymbol{\lambda}) \boldsymbol{\lambda} (1 - c_3) \\ \quad = \mathbf{i}_2 (-c_1 c_2 s_3 - s_1 s_2 c_2 + s_1 s_2 c_2 c_3) + \mathbf{j}_2 (c_3 + s_1^2 c_2^2 - s_1^2 c_2^2 c_3) + \mathbf{k}_2 (-s_2 s_3 + s_1 c_1 c_2^2 - s_1 c_1 c_2^2 c_3) \\ \mathbf{k}_3 = \mathbf{k}_2 c_3 - (\mathbf{k}_2 \times \boldsymbol{\lambda}) s_3 + (\mathbf{k}_2 \cdot \boldsymbol{\lambda}) \boldsymbol{\lambda} (1 - c_3) \\ \quad = \mathbf{i}_2 (s_1 c_2 s_3 - c_1 s_2 c_2 + c_1 s_2 c_2 c_3) + \mathbf{j}_2 (s_2 s_3 + s_1 c_1 c_2^2 - s_1 c_1 c_2^2 c_3) + \mathbf{k}_2 (c_3 + c_1^2 c_2^2 - c_1^2 c_2^2 c_3) \end{array} \right. \quad (\text{A.17})$$

namely

$$\begin{aligned} & (\mathbf{i}_3 \ \mathbf{j}_3 \ \mathbf{k}_3) \\ &= (\mathbf{i}_2 \ \mathbf{j}_2 \ \mathbf{k}_2) \begin{bmatrix} c_3 + s_2^2 - c_3 s_2^2 & -c_1 c_2 s_3 - s_1 s_2 c_2 + s_1 s_2 c_2 c_3 & s_1 c_2 s_3 - c_1 s_2 c_2 + c_1 s_2 c_2 c_3 \\ c_1 c_2 s_3 - s_1 s_2 c_2 + s_1 s_2 c_2 c_3 & c_3 + s_1^2 c_2^2 - s_1^2 c_2^2 c_3 & s_2 s_3 + s_1 c_1 c_2^2 - s_1 c_1 c_2^2 c_3 \\ -s_1 c_2 s_3 - c_1 s_2 c_2 + c_1 s_2 c_2 c_3 & -s_2 s_3 + s_1 c_1 c_2^2 - s_1 c_1 c_2^2 c_3 & c_3 + c_1^2 c_2^2 - c_1^2 c_2^2 c_3 \end{bmatrix} \\ &= (\mathbf{i} \ \mathbf{j} \ \mathbf{k}) \begin{bmatrix} c_2 c_3 & s_1 s_2 c_3 - c_1 s_3 & c_1 s_2 c_3 + s_1 s_3 \\ c_2 s_3 & s_1 s_2 s_3 + c_1 c_3 & c_1 s_2 s_3 - s_1 c_3 \\ -s_2 & s_1 c_2 & c_1 c_2 \end{bmatrix} \end{aligned} \quad (\text{A.18})$$

So we get the coordinate transformation matrix from the body-fixed coordinate system to the inertia coordinate system

$$\mathbf{A} = \begin{bmatrix} c_2 c_3 & s_1 s_2 c_3 - c_1 s_3 & c_1 s_2 c_3 + s_1 s_3 \\ c_2 s_3 & s_1 s_2 s_3 + c_1 c_3 & c_1 s_2 s_3 - s_1 c_3 \\ -s_2 & s_1 c_2 & c_1 c_2 \end{bmatrix} \quad (\text{A.19})$$

Appendix III

List of Symbols

A	Transverse inertia moment of the projectile, cross-section area, linearization coefficient
\mathbf{A}	Matrix of system, rotation matrix
a	Acceleration of the mass center of the projectile
a_p	Axial acceleration of original point o_0 of rocket launcher coordinate system $o_0x_0y_0z_0$ relative to the launching guider
B_z, \mathbf{B}_z	Linearization coefficients
C	Polar inertia moment of the projectile, mass center of the rigid body, linearization coefficient
C_j	Damping coefficient of damper j
C'_j	Damping coefficient of torsional damper j
\mathbf{C}	Damping matrix
D	Action point of exterior forces, interphase drag
D^1, D^3	Operator
D_x, D_y, D_{xy}	Bending stiffness of the plate
d_p	Equivalent diameter of the propellant grain
D_p	Diameter of the propellant grain
D_z, \mathbf{D}_z	Linearization coefficients
d^1, d^3	Operator
d_0	Rotating band diameter of the projectile
E	Young's modulus
\mathbf{E}	Transform matrix
EA	Tensile stiffness
EI	Bending stiffness of the beam
E_X, E_Y, E_Z	Longitudinal, vertical, lateral mean square
e_1	Half the web size of the propellant

e_g	Internal energy of gas
\mathbf{f}	External forces matrix acting on the system
\mathbf{f}_i	External force (including external torque) matrix acting on element i
f_p	Impetus of the propellant
$\mathbf{F}_i, \mathbf{F}_i$	External forces acting on element i
\mathbf{F}^{sf}	Contact force between the front bourrelet and the launching tube
\mathbf{F}_2^{sf}	Contact force between the rear bourrelet and the launching tube
F_p	Engine thrust
G	Shear elastic modulus
GJ_p	Torsional rigidity of axis
GA_s	Shearing rigidity
g	Gravity acceleration
h	Thickness of plate
\mathbf{H}	Coordinate transformation matrix
H_c	Burned released enthalpy of principal charge per unit mass
h_p	Convective heat transfer coefficient
h_{re}	Radiative heat interchange coefficient
i, i	Number of element, imaginary unit
I	Input point of element
\mathbf{I}_n	Unit matrix of order n
j	Number of element
J_p	Polar product of inertia of axial section
\mathbf{J}	Inertia matrix
k	Modal order
\mathbf{K}	Augmented operator
K_j	Stiffness coefficient of the spring j
K'_j	Stiffness coefficient of the torsional spring j
K^*	Winckler (elastic) basic modulus
K'^*	Rotating basic modulus
k_p	Coefficient of thermal conductance of the propellant
\mathbf{L}	Eccentricity of thrust
\mathbf{L}_m	Eccentricity of mass
L_p	Length of the propellant grain
\mathbf{l}	Position coordinate matrix
$\tilde{\mathbf{l}}$	Skew symmetric matrix of position vector
l_1	Distance between the mass center of the projectile and the front end plane of front bourrelet of the projectile

l_R	Distance between the mass center of the projectile and the rear end plane of rear bourrelet of the projectile
l_α	Distance between the interface point of the combined rifling and rifling initial point
M	Bending moment, moment, augmented operator, internal moment matrix under modal coordinate
M_j	Mass parameter matrix of the body j
m	Mass of body element, mass of the projectile
\mathbf{m}	Internal moment matrix under physics coordinate
\dot{m}_c	Rate of gas mass production of principal charge per unit volume
\bar{m}	Linear density of the beam
o	Rear bourrelet center of the projectile
O	Output point of element
$\mathbf{O}_{m \times n}$	$m \times n$ zero matrix
O_1	Geometric center of the projectile
o_2	Front bourrelet center of the projectile
O_3	Intersection point of the bore axis and the vertical plane of the bore axis with the mass center
P	Gas pressure
$P_{i,j}$	Connection point in the system
p	Distributed load intensity
Q	Internal force matrix under modal coordinate
q	Internal force matrix under physics coordinate
q^k	Generalized coordinate
Q_s	Heat exchange capacity between solid phase and gas phase per unit volume
R	Gas constant
R	Linear displacement matrix under modal coordinate
r	Linear displacement matrix under physics coordinate
r_b	Radius of neutral circularity of guide pin
Re	Gas motion Reynold's number
R_p	Stress of solid phase intergranular
T	Temperature
t	Time
ΔT	Time step
t_g	The time when the projectile flies out of the muzzle (or the muzzle of the launching tube)
U_i, U_x	Transfer matrix of the element
\hat{U}	Extended transfer matrix

$\bar{\mathbf{U}}$	Complex transfer matrix
$\hat{\mathbf{U}}$	Complex extended transfer matrix
\mathbf{U}_{all}	Overall transfer matrix of the system
\mathbf{V}^k	Augmented eigenvector corresponding to the k th eigenfrequency of the system
u_1	Burning rate coefficient of the propellant
u_p	Solid phase rate
u_g	Gas phase rate
\mathbf{v}	Augmented eigenvector matrix under physics coordinate
ν	Burning rate exponent of the propellant
v_0	Muzzle velocity of the projectile
v_p	Velocity of the origin o_0 of rocket launcher coordinate system $o_0x_0y_0z_0$ relative to the launching tube
v_g	Axial component of the velocity of the mass center of the projectile relative to the muzzle (muzzle of the launching tube)
w	Deflection of transverse vibration plate
X'	Artillery recoil displacement
x_q	Longitudinal displacement of the projectile relative to the barrel
y_{O_3C}, z_{O_3C}	Vertical and lateral component of displacement of the mass center of the projectile relative to the artillery coordinate system
$x'_{oc}, y'_{oc}, z'_{oc}$	Longitudinal, vertical and lateral components of displacement of the mass center of the rocket relative to the rocket launcher coordinate system
Z	Relative burned thickness of the propellant
$\mathbf{Z}_{i,j}$	State vector of connection point $P_{i,j}$ or (i,j) under modal coordinate
$\mathbf{z}_{i,j}$	State vector of connection point $P_{i,j}$ or (i,j) under physics coordinate
α	Rifling (guide slot of launching tube) twist angle
α_0	Twist angle of the rifling initial point
α_g	Muzzle rifling twist angle
β_D	Dynamic unbalance angle
β_p	Thrust malalignment angle
γ	Spin angle of projectile, gas adiabatic exponent
$\dot{\gamma}$	Spin angular speed of projectile
γ_0	Initial orientation angles of guide slot
δ	Nutation angle
Δ	Attack angle
δ_1^l	Vertical swing angle of the projectile axis relative to the launching tube
δ_2^l	Lateral swing angle of the projectile axis relative to the launching tube
ε	Strain

Θ	Angular displacement matrix under modal coordinate
θ	Angular displacement matrix under physics coordinate
θ_1	Departure angle of the rocket launcher
$\theta_x, \theta_y, \theta_z$	Generalized angle of the rigid body for describing orientation
μ	Friction coefficient between the guide pin and the tube wall of the launching tube, Poisson's ratio of material
μ_g	Kinematic viscosity coefficient of gas
ρ	Material density, distributed density
ρ_g	Gas phase density
ϕ	Voidage
ϕ_0	Criticality voidage of propellant charge with free loading
Φ	Projectile oscillation angle
φ_1	Vertical swing angle of the projectile
φ_2	Lateral swing angle of the projectile
ψ	Deflection angle of the projectile
ψ_1	Vertical deflection angle of the projectile
ψ_2	Lateral deflection angle of the projectile
ψ_1^I	Vertical spin angle of barrel (launching tube)
ψ_2^I	Lateral spin angle of barrel (launching tube)
ω	Angle velocity
ω_k	The k th order eigenfrequency of system
Ω	Excitation frequency

Appendix IV

International Academic Communion for the Transfer Matrix Method for Multibody Systems



Figure AIV.1 Professor Xiaoting Rui was invited by Professor Werner Schiehlen, President of IUTAM, to give lectures at Stuttgart University in 1999, 2001, 2003 and 2006.



Figure AIV.2 Professor Xiaoting Rui was invited by Professor Jens Wittenburg, Head of the Insititue of Applied Mechanics in Karlsruhe University, to give lectures in 1999 and 2002.



Figure AIV.3 Professor Xiaoting Rui was invited by Professor Erwin Stein, President of the German Mechanics Society, to give lectures at Hannover University in 1995.



Figure AIV.4 Professor Xiaoting Rui was invited by Professor Peter Eberhard to give lectures at Erlangen-Nurnberg University and Stuttgart University in 1999, 2002 and 2011.

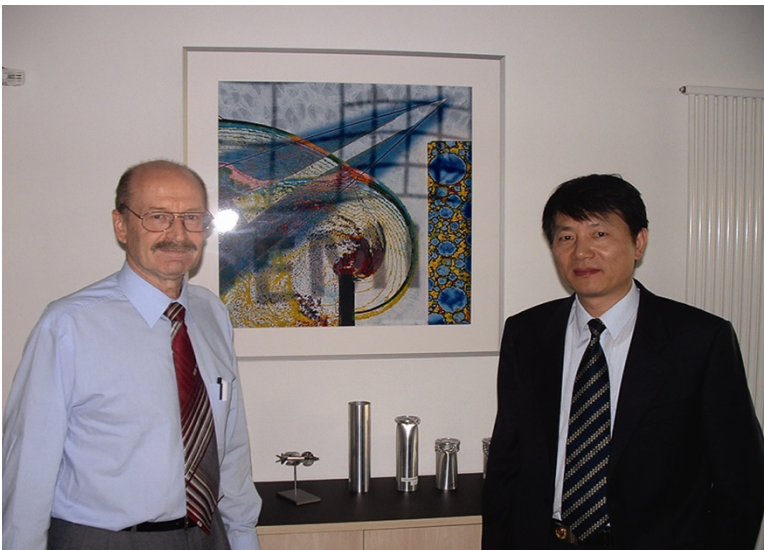


Figure AIV.5 Professor Xiaoting Rui was invited by Professor Klaus Thoma, Head of the Ernst-Mach Institute, to give lectures in 2003 and 2011.



Figure AIV.6 Professor Xiaoting Rui was invited by Professor Dieter Bestle, Head of the Institute of Engineering and Vehicle Dynamics in Cottbus Technology University, to give lectures in 2001, 2003, 2006 and 2011.



Figure AIV.7 Professor Xiaoting Rui was invited by Professor Bodo Heimann of Hannover University to give lectures in 2006.



Figure AIV.8 Professor Xiaoting Rui was invited by Professor Edwin Kreuzer, President of Hamburg-Hurburg Technology University, to give lectures in 1999, 2001 and 2003.

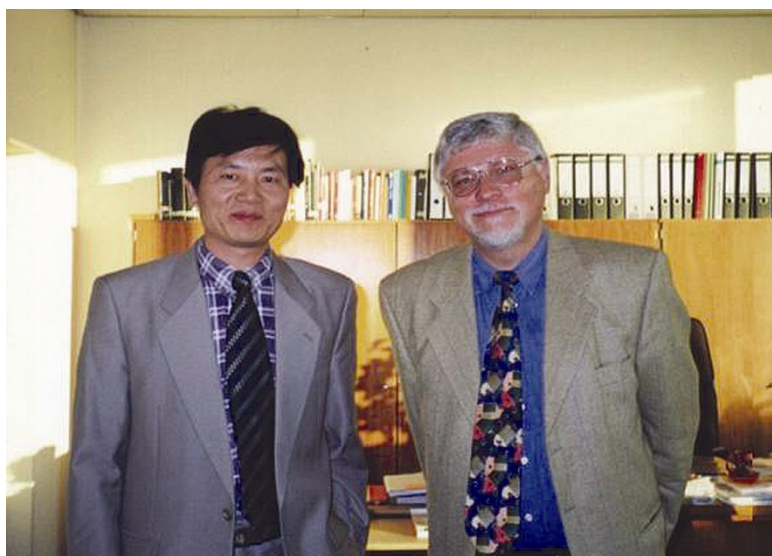


Figure AIV.9 Professor Xiaoting Rui was invited by Professor Karl Popp, Head of the Institute of Mechanics in Hannover Univeristy, to give lectures in 2002.



Figure AIV.10 Professor Xiaoting Rui was invited by Professor Friedrich Pfeiffer, Lead Editor of *Archive of Applied Mechanics*, to give lectures at Munich Technology University in 2002.



Figure AIV.11 Professor Xiaoting Rui was invited by Professor Joachim Luckel, Head of the Institute of Mechanical Control in Paderborn University, to give lectures in 2002. Professor Joachim Luckel is on the right of the photograph.



Figure AIV.12 Professor Xiaoting Rui was invited by Professor Peter Maisser, Head of the Institute of Mechanical Control at Chemnitz Technology University, to give lectures in 2002.

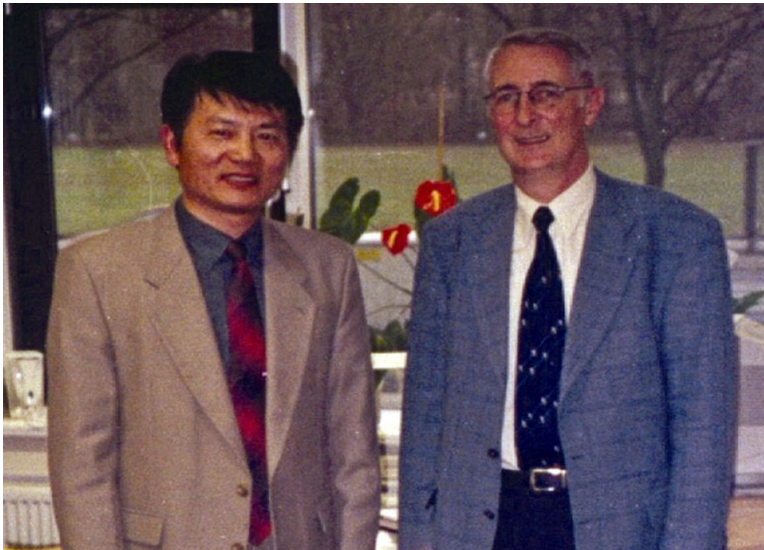


Figure AIV.13 Professor Xiaoting Rui was invited by Professor Lutz Sperling, Head of the Institute of Engineering Mechanics at Magdeburg University, to give lectures in 2002 and 2003.

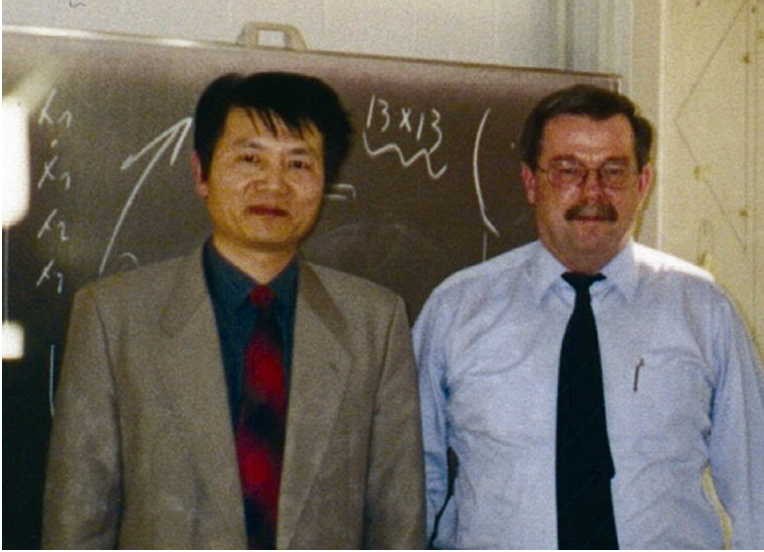


Figure AIV.14 Professor Xiaoting Rui was invited by Professor Horst Irreties to give lectures at Kassel University in 2002 and 2003.

Kooperationsvertrag in Erlangen unterzeichnet

Partnerschaft mit Uni in Nanjing



FAU-Prorektor Prof. Dr. Bernd Naumann (links) und Prof. Dr. Xiaoting Rui (rechts) von der Nanjing University of Science and Technology unterzeichneten im Dezember einen Kooperationsvertrag zwischen beiden Universitäten. Prof. Rui arbeitet bereits seit Jahren mit Prof. Dr. Peter Eberhard (Mitte) vom Institut für Maschinenbau und Fertigungstechnik zusammen. Im Sommer 2002 wird Prof. Eberhard in Nanjing einen Kurs zur Kontaktmechanik halten. Auch bei der Studentenausbildung will man zusammenarbeiten.

Foto: SG Öff

Figure AIV.15 Overseas report in 2001 about Professor Xiaoting Rui's lectures in Germany and his making an agreement on behalf of NUST with the President of Erlangen-Nurnberg University.

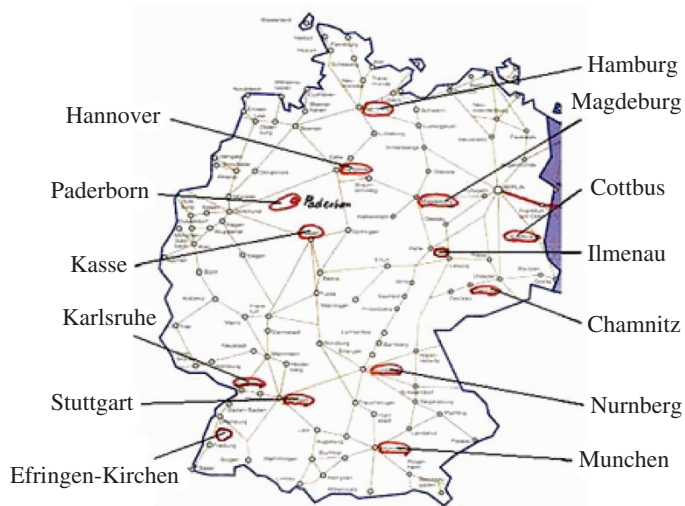


Figure AIV.16 The locations where Professor Xiaoting Rui has given lectures in Germany.



Figure AIV.17 Professor Xiaoting Rui was invited by Professor Kluse Zimmermann of Ilmenau Technology University to visit Ilmenau Technology University in 2001.



Figure AIV.18 Professor Xiaoting Rui was invited to participate in the IUTAM Symposium on Multiscale Problems in Multibody System Contacts 2006. This photograph shows all the Chinese representatives at the conference.



Figure AIV.19 As the only member of the Scientific Committee of Asia at the IUTAM Symposium on Multiscale Problems in Multibody System Contacts 2006, Professor Xiaoting Rui presided over the conference and gave a lecture.



Figure AIV.20 As an academic committee member of the International Conference on Mechanical Engineering and Mechanics 2005, Professor Xiaoting Rui gave the keynote address.



Figure AIV.21 As an academic committee member of the International Conference on Mechanical Engineering and Mechanics 2007, Professor Xiaoting Rui gave the keynote address.



Figure AIV.22 As an academic committee member of the International Conference on Dynamics, Vibration and Control 2006, Professor Xiaoting Rui presided over the conference and gave the keynote address.



Figure AIV.23 The appraisal meeting for the transfer matrix method of multibody systems was held in Beijing by the Technical Committee of the National Defense Industry. From the left: Professor Yao Zhijun (China Baicheng Weapon Testing Center), Professor Li XinLong (China Weapon Science Research Institute), lecturer Huang Wenhui (Harbin Techonology University), lecturer Huang Kezhi (Tsinghua University), lecturer Wang Zherong (Chian North Vehicle Institute), director An Haitao (Technical Committee of the National Defense Industry), lecturer Su Zhezi (China Weapon Science Research Institute), lecturer Duo Yingxian(Peking Institute of Technology), Professor Zhao Youli (Hubei Jiangshan Heavy Industry Limited), academic Chen Bin (Peking University), Professor Ma Baohua (Peking Institute of Technology), General Ma Dianrong (Science and Technical Committee of General Armament Department), Professor Huang Kaoli (Technical Institute of Armament), Professor Rui Xiaoting (Nanjing University of Science and Technology).



Figure AIV.24 Professor Dieter Bestle of Brandenburg University of Technology Cottbus was invited by Professor Xiaoting Rui for a five-month stay in Nanjing as guest professor to study the transfer matrix method for a multibody system in 2012.

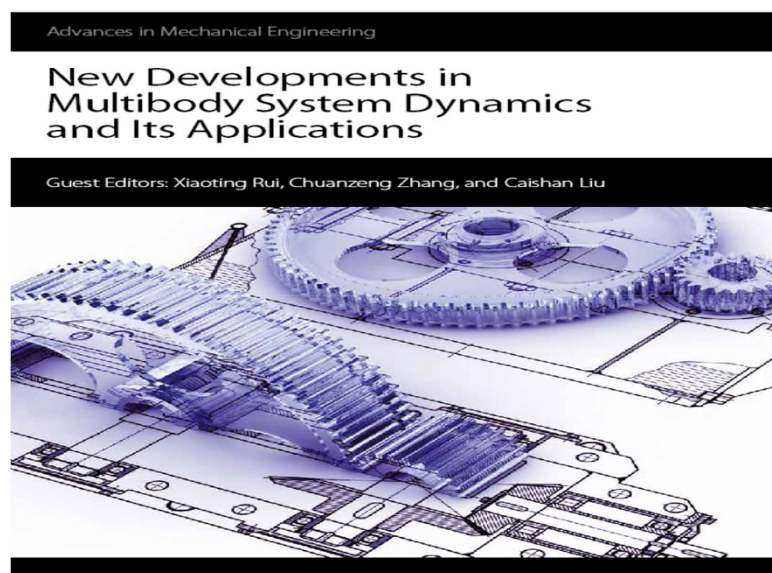


Figure AIV.25 Since 2013 Professor Xiaoting Rui has been invited as the lead guest editor by the SCI indexed Journal *Advance in Mechanical Engineering* for an annual special collection *New Developments in Multibody System Dynamics and its Applications*.



Figure AIV.26 Professor Xiaoting Rui was invited to visit the Military Technical College in Cairo, Egypt, in 2015.

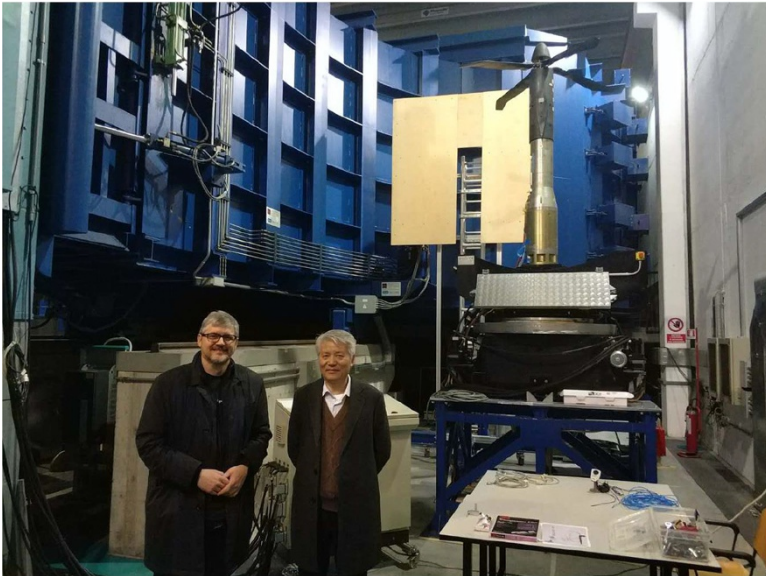


Figure AIV.27 Professor Xiaoting Rui was invited by Professor Pierangelo Masarati of Politecnico di Milano as a member of defense committee of doctoral thesis and to visit his university in 2018.

References

- 1 Rui Xiaoting, Lu Yuqi, Wang Guoping, et al. *Simulation and Test Methods of Launch Dynamics of Multiple Launch Rocket System*. Beijing: National Defense Industry Press, 2003.
- 2 Rui Xiaoting. *Launch Dynamics of Multibody System*. Beijing: National Defense Industry Press, 1995.
- 3 Rui Xiaoting, He Bin, Lu Yuqi, et al. Discrete time transfer matrix method for multibody system dynamics. *Multibody System Dynamics*, 2005, 14(4): 317–344.
- 4 Rui Xiaoting, Wang Guoping, Lu Yuqi, et al. Transfer matrix method for linear multibody system. *Multibody System Dynamics*, 2008, 19(3): 179–207.
- 5 Rui Xiaoting, Jianshu Zhang, Qinbo Zhou. Automatic deduction theorem of overall transfer equation of multibody system. *Advance in Mechanical Engineering*, 2014, ID 378047.
- 6 Schiehlen W. *Multibody Systems Handbook*. Berlin: Springer-Verlag, 1990.
- 7 Wittenburg J. *Dynamics of Systems of Rigid Bodies*. Stuttgart: B.G. Teubner, 1977.
- 8 Huang Wenhui, Shao CX. *Flexible Multibody System Dynamics*. Beijing: Science Press, 1996.
- 9 Kane TR, Likins PW, Levinson DA. *Spacecraft Dynamics*. New York: McGraw-Hill Book Company, 1983.
- 10 Eberhard P., Hu Bin. *Modern Impact Dynamics*. Nanjing: Southeast University Press, 2003.
- 11 Liu Yanzhu, Hong Jiazhen, Yang Haixing. *Multi-rigid-body System Dynamics*. Beijing: Higher Education Press, 1989.
- 12 Lu Youfang. *Multi-Flexible-Body System Dynamics*. Beijing: Higher Education Press, 1996.
- 13 Zienkiewicz OC. *The Finite Element Method*. New York: McGraw-Hill Book Company, 1987.
- 14 Ying AL. *Infinite Element Method*. Beijing: Peking University Press, 1992.
- 15 Huang KZ. *Nonlinear Continuum Mechanics*. Beijing: Tsinghua University Press, 1989.
- 16 Dai CX, Le TY, Duo YX. *New Automatic Weapon*. Beijing: National Defense Industry Press, 1990.
- 17 Chen YS. *Nonlinear Vibration*. Beijing: Higher Education Press, 2002.
- 18 Bestle D, Eberhard P. Analyzing and optimizing multibody systems. *Mechanics of Structures and Machines*, 1992, 20: 67–92.
- 19 Michaelsen A, Popp K. Kinematics and control of a stair climbing robot. *Proceedings of the 7th International Conference on Motion and Vibration Control*. St. Louis. CR-Rom Publication, 2004.
- 20 Maissner P. About some aspects in mathematical modeling of mechatronic systems. *International Symposium on Dynamics and Control*, 2003: 15–17.
- 21 Thoma K, Schäfer F, Hiermaier S, et al. An approach to achieve progress in spacecraft shielding. *Advances in Space Research*, 2004, 34(5): 1063–1075.
- 22 Joachim L, Jürgen G, Reiner A, et al. Computer-aided design of mechatronic systems, exemplified by the integrated wheel suspension of an innovative service vehicle. *The 1st IFAC Conference on Mechatronic Systems, Darmstadt*, 2000.

- 23 Sperling L, Ryzhik B, Duckstein H, et al. Auto-balancing of rotors with a rigid bearing. *Machine Dynamics Problems*, 2004, 28(2): 45–64.
- 24 Wauer J, Bührle P. Dynamics of a flexible slider-crank mechanism driven by a non-ideal source of energy. *Nonlinear Dynamics*, 1997, 13(3): 221–242.
- 25 Pfeiffer F. The idea of complementarity in multibody dynamics. *Archive of Applied Mechanics*, 2003, 72: 8097–8106.
- 26 Liu Caishan, Chen Bin. A global review for the impact dynamics research of flexible multibody system. *Advances in Mechanics*, 2000, 30(1): 7–14.
- 27 Chen Bin. *Analytical Dynamics*. Beijing: Peking University Press, 1987.
- 28 Jia Shuhui. *Rigid Body Dynamics*. Beijing: Higher Education Press, 1986.
- 29 Wang Zherong. On the technical features and development trend of main battle tank. *Engineering Science*, 2002, 4(11): 7–11.
- 30 Su Zhezi. Present status and the gaming of self-propelled guns. *Symposium of the Third Academic Annual Meeting of China Arms Society*, 1993, 198–204.
- 31 Li Hongzhi, Liu Xiaoli. The state of the development of foreign airborne throwing weapons. *Symposium of the Third Academic Meeting of China Astronautics Society*, 1999: 47–54.
- 32 Huang Xianxiang, Gao Qinhe, Guo Xiaosong. Dynamic modeling of erected process for large mechanism. *Journal of System Simulation*, 2002, 14(3): 271–274.
- 33 Liu Yixin. Study of the method for the definition of the firing dispersion index of intermediate range multiple launch rocket system. *Journal of Rockets and Guidance*, 1996, 2: 1–4.
- 34 Zhu Weiqiu, Ren Yongjian. The transfer matrix method for dynamic analysis of one-dimensional lattice structures. *Chinese Journal of Applied Mechanics*, 1991, 8(3): 88–97.
- 35 Zhong Wanxie. Vibration wave and symplectic mathematics, in *The Latest Development of General Mechanics (Dynamics, Vibration and Control)* (Huang WH, Chen B, Wang ZL, eds). Beijing: Science Press, 1994.
- 36 Pestel EC, Leckie FA. *Matrix Method in Elastomechanics*. New York: McGraw-Hill Book Company, 1963.
- 37 Uhrig R. *Elastostatik und Elastokinetik in Matrizenschreibweise das Verfahren der Übertragungsmatrizen*. Berlin: Springer Verlag, 1973.
- 38 Pilkey WD, Chang PY. *Modern Formulas for Statics and Dynamics*. New York: McGraw-Hill Book Company, 1978.
- 39 Eberhard P, Neerpashch U. Interactive modeling of multibody systems with an object oriented data model. *Mathematical Modeling of Systems*, 1996, 2(1): 55–68.
- 40 Kreuzer E, Kust O. Analysis of long torsional strings by proper orthogonal decomposition. *Archive of Applied Mechanics*, 1996, 67: 68–80.
- 41 Rui Xiaoting, Lu Yuqi, Dong Dianjun. A method for the exact solution of the transverse vibration of beam system with lumped mass, in *Application of Modern Mathematical Theory in Dynamics, Vibration and Control*. Beijing: Science Press, 1992: 213–219.
- 42 Rui Xiaoting. The natural vibration characteristics of the gun system. *Journal of Nanjing University of Science and Technology*, 1993, 5: 44–48.
- 43 Rui Xiaoting, Liu Yafei. Transfer matrix method of beam systems. *Mechanics in Engineering*, 1993, 5: 66–67.
- 44 Rui Xiaoting, Wang Shiming, Sun Yiping. Transfer matrix method of vibration of beam system with spring, rigid body, lumped mass and distributed mass. *Journal of Nanjing University of Science and Technology*, 1993, 6: 76–80.
- 45 Rui Xiaoting, Sui Wenhui, Shao Yunzhong. Transfer matrix method of rigid body and its application in multibody system dynamics. *Journal of Astronautics*, 1993, 4: 82–87.
- 46 Rui Xiaoting, Liu Yafei, Zhang Dianyin. Free vibration of rigid and flexible system with arbitrary elastic support. *Journal of Vibration and Shock*, 1994, 2: 82–87.

- 47 Rui Xiaoting, Liu Zhengfu, Lu Yuqi. Some issues of transfer matrix method of multibody system, in *Symposium of the Fifth National General Mechanics Academic Meeting* (Chen B, ed.). Beijing: Peking University Press, 1994: 121–124.
- 48 Rui Xiaoting, Lu Yuqi. Transfer matrix method of multibody system vibration. *Journal of Astronautics*, 1995, 3: 41–47.
- 49 Stein E, Huang Yuejun, Rui Xiaoting, et al. Transfer matrix method of damping multibody systems vibration. *Journal of Astronautics*, 1996, 2: 28–35.
- 50 Lu Yuqi, Wang Xiaofeng, Zhang Yanjiao, Rui Xiaoting. Natural vibration of variable cross section continuous beam with arbitrary lumped mass, elastical and rigid supports. *Journal of Ballistics*, 1997, 4: 23–28.
- 51 He Bin, Rui Xiaoting, Wang Guoping. Riccati discrete time transfer matrix method of multibody system for elastic beam undergoing large overall motion. *Multibody System Dynamics*, 2007, 18(4): 579–598.
- 52 Lu Yuqi, Rui Xiaoting, Liu Zhengfu, et al. Dynamic response of the coupled multibody system. *Journal of Astronautics*, 1998, 1: 44–48.
- 53 Rui Xiaoting, Lu Yuqi, Huang Baohua, et al. Vibration analysis of multibody systems. *Acta Armamentarii*, 1999, 1: 28–31.
- 54 Rui Xiaoting, Wang Guoping, Lu Yuqi. Vibration analysis of a multibody system with the transfer matrix method. *The 5th EUROMECH Solid Mechanics Conference, Thessaloniki, Greece*, 2003.
- 55 Lu Yuqi, Rui Xiaoting, Zhang Wei, et al. The orthogonality of the eigen vector of a multibody system, in *Study of Dynamics, Vibration and Control* (Chen B, ed.). Changsha: Hunan University Press, 1998: 167–171.
- 56 Lu Yuqi, Rui Xiaoting. Eigenvalue problem, orthogonal and response of multibody system. *Proceedings of the International Conference on Advanced Problems in Vibration Theory and Applications*. Beijing: Science Press, 2000: 711–714.
- 57 Rui Xiaoting, Wang Guoping, Lu Yuqi, et al. Vibration characteristics and orthogonality of linear multibody system. *Proceedings of the International Conference on Mechanical Engineering and Mechanics*. New York: Science Press USA Inc., 2005: 916–920.
- 58 Rui Xiaoting, Yun Laifeng, Lu Yuqi. Augmented eigenvector of multibody system coupled with rigid and elastic bodies and its orthogonality. *Acta Armamentarii*, 2007, 28(5): 581–586.
- 59 Rui Xiaoting, Edwin Kreuzer, Bao Rong, et al. Discrete time transfer matrix method for dynamics of multibody system with flexible beams moving in space. *Acta Mechanica Sinica*, 2012, 28(2): 490–504.
- 60 Yun Laifeng, Rui Xiaoting, Lu Yuqi, et al. Extended transfer matrix method to solute steady state response of multibody system. *Journal of Nanjing University of Science and Technology*, 2006, 30(4): 419–423.
- 61 Yun Laifeng, Rui Xiaoting, Wang Gonglian, et al. Method for structure parameter identification of coupled flexible-rigid multibody system. *Journal of Nanjing University of Science and Technology*, 2006, 30(4): 424–428.
- 62 Rui Xiaoting, Bao Rong, Guoping Wang, et al. Discrete time transfer matrix method for dynamics analysis of complex weapon systems. *SCIENCE CHINA Technological Sciences*, 2011, 54(5): 1061–1071.
- 63 Rui Xiaoting, He Bin, Rong Bao, Wang Guoping, Lu Yuqi. Discrete time transfer matrix method for dynamics of multi-rigid-flexible-body system moving in plane. *Journal of Multi-body Dynamics*, 2009, 23(K1): 23–42.
- 64 Rui Xiaoting, Lu Yuqi, He Feiyue, et al. Discrete time transfer matrix method of multibody system, in *Study of Dynamics, Vibration and Control* (Chen B, ed.). Changsha: Hunan University Press, 1998: 279–283.

- 65 Rui Xiaoting, Lu Yuqi, Pan Ling, et al. Discrete time transfer matrix method for multibody system dynamics. *Advances in Computational Multibody Dynamics, Lisbon, Portugal*, 1999, 93–108.
- 66 Li Chongming, Rui Xiaoting. Validating on the transfer matrix method of multibody system without considering constraint violation correction. *Journal of Dynamics and Control*, 2005, 3(3): 8–13.
- 67 Li Chongming, Rui Xiaoting. Improvement of the accuracy of computation for the discrete time transfer matrix method of multibody system. *Chinese Journal of Applied Mechanics*, 2004, 21(1): 56–61.
- 68 Rui Xiaoting, Rong Bao, He Bin, et al. Discrete time transfer matrix method of multi-rigid-flexible-body system. *Proceedings of the International Conference on Mechanical Engineering and Mechanics*. New York: Science Press USA Inc., 2007: 2244–2250.
- 69 Rui Xiaoting, He Bin, Lu Yuqi, et al. Discrete time transfer matrix method for rigid-flexible multibody system dynamics. *Journal of Nanjing University of Science and Technology*, 2006, 30(4): 389–394.
- 70 Dieter Bestle, Laith Abbas, Rui Xiaoting. Recursive eigenvalue search algorithm for transfer matrix method of linear flexible multibody systems. *Multibody System Dynamics*, 2014, 32(4): 429–444.
- 71 Rui Xiaoting, He Bin. Advanced in discrete time transfer matrix method for multibody system dynamics. *IUTAM Symposium on Multiscale Problems in Multibody System Contacts, Stuttgart, Germany*, 2006.
- 72 Laith K. Abbas, Rui Xiaoting. Free vibration characteristic of multi-level beam based on transfer matrix method of multibody systems. *Advance in Mechanical Engineering*, 2014, ID 792478.
- 73 Gangli Chen, Rui Xiaoting, Fufeng Yang, et al. Study on the dynamics of laser gyro strapdown inertial measurement unit system based on transfer matrix method for multibody system. *Advance in Mechanical Engineering*, 2014, ID 854583.
- 74 Yun Laifeng, Rui Xiaoting, He Bin, et al. Transfer matrix method for a two-dimensional system. *Chinese Journal of Theoretical and Applied Mechanics*, 2006, 38(5): 712–720.
- 75 Rui Xiaoting, Yun Laifeng, Tang Jingjing, et al. Transfer matrix method for 2-dimensional system. *Proceedings of the International Conference on Mechanical Engineering and Mechanics*. New York: Science Press USA Inc., 2005: 93–99.
- 76 He Bin, Rui Xiaoting, Lu Yuqi. Hybrid method of discrete time transfer matrix method for multibody system dynamics and finite element method. *Journal of Nanjing University of Science and Technology*, 2006, 30(4): 395–399.
- 77 Lu Weijie, Rui Xiaoting, Yun Laifeng, et al. Transfer matrix method for linear controlled multibody system. *Journal of Vibration and Shock*, 2006, 25(5): 25–30.
- 78 Yang Fufeng, Rui Xiaoting, Yun Laifeng, et al. Transfer matrix method of controlled multibody system. *Journal of Nanjing University of Science and Technology*, 2006, 30(4): 414–418.
- 79 He Bin, Rui Xiaoting, Lu Yuqi. Riccati discrete time transfer matrix method for huge chain multi-rigid-body system dynamics. *Proceedings of the International Conference on Mechanical Engineering and Mechanics*. New York: Science Press USA Inc., 2005: 726–731.
- 80 He Bin, Rui Xiaoting, Lu Yuqi. Riccati discrete time transfer matrix method for multibody system dynamics. *Acta Armamentarii*, 2006, 27(4): 622–625.
- 81 He Bin, Rui Xiaoting, Yu Hailong. Finite segment transfer matrix method for nonlinear mechanics arm. *Fire Control and Command Control*, 2007, 32(4): 15–17.
- 82 Rui Xiaoting, Yu Hailong, He Bin, et al. Finite element transfer matrix method of multibody system for naval gun vibration analysis. *Acta Armamentarii*, 2007, 28(9): 1036–1040.
- 83 Yu Hailong, Rui Xiaoting, He Bin, et al. Finite element transfer matrix method of gun tube natural vibration characteristic. *Journal of Ballistics*, 2006, 18(3): 62–64.

- 84 Yang Fufeng, Rui Xiaoting, Zhan Zhihuan. Study on dynamics of controlled multibody system with branch based on transfer matrix method of controlled multibody system. *Proceedings of the International Conference on Mechanical Engineering and Mechanics*. New York: Science Press USA Inc., 2007: 1367–1371.
- 85 Yang Fufeng, Rui Xiaoting, Gu Jinliang, et al. Study on the controled multibody system dynamics of mooring supply systems. *Proceedings of the International Conference on Mechanical Engineering and Mechanics*. New York: Science Press USA Inc., 2005: 749–752.
- 86 Li Chongming, Rui Xiaoting. Study on holonomic system with discrete time transfer matrix method. *Chinese Quarterly of Mechanics*, 2003, 24(3): 411–415.
- 87 Rui Xiaoting, Wang Guoping, Lu Yuqi, et al. Advances in rocket launch dynamics. *The 20th International Symposium on Ballistics*. Florida: DEStech Publications, 2002: 408–415.
- 88 Rui Xiaoting, Wang Guoping, Chen Weidong, et al. Simulation of random launch and flight dynamics of MLRS. *Journal of Nanjing University of Science and Technology*, 2003, 27(5): 616–620.
- 89 Wang Guoping, Rui Xiaoting. Study on dynamics of long range multiple launch rocket system. *Journal of Dynamics and Control*, 2004, 2(1): 59–63.
- 90 Zhihuan Zhan, Rui Xiaoting, Bao Rong, et al. Design of active vibration control for launcher of multiple launch rocket system. *Journal of Multi-body Dynamics*, 2011, 225(3): 280–293.
- 91 Yun Laifeng, Rui Xiaoting, Lu Yuqi, et al. A study on the vibration characteristics of multiple launch rocket system. *Acta Armamentarii*, 2004, 25(1): 9–13.
- 92 Wang Guoping, Rui Xiaoting, Lu Yuqi. Influence of firing orders on performance of MLRS. *Journal of Nanjing University of Science and Technology*, 2004, 28(4): 364–368.
- 93 Wang Guoping, Rui Xiaoting, Chen Weidong. Technology of the simulation of the firing dispersion of multipl launch rocket. *Journal of System Simulation*, 2004, 16(5): 963–966.
- 94 Wang Guoping, Rui Xiaoting, Cheng Weidong, et al. Simulation in the reduction of rocket consumption in multiple launch rocket system tests. *Acta Armamentarii*, 2004, 25(6): 786–789.
- 95 Wang Guoping; Rui Xiaoting. Simulation of launch dynamics of LRMLRS. *Journal of System Simulation*, 2006, 18(5): 1097–1100.
- 96 Wang Guoping, Rui Xiaoting, Yang Fan, et al. Application of transfer matrix method of multibody system in dynamics of multiple launch rocket system. *Journal of Nanjing University of Science and Technology*, 2006, 30(4): 434–438.
- 97 Rui Xiaoting, Yun Laifeng, Lu Yuqi, et al. Study on the launch dynamics of multiple launch rocket system. *Acta Armamentarii*, 2004, 25(5): 556–561.
- 98 Rui Xiaoting, Wang Guoping, Yun Laifeng. Study on the vibration characteristics of LRMLRS. *Journal of Vibration and Shock*, 2005, 24(1): 9–12.
- 99 Rui Xiaoting, Wang Guoping, Lu Yuqi. New technology to improving firing dispersion of multiple launch rocket system. *Acta Armamentarii*, 2006, 27(2): 301–305.
- 100 Yang Fan, Wang Guoping, Rui Xiaoting, et al. Influence of firing interval on dynamics characteristic of MLRS. *Journal of Nanjing University of Science and Technology*, 2006, 30(4): 401–404.
- 101 Hong Jun, Rui Xiaoting. Numerical simulation for granular system in barrel under ladder load. *Journal of System Simulation*, 2007, 19(5): 1007–1010.
- 102 Rui Xiaoting, Qiu Fengchang. Natural vibration of multibody gun system. *International Symposium on Cannon and Gun Technology, Nanjing, China*, 1993: 494–502.
- 103 Rui Xiaoting, Xu Mingyou. Application of transfer matrix in launching dynamics. *The 14th International Symposium on Ballistics, Quebec, Canada*, 1993.
- 104 Rui Xiaoting, Qin Yingxiao, Zhao Hailin, et al. Natural vibration of spin tube gun with multilumped masses. *Acta Armamentarii*, 1994, 2: 1–5.

- 105 Rui Xiaoting, Zeng Shilong, Qin Yingxiao. Vibration of rotating a beam off-axially with moving load and mass. *ACTA Armamentarii Sinica*, 1994, 4: 1–4.
- 106 Rui Xiaoting, Qiu Fengchang. Natural vibration of multibody gun system. *Acta Armamentarii*, 1995, 2: 7–12.
- 107 Rui Xiaoting, Dang Shuangxi, Zhang Jinkui, et al. Application of transfer matrix method in the dynamcis of guns. *Mechanics in Engineering*, 1995, 4: 42–44.
- 108 Rui Xiaoting, Lu Yuqi, Lu Wenguang, et al. A study on the launch dynamics of self-propelled artillery. *Acta Armamentarii*, 2000, 12: 38–40.
- 109 Tang Jingjing, Rui Xiaoting, Lu Yuqi, et al. Calculation of the self-propelled artillery vibration characteristics. *Journal of Ballistics*, 2003, 15(2): 23–27.
- 110 Rui Xiaoting, Qin Yingxiao, Yi Zengqi, et al. Vibration characteristics of gun systems studied through the transfer matrix method. *Acta Armamentarii*, 1996, 1: 75–78.
- 111 Yun Laifeng, Rui Xiaoting, Hou Risheng, et al. Calculation of launch dynamics with two-phase flow interior ballistic model for self-propelled artillery. *Explosion and Shock Waves*, 2007, 27(1): 12–17.
- 112 He Bin, Rui Xiaoting, Lu Yuqi, Yu Hailong. A blocking method for lurching dynamics of shipboard gun. *Journal of Dynamics and Control*, 2004, 2(2): 34–37.
- 113 Yu Hailong, Rui Xiaoting, He Bin, et al. Study on dynamic simulation of launch and flight for naval gun. *Journal of System Simulation*, 2007, 19(5): 956–958.
- 114 Yu Hailong, Rui Xiaoting, Li Sulong, et al. Application of transfer matrix method of multibody system in launch dynamics for super-high firing frequency weapon. *Journal of Nanjing University of Science and Technology*, 2006, 30(4): 445–450.
- 115 Lu Yuqi, Wang Xiaofeng, Rui Xiaoting, et al. Study on the dynamics of the fuze mechanism. *Journal of Nanjing University of Science and Technology*, 2000, 24(6): 528–531.
- 116 Lu WenGuang, Rui XiaoTing, Lu YuQi, et al. Study on the runaway escapement dynamics. *Acta Armamentarii*, 2005, 26(3): 401–404.
- 117 Rui Xiaoting, Huang Kechao, Qin Yingxiao. Transfer matrix method of multibody system and its application in spacecraft dynamics. *Proceedings of the Third China-Russia-Ukraine Symposium on Astronautical Science and Technology*. Xi'An: Northwestern Polytechnical University Press, 1994, 933–935.
- 118 Yang Fan, Rui Xiaoting, Wang Guoping. Methods to improve firing accuracy of ballistic missiles. *Journal of Nanjing University of Science and Technology*, 2007, 31(1): 10–16.
- 119 Hossam Hendy, Rui Xiaoting, Qinbo Zhou, et al. Controller parameters tuning based on transfer matrix method for multibody systems. *Advance in Mechanical Engineering*, 2014, ID 957684.
- 120 Wei Zhu, Gangli Chen, Leixiang Bian, Rui Xiaoting. Transfer matrix method for multibody systems for piezoelectric stack actuators. *Smart Materials and Structures*, 2014, 23(9): 095043.
- 121 Chen Weidong, Rui Xiaoting, Wang Guoping. Discrete optimum design based on statistics. *Journal of Harbin Institute of Technology*, 2005, 37(3): 359–361.
- 122 Wang Guoping, Rui Xiaoting, Chen Weidong. Simulation of dispersion of MLRS by using the maximum entropy method. *Journal of Ballistics*, 2007, 19(2): 13–15.
- 123 Wang Guoping, Rui Xiaoting. Influence of windage of tubular launcher to dispersion of MLRS. *Journal of Ballistics*, 2003, 15(4): 27–31.
- 124 Wang Guangwei, Rui Xiaoting, Wang Guoping. Test method for vertical target dispersion of ammunition. *Journal of Nanjing University of Science and Technology*, 2006, 30(4): 482–485.
- 125 Chen Weidong, Rui Xiaoting, Wang Guoping. Judgment of the reliability of stochastic system based on maximum entropy. *Acta Armamentarii*, 2002, 23(s1): 17–20.
- 126 Rui Xiaoting, Chen Weidong, Wang Guoping. The analysis of dispersion of weapon system based on the maximum entropy method. *Journal of Ballistics*, 2002, 14(3): 51–56.

- 127 Bao Rong, Rui Xiaoting, Ling Tao. Discrete time transfer matrix method for launch dynamics modeling and cosimulation of self-propelled artillery system. *Journal of Applied Mechanics*, 2013, 80(1): 011008.
- 128 Abbas, L.K., Li Min-Jiao, Rui Xiaoting. Transfer matrix method for the determination of the natural vibration characteristics of realistic thrusting launch vehicle-part I. *Mathematical Problems in Engineering*, 2013, ID 764673.
- 129 Mostafa Khalil, Rui Xiaoting, Hossam Hendy. Discrete time transfer matrix method for projectile trajectory prediction. *Journal of Aerospace Engineering*, 2013, ID 153913.
- 130 Rui Xiaoting, Yang Fufeng, Sha Nansheng, et al. Wavelet analysis of fuze test data. *Acta Armamentarii*, 2005, 26(6): 838–841.
- 131 Lu Wenguang, Rui Xiaoting, Gu Jinliang, et al. Test and analysis of attitude and movement of projectile in bore. *Acta Armamentarii*, 2006, 27(1): 149–153.
- 132 Rui Xiaoting, Yang Qiren. *Theory of Projectile Launch Process*. Nanjing: Southeast University Press, 1992.
- 133 Pu Fa, Rui Xiaoting. *Exterior Ballistics*. Beijing: National Defense Industry Press, 1989.
- 134 Lu Yuqi, Rui Xiaoting, Sui Wenhai, et al. Vibration characteristics of a time variant system, in *Proceedings of the International Conference on Vibration Engineering, Beijing* (Hu HC, Zheng ZC, eds), 1994, 893–896.
- 135 Bao Rong, Rui Xiaoting, Ling Tao. Dynamics and genetic fuzzy neural network vibration control design of a smart flexible four-bar linkage mechanism. *Multibody System Dynamics*, 2012, 28(2): 291–311.
- 136 Lu Weijie, Rui Xiaoting, Yang Fufeng, et al. Study on dynamic simulation of container replenishment systems. *Proceedings of the International Conference on Mechanical Engineering and Mechanics*. New York: Science Press USA Inc., 2005, 742–745.
- 137 Tang Jingjing, Yun Laifeng, Lu Yuqi. A comparison of the dynamic method of multibody system. *Transactions of Shenyang Ligong University*, 2003, 22(3): 81–84.
- 138 Yang Fufeng, Rui Xiaoting, Wei Weibo. A wavelet estimation method of density function. *Acta Armamentarii*, 2006, 27(3): 83–87.
- 139 Liu Wei, Rui Xiaoting, Wang Guoping. Terminal trajectory correction capability analysis and optimization design for simple control projectile. *Journal of Nanjing University of Science and Technology*, 2006, 30(4): 449–453.
- 140 Dong Mancai, Rui Xiaoting, Wang Guoping. Analysis methods of random eigenvalue of multibody system with random parameters. *Journal of Nanjing University of Science and Technology*, 2006, 30(4): 458–461.
- 141 Bao Rong, Rui Xiaoting, Ling Tao, et al. Perturbation finite element transfer matrix method for random eigenvalue problems of uncertain structures. *Journal of Applied Mechanics*, 2012, 79(2): 021005.1–8.
- 142 Guoping Wang, Bao Rong, Ling Tao, et al. Riccati discrete time transfer matrix method for dynamics of underwater towed system. *Journal of Applied Mechanics*, 2012, 79(4): 041014.1–9.
- 143 Bao Rong, Rui Xiaoting, Guoping Wang. Discrete time transfer matrix method for dynamic modeling of complex spacecraft with flexible appendages. *Journal of Computational and Nonlinear Dynamics*, 2011, 6(1): 011013.
- 144 Bao Rong, Rui Xiaoting, Guoping Wang. Modified finite element transfer matrix method for eigenvalue problem of flexible structures. *Journal of Applied Mechanics*, 2011, 78(2): 021016.
- 145 Bao Rong, Rui Xiaoting, Guoping Wang, et al. Dynamic modeling and H_∞ independent modal space vibration control of laminate plates. *SCIENCE CHINA Physics, Mechanics & Astronomy*, 2011, 54(6): 1–13.

- 146 Bao Rong, Rui Xiaoting, Guoping Wang, et al. New efficient method for dynamics modeling and simulation of flexible multibody systems moving in plane. *Multibody System Dynamics*, 2010, 24(2): 181–200.
- 147 He Bin, Rui Xiaoting, Yu Hailong. Finite element transfer matrix method for analyzing natural vibration characteristics of slender rocket/projectile. *Journal of Dynamics and Control*, 2005, 3(4): 67–71.
- 148 He Bin, Rui Xiaoting, Lu Yuqi. Study on flight dynamic modeling of flexible shell/rocket. *Journal of Ballistics*, 2006, 18(1): 22–24.
- 149 Yang Fufeng, Rui Xiaoting, Zhou Xiaoli. Model and simulation of discarding and collision of APFSDS. *Journal of System Simulation*, 2005, 17(10): 2493–2495.
- 150 Hailong Yu, Rui Xiaoting. Study on launch dynamics of self-propelled artillery based on transfer matrix method of multibody system. *Advance in Mechanical Engineering*, 2014, ID 308049.
- 151 Lu Weijie, Rui Xiaoting, Liu Jun. Analysis of mechanical characteristics of ballistic spring under high rotation speed. *Acta Armamentarii*, 2006, 27(5): 802–806.
- 152 Lu Weijie, Rui Xiaoting, Lu Wenguang. Research on an automatic fuze failure analysis system based on dynamics simulation. *Acta Armamentarii*, 2007, 28(1): 15–19.
- 153 Wei Weibo, Rui Xiaoting, Liu Jun. Simulation of changes of gun pressure based on OpenGL. *Journal of System Simulation*, 2006, 18(3): 666–668.
- 154 Yun Laifeng, Rui Xiaoting, et al. Discussion on mechanism of breech-blow caused by propellant charge. *Journal of China Ordnance*, 2007, 3(4): 256–261.
- 155 Yun Laifeng, Rui Xiaoting, Wang Hao. Discussion about mechanism of breech-blow caused by gun propellant charge. *Acta Armamentarii*, 2007, 28(2): 153–157.
- 156 Hong Jun, Rui Xiaoting, Liu Jun. Three dimensional numerical simulation on collision and press process of propellant bed. *Acta Armamentarii*, 2007, 28(3): 305–308.
- 157 Hong Jun, Rui Xiaoting. Numerical simulation for granular system in barrel under ladder load. *Journal of System Simulation*, 2007, 19(5): 1007–1010.
- 158 Shiping Jiang, Rui Xiaoting, Hong Jun, Guoping Wang, Bao Rong, et al. Numerical simulation of impact breakage of gun propellant charge. *Granular Matter*, 2011, 13(5): 611–622.
- 159 Rui Xiaoting, Yun Laifeng, Wang Hao, et al. Experimental simulation for fracture of gun propellant charge bed. *Journal of China Ordnance*, 2005, 1(2): 151–155.
- 160 Rui Xiaoting, Yun Laifeng, Sha Nansheng, et al. Advance on launch safety for gun propellant charge. *Acta Armamentarii*, 2005, 26(5): 690–696.
- 161 Chen Tao, Rui Xiaoting, Ling Jian. Dynamic extrusion and fracture simulation of propellant charge bed. *Journal of Nanjing University of Science and Technology*, 2006, 30(4): 467–471.
- 162 Ling Jian, Rui Xiaoting, Yun Laifeng. Simulation of status of combustion and mechanics of propellant charge in chamber. *Journal of Nanjing University of Science and Technology*, 2006, 30(4): 512–516.
- 163 Rui Xiaoting, Yun Laifeng, Wang Ha, et al. A study on the experimental simulation for bursting of the charge bed. *Acta Armamentarii*, 2004, 4: 498–502.
- 164 Rui Xiaoting, Liu Jun, Chen Tao. Dynamic analysis on the extrusion and rupture of propellants. *Acta Armamentarii*, 2004, 25(6): 679–683.
- 165 Bao Rong, Rui Xiaoting, Guoping Wang. New method for dynamics modelling and analysis on flexible plate undergoing large overall motion. *Journal of Multi-body Dynamics*, 2010, 224(K1): 33–44.
- 166 Bao Rong, Rui Xiaoting, Guoping Wang, et al. Discrete time transfer matrix method for dynamics of multibody system with real-time control. *Journal of Sound and Vibration*, 2010, 329(6): 627–643.
- 167 Rui Xiaoting, Zhang Wei, Lu Yuqi. Study on the launch environment of the fuze. *Journal of Ballistics*, 2000, 4: 12–16.

- 168 Rui Xiaoting, Liu Zhengfu, Lu Yuqi. A study on projectile motion in bore. *Acta Armamentarii*, 1991, 4: 1–6.
- 169 Rui Xiaoting, Zeng Shilun, Ge Guangjun. Application of artificial intelligence in launching dynamics. *Acta Armamentarii*, 1996, 2: 173–176.
- 170 Rui Xiaoting, Liu Zhengfu. A study on projectile motion of spin bore. *Mechanics and Practice*, 1990, 5: 28–31.
- 171 Rui Xiaoting, Lu Yuqi. Lateral vibration of rotating beam, in *Engineering Mechanics*. Beijing: Science Press, 1992, 386–390.
- 172 Rui Xiaoting, Liu Zhengfu. A study on projectile motion of spin bore. *Proceedings of the International Conference on Dynamics, Vibration and Control*. Beijing: Beijing University Press, 1990, 161–166.
- 173 Rui Xiaoting, Zhang Yanjiao, Liu Zhengfu, Lu Yuqi. A study on a unified differential equation of the projectile motion. *Acta Armamentarii*, 1993, 4: 23–27.
- 174 Sui Wenhai, Rui Xiaoting, Xu Buzheng. A study on the general motion of a projectile touching an increasing twist rifled bore. *Acta Armamentarii*, 1994, 1: 10–14.
- 175 Rui Xiaoting, Xu Mingyou, Liu Yafei, Zeng Shilun. A general dynamic model for a projectile in an increasing twist rifled bore. *Acta Armamentarii*, 1993, 3: 1–5.
- 176 Rui Xiaoting, Liu Yafei. Projectile's motion touching the wall of increasing twist rifled bore. *Acta Armamentarii*, 1993, 1: 13–16.
- 177 Rui Xiaoting, Huang Baohua, Yu Zhanhong. Effects of projectile nutation within the bore on the launching safety of high explosives charges. *Acta Armamentarii*, 1997, 1: 230–233.
- 178 Rui Xiaoting, Zeng Shilong, Qin Yingxiao. Projectile launching dynamics and its expert system. *The 13th International Symposium on Ballistics, Sweden*, 1992, 1(2): 73–80.
- 179 Rui Xiaoting. Study on missile axis motion caused by forced force. *Acta Armamentarii (Missile Fascicle)*, 1989, 3: 59–61.
- 180 Rui Xiaoting, Lu Yuqi. Projectile motion in an increasing twist rifled bore. *Acta Armamentarii*, 1992, 4: 15–20.
- 181 Rui Xiaoting, Zong Yunqing. Mechanic problems in the exterior ballistics. *Mechanics and Practice*, 1992, 2: 76–78.
- 182 Rui Xiaoting, Xu Mingyou. The general motion of missiles, in *Engineering Mechanics (Supplement)*. Beijing: Science Press, 1992, 380–385.
- 183 Rui Xiaoting, Yang Qiren. The analysis of the motion of sabot discarding. *Acta Armamentarii*, 1992, 2: 49–54.
- 184 Rui Xiaoting, Yang Qiren. Study on theory of projectile initial disturbance. *Journal of Engineering Mechanics*, 1991, 2: 136–143.
- 185 Rui Xiaoting, Qin Wenpei, Qin Yingxiao. On influence of ulterior period to missile initial disturbance, in *Engineering Mechanics*. Beijing: Science Press, 1992, 755–757.
- 186 Rui Xiaoting, Zhang Yanjiao. On correct method applied assumption of mathematics and dynamics in engineering, in *Engineering Mechanics (Supplement)*. Beijing: Science Press, 1992, 391–395.
- 187 Rui Xiaoting, Lu Yuqi. Effects of gravity and its acting position on missile motion, in *Engineering Mechanics (Supplement)*. Beijing: Science Press, 1992, 744–747.
- 188 Rui Xiaoting. On the motion of projectile axis caused by gravity. *Acta Armamentarii*, 1991, 3: 8–12.
- 189 Rui Xiaoting. Approximate method for studying lateral motion of a projectile in bore. *Journal of East China Institute of Technology*, 1992, 2: 33–36.
- 190 Rui Xiaoting, Zhang Yanjiao. Study on motion states and handling methods for projectile motion in the bore. *Journal of Ballistics*, 1990, 3: 24–30.
- 191 Rui Xiaoting. The interaction between the lateral vibration of gun tube and the motion of projectile. *Journal of Jiangxi Polytechnic University*, 1991, 2: 446–453.

- 192 Rui Xiaoting. A study on projectile motion in bore II. *Acta Armamentarii*, 1987, 2: 23–38.
- 193 Rui Xiaoting. A study on projectile motion in bore I. *Acta Armamentarii*, 1987, 1: 1–16.
- 194 Rui Xiaoting, Lu Yuqi. The general pattern of projectile motion in the bore. *Engineering Mechanics*, 1991, 4: 60–67.
- 195 Rui Xiaoting, Yang Qiren. Motion of projectile with smaller diameter of bourrelet than bore diameter in bore. *Journal of Jiangxi Polytechnic University*, 1991, 2: 454–459.
- 196 Rui Xiaoting. The general differential equations of projectile moving in the bore. *Journal of Ballistics*, 1991, 3: 28–36.
- 197 Rui Xiaoting, Qin Yingxiao, Zhao Hailing. Study on projectile general motion touching the bore wall and the approaches reducing the projectiles dispersion. *Engineering Mechanics*, 1991, 3: 94–100.
- 198 Rui Xiaoting. Study on projectile motion touching the bore wall. *Journal of Ballistics*, 1991, 1: 19–22.
- 199 Liu Zhengfu, Rui Xiaoting. Motion of asymmetric projectile during after effect. *Acta Armamentarii*, 1991, 2: 34–41.
- 200 Rui Xiaoting. A study on projectile motion in aftereffect period of propellant gas. *Journal of East China Institute of Technology*, 1989, 4: 64–73.
- 201 Holzer H. *Die Berechnung der Drehschwingungen*. Berlin: Springer, 1921.
- 202 Myklestad NO. A new method of calculating natural modes of uncoupled bending vibration of airplane wings and other types of beams. *Journal of Aeronautics Science*, 1944, 11: 153–162.
- 203 Proh MA. A general method for calculating critical speeds of flexible rotors. *Journal of Applied Mechanics*, 1945, 12(3): 142–148.
- 204 Thomson WT. Matrix solution for the vibration of non-uniform beams. *Journal of Applied Mechanics*, 1950: 337–339.
- 205 Rubin S. On transmission matrices for vibration and their relation to admittance and impedance. *Journal of Engineering for Industry*, 1964, 86: 9–21.
- 206 Targoff WP. The associated matrices of bending and coupled bending-torsion vibrations. *Journal of Aeronautics Science*, 1947, 14: 579–582.
- 207 Lin YK. *Probabilistic Theory of Structure Dynamics*. New York: McGraw-Hill Book Company, 1967.
- 208 Mercer CA, Seavey C. Prediction of natural frequencies and normal modes of skin-stringer panel rows. *Journal of Sound and Vibration*, 1967, 6: 149–162.
- 209 Lin YK, McDaniel TJ. Dynamics of beam-type periodic structures. *Journal of Engineering Materials and Technology*, 1969, 91: 1133–1141.
- 210 Mead DJ, Gupta GS. Propagation of flexural waves in infinite, damped rib-skin structures. *United States Air Force Report*, AFML-TR-70-13, 1970.
- 211 Mead DJ. Vibration response and wave propagation in periodic structures. *Journal of Engineering Materials and Technology*, 1971, 93: 783–792.
- 212 Henderson JP, McDaniel TJ. The analysis of curved multi-span structures. *Journal of Sound and Vibration*, 1971, 18: 203–219.
- 213 McDaniel TJ. Dynamics of circular periodic structures. *Journal of Aircraft*, 1971, 8: 143–149.
- 214 McDaniel TJ, Logan JD. Dynamics of cylindrical shells with variable curvature. *Journal of Sound and Vibration*, 1971, 19: 39–48.
- 215 Murthy VR, Nigam NC. Dynamics characteristics of stiffened rings by transfer matrix approach. *Journal of Sound and Vibration*, 1975, 39: 237–245.
- 216 Murthy VR, McDaniel TJ. Solution bounds to structural systems. *AIAA Journal*, 1976, 14: 111–113.
- 217 McDaniel TJ, Murthy VR. Solution bounds for varying geometry beams. *Journal of Sound and Vibration*, 1976, 44: 431–448.

- 218 Horner GC, Pilkey WD. The Riccati transfer matrix method. *Journal of Mechchanics Design*, ASME, 1978, 1(100): 297–302.
- 219 Fang HL. Solution of the three dimensional seismic wave problems of stratified foundation by transfer matrix method. *Journal of Hydraulic Engineering*, 1990, 8: 64–71.
- 220 Zhou Xinzhu, Zheng Jianjun, Jiang Lu. Transfer matrix method for the analysis of annular plates with variable thickness on an elastic foundation. *Journal of Zhejiang University of Technology*, 2005, 33(1): 8–12.
- 221 Wang XC, Shao M. *Basic Theory of Finite Element Method*. Beijing: Tsinghua University Press, 1988.
- 222 Kumar AS, Sankar TS. A new transfer matrix method for response analysis of large dynamic systems. *Computers & Structures*, 1986, 23(4): 545–552.
- 223 Dokanish MA. A new approach for plate vibration: combination of transfer matrix and finite element technique. *Journal of Mechanical Design*, 1972, 94: 526–530.
- 224 Zhen Fang, Chen Jirong. Calculating the natural frequencies of elastic thin plates of variable thickness by finite strip-riccati transfer substructure method. *Journal of Yanshan University*, 1997, 21(3): 249–252.
- 225 Chen YH, Xue HY. Dynamic large deflection analysis of structures by a combined finite element Riccati transfer matrix method on a microcomputer. *Computers & Structures*, 1991, 39(6): 699–703.
- 226 Ohga M, Shigematus T. Transient analysis of plates by a combined finite element transfer matrix method. *Computers & Structures*, 1987, 26: 543–549.
- 227 Xue HY. A combined dynamic finite element Riccati transfer matrix method for solving non-linear eigenproblems of vibrations. *Computers & Structures*, 1994, 53: 1257–1261.
- 228 Loewy RG, Bhntani N. Combined finite element-transfer matrix method. *Journal of Sound and Vibration*, 1999, 226(5): 1048–1052.
- 229 Loewy RG, Degen EE, Shephard MS. Combined finite element-transfer matrix method based on a mixed formulation. *Computers & Structures*, 1985, 20: 173–180.
- 230 Hu Haichang. *Theory of Natural Vibration of Multi-degree of Freedom Structures*. Beijing: Science Press, 1987.
- 231 Yang B. Linear vibration of a coupled string-rigid body system. *Proceedings of the International Conference on Vibration Engineering*. Beijing: International Academic Publishers, 1994, 91–96.
- 232 Xie BJ. *Linear Algebra*. Beijing: People's Education Press, 1978.
- 233 Fraeijs de Veubeke BM. Influence of internal damping on aircraft resonance, in *Manual on Aeroelasticity*. North Atlantic Treaty Organization, 1960, 1.
- 234 Ramkrishna D, Amvndson NR. On vibration problems with discretely distributed loads-a rigorous formalism. *Journal of Applied Mechanics*, 1974, (41): 1106–1112.
- 235 Chenwen Cai. *Theory of Vibration*. Beijing: People's Education Press, 1963.
- 236 Yasuda K, Torii T, Kasahara M. Proposition of an incremental transfer matrix method for nonlinear vibration analysis. *JSME, Series III*, 1991, 34(1): 12–18.
- 237 Chen Jirong, Du Guojun. Finite strip–transfer matrix method about vibration analysis of rectangular plate. *Journal of Yanshan University*, 1993, 17(2): 95–99.
- 238 Wang SW. *Structural Dynamics of Aircraft*. Xi'an: Northwest Polytechnical University Press, 1985.
- 239 The Editorial Board of the Notebook of Vibration and Shock. *Notebook of Vibration and Shock*. Beijing: National Defense Industry Press, 1988, (1): 90–99.
- 240 Ni ZH. *Vibration Mechanics*. Xi'an: Xi'an Jiaotong University, 1989.
- 241 Chen Yuhau. Finite element transfer matrix method combined with finite element method for the analysis of plate. *Journal of Suzhou University*, 1994, 10(1): 69–71.
- 242 Zheng ZC. *Mechanical Vibration*. Beijing: China Machine Press, 1986.

- 243 Mustoe GW, Miyata M. Material flow analyses of non-circular shaped granular media using discrete element methods. *Journal of Engineering Mechanics*, 2001, 127(10): 1017–1026.
- 244 Eberhard E, Stead D, Coggan JS, et al. Hybrid finite-/discrete-element modelling of progressive failure in massive rock slopes. *ISRM 2003 – Technology Roadmap for Rock Mechanics, South African Institute of Mining and Metallurgy*, 2003, 279–280.
- 245 Liu HW. *Material Mechanics*, 3rd edition. Beijing: Higher Education Press, 1992.
- 246 Donald LK. Multibody system analysis based on Hamilton's weak principle. *AIAA Journal*, 2001, 39(12): 2382–2388.
- 247 Dokainish MA, Subbaraj K. A survey of direct time-integration methods in computational structural dynamics. I. Explicit methods. *Computers & Structures*, 1989, 32(6): 1371–1386.
- 248 Subbaraj K, Dokainish MA. A survey of direct time-integration methods in computational structural dynamics. II. Implicit methods. *Computers & Structures*, 1989, 32(6): 1387–1401.
- 249 Wang YL. Analysis of improving firing dispersion extent of tactical rocket. *Acta Armamentarii*, 1979, (1): 51–61.
- 250 Liu YW, Yan SZ, Zhang DJ. Dynamics of flexible bodies considering the dynamic stiffening terms. *China Mechanical Engineering*, 1997, 8(4): 81–84.
- 251 Hung SCC, Weng CI. Model analysis of controlled multilink systems with flexible link and joints. *Journal of Guidance, Control and Dynamics*, 1992, 15(3): 634–641.
- 252 Li Yan. Improvement in solution of eigenvalues with transfer matrix method on computer. *Journal of Aerospace Power*, 1991, 6(3): 249–250.
- 253 Munjal ML, Doige AG. Symmetry of one dimensional dynamical systems in terms of transfer matrix parameters. *Journal of Sound and Vibration*, 1990, 136(3): 467–475.
- 254 Snowdon JC. Mechanical four pole parameters and its application. *Journal of Sound and Vibration*, 1971, 15: 307–323.
- 255 Munjal ML. Velocity ratio-cum-transfer matrix method for the evaluation of a muffler with mean flow. *Journal of Sound and Vibration*, 1975, 39(1): 105–119.
- 256 Lung TY, Doige GA. A time-averaging, transient-testing method for acoustic properties of piping systems and mufflers with flow. *Journal of the Acoustical Society of America*, 1983, 73(3): 867–876.
- 257 Munjal ML. *Acoustics of Ducts and Mufflers*. New York: Wiley-Interscience, 1987.
- 258 Uhrig R. The transfer matrix method seen as one method of structural analysis among others. *Journal of Sound and Vibration*, 1966, 4(2):136–148.
- 259 Loewy RG. Analysis and vibration control of a helicopter rotor blade. *Conference Publication*, 1994, (389): 1290–1295.
- 260 Hu PM. Analysis of high frequency vibration by transfer matrix method. *Chinese Journal of Vibration and Shock*, 1996, 15(4): 50–52.
- 261 Chen YH. Large deflection analysis of structures by an improved combined finite element-transfer matrix method. *Computers & Structures*, 1995, 55 (1): 167–171.
- 262 Euler L. Nova methods motum corporum rigidarum determinandi. *Novi Commentarii Academiae Scientiarum Petropolitanae*, 1776, 20: 208–238.
- 263 Pereira MFOS, Ambrosio JAC. *Computer-Aided Analysis of Rigid and Flexible Mechanical Systems*. Dordrecht: Kluwer Academic Publishers, 1994.
- 264 Xu SL. *Fortran Program Set of Common Algorithm (II)*. Beijing: Tsinghua University Press, 1995.
- 265 He BD. *Design of Rocket Launcher*. Beijing: National Defense Industry Press, 1988.
- 266 Marting TS, Robert SB. *Projectile motion in a flexible gun tube*. ADA140737, 1984.
- 267 Song PJ. *The Exterior Ballistics of Rockets and Guns*. Beijing: Weapon Industry Press, 1992.
- 268 Xu MY. *The Exterior Ballistics of Rockets*. Beijing: Weapon Industry Press, 1989.
- 269 GJB349.13A-97, Rocket Stereotypes Test Procedures. Science Technology and Industry for National Defense Committee, 1997.

- 270 Cochran JE. Investigation of factors which contribute to mallaunch of free rockets. AD-A024570, 1976.
- 271 Cochran JE. Artillery research missile launch development program. AD-771066, 1977.
- 272 Cochran JE, Gunnels RT, McCutchen K. Rocket launchers as passive controls. AD-A112571, 1981.
- 273 Zhou YH, Wang SC. *Applied Two-Phase Flow Interior Ballistics*. Beijing: National Defense Industry Press, 1990.
- 274 Zhang YL. *Design of Gun Anti-recoil Mechanism*. Beijing: National Defense Industry Press, 1984.
- 275 Rui Xiaoting, Liu Yixin, Yu Hailong. *Launch Dynamics of Tank/Self-propelled Gun*. Beijing: Science Press, 2011.
- 276 Rui Xiaoting, Yun Laifeng, Wang Guoping, et al. *Direction to Launch Safety of Ammunition*. Beijing: National Defense Industry Press, 1986.
- 277 Wang MD, Zhao YQ, Zhu JG. *Principle of Tank Driving*. Beijing: National Defense Industry Press, 1983.
- 278 Li DP. *Motion of Ship and its Modeling*. Harbin: Harbin Engineering University Press, 1999.
- 279 Rui, X., Wang, G., Yun, L., et al. (2009). Advances in transfer matrix method of multibody system. Proceedings of the ASME Design Engineering Technical Conference, August 30–September 2, 2009, San Diego, California, USA, 861–869.
- 280 Rui, X., Rong, B., and Wang, G. (2009). New method for dynamics modeling and simulation of flexible multibody system. Proceedings of the 3rd International Conference on Mechanical Engineering and Mechanics, October 21–23, 2009, Beijing, P.R. China, 17–23.
- 281 Rui, X. (2011). Launch dynamics of multibody system and its applications. *Engineering Sciences* 13 (10): 76–82.
- 282 Rui, X., Zhang, C., and Liu, C. (2014). New developments in multibody system dynamics and its applications. *Advances in Mechanical Engineering*, 2014 (2). Article ID: 671604.
- 283 Rui, X., Abbas, L.K., Yang, F. et al. (2017). Flapwise vibration computations of coupled helicopter rotor/fuselage: application of multibody system dynamics. *AIAA Journal* 56 (2): 1–18.
- 284 Rui, X., Yun, L., Chen, T., and Feng, B. (2009). Evaluating method for launch safety of propellant charge. International Autumn Seminar on Propellants, Explosives and Pyrotechnics, September 22–25, 2009, Kunming, P.R. China, 656–659.
- 285 Rui, X. (2017). New developments in launch dynamics of multibody system and its applications. *Journal of Vibration, Measurement & Diagnosis*, 37 (2): 213–220.
- 286 Rui, X., Wang, X., Zhou, Q., and Zhang, J. (2018). Developments in transfer matrix method for multibody systems (Rui method) and its applications. Proceedings of the ASME 2018 International Design Engineering Technical Conferences and Computers and Information in Engineering Conference, August 26–29, 2018, Quebec City, Quebec, Canada.
- 287 Chen, G., Rui, X., Yang, F. et al. (2016). Study on the natural vibration characteristics of flexible missile with thrust by using riccati transfer matrix method. *Journal of Applied Mechanics* (3): 83. Article ID: 031006-1~031006-8.
- 288 Gu, J., Rui, X., Zhang, J. et al. (2016). Riccati transfer matrix method for linear tree multibody systems. *Journal of Applied Mechanics* 84 (1). Article ID: 011008-1~011008-7.
- 289 Wang, G., Rui, X., Rong, B., et al. (2009). Stochastic transfer matrix method for random eigenvalue problems. Proceedings of the 3rd International Conference on Mechanical Engineering and Mechanics, October 21–23, 2009, Beijing, P.R. China, 592–597.
- 290 Wang, G., Rui, X., and Rong, B. (2011). Evaluation of PDF of eigenvalue for multibody system with random parameters. Proceedings of the 4th International Conference on Mechanical Engineering and Mechanics, August 10–12, 2011, Suzhou, P.R. China, 443–447.

- 291 Rong, B., Rui, X., Wang, G., and Yin, Z. (2012). Study on random eigenvalue problems of slender rocket with uncertain parameters. *Engineering Mechanics* 29 (7): 341–346.
- 292 Zhang, J., Rui, X., Wang, G., and Yang, F. (2013). Riccati transfer matrix method for eigenvalue problem of the system with antisymmetric boundaries. ECCOMAS Thematic Conference on Multibody Dynamics, July 1–4, 2013, Zagreb, Croatia.
- 293 Gu, J., Rui, X., Chen, G. et al. (2016). Distributed parallel computing of the recursive eigenvalue search in the context of transfer matrix method for multibody systems. *Advances in Mechanical Engineering* 8 (11): 1–15.
- 294 Abbas, L.K., Chen, D., and Rui, X. (2014). Numerical calculation of effect of elastic deformation on aerodynamic characteristics of a rocket. *International Journal of Aerospace Engineering* 3–4: 1–11.
- 295 Abbas, L.K., Rui, X., and Marzocca, P. (2015). Aerothermoelastic analysis of panel flutter based on the absolute nodal coordinate formulation. *Multibody System Dynamics* 33 (2): 163–178.
- 296 Abbas, L.K., Zhou, Q., Hendy, H., and Rui, X. (2015). Transfer matrix method for determination of the natural vibration characteristics of elastically coupled launch vehicle boosters. *Acta Mechanica Sinica* 31 (4): 570–580.
- 297 Li, M., Rui, X., and Abbas, L.K. (2015). Elastic dynamic effects on the trajectory of a flexible launch vehicle. *Journal of Spacecraft and Rockets* 52 (6): 1–17.
- 298 Abbas, L.K. and Rui, X. (2014). Free vibration characteristic of multilevel beam based on transfer matrix method of linear multibody systems. *Advances in Mechanical Engineering*, 2014 (1). Article ID: 792478.
- 299 Abbas, L.K., Zhou, Q., Bestle, D., and Rui, X. (2017). A unified approach for treating linear multibody systems involving flexible beams. *Mechanism and Machine Theory* 107: 197–209.
- 300 Chen, D., Abbas, L.K., Rui, X. et al. (2017). Aerodynamic and static aeroelastic computations of a slender rocket with all-movable canard surface. *Proceedings of the Institution of Mechanical Engineers, Part G: Journal of Aerospace Engineering*, 232(6): 1103–1119.
- 301 Chen, D., Abbas, L.K., Rui, X. et al. (2017). Dynamic modeling of sail mounted hydroplanes system – Part I: modal characteristics from a transfer matrix method. *Ocean Engineering* 130: 629–644.
- 302 Chen, D., Abbas, L.K., Rui, X. et al. (2017). Dynamic modeling of sail mounted hydroplanes system – Part II: hydroelastic behavior and the impact of structural parameters and free-play on flutter. *Ocean Engineering* 131: 322–337.
- 303 Abbas, L.K. and Rui, X. (2017). Vibration of spinning beam based on transfer matrix method of linear multibody systems. International Conference on Mechanical, System and Control Engineering. IEEE, 67–71.
- 304 Abbas, L.K., Rui, X., Marzocca, P. et al. (2012). Static/dynamic edge movability effect on non-linear aerothermoelastic behavior of geometrically imperfect curved skin panel: flutter and post-flutter analysis. *Journal of Applied Mechanics – Transactions of the ASME* 79 (4): 1004.
- 305 Abbas, L.K., Rui, X., Marzocca, P. et al. (2011). A parametric study on supersonic/hypersonic flutter behavior of aero-thermo-elastic geometrically imperfect curved skin panel. *Acta Mechanica* 222 (1–2): 41–57.
- 306 Abbas, L.K., Li, M., and Rui, X. (2013). Transfer matrix method for the determination of the natural vibration characteristics of realistic thrusting launch vehicle—Part I. *Mathematical Problems in Engineering* 2: 388–400.
- 307 Abbas, L.K., Rui, X., and Hammoudi, Z.S. (2010). Plate/shell element of variable thickness based on the absolute nodal coordinate formulation. *Proceedings of the Institution of Mechanical Engineers, Part K – Journal of Multi-Body Dynamics* 224 (K2): 127–141.

- 308 Abbas, L.K., Ma, L., and Rui, X. (2010). Natural vibrations of open-variable thickness circular cylindrical shells in high temperature field. *Journal of Aerospace Engineering* 23 (3): 205–212.
- 309 Abbas, L.K., Bestle, D., and Rui, X. (2013). Transfer matrix method for the determination of the free vibration of two elastically coupled beams. Proceedings of the 2013 International Conference on Applied Mechanics and Materials (ICAMM 2013), November 23–24, 2013, Zhuhai, China, 372: 301–304.
- 310 Abbas LK., Zhou Q, Rui X. (2015). Frequency determination of beams coupled by a double spring-mass system using transfer matrix method of linear multibody systems. Proceedings of the 5th International Symposium on Knowledge Acquisition and Modeling, July 27–28, 2015, London, England, 21–24.
- 311 Abbas, L.K., Rui, X., and Marzocca, P. (2012). Panel flutter analysis of plate element based on the absolute nodal coordinate formulation. *Multibody System Dynamics* 27 (2): 135–152.
- 312 Li, M., Abbas, L.K., Rui, X., et al. (2015). The wet mode analysis of rudder system. International Conference on Electrical, Automation and Mechanical Engineering, July 26–27, 2015, Phuket, Thailand, 1586–1602.
- 313 Xie, K., Abbas, L.K., and Chen, D., et al.(2017). Numerical investigations on dynamic stall of a pitching-plunging helicopter blade airfoil. ICCFD.
- 314 Chen, D., Abbas, L.K., Wang, G., and Rui, X. (2017). Influence of flow field environment on wet modal vibration of flexible riser. *Journal of Harbin Engineering University*, 38 (10): 1587–1594.
- 315 Chen, D., Abbas, L.K., and Rui, X. (2014). Aerodynamic derivative and aerodynamic heating simulation and computation of spinning vehicle. *Computer Simulation* 31 (5): 26–30.
- 316 Chen, D., Abbas, L.K., Rui, X., and Wang, G. (2014). Numerical simulation of a spinning stabilized projectile aerodynamic characteristics effected by structure errors. *Acta Aerodynamica Sinica* 32 (5): 705–711.
- 317 Abbas, L.K., Chen, D., and Rui, X. (2013). Normal force computation for axisymmetric multistage launch vehicle. In: *Proceedings of the 2013 International Conference on Applied Mechanics and Materials (ICAMM 2013)*, Zhuhai, China (23–24 November 2013), vol. 419, 23–29.
- 318 Ma, L., Rui, X., Abbas, L.K. et al. (2012). Free vibration analysis and physical parameter identification of non-uniform beam carrying spring-mass systems. *Transactions of Nanjing University of Aeronautics and Astronautics* 29 (4): 345–353.
- 319 Abbas, L.K., Rui, X., and Marzocca, P. (2012). Absolute nodal coordinate formulation for aeroelastic analysis of panel. *Advanced Materials Research* 588–589: 1817–1821.
- 320 Liu, Z., Rui, X., and Abbas, L.K. (2012). Application of chebyshev series to solution of cable vibration problems. In: *Proceedings of the 2012 International Conference on Applied Mechanics and Materials (ICAMM 2012)*, Sanya, China (24–25 November 2012), vol. 101–102, 1173–1176.
- 321 Abbas, L.K., Rui, X., and Marzocca, P. (2009). Non-linear aerothermoelastic modeling and behavior of a double-wedge lifting surface. *Journal of Shanghai Jiaotong University (Science)* 14 (5): 620–625.
- 322 Tang, W., Rui, X., Wang, G. et al. (2016). Dynamics design for multiple launch rocket system using transfer matrix method for multibody system. *Proceedings of the Institution of Mechanical Engineers, Part G: Journal of Aerospace Engineering* 230 (14): 2557–2568.
- 323 Tang, W., Rui, X., Wang, G., and Yang, F. (2015). Quantitative analysis for affecting factors firing dispersion of multiple launch rockets system. *Journal of Nanjing University of Science and Technology* 9 (6): 704–710.
- 324 Tang, W., Rui, X., Wang, G., and Wang, G. (2016). Launching technique with variant firing orders and variant firing intervals for multiple launch rockets system. *Journal of Vibration and Shock* 35 (2): 51–57.

- 325 Tang, W., Rui, X., Yang, F., and Liu, F. (2016). Study on the vibration characteristics of a complex multiple launch rocket system. Proceedings of the 6th International Conference on Electronic, Mechanical, Information and Management Society, April 1–3, 2016, Shenyang, China, 360–365.
- 326 Xin, S., Rui, X., Zhang, J. et al. (2014). Method of improving firing precision for shipborne multiple launch rocket systems. *Journal of Ballistics* 26 (1): 40–44.
- 327 Xin, S., Rui, X., and Rui, X. (2015). Automatic deduction for overall transfer equation of a multiple launch rocket system and its dynamic visual simulation method. *Journal of Vibration and Shock* 34 (4): 30–34.
- 328 Han, X., Rui, X., Wang, G. et al. (2008). Research of fuze overload in bore of flexibility pills based on wavelet method. *Journal of System Simulation* 20 (13): 3496–3499.
- 329 Rui, X., Wang, G., Gu, J. et al. (2016). Study on system design method of firing precision for multiple rocket launcher. *Journal of Mechanical Engineering* 52 (7): 164–177.
- 330 He, J., Rui, X., Wang, G., and Gu, J. (2011). Research on technology of variable firing-order and firing-interval and actualization of firing device. *Journal of Ballistics* 23 (3): 79–83.
- 331 Yang, F., Rui, X., Wang, G., and Zhang, C. (2009). Test method of non-full loading firing dispersion. *Journal of Nanjing University of Science and Technology (Natural Science)* 33 (1): 83–87.
- 332 Wang, G., Rui, X., and Wang, G. (2008). New estimation method for dispersion of firing. *Modern Defence Technology* 36 (4): 42–45.
- 333 Wang, G., Rui, X., Wang, G., and Zhang, Y. (2008). Firing accuracy evaluation method of multiple launch rocket system. *Journal of Gun Launch & Control* 2008 (2): 82–84.
- 334 Wang, G., Rui, X., and Wang, G. (2009). High and low temperature environment test method of rockets based on Bayes. *Journal of Nanjing University of Science and Technology (Natural Science)* 33 (1): 88–92.
- 335 Wang, G. and Rui, X. (2012). Influence of jet flow on dynamic behavior of a MLRS. *Journal of Vibration and Shock* 31 (21): 143–145, 151.
- 336 Wang, G., Rui, X., Yang, F., and Xu, H. (2012). Dynamics analysis for wheeled and tracked multiple launch rocket system. *Acta Armamentarii* 33 (11): 1286–1290.
- 337 Wang, G., Rui, X., and Yang, F. (2012). Simulations and test validations for initial disturbances of rocket. *Journal of Vibration Engineering* 25 (5): 527–531.
- 338 Wang, G., Rui, X., Zhang, C., and Xin, S. (2011). Simulation of ballistic characteristics of long-range-rocket target-sensitivity-projectile. *Journal of Ballistic* 30 (07): 178–187.
- 339 Wang, G. and Rui, X. (2011). Rocket initial disturbance of LRMLRS. *Journal of Nanjing University of Science and Technology (Natural Science)* 35 (01): 62–65.
- 340 Wang, G., Rui, X., Liu, L., and Yang, F. (2016). Evaluation method for firing precision of LRMLRS. *Journal of Nanjing University of Science and Technology* 37 (6): 907–910.
- 341 Rui, X. and Rong, B. (2012). Advances in transfer matrix method for multibody system dynamics. *Advances in Mechanic* 42 (1): 4–17.
- 342 Wang, X., Rui, X., Yang, F. et al. (2018). Launch dynamics modeling and simulation of vehicular missile system. *Journal of Guidance, Control, and Dynamics*, 2018 (5): 1–10.
- 343 Zha, Q., Rui, X., Yu, H., and Zhou, Q. (2017). Study on the impact sensitivity of firing factors of self-propelled gun. *Journal of Vibration Engineering*, 30 (6): 938–946.
- 344 Liu, W., Rui, X., and Yu, H. (2008). Model and simulation of launch dynamics of automatic cannon in helicopter. *Journal of System Simulation* 20 (8): 1983–1985.
- 345 Liu, W., Rui, X. et al. (2008). Influence to ballistics of helicopter-carried rocket by aerodynamic characteristics. *Journal of System Simulation* 20 (14): 3873–3875, 3880.
- 346 Han, X., Rui, X., and Zhao, G. (2009). The analytic hierarchy process and the grey relevancy method on the multi-decision-making targets. *Fire Control & Command Control* 34 (9): 80–83.

- 347 Han, X., Rui, X., Yang, F. et al. (2009). Design and simulation on projectile-borne storage testing system based on embedded system. *Journal of System Simulation* 21 (1): 84–87.
- 348 Rui, X., Gu, J., Zhang, J. et al. (2017). Visualized simulation and design method of mechanical system dynamics based on transfer matrix method for multibody systems. *Advances in Mechanical Engineering* 9 (8).
- 349 Yang, H., Rui, X., Liu, Y. et al. (2013). Visual simulation software for multibody system dynamics based on MBDyn. *Journal of Nanjing University of Science and Technology* 37 (6): 785–791.
- 350 Yang, H., Rui, X., Zhan, Z. et al. (2015). Virtual design software for mechanical system dynamics using transfer matrix method of multibody system and its application. *Advances in Mechanical Engineering*, 7 (9): 1–24.
- 351 Yang, H., Rui, X., Liu, Y., and He, J. (2013). Business software rapid development platform based on SOA. *International Journal of Database Theory and Application* 6 (3): 21–32.
- 352 Yang, H., Rui, X., Liu, Y., and Liu, F. (2013). Study on robotics simulation based on ODE. *ICIC Express Letters* 7 (10): 2873–2879.
- 353 Yang, H., Rui, X., Liu, Y. et al. (2014). Study on distributed parallel computing of transfer matrix method for multibody systems. *Journal of Vibration Engineering* 27 (1): 9–15.
- 354 Ma, L., Rui, X., Yang, F., and Rong, B. (2009). Power spectrum analysis for laser gyro damping system of strap down inertial navigation. *Journal of Vibration Engineering* 22 (6): 603–607.
- 355 Ma, L., Rui, X., Yang, F. et al. (2011). A physical parameter identification method based on transfer matrix method of multibody system and genet IC algorithm. *Journal of Vibration Engineering* 24 (06): 607–612.
- 356 Ma, L., Rui, X., Yang, F., et al. (2009). Numerical investigation of laser gyro damping system of strap-down inertial navigation. Proceedings of the 3rd International Conference on Mechanical Engineering and Mechanics, October 21–23, 2009, Beijing, P.R. China, 1005–1009.
- 357 Yang, F., Rui, X., and Zhang, H. (2011). Study on combined environment adaptability of strapdown inertial measure unit by MS-TMM. Proceedings of the 4th International Conference on Mechanical Engineering and Mechanics, August 10–12, 2011, Suzhou, P.R. China, 598–603.
- 358 Yang, F., Rui, X., and Ma, L. (2008). Dynamical model and simulation of laser gyro strapdown inertial navigation system. *Journal of Chinese Inertial Technology* 16 (3): 301–305.
- 359 He, J., Rui, X., Wang, G. et al. (2012). Vibration characteristic of launch guider of a MLRS in firing process. *Journal of Vibration and Shock* 31 (1): 35–38, 139.
- 360 He, J., Rui, X., Wang, G. et al. (2011). Design technology of improving firing dispersion of MLRS. *Journal of Vibration Engineering* 24 (06): 676–681.
- 361 Yu, H., Rui, X., Wang, G., and Rong, B. (2011). The effect of firing order and firing interval to firing dispersion by metal storm weapon. *Journal of Projectiles, Rockets, Missiles and Guidance* 31 (1): 91–93.
- 362 Yu, H., Rui, X., Wang, G., and Liu, Z. (2011). The study on vibration characteristic for multiple tandem weapon. *Journal of Projectiles, Rockets, Missiles and Guidance* 31 (3): 195–199, 202.
- 363 Yu, H., Rui, X., Wang, G., and Liu, Z. (2010). Analysis of factors influencing firing precision of ‘Metal Storm’ weapons. *Journal of Nanjing University of Science and Technology (Natural Science)* 34 (4): 524–527.
- 364 Yu, H., Rui, X., Yang, F. et al. (2010). Modeling and simulation of launch dynamics for ‘Metal Storm’ weapon. *Journal of Nanjing University of Aeronautics & Astronautics* 42 (5): 574–577.
- 365 Yun, L., Rui, X., Wang, G., and Chen, T. (2010). Application of DCD scheme to computation of two-phase flow interior ballistics for fractured propellant bed. *Explosion and Shock Waves* 30 (3): 295–300.
- 366 Yun, L., Rui, X., and Feng, K. (2009). Interior ballistic performances of equilibrium launcher. *Journal of Nanjing University of Science and Technology (Natural Science)* 33 (2): 258–261. 271.

- 367 Yun, L., Rui, X., and Chen, T. (2009). Application of DCD scheme in computation of gas-solids two-phase flow. *Journal of Ballistics* 21 (2): 107–110.
- 368 Yun, L., Rui, X., and Feng, K. (2009). Analysis of abnormal interior ballistic performance of an equilibrium launcher at high and low temperature. *Chinese Journal of Explosives & Propellants* 32 (2): 68–71.
- 369 Li, Y., Yu, H., and Rui, X. (2014). Numerical study on penetration of rotating projectile into steel plate. *Fire Control & Command Control* 14 (12): 31–35.
- 370 Li, Y., Yu, H., and Rui, X. (2014). Numerical simulation of angle of attack on body projectile penetrating composite target effects. *Computer Simulation* 31 (4): 1–4. 13.
- 371 Zhang, C., Rui, X., Rong, B., and Wang, G. (2013). Vibration characteristics of airborne multiple launch rocket systems. *Journal of Vibration Engineering* 26 (1): 15–19.
- 372 Zhang, C., Rui, X., Rong, B. et al. (2013). Test method of non-full loading firing dispersion for an airborne multiple launch rocket system. *Journal of Vibration and Shock* 32 (2): 1–5.
- 373 Jiang, S., Yu, H., Rui, X. et al. (2014). Dynamic analysis on impact fragmentation of granular systems. *Explosion and Shock Waves* 34 (2): 247–251.
- 374 Jiang, S., Chen, P., Rui, X., and Zhang, M. (2011). Meet irreducible d-modules in strongly maximal taf algebras. *Journal of Mathematics* 31 (4): 763–769.
- 375 Han, X., Rui, X., Hong, J., and Yang, F. (2008). Test analysis and numerical simulation of fuse inertia components falling dynamics. *Journal of System Simulation* 20 (8): 1990–1994.
- 376 Zhou, Z., Wang, G., Rui, X. et al. (2016). Interior ballistic simulation and optimization of solid pulse thruster. *Journal of Ballistics* 28 (1): 8–13.
- 377 Zhang, J., Wang, G., and Rui, X. (2015). Vibration analysis of systems with random parameter using perturbation transfer matrix method. *Journal of Machine Design* 32 (10): 86–90.
- 378 Liu, Z., Rui, X., and Yang, H. (2012). Application of symbolic computation in natural vibration analysis of cables and suspenders. *Mechanics and Engineering* 34 (1): 62–65.
- 379 Zhou, X., Rui, X., and Zhang, S. (2008). Implement of tracking system of moving target based on DSP. *Microcomputer Information* 24 (23): 189–191.
- 380 Wei, W., Rui, X., and Chen, Y. (2008). Study on millimeter wave radar homing head. *Tactical Missile Technology* 2: 83–87.
- 381 Dong, M. and Rui, X. (2008). Study on distribution law of mutiple launch rocket falling points. *Journal of Gun Launch & Control* 3: 1–5.
- 382 Zhou, Q., Rui, X., Yang, F. et al. (2017). Measurement for projectile's in-bore yaw based on optical lever principle. *Journal of Aerospace Engineering*.
- 383 Rong, B., Rui, X., Wang, G., and Yang, F. (2010). New efficient method for dynamic modeling and simulation of flexible multibody systems moving in plane. *Multibody System Dynamics* 24 (2): 181–200.
- 384 Rui, X. and Schiehlen, W. (2007). Multibody system dyanamics: preface. *Multibody System Dynamics* 18 (4): 485.
- 385 Khalil, M., Rui, X., Zha, Q., and Hendy, H. (2014). Investigation on spin-stabilized projectile trajectory observability based on flight stability. In: *Proceedings of the 3rd International Conference on Applied Mechanics and Materials (ICAMM 2014)*, Shenzhen, China (15–16 November 2014), vol. 530–531, 175–180.
- 386 Hendy, H., Rui, X., and Khalil, M. (2013). An integrated GPS/INS navigation system for land vehicle. In: *Proceedings of the 2013 International Conference on Applied Mechanics and Materials (ICAMM 2013)*, Zhuhai, China (23–24 November 2013), vol. 336–338, 221–226.
- 387 Li, H., Feng, Z., Li, K., and Rui, X. (2003). Object-oriented simulation of antiaircraft missile. *Proceedings of the International Symposium on Test and Measurement* 4: 2877–2880.

- 388 Li, M., Abbas, L.K., Rui, X., and Wang, G. (2016). The prediction of flexible rocket's aerodynamic force computational accuracy. *Journal of Harbin Institute of Technology* 48 (10): 91–96.
- 389 Liu, F., Rui, X., Yu, H., and Zhang, J. (2016). Study on launch dynamics of the self-propelled artillery marching fire. *Journal of Vibration Engineering* 29 (3): 380–385.
- 390 Liu, F., Rui, X., Yu, H. et al. (2016). Influence of barrels' flexibility on the launch dynamics of tank during marching fire. *Journal of Vibration and Shock* 35 (2): 58–63.
- 391 Liu, Z., Rui, X., Zhan, Z. et al. (2012). Improved EMD-based structural damage feature extraction. *Journal of Vibration, Measurement and Diagnosis* 32 (04): 634–639. 692.
- 392 Rong, B., Rui, X., Wang, G., and Yang, F. (2011). Developments of studies on multibody system dynamics. *Journal of Vibration and Shock* 30 (07): 178–187.
- 393 Rong, B., Rui, X., and Zhu, L. (2011). Dynamic simulation of granular system dynamic simulation of granular system. *Journal of Vibration Engineering* 24 (02): 146–150.
- 394 Jiang, S., Rui, X., Hong, J. et al. (2011). Dynamic simulation of granular system. *Rock and Soil Mechanics* 32 (08): 2529–2532, 2538.
- 395 Liu, Z., Rui, X., Yang, F. et al. (2011). Transfer matrix method for vibration measurement of cable tension. *Journal of Vibration and Shock* 30 (10): 270–273.
- 396 He, B., Rui, X., Yun, L. et al. (2008). Discussion on the methods of estimating structural vibration from railway lines and the determination of damping matrix. *Journal of Vibration and Shock* 27 (11): 83–86.
- 397 Liu, F., Rui, X., Yu, H., and Zhang, J. (2016). Study on the theory of projectile firing process during marching fire. International Conference on Education, Management, Computer and Society (EMCS 2016), 1341–1345.
- 398 Rong, B., Rui, X., and Wang, G. (2009). Dynamics modeling and simulation of spacecrafts with flexible solar panels. Proceedings of the 3rd International Conference on Mechanical Engineering and Mechanics, October 21–23, 2009, Beijing, P.R. China, 807–812.
- 399 Liu, Z., Rui, X., Wang, G., and Yu, H. (2013). Transfer matrix method for vibration measurement of cable tension considering sag. *Journal of Nanjing University of Science and Technology* 37 (4): 608–612.
- 400 Zhang, C., Rui, X., Rong, B., and Wang, G. (2013). Method to improve firing dispersion of airborne multiple launch rocket systems. *Journal of Nanjing University of Science and Technology* 37 (2): 233–238.
- 401 Jiang, S., Rui, X., Wang, Y., and Li, C. (2013). Dynamics simulation of gun propellant charge with compress and fracture based on discrete element method. *Scientia Sinica* 43 (8): 965–970.
- 402 Feng, B., Rui, X., Xu, H. et al. (2012). Dynamic compression fracture condition of one nitroamine propellant charge during launch course. *Chinese Journal of Explosives & Propellants* 35 (2): 70–73, 85.
- 403 Hong, J., Rui, X., and Fei, Q. (2010). Dynamic simulation for propellant bed with press and fracture. *Journal of System Simulation* 22 (4): 1018–1021.
- 404 Khalil, M., Rui, X., Zha, Q. et al. (2013). Projectile impact point prediction based on self-propelled artillery dynamics and Doppler radar measurements. *Advances in Mechanical Engineering*, 2013 (3). Article ID: 153913.
- 405 He, B., Rui, X., and Zhang, H. (2012). Transfer matrix method for natural vibration analysis of tree system. *Mathematical Problems in Engineering* 1: 59–63.
- 406 Bestle, D. and Rui, X. (2013). Application of the transfer matrix method to control problems. Proceedings of the ECCOMAS Thematic Conference on Multibody Dynamics, 259–268.
- 407 Zhu, W., Bian, L., and Rui, X. (2014). Online parameter identification of the asymmetrical Bouc–Wen model for piezoelectric actuators. *Precision Engineering – Journal of the International Societies for Precision Engineering and Nanotechnology* 38 (4): 921–927.

- 408 Zhu, W. and Rui, X. (2014). Semiactive vibration control using a magnetorheological damper and a magnetorheological elastomer based on the Bouc–Wen model. *Shock and Vibration* 2: 1–10.
- 409 Zhu, W. and Rui, X. (2015). Online parameter identification of Bouc–Wen model for piezoelectric actuators. *Optics and Precision Engineering* 23 (1): 110–116.
- 410 Zhu, W., Bian, L., An, Y. et al. (2015). Modeling and control of a two-axis fast steering mirror with piezoelectric stack actuators for laser beam tracking. *Smart Materials and Structures* 24 (7): 1–12.
- 411 Zhu, W., Chen, G., and Rui, X. (2015). Modeling of piezoelectric stack actuators considering bonding layers. *Journal of Intelligent Material Systems and Structures* 26 (17): 2418–2427.
- 412 Zhu, W. and Rui, X. (2016). Hysteresis modeling and displacement control of piezoelectric actuators with the frequency-dependent behavior using a generalized Bouc–Wen model. *Precision Engineering – Journal of the International Societies for Precision Engineering and Nanotechnology* 43: 299–307.
- 413 Zhou, Q., Rui, X., Tao, Y. et al. (2016). Deduction method of the overall transfer equation of linear controlled multibody systems. *Multibody System Dynamics* 38 (3): 263–295.
- 414 Zhu, W., Zhou, Q., and Rui, X. (2016). Angle hybrid control for a two-axis piezo-positioning system and its application. *Smart Materials and Structures* 25 (9). Article ID: 095002.
- 415 Zhu, W., Bian, L., Chen, G. et al. (2017). Hysteresis modelling and experimental verification of a Fe–Ga alloy magnetostrictive actuator. *Smart Materials and Structures* 26 (3). Article ID: 035039.
- 416 Zhu, W., Yang, F., and Rui, X. (2017). A fully dynamic model of a multi-layer piezoelectric actuator incorporating the power amplifier. *Smart Materials and Structures* 26 (12). Article ID: 125008.
- 417 Zhang, H., Rui, X., Yang, F. et al. (2017). Research on the adaptive damping method of strap-down inertial measurement unit based on the magneto rheological technology. *Shock and Vibration* 1–14.
- 418 Zhang, H., Rui, X., Yang, F., and Chen, G. (2017). Adaptive estimation and simulation on the vibration frequency of missile system. *Journal of Vibration and Shock*, 36 (10): 212–216.
- 419 Tao, Y., Rui, X., Yang, F. et al. (2017). Design and experimental research of a magnetorheological elastomer isolator working in squeeze/elongation-shear mode. *Journal of Intelligent Material Systems and Structures*, 29(7): 1418–1429.
- 420 Hendy, H., Rui, X., Zhou, Q. et al. (2014). Transfer matrix method for multibody systems of TITO system control applications. In: *Proceedings of the 3rd International Conference on Applied Mechanics and Materials (ICAMM 2014)*, Shenzhen, P.R. China (15–16 November 2014), vol. 530–531, 1043–1048.
- 421 Zhan, Z., Rui, X., Rong, B. et al. (2011). Design of vibration control of launcher for multiple launch rocket system. *Journal of Vibration Engineering* 24 (03): 327–332.
- 422 Zhan, Z., Rui, X., Wang, G. et al. (2010). Vibration control for launcher of multiple launch. *Chinese Journal of Theoretical and Applied Mechanics* 42 (03): 583–590.
- 423 He, J., Rui, X., Wang, G. et al. (2013). Research on design and actualization of vibration controlled system of launch guider of MLRS. *Fire Control & Command Control* 38 (11): 129–133.
- 424 Yang, F., Rui, X., Wang, Q., and Wang, G. (2010). Initial disturbance control for multiple launching rocket system. *Journal of Nanjing University of Science and Technology (Natural Science)* 34 (1): 61–65.
- 425 Rui, X. and Rong, B. (2011). Dynamic modeling and LQR-based active vibration control of piezoelectric structures. *Proceedings of the 4th International Conference on Mechanical Engineering and Mechanics*, August 10–12, 2011, Suzhou, P.R. China, 31–36.

- 426 Zhan, Z., Rui, X., Yang, F., and Wang, G. (2009). Optimum pulse control of multibody system. *Proceedings of the 3rd International Conference on Mechanical Engineering and Mechanics*, October 21–23, 2009, Beijing, P.R. China, 1039–1043.
- 427 Xin, S., Rui, X., Wang, G. et al. (2015). Vibration control of shipborne multiple launch rocket systems. *Journal of Nanjing University of Science and Technology* 1: 1–6.
- 428 Li, B., Rui, X., and Zhou, Q. (2017). Study on simulation and experiment of control for multiple launch rocket system by computed torque method. *Nonlinear Dynamics*, 91 (3): 1639–1652.
- 429 Li, B. and Rui, X. (2018). Vibration control of uncertain multiple launch rocket system using radial basis function neural network. *Mechanical Systems and Signal Processing* 98: 702–721.
- 430 Li, B., Rui, X., Yang, F. et al. (2017). Design and implementation of an adaptive Kalman filtering for the launcher of multiple launch rocket system. *International Journal of Adaptive Control and Signal Processing*, 31 (2): 1–17.
- 431 Han, X., Rui, X., Yang, F. et al. (2008). Fuze mechanism control and testing system based on Labview. *Microcomputer Information* 24 (16): 81–83.
- 432 Wang, G., Rui, X., and Tang, W. (2017). Active vibration control design method based on transfer matrix method for multibody systems. *Journal of Engineering Mechanics* 143 (6).
- 433 Wang, G., Rui, X., Xu, H. et al. (2013). PVDF sensor for total pressure of projectile base. *Ordnance Industry Automation* 32 (1): 71–74. 78.
- 434 Yang, F., Rui, X., and Zhan, Z. (2008). The transfer matrix method of controlled multibody system with branch. *Journal of Dynamics and Control* 6 (3): 213–218.
- 435 Yang, F., Rui, X., Ma, L., and He, J. (2009). Study on control design for linear transfer matrix method of controlled multibody system. *Proceedings of the 3rd International Conference on Mechanical Engineering and Mechanics*, October 21–23, 2009, Beijing, P.R. China, 1153–1158.
- 436 Rong, B., Rui, X., Yang, F., and Zhan, Z. (2009). Dynamics modeling and simulation for controlled flexible manipulator. *Journal of Vibration Engineering* 22 (2): 168–174.
- 437 Rong, B., Rui, X., Wang, G., and Yang, F. (2011). Dynamic modeling and H_∞ independent modal space vibration control of laminate plates. *Science China – Physics Mechanics & Astronomy* 54 (9): 1638–1650.
- 438 Chen, Z., Zhu, W., and Rui, X. (2017). Study on vibration reduction of the tank engines based on MRE. *Noise and Vibration Control* 37 (1): 72–75. 116.
- 439 Meng, X., Yu, H., Rui, X. et al. (2017). MRD modeling and its application in seat cushioning. *Noise and Vibration Control* 37 (1): 58–62.
- 440 Rui, X., He, B., Yun, L. et al. (2007). Advances in discrete time transfer matrix method of multibody system. *Solid Mechanics and its Applications* 1: 227–241.
- 441 Rui, X., He, B., Rong, B. et al. (2009). Discrete time transfer matrix method for dynamics of a multi-rigid-flexible-body system moving in plane. *Proceedings of the Institution of Mechanical Engineers, Part K – Journal of Multi-Body Dynamics* 223 (1): 23–42.
- 442 He, B., Rui, X., and Wang, G. (2007). Riccati discrete time transfer matrix method for elastic beam undergoing large overall motion. *Multibody System Dynamics* 18 (4): 579–598.
- 443 Wang, G., Rong, B., Tao, L., and Rui, X. (2012). Riccati discrete time transfer matrix method for dynamic modeling and simulation of an underwater towed system. *Journal of Applied Mechanics – Transactions of the ASME* 79 (4): 1014.
- 444 Rui, X., Bestle, D., and Zhang, J. (2013). A new form of the transfer matrix method for multibody systems. *Proceedings of the ECCOMAS Thematic Conference on Multibody Dynamics*, 643–654.

- 445 Rui, X., Bestle, D., Zhang, J. et al. (2016). A new version of transfer matrix method for multibody systems. *Multibody System Dynamics* 38 (2): 137–156.
- 446 Rui, X., Wang, G., Zhang, J., and Rui, X. (2016). Study on automatic deduction method of overall transfer equation for branch multibody system. *Advances in Mechanical Engineering* 8 (6): 1–16.
- 447 Zhang, J., Rui, X., Li, B. et al. (2016). Study on the stress stiffening effect and modal synthesis methods for the dynamics of a spatial curved beam. *Journal of Applied Mechanics* 83 (8). Article ID: 081004-1~081004-8.
- 448 Zhang, J., Rui, X., and Chen, G. (2016). Dynamics modeling and analysis of a spatial curved beam with stress stiffening. *Journal of Vibration and Shock* 35 (14): 27–33.
- 449 Zhang, J., Rui, X., and Gu, J. (2016). Eigenvalue analysis of the stress stiffening effect for a curved beam with large rigid motion. *Journal of Vibration Engineering* 29 (5): 779–786.
- 450 Zhang, J., Rui, X., Liu, F. et al. (2017). Substructuring technique for dynamics analysis of flexible beams with large deformation. *Journal of Shanghai Jiaotong University* 22 (5): 562–569.
- 451 Rong, B., Rui, X., and Tao, L. (2012). Perturbation finite element transfer matrix method for random eigenvalue problems of uncertain structures. *Journal of Applied Mechanics – Transactions of the ASME* 79 (2): 1005.
- 452 Rong, B., Rui, X., and Wang, G. (2010). New method for dynamics modelling and analysis on a flexible plate undergoing large overall motion. *Proceedings of the Institution of Mechanical Engineers, Part K – Journal of Multi-Body Dynamics* 224 (K1): 33–44.

Index

a

absolute nodal coordinate approach 265
 acceleration 82
 ADMAS 8
 amplitude resonance 72
 angle 12, 15–17, 84
 angular acceleration 183, 184
 angular displacement 8, 15–17
 angular velocity 12, 207, 225, 243
 ANSYS 2
 applied force 591
 assumed modes method 11
 attack angle 12, 578, 579
 augmented eigenvector 6–10, 17, 86–115
 augmented operator 6, 7, 14, 17, 87

b

beam theory 67, 296
 bending stiffness 29
 body 1
 body dynamics equation of body
 element 8–14, 80
 body dynamics equations of system 8–14,
 79, 87
 body-fixed coordinate system 15, 16, 185,
 187, 266
 boundary conditions 31, 32
 boundary element method 2
 boundary ends 9, 15, 23, 434, 435, 442
 branch multibody system 356, 607

c

Cartesian coordinates 144
 center of mass 579
 centrifugal force 2

chain multi-rigid-flexible-body
 system 100, 443
 chain system 9, 11, 23, 55, 185, 442
 characteristic equation 22, 32
 chessboard rule 378, 408–412
 classical transfer matrix method
 (classical TMM) 3
 closed-loop system 129, 435, 442
 complex transfer matrix 59, 73, 404
 component mode synthesis method 270
 computational efficiency 5, 6, 8, 14
 computational scale 2, 3, 5, 10–14, 21, 22
 computer-aided design (CAD) 4
 conjugate complex numbers 59
 conjugate operator 85
 conjugate transformation 84, 85
 constitutive relations 93, 97, 98, 100, 101, 646
 continuity assumption 270
 continuous functions 84, 87, 89
 continuous system 6, 12
 controlled multibody system 327, 348–375
 Coriolis acceleration 269
 Coriolis forces 2
 corotational coordinate approach 265
 cross-product matrix 15

d

damped system 22, 33, 57
 damper 2, 56
 damping coefficient 56, 58, 112, 254
 damping linear operator 113, 114
 damping ratio 21, 71, 112
 deflection angle 12, 541, 578
 degrees of freedom (DOF) 2
 dichotomy method 36

differential-algebraic equations 219
 discrete system 5, 11, 41
 discrete time transfer matrix method
 (DTTMM) 5, 183
 discrete time transfer matrix method for
 multibody systems (MSDTMM) 6,
 217–266
 discrete time transfer matrix method for multi-
 rigid-body systems (MRSDTTMM) 6,
 217–220, 259
 discrete time transfer matrix method for multi-
 rigid-flexible-body systems 6, 217
 displacements 22
 disturbance factors 12, 491, 493
 dynamics design 7, 12–14, 79
 dynamics response 79, 102

e

eigenequation 9, 10, 358, 505
 eigenfrequency 21, 25, 26, 33, 40, 89
 eigenfunctions 87, 96, 107
 eigenvalue problem 5, 7, 14, 21, 22
 eigenvector orthogonality 2
 elastic coefficient 105, 329, 336, 346, 583, 622
 elastic force 60, 154, 329, 557, 646
 entire elasticity assumption 271
 equation of motion 60
 Euclidean space 84, 85
 Euler–Bernoulli beam 41, 44–53
 Eulerian formula 59
 extended MSTMM 8, 120
 extended state vectors 68, 73, 122, 134
 extended transfer equation 63, 64, 72, 122,
 350, 404
 extended transfer matrix 73, 74, 120, 350,
 396–401
 exterior ballistics 12, 517, 518

f

finite difference 167
 finite element method (FEM) 1
 finite element transfer matrix method 5,
 140–153
 finite element transfer matrix method for a
 multibody system (FE-MSTMM) 129, 338
 finite segment discrete time transfer matrix
 method for multibody systems 341
 finite segment method 265, 341, 342

firing dispersion 6, 489
 firing frequency 21, 504
 firing orders 21
 firing precision 21, 489
 firing sequence 492, 519
 flexible body 1, 2, 199
 floating frame of reference
 formulation 199, 266
 forced vibration 63
 forced vibration systems 378
 Fourier coefficients 130, 132
 Fourier series 120, 130–132, 162
 framework system 129
 free end 50
 free vibration 25, 40

g

generalized coordinate 6, 9, 16, 17, 87, 199,
 217, 265, 269
 generalized force 148
 geometrical equation 185
 geometric equation 436, 442
 geometry relations 92, 97
 global dynamics equation 6–13, 79, 88, 183,
 199, 266, 433

h

harmonic balance principle 132
 harmonic function 89
 hinge 1, 22
 homogeneity assumption 271
 homogeneous equations 32, 38, 39, 40, 69, 419
 hybrid coordinate approach 265
 hypothesis modal shape method 2

i

ideal trajectory 12
 ill-condition 2, 5, 7, 11, 13, 14, 21, 22, 140
 inboard body 14, 189
 incremental method 131
 incremental TMM 130
 incremental transfer matrix 131, 134
 inertia coordinate system 23, 266, 267, 683
 initial condition 10
 initial disturbance 12, 489
 inner product space 83
 input end 15, 24
 interior ballistic 12, 517, 548

internal forces 15
 internal moments 32, 34, 82, 189–193, 206
 International System of Units (SI) 17
 isotropy assumption 271

j

joint 88, 171, 219, 225, 258, 262, 553, 561, 585–587

k

Kane's method 105
 kinematic equations 271
 kinetic energy 147, 339
 Kirchhoff's hypothesis 143

l

Lagrange equation 146, 148
 Lagrange interpolation polynomial 228
 Lagrange multipliers 219
 Lagrangian equations 219
 large motion 1
 launch dispersion 13
 launch dynamics 1, 12
 launch dynamics of multibody systems 5
 launching frequency 7
 launch system 2, 3, 5–7, 12–14
 light damped system 58
 linearization 225
 linear multibody system dynamics 21, 79
 linear operator 81, 82, 85, 113, 114
 linear space 83, 84, 86
 linear system 3, 14, 15
 linear time-invariant multibody systems 225, 607
 linear transformation 4, 85
 longitudinal stiffness 88, 646
 longitudinal vibration 23, 26–28
 lumped mass 1, 27

m

Marting's equation 514
 modal analysis method 13, 21, 79, 265, 276, 277, 305, 318
 modal coordinates 6, 16, 22, 26
 modal synthesis method 2, 7, 13, 21
 mode superposition method 40, 114
 multibody system (MS) 1
 multibody system dynamics (MSD) 1
 multi-degree-of-freedom system 138

multi-flexible-body system (MFS) 2, 21, 199
 multi-flexible-body system dynamics (MFSD) 2
 multiple launch rocket system (MLRS) 3, 491
 multi-rigid-body system (MRS) 1, 183
 multi-rigid-body system dynamics (MRSD) 1
 multi-rigid-flexible-body system (MRFS) 1
 multi-rigid-flexible-body systems dynamics (MRFSD) 80
 multi-rigid-launch-body systems dynamics (MRLSD) 79

n

natural vibration characteristics 2
 Newton–Euler method 186, 187
 Newton–Raphson method 154, 159
 Newton's second law 27
 Newton's third law 185, 188
 nonlinear system 8, 129
 nonlinear time-variant systems 221
 nontrivial solution 33
 numerical algorithm 220, 328
 numerical integration 6, 139, 183

o

ordinary differential equations 10
 orthogonality 2
 orthogonality of augmented eigenvectors 6, 89
 orthogonality of eigenvectors 5, 7, 13, 14, 79–83
 outboard body 14, 188–193
 output end 15, 24
 overall transfer equation 9, 31, 442
 overall transfer matrix 9, 31, 442

p

parameter matrix 80
 parameter matrix of damping 80
 parameter matrix of mass 80
 parameter matrix of stiffness 80
 partial differential equations 10
 phase resonance 72
 physical coordinates 6, 15–17
 planar motion 25
 potential energy 147
 principal coordinates 8, 40
 principal modals 25
 principal mode shape 40
 principal vibration 40

q

quasi-linear system 130

r

Rayleigh–Ritz method 265, 269

real trajectory 12

Riccati discrete time transfer matrix method for
multibody systems (Riccati MSDTTMM) 6,
423–429

Riccati finite element transfer matrix
method 417

Riccati transfer matrix method (Riccati
TMM) 3, 154, 417

Riccati transfer matrix method for multibody
systems (Riccati MSTMM) 378, 417

Riccati transformation 8, 158, 418

rigid body 1

Runge–Kutta method 108

s

self-propelled artillery 3, 545

shape function 146

Shear deformations 142

shipboard gun 489

simple-harmonic excitation 63

simple harmonic external force 349

small deformation assumption 199, 271

smooth hinge 14, 225

spatial motion 41, 269, 274

spin angle 12

state variables 6, 22

state vector 22–26, 184, 200, 222–224, 276

static response 80, 124

steady-state oscillations 139

steady-state response 7, 63

steady-state vibration 63

step-by-step scanning method 36

step-by-step time integration method 225

stiffness gradient 2

stiffness matrix 5, 146, 147, 154, 339, 340, 377

structural damping 56, 72

structural dynamics 3

swing angle 12, 518

symmetric transformation 84

symmetry operator 85

t

Taylor expansion theorem 226

Timoshenko beam 41, 390

topology figure 433–436

torsional stiffness 48

torsional vibration 3

transfer direction 15

transfer equations 9, 26

transfer matrix 3, 26

transfer matrix library 12, 377, 607

transfer matrix method (TMM) 3

transfer matrix method for linear multibody
systems 22

transfer matrix method for multibody systems
(MSTMM) 3, 5

transient response 63, 102

transpose transformation 85

transverse vibration 3, 29

tree system 129, 435

trigonometric series 165

two-dimensional system 5, 140, 162,
167, 170

two-phase flow 548, 563, 565

u

undamped free vibration 25

undamped system 22

v

velocity 12, 70, 154–156

vibration characteristics 2, 21

viscous damping 56

WILEY END USER LICENSE AGREEMENT

Go to www.wiley.com/go/eula to access Wiley's ebook EULA.